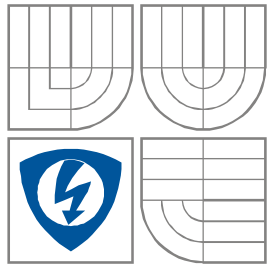


BRNO UNIVERSITY OF TECHNOLOGY
VYSOKÉ UČENÍ TECHNICKÉ V BRNĚ



**FACULTY OF ELECTRICAL ENGINEERING AND
COMMUNICATION**
DEPARTMENT OF RADIO ELECTRONICS

FAKULTA ELEKTROTECHNIKY A KOMUNIKAČNÍCH TECHNOLOGIÍ
ÚSTAV RADIOELEKTRONIKY

**APPLICATIONS OF ADVANCED CONTROLLABLE
ACTIVE ELEMENTS IN ELECTRONIC CIRCUITS**
APLIKACE POKROČILÝCH ŘIDITELNÝCH AKTIVNÍCH PRVKŮ V ELEKTRONICKÝCH OBVODECH

HABILITATION THESIS
HABILITAČNÍ PRÁCE

AUTHOR
AUTOR PRÁCE

Ing. Roman Šotner, Ph.D.

BRNO, 2016

ABSTRACT

This habilitation thesis describes research and pedagogical activities in the field of active elements and their applications in analog signal processing. The first part concerns research and development which is focused on signal generation, reconfigurable active filters providing different transfer responses without the necessity of reconnecting input and output ports. A short text has been added to the contribution dealing with the area of synthesis of fractional-order circuits. The results of modeling and development of active elements in CMOS technologies are described in a further subpart. The research and development activities are supported by a short overview of selected practical products. The discussed topics present an overview of the author/applicant's activities especially in the years after the defense of his Ph.D. thesis. References of older results (2-3 cases) are required for context in explanations and discussions. The part focused on pedagogical activities deals with the engagement of the applicant in education and teaching at his workplace, creation of teaching aids/materials for students (HW and lecture notes/guidance documents for practical lessons), brief description of selected final works of bachelor and master students and their contribution to research activities of the applicant.

KEYWORDS

Active elements, active filters, CMOS, electronic control, modeling of active elements and analog systems, oscillators, reconfiguration, synthesis and design of circuits.

ABSTRAKT

Tato habilitační práce popisuje výzkumné a výukové (pedagogické) aktivity v oblasti aktivních prvků a jejich aplikací v analogovém zpracování signálů. Část věnovaná výzkumu a vývoji se zabývá generací signálů, rekonfigurovatelnými aktivními filtry realizujícími různé přenosové funkce bez nutnosti přepojení vstupní a výstupní brány. Menší část je věnována přínosu v oblasti syntézy obvodů neceločíselného řádu. Další část stručně pojednává o výsledcích v modelování a vývoji aktivních prvků v technologiích CMOS. Výzkumné a vývojové aktivity jsou podpořeny krátkým popisem vybraných produktů. Popisovaný výzkum shrnuje aktivity uchazeče především v době po obhajobě doktorské práce. Pokud je odkazováno na starší výsledky (asi 2-3 případy), je to z důvodu kontextu a návaznosti. Část zaměřená na výukové aktivity pojednává o zapojení uchazeče do výuky na pracovišti, tvorbě výukových pomůcek (přípravky pro praktickou výuku a skripta/návody do cvičení) a podává krátký popis vybraných závěrečných prací a jejich přínosu pro výzkumné aktivity uchazeče.

KLÍČOVÁ SLOVA

Aktivní filtry, aktivní prvky, CMOS, elektronické řízení, modelování aktivních prvků a analogových systémů, oscilátory, rekonfigurace, syntéza a návrh obvodů.

Experimentální část této habilitační práce byla realizována na výzkumné infrastruktuře
vybudované v rámci projektu CZ.1.05/2.1.00/03.0072

Centrum senzorických, informačních a komunikačních systémů (SIX)
operačního programu Výzkum a vývoj pro inovace.

CONTENT

ACKNOWLEDGEMENTS	1
1 PREFACE	2
2 RESEARCH AND DEVELOPMENT	3
2.1 Introduction and motivation.....	3
2.2 Signal generation	5
2.3 Reconfigurable reconnection-less filters	13
2.4 Synthesis of fractional-order circuits	16
2.5 Modeling and development of active devices.....	17
2.6 Selected practical results and products	19
3 PEDAGOGICAL ACTIVITIES	21
3.1 Lessons and lectures in courses at workplace.....	21
3.2 Supervised works of bachelor and master students	23
4 APPLICANT'S PERSONAL PROFILE	26
BIBLIOGRAPHY	29
LIST OF ABBREVIATIONS	33
FABRICATED INTEGRATED CIRCUITS	34
ENCLOSED COPIES OF PAPERS	35

ACKNOWLEDGEMENTS

I would like to express many thanks to my colleague *Dr. Jan Jeřábek* for his kind cooperation on many research works and projects and especially for his patience. Many thanks belong to *assoc. prof. Norbert Herencsár* and *assoc. prof. Jiří Petržela* for useful discussions about a variety of interesting topics. I would like to thank *Dr. Roman Prokop*, *Dr. Vilém Kledrowetz* and *assoc. prof. Lukáš Fucik*. I really appreciate their guidance and help with IC design and the opportunity to develop and fabricate our own cells for constructing advanced active elements based on a modular approach. Sincerest thanks go to my mentor and supervisor *prof. Tomáš Dostál* for his support, patience, and opportunity to work with him in the field of analog signal processing since my bachelor studies at the faculty. My great gratitude goes to *Dr. Zdeněk Hruboš*, *Dr. Tomáš Götthans*, *assoc. prof. Jaroslav Koton*, *prof. Kamil Vrba*, *prof. Lubomír Brančík*, and *M.Sc. Aslihan Kartci* for their cooperation and help with my research in recent years. I also greatly appreciate working with bachelor and master students. Interaction between me and students brings interesting ideas and future cooperation.

I really appreciate fruitful international cooperation with *assoc. prof. Winai Jaikla* (King Mongkut's Institute of Technology Ladkrabang, Bangkok), *Dr. Abhirup Lahiri* (ST Microelectronics, India), and *assoc. prof. Jiun-Wei Horng* (Chung Yuan Christian University, Taiwan).

I would like to thank highly recognized experts *prof. Raj Senani* (Netaji Subhas Institute of Technology, India) and *prof. Costas Psychalinos* (University of Patras, Greece) for their support and encouragement.

Special thanks go to my family for their support and providing ideal foundation for my hard scientific work.

Roman Šotner

Vémyslice, July 28, 2016

1 PREFACE

Research and pedagogical activities forms two main directions of this thesis. The area focused on achieved research results is thematically divided to five topics (analog signal generation, advanced reconnection-less reconfigurable filtering, small-contribution to synthesis of fractional-order circuits, modeling and development of advanced active devices and selected practical results and products). The area focused on pedagogical activities describes courses and pedagogical activities of the applicant as well as works of students where the applicant served as supervisor and these works significantly contributed to the described research.

This thesis has the title “**Applications of advanced controllable active elements in electronic circuits**”. It means that cores of proposed circuit solutions presented in this work and enclosed copies of research papers are types of active devices generally different from standard and most-known operational amplifiers typical for many common circuitries widely used by designers and scholars in constructions and in processes of education. The research part of this thesis is written with an accompanying commentary of achieved results.

Topics discussed in this work are focused on advanced active elements and their applications in analog systems concerning signal generation, advanced filtering and advanced circuit solutions for purposes of modulation and fractional-order circuit synthesis. Results (details in enclosed papers) are described in the form of circuit structures and their simulation or experimental (laboratory) results based on commercially available active and passive devices. Several parts of the described research are supported by IC implementation of newly designed and fabricated advanced active elements within the frame of the project of Czech Scientific Foundation no. P102/14-24186P (2014-2016). This work covers achieved research results of the author/applicant obtained between the years 2011 and 2016. The majority of results obtained during the Ph.D. study of the author (from 2008 to 2011) is excluded. The presented results include 39 papers in total (25 papers in SCI-E journals with impact factor and 14 papers presented at international conferences) written by the applicant (author or coauthor) published since 2011.

2 RESEARCH AND DEVELOPMENT

Research activities of the applicant can be briefly summarized by the following four topics (accompanying comments of achieved results). The first topic deals with signal generation focused on aspects of the simplest solutions of harmonic (sine wave) oscillators, specific aspects of the design for operation in units and tens of MHz, solutions for enlargement of tunability range, simple multiphase structures (reducing general complexity of standard chains of subsequently phase-shifted loops of integrators) and triangular and square waver generation.

The second topic discusses advanced electronically reconfigurable reconnection-less (different transfer functions available in the same single-input and single-output circuit topology without reconnection of input and output terminals) filters of the first- and second-order (biquads).

The third topic discusses the author's other interests and already achieved results in the field of fractional-order circuit synthesis and design.

The fourth topic includes modeling and development of new original active devices with electronically independently controllable parameters especially at the level of behavioral modeling (utilization of commercially available devices) as well as development of own active elements in CMOS technologies that is required for further experiments.

Selected practical results achieved within the frame of the national (Czech Scientific Foundation) project and European project (FP7) are discussed at the end of the part describing research activities

2.1 Introduction and motivation

The operational amplifier has been a practically available part (active element) in analog signal processing for decades. Lack of adjustability of parameters (by external electronic control) of applications designed with an operational amplifier is an important drawback for many applications (variable gain amplifier, filter, oscillator, ...). Therefore other active elements were formed and began to be used in circuit design. These active elements are still being developed and interesting modifications or elements working with different principles are still appearing. These active elements with controllable features have received increasing attention in recent years. Active elements are very important parts of communication systems for analog signal processing, amplification, filtering, generating, mixing, shaping, etc. of signals in almost all electronic devices. They cover frequency ranges from audio to microwave systems. The analog way is still used in many cases and the search for new active elements and approaches is an actual topic in many research and developing teams all over the world.

Novel approaches in active element conceptions could bring interesting results in the field of standard circuit synthesis, fractional-order circuit synthesis or dynamical nonlinear circuits and unconventional design and modeling of real physical systems.

The modular approach of designing active elements allows simplification of the resulting circuit structures (filter, oscillator, ...) and design procedures. The modular approach supposes the utilization of more elementary active parts (active cells) in one complex element.

There are several reasons for development of analog solutions of communication subsystems. Requirements for variability and adaptability of complex electronic systems increase constantly. It is the reason for the utilization of direct electronic control, i.e. adjusting of application directly by parameters of active elements (transconductance, gain, input/output resistance). Electronic adjustability of parameters in an analog solution allows to compensate the influences of temperature, fluctuations of supply voltage, etc. in quite a simple way. The typical problems of analog solutions (thermal issues, aging of parameters, etc.) could be several-times lower and suppressed or even compensated in the case of on-chip implementation. Modern approaches in the design of active circuits allow to target all requirements for control into active element(s). Only a few (or even no) external passive elements with fixed values are necessary in applications. Analog solutions are able to offer lower cost, higher efficiency in some cases (high frequencies) and lower power consumption (on a chip) in comparison to digital solutions. A digital solution also has a certain processing delay and it is not able to react to changes in the system immediately. A digital signal processor (DSP) brings many advantages also for higher frequencies but high power consumption is a price for these benefits. A solution employing DSP can not be adequate if particular specifications are given (DSP and its accessories requires a larger area, high power consumption (hundreds of mA of power supply current) and it is more complicated in comparison to a simple analog circuit). Implementation of digital processing may not always be optimal if a simpler, cheaper and sufficient analog way exists.

Electronic control has been a topic of interest for many years. We can divide electronic control in analog circuits into two groups. The first group includes solutions where control (referred to as indirect) employs digital potentiometers, field effect transistors (FET) in linear regime (ohmic) of operation or other active elements (operational transconductance amplifier/transconductor¹ abbreviated as OTA for example), which replace grounded or floating resistors. The worst situation occurs if it is necessary to replace a floating resistor because such a solution could be quite complicated.

Digital potentiometers are very useful in adjustable circuits where parameters are controlled by the value of the resistor. Implementation of digital potentiometers seems to be one of the best methods for electronic control (indirect) of circuits in audio-bandwidth (several tens of kHz) with classic operational amplifiers. Unfortunately, digital potentiometers are not suitable for higher frequency bands due to their large parasitic capacitances (tens of pF). Discontinuous changes of resistance values and a low number of steps may cause further problems and inaccuracies. Discrete digital to analog converters (DAC) also offer the possibility of electronic control. However, high cost and other complications (area, additional power consumption, sufficient number of bits, discontinuous control, ...) in the circuit are the main disadvantages for low-power

¹ BIOLEK, D., SENANI, R., BIOLKOVA, V., KOLKA, Z. Active elements for analog signal processing: Classification, Review, and New Proposals. *Radioengineering*, 2008, vol. 17, no. 4, p. 15-32.

systems at high frequencies.

Approaches, where the parameters of an active element are directly controlled by an external force (bias or control DC current, voltage), belongs to the second group. Some suitable approaches are accessible in literature. These approaches have one of the following typical characteristics. Many new and modified active elements are feasible for voltage, current and mixed mode operation¹. Many theoretical solutions of active elements were discussed that are convenient for direct electronic control in circuit structures (active frequency filters for example). We can mention multi-output current conveyors (MOCCII)^{1,2}, current differencing transconductance amplifiers (CDTA)^{1,3}, multi-output transconductors (MOTA)^{1,4} and other elements which are applied in analog systems. Many interesting conceptions of new non-standard active elements were also introduced¹. Nevertheless, many of them are still only hypothetical, they are not commercially available and have not been investigated yet and used for circuit synthesis. Bias currents are used very often for electronic control of parameters of these active elements. The common approach is based on controlling the intrinsic resistance of current input (RX)² and transconductance (gm)³.

Taking into account the above discussed problems, it is observable that several fields are open for further research in analog signal processing. In addition, it is really important to introduce the obtained results to students in the form of computer and practical exercises in courses and lectures focused on analog signal processing and circuit theory because these approaches should be disseminated between a modern technical society of young workers, designers and experts in the field. Unfortunately, their knowledge is limited to an operational amplifier and its applications in most cases.

2.2 Signal generation

The author's biggest interest (in recent years) has been given to synthesis, design and development of new and improved types of harmonic oscillators of various structures, employing various electronically controllable active elements and providing interesting features. Harmonics (sine wave) oscillators form the majority of the content of this research part. Moreover, several works concerning triangular and square wave generators have been prepared and published.

2.2.1 Sine-wave oscillators

A part of these results can be divided according to the purpose of the specific solution. Attention of the author in this topic is focused on simplicity, direct electronic control (parameters of the circuit are adjustable by electronically controllable parameter of used active element – single device or more than one device), tunability range enlargement, and multiphase generation. Of course, all features can be achieved simultaneously only

² PANDEY, N., PAUL, S. K., JAIN, S. B. A new electronically tunable current mode universal filter using MO-CCCII. *Analog Integrated Circuits and Signal Processing*, 2009, vol. 58, no. 2, p. 171-178.

³ KESKIN, A. U., BIOLEK, D., HANCIUGLU, E., BIOLKOVA, V. Current-mode KHN filter employing Current Differencing Transconductance Amplifiers, *AEU - Int. Journal of Electronics and Communications*, 2006, vol. 60, no. 6, p. 443-446.

⁴ BHASKAR, D. R., SINGH, A. K., SHARMA, R. K., SENANI, R. New OTA-C universal current-mode/trans-admittance biquad. *IEICE Electronics Express*, 2005, vol. 2, no. 1, p. 8-13.

in a limited number of solutions. Therefore, specific approaches to the synthesis and design have to be used. Another reason for the investigation in this research field arises from the lack of simple systems serving for amplitude stabilization and gain control during the tuning process. Because these important systems were missing in the majority of already published designs, the author's interests were also focused on the simplest and logical implementation of these systems in proposed structures of circuits. It is impossible to obtain a pure sine waveform with minimal total harmonic distortion (THD) and with almost constant amplitude during the tuning process without these systems for amplitude stabilization.

Research in the field of simple (simple means utilization of three active elements with a low-number of terminals maximally) electronically tuneable oscillators starts with the development of oscillator structures employing two independent active parameters (current gains) for control of condition for oscillation (CO) and adjusting of frequency of oscillation (FO). Research work [1] deals with utilization of three-terminal-based advanced active elements so-called current follower buffered amplifier (CFBA) or current inverter buffered amplifier (CIBA), both with electronically controllable current gain, and current and voltage amplifier (CVA), where both gains (current and voltage) are electronically adjustable. These elements have low-impedance current input, auxiliary high-impedance terminal and low-impedance voltage output (consisting adjustable current amplifier and voltage buffer/inverter or voltage adjustable amplifier). Literature [1] discusses two solutions where FO (nonlinear control) and CO are controllable independently by current gain of used CIBA and CFBA. The third solution offers linear tuning of FO by two current gains in the frame of both used active elements (CFBA and inverting CVA) simultaneously and the second controllable parameter of inverting CVA (voltage gain) serves for CO control. Due to space limitations, the third solution was not tested in [1]. The presented circuits provide quadrature outputs.

A simple solution of similar complexity (only two active elements and two resistors and capacitors are used) was presented in [2]. In comparison to [1], there were used only commercially available devices as such (not their combinations for behavioral modeling of a complex active device as will be discussed in further text) as voltage- and current-mode multipliers (AD835 and EL2082 for example) are. The variable gain voltage amplifier (VGA) and electronically controllable current conveyor of second generation (ECCII) were easily established. The main intention of this work consists in a special type of enlargement of the tuning range by specific form of symbolical equation for FO. Voltage controllable gain (in both polarities – negative and positive) of the VGA based on voltage-mode multiplier ensures wider control of FO than available for one polarity of voltage gain. Design of this oscillator was provided for tens of MHz due to high-frequency transfer responses of used active devices. Unfortunately, this circuit structure serves for single phase generation only (theoretical drawback of topology).

The simplest example of the quadrature oscillator solution has been found and published in literature [3]. Only a single active device has been implemented in the oscillator core. The newly proposed active device, so-called voltage differencing current conveyor (VDCC), has also real CMOS implementation fabricated in ON Semiconductor I2T100 0.7 μm technology in 2015. This advanced active element consists of two subparts (OTA based on voltage-mode Gilbert multiplier and current

controlled current conveyor of second generation) that offer direct electronic control of transconductance and input resistance (two independent parameters). It means simple and independent electronic control of FO in the proposed application (oscillator).

Three active elements (two with controllable features - voltage and current gain) have also been implemented in a simple oscillator structure (three passive elements only) presented in [4]. The main purpose of the design was focused on the high-frequency features that was confirmed by experiments in tens of MHz. This circuit offers control of FO by adjustable voltage gain and CO by adjustable current gain, similarly as in [2], but circuit structure is completely different.

Enlargement of FO tunability range in oscillators has been the subject of interest also in work [5]. In comparison to previous approaches [2]-[4], simultaneous control of two parameters for control of FO has been used here. The presented circuit employs two special types of current feedback amplifiers (CFA) with so-called dual current control (internal transistor structure proposed). It brings the possibility of control of current gain of the current conveyor part as well as input resistance of the current input terminal. In comparison to [2], this structure provides quadrature outputs.

The majority of other works regarding this topic has the same aim. This aim consists in proposing multiphase solutions (other phase shifts than quadrature only). Logical limitation of the design on simple solutions (number of active and passive elements as minimal as possible) cannot be fulfilled in many cases. Therefore, also several solutions providing quadrature signal generation utilizing complex circuitry are also included in these discussions. In addition, they have other benefits (despite increased complexity), for example, linear control of FO while output amplitudes are constant during the tuning process and simple implementation of the system for amplitude stabilization.

Literature [6] deals with an interesting solution of the simple multiphase oscillator producing output signals with specific phase shifts of 45 and 90 degrees between three output signals that is not available in similarly simple structures employing commercially available active devices (diamond transistors OPA860 and current conveyors of second generation). Unfortunately, only CO can be controlled electronically. The main reason for investigation arises from lack of these simple solutions providing multiphase outputs (except quadrature). Multiples of $k\pi/4$ and $k\pi/2$ phase shifts in simple second-order circuits are not subjects of investigation in literature very often. Of course, there are many multiphase solutions based on cascades (chains) of lossy blocks in one loop that allow various integer phase shifts but circuits are very extensive (many active and passive elements) and tunability complicated in some cases.

Paper [7] introduces an oscillator producing three output signals with mutual phase shift of 45, 90 and 135 degrees. The solution of the circuitry is really simple (only single active device and four passive elements). The active element, so-called current and differential voltage amplifier (CDVA), offers control of current and voltage gain (two independent parameters provided by an adjustable current amplifier section and adjustable voltage amplifier section). Operation of the device was confirmed experimentally by a behavioral model employing an adjustable current amplifier and differential input variable gain voltage amplifier.

Quadrature oscillator proposed in [8] utilizes quite a large number of active elements (majority of them are electronically controllable current conveyors with

adjustable current gain) and five passive elements. However, all of them are really simple (three terminal devices). The frequency of oscillations can be tuned linearly while produced waveforms have constant amplitudes during the tuning process. Two current gains serve for linear tuning of FO and the third for control of CO from an external automatic gain control circuit (AGC) for amplitude stabilization (two solutions tested) keeping almost a constant level of output amplitudes during the tuning process. Very stable output levels during the tuning process, low THD, and FO tuning range larger than one decade (almost two decades) are beneficial.

Work [9] brings new simple structures of a multiphase oscillator utilizing single or two so-called voltage differencing buffered amplifiers (VDBAs) with differential outputs and five passive elements producing phase shifts of 45, 90, 135, and 180 degrees. A simple OTA and voltage buffer in single or differential output version is composed of a VDBA device. However, electronic tunability is not easily possible. CO is electronically controllable by value of transconductance. A special version of VDBA (extended by variable gain voltage amplifier – so-called voltage differencing buffered voltage amplifier, abbreviated VDBVA) offers an additional parameter for electronic control (voltage gain) in the frame of a single active device that was used (together with simple VDBA) in the quadrature oscillator allowing differential output waveforms or single ended phase shifts of 90, 180, and 270 degrees. Both transconductances (in VDBA and VDBVA) are used for linear control of FO and variable voltage gain of VDBVA serves for CO control while output levels are constant during the tuning process. Active elements can be established as behavioral models created by commercially available devices but full CMOS structures of these devices were proposed in this work [9].

Multiphase oscillator presented in [10] utilizes a single active device VDCC (already noted). However, this device has been modified in order to obtain various controllability of more than two parameters. Similarly as the device introduced in [3] conceptual subparts are OTA and current conveyor of second generation (CCII). In addition, the current conveyor subsection also allows electronic controllability of current gain between current input and current output terminals (it behaves like ECCII). Therefore, three parameters (transconductance, resistance of current input terminal and current gain) are now available for independent electronic control that gives beneficial possibilities for applications where this modification of VDCC will be used. An application example presented in [10] introduces a new type of harmonic oscillator providing linear control of FO (special simultaneous control of transconductance and input resistance) and phase shifts of 45, 90, 135 and 180 degrees. Simultaneous control of both discussed parameters ensures invariant output levels of two signals with phase distance 45 degree during the tuning process. Simulations with full CMOS structure of VDCC were used for verification of theoretical presumptions.

The circuit presented in [11] has been derived from a known structure of the so-called Collpits LC concept employing an inductor, two capacitors and a single bipolar transistor. This circuit is not discussed in the group of simple solutions because it belongs to third-order structures. It was found and proved that a bipolar transistor can be easily replaced by a current amplifier with adjustable gain in this structure to obtain the parameter for controlling CO. Replacement of the inductor by a synthetic emulator based on two OTAs offers simple electronic control (linear) of FO and accessibility of additional nodes (are not available in general Collpits circuit) where a quadrature phase

shift between two from three produced signals can be easily accessed. Tunability of FO was tested in the frame of more than one decade. The circuit was tested by Spice simulations (CMOS structures of controllable current amplifier and OTAs were designed) as well as by experiments with commercially available devices (diamond transistors and current amplifier established by current-mode multiplier).

Progress has been moving forward in simple multiphase solutions of the second-order oscillator [12]. The presented circuit utilizes two active devices (so-called voltage controlled current follower differential input transconductance amplifiers, abbreviated as VCCFDITAs) and provides phase shifts of 45 and 135 degrees between produced signals. An important finding consists in all unchangeable output levels during the tuning process. The previously discussed simple structures provided only one phase distance where both output levels are constant during the tuning process given by theoretical expectation of synthesis. In addition, FO can be easily controlled linearly by two parameters (simultaneous change of their values). The presented results were confirmed by simulations (quite extensive behavioral model based on ECCIs, current followers/inverters, and a variable gain voltage amplifier) as well as experimentally. However, experimental results have not been published yet.

As discussed in the previous text, an interesting circuit employing two advanced active elements (current follower differential output buffered amplifier with controllable current gain abbreviated as CG-CFDOBA, and buffered current and voltage amplifier with controllable current and voltage gains abbreviated as CG-BCVA) presented in [1] was not deeply studied. Only a theoretical concept of operation has been indicated in [1]. Therefore, a detailed study of the modified solution has been prepared in [13]. The modification consists of outputs of both polarities for multiphase (90, 180, 270 degrees) or differential output mode purposes (quadrature phase shift with two times higher output level). Two adjustable current gains serve for electronic control of FO (in a range of more than one decade) and voltage gain of BCVA for control of CO. All output levels are unchangeable (and very stable) during the tuning process due to simple implementation of an inertial system for amplitude stabilization. Detailed symbolical and computer (simulation) studies as well as experimental verifications have been presented. Full CMOS implementations of used active elements have been designed. A deep discussion on oscillation condition fulfillment in these structures has been provided and verifications illustrated on the proposed circuit.

A similarly complex circuit has been published in reference [14]. However, the main aim was in utilizing the same active elements in places of integrators in a single loop. Dual output controlled gain current follower buffered amplifiers (DO-CG-CFBA) are used at these places and ensure linear electronic controllability of FO by two controllable current gains. However, the necessity of an additional loop creating negative resistance from an additional adjustable current amplifier is the price for simplicity of the main active elements in a closed loop in comparison to [13]. Active elements can be emulated (implemented) by commercially available devices (current-mode multipliers and differential output differential input operational amplifiers). A full CMOS structure of DO-CG-CFBA has been shown and used for simulations. Moreover, experimental results based on the above discussed commercially available devices also supported theoretical presumptions. Multiphase outputs of 90, 180, and 270 degrees suitable also for differential mode were tested for FOs in the range of more than 3 decades.

A detailed investigation of possibilities for multiphase generation in second-order multi-loop structures is provided in paper [15]. These structures suppose OTAs in basic building blocks (integrator in loops) and adjustable current amplifier for fulfillment of CO. Two presented structures of oscillators are suitable for generation of phase shifts in multiples of 90 and 45 degrees. The difference in both structures is in utilization of both lossless or one lossy integrator in a loop. All produced output levels are theoretically unchangeable during the tuning process of FO and both circuits offer linear control of FO by two transconductances simultaneously. All expectations were confirmed by simulations with proposed CMOS structures.

An interesting and simple structure of an oscillator providing 45 degree phase shift has been presented in [16]. The circuit consists of a single active device – so-called modified current differencing unit (MCDU). The basic principle of the MCDU creates a difference of two input currents weighted by two independently controllable current gains. In addition, inputs of the MCDU are intended as inputs of two current conveyors of second generation (additional voltage terminals). Even the input resistances of current input terminals are also adjustable. These features give various advantages of controllability for further applications. Exemplary implementation of MCDU in a simple oscillator uses only two external capacitors. One current gain of the MCDU serves for CO control and both controllable internal resistances (adjustable by DC voltage) of current input terminals serve for linear tuning of FO. Both output signals keep a constant phase distance of 45 degrees and levels are unchangeable during the tuning process of FO. This behavior was confirmed experimentally by a quite complex model of the MCDU based on commercially available devices (ECCII – current-mode multipliers, and diamond transistors).

Linear controllability of second-order quadrature oscillators is a very interesting topic for further studies. Linear controllability of FO does not directly mean also constant value of output amplitudes during the tuning process of FO. Therefore, a study of this aspect has been provided in [17]. It was revealed that the resulting behavior always depends on the position of controllable parameters in the loop. Comparison of two almost identical structures (only position of controllable parameters in a loop was different) confirmed expected results. We found that implementing both controllable parameters in a lossless integrator creates linear dependence of FO on these parameters (simultaneous change). However, it damages the relation between the produced output responses and amplitude ratio depends on these parameters also under the condition of their equality (simultaneous control for linear tuning). Nevertheless, specific implementation of controllable parameters on different places (to both integrators – lossless and lossy) may remove this drawback. Expected behavior has been verified experimentally by implementation of commercially available devices (current and voltage-mode multipliers, differential input voltage buffer) up to frequencies of tens of MHz. Similar studies are missing in recent literature.

Generating an arbitrary phase shift between two signals seems to be a very interesting topic for discussion. A logical way in implementing an all-pass filter connected to the output of a signal generator exists. However, such an approach significantly complicates overall circuitry in many cases (oscillator core can be very simple). Therefore, the author's interests were also focused on arbitrary generation of two signals with a continuously settable phase shift directly in the oscillator structure. Some attempts are available in recent literature. However, circuits producing multiples

of the minimal integer phase step (discontinuous multiples of basic phase distance available in nodes of subsequently connected lossy sections in loop) and its multiples ($\pi/6$, $\pi/4$, etc.) are also called arbitrary phase shift oscillators. The main goal of this research was to find the simplest circuit where the phase shift between two generated signals will be adjustable continuously by an electronically controllable parameter (at least in a theoretical range from 0 to 180 degrees). A possible concept of synthesis is described in [18]. These types of oscillators can be designed by utilizing two all-pass sections with a controllable zero/pole characteristic frequency (simultaneously) and a variable amplifier in a single loop. The main idea of control inheres in independent control of each all-pass section. Symbolical analysis of phase relations in the circuit revealed dependence of phase shifts on the ratio of controllable parameters serving for adjusting of characteristic frequency. Unfortunately, oscillation frequency of the system depends on multiplication of these parameters. Therefore, correct design requires careful calculation of parameters and their accurate setting in order to obtain precise values of oscillation frequency and phase shift. An example of such an oscillator was given in [18] where OTAs were used for practical tests. Real active elements limit the presented method. It results from constraints of adjusting real parameters of active elements. Therefore, the actual available range of phase shift setting is always limited. The worst situation occurs in the corners of control (very high ratios of both parameters) where dependence reaches targeted values (0 and 180 degrees) asymptotically.

Experience from design of phase shifters and oscillators was also applied in the study of these signal generators for phase shift modulation and keying. The previously discussed circuit can be easily used for these purposes as presented in literature [19]. "Oscillator core" only (presented in [18]) can be used by itself. However, design requires development of a quite complicated control (logic circuits, comparators and conversions) system that transforms TTL levels to DC control voltages desired by the oscillator. As discussed in [18], independent adjusting of parameters (ratio) responsible for phase shift setting also influences FO. Therefore, very precise adjusting of both transconductances (very accurate values) is required in order to obtain required phase shift as well as expected FO (given by the product of both parameters), because FO and phase shift are (and must be in such simple structures) mutually dependent. Inaccuracy may cause two-tone modulation (short "hopping" of frequency FO around intended value) except phase shift switching in the worst case that can be evaluated as the most important drawback of the proposed method. This type of phase shift keying modulator has been presented in [19], where the described results were supported by simulations employing macromodels of commercially available devices. Detailed tests provided by real experiments with these active devices (current-mode multipliers, diamond transistors, differential input voltage buffers) as well as CMOS representations of required active elements were published in [20].

2.2.2 Triangular and square wave generators

Not only sine wave generators (oscillators) but also triangular and square wave generators are very important sources of very useful shapes of waveforms useful in analog signal processing. Square wave signals are really important for pulse width modulation (power supply sources - DC-DC converters for example, audio amplifiers in advanced classes D, E, F, ..., etc.), converters, for digital signal processing as clock, sources of ramps and impulses for various analog/digital systems, etc. Circuitry of

triangular and square wave generators is less complex than circuitry of harmonic oscillators due to their generally pure nonlinear principle of operation (charging of C by constant current). In fact, the basic structure requires only an integrator and comparator with hysteresis in a single closed loop (positive feedback ensured). Any other additional circuitry, for example, for amplitude stabilization typical for sine wave oscillators, is not required. The basic concept regarding operational amplifiers (no electronic control, external passive elements, etc.) can be significantly improved (electronic controllability, reduced complexity, minimal number of active and passive elements) by utilizing advanced active elements similarly as we already discussed in harmonic oscillators. The author's interests are focused on really minimal solutions (minimal number of active and passive elements) of these generators. These reductions are available due to specific features of advanced active elements (independent electronic controllability of several parameters and combination of principle of several active devices/sub-blocks in single active element).

The solution of the generator presented in [21] introduces how to implement the beneficial device CDVA (already discussed in [7]) here. The adjustable voltage amplifier section serves as a comparator with hysteresis (positive feedback) and adjustable current amplifier as the source of settable constant current charging C. Overall circuitry is really simple (grounded capacitor, single resistor and single CDVA device). Control of repeating frequency can be provided by the adjustable current gain and the voltage gain serves for setting the width of the hysteresis window. An additional DC current source may influence the duty cycle easily.

A fully differential (two-times higher output amplitudes) triangle and square wave generator employing dual output and fully balanced VDBA (active device with single controllable parameter - transconductance), single capacitor and two resistors was presented also in [9]. The structure utilizes OTA subparts of VDBAs (one serves for integrator and second for comparator operations) for control and voltage buffered (low-impedance) outputs

The next paper [22] introduces a similarly complex generator (also based on a single active device) utilizing the already discussed VDCC. VDCC has been implemented in the form of a CMOS structure consisting OTA and ECCII (controllable resistance of current input terminal and current gain) subsections. Two grounded external resistors and grounded capacitor are used in the resulting circuit. The OTA subsection serves as comparator and current conveyor section as current source charging C. Output current is busted by adjustable current gain serving for control of the repeating frequency. The designed generator offers square wave outputs in the form of voltage and current simultaneously. Application of the generator was verified in a simple pulse width modulator, where additional VDCC serves as a comparator (without hysteresis) of triangular output waveform with input signal.

The order of subsections in the frame of the VDCC can be interchanged (the current conveyor ECCII part also serves as comparator and the OTA part as integrator/current source) to create a generator. Verification of this modification was published in [23]. Overall circuitry of this solution is really simple (single VDCC and external grounded capacitor). Maximal output current of the OTA subsection drives C (and directly controls repeating frequency) and setting of current gain in the frame of the VDCC controls the hysteresis window. A behavioral model of the VDCC has been

established in order to prove expected and simulated operation of the generator and its application (pulse width modulator) experimentally. Variable gain voltage amplifiers, current-mode multipliers and voltage buffers were used to construct the model.

2.3 Reconfigurable reconnection-less filters

Classic multifunctional filters offer one input and several outputs accessible simultaneously or several inputs and one output. It means that such a structure requires reconnection of the input/output terminal in order to obtain a different transfer response. Therefore, such an approach is not very beneficial for solutions of systems where additional (mechanical for example) change in circuitry (reconnection) is not easily allowed. This is a typical problem for on-chip implementation – after fabrication when changes of topology are not possible. Of course, there are some ways how to provide reconnection. However, switching may bring some undesired problems – increasing of the level of distortion from interferences (close position of analog and digital signal paths) of the clock and useful signal (if required changes are fast), overshoots, additional complication of the design, additional area, additional control logic, additional power consumption, etc. Therefore, other ways how to avoid the above noted problems are welcomed, especially in low-voltage and low-power systems.

Beneficial behavior of reconnection-less reconfigurable filters allows immediate and continuous reaction to changes in the processed useful signal (temporarily increasing distortion, noise floor, and undesired spectral components in some parts of the band). Such processing is also suitable for some kinds of adaptive control. We can imagine a useful signal that needs to be digitized in an analog to digital converter (ADC) and some undesirable frequency components suddenly occur. Now, the signal path with constant/flat frequency response should be changed to high-pass, low-pass or band-reject (for example) response and tuned (bandwidth change) in order to remove undesired signals and noises. Unfortunately, circuit systems with these features do not seem to be feasible using standard operational amplifiers due to lack of electronically controllable parameters. However, advanced special active elements with controllable features can be very useful for purposes of this synthesis. Electronically controllable reconnection-less filters allow some kind of multifunctionality even in the case when one input and one output terminal are the same for the entire time.

This research focuses on a filtering solution that allows control (or selection) of the type of the transfer function as well as parameters (pole frequency, etc.) of the filter electronically by parameter(s) of an advanced active element.

2.3.1 First-order filters

A voltage differencing current conveyor has various advantages in versatility and multi-parameter controllability. This device can also be easily implemented in reconnection-less electronically reconfigurable filters as shown in ref. [24]. The filtering structure consists of only a single VDCC and external grounded capacitor. Three electronically adjustable parameters can be used for control and reconfiguration of the first-order filter. Suitable configuration of values of resistance of a current input terminal, transconductance and current gain provides reconfiguration of the filter response

between all-pass, low-pass and inverting direct (unity gain) transfer responses. Tuning of the pole frequency (all-pass and low-pass response) is available by current gain. Experiments were performed for the designed CMOS structure as well as for the established behavioral model (in laboratory) based on commercially available devices (diamond transistors and current-mode multiplier).

Reference [25] introduces a filter utilizing the same subparts as VDCC (OTA and ECCII). However, their interconnection differs from the general convention prescribed for VDCC (OTA connected to z terminal of ECCII). The proposed circuit provides all-pass and low-pass response, inverting direct transfer, adjustable zero and adjustable low-pass filter with zero. Unfortunately, all responses are not available at the same output terminal. Two output terminals are accessible. Simulations with macromodels of diamond transistors and a current-mode multiplier confirmed intended behavior.

The modified current differencing unit with various controllable parameters and interesting signal operation of subtraction, as already discussed in topics regarding oscillators, can also be beneficially used in the design of reconfigurable reconnection-less filters. The first circuit reported in [26], representing this family of filters, employs only a single MCDU and single floating capacitor. The filter operates in current-mode and offers all-pass, inverting high-pass, low-pass and direct transfer responses in single-input and single-output structure. Zero/pole frequencies of responses are controllable electronically. The behavioral model of the active element based on current-mode multipliers (EL2082) and diamond transistor confirmed intended features in simulations and laboratory experiments. Note that full controllability of the MCDU is not necessary in this structure (only single current input resistance is electronically adjustable). Two other solutions of the MCDU-based filters have been reported in [27]. Full controllability of current-input resistances (of MCDU) is now required. Paper [27] introduces three additional solutions (one voltage-mode and two current-mode circuits). The complexity of circuitries is identical to [26], only feedback interconnections are different. However, it yields completely different transfer responses. The first solution operates with inverting all-pass, high-pass and direct transfer responses, the second filter provides almost identical transfers (only output inversion) because the structure is the same (also general symbolical transfer response has very slight modification), only working in current-mode. The last current-mode circuit operates as direct transfer, low-pass filter, inverting high-pass filter and all-pass filter. All solutions utilize a single MCDU and floating capacitor.

Active elements with multiparameter controllability seem to be very useful for these purposes as shown also in [28] where a different type of active device has been implemented in these types of reconfigurable filters. So-called current follower differential input transconductance amplifier (CFDITA), in the version controllable by bias currents and having copy of auxiliary terminal, has been implemented together with an adjustable current amplifier in reconfigurable filters. The principle of this active device is different (current inputs and outputs) than VDCC, as already noted in previous text (oscillators). The behavioral model of the active element has been established from variable gain voltage amplifiers, differential voltage buffer, current-mode multiplier and diamond transistors and employed for simulations and laboratory experiments. The active element consists of two controllable features (resistance of current input terminal and transconductance). Also, CMOS implementation of the device is available. Two almost identical structures (difference only in polarity of some terminals of active

devices) of reconfigurable reconnection-less first-order filters are studied in [28]. However, their general symbolical transfer functions are different. The first solution of the filter allows inverting high-pass, all-pass and inverting direct transfer responses. The second solution has similar capabilities to obtain previously noted transfer functions. However, an important disadvantage of the first structure consists in the requirement for current gain (current amplifier) in both polarities (positive and negative) in order to change transfer type. The second solution solves this problem (negative gain is not necessary) but requirements for current gain are higher (maximal value of gain).

2.3.2 Second-order filters

Development of first-order structures is quite simple and may not be sufficient for requirements on rapid increase of attenuation (slope of magnitude response between pass and stop band). Therefore, filters of higher order (biquads especially) are welcomed. However, their synthesis is not such an easy task as will be discussed.

Work on this topic started in paper [29], where a simple (two active elements based) voltage-mode solution of the biquadratic (second-order) reconnection-less reconfigurable all-pass and band-reject (notch) filter has been introduced. Difficulties (complexity) of standard synthesis based on multiple-loop integrator structures for these purposes were indicated. Therefore, partial general autonomous admittance network and proper selection of passive elements has been used for synthesis in order to obtain a simple solution. The resulting circuit employs two active elements (two current conveyors of second generation - one of them with controllable current gain between X and Z terminal, second utilizes only a voltage follower part between Y and X; two resistors and two capacitors). The final structure allows reconfiguration between all-pass and band reject response. Continuous change of transfer type between both responses is observed and studied. Nevertheless, the circuit has many drawbacks. Topology does not allow a higher quality factor than 0.5 (not controllable electronically), pole frequency is not easily tunable without utilization of electronically adjustable replacements of resistors. The input and output impedance is frequency dependent (and dependent also on intentionally adjustable parameters). Therefore, practical utilization requires additional buffers for impedance separation. However, the value of maximal attenuation (in band-reject configuration) is not given by the equality of current gain to 0. Therefore, quite high attenuation can be obtained (almost 50 dB at 1.69 MHz in experiments based on utilization of current-mode multipliers).

Drawbacks of the second-order circuit reported in [29] lead to searching for another way of synthesis (standard multiple-loop integrator structure [30]). Almost all reported disadvantages of the circuit in [29] were removed. However, complexity (2 active devices in [29] vs. at least 6 active devices in [30]) is the price for these benefits. Signal-flow graphs directly indicates purposes of synthesis for reconfigurability of band-reject and all-pass response. The structure reported in [30] uses ECCIIs, current followers/inverters and voltage buffer or OTAs and buffer (two solutions available from the same topology). Quality factor, pole frequency and pass-band gain can be set independently. However, the parameter serving for reconfiguration (gain or transconductance at linear member of numerator of the second-order transfer response) may reach a value of 0 for band-reject configuration. It means disconnection of one transfer branch. Nevertheless, ideal disconnection is not possible due to real parasitic

features of active devices. Current gain of the amplifier will not be accurately equal to zero, even transconductance of OTA cannot be set directly equal to zero.

Complexity of previously reported synthesis led to other ways how to design biquadratic types of reconfigurable reconnection-less filters. The matrix method of unknown nodal voltages seems to be a very powerful tool for the intended tasks. It allows almost directly to establish the required form of the second-order transfer function (numerator and denominator). Based on these formulas (modified to sub-determinants), the creation of a general circuit structure is quite straightforward. Only knowledge about the position of capacitors (floating/grounded) in nodes (in admittance matrix) must be known as the initial step. This method has been firstly used for synthesis of reconfigurable reconnection-less biquads in [31]. Three structures (each employing four OTAs) are introduced. Two of them utilize only active devices and two capacitors (floating and grounded). The third solution also requires floating resistance (but it can be replaced by OTA too). Specific electronic configuration of transconductances allows various operations (for example: band-reject, all-pass, high-pass, low-pass with zero, high-pass with zero and asymmetric band-pass response available in the first type of the circuit). For detailed discussions see ref. [31]. All structures reported in [31] use four differential-input single-output OTAs. One differential-input and differential-output OTA has replaced one of them in [32]. Features available in this circuit are almost identical to the above noted. Intentions of the synthesis were verified experimentally (diamond transistors as OTAs). Synthesis and design of higher-order (higher than biquads) reconfigurable reconnection-less filters was not solved in current-state-of-the-art.

2.4 Synthesis of fractional-order circuits

Fractional-order⁵ circuit synthesis and applications of fractional-order systems are really up-to-date topics of interest and activities of many researchers today. Many works in this field are focused on the design of active filters. However, in my opinion, practical applications of these filters are really limited. The designer will rather select an integer-order solution than a complicated fractional-order structure requiring many subsections and active devices in order to emulate the intended frequency response (in magnitude and phase) in a wide frequency bandwidth. Complexity of the circuit is directly proportional to desired accuracy and bandwidth of valid approximation^{6,7}. On the other hand, fractional-order systems for applications in oscillators and phase shifters as well as emulation of fractional-order immittances can be found as useful also in industry (analogue control systems⁸ and voltage regulators⁹ for example). Therefore, space for further research is still open here. As already stated, emulation of fractional-

⁵ ELWAKIL, A. S. Fractional-order circuits and systems: An emerging interdisciplinary research area. *IEEE Circuits and Systems Magazine*, 2010, vol. 10, no. 4, pp. 40-50.

⁶ VALSA, J., DVORAK, P., FRIEDL, M. Network model of CPE. *Radioengineering*, 2011, vol. 20, no. 3, p. 619-626.

⁷ VALSA, J., VLACH, J. RC models of a constant phase element. *International Journal of Circuit Theory and Applications*, 2013, vol. 41, no. 1, p. 59-67.

⁸ PETRAS, J. Fractional-order feedback control of a DC motor. *Journal of Electrical Engineering*, 2009, vol. 60, no. 3, p. 117-128.

⁹ KADLČIK, L., HORSKY, P. A low-dropout voltage regulator with a fractional-order control. *Radioengineering*, 2016, vol. 25, no. 2, p. 312-320.

order devices by electronic circuits is a quite complex task. However, there is no other way. Many researchers believe that commercially produced fractional-order elements will be available soon. Several concepts of electrochemical and polymer materials (layers of organic and inorganic matter) that are capable of creating a fractional-order device have also been published quite recently^{10,11}.

Our team contributed to this field with several works regarding fractional-order filters. Works where the applicant took larger part of effort are focused on development of first-order bilinear transfer sections with independently electronically controllable zero and pole locations. These structures may serve for emulation of fractional-order devices if they are connected in cascade. Work [33] introduces several simple structures of bilinear sections for emulation of fractional-order transfers in the form of fractional-order integrator or differentiator. An example of the so-called “half integrator” ($ks^{0.5}$) is verified in [33] by cascade of five bilinear sections and their proper setting (zero and pole locations in accordance to prescribed approximation).

A similar approach can be used for emulating fractional-order immittance. Special bilinear grounded impedance with electronically and independently adjustable zero and pole location was developed and presented in [34]. A special type of feedback system for multiplication of impedances/admittances, where a specific number of proposed bilinear grounded impedances is inserted, allows quite simple emulation of fractional-order impedance (verified as so-called fractional-order half inductance). Seven sections have been used in order to emulate accurate behavior in the frame of approximately four decades with a phase ripple of 1.5 degrees. As noted, complexity of this circuit is really huge. Requirements of synthesis include seven grounded capacitors and 29 OTAs based on diamond transistors.

2.5 Modeling and development of active devices

An important part of the author’s work is focused on modeling, behavioral modeling of active elements based on commercially available parts and development of CMOS advanced active elements (these activities started in 2014 based on close cooperation with colleagues at department of Microelectronics).

Many behavioral models (from recent years) served for experimental verification of complex single-purpose systems included in many published papers. However, it was necessary to develop behavioral models of active elements in the frame of the received post-doctoral project (2014). Advanced active elements suppose electronic controllability of several parameters that must be modeled and emulated by features of commercially available devices. Emulation of electronically controllable resistance of current input terminal of current conveyor (CCCII) or current amplifier (for example) seems to be the most difficult task. This difficulty consists in intended independence of input resistance on current gain and vice versa.

¹⁰ ELSHURFA, A. M., ALMADHOUN, M. N., SALAMA, K. N., ALSHAREEF, H. N. Microscale electrostatic fractional capacitors using reduced graphene oxide percolated polymer composites. *Applied Physics Letters*, 2013, vol. 102, no. 23, article no. 232901.

¹¹ ADHIKARY, A., KHANRA, M., SEN, S., BISWAS, K. Realization of carbon nanotube based electrochemical fractor. In *Proceedings of IEEE Int. symposium on Circuits and Systems (ISCAS)*, Lisbon (Portugal), pp. 2329-2332, 2015.

We solved these problems in paper [35] where several suitable approaches were presented. The first approach utilizes ECCIIs (current-mode multipliers EL2082) and the second employs variable gain voltage amplifiers (VCA810). The range of resistance control, dependence of resistance on DC control voltage, linearity, stability, AC responses (bandwidth), complexity are evaluated experimentally (measured) and discussed in [35]. The disadvantage consists in matching two controllable current gains in the case of using ECCIIs. Based on key information reported in [35], many further behavioral models of active elements have been prepared, for example control of input resistance of an MCDU model in [16], [26] utilizes this approach (two-three ECCIIs).

Paper [36] reports a complex behavioral model for an advanced type of current conveyor having input resistance(s) controllable in accordance to a different principle than presented in [35]. This principle has also been implemented in the behavioral model of VDCC presented in [23] for example. In comparison to [35], matching two current gains in the frame of ECCIIs is not required but two additional voltage buffers are used. The model of an advanced current conveyor presented in [36] offers special inter-terminal features (not available in standard concept), i.e.: adjustable voltage gain between the Y and X terminal (including weighted voltage difference of two pairs of input voltages – 4 voltage input terminals available), adjustable current gain (weighted) between three current inputs and one output Z terminal and adjustable input resistances of X terminals (each independently). The VDCC device has been modeled also by simpler behavioral models than the structure reported in [35] (for example [24], [37]). However, their electronic controllability is limited to features (parameters) required for target applications shown in these works only.

The VDCC device can be implemented in single purpose all-pass filters quite easily as shown in [37]. Various application field, variability and beneficial features of VDCC led to selecting this device (in 2014) for further design and fabrication in a CMOS process as a really available IC device for analog signal processing. As already noted several times, VDCC covers two subparts (OTA and CCCII) suitable for a modular approach. We designed both subparts in ON Semiconductor 0.7 μm I2T100 technology (5V supply voltage). Design specifications of the current conveyor part with controllable input resistance at the X terminal, taking into account all aspects of precise design (large dynamic range, DC accuracy, ESD protection), were presented in [38]. The OTA section employing voltage-mode multiplier of Gilbert's type^{12,13} (supplemented by current output) offers transconductance adjusting in both polarities. These sections itself were applied for designing simple reconfigurable first-order filters as discussed in [39]. Finally, full VDCC implementation (both subparts together) has been presented in the application of the quadrature oscillator in [3]. Two papers regarding VDCC have already been accepted for the prestigious 59th IEEE Midwest Symposium on Circuits and Systems held in Abu Dhabi in October 2016.

Our team is working on developing active devices in the ON Semiconductor 0.35 μm I3T25 process in the frame of the postdoctoral project P102/14-24186P. Our works are focused on experimental verification of developed cells (subparts suitable for

¹² GILBERT, B. A precise four-quadrant multiplier with subnanosecond response. *IEEE Journal of Solid-State Circuits*, 1968, vol. SC-3, no. 4, p. 365-373.

¹³ GILBERT, B. A high-performance monolithic multiplier using active feedback. *IEEE Journal of Solid-State Circuits*, 1974, vol. SC-9, no. 6, p. 364-373.

a modular approach) in current state. The proposed subparts in the frame of the new IC are also suitable to establish a VDCC device with significantly better frequency features than cells in I2T100. We expect dissemination of the first results from the fourth quarter of 2016.

2.6 Selected practical results and products

The applicant took part in several research projects connected with basic and applied research. He has coauthored several products. The selected products are listed in the following text. Full records of products are available at websites^{14,15}.

Six-channel bondwire tester

Six-channel tester of bondwire (authored by: R. Sotner, J. Petrzela, T. Gotthans, J. Drinovsky, T. Kratochvil)¹⁶ provides current stress tests of metallic bonding wires (different materials) between substrate surface and IC package pads. The tester ensures continuous DC current flow or pulsed current with adjustable amplitude of pulse (square wave) shape through bondwire, sensing of this current together with sensing of voltage drop across the bondwire and further processing. The tester allows sequential measurement in six channels, i.e. six bonding wires that are included in the SOIC28 IC package (provided by our partner ON Semiconductor BVBA, Oudenaarde). A powerful computer workstation with a measuring card is responsible for amplitude control, duty cycle, number of pulse repetitions of current flowing through bondwire, addressing of specific bondwire, gain control of internal amplifiers and processing of sensed signals. This product was created in 2014 for nanoCOPS FP7-ICT project “Nanoelectronic COupled Problems Solutions” no. 619166 (2014-2016) solved by Centre of Sensor, Information and Communication Systems (SIX).

Experimental prototype of modified CMOS Gilbert multiplier with current output

This cell (authored by: R. Sotner, R. Prokop, V. Kledrowetz, J. Jerabek, L. Fucik)¹⁷ was designed (2014) and fabricated (2015) in AMIS/ON Semiconductor CMOS07 0.7 μm I2T100 (5 V supply) technology in the frame of the Europractice (mini@sic) academic consortium. The designed circuit serves for experimental verifications of advanced multi-parameter electronically controllable active devices based on a modular approach (interconnection of several basic sub-blocks) and their applications. The multiplying core utilizes the modified Gilbert conception and the differential voltage to current converter is used at the output of the circuit in addition. Input range of both differential voltage pairs (X and Y) is up to ± 300 mV approximately and 3 dB bandwidth of current transfer (to short) up to 2 MHz. The range of adjustable

¹⁴ <https://www.vutbr.cz/lide/roman-sotner-88799/tvurci-aktivita>

¹⁵ <http://www.urel.feec.vutbr.cz/index.php?page=products&lang=eng>

¹⁶ http://www.urel.feec.vutbr.cz/web_documents/produkty/2014/Sotner_bondwire_tester_EN.pdf

¹⁷ http://www.urel.feec.vutbr.cz/web_documents/produkty/2015/Sotner_MLT_EN.pdf

transconductance (by DC voltage – one input voltage is used for control) is 0 to ± 2.8 mS (for 0 to ± 1.4 V). This product was tested in 2015 for the project of Czech Scientific Foundation no. P102/14-24186P “Research for electronically adjustable advanced active elements for circuit synthesis” (2014-2016) solved by Centre of Sensor, Information and Communication Systems (SIX).

Experimental prototype of CMOS current conveyor (CCCII) with current controllable resistance of current input terminal

AMIS/ON Semiconductor CMOS07 0.7 μm I2T100 (5 V supply) technology (mini@sic Europractice) was used for the design (2014) and fabrication (2015) of this active cell (authored by: R. Sotner, R. Prokop, V. Kledrowetz, J. Jerabek, L. Fajcik)¹⁸. The presented active part is specified for experiments focused on advanced multi-parameter electronically controllable active elements based on a modular approach (interconnection of several basic sub-blocks) and their applications. The unity-gain transfer between X and Z terminals achieves a 3 dB bandwidth up to 18 MHz, unity-gain transfer between Y and X terminals achieves a bandwidth up to 30 MHz (in dep. on DC control/bias current: tested from 5 to 300 μA - the input resistance (X) is adjusted from 2.1 to 0.3 k Ω). The active part has great linearity and dynamical range of the current transfer (more than ± 1000 μA). This product was tested in 2015 for the project of Czech Scientific Foundation no. P102/14-24186P “Research for electronically adjustable advanced active elements for circuit synthesis” (2014-2016) solved by Centre of Sensor, Information and Communication Systems (SIX).

¹⁸ http://www.urel.feec.vutbr.cz/web_documents/produkty/2015/Sotner_CCCII_EN.pdf

3 PEDAGOGICAL ACTIVITIES

3.1 Lessons and lectures in courses at workplace

The applicant's pedagogical activities (from 2008) are spread over several areas of analog and digital circuits and systems. He serves as lecturer of several topics in fields of analog filter design, electronic circuits theory, modern wireless communication and pulse and digital techniques taught for bachelor and master students in the field of Electronics and Communication (M-EST, B-EST) in the programme Electrical, Electronic, Communication and Control Technology at the Faculty of Electrical Engineering and Communication, Brno University of Technology. In addition, he serves as supervisor for master and bachelor theses in mentioned areas.

He is responsible for lectures focused on signal flow graph approach in analysis and synthesis of linear electronic circuits (in Electronic Circuit Theory – MTEO, winter semester) from 2009. Lectures includes graphical description of topology of linear electronic circuits (from elementary passive elements to chains and loops of active building blocks) Mason, Coates, Mason-Coates (MC) graphs, rules for evaluations (transfers, impedances, characteristic equation), simplifications and work with these graphs (Mason rule, etc.), definition of graphs for basic building elements (two-terminal, two-port, loop and self-loop), mutual conversion between voltage and current (description by signal flow graph), analysis of passive (regular) circuits by MC graphs, analysis of irregular circuits (graphs of active elements, transformation rules for irregular elements), graphs without self-loops for analysis, synthesis and description of blocks (Mason) in voltage-, current- and mixed-mode of operation, examples of synthesis of multi-loop feedback based filters (follow-the-leader structures with lossless integrators). Correspondence of graph methods with matrix method of unknown nodal voltages is clearly explained. Practical examples and results (experimental/simulation) complement explanations and intentions of synthesis and design. The author also provides practical lessons in the laboratory/experimental part of this course (from 2008). During his work (Ph.D. study), he prepared several innovations of these lessons in the frame of projects of the Council of Higher Education Institutions (FRVŠ) entitled “New laboratory exercises based on modern active elements (103/2009/G1)” and “Enlargement of laboratory education in the field of signal generation (450/2011/G1)”. Financial support of these projects significantly improved practical exercises and the experimental workplace. It allowed to prepare new topics (instructions + forms + hardware devices) in the field of multifunctional and electronically controllable active filters using different principles (also including the switched capacitor principle), autonomous circuits, oscillators (also unconventional chaotic dynamical systems) and generators. Many of them use modern active elements (current conveyors, multipliers, transconductance amplifiers, etc.) because the author's effort is also concentrated on transferring obtained research results to the process of education. It means that some of the author's solutions published in literature (where hardware was created in order to verify operation experimentally) were modified (protections and precise mechanical construction), fabricated in several samples and complemented by precise instructions how to measure and evaluate required features. Therefore, absolvents of these lessons should be informed about the existence of active devices with electronically controllable

parameters in most cases (they know only opamps from their past experience). Students learn their typical as well as special implementations in linear and nonlinear electronic circuits. The applicant (main author) with his colleagues prepared an electronic tutorial and instructions (202 pages) entitled “Laboratorní cvičení kurzu teorie elektronických obvodů” including theory and principle, precise instructions (step-by-step) and blank forms (with empty tables and graphs) for evaluating measured results. Therefore, the electronic text also serves as a workbook. Topics (18 lessons) included in this workbook are concentrated on active filters (Sallen key, gyrators and impedance converters in active filters, biquads with current conveyors, Kerwin Huelsman Newcomb structure, fourth-order multifunctional filter with transconductance amplifiers, integrated filter based on switched capacitors, current-mode biquad with transconductors), oscillators and generators (RC Wien oscillator with operational amplifier, design of the oscillator with current feedback amplifier, operational transconductance amplifier based electronically tunable oscillator with stepwise shifted phase, oscillator based on tunable active band-pass biquad filter, second-order oscillator with multiphase outputs – study of oscillation condition, tunable quadrature oscillator with electronically controllable current conveyors, tunable triangular and square wave generator in discrete and integrated solution, analog computer – nonlinear dynamical systems) and simple applications (capacitive load compensation in amplifiers, analog voltage-mode multiplier and its applications).

The next pedagogical engagement (less than half of a semester) of the applicant (from 2013/14) consists of computer lessons for bachelor students in the course Pulse and Digital Techniques (BICT, summer semester) and it covers the transfer of impulse signals through linear and nonlinear transmission systems, design of power switches (diodes and transistors in pulse circuits), comparators and basic work with the simulation software LTspice.

The applicant serves as lecturer (from 2010/11) in the bachelor course Analog Filter Design (BELF, summer semester) where he focuses his talks on topics regarding multifunctional active filters (in all modes of operation – explanation of voltage and current mode) with various active elements (their synthesis, analysis and design with attention on correct selection of proper type of the filter and active devices) and he deals especially with multifunctional active filters based on loop and multi-loop integrator structures allowing various electronic control of their features (pole frequency, quality factor, pass-band and stop-band gain, reconfigurability, etc.) and study of real parasitic influences in these structures. The applicant also gives lessons in computer trainings of this course occasionally.

He also provides one lecture yearly (from 2014/15) in a course for bachelor students Modern Wireless Communication (BMBK, winter semester). The lecture called “Design and analysis of analog electronic circuits” generally summarizes important aspects and topics of analog electronic circuits for purposes of modern communication systems. This lecture presents some overview starting from basic simple linear circuits and proofs of elementary facts, laws and principles (superposition, reciprocity, duality, Thevenin and Norton theorem, Kirchhoff’s laws, matrix methods, signal flow graphs) in these circuits to complex computer supported modeling and analyses (DC, AC, bias point, transient, parametric, noise, Worst Case, Monte Carlo, etc.) of large circuit structures. Attention is given to demonstrating these analyses in modern simulation software, especially on: NAF, FilterCAD and FilterSolution for

computer aided design of filters, Snap for symbolical solution of linear and linearized circuits, OrCAD PSpice for standard discrete active and passive circuits and Cadence CDS-IC design tools (virtuoso, spectre) for design, simulation and layout preparation of analog integrated circuits.

3.2 Supervised works of bachelor and master students

The applicant supervised 28 successfully defended bachelor and master theses (from 2009). Several topics of these works directly supported his research activities or developments in the frame of several projects. Selected examples of interesting and useful theses are briefly discussed in the following text. Interests of students were focused on digitally controllable resistors/potentiometers and their features. Students selected commercially available types with various types of control (buttons, I2C, etc.), applied these devices in standard operational amplifier based filtering applications^{19,20} and compared obtained features to analog control (potentiometer). Some works were focused on modern multi-terminal active devices applied in multifunctional filters^{21,22} and electronically controlled multifunctional filters of Kerwin Huelsman Newcomb structures²³. Several students' works contributed to investigating commercially available voltage and current-mode multipliers in the form of active elements^{24,25}. Practical experiments provided by the developed circuit²⁵ significantly supported the acceptance of research paper [4]. Controllable generators (analog and digital solutions) of current impulses were investigated^{26,27} due to requirements of our industrial partner for possible future cooperation on the development of these systems (tests of detonators). I really appreciate work where a student²⁸ provided a complete "retranslation" (manual creation of models from simulated results in many cases) of

¹⁹ ŠEVČÍK, B. Elektronicky říditelný aktivní filtr 2. řádu. Brno: Vysoké učení technické v Brně, Fakulta elektrotechniky a komunikačních technologií. Ústav radioelektroniky, 2009. 54 s., Diplomová práce. Vedoucí diplomové práce Ing. Roman Šotner

²⁰ SEDLÁŘ, P. Digitálně řízený rezistor. Brno: Vysoké učení technické v Brně, Fakulta elektrotechniky a komunikačních technologií. Ústav radioelektroniky, 2009. 55 s., Diplomová práce. Vedoucí práce: Ing. Roman Šotner

²¹ MIKSL, J. Toleranční analýza filtrů s CDTA. Brno: Vysoké učení technické v Brně, Fakulta elektrotechniky a komunikačních technologií. Ústav radioelektroniky, 2009. 51 s., Bakalářská práce. Vedoucí práce: Ing. Roman Šotner

²² MAŇAS, S. Více-výstupové aktivní bloky a jejich aplikace v proudovém módu. Brno: Vysoké učení technické v Brně, Fakulta elektrotechniky a komunikačních technologií. Ústav radioelektroniky, 2010. 50 s., Bakalářská práce. Vedoucí práce: Ing. Roman Šotner

²³ HARSA, J. Multifunkční elektronicky nastavitelné filtry KHN. Brno: Vysoké učení technické v Brně, Fakulta elektrotechniky a komunikačních technologií. Ústav radioelektroniky, 2010. 45 s., Bakalářská práce. Vedoucí práce: Ing. Roman Šotner

²⁴ MIKSL, J. Analýza, vlastnosti a aplikace komerčně dostupných proudových násobiček. Brno: Vysoké učení technické v Brně, Fakulta elektrotechniky a komunikačních technologií. Ústav radioelektroniky, 2011. 79 s., Diplomová práce. Vedoucí práce: Ing. Roman Šotner

²⁵ KOPEČEK, P. Analýza, vlastnosti a aplikace komerčně dostupných napěťových násobiček. Brno: Vysoké učení technické v Brně, Fakulta elektrotechniky a komunikačních technologií. Ústav radioelektroniky, 2011. 68 s., Diplomová práce. Vedoucí práce: Ing. Roman Šotner

²⁶ SVOBODA, K. Zdroj generující definovatelné proudové impulzy. Brno: Vysoké učení technické v Brně, Fakulta elektrotechniky a komunikačních technologií, 2014. 34 s., Bakalářská práce. Vedoucí bakalářské práce Ing. Roman Šotner, Ph.D.

²⁷ DUJÍČEK, M. Digitálně řízený zdroj generující proudové impulzy nastavitelného náběhu a trvání. Brno: Vysoké učení technické v Brně, Fakulta elektrotechniky a komunikačních technologií, 2014. 46 s., Diplomová práce. Vedoucí práce: Ing. Roman Šotner, Ph.D.

²⁸ VEVERKA, V. Modely tranzistorů technologie CMOS 0,35um I3T. Brno: Vysoké učení technické v Brně, Fakulta elektrotechniky a komunikačních technologií. Ústav radioelektroniky, 2014. 106 s., Diplomová práce. Vedoucí práce: Ing. Roman Šotner, Ph.D.

transistors from ON Semiconductor 0.35 μm I3T process in Cadence Spectre simulator to PSpice simulator. It was necessary for further works and designs with this CMOS technology on common workstations without linux operational system and installed Cadence IC tools that is expensive and extremely demanding on maintenance (access to local area network with license server and project server). Models from Spectre are not directly compatible with PSpice. Significant attention has been given to modeling (create behavioral models based on commercially available devices – variable gain voltage amplifiers and diamond transistors) of current amplifiers²⁹ and modeling and applications of high-speed voltage-mode multiplier (PSpice model not available in general libraries not even available at the website of the producer)³⁰. Some of the obtained results (improved features and controllability of some applications) should be processed in future publications. Despite several problems and lower quality of formal point of view, significant contribution to further research can be found in a master thesis³¹ finished quite recently. Advanced active elements that were only hypothetical in recent scientific literature are discussed there. A student prepared several real behavioral models of these controllable devices and he has also shown basic experimentally tested features of these models. Further progress and works with developed models are expected in the future. Experiments with newly derived triangular and square wave generator structure have been obtained in the work of a bachelor student³². The structure improves some features of already known solutions in literature. In conclusion, it seems that cooperation with students can be really useful for further growth, interesting hints and ideas for research.

Several students attended competitions and conferences for young designers and researchers EEICT (Electrical Engineering, Information and Communication Technologies) between 2009 and 2016 under the applicant's supervision. Part of a master thesis¹⁹ has been published and presented at a conference in the form of a paper entitled "Universal interface for control of digital potentiometers in analog systems"³³. Part of the thesis²¹ has been presented in the section of bachelor contributions entitled "Universal KHN filter with CDTA"³⁴. A student's work on an audio power amplifier "Simulation and implementation of the audio power amplifier – class A"³⁵ was also

²⁹ KOS, D. Model říditelného proudového zesilovače s diamantovými tranzistory a napětovými zesilovači. Brno: Vysoké učení technické v Brně, Fakulta elektrotechniky a komunikačních technologií, Ústav radioelektroniky, 2015. 41 s., Bakalářská práce. Vedoucí práce: Ing. Roman Šotner, Ph.D.

³⁰ KUŘÁTKO, D. Model čtyř-kvadrantové analogové násobičky AD835 pro Pspice. Brno: Vysoké učení technické v Brně, Fakulta elektrotechniky a komunikačních technologií, Ústav radioelektroniky, 2015. 41 s., Bakalářská práce. Vedoucí práce: Ing. Roman Šotner, Ph.D.

³¹ NOVOTNÝ, J. Behaviorální modely aktivních prvků s nezávislým víceparametrovým elektronickým řízením. Brno: Vysoké učení technické v Brně, Fakulta elektrotechniky a komunikačních technologií, Ústav radioelektroniky, 2016. 88 s., Diplomová práce. Vedoucí práce: Ing. Roman Šotner, Ph.D.

³² ŠUSTEK, V. PWM modulátory s moderními více-branovými aktivními prvky. Brno: Vysoké učení technické v Brně, Fakulta elektrotechniky a komunikačních technologií, Ústav radioelektroniky, 2016. 60 s., Bakalářská práce. Vedoucí práce: Ing. Roman Šotner, Ph.D.

³³ ŠEVČÍK, B. Universal interface for control of digital potentiometers in analog systems. In proceedings of the Student EEICT 2009 conference, available at [www: http://www.feec.vutbr.cz/EEICT/2009/sbornik/02-Magisterske%20projekty/01-Elektronika%20a%20komunikace/13-xsevci34.pdf](http://www.feec.vutbr.cz/EEICT/2009/sbornik/02-Magisterske%20projekty/01-Elektronika%20a%20komunikace/13-xsevci34.pdf)

³⁴ MIKSL, J. Universal KHN filter with CDTA. In proceedings of the Student EEICT 2009 conference, available at [www: http://www.feec.vutbr.cz/EEICT/2009/sbornik/01-Bakalarske%20projekty/01-Elektronika%20a%20komunikace/09-xmiks100.pdf](http://www.feec.vutbr.cz/EEICT/2009/sbornik/01-Bakalarske%20projekty/01-Elektronika%20a%20komunikace/09-xmiks100.pdf)

³⁵ SVADBÍK, P. Simulation and implementation of the audio power amplifier – class A. In proceedings of the Student EEICT 2010 conference, available at [www: http://www.feec.vutbr.cz/EEICT/2010/sbornik/01-Bakalarske_projekty/01-Elektronika_a_komunikace/10-xsvadb01.pdf](http://www.feec.vutbr.cz/EEICT/2010/sbornik/01-Bakalarske_projekty/01-Elektronika_a_komunikace/10-xsvadb01.pdf)

finalized as an excellent hardware prototype for practical laboratory education. Partial results from master theses^{24,25} were presented in the paper “Adjustable square-triangle wave generator”³⁶ as well as application of commercially available current-mode multipliers in the paper entitled “Electronically adjustable oscillator employing commercially accessible current mode multipliers”³⁷. Results of a new active element based on a lossy inductance simulator applied in multifunctional filter were presented as a doctoral contribution called “Current-mode multifunction filters utilizing losses of inductor simulator”³⁸. Papers were presented in sections of Electronics and communications and Signal processing.

The applicant also served as consultant for students of high schools with technical scope of interest (in electronics) in the frame of a competition called “Středoškolská odborná činnost (SOČ)”³⁹. Results of the work of these students were presented as posters at the EEICT conference in 2011 (section Microelectronics⁴⁰) and 2013 (section Electronics and communications⁴¹) and included to proceedings as papers.

³⁶ KOPEČEK, P. Adjustable square-triangle wave generator. In proceedings of the Student EEICT 2011 conference, available at www: <http://www.feec.vutbr.cz/EEICT/2011/sbornik/02-Magisterske%20projekty/01-Elektronika%20a%20komunikace/05-xkopec01.pdf>

³⁷ MIKSL, J. Electronically adjustable oscillator employing commercially accessible current mode multipliers. In proceedings of the Student EEICT 2011 conference, available at www: <http://www.feec.vutbr.cz/EEICT/2011/sbornik/02-Magisterske%20projekty/02-Zpracovani%20signalu.%20obrazu%20a%20dat/08-xmiksl00.pdf>

³⁸ KARTCI, A. Current-mode multifunction filters utilizing losses of inductor simulator. In proceedings of the Student EEICT 2016 conference, available at www: <http://www.feec.vutbr.cz/EEICT/2016/sbornik/EEICT-2016-sborn%C3%ADk-komplet.pdf>

³⁹ <http://www.jcmm.cz/cz/podpora-soc.html>

⁴⁰ BAŠTA, M. Aplikace analogových proudových násobiček v elektronicky říditelném oscilátoru. In proceedings of the Student EEICT 2011 conference, available at www: <http://www.feec.vutbr.cz/EEICT/2011/sbornik/04-Stredoskolske%20projekty/06-Mikroelektronika%20a%20technologie/01-bastamilos.pdf>

⁴¹ ŠOUKAL, P. Microprocessor-based control module for four-channel audio amplifier. In proceedings of the Student EEICT 2013 conference, available at www: <http://www.feec.vutbr.cz/EEICT/2013/sbornik/04stredoakolskeprojekty/01elektronikaakomunikace/10-soukal23.pdf>

4 APPLICANT'S PERSONAL PROFILE

Education and employment overview

Roman Šotner was born in Znojmo in 1983. He attended high school focused on electronics (Integrovaná střední škola, Purkyňova 97, Brno) between the years 1999 and 2003. He studied at the Faculty of Electrical Engineering and Communication, BUT Brno in the bachelor programme Electrical, Electronic, Communication and Control Technology (branch: Electronics and Communication) from 2003. He obtained his bachelor degree in 2006 (thesis: Oscillators based on modern active elements, supervised by prof. Tomáš Dostál) and continued his education in the master degree programme (the same branch). He graduated in 2008 (thesis: Multifunctional tunable active filter, supervised by prof. Tomáš Dostál). His Ph.D. study started in 2008 in the programme Electrical Engineering and Communication (branch Electronics and Communications) at the same faculty (Dept. of Radio Electronics) under supervision of prof. Tomáš Dostál in the topics of innovative applications of modern active devices in communications. When prof. Dostál retired (professor emeritus now), assoc. prof. Jiří Petržela was appointed as his new supervisor in 2010. He finished studies in February 2012 by defense of doctoral thesis "Study of electronic control and real behavior in variable filtering and oscillating applications of modern active elements".

He was a part-time employee at the Dept. of Radio Electronics and Dept. of Telecommunications from 2008 to 2012 during his Ph.D. study in the frame of research projects. He serves as researcher and lecturer or instructor in practical (laboratory and computer) lessons at the Dept. of Radio Electronics from 2012 (full-time employee) and researcher at Dept. of Telecommunications from 2016 (part-time employee).

He has taken part in several highly practically oriented activities during his career. He has been engaged as technician (serviceman of electronic equipment and instruments for measurement of electrical quantities – diagnostic and repairs) in the company ELEX (Richard Hrozek, Brno) many times from 2002 to 2007.

Research interests and scientific aspects

Modern analogue adjustable active elements, electronic control of circuits, circuit synthesis and design (including also IC design and layout), computer simulations and modeling, behavioral modeling and representation, real circuit behavior, parasitic analysis and experimental work belong to the applicant's research interest. He has been a member of IEEE since 2008 and IEICE (Japan) since 2015. His record at the Web of Science (Thomson Reuters) database contains 72 items (2016-07-28). He is author or coauthor of 44 articles (first author in 33 papers) in journals with impact factor (SCI-E) and 28 conference contributions indexed by this database. These papers received 121 citations without self-citations. His current h-index: 12. He serves as invited reviewer for many conferences (Telecommunications and Signal Processing, Radioelektronika/MAREW, Design and Diagnostic of Electronic Circuits and Systems, Midwest Symposium on Circuits and Systems, Electronics, International Conference on Electrical and Electronic Engineering, etc.) and renowned international journals (Int. Journal of Electronics, Microelectronics Journal, Analog Integrated Circuits and Signal Processing, Circuits Systems and Signal Processing, IEEE Transactions on

Instrumentation and Measurement, IEEE Transactions on Industrial Electronics, Journal of Electrical Engineering, Radioengineering, IET Circuits Devices and Systems, IET Electronics Letters, Journal of Circuits Systems and Computers, Measurement Science Review, etc.). He has also been editorial board member/associate editor (section circuits) of Radioengineering Journal since 2014.

Participation in research projects (selected)

The applicant was member of a team in the following projects of fundamental research (supported by the Czech Scientific Foundation): Advanced methods, structures and components of electronic wireless communication (no. GD102/08/H027, project leader: prof. Aleš Prokeš, 2008-2011), Computer automation of methods for linear circuit synthesis and research for novel active elements (no. GA102/09/1681, project leader: prof. Kamil Vrba, 2009-2013). Currently, he acts as project leader in the project: Research for electronically adjustable advanced active elements for circuit synthesis (no. P102/14-24186P, 2014-2016).

The applicant also participated on internal grants of Brno University of Technology (specific research): Research for robust hardware solutions for wireless communication systems (no. FEKT-S-10-9, project leader: prof. Lubomír Brančík, 2010), and Perspective circuit solutions and algorithms for communication systems (no. FEKT-S-14-2281, project leader: assoc. prof. Jiří Petržela, 2014-2016).

He has been member of a team in a project of the European Union (Seventh Framework Programme, FP7-ICT STREP) Nanoelectronic COupled Problems Solutions (nanoCOPS, no. 619166, project leader: prof. Tomáš Kratochvíl, 2014-2016).

Pedagogical activities

The applicant works as an instructor in the laboratory and computer exercises in the courses Electronic Circuit Theory, Design of Analog Filters and Pulse and Digital Techniques. He is also a lecturer of selected topics in these fields. He supervised 13 bachelor and 15 master final theses from 2008 to 2016. He obtained two projects from the Council of Higher Education Institutions (FRVŠ): New laboratory exercises based on modern active elements (no. 103/2009/G1, 2009, project leader: Dr. Josef Slezák), and Enlargement of laboratory education in the field of signal generation (no. 450/2011/G1, 2011), where the applicant served as project leader. Both projects significantly supported education (new hardware units and materials for education of modern active elements and their applications) in courses focused on analog electronics and circuit theory in recent years. He also served as exhibitor of special analog models creating real physical dynamical systems for inexperienced public community in the form of real hardware solutions observable by oscilloscopes at Noc vědců in the Technical museum in Brno (2013) and Science Show Olympia (2014).

International cooperation

There are several joint works with assoc. prof. Winai Jaikla from King Mongkut's Institute of Technology Ladkrabang, Bangkok, Thailand and also assoc. prof. Jiun-Wei

Hornig from Chung Yuan Christian University, Taoyuan, Taiwan. Dr. Abhirup Lahiri from ST Microelectronics, India is an appreciated colleague in the field of CMOS integrated circuits design. Cooperation with assoc. prof. Bilgin Metin from the Dept. of Management Information Systems, Bogazici University, Turkey in the field of filtering structures and circuit synthesis based on utilization of simple transistors started quite recently. Support, encouragement and great hints from prof. Raj Senani (Netaji Subhas Institute of Technology, India) in the field of oscillators and prof. Costas Psychalinos (University of Patras, Greece) in the field of fractional-order systems are highly appreciated.

International internship

The applicant visited (March 2012) the ASIC design center of the company ON Semiconductor in Vilvoorde-Brussels (Belgium) and cooperated on preparing small-signal AC models for stability tests of control loops in DC-DC converters. He also visited Yildiz Technical University in Istanbul (Turkey) as an invited lecturer (September 2015) in the frame of Erasmus+ teaching a mobility program (invited lectures: Advanced active elements in active filters with electronically reconfigurable transfer responses and in signal generation).

Other experience

He passed a course focused on the essentials of scientific work organized by the Academy of Sciences of the Czech Republic in Brno (May 2009). He also attended additional pedagogical courses (accredited) at Lifelong Learning Institute of BUT Brno (Institut celoživotního vzdělávání) from 2011 to 2012 for future possibility of teaching at technically oriented high schools.

Practical skills

The applicant has vast experience with design (Eagle) and manual manufacturing, assembling of PCB and measurement with laboratory equipment. He is an experienced user of many simulation tools: OrCAD PSpice (advanced knowledge); LTSpice (user knowledge); Cadence IC tools versions 5 and 6 (system for design of IC for linux): virtuoso editor, spectre simulator, layout editor (user knowledge); MicroCap (basic knowledge); Ansoft Designer (basic knowledge).

Foreign languages

English (intermediate), German (elementary).

Further skills and activities

Fishing, watermanship (rowing), camping, traveling and sightseeing, amateur electronic constructions, musical instrument (clarinet).

BIBLIOGRAPHY

- [1] SOTNER, R., JERABEK, J., HERENC SAR, N., HRUBOS, Z., DOSTAL, T., VRBA, K. Study of Adjustable Gains for Control of Oscillation Frequency and Oscillation Condition in 3R-2C Oscillator. *Radioengineering*, 2012, vol. 21, no. 1, p. 392-402. ISSN: 1210-2512.
- [2] SOTNER, R., JERABEK, J., HERENC SAR, N., HORNG, J-W., VRBA, K., DOSTAL, T. Simple Oscillator with Enlarged Tunability Range Based on ECCII and VGA Utilizing Commercially Available Analog Multiplier. *Measurement Science Review*, 2016, vol. 16, no. 2, p. 35-41. ISSN: 1335-8871.
- [3] SOTNER, R., JERABEK, J., PROKOP, R., KLEDROWETZ, V. Simple CMOS voltage differencing current conveyor-based electronically tuneable quadrature oscillator. *Electronics Letters*, 2016, vol. 52, no. 12, p. 1016-1018. ISSN: 0013-5194.
- [4] SOTNER, R., JERABEK, J., JAIKLA, W., HERENC SAR, N., VRBA, K., DOSTAL, T. Novel Oscillator Based on Voltage and Current- Gain Adjusting Used for Control of Oscillation Frequency and Oscillation Condition. *Elektronika Ir Elektrotechnika*, 2013, vol. 19, no. 6, p. 75-80. ISSN: 1392-1215.
- [5] SOTNER, R., HERENC SAR, N., JERABEK, J., DVORAK, R., KARTCI, A., DOSTAL, T., VRBA, K. New double current controlled CFA (DCC-CFA) based voltage- mode oscillator with independent electronic control of oscillation condition and frequency. *Journal of Electrical Engineering*, 2013, vol. 64, no. 2, p. 65-75. ISSN: 1335-3632.
- [6] SOTNER, R., LAHIRI, A., JERABEK, J., HERENC SAR, N., KOTON, J., DOSTAL, T., VRBA, K. Special Type of Three- Phase Oscillator Using Current Gain Control for Amplitude Stabilization. *International Journal of Physical Sciences*, 2012, vol. 7, no. 25, p. 3089-3098. ISSN: 1992-1950.
- [7] SOTNER, R., JERABEK, J., GOTTHANS, T., PROKOP, R., DOSTAL, T., VRBA, K. Controlled Gain Current and Differential Voltage Amplifier and Study of Its Application in Simple Adjustable Oscillator. In *Proceedings of the 36th International Conference on Telecommunications and Signal Processing (TSP 2013)*, Rome (Italy), 2013, p. 407-411. ISBN: 978-1-4799-0403-7.
- [8] SOTNER, R., LAHIRI, A., KARTCI, A., HERENC SAR, N., JERABEK, J., VRBA, K. Design of Novel Precise Quadrature Oscillators Employing ECCIIs with Electronic Control. *Advances in Electrical and Computer Engineering*, 2013, vol. 13, no. 2, p. 65-72. ISSN: 1582-7445.
- [9] SOTNER, R., JERABEK, J., HERENC SAR, N. Voltage Differencing Buffered/ Inverted Amplifiers and Their Applications for Signal Generation. *Radioengineering*, 2013, vol. 22, no. 2, p. 490-504. ISSN: 1210-2512.
- [10] SOTNER, R., JERABEK, J., PETRZELA, J., HERENC SAR, N., PROKOP, R., VRBA, K. Second-order Simple Multiphase Oscillator Using Z-Copy Controlled- Gain Voltage Differencing Current Conveyor. *Elektronika Ir Elektrotechnika*, 2014, vol. 20, no. 9, p. 13-18. ISSN: 1392-1215.
- [11] SOTNER, R., JERABEK, J., HERENC SAR, N., PETRZELA, J., VRBA, K., KINCL, Z. Linearly Tunable Quadrature Oscillator Derived from LC Colpitts Structure Using Voltage Differencing Transconductance Amplifier and Adjustable Current Amplifier. *Analog Integrated Circuits and Signal Processing*, 2014, vol. 81, no. 1, p. 121-136. ISSN: 0925-1030.
- [12] SOTNER, R., JERABEK, J., HERENC SAR, N., HORNG, J-W., VRBA, K. Electronically Linearly Voltage Controlled Second-Order Harmonic Oscillator With Multiples of $\pi/4$

- Phase Shifts. In *Proceedings of the 38th International Conference on Telecommunication and Signal Processing (TSP 2014)*, Berlin (Germany), 2014, p. 708-712. ISBN: 978-1-4799-8497-8.
- [13] SOTNER, R., HRUBOS, Z., HERENC SAR, N., JERABEK, J., DOSTAL, T., VRBA, K. Precise Electronically Adjustable Oscillator Suitable for Quadrature Signal Generation Employing Active Elements with Current and Voltage Gain Control. *Circuits Systems and Signal Processing*, 2014, vol. 33, no. 1, p. 1-35. ISSN: 0278-081X.
- [14] SOTNER, R., HERENC SAR, N., JERABEK, J., KOTON, J., DOSTAL, T., VRBA, K. Electronically controlled oscillator with linear frequency adjusting for four-phase or differential quadrature output signal generation. *International Journal of Circuit Theory and Applications*, 2014, vol. 42, no. 12, p. 1264-1289. ISSN: 0098-9886.
- [15] SOTNER, R., JERABEK, J., HERENC SAR, N., VRBA, K., DOSTAL, T. Features of multi-loop structures with OTAs and adjustable current amplifier for second-order multiphase/ quadrature oscillators. *AEU - International Journal of Electronics and Communications*, 2015, vol. 69, no. 5, p. 814-822. ISSN: 1434-8411.
- [16] SOTNER, R., JERABEK, J., HERENC SAR, N., VRBA, K. Design of the simple oscillator with linear tuning and $\pi/4$ phase shift based on emulator of the modified current differencing unit. *IEICE Electronics Express*, 2015, vol. 12, no. 19, p. 1-7. ISSN: 1349-2543.
- [17] SOTNER, R., JERABEK, J., LANGHAMMER, L., POLAK, J., HERENC SAR, N., PROKOP, R., PETRZELA, J., JAIKLA, W. Comparison of two solutions of quadrature oscillators with linear control of frequency of oscillation employing modern commercially available devices. *Circuits Systems and Signal Processing*, 2015, vol. 34, no. 11, p. 3449-3469. ISSN: 0278-081X.
- [18] SOTNER, R., JERABEK, J., PETRZELA, J., PROKOP, R., VRBA, K., KARTCI, A., DOSTAL, T. Quadrature Oscillator Solution Suitable with Arbitrary and Electronically Adjustable Phase Shift. In *Proceedings of the IEEE International Symposium on Circuits and Systems (ISCAS)*, Lisbon (Portugal), 2015, p. 3056-3059. ISBN: 978-1-4799-8391-9, ISSN: 0271-4310.
- [19] SOTNER, R., KARTCI, A., JERABEK, J., HERENC SAR, N., PETRZELA, J. Modulator Based on Electronic Change of Phase Shift in Simple Oscillator. In *ELECO 2015 9th International Conference on Electrical and Electronics Engineering*, Bursa (Turkey), 2015. p. 101-105. ISBN: 978-605-01-0737-1.
- [20] KARTCI, A., SOTNER, R., JERABEK, J., HERENC SAR, N., PETRZELA, J. Phase shift keying modulator design employing electronically controllable all- pass sections. *Analog Integrated Circuits and Signal Processing*, 2016, online first (in press), p. 1-20. ISSN: 0925-1030.
- [21] SOTNER, R., JERABEK, J., HERENC SAR, N., PROKOP, R., VRBA, K., PETRZELA, J., DOSTAL, T. Simply Adjustable Triangular and Square Wave Generator Employing Controlled Gain Current and Differential Voltage Amplifier. In *Proceedings of the 23th international conference Radioelektronika 2013*, Pardubice (Czech Republic), 2013, p. 109-114. ISBN: 978-1-4673-5517-9.
- [22] SOTNER, R., JERABEK, J., HERENC SAR, N., DOSTAL, T., VRBA, K. Design of Z-copy controlled- gain voltage differencing current conveyor based adjustable functional generator. *Microelectronics Journal*, 2015, vol. 46, no. 2, p. 143-152. ISSN: 0026-2692.
- [23] JERABEK, J., SOTNER, R., DOSTAL, T., VRBA, K. Simple Resistor-less Generator Utilizing Z- copy Controlled Gain Voltage Differencing Current Conveyor for PWM

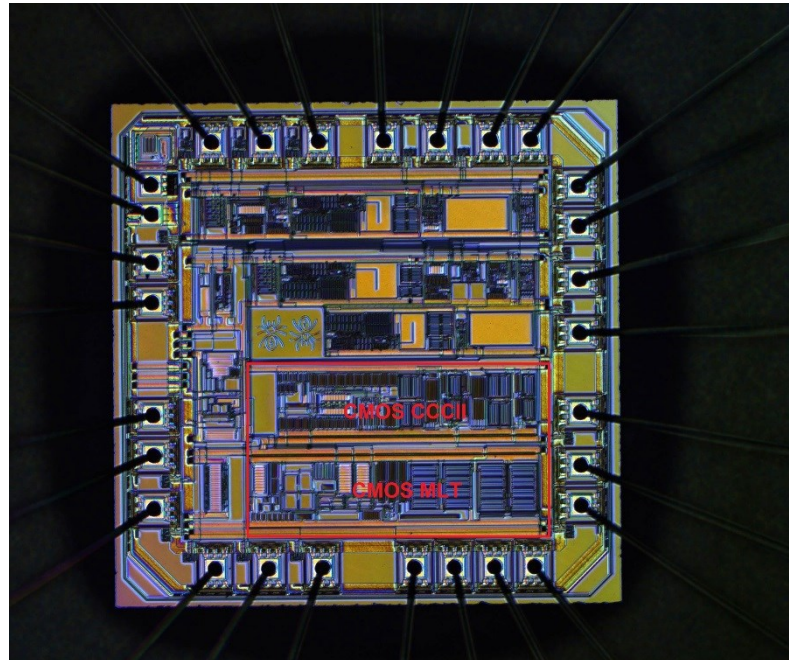
- Generation. *Elektronika Ir Elektrotechnika*, 2015, vol. 21, no. 5, p. 28-34. ISSN: 1392-1215.
- [24] SOTNER, R., HERENC SAR, N., JERABEK, J., PROKOP, R., KARTCI, A., DOSTAL, T., VRBA, K. Z-Copy Controlled-Gain Voltage Differencing Current Conveyor: Advanced Possibilities in Direct Electronic Control of First- Order Filter. *Elektronika Ir Elektrotechnika*, 2014, vol. 20, no. 6, p. 77-83. ISSN: 1392-1215.
- [25] SOTNER, R., JERABEK, J., HERENC SAR, N., PROKOP, R., VRBA, K., DOSTAL, T. Resistor-less First- Order Filter Design with Electronical Reconfiguration of its Transfer Function. In *Proceedings of the 24th International Conference Radioelektronika 2014*, Bratislava (Slovakia), 2014. p. 63-66. ISBN: 978-1-4799-3715-8.
- [26] SOTNER, R., JERABEK, J., HERENC SAR, N., ZAK, T., JAIKLA, W., VRBA, K. Modified Current Differencing Unit and its Application for Electronically Reconfigurable Simple First-order Transfer Function. *Advances in Electrical and Computer Engineering*, 2015, vol. 15, no. 1, p. 3-10. ISSN: 1582-7445.
- [27] SOTNER, R., JERABEK, J., HERENC SAR, N., PROKOP, R., VRBA, K., DOSTAL, T. First-order Reconfigurable Reconnection- less Filters Using Modified Current Differencing Unit. In *Proceedings of 25th International Conference Radioelektronika 2015*. Pardubice (Czech Republic), 2015, p. 46-50. ISBN: 978-1-4799-8117-5.
- [28] SOTNER, R., JERABEK, J., HERENC SAR, N., PROKOP, R., LAHIRI, A., DOSTAL, T., VRBA, K. First-order transfer sections with reconnection-less electronically reconfigurable high-pass, all-pass and direct transfer character. *Journal of Electrical Engineering*, 2016, vol. 67, no. 1, p. 12-20. ISSN: 1335-3632.
- [29] SOTNER, R., JERABEK, J., SEVCIK, B., DOSTAL, T., VRBA, K. Novel Solution of Notch/All- pass Filter with Special Electronic Adjusting of Attenuation in the Stop Band. *Elektronika Ir Elektrotechnika*, 2011, vol. 17, no. 7, p. 37-42. ISSN: 1392- 1215.
- [30] SOTNER, R., JERABEK, J., PETRZELA, J., VRBA, K., DOSTAL, T. Design of Fully Adjustable Solution of Band-Reject/All- Pass Filter Transfer Function Using Signal Flow Graph Approach. In *Proceedings of the 24th International Conference Radioelektronika 2014*, Bratislava (Slovakia), 2014. p. 67-70. ISBN: 978-1-4799-3715-8.
- [31] SOTNER, R., PETRZELA, J., JERABEK, J., VRBA, K., DOSTAL, T. Solutions of Reconnection-less OTA- based Biquads with Electronical Transfer Response Reconfiguration. In *Proceedings of 25th International Conference Radioelektronika 2015*, Pardubice (Czech Republic), 2015. p. 40-45. ISBN: 978-1-4799-8117-5.
- [32] SOTNER, R., PETRZELA, J., JERABEK, J., DOSTAL, T. Reconnection-less OTA- based Biquad Filter with Electronically Reconfigurable Transfers. *Elektronika Ir Elektrotechnika*, 2015, vol. 21, no. 3, p. 33-37. ISSN: 1392-1215.
- [33] SOTNER, R., JERABEK, J., HERENC SAR, N., PETRZELA, J., DOSTAL, T., VRBA, K. First-order adjustable transfer sections for synthesis suitable for special purposes in constant phase block approximation. *AEU - International Journal of Electronics and Communications*, 2015, vol. 69, no. 9, p. 1334-1345. ISSN: 1434-8411.
- [34] SOTNER, R., JERABEK, J., PETRZELA, J., DOSTAL, T. Simple Approach for Synthesis of Fractional- Order Grounded Immittances Based on OTAs. In *Proceedings of 39th International Conference on Telecommunications and Signal Processing (TSP 2016)*, Vienna (Austria), 2016, p. 563-568. ISBN: 978-1-5090-1287-9.
- [35] SOTNER, R., KARTCI, A., JERABEK, J., HERENC SAR, N., DOSTAL, T., VRBA, K. An Additional Approach to Model Current Followers and Amplifiers with Electronically Controllable Parameters from Commercially Available ICs. *Measurement Science Review*,

- 2012, vol. 12, no. 6, p. 255-265. ISSN: 1335-8871.
- [36] SOTNER, R., JERABEK, J., KARTCI, A., HERENC SAR, N., PROKOP, R., PETRZELA, J., VRBA, K. Behavioral Models of Current Conveyor of Second Generation with Advanced Controllable Inter-Terminal Relations. In *Proceedings of the 38th International Conference on Telecommunications and Signal Processing (TSP 2015)*, Prague (Czech Republic), 2015, p. 360-365. ISBN: 978-1-4799-8497-8.
- [37] SOTNER, R., HERENC SAR, N., JERABEK, J., VRBA, K., DOSTAL, T., JAIKLA, W., METIN, B. Novel first-order all-pass filter applications of z- copy voltage differencing current conveyor. *Indian Journal of Pure and Applied Physics*, 2015, vol. 53, no. 8, p. 537-545. ISSN: 0019-5596.
- [38] SOTNER, R., PROKOP, R., JERABEK, J., KLEDROWETZ, V., FUJCIK, L., DOSTAL, T. Design of Current-Controlled Current Conveyor Stage With Systematic Current Offset Reduction. In *Proceedings of International Conference on Applied Electronics (APPEL 2015)*, Pilsen (Czech Republic), 2015, p. 225-228. ISBN: 978-80-261-0385-1.
- [39] SOTNER, R., JERABEK, J., PROKOP, R., KLEDROWETZ, V., FUJCIK, L., DOSTAL, T. Reconfigurable 1st Order Filters Based on Differential Voltage Input and a Single Current Output Transconductance Multiplier. In *PROCEEDINGS EUROCON 2015 (IEEE Region 8, 16th International Conference on Computer as a Tool)*, Salamanca (Spain), 2015, p. 324-327. ISBN: 978-1-4799-8569-2.

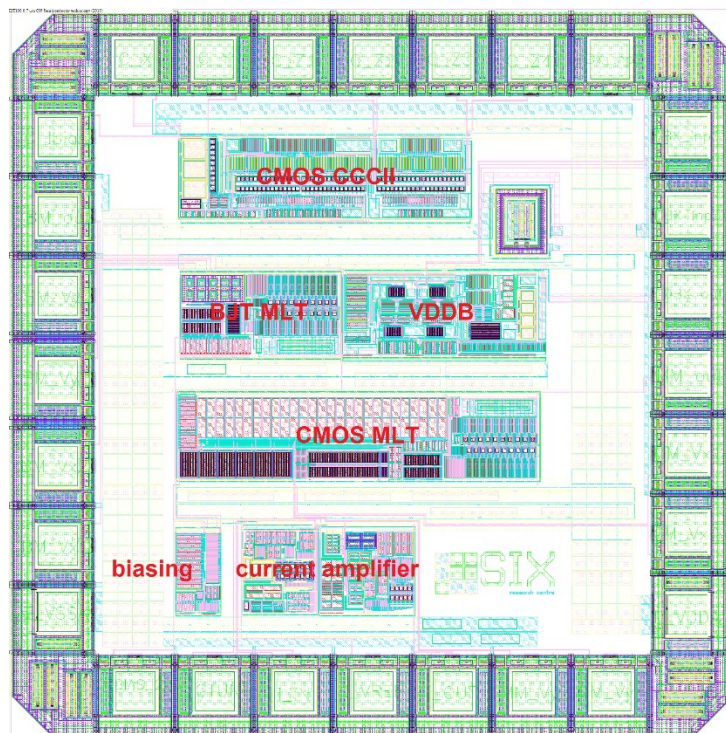
LIST OF ABBREVIATIONS

ADC	analog to digital converter
CCCII	current controllable current conveyor of second generation
CCII	current conveyor of second generation
CDTA	current differencing transconductance amplifier
CDVA	current and differential voltage amplifier
CFA	current feedback amplifier
CFBA	current follower buffered amplifier
CG-BCVA	buffered current and voltage amplifier with controllable current and voltage gains
CG-CFDOBA	current follower differential output buffered amplifier with controllable current gain
CIBA	current inverter buffered amplifier
CO	condition of oscillations
CVA	current and voltage amplifier
DAC	digital to analog converter
DO-CG-CFBA	dual output controlled gain current follower buffered amplifiers
DSP	digital signal processor
ECCII	electronically controllable current conveyor of second generation (current gain control)
FET	field effect transistor
FO	frequency of oscillations
gm	transconductance
MCDU	modified current differencing unit
MOCCII	multiple-output current conveyor of second generation
MOTA	multiple-output operational transconductance amplifier
OTA	operational transconductance amplifier
RX	resistance of current input terminal
THD	total harmonic distortion
TTL	transistor-transistor-logic
VCCFDITA	voltage controlled current follower differential input transconductance amplifier
VDBA	voltage differencing buffered amplifier
VDBVA	voltage differencing buffered voltage amplifier
VDCC	voltage differencing current conveyor
VGA	variable gain voltage amplifier

FABRICATED INTEGRATED CIRCUITS



Microphotograph of cells in I2T100 0.7 μm ON Semiconductor technology (2014/15)



Top-layout of IC fabricated in I3T25 0.35 μm ON Semiconductor technology (2015/16)

ENCLOSED COPIES OF PAPERS

[1] SOTNER, R., JERABEK, J., HERENC SAR, N., HRUBOS, Z., DOSTAL, T., VRBA, K. Study of Adjustable Gains for Control of Oscillation Frequency and Oscillation Condition in 3R-2C Oscillator. *Radioengineering*, 2012, vol. 21, no. 1, p. 392-402. ISSN: 1210-2512.

Study of Adjustable Gains for Control of Oscillation Frequency and Oscillation Condition in 3R-2C Oscillator

Roman SOTNER¹, Jan JERABEK², Norbert HERENC SAR²,
Zdenek HRUBOS¹, Tomas DOSTAL^{1,3}, Kamil VRBA²

¹Dept. of Radio Electronics, Brno University of Technology, Purkynova 118, 612 00 Brno, Czech Republic

²Dept. of Telecommunications, Brno University of Technology, Purkynova 118, 612 00 Brno, Czech Republic

³Dept. of Electronics and Informatics, College of Polytechnics Jihlava, Tolsteho 16, Jihlava 586 01, Czech Republic

{sotner; jerabekj; herencsn; dostal; vrbak}@feec.vutbr.cz, xhrubo00@stud.feec.vutbr.cz

Abstract. An idea of adjustable gain in order to obtain controllable features is very useful for design of tunable oscillators. Several active elements with adjustable properties (current and voltage gain) are discussed in this paper. Three modified oscillator conceptions that are quite simple, directly electronically adjustable, providing independent control of oscillation condition and frequency were designed. Positive and negative aspects of presented method of control are discussed. Expected assumptions of adjustability are verified experimentally on one of the presented solutions.

Keywords

Electronic tuning, adjustable current and voltage amplifiers, voltage and current followers, oscillators.

1. Introduction

Many active elements that are suitable for analog signal processing were introduced in [1]. Some of them have interesting features, which allow electronic control of their parameters. Therefore, these elements have also favorable features in applications. There are several common ways of electronic control of parameters in particular applications. One of the basic approaches is based on replacing grounded or floating resistors in so-called single-resistance-controlled oscillator types (SRCO) [2]-[6], where resistors can be replaced by FET [3]. It could be useful, if there are solutions of active element that allows direct control of any parameter. Control of bias current and therefore of the input resistance is also very popular [7], [8] nowadays. Bias control of transconductance (for example [9-11]) and application of electronically adjustable gain in current conveyors and similar active elements [1], [12]-[20] is another way for direct electronic adjusting. Recently introduced adjustable current transfers in feedback loops [21], [22] of electronic circuit are very suitable not only for the design of adjustable filters, but also for oscillator synthesis. We can recognize two general ways of control.

Direct control means that the functional block is adjustable (tunable) by externally controlled parameter(s) of active element (i.e. current gain, intrinsic resistance, transconductance, etc.). Indirect control is usually provided by some kind of controllable replacement. Simple resistor is replaced by FET transistor, digital to analog converter, or digital potentiometer, etc.

The most important active elements for our approach are current followers (CF) [1], [23], current amplifiers (CA) [1], [24], [25], and voltage buffers/followers (VB/VF) [1]. Many applications were focused on current mode filters (for example [26]-[28]) or inductance simulators (for example [24]). There are also attempts to control some of the parameters digitally and therefore the digitally adjustable current amplifier (DACA) was introduced in [26], [27]. The use of digitally controlled current transfers was given in so-called Z-Copy Controlled-Gain Current Differencing Buffered Amplifier (ZC-CG-CDBA) [29]. Similarly, digital control was also used in case of differential current conveyors [30].

Current followers were used many times as basic elements of oscillators. Some important works that are following last development are discussed below. Chen *et al.* [31] introduced oscillator employing one CF with two capacitors and resistors providing quadrature outputs. However, condition of oscillation (CO) and oscillation frequency (f_0) are complicated and therefore conception is not suitable for electronic adjusting. Abuelma'atti [32] proposed conception with one CF and autonomous passive section, but CO and f_0 have complicated equation and parameters unsuitable for electronic control. However, the oscillator provides multiphase output responses. Similarly, Soliman [33] developed oscillator using CF and also VB. Finally, Gupta *et al.* [34] focused their research on adjustability in oscillator circuits based on CFs and presented solutions utilizing four CFs, three or four resistors, and two grounded capacitors. Their solutions allow tunability by single resistor (SRCO), as it is similarly shown in [35]. Lately, interesting conception was published by Martinez *et al.* [36], where three or four CFs, two VBs, three resistors, and two grounded capacitors in another SRCO type are used. Two multiphase SRCO oscillator realizations

with independent CO and f_0 control were recently introduced by Biolkova *et al.* [37], which also use the combination of two current followers/inverters and VBs, so-called current inverter buffered amplifier (CIBA), three and four floating resistors, and two grounded capacitors.

There are not many conceptions that use the possibility to control the current gain of active element. We can discuss and compare the following solutions: Souliotis *et al.* [38] used three electronically controllable dual-output CAs (integrators) in generalized arbitrary-multiphase current-mode oscillator as an example of directly electronically tunable oscillator. The oscillator is tunable by control current I_{bias} . Kumngern *et al.* [19] used current conveyor based integrators for generalized multiphase oscillator design similarly. The proposed conception is based on current conveyors with adjustable current gain between X and Z ports. Number of phases is reconfigurable by simple switches. Bias control of the current gain is used for matching of time constant of each integrator section. Synthesis and results are not focused on electronic adjusting oscillation frequency. Kumngern *et al.* [39] also proposed the circuit, where combination of intrinsic input resistance and current gain was used for f_0 and CO control. Electronic control of f_0 in [18] is possible by adjustable current gain, but CO control is available only by adjusting of grounded resistor. Solution in [18] employs only one active element, but its disadvantage is the dependence of one of produced amplitude on tuning process and nonlinear control of f_0 . The same type of f_0 control was also used in [40] and [41] in oscillators employing so-called Z-Copy Controlled-Gain Current Differencing Buffered Amplifier (ZC-CG-CDBA). Solution in [40] uses two active elements and five passive elements (capacitors are grounded). Discrete model of one active element employs four diamond transistors [42], [43], [61] and voltage buffer. It is not a problem for future on-chip implementation. Oscillation frequency is controllable linearly by current gain, CO and f_0 are mutually independent. Output amplitude is not dependent on tuning process and CO is controllable just by floating resistors. Solution in [41] requires two ZC-CG-CDBAs and 6 passive elements. CO is also controllable by floating resistor, but f_0 is adjustable digitally (dependence of f_0 on current gain is linear). In comparison to solutions presented in this paper, oscillators in [40], [41] require more sophisticated active elements (4-5 ports per active element). It is worth mentioning that our solutions require active elements that consist of only 3 ports and therefore final chip area of our solution in comparison with oscillators in [40] and [41] will be smaller. Subsequently, the power consumption is also significantly decreased. Oscillation frequency and condition of oscillation are controllable directly, electronically, and independently.

Oscillator solutions utilizing different active elements were presented in literature. Transconductor (OTA) [1], [9] is also useful active element for design of oscillators. We can discuss the following popular solutions. Directly electronically adjustable oscillators were proposed in [44]-[48]. Solutions use at least three active elements. Interesting

circuits were published in [48]-[51], where grounded and floating, two-four capacitor and three or four OTAs were used. Quite complicated solutions (many passive elements) were presented in [52] and [53]. Oscillator utilizing dual-output OTAs and four capacitors was discussed in [54]. Interesting current-mode types were published in [55]. Discussed solutions allow direct electronic control and independently adjustable CO and f_0 (in many cases). However, all OTA-based solutions have one important disadvantage: additional voltage buffering of high-impedance nodes is necessary, if we require voltage (low-impedance) outputs.

Typical representative of active element with similar type of low-impedance output (as our solutions) is current feedback amplifier (CFA) [1]. Oscillators consisting of two CFAs were widely investigated in the past. Important examples are included in [56]-[60]. CFA-based oscillators employing two active elements and grounded capacitors were proposed by Gupta and Senani in [59], [60]. Circuit topology with similar features is in Fig. 3 a, b in [60]. However, oscillators in mentioned literature [56]-[60] require additional voltage input (Y) of active element (CFA contains four ports - X, Y, Z, o) [1]. Our solutions use only current inputs and active element requires only three ports in contrary. Solutions presented in [59], [60] allow the control only by resistors (SRCO types). Direct electronic control with classical CFA is not possible. On the other hand, circuits in [59], [60] have some of resistors grounded when compared to our solutions, where all resistors are floating. Our approach uses direct electronic control (by the DC control voltage of active element) and characteristic equations contain different members and adjustable parameters of active elements. No additional circuit is necessary, except simple AGC.

Oscillator conceptions that are focused mainly on direct electronic control are presented in this paper. Oscillators provide the following important features: a) all capacitors are grounded (required for on-chip implementation); b) active elements with single current input and single voltage output are sufficient; c) only two active elements are required; d) independent control of oscillation frequency and condition of oscillations without mutual disturbance; e) f_0 and CO controlled without changes of any passive element; f) buffered outputs - no additional buffering is necessary; g) simple implementation of amplitude (automatic) gain control (AGC) for f_0 adjusting and satisfying total harmonic distortion (THD) - only rectified output voltage is required; h) real parts of current input (intrinsic) impedance of active elements are absorbed to values of working (external) resistors.

Above discussed solutions were the most important for our approach although many others were presented in literature. Current gain based approaches have not been frequently used for control the oscillators. It is clear that some of discussed solutions use less number of active elements, but direct frequency control and other advantages discussed below are not simultaneously allowed. Last

research was focused also on current-mode solutions (high-impedance outputs, for example [55]). Solutions providing voltage (low-impedance) outputs are discussed in this paper. Necessity of additional voltage buffers or current to voltage converters for voltage-mode operation is the most important problem of some previous works. Some hitherto published realizations are really economical (minimal number of active elements), but characteristic equation is not suitable for electronic control, active elements are quite complicated (many inputs and outputs), many of them do not provide quadrature outputs and in the most cases relation between produced amplitudes and total harmonic distortion in dependence on f_0 adjusting are not mentioned or investigated.

2. Elements with Controlled Gain

Biolkova *et al.* [37] introduced novel active element, so-called dual output current inverter buffered amplifier (DO-CIBA). Application field of such active element is very spread, but possibility of direct electronic control was not discussed (direct electronic control in the frame of the active element). We used several modified versions of DO-CIBA.

Symbol of so-called controlled gain current follower differential output buffered amplifier (CG-CFDOBA) [1] is depicted in Fig. 1 (a). The element contains four ports. Basic principle is explained in Fig. 1 (b). Low-impedance current input is labeled p , auxiliary high-impedance port as z , and buffered outputs (after voltage buffer/inverter) as $w+$ and $w-$, respectively. The output current at auxiliary port (z) is positive, which means that it flows out of the terminal. The current gain (B) between current input port (p) and auxiliary port (z) can be adjusted electronically via external voltage. Possible implementation of CG-CFDOBA with commercially available devices [62]-[66] is shown in Fig. 1 (c).

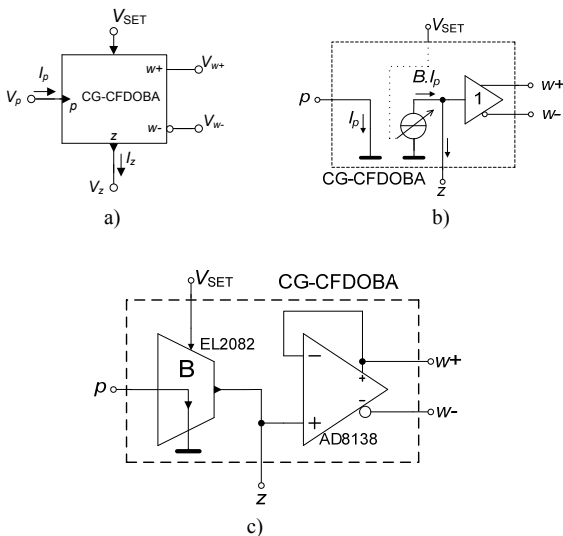


Fig. 1. Controlled gain current follower differential output buffered amplifier (CG-CFDOBA): a) symbol, b) behavioral model, c) possible implementation.

Simplified version (Fig. 2), where only one output w is necessary, should be also noted. This modification is usually called as controlled gain current follower buffered amplifier (CG-CFBA) [1]. Modification, where current at auxiliary terminal (Fig. 3) z is inverted, is marked as controlled gain current inverter buffered amplifier (CG-CIBA) [1], [37].

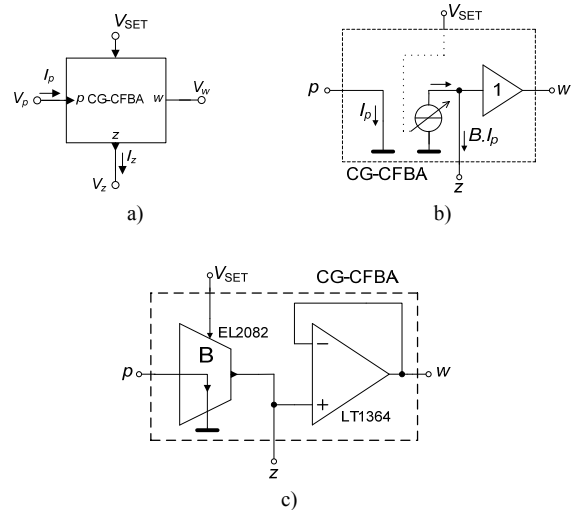


Fig. 2. Controlled gain current follower buffered amplifier (CG-CFBA): a) symbol, b) behavioral model, c) possible implementation.

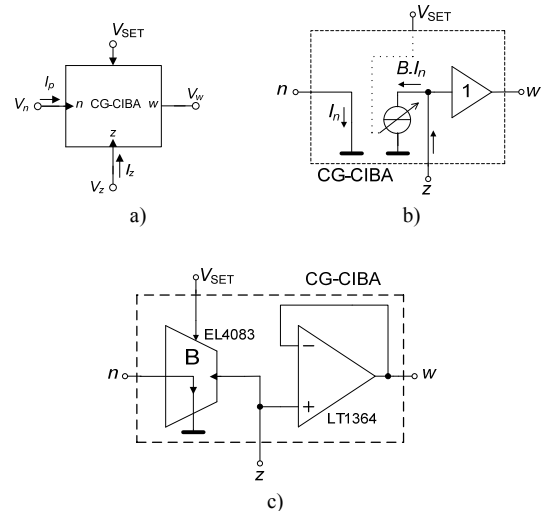


Fig. 3. Controlled gain current inverter differential output buffered amplifier (CG-CIBA): a) symbol, b) behavioral model, c) possible implementation.

The following hybrid matrices describe generally our intention in order to obtain adjustability very well. Equation (1a) describes the modified DO-CIBA with adjustable current gain (B), (1b) explains extension providing adjustable current (B) and voltage gain (A) simultaneously

$$\begin{bmatrix} I_z \\ V_{w+} \\ V_{w-} \\ V_p \end{bmatrix} = \begin{bmatrix} 0 & 0 & 0 & \pm B \\ 1 & 0 & 0 & 0 \\ -1 & 0 & 0 & 0 \\ 0 & 0 & 0 & 0 \end{bmatrix} \begin{bmatrix} V_z \\ I_{w+} \\ I_{w-} \\ I_p \end{bmatrix}, \tag{1a}$$

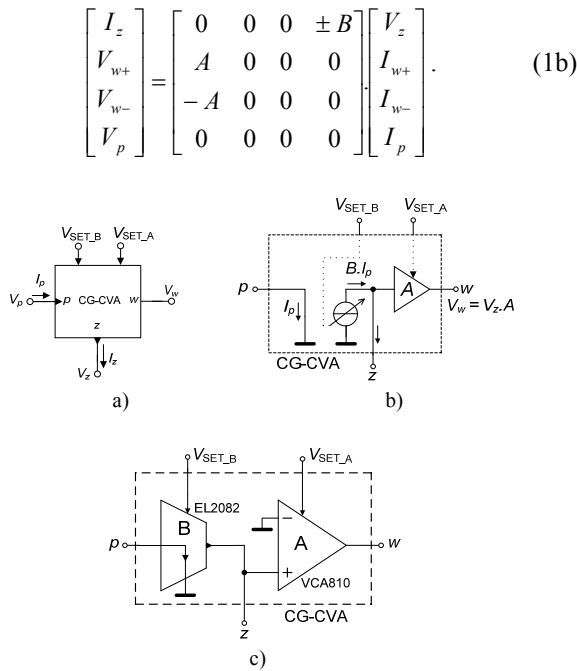


Fig. 4. Controlled gain current amplified voltage amplifier (CG-CVA): a) symbol, b) behavioral model, c) possible implementation.

General adjustable element can be created if adjustable voltage amplifier is used instead of voltage buffer (Fig. 4). It provides full control, i.e. current gain (B) and voltage gain (A). We called this element as controlled gain current and voltage amplifier (CG-CVA). Version with inverting current amplifier is called controlled gain inverted current and voltage amplifier (CG-ICVA). Possible modification with dual voltage output ($w+$, $w-$) could be called dual output controlled gain current and voltage amplifier (DO-CG-CVA). Ideal behavior is clear from (1b).

3. Proposed Oscillators

We have used well-know and popular method for synthesis and design of oscillators. Approach is based on lossless and lossy integrators in the loop. Approach using state variable methods [2], [58]-[61] could also be used for this synthesis and results are identical. Elementary circuit presented in Fig. 5 represents basic building block with transfer constant $I_z/V_i = B/R$. This building block with grounded capacitors at z ports is the main core of future applications (oscillators).

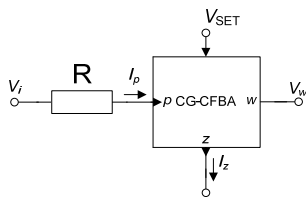


Fig. 5. Elementary building block.

The first designed circuit is shown in Fig. 6. It was created on the basis of discussed approach and elementary

building block from Fig. 5, with the following characteristic equation:

$$s^2 + \frac{-G_1 - G_2 - G_3 + G_3 B_2}{C_2} s + \frac{B_1 G_1 G_2}{C_1 C_2} = 0. \quad (2)$$

Condition of oscillation and oscillation frequency are:

$$B_2 = 1 + \frac{G_1 + G_2}{G_3}, \quad (3)$$

$$\omega_0 = \sqrt{\frac{B_1 G_1 G_2}{C_1 C_2}} \quad (4)$$

where adjustable current gain B_1 stands for current gain of the first active element (CG-CIBA) and B_2 represents current gain of the second active element (CG-CFBA).

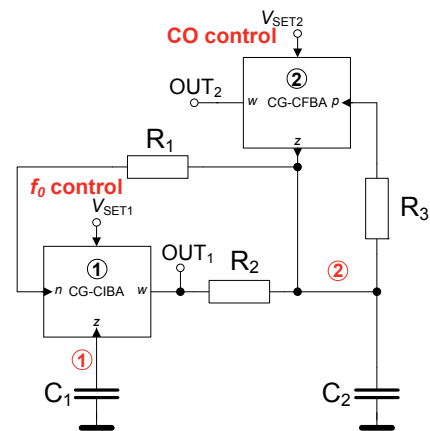


Fig. 6. The first proposed oscillator.

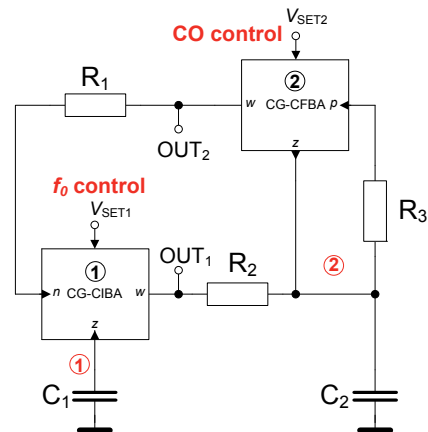


Fig. 7. The second version of the oscillator.

The second solution of the oscillator shown in Fig. 7 was derived from the circuit in Fig. 6 when the resistor R_1 is directly connected to the voltage output of the CG-CFBA. This modification of the oscillator has positive effect on the characteristic equation, which has now the following form:

$$s^2 + \frac{-G_2 - G_3 + G_3 B_2}{C_2} s + \frac{B_1 G_1 G_2}{C_1 C_2} = 0. \quad (5)$$

Oscillation frequency has the same form as in (4), but condition of oscillation is now:

$$B_2 = 1 + \frac{G_2}{G_3}. \tag{6}$$

As shown later, we suppose equality of passive elements for further simplification: $R_1 = R_2 = R$ and $C_1 = C_2 = C$. We used discussed simplifications and compared COs (3) and (6). Theoretical gains $B_2 = 3$ (Fig. 6) and $B_2 = 2$ (Fig. 7) are required to start the oscillations. Possibility of independent adjusting of f_0 and CO by B_1 or R_1 and B_2 is obvious. Control of f_0 by only one parameter (B_1) without another matching condition is advantageous. We are interested only in direct electronic control. Therefore, tuning by passive element is not appropriate for our approach. The oscillators also belong to SRCO types due to the controllability by R_1 . The ideal relative sensitivities of f_0 on circuit parameters are

$$S_{B_1}^{o_0} = -S_{R_1}^{o_0} = -S_{R_2}^{o_0} = -S_{C_1}^{o_0} = -S_{C_2}^{o_0} = 0.5, \tag{7}$$

$$S_{B_2}^{o_0} = S_{R_3}^{o_0} = 0. \tag{8}$$

The ratio between amplitude of state voltages v_1 and v_2 (therefore also between V_{OUT1} and V_{OUT2}) is

$$\frac{V_{OUT1}}{V_{OUT2}} = \frac{-B_1}{sR_1C_1} = \frac{-B_1}{j\omega R_1C_1}. \tag{9}$$

Substitution of the ω by ω_0 from (4) to (9) leads to

$$\frac{V_{OUT1}}{V_{OUT2}} = \frac{-B_1}{j\sqrt{\frac{B_1}{R_1R_2C_1C_2}}R_1C_1} = jB_1\sqrt{\frac{R_2C_2}{R_1C_1B_1}}. \tag{10}$$

It confirms the fact that both produced signals are in quadrature. If we suppose equality $R_1 = R_2 = R$ and $C_1 = C_2 = C$ then the relation between both voltages is given by

$$\frac{V_{OUT1}}{V_{OUT2}} = j\sqrt{B_1}, \tag{11}$$

therefore amplitude of V_{OUT1} is dependent on B_1 and in fact on adjusted f_0 . Produced signals have equal amplitudes for $B_1 = 1$. This problem is not often discussed and studied in detail, but it is usually presented in many hitherto published simple oscillator solutions (for example [18], [20]). Nonlinear dependence of f_0 on parameter B_1 (suitable for tuning) is next consequence.

We also proposed a solution where dependence of produced amplitudes on tuning process is eliminated and tuning characteristic is linear. However, necessity of matching of two gains is now important [40]. The third oscillator (Fig. 8) is described by the following characteristic equation:

$$s^2 + \frac{G_1 + G_3 - G_3A_2}{C_2}s + \frac{B_1B_2G_1G_2}{C_1C_2} = 0. \tag{12}$$

The CO and f_0 determined from (12) have forms:

$$A_2 = 1 + \frac{G_1}{G_3}, \quad \omega_0 = \sqrt{\frac{B_1B_2G_1G_2}{C_1C_2}}. \tag{13}, (14)$$

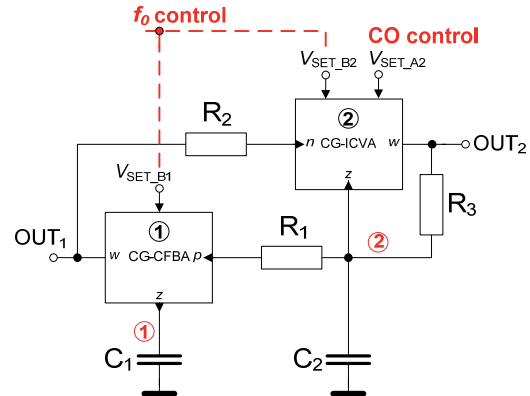


Fig. 8. The third version of oscillator with direct electronic adjusting.

The parameter A_2 is the voltage gain of the CG-ICVA in Fig. 8. For more details see principle in Fig. 4. Relation between produced amplitudes is

$$\frac{V_{OUT1}}{V_{OUT2}} = \frac{B_1}{sR_1C_1} = \frac{B_1}{j\omega R_1C_1}, \tag{15}$$

and after modification it leads to

$$\frac{V_{OUT1}}{V_{OUT2}} = \frac{B_1}{j\sqrt{\frac{B_1B_2}{R_1R_2C_1C_2}}R_1C_1} = -jB_1\sqrt{\frac{R_2C_2}{R_1C_1B_1B_2}}. \tag{16}$$

We suppose $B_1 = B_2 = B$ and therefore (16) simplifies to

$$\frac{V_{OUT1}}{V_{OUT2}} = -j\sqrt{\frac{R_2C_2}{R_1C_1}}. \tag{17}$$

We also suppose above discussed simplification of equality of passive elements ($R_1 = R_2 = R$ and $C_1 = C_2 = C$). Therefore output amplitudes are equal to each other even if f_0 is tuned.

The ideal relative sensitivities of f_0 in (14) on circuit parameters are very similar to the previous case:

$$S_{B_1}^{o_0} = S_{B_2}^{o_0} = -S_{R_1}^{o_0} = -S_{R_2}^{o_0} = -S_{C_1}^{o_0} = -S_{C_2}^{o_0} = 0.5, \tag{18}$$

$$S_{A_2}^{o_0} = S_{R_3}^{o_0} = 0. \tag{19}$$

Implementation of adjustable current gain is very favorable for direct electronically controllable applications, for example oscillators. For instance, both circuits in [37] allow tuning by changing the values of resistors only. For example, the second circuit in [37] does not allow tuning without changes of one amplitude as discussed by authors in [37]. Changing the value of only one resistor is suitable for f_0 tuning. However, this approach [40] allows to control f_0 similarly as it is shown in Fig. 8 (B_1 and B_2 for tuning of f_0). This control approach removes remaining drawback of the second circuit in [37].

4. Experiments and Real Behavior

The second solution of the oscillator (Fig. 7) was chosen as an example for experimental verification and detailed analysis. This selection is also caused by the reason that we would like to show some drawbacks of the second solution (dependence of amplitude on gain B in case of quadrature signals is documented).

Behavior of each circuit is affected by real features of active elements. Input resistance (port p or n) of both active elements is labeled as R_p or R_n . Output resistances R_w (at port w) are in most cases negligible because opamp (as voltage buffer) has values $< 1 \Omega$ in wide frequency range. Input capacitances of active elements have minimal impact because they are together with quite small resistance. Impedances of auxiliary port z consist of high resistive and capacitive part. High impedance node 1 and node 2 are influenced by output resistance of the used current amplifier and by input resistance of voltage buffer. We labeled this parameter as R_z . Capacitances in auxiliary port are labeled as C_z . Basic models of used active elements for non-ideal analysis are in Fig. 9.

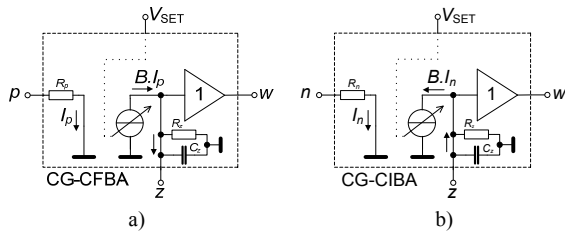


Fig. 9. Non-ideal models of used active elements.

CG-CIBA was built from four-quadrant current-mode multiplier EL4083 [62] (it allows both negative and positive current output). However, current gain adjusting is limited only to unity [62]. The second part (voltage buffer) was constructed by dual opamp LT1364 [63]. CG-CFBA was created from current-mode multiplier EL2082 [64] because it allows larger range of current gain. Opamp LT1364 was also used. In our case is $R_z \approx 830 \text{ k}\Omega$. Output impedances of EL4083 and EL2082 are approximately $1 \text{ M}\Omega / 5 \text{ pF}$ and input impedance of LT1364 is approximately $5 \text{ M}\Omega / 3 \text{ pF}$ [63]. Both parasitic capacitances have approximately values $C_z \approx 8 \text{ pF}$. Input resistance of inverting CG-CIBA (R_n) is dependent on auxiliary bias current and varies in range from 40 to 700 Ω if auxiliary bias current is changed from 2.5 mA to 0.2 mA. It was tested experimentally, because it is not discussed in [62]. Expected value of R_n is approximately 300 Ω in our case (it is quite high value). Input resistance of CG-CFBA has fixed and lower value, $R_p \approx 95 \Omega$.

Passive external elements of oscillator (Fig. 7) were selected as $R_1 = R_2 = R_3 = 1 \text{ k}\Omega$, $C_1 = C_2 = 100 \text{ pF}$ and parameters of active elements were designed as $B_1 = 1$, $B_2 = 2$, respectively. The model of oscillator in Fig. 10 takes into account also important parasitic elements placed

in critical parts of the circuit ($R_{z1} = R_{z2} = 830 \text{ k}\Omega$, $C_{z1} = C_{z2} = 8 \text{ pF}$).

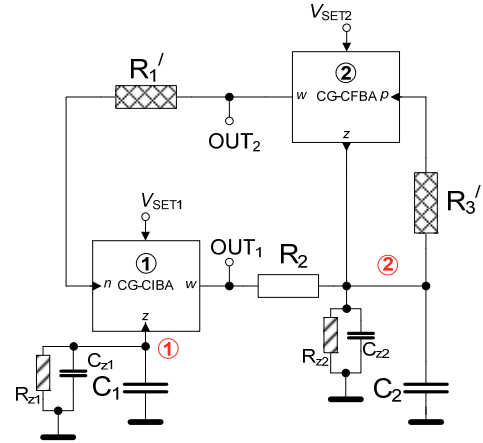


Fig. 10. Important parasitic influences in the circuit.

Real values of passive elements are $R_1' = R_1 + R_n \approx 1.3 \text{ k}\Omega$, $R_3' = R_3 + R_p \approx 1.1 \text{ k}\Omega$, $C_1' = C_1 + C_{z1} \approx 108 \text{ pF}$, $C_2' \approx 108 \text{ pF}$. CO and f_0 have now the following and more complex forms:

$$B_2 \geq \frac{R_1' R_{z1} R_{z2} C_1' (R_2 + R_3') + R_1' R_2 R_3' (R_{z1} C_1' + R_{z2} C_2')}{R_1' R_2 R_3' R_{z1} R_{z2} C_1'} \quad (20)$$

$$\omega_0' = \sqrt{\frac{R_3' R_{z2} (B_1 R_{z1} + R_1') + R_1' R_2 (R_{z2} - B_2 R_{z2} + R_3')}{R_1' R_2 R_3' R_{z1} R_{z2} C_1' C_2'}} \quad (21)$$

From (21) it is clear that B_2 could influence oscillation frequency. Nevertheless, impact of the second sum term in (21) is very small because it has several times lower value in comparison with the first term and B_2 has quite constant value (in comparison to B_1). Possible influence on exact value of f_0 appears for $B_1 < 0.1$ only. Tab. 1 provides comparison of the order of terms magnitude in nominator from (21).

B_1 [-]	$R_3' R_{z2} (B_1 R_{z1} + R_1')$	$R_1' R_2 (R_{z2} - B_2 R_{z2} + R_3')$
10	10^{15}	10^{12}
1	10^{14}	10^{12}
0.1	10^{13}	10^{12}
0.01	10^{12}	10^{12}

Tab. 1. Magnitude difference of members of (21).

Influences of imperfections of voltage followers were also found in f_0 . Modified equation (21), considering this problem is in form:

$$\omega_0' = \sqrt{\frac{R_3' R_{z2} (B_1 R_{z1} \alpha_1 \alpha_2 + R_1') + R_1' R_2 (R_{z2} - B_2 R_{z2} + R_3')}{R_1' R_2 R_3' R_{z1} R_{z2} C_1' C_2'}} \quad (22)$$

where α_1 and α_2 are non-ideal voltage gains. Practically, these gains are not equal to 1. Tab. 2 shows impact on non-accurate gain (buffering) on deviation $f_0 \pm \Delta f_0$ (worst case) based on calculation (22) for $f_0 = 1.293 \text{ MHz}$. Tolerances of these undesired gains (larger than 5%) could cause additional significant problems with accuracy of f_0 (Tab. 2).

Toler. $\alpha_{1,2}$ [%]	$\alpha_{1,2}$ [-]	$\pm\Delta f_0$ [kHz]
± 10	0.90-1.10	130
± 5	0.95-1.05	65
± 2	0.98-1.02	26

Tab. 2. Impact of non-accurate voltage buffering on f_0 .

The circuit was complemented by AGC system (Fig. 11) employing simple common-source transistor stage, which allows control of B_2 through V_{SET2} by rectified output signal. Common bipolar transistor BC547B and diode 1N4148 was used in AGC. Voltage V_h in ACG circuit is derived from voltage setting the CO and its value is between 2 - 2.5 V. Increasing of output level causes larger base-emitter voltage and causes decreasing of V_{SET2} (therefore also B_2). Decreasing of V_{OUT2} causes increasing of V_{SET2} . A very precise and careful setting is necessary for correct operation of AGC.

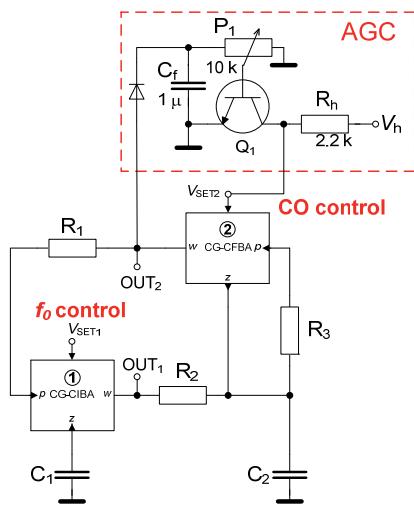
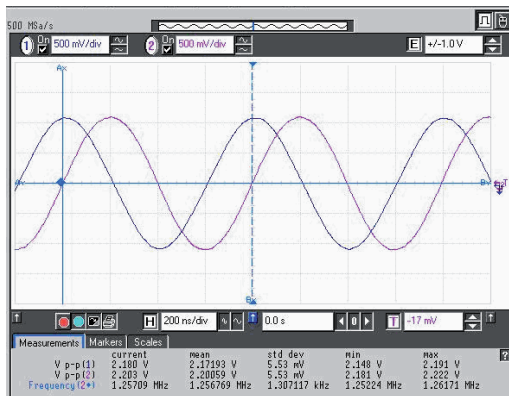
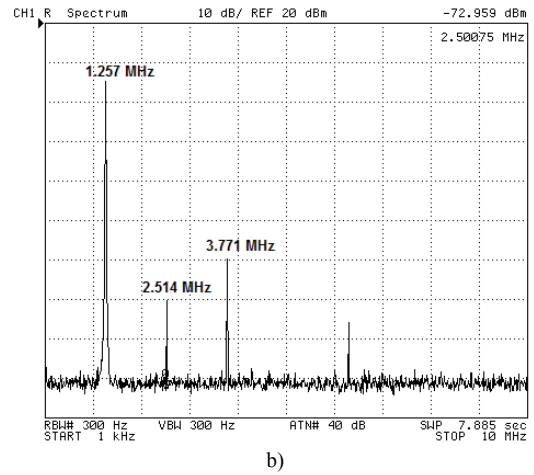


Fig. 11. Important parasitic influences in the circuit.

Results of experiments were obtained by oscilloscope Agilent Infinium 54820A and vector network/spectrum analyzer Agilent 4395A. Supply voltage was $V_{DD} = +5\text{ V}$ and $V_{SS} = -5\text{ V}$. Real active elements and their properties are considered. Expected oscillation frequency is $f_0 = 1.293\text{ MHz}$ (21) for selected and designed parameters (if $B_1 = 1$). Measured value was 1.257 MHz. Deviation is mostly caused by inaccuracy of expected value of R_{n1} . This parameter is also dependent on bias current [62]. Transient response and spectrum of V_{OUT2} are shown in Fig. 12.



a)



b)

Fig. 12. Measured results: a) transient responses, b) spectrum of V_{OUT2} .

Relation between control voltages and current gains are $B_1 \approx V_{SET1}/V_{DD}$ [62] and $B_2 \approx V_{SET2}$ [64]. Range of tunability was measured from 100 kHz to 1.257 MHz for B_1 changed from 0.01 to 1, see Fig. 13.

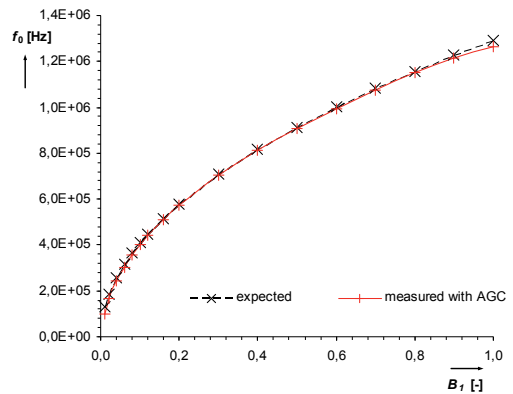
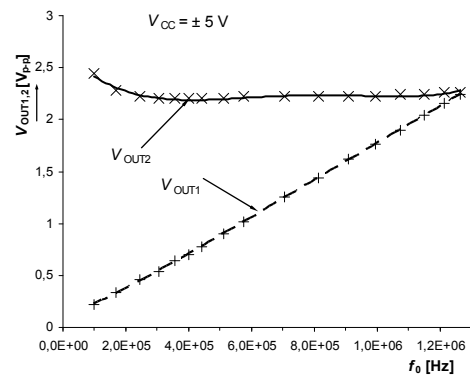


Fig. 13. Dependence of f_0 on current gain B_1 .

Output level (V_{OUT2}) has quite constant value $2.22 \pm 0.06\text{ V}_{p-p}$ in frequency range between 400 kHz and 1.257 MHz ($B_1 \in \{0.1; 1\}$), see Fig. 14 (a). Attenuation of higher harmonic components is greater than 40 dB (Fig. 12 (b)) and THD is in range from 0.6 to 1 % (Fig. 14 (b)). THD of V_{OUT1} is about 1 - 1.3 % in almost whole range of f_0 adjusting (Fig. 14 (b)). Output level of V_{OUT1} changes according to B_1 from 0.22 to 2.24 V, see Fig. 14 (a).



a)

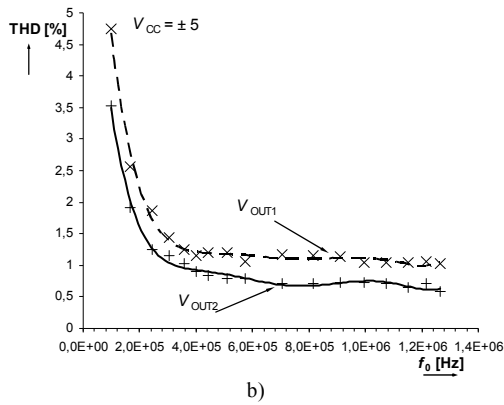


Fig. 14. Results of tuning process: a) dependence of output levels on controlled current gain B_1 , b) dependence of THD on oscillation frequency.

Dependence of V_{OUT1} on B_1 is depicted in Fig. 15. It confirms (11) very well. Measured prototype is shown in Fig. 16.

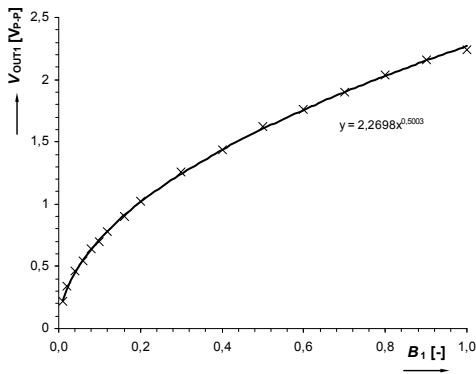


Fig. 15. Dependence of V_{OUT1} on B_1 .

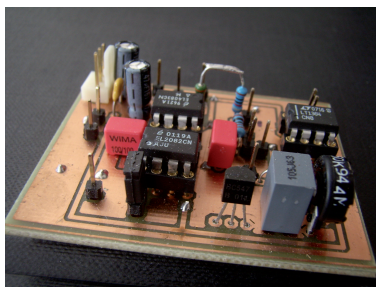


Fig. 16. Measured prototype.

5. Conclusion

The most important contributions of presented solutions are direct electronic and also independent control of CO and f_0 , suitable AGC circuit implementation, buffered low-impedance outputs, and of course, grounded capacitors. Independent tunability by only one parameter is very useful, but tuning characteristic is nonlinear. The most important drawback is dependence of amplitude V_{OUT1} on current gain B_1 (if quadrature outputs are required), which was confirmed by experimental measurements. Circuit in Fig. 7 was selected in order to show all features and docu-

ment the expected behavior, which was first derived theoretically (equations). It is quite hidden problem at first sight without precise analyses. This problem was solved and possible conception (Fig. 8) was introduced. It is necessary to change oscillation frequency simultaneously by two parameters (adjustable current gains) and oscillation condition by adjustable voltage gain (all in frame of two active elements). Equality (and invariability) of generated amplitudes and linearity of tuning characteristic during the tuning process are required aspects. This feature is not novel advantage of circuit in Fig. 8. Detailed discussion is available in [40] for example. All favorable features were obtained without further extension of proposed circuit. Future work will be focused on detailed tests of proposed circuit in Fig. 8. However, controllability of f_0 by one parameter (Fig. 8) was lost and simultaneous change of two parameters is necessary [40].

Acknowledgements

The research leading to these results has received funding from the European Community's Seventh Framework Programme (FP7/2007-2013) under grant agreement no. 230126. The research described in the paper was also supported by the Czech Science Foundation projects under No. 102/11/P489 and No. 102/09/1681. The research described in the paper is a part of the COST Action IC0803 RF/Microwave communication subsystems for emerging wireless technologies, financed by the Czech Ministry of Education by the grant no. OC09016. The support of the project CZ.1.07/2.3.00/20.0007 WICOMT, financed from the operational program Education for Competitiveness, is gratefully acknowledged. The described research was performed in laboratories supported by the SIX project; the registration number CZ.1.05/2.1.00/03.0072, the operational program Research and Development for Innovation. Authors wish to thank the anonymous reviewers for their useful and constructive comments that helped to improve the paper. Authors are also thankful to Dr. Jaroslav Koton from the Brno University of Technology, Czech Republic, for his comments and corrections made on the paper.

References

- [1] BIOLEK, D., SENANI, R., BIOLKOVA, V., KOLKA, Z. Active elements for analog signal processing: Classification, review, and new proposal. *Radioengineering*, 2008, vol. 17, no. 4, p. 15 – 32.
- [2] GUPTA, S. S., SHARMA, R. K., BHASKAR, D. R., SENANI, R. Sinusoidal oscillators with explicit current output employing current-feedback op-amps. *International Journal of Circuit Theory and Applications*, 2010, vol. 38, no. 2, p. 131-147.
- [3] GUPTA, S. S., BHASKAR, D. R., SENANI, R. New voltage controlled oscillators using CFOAs. *AEU – International Journal of Electronics and Communications*, 2009, vol. 63, no. 3, p. 209-217.
- [4] MARTINEZ, P. A., SABADELL, J., ALDEA, C. Grounded resistor controlled sinusoidal oscillator using CFOAs. *Electronics Letters*, 1997, vol. 33, no. 5, p. 346-348.

- [5] MAHESHWARI, S., CHATUVERDI, B. High output impedance CMQOs using DVCCs and grounded components. *International Journal of Circuit Theory and Applications*, 2011, vol. 39, no. 4, p. 427-435.
- [6] HERENC SAR, N., VRBA, K., KOTON, J., LAHIRI, A. Realizations of single-resistance-controlled quadrature oscillators using a generalized current follower transconductance amplifier and a unity gain voltage-follower. *Int. Journal of Electronics*, 2010, vol. 97, no. 8, p. 879-906.
- [7] SIRIPRUCHYANUN, M., CHANAPROMMA, C., SILAPAN, P., JAIKLA, W. BiCMOS Current-Controlled Current Feedback Amplifier (CC-CFA) and its applications. *WSEAS Transactions on Electronics*, 2008, vol. 6, no. 5, p. 203-219.
- [8] HORNG, J. W. A sinusoidal oscillator using current-controlled current conveyors. *Int. Journal of Electronics*, 2001, vol. 88, no. 6, p. 659-664.
- [9] GEIGER, R. L., SANCHEZ-SINENCIO, E. Active filter design using operational transconductance amplifiers: a tutorial. *IEEE Circuits and Devices Magazine*, 1985, vol. 1, p. 20-32.
- [10] LAHIRI, A. Explicit-current-output quadrature oscillator using second-generation current conveyor transconductance amplifier. *Radioengineering*, 2009, vol. 18, no. 4, p. 522-526.
- [11] SOTNER, R., JERABEK, J., PETRZELA, J., DOSTAL, T., VRBA, K. Electronically tunable simple oscillator based on single-output and multiple output transconductor. *IEICE Electron. Express*, 2009, vol. 6, no. 20, p. 1476-1482.
- [12] SURAKAMPONTORN, W., THITIMAJSHIMA, W. Integrable electronically tunable current conveyors. *IEE Proceedings-G*, 1988, vol. 135, no. 2, p. 71-77.
- [13] FABRE, A., MIMECHE, N. Class A/AB second-generation current conveyor with controlled current gain. *Electronics Letters*, 1994, vol. 30, p. 1267-1268.
- [14] MINAEI, S., SAYIN, O. K., KUNTMAN, H. A new CMOS electronically tunable current conveyor and its application to current-mode filters. *IEEE Transaction on Circuits and Systems I - Regular papers*, 2006, vol. 53, no. 7, p. 1448-1457.
- [15] TANGSRIRAT, W. Electronically tunable multi-terminal floating nullor and its application. *Radioengineering*, 2008, vol. 17, no. 4, p. 3-7.
- [16] SHI-XIANG, S., GUO-PING, Y., HUA, C. A new CMOS electronically tunable current conveyor based on translinear circuits. In *Proc. of 7th Int. Conf. on ASIC (ASICON 2007)*, 2007, p. 569-572.
- [17] SOTNER, R., HRUBOS, Z., SLEZAK, J., DOSTAL, T. Simply adjustable sinusoidal oscillator based on negative three-port current conveyors. *Radioengineering*, 2010, vol. 19, no. 3, p. 446 to 453.
- [18] SOTNER, R., JERABEK, J., PROKOP, R., VRBA, K. Current gain controlled CCTA and its application in quadrature oscillator and direct frequency modulator. *Radioengineering*, 2011, vol. 20, no. 1, p. 317-326.
- [19] KUMNGERN, M., CHANWUTIUM, J., DEJHAN, K. Electronically tunable multiphase sinusoidal oscillator using translinear current conveyors. *Analog Integrated Circuits and Signal Processing*, 2010, vol. 65, no. 2, p. 327-334.
- [20] HERENC SAR, N., LAHIRI, A., VRBA, K., KOTON, J. An electronically tunable current-mode quadrature oscillator using PCAs. *Int. Journal of Electronics*, 2011, available online, DOI: 10.1080/00207217.2011.643489.
- [21] BIOLKOVA, V., BIOLEK, D. Shadow filters for orthogonal modification of characteristic frequency and bandwidth. *Electronics Letters*, 2010, vol. 46, no. 12, p. 830-831.
- [22] LAKYS, Y., FABRE, A. Shadow filters - new family of second-order filters. *Electronics Letters*, 2010, vol. 46, no. 4, p. 276-277.
- [23] TANGSRIRAT, W., PUKKALANUN, T. Digitally programmable current follower and its applications. *AEU - International Journal of Electronics and Communications*, 2009, vol. 63, no. 5, p. 416 to 422.
- [24] PSYCHALINOS, C., SPANIDOU, A. Current amplifier based grounded and floating inductance simulators. *AEU - International Journal of Electronics and Communications*, 2006, vol. 60, no. 2, p. 168-171.
- [25] SEDIGHI, B., BAKHTIAR, M. S. Variable gain current mirror for high-speed applications. *IEICE Electronics Express*, 2007, vol. 4, no. 8, p. 277-281.
- [26] JERABEK, J., VRBA, K. Fully differential universal filter with differential and adjustable current followers and transconductance amplifiers. In *Proc. of the 33rd Int. Conf. on Telecommunications and Signal Processing - TSP 2010*. Baden (Austria), 2010, p. 5-9.
- [27] JERABEK, J., SOTNER, R., VRBA, K. Fully-differential current amplifier and its application to universal and adjustable filter. In *International Conference on Applied Electronics APPEL 2010*. Plzeň (Czech Republic), 2010, p. 141-144.
- [28] KOTON, J., VRBA, K., HERENC SAR, N. Tuneable filter using voltage conveyors and current active elements. *Int. J. Electronics*, 2009, vol. 96, no. 8, p. 787-794.
- [29] BIOLEK, D., BAJER, J., BIOLKOVA, V., KOLKA, Z., KUBICEK, M. Z copy-controlled gain-current differencing buffered amplifier and its applications. *International Journal of Circuit Theory and Applications*, 2011, vol. 39, no. 3, p. 257-274.
- [30] MAHMOUD, S., HASHIES, M., SOLIMAN, A. Low-voltage digitally controlled fully differential current conveyor. *IEEE Transactions on Circuits and Systems I*, 2005, vol. 52, no. 10, p. 2055-2064.
- [31] CHEN, J. J., CHEN, C. C., TSAO, H. W., LIU, S. I. Current-mode oscillators using single current follower. *Electronics Letters*, 1991, vol. 27, no. 22, p. 2056-2059.
- [32] ABUELMA'ATTI, M. T. Grounded capacitor current-mode oscillator using single current follower. *IEEE Transaction on Circuits and Systems I: Fundamental Theory and Applications*, 1992, vol. 39, no. 12, p. 1018-1020.
- [33] SOLIMAN, A. M. Novel oscillators using current and voltage followers. *Journal of the Franklin Institute*, 1998, vol. 335, no. 6, p. 997-1007.
- [34] GUPTA, S. S., SENANI, R. New single-resistance-controlled oscillator configurations using unity-gain cells. *Analog Integrated Circuits and Signal Processing*, 2006, vol. 46, no. 2, p. 111-119.
- [35] GUPTA, S. S., SENANI, R. New single resistance controlled oscillators employing a reduced number of unity-gain cells. *IEICE Electron. Express*, 2004, vol. 1, no. 16, p. 507-512.
- [36] MARTINEZ, P. A., MONGE-SANZ, B. M. Single resistance controlled oscillator using unity gain cells. *Microelectronics Reliability*, 2005, vol. 45, no. 1, p. 191-194.
- [37] BIOLKOVA, V., BAJER, J., BIOLEK, D. Four-phase oscillators employing two active elements. *Radioengineering*, 2011, vol. 20, no. 1, p. 334-339.
- [38] SOULIOTIS, G., PSYCHALINOS, C. Electronically controlled multiphase sinusoidal oscillators using current amplifiers. *International Journal of Circuit Theory and Applications*, 2009, vol. 37, no. 1, p. 43-52.
- [39] KUMNGERN, M., JUNNAPIYA, S. A sinusoidal oscillator using translinear current conveyors. In *Asia Pacific Conference on Circuits and Systems (APCCAS 2010)*, 2010, p. 740-743.

- [40] BIOLEK, D., LAHIRI, A., JAIKLA, W., SIRIPRUCHYANUN, M., BAJER, J. Realisation of electronically tunable voltage-mode/current-mode quadrature sinusoidal oscillator using ZC-CG-CDBA. *Microelectronics Journal*, 2011, vol. 42, no. 10, p. 1116 to 1123.
- [41] BAJER, J., BIOLEK, D. Digitally controlled quadrature oscillator employing two ZC-CG-CDBAs. In *Proc. of International Conference on Electronic Devices and Systems EDS'09 IMAPS CS*. Brno (Czech Republic), 2009, p. 298-303.
- [42] BIOLEK, D., BIOLKOVA, V. Implementation of active elements for analog signal processing by diamond transistors. In *Proc. of International Conference on Electronic Devices and Systems EDS'09 IMAPS CS*. Brno (Czech Republic), 2009, p. 304-309.
- [43] *OPA860: Wide Bandwidth Operational Transconductance Amplifier and Buffer*, Texas Instruments. [Online]. 2005, last modified 8/2008 [Cited 2011-07-28]. Available at URL: <<http://focus.ti.com/lit/ds/symlink/opa860.pdf>>
- [44] KUNTMAN, H., OZPINAR, A. On the realization of DO-OTA-C oscillators. *Microelectronics Journal*, 1998, vol. 29, no. 12, p. 991 to 997.
- [45] RODRIGUEZ-VAZQUEZ, A., LINAREZ-BARRANCO, B., HUERTAS, L., SANCHEZ-SINENCIO, E. On the design of voltage-controlled sinusoidal oscillators using OTA's. *IEEE Transactions on Circuits and Systems*, 1990, vol. 37, no. 2, p. 198-211.
- [46] SWAMY, M., RAUT, R., TANG, Z. Generation of OTA-C oscillator structures using network transposition. In *Proceedings of 47th IEEE International Midwest Symposium on Circuits and Systems*. Hiroshima (Japan), 2004, p. 73-76.
- [47] LINAREZ-BARRANCO, B., SERANO-GARRREDONA, T., RAMOS-MARTOS, J., CEBALLOS-CACERES, J., MORA, J., LINAREZ-BARRANCO, A. A precise 90 quadrature OTA-C oscillator tunable in the 50-130 MHz range. *IEEE Transactions on Circuits and Systems I: Regular papers*, 2004, vol. 51, no. 4, p. 649-663.
- [48] CAM, U., KUNTMAN, H., ACAR, C. On the realization of OTA-C oscillators. *International Journal of Electronics*, 1998, vol. 85, no. 3, p. 313-326.
- [49] SINGH, V. Equivalent forms of dual-OTA RC oscillators with application to grounded-capacitor oscillators. *IEE Proc - Circuits Devices Systems*, 2006, vol. 153, no. 2, p. 95-99.
- [50] LINAREZ-BARRANCO, B., RODRIGUEZ-VAZQUEZ, A., SANCHEZ-SINENCIO, E., HUERTAS, L., J. CMOS OTA-C high frequency sinusoidal oscillators. *IEEE Journal of Solid-State Circuits*, 1991, vol. 26, no. 2, p. 160-165.
- [51] SOLIMAN, A. M. CMOS balanced output transconductor and applications for analog VLSI. *Microelectronics Journal*, 1999, vol. 30, no. 1, p. 29-39.
- [52] TAO, Y., FIDLER, J. K. Electronically tunable dual-OTA second-order sinusoidal oscillators/filters with non-interacting controls: A systematic synthesis approach. *IEEE Transaction on Circuits and Systems I: Fundamental Theory and Applications*, 2000, vol. 47, no. 2, p. 117-129.
- [53] PROMEE, P., ANGKEAW, K., CHANWUTIUM, J., DEJHAN, K. Dual input all-pass networks using MO-OTA and its application. In *ECTI-CON Conference*, 2007, p. 129-132.
- [54] GALAN, J., CARVALAJ, R. G., TORRALBA, A., MUNOZ, F., RAMIREZ-ANGULO, J. A low-power low-voltage OTA-C sinusoidal oscillator with large tuning range. *IEEE Transaction on Circuits and Systems I: Fundamental Theory and Applications*, 2005, vol. 52, no. 2, p. 283-291.
- [55] BHASKAR, D. R., ABDALLA, K. K., SENANI, R. Electronically-controlled current-mode second order sinusoidal oscillators using MO-OTAs and grounded capacitors. *Circuits and Systems*, 2011, vol. 2, no. 2, p. 65-73.
- [56] BHASKAR, D. R., SENANI, R. New CFOA-based single-element-controlled sinusoidal oscillators. *IEEE Transaction on Instrumentation and Measurement*, 2006, vol. 55, no. 6, p. 2014 to 2021.
- [57] SENANI, R., SINGH, V. K. Novel single-resistance-controlled-oscillator configuration using current feedback Amplifiers. *IEEE Transactions on Circuits and Systems - I: Fundamental Theory and Applications*, 1996, vol. 43, no. 8, p. 698-700.
- [58] SENANI, R., GUPTA, S. S. Synthesis of single-resistance-controlled oscillators using CFOAs: simple state-variable approach. *IEE Proceedings on Circuits Devices and Systems*, 1997, vol. 144, no. 2, p. 104-106.
- [59] GUPTA, S. S., SENANI, R. State variable synthesis of single resistance controlled grounded capacitor oscillators using only two CFOAs. *IEE Proceedings on Circuits, Devices and Systems*, 1998, vol. 145, no. 2, p. 135-138.
- [60] GUPTA, S. S., SENANI, R. State variable synthesis of single-resistance-controlled grounded capacitor oscillators using only two CFOAs: additional new realisations. *IEE Proceedings on Circuits Devices and Systems*, 1998, vol. 145, no. 6, p. 415-418.
- [61] PETRZELA, J., VYSKOCIL, P., PROKOPEC, J. Fundamental oscillators based on diamond transistors. In *Proceedings of 20th International Conference Radioelektronika 2010*. Brno (Czech Republic), 2010, p. 217-220.
- [62] *EL4083: Current-Mode Four-Quadrant Multiplier*, Intersil (Elantec) [Online]. 1995, last modified 2003 [Cited 2011-07-28]. Available at: <http://www.intersil.com/data/fn/fn7157.pdf>>
- [63] *LT1364: Dual and Quad 70 MHz, 1000 V/μs, Op Amps*, Linear Technology [Online]. 1994 [Cited 2011-07-28]. Available at URL: <<http://cds.linear.com/docs/Datasheet/13645fa.pdf>>
- [64] *EL2082: Current-Mode Multiplier*, Intersil (Elantec) [Online]. 1996, last modified 2003 [Cited 2011-07-28]. Available at URL: <<http://www.intersil.com/data/fn/fn7152.pdf>>
- [65] *AD8138: Low Distortion Differential ADC Driver*, Analog Devices [Online]. Last modified 1/2006 [Cited 2011-07-28]. Available at: <http://www.analog.com/static/imported-files/data_sheets/AD8138.pdf>
- [66] *VC4810: High Gain Adjust Range, Wideband, Variable Gain Amplifier*, Texas Instruments [Online]. 2003, last modified 12/2010 [Cited 2011-07-28]. Available at URL: <http://focus.ti.com/lit/ds/sbos275f/sbos275f.pdf>>

About Authors ...

Roman SOTNER was born in Znojmo, Czech Republic, in 1983. He received his M.Sc. and Ph.D. degrees from Brno University of Technology, Czech Republic, in 2008 and 2012, respectively. Currently, he is a technical worker at the Department of Radio Electronics, Faculty of Electrical Engineering and Communication, Brno University of Technology, Brno, Czech Republic. His interests are analog circuits (active filters, oscillators, audio, etc.), circuits in the current mode, circuits with direct electronic controlling possibilities especially and computer simulation.

Jan JERABEK was born in Bruntal, Czech Republic, in 1982. He received his Ph.D. degree in Electrical Engineering in 2011 from Brno University of Technology, Czech Republic. He received M.Sc. and B.Sc. degree from the same university in 2007 and in 2005, respectively. He is currently an assistant professor at the Department of

Telecommunications, Faculty of Electrical Engineering and Communication, Brno University of Technology. His research interests are focused on circuit applications of modern active elements such as current amplifiers and multiple output current followers. Dr. Jerabek is a member of IEEE.

Norbert HERENC SAR received his M.Sc. and Ph.D. degrees in Electronics & Communication and Teleinformatics from Brno University of Technology, Czech Republic, in 2006 and 2010, respectively. Currently, he is an Assistant Professor at the Department of Telecommunications, Faculty of Electrical Engineering and Communication, Brno University of Technology, Brno, Czech Republic. From September 2009 through February 2010 he was an Erasmus Exchange Student with the Department of Electrical and Electronic Engineering, Bogazici University, Istanbul, Turkey. His research interests include analog filters, current-mode circuits, tunable frequency filter design methods, and oscillators. He is an author or co-author of about 75 research articles published in international journals or conference proceedings. Dr. Herencsar is Senior Member of the IACSIT and Member of the IAENG and ACEEE.

Zdenek HRUBOS was born in Uherske Hradiste, Czech Republic, in 1984. He received his M.Sc. degree in 2009 from Brno University of Technology, Czech Republic. He is currently studying his Ph.D. study at the same university. His research interest is in computer analysis and synthesis of electronics circuits and nonlinear systems.

Tomas DOSTAL (*1943) received his Ph.D. degree in 1976 and DrSc. degree in 1989. He was with the University of Defense Brno (1976-1978 and 1980-1984), with the Military Technical College Baghdad (1978-1980), with the Brno University of Technology (1984-2008) and with the European Polytechnic Institute, Kunovice, Czech Republic (2008 - 2009). Since 2009 he has been with the College of Polytechnics, Jihlava as Professor of Electronics. His interests are in circuit theory, analog filters, switched capacitor networks and circuits in the current mode.

Kamil VRBA received his Ph.D. degree in Electrical Engineering in 1976, and the Prof. degree in 1997, both from the Technical University of Brno. Since 1990 he has been Head of the Department of Telecommunications, Faculty of Electrical Engineering and Computer Science, Brno University of Technology, Brno, Czech Republic. His research work is concentrated on problems concerned with accuracy of analog circuits and mutual conversion of analog and digital signals. In cooperation with AMI Semiconductor Czech, Ltd. (now ON Semiconductor Czech Republic, Ltd.) he has developed number of novel active function blocks for analog signal processing such as universal current conveyor (UCC), universal voltage conveyor (UVC), programmable current amplifier (PCA), digitally adjustable current amplifier (DACA), and others. He is an author or co-author of more than 700 research articles published in international journals or conference proceedings. Professor Vrba is a Member of IEEE and IEICE.

[2] SOTNER, R., JERABEK, J., HERENC SAR, N., HORNG, J-W., VRBA, K., DOSTAL, T. Simple Oscillator with Enlarged Tunability Range Based on ECCII and VGA Utilizing Commercially Available Analog Multiplier. *Measurement Science Review*, 2016, vol. 16, no. 2, p. 35-41. ISSN: 1335-8871.

Simple Oscillator with Enlarged Tunability Range Based on ECCII and VGA Utilizing Commercially Available Analog Multiplier

Roman Sotner¹, Jan Jerabek², Norbert Herencsar², Jiun-Wei Horng³, Kamil Vrba², Tomas Dostal^{1,4}

¹*Dept. of Radio Electronics, Faculty of Electrical Engineering and Communication, Brno University of Technology, Technicka 3082/12, 616 00, Brno, Czech Republic, sotner@feec.vutbr.cz*

²*Dept. of Telecommunications, Faculty of Electrical Engineering and Communication, Brno University of Technology, Technicka 3082/12, 616 00, Brno, Czech Republic*

³*Dept. of Electronic Engineering, Chung Yuan Christian University, 32023, Chung-Li, Taiwan*

⁴*Dept. of Technical Studies, College of Polytechnics Jihlava, Tolsteho 16, 586 01, Jihlava, Czech Republic*

This work presents an example of implementation of electronically controllable features to an originally unsuitable circuit structure of oscillator. Basic structure does not allow any electronic control and has mutually dependent condition of oscillation (CO) and frequency of oscillation (FO) if only values of passive elements are considered as the only way of control. Utilization of electronically controllable current conveyor of second generation (ECCII) brings control of CO independent of FO. Additional application of voltage amplifier with variable gain in both polarities (voltage-mode multiplier) to feedback loop allows also important enlargement of the range of the independent FO control. Moreover, our proposal was tested and confirmed experimentally with commercially available active elements ("Diamond transistor", current-mode multiplier, voltage-mode multiplier) in working range of tens of MHz.

Keywords: Current- and voltage-mode multipliers, oscillators, electronic control, mutual dependence of condition and frequency, diamond transistor, variable gain, voltage amplifier.

1. INTRODUCTION

Mutual dependence of condition of oscillation (CO) and frequency of oscillation (FO) is a problem of several conceptions of sinusoidal oscillators. This group of circuits has parameters (circuit element values) of FO included also in CO and vice versa. Typical examples can be found in [1]-[2], for example.

Another situation is when control of FO is provided by one parameter separated from others included in CO relation. Thus, control of FO seems to be really independent of CO. Unfortunately, parameter(s) required for CO control (startup of oscillations and amplitude stabilization during the tuning process) occur in the FO formula. Parameter that is unchangeable only seemingly may have impact on FO (it depends on specific solution and design, whether real frequency is influenced significantly, slightly or even insignificantly). It is significant especially if wideband tuning is required and, at least, stability of FO is affected. Typical examples can be found in [3]-[5].

On the other hand, simple solutions where CO is independently controllable are also available [6]. However, FO tuning has direct impact on CO fulfillment (parameter from FO is present in CO) and therefore the independent parameter that keeps CO fulfilled must be adjusted during the tuning process too. This is also unsuitable.

Some of the previous works discuss also specific solutions with theoretically independent CO and FO. CO of such solutions is theoretically always fulfilled if equality of working capacitors and other passive or/and active elements is ensured (for example [7]). Theoretical control of FO without impact on CO and vice versa is available only if exact matching (equality) of two parameters simultaneously used for FO tuning and CO fulfillment is ensured. In most cases, the same passive elements (parameters of active elements) are included in CO and also in FO term (for example [7]-[12]) and critical matching of two parameters is required for simultaneous fulfillment of CO and tuning of FO (typical example: CO : $g_{m1} = g_{m2}$; FO : $\sqrt{(g_{m1}g_{m2}/(C_1C_2))}$, see [8], [11], [12], for example).

Unfortunately, startup of oscillations requires slight inequality of both parameters in CO relation which can be theoretically preserved during the FO tuning. In addition, CO driving is required in real situation for amplitude stabilization during the tuning process ([13] and references cited therein) and additional independent parameter suitable for this operation is not available in this kind of solution. Thus, CO and FO are mutually dependent also in this case. This dependence is not so obvious but it is caused by problematic matching (and driving) of two suitable parameters serving for FO control and CO fulfillment simultaneously. It is a common problem of very simple solutions having low number of active elements. This drawback is typical also for some of the simple or complex third- or higher-order systems (selected solutions available for example in [14]-[17]).

Some of the above discussed circuits were designed in order to be very simple (minimal number of active and passive elements) and to provide linear control of FO ([10], [12] for example). However, lack of independently controllable parameter for CO control complicates their practical utilization. Very simple oscillator solutions (up to two simple active elements) usually offer only nonlinear control of FO (if CO and FO are really independent). Some types of the nonlinearly controllable oscillators have also minimal available FO [3]-[5] given by special relation in numerator of FO equation. Some realizations have even more unsuitable equation for FO, where FO control is quite limited even by two borders [4]. Important goal of this paper is to show that slight modification of these simple solutions could bring significant improvements.

Table 1. Comparison of recently published tunable oscillators.

Reference	Number of active/passive elements	Construction type/technology	FO range [MHz]	Amplitude change in tunable range [mV _{p-p}]	THD range [%]	Approximate power consumption [mW]	AGC type	Parameter for FO control	Extension of tunability range by special form of FO
[3]	3/4	discrete	0.6 – 2.2	N/A	0.4 – 0.9	250	internal nonlinearity	<i>B</i>	No
[4]	2/4	discrete	0.3 – 1.8	N/A	0.3 – 10	180	manual adjusting	<i>B</i>	No
[5]	2/3	CMOS	0.6 – 2.5	350 – 410	0.8	N/A	internal nonlinearity	<i>g_m</i>	No
[10]	1/2	CMOS	N/A	N/A	2.9	N/A	N/A	<i>R_X</i>	No
[11]	3/2	N/A	N/A	N/A	N/A	N/A	N/A	<i>g_m</i>	No
[12]	1/2	BJT	N/A	N/A	N/A	N/A	internal nonlinearity	<i>g_m</i>	No
[13]	2/5	CMOS/discrete	0.3 – 8.0	180 – 240	0.3 – 5 (0.3 – 0.5)*	450	inertial AGC	<i>B, A</i>	No
[14]	2-4/2-4	CMOS	up to 69.0	200 – 500	0.2 – 2.8	N/A	inertial AGC	<i>g_m</i>	No
[15]	3/3	CMOS	0.1 – 4.0	500 – 1 700 0 – 3 000	> 1	N/A	el. resistor	<i>g_m</i>	No
[16]	3/3	CMOS	0.03 – 0.09	N/A	up to 2.6	4	N/A	<i>g_m</i>	No
[17]	3/5	CMOS	4.0 – 9.0	N/A	0.5 – 1.8	N/A	N/A	<i>R</i>	No
[26]	1/4	CMOS	1.3 – 7.4	50 – 60 60 – 90	0.5 – 3.8	5.8 – 6.8	inertial AGC	<i>g_m/R_X</i>	No
[27]	2/2	discrete	0.5 – 1.8	600 – 700 700 – 750 950 – 1 150	0.5 – 1	N/A	inertial AGC	<i>g_m/R_X</i>	No
prop.	2/4	discrete	3.7 - 27.1	175 – 205	0.2 – 3.7 (0.2 – 1.5)*	300	inertial AGC	<i>A</i>	Yes

*in slightly reduced bandwidth

B – current gain controllable by DC voltage

A – voltage gain controllable by DC voltage

R_X – control of internal resistance of current input terminal by DC bias current

R – passive resistance value change

g_m – transconductance controllable by DC bias current

N/A – not available, not tested

Detailed qualitative comparison of previously reported related works is given in Table 1. It can be seen that only circuits in ref. [14] have better frequency features. However, in accordance with the results in [14], produced signals significantly change level during the tuning process and the structures with the best performances have more active devices (without considering AGC loop) than the solution presented in this paper. Higher power consumption of discrete active devices utilized in our circuit is the cost for utilization of commercially available devices based on BJT and technology target on great dynamical range and great linearity. It allows production of output signal level in hundreds of mV_{p-p} in comparison to many CMOS solutions (highly nonlinear and with limited output swing to several tens of mV or μ V in many cases) presented in literature. It is worth mentioning that none from the compared and other known solutions in literature utilizes additional tunability extension in nonlinearly tunable oscillators by both polarities of voltage gain available in simple voltage multiplier presented in the frame of the VGA structure used in this oscillator.

Presented example shows that some initially unsuitable solutions (with mutually dependent CO and FO given by passive elements in many cases) for electronically adjustable applications can be also modified to perform better. This modification consists only of additional feedback loop. Alternate polarity of gain in this loop brings extension of the range of FO control that was originally not possible and similarly simple circuits [3]-[5] have limit at the low corner of FO range (FO cannot be tuned from zero in ideal case).

This paper focuses on implementation of electronic control to a simple type of the second-order harmonic oscillator, where independent (or even electronic) control of CO and FO is not possible in initial state. However, implementation of controlled current and voltage gains helps to control CO and FO independently. It also directly prepares for amplitude stabilization by a quite simple amplitude automatic gain control circuit (AGC).

The paper is organized as follows: Reasons for this research and improvements in this area of simple oscillators and explanation of situation are given in the introductory section. Next chapter deals briefly with the principle of active elements used in our design. Proposal of the controllable oscillator is discussed in section 3. Real behavior and experiments are given in chapter 4 and finally, concluding remarks are in section 5.

2. INTRODUCTION TO THE PRINCIPLE OF USED ACTIVE ELEMENTS

Basic ideal principles of used active elements are explained in Fig.1. and the following text. The function of electronically controllable current conveyor of second generation (ECCII+) [18]-[20] (Fig.1.a) is described by quite common and simple equations (in ideal case): $V_Y = V_X$, $I_Y = 0$, $I_{Z+} = BI_X$. The current gain between X and Z ports (B) is adjustable by DC voltage (V_{SETB}) and voltage gain (transfer) from Y to X port is fixed (equal to 1). Variable

Gain Amplifier (VGA) in Fig.1.b) with gain (A) controllable by DC voltage V_{SETA} in both polarities was constructed by high-speed voltage-mode four-quadrant multiplier that contains also additional summing point. Detailed connection of multiplier (AD835 in our case) as amplifier with $\pm A$ is shown in Fig.1.c). Transfer function of the amplifier has the form:

$$\pm A = \pm V_{SETA} \left(\frac{R_{f1} + R_{f2}}{R_{f2}} \right), \quad (1)$$

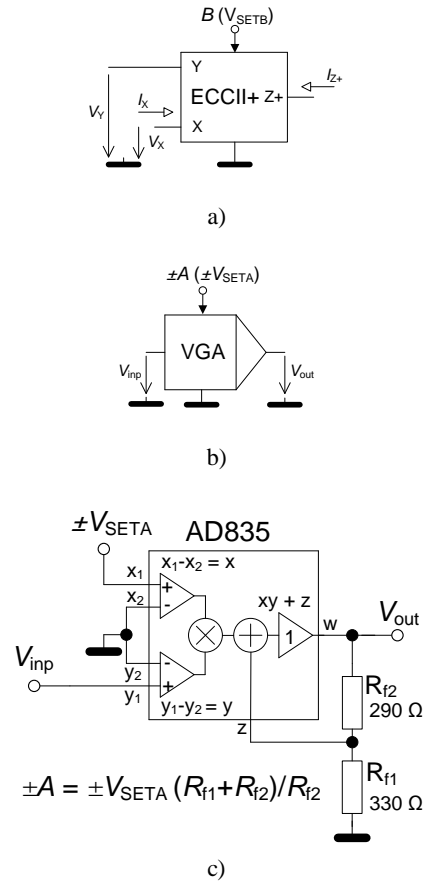


Fig.1. Principles of used active elements: a) ECCII+, b) variable gain amplifier, c) detailed application of multiplier as VGA.

3. OSCILLATOR PROPOSAL

Our goal is to not show a fully linearly controllable and multiphase type of oscillator. Instead we want to discuss useful application of the voltage mode multiplier in oscillator structure that is not normally suitable for electronic control. Structure shown in Fig.2. employs ECCII, two resistors and two grounded capacitors. It has no capability of electronic control of FO. When using classical positive current conveyor of second generation (CCII+) [21], [22], CO and FO are mutually dependent and the solution is not really suitable for practice. In our case, CO is adjustable by current gain B of the ECCII. In addition, control by passive elements is also not possible due to their mutual appearance in equations for FO and CO.

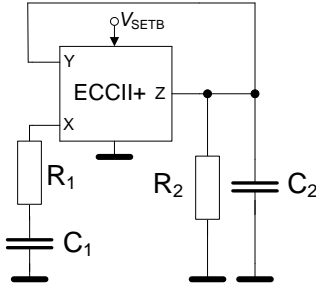


Fig.2. Simple single ECCII-based oscillator.

Characteristic equation of the circuit in Fig.2. has the following form:

$$s^2 + \frac{R_1 C_1 + R_2 C_2 - R_2 C_1 B}{R_1 R_2 C_1 C_2} s + \frac{1}{R_1 R_2 C_1 C_2} = 0. \quad (2)$$

Initial circuit in Fig.2. is a good starting point for our modification, which consists of insertion of an additional voltage gain A (one active device to the circuit, VGA connected as in Fig.1.c). Resulting circuit has independently adjustable FO and CO by electronically controllable parameters. The number of passive elements remains the same, only resistors are floating as is obvious from Fig.3.

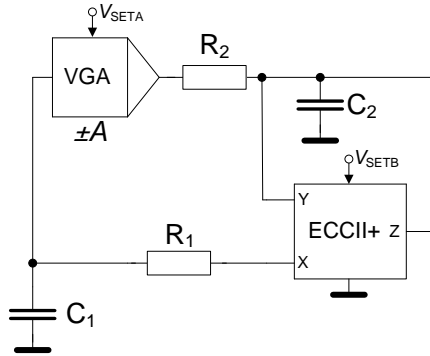


Fig.3. Proposed modification of circuit from Fig.2. to fully and independently controllable oscillator.

Characteristic equation is modified from (2) to:

$$s^2 + \frac{R_1 C_1 + R_2 C_2 - R_2 C_1 B}{R_1 R_2 C_1 C_2} s + \frac{1 \pm A}{R_1 R_2 C_1 C_2} = 0, \quad (3)$$

where CO and FO are as follows:

$$B \geq \frac{R_1 C_1 + R_2 C_2}{R_2 C_1}, \quad (4)$$

$$\omega_0 = \sqrt{\frac{1 \pm A}{R_1 R_2 C_1 C_2}} = \sqrt{\frac{1 \pm V_{SETA} \left(\frac{R_{f1} + R_{f2}}{R_{f2}} \right)}{R_1 R_2 C_1 C_2}}. \quad (5)$$

Gain polarity of the voltage amplifier can be considered as positive only ($+A$). In this case, FO has lower limit given by 1 (for $A = 0$) in numerator, as we can see from equation (5). Therefore, FO cannot be equal to 0 in ideal case. This fact also reduces frequency range of FO control. Due to root square, FO is not controllable linearly. But this is an obvious problem in such a simple circuit. Utilization of standard VGA, for example VCA810 [23], LMH6505 [24], leads to reduced FO control range. Fortunately, high-speed analog multiplier (AD835 [25]) applied as VGA in our case allows simultaneous change of gain polarity ($\pm A$), which seems to be very beneficial in this application. It offers enlargement of FO control (below 1 in numerator of (5)) with limit of $A > -1$.

Relation between nodal voltages on both capacitors is:

$$\frac{V_{C2}}{V_{C1}} = \frac{R_1 A - R_2 B}{R_1 - R_2 B + s C_2 R_1 R_2}. \quad (6)$$

It indicates that FO control by A has direct impact on one generated amplitude (V_{C2}) and compensation changes of gain in the structure for CO control (amplitude stabilization) by B also cause impact on phase shift. Therefore, similar simple oscillators are not suitable for tunable multiphase/quadrature signal generation, with some exceptions [26], [27]. Nevertheless, this solution is sufficient for single-output oscillator type (output voltage on C_1) with mutually independent CO a FO.

4. REAL BEHAVIOR AND EXPERIMENTAL VERIFICATION

Real solution of the oscillator from Fig.3. can be formed by commercially available devices as shown in Fig.4. We have to use ECCII- type (EL2082 [28]) and current inverter formed by "Diamond circuit", well-known as "Diamond transistor" (DT) OPA860 [29], because ECCII+ is not directly available. Voltage buffer (subpart of OPA860) connected to the node with C_1 ensures low-impedance voltage output for measurement purposes. AGC is also implemented in this real solution shown in Fig.4.

Our aim is to design an oscillator operating in range of tens of MHz (used active elements allow it). Thus, working capacitors and resistors with very low values were selected ($C_1 = C_2 = C = 33$ pF, $R_1 = 120 + 95 \Omega$ and $R_2 = 220 \Omega$), where R_1 includes internal resistance of terminal X of ECCII (95 Ω) [28]. High-frequency design requires the best knowledge of all parasitic influences. Non-ideal model of the oscillator with important parasitic features is shown in Fig.5. The most important are parasitic capacitances in nodes, because they have values comparable with working capacitors. Therefore, their impact is substantial and they cause a very large difference between ideal and real FO. They are formed by capacitances of terminals of active elements [25], [28], [29] and also by PCB capacitances and parasitic feedback crosstalks. Thus, we expect them to be ~20 pF. Estimated values are noted in Fig.5. (purple color).

FO in influenced (real) case can be calculated as:

$$\omega_0' = \sqrt{\frac{AR_{p1}R_{p2} + R_{p1}R_{p2} + R_1R_2 + R_{p1}R_2 - BR_{p2}R_2}{R_1R_2R_{p1}R_{p2}C_1C_2}}, \quad (7)$$

and real CO has the form:

$$B \geq \frac{R_{p1}R_{p2}(R_1C_1' + R_2C_2') + R_1R_2(R_{p1}C_1' + R_{p2}C_2')}{R_2R_{p1}R_{p2}C_1'} \quad (8)$$

CO actually influences FO in real case, see (7). Fortunately, impact of negative term $-BR_{p2}R_2$ is significantly lower than term $AR_{p1}R_{p2}$. Therefore, its influence on FO is significant only for very low A or for large change of B while A is constant (not allowed by AGC).

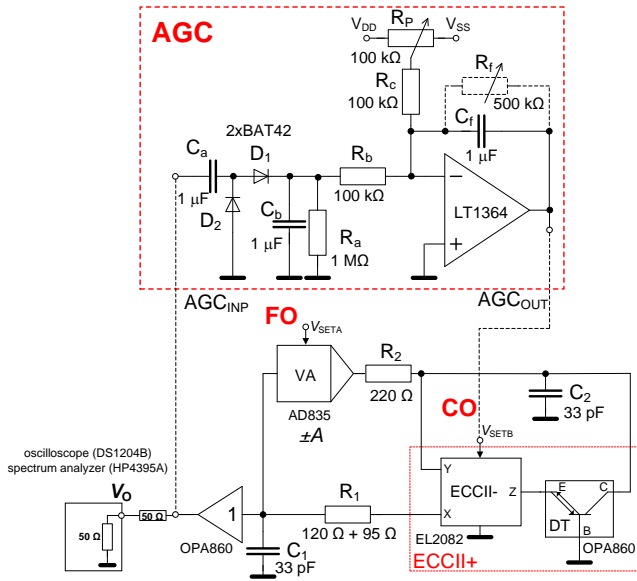


Fig. 4. Real circuit for experimental tests.

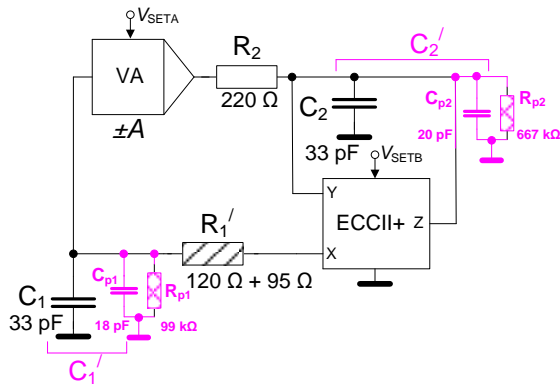
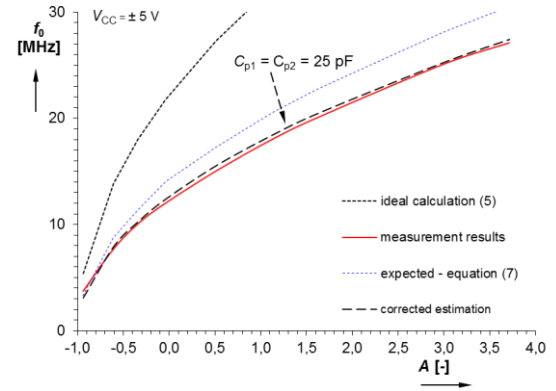


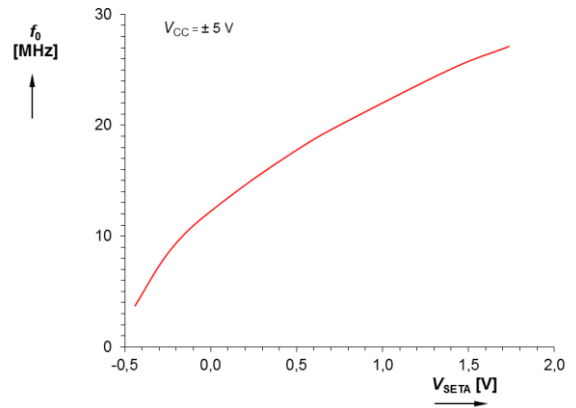
Fig. 5. Model for estimation of parasitic influences in the structure of oscillator.

Ideal range of tunability (for discussed ideal values of R , C) and A in range from -0.94 to 3.71 (V_{SETA} from -0.44 to 1.74 V) was calculated from 5.4 to 48.2 MHz. Results are shown in Fig. 6. Estimation of FO range, based on analysis of model in Fig. 5., was provided from a full representation of real FO (7). It provides range of FO from 3.3 to 30.6 MHz. FO range from 3.7 to 27.1 MHz was obtained from experimental measurements (setup was shown in Fig. 4.). Overlying of estimated and measured trace in Fig. 6.

occurs for $C_{p1} = C_{p2} = 25$ pF in (7). If gain A was available only in positive polarity, tunability range would be restricted only to 12 – 27 MHz. Note: We used RIGOL DS1204B oscilloscope and HP4395A spectrum analyzer. Condition of oscillation is ideally fulfilled for $B = 2$ (in case of equal C and R as stated above). However, as we can see in Fig. 7., V_{SETB} (practically equal to gain B , see [28]) indicates that the gain changes during the tuning process as was explained in [13].



a)



b)

Fig. 6. Dependence of FO on: a) voltage gain A – comparison, b) DC control voltage V_{SETA} .

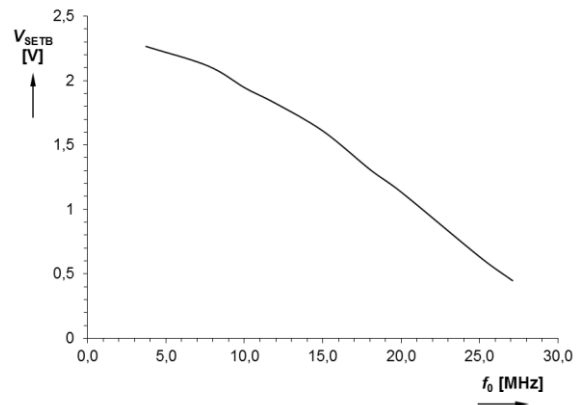


Fig. 7. Dependence of $V_{SETB} \cong B$ (actually CO) on FO.

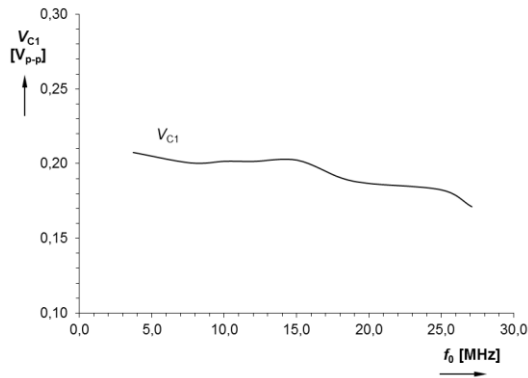


Fig. 8. Dependence of output voltage on FO.

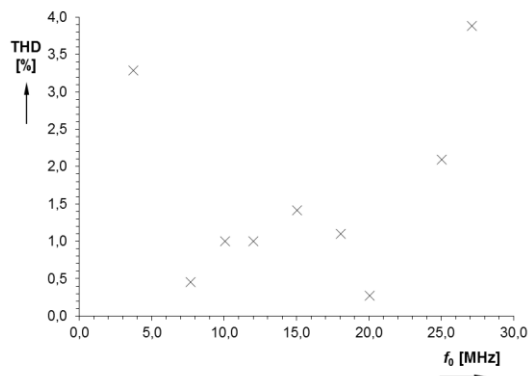
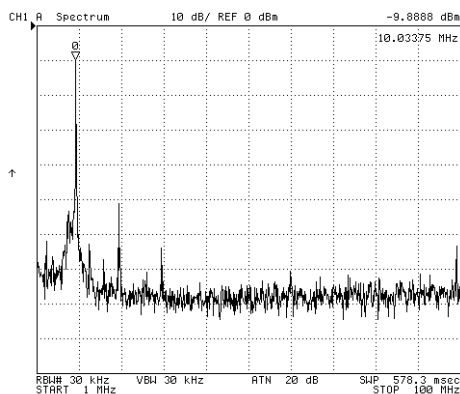
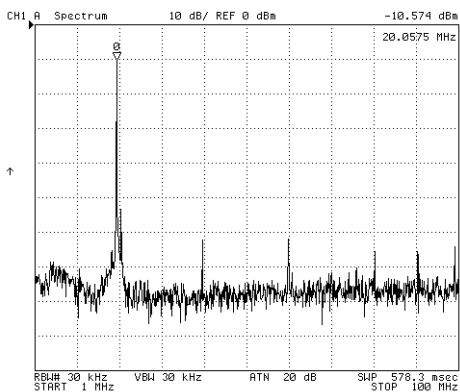


Fig. 9. Dependence of THD on FO.



a)



b)

Fig. 10. Frequency spectrum for two selected frequencies: a) 10 MHz, b) 20 MHz.

Fig. 8. shows the dependence of output voltage (V_{C1}) on FO and Fig. 9. indicates total harmonic distortion (THD), both in the observed range of FO. Higher THD (above 1 %) is given by low and limited dynamical range of AD835 [25] and nonlinearity (DC transfer characteristic) of active device itself (second and third harmonic components at the output of AD835 are suppressed by 40 dB only for very high frequencies).

Exemplary spectrum analysis results are shown in Fig. 10. for two selected frequencies of oscillation: 10 MHz ($V_{SETA} = -0.16$ V, $A = -0.34$) and 20 MHz ($V_{SETA} = 1.74$ V, $A = 3.71$).

5. CONCLUSION

Proposed oscillator offers interesting features for high-frequency design despite the lack of multiphase outputs. However, this feature is not commonly available in case of very simple circuits utilizing only basic elements (with respect to many still hypothetical structures [30]). Output level slightly fluctuates but change of output peak-to-peak voltage in observed range of FO (3.7–27.1 MHz) is maximally 30 mV. THD varies between 0.2–3.7 %. Higher values are given especially by internal nonlinearity of AD835 (indicated in datasheet [25]), inappropriate time constant of AGC that is insufficient for very low and high FO (corners of tunability range) and achievement of limits of gain slope B (EL2082), see Fig. 7. THD achieving maximally 1.5 % is allowed in narrower range (7–20 MHz) of FO change. Both polarities of DC control voltage V_{SETA} (utilization of voltage multiplier) allow important extension of FO control in comparison to single polarity control of gain A (only FO range from 12 to 27.1 MHz allowed for single/positive polarity of A). Power consumption is quite high in discrete solution (hundreds of mW).

Parasitic analysis of real influences in the circuit is highly required for working capacitors below 100 pF. Results show that estimation is quite problematic and minimal deviation of expected and real values (combined with fabrication tolerances of active and passive elements) can be very large. In conclusion we can see that commercially available devices are really able to overcome the border of 10 MHz. Therefore, we can utilize them sufficiently for behavioral modeling of complex devices and systems [31], [32] operating in these bands. High-frequency features predetermine the proposed circuit, for example, as an easily tunable signal source in short wave and medium wave transmitters with amplitude or frequency modulation or digital amplitude keying.

ACKNOWLEDGMENT

Research described in the paper was supported by Czech Science Foundation project under No. 14-24186P.

REFERENCES

- [1] Soliman, A.M. (1998). Novel oscillators using current and voltage followers. *Journal of the Franklin Institute*, 335 (6), 997-1007.

- [2] Keskin, A.U., Aydin, C., Hancioglu, E., Acar, C. (2006). Quadrature oscillator using current differencing buffered amplifiers (CDBA). *Frequenz*, 60 (6), 21-23.
- [3] Sotner, R., Sevcik, B., Slezak, J., Petrzela, J., Brancik, L. (2011). Sinusoidal oscillator based on adjustable current amplifier and diamond transistors with buffers. *Przeglad Elektrotechniczny*, 87 (1), 266-270.
- [4] Sotner, R., Hrubos, Z., Slezak, J., Dostal, T. (2010). Simply adjustable sinusoidal oscillator based on negative three-port current conveyors. *Radioengineering*, 19 (3), 446-453.
- [5] Sotner, R., Jerabek, J., Petrzela, J., Dostal, T., Vrba, K. (2009). Electronically tunable simple oscillator based on single-output and multiple output transconductor. *IEICE Electronics Express*, 6 (20), 1476-1482.
- [6] Herencsar, N., Minaei, S., Koton, J., Yuce, E., Vrba, K. (2013). New resistorless and electronically tunable realization of dual-output VM all-pass filter using VDIBA. *Analog Integrated Circuits and Signal Processing*, 74 (1), 141-154.
- [7] Jaikla, W., Siripruchyanun, M., Bajer, J., Biolek, D. (2008). A simple current-mode quadrature oscillator using single CDTA. *Radioengineering*, 17 (4), 33-40.
- [8] Pandey, N., Paul, S.K. (2011). Single CDTA-based current mode all-pass filter and its applications. *Journal of Electrical and Computer Engineering*, 2011, art. ID 897631.
- [9] Songkla, S.N., Jaikla, W. (2012). Realization of electronically tunable current-mode first-order allpass filter and its application. *International Journal of Electronics and Electrical Engineering*, 2012 (6), 40-43.
- [10] Keawon, R., Jaikla, W. (2011) A resistor-less current-mode quadrature sinusoidal oscillator employing single CCCDTA and grounded capacitors. *Przeglad Elektrotechniczny*, 87 (8), 138-141.
- [11] Senani, R. (1989). New electronically tunable OTA-C sinusoidal oscillator. *Electronics Letters*, 25 (4), 286-287.
- [12] Li, Y. (2010). Electronically tunable current-mode quadrature oscillator using single MCDTA. *Radioengineering*, 19 (4), 667-671.
- [13] Sotner, R., Hrubos, Z., Herencsar, N., Jerabek, J., Dostal, T., Vrba, K. (2014). Precise electronically adjustable oscillator suitable for quadrature signal generation employing active elements with current and voltage gain control. *Circuits Systems and Signal Processing*, 33 (1), 1-35.
- [14] Linares-Barranco, B., Rodriguez-Vazquez, A., Sanchez-Sinencio, E., Huertas, J.L. (1991). CMOS OTA-C high-frequency sinusoidal oscillators. *IEEE Journal of Solid-State Circuits*, 26 (2), 160-165.
- [15] Prommee, P., Dejhan, K. (2002). An integrable electronic-controlled quadrature sinusoidal oscillator using CMOS operational transconductance amplifier. *International Journal of Electronics*, 89 (5), 365-379.
- [16] Horng, J-W. (2009). Current-mode third-order quadrature oscillator using CDTAs. *Active and Passive Electronic Components*, 2009, art. ID 789171.
- [17] Chatuverdi, B., Maheshwari, S. (2013). Third-order quadrature oscillators circuit with current and voltage outputs. *ISRN Electronics*, 2013, art. ID 385062.
- [18] Surakamponorn, W., Thitimajshima, W. (1988). Integrable electronically tunable current conveyors. *IEE Proceedings-G*, 135 (2), 71-77.
- [19] Fabre, A., Mimeche, N. (1994). Class A/AB second-generation current conveyor with controlled current gain. *Electronics Letters*, 30 (16), 1267-1268.
- [20] Minaei, S., Sayin, O.K., Kuntman, H. (2006). A new CMOS electronically tunable current conveyor and its application to current-mode filters. *IEEE Transaction on Circuits and Systems - I*, 53 (7), 1448-1457.
- [21] Sedra, A., Smith, K.C. (1970). A second generation current conveyor and its applications. *IEEE Transaction on Circuit Theory*, CT-17 (2), 132-134.
- [22] Svoboda, J.A., McGory, L., Webb, S. (1991). Applications of a commercially available current conveyor. *International Journal of Electronics*, 70 (1), 159-164.
- [23] Texas Instruments. *VCA810: High gain adjust range, wideband and variable gain amplifier*. <http://www.ti.com/lit/ds/symlink/vca810.pdf>.
- [24] Texas Instruments. *LMH6505: Wideband, low power, linear-in-dB, variable gain amplifier*. <http://www.ti.com/lit/ds/symlink/lmh6505.pdf>.
- [25] Analog Devices. *AD835: 250 MHz, voltage output 4-quadrant multiplier*. http://www.analog.com/static/imported-files/data_sheets/AD835.pdf.
- [26] Sotner, R., Jerabek, J., Petrzela, J., Herencsar, N., Prokop, R., Vrba, K. (2014). Second-order simple multiphase oscillator using Z-copy controlled-gain voltage differencing current conveyor. *Elektronika ir Elektrotechnika*, 20 (9), 13-18.
- [27] Sotner, R., Jerabek, J., Herencsar, N., Horng, J-W., Vrba, K. (2015). Electronically linearly voltage controlled second-order harmonic oscillators with multiples of pi/4 phase shifts. In *38th International Conference on Telecommunications and Signal Processing (TSP)*, 9-11 July 2015. IEEE, 708-712.
- [28] Intersil. *EL2082: Current-mode multiplier*. <http://www.intersil.com/data/fn/fn7152.pdf>.
- [29] Texas Instruments. *OPA860: Wide-bandwidth, operational transconductance amplifier (OTA) and buffer*. <http://www.ti.com/lit/ds/symlink/opa860.pdf>.
- [30] Biolek, D., Senani, R., Biolkova, V., Kolka, Z. (2008). Active elements for analog signal processing: Classification, review, and new proposal. *Radioengineering*, 17 (4), 15-32.
- [31] Sotner, R., Kartci, A., Jerabek, J., Herencsar, N., Dostal, T., Vrba, K. (2012). An additional approach to model current followers and amplifiers with electronically controllable parameters from commercially available ICs. *Measurement Science Review*, 12 (6), 255-265.
- [32] Odon, A. (2010). Modelling and simulation of the pyroelectric detector using MATLAB/Simulink. *Measurement Science Review*, 10 (6), 195-199.

Received September 3, 2015.

Accepted March 22, 2016.

[3] SOTNER, R., JERABEK, J., PROKOP, R., KLEDROWETZ, V. Simple CMOS voltage differencing current conveyor-based electronically tuneable quadrature oscillator. *Electronics Letters*, 2016, vol. 52, no. 12, p. 1016-1018. ISSN: 0013-5194.

Simple CMOS voltage differencing current conveyor-based electronically tunable quadrature oscillator

R. Sotner[✉], J. Jerabek, R. Prokop and V. Kledrowetz

A brief example of application of recently introduced concept of electronically controllable CMOS voltage differencing current conveyor of second generation in electronically tunable second-order oscillator is shown. On-chip experimental results confirm theory and design intentions.

Introduction: Recent findings in approach to electronic control of circuit's features consist of many interesting single and multiple-parameters concepts, utilised in useful active elements, have been reported in recent years [1, 2]. However, majority of them is still hypothetical (basic simulations available) only [3]. Only several of these concepts have been really fabricated and tested experimentally. A typical example is current differencing transconductance amplifier (CDTA) [3] experimentally applied in [4, 5] for instance. Unfortunately, its key internal parameter (transconductance) has fixed values [4]. Therefore, any control in frame of their application supposes only change of value of external passive elements or their electronically adjustable replacements. Many hypothetical active elements, allowing electronic control of more than one internal parameter (transconductance, intrinsic resistance, voltage, current gain etc.) have been theoretically prepared and can be controlled independently and simultaneously. The interesting examples employing current conveyor core are shown in [1].

Our contribution presents oscillator based on the (to the best of author's knowledge) first really fabricated (in CMOS process) so-called voltage differencing current conveyor of second generation (VDCC) that offers independent electronic control of transconductance (g_m) and also resistance of current input terminal (R_X). Only several solutions of oscillator based on single active device (VDCC and CDTA as the examples) have been introduced in recent literature [2, 4–7]. However, these simple circuit topologies (generally [2]) suffer from several typical drawbacks: (a) floating passive elements [4], (b) fixed (not externally controllable) values of internal on-chip parameters [4, 5], (c) frequencies of oscillations (FOs) and conditions of oscillations (COs) controllable only by values of external passive elements while electronically controllable on-chip parameter is available but topology of the circuit does not allow using it [6], (d) many additional auxiliary terminals and features leading to complexity not necessary for simple applications [7], (e) reduced output level of oscillations [only tens of millivolts (mV)] due to limited dynamical range and linearity of active element [7]. Therefore, a presented oscillator improves some features of the recently reported solutions including simple voltage control of an FO, simple implementation of amplitude stabilisation, compact solution and larger output level that are not available simultaneously in the recent results focused on implementation of this device.

Voltage differencing current conveyor: The device was first defined as hypothetical by Biolek *et al.* [3]. We used I2T100 CMOS (of ON Semiconductor) 0.7 μm process for design and fabrication of the VDCC prototype. Symbol, explanation of basic small-signal behaviour, implementation using operational transconductance amplifier [3] and current controlled current conveyor of second generation (CCCII) [1, 3] and microphotograph of the VDCC layout are shown in Fig. 1. In comparison with standard VDCC definition there are several important modifications. The transconductance (g_m) has dual polarity character (easily settable by DC control voltage). Transfer relation between input (differential) voltages to auxiliary current is: $(V_p - V_n) \cdot (\pm g_m) = \pm I_{z_TA}$. CCCII part has two outputs with both polarities and available external control of bias current in order to adjust resistance (R_X) of current input terminal (X). This gives relation: $V_X = V_{z_TA} + R_X I_X$. Standard transfer function of CCCII is: $I_{zp} = I_X$ and $I_{zn} = -I_X$. The rest of the features are clear from Fig. 1. Our VDCC device was designed with attention to DC accuracy, improved linearity and dynamics, disabling to obtain very high gain bandwidth product (GBW). Frequency features of fabricated VDCC (roll-off of frequency responses) predetermine application field to hundreds of kilohertz (kHz) (GBW of the g_m is around 2 MHz).

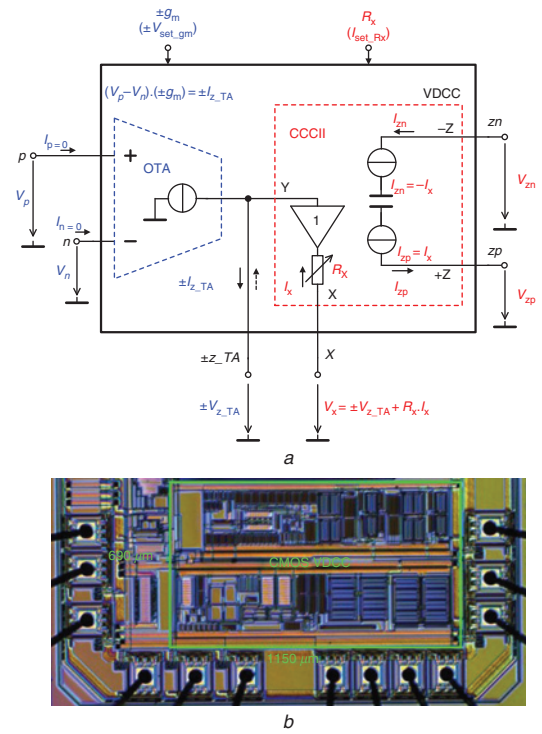


Fig. 1 VDCC block structure, explanation and on-chip implementation
a Symbol and behavioural explanation (internal subparts)
b Microphotograph of fabricated VDCC prototype (0.79 mm²)

Application of VDCC in quadrature oscillator: Simple circuitry of the oscillator is shown in Fig. 2 including automatic gain control circuit (AGC) for amplitude stabilisation. Characteristic equation has form

$$s^2 + \frac{R_X - R'}{C_2 R_X R'} s + \frac{g_m}{C_1 C_2 R_X} = 0, \quad (1)$$

where CO has form $R_X \leq R'$ and the FO is

$$\omega_0 = \sqrt{\frac{g_m}{C_1 C_2 R_X}}. \quad (2)$$

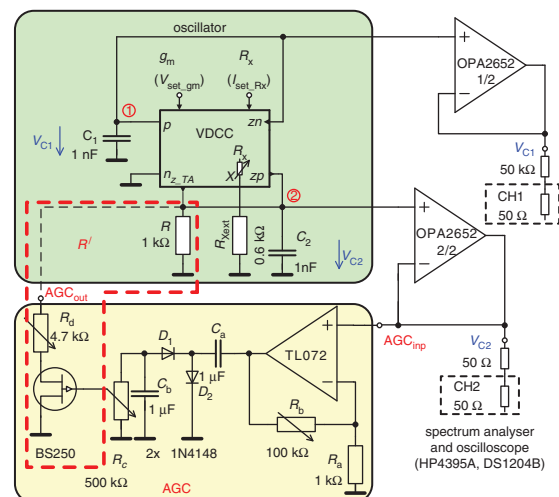


Fig. 2 Experimental setup of oscillator structure with external AGC

Thus, the FO can be controlled independently on CO. Parameter R' has specific purpose (is suitable for CO control). It is created by parallel combination of R and R_d in series to R_{DS} of used FET [$R' = R \parallel (R_d + R_{DS})$] in order to ensure simple amplitude stabilisation. Orthogonally generated amplitudes across V_{C1} and V_{C2} have the following relation: $V_{C2}/V_{C1} = g_m/sC_2$. The oscillator generates quadrature (orthogonal) waveforms with equal amplitudes when $C_1 = C_2 = C$ and $R_X = 1/g_m$.

Experimental results: The presented circuit in Fig. 2 was experimentally tested with the parameters indicated in Fig. 2 in detail ($C_1 = C_2 = C = 1$ nF, $R = 1$ k Ω , $R_{Xext} = 0.6$ k Ω). The DC bias current $I_{set,Rx}$ was set to 160 μ A that yields internal $R_X \cong 500$ Ω and it creates $R'_X \cong R_X + R_{Xext} \cong 1.1$ k Ω . Transient responses of output waveforms are shown in Fig. 3 together with spectral analysis of each output wave (V_{C1} , V_{C2}) for setting: $g_m = 1.07$ mS ($V_{set-gm} = 0.54$ V) and ideal value of $f_0 = 157$ kHz. Measured frequency was 150 kHz in this particular case. Total harmonic distortion (THD) of produced signals is only 0.8%.

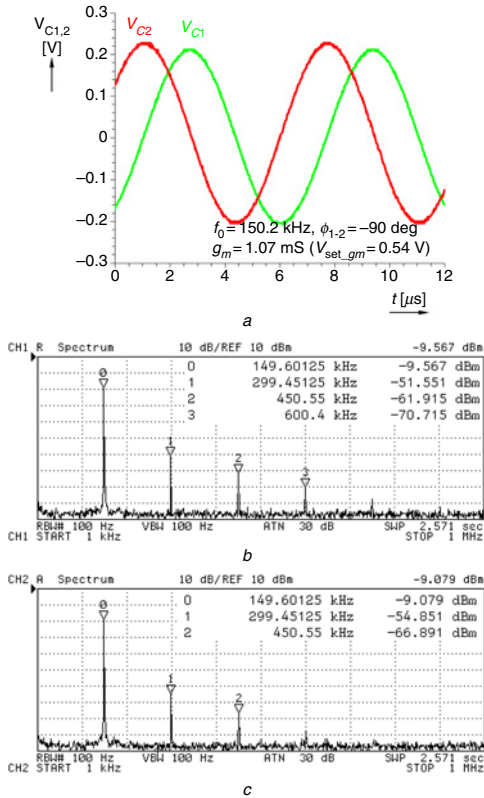


Fig. 3 Measured transient characteristics and their spectral analysis

- a Generated transient responses
- b Spectrum of V_{C1}
- c Spectrum of V_{C2}

Tunability range of the oscillator was tested from 29 to 230 kHz by change of g_m from 14 μ S to 2.8 mS (7 mV $\leq V_{set-gm} \leq 1.4$ V; $g_m \cong 2V_{set-gm}$). Comparison of ideal and measured dependence of the FO on g_m is shown in Fig. 4 as well as dependence of phase shift (quadrature) error between produced waveforms on g_m . Power consumption of the oscillator without AGC reaches 45 mW maximally at supply voltage ± 2.5 V.

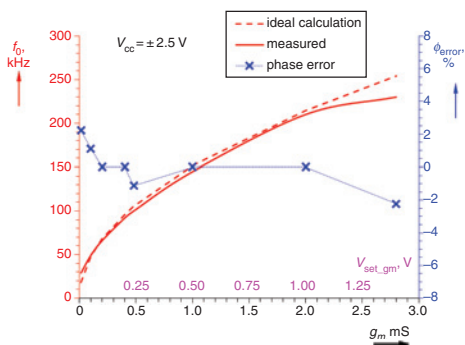


Fig. 4 Measured dependences of f_0 and phase error while adjusting g_m

Conclusion: This Letter presented simple quadrature oscillator application of the recently introduced concept of CMOS VDCC device. The benefits of presented solution are: (a) voltage controllable on-chip transconductance allowing simple tuning of the oscillator, (b) improved

output levels (with respect to the results in [7]), (c) only one on-chip active device required, (d) simple implementation of elementary and low-cost external AGC (oscillator can work without AGC but is always required for low THD), (e) all grounded passive external components, (f) electronic controllability of R_X offers simple disabling/enabling of the output waveforms generation without overshoots and ripple in standard case when oscillator is disabled/activated by disconnection/connection of supply voltage. Functionality of the oscillator was confirmed experimentally with VDCC chip.

Acknowledgment: This work was supported by the Czech Scientific Foundation project no. 14-24186P.

© The Institution of Engineering and Technology 2016

Submitted: 24 March 2016 E-first: 13 May 2016

doi: 10.1049/el.2016.0935

One or more of the Figures in this Letter are available in colour online.

R. Sotner, J. Jerabek, R. Prokop and V. Kledrowetz (*Faculty of Electrical Engineering and Communication, Brno University of Technology, Brno, Czech Republic*)

✉ E-mail: sotner@feec.vutbr.cz

References

- 1 Senani, R., Bhaskar, D.R., and Singh, A.K.: 'Current conveyors: variants, applications and hardware implementations' (Springer, Switzerland, 2015), doi: 10.1007/978-3-319-08684-2
- 2 Senani, R., Bhaskar, D.R., and Singh, A.K.: 'Sinusoidal oscillators and waveform generators using modern electronic circuit building blocks' (Springer, Switzerland, 2016), doi: 10.1007/978-3-319-23712-1
- 3 Biolek, D., Senani, R., Biolkova, V., and Kolka, Z.: 'Active elements for analog signal processing: classification, review, and new proposals', *Radioengineering*, 2008, **17**, (4), pp. 15–32
- 4 Jaikla, W., Siripruchyanun, M., Bajer, J., and Biolek, D.: 'A simple current-mode quadrature oscillator using single CDTA', *Radioengineering*, 2008, **17**, (4), pp. 33–40
- 5 Biolek, D., and Biolkova, V.: 'Allpass filter employing one grounded capacitor and one active element', *Electron. Lett.*, 2009, **45**, (16), pp. 807–808, doi: 10.1049/el.2009.0575
- 6 Prasad, D., Bhaskar, D.R., and Srivastava, M.: 'New single VDCC-based explicit current-mode SRCO employing all grounded passive components', *Electronics*, 2014, **18**, (2), pp. 81–88
- 7 Sotner, R., Jerabek, J., Petrzela, J., Herencsar, N., Prokop, R., and Vrba, K.: 'Second-order simple multiphase oscillator using z-copy controlled-gain voltage differencing current conveyor', *Elektron. Elektrotech.*, 2014, **20**, (9), pp. 13–18, doi: 10.5755/j01.eee.20.9.8709

[4] SOTNER, R., JERABEK, J., JAIKLA, W., HERENC SAR, N., VRBA, K., DOSTAL, T. Novel Oscillator Based on Voltage and Current- Gain Adjusting Used for Control of Oscillation Frequency and Oscillation Condition. *Elektronika Ir Elektrotechnika*, 2013, vol. 19, no. 6, p. 75-80. ISSN: 1392-1215.

Novel Oscillator Based on Voltage and Current-Gain Adjusting Used for Control of Oscillation Frequency and Oscillation Condition

R. Sotner¹, J. Jerabek², W. Jaikla³, N. Herencsar², K. Vrba², T. Dostal^{1,4}

¹*Department of Radio Electronics, Faculty of Electrical Engineering and Communication, Brno University of Technology, Technicka 12, Brno, 616 00, Czech Republic*

²*Department of Telecommunications, Faculty of Electrical Engineering and Communication, Brno University of Technology, Technicka 12, Brno, 616 00, Czech Republic*

³*Department of Engineering Education, Faculty of Industrial Education, King Mongkut's Institute of Technology Ladkrabag, Ladkrabag, Bangkok 105 20, Thailand*

⁴*Department of Electrical Engineering and Computer Science, College of Polytechnics Jihlava, Tolsteho 16, Jihlava 586 01, Czech Republic*

sotner@feec.vutbr.cz

Abstract—The paper deals with novel controllable oscillator where two types of electronic control are used. Proposed second-order circuit contains current follower, adjustable current amplifier, adjustable voltage amplifier, two resistors and two grounded capacitors. Oscillation frequency is tuned by voltage gain of used voltage amplifier that is represented by high-frequency voltage-mode multiplier. Oscillation condition is automatically regulated by current gain of the adjustable current amplifier which is based on current-mode multiplier. Experimental results confirmed workability of the circuit.

Index Terms—Electronic control, oscillator, adjustable current amplifier, current follower/inverter, adjustable voltage amplifier.

I. INTRODUCTION

Many active elements which are suitable for electronic control could be found in open literature [1]. Several ways how to control parameters of applications have been described [2]–[9]. Surakamponton et al. [2] and Fabre et al. [3] introduced active elements with possibility of current gain control. This active element is referred to as electronically controllable current conveyor of second generation (ECCII) and it allows adjusting of current transfer between current input and current output of the current conveyor [1], [4], [5]. Another way of control is change of transconductance [1], [6] by bias current. Geiger

et al. [6] described several basic applications of transconductors (OTAs) and formulated background of knowledge in this topic. Fabre et al. [7] presented active element with different possibility of control. The biasing current in internal structure of the current conveyor was used for control of intrinsic resistance of current input. Minaei et al. [8] proposed ECCII with combination of two methods of control in one device (intrinsic resistance and current gain). Marcellis et al. [9] implemented control of the current and voltage gains. Digital potentiometers are popular solutions for control of applications with standard voltage opamps at low frequencies (hundreds of kHz maximally) because their frequency features are not satisfactory in this particular case. Methods how to control frequency of oscillation (FO) and condition of oscillation (CO), that were sketched out, are discussed in more detail in the following text. All discussed ways of control suppose direct electronic adjusting in frame of parameter of active element. Other ways which use passive elements (resistors in many cases) and their replacements (FETs, digital potentiometers, ...) belong to group of indirect methods.

The first group of oscillator solutions employs controllable transconductances (g_m). In the past, only simple transconductors (voltage controlled current sources) with differential input and single output were used. Rodriguez-Vazquez et al. [10], Linarez-Barranco et al. [11], [12], Senani [13], Abuelmaatti [14] and many others presented simple and flexible solutions using at least two transconductors. Over the years, transistor conceptions have been improved and also novel modified types were developed. Biolek [15], [16] introduced so-called current differencing transconductance amplifier (CDTA), where current differencing unit at the input of transistor is used. Lahiri [17] proposed controllable oscillator with two CDTAs and two grounded capacitors or oscillator employing only one active element [18], [19]. Three CDTAs

Manuscript received January 27, 2013; accepted April 9, 2013.

Research described in the paper was supported by Czech Science Foundation projects No. 102/11/P489, 102/09/1681 by internal grant FEKT-S-11-15 and project Electronic-biomedical co-operation ELBIC M00176. Dr. Herencsar was supported by the project CZ.1.07/2.3.00/30.0039 of Brno University of Technology. The support of the project CZ.1.07/2.3.00/20.0007 WICOMT, financed from the operational program Education for competitiveness, is gratefully acknowledged. The described research was performed in laboratories supported by the SIX project; the registration number CZ.1.05/2.1.00/03.0072, the operational program Research and Development for Innovation.

were used by Tangsrirat et al. in [20]. Solutions of third order oscillators were also investigated. Horng [21], [22] built oscillator with three grounded capacitors. Prasad et al. [23] utilized novel approach in oscillator with one multiple-output current controlled current differencing transconductance amplifier (MO-CCCDTA).

TABLE I. COMPARISON OF IMPORTANT PREVIOUSLY REPORTED CONTROLLABLE OSCILLATORS

Work	Active element	No. of active/passive elements	Simple equations for FO / CO	AGC proposed	FO range	THD	Type of FO / CO control	DC voltage control of FO
[11]	OTA	4 / 3	YES / YES	YES	3-10.3 MHz	0.2 %	g_m / g_m	NO (I_b)
[12]	OTA	2-4 / 2-4	NO / NO	YES	12-56 MHz	2.5 %	g_m / g_m	NO (I_b)
[13]	OTA	3 / 2	YES / YES	N/A	N/A	N/A	g_m / g_m	NO (I_b)
[14]	OTA	2 / 3	YES / YES	N/A	N/A (300 kHz)*	N/A	g_m / R	NO (I_b)
[16]	CDTA	2 / 6	YES / YES	N/A	N/A (1 MHz)*	N/A	$R / R, g_m$	NO
[17]	CDTA	2 / 3	YES / YES	N/A	N/A (10 MHz)*	N/A	$g_m / R, g_m$	NO (I_b)
[18]	CCTA	1 / 4	YES / YES	N/A	21-682 kHz	N/A	g_m / R	NO (I_b)
[19]	DVCCTA	1 / 4	YES / YES	N/A	20-700 kHz	4.6 %	g_m / R	NO (I_b)
[20]	CDTA	3 / 2	YES / YES	N/A	0.2-1.8 MHz	2.5 %	g_m / g_m	NO (I_b)
[21]	CDTA	3 / 3	YES / NO	N/A	3-9 kHz	1 - 2.6 %	g_m / g_m	NO (I_b)
[22]	CDTA	3 / 3	YES / YES	N/A	0.4-0.8 MHz	10 %	g_m / g_m	NO (I_b)
[23]	MO-CCCDTA	1 / 3	YES / YES	N/A	N/A (114 kHz)*	0.6 %	g_m / R	NO (I_b)
[26]	CCCDTA	2 / 2	YES / YES	N/A	0.1-5 MHz	N/A	g_m / R_X	NO (I_b)
[27]	CCCDTA	2 / 2	YES / YES	YES	1-4 MHz	1.6 %	g_m / R_X	NO (I_b)
[28]	CCCII	2 / 2	YES / YES	N/A	0.1-1.7 MHz	1 - 7 %	R_X / B	NO (I_b)
[29]	ZC-CG-CDBA	2 / 5	YES / YES	YES	0.25-2.75 MHz	0.2 %	B_G / R	NO (digital)
[30]	CCTA	1 / 4	YES / YES	N/A	0.25-1.23 MHz	0.6 - 4 %	B_G / R	YES
[31]	DT, CA	3 / 4	YES / NO	N/A	0.6-2.2 MHz	0.4 - 0.9 %	B_G / R	YES
[32]	ECCII-, CCII+	3 / 5	YES / YES	N/A	0.26-1.25 MHz	0.2 - 1.5 %	B_G / B_G	YES
[33]	CG-CIBA/CFBA	2 / 5	YES / YES	YES	0.1-1.26 MHz	0.6 - 1.3 %	B_G / B_G	YES
[34]	PCA	3 / 4	YES / YES	N/A	50-300 kHz	N/A	B_G / B_G	NO (I_b)
Prop.	VA, CA, MO-CF/I	3 / 4	YES / YES	YES	12-25.5 MHz	0.3 - 2 %	A_G / B_G	YES

Notes (parameters and abbreviations which are not explained in text of the introductory section):

I_b - bias current (type of control)

g_m / g_m - two different transconductances are used for independent FO and CO control

g_m / R - transconductance suitable for FO and resistance value for CO control

$R / R, g_m$ - resistance value(s) suitable for FO control and resistance or/and transconductance suitable for CO control

$g_m / R, g_m$ - two different transconductances and also one transconductance and resistance are suitable for independent FO and CO control

g_m / R_X - transconductance suitable for FO and electronically controllable intrinsic resistance suitable for CO control

B_G / R - current gain suitable for FO and resistor value for CO control

B_G / B_G - two different current gains are used for independent FO and CO control

A_G / B_G - voltage gain suitable for FO and current gain for CO control

CCCDTA - current controlled CDTA; DVCCTA - differential voltage CCTA; CCCII - current controlled (translinear) current conveyor of second generation; CA - current amplifier (controllable); VA - voltage amplifier (controllable); MO-CF/I - multi-output current follower/inverter; DT - diamond transistor; CG-CIBA/CFBA - controlled gain current inverted buffered amplifier / current follower buffered amplifier

N/A - not possible, not available or not verified

* verified only at stable FO (discrete value sets)

The second group consists of oscillators which are controllable by adjustable intrinsic resistance of current input (R_X) in novel modified active elements. Current conveyor transconductance amplifier (CCTA) introduced by Prokop et al. [24] was also frequently used in adjustable oscillators. Siripruchyanun et al. [25] introduced possibility of R_X control and its usefulness in applications together with g_m adjusting. The CDTA element was also extended and controllable R_X and g_m parameters were determined for control of resistor-less oscillator by Jaikla et al. [26]. Similar oscillator was proposed also by Sakul et al. in [27]. The third group contains solutions employing adjusting of the current gain (B_G) in order to control the application. Kumngern et al. implemented combination of two methods, i.e. control of R_X and current gain (B_G) for adjusting of FO and CO in [28]. Biolek et al. [29] proposed oscillator with so-called z-copy controlled-gain current differencing buffered amplifier (ZC-CG-CDBA) where they also implemented possibility of current gain adjusting. Several applications of adjustable current gain were also discussed in [30]–[33]. Herencsar et al. [34] introduced programmable current amplifier (PCA, DACA) [35] and its application in

oscillator.

Several solutions of the controllable oscillators based on above discussed methods are compared in Table I. Following problems of the discussed results are evident: I. some solutions require larger number of passive elements [12], [16], [29], [32], [33]; II. only few works deal with applications that operate in frequency range above 10 MHz [11], [12], [17]; III. many solutions were designed as tunable (or have these abilities), but their verification was not provided [13], [14], [16], [17], [23]; IV. some variants suffer from high total harmonic distortion (THD) [19], [22], [28], [30]; V. automatic gain control (AGC) for amplitude stabilization was proposed in minimum conceptions [11], [12], [27], [29], [33]; VI. additional conversion of DC control voltage to bias current (controlling g_m for example) is required [11]–[28], [34]; VII. in some cases equations for FO or CO are complicated - matching of several parameters (equality of several C or g_m) required for electronic control [12], [21], [31]; VIII. intrinsic resistance (R_X) is generally nonlinear temperature dependent parameter and intended control by R_X [25]–[28] may cause problems for higher amplitudes of processed signals in some applications; IX.

some solutions require controllable replacement of passive resistor to control of CO [16], [18], [19], [23], [29]–[31].

We prepared a solution that solves several above discussed problems simultaneously. Independent direct electronic control of FO and CO by adjustable voltage and current gain that was not discussed in hitherto published works is used in our approach. Advantages (fulfilled together) of proposed circuit are: I. direct electronic DC voltage control of FO allows comfortable driving from digital systems; II. simple oscillation condition suitable for direct electronic control; III. approach based on high-speed voltage- and current-mode multipliers (used as behavioral representation of active elements) allows operation range in tens of MHz; IV. precise AGC allows sufficient THD in adjusted frequency range; V. we avoid the R_X control (for adjustable purposes) in this work; VI. CO is directly controllable by parameters of active element (no replacement of resistor is required). When on-chip implementation is performed, one resistor with low value is "absorbable" to the current input intrinsic resistance. Of course, other simpler circuits (Table I), controlled by several different ways exist, but above listed features are not fulfilled simultaneously in many of discussed solutions.

II. PROPOSED OSCILLATOR

The basic principle of active elements (adjustable voltage amplifier, adjustable current amplifier and current distributor - current follower/inverter) is explained in Fig. 1.

We implemented two integrator loops with controllable current feedback in order to design simple type of the adjustable oscillator with minimum passive elements and grounded capacitors. Possibility of current and voltage gain control is very useful for tuning of FO and control of CO in our solution that is shown in Fig. 2. Basic component of the signal flow graph (SFG) is the current follower and inverter (MO-CF/I). Combined arrows substitute voltage to current (open-closed) and current to voltage (closed-open) conversion in Fig. 2(a).

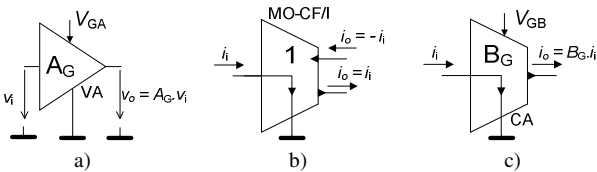


Fig. 1. Active elements applied in proposed oscillator: a) adjustable voltage amplifier, b) current distributor c) adjustable current amplifier.

We can briefly explain principle of the circuit in Fig. 2(b). The node 1, where three passive elements are connected together, is the most important part. These elements form significant impedance (conversion constant between current and voltage). Voltage in node 1 is transformed to the current through R_1 . The MO-CF/I produces identical copies of its input current (inverting or non-inverting output). Negative output is connected to C_2 , where current is changed to voltage (node 2). This voltage is amplified or attenuated by adjustable voltage amplifier (VA) with voltage gain A_G . Finally, the output voltage of the VA is transferred through divider (R_1 , R_2) with capacitive load (C_1). The second loop

(S_2) contains current amplifier (CA) with the current gain B_G and it is connected directly to positive output of the MO-CF/I. The CA represents the feedback path which is connected back to the node 1. Output current of the CA is transformed from current to voltage at the impedance formed by R_1 , R_2 and C_1 .

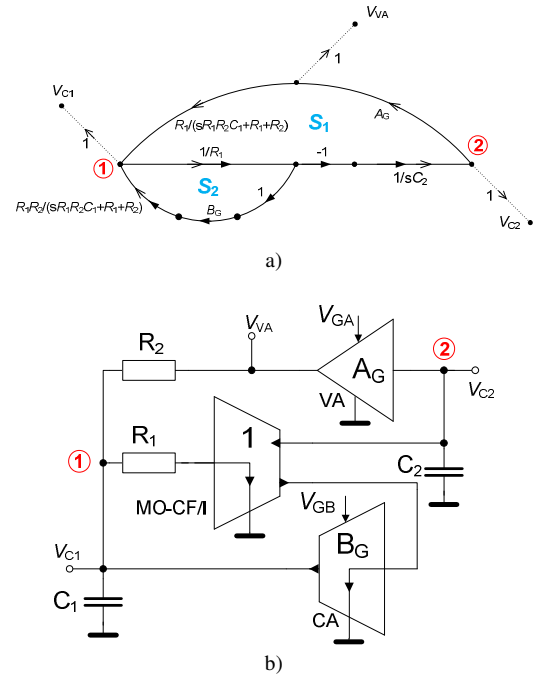


Fig. 2. Proposed oscillator: a) SFG for explanation; b) circuit representation.

Analysis of the SFG in Fig. 2 (by Mason rule [36], [37]) yields to following characteristic equation

$$\begin{aligned} \Delta &= 1 - (S_1 + S_2) = \\ &= 1 - \left[\frac{-A_G}{sR_1C_2} \left(\frac{R_1}{sR_1R_2C_1 + R_1 + R_2} \right) + \frac{B_G}{R_1} \left(\frac{R_1R_2}{sR_1R_2C_1 + R_1 + R_2} \right) \right] = \\ &= s^2 + \frac{R_1 + R_2 - B_G R_2}{R_1 R_2 C_1} s + \frac{A_G}{R_1 R_2 C_1 C_2} = 0. \end{aligned} \quad (1)$$

We can determine CO and FO as follows:

$$B_G \geq 1 + \frac{R_1}{R_2}, \quad (2)$$

$$\omega_0 = \sqrt{\frac{A_G}{R_1 R_2 C_1 C_2}}. \quad (3)$$

It is obvious that CO is controllable by B_G and FO by A_G and they are mutually independent. The relative sensitivities of FO on values of passive elements and gains, that are evident from (3), are:

$$S_{A_G}^{\omega_0} = -S_{R_1}^{\omega_0} = -S_{R_2}^{\omega_0} = -S_{C_1}^{\omega_0} = -S_{C_2}^{\omega_0} = 0,5, \quad (4)$$

$$S_{B_G}^{\omega_0} = 0. \quad (5)$$

III. REAL IMPLEMENTATION AND EXPERIMENTAL VERIFICATION

We created non-ideal model of the proposed circuit from Fig. 2(b). Additional nodal impedances that are caused by

real active elements and additional voltage buffers for impedance separation were added. Complete model is shown in Fig. 3. We implemented commercially available active elements for experimental verifications. The MO-CF/I element was implemented by EL4083 [38] current mode multiplier. The current amplifier (CA) with adjustable current gain is represented by EL2082 [39] current mode multiplier. We constructed adjustable voltage amplifier from high frequency voltage mode multiplier AD834 [40] and high speed opamp AD8045 [41].

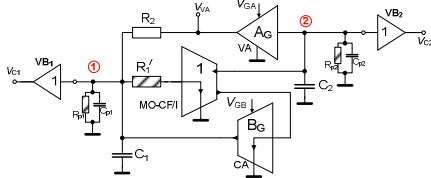


Fig. 3. Analysis of parasitic influences of proposed oscillator.

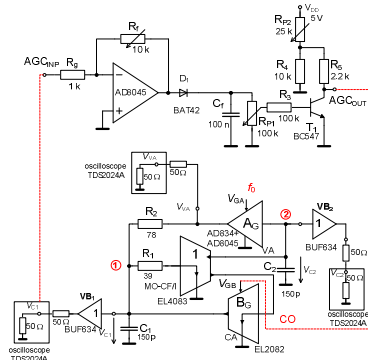
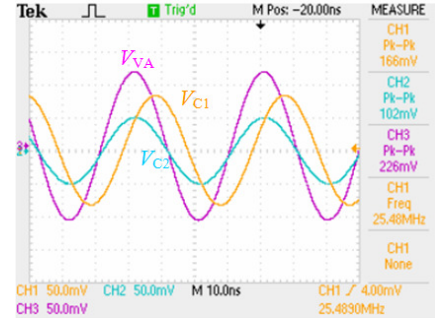


Fig. 4. Measuring setup for experimental tests.

Additional (separation) buffers were BUF634 types [42]. We selected values of passive elements as follows: $R_1 = 39 \Omega$ (real input resistance of MO-CF/I is considered), $R_2 = 78 \Omega$, $C_1 = C_2 = C = 150 \text{ pF}$, $B_G = 2$. Important parameters of the MO-CF/I (EL4083 [38]) are output impedances, both are characterized by $R_{\text{out_MO-CF}} \approx 1 \text{ M}\Omega$, $C_{\text{out_MO-CF}} \approx 5 \text{ pF}$ and also input resistance, $R_{\text{inp_MO-CF}} \approx 40 \Omega$. Producer of EL2082 (modeling CA) indicates output properties as follows: $R_{\text{out_CA}} \approx 1 \text{ M}\Omega$, $C_{\text{out_CA}} \approx 5 \text{ pF}$, $R_{\text{inp_CA}} \approx 95 \Omega$. We suppose that influence of $R_{\text{inp_CA}}$ is negligible because $R_{\text{inp_CA}} \ll R_{\text{out_MO-CF}}$. The voltage amplifier (VA) is characterized by input resistance $R_{\text{inp_VA}} \approx 25 \text{ k}\Omega$ (AD834). High speed VA was built in accordance with recommendations in [40]. Output resistance of VA is negligible (datasheet of AD8045 shows value $< 4 \Omega$ up to 100 MHz). Input impedance of additional separation voltage buffer is $R_{\text{inp_VB}} \approx 8 \text{ M}\Omega$, $C_{\text{inp_VB}} \approx 8 \text{ pF}$ (BUF634). Outputs of the MO-CF/I are dominant in the node 1 where $R_{p1} \approx R_{\text{out_CA}} \parallel R_{\text{inp_VB}} \approx 890 \text{ k}\Omega$ and $C_{p1} \approx C_{\text{out_CA}} + C_{\text{inp_VB}} \approx 13 \text{ pF}$.

The main problem is in the node 2, because input resistance of VA (AD834) is only $25 \text{ k}\Omega$ i.e. $R_{p2} \approx R_{\text{inp_VA}} \parallel R_{\text{out_MO-CF}} \parallel R_{\text{inp_VB}} \approx 24 \text{ k}\Omega$. Capacitances in the node 2 have overall values $C_{p2} \approx C_{\text{inp_VA}} + C_{\text{out_MO-CF}} + C_{\text{inp_VB}} \approx 18 \text{ pF}$. Value of R_1 is also influenced by $R_{\text{inp_MO-CF}} \approx 40 \Omega$, i.e. real $R_1' \approx R_1 + R_{\text{inp_MO-CF}} \approx 79 \Omega$. We can include parasitic capacitances to "working" values as $C_1' \approx C_1 + C_{p1} \approx 163 \text{ pF}$, $C_2' \approx C_2 + C_{p2} \approx 168 \text{ pF}$. However,

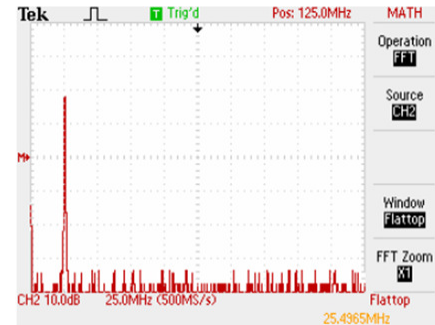
estimation of parasitic features given by printed circuit board (PCB) is very problematic.



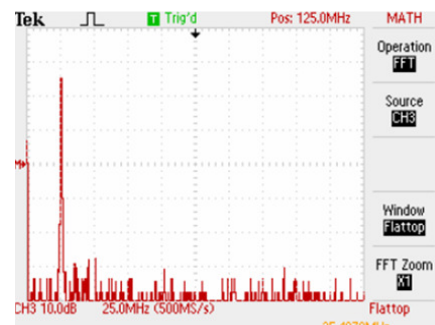
a)



b)



c)



d)

Fig. 5. Experimental results for $f_0 = 25.5 \text{ MHz}$, $A_G = 4$: a) all transient responses, b) spectrum of V_{C1} , c) spectrum of V_{C2} , d) spectrum of V_{VA} .

Analysis of parasites in circuit in Fig. 3 leads to more real forms of CO and FO:

$$B_G' \geq \frac{R_1' R_2 R_{p1} C_1' + R_2 R_{p1} R_{p2} C_2' + R_1' R_2 R_{p2} C_2' + R_1' R_{p1} R_{p2} C_2'}{R_2 R_{p1} R_{p2} C_2'} \quad (6)$$

$$\omega_0' = \sqrt{\frac{A_G R_{p1} R_{p2} + R_1' R_2 + R_{p1} R_2 + R_{p1} R_1' - B_G' R_{p1} R_2}{R_1' R_2 R_{p1} R_{p2} C_1' C_2'}} \quad (7)$$

The term $A_G R_{p1} R_{p2}$ in (7) has more than hundred times higher value than term $B_G' R_{p1} R_2$ for $B_G = 2$ and $A_G > 1$.

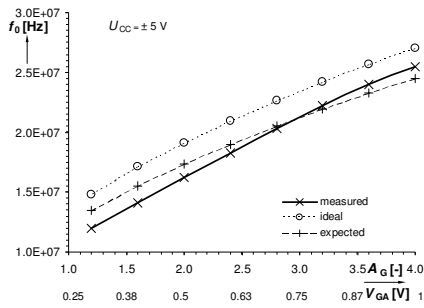


Fig. 6. Measured dependence of FO on A_G .

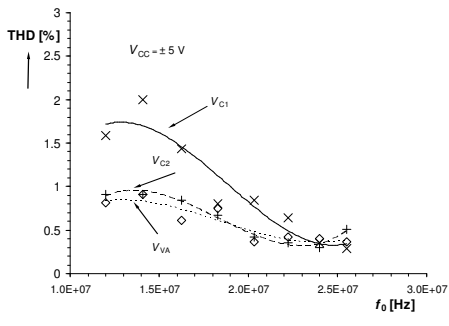


Fig. 7. Measured dependence of THD on FO.

Therefore, its influence on FO is insignificant. Nevertheless, significant effects appear for lower A_G ($\ll 1$). This drawback increases with lower value of R_{p2} ($R_{p1} \gg R_{p2}$ in our equivalent circuit model). It is caused by specific feature of used VA. The next important problem is quite high value of C_{p2} .

We tested proposed circuit in laboratory and find out the following results. The oscillator was modified (supplemented by automatic gain control circuit - AGC for amplitude stabilization, impedance matching) and carefully adjusted for adequate operation. The tested device was connected to measuring installation included in Fig. 4. Additional opamp in the AGC loop (pre-amplification) was necessary because output level of VB_1 is quite low (about 100 mV_{p,p}) for sufficient THD (AD834 has restricted linear dynamical range of input voltage) and does not reach threshold voltage of the diode in the rectifier. Time domain results and spectral analyses for the highest achieved FO are shown in Fig. 5.

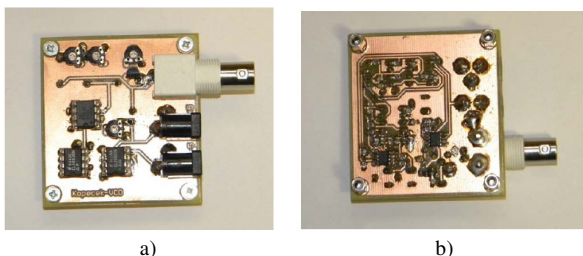


Fig. 8. Measured prototype: a) top side, b) bottom side.

The dependence of FO on A_G is depicted in Fig. 6. Ideal range (when only R_{imp_MO-CF} is included) of FO tuning was calculated between 14.81 and 27.05 MHz. Expected range (calculation from (7)) of FO control is from 13.43 to 24.52 MHz. Measurements provided range from 12.01 to 25.50 MHz. All results were obtained for A_G adjusted from

1.2 to 4. THD was evaluated as 0.3 to 2% (Fig. 7). Measured prototype is shown in Fig. 8.

IV. CONCLUSIONS

Presented work shows that two different ways of control (voltage and current gain) are also possible for tunable oscillator in comparison to classical method based on change of resistor(s) value or standard methods of electronic control by transconductance (g_m) [10]–[23], intrinsic resistance [7], [8], [25] or their combination [26], [27] for example. Researchers try to find alternative methods of control of FO and CO (as we can see in [29]–[35]). Such methods may avoid using some not-generally advantageous ways of direct electronic control of parameters (control of intrinsic resistance R_X for example). Presented solution is also an attempt, which shows how to avoid necessity of R_X control in mixed-mode applications utilizing current-mode active elements (compared to [26]–[28]).

Presented solution has several conveniences that are not fulfilled in many above compared solutions (Table I) simultaneously. Main advantages of the proposed solution are: I. direct simple DC voltage control of FO; II. simple and specially established CO - easy implementation of AGC by DC control voltage (no replacement of passive resistor is required); III. proposal of precise AGC system, which ensures sufficient THD level (0.3 - 2 %) in intended frequency range; IV. additional simplification for on-chip implementation - one resistor (R_1) is "absorbable" to fixed value of intrinsic resistance of current input; V. no additional conversion of control voltages to bias current etc. is required - DC voltage is directly available to adjust the oscillator from control part or other device; VI. due to the high-frequency devices and low values of passive elements, operational range of FO adjusting was at frequencies of several tens of MHz (between 12 - 25.5 MHz). In real case, an attention to sufficient values of nodal impedances (resistances and capacitances) and undesirable couplings must be given.

Active elements were modeled by commercially available current multipliers, voltage amplifiers and buffers. This approach allows preliminary laboratory tests. The authors believe that if the circuit built from discrete commercially available elements works well, then appropriate and future on-chip implementation will work even better.

ACKNOWLEDGMENT

We would like to thank to Pavel Kopecek, M.Sc. for his help with experimental work and measurements.

REFERENCES

- [1] D. Biolek, R. Senani, V. Biolkova, Z. Kolka, "Active elements for analog signal processing: Classification, Review and New Proposals", *Radioengineering*, vol. 17, no. 4, pp. 15–32, 2008.
- [2] W. Surakampontorn, W. Thitimajshima, "Integrable electronically tunable current conveyors", *IEE Proceedings-G*, vol. 135, no. 2, pp. 71–77, 1988.
- [3] A. Fabre, N. Mimeche, "Class A/AB Second-generation Current Conveyor with Controlled Current Gain", *Electronics Letters*, vol. 30, no. 16, pp. 1267–1268, 1994. [Online]. Available: <http://dx.doi.org/10.1049/el:19940878>
- [4] A. Sedra, K. C. Smith, "A second generation current conveyor and its

- applications”, *IEEE Transaction on Circuit Theory*, vol. CT-17, no. 2, pp. 132–134, 1970. [Online]. Available: <http://dx.doi.org/10.1109/TCT.1970.1083067>
- [5] J. A. Svoboda, L. McGory, S. Webb, “Applications of a commercially available current conveyor”, *Int. Journal of Electronics*, vol. 70, no. 1, pp. 159–164, 1991. [Online]. Available: <http://dx.doi.org/10.1080/00207219108921266>
- [6] R. L. Geiger, E. Sánchez-Sinencio, “Active filter design using operational transconductance amplifiers: a tutorial”, *IEEE Circ. and Devices Magazine*, vol. 1, pp. 20–32, 1985. [Online]. Available: <http://dx.doi.org/10.1109/MCD.1985.6311946>
- [7] A. Fabre, O. Saaid, F. Wiest, C. Boucheron, “High frequency applications based on a new current controlled conveyor”, *IEEE Trans. on Circuits and Systems – I*, vol. 43, no. 2, pp. 82–91, 1996.
- [8] S. Minaei, O. K. Sayin, H. Kuntman, “A new CMOS electronically tunable current conveyor and its application to current-mode filters”, *IEEE Trans. on Circuits and Systems – I*, vol. 53, no. 7, pp. 1448–1457, 2006.
- [9] A. Marcellis, G. Ferri, N. C. Guerrini, G. Scotti, V. Stornelli, A. Trifiletti, “The VGC-CCII: a novel building block and its application to capacitance multiplication”, *Analog Integrated Circuits and Signal Processing*, vol. 58, no. 1, pp. 55–59, 2009. [Online]. Available: <http://dx.doi.org/10.1007/s10470-008-9213-6>
- [10] A. Rodriguez-Vazquez, B. Linares-Barranco, J. L. Huertas, E. Sanchez-Sinencio, E. “On the design of voltage-controlled sinusoidal oscillators using OTAs”, *IEEE Trans. Circuits and Systems*, vol. 37, no. 2, pp. 198–211, 1990. [Online]. Available: <http://dx.doi.org/10.1109/31.45712>
- [11] B. Linares-Barranco, A. Rodriguez-Vazquez, E. Sanchez-Sinencio, J. L. Huertas, “10 MHz CMOS OTA-C voltage-controlled quadrature oscillator”, *Electronics Letters*, vol. 25, no. 12, pp. 198–211, 1989. [Online]. Available: <http://dx.doi.org/10.1049/el:19890517>
- [12] B. Linares-Barranco, A. Rodriguez-Vazquez, E. Sanchez-Sinencio, J. L. Huertas, “CMOS OTA-C high-frequency sinusoidal oscillators”, *IEEE Journal of Solid-State Circuits*, vol. 26, no. 2, pp. 160–165, 1991. [Online]. Available: <http://dx.doi.org/10.1109/4.68133>
- [13] R. Senani, “New electronically tunable OTA-C sinusoidal oscillator”, *Electronics Letters*, vol. 25, no. 4, pp. 286–287, 1989. [Online]. Available: <http://dx.doi.org/10.1049/el:19890199>
- [14] M. T. Abuelma’atti, “A new minimum component active-C OTA-based linear voltage (current)-controlled sinusoidal oscillator”, *IEEE Transactions on Instrumentation and Measurement*, vol. 39, no. 5, pp. 795–797, 1990. [Online]. Available: <http://dx.doi.org/10.1109/19.58629>
- [15] D. Biolek, “CDTA – building block for current-mode analog signal processing”, in *Proc. of European Conf. Circuits Theory and Design (ECCTD 03)*, Krakow, 2003, pp. 397–400.
- [16] A. U. Keskin, D. Biolek, “Current mode quadrature oscillator using current differencing transconductance amplifiers (CDTA)”, *IET – Circuits, Devices and Systems*, vol. 153, no. 3, pp. 214–217, 2006. [Online]. Available: <http://dx.doi.org/10.1049/ip-cds:20050304>
- [17] A. Lahiri, “New current-mode quadrature oscillators using CDTA”, *IEICE Electronics Express*, vol. 6, no. 3, pp. 135–140, 2009. [Online]. Available: <http://dx.doi.org/10.1587/ele6.135>
- [18] A. Lahiri, “Explicit-current-output Quadrature Oscillator Using Second-generation Current Conveyor Transconductance Amplifier”, *Radioengineering*, vol. 18, no. 4, pp. 522–526, 2009.
- [19] A. Lahiri, W. Jaikla, M. Siripruchyanun, “Voltage-mode quadrature sinusoidal oscillator with current tunable properties”, *Analog Integrated Circuits and Signal Processing*, vol. 65, no. 2, pp. 321–325, 2010. [Online]. Available: <http://dx.doi.org/10.1007/s10470-010-9488-2>
- [20] W. Tangsrirat, W. Tanjaroen, “Current-mode sinusoidal quadrature oscillator with independent control of oscillation frequency and condition using CDTAs”, *Indian Journal of Pure and Applied Physics*, vol. 45, no. 5, pp. 363–366, 2010.
- [21] J. W. Horng, “Current-Mode Third-order Quadrature Oscillator Using CDTAs”, *Active and Passive Electronic Components*, vol. 2009, pp. 1–5, 2009. [Online]. Available: <http://dx.doi.org/10.1155/2009/789171>
- [22] J. W. Horng, H. Lee, J. Wu, “Electronically tunable third-order quadrature oscillator using CDTAs”, *Radioengineering*, vol. 19, no. 2, pp. 326–330, 2010.
- [23] D. Prasad, D. R. Bhaskar, A. K. Singh, “Electronically controllable Crouded Capacitor Current-Mode Quadrature Oscillator Using Single MO-CCCDA”, *Radioengineering*, vol. 20, no. 1, pp. 354–359, 2011.
- [24] R. Prokop, V. Musil, “Modular approach to design of modern circuit blocks for current signal processing and new device CCTA”, in *Proc. Conf. on Signal and Image Processing IASTED*, Anaheim, 2005, pp. 494–499.
- [25] M. Siripruchyanun, W. Jaikla, “Current controlled current conveyor transconductance amplifier (CCCCTA): a building block for analog signal processing”, *Electrical Engineering*, vol. 90, no. 6, pp. 443–453, 2008. [Online]. Available: <http://dx.doi.org/10.1007/s00202-007-0095-x>
- [26] W. Jaikla, A. Lahiri, “Resistor-less current-mode four-phase quadrature oscillator using CCCDTAs and grounded capacitors”, *AEU – International Journal of Electronics and Communications*, vol. 66, no. 3, pp. 214–218, 2011. [Online]. Available: <http://dx.doi.org/10.1016/j.aeu.2011.07.001>
- [27] Ch. Sakul, W. Jaikla, K. Dejhan, “New resistorless current-mode Quadrature Oscillators Using 2 CCCDTAs and Grounded Capacitors”, *Radioengineering*, vol. 20, no. 4, pp. 890–896, 2011.
- [28] M. Kummern, S. Junnapiya, “A sinusoidal oscillator using translinear current conveyors”, in *Proc. of Asia Pacific Conf. on Circuits and Systems APPCAS2010*, Kuala Lumpur, 2010, pp. 740–743.
- [29] D. Biolek, A. Lahiri, W. Jaikla, M. Siripruchyanun, J. Bajer, “Realisation of electronically tunable voltage-mode/current-mode quadrature sinusoidal oscillator using ZC-CG-CDBA”, *Microelectronics Journal*, vol. 42, no. 10, pp. 1116–1123, 2011. [Online]. Available: <http://dx.doi.org/10.1016/j.mejo.2011.07.004>
- [30] R. Sotner, J. Jerabek, R. Prokop, K. Vrba, “Current gain controlled CCTA and its application in quadrature oscillator and direct frequency modulator”, *Radioengineering*, vol. 20, no. 1, pp. 317–326, 2011.
- [31] R. Sotner, B. Sevcik, J. Slezak, J. Petrzela, L. Brancik, “Sinusoidal Oscillator based on Adjustable Current Amplifier and Diamond Transistors with Buffers”, *Przeglad Elektrotechniczny*, vol. 87, no. 1, pp. 266–270, 2011.
- [32] R. Sotner, Z. Hrubos, B. Sevcik, J. Slezak, J. Petrzela, T. Dostal, “An example of easy synthesis of active filter and oscillator using signal flow graph modification and controllable current conveyors”, *Journal of Electrical Engineering*, vol. 62, no. 5, pp. 258–266, 2011. [Online]. Available: <http://dx.doi.org/10.2478/v10187-011-0041-z>
- [33] R. Sotner, J. Jerabek, N. Herencsar, Z. Hrubos, T. Dostal, K. Vrba, “Study of Adjustable Gains for Control of Oscillation Frequency and Oscillation Condition in 3R-2C Oscillator”, *Radioengineering*, vol. 21, no. 1, pp. 392–402, 2012
- [34] N. Herencsar, A. Lahiri, K. Vrba, J. Koton, “An electronically tunable current-mode quadrature oscillator using PCAs”, *Int. Journal of Electronics*, vol. 99, no. 5, pp. 609–621, 2011. [Online]. Available: <http://dx.doi.org/10.1080/00207217.2011.643489>
- [35] J. Jerabek, J. Koton, R. Sotner, K. Vrba, “Adjustable band-pass filter with current active elements: two fully-differential and single-ended solutions”, *Analog Integrated Circuits and Signal Processing*, vol. 74, no. 1, pp. 129–139, 2013. [Online]. Available: <http://dx.doi.org/10.1007/s10470-012-9942-4>
- [36] S. Mason, “Feedback Theory: Further properties of Signal Flow Graphs”, *Proceedings of IRE*, vol. 44, no. 7, pp. 920–926, 1956. [Online]. Available: <http://dx.doi.org/10.1109/JRPROC.1956.275147>
- [37] C. L. Coates, “Flow-graph Solution of Linear Algebraic Equations”, *IRE Transactions on Circuit Theory*, vol. 6, no. 2, pp. 170–187, 1959. [Online]. Available: <http://dx.doi.org/10.1109/TCT.1959.1086537>
- [38] *EL4083 CN Current-mode four-quadrant multiplier* (datasheet), Intersil (Elantec), 1995, p. 14. [Online]. Available: <http://www.intersil.com/data/fn/fn7157.pdf>
- [39] *EL2082 CN Current-mode multiplier* (datasheet), Intersil (Elantec), 1996, p. 14. [Online]. Available: <http://www.intersil.com/data/fn/fn7152.pdf>
- [40] *AD834 500 MHz Four-Quadrant Multiplier* (datasheet), Analog Devices, 2005, p. 20. [Online]. Available: http://www.analog.com/static/imported-files/data_sheets/AD834.pdf
- [41] *AD8045 Ultra-low Distortion Voltage Feedback High Speed Amplifier* (datasheet), Analog Devices, 2004, p. 24. [Online]. Available: http://www.analog.com/static/imported-files/data_sheets/AD8045.pdf
- [42] *BUF 634 250 mA High-speed buffer* (datasheet), Texas Instruments, 1996, p. 20. [Online]. Available: <http://focus.ti.com/lit/ds/symlink/buf634.pdf>

[5] SOTNER, R., HERENCŠAR, N., JERABEK, J., DVORAK, R., KARTCI, A., DOSTAL, T., VRBA, K. New double current controlled CFA (DCC-CFA) based voltage- mode oscillator with independent electronic control of oscillation condition and frequency. *Journal of Electrical Engineering*, 2013, vol. 64, no. 2, p. 65-75. ISSN: 1335-3632.

NEW DOUBLE CURRENT CONTROLLED CFA (DCC–CFA) BASED VOLTAGE–MODE OSCILLATOR WITH INDEPENDENT ELECTRONIC CONTROL OF OSCILLATION CONDITION AND FREQUENCY

Roman Šotner^{*} — Norbert Herencsár^{**} —
 Jan Jeřábek^{**} — Radek Dvořák^{*} — Aslihan Kartci^{***}
 — Tomáš Dostál^{*} — Kamil Vrba^{**}

In this paper, a new electronically tunable quadrature oscillator (ETQO) based on two modified versions of current feedback amplifiers (CFAs), the so called double current controlled CFA (DCC-CFAs) is presented. The frequency of oscillation (FO) of the proposed voltage-mode (VM) ETQO is electronically adjustable by current gain or by varying the intrinsic resistance of the X terminal of the active element used. The condition of oscillation (CO) is adjustable by current gain independently with respect to frequency of oscillation. Simultaneous control of current gain and intrinsic resistance allows linear control of FO and provides extension of frequency tuning range. In the proposed circuit all the capacitors are grounded. The use of only grounded capacitors makes the proposed circuit ideal for integrated circuit implementation. The presented active element realized by using BiCMOS technology and the behavior of proposed circuit are discussed in details. The theoretical results are verified by SPICE simulations based on CMOS ON-Semi C5 0.5 μm and bipolar ultra high frequency transistor arrays Intersil HFA 3096 process parameters.

Key words: electronic control, sinusoidal oscillator, current feedback amplifier (CFA), double current controlled CFA (DCC-CFA)

1 INTRODUCTION

Recently, in [1], the fact of plenty available analog building blocks (ABBs) for analog signal processing is discussed. In [1], the review of basic, modified, and novel active elements is also given. In the last years in the literature interesting applications of components mentioned in [1], such as operational transconductance amplifier (OTA) [2, 3], current controlled second-generation current conveyor (CCCII) [4, 5], dual-X second-generation current conveyor (DXCCII) [6, 7], fully-differential second-generation current conveyor (FDCCII) [8, 9], current feedback amplifier (CFA) [10], current controlled CFA (CC-CFA) [11], modified current feedback operational amplifier (MCFOA) [12], current differencing buffered amplifier (CDBA) [13, 14], current differencing transconductance amplifier (CDTA) [15, 16], current follower transconductance amplifier (CFTA) [17, 18], programmable current amplifiers [19, 20], adjustable current followers [21], *etc.*, have been published. Many of these components offer features for electronic control and great frequency response. Mentioned elements find wide range of applications in the field of sensor, control, measuring, automotive electronics, acoustic, and high-speed & radio-communication systems (amplifiers, filters, oscillators, modulators, active rectifiers, *etc.*) [22–28].

The possibilities of electronic tunability of ABBs are today focused to several ways. As an example internal (intrinsic) resistance R_X control by bias current I_b [5, 11,

29], transconductance (g_m) control by bias current I_b [30–33], control by one passive element (grounded or floating resistor), so-called single resistance controlled oscillators (SRCO) [34–38] can be mentioned. Some suitable solutions allow replacement of the resistor by FET and easy voltage control of frequency of oscillation (FO) [35, 37]. Interesting approach based on synthetic negative capacitance control is published in [39]. Switching of working capacitors is also suitable method, if continuous control of FO is not necessary [40]. Another interesting way is the use of current gain control, which is not so common. Several solutions of electronically controllable current conveyors were proposed [41–45] and applied for electronic control of frequency of oscillation [44, 45].

Short review of several important previously presented solutions of oscillators with CFAs is summarized below. Siripruchyanun *et al* [11] proposed oscillator employing two CFAs and two capacitors with g_m and R_X control, but FO tunability has not been verified. Verification was provided by simulation at $f_0 = 820$ kHz with total harmonic distortion (THD) 2.7%. In [34], Gupta *et al* presented SRCO solutions based on two CFA and five passive elements, where one of two capacitors is floating. Tunability range of the verified type was from 45 to 150 kHz with THD = 0.6%. In [35], Gupta *et al* presented similar types of SRCO oscillators employing two CFAs and 5–6 passive elements. Oscillation frequency is tunable by FET replacement of specific resistor approximately from 230 to 300 kHz with THD = 1.6%. Lahiri *et al* proposed several

^{*} Department of Radio Electronics, ^{**} Department of Telecommunications, Brno University of Technology, Technická 12, 616 00 Brno, Czech Republic, sotner@feec.vutbr.cz ^{***} Department of Electronics and Telecommunication Engineering, Corlu Engineering Faculty, Namik Kemal University, Cerkezkooy Yolu, 3. km, 59860 Corlu, Turkey

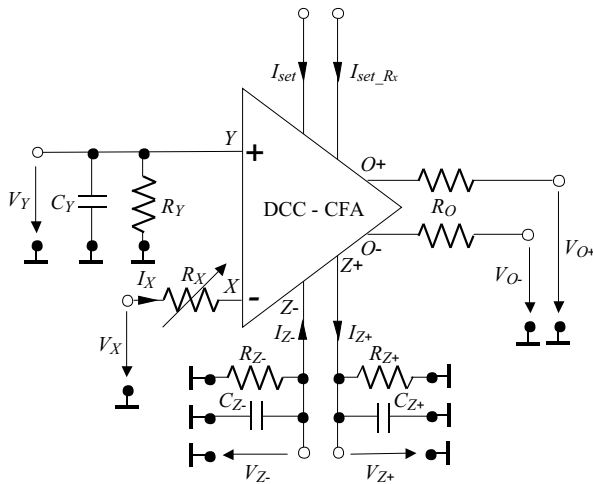


Fig. 1. Circuit symbol of the DCC-CFA including parasitic elements representing small-signal properties

Table 1. Dimensions of CMOS transistors in Figs. 3(a) and (b)

Transistor	W/L (μm)
$M_1, M_2, M_{35}-M_{44}, M_{53}, M_{54}, M_{60}, M_{61}, M_{65}, M_{66}$	20/1
$M_3, M_4, M_7-M_{25}, M_{47}, M_{48}, M_{51}, M_{52}, M_{55}, M_{56}$	40/1
$M_5, M_6, M_{45}, M_{46}, M_{49}, M_{50}$	10/1
$M_{26}-M_{34}, M_{57}-M_{59}, M_{62}-M_{64}$	5/1

Table 2. Dimensions of CMOS transistors in Fig. 3(c) (voltage buffer)

Transistor	W/L (μm)
$M_1-M_3, M_8, M_9, M_{12}, M_{13}$	5/1
$M_4-M_7, M_{10}, M_{11}, M_{14}-M_{17}$	10/1

variants of oscillators using two CFAs and 5 passive elements with grounded capacitors [36]. Furthermore, some of them have FO controllable by a single resistor. Verification was provided at $f_0 = 1.3$ MHz with THD = 3%. Bhaskar *et al* [37] showed several conceptions of SRCO types employing two CFAs with 4–5 passive elements and 2 or 3 capacitors included. Tunability is based on FET replacement of resistor. The change of FO was verified approximately from 3 to 35 kHz with THD between 0.5–2%. Herencsar *et al* [38] presented SRCO quadrature solutions based on two CFAs and 5 passive elements. Tunability was verified from 100 to 400 kHz with THD = 0.7%. In [39], Lahiri *et al* introduced quadrature realizations using two CFAs and 4 passive elements, where one capacitor is replaced by negative synthetic equivalent for purposes of adjustability. In fact, the circuit contains three active and 6 passive elements. The THD values in both outputs are under 2%. Soliman presented solutions based on 2–3 CFAs and 4–6 passive elements (all C grounded) [46]. The condition of oscillation (CO) of some of the proposed circuits is quite complicated and the independent control of the FO and CO is not allowed. Several realizations in

[46] of them have quadrature outputs and the feasibility was verified on $f_0 = 159$ kHz. In [47], Singh *et al* introduced interesting solutions of SRCOs employing only one CFA and 5 passive elements. Tunability was verified from 5 to 35 kHz and 123–270 kHz with THD 1.4% and 3%, respectively. Senani *et al* published SRCO solution based on two CFAs and 5 passive elements with FO adjustability from 50 to 450 kHz [48]. In [49] it is introduced a SRCO, which is designed by Martinez *et al*, wherein two CFAs and 5 passive elements were used. The circuit is tunable from 40 to 400 kHz with THD < 1%. The SRCO conception presented in [50] by Shen-Iuan *et al* contains two CFAs and 6 passive elements and it is designed for low frequencies — tunability from 10 Hz up to 550 Hz. Theoretical work [51] by Celma *et al* deals with comparison of CFA based oscillators versus classical Op-Amp solutions. The proposed SRCO solution [52] employing one CFA and 5 passive elements is tunable from 330 kHz to 1 MHz. Senani *et al* proposed several SRCO solutions published in [53], where 3 CFAs and 5 passive elements were used. Adjusting of FO is possible from 5 to 15 kHz. Some theoretical information about synthesis was given by Gupta *et al* in [54]. In [55], Abuelmaatti introduced novel oscillator solutions based on partial admittance autonomous networks with 1 and 2 CFAs and verified circuits employ 3 and 4 passive elements, respectively. Unfortunately, equations for FO and CO are quite complicated. Workability was proved at frequencies around 150 kHz. Gunes *et al* [56] presented interesting approach about several realizations of SRCO oscillators using one CFA and 5 passive elements with favorable and also with complicated design equations. Tunability was verified by R control from 5 kHz to 2 MHz by switching of the working capacitors. Very interesting solution of controllable oscillator was introduced by Bhaskar *et al* in [57], which is based on one CFA, 5 passive elements and two voltage multipliers for electronic control of FO. The tuning of FO by control voltage was verified from 15 to 73 kHz with THD in range 1.5–1.9%. Summarization of suitable voltage controlled solutions is in [58], where two CFAs are used with two voltage multipliers and 5–6 passive elements. The tunability of the selected circuits was verified from 18 to 130 kHz and for the other variants approximately from 20 to 330 kHz. The THD is between 0.8–3.9%. Senani *et al* [59] also proposed several conceptions employing one CFA and 6 passive elements (3C/3R), however, tuning of FO is unfortunately not allowed (the circuit is tested at fixed FO of 11.4 kHz). In both cases the obtained THD is 0.6 and 1.2%.

In general it can be seen that in some of introduced circuits (for example in [36, 37, 46]) the CO is very complicated, and overwhelming majority of presented solutions use R control (SRCO) for FO tuning. Hence, in case of floating resistor the adequate voltage control by FET or digital potentiometers can be difficult to implement. Therefore, to eliminate above mentioned disadvantages in the implementation of R control, we present a modified

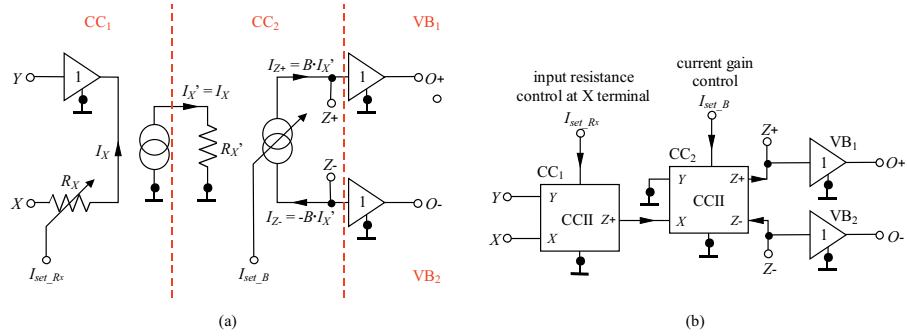


Fig. 2. (a) – behavioral model and, (b) – block diagram of DCC-CFA

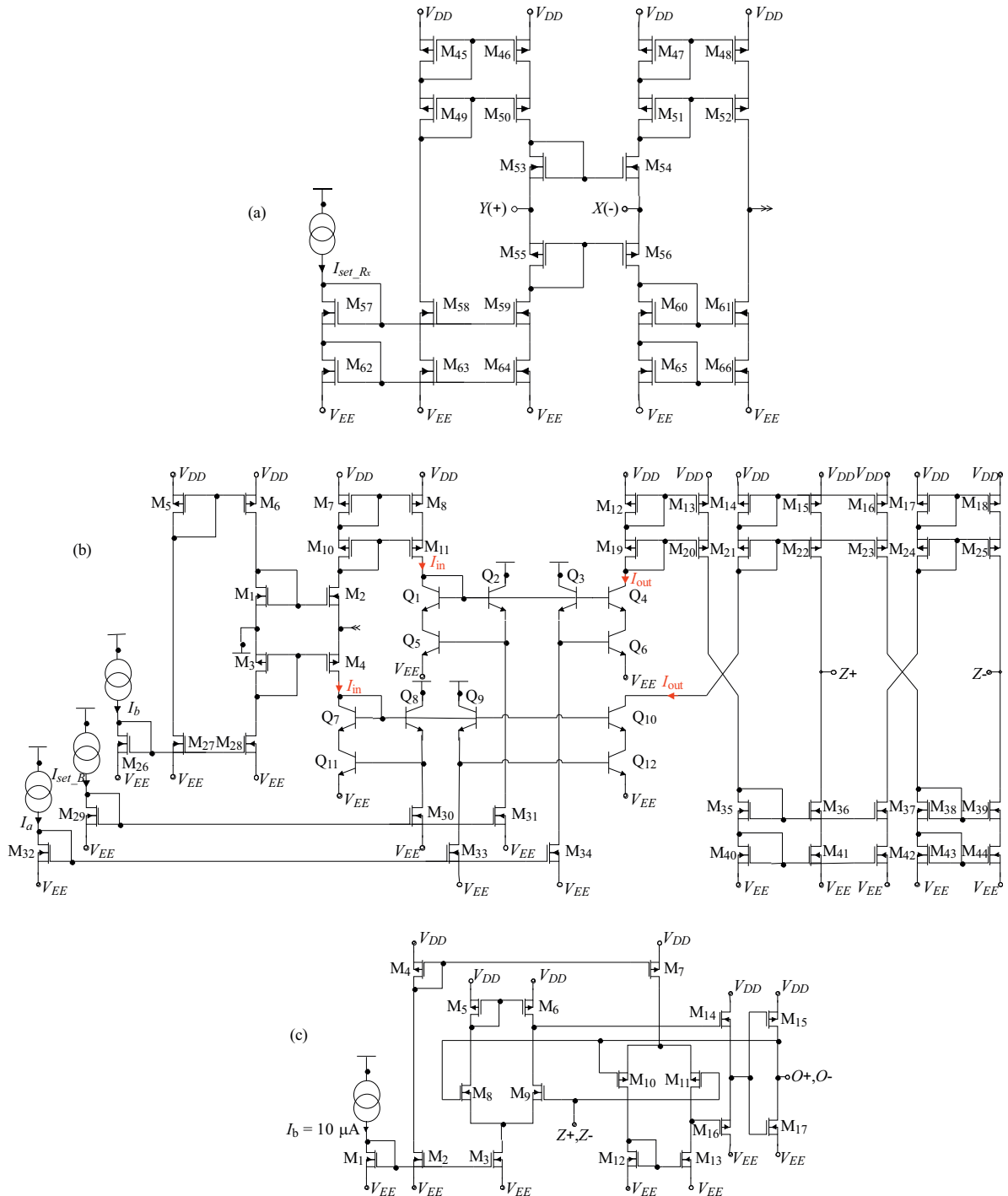


Fig. 3. Conception of the three internal parts of DCC-CFA: (a) – CC1, (b) – CC2, (c) – VB

ABB of well known CFA so-called Double Current Controlled CFA (DCC-CFA) in this paper. Main advantages of presented active element is the current gain control between ports X and Z terminals and control of input (intrinsic) resistance (R_X) of current input X terminal without mutually affection that allow simple electronically tunable quadrature oscillator (ETQO) design with fine tuning. Moreover, this paper presents another point of view on frequency of oscillation and condition of oscillation adjusting than use oscillators in many hitherto published CFA based solutions. Hence, combination of two ways of control is possible. Here proposed ETQO provides electronic CO and except “classical” SRCO type of control allows also two another types of electronic control of FO via R_X (I_{set_RX}) and current gain B (I_{set_B}). In addition, simultaneous change of both parameters (their invariant ratio) allows linear FO tuning. Hence, independent control of the CO and FO without any matching conditions and without changes of any passive elements are very useful features. For wider range of FO tuning and for electronic CO control via current controlled current gain, a simple implementation of automatic amplitude gain control circuit (AGC) is presented.

2 DOUBLE CURRENT CONTROLLED CFA (DCC-CFA)

The CFA device [1,10,11] is equivalent circuit to second-generation current conveyor (CCII), which is followed by voltage buffer. Principle of electronic control of input (intrinsic) resistance (labeled as R_X) of current input terminal X is already well known [11,29], where only one CCII and bias control (I_b) is sufficient [4,29]. Implementation of current gain control is more complicated [42]. Previously, in the four terminal floating nullor (FTFN) [60–62] has been implemented such solution, which internal structure contains CCII with special type of controlled current mirror sections, two auxiliary DC currents (gain is given by ratio of these currents), and also standard bias current. Therefore, theoretically it is possible to change current gain and intrinsic resistance R_X in one modified CCII without their mutual affection. However, our further analyses demonstrate that R_X (I_b) bias current control causes increase of nonlinearity of input dynamical range and current gain interference ($R_X-I_{set_RX}$ control affects linearity of B control by I_{set_B}), if current gain (in this paper labeled by symbol B) is not unity. Therefore, in our design the section for adjusting R_X (I_{set_RX}) and gain control B (I_{set_B}) are separated and all interferences between R_X and B control are eliminated.

Circuit symbol of the DCC-CFA including parasitic elements representing small-signal properties is shown in Fig. 1, which can be described by the following hybrid

matrix

$$\begin{bmatrix} I_Y \\ V_X \\ I_{Z+} \\ I_{Z-} \\ V_{O+} \\ V_{O-} \end{bmatrix} = \begin{bmatrix} Y_Y & 0 & 0 & 0 & 0 & 0 \\ \alpha & R_X & 0 & 0 & 0 & 0 \\ 0 & \beta_1 B & Y_{Z+} & 0 & 0 & 0 \\ 0 & -\beta_2 B & 0 & Y_{Z-} & 0 & 0 \\ 0 & 0 & \gamma_1 & 0 & Z_{O+} & 0 \\ 0 & 0 & \gamma_2 & 0 & 0 & Z_{O-} \end{bmatrix} \begin{bmatrix} V_Y \\ I_X \\ V_{Z+} \\ V_{Z-} \\ I_{O+} \\ I_{O-} \end{bmatrix}, \quad (1)$$

where $Y_Y = sC_Y + 1/R_Y$, $Y_{Z+} = sC_{Z+} + 1/R_{Z+}$, $Y_{Z-} = sC_{Z-} + 1/R_{Z-}$, $Z_{O+} = R_{O+}$, $Z_{O-} = R_{O-}$ are parallel admittances and resistances at their relevant terminals. The α is voltage tracking error between Y and X terminals ($\alpha = 1 - \varepsilon$, $|\varepsilon| \ll 1$), $\beta_{1,2}$ are current tracking errors ($\beta = 1 - \delta$, $|\delta| \ll 1$) between X and $Z_{1,2}$ terminals, and $\gamma_{1,2}$ are voltage tracking errors between Z and O terminals ($\gamma = 1 - \eta$, $|\eta| \ll 1$), respectively.

The behavioral model, the block diagram, and the proposed internal structure of DCC-CFA are shown in Figs. 2 and 3, respectively. The internal structure contains two current conveyors (CC_1 and CC_2) and two voltage buffers (VBs). In Fig. 3(a) the CC_1 section is classical CCII with cascoded mirrors [63–65]. The core of the CC_2 , shown in Fig. 3(b), is based on modified CCII with additional mirrors for current gain control, which was introduced in [60–63]. In Fig. 3(c), the last part of DCC-CFA, the voltage buffer employing two classical transconductance sections is shown [65,66]. The supply voltages of DCC-CFA were chosen as ± 2.5 V.

The input intrinsic resistance of CC_1 stage is given by the following equation

$$R_X \approx \frac{1}{g_{m_M54} + g_{m_M56}} = \frac{1}{\sqrt{2KP_N \left(\frac{W_{M54}}{L_{M54}}\right) I_{set_RX} + \sqrt{2KPP \left(\frac{W_{M56}}{L_{M56}}\right) I_{set_RX}}}}, \quad (2)$$

where W and L are the channel width and length, respectively, and $KP = \mu_0 C_{OX}$ (μ_0 is carrier mobility, C_{OX} is the gate-oxide capacitance per unit area) for the used CMOS ON-Semi C5 0.5 μm technology model (LOT: T22Y_TT, WAF: 3104) [67]. The dimensions of the MOS transistors used in the DCC-CFA implementation are listed in Tab. 1 (CC_1 and CC_2 stages) and Tab. 2 (voltage buffer), respectively.

The current gain control of DCC-CFA, which is implemented in the stage CC_2 shown in Fig. 3(b), is done by special current mirrors formed by group of transistors Q_1 – Q_{12} for purposes of electronic adjustability. Moreover, in comparison with PNP types of transistors, NPN types have much better properties in particular technology, and therefore, design is done with NPN types only. In the simulations the commercially available models of ultra high frequency transistor arrays Intersil HFA 3096 were used [68]. Applying the translinear principle [20,60,61,69–71] and assuming that all transistors are well matched with the common-emitter current gains

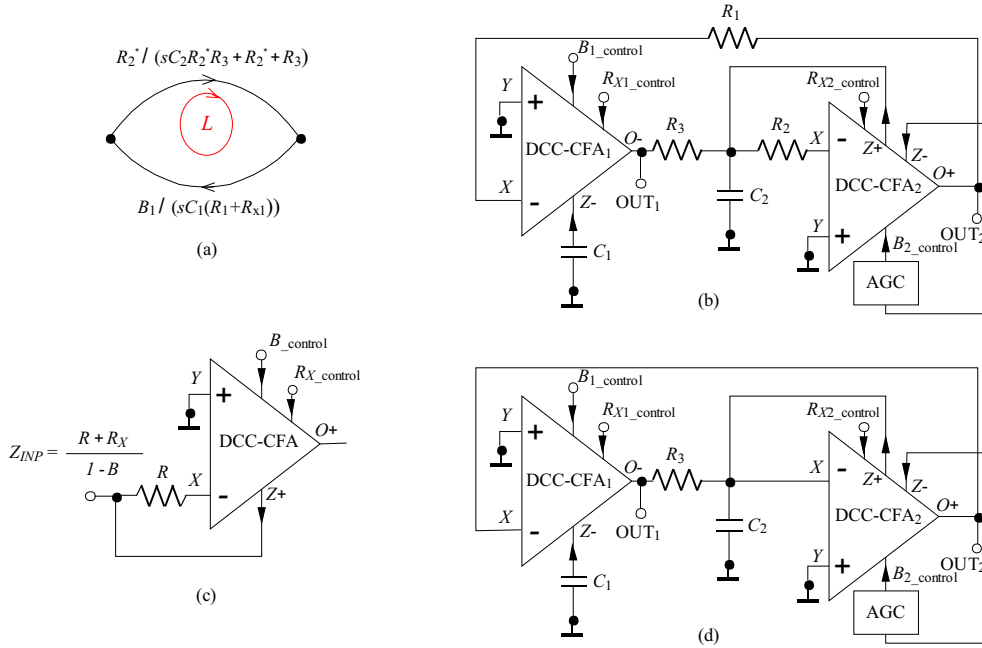


Fig. 4. (a)– signal flow graph of the proposed oscillator, (b) – the proposed oscillator, (c) – controllable negative resistance based on DCC-CFA, (d) – minimal realization of proposed oscillator using intrinsic resistances of current inputs

$h_{21e} \gg 1$, then the relationship of the collector currents can be characterized by the following equations

$$\prod_{n \in CW} I_n = \prod_{n \in CCW} I_n, \quad (3)$$

$$I_{C-Q5} I_{C-Q2} = I_{C-Q3} I_{C-Q6}, \quad (4)$$

$$I_{C-Q11} I_{C-Q8} = I_{C-Q9} I_{C-Q12}, \quad (5)$$

where CW means clockwise and CCW counter clockwise direction of calculation in translinear approach. In (4) and (5) I_{C-Q5} and I_{C-Q11} are input currents of the so-called “gain producing bipolar section” and I_{C-Q6} and I_{C-Q12} are the output currents. According to the previous statement, (4) and (5) can be express as

$$I_{in} I_{C-Q2} = I_{C-Q3} I_{out}, \quad I_{in} I_{C-Q8} = I_{C-Q9} I_{out}. \quad (6)$$

Assuming that $I_{C-Q2} = I_{C-Q8} = I_{set_B}$ and $I_{C-Q3} = I_{C-Q9} = I_a$, the current gain can be calculated as follows

$$B \approx \frac{I_{out}}{I_{in}} = \frac{I_{C-Q8}}{I_{C-Q9}} = \frac{I_{C-Q2}}{I_{C-Q3}} = \frac{I_{set_B}}{I_a}. \quad (7)$$

From (7), it is evident that the current gain can be easily controlled by either I_{set_B} and/or I_a .

3 OSCILLATOR DESIGN WITH TWO WAYS OF FO AND CO TUNING

There are many approaches leading to synthesis of oscillators in current technical literature [72]. As an example, loop and multi-loop integrator systems, autonomous circuit nodal analysis, or the state variable method can be

mentioned [34, 37, 46]. Here proposed quadrature oscillator is based on very common approach employing integrators in the loop. The signal flow graph (SFG) of proposed oscillator and the corresponding circuit employing two DCC-CFAs and five passive elements is shown in Figs. 4(a) and (b), respectively. It is based on loop feedback system with one lossless voltage integrator (DCC-CFA₁, R_1 , and C_1) and passive lossy voltage integrator (PLVI), which is formed by R_3 and C_2 . In addition, the PLVI requires a negative resistance that is realized by another current amplifier included in frame of the DCC-CFA₂, as it is shown in Fig. 4(c).

The determinant of SFG [73] for the oscillator from Fig. 4(b) is shown in Fig. 4(a) and has a form

$$\Delta = 1 - \left[\frac{-B_1}{sC_1(R_1 - R_{X1})} \frac{R_2^*}{sC_2 R_2^* R_3 + R_2^* + R_3} \right] = 0, \quad (8)$$

where R_2^* represents a negative resistance given by

$$R_2^* = \frac{R_2 + R_{X2}}{1 - B_2}. \quad (9)$$

By substituting (9) into (8) we obtain the characteristic equation (CE) of the circuit in the following simple form

$$\text{CE: } s^2 + s \frac{R_3 + (R_2 + R_{X2}) - R_3 B_2}{R_2 R_3 C_2} + \frac{B_1}{R_3 C_1 C_2 (R_1 + R_{X1})} = 0, \quad (10)$$

where the condition of oscillation and the frequency of oscillation are

$$\text{CO: } B_2 \geq \frac{R_3 + (R_2 + R_{X2})}{R_3}, \quad (11)$$

$$\text{FO: } \omega_0 = \sqrt{\frac{B_1}{R_3 C_1 C_2 (R_1 + R_{X1})}}. \quad (12)$$

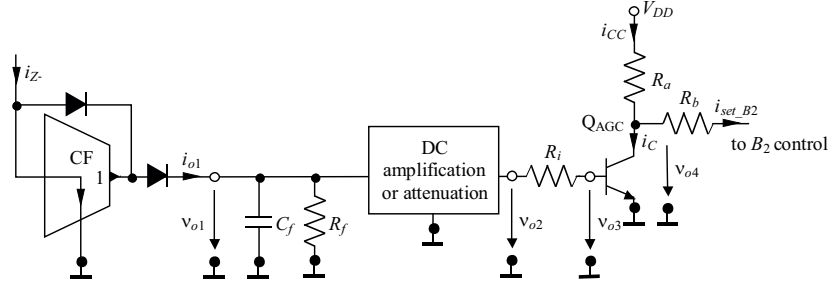


Fig. 5. Detailed AGC circuit

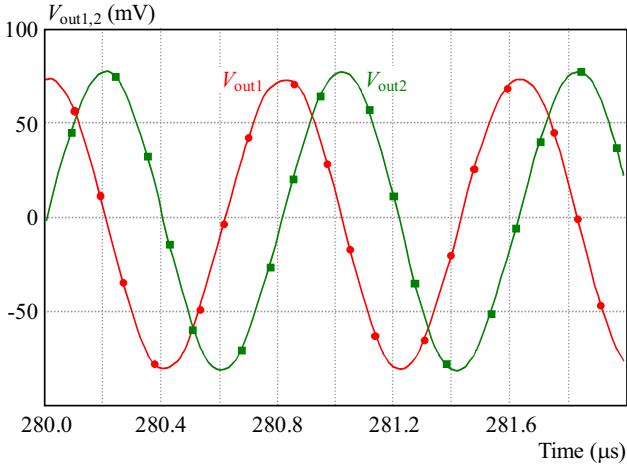


Fig. 6. Stable state output oscillations

From (11) and (12) it can be seen that in ideal case the CO and FO are independently adjustable by current gains of DCC-CFAs. Moreover, the FO can be adjustable by floating resistor R_1 , therefore, this oscillator can also be added to the group of oscillators referred as SRCO types. Unfortunately, the replacement or adjusting of floating element can be complicated. Therefore, in our case we can also use intrinsic resistance control of DCC-CFA (R_X), which allows tuning by very simple way. Assuming that the current gain of DCC-CFA₁ is equal to 1 (fixed gain), the FO in (12) turns to

$$\text{FO: } \omega_0 = \sqrt{\frac{1}{R_3 C_1 C_2 [R_1 + R_X (I_{\text{set_RX}})]}}. \quad (13)$$

The equivalent minimal oscillator circuit is shown in Fig. 4(d) in case of only internal intrinsic resistances R_{X1}, R_{X2} ($R_1 = R_2 = 0$) and one external R_3 are considered.

The relative sensitivities of the frequency of oscillation (12) on circuit parameters can be calculated as

$$S_{R_1}^{\omega_0} = -0.5 \frac{R_1}{R_1 + R_{X1}}, \quad S_{R_{X1}}^{\omega_0} = -0.5 \frac{R_{X1}}{R_1 + R_{X1}}, \quad (14)$$

$$S_{R_3, C_1, C_2}^{\omega_0} = -S_{B_1}^{\omega_0} = -0.5, \quad S_{B_2, R_{X2}, R_2}^{\omega_0} = 0.$$

Equation (14) indicates that the ω_0 passive and active sensitivities are equal or not higher than 0.5 in absolute value, and hence, the circuit exhibits an attractive sensitivity performance.

4 SIMULATION RESULTS

In this Section, results concerning oscillator from Fig. 4(b), *ie* time domain, tuning properties and quality of produced signal are presented. Input resistances $R_{X1,2}$ were set to 760Ω ($I_{\text{set_RX}} = 50 \mu\text{A}$). External resistors have values 200Ω , therefore real values of $(R_1 + R_{X1})$ and $(R_2 + R_{X2})$ can be considered as 960Ω . The proposed oscillator is also able to operate without external resistors, as it is shown in Fig. 4(d). However, the analyses showed that the solution with external resistors of small values is better in THD. Therefore, the usage of external resistors R_1 and R_2 is matter of spectral quality of generated waveform. The current transfer $B_1 = 0.8$ is set by $I_{\text{set_B1}} = 40 \mu\text{A}$. To fulfill the CO in (11) and to start the oscillation, the $B_2 \geq 2$ must be satisfied, which corresponds in the ideal case to $I_{\text{set_B2}} \geq 100 \mu\text{A}$.

Since we expect wider range of electronic tuning of FO, stable output level, and lower THD, a precise automatic amplitude gain control circuit (AGC) implementation (Fig. 4(b)) is necessary. In low-voltage CMOS and BiCMOS technologies there is always problem with linearity and amplitude of output signal, which is quite small (tens - hundreds mV maximally). The implementation of AGC is quite easy, since the CO is controlled by B_2 parameter. Theoretically, the rectified output voltage is able to control B_2 , but here proposed and similar types of oscillators provides output amplitude with several tens or hundreds of mV. Hence, before the rectification a sufficiently larger level amplification (several times) is necessary. Subsequently, the used amplifier before rectification must have great frequency features and also great slew rate. Such conception is better for higher output oscillation level, where pre-amplification (before rectifier) is not necessary. Therefore, we utilized the current-mode rectifier (based on current follower [74]) as it is shown in Fig. 5. We engaged unused (grounded in practice) current output Z- of DCC-CFA₂ in this case. The current follower in Fig. 5 was modeled by the diamond transistor OPA860 [75]. An advantage of this rectifier is in precise rectification suitable for low current amplitudes (tens of μA). In the simulations, the BAS70 [76] high speed diode with minimal threshold voltage and short recovery time was used, which provides low output amplitudes.

Figure 6 shows the output oscillation at both outputs for $B_1 = 0.8$ ($I_{\text{set_B1}} = 40 \mu\text{A}$). Oscillator pro-

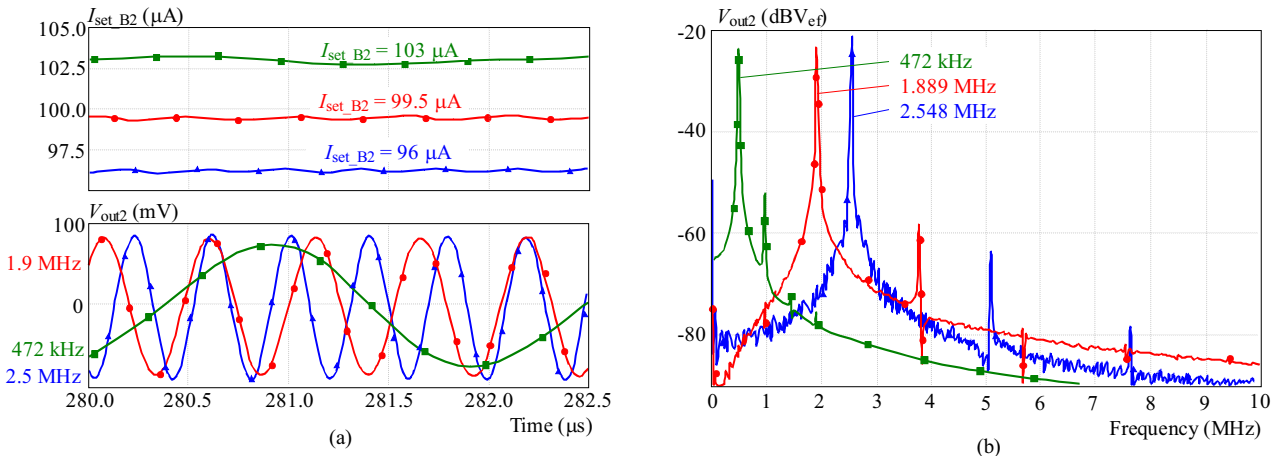


Fig. 7. (a) Tuning process observed on OUT₂ and corresponding AGC response, (b) spectrum of OUT₂ output oscillations

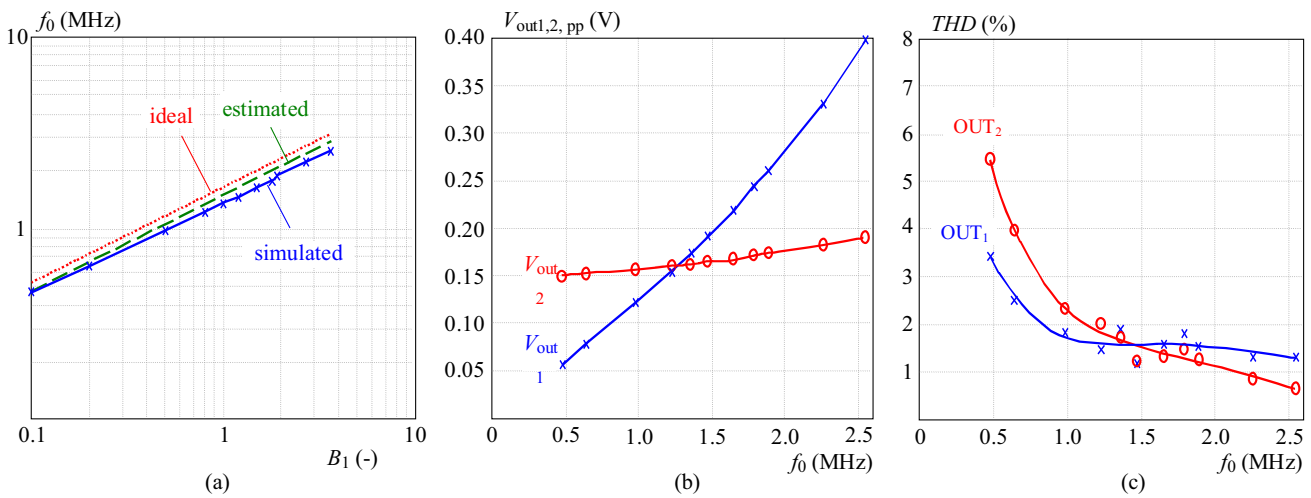


Fig. 8. Current gain control of oscillation frequency: (a) – dependence of FO on controlled current gain B_1 , (b) – dependence of output amplitudes on frequency of oscillation, (c) – THD versus oscillation frequency

duces quadrature outputs (see SFG in Fig. 4(a) – relation between outputs) in steady state operation. Simulations provided oscillation frequency 1.23 MHz. Theoretical value is 1.45 MHz. Considering the parasitic influences of the circuit, the obtained frequency of oscillation is 1.32 MHz for both outputs with amplitudes about 160 mV peak-to-peak.

4.1 FO control via current gain

The first way of control the FO of the oscillator from Fig. 4(b) is via current gain B_1 (I_{set_B1}). The output level of V_{OUT2} achieved values between 150-190 mV peak-to-peak, in the tuning range approximately from 470 kHz to 2.5 MHz for B_1 from 0.1 to 3.6. Figure 7 shows three output waveforms for different oscillation frequencies together with corresponding responses of AGC (I_{set_B2}) on change of output amplitude and spectrum of V_{OUT2} . The output V_{OUT1} changed voltage level rapidly from 56 to 400 mV, peak-to-peak (in the same frequency range of FO adjusting). The difference between the approximately determined, when small-signal parasitic influences C_p of DCC-CFA are considered and simulated FO is caused by

non-ideal properties of active elements used and nonlinearity of B control. Figure 8 shows graphical representations of the obtained results *ie* dependence of FO on B_1 , dependence of output level on FO, and THD versus FO, respectively. Obtained results are in good agreement with theory. Better results can be obtained by more careful CO and AGC settings. However, due to complex DCC-CFA transistor model, the optimization of oscillator parameters is time consuming.

4.2 FO control by intrinsic resistance

In case of the second possibility of FO control, the FO, given by (13), can be easily controlled by means of control current I_{set_RX1} of DCC-CFA₁. The dependences of FO on R_{X1} and dependences of output amplitudes on FO are shown in Fig. 9, respectively. Output level of V_{OUT2} is greater than in previous case of control, *ie* between 160–175 mV peak-to-peak. The output signal level of V_{OUT1} is changed in narrower range from 110 to 260 mV_{P-P}. However, the tunability range is narrower than in previous case and it is approximately from

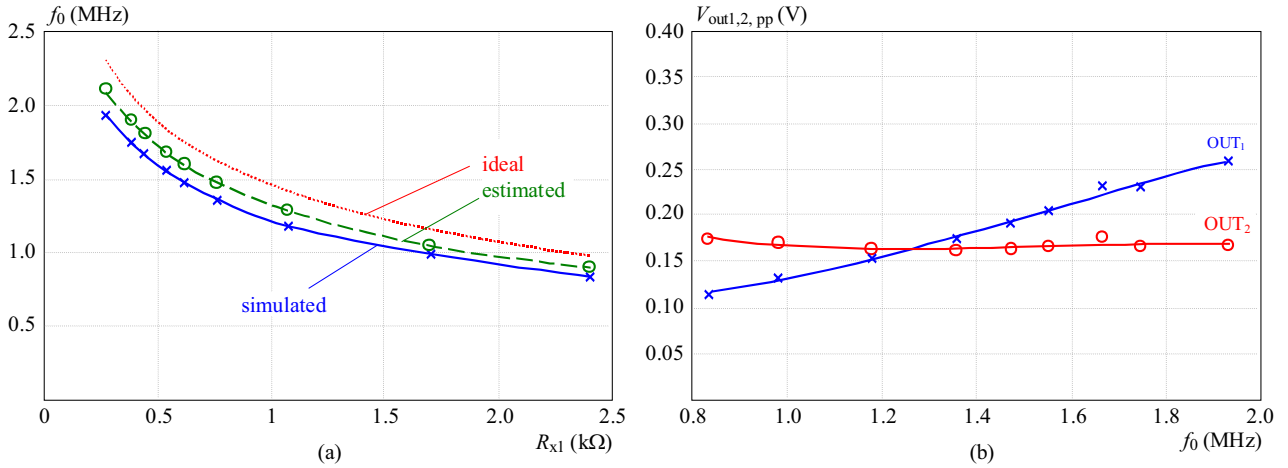


Fig. 9. Intrinsic resistance control of oscillation frequency: (a) – dependence of frequency of oscillation on intrinsic resistance, (b)– dependence of output amplitudes on frequency of oscillation

830 kHz to 1.93 MHz. The THD values are close to the THD of the first type of adjusting.

5 DISCUSSION

First type of electronic control of frequency of oscillation via B_1 is suitable for wider range of tuning. Results show that the frequency is tunable approximately from 470 kHz to 2.5 MHz. The AGC system defends oscillator against large fluctuations or outages of output amplitudes, however, in direction to higher frequencies it still brings small (40 mV) change of V_{OUT2} amplitude. The second variant of electronic control by intrinsic resistance R_X is suitable for shorter range of adjusting with better stability of the output level (V_{OUT2}) in the range of interest. In this case the variance of V_{OUT2} is only about 15 mV and, in comparison to B_1 control of FO, the range of oscillation frequency adjusting is approximately two times narrower, *ie* from 830 kHz to 1.93 MHz. This weakness is given by the constraining technological limits of R_X caused by smaller and restricted changes of R_X (range between saturation and linear region of transistors). The effect of R_X on frequency of oscillation is also determined by sensitivity of R_X on FO that is decreasing, if $R_1 \gg R_{X1}$. In both cases the THD is comparable. If simultaneous adjusting of both parameters in Fig. 4(b) (B_1 and also R_X) is applied, it allows spreading of FO range from 283 kHz ($I_{set_B1} = 5 \mu A$, $I_{set_RX} = 5 \mu A$) to 3.48 MHz ($I_{set_B1} = 200 \mu A$, $I_{set_RX} = 400 \mu A$), and also linear control of FO (if B_1 and $(R_1 + R_{X1})$ ratio keeps preserved).

Analyzing of (12) from Fig. 4(a) and assuming that $C_1 = C_2 = C$, the relation between V_{OUT2} and V_{OUT1} can be given as

$$V_{OUT1} = V_{OUT2} \sqrt{B_1 \frac{R_3}{(R_1 + R_{X1})}}. \quad (15)$$

From (15) it is evident that the output voltage level at OUT_1 (V_{OUT1}) is dependent on current gain B_1 ,

which affects the frequency of oscillation. Moreover, the V_{OUT1} is also dependent on $(R_1 + R_{X1})$, which appears in DCC-CFA₁ based lossless integrator unit and both amplitudes (V_{OUT1} and V_{OUT2}) are unchangeable (or even equal) during the tuning process if invariant ratio of B_1 and $(R_1 + R_{X1})$ is ensured.

6 CONCLUSION

In this paper, easy construction of oscillator with mutually independent control of frequency of oscillation and condition of oscillation was demonstrated. Used approach employs standard loop integrator system with controllable negative resistance based double current controlled CFAs. Advantage of introduced specific modification of CFA in signal processing and electronically tunable applications is clear. Proposed ABB allows current gain and internal (intrinsic) resistance control simultaneously. The proposed oscillator in minimal configuration employs three passive elements and it is tunable by current gain (B) or by internal resistance (R_X), both controlled by auxiliary DC control currents. The full realization of the oscillator with five passive elements belongs to the category of the so-called SRCO types, because FO control is also allowed by external floating resistor R_1 . The tunability range was verified by simulations from 283 kHz to 3.48 MHz by both ways of the electronic FO control simultaneously. For stable output voltage levels and wider range of frequency tuning, a precise AGC system was designed. Amplitudes of output oscillations and total harmonic distortion are adequate to the used low voltage technology, low dynamic ranges of used active elements and quality of AGC circuit. Advantages of proposed solution are the following: sufficient range of tunability with possible extension by two types of FO control, possibility of linear control of FO, possibility of operation with equal amplitudes, grounded capacitors, easy final construction, and low sensitivities on passive components. Theoretical study was confirmed by detailed SPICE simulations.

Acknowledgments

Research described in the paper was supported by Czech Science Foundation projects under No. 102/11/P489 and No. 102/09/1681. The support of the project CZ.1.07/2.3.00/20.0007 WICOMT, financed from the operational program Education for competitiveness, is gratefully acknowledged. The described research was performed in laboratories supported by the SIX project; the registration number CZ.1.05/2.1.00/03.0072, the operational program Research and Development for Innovation. Dr. Norbert Herencsár was supported by the project CZ.1.07/2.3.00/30.0039 of Brno University of Technology.

Part of this work was done while Ms. Aslihan Kartci was on Erasmus training mobility at the Brno University of Technology, Czech Republic.

REFERENCES

- [1] BIOLEK, D.—SENANI, R.—BIOLKOVA, V.—KOLKA, Z.: Active Elements for Analog Signal Processing: Classification, Review, and New Proposals.
- [2] GEIGER, R. L.—SANCHEZ-SINENCIO, E.: Active Filter Design using Operational Transconductance Amplifiers: A Tutorial, *IEEE Circuits and Devices Magazine* **1** (1985), 20–32.
- [3] BIOLEK, D.—BIOLKOVA, V.—KOLKA, Z.: Universal Current-Mode OTA-C KHN Biquad.
- [4] FABRE, A.—SAAID, O.—WIEST, F.—BOUCHERON, C.: High Frequency Applications Based on a New Current Controlled Conveyor.
- [5] TANGSRIRAT, W.: Current-Tunable Current-Mode Multifunctional Filter Based on Dual-Output Current-Controlled Conveyors, *AEU – International Journal of Electronics and Communications* **61** No. 8 (2007), 528–533, doi:10.1016/j.aeue.2006.09.005..
- [6] ZEKI, A.—TOKER, A.: The Dual-X Current Conveyor (DXCCII): A New Active Device for Tunable Continuous-Time Filters, *International Journal of Electronics* **89** (2002), 913–923.
- [7] KACAR, F.—METIN, B.—KUNTMAN, H.: A new CMOS Dual-X Second-Generation Current Conveyor (DXCCII) with an FDNR Circuit Application, *AEU – International Journal of Electronics and Communications* (2009), DOI: 10.1016/j.aeue.2009.05.007.
- [8] SOLIMAN, A. M.: New Fully-Differential CMOS Second-Generation Current Conveyor, *ETRI Journal* **28** No. 4 (2006), 495–501.
- [9] METIN, B.—HERENCsAR, N.—PAL, K.: Supplementary First-Order All-Pass Filters with Two Grounded Passive Elements using FDCCII, *Radioengineering* **20** No. 2 (2011), 433–437.
- [10] SVOBODA, J. A.—McGORY, L.—WEBB, S.: Applications of a Commercially Available Current Conveyor, *Int. Journal of Electronics* **70** No. 1 (1991), 159–164.
- [11] SIRIPRUCHYANUN, M.—CHANAPROMMA, C.—SILAPAN, P.—JAIKLA, W.: BiCMOS Current-Controlled Current Feedback Amplifier (CC-CFA) and its Applications, *WSEAS Transactions on Electronics* **6** No. 5 (2008), 203–219.
- [12] YUCE, E.—MINAEI, S.: A Modified CFOA and its Applications to Simulated Inductors, Capacitance Multipliers, and Analog Filters, *IEEE Transaction on Circuits and Systems–I* **55** No. 1 (2008), 266–275.
- [13] ACAR, C.—OZOGUZ, S.: A new Versatile Building Block: Current Differencing Buffered Amplifier, *Microelectronics Journal* **30** (1999), 157–160.
- [14] KESKIN, A. U.: A Four Quadrant Analog Multiplier Employing Single CDBA, *Analog Integrated Circuits and Signal Processing* **40** (2004), 99–101.
- [15] BIOLEK, D.: CDTA – Building Block for Current-Mode Analog Signal Processing, In *Proceedings of the 16th European Conference on Circuit Theory and Design (ECCTD 2003)*, Krakow, Poland, 2003, pp. 397–400.
- [16] KESKIN, A. U.—BIOLEK, D.—HANCIOGLU, E.—BIOLKOVA, V.: Current-Mode KHN Filter Employing Current Differencing Transconductance Amplifiers, *AEU – Int. J. Electronics and Communications* **60** No. 6 (2006), 443–446, DOI: 10.1016/j.aeue.2005.09.003.
- [17] HERENCsAR, N.—KOTON, J.—VRBA, K.: Realization of Current-Mode KHN-Equivalent Biquad using Current Follower Transconductance Amplifiers (CFTAs), *IEICE Transaction on Fundamentals* **E93–A** No. 10 (2010), 1816–1819.
- [18] HERENCsAR, N.—VRBA, K.—KOTON, J.—LAHIRI, A.: Realisations of Single-Resistance-Controlled Quadrature Oscillators using Generalised Current Follower Transconductance Amplifier and Unity-Gain Voltage-Follower, *International Journal of Electronics* **97** No. 8 (2010), 897–906.
- [19] KOTON, J.—VRBA, K.—HERENCsAR, N.: Tuneable Filter using Voltage Conveyors and Current Active Elements, *International Journal of Electronics* **96** No. 8 (2009), 787–794.
- [20] HERENCsAR, N.—LAHIRI, A.—VRBA, K.—KOTON, J.: An Electronically Tunable Current-Mode Quadrature Oscillator using PCAs, *International Journal of Electronics* **99** No. 5 (2012), 609–621.
- [21] JERABEK, J.—VRBA, K.: Fully Differential Universal Filter with Differential and Adjustable Current Followers and Transconductance Amplifiers, In *Proceeding of the 33rd International Conference on Telecommunications and Signal Processing – TSP10*, Baden near Vienna, Austria, 2010, pp. 5–9.
- [22] VAINIO, O.—OVASKA, S. J.: A Class of Predictive Analog Filters for Sensor Signal Processing and Control Instrumentation, *IEEE Transactions on Industrial Electronics* **44** No. 4 (1997), 565–578.
- [23] SAMITIER, J.—PUIG-VIDAI, M.—BOTA, S. A.—RUBIO, C.—SISKOS, S. K.—LAPOULOS, T.: A Current-Mode Interface Circuit for a Piezoresistive Pressure Sensor, *IEEE Transactions on Instrumentation and Measurement* **47** No. 3 (1998), 708–710.
- [24] FERRI, G.—GUERRINI, N. C.: *Low-Voltage Low-Power CMOS Current Conveyors*, Kluwer Acad. Publ., London, 2003.
- [25] UYGUR, A.—KUNTMAN, H.: Seventh-Order Elliptic Video Filter with 0.1 dB Pass Band Ripple Employing CMOS CDTAs, *AEU – International Journal of Electronics and Communications* **61** No. 5 (2007), 320–328.
- [26] LO, T. Y.—KAO, C. S.—HUNG, C. C.: A Gm-C Continuous-Time Analog Filter for IEEE 802.11 a/b/g/n Wireless LANs, *Analog Integrated Circuits and Signal Processing* **58** No. 3 (2009), 197–204.
- [27] FABRE, A.—SAAID, O.—WIEST, F.—BOUCHERON, C.: Low Power Current-Mode Second-Order Bandpass IF Filter, *IEEE Transactions on Circuits and Systems–II* **44** No. 6 (1997), 436–446.
- [28] RUDELL, J. C.—OU, J. J.—CHO, T. B.—CHIEN, G.—BRIANTI, F.—WELDON, J. A.—GREY, P.: A 1.9-GHz Wide-Band IF Double Conversion CMOS Receiver for Cordless Telephone Applications, *IEEE Journal of Solid-State Circuits* **32** No. 12 (1997), 2071–2088.
- [29] HORNG, J. W.: A Sinusoidal Oscillator using Current-Controlled Current Conveyors, *Int. Journal of Electronics* **88** No. 6 (2001), 659–664, DOI: 10.1080/00207210110044369.
- [30] LAHIRI, A.: Explicit-Current-Output Quadrature Oscillator using Second-Generation Current Conveyor Transconductance Amplifier, *Radioengineering* **18** No. 4 522–526 (2009).

- [31] HORNG, J. W.—LEE, H.—WU, J.: Electronically Tunable Third-Order Quadrature Oscillator using CDTAs, *Radioengineering* **19** No. 2 (2010), 326–330.
- [32] HERENC SAR, N.—KOTON, J.—VRBA, K.—LATTENBERG, I.: New Voltage-Mode Universal Filter and Sinusoidal Oscillator using Only Single DBTA, *International Journal of Electronics* **97** No. 4 (2010), 365–379, DOI: 10.1080/00207210903325229.
- [33] SOTNER, R.—JERABEK, J.—PETRZELA, J.—DOSTAL, T.—VRBA, K.: Electronically Tunable Simple Oscillator based on Single-Output and Multiple-Output Transconductor, *IEICE Electronics Express* **6** No. 20 (2009), s 1476–1482, DOI: 10.1587/elex.6.1476.
- [34] GUPTA, S. S.—SHARMA, R. K.—BHASKAR, D. R.—SENANI, R.: Sinusoidal Oscillators with Explicit Current Output Employing Current-Feedback op-amps, *International Journal of Circuit Theory and Applications* **38** No. 2 (2010), 131–147, DOI: 10.1002/cta.531.
- [35] GUPTA, S. S.—BHASKAR, D. R.—SENANI, R.: New Voltage Controlled Oscillators using CFOAs, *AEU – International Journal of Electronics and Communications* **63** No. 3 (2009), 209–217, DOI:10.1016/j.aeue.2008.01.002.
- [36] LAHIRI, A.—JAIKLA, W.—SIRIPRUCHYANUN, M.: Explicit-Current-Output Second-Order Sinusoidal Oscillators using Two CFOAs and Grounded Capacitors, *AEU – International Journal of Electronics and Communications* **65** No. 7 (2011), 669–672, DOI: 10.1016/j.aeue.2010.09.003.
- [37] BHASKAR, D. R.—SENANI, R.: New CFOA-Based Single-Element-Controlled Sinusoidal Oscillators, *IEEE Transaction on Instrumentation and Measurement* **55** No. 6 (2006), 2014–2021, DOI:10.1109/TIM.2006.884139.
- [38] HERENC SAR, N.—LAHIRI, A.—KOTON, J.—VRBA, K.: VM and CM Quadrature Sinusoidal Oscillators using Commercially Available Active Devices, In *Proceedings of International Conference on Applied Electronics 2010, Pilsen, Czech Republic, 2010*, pp. 125–128.
- [39] LAHIRI, A.—GUPTA, M.: Realizations of Grounded Negative Capacitance using CFOAs, *Circuits, Systems and Signal Processing* **30** No. 1 (2011), 134–155, DOI: 10.1007/s00034-010-9215-3.
- [40] LAHIRI, A.: Current-Mode Variable Frequency Quadrature Sinusoidal Oscillator using Two CCs and Four Passive Components Including Grounded Capacitors, *Analog Integrated Circuits and Signal Processing* **68** No. 1 (2011), 129–131, DOI: 10.1007/s10470-010-9571-8.
- [41] JERABEK, J.—SOTNER, R.—VRBA, K.: Fully-Differential Current Amplifier and its Application to Universal and Adjustable Filter, In *Proceedings of International Conference on Applied Electronics 2010, Pilsen, Czech Republic, 2010*, pp. 141–144.
- [42] MINAEI, S.—SAYIN, O. K.—KUNTMAN, H.: A New CMOS Electronically Tunable Current Conveyor and its Application to Current-Mode Filters, *IEEE Transaction on Circuits and Systems-I* **53** No. 7 (2006), 1448–1457, DOI: 10.1109/TCSI.2006.875184.
- [43] MARCELLIS, A.—FERRI, G.—GUERRINI, N. C.—SCOTTI, G.—STORNELLI, V.—TRIFILETTI, A.: The VGC-CCII: a Novel Building Block and its Application to Capacitance Multiplication, *Analog Integrated Circuits and Signal Processing* **58** No. 1 (2009), 55–59, DOI: 10.1007/s10470-008-9213-6.
- [44] SOTNER, R.—HRUBOS, Z.—SLEZAK, J.—DOSTAL, T.: Simply Adjustable Sinusoidal Oscillator based on Negative Three-Port Current Conveyors, *Radioengineering* **19** No. 3 (2010), 446–453.
- [45] SOTNER, R.—SEVCIK, B.—SLEZAK, J.—PETRZELA, J.—BRANCIK, L.: Sinusoidal Oscillator based on Adjustable Current Amplifier and Diamond Transistors with Buffers, *Przegład Elektrotechniczny (Electrical Review)* **87** No. 1 (2011), 266–270.
- [46] SOLIMAN, A. M.: Current Feedback Operational Amplifier Based Oscillators, *Analog Integrated Circuits and Signal Processing* **23** No. 1 (2000), 45–55, DOI: 10.1023/A:1008391606459.
- [47] SINGH, V. K.—SHARMA, R. K.—SINGH, A. K.—BHASKAR, D. R.—SENANI, R.: Two New Canonic Single-CFOA Oscillators with Single Resistor Controls, *IEEE Transaction on Circuits and Systems-II* **52** No. 12 860–864 (2005), DOI: 10.1109/TC-SII.2005.853964.
- [48] SENANI, R.—SINGH, V. K.: Novel Single-Resistance-Controlled Oscillator Configuration using Current Feedback Amplifiers, *IEEE Transactions on Circuits and Systems-I* **43** No. 8 (1996), 698–700, DOI: 10.1109/81.526688.
- [49] MARTINEZ, P. A.—SABADELL, J.—ALDEA, C.: Grounded Resistor Controlled Sinusoidal Oscillator using CFOAs, *Electronics Letters* **33** No. 5 (1997), 346–348, DOI: 10.1049/el:19970229.
- [50] SHEN-IUAN, L.—JIANN-HORNG, T.: Single-Resistance-Controlled Sinusoidal Oscillator using Current-Feedback-Amplifiers, *International Journal of Electronics* **80** No. 5 (1996), 661–664, DOI: 10.1080/002072196137101.
- [51] CELMA, S.—CARLOSENA, A.—MARTINEZ, P. A.: High-Quality Sinusoidal Oscillator using Current Feedback Amplifiers, In *Instrumentation and Measurement Technology Conference - IMTC93, 1993*, pp. 741–744, DOI: 10.1109/IMTC.1993.382545.
- [52] CELMA, M.—MARTINEZ, P. A.—SABADELL, J.: On the Design of CFA-Based Sinusoidal Oscillators, In *Proceedings of the 20th International Conference on Microelectronics - MIEL95, 1995*, pp. 731–736, DOI: 10.1109/ICMEL.1995.500958.
- [53] SENANI, R.—GUPTA, S. S.: Synthesis of Single-Resistance-Controlled Oscillators using CFOAs: Simple State-Variable Approach, *IEE Proceedings on Circuits Devices and Systems* **144** No. 2 (1997), 104–106, DOI: 10.1049/ip-cds:19971006.
- [54] GUPTA, S. S.—SENANI, R.: State Variable Synthesis of Single Resistance Controlled Grounded Capacitor Oscillators using only Two CFOAs, *IEE Proceedings on Circuits, Devices and Systems* **145** No. 2 (1998), 135–138, DOI: 10.1049/ip-cds:19981667.
- [55] ABUELMAATTI, M. T.: New Two CFOA-Based Sinusoidal RC Oscillator with Buffered Outlet, *Analog Integrated Circuits and Signal Processing* **66** No. 3 (2011), 475–482, DOI: 10.1007/s10470-010-9582-5.
- [56] GUNES, E. O.—TOKER, A.: On the Realization of Oscillators using State Equations, *AEU – International Journal of Electronics and Communications* **56** No. 5 (2002), 317–326, DOI: 10.1078/1434-8411-54100119.
- [57] BHASKAR, D. R.—SENANI, R.—SINGH, A. K.—GUPTA, S. S.: Two Simple Analog Multiplier Based Linear VCOs using Single Current Feedback op-amp, *Circuit and Systems* **1** No. 1 (2010), 1–4, DOI: 10.4236/cs.2010.11001.
- [58] BHASKAR, D. R.—SENANI, R.—SINGH, A. K.: Linear Sinusoidal VCOs: New Configurations using Current-Feedback op-amps, *Int. Journal of Electronics* **97** No. 3 (2010), 263–272, DOI: 10.1080/00207210903286173.
- [59] SENANI, R.—SHARMA, R. K.: Explicit-Current-Output Sinusoidal Oscillators Employing Only a Single Current-Feedback op-amp, *IEICE Electronics Express* **2** No. 1 (2004), 14–18, DOI: 10.1587/elex.2.14.
- [60] TANGSRIRAT, W.—UNHAVANICH, S.—DAMAWIPATA, T.: FTFN with Variable Current Gain, In *Proceedings of the 10th International Conference on Electrical and Electronic Technology - TENCON01, 2001*, pp. 209–212, DOI: 10.1109/TENCON.2001.949582.
- [61] TANGSRIRAT, W.: Electronically Tunable Multi-Terminal Floating Nullor and its Application, *Radioengineering* **17** No. 4 (2008), 3–7.

- [62] KUMNGERN, M.—CHANWUTIUM, J.—DEJHAN, K.: Electronically Tunable Multiphase Sinusoidal Oscillator using Translinear Current Conveyors, *Analog Integrated Circuits and Signal Processing* **65** No. 2 (2010), 327–334.
- [63] TOUMAZOU, C.—LIDGEY, F. J.—HAIGH, D. G.: *Analog IC design: The current mode approach*, Peter Peregrinus Ltd, London, 1990.
- [64] ELDBIB, I, MUSIL, V.: Self-Cascoded Current Controlled CCII Based-Tunable Band Pass Filter, In *Proceedings of the 18th International Conference Radioelektronika 2008*, 2008, pp. 1–4, DOI: 10.1109/RADIOELEK.2008.4542706.
- [65] BAKER, J.: *CMOS Circuit Design, Layout and Simulation*, IEEE Press Series on Microelectronic Systems, 2005.
- [66] PROKOP, R.: *Modular Approach to Design of Modern Analog Devices in CMOS Technology*, 2009, PhD thesis, Dept. of Microelectronics FEED BUT Brno, Czech Republic.
- [67] The Mosis Service, ON-Semi C5 0.5 μ m Wafer Electrical Test Data and SPICE Model Parameters, available on www [online 16.4.2011]: http://www.mosis.com/Technical/Testdata/ami_c5n_corner_bsim3.txt.
- [68] Linear Technology, Ultra high frequency transistor arrays HFA 3046/3096/3127/3128, datasheet, 1–13 (2005), available on www [online 16.4.2011]: <http://www.intersil.com/products/deviceinfo.asp?pn=HFA3096>.
- [69] GILBERT, B.: Translinear Circuits: a Historical Overview, *Analog Integrated Circuits and Signal Processing* **9** No. 2 (1996), 95–118, DOI: 10.1007/BF00166408.
- [70] BRADLEY, A.: MOS Translinear Principle for All Inversion Levels, *IEEE Transaction on Circuits and Systems-II* **55** No. 2 (2008), 121–125, DOI: 10.1109/TCSII.2007.910904.
- [71] SHU-XIANGS.—GUO-PING, Y.—HUA, C.: A New CMOS Electronically Tunable Current Conveyor Based on Translinear Circuits, In *Proceeding of 7th International Conference on ASIC - ASICON07*, 2007, pp. 569–572, DOI: 10.1109/ICA-SIC.2007.4415694.
- [72] CHEN, W. K.: *The Circuits and Filters Handbook*, CRC Press, Florida, 1995.
- [73] MASON, S. J.: Feedback Theory: Further Properties of Signal Flow Graphs, *Proc. IRE* **44** No. 7 (1956), 920–926.
- [74] TANGSRIRAT, W.: Current Limiters using Single Current Follower and Applications to Precision Rectifiers, *Indian Journal of Pure and Applied Physics* **49** No. 4 (2011), 284–287.
- [75] Texas Instruments Wide-Bandwidth Operational Transconductance Amplifier and Buffer OPA 860, Datasheet, 1–3, 2008, available on www [online: 16.4.2011]: <http://focus.ti.com/docs/prod/folders/print/opa860.html>.
- [76] ST Microelectronics, BAS 70 – Small Signal Schottky Diodes, Datasheet, 1–4, 2001, available on www [online 16.4.2011]: http://www.datasheetcatalog.com/datasheets_pdf/B/A/S/7/BAS70-04.shtml.

Received 8 January 2012

Roman Šotner was born in Znojmo, Czech Republic, in 1983. He received the MSc and PhD degrees from Brno University of Technology, Czech Republic, in 2008 and 2012, respectively. Currently, he is a technical worker at the Department of Radio electronics, Faculty of Electrical Engineering and Communication, Brno University of Technology, Brno, Czech Republic. His interests are analogue circuits (active filters, oscillators, audio, etc), circuits in the current mode, circuits with direct electronic controlling possibilities especially and computer simulation.

Norbert Herencsár received MSc and PhD degrees in Electronics, Communication and Teleinformatics from Brno University of Technology, Czech Republic, in 2006 and 2010, respectively. Currently, he is an Assistant Professor at the Department of Telecommunications, Faculty of Electrical Engineering and Communication, Brno University of Technology, Brno, Czech Republic. From September 2009 through February 2010 he was an Erasmus exchange student with the Department of Electrical and Electronic Engineering, Bogazici University, Istanbul, Turkey. His research interests include analog filters, current-mode circuits, tunable frequency filter design methods, and oscillators. He is an author or co-author of about 75 research articles published in international journals or conference proceedings. Dr. Herencsár is a Member of IEEE, ACEEE, IAENG, and Senior Member of IACSIT.

Jan Jeřábek received the BSc, MSc and PhD degrees in Electrical Engineering from the Brno University of Technology, Czech Republic in 2005, 2007, and 2011, respectively. Currently, he is an Assistant Professor at the Department of Telecommunications. His research interests are focused on circuit applications of modern active elements such as current operational amplifiers and multiple-output current followers.

Radek Dvořák was born in Třebíč, Czech Republic. He received his MSc from Brno University of Technology in 2007. His research interests include alternative microwave measurement methods.

Aslihan Kartci is currently working toward the Bachelor of Engineering (BE) degree from the Department of Electronics & Telecommunication Engineering, Corlu Engineering Faculty, Namik Kemal University, and from September 2010 through February 2011 she was an Erasmus exchange student with the Faculty of Electrical Engineering and Communication of Brno University of Technology, Brno, Czech Republic. Her research interests include signal processing and telecommunications.

Tomáš Dostál received his PhD (1976) and DrSc degree (1989). He was with the University of Defense Brno (1976–1978 and 1980–1984), with the Military Technical College Baghdad (1978–1980), with the Brno University of Technology (1984–2008) and with the European Polytechnic Institute (2008–2009). Since 2009 he has been with the College of Polytechnics, Jihlava as Professor of Electronics. His interests are in circuit theory, analog filters, switched capacitor networks and circuits in the current mode.

Kamil Vrba received the PhD degree in Electrical Engineering in 1976, and the Prof. degree in 1997, both from the Technical University of Brno. Since 1990 he has been Head of the Department of Telecommunications, Faculty of Electrical Engineering and Computer Science, Brno University of Technology, Brno, Czech Republic. His research work is concentrated on problems concerned with accuracy of analog circuits and mutual conversion of analog and digital signals. In cooperation with AMI Semiconductor Czech, Ltd. (now ON Semiconductor Czech Republic, Ltd.) he has developed number of novel active function blocks for analog signal processing such as universal current conveyor (UCC), universal voltage conveyor (UVC), programmable current amplifier (PCA), digitally adjustable current amplifier (DACA), and others. He is an author or co-author of more than 700 research articles published in international journals or conference proceedings. Professor Vrba is a Member of IEEE and IEICE.

[6] SOTNER, R., LAHIRI, A., JERABEK, J., HERENC SAR, N., KOTON, J., DOSTAL, T., VRBA, K. Special Type of Three- Phase Oscillator Using Current Gain Control for Amplitude Stabilization. *International Journal of Physical Sciences*, 2012, vol. 7, no. 25, p. 3089-3098. ISSN: 1992-1950.

Review

Special type of three-phase oscillator using current gain control for amplitude stabilization

Roman Sotner^{1*}, Abhirup Lahiri², Jan Jerabek³, Norbert Herencsar³,
Jaroslav Koton³, Tomas Dostal^{1,4} and Kamil Vrba³

¹Department of Radio Electronics, Brno University of Technology, Purkynova 118, 612 00 Brno, Czech Republic.
²36-B, J and K Pocket, Dilshad Garden, Delhi, India.

³Department of Telecommunications, Brno University of Technology, Purkynova 118, 612 00 Brno, Czech Republic.

⁴Department of Electronics and Computer Science, College of Polytechnics Jihlava, Tolsteho 16, Jihlava 586 01, Czech Republic.

Accepted 18 June, 2012

The main aim of this work is to demonstrate the use of electronically controlled second-generation current conveyor in providing electronic control to the condition of oscillation (CO) of a new active RC sinusoidal oscillator. Electronic control of the CO, which is independently set and does not affect the oscillation frequency, is enabled by the use of an auxiliary amplitude control loop to regulate the amplitude and provide very good total harmonic distortion performance. The proposed oscillator employs only one standard second-generation current conveyor, one electronically controlled second-generation current conveyor, five passive elements and is capable of providing three voltage outputs having phase shifts 45 and 90°, if specific design requirements are fulfilled. Similar simple types of oscillators do not provide such features. Non-ideal analysis of the circuit has also been carried out and the proposed oscillator has been verified by both PSpice simulations and experimental measurements using commercially available integrated circuits.

Key words: Three-phase oscillator, special features, electronic control, electronically controllable current conveyor (ECCII), second generation current conveyor (CCII).

INTRODUCTION

The second generation current conveyor (CCII) (Sedra and Smith, 1970; Biolek et al., 2008) and its practical utilization (Svoboda et al., 1991) is a very popular active element for the realizations of variety of circuit solutions. However, active RC circuits based on CCII typically lack in inherent electronic control of the circuit parameters. Electronic control for such CCII based RC solutions is made possible by simulating resistor through metal-oxide-semiconductor field-effect transistor (MOSFET) in triode region and thereby creating a voltage-controlled-resistor. A unique way of creating electronically controlled RC circuits is to provide electronic control within the CCII,

which was first attempted by Surakampontrorn and Thitimahshima (1988) by creating the so called electronically controllable current conveyor (ECCII). ECCII has controllable current gain between X and Z terminals. One of the most recent Complementary metal-oxide-semiconductor (CMOS) implementations of the ECCII was presented by Minaei et al. (2006). To improve the features and adjustability other active elements were developed, that is, voltage gain controlled current conveyors (VGC-CCII) (Marcellis et al., 2009), that enables the gain control between X and Z terminals and furthermore the control of gain between Y and X terminals, and other active elements providing current-gain (Kumngern et al., 2010a; Tangsrirat, 2008; Koton et al., 2010). Biolek et al. (2008) also lists many active elements for direct electronic control of circuits, but many of them are only hypothetical and not commonly available

*Corresponding author. E-mail: sotner@feec.vutbr.cz. Tel: +420 541 149 140.

for designers without microelectronic technology and production.

As shown subsequently, ECCII is a very useful active element for the design of sinusoidal oscillators. It can provide direct electronic control of the frequency of oscillation (FO) and the condition of oscillation (CO) (Kumngern et al., 2010a; Sotner et al., 2011a, b, 2010). Electronic control of the FO is very useful for applications requiring variable frequency sources and frequency control on the fly. The control of CO can be very useful for applications requiring tight control of the amplitude of oscillation and having very tight total harmonic distortion (THD) requirements. Electronic control of the CO can be used to regulate the amplitude by sensing the peak of the amplitude and reducing the loop gain, thereby controlling the oscillation amplitude.

In this paper, a simple three-phase oscillator employing a single ECCII- and CCII+ is presented, wherein electronic control of the CO has been enabled using ECCII. Thus, the proposed oscillator is able to achieve very good THD performance. Due to the very large number of works dealing with controlled current (CC) based oscillators, it is impossible to discuss all the previously published results and we restrict this discussion to state-of-the-art solutions. It should be pointed out that many of the RC oscillators do not discuss the control mechanism and just state that the oscillation condition and oscillation frequency can be changed by varying the passive element values (e.g. resistors and thereby coming with terminologies like resistance-controlled-oscillators, etc). We divide RC oscillators based on CCs to the three following types:

Type I: The first group contains mainly non-adjustable oscillators. It means that tuning of FO is complicated (simultaneous changes of several values of resistors) or is not allowed. These oscillators are more suitable to be used as fixed frequency oscillators. Several works can be introduced as examples (Nandi, 1977; Abuelmaatti and Humood, 1987; Martinez et al., 1995; Soliman, 1998; Soliman and Elwakil, 1999). Many circuits were designed as modifications of well known Wien-bridge oscillator. In the mentioned works two or more active and four or more passive elements were used. Soliman (1999) verified several solutions, where two or three CCII±-s and four or six grounded passive elements were used. We can suppose that the current feedback amplifier (CFA) is also CCII with additional voltage buffer. Many authors were interested in this field for years. For example Senani and Sharma (2004) used one CCII/CFA and six passive elements (floating and grounded) in simple oscillators, where CO is adjustable independently with respect to FO by one resistor.

Type II: All solutions that provide control of FO and CO by floating or grounded resistors to the second group were clubbed. This type of oscillators is classified as single resistance controlled oscillator (SRCO). Celma et

al. (1992) utilized only one CCII+, two grounded capacitors and three resistors in simple oscillator. There exist possibilities of FO and CO control, but the elements that provide adjusting are floating. Senani and Singh (1996) proposed solution, which allows the control of FO and CO separately by two resistor values. The circuit employs two CFAs, two capacitors and three resistors. Also Horng (2005) published several solutions, where SRCO oscillators using three CCII (positive and negative types) and grounded passive elements were proposed. Similarly, Chang (1994) showed us SRCO oscillator using three CCII (both types), two grounded capacitors and resistors. Toker et al. (2002) proposed SRCO types, where inverting type of CC (ICCI±) was used. Martinez et al. (1999) built his SRCO with three CCII+s, two grounded capacitors, and four resistors. Similarly, Khan et al. (2005) used commercially available CCII/CFA elements with four resistors and two grounded capacitors for SRCO design. Quite large and difficult solutions were presented by Soliman (2010). Circuits contain four CCII and maximally 6 passive elements, most of them are grounded. Recently, several solutions of SRCOs employing two current conveyors and maximally four passive elements are summarized by Lahiri (2011).

Type III: This group covers such realizations, where FO and CO are adjustable electronically in direct way. One possibility is to control the intrinsic resistance (R_x) of input terminal X of CCII (Fabre et al., 1996; Salem et al., 2006; Barthelemy et al., 2007; Eldbib and Musil, 2008) or simulate resistors by transconductance elements, e.g. operational transconductance amplifier (OTA). Of course, there exist many solutions with more sophisticated active elements like current follower transconductance amplifier (CFTA) (Herencsar et al., 2010), current controlled current differencing transconductance amplifier (CCCDTA) (Jaikla and Lahiri, 2012), etc., Bielek et al. (2008) worked on it, but it is not the intention of this work to discuss all of them. An example of such oscillator solution was published (Horng, 2001), where FO and CO are controlled by bias current setting R_x of the active element. Abuelmaatti and Al-Qahtani (1998) presented multiphase (n-phases) oscillator using lossy integrators. Each integrator is based on CCCII and two grounded capacitors and hence, oscillator employs only capacitors as external components. Another way is to use adjustable current gain to control FO and CO. Recently, several active elements with this feature were published (Minaei et al., 2006; Marcellis et al., 2009; Kumngern et al., 2010a; Tangsrirat, 2008; Shi-Xiang et al., 2007). Kumngern et al. (2010a) proposed multiphase oscillator with oscillation frequency controlled by current gain in each integrator section. Similar solution is provided by Souliotis et al. (2009) with controllable current amplifiers. Biolkova et al. (2011) proposed two "SRCO compatible" oscillators with differential-output current inverter buffered amplifiers (DO-CIBAs). The circuit is quite simple and provides four-phase outputs, which is suitable for

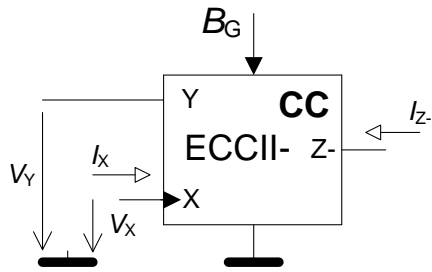


Figure 1. Electronically controllable current conveyor of second generation (ECCII-).

comparison to some of the previously published solutions, CO control in our circuit is simpler and more effective, since the current gain of the ECCII is controlled by direct current (DC) voltage. This also provides compatibility with an auxiliary amplitude control loop to regulate the oscillation amplitude. The proposed oscillator has been experimentally verified by using commercially available Integrated circuits (ICs) and with an auxiliary amplitude control loop to prove the concept of the used ECCII in controlling the CO, to regulate the amplitude and provide very good THD performance.

PROPOSED THREE-PHASE OSCILLATOR

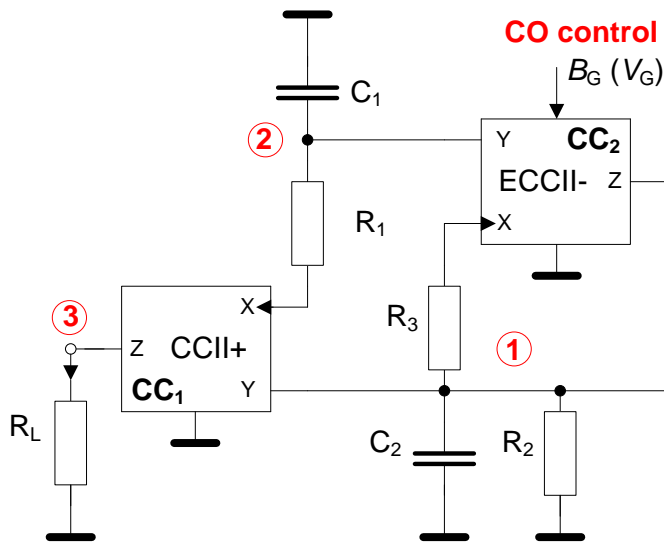


Figure 2. Proposed oscillator.

B_G (adjustable transfer between X and Z port of the ECCII) was used in our contribution, which allows us to set the CO without disturbing the FO. It can remove the earlier discussed drawback also in some hitherto published solutions. However, it can not be always helpful. Specific solution (concerning controllable B_G) is based on type of circuit topology. After this modification and proper design, FO is set by the passive elements and CO by the current gain (B_G) in our circuit. As pointed earlier, the electronic control of the CO enables the use of auxiliary amplitude control loop to regulate the amplitude. Figure 1 explains the general principle of the ECCII element. The transfer relations between terminal voltages and currents are described as follows (Surakamponorn and Thitimahshima, 1988; Minaei et al., 2006): $V_Y = V_X, I_Y = 0, I_Z = -B_G I_X$. The CCII+ behaves as the ECCII only, it does not feature with the current gain possibility, and the relation between X and Z currents is $I_Z = I_X$ (Sedra and Smith, 1970).

differential outputs. Kumngern and Junnapiya, (2010b) discussed the combination of both intrinsic resistance and current gain control to adjust the FO and CO in oscillator using only two current conveyors and two grounded capacitors. Main design approaches in most of the aforementioned types of oscillators are loop and multi-loop integrator structures, nodal admittance analysis (autonomous circuit) or state variable synthesis. Also, many of the discussed multiphase oscillator circuits provide phase shifts either in 90 or 180°(that is, inversion). This is provided by the presence of integrators in the circuit loop in most cases (Kumngern et al., 2010a; Sotner et al., 2011a, b; Abuelmaatti and Al-Qahtani, 1998; Souliotis et al., 2009; Biolkova et al., 2011) or based on multifunctional biquad filter-band pass response (Bajer et al., 2011a) for example. Our oscillator provides both 45 and 90° phase shift, which is a special feature of our circuit. Two produced signals are accessible from high- impedance nodes and the third is the current response through grounded resistive load. In

Common design approaches discussed in introductory part are loop and multi-loop integrator structures, nodal admittance analysis (autonomous circuit) or state variable synthesis (Gupta and Senani, 1998a, b; Senani and Gupta, 1997). We used classical nodal analysis (instructive example of this kind of synthesis was used by Toker et al. (2002)) and found characteristic equation which provides possibility to control the condition for oscillation by B_G . Proposed circuit is as shown in Figure 2. The main advantage is that oscillator uses current gain of ECCII for automatic gain control (AGC). Five (six including R_L) passive elements, ECCII- and CCII+ together form whole oscillator circuit. All capacitors are grounded. In the proposed oscillator, both floating resistors are in series to X terminals, which is advantageous, because unwanted effects of the parasitic resistances at X terminals can be compensated by choosing sufficiently high resistor values.

Characteristic equation has the form:

$$s^2 + \frac{R_1 R_2 C_1 + R_1 R_3 C_1 + R_2 R_3 C_2 - R_1 R_2 C_1 B_G}{R_1 R_2 R_3 C_1 C_2} s + \frac{1}{R_1 R_2 C_1 C_2} = 0 \tag{1}$$

The CO derived from Equation 1 is:

$$B_G \geq \frac{R_1 C_1 (R_2 + R_3) + R_2 R_3 C_2}{R_1 R_2 C_1} \tag{2}$$

The oscillation frequency has very common form for these types of oscillators:

$$\omega_0 = \sqrt{\frac{1}{R_1 R_2 C_1 C_2}} \tag{3}$$

The sensitivities of oscillation frequency on all parameters are in ideal case low:

$$S_{R_1}^{\omega_0} = S_{R_2}^{\omega_0} = S_{C_1}^{\omega_0} = S_{C_2}^{\omega_0} = -0.5 \tag{4}$$

$$S_{R_3}^{\omega_0} = S_{B_G}^{\omega_0} = 0 \tag{5}$$

CCII+ (CC₁) provides not only the buffer functionality between terminal Y and X, but further enables the generation of an explicit-current-output (ECO) (Senani and Sharma, 2004) from the Z terminal. This current can be flown into an external resistive load to provide a third voltage output.

Simple circuit analysis of the relationship between the produced voltage signals at the nodes (highlighted by red color) shows that:

$$\frac{V_3}{V_2} = \frac{-R_3 R_L (1 + sC_2 R_2)}{R_1 R_2 (1 - B_G) + R_1 R_3 + sC_2 R_1 R_2 R_3} \tag{6}$$

$$\frac{V_3}{V_1} = \frac{sC_1 R_L}{1 + sC_1 R_1} \tag{7}$$

$$\frac{V_2}{V_1} = \frac{1}{1 + sC_1 R_1} \tag{8}$$

If we suppose that all resistors in the oscillator structure are equal, that is, $R_1 = R_2 = R_3 = R$ and also both the capacitors have same value, that is, $C_1 = C_2 = C$, then the CO simplifies to $B_G = 3$ and $\omega_0 = 1/RC$. If the CO is fulfilled ($B_G = 3$), we can obtain:

$$\frac{V_3}{V_2} = \frac{-RR_L(1 + sCR)}{-R^2 + sCR^3} = \frac{R_L}{R} \left(\frac{1 + sCR}{1 - sCR} \right) \tag{9}$$

$$\frac{V_3}{V_2} = \frac{R_L}{R} \left(\frac{1 + j\omega_0 CR}{1 - j\omega_0 CR} \right) = \frac{R_L}{R} \left(\frac{1 + j}{1 - j} \right) = \frac{R_L}{R} j \tag{10}$$

$$V_3 = V_2 \frac{R_L}{R} e^{\frac{\pi}{2}j} \tag{11}$$

From Equation 11, it can be seen that the phase shift between V_3 and V_2 is 90° , that is, they are quadrature in nature. Similarly, relation between V_3 and V_1 can be derived as:

$$\frac{V_3}{V_1} = \frac{R_L}{2R} (1 + j) \tag{12}$$

$$V_3 = V_1 \frac{\sqrt{2}}{2} \left(\frac{R_L}{R} \right) e^{\frac{\pi}{4}j} \tag{13}$$

From Equation 13, it is evident that the phase shift between these signals is 45° . The same phase shift is between V_1 and V_2 because

$$\frac{V_2}{V_1} = \frac{1}{1 + j} = \frac{1}{2} (1 - j) \tag{14}$$

$$V_2 = V_1 \frac{\sqrt{2}}{2} e^{-\frac{\pi}{4}j} \tag{15}$$

The relations between the amplitudes of the produced signals are given mainly by mutual ratio of R_L and R .

At this point, we should take note of the circuit proposed by Senani et al. (1990) (Figure 2c in discussed literature), where three OTAs were used. From circuit synthesis point of view, the circuit could be considered as similar. However, there are important practical differences. First of all, circuit discussed by Senani et al. (1990) contains three active elements (and any resistor, only two capacitors), but our solution contains only two active elements, three (four including R_L) resistors and two capacitors.

Two high-impedance nodes only are in Senani's solution, but three nodes (including high-impedance ECO output) are in our contribution. Practically, it allows us to obtain outputs of three phases. This possibility is not discussed neither was it allowed in Senani's solution. Additionally, characteristic equations of both circuits (our and Figure 2c) are completely different.

Similar to the proposed circuit solution, recently Bajer et al. (2011b) discussed an oscillator, which is a derivation of Wien-bridge type with two CCII's. It does not allow direct electronic control of FO, but CO is adjustable electronically using an opto-coupler (replacement of floating resistor). Our solution provides several advantages with respect to Bajer et al. (2011b). Our circuit contains less number of resistors, it is not necessary to drive floating resistor for CO control and features with already mentioned properties.

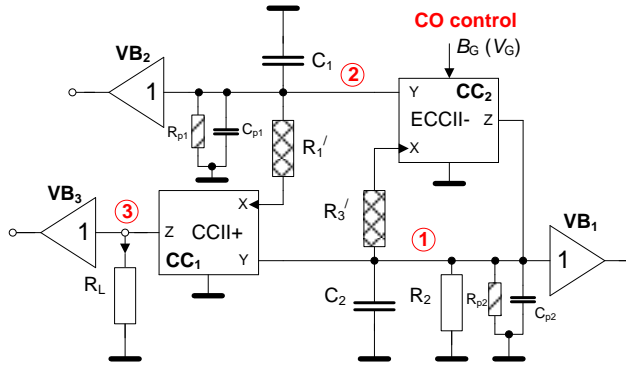


Figure 3. Important parasitic influences in the analyzed circuit.

REAL ACTIVE ELEMENTS NON-IDEALITIES

For the description of the proposed oscillator under the earlier discussed proposed three-phase oscillator, we assume ideal active elements, as they were presented in the first paragraph. According to Equation 3 for $R_1 = R_2 = R_3 = 1 \text{ k}\Omega$; $C_1 = C_2 = 220 \text{ pF}$, the ideal value of oscillation frequency is 723 kHz. However, the real active elements feature with their non-ideal behavior. For the simulations and experimental measurements, these results are given subsequently in the simulations and experimental measurements. We use the current mode multiplier EL2082 as ECCII- and the diamond transistor OPA860 as CCII+.

High-impedance nodes 1 and 2 (Figure 2) are important in the presented circuit. Input and output impedances of active elements cause problems in these nodes. Parasitic influences in the circuit are as shown in Figure 3. We can notice $R_{p1} \approx R_{Y_{CC2}}$, $C_{p1} \approx C_{Y_{CC2}}$, and $R_{p2} \approx R_{Y_{CC1}} \parallel R_{Z_{CC2}}$, $C_{p2} \approx C_{Y_{CC1}} + C_{Z_{CC2}}$. Datasheet information indicates values as follows: $R_{Y_{CC1}} \approx 450 \text{ k}\Omega$, $C_{Y_{CC1}} \approx 2 \text{ pF}$ (OPA860) and $R_{Y_{CC2}} \approx 2 \text{ M}\Omega$, $R_{Z_{CC2}} \approx 1 \text{ M}\Omega$, and $C_{Y_{CC2}} \approx 2 \text{ pF}$, $C_{Z_{CC2}} \approx 5 \text{ pF}$ (EL2082). We also have to consider input impedances of voltage buffer in these high-impedance nodes. We used LT1364 for experimental purposes. This operational amplifier has input impedance $Z_{\text{inp_buff}} \approx 5 \text{ M}\Omega / 3 \text{ pF}$. In summary it means that $R_{p1} \approx R_{Y_{CC2}} \parallel R_{\text{inp_buff}} \approx 1.4 \text{ M}\Omega$, $C_{p1} \approx C_{Y_{CC2}} + C_{\text{inp_buff}} \approx 5 \text{ pF}$, $R_{p2} \approx R_{Y_{CC1}} \parallel R_{Z_{CC2}} \parallel R_{\text{inp_buff}} \approx 295 \text{ k}\Omega$, $C_{p2} \approx C_{Y_{CC1}} + C_{Z_{CC2}} + C_{\text{inp_buff}} \approx 10 \text{ pF}$.

The following equations were derived from Figure 3 where $C_1' \approx C_1 + C_{p1}$, $C_2' \approx C_2 + C_{p2}$, $R_1' \approx R_1 + R_{X_{CC1}} \approx 1013 \text{ }\Omega$ and $R_3' \approx R_3 + R_{X_{CC2}} \approx 1005 \text{ }\Omega$ ($R_{X_{CC1}} \approx 13 \text{ }\Omega$, $R_{X_{CC2}} \approx 95 \text{ }\Omega$). It is clear that we choose $R_1 = 1 \text{ k}\Omega$ and $R_3 = 910 \text{ }\Omega$. The characteristic equation is now in the form:

$$a_2' s^2 + a_1' s + a_0' = 0 \quad (16)$$

where

$$a_0' = R_3' R_{p1} R_{p2} + R_1' R_{p2} [R_2 (1 - B_G) + R_3'] + R_2 R_3' (R_1' + R_{p1}) \quad (17)$$

$$a_1' = R_{p1} R_{p2} [C_1' R_1' (R_2 + R_3) + C_2' R_2 R_3'] + R_1' R_2 R_3' (C_1' R_{p1} + C_2' R_{p2}) - C_1' R_1' R_2 R_{p1} R_{p2} B_G \quad (18)$$

$$a_2' = R_1' R_2 R_3' R_{p1} R_{p2} C_1' C_2' \quad (19)$$

New formulas include discussed parameters. The oscillation condition and the oscillation frequency change to

$$B_G' \geq \frac{R_{p1} R_{p2} [C_1' R_1' (R_2 + R_3) + C_2' R_2 R_3'] + R_1' R_2 R_3' (C_1' R_{p1} + C_2' R_{p2})}{C_1' R_1' R_2 R_{p1} R_{p2}} \quad (20)$$

$$\alpha_0' = \sqrt{\frac{R_3' R_{p1} R_{p2} + R_1' R_{p2} [R_2 (1 - B_G) + R_3'] + R_2 R_3' (R_1' + R_{p1})}{R_1' R_2 R_3' R_{p1} R_{p2} C_1' C_2'}} \quad (21)$$

R_1' and R_3' are problematic, because they can be influenced by large manufacturing tolerance. Literature (OPA860) shows dependence of $R_{X_{CC1}}$ on bias current in range of 8 to 55 Ω . Therefore, we are not able to determine actual value with adequate accuracy. Nevertheless, for $R_1' = 1013 \text{ }\Omega$ we calculated Equation 3 as $f_0' = 719 \text{ kHz}$. When more accurate calculation of Equation 21 is done, $f_0' = 695 \text{ kHz}$ is obtained. Additional parasitic capacitances of C_{p1} and C_{p2} and value of $R_{X_{CC1}}$ have main effects on FO accuracy.

SIMULATIONS AND EXPERIMENTAL MEASUREMENTS

The final connection of the proposed oscillator supplemented by the amplitude gain control circuit (AGC) is as shown in Figure 4. Voltages generated in all nodes are available through additional voltage buffers. We used operational amplifier LT1364 together with internal buffer in OPA860 for this purpose. The AGC circuit contains cascade diode doubler and very simple common-emitter DC amplifier with bipolar transistor. The function of the AGC is based on nonlinear input-output transfer characteristic of this amplifier. Potentiometers are necessary for careful and very fine adjusting of CO. Power supply was $\pm 5 \text{ V}$. We used professional macromodels of the mentioned active elements for PSpice simulations and $f_0 = 695 \text{ kHz}$ was obtained. Transient responses and frequency spectrum are as shown in Figure 5. Accordingly to Figure 5b, the THD values obtained from simulations for output amplitudes V_{OUT1} , V_{OUT2} , and V_{OUT3} are 0.07, 0.05, and 0.43%, respectively.

The subsequent experimental measurements were carried out using RIGOL DS1204B oscilloscope and HP4395A network vector/spectrum analyzer. The spectrum analyzer requires impedance matching (50 Ω)

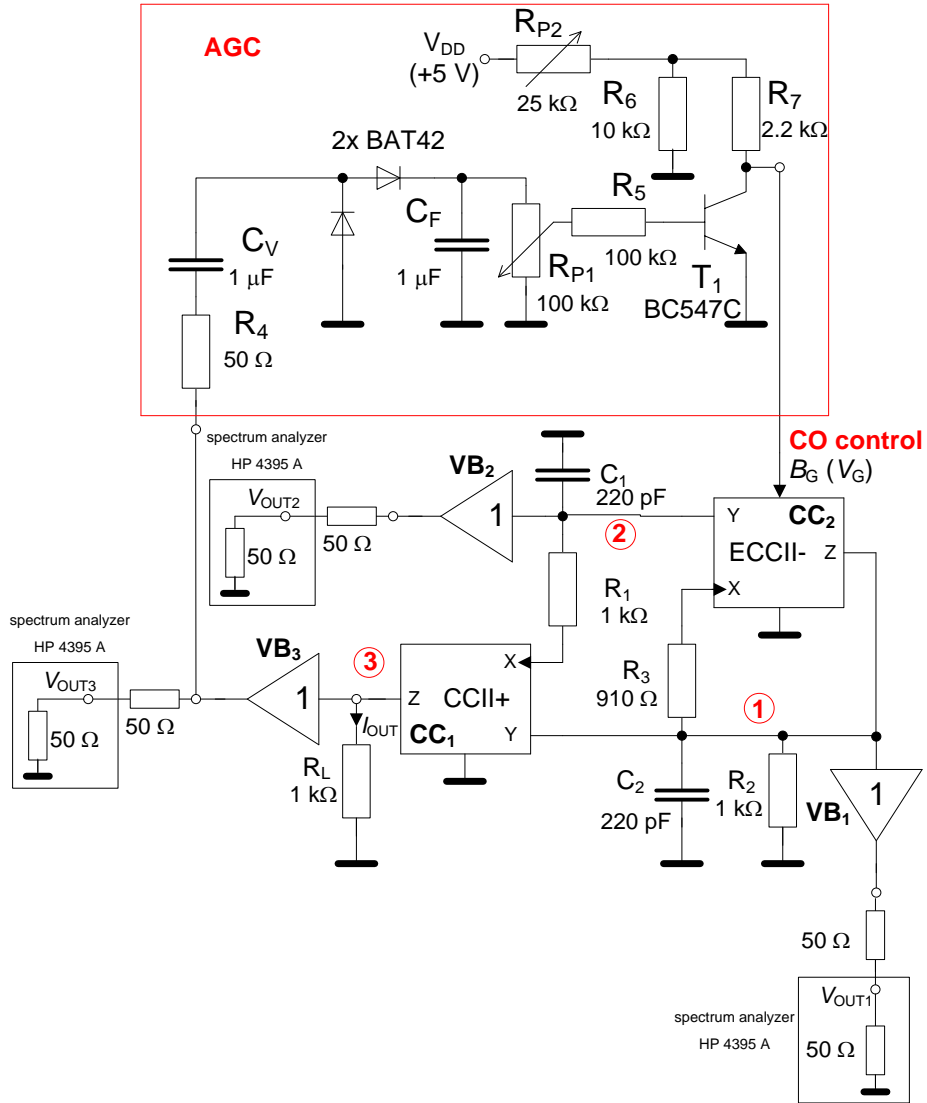


Figure 4. Measured circuit with complete accessories.

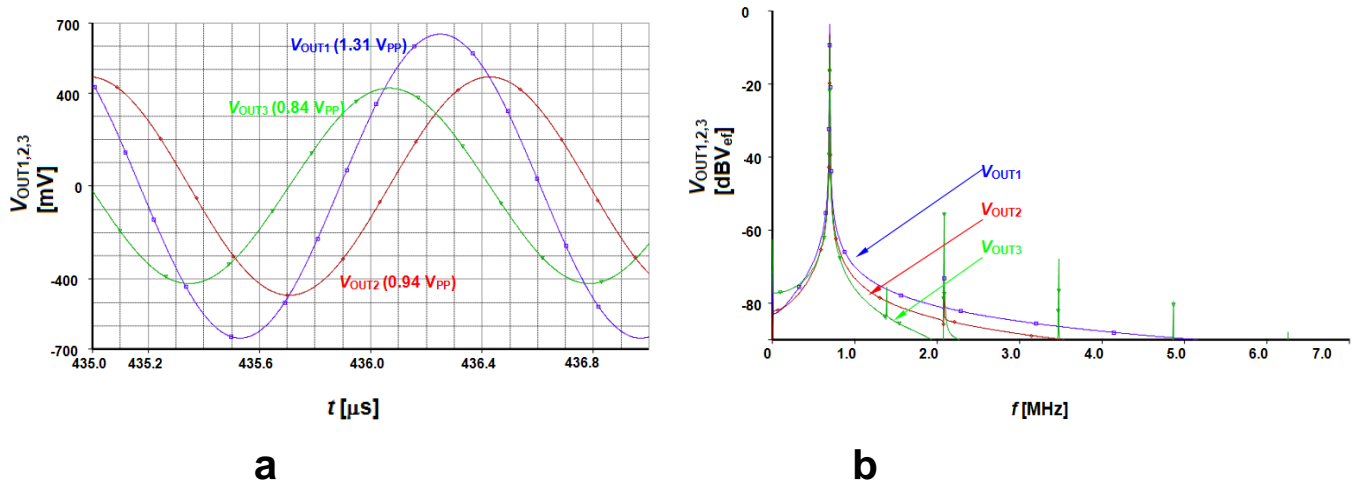


Figure 5. Simulation results: (a) transient responses, and (b) frequency spectrum.

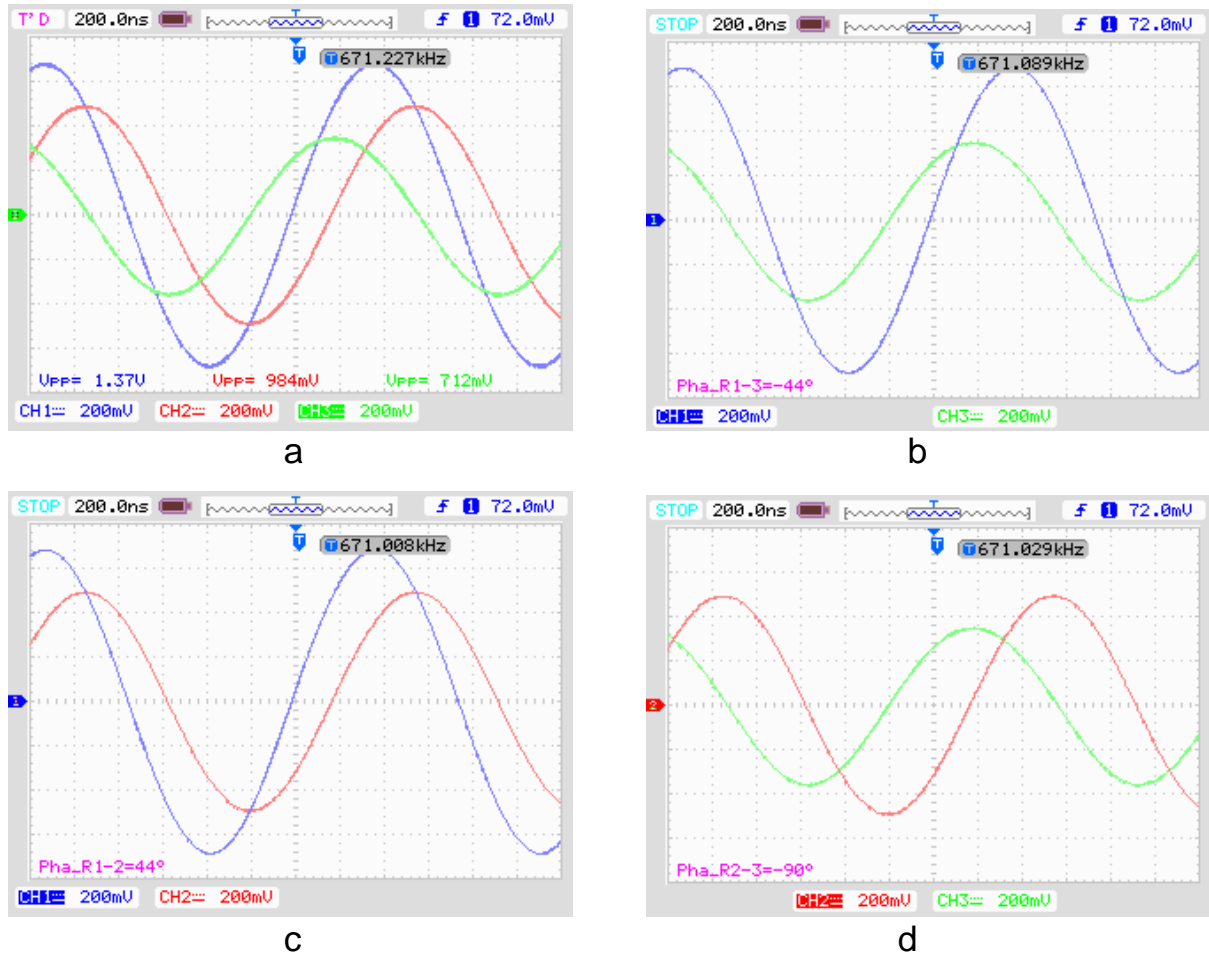


Figure 6. Measured transient responses: (a) all produced signals, (b) phase shift between V_{OUT1} and V_{OUT3} , (c) phase shift between V_{OUT1} and V_{OUT2} , and (d) phase shift between V_{OUT2} and V_{OUT3} .

and therefore the voltage buffers were very important.

Measurement results are as shown in Figure 6. Figure 6a shows all available transient responses together. Figure 6b presents phase shift between V_{OUT1} and V_{OUT3} ; Figure 6c shows the responses of V_{OUT1} and V_{OUT2} , and finally Figure 6d shows voltages V_{OUT2} and V_{OUT3} . Experimentally measured oscillation frequency was 671 kHz, which matches well the simulation results. The difference between PSpice predicted FO (and also FO expected from Equation 21) and the experimentally obtained FO is about 3.5%, which can be accounted by the additional printed circuit board parasitic capacitances and tolerances of used working capacitors were not taken into account.

The AGC circuit preserved V_G (DC value, which is approximately representing B_G) on value 2.95 V. Spectral analyses provide information of THD at all outputs (Figure 7). Figure 7a shows the spectral analysis of V_{OUT1} . Suppression of higher harmonics (dominant is second) is about 52 dB and its calculated THD is lower than 0.25%. In Figure 7b, the spectral analysis of V_{OUT2} is

depicted. Suppression of the second harmonic is more than 54 dB and THD is approximately 0.2%. The worst situation is at V_{OUT3} where suppression is only 43 dB (Figure 7c), with resulting THD of 0.75%. Photos of measured experimental circuit are as shown in Figure 8.

CONCLUSION

An oscillator with electronically controllable CO using ECCII has been demonstrated. The electronic control of the CO enables the use of an auxiliary amplitude control loop to regulate the amplitude and provide very good THD performance. It is clear from symbolical analysis that control of FO is very complicated, but proposal of fully controllable oscillator was not the intention of this contribution. We have shown other special features of circuit. The proposed oscillator employs one ECCII, one CCII and five (six, including R_L) passive components, and is capable to provide voltage outputs with either 45 or 90° phase shift, which is a special feature and interesting

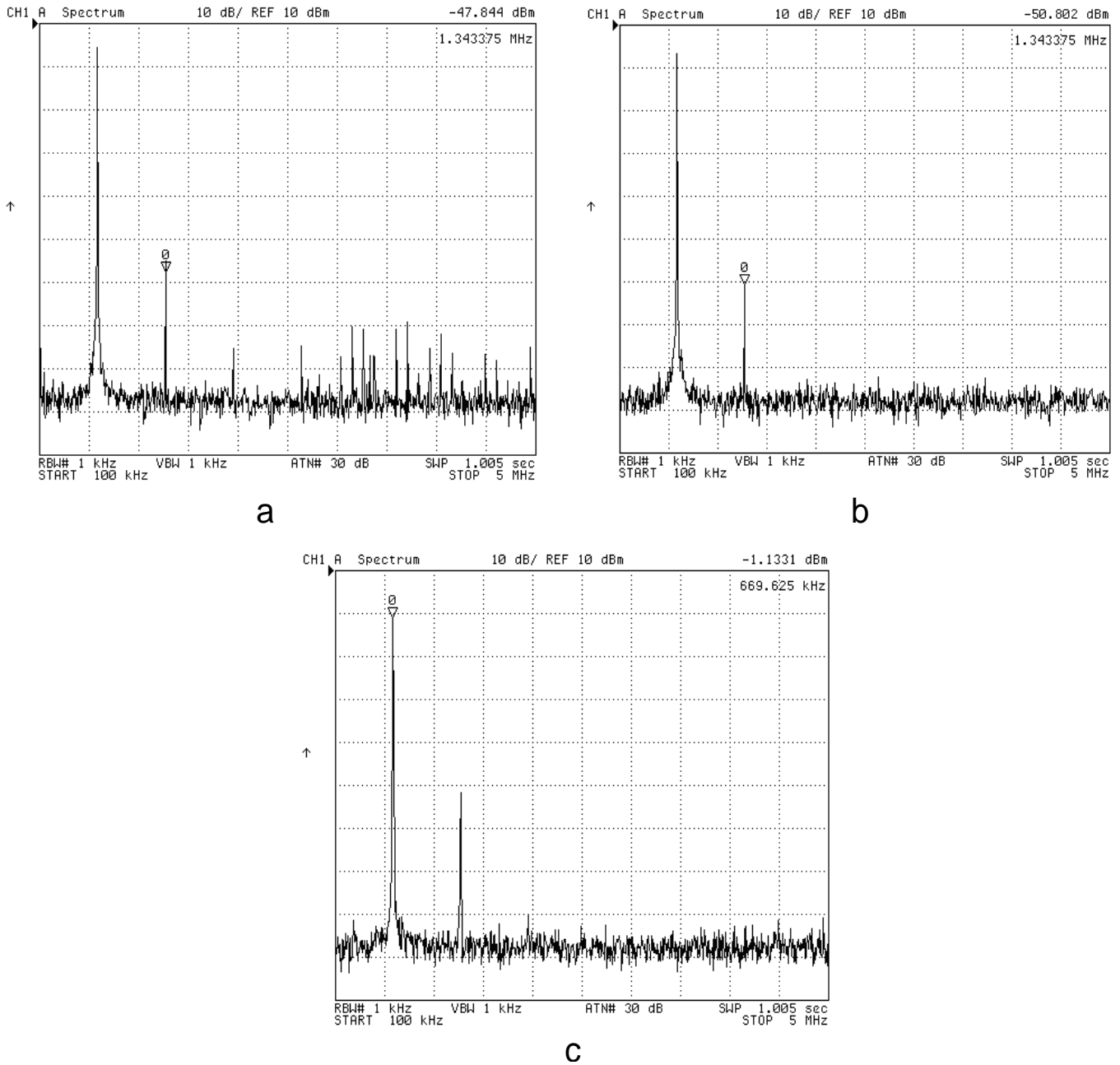


Figure 7. Measured spectral analysis: (a) V_{OUT1} (b) V_{OUT2} , and (c) V_{OUT3} .

curiosity in simple type of the oscillator. Simulation and experimental results have verified the workability of the proposed oscillator.

ACKNOWLEDGEMENTS

The research described in this paper was supported by the Czech Science Foundation projects under No. 102/11/489, No. 102/09/1681, and No. 102/10/P561. This paper is part of the COST Action IC0803 RF/Microwave

communication subsystems for emerging wireless technologies, financed by the Czech Ministry of Education by the grant no. OC09016. The support of the project CZ.1.07/2.3.00/20.0007 WICOMT, financed from the operational program education for competitiveness, is gratefully acknowledged. This research was performed in laboratories supported by the six project; the registration number CZ.1.05/2.1.00/03.0072, the operational program Research and Development for Innovation. The authors would like to thank the reviewers for their valuable comments.

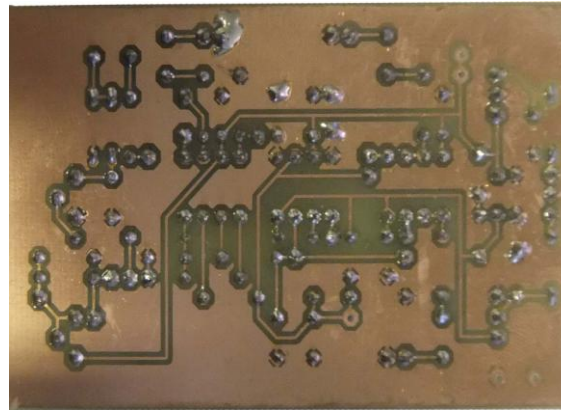
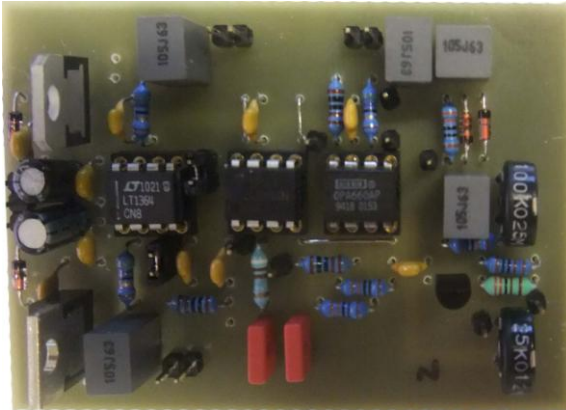


Figure 8. Measured prototype.

REFERENCES

- Abuelmaatti MT, Al-Qahtani MA (1998). New current-controlled multiphase sinusoidal oscillator using translinear current-conveyors. *IEEE Trans. Circuits Syst. II: Analog Digital Signal Process*, 45(7): 881-885.
- Abuelmaatti MT, Humood NA (1987). Two new minimum-component Wien-bridge oscillators using current conveyors. *Int. J. Electron.*, 63(5): 669-672.
- Bajer J, Vavra J, Biolek D, Hajek K (2011a). Low-distortion current-mode quadrature oscillator for low-voltage low-power applications with non-linear non-inertial automatic gain control. *Proc. Eur. Conf. Circuit Theory Design (ECCTD)*, Linköping, Sweden, pp. 441-444.
- Bajer J, Lahiri A, Biolek D (2011b). Current-mode CCII+ based oscillator circuits using a conventional and modified Wien-bridge with all capacitors grounded. *Radioengineering*, 20(1): 245-250.
- Barthelemy H, Fillaud M, Bourdel S, Gaunery J (2007). CMOS inverters based positive type second generation current conveyors. *Analog Integr. Circuits Signal Process*, 50(2): 141-146.
- Biolek D, Senani R, Biolkova V, Kolka Z (2008). Active elements for analog signal processing: classification, review, and new proposal. *Radioengineering*, 17(4): 15-32.
- Biolkova V, Bajer J, Biolek D (2011). Four-phase oscillators employing two active elements. *Radioengineering*, 20(1): 334-339.
- Celma S, Martinez PA, Carlosena A (1992). Minimal realisation for single resistor controlled sinusoidal oscillator using single CCII. *Electron. Lett.*, 28(5): 443-444.
- Chang CM (1994). Novel current-conveyor-based single-resistance-controlled/voltage-controlled oscillator employing grounded resistors and capacitors. *Electron. Lett.*, 30(3): 181-183.
- EL2082: Current-mode multiplier, Intersil (Elantec) [online]. 1996, last modified 2003, available at URL: <<http://www.intersil.com/data/fn/fn7152.pdf>>
- Eldib I, Musil V (2008). Self-cascoded current controlled CCII based tunable band pass filter. *Proceedings of the 18th Int. Conf. Radioelektronika, Praha, Czech Republic*, pp. 1-4.
- Fabre A, Saaid O, Wiest F, Boucheron C (1996). High frequency applications based on a new current controlled conveyor. *IEEE Trans. Circuits Syst.*, - I, 43(2): 82-91.
- Gupta SS, Senani R (1998a). State variable synthesis of single resistance controlled grounded capacitor oscillators using only two CFOAs. *IEE Proc. Circuits Devices Syst.*, 145(2): 135-138.
- Gupta SS, Senani R (1998b). State variable synthesis of single-resistance-controlled grounded capacitor oscillators using only two CFOAs: additional new realisations. *IEE Proc. Circuits Devices Syst.*, 145(6): 415-418.
- Herencsar N, Vrba K, Koton J, Lahiri A (2010). Realisations of single-resistance-controlled quadrature oscillators using generalised current follower transconductance amplifier and unity-gain voltage-follower. *Int. J. Electron.*, 97(8): 897-906.
- Hong JW (2001). A sinusoidal oscillator using current-controlled current conveyors. *Int. J. Electron.*, 88(6): 659-664.
- Hong JW (2005). Current conveyors based allpass filters and quadrature oscillators employing grounded capacitors and resistors. *Comput. Electrical Eng.*, 31(1): 81-92.
- Jaikla W, Lahiri A (2012). Resistor-less current-mode four-phase quadrature oscillator using CCCDTAs and grounded capacitors. *AEU – Int. J. Electron. Commun.*, 66(3): 214-218.
- Khan AA, Bimal S, Dey KK, Roy SS (2005). Novel RC sinusoidal oscillator using second-generation current conveyor. *IEEE Trans. Instrum. Meas.*, 54(6): 2402-2406.
- Koton J, Herencsar N, Cicekoglu O, Vrba K (2010). Current-mode KHN equivalent frequency filter using ECCIIs. *Proceedings of the 33th International Conference on Telecommunications and Signal Processing (TSP)*, Baden, Austria, pp. 27-30.
- Kumngern M, Chanwutium J, Dejhon K (2010a). Electronically tunable multiphase sinusoidal oscillator using translinear current conveyors. *Analog Integr. Circuits Signal Process*, 65(2): 327-334.
- Kumngern M, Junnapiya S (2010b). A sinusoidal oscillator using translinear current conveyors. *Proceedings of the Asia Pacific Conference on Circuits and Systems (APCCAS)*, Kuala Lumpur, Malaysia, pp. 740-743.
- Lahiri A (2011). Current-mode variable frequency quadrature sinusoidal oscillator using two CCs and four passive components including grounded capacitors. *Analog Integr. Circuits Signal Process*, 68(1): 129-131.
- LT1364: Dual and Quad 70 MHz, 1000 V/us, Op Amps, Linear Technology [online]. 1994, available at URL: <<http://cds.linear.com/docs/Datasheet/13645fa.pdf>>
- Marcellis A, Ferri G, Guerrini NC, Scotti G, Stornelli V, Trifiletti A (2009). The VGC-CCII: a novel building block and its application to capacitance multiplication. *Analog Integr. Circuits Signal Process*, 58(1): 55-59.
- Martinez PA, Celma S, Gutierrez I (1995). Wien-type oscillators using CCII+. *Analog Integr. Circuits Signal Process*, 7(2): 139-147.
- Martinez PA, Sabadell J, Aldea C, Celma S (1999). Variable frequency sinusoidal oscillators based on CCII+. *IEEE Trans. Circuits Syst. I: Fundam. Theory Appl.*, 46(11): 1386-1390.
- Minaei S, Sayin OK, Kuntman H (2006). A new CMOS electronically tunable current conveyor and its application to current-mode filters. *IEEE Trans. Circuits Syst. I—Regul. Pap.*, 53(7): 1448-1457.
- Nandi R (1977). Wien bridge oscillators using current conveyors. *Proc. IEEE*, 65(11): 1608-1609.
- OPA860: Wide Bandwidth Operational Transconductance Amplifier and Buffer, Texas Instruments [online]. 2005, last modified 8/2008, available at URL: <<http://focus.ti.com/lit/ds/symlink/opa860.pdf>>
- Salem SB, Fakhfakh M, Masmoudi DS, Loulou M, Loumeau P, Masmoudi N (2006). A high performance CMOS CCII and high frequency applications. *Analog Integr. Circuits Signal Process*, 49(1): 71-78.

- Sedra A, Smith KC (1970). A second generation current conveyor and its applications. *IEEE Trans. Circuit Theory*, 17(2): 132-134.
- Senani R, Gupta SS (1997). Synthesis of single-resistance-controlled oscillators using CFOAs: simple state-variable approach. *IEE Proc. Circuits Devices Syst.*, 144(2): 104-106.
- Senani R, Kumar BA, Tripathi MP (1990). Systematic generation of OTA-C sinusoidal oscillators. *Electron. Lett.*, 26(18): 1457-1459.
- Senani R, Sharma RK (2004). Explicit-current-output sinusoidal oscillators employing only a single current-feedback op-amp. *IEICE Electron. Express*, 2(1): 14-18.
- Senani R, Singh VK (1996). Novel single-resistance-controlled-oscillator configuration using current feedback amplifiers. *IEEE Trans. Circuits Syst.- I: Fundam. Theory Appl.*, 43(8): 698-700.
- Shi-Xiang S, Guo-Ping Y, Hua C (2007). A new CMOS electronically tunable current conveyor based on translinear circuits. *Proceedings of the 7th Int. Conf. on ASIC (ASICON 2007)*, Guilin, China, pp. 569-572.
- Soliman AM (1998). Novel generation method of current mode Wien-type oscillators using current conveyors. *Int. J. Electron.*, 85(6): 737-747.
- Soliman AM (1999). Synthesis of grounded capacitor and grounded resistor oscillators. *J. Franklin Inst.*, 336(4): 735-746.
- Soliman AM (2010). On the generation of CCII and ICCII oscillators from three Op Amps oscillator. *Microelectron. J.*, 41(10): 680-687.
- Soliman AM, Elwakil AS (1999). Wien oscillators using current conveyors. *Comput. Electr. Eng.*, 25(1): 45-55.
- Sotner R, Hrubos Z, Sevcik B, Slezak J, Petrzela J, Dostal T (2011a). An example of easy synthesis of active filter and oscillator using signal flow graph modification and controllable current conveyors. *J. Electrical Eng.*, 62(5): 258-266.
- Sotner R, Hrubos Z, Slezak J, Dostal T (2010). Simply adjustable sinusoidal oscillator based on negative three- port current conveyors. *Radioengineering*, 19(3): 446-453.
- Sotner R, Jerabek J, Prokop R, Vrba K (2011b). Current gain controlled CCTA and its application in quadrature oscillator and direct frequency modulator. *Radioengineering*, 20(1): 317-326.
- Souliotis G, Psychalinos C (2009). Electronically controlled multiphase sinusoidal oscillators using current amplifiers. *Int. J. Circuit Theory Appl.*, 37(1): 43-52.
- Surakampontrorn W, Thitimahshima W (1988). Integrable electronically tunable current conveyors. *IEE Proceedings-G*, 135(2): 71-77.
- Svoboda JA, McGory L, Webb S (1991). Applications of commercially available current conveyor. *Int. J. Electron.*, 70(1): 59-64.
- Tangsrirat W (2008). Electronically tunable multi-terminal floating nullor and its application. *Radioengineering*, 17(4): 3-7.
- Toker A, Kuntman H, Cicekoglu O, Discigil M (2002). New oscillator topologies using inverting second-generation current conveyors. *Turk. J. Electr. Eng.*, 10(1): 119-129.

[7] SOTNER, R., JERABEK, J., GOTTHANS, T., PROKOP, R., DOSTAL, T., VRBA, K. Controlled Gain Current and Differential Voltage Amplifier and Study of Its Application in Simple Adjustable Oscillator. In *Proceedings of the 36th International Conference on Telecommunications and Signal Processing (TSP 2013)*, Rome (Italy), 2013, p. 407-411. ISBN: 978-1-4799-0403-7.

Controlled Gain Current and Differential Voltage Amplifier and Study of Its Application in Simple Adjustable Oscillator

Roman Sotner, Jan Jerabek, Tomas Gotthans, Roman Prokop, Tomas Dostal, and Kamil Vrba

Abstract—Presented contribution of the paper deals with novel active element Controlled Gain Current and Differential Voltage Amplifier (CG-CDVA) and its implementation in a very simple adjustable oscillator. Explanation of principle of the active element is complemented by possible behavioral model based on commercially available active elements. Therefore we are able to establish measurement setup that is suitable for preliminary experimental purposes. The proposed oscillator was analyzed by common symbolic approaches and as well verified experimentally. Important results of typical analyses were discussed.

Keywords—Adjustable oscillator, current gain control, electronic control, voltage gain control.

I. INTRODUCTION

Actual needs in analog signal processing requires compact and controllable active elements. Many novel conceptions and approaches were presented in literature [1] quite briefly but many of discussed approaches have not been studied in detail yet. Main aim of such approach is evident. More than one controllable parameter allows more possibilities of control in resulting application. Therefore, for synthesis and construction of application, lower number of active elements with equivalent abilities of adjustability is sufficient in many cases.

Two basic approaches of control of active elements were proposed in the past, namely transconductance (g_m) control and intrinsic resistance control (R_x) by control of DC current of biasing circuits (I_b). Development of controllable elements

starts with discovery of current conveyor [2]. These elements allow adjustable current input resistance as showed Fabre et al. [3], for example. Operational transconductance amplifiers are disposable as voltage controllable current sources with controllable transconductance. Brief summary of basic features and applications was given in [4]. Unfortunately, current conveyors and also transconductance amplifiers are basic elements and do not provide additional voltage buffering which is required in many applications.

Current gain control achieved attention of many researchers, especially in recent years, and it seems to be also very rich topic today. The first attempts were given by Surakamponorn et al. [5] and Fabre et al. [6] that deal with these possibilities in frame of current conveyors. Many of more sophisticated elements with controllable current amplification were developed in recent years. A basic structures of continuously adjustable current amplifiers or advanced blocks with various multi-terminal possibilities were given in [7]-[11], for example. Digital control is modern method of gain adjusting [12]-[13] of these and similar devices. Development of elements with current gain control started evolution in synthesis of current mode and also voltage mode circuits.

Our activities in this field are focused on combination of several different methods of control. Some interesting conceptions have been presented. Combination of several methods of control in frame of simple common active element like current conveyor is not so old idea. Minaei et al. [14] developed electronically controllable current conveyor where possibility of adjusting of current input resistance of x terminal and also current gain between x and z terminal was available. Marcellis et al. [15] implemented methods of current and also voltage gain control between terminals of current conveyor. Similarly Kumngern et al. [16] proposed very simple current conveyor where intrinsic resistance and current gain are separately controllable but by different way in comparison to [14]. Proposed principles of combined control seem to be very useful for design of parts of advanced elements with various types of adjusting.

Our research is focused on combined active elements utilizing at least two basic principles because it allows to design interesting applications as explains following works. The frequently used active element with combined sections (current conveyor of second generation section and transconductance section) is so-called current conveyor transconductance amplifier (CCTA) [17] which was modified many times, for example [18]-[20]. Siripruchyanun et al. [18] utilized adjustable current conveyor and transconductance

Manuscript received February 21, 2013. Research described in the paper was supported by Czech Science Foundation project under No. 102/09/1681 and by internal grant No. FEKT-S-11-13. The support of the project CZ.1.07/2.3.00/20.0007 WICOMT, financed from the operational program Education for competitiveness, is gratefully acknowledged. The described research was performed in laboratories supported by the SIX project; the registration number CZ.1.05/2.1.00/03.0072, the operational program Research and Development for Innovation.

R. Sotner (corresponding author) and T. Gotthans are with the Dept. of Radio Electronics, Brno University of Technology, Brno, Technicka 12, 616 00 Czech Republic. (e-mail: sotner@feec.vutbr.cz, xgotth00@stud.feec.vutbr.cz).

J. Jerabek and K. Vrba are with the Dept. of Telecommunications, Brno University of Technology, Brno, Technicka 12, 616 00 Czech Republic (e-mails: {jerabekj, vrbak}@feec.vutbr.cz).

R. Prokop is with the Dept. of Microelectronics, Brno University of Technology, Brno, Technicka 10, 616 00 Czech Republic (e-mail: prokop@feec.vutbr.cz).

T. Dostal is with the Dept. of Electrical Engineering and Computer Science, College of Polytechnics Jihlava, Jihlava, Tolsteho 16, 586 01 Czech Republic (e-mail: dostal@vspj.cz).

section in the CCTA and also obtain two possibilities (R_x and g_m) of control in frame of one active element.

Similar modifications were used in advanced version of so-called current differencing transconductance amplifier (CDTA) [21], where current differencing unit with controllable intrinsic resistances complemented by adjustable transconductance section was designed by Jaikla et al. [22], [23].

However, the discussed and similar works are not employing current gain and voltage gain control in frame of combined active element that allows interesting features thanks to differential voltage input (another auxiliary terminal which means advantages in synthesis). We will present example of application of such active element in very simple oscillator.

In comparison to examples of some quite complicated solutions consisting of many active elements [24]-[25], our solution of oscillator allows simplicity, just one buffered voltage output and very simple utilization of automatic gain control circuit for amplitude stabilization (DC voltage control). Non-buffered high-impedance outputs are quite common problems which require additional buffering [26]. There were published also multiphase types of oscillators [7], but proposed structure belongs to quadrature types (as was shown for example in [9], [10], [20], [22], [23], [27], [28]) in theoretical point-of-view. However, utilization of only one active element is beneficial advantage (considering available adjustabilities). Similar electronically controllable features were achieved in [18], [29]-[30] where adjustable oscillators based on single active element were also presented. However, they used different methods of control and none output has been automatically buffered and ready for low-impedance load (50 Ω typically).

II. CONTROLLED GAIN CURRENT AND DIFFERENTIAL VOLTAGE AMPLIFIER

The controlled gain current and differential voltage amplifier (CG-CDVA) seems to be novel active element that completes family of devices briefly summarized by Biolek et al. in [1].

Presented active element consists of current input terminal p , auxiliary terminal (output of current amplifier section) z , auxiliary terminal v (voltage terminal) and output terminal w . Two terminals V_{SETA} and V_{SETB} are determined for purposes of control.

So called current differencing differential input buffered amplifier (CDDIBA), current differencing differential input differential output buffered amplifier (CDDIDIBA), current differencing operational amplifier (CDOA) and current voltage differential input buffered amplifier (CVDIBA) are the most similar devices to our proposal. However, some of them have more complicated input section (current differencing unit) than our device and do not allow any possibility of control of parameters [1].

Our proposal combines simpler sections (controllable current and voltage amplifier) and enables two ways of control in frame of active element i.e. current gain (B) control and voltage gain (A) control. Fundamental principle of the

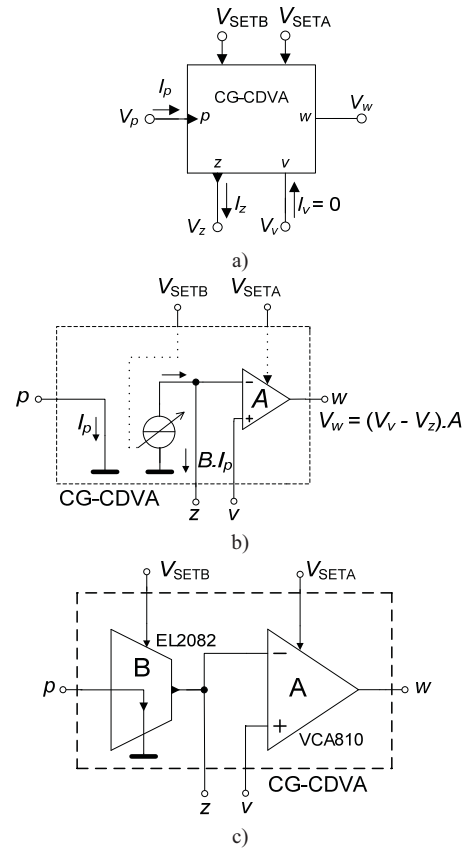


Fig. 1. Controlled gain current and differential voltage amplifier: a) symbol, b) behavioral model, c) possible implementation from commercially available devices.

current and voltage gain control in frame of so-called controlled gain current and voltage amplifier (CG-CVA) was briefly discussed in [27]. Proposed CG-CDVA has availability of combined current output and differential voltage input. The basic mathematical description of this element has form:

$$I_z = B \cdot I_p, V_w = A \cdot (V_v - V_z). \quad (1), (2)$$

Symbol, behavioral model and possible implementation of CG-CDVA was shown in Fig. 1. Behavioral model of CG-CDVA employs current-mode multiplier EL2082 [31] and voltage controlled amplifier VCA810 [32].

III. PROPOSED SIMPLE OSCILLATORS

Proposed circuit is shown in Fig. 2 and has following characteristic equation:

$$s^2 + \frac{R_1 + R_2 - R_1 A}{R_1 R_2 C_2} s + \frac{AB}{R_1 R_2 C_1 C_2} = 0. \quad (3)$$

Condition of oscillations (CO) and frequency of oscillations (FO) are:

$$1 + \frac{R_2}{R_1} \leq A, \omega_0 = \sqrt{\frac{AB}{R_1 R_2 C_1 C_2}}. \quad (4), (5)$$

It is obvious that FO can be controlled by B and CO by A . However, FO depends also on gain A (CO) in case of this simple oscillator shown in Fig. 2. Therefore we modified circuit in Fig. 2 to following realization that is presented in

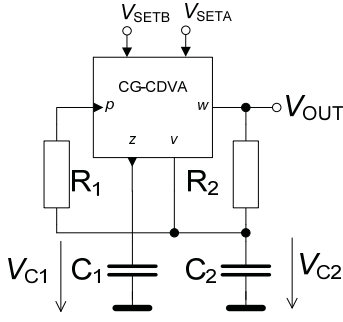


Fig. 2. Proposed simple second order oscillator using CG-CDVA.

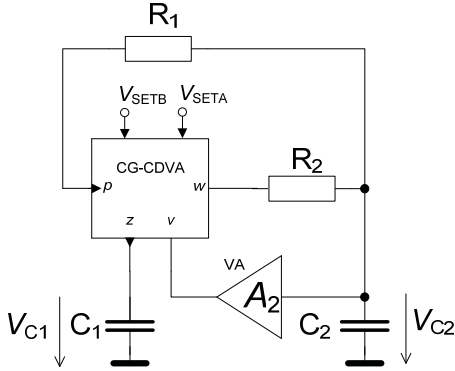


Fig. 3. Modification of simple second order oscillator using CG-CDVA with independent CO and FO.

Fig. 3 which is more suitable for purposes of tunability. Circuit has characteristic equation:

$$s^2 + \frac{R_1 + R_2 - R_1 A_1 A_2}{R_1 R_2 C_2} s + \frac{A_1 B}{R_1 R_2 C_1 C_2} = 0, \quad (6)$$

where A_1 is internal controllable gain inside of CG-CDVA and A_2 is adjustable voltage gain realized outside of CG-CDVA. Oscillation frequency has same form as (5) but CO is different: $A_2 \geq (R_1 + R_2)/R_1 A_1$. Proposed modification allows separated control of CO (considering fixed $A_1 = 1$) without influence on FO by A_2 because this parameter affects CO only. Block of amplifier with adjustable gain A_2 can be designed as non-inverting voltage amplifier with operational amplifier, for example. It allows gain control by simple replacement of grounded resistor by FET transistor. Our further attention is focused on detailed analysis of circuit in Fig. 2.

IV. EXPERIMENTAL VERIFICATION

We created experimental PCB and measuring setup with commercially available devices (in accordance with behavioral implementation of CG-CDVA in Fig. 1c) and documented functionality of oscillator in Fig. 2 by real behavior. We designed measurement setup (Fig. 4) which is suitable for all necessary tests. High-impedance nodes of the oscillator were buffered by voltage buffers BUF634 [33] and matched to 50Ω load (spectrum analyzer). Well-known low-cost and low-frequency opamps TL072 [34] were used in automatic gain control circuit for amplitude stabilization (AGC).

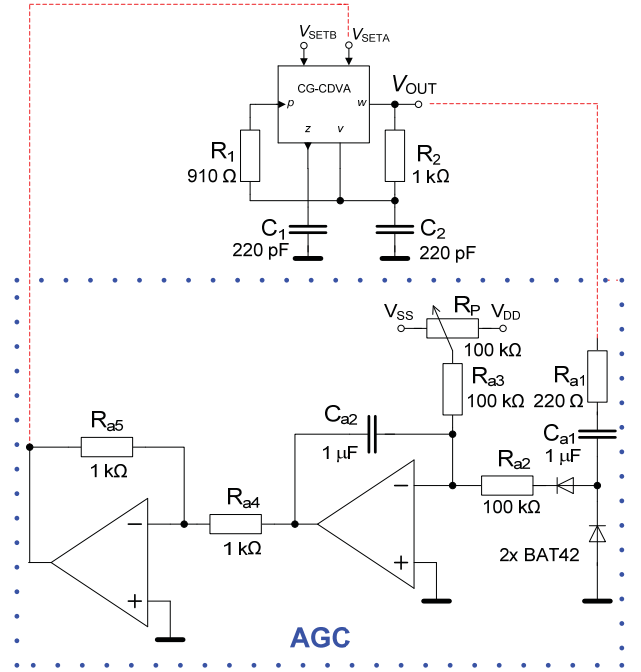


Fig. 4. Measurement setup of simple oscillator.

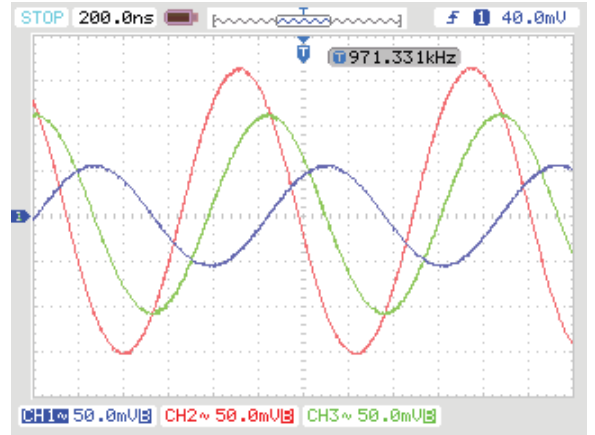


Fig. 5. Measured transient responses ($f_0 = 0.971$ MHz, $V_{SETB} = 1.0$ V, $V_{SETA} \approx -1.136$ V).

Parameters had following values: $R_1 = 910 \Omega$ (internal resistance of p terminal has 95Ω [31]), $R_2 = 1$ k Ω , $C_1 = C_2 = 220$ pF and minimal voltage gain which is necessary for start of oscillation:

$$-V_{SETA} \approx \frac{\log\left(1 + \frac{R_2}{R_1}\right) + 2}{2} \approx \frac{\log(2) + 2}{2} \approx 1.15 \text{ V}, \quad (7)$$

that was calculated from eq. for gain of VCA810 [32]. We calculated ideal FO as $f_0 = 1.023$ MHz for $B = 1.0$ ($V_{SETB} = 1.0$ V). However, necessary gain A was ≈ 1.87 ($V_{SETA} \approx -1.136$ V) and measured frequency $f_0 = 0.971$ MHz. Expected calculation from (5) considering measured value of A (provided by AGC) gives $f_0 = 0.987$ MHz. However, parasitic capacitances of PCB plays important role and they were not included to this estimation.

Results in time domain are in Fig. 5. There are three signals. Voltage V_{OUT} is represented by red color, V_{C1} is highlighted by blue color and V_{C2} by green color. Spectral

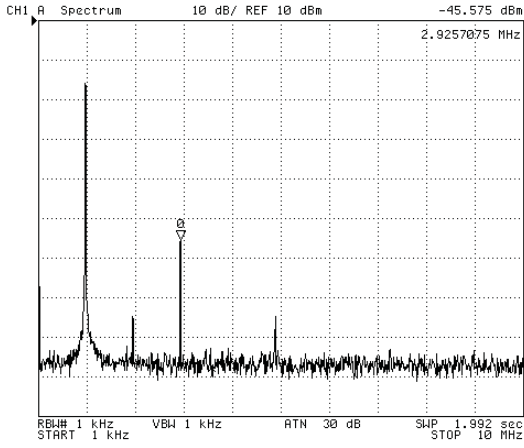


Fig. 6. Frequency spectrum of V_{OUT} .

features of selected output V_{OUT} are observed in Fig. 6 where results of vector-network/spectral analyzer HP4395A are shown. This output has the worst-case total harmonic distortion (THD) $\approx 1\%$.

Experimental results and also further symbolic analysis (considering equality $C_1 = C_2 = C$ and $R_1 = R_2 = R$) shown that quadrature phase shift between voltages across capacitors exists because:

$$\frac{V_{C1}}{V_{C2}} = -j\sqrt{\frac{B}{A}} \approx -j\sqrt{\frac{V_{SETB}}{10^{-2}(V_{SETA}+1)}}. \quad (8)$$

However, amplitude of V_{C1} highly depends on tuning process and also on small changes of A . The main aim of our selection (oscillator in Fig. 2) is demonstrations of main features of practical impact of interactive influence of A in FO caused by automatic (by AGC circuit) compensation of CO. Impact on dependence of FO on controlling parameter is evident because:

$$\omega_0 \approx \sqrt{\frac{V_{SETB} \cdot 10^{-2}(V_{SETA}+1)}{(R_1 + R_p)R_2 C_1 C_2}}. \quad (9)$$

However, experimental results reveal that influence is not significant in observed range of FO tuning. There are three traces in Fig. 7. The first trace (blue color) is ideal representation of equation (5) with fixed $A = 2$, the second trace (dotted purple color) represents so-called expected representation of (9) with influence of compensated A (CO control) and the third trace (red color) shows measured values. Observed impact of compensations of A on FO seems to be insignificant for lower B (V_{SETB} is under 1.5 V and range of adjusting is approximately 1 MHz).

Compensated value of A was obtained experimentally as we documented in Fig. 8. Range of FO adjusting was tested from 0.23 MHz to 1.7 MHz by V_{SETB} changed from 0.05 to 3.61 V.

AGC system keeps V_{OUT} in one low-impedance output nearly constant. However, both voltages in high-impedance nodes (across capacitors) changed when tuning. THD achieves values maximally 1% between 0.75 MHz and 1.7 MHz at V_{OUT} and about 0.3% at V_{C1} . We also analyzed dependence of phase shift between V_{C1} and V_{C2} . The oscillator kept quadrature voltages in observed frequency range with deviation of ± 2 degrees maximally, see Fig. 9.

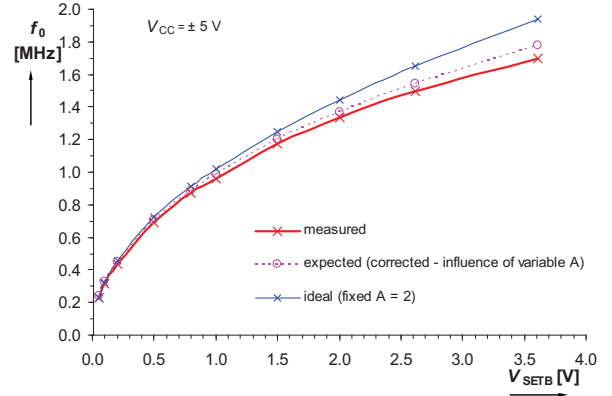


Fig. 7. Dependence of FO on control voltage V_{SETB} .

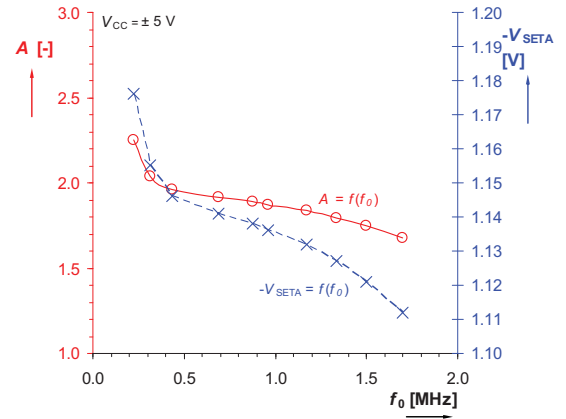


Fig. 8. Dependence of A and control voltage V_{SETB} on FO (response of AGC circuit).

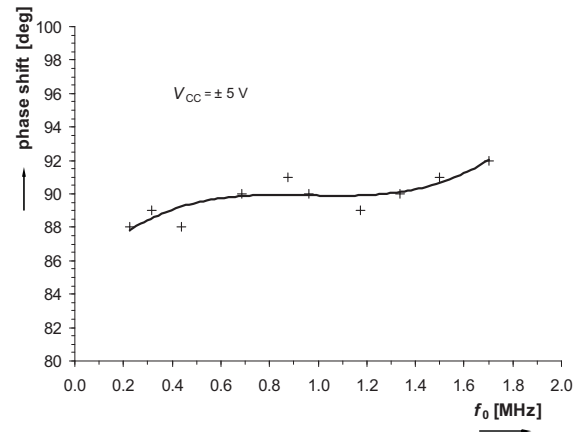


Fig. 9. Measured phase shift between V_{C1} and V_{C2} .

V. CONCLUSION

The paper presents novel active element Controlled Gain Current and Differential Voltage Amplifier (CG-CDVA) and demonstrates its suitability in the adjustable oscillator. The presented type of oscillator satisfy simply one output (we do not expect direct quadrature engagement due to dependence of one generated amplitude on B) tasks in wider range of FO adjusting. This range is not so wideband because control of FO has quadrature character, linear dependence is more

suitable [9], [27] but not possible in such simple case of oscillator. Precise operation is possible for only slightly tuned (or fixed) applications where impact of changes B (moderately also A) on generated amplitudes (8) is not critical (Fig. 7) and amplitudes are affected minimally. Despite of some discussed theoretical problems measured performances of the prototype are interesting and brought useful knowledge of behavior of these types of oscillators. Nevertheless, problem of interactive dependence of FO on CO can be easily overcome by additional controllable voltage amplifier. Further work will be focused on study of the second type of proposed oscillator (with additional amplifier A_2), development and testing of CMOS implementation of proposed CG-CDVA and synthesis of novel applications in the field of controllable filters, oscillators, triangle and square wave generators, etc.

REFERENCES

- [1] D. Biolek, R. Senani, V. Biolkova, Z. Kolka, "Active elements for analog signal processing: Classification, Review and New Proposals," *Radioengineering*, vol. 17, no. 4, pp. 15–32, 2008.
- [2] A. Sedra, K. C. Smith, "A second generation current conveyor and its applications," *IEEE Transaction on Circuit Theory*, vol. CT-17, no. 2, pp. 132–134, 1970.
- [3] A. Fabre, O. Saaïd, F. Wiest, C. Boucheron, "High frequency applications based on a new current controlled conveyor," *IEEE Trans. on Circuits and Systems - I*, vol. 43, no. 2, pp. 82–91, 1996.
- [4] R. L. Geiger, E. Sánchez-Sinencio, "Active filter design using operational transconductance amplifiers: a tutorial," *IEEE Circ. and Devices Magazine*, vol. 1, pp. 20–32, 1985.
- [5] W. Surakampontrorn, W. Thitimaishima, "Integrable electronically tunable current conveyors," *IEE Proceedings-G*, vol. 135, no. 2, pp. 71–77, 1988.
- [6] A. Fabre, N. Mimeche, "Class A/AB Second-generation Current Conveyor with Controlled Current Gain," *Electronics Letters*, vol. 30, no. 16, pp. 1267–1268, 1994.
- [7] G. Soulitis, C. Psychalinos, "Electronically controlled multiphase sinusoidal oscillators using current amplifiers," *International Journal of Circuit Theory and Applications*, vol. 37, no. 1, pp. 43–52, 2009.
- [8] W. Tangsrirat, "Electronically Tunable Multi-Terminal Floating Nullor and Its Application," *Radioengineering*, vol. 17, no. 4, pp. 3–7, 2008.
- [9] D. Biolek, A. Lahiri, W. Jaikla, M. Siripruchyanun, J. Bajer, "Realisation of electronically tunable voltage-mode/current-mode quadrature sinusoidal oscillator using ZC-CG-CDBA," *Microelectronics Journal*, vol. 42, no. 10, pp. 1116–1123, 2011.
- [10] N. Herencsar, A. Lahiri, K. Vrba, J. Koton, "An electronically tunable current-mode quadrature oscillator using PCAs," *Int. Journal of Electronics*, vol. 99, no. 5, pp. 609–621, 2012.
- [11] J. Jerabek, J. Koton, R. Sotner, K. Vrba, "Adjustable band-pass filter with current active elements: two fully-differential and single-ended solutions," *Analog Integrated Circuits and Signal Processing*, vol. 74, no. 1, pp. 129–139, 2013.
- [12] W. Tangsrirat, T. Pukkalanun, "Digitally programmable current follower and its applications," *AEU – International Journal of Electronics and Communications*, vol. 63, no. 5, pp. 416–422, 2009.
- [13] H. Alzahr, N. Tasadduq, O. Al-Ees, F. Al-Ammari, "A complementary metal-oxide semiconductor digitally programmable current conveyor," *International Journal of Circuit Theory and Applications*, available online, 2011, DOI: 10.1002/cta.786.
- [14] S. Minaei, O. K. Sayin, H. Kuntman, "A new CMOS electronically tunable current conveyor and its application to current-mode filters," *IEEE Trans. on Circuits and Systems - I*, vol. 53, no. 7, pp. 1448–1457, 2006.
- [15] A. Marcellis, G. Ferri, N. C. Guerrini, G. Scotti, V. Stornelli, A. Trifiletti, "The VGC-CCII: a novel building block and its application to capacitance multiplication," *Analog Integrated Circuits and Signal Processing*, vol. 58, no. 1, pp. 55–59, 2009.
- [16] M. Kummngern, S. Junnapiya, "A sinusoidal oscillator using translinear current conveyors," in *Proc. Asia Pacific Conf. on Circuits and Systems APPCAS2010*, Kuala Lumpur, 2010, pp. 740–743.
- [17] R. Prokop, V. Musil, "Modular approach to design of modern circuit blocks for current signal processing and new device CCTA," in *Proc. Conf. on Signal and Image Processing IASTED*, Anaheim, 2005, pp. 494–499.
- [18] M. Siripruchyanun, W. Jaikla, "Current controlled current conveyor transconductance amplifier (CCCCTA): a building block for analog signal processing," *Electrical Engineering*, vol. 90, no. 6, pp. 443–453, 2008.
- [19] M. Siripruchyanun, P. Silapan, W. Jaikla, "Realization of CMOS Current Controlled Current Conveyor Transconductance amplifier (CCCCTA) and its applications," *Journal of Active and Passive Electronic Devices*, vol. 4, no. 1-2, pp. 35–53, 2009.
- [20] R. Sotner, J. Jerabek, R. Prokop, K. Vrba, "Current gain controlled CCTA and its application in quadrature oscillator and direct frequency modulator," *Radioengineering*, vol. 20, no. 1, pp. 317–326, 2011.
- [21] D. Biolek, "CDTA – building block for current-mode analog signal processing," in *Proc. European Conf. Circuits Theory and Design ECCTD03*, Krakow, 2003, pp. 397–400.
- [22] W. Jaikla, A. Lahiri, "Resistor-less current-mode four-phase quadrature oscillator using CCCDTAs and grounded capacitors," *AEU - International Journal of Electronics and Communications*, vol. 66, no. 3, pp. 214–218, 2011.
- [23] Ch. Sakul, W. Jaikla, K. Dejhan, "New resistorless current-mode Quadrature Oscillators Using 2 CCCDTAs and Grounded Capacitors," *Radioengineering*, vol. 20, no. 4, pp. 890–896, 2011.
- [24] A. Rodriguez-Vazquez, B. Linares-Barranco, J. L. Huertas, E. Sanchez-Sinencio, E. "On the design of voltage-controlled sinusoidal oscillators using OTAs," *IEEE Trans. Circuits and Systems*, vol. 37, no. 2, pp. 198–211, 1990.
- [25] B. Linares-Barranco, A. Rodriguez-Vazquez, E. Sanchez-Sinencio, J. L. Huertas, "CMOS OTA-C high-frequency sinusoidal oscillators," *IEEE Journal of Solid-State Circuits*, vol. 26, no. 2, pp. 160–165, 1991.
- [26] J. W. Horng, "A sinusoidal oscillator using current-controlled current conveyors," *Int. Journal of Electronics*, vol. 88, no. 6, pp. 659–664, 2001.
- [27] R. Sotner, J. Jerabek, N. Herencsar, Z. Hrubos, T. Dostal, K. Vrba, "Study of Adjustable Gains for Control of Oscillation Frequency and Oscillation Condition in 3R-2C Oscillator," *Radioengineering*, vol. 21, no. 1, pp. 392–402, 2012.
- [28] R. Sotner, Z. Hrubos, B. Sevcik, J. Slezak, J. Petrzela, T. Dostal, "An example of easy synthesis of active filter and oscillator using signal flow graph modification and controllable current conveyors," *Journal of Electrical Engineering*, vol. 62, no. 5, pp. 258–266, 2011.
- [29] Y. Li, "Electronically tunable current-mode quadrature oscillator using single MCDTA," *Radioengineering*, vol. 19, no. 4, pp. 667–671, 2010.
- [30] R. Keawon, W. Jaikla, "A Resistor-less Current-mode Quadrature Sinusoidal Oscillator Employing Single CCCDTA and Grounded Capacitors," *Przeglad Elektrotechniczny*, vol. 87, no. 8, pp. 138–141, 2011.
- [31] *Intersil (Elantec). EL2082 CN Current-mode multiplier* (datasheet), 1996, 14 p., accessible on [www: http://www.intersil.com/data/fn/fn7152.pdf](http://www.intersil.com/data/fn/fn7152.pdf)
- [32] *Texas Instruments. VCA810 High Gain Adjust Range, Wideband, variable gain amplifier* (datasheet), 2003, 30 p., accessible on [www: http://focus.ti.com/lit/ds/sbos275f/sbos275f.pdf](http://focus.ti.com/lit/ds/sbos275f/sbos275f.pdf)
- [33] *Texas Instruments. BUF 634 250 mA High-speed buffer* (datasheet), 1996, 20 p., accessible on [www: http://focus.ti.com/lit/ds/symlink/buf634.pdf](http://focus.ti.com/lit/ds/symlink/buf634.pdf)
- [34] *National Semiconductor. TL072 - Low-noise JFET-input operational amplifiers* (datasheet), 2005, 48 p. accessible on [www: http://www.ti.com/lit/ds/symlink/tl072.pdf](http://www.ti.com/lit/ds/symlink/tl072.pdf)

[8] SOTNER, R., LAHIRI, A., KARTCI, A., HERENC SAR, N., JERABEK, J., VRBA, K. Design of Novel Precise Quadrature Oscillators Employing ECCIs with Electronic Control. *Advances in Electrical and Computer Engineering*, 2013, vol. 13, no. 2, p. 65-72. ISSN: 1582-7445.

Design of Novel Precise Quadrature Oscillators Employing ECCIIs with Electronic Control

Roman SOTNER¹, Abhirup LAHIRI², Aslihan KARTCI³, Norbert HERENC SAR¹,
Jan JERABEK¹, Kamil VRBA¹

¹Faculty of Electrical Engineering and Communication, Brno University of Technology, Czech Republic
²36-B, J and K Pocket, Dilshad Garden, Delhi, India.

³Corlu Engineering Faculty, Namik Kemal University, Cerkezko y, Turkey
sotner@feec.vutbr.cz

Abstract—In this paper, an interesting design of precise quadrature oscillator employing electronically controllable current conveyors of the second generation (ECCII) is presented. The main purpose of this paper is to show advantages and features of direct electronic control of application by an adjustable current gain where help of signal flow graph approach was used to clearer and visual understanding of the design. The discussed circuit and its presented modification have several favorable features such as grounded capacitors, independent electronic adjusting of oscillation frequency and condition of oscillation by the current gain and easy automatic gain control circuit (AGC) implementation (non-ideal effects of tuning process on output amplitudes are suppressed). Oscillator was designed for frequency band of units of MHz and tested with two types of inertial AGCs. Theoretical presumptions were confirmed by laboratory experiments.

Index Terms—Direct electronic control, current gain adjusting, electronically controllable current conveyors, quadrature oscillators, signal flow graph approach.

I. INTRODUCTION

A. Overview of controlling possibilities in current conveyors and amplifiers

Current or voltage-mode integrators employing current conveyors CCII [1-4] are very often used in modern analog circuit design. However, resistors (in most cases grounded) or adjustable resistance of current input called R_X is the only way how to change the time constant. This parameter can be adjusted by the bias current I_b in limited range. This solution is very popular in novel on-chip implementations of new active elements. The examples of such elements, their definitions and descriptions can be found in [3-8]. Adjusting of current gain in current active elements and in current conveyors (CC) was firstly introduced in [9]. This approach is built on the adjustable transfer between X and Z ports in the CCII type. Authors defined so-called electronically controllable current conveyor of second generation (ECCII). There are already some works on this topic in the open

literature. Nevertheless, it is still not so common way how to adjust circuit parameters and many solutions still use the R_X (I_b) control. Minaei et al. [10] introduced novel element called ECCII, where current gain control was also possible. Similarly, Marcellis et al. in [11], Tangsrirat in [12], Shi-Xiang et. al in [13] and Herencsar in [14] proposed active elements with this useful feature. It provides interesting and special feature in many applications. In some recently published works that focus on the oscillator and filter design [14-25], the implementation of adjustable current gain (B_G) for control of parameters in application is quite a beneficial solution.

B. Recently reported oscillators employing current gains

We focused on state-of-the-art of oscillator solutions, which use current gain control for electronic adjusting in applications. Of course, there are many oscillators based on active elements working with different principles in contemporary literature. Hitherto published solutions employs such elements, e.g. transconductors (OTAs), current differencing transconductance amplifiers (CDTAs), current follower transconductance amplifiers (CFTA), and many others [3]. Our discussion will be specialized on solutions employing current-gain control.

This work focuses on oscillator design, where the main aim is the electronic control of oscillation frequency (f_0) and condition of oscillation (CO) using B_G simultaneously. Several hitherto published works were presented in this area. Souliotis et al. presented multiphase oscillator using lossy integrators based on the adjustable current amplifiers in [15]. All capacitors are grounded, CO and oscillation frequency are electronically and independently adjustable. The oscillator produces current output signals. Multiphase solution with cascade connection of lossy integrators based on translinear current conveyors (CCCII) was introduced by Kumngern et al. in [16]. Kumngern et al. also published work [17], where combination of both methods (intrinsic resistance and current gain control) was verified. A solution presented in [17] requires two active elements. CO is driven by current gain and f_0 by R_X (I_b). The oscillator does not provide quadrature outputs and linear control of f_0 . In [20], the ECCII was a functional part of modified active element, CCTA [3] and B_G control was used for the oscillation frequency adjusting in simple quadrature oscillator. Electronic control of f_0 is possible by B_G , but CO control is available only by adjusting of grounded resistor. It is a very simple solution employing only one active element, but

Research described in the paper was supported by Czech Science Foundation projects under No. 102/11/P489 and No. 102/09/1681. The support of the project CZ.1.07/2.3.00/20.0007 WICOMT, financed from the operational program Education for competitiveness, is gratefully acknowledged. The described research was performed in laboratories supported by the SIX project; the registration number CZ.1.05/2.1.00/03.0072, the operational program Research and Development for Innovation and supported by the project CZ.1.07/2.3.00/30.0039. This research work is also funded by projects EU ECOP EE.2.3.20.0094, CZ.1.07/2.2.00/28.0062.

there are some drawbacks in this solution. The first problem is dependence of one produced amplitude on tuning process (B_G which tunes f_0) and the second problem is nonlinear control of f_0 . Very interesting oscillator in [22] provides control of f_0 and CO by B_G , but these parameters are not independent and control of f_0 is also not linear. In addition, only one capacitor is grounded. Independence between f_0 and CO parameters was achieved in [23]. However, there is dependence of one of produced amplitudes on B_G under tuning process and control of f_0 is not linear. It is a problem of very simple solutions using minimal number of active elements and grounded capacitors. Current-gain control suitable for f_0 control was used also in [24] and [25] in quadrature oscillators employing so-called z-copy controlled-gain current-differencing buffered amplifier (ZC-CG-CDBA). The solution in [24] is based on two active elements and five passive elements (capacitors are grounded). Nevertheless, active element is quite complicated. Discrete model requires four diamond transistors [26-27] and voltage buffer, but it is not a problem for future on-chip implementation. The oscillation frequency is controllable by B_G linearly. CO and f_0 are completely independent. There is no dependence of output amplitude on tuning process. CO is controllable via floating resistors only (it is a small drawback of this solution). The authors used optocoupler for amplitude stabilization and automatic gain control circuit (AGC). The solution in [25] requires two ZC-CG-CDBAs and 6 passive elements (capacitors are also grounded). CO is also controllable by floating resistor, and f_0 is even adjustable digitally (dependence of f_0 on B_G is linear). Alzahr in [28] introduced interesting solution where digital adjusting of current gains was used to ensure linear f_0 control and simple CO control (both by current gains). Complexity of circuit is similar to the discussed solutions (four resistors, two grounded capacitors).

C. Our proposal and comparison

We can summarize the important features of previous works focused on current gain control for adjustability and tuning purposes. There is linear dependence of f_0 on B_G in our solution and output amplitude is not affected by tuning process in comparison to the work [17] or [20]. Only CO is controllable by B_G in [17]. In [20] is still necessary to control CO by adjusting of passive element. A very simple solution in [22] allows to control f_0 and CO by B_G , but f_0 is dependent on CO. Both parameters are independent in [23], but dependence of f_0 on B_G is not linear and one of output amplitudes is changing if f_0 is adjusted. Finally, in [24] and [25], there were many from previous drawbacks removed. However, CO is still controllable only by floating resistor. Digital control of current gain in order to adjust f_0 and also CO was introduced in [28]. There were also almost all drawbacks solved but solution requires four resistors and similar number of active elements as in our case. A digital discontinuous control of CO (by current gain) may not be the best solution. Accuracy and precision of AGC require also careful and soft gain adjusting to minimize fluctuances of output amplitudes and obtain acceptable THD. Continuous control is better and maybe simpler than digital control because appropriate bit resolution of gain control is necessary for soft adjusting of CO. Linear control of f_0 ,

mutual independence of CO and f_0 and direct continuous electronic control of f_0 and CO only by current gain (B_G) simultaneously are possible in our solution with respect to works discussed above. CO and f_0 are controllable by DC voltage and therefore easy implementation of inertial AGC is possible. There are no problems with dependences of one output amplitude on B_G . Our work practically complements the family of oscillators [22-25] employing current gain (B_G) for direct electronic control of oscillator parameters. Powerful approach using state variable methods ([29-31] for example) could also be used for this design and results should be identical. We can discuss examples regarding very impressive works written by Gupta et al. [29-30]. Many oscillator structures including current feedback amplifier based integrators (in fact) in the loops constructed by the state variable methods were introduced in both works [29-30]. Oscillators in [29] are simpler (only two active elements, grounded capacitors) than solution described in our contribution. Unfortunately, oscillators in [29-30] belong to single resistance controllable types (electronic control is more complicated) and relations between amplitudes exist in case of tuning. Both stable output amplitudes while oscillator is tuned are required in many communication systems [24]. It is not novelty of our solution but this requirement was not considered for oscillator synthesis in many hitherto published works. Clarity of signal flow graph methods and descriptions is more suitable for help with design, better understanding of the behavior in the circuit (direct and feedback branches) and correct insertion of controllable active elements to the circuit in order to control f_0 without influencing amplitudes through tuning process.

The main aim of this paper is not to propose novel method of synthesis. This work focuses on investigation of controllable features in oscillators employing electronically adjustable current conveyors with current gain control for precise quadrature oscillator design operating without standard problems (non-linear control of oscillation frequency and amplitudes dependent on tuning process) of many reported and simpler solutions. The main result of our proposal is novel and precise quadrature oscillator (based on clear design and principle of operation) with wideband and linear f_0 control, with easy implementation of AGC, acceptable THD level and unchangeable amplitudes during the tuning process.

The paper is organized as follows: Known ways of electronic control in current conveyors and amplifiers, recent progress in the oscillator design based on continuous current gain control and comparisons are introduced in the Introductory section. Proposed circuit and design steps are discussed in details in the Section 2. Specific design, real behavior and experimental results are summarized in the Section 3. Concluding notes are in the Section 4.

II. PROPOSED OSCILLATOR DESIGN

We used two types of active elements (current conveyors, see Fig. 1) in proposed oscillator. The first is electronically controllable current conveyor of second generation (ECCII) [9]. The function is described by quite common and simple equations (in ideal case): $V_Y = V_X$, $I_Y = 0$, $I_Z = -B_G I_X$. The current gain between X and Z ports is adjustable and voltage

gain (transfer) from Y to X port is fixed (equal to 1). The second type is well-known current conveyor of second generation (CCII+/-) [1-3] with one or two outputs of both polarities (Z+/Z-). Transfer between X and Z ports and between Y and X ports of CCII+/- are fixed (equal to ± 1): $V_Y = V_X, I_Y = 0, I_{Z+} = I_X, I_{Z-} = -I_X$.

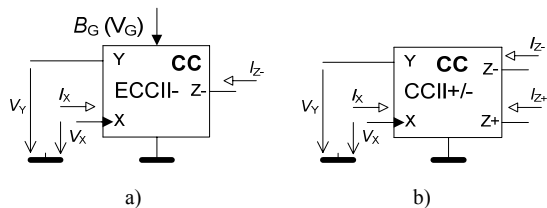


Figure 1. Current conveyors used in proposed oscillators: a) ECCII-, b) CCII+/-

Design was based on frequently used integrators (loss-less and lossy) in two feedback loops (similarly to multifunctional filters [32-37]). The first attempt [23] of design of this type oscillator was provided with only two ECCII- and one CCII+. The first ECCII allows to control f_0 and the second was used for CO control and future implementation of AGC. However, detailed analysis shows one disadvantage in [23], which is caused by driving gain B_G influencing the amplitude of produced signal (therefore amplitude changed with adjusting of f_0). While one of generated amplitudes has constant value, the second output amplitude is varying in dependence on tuning. Therefore, we improved this type of the oscillator in [23] and result is presented in this paper (two structures in Fig. 2 and Fig. 3). Our approach is based on the aid of signal flow graph (SFG) [38-39] which represents the two-loop circuit structure (Fig. 2) with current distribution [34], similarly as in [23]. The characteristic equation can be easily obtained by application of Mason rule [38-39] (Δ - determinant of SFG):

$$\Delta = 1 - (L_1 + L_2) = 1 - [F_1 H_1(s) H_2(s) + F_2 H_2(s)] = 0, \quad (1)$$

where

$$H_1(s) = k_1 \frac{1}{s}, \quad H_2(s) = k_1 \frac{1}{s + k_2}. \quad (2), (3)$$

New modification (Fig. 3) contains additional ECCII, in order to eliminate the disadvantage of amplitude dependence and extend f_0 range of adjusting. Dependence of f_0 on $B_{G1,2}$ is linear, which is more suitable and typical in controllable oscillators. Simultaneous changes of two current gains $B_{G1,2}$ is the only disadvantage of this solution. Transfers of the branches have the following forms:

$$H_1(s) = \frac{B_{G1}}{sC_1 R_1}, \quad H_2(s) = \frac{-R_2}{R_3(sC_2 R_2 + 1)}, \quad (4), (5)$$

$$F_1 = -B_{G2}, \quad F_2 = -B_{G3}. \quad (6), (7)$$

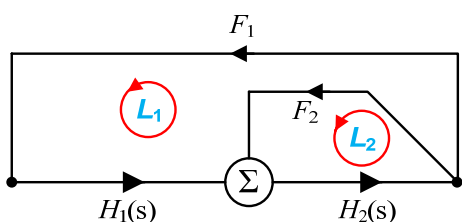


Figure 2. General two loop system

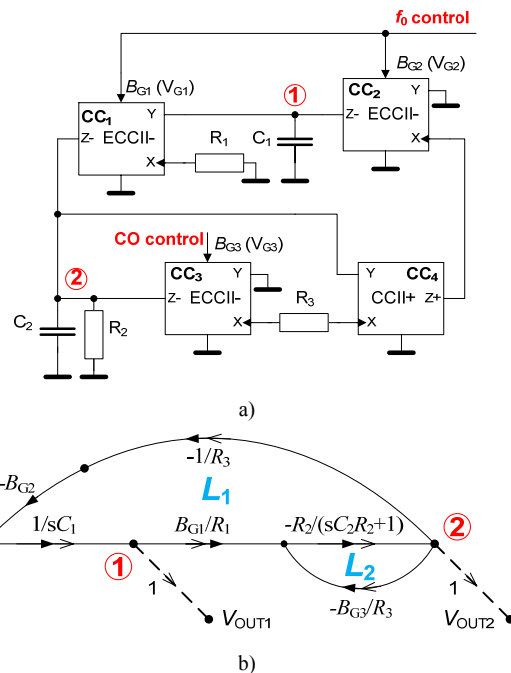


Figure 3. Proposed quadrature oscillator: a) circuit, b) detailed SFG

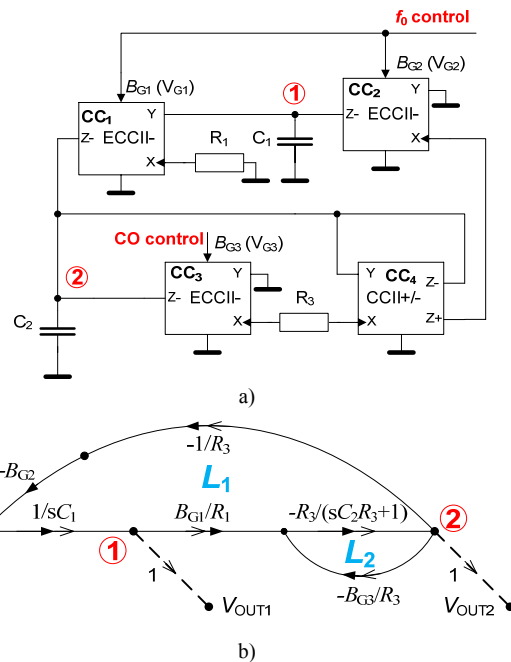


Figure 4. Proposed modified oscillator with reduced number of passive components: a) circuit, b) detailed SFG

We can discuss principle in more detail. In Fig. 3 we can see solution of the quadrature oscillator (autonomous circuit). Figure 3b shows simple signal flow graph (SFG), where conversion between voltage and current is documented by dotted and full arrows. The CC₁, CC₂ with R₁ and C₁ presents current-mode loss-less integrator. CC₄ and C₂, R₂, R₃ create lossy integrator (node 2). Useful feature of such integrator with current distribution (CC₃ + CC₄) is the possibility to change current gain of one path and therefore also gain of one feedback branch (CC₃ presents adjustable feedback path). Our requirement is to achieve solution without problem of varying amplitudes during the tuning process. Therefore, we need two adjustable parameters in large loop L₁ (F₁H₁H₂). Adjustable gain B_{G1} was implemented directly in current integrator

formed by CC_1 and R_1 and C_1 . Lossy integrator H_2 was not primary constructed as adjustable. Product of F_2H_2 must not include any adjustable parameter which is determined for f_0 control, as we can see from (1) and also from the example (8). Mutually independent control of CO and f_0 is the reason for this presumption. The second gain B_{G2} (CC_2) was solved as separate adjustable path (from output of CC_4 to node 1). Additionally, CC_2 could be considered as another complication (extra active element) but it brings also beneficial feature. Simultaneous adjusting of B_{G1} and B_{G2} allows linear and wide-range f_0 adjusting in comparison to the single-parameter-controllable oscillators and removes obstacle with amplitude dependences. The second loop created by F_2H_2 (1) has to ensure CO control without affection on f_0 . Separated feedback path created by CC_3 (B_{G3}) allows easy CO control, see (8). This step is really necessary. Therefore, we cannot use one simple CC instead of CC_3 and CC_4 . The characteristic equation of the oscillator in Fig. 3 has the following form:

$$\Delta_1 = 1 - (L_1 + L_2) = 1 - \left[-\frac{1}{R_3} B_{G2} \frac{1}{sC_1} \frac{B_{G1}}{R_1} \frac{R_2}{(sC_2R_2 + 1)} \right] + \frac{B_{G3}}{R_3} \frac{R_2}{(sC_2R_2 + 1)} = s^2 + \frac{R_3 - R_2 B_{G3}}{R_2 R_3 C_2} s + \frac{B_{G1} B_{G2}}{R_1 R_3 C_1 C_2} = 0. \quad (8)$$

Condition of oscillation and oscillation frequency are:

$$B_{G3} \geq \frac{R_3}{R_2}, \quad (9)$$

$$\omega_0 = \sqrt{\frac{B_{G1} B_{G2}}{R_1 R_3 C_1 C_2}}. \quad (10)$$

Relation between generated amplitudes is:

$$\frac{V_{OUT1}}{V_{OUT2}} = \frac{B_{G2}}{j\omega_0 C_1 R_3} = -j \sqrt{\frac{R_1 C_2 B_{G2}}{R_3 C_1 B_{G1}}}, \quad (11)$$

$$V_{OUT1} = V_{OUT2} \sqrt{\frac{R_1 C_2 B_{G2}}{R_3 C_1 B_{G1}}} e^{\frac{\pi}{2}j}. \quad (12)$$

Simultaneous change of B_{G1} and B_{G2} ($B_{G1} = B_{G2} = B_{G1,2}$) tunes oscillation frequency linearly without influence of output amplitudes as is clear from (12). Sensitivities of ω_0 on parameters of active and passive elements are following:

$$S_{R_1}^{\omega_0} = S_{R_3}^{\omega_0} = S_{C_1}^{\omega_0} = S_{C_2}^{\omega_0} = -0.5, \quad (13)$$

$$S_{B_{G1}}^{\omega_0} = S_{B_{G2}}^{\omega_0} = 0.5, \quad S_{B_{G3}}^{\omega_0} = S_{R_2}^{\omega_0} = 0. \quad (14)$$

The modified solution of the oscillator from Fig. 3 is shown in Fig. 4. Resistor R_2 was saved in this modification and only 2R-2C based oscillator with four CC was obtained. This designation (2R-2C) was used in [40-41] for oscillators which contain only two resistors and two capacitors. However, CC_4 must be extended to two-output type (two Z ports) and then only four passive elements are needed. The CC_4 is more complicated than simple three-port CCII+ but for internal topology of CC it is no problem [4-5], [15-16]. The characteristic equation for the modified oscillator in Fig. 4 is:

$$\Delta_2 = s^2 + \frac{1 - B_{G3}}{R_3 C_2} s + \frac{B_{G1} B_{G2}}{R_1 R_3 C_1 C_2} = 0. \quad (15)$$

Oscillation frequency is given by formula (10) and CO is very simple: $B_{G3} \geq 1$. A relation between both produced

amplitudes equals to (11) and (12). Sensitivities of f_0 on circuit parameters are the same as in the first type of oscillator.

III. REAL BEHAVIOR AND DISCUSSION OF EXPERIMENTAL RESULTS

We choose first type of the oscillator for a detailed analysis, because it can be realized easily by available active elements. A circuit from Fig. 3 was extended by several passive elements. These elements are modeling the most important parasitic influences in the real circuit. Hatched resistors in Fig. 5 include intrinsic resistances of current inputs of used active elements or resistances of current outputs. Capacitors C_{p1} and C_{p2} were also added in order to represent important parasitic behavior. We used current mode multiplier EL2082 [42], diamond transistor OPA860 [27] and buffer OPA633 [43] for experimental purposes. The expected values of parasitics are derived from their models.

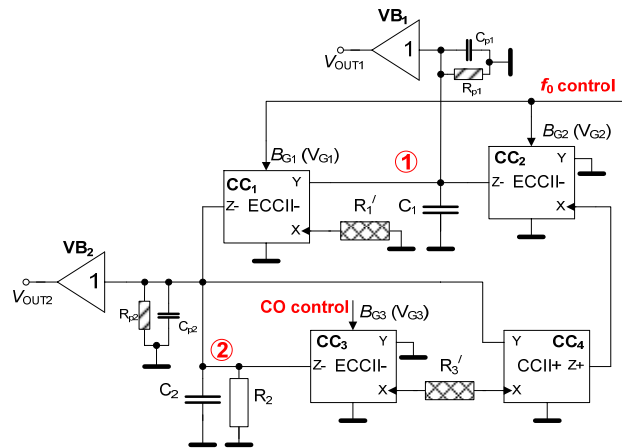


Figure 5. Important parasitic influences in the analyzed oscillator from Fig. 3

From Fig. 5 we can determine the following parameters: $R_{p1} \approx R_{Y_CC1} \parallel R_{Z_CC2} \parallel R_{inp_buff1}$, $C_{p1} \approx C_{Y_CC1} + C_{Z_CC2} + C_{inp_buff1}$, $R_{p2} \approx R_{Z_CC1} \parallel R_{Z_CC3} \parallel R_{Y_CC4} \parallel R_{inp_buff2}$, $C_{p2} \approx C_{Z_CC1} + C_{Z_CC3} + C_{Y_CC4} + C_{inp_buff2}$, $R_1' \approx R_1 + R_{X_CC1}$, $R_3' \approx R_3 + R_{X_CC3} + R_{X_CC4}$. Datasheet information indicates values as follows: $R_{Y_CC1,2,3} \approx 2 \text{ M}\Omega$, $R_{Z_CC1,2,3} \approx 1 \text{ M}\Omega$ and $C_{Y_CC1,2,3} \approx 2 \text{ pF}$, $C_{Z_CC1,2,3} \approx 5 \text{ pF}$, $R_{X_CC1,2,3} \approx 95 \Omega$ (EL2082 [42]); $R_{Y_CC4} \approx 0.455 \text{ M}\Omega$, $C_{Y_CC4} \approx 2 \text{ pF}$, $R_{Z_CC4} \approx 54 \text{ k}\Omega$, $C_{Z_CC4} \approx 2 \text{ pF}$, $R_{X_CC4} \approx 13 \Omega$ (OPA860 [27]); input diamond buffer of OPA860 [27] characteristics $Z_{inp_buff2} \approx 1 \text{ M}\Omega / 2 \text{ pF}$; $Z_{inp_buff1} \approx 1.5 \text{ M}\Omega / 1.6 \text{ pF}$ (OPA633 [43]). The resulting values are: $R_{p1} \approx 462 \text{ k}\Omega$, $R_{p2} \approx 192 \text{ k}\Omega$, $R_1' \approx 915 \Omega$, $R_3' \approx 928 \Omega$; $C_{p1} \approx 8.6 \text{ pF}$, $C_{p2} \approx 14 \text{ pF}$. We suppose $R_{X_CC2} \ll R_{Z_CC4}$. We can neglect these parameters because $95 \Omega \ll 54 \text{ k}\Omega$. Equations for oscillation frequency and CO considering real influences are:

$$\omega_0' = \sqrt{\frac{B_{G1} B_{G2} \left(\frac{R_2 R_{p2}}{R_2 + R_{p2}} \right) R_{p1} + R_1' \left[R_3' - B_{G3} \left(\frac{R_2 R_{p2}}{R_2 + R_{p2}} \right) \right]}{R_1' \left(\frac{R_2 R_{p2}}{R_2 + R_{p2}} \right) R_3' R_{p1} C_1' C_2'}}}, \quad (16)$$

$$B'_{G3} \geq \frac{R'_3 \left[\left(\frac{R_2 R_{p2}}{R_2 + R_{p2}} \right) C'_2 + R_{p1} C'_1 \right]}{\left(\frac{R_2 R_{p2}}{R_2 + R_{p2}} \right) R_{p1} C'_1} \quad (17)$$

Careful analysis reveals in equation (16) that

$$B_{G1} B_{G2} \left(\frac{R_2 R_{p2}}{R_2 + R_{p2}} \right) R_{p1} \gg R'_1 \left[R'_3 - B_{G3} \left(\frac{R_2 R_{p2}}{R_2 + R_{p2}} \right) \right] \quad (18)$$

Significant influence exists only for $B_{G1,2} \rightarrow 0$.

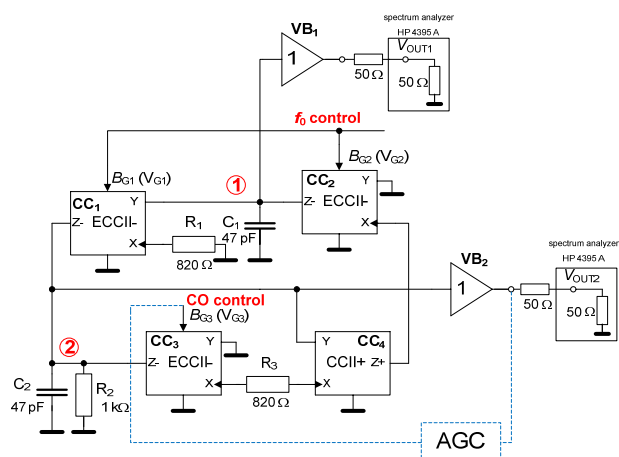


Figure 6. Configuration of experimentally tested oscillator

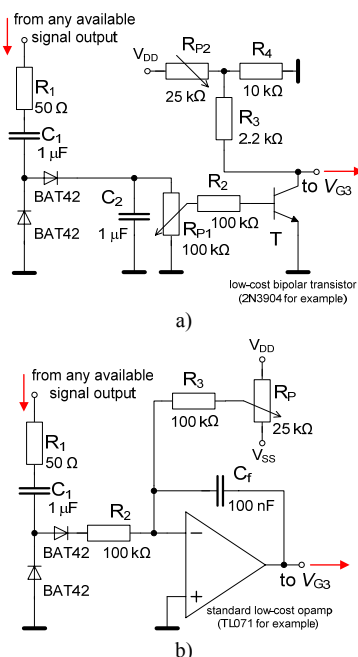


Figure 7. Two types of AGC for experimental purposes: a) based on BJT, b) based on opamp

The circuit shown in Fig. 3 was experimentally tested and we obtained the following results. For better and clearer understanding, particular measured circuit with designed values and measuring devices included is shown in Fig. 6. For ECCIIs (CC₁-CC₃), modeled by EL2082 multiplier, $B_G \approx V_G$ [42] is valid. Selected values of passive elements are $R_1 = R_3 = 820 \Omega$, $R_2 = 1 \text{ k}\Omega$, $C_1 = C_2 = 47 \text{ pF}$. Supply voltage is symmetrical $V_{DD} = +5 \text{ V}$ and $V_{SS} = -5 \text{ V}$. In accordance to analysis of parasitic influences, it is clear that real parameters of active elements play important role. Parasitic capacitances have main impact on accuracy of f_0

because they are comparable to the working values C_1 and C_2 . Tolerances of C_1 and C_2 are very important too. Some estimations based on above discussion of parasitic elements are given: $R'_1 \approx 915 \Omega$, $R'_3 \approx 928 \Omega$, $C'_1 \approx 56 \text{ pF}$, $C'_2 \approx 61 \text{ pF}$.

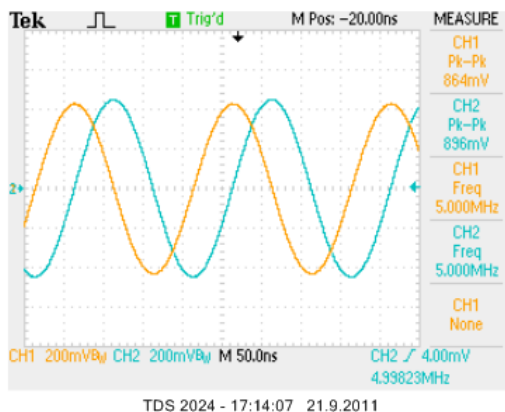


Figure 8. Transient responses of oscillator (when AGC from Fig. 7a was used) for $f_0 = 5 \text{ MHz}$

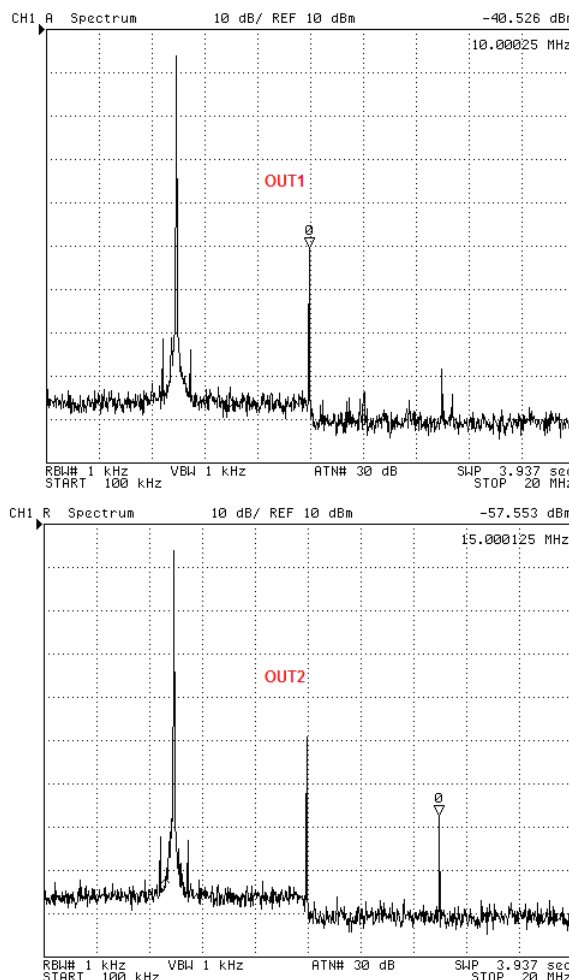


Figure 9. Spectral analysis for both outputs (AGC from Fig. 7a) for $f_0 = 5 \text{ MHz}$

However, tolerances of passive elements and parasitics of printed circuit board (PCB) were not considered. Experimental verification was made with two different types of very simple inertial AGC circuit (Fig. 7). These circuits are suitable for voltage control of CO in similar oscillator solutions. The AGC circuits contain cascade diode doubler. The first type of AGC is based on very simple common-emitter DC amplifier with bipolar transistor. The function is

based on nonlinear input-output transfer characteristic of this amplifier. The second type of AGC uses common opamp. Potentiometers are necessary for careful and very fine adjusting of CO.

The transient responses and spectral analysis of the oscillator with first type of AGC (Fig. 7a) are in Fig. 8 and Fig. 9. Results are for $f_0 = 5$ MHz ($B_{G1,2} = 1.63$).

The transient responses and spectral analysis of the oscillator with second type of AGC (Fig. 7b) are shown in Fig. 10 and Fig. 11 for same values of $B_{G1,2}$ as in previous case. The second type of AGC (Fig. 7b) offers larger suppression of higher harmonic components and therefore lower THD for nearly equal amplitudes, see Fig. 8 - Fig. 11.

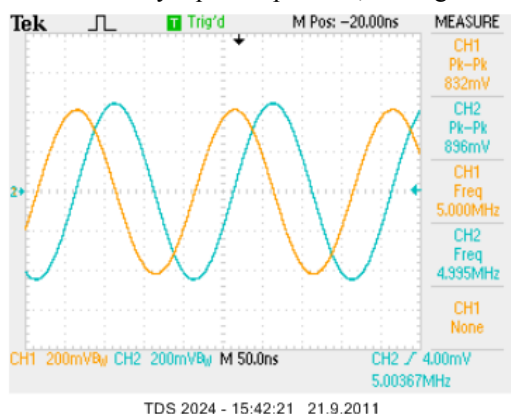


Figure 10. Transient responses of oscillator (when AGC from Fig. 7b was used) for $f_0 = 5$ MHz

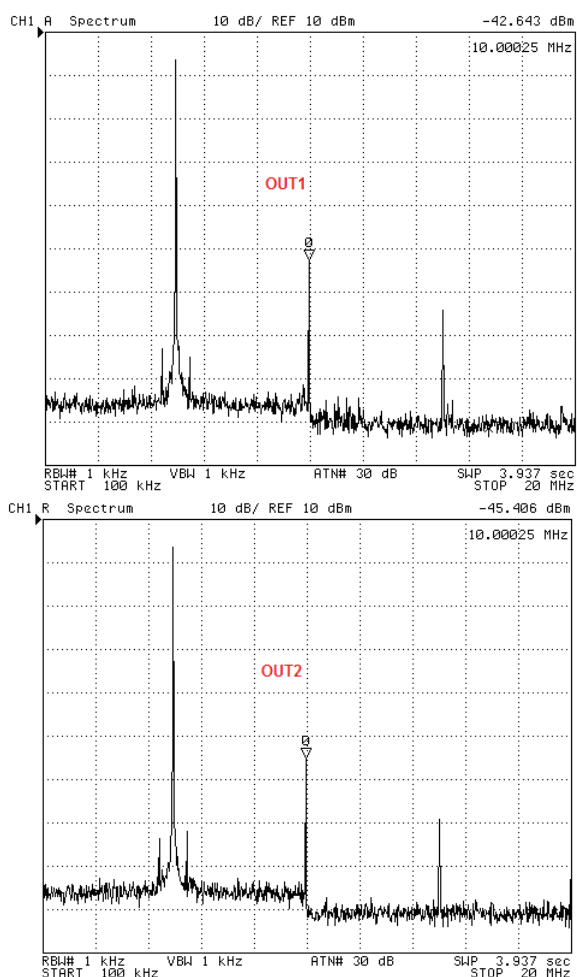


Figure 11. Spectral analysis for both outputs (AGC from Fig. 7b) for $f_0 = 5$ MHz

In Fig. 12 ideal, expected and measured dependences of f_0 on current gain $B_{G1,2}$ are compared. Ideal dependence was obtained from eq. (10), where only expected values $R_1' \approx 915 \Omega$, $R_3' \approx 928 \Omega$ were considered. Ideal range of f_0 adjusting is from 0.25 MHz to 8.84 MHz. Expected range is from 0.20 MHz to 7.13 MHz. The expected curve was calculated from (16). Range of f_0 adjusting from 0.13 MHz to 7.87 MHz was gained from measurement. All traces in Fig. 12 were obtained for $B_{G1,2}$ from 0.06 to 2.4 ($V_{G1,2}$ from 0.06 to 2.6 V). We have measured and evaluated dependences of output level and total harmonic distortion (THD) on f_0 . Results are in Fig. 13 and Fig. 14.

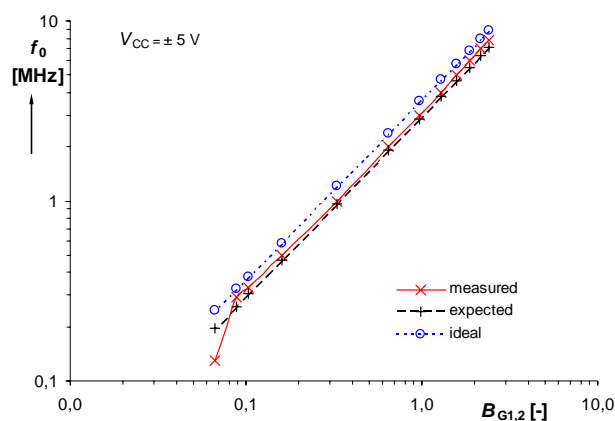


Figure 12. Dependence of f_0 on $B_{G1,2}$

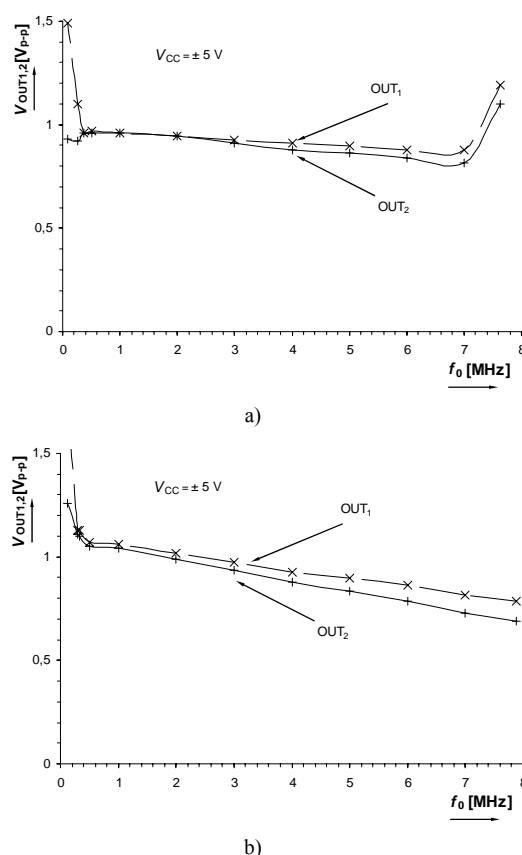


Figure 13. Dependence of voltage level of output signals on f_0 for oscillator using: a) AGC in Fig. 7a, b) AGC in Fig. 7b

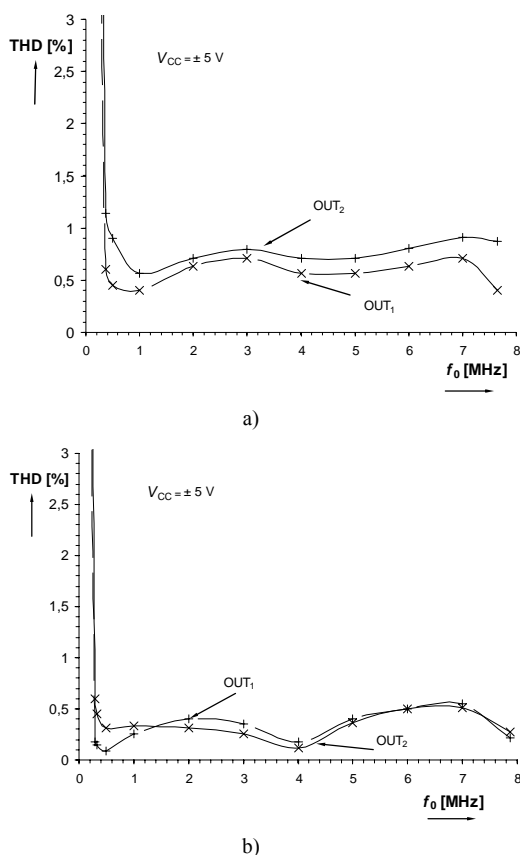


Figure 14. Dependence of THD on f_0 for oscillator using: a) AGC in Fig. 7a, b) AGC in Fig. 7b

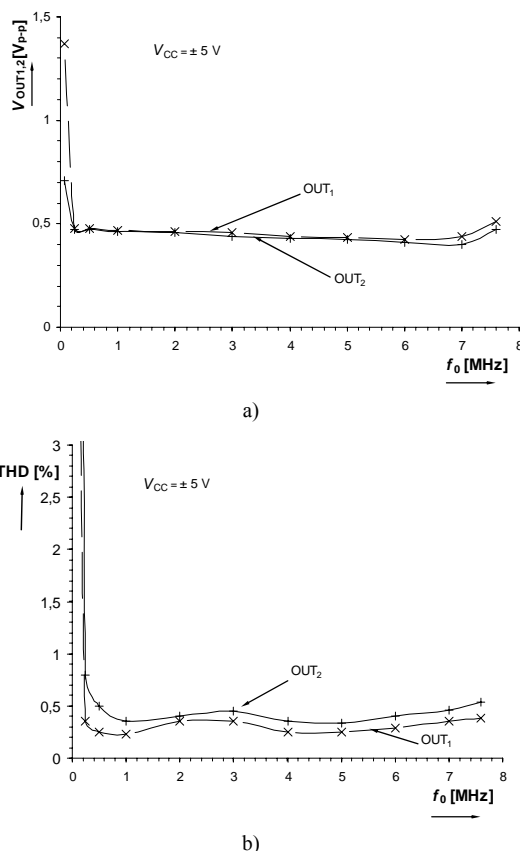


Figure 15. Results of readjusted AGC (Fig. 7a): a) output levels in dependence on f_0 , b) dependence of THD on f_0

We can see fluctuation of THD between 0.4 and 0.9 % in almost whole range of f_0 (AGC type from Fig. 7a). AGC type in Fig. 7b (with opamp) provides lower THD between

0.1 and 0.6 %, but falling of output level with increasing of f_0 is slightly faster. Therefore, better setting of the AGC circuit in Fig. 7a for next experiments was used. Output voltage was changed to half of values used in measurement documented in Fig. 13a and THD was decreased. Values are then between 0.2 and 0.5 %. This setting also improves stability of output level. The dependence of $V_{OUT1,2}$ on f_0 is now nearly constant. The results are shown in Fig. 15.

The proposed circuit in Fig. 6 can be easily simulated in PSpice program. All used commercially available active elements (EL2082, OPA860, etc.) have models that are included in PSpice libraries. We provided statistical Monte-Carlo analyses of the discussed oscillator for typical fabrication tolerances of passive elements (see Tab. 1) and Gaussian distribution. Fabrication uncertainty of key parameters of the active elements, that are responsible for control of oscillation frequency ($B_{1,2}$), was simulated by variation of $V_{G1,2}$ (also in Tab. 1). The initial settings of oscillator was provided for $f_0 = 5$ MHz. Table 1 contains the maximal and minimal (the most pessimistic case) f_0 , more optimistic (close to the real case) standard deviation (sigma) and mean value of f_0 . The analyses confirmed expected sensitivities of f_0 on passive and active parameters in equations (13) and (14). High tolerances of $V_{G1,2}$ ($B_{1,2}$) mean high dispersion of expected f_0 . Figure 16 shows an example of Monte-Carlo set results.

Tab. 1. Results of Monte-Carlo analysis (100 runs)

tolerances [%]			mean	min	max	sigma
R_1, R_2, R_3	C_1, C_2	V_{G1}, V_{G2}	[MHz]	[MHz]	[MHz]	[kHz]
1	5	5	4.986	4.809	5.157	70.4
1	5	10	4.982	4.682	5.249	111.6

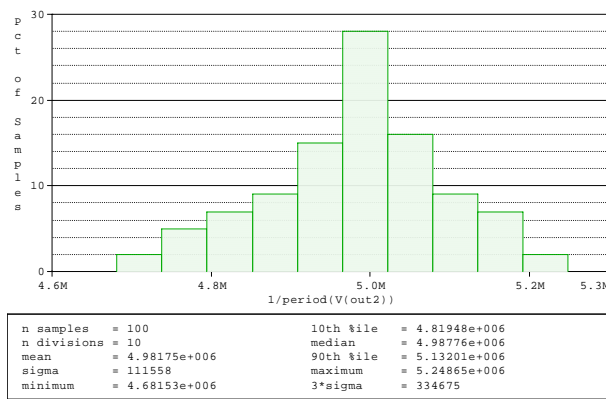


Figure 16. Histogram of Monte-Carlo analysis (tol. 10% $V_{G1,2}$, 5% C , 1% R)

IV. CONCLUSION

In this paper, we discussed features of quadrature oscillator using ECCII and CCII elements, which was systematically designed by two-loop integrators synthesis and help of signal-flow graph approach for better understanding. In recent years, many works dealing with the quadrature oscillator synthesis and design have been published. However, our approach to this problem was based more practically and mainly on quality of produced signals, i.e. precise electronic adjusting of the CO (two AGCs) and tuning of f_0 with minimal fluctuances of output level and low THD in comparison to common similar research works (simpler solutions employing minimal number of active elements for example). We obtained more accurate equations for oscillator design from more detailed

analyses of influences of real active elements which are useful for calculation of expected results. Experimental verifications with two very simple AGC circuits were provided and compared. Output amplitudes are not influenced by tuning of f_0 (this is typical for simpler types of oscillators) and the proposed method of current gain control of CO allows simple implementation of AGC. Really good results (nearly constant output amplitudes for wideband tuning of oscillation frequency and low THD) were obtained for optimal setting of AGC.

REFERENCES

- [1] A. Sedra, K. C. Smith, "A second generation current conveyor and its applications," *IEEE Transaction on Circuit Theory*, vol. CT-17, no. 2, pp. 132-134, 1970.
- [2] J. A. Svoboda, L. M. McGory, S. Webb, "Applications of commercially available current conveyor," *Int. Journal of Electronics*, vol. 70, no. 1, pp. 159-164, 1991.
- [3] D. Biolek, R. Senani, V. Biolkova, Z. Kolka, "Active elements for analog signal processing: Classification, Review, and New Proposal," *Radioengineering*, vol. 17, no. 4, pp. 15-3, 2008.
- [4] R. Raut, M. N. S. Swamy, *Modern Analog Filter Analysis and Design: A practical approach*. Weinheim, Germany: Wiley-VCH Verlag GmbH and Co. KGaA, 2010.
- [5] A. Fabre, O. Saaid, F. Wiest, C. Boucheron, "High frequency applications based on a new current controlled conveyor," *IEEE Trans. on Circuits and Systems - I*, vol. 43, no. 2, pp. 82-91, 1996.
- [6] S. B. Salem, M. Fakhfakh, D. S. Masmoudi, M. Loulou, P. Loumeau, N. Masmoudi, "A high performance CMOS CCII and high frequency applications," *Analog Integrated Circuits and Signal Processing*, vol. 49, no. 1, pp. 71-78, 2006.
- [7] H. Barthelemy, M. Fillaud, S. Bourdel, J. Gaunery, "CMOS inverters based positive type second generation current conveyors," *Analog Integrated Circuits and Signal Processing*, vol. 50, no. 2, pp. 141-146, 2007.
- [8] I. Eldbib, V. Musil, "Self-cascoded Current Controlled CCII Based Tunable Band Pass Filter," in *Proc. 18th Int. Conf. Radioelektronika*, Praha, 2008, pp. 1-4.
- [9] W. Surakampontorn, W. Thitimajshima, "Integrable electronically tunable current conveyors," *IEE Proceedings-G*, vol. 135, no. 2, pp. 71-77, 1988.
- [10] S. Minaei, O. K. Sayin, H. Kuntman, "A new CMOS electronically tunable current conveyor and its application to current-mode filters," *IEEE Trans. on Circuits and Systems - I*, vol. 53, no. 7, pp. 1448-1457, 2006.
- [11] A. Marcellis, G. Ferri, N. C. Guerrini, V. Scotti, A. Trifiletti, "The VGC-CCII: a novel building block and its application to capacitance multiplication," *Analog Integrated Circuits and Signal Processing*, vol. 58, no. 1, pp. 55-59, 2009.
- [12] W. Tangsrirat, "Electronically Tunable Multi-Terminal Floating Nullor and Its Application," *Radioengineering*, vol. 17, no. 4, pp. 3-7, 2008.
- [13] S. Shi-Xiang, Y. Guo-Ping, C. Hua, "A new CMOS electronically tunable current conveyor based on translinear circuits," in *Proc. 7th Int. Conf. on ASIC*, Guilin, 2007, pp. 569-572.
- [14] N. Herencsar, A. Lahiri, K. Vrba, J. Koton, "An electronically tunable current-mode quadrature oscillator using PCAs," *Int. Journal of Electronics*, vol. 99, no. 5, pp. 609-621, 2012.
- [15] G. Souliotis, C. Psychalinos, "Electronically controlled multiphase sinusoidal oscillators using current amplifiers," *International Journal of Circuit Theory and Applications*, vol. 37, no. 1, pp. 43-52, 2009.
- [16] M. Kumngern, J. Chanwutium, K. Dejhan, "Electronically tunable multiphase sinusoidal oscillator using translinear current conveyors," *Analog Integrated Circuits and Signal Processing*, vol. 65, no. 2, pp. 327-334, 2010.
- [17] M. Kumngern, S. Junnapiya, "A sinusoidal oscillator using translinear current conveyors," in *Proc. Asia Pacific Conference on Circuits and Systems (APPCAS)*, Kuala Lumpur, 2010, pp. 740-743.
- [18] J. Koton, N. Herencsar, O. Cicekoglu, K. Vrba, "Current-mode KHN equivalent frequency filter using ECCII," in *Proc. 33th Telecommunication and Signal Processing Conf.*, Vienna, 2010, pp. 27-30.
- [19] J. Jerabek, R. Sotner, K. Vrba, "Fully-differential current amplifier and its application to universal and adjustable filter," in *Proc. International Conference on Applied Electronics APPEL*, Pilsen, 2010, pp. 141-144.
- [20] R. Sotner, J. Jerabek, R. Prokop, K. Vrba, "Current gain controlled CCTA and its application in quadrature oscillator and direct frequency modulator," *Radioengineering*, vol. 20, no. 1, pp. 317-326, 2012.
- [21] R. Sotner, J. Jerabek, B. Sevcik, T. Dostal, K. Vrba, "Novel Solution of Notch/All-pass Filter with Special Electronic Adjusting of Attenuation in the Stop Band," *Elektronika I Ir Elektrotechnika*, vol. 16, no. 7 (113), pp. 37-42, 2011.
- [22] R. Sotner, Z. Hrubos, J. Slezak, T. Dostal, "Simply Adjustable Sinusoidal Oscillator Based on Negative Three-Port Current Conveyors," *Radioengineering*, vol. 19, no. 3, pp. 446-453, 2010.
- [23] R. Sotner, Z. Hrubos, B. Sevcik, J. Slezak, J. Petrzela, T. Dostal, "An example of easy synthesis of active filter and oscillator using signal flow graph modification and controllable current conveyors," *Journal of Electrical Engineering*, vol. 62, no. 5, pp. 258-266, 2011.
- [24] D. Biolek, A. Lahiri, W. Jaikla, M. Siripruchyanun, J. Bajer, "Realization of electronically tunable voltage-mode/current-mode quadrature sinusoidal oscillator using ZC-CG-CDBA," *Microelectronics Journal*, vol. 42, no. 10, pp. 1116-1123, 2011.
- [25] J. Bajer, D. Biolek, "Digitally Controlled Quadrature Oscillator Employing Two ZC-CG-CDBAs," in *Proc. Conference on Electronic Devices and Systems EDS IMAPS CS*, Brno, 2009, pp. 298-303.
- [26] D. Biolek, V. Biolkova, "Implementation of Active Elements for Analog Signal Processing by Diamond Transistors," in *Proc. Conference on Electronic Devices and Systems EDS IMAPS CS*, Brno, 2009, pp. 304-309.
- [27] OPA860: Wide Bandwidth Operational Transconductance Amplifier and Buffer, Texas Instruments [online]. 2005, last modified 8/2008 [cit.28.7.2011]. available at URL: <<http://focus.ti.com/lit/ds/symlink/opa860.pdf>>
- [28] H. Alzahrer, "CMOS Digitally Programmable Quadrature Oscillators," *International Journal of Circuit Theory and Applications*, vol. 36, no. 8, p. 953-966, 2008. DOI: 10.1002/cta.479.
- [29] S. S. Gupta, R. Senani, "State variable synthesis of single resistance controlled grounded capacitor oscillators using only two CFOAs," *IEE Proceedings on Circuits, Devices and Systems*, vol. 145, no. 2, p. 135-138, 1998.
- [30] S. S. Gupta, R. Senani, "State variable synthesis of single-resistance-controlled grounded capacitor oscillators using only two CFOAs: additional new realizations," *IEE Proceedings on Circuits Devices and Systems*, vol. 145, no. 6, pp. 415-418, 1998.
- [31] A. Lahiri, "Deriving (MO) (I) CCCII Based Second-order Sinusoidal Oscillators with Non-interactive Tuning Laws using State Variable Method," *Radioengineering*, vol. 20, no. 1, pp. 349-353, 2011.
- [32] T. Tsukutani, Y. Sumi, Y. Fukui, "Electronically tunable current-mode OTA-C biquad using two-integrator loop structure," *Frequenz*, vol. 60, no. 3-4, pp. 53-56, 2006.
- [33] J. Jerabek, K. Vrba, "Multiple-Input Multiple-Output Universal Filter Using Current Followers," in *Proc. 31th Telecommunication and Signal Processing Conf.*, Budapest, 2008, pp. 29-32.
- [34] T. Dostal, "Filters with multi-loop feedback structure in current mode," *Radioengineering*, vol. 12, no. 3, pp. 6-11, 2003.
- [35] T. Tsukutani, Y. Sumi, Y. Fukui, "Novel current-mode biquad filter using OTAs and DO-CCII," *Int. Journal of Electronics*, vol. 94, no. 2, pp. 99-105, 2007.
- [36] M. T. Abuelmaatti, A. Bentrchia, "A novel mixed-mode OTA-C universal filter," *Int. Journal of Electronics*, vol. 92, no. 7, pp. 375-383, 2005.
- [37] Y. Sun, J. K. Fidler, "Structure Geretion of Current-Mode Two Integrator Dual output-OTA Grounded Capacitor Filters," *IEEE Transaction on Circuits and Systems II: Analog and Digital Signal Processing*, vol. 43, no. 9, pp. 659-663, 1996.
- [38] S. J. Mason, "Feedback Theory: Further properties of Signal Flow Graphs," *Proceedings of IRE*, vol. 44, no. 7, pp. 920-926, 1956.
- [39] C. J. Coates, "Flow-graph Solution of Linear Algebraic Equations," *IRE Transactions on Circuit Theory*, vol. 6, no. 2, pp. 170-187, 1959.
- [40] A. Lahiri, "Current-mode variable frequency quadrature sinusoidal oscillator using two CCs and four passive components including grounded capacitors," *Analog Integrated Circuits and Signal Processing*, vol. 71, no. 2, pp. 303-311, 2012.
- [41] A. Lahiri, "Current-mode variable frequency quadrature sinusoidal oscillator using two CCs and four passive components including grounded capacitors: a supplement," *Analog Integrated Circuits and Signal Processing*, vol. 68, no. 1, pp. 129-131, 2011.
- [42] EL2082: Current-Mode Multiplier, Intersil (Elantec) [online]. 1996, last modified 2003 [cit.28.7.2011]. available at URL: <<http://www.intersil.com/data/fn/fn7152.pdf>>
- [43] OPA633: High speed buffer amplifier, Texas Instruments [online]. 1993, last modified 9/2000 [cit.28.7.2011]. available at URL: <<http://focus.ti.com/lit/ds/symlink/opa633.pdf>>

[9] SOTNER, R., JERABEK, J., HERENCŠAR, N. Voltage Differencing Buffered/ Inverted Amplifiers and Their Applications for Signal Generation. *Radioengineering*, 2013, vol. 22, no. 2, p. 490-504. ISSN: 1210-2512.

Voltage Differencing Buffered/Inverted Amplifiers and Their Applications for Signal Generation

Roman SOTNER¹, Jan JERABEK², Norbert HERENC SAR²

¹Dept. of Radio Electronics, Brno University of Technology, Technicka 3082/12, 616 00 Brno, Czech Republic

²Dept. of Telecommunications, Brno University of Technology, Technicka 3082/12, 616 00 Brno, Czech Republic

{sotner; jerabekj; herencsn}@feec.vutbr.cz

Abstract. This paper presents some interesting new applications in the field of analog signal processing focused on signal generation. A novel modifications of recently developed and studied family of active elements, called voltage differencing buffered amplifier (VDBA) and voltage differencing inverted buffered amplifier (VDIBA) are discussed. Our attention is focused on simple application of active elements like dual output VDBAs (DO-VDBAs) and fully balanced VDBAs (FB-VDBAs), where one or two z terminals and always voltage outputs of both polarities are present. The last modification of VDBA allows additional electronic control of voltage gain in frame of active element except standard transconductance control. Discussed active elements were used to build very simple multiphase oscillators with minimal complexity as a simple non-tunable alternative to classical conceptions utilizing lossy integrators in phase-shifted loop. Linearly tunable quadrature differential mode (balanced) oscillator or balanced simple triangle and square wave generator were chosen as other useful examples. Features of proposed circuits are discussed and selected examples verified and evaluated by computer simulations with appropriate low-voltage TSMC 0.18 μm CMOS technology models.

Keywords

Analog signal processing, low-voltage circuit, voltage differencing inverted buffered amplifier, VDIBA, voltage differencing buffered amplifier, VDBA, multiphase oscillators, quadrature oscillator, triangle and square wave generator, differential output responses, electronic control.

1. Introduction

There are many active elements in the field of analog signal processing, however new ideas in this area help to provide further improvements in order to obtain more effective and interesting circuits. Plenty of novel active elements were introduced by Biolek et al. [1]. Nevertheless, many of them are only hypothetical elements and offer further research mainly from practical point of view. Main

aim of this paper is to show simple alternatives allowing multiphase generation, simple quadrature generation and square and triangle wave differential mode generation with help of modifications of novel active elements known as voltage differencing buffered amplifier (VDBA) [1]-[4] or voltage differencing inverted amplifier (VDIBA) [5]. Presented active elements and their modifications allow interesting utilization and design of more profitable or more challenging application (differential mode operation, advanced electronic control, etc.) in comparison to classical VDBA or VDIBA elements.

This paper is divided to three parts. The first part deals with behavioral principles of used active elements. The second part discusses possible applications in analog signal generation (there are three areas: multiphase oscillators, quadrature/differential mode oscillator and simple functional generator). The third part deals with possible structures of discussed active elements that are mostly used in presented designs, their behavior and simulation results, and features of selected of proposed applications (multiphase oscillator and functional generator).

Several approaches to design of multiphase oscillators are available in the open literature. The first way uses integrators or similar selective sections in the loop [6]-[8]. Classical integrator phase shifted loops [6]-[8] were key circuits for generation signals with several phase shifts between them for many years. However, such circuits require many lossy integrators or selective sections (it depends on the number of multiplicand of basic shift - $\pi/2$, $\pi/4$ or $\pi/6$ typically). Such structures were based on classical simple active elements like current conveyors (CC) [6], [8], current amplifiers [7], etc. However, complexity and number of sections required for such type of oscillators is high. It means at least 4 sections (4 capacitors and 4 active elements) for phase shifts 45, 90, 135 and 180 degrees for example in classical loop way of synthesis. The second possibility of construction of multiphase oscillators (unfortunately number of phases is more limited) utilizes all-pass sections (for example [9]-[11]). Here simple (operational amplifiers for example [9]) or more complex active elements like current differencing transconductance amplifiers (CDTAs) have been employed [10]. These already studied circuits usually allow quadrature phase shifts (or

multiple of $\pi/2$) [11]. However, they usually do not allow nonstandard phase shifts such as 45, 90, 135 and 180 degrees simultaneously in comparison to classical types employing phase shifted integrator loops. The last used approach is based on combination of active all-pass section with lossy or lossless integrators or differentiators or similar sections. This approach is also in field of our interest in design of multiphase oscillator used in this paper. Unfortunately, our study below shows that not all published oscillator structures have been analyzed carefully in the past and many other circuits with similar features probably exist in the literature. In addition, the analysis of possible outputs of oscillator circuits or analysis of the relation between them is also not provided in many papers. In the following paragraphs we summarized the most important features of approaches used in recent literature and also by us:

a) Phase shifted loops with integrators or similar selective sections and typical examples

Advantages: tunability; easy synthesis; easy CO (condition of oscillation) control by gain of amplifier cascaded in the loop; even and odd phases of $\pi/2$, $\pi/4$ or $\pi/6$.

Disadvantages: many sections (one section = the lowest available phase shift) for required number of phase shifts; higher power consumption (many active elements); in some cases simultaneously matched control of parameter of each elementary transfer in each section - complication of FO (frequency of oscillation) and CO control (some types are controllable by simultaneous changes of each time constant [7], some require special matching conditions [6], [8]).

Abuelmaatti et al. [6] proposed multiphase current-mode oscillator employing controllable current conveyors in lossy integrators. Loop structure utilizes two capacitors per section and FO, CO control require matching condition between capacitor values. Voltage-mode multiphase oscillator based on classical operational amplifiers was presented by Gift [9] where all-pass sections with adjustable time constants (by R and C values only) were used for construction. However, number of passive elements seems to be very high for large number of phase shifts. Souliotis et al. utilized current amplifiers in cascade of lossy integrators creating current-mode multiphase oscillator [7]. Adjusting of FO is quite simple by bias current of active elements. Kumnigern et al. [8] also built their current-mode oscillator with lossy integrators utilizing current conveyors, where intrinsic resistance of the x -terminal and gain between z and x terminal simultaneously is possible. However, matching between capacitors is also required for realization of higher number of phases and therefore accuracy of such matching condition influences also accuracy of the phase shift.

b) All-pass section in the loop based oscillators and typical examples

Advantages: simpler circuits; lower number of pas-

sive and active elements (in many cases two sections are sufficient [10]); lower power consumption.

Disadvantages: complicated tunability or CO control and matching in parameter values is required in many cases; accuracy of relation (transfers) between available outputs for accurate phase shifts required; phase shifts are available as multiple of $\pi/2$ almost in all cases.

Keskin et al. [10] published the perfect example of oscillator based on two all-pass sections employing two CDTAs and 6 passive elements that serve for CO and FO control. The oscillator produces output signals also in form of currents. The discussed circuit provides quadrature phase shifts only. Similarly, Songsuwankit et al. [11] also deal with phase shifter-based (all-pass section consists of three OTAs and one floating capacitor) oscillator design. Here, arbitrary setting of phase shift is possible, but the proposed oscillator provides only two outputs.

c) All-pass sections in combination with integrators or integrators/differentiators in simple loops and typical examples

Advantages: similar to the previous group; produced phase shifts are available similarly as in phase shifted loop oscillators (it depends on construction of particular circuit); CO control independent on FO in some cases.

Disadvantages: similar to the previous discussion; if FO is controllable by specific parameter it influences phase or at least amplitude relations.

Keawon et al. [12] proposed an oscillator employing single current controlled current differencing transconductance amplifier (CCCDTA), where two capacitors are required. Control of FO and CO is established by intrinsic resistance and transconductance control. Output signals are in form of currents. Jaikla et al. [13] designed a circuit utilizing single CDTA and three passive elements. The independent CO and FO control is not possible and their adjustment is possible only by passive elements (also floating capacitor). Quadrature oscillator produces signals in form of currents. Also Pandey et al. [14] presented a circuit, which produces currents in quadrature phase shift with two CDTAs and two passive elements, where control is given by transconductances. Herencsar et al. [5] also discussed an oscillator, where one simple all-pass section and lossy integrator employing two VDIBA elements and three passive elements with control of CO were used. Keskin et al. [15] also presented an oscillator producing voltage signals, which is based on two current differencing buffered amplifiers (CDBAs) in which 8 passive elements are required and independent control of CO is difficult. Songkla et al. [16] presented an oscillator, where three current controlled current conveyors (controlled by intrinsic resistance) of second generation and two passive elements generate current output signals. Minaei et al. [17] utilized differential voltage current conveyor (DVCC) and the circuit requires three DVCCs, four passive elements, and produces voltage output responses. All discussed

examples provide quadrature outputs. None of them show production of phase shifts such as 45, 90, 135, 180 degrees, which is the main contribution of our circuits.

General conclusions from above discussions are that tunability of cascaded phase shifted loop is better, but complexity is several times higher. Therefore, simpler structures that utilize another design approaches are more interesting in some cases. Therefore, our intention in this paper is to design simpler solutions that have not been developed so far.

The next part of our contribution deals with quadrature oscillator design. Important quadrature oscillators with independent CO and FO adjusting, grounded capacitors, and voltage output responses are compared in the following text.

Many from recently investigated structures use passive elements for control of CO and FO, therefore their replacement by electronically adjustable equivalents is necessary. Soliman [18] utilizes current conveyors (two or three) and 5-6 passive elements in solution of an oscillator, where differential output signals are not easily available. Oscillator presented by Herencsar et al. based on generalized current follower transconductance amplifier (GCFTA) and voltage buffer employs two active and four passive elements. However, it does not provide linear control of FO (produced amplitude is dependent on tuning process) [19]. Tuning is realized by changes of passive elements. Similar type of FO and CO control is used in works [20]-[22] as well. Gupta et al. [20] developed an oscillator based on current and voltage followers as active elements (2-4 in the proposed circuits) and 5 passive elements. Amplitude of generated signal was influenced by FO adjusting without possibility of linear control. Oscillator with differential output signals and quadrature phase shift is proposed by Biolkova et al. in [21]. The circuit is based on two dual output current inverter buffered amplifiers (DO-CIBAs) and 5-6 passive elements. The FO control without influence on produced amplitudes is linear, but simultaneous change of floating resistor values is necessary. Lahiri [22] proposed an oscillator employing three current feedback amplifiers (CFAs) and 6 passive elements, where adjusting of resistor values is the only way how to control CO and FO. Lahiri et al. [23] also proposed another oscillator based on single current conveyor transconductance amplifier (CCTA) and four passive elements, where electronic control is realized by g_m . Nevertheless, generated amplitude is influenced by tuning of FO and dependence of control is not linear. The same features were achieved in solution presented in [24], where two CDTAs and three passive elements were used. Rodriguez-Vazquez et al. [25] presented an oscillator based on 3-4 transconductors (OTAs) and two capacitors. Linear control of FO without influence on generated amplitudes is possible electronically by transconductances. The oscillator in [26] utilizes special configuration of three specially modified CFAs and five passive elements, which allows linear control of FO without impact on generated amplitudes. Digital control of such

application has been also discussed in the past, for example by Alzahrer et al. [27], where 3 or 5 active elements (current amplifiers and voltage buffers) and 6 passive elements were used and linear control of FO without impact on generated amplitudes is allowed. Interesting digitally controllable solution was presented by Biolek et al. [28], where two active elements - so called z-copy controlled gain current differencing buffered amplifiers (ZC-CG-CDBAs), five passive elements are used and allow linear control of FO. Several solutions of quadrature oscillators, where control procedure was focused on current and voltage gain adjusting in frame of active elements called controlled gain current follower differential output buffered amplifiers (CG-CFDOBA), controlled gain current inverter buffered amplifiers (CG-CIBAs) and controlled gain current amplified voltage amplifier (CG-CVA), are discussed in [29] (five passive and two active elements are used in the proposed oscillators). Some of them allow differential output responses and linear control of FO. Galan et al. [30] utilizes four dual output OTAs (g_m control) and four capacitors to achieve fully differential output oscillator. The first note about utilization of FB-VDBA in differential (balanced) quadrature was discussed by Bajer et al. [31]. The oscillator consists of two FB-VDBAs, two resistors, four grounded capacitors and allows linear electronic control of FO and independent control of CO (unfortunately by a floating resistor).

Oscillator structure presented in this contribution seems to be very economical in comparison to above discussed circuits, because only single DO-VDBA and dual output controlled gain voltage differencing buffered voltage amplifier (DO-CG-VDBVA) and three passive elements (only one of them is floating) are required. The proposed oscillator provides differential outputs, linear control of FO by simultaneous adjusting of both g_m , and CO control by adjustable voltage gain. In some above discussed solutions utilizing other type of active elements the potential possibility to obtain voltage or even voltage differential (balanced) outputs also exists, but additional current to voltage conversion or voltage buffering/inversion (out of active element) is required. However, if it is possible, than these discussed oscillators have other drawbacks such as control by passive elements [21] or high number of active elements [30].

Principle of triangle and square generator (called functional) is known very well. There were interesting attempts to build very simple generator from active elements like basic operational amplifiers, current conveyors, etc. [1]. However, these simple circuits have some drawbacks (many passive elements) and lack of electronic controllability. The following discussion deals with typical examples.

Biolek et al. [32] introduced an interesting circuit with single CDTA, 3 resistors and one capacitor which provides FO in range of MHz tunable by resistor value. De Marcellis et al. [33] proposed generator employing 2 CCIIIs, 6 resistors and one capacitor. Control of FO is also

possible by adjusting of resistor value. Chien et al. [34] presented solution based on two differential voltage current conveyors (DVCCs) [1], three resistors and control of duty cycle is also allowed. Almashary et al. [35] presented a generator, where 2 CCIs, 3 resistors, and 2 capacitors are required. Tunability of FO is possible by value of resistor. Pal et al. [36] employed two CCIs, three resistors and floating capacitor in his approach. Two current feedback operational amplifiers (CFOAs) [1] with two capacitors and two resistor utilized generator presented by Saque et al. [37]. Minaei et al. [38] introduced similar approach based on CFOAs and DVCCs. Two operational transresistance amplifiers (OTRAs), three resistors and one floating capacitor based generator is shown by Lo et al. [39].

Electronically controllable active elements allow better performance in these types of generators. Works [40]-[42] brought key information for design of generators with transconductance (OTA) sections (controlled by DC bias currents) and special comparators with hysteresis (so called Schmitt trigger [40]), for example). Our presented topology of triangular and square wave generator is based on similar principles. Kim et al. [41] and Chung et al. [42] utilized 3 OTA sections, one capacitor and two resistors, similarly Siripruchyanun et al. [43].

Several generators were designed with current-mode outputs. Kumbun et al. [44] employed two multiple outputs through transconductance amplifiers (MO-CTTAs) only to realize adjustable generator. Two multiple output current controlled current differencing amplifiers (MO-CCCDTAs) were used for design of generator by Silapan et al. [45] and Sristakul et al. [46]. Silapan et al. [45] published a very excellent work (fundamentally very similar to our solution), where two controllable multi-output CDTA (MO-CCCDTA) elements, and one capacitor is sufficient. In fact, there were used two independently adjustable OTA sections in each MO-CCCDTA and it allows to "integrate" resistor inside of the active element. The generator is designed with current output responses.

In our topology only two OTA sections, one capacitor and one resistor are sufficient (reasons for the second are explained in a specific chapter - Schmitt comparator in our contribution is adapted for differential output purposes). Differential output means two times higher output signals and immunity to common mode disturbances, which is really important in modern low-voltage CMOS technologies. The resulting conclusion from hitherto published works is clear - to the best of the authors' knowledge no generator (with electronic control of repeating frequency and duty cycle) for differential (balanced output) signal generation that is simpler exists in the literature and many presented single-ended solutions seem to be quite complicated and use also floating passive elements ([33], [36] for example).

2. Controllable Voltage Differencing Buffered Amplifiers

Conceptions of VDBA/VDIBA [1]-[5] and their behavioral model are discussed in this chapter. Advantageous differences from classical VDBA [1]-[4] or VDIBA approach based on OTA and inverter section [5] are discussed and explained. Classical VDBA/VDIBA employs high-impedance voltage differencing input terminals (in this paper labeled as p and n), auxiliary high-impedance z terminal, and low-impedance output of voltage buffer/inverter noted as $+w/-w$. Modified conception uses transconductance section with one output polarity (one z terminal) and cascade of two voltage inverters. Therefore, both inverting ($-w$) and direct voltage outputs ($+w$) are available. However, some applications require two auxiliary terminals z for special purposes of circuit synthesis. Internal structure of FB-VDBA [2] is more complicated, because different transconductance section with current mirrors is required. Advanced VDBA/VDIBA modification allows several types of electronic control as will be shown in more details.

2.1 DO-VDBA

The first possible modification of VDBA/VDIBA [1]-[6] is created very simply by additional voltage inverter. Therefore, we have now also direct voltage buffered output, which is very useful for differential mode signal operations. Symbol and behavioral model is shown in Fig. 1.

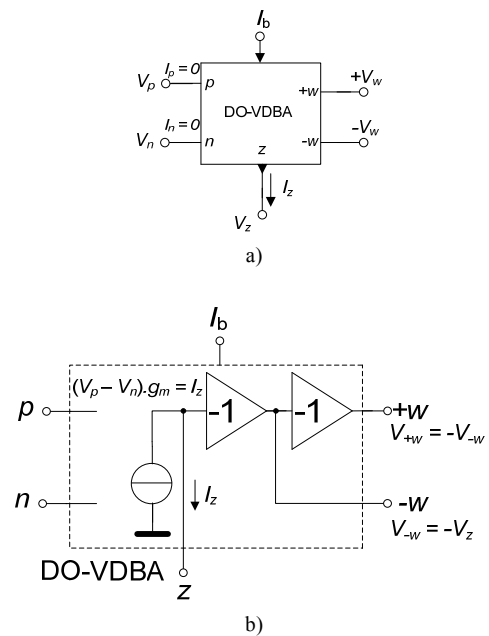


Fig. 1. Dual output voltage differencing buffered amplifier (DO-VDBA): a) symbol, b) behavioral model.

We called this element dual output voltage differencing buffered amplifier (DO-VDBA) in accordance to [1]. The main principle is obvious from behavioral model (see Fig. 1b). Control of transconductance is possible by external biasing (I_b). Relation between terminals can be written in hybrid matrix as follows:

$$\begin{bmatrix} I_p \\ I_n \\ I_z \\ V_{+w} \\ V_{-w} \end{bmatrix} = \begin{bmatrix} 0 & 0 & 0 & 0 & 0 \\ 0 & 0 & 0 & 0 & 0 \\ g_m & -g_m & 0 & 0 & 0 \\ 0 & 0 & 1 & 0 & 0 \\ 0 & 0 & -1 & 0 & 0 \end{bmatrix} \begin{bmatrix} V_p \\ V_n \\ V_z \\ I_{+w} \\ I_{-w} \end{bmatrix} \quad (1)$$

2.2 FB-VDBA

In some cases of circuit synthesis two auxiliary z terminals (both polarities for example) are required. A very useful and easily obtainable version [2], [3] is shown in Fig. 2.

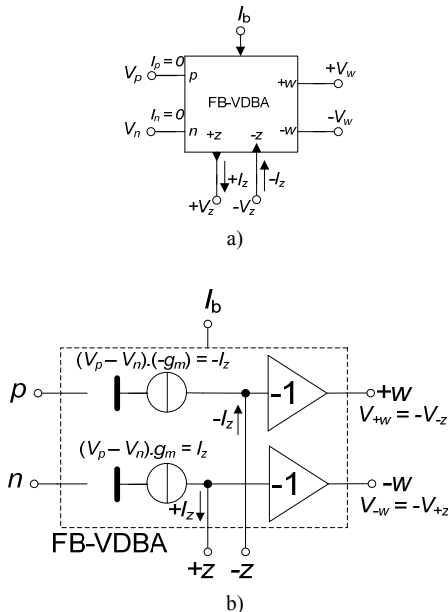


Fig. 2. Fully balanced voltage differencing buffered amplifier (FB-VDBA): a) symbol, b) behavioral model.

$$\begin{bmatrix} I_p \\ I_n \\ I_{+z} \\ I_{-z} \\ V_{+w} \\ V_{-w} \end{bmatrix} = \begin{bmatrix} 0 & 0 & 0 & 0 & 0 & 0 \\ 0 & 0 & 0 & 0 & 0 & 0 \\ g_m & -g_m & 0 & 0 & 0 & 0 \\ -g_m & g_m & 0 & 0 & 0 & 0 \\ 0 & 0 & 0 & -1 & 0 & 0 \\ 0 & 0 & -1 & 0 & 0 & 0 \end{bmatrix} \begin{bmatrix} V_p \\ V_n \\ V_{+z} \\ V_{-z} \\ I_{+w} \\ I_{-w} \end{bmatrix} \quad (2)$$

Matrix description is very similar to (1), but main difference is in additional equation for the second output current from the second z terminal, see (2).

2.3 DO-CG-VDBVA

Previous types of VDBAs (DO-VDBA and FB-VDBA) [1]-[6] allow only one possibility of electronic control. However, in many applications various possibilities of controls are required. As an example, sinusoidal oscillators can be mentioned, where one controllable parameter serves for control of oscillation condition and the second one adjusts oscillation frequency. Therefore, introduced modification contains two adjustable parameters. These parameters can be obtained by additional voltage amplifier together with buffer/inverter in behavioral structure or by replacement of inverter/buffer by this controllable voltage amplifier. This active element received a typical name consisting of main features typical for classical VDBA or VDIBA [1]-[6] but considering also controllability of voltage gain (A). Symbol and behavioral model of the dual output controlled gain voltage differencing buffered voltage amplifier (DO-CG-VDBVA) is depicted in Fig. 3.

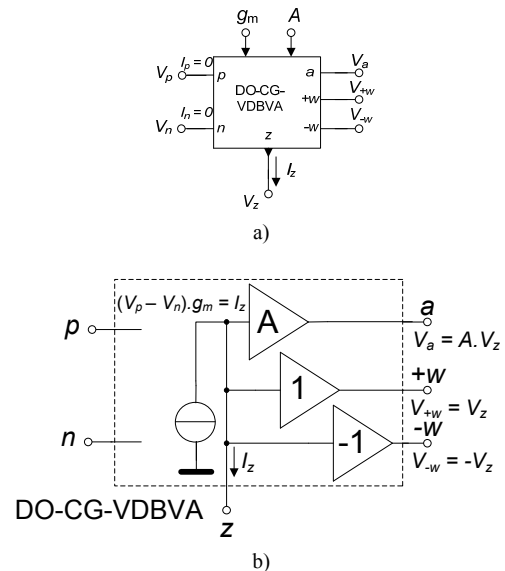


Fig. 3. Dual output controlled gain voltage differencing buffered voltage amplifier: a) symbol, b) behavioral model.

Matrix equations also include a new parameter - adjustable voltage gain as follows:

$$\begin{bmatrix} I_p \\ I_n \\ I_z \\ V_a \\ V_{+w} \\ V_{-w} \end{bmatrix} = \begin{bmatrix} 0 & 0 & 0 & 0 & 0 & 0 \\ 0 & 0 & 0 & 0 & 0 & 0 \\ g_m & -g_m & 0 & 0 & 0 & 0 \\ 0 & 0 & A & 0 & 0 & 0 \\ 0 & 0 & 1 & 0 & 0 & 0 \\ 0 & 0 & -1 & 0 & 0 & 0 \end{bmatrix} \begin{bmatrix} V_p \\ V_n \\ V_z \\ I_a \\ I_{+w} \\ I_{-w} \end{bmatrix} \quad (3)$$

from which it is obvious that direct voltage buffering can be achieved by a simple way shown in Fig. 1 (two inverters in cascade).

3. Applications for Signal Generation

The discussed active elements can be used in interesting applications in analog signal processing and mainly in signal generation. Several types of sinusoidal oscillators and functional (triangle and square wave) generators based on the discussed active elements are presented in this section.

3.1 Multiphase Harmonic Oscillator SRCO

So-called single resistance controllable oscillators (SRCO) [20] were very popular for many years due to their simplicity (one-two active elements maximally) and simultaneously independent control of CO and FO by resistor values. The basic conception employs lossy integrator (R_1, C_1), one DO-VDBA and special impedance constructed from $-R_2$ and C_2 in an interesting circuit configuration (Fig. 4).

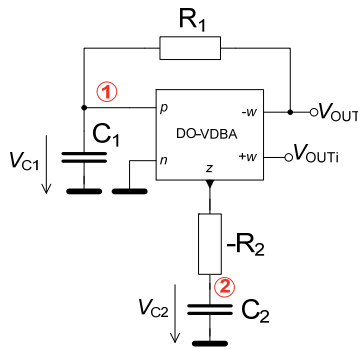


Fig. 4. Simple multiphase oscillator using single DO-VDBA.

Characteristic equation of the discussed oscillator has form:

$$s^2 + \frac{(1-g_m R_2)}{R_1 C_1} s + \frac{g_m}{R_1 C_1 C_2} = 0, \quad (4)$$

where CO is controllable by $-R_2$ value and FO by value of R_1 . Therefore, specifications for SRCO type of oscillator are fulfilled. Practical utilization of floating resistance $-R_2$ is different, because Fig. 4 serves only for theoretical and simple explanation of the principle. Controllability of $-R_2$ value in order to ensure soft CO control is not very comfortable. Therefore, we implemented the second active element to replace inconvenient floating negative passive element from another FB-VDBA. Transconductance control now realizes CO adjusting by a simple electronic way. Replacement of the impedance connected to z terminal of DO-VDBA is shown in Fig. 5. The principle of the design of the basic (Fig. 4) and modified circuit is clear from the diagram in Fig. 5. Two blocks with specific transfers (lossy integrator and special synthetic function) between current and voltage (transadmittance Y_T and transimpedance Z_T) were used for synthesis of the discussed circuit. Impedance of serial $R_2 C_2$ combination in Fig. 5 has form:

$$Z_{INP_RC} = \frac{1-sR_2C_2}{sC_2}, \quad (5)$$

and from equivalent circuit resulting impedance:

$$Z_{INP_EQ} = \frac{1-s\frac{C_2}{g_{m2}}}{sC_2}. \quad (6)$$

The improved characteristic equation is now:

$$s^2 + \frac{g_{m2}-g_{m1}}{R_1 C_1 g_{m2}} s + \frac{g_{m1}}{R_1 C_1 C_2} = 0 \quad (7)$$

where CO and FO can be easily obtained as:

$$g_{m2} \leq g_{m1}, \quad \omega_0 = \sqrt{\frac{g_{m1}}{R_1 C_1 C_2}}. \quad (8), (9)$$

We can determine transfers between outputs of the oscillator and get relations between produced amplitudes and phase shifts respectively as:

$$\frac{V_{OUT_0}}{V_{C1}} = \frac{g_{m1} \left(-1 + s \frac{C_2}{g_{m2}} \right)}{sC_2}, \quad (10)$$

$$\frac{V_{OUT_0}}{V_{C2}} = -\frac{1 + sC_1 R_1}{1 - \frac{g_{m1}}{g_{m2}} + sC_1 R_1}, \quad (11)$$

$$\frac{V_{C2}}{V_{C1}} = -\frac{g_{m1}}{sC_2}. \quad (12)$$

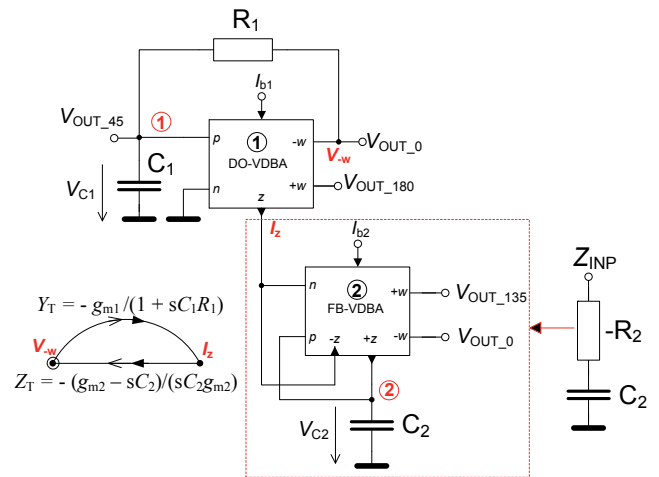


Fig. 5. Modification of the oscillator in Fig. 4 with electronically controllable CO.

We can simplify these equations considering fulfilled CO (8) and equality of $C_1 = C_2 = C$ and determine relations as:

$$\frac{V_{OUT_0}}{V_{C1}} = \frac{g_{m1}(-1+sC)}{sC}, \quad (13)$$

$$V_{OUT_0} = \sqrt{1+g_{m1}R_1} e^{\sqrt{g_{m1}R_1}j} V_{C1}, \quad (14)$$

$$\varphi_{V_{OUT_0_C1}} = \arctg(\sqrt{g_{m1}R_1}), \quad (15)$$

which leads to 45° phase shift in case of equality $g_{m1} = 1/R_1$. The next relation has form:

$$\frac{V_{OUT_0}}{V_{C2}} = -\frac{1+sCR_1}{sCR_1}, \quad (16)$$

$$V_{OUT_0} = -\sqrt{1+\frac{1}{g_{m1}R_1}} e^{\frac{1}{\sqrt{g_{m1}R_1}}j} V_{C2}, \quad (17)$$

$$\varphi_{V_{OUT_0_C2}} = 180 + \arctg\left(-\frac{1}{\sqrt{g_{m1}R_1}}\right), \quad (18)$$

which leads to 135° for fulfilled $g_{m1} = 1/R_1$. The last relation that we can find between voltages across capacitors is:

$$\frac{V_{C2}}{V_{C1}} = -\frac{g_{m1}}{sC}, \quad (19)$$

$$V_{C2} = \sqrt{g_{m1}R_1} e^{\frac{\pi}{2}j} V_{C1}, \quad (20)$$

$$\varphi_{C2_C1} = \arctg\left(\frac{\sqrt{g_{m1}R_1}}{0}\right) = \frac{\pi}{2} \quad (21)$$

where only amplitude relation depends on R_1 value (FO control). We can find out that the proposed oscillator produces signals with phase shifts 45, 90, 135 and 180 degrees for fulfilled CO and $g_{m1} = 1/R_1$ as conclusion of this analysis.

This type of oscillators is not very suitable for FO adjusting, if multiphase outputs are also required. Any change of FO leads to inequality of $g_{m1} = 1/R_1$ through R_1 and causes disturbance of phase and amplitude proportions in the circuit. Only phase relation between V_{C1} and V_{C2} keeps preserved (but not amplitude). Additional voltage buffering of V_{OUT_45} is also a complication for practical utilization. However, obtaining of four-phase outputs is possible by quite a simple way (similarly as in [5], where one disadvantage remains – floating capacitor) without necessity of many active elements in comparison to [6]-[8], for example. Therefore, the presented solution offers some benefits and improvements.

3.2 Multiphase Oscillator - Special Requirements

The previous type of the oscillator requires synthetic replacement of floating negative resistance. Therefore, in Fig. 6 another solution with similar phase shifts like the above discussed circuit is introduced, but usage of floating negative resistance is not required. This oscillator uses conversion ($V \rightarrow I, I \rightarrow V$) transfer sections in the loop based on only lossy integrators and additional positive feedback in comparison to the previous type (diagram in Fig. 6). The second DO-VDBA₂ with R_3 serves as a sub-

tractor, which allows to obtain required outputs with appropriate phase shifts. Characteristic equation, CO and elementary FO have forms:

$$s^2 + \frac{R_2C_2 + R_1C_1(1 - R_2g_{m1})}{R_1R_2C_1C_2}s + \frac{1}{R_1R_2C_1C_2} = 0, \quad (22)$$

$$g_{m1} \geq \frac{R_1C_1 + R_2C_2}{R_1R_2C_1}, \quad \omega_0 = \sqrt{\frac{1}{R_1R_2C_1C_2}}. \quad (23), (24)$$

Relations between generated signals are:

$$\frac{V_{C1}}{V_{C2}} = \frac{1}{1+sC_1R_1}, \quad (25)$$

$$\frac{V_{OUT_135}}{V_{C1}} = R_3g_{m2} \left(\frac{1+sC_2R_2}{-R_2g_{m1} + 1+sC_2R_2} \right), \quad (26)$$

$$\frac{V_{OUT_135}}{V_{C2}} = -R_3g_{m2} \left(\frac{sC_1R_1}{1+sC_1R_1} \right), \quad (27)$$

which leads to (considering $C_1 = C_2 = C$, fulfilled CO: $R_2g_{m1} = 2$ and $R_3g_{m2} = 1$):

$$V_{C1} = \frac{\sqrt{2}}{2} e^{\frac{\pi}{4}j} V_{C2}, \quad (28)$$

$$V_{OUT_135} = e^{\frac{\pi}{2}j} V_{C1}, \quad (29)$$

$$V_{OUT_135} = -\frac{\sqrt{2}}{2} e^{\frac{\pi}{4}j} V_{C2} = \frac{\sqrt{2}}{2} e^{\frac{3\pi}{4}j} V_{C2}. \quad (30)$$

Simple solution of both DO-VDBAs (only one positive z terminal) is sufficient in this modification of the oscillator in comparison to the previous type.

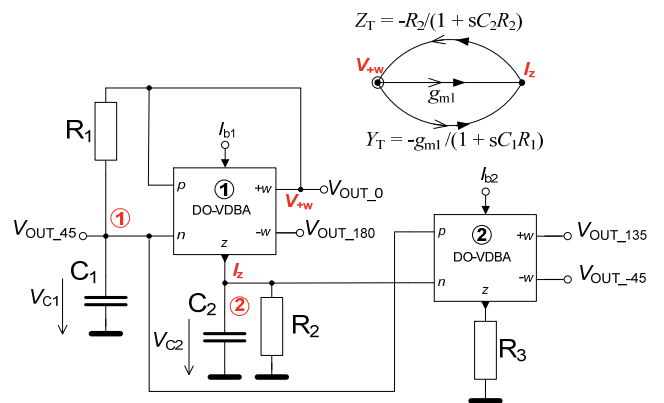


Fig. 6. Modification of the proposed oscillator without necessity of employing floating negative resistance.

3.3 Adjustable Harmonic Quadrature Oscillator

The solution presented in this section offers more benefits in comparison to the previous multiphase type,

where FO adjusting was limited or not possible due to request of four multiphase outputs (45, 90, 135, 180 degrees). The main requirement of the intended synthesis is the design of fully electronically controllable (CO and linear control of FO) oscillator with multiphase purposes (90, 180, 270 degrees) or quadrature differential (balanced) mode oscillator. The presented circuit consists of lossy and loss-less integrators in one loop complemented by negative resistance controllable by voltage gain. This application (Fig. 7) is the perfect example of utilization of the DO-CG-VDBVA. Loss-less controllable (by g_{m2}) voltage integrator forms the first part (C_2 and DO-VDBA) of the oscillator. The second important part is the lossy integrator (controllable by g_{m1}) together with negative resistance supplementary simulating circuit (R_1 , C_1 and DO-CG-VDBVA), where negative resistance is adjustable by voltage gain A_1 . Characteristic equation, CO and FO have the following forms:

$$s^2 + \frac{(1-A_1)}{R_1 C_1} s + \frac{g_{m1} g_{m2}}{C_1 C_2} = 0, \quad (31)$$

$$A_1 \geq 1, \quad \omega_0 = \sqrt{\frac{g_{m1} g_{m2}}{C_1 C_2}}. \quad (32), (33)$$

Relative sensitivities of oscillation frequency on parameters in (33) achieve typical values (± 0.5). Linear control of FO is ensured by simultaneous adjusting of g_{m1} and g_{m2} ($g_{m1} = g_{m2}$) and independent control of CO by A_1 . The oscillator provides low impedance at each of the outputs, therefore, easy connection to low-resistance loads is allowed. The relation between produced signals across the capacitors has form:

$$\frac{V_{C2}}{V_{C1}} = -\frac{g_{m2}}{s C_2} = j \sqrt{\frac{g_{m2} C_1}{g_{m1} C_2}}, \quad (34)$$

which means quadrature phase shift and equal amplitudes during the tuning process (FO) at all outputs in case of simultaneous control of both g_m and when capacitors have equal values. Single-ended operation mode allows to obtain the oscillator with unchangeable amplitudes providing four phase shifts (multiples of $\pi/2$). Differential operation mode has benefit of two-times higher output amplitudes, but in quadrature form only.

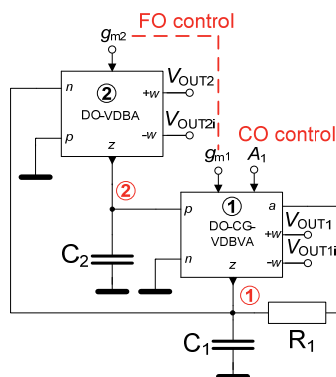


Fig. 7. Fully controllable multiphase/quadrature differential mode (balanced) oscillator.

3.4 Triangle and Square Wave Generator

The last presented useful and quite simple application of the discussed active elements is a differential output (balanced) triangle and square wave generator. Explanations of processes in the function of the generator are provided by charging of a capacitor and switching (turn-over) at reference levels. The loss-less integrator and comparator with hysteresis (Schmitt trigger) in the feedback loop are main building blocks of these types of non-harmonic signal sources [32]-[46]. We show possibilities how to build loss-less integrator with VDBA elements (partial block of the oscillator in Fig. 7).

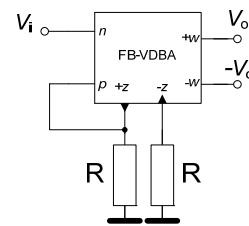


Fig. 8. Schmitt comparator with hysteresis employing FB-VDBA.

For construction of a dual-output Schmitt comparator (Fig. 8) one FB-VDBA with two z terminals was employed. Theoretically, the DO-VDBA (one z terminal) is also possible for construction of a comparator (we can save one resistor). However, the FB-VDBA (with current multiplying performed by current mirrors in internal topology - we will present it in experimental/simulation part of this paper) allows higher gain of the whole voltage feedback system, which is the key factor (in low-power and low-supply voltage technology) for precise flip-over process of the comparator. Quality of the comparator has a direct impact on accuracy of oscillation/repeating frequency (also noted by abbreviation FO) and accuracy of reference levels.

The following equation is valid between the input and output voltage of FB-VDBA in the comparator (Fig. 8):

$$(\mp V_{o_sat}) = \frac{g_m R}{g_m R - 1} (\pm V_i), \quad (35)$$

which leads to

$$\mp V_{o_sat} = \pm V_i, \quad (36)$$

if validity of $g_m R \gg 1$ is ensured. We found referencing value (V_{ref}) for very high gains (given by transconductance g_m and resistor R) which is necessary for turnover of the output of the comparator from a high output voltage level to a low output voltage level respectively in (36). The output voltage (in ideal case also reference threshold voltage) is given by maximum output current $\pm I_{+z_max}$, which means maximum of positive or negative output saturation: $\pm V_{+z} = \pm R \cdot I_{+z_max}$. Dynamical characteristic of the comparator has two comparative reference voltages determined as $\pm R \cdot I_{+z_max}$, thanks to positive feedback from voltage across R and very high gain ($g_m R$).

Fig. 9 shows the complete generator, where the lossless integrator employs the first type of DO-VDBA and the comparator presents the same circuit as we discussed in Fig. 8.

Linear charging of the capacitor C starts at the negative reference voltage level ($-V_{C_max}$) and is given by $+I_{C_max} = +I_{z1_max} + I_d = k_1 I_{b1} + n.k_1 I_{b1}$, where constant k represents current gain in the internal topology of VDBA (multiplying by current mirrors), I_d is auxiliary controlled DC current and n is the ratio between I_d and I_{b1} ($I_d = n.I_{b1}$). The input voltage linear range of DO-VDBA is very small for higher g_m and the slope of the DC transfer characteristic very sharp.

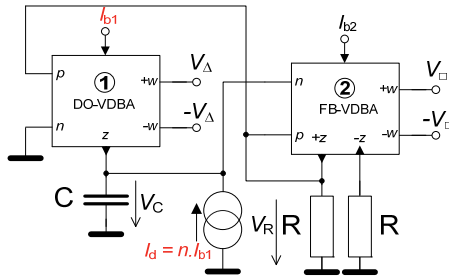


Fig. 9. Differential mode triangle and square wave generator employing DO-VDBA and FB-VDBA.

Therefore, the output currents are given by one from both saturation corners limited by bias current I_b as $\pm I_{z1_max} = \pm k_1 I_{b1}$ (DO-VDBA) and $\pm I_{z2_max} = \pm k_2 I_{b2}$ (FB-VDBA), see Fig. 11a and Fig. 13a. Discharging that starts at $+V_{C_max}$ is given similarly, because $-I_{C_max} = -I_{z1_max} + I_d$. Both time intervals per one signal period are obtained from:

$$\Delta V_C = \frac{I_{z1_max} + I_d}{C} T_1, \tag{37}$$

$$\Delta V_C = \frac{-(-I_{z1_max} + I_d)}{C} T_2. \tag{38}$$

The distance between the negative and positive threshold values ($-V_{C_max} = +RI_{z2_max}$ and $+V_{C_max} = -R.I_{z2_max}$) can be expressed as:

$$\Delta V_C = \Delta V_R = +V_{C_max} - (-V_{C_max}) = 2V_{C_max}, \tag{39}$$

$$2V_{R_max} = +RI_{z2_max} - (-RI_{z2_max}). \tag{40}$$

Both time intervals are stated as:

$$T_1 = \frac{\Delta V_C C}{I_{z1_max} + I_d} = \frac{2RCk_2 I_{b2}}{k_1 I_{b1} + n.k_1 I_{b1}}, \tag{41}$$

$$T_2 = \frac{\Delta V_C C}{I_{z1_max} - I_d} = \frac{2RCk_2 I_{b2}}{k_1 I_{b1} - n.k_1 I_{b1}}. \tag{42}$$

The repeating period and frequency have forms:

$$T = T_1 + T_2 = \frac{4RCk_1 I_{b1} k_2 I_{b2}}{(k_1 I_{b1} + n.k_1 I_{b1})(k_1 I_{b1} - n.k_1 I_{b1})}, \tag{43}$$

$$f_0 = \frac{k_1 I_{b1} (1+n)(1-n)}{4RCk_2 I_{b2}} = \frac{k_1 I_{b1} (1-D)D}{RCk_2 I_{b2}}. \tag{44}$$

It is obvious that current I_d is DC component, which shifts linear trace (triangular signal), i.e. offset. It influences the duty cycle of the produced wave as:

$$D = \frac{T_1}{T} = \frac{1}{2} \left(1 - \frac{I_d}{I_{b1}} \right) = \frac{1}{2} (1-n). \tag{45}$$

The maximal theoretical limits of I_d are given by $\pm I_{b1}$ ($n = 1$ for $D = 0\%$ and $n = -1$ for $D = 100\%$). Therefore, change of the polarity of I_d is required. The repeating frequency can be controlled independently with respect to the duty cycle if ratio $I_d/I_{b1} = n$ is kept strictly constant while frequency f_0 is tuned by I_{b1} .

4. Simulation Results

4.1 Possible CMOS Implementations of Selected DO-VDBA Solutions

We designed internal topologies of DO-VDBA and FB-VDBA to demonstrate functionality and practical features of the designed applications. Models of TSMC 0.18 μm CMOS technology parameters [47] were used for our simulations. The first topology uses classical transconductance section with active load (PMOS mirror) and two simple voltage inverters, see Fig. 10. Lower gain of one transconductance section (higher gain requires cascading) and only one z terminal are the main disadvantages of this solution. Nevertheless, it is a useful solution in a specific situation and power consumption is lower in comparison to the second solution (it will be discussed later). PSpice analyses provided the following results ($I_b = 50 \mu\text{A}$, $V_{CC} = \pm 1.2 \text{ V}$): $g_m = 500 \mu\text{S}$, $R_z \approx 170 \text{ k}\Omega$, $C_z \approx 0.35 \text{ pF}$, $R_{\pm w} \approx 53 \Omega$, voltage gain between z and $+w$ has value 0.926 and gain between z and $-w$ is 0.962. Differential input resistance of OTA section is high - at 1 MHz has values higher than 1.1 $\text{M}\Omega$ (parasitic capacitance $\approx 0.27 \text{ pF}$). Adjusting of I_b influences R_z value, for $I_b = 200 \mu\text{A}$ R_z value is approx. 46 $\text{k}\Omega$ (value decreases with higher I_b).

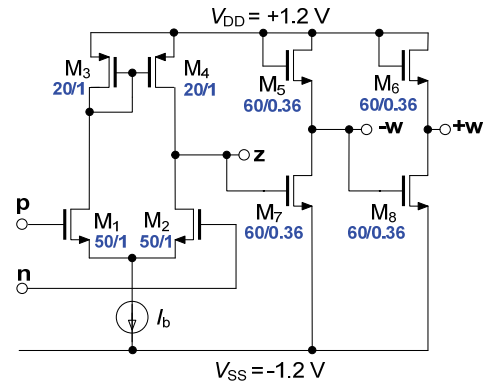


Fig. 10. DO-VDBA with one z terminal.

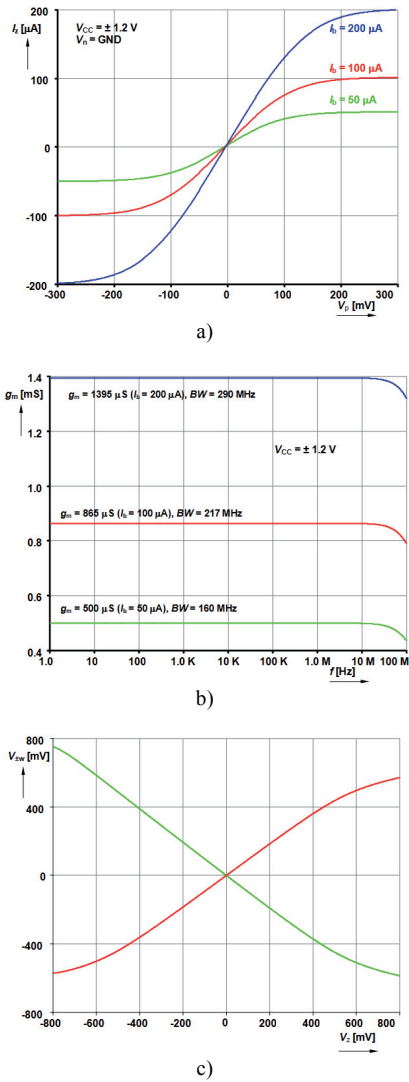


Fig. 11. Selected features of the proposed DO-VDBA: a) DC transfer characteristic of OTA section, b) dependence of g_m on frequency, c) DC transfer characteristics of inverter/buffer.

Adjusting of I_b in the range of 5 - 200 μA causes changes of g_m from 60 μS to 1.4 mS. Some of the simulation results are documented graphically in Fig. 11.

The FB-VDBA has a different construction (Fig. 12). Function of the second type (FB-VDBA) is practically similar, only internal topology is slightly complicated due to necessity of z terminals of both polarities and k -times higher gain of transconductance section and mirrors of FB-VDBA. Many parameters of the second type of DO-VDBA are practically identical to the previously discussed type (parameters of voltage inverters). Simulations provided the following results ($I_b = 50 \mu\text{A}$, $V_{CC} = \pm 1.2\text{V}$): $g_m = 1030 \mu\text{S}$, $R_{\pm w} \approx 130 \text{k}\Omega$, $C_{\pm z} \approx 0.38 \text{pF}$. The differential input resistance of OTA section has higher values than 0.64 M Ω at 1 MHz (parasitic capacitance $\approx 0.25 \text{pF}$). Adjusting of g_m from 132 μS to 2.76 mS was verified (I_b between 5 and 200 μA). The highest tested $I_b = 200 \mu\text{A}$ decreases $R_{\pm z}$ value to 53 k Ω approximately. Selected results are documented in Fig. 13.

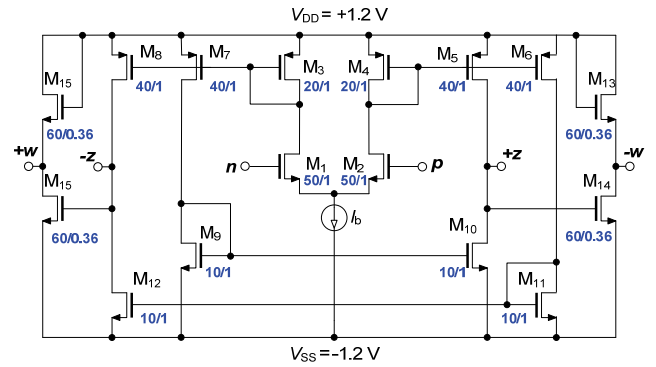


Fig. 12. FB-VDBA with z terminals of both polarities.

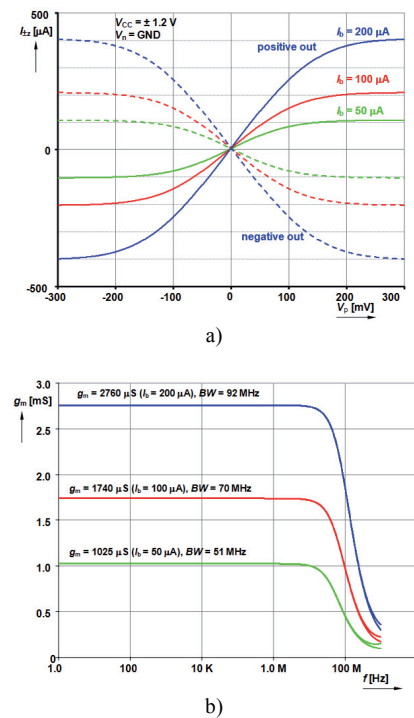


Fig. 13. Selected features of FB-VDBA: a) DC transfer characteristic of OTA section, b) dependence of g_m on frequency.

4.2 Detailed PSpice Analysis of Some Proposed Applications

Multiphase oscillator - type without necessity of floating negative resistance

Oscillator from Fig. 6 we designed for operation at $f_0 = 1.539 \text{ MHz}$ with parameters: $R_1 = R_2 = R = 2.2 \text{ k}\Omega$, $C_1 = C_2 = C = 47 \text{ pF}$, $R_3 = 1 \text{ k}\Omega$, and $g_{m2} = 1 \text{ mS}$. Obtained results of simulation are shown in Fig. 14. Voltage gain of subtracting point created by DO-VDBA₂ and R_3 is approximately equal to 1. Real value of g_{m1} necessary for start of oscillation was increased to 1.133 mS ($I_{b1} = 146 \mu\text{A}$). Oscillation frequency 1.506 MHz was obtained, which is very close to the ideal value (error about 2%). Achieved total harmonic distortion (THD) was 0.40%, 0.39%, 0.26%, 0.81% and 0.81% for all outputs namely: V_{OUT0} , V_{OUT180} , V_{OUT45} , V_{OUT135} , V_{OUT-45} .

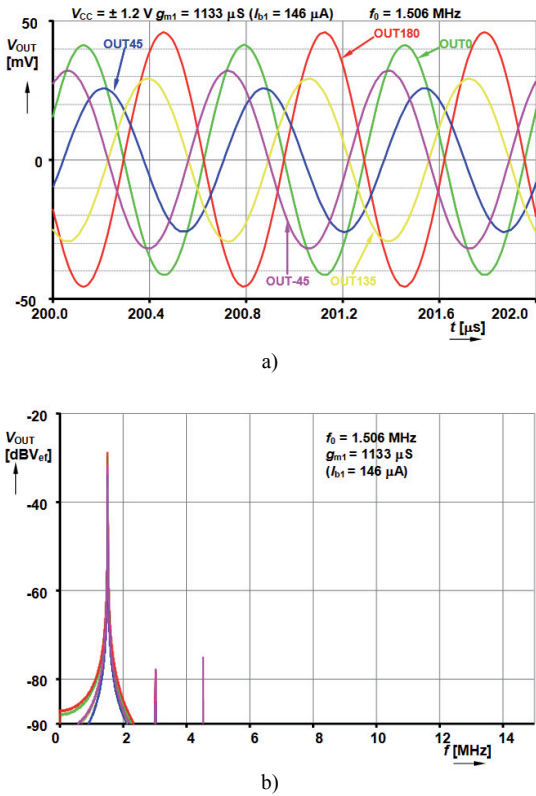


Fig. 14. Results of simulation of the oscillator from Fig. 6: a) transient responses, b) frequency spectrum.

Functional generator

We require operation in hundreds of kHz, therefore parameters of the design (considering solution shown in Fig. 9) are the following: $C = 22$ pF, $R = 10$ kΩ, $I_{b2} = 20$ μA, $k_2 = 2$ and suitable range of maximal output current (given by $k_1 I_{b1}$, where $k_1 = 1$) adjusting between 5 μA and 100 μA. Duty cycle was set to 50% ($n = 0$). Load resistances $R_L = 1$ kΩ were connected at the output ports (w) in simulations. We used FB-VDBA based comparator. This solution has one disadvantage, which is the necessity of the second resistor. However, such OTA section with mirrors in FB-VDBA structure has higher available voltage gain (bias mirroring with gain $k_2 = 2$, see Fig. 12) than simpler OTA section in the DO-VDBA. Of course, there is possibility to use simpler DO-VDBA, but validity of (36) is highly influenced by insufficient gain of the comparator in low-power solution. In fact, we are discussing a specific design for our requirements in the following text. Quality of the comparator directly influences oscillation frequency (threshold referencing voltage for changing of output polarity). The transconductance of OTA section of FB-VDBA has value 470 μS for $I_{b2} = 20$ μA. This value is quite low for sufficient voltage amplification in the comparator (it is better than for the same solution with DO-VDBA). We expected equality between input threshold voltage and output voltage of the comparator. Unfortunately, gain is not sufficient and therefore we achieved only $V_{\square} \approx 1.3V_{\Delta}$. In addition this gain is not valid in the whole DC transfer characteristic due to its nonlinearity in frame of the OTA section as part of the FB-VDBA based

comparator. AC analysis allows finding small-signal g_m for ideal calculation (35) of the comparator behavior. Nevertheless, g_m has a lower value than in the origin of the characteristic (around 0) in case of comparator in overturn corners (reference voltages) of DC transfer characteristic. The new equation for repeating frequency considering the above discussed inequality of input (reference) and output voltage of the comparator and $D = 50\%$ has the following form:

$$f_{0_exp} = \frac{I_{b1}}{4C \frac{V_R}{\left(\frac{g_{m2}R}{g_{m2}R-1}\right)}} = \frac{I_{b1}}{\frac{4RCk_2I_{b2}}{\left(\frac{g_{m2}R}{g_{m2}R-1}\right)}} \cong \frac{I_{b1}}{\frac{8RCI_{b2}}{1.3}} \quad (46)$$

Maximal output voltage at terminal $+z_2$ (V_R) of FB-VDBA has amplitude value $V_R = V_{\square} = I_{b2} \cdot k_2 \cdot R \approx 400$ mV. This value is also expected for output amplitude of square wave signal (in case of single-ended solution). Considering the practical inequality of (36) given by (35) means that input reference voltage (causing overturn of the comparator) is 1.3 times lower (approximately 300 mV) than V_{\square} . This value is expected for amplitude of triangle (symmetrical ramp) wave signal. All these presumptions expect unity-gain followers/inverters and symmetrical referencing voltage (it is given by quality of the comparator), in real case it can be slightly different (non-unity gains of followers/inverters causes changes of expected amplitudes). Repeating frequency f_0 is expected for selected parameters and $I_{b1} = 30$ μA and with help of (46) as $f_0 = 1.108$ MHz. Simulated value of generator with models of VDBAs discussed above was obtained as 1.031 MHz. Results are in Fig. 15.

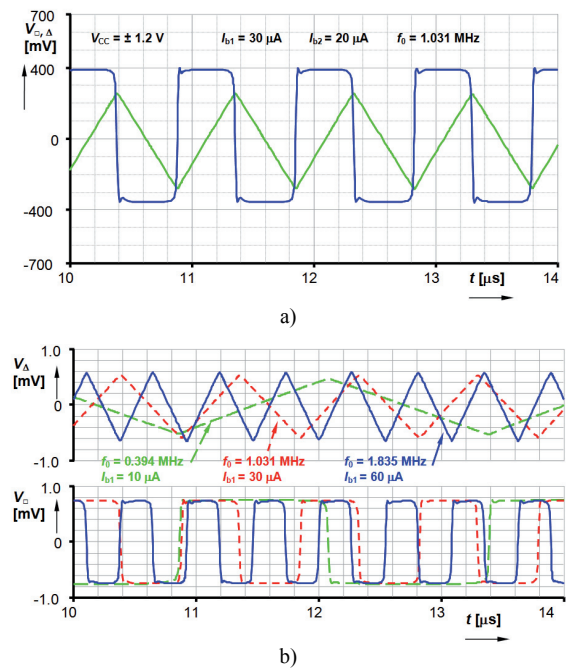


Fig. 15. Simulated transient responses of the proposed generator: a) single-ended mode, b) example of electronic control of f_0 (differential-balanced output mode).

Differential mode of operation has advantage of two-times higher produced amplitude. Electronic adjusting of f_0 was verified between 211 kHz and 2.83 MHz (I_{b1} changed from 5 μA to 100 μA), see Fig. 16 where comparison of calculated f_0 (46) and simulation results are depicted.

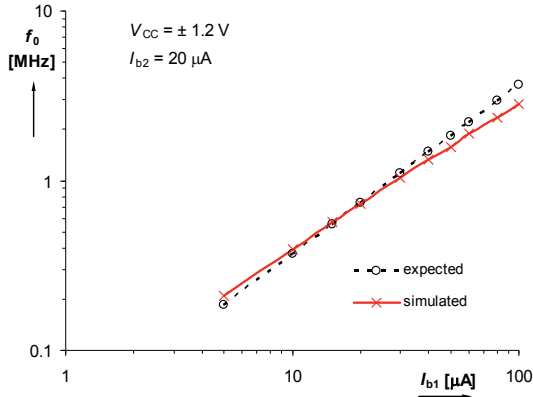


Fig. 16. Calculated and simulated dependence of f_0 on I_b .

An example of operation of the generator with $D = 24.5\%$ at $f_0 = 1$ MHz was provided. Expected f_0 can be expressed by the following equation considering a finite gain similarly as (46):

$$f_{0_exp} = \frac{I_{b1}(1-D)D}{2RCI_{b2}} \left(\frac{g_{m2}R-1}{g_{m2}R} \right). \quad (47)$$

Analysis used the same values of the rest of parameters as in the previous case. The bias current $I_{b1} = 39 \mu\text{A}$ was set in accordance to (47) for the above discussed assignment. Results in differential output mode are shown in Fig. 17 where possibility of adjusting of f_0 between two values is documented while D keeps unchangeable.

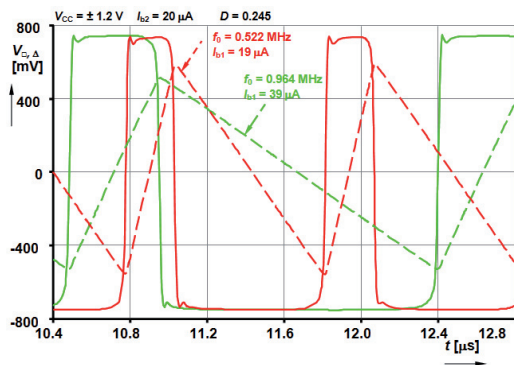


Fig. 17. Examples of variability f_0 in simulated transient responses with $D = 24.5\%$.

5. Experimental Results

The comparator in Fig. 8 was tested experimentally with behavioral model (Fig. 18) based on commercially available devices. All parameters and values are noted in Fig. 18. The circuit was tested for ramp-pulse excitation (± 0.7 V, 1 kHz) and the results are in Fig. 19.

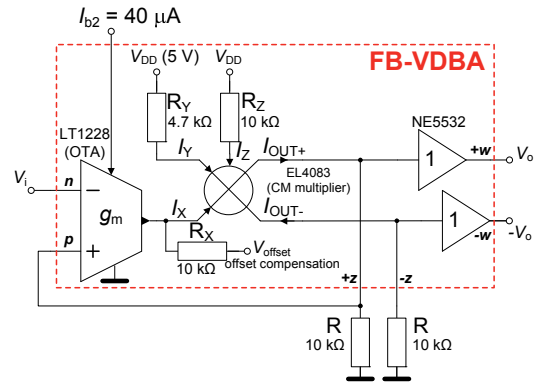
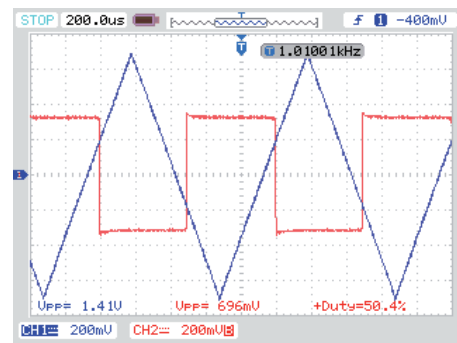
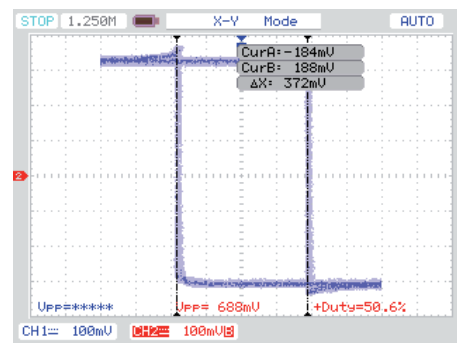


Fig. 18. Schmitt comparator employing behavioral model of FB-VDBA (based on commercially available devices).



a)



b)

Fig. 19. Measurement results of the comparator: a) transient responses V_i (triangular), V_o , b) hysteresis characteristic of the comparator.

6. Conclusion

The designed active elements allow beneficial features in specific applications. They were intended for utilization in multiphase oscillators, quadrature oscillators (single-ended or differential mode) or triangle and square wave generators for example, where provided modifications of VDBA and VDIBA elements [1]-[5] with standard transconductance control or also additional electronic control of voltage gain in frame of active element were employed. Some of the presented circuits allow benefits of simplicity (multiphase oscillators for example) in comparison to classical design methods based on cascading lossy integrators or similar sections in phase shifted loop [6]-[8],

where higher number of active and passive elements is necessary. Higher demands on precise accuracy of relations between generated outputs and necessity of several matching conditions is cost of these benefits. Nevertheless, matching conditions are also drawback of some more sophisticated phase-shifted solutions. Both introduced quadrature oscillators and triangle and square wave generator offer advantages of simplicity and differential output responses. The proposed circuits were verified by simulations at frequencies of several MHz and complemented by detailed discussions.

Acknowledgements

The research described in the paper was supported by Czech Science Foundation projects under No. 102/09/1681 and No. 102/11/P489 and by project (Brno University of Technology) of specific research FEKT-S-11-15. Dr. Herencsar was supported by the project of the Brno University of Technology CZ.1.07/2.3.00/ 30.0039. The support of the project CZ.1.07/2.3.00/20.0007 WICOMT, financed from the operational program Education for Competitiveness is gratefully acknowledged. The described research was performed in laboratories supported by the SIX project; registration number CZ.1.05/2.1.00/03.0072, the operational program Research and Development for Innovation. This research work is funded also by projects EU ECOP EE.2.3.20.0094, CZ.1.07/2.2.00/28.0062.

References

- [1] BIOLEK, D., SENANI, R., BIOLKOVA, V., KOLKA, Z. Active elements for analog signal processing: Classification, review, and new proposal. *Radioengineering*, 2008, vol. 17, no. 4, p. 15-32.
- [2] BIOLKOVA, V., KOLKA, Z., BIOLEK, D. Fully balanced voltage differencing buffered amplifier and its applications. In *Proc. of 52nd MWSCAS*. Cancun (Mexico), 2009, p. 45-48.
- [3] BIOLEK, D., BIOLKOVA, V., KOLKA, Z. All-pass filter employing fully balanced voltage differencing buffered amplifier. In *Proc. of the IEEE Latin American Symposium on Circuits and Systems (LASCAS 2010)*. Iguacu (Brazil), 2010. p. 232-235.
- [4] KACAR, F., YESIL, A., NOORI, A. New CMOS realization of voltage differencing buffered amplifier and its biquad filter applications. *Radioengineering*, 2012, vol. 21, no. 1, p. 333-339.
- [5] HERENC SAR, N., MINAEI, S., KOTON, J., YUCE, E., VRBA, K. New resistorless and electronically tunable realization of dual-output VM all-pass filter using VDIBA. *Analog Integrated Circuits and Signal Processing*, 2013, vol. 74, no. 1, p. 141-154.
- [6] ABUELMAATTI, M. T., AL-QAHTANI, M. A. A new current-controlled multiphase sinusoidal oscillator using translinear current conveyors. *IEEE Transactions on Circuits and Systems II: Analog and Digital Signal Processing*, 1998, vol. 45, no. 7, p. 881-885.
- [7] SOULIOTIS, G., PSYCHALINOS, C. Electronically controlled multiphase sinusoidal oscillators using current amplifiers. *International Journal of Circuit Theory and Applications*, 2009, vol. 37, no. 1, p. 43-52.
- [8] KUMNGERN, M., CHANWUTIUM, J., DEJHAN, K. Electronically tunable multiphase sinusoidal oscillator using translinear current conveyors. *Analog Integrated Circuits and Signal Processing*, 2010, vol. 65, no. 2, p. 327-334.
- [9] GIFT, S. J. G. The application of all-pass filters in the design of multiphase sinusoidal systems. *Microelectronics Journal*, 2000, vol. 31, no. 1, p. 9-13.
- [10] KESKIN, A. U., BIOLEK, D. Current mode quadrature oscillator using current differencing transconductance amplifiers (CDTA). *IEE Proc. Circuits Devices and Systems*, 2006, vol. 153, no. 3, p. 214-218.
- [11] SONGSUWANKIT, K., PETCHMANEELUMKA, W., RIWRUJA, V. Electronically adjustable phase shifter using OTAs. In *Proc. of the International Conference on Control, Automation and Systems (ICCAS2010)*. Gyeonggi-do (Korea), 2010, p. 1622-1625.
- [12] KEAWON, R., JAIKLA, W. A resistor-less current-mode quadrature sinusoidal oscillator employing single CCCDTA and grounded capacitors. *Przeglad Elektrotechniczny*, 2011, vol. 87, no. 8, p. 138-141.
- [13] JAIKLA, W., SIRIPRUCHYANUN, M., BAJER, J., BIOLEK, D. A simple current-mode quadrature oscillator using single CDTA. *Radioengineering*, 2008, vol. 17, no. 4, p. 33-40.
- [14] PANDEY, N., PAUL, S. K. Single CDTA-based current mode all-pass filter and its applications. *Journal of Electrical and Computer Engineering*, 2011, vol. 2011, p. 1-5.
- [15] KESKIN, A. U., AYDIN, C., HANCIOGLU, E., ACAR, C. Quadrature oscillator using current differencing buffered amplifiers (CDBA). *Frequenz*, 2006, vol. 60, no. 3, p. 21-23.
- [16] SONGKLA, S. N., JAIKLA, W. Realization of electronically tunable current-mode first-order allpass filter and its application. *International Journal of Electronics and Electrical Engineering*, 2012, vol. 2012, no. 6, p. 40-43.
- [17] MINAEI, S., YUCE, E. Novel voltage-mode all-pass filter based on using DVCCs. *Circuits, Systems and Signal Processing*, 2010, vol. 29, no. 3, p. 391-402.
- [18] SOLIMAN, A. M. Synthesis of grounded capacitor and grounded resistor oscillators. *Journal of the Franklin Institute*, 1999, vol. 336, no. 4, p. 735-746.
- [19] HERENC SAR, N., VRBA, K., KOTON, J., LAHIRI, A. Realizations of single-resistance-controlled quadrature oscillators using a generalized current follower transconductance amplifier and a unity gain voltage-follower. *Int. Journal of Electronics*, 2010, vol. 97, no. 8, p. 879-906.
- [20] GUPTA, S. S., SENANI, R. New single-resistance-controlled oscillator configurations using unity-gain cells. *Analog Integrated Circuits and Signal Processing*, 2006, vol. 46, no. 2, p. 111-119.
- [21] BIOLKOVA, V., BAJER, J., BIOLEK, D. Four-phase oscillators employing two active elements. *Radioengineering*, 2011, vol. 20, no. 1, p. 334-339.
- [22] LAHIRI, A., GUPTA, M. Realizations of grounded negative capacitance using CFOAs. *Circuits, Systems and Signal Processing*, 2011, vol. 30, no. 1, p. 134-155.
- [23] LAHIRI, A. Explicit-current-output quadrature oscillator using second-generation current conveyor transconductance amplifier. *Radioengineering*, 2009, vol. 18, no. 4, p. 522-526.
- [24] LAHIRI, A. Novel voltage/current-mode quadrature oscillator using current differencing transconductance amplifier. *Analog Integrated Circuits and Signal Processing*, 2009, vol. 61, no. 2, p. 199-203.
- [25] RODRIGUEZ-VAZQUEZ, A., LINAREZ-BARRANCO, B., HUERTAS, L., SANCHEZ-SINENCIO, E. On the design of volt-

- age-controlled sinusoidal oscillators using OTA's. *IEEE Transaction on Circuits and Systems*, 1990, vol. 37, no. 2, p. 198-211.
- [26] SOTNER, R., HERENC SAR, N., JERABEK, J., KOTON, J., DOSTAL, T., VRBA, K. Quadrature oscillator based on modified double current controlled current feedback amplifier. In *Proc. of 22nd Int. Conf. Radioelektronika*. Brno (Czech Republic), 2012, p. 275-278.
- [27] ALZAHER, H. CMOS digitally programmable quadrature oscillators. *International Journal of Circuit Theory and Applications*, 2008, vol. 36, no. 8, p. 953-966.
- [28] BIOLEK, D., LAHIRI, A., JAIKLA, W., SIRIPRUCHYANUN, M., BAJER, J. Realization of electronically tunable voltage-mode/current-mode quadrature sinusoidal oscillator using ZC-CG-CDBA. *Microelectronics Journal*, 2011, vol. 42, no. 10, p. 1116-1123.
- [29] SOTNER, R., JERABEK, J., HERENC SAR, N., HRUBOS, Z., DOSTAL, T., VRBA, K. Study of adjustable gains for control of oscillation frequency and oscillation condition in 3R-2C oscillator. *Radioengineering*, 2012, vol. 21, no. 1, p. 392-402.
- [30] GALAN, J., CARVALAJ, R. G., TORRALBA, A., MUNOZ, F., RAMIREZ-ANGULO, J. A low-power low-voltage OTA-C sinusoidal oscillator with large tuning range. *IEEE Transaction on Circuits and Systems I: Fundamental Theory and Applications*, 2005, vol. 52, no. 2, p. 283-291.
- [31] BAJER, J., BIOLEK, D., BIOLKOVA, V., KOLKA, Z. Voltage-mode balanced-outputs quadrature oscillator using FB-VDBAs. In *Proc. of Int. Conf. on Microelectronics (ICM)*, 2010, p. 491-494.
- [32] BIOLEK, D., BIOLKOVA, V. Current-mode CDTA-based comparators. In *Proc. of the 13th International Conference on Electronic Devices and Systems EDS IMAPS*. Brno (Czech Republic), 2006, p. 6-10.
- [33] DE-MARCELLIS, A., DI-CARLO, C., FERRI, G., STORNELLI, V. A CCI-based wide frequency range square waveform generator. *International Journal of Circuit Theory and Applications*, 2013, vol. 41, no. 1, p. 1-13.
- [34] CHIEN, H-CH. Voltage-controlled dual slope operation square/triangular wave generator and its application as a dual mode operation pulse width modulator employing differential voltage current conveyors. *Microelectronics Journal*, 2012, vol. 43, no. 12, p. 962-974.
- [35] ALMASHARY, B., ALHOKAIL, H. Current-mode triangular wave generator using CCII's. *Microelectronics Journal*, 2000, vol. 31, no. 4, p. 239-243.
- [36] PAL, D., SRINIVASULU, B. B., PAL, A., DEMOSTHENOUS, B., DAS, N. Current conveyor-based square/triangular waveform generators with improved linearity. *IEEE Transaction on Instrumentation and Measurement*, 2009, vol. 58, no. 7, p. 2174-2180.
- [37] SAQUE, A. S., HOSSAIN, M. M., DAVIS, W. A., RUSSELL, H. T., CARTER, R. L. Design of sinusoidal, triangular, and square wave generator using current feedback amplifier (CFOA). In *Proc. of IEEE Region 5 Conference*. Kansas City (USA), 2008, p. 1-5.
- [38] MINAEI, S., YUCE, E. A simple Schmitt trigger circuit with grounded passive elements and its application to square/triangular wave generator. *Circuits, Systems, and Signal Processing*, 2012, vol. 31, no. 3, p. 877-888.
- [39] LO, Y. K., CHIEN, H. C. Switch-controllable OTRA-based square/triangular waveform generator. *IEEE Transaction on Circuits, Systems and Signal Processing II*, 2007, vol. 54, no. 12, p. 1110-1114.
- [40] KIM, K., CHA, H. W., CHUNG, W. S. OTA-R Schmitt trigger with independently controllable threshold and output voltage levels. *Electronics Letters*, 1997, vol. 33, no. 13, p. 1103-1105.
- [41] CHUNG, W. S., KIM, H., CHA, H. W., KIM, H. J. Triangular/square-wave generator with independently controllable frequency and amplitude. *IEEE Transactions on Instrumentation and Measurement*, 2005, vol. 54, no. 1, p. 105-109.
- [42] CHUNG, W. S., CHA, H. W., KIM, H. J. Current-controllable monostable multivibrator using OTAs. *IEEE Transactions on Circuits and Systems I: Fundamental Theory and Applications*, 2002, vol. 49, no. 5, p. 703-705.
- [43] SIRIPRUCHYANUN, M., WARDKEIN, P. A full independently adjustable, integrable simple current controlled oscillator and derivative PWM signal generator. *IEICE Trans. Fundam. Electron. Commun. Comput. Sci.*, 2003, vol. E86-A, no. 12, p. 3119-3126.
- [44] KUMBUN, J., SIRIPRUCHYANUN, M. MO-CTTA-based electronically controlled current-mode square/triangular wave generator. In *Proc. of the 1st International Conf. on Technical Education (ICTE2009)*, 2010, p. 158-162.
- [45] SILAPAN, P., SIRIPRUCHYANUN, M. Fully and electronically controllable current-mode Schmitt triggers employing only single MO-CCCDTA and their applications. *Analog Integrated Circuits and Signal Processing*, 2011, vol. 68, no. 11, p. 111-128.
- [46] SRISAKUL, T., SILAPAN, P., SIRIPRUCHYANUN, M. An electronically controlled current-mode triangular/square wave generator employing MO-CCCCTAs. In *Proc. of the 8th Int. Conf. on Electrical Engineering/ Electronics, Computer, Telecommunications, and Information Technology*. 2011, p. 82-85.
- [47] MOSIS parametric test results of TSMC LO EPI SCN018 technology. [Online] Cited 2012-05-24. Available at: <ftp://ftp.isi.edu/pub/mosis/vendors/tsmc-018/t44e10epi-params.txt>.
- [48] BAKER, J. *CMOS Circuit Design, Layout and Simulation*. IEEE Press Series on Microelectronic Systems, 2005.

About Authors ...

Roman SOTNER was born in Znojmo, Czech Republic, in 1983. He received the M.Sc. and Ph.D. degrees from the Brno University of Technology, Czech Republic, in 2008 and 2012, respectively. Currently, he is a technical worker at the Department of Radio Electronics, Faculty of Electrical Engineering and Communication, Brno University of Technology, Brno, Czech Republic. His interests are analog circuits (active filters, oscillators, audio, etc.), circuits in the current mode, circuits with direct electronic controlling possibilities especially and computer simulation.

Jan JERABEK was born in Bruntal, Czech Republic, in 1982. He received the Ph.D. degree in Electrical Engineering in 2011 from the Brno University of Technology, Czech Republic. He received M.Sc. and B.Sc. degree from the same university in 2007 and 2005, respectively. He is currently an Assistant Professor at the Department of Telecommunications, Faculty of Electrical Engineering and Communication, Brno University of Technology. His research interests are focused on circuit applications of modern active elements such as current amplifiers and multiple output current followers.

Norbert HERENC SAR received the M.Sc. and Ph.D. degrees in Electronics & Communication and Teleinformatics from the Brno University of Technology, Czech Republic, in 2006 and 2010, respectively. Currently, he is

an Assistant Professor at the Department of Telecommunications and employee at the Centre of Sensor, Information and Communication Systems (SIX), Faculty of Electrical Engineering and Communication, Brno University of Technology, Brno, Czech Republic. From September 2009 through February 2010 he was an Erasmus Exchange Student with the Department of Electrical and Electronic Engineering, Bogazici University, Istanbul, Turkey, where he is now a Visiting Researcher since February 2013. His research interests include analog filters, current-, voltage- and mixed-mode circuits, new active elements and their circuit applications, and oscillators. He is an author or co-author of 28 research articles published in SCI-E international journals, 20 articles published in other journals, and 61 papers published in proceedings of international conferences. In 2011 and 2012, he received the Rector Award in the University competition "Top 10 Excellence VUT" for

the 9th and 8th most productive scientist at the Brno University of Technology, category "Publications", respectively. His paper "Novel resistorless dual-output VM all-pass filter employing VDIBA", presented and published at the 7th International Conference on Electrical Electronics Engineering - ELECO 2011, Bursa, Turkey, received "The best paper award in memory of Prof. Dr. Mustafa Bayram". Since 2008, Dr. Herencsar serves in the organizing and technical committee of the International Conference on Telecommunications and Signal Processing (TSP). In 2011, he was a guest co-editor of TSP 2010 Special Issue on Telecommunications, published in the Telecommunication Systems journal of Springer. In 2011-2013, he was a guest co-editor of TSP 2010, TSP 2011, and TSP 2012 Special Issues on Signal Processing, published in the Radioengineering journal. He is Senior Member of the IACSIT and Member of the IEEE, IAENG, and ACEEE.

[10] SOTNER, R., JERABEK, J., PETRZELA, J., HERENC SAR, N., PROKOP, R., VRBA, K. Second-order Simple Multiphase Oscillator Using Z-Copy Controlled- Gain Voltage Differencing Current Conveyor. *Elektronika Ir Elektrotechnika*, 2014, vol. 20, no. 9, p. 13-18. ISSN: 1392-1215.

Second-Order Simple Multiphase Oscillator Using Z-Copy Controlled-Gain Voltage Differencing Current Conveyor

R. Sotner¹, J. Jerabek², J. Petrzela¹, N. Herencsar², R. Prokop³, K. Vrba²

¹Department of Radio Electronics, Faculty of Electrical Engineering and Communication,
Brno University of Technology,
Technická 12, Brno, 616 00, Czech Republic

²Department of Telecommunications, Faculty of Electrical Engineering and Communication,
Brno University of Technology,
Technická 12, Brno, 616 00, Czech Republic

³Department of Microelectronics, Faculty of Electrical Engineering and Communication,
Brno University of Technology,
Technická 10, Brno, 616 00, Czech Republic
sotner@feec.vutbr.cz

Abstract—Interesting type of the second-order electronically controllable multiphase oscillator is introduced in this paper. Modified voltage differencing current conveyor, so-called z-copy controlled gain voltage differencing current conveyor (ZC-CG-VDCC), offers interesting features for synthesis of this type of multiphase oscillator. Available controllable parameters of the ZC-CG-VDCC (intrinsic resistance, transconductance and current gain) are fully utilized for independent adjusting of oscillation condition and oscillation frequency. Specific matching condition allows linear control of oscillation frequency that is not so typical in such simple types of oscillators. Available phase shifts are 45, 90, 135 and 180 degree. Simulation results based on CMOS model of active element confirms intentions of the proposal in the bandwidth of several MHz.

Index Terms—Electronic control, current-gain, intrinsic resistance, second-order multiphase oscillators, transconductance, voltage differencing current conveyor, z-copy.

I. INTRODUCTION

Applications of more than one type of controllable parameter in frame of one active device have increasing attention of many researchers. Several interesting solutions of active element with these features were reported in literature. For example, Minaei et al. [1], Marcellis *et al.* [2], Kumngern et al. [3] and others presented interesting

conceptions. Extended version of the current conveyor introduced in [1] allows adjustable current gain (B) between x and z terminals and adjustable intrinsic resistance (R_x) of the current input terminal x . Modified current conveyor introduced in [2] disposes controllable features of current gain between x and z terminals and voltage gain between y and x terminals. Combination of R_x and B control is available in interesting version of translinear current conveyor [3]. Typical examples of active elements with two-parameter control are also modifications of the current differencing transconductance amplifier (CDTA) [4], [5]. DC bias currents are also used for control of R_x and transconductance g_m [6], [7]. Transconductance section [4], [8] combined with current conveyor of second generation [4], [9], [10] are common subparts in so-called current conveyor transconductance amplifier (CCTA) [4], [11], where independent R_x and g_m control is also possible [12]. Some modifications of CCTA provide also adjustable current gain control [13].

Active element presented in this paper and used in proposed application offers possibility of control of three independent parameters. In case of oscillator, it is fully utilized for control of oscillation condition and linear tuning of oscillation frequency.

The reasons for utilization of active elements employing several types of electronic control came from requirements for comfortable electronic control in applications. The important applications in the field of signal generation are oscillators. Therefore, we provided detailed study of several oscillator solutions and found following drawbacks concerning mainly lack of electronically controllable features of proposed circuits:

1. too many passive elements (for example [14]–[17]),
2. condition of oscillation given by equality of capacitors only (for example [18]–[22]),

Manuscript received April 8, 2014; accepted September 14, 2014.

Research described in the paper was supported by Czech Science Foundation project under No. 14-24186P and by internal grant No. FEKT-S-14-2281 and project Electronic-biomedical co-operation ELBIC M00176. The support of the project CZ.1.07/2.3.00/20.0007 WICOMT, financed from the operational program Education for competitiveness, is gratefully acknowledged. The described research was performed in laboratories supported by the SIX project; the registration number CZ.1.05/2.1.00/03.0072, the operational program Research and Development for Innovation. Dr. Herencsar was supported by the project CZ.1.07/2.3.00/30.0039 of the Brno University of Technology.

TABLE I. SOME OF RECENTLY REPORTED SOLUTIONS OF SIMPLE SECOND-ORDER MULTIPHASE OSCILLATORS.

Reference	Year	No. of active elements	No. of passive elements	Type of active element	Tunable type	Grounded C	Mutual dependence of oscillation frequency and condition	Electronic control of oscillation frequency	Electronic control of oscillation condition	Type of control (PE- passive elements-resistor; DC V - DC bias voltage; DC I - DC bias current)	Type of the phase shift (multiplicand)	Type of output signals (current or voltage)
[6]	2012	2	2	CCCDTA	Yes	Yes	No	Yes (g_m)	Yes (g_m)	DC I	$kf/2$	current
[31]	2011	2	5 or 6	DO-CIBA	Yes	Yes	No	No (R)	No (R)	PE	$kf/2$	voltage
[32]	2013	2	3	VDIBA	No	No	Yes	Yes (g_m)	Yes (g_m)	DC I	$kf/2$	voltage
[33]	in press	3	5	DO-CG-CFBA	Yes	Yes	No	Yes (B)	Yes (B)	DC V	$kf/2$	voltage
[34]	2014	2	5	CG-CFDOBA, CG-BCVA	Yes	Yes	No	Yes (B)	Yes (A)	DC V	$kf/2$	voltage
[35]	2012	1	3	VDTA	Yes	Yes	No	Yes (g_m)	No (R)	DC I	$kf/2$	current
[36]	2013	1	5	VDTA	Yes	Yes	No	Yes (g_m)	No (R)	DC I	$kf/2$	voltage
[37]	2012	2	6	CCII+, ECCII-	No	Yes	No	No	Yes (B)	DC V	$kf/4$	voltage
[38]*	2013	2	3; 5	DO-VDBA, FB-VDBA	No	Yes	No; Yes	Yes(g_m); No	Yes (g_m)	DC I	$kf/4$	voltage
proposed		1	4	ZC-CG-VDCC	Yes	Yes	No	Yes (g_m, R_x)	Yes (B)	DC I	$kf/4$	voltage

Notes: A – voltage gain; B – current gain; g_m – transconductance; R – resistor value
 * ref. [38] deals with two types of the oscillator with phase shift $kf/4$

3. matching of two controllable parameters or values of passive elements required in order to fulfill oscillation condition, and tuning of oscillation frequency is required simultaneously [18]–[22],

4. linear control of oscillation frequency is not possible especially in simple solutions having minimal number of active elements [23]–[28],

5. none of discussed simple second-order solution allow four-phase outputs with $\pi/4$ shift i.e. 45, 90, 135, and 180 degree of phase shifts.

Of course, there are many multiphase solutions based on cascades (chains) of lossy blocks in one loop (for example [29] and references cited therein) that allow various phase shifts, but circuit realization is very extensive (many active and passive elements) and tunability complicated in some cases [30]. Therefore, we focused our attention on simple (minimal number of active element) electronically adjustable solutions. Despite of fact that several second-order multiphase and tunable oscillators were introduced [6], [31]–[36], any solution from them does not allow to realize phase shift between produced signals different than $f/2$. Detailed comparison is shown in Table I. Our solution produces phase shift $f/4$ between generated signals. The same feature is available in [37], [38], but discussed solutions do not have capability of electronic control (or any other method) of oscillation frequency or they do not have independent control of oscillation frequency (element suitable for frequency control influences oscillation condition). Therefore, oscillator presented in this paper provides significant advantages (electronic control of oscillation frequency independently on oscillation condition and minimal number of active elements) in comparison to previous works that realizes phase shift in multiples of $f/4$ [37], [38].

II. SECOND-ORDER MULTIPHASE OSCILLATOR USING Z-COPY CONTROLLED-GAIN VOLTAGE DIFFERENCING CURRENT CONVEYOR

Presented second-order multiphase oscillator utilizes active element referred as z-copy controlled gain voltage differencing current conveyor (ZC-CG-VDCC). Detailed description of the active element and its parameters are discussed in [39]. Therefore, only very brief introduction is given here. ZC-CG-VDCC is multi-terminal mixed-mode active device that provides three independent types of controllable parameters (R_x , g_m , B). These parameters are adjustable by DC bias currents. Difference of voltages V_p and V_n at high-impedance input terminals is transformed to current I_{z_TA} by transconductance section (g_m). The identical copy is provided for auxiliary purposes (high-impedance terminal z_c_TA). Voltage at low-impedance current input terminal x is directly given by intrinsic resistance R_x and V_{z_TA} . Current $I_x = (V_x - V_{z_TA})/R_x$ is amplified by adjustable gain B to positive and negative output (high-impedance terminals z_p , z_n). Symbol, including internal behavioral model, is shown in Fig. 1. Outgoing current (arrow in direction out of the device) is meant as positive. Inter-terminal relations are also included in Fig. 1. Possible CMOS implementation and its features are shown in [39].

Circuit structure of the multiphase voltage-mode oscillator is given in Fig. 2. Here it is worth to note that the circuit can also work in current-mode if the load resistances R_{L1} and R_{L2} are omitted. In this case current responses are taken from terminals z_p and z_c_TA . Characteristic equation of the oscillator in Fig. 2 has very favorable form

$$s^2 + \frac{C_2 - C_1 B}{R_x C_1 C_2} s + \frac{g_m}{R_x C_1 C_2} = 0, \quad (1)$$

where condition of oscillation (CO) and frequency of oscillation (FO) are:

$$B \geq \frac{C_2}{C_1}, \quad (2)$$

$$\tilde{S}_0 = \sqrt{\frac{g_m}{R_x C_1 C_2}}. \quad (3)$$

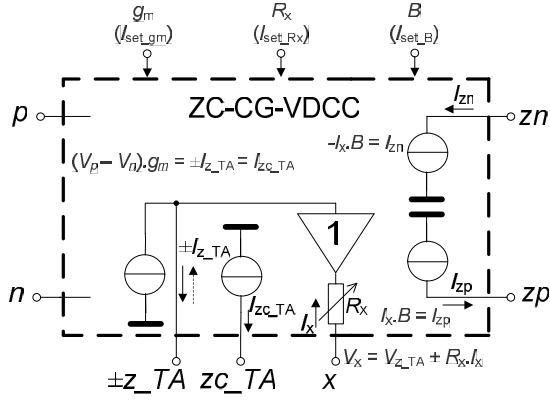


Fig. 1. Symbol and behavioral model of the ZC-CG-VDCC.

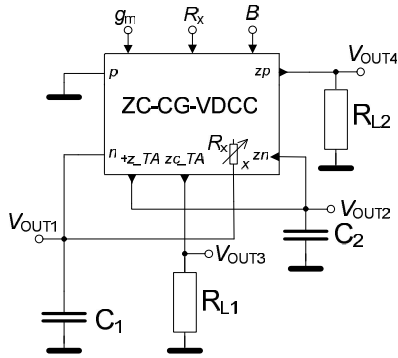


Fig. 2. ZC-CG-VDCC based second-order simple multiphase oscillator.

The relation between outputs V_{OUT2} and V_{OUT1} is represented by following expression

$$\frac{V_{OUT2}}{V_{OUT1}} = \frac{B + R_x g_m}{B - s C_2 R_x}. \quad (4)$$

If CO ($B = 1$) is fulfilled and $g_m = 1/R_x$, $C_1 = C_2 = C$, (4) can be simplified to

$$\frac{V_{OUT2}}{V_{OUT1}} = 1 + j, \quad (5)$$

that gives

$$V_{OUT2} = \sqrt{2} \exp(jf/4) V_{OUT1}. \quad (6)$$

Relation for V_{OUT4} and V_{OUT1} has a form

$$\frac{V_{OUT4}}{V_{OUT1}} = R_{L2} B \frac{s C_2 + g_m}{s C_2 R_x - B}. \quad (7)$$

Simplified relation ($g_m = 1/R_x$, $C_1 = C_2 = C$, $B = 1$), valid at FO, has a form:

$$\frac{V_{OUT4}}{V_{OUT1}} = -R_{L2} g_m j = -\frac{R_{L2}}{R_x} j, \quad (8)$$

$$V_{OUT4} = R_{L2} g_m \exp(-jf/2) V_{OUT1}. \quad (9)$$

Between V_{OUT3} and V_{OUT1} we achieve very simple relation (for discussed simplification):

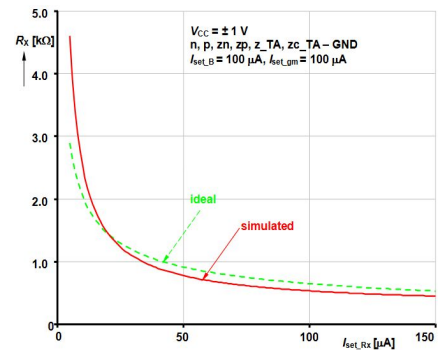
$$\frac{V_{OUT3}}{V_{OUT1}} = -\frac{R_{L1}}{R_x} = -R_{L1} g_m, \quad (10)$$

$$V_{OUT3} = R_{L1} g_m \exp(jf) V_{OUT1}. \quad (11)$$

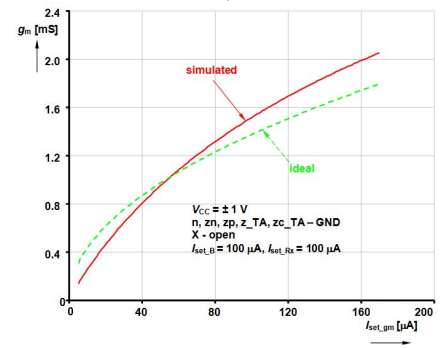
Detailed evaluation of above noted relations shows that phase shifts keep preserved during the tuning process if considered conditions ($g_m = 1/R_x$, $C_1 = C_2 = C$) are ensured. However, as we can see, amplitudes of two of produced signals (V_{OUT3} , V_{OUT4}) vary during the tuning process. Oscillation frequency can be adjusted linearly by g_m and R_x simultaneously while their ratio is kept constant.

III. SIMULATION RESULTS

We used CMOS model of the ZC-CG-VDCC introduced in [39] for verification and analysis of proposed circuit. Controllability of discussed parameters (R_x , g_m , B) of the ZC-CG-VDCC CMOS model from [39] is documented in Fig. 3. Ideal traces are determined from theoretical equations for R_x , g_m , and B in accordance with the CMOS model specifications [39]. Adjusting of the DC bias current I_{set_Rx} between $5.9 \mu\text{A}$ and $80 \mu\text{A}$ allows control of R_x in approximate range from $4 \text{ k}\Omega$ to $0.67 \text{ k}\Omega$. Transconductance control is in case of this proposed oscillator sufficient from $250 \mu\text{S}$ to $1500 \mu\text{S}$ by I_{set_gm} between $9.7 \mu\text{A}$ and $99 \mu\text{A}$. Current gain control B is in range 0.4 to 4 (I_{set_B} from $100 \mu\text{A}$ to $10 \mu\text{A}$).



a)



b)

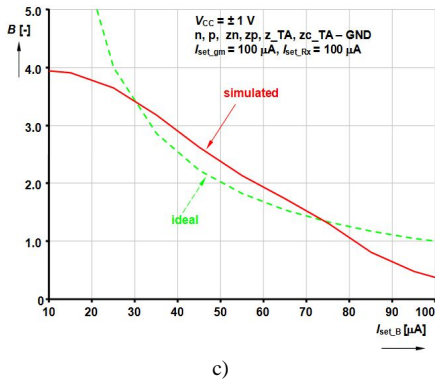


Fig. 3. Typical dependences of controllable parameters of ZC-CG-VDCC element [39] on DC bias control currents: a) R_x , b) g_m , c) B .

The oscillator in Fig. 4 (including circuit for amplitude stabilization) was designed with following parameters: $C_1 = C_2 = 30$ pF, $R_x = 2$ k Ω ($I_{set_Rx} = 13.3$ μ A), $g_m = 500$ μ S ($I_{set_gm} = 22$ μ A), $B = 1$ (control current had to be varied in range $I_{set_B} = 79$ μ A–81 μ A). Supply voltage was ± 1 V. Values of load resistance are $R_{L1} = R_{L2} = 2$ k Ω . Ideal oscillation frequency has value 2.654 MHz.

Ideal phase and amplitude relations based on analysis in (4)–(11) for these initial parameters and discrete frequency are given in Fig. 5. Dots at the ends of lines of the constant vectors mean constant unchangeable positions (obvious at single FO value). Nonlinear tuning process based on fixed R_x and adjusted g_m is possible. However, amplitude (V_{OUT3} and V_{OUT4}) and also additional amplitude and phase changes between V_{OUT1} and V_{OUT2} occur, see Fig. 6 for further information, where dynamical output vectors in polar plot are shown (arrows signalize trends of amplitude changes with increasing g_m from 100 μ S to 1 mS). Voltage V_{OUT1} has always constant value. Simultaneous control of both parameters ($g_m = 1/R_x$) is the best choice for the operation of proposed system. Figure 7 shows that V_{OUT2} keeps constant for $g_m = 1/R_x$ control of FO. Amplitudes of V_{OUT1} and V_{OUT2} are not equal but their ratio keeps invariant in process of tuning and levels are constant (dot at the end of line of the vectors). Unfortunately, V_{OUT3} and V_{OUT4} are still dependent on FO control.

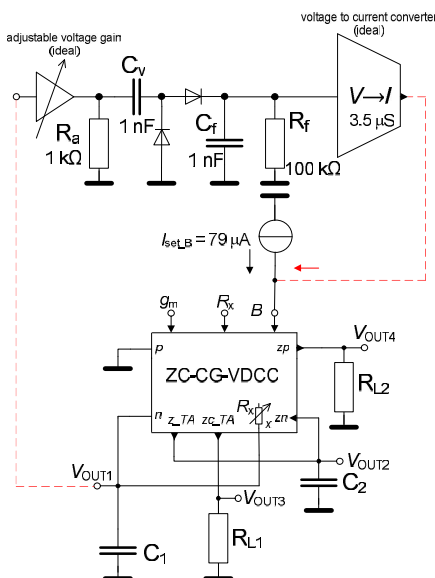


Fig. 4. Simulated oscillator circuit including automatic gain control circuit for amplitude stabilization.

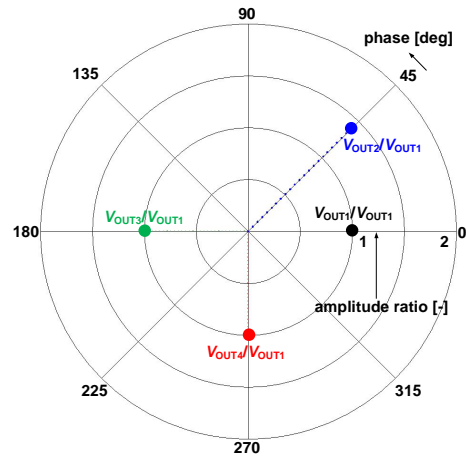


Fig. 5. Phase and amplitude relations between available outputs of ideal oscillator ($f_0 = 2.65$ MHz) in polar plot.

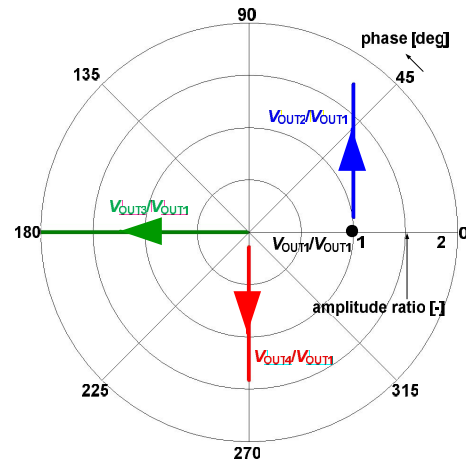


Fig. 6. Polar plot of output vector voltage relations for g_m and FO adjusting from 100 μ S to 1 mS (fixed $R_x = 2$ k Ω).

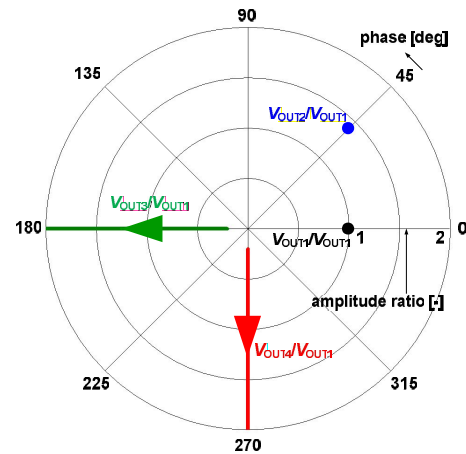


Fig. 7. Polar plot of output vector voltage relations for control of FO by $g_m = 1/R_x$ simultaneous adjusting from 100 μ S to 1 mS.

Value of FO, obtained from simulation, achieved 2.566 MHz. Simulation results are shown in Fig. 8, where transient responses for all four outputs are available. Simulated phase shifts were 44 degrees (V_{OUT1} - V_{OUT2}), 86 degrees (V_{OUT1} - V_{OUT4}), 181 degrees (V_{OUT1} - V_{OUT3}) and 139 degrees (V_{OUT2} - V_{OUT4}).

The FO control supposes simultaneous change of g_m and R_x . Theoretical range of FO control allows control in between 1.327 MHz–7.960 MHz ($g_m = 1/R_x = <0.25; 1.5>$ mS). Simulations provided adjusting from 1.331 MHz to 7.391 MHz. Corresponding results are in Fig. 9. Amplitudes

of V_{OUT3} and V_{OUT4} still changes in accordance to discussed theoretical relations (V_{OUT1} and V_{OUT2} are unchangeable if equality $g_m = 1/R_x$ is ensured).

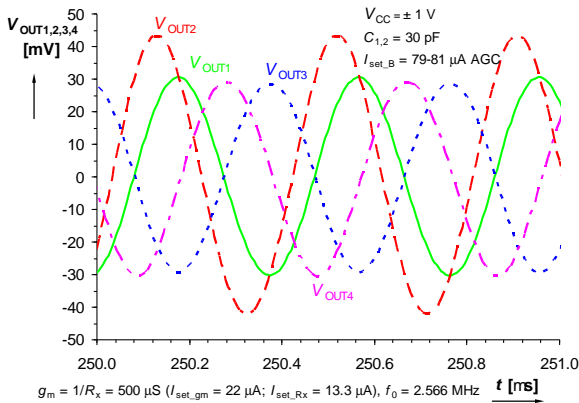


Fig. 8. Transient responses of all available outputs.

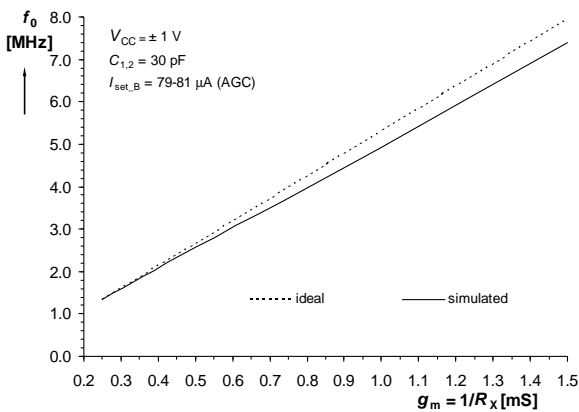


Fig. 9. Dependence of oscillation frequency on $g_m = 1/R_x$.

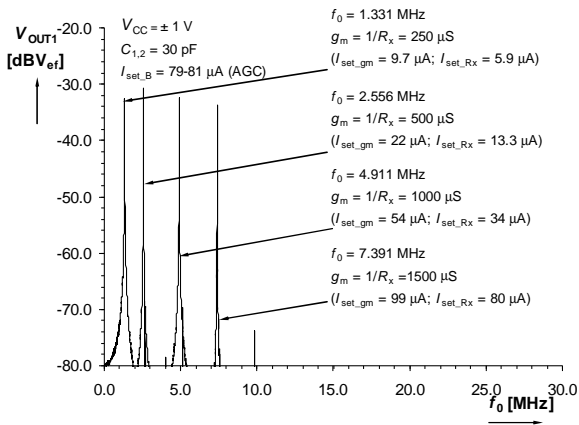


Fig. 10. Frequency spectrum of V_{OUT1} for selected oscillation frequencies.

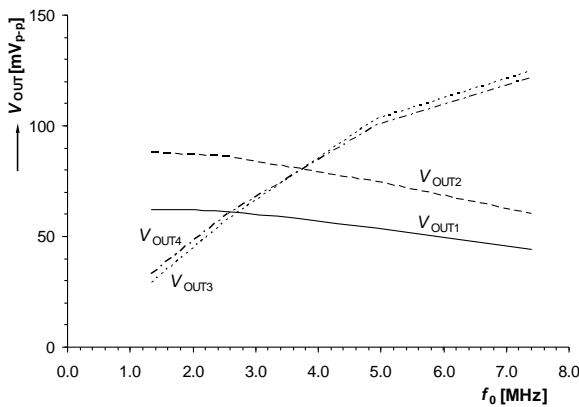


Fig. 11. Dependences of output levels on oscillation frequency.

Frequency spectrum of V_{OUT1} for four discrete frequencies is shown in Fig. 10. Figure 11 shows dependence of output levels on tuning process. It confirms theoretical relations (4)–(15). Total harmonic distortion (THD) results obtained at all available outputs are shown in Fig. 12 and reach 0.45 %–3.8 % (V_{OUT1} : 0.45 %–1.48 %; V_{OUT2} : 0.45 %–2.28 %; V_{OUT3} : 0.58 %–3.81 %; V_{OUT4} : 1.17 %–3.15 %) in whole range of oscillation frequency tuning. Last plot shows power consumption of the oscillator that has very slight dependence on tuning process (Fig. 13).

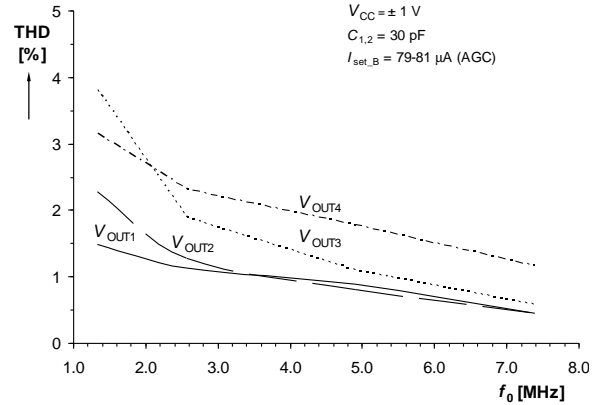


Fig. 12. Dependences of THD on oscillation frequency.

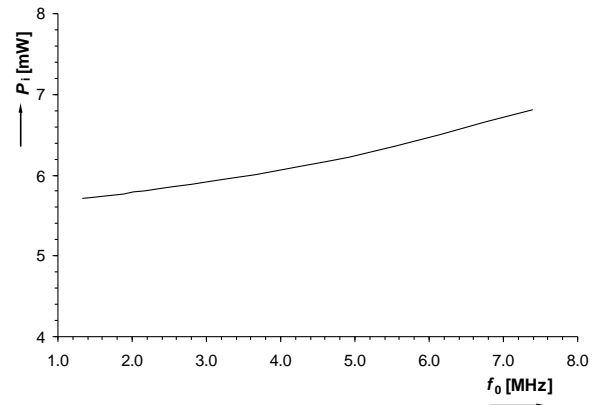


Fig. 13. Dependence of power consumption on oscillation frequency.

IV. CONCLUSIONS

The proposed simple second-order sinusoidal oscillator fulfils multiphase requirements (produces 45, 90, 135 and 180 degree phase shifts simultaneously) and can work also as the quadrature type. The matching of two parameters is required for linear electronic control of the oscillation frequency. Nevertheless, this matching is easily accessible by adjusting of both parameters (transconductance g_m and intrinsic resistance of the current input R_x). The third parameter (current gain B) controls the condition of oscillation. All parameters are controlled electronically. Verification of tuning was provided from 1.331 to 7.391 MHz.

REFERENCES

- [1] S. Minaei, O. K. Sayin, H. Kuntman, "A new CMOS electronically tunable current conveyor and its application to current-mode filters", *IEEE Trans. on Circuits and Systems - I*, vol. 53, no. 7, pp. 1448–1457, 2006.
- [2] A. Marcellis, G. Ferri, N. C. Guerrini, G. Scotti, V. Stornelli, A. Trifiletti, "The VGC-CCII: a novel building block and its application to capacitance multiplication", *Analog Integrated Circuits and Signal Processing*, vol. 58, no. 1, pp. 55–59, 2009. [Online].

- Available: <http://dx.doi.org/10.1007/s10470-008-9213-6>
- [3] M. Kumngern, S. Junnapiya, "A sinusoidal oscillator using translinear current conveyors", in *Proc. Asia Pacific Conf. on Circuits and Systems APPCAS2010*, Kuala Lumpur, 2010, pp. 740–743.
 - [4] D. Biolk, R. Senani, V. Biolkova, Z. Kolka, "Active elements for analog signal processing: classification, review and new proposals", *Radioengineering*, vol. 17, no. 4, pp. 15–32, 2008.
 - [5] A. U. Keskin, D. Biolk, E. Hancioglu, V. Biolkova, "Current-mode KHN filter employing Current Differencing Transconductance Amplifiers", *AEU – Int. Journal of Electronics and Communications*, vol. 60, no. 6, pp. 443–446, 2006. [Online]. Available: <http://dx.doi.org/10.1016/j.aue.2005.09.003>
 - [6] W. Jaikla, A. Lahiri, "Resistor-less current-mode four-phase quadrature oscillator using CCCDTAs and grounded capacitors", *AEU – Int. Journal of Electronics and Communications*, vol. 66, no. 3, pp. 214–218, 2012. [Online]. Available: <http://dx.doi.org/10.1016/j.aue.2011.07.001>
 - [7] Ch. Sakul, W. Jaikla, K. Dejhan, "New resistorless current-mode quadrature oscillators using 2 CCCDTAs and grounded capacitors", *Radioengineering*, vol. 20, no. 4, pp. 890–896, 2011.
 - [8] R. L. Geiger, E. Sanchez-Sinencio, "Active filter design using operational transconductance amplifiers: a tutorial", *IEEE Circ. and Devices Magazine*, vol. 1, pp. 20–32, 1985. [Online]. Available: <http://dx.doi.org/10.1109/MCD.1985.6311946>
 - [9] A. Fabre, O. Saaid, F. Wiest, C. Boucheron, "High frequency applications based on a new current controlled conveyor", *IEEE Trans. on Circuits and Systems - I*, vol. 43, no. 2, pp. 82–91, 1996.
 - [10] A. Sedra, K. C. Smith, "A second generation current conveyor and its applications", *IEEE Trans. Circuit Theory*, vol. CT-17, no. 2, pp. 132–134, 1970. [Online]. Available: <http://dx.doi.org/10.1109/TCT.1970.1083067>
 - [11] R. Prokop, V. Musil, "Modular approach to design of modern circuit blocks for current signal processing and new device CCTA", in *Proc. Conf. on Signal and Image Processing IASTED*, Anaheim, 2005, pp. 494–499.
 - [12] M. Siripruchyanun, W. Jaikla, "Current controlled current conveyor transconductance amplifier (CCCTA): a building block for analog signal processing", *Electrical Engineering Springer*, vol. 90, no. 6, pp. 443–453, 2008. [Online]. Available: <http://dx.doi.org/10.1007/s00202-007-0095-x>
 - [13] R. Sotner, J. Jerabek, R. Prokop, K. Vrba, "Current gain controlled CCTA and its application in quadrature oscillator and direct frequency modulator", *Radioengineering*, vol. 20, no. 1, pp. 317–326, 2011.
 - [14] A. Lahiri, M. Gupta, "Realizations of grounded negative capacitance using CFOAs", *Circuits, Systems and Signal Processing*, vol. 30, no. 1, pp. 134–155, 2011. [Online]. Available: <http://dx.doi.org/10.1007/s00034-010-9215-3>
 - [15] A. U. Keskin, C. Aydin, E. Hancioglu, C. Acar, "Quadrature oscillator using current differencing buffered amplifiers (CDBA)", *Frequenz* vol. 60, no. 3, pp. 21–23, 2006.
 - [16] B. Linares-Barranco, A. Rodriguez-Vazquez, E. Sanches-Sinencio, J. L. Huertas, "CMOS OTA-C high-frequency sinusoidal oscillators", *IEEE Journal of Solid-State Circuits*, vol. 26, no. 2, pp. 160–165, 1991. [Online]. Available: <http://dx.doi.org/10.1109/4.68133>
 - [17] Y. Tao, J. K. Fidler, "Electronically tunable dual-OTA second order sinusoidal oscillators/filters with non-interacting controls: A systematic synthesis approach", *IEEE Trans. on Circuits and Systems - I*, vol. 47, no. 2, pp. 117–129, 2000.
 - [18] Y. Li, "Electronically tunable current-mode quadrature oscillator using single MCDTA", *Radioengineering*, vol. 19, no. 4, pp. 667–671, 2010.
 - [19] R. Keawon, W. Jaikla, "A Resistor-less current-mode quadrature sinusoidal oscillator employing single CCCDTA and grounded capacitors", *Przegląd Elektrotechniczny*, vol. 87, no. 8, pp. 138–141, 2011.
 - [20] N. Pandey, S. K. Paul, "Single CDTA-based current mode all-pass filter and its applications", *Journal of Electrical and Computer Engineering*, vol. 2011, pp. 1–5, 2011.
 - [21] S. N. Songkla, W. Jaikla, "Realization of electronically tunable current-mode first-order allpass filter and its application", *Int. Journal of Electronics and Electrical Engineering*, vol. 2012, no. 6, pp. 40–43, 2012.
 - [22] S. Minaei, E. Yuce, "Novel voltage-mode all-pass filter based on using DVCCs", *Circuits Systems and Signal Processing*, vol. 29, no. 3, pp. 391–402, 2010. [Online]. Available: <http://dx.doi.org/10.1007/s00034-010-9150-3>
 - [23] N. Herencsar, J. Koton, K. Vrba, A. Lahiri, "New voltage-mode quadrature oscillator employing single DBTA and only grounded passive elements", *IEICE Electronics Express*, vol. 6, no. 24, pp. 1708–1714, 2009. [Online]. Available: <http://dx.doi.org/10.1587/elex.6.1708>
 - [24] J. W. Horng, "A sinusoidal oscillator using current-controlled current conveyors", *Int. Journal of Electronics*, vol. 88, no. 6, pp. 659–664, 2001. [Online]. Available: <http://dx.doi.org/10.1080/00207210110044369>
 - [25] A. Lahiri, "A. Novel voltage/current-mode quadrature oscillator using current differencing transconductance amplifier", *Analog Integrated Circuits and Signal Processing*, vol. 61, no. 2, pp. 199–203, 2009. [Online]. Available: <http://dx.doi.org/10.1007/s10470-009-9291-0>
 - [26] S. I. Liu, "Single-resistance-controlled/ voltage-controlled oscillator using current conveyors and grounded capacitors", *Electronics Letters*, vol. 31, no. 5, pp. 337–338, 1995. [Online]. Available: <http://dx.doi.org/10.1049/el:19950259>
 - [27] M. T. Abuelmaatti, M. H. Khan, "New electronically-tunable oscillator circuit using only two OTAs", *Active and Passive Electronic Components*, vol. 20, no. 4, pp. 189–194, 1998. [Online]. Available: <http://dx.doi.org/10.1155/1998/63168>
 - [28] S. Maheshwari, B. Chatuverdi, "High output impedance CMQOs using DVCCs and grounded components", *Int. Journal of Circuit Theory and Applications*, vol. 39, no. 4, pp. 427–435, 2011. [Online]. Available: <http://dx.doi.org/10.1002/cta.636>
 - [29] S-H. Tu, Y-S. Hwang, J-J. Chen, A. M. Soliman, C-M. Chang, "OTA-C arbitrary-phase-shift oscillators", *IEEE Trans. on Instrumentation and Measurement*, vol. 61, no. 8, pp. 2305–2319, 2012. [Online]. Available: <http://dx.doi.org/10.1109/TIM.2012.2184958>
 - [30] M. Kumngern, J. Chanwutium, K. Dejhan, "Electronically tunable multiphase sinusoidal oscillator using translinear current conveyors", *Analog Integrated Circuits and Signal Processing*, vol. 65, no. 2, pp. 327–334, 2010. [Online]. Available: <http://dx.doi.org/10.1007/s10470-010-9470-z>
 - [31] V. Biolkova, J. Bajer, D. Biolk, "Four-phase oscillator employing two active elements", *Radioengineering*, vol. 20, no. 1, pp. 334–339, 2011.
 - [32] N. Herencsar, S. Minaei, J. Koton, E. Yuce, K. Vrba, "New resistorless and electronically tunable realization of dual-output VM all-pass filter using VDIBA", *Analog Integrated Circuits and Signal Processing*, vol. 74, no. 1, pp. 141–154, 2013. [Online]. Available: <http://dx.doi.org/10.1007/s10470-012-9936-2>
 - [33] R. Sotner, N. Herencsar, J. Jerabek, J. Koton, T. Dostal, K. Vrba, "Electronically controlled oscillator with linear frequency adjusting for four-phase or differential quadrature output signal generation", *Int. Journal of Circuit Theory and Applications*, 2013. (in press) [Online]. Available: <http://dx.doi.org/10.1002/cta.1919>
 - [34] R. Sotner, Z. Hrubos, N. Herencsar, J. Jerabek, T. Dostal, "Precise electronically adjustable oscillator suitable for quadrature signal generation employing active elements with current and voltage gain control", *Circuits Systems and Signal Processing*, vol. 33, no. 1, pp. 1–35, 2014. [Online]. Available: <http://dx.doi.org/10.1007/s00034-013-9623-2>
 - [35] D. Prasad, D. R. Bhaskar, "Electronically controllable explicit current output sinusoidal oscillator employing single VDTA", *ISRN Electronics*, vol. 2012, pp. 1–5, 2012. [Online]. Available: <http://dx.doi.org/10.5402/2012/382560>
 - [36] N. Herencsar, R. Sotner, J. Koton, J. Misurec, K. Vrba, "New compact VM four-phase oscillator employing only single z-copy VDTA and all grounded passive elements", *Elektronika ir Elektrotechnika*, vol. 19, no. 10, pp. 87–90, 2013.
 - [37] R. Sotner, A. Lahiri, J. Jerabek, N. Herencsar, J. Koton, T. Dostal, K. Vrba, "Special type of three-phase oscillator using current gain control for amplitude stabilization", *Int. Journal of Physical Sciences*, vol. 7, no. 25, pp. 3089–3098, 2012.
 - [38] R. Sotner, J. Jerabek, N. Herencsar, "Voltage differencing buffered/inverted amplifiers and their applications for signal generation", *Radioengineering*, vol. 22, no. 2, pp. 490–504, 2013.
 - [39] R. Sotner, N. Herencsar, J. Jerabek, R. Prokop, A. Kartci, T. Dostal, K. Vrba, "Z-Copy controlled-gain voltage differencing current conveyor: Advanced possibilities in direct electronic control of first-order filter", *Elektronika ir Elektrotechnika*, vol. 20, no. 6, pp. 77–83, 2014.

[11] SOTNER, R., JERABEK, J., HERENC SAR, N., PETRZELA, J., VRBA, K., KINCL, Z. Linearly Tunable Quadrature Oscillator Derived from LC Colpitts Structure Using Voltage Differencing Transconductance Amplifier and Adjustable Current Amplifier. *Analog Integrated Circuits and Signal Processing*, 2014, vol. 81, no. 1, p. 121-136. ISSN: 0925-1030.

Linearly tunable quadrature oscillator derived from LC Colpitts structure using voltage differencing transconductance amplifier and adjustable current amplifier

Roman Sotner · Jan Jerabek · Norbert Herencsar ·
Jiri Petrzela · Kamil Vrba · Zdenek Kincl

Received: 19 February 2014/Revised: 13 May 2014/Accepted: 12 June 2014/Published online: 3 July 2014
© Springer Science+Business Media New York 2014

Abstract The paper deals with an interesting oscillator solution derived from LC Colpitts circuit structure. Electronically controllable current gain of the current amplifier is utilized for driving of oscillation condition together with two transconductances in frame of voltage differencing transconductance amplifier for adjusting of frequency of oscillation. In the proposed structure these elements replace common bipolar transistor and metal coil. Designed circuit offers important advantages, i.e. absence of metal coil, quadrature outputs, amplitudes of generated signals independent of tuning process, linear electronic control of oscillation frequency (independent of oscillation condition). Implementation of circuit for amplitude stabilization and automatic control of oscillation condition for designed circuit is simple. These benefits are not available in classical LC Colpitts structures or in many well-known third-order oscillators. The theoretical conclusions are supported by experiments with behavioral representation employing

commercially available devices and also by simulations using CMOS model.

Keywords Adjustable current amplifier · Voltage differencing transconductance amplifier · Quadrature oscillator · Electronic control · Third-order oscillator · Colpitts oscillator

1 Introduction

1.1 Brief review of adjustable possibilities in active circuits and motivation

It is well known that classical LC sinusoidal oscillators are important parts in analog and mixed-signal processing. However, these types require metal coil(s). Therefore, only complicated tuning is possible (external passive elements L and C value change) and this is the main drawback of such solutions, where electronic control is not directly and easily possible. Fortunately, there are many types of active elements that allow direct electronic control of some of its parameter(s) [1] and therefore are suitable for control of features of particular application. Frequently controlled parameters are current gain [1, 2–4], intrinsic resistance of current input [1, 5, 6] and transconductance [1, 7]. More than one parameter could be controlled in frame of one active device available in [2–7]. Advanced active elements with interesting and useful features were introduced for example in [8–12].

In this paper, our effort focuses on direct electronic control of parameters of the Colpitts LC circuit/oscillator [13]. Control of transconductance and current gain was used in resulting circuit and proposed oscillator. Thanks to the control features, the proposed oscillator has several

R. Sotner (✉) · J. Petrzela · Z. Kincl
Department of Radio Electronics, Brno University of
Technology, Technicka 3082/12, 616 00 Brno, Czech Republic
e-mail: sotner@feec.vutbr.cz

J. Petrzela
e-mail: petrzelj@feec.vutbr.cz

Z. Kincl
e-mail: kincl@feec.vutbr.cz

J. Jerabek · N. Herencsar · K. Vrba
Department of Telecommunications, Brno University of
Technology, Technicka 3082/12, 616 00 Brno, Czech Republic
e-mail: jerabekj@feec.vutbr.cz

N. Herencsar
e-mail: herencsn@feec.vutbr.cz

K. Vrba
e-mail: vrbak@feec.vutbr.cz

Table 1 Comparison of selected controllable third-order oscillators which generate quadrature outputs

Reference	Active elements	Number of passive elements	Fully independent CO and FO	Matching of parameters for independent CO and FO required	Linear electronic control of FO possible (yes, no, conditionally)	Linear electronic control of FO proved	Quadrature amplitude dependent on tuning process	Type of output signal (current, voltage or both available)
[16]	2, 4 OTA (Fig. 2a, e)	3, 4	No	Yes	Conditionally	No	N/A	Voltage
[17]	3 CDTA	3	No	Yes	Conditionally	No	N/A	Current
[18]	3 CDTA	3	Yes	No	Conditionally	No	N/A	Both
[19]	3 CCCII	3	Yes	No	Conditionally	No	N/A	Both
[20]	4 CCCII	3	Yes	No	No	No	N/A	Current
[21]	3 DVCC	6	Yes	No	Conditionally	No	N/A	Both
[22]	3 DVCC	6	No	Yes	Conditionally	No	N/A	Both
[23]	3 OTA	3	No	Yes	Conditionally	No	N/A	Voltage
[24]	1 DDCC, 2 OTA	4	Yes	No	No	No	N/A	Voltage
[25]	2 CCII	6	Yes	No	No	No	N/A	Both
[26]	1 CCCDTA, 1 OTA	3	Yes	No	Conditionally	No	N/A	Both
[27]	2 CCII, 1 UVC	6	Yes	No	No	No	N/A	Both
Proposed	1 CA, 1 VDTA (2 OTA)	3 + R_1	Yes	No	Yes	Yes	No	Voltage

Abbreviations: CA current amplifier, CCII current conveyor of second generation, CCIII current controlled current conveyor of second generation, CCCDTA current controlled current differencing transconductance amplifier, CDTA current differencing transconductance amplifier, DDCC differential difference current conveyor, DVCC differential voltage current conveyor, OTA operational transconductance amplifier, UVC universal voltage conveyor, VDTA voltage differencing transconductance amplifier

favorable features in comparison with standard LC solution and also in comparison with some other adjustable third-order oscillators.

1.2 Comparison of important third-order oscillators

It is not easy to compare structures based on different design approaches. Nevertheless, important third-order oscillators producing signals with quadrature phase shift are qualitatively compared in the following text. Unfortunately, some of third-order circuits do not allow control of parameters and deeper analysis is also not given (for example in [14, 15]) and evaluation of phase shifts is not possible. Similarly in [16], where two realizations of third- and fourth-order circuit were introduced, their condition of oscillation (CO) and frequency of oscillation (FO) are electronically controllable by transconductances (g_m). However, CO and FO are controllable independently only if a problematic condition (CO: $g_{m1} = g_{m2}$) is fulfilled. Since $FO^2 = g_{m1}g_{m2}/(C_1C_2)$, controllability is difficult in real solution. Fully independent CO and FO means that parameter(s) controlling FO are not present in CO and vice versa.

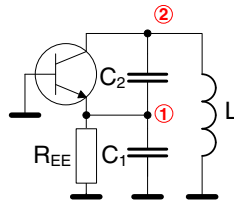
Table 1 compares discussed solutions available in [16–27] clearly. We can give a summarization of the following

drawbacks, which are present in known third-order circuits, as follows:

- mutual dependence of FO and CO [16, 17, 22, 23];
- nonlinear control of FO [17–27];
- not proved independence of one generated amplitude on tuning process [16–27];
- too many active elements [16, 20];
- too many passive elements [21, 22, 25, 27].

Presented research is a significant extension of the study briefly given in [28]. Our solution of third-order oscillator has quadrature outputs with amplitudes independent of the tuning process and linear control of FO. Quadrature oscillators operating at RF bands and generating unchangeable output signals are mainly determined for applications in modern digital multi-state modulations and demodulations (quadrature phase shift keying—QPSK for example) as source of carrier signal (coherent cosine and sine wave components) in many communication systems. All above discussed circuits employ grounded capacitors. One floating capacitor in the structure is a drawback which is characteristic also for standard Colpitts structure that was used for synthesis of this oscillator. Nevertheless, in comparison to all discussed circuits, important benefits of our structure overcome this drawback. The following text

Fig. 1 Adapted LC Colpitts circuit based on idea presented in [13]



is divided as follows: chapter 2 presents an idea used to obtain proposed circuit; design of fully controllable oscillator with synthetic inductor is discussed in chapter 3; real behavior considering main parasitic influences is commented in Sect. 4; experimental results of measurements with behavioral models utilizing commercially available devices are evaluated in Sect. 5; CMOS-based structure is introduced in Sect. 6 together with simulation results and study of parameters dispersion and uncertainty and concluding remarks are given in Sect. 7.

2 Classical LC Colpitts circuit and its enhancements

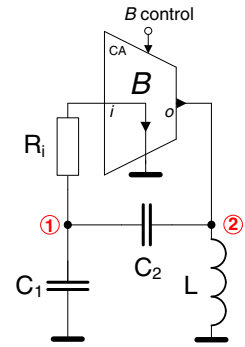
Classical Colpitts oscillator [29] uses metal coil and its tunability is possible due to values of passive elements (LC). Therefore, direct electronic control of FO and CO is not easily possible. Common active element used in such oscillator is bipolar transistor. It is not promising element from the point of view of direct electronic control of final application. Hence motivation of our work is to focus on extension of Colpitts circuit to electronically controllable system where parameters of active elements serve for FO and CO control. Several suitable modifications of bipolar-transistor-based Colpitts circuit were presented in the past. One of them is a model discussed by Kennedy [13] that attracts our attention because connection of bipolar transistor to the LC circuit is quite unique. The circuit model presented in [13] can be simplified and adapted to structure shown in Fig. 1.

In common base configuration of bipolar transistor, current transfer between emitter and collector is given by its current gain (β , h_{21e} , h_{FE}) and is equal to 1 for very high β [30] ($\beta = i_{collector}/i_{base}$). Therefore, we can replace bipolar transistor in Fig. 1 by simple current follower (emitter of a bipolar transistor serves as low-impedance input and collector as high-impedance output). Analysis of the circuit provided the following characteristic equation:

$$s^3 + \frac{C_1 + C_2}{LC_1C_2}s + \frac{1}{R_iLC_1C_2} = 0, \tag{1}$$

where R_i is an input resistance of real current follower. Unfortunately, Eq. (1) does not represent characteristic equation of the oscillator. However, we can set the current transfer between input and output of the current follower as

Fig. 2 Modification of the oscillator employing controlled current amplifier



general variable and repeat the analysis. Characteristic equation is now in form:

$$s^3 + \left(\frac{1-B}{R_iC_1}\right)s^2 + \frac{C_1 + C_2}{LC_1C_2}s + \frac{1}{R_iLC_1C_2} = 0, \tag{2}$$

where B is generally controllable current transfer (gain/loss). As we can see in (2), proper value of B can bring this circuit (Fig. 2) to boundary of stability (oscillation), R_i is now input resistance of the adjustable current amplifier (CA).

Characteristic Eq. (2) of the oscillator in Fig. 2 has very favorable CO:

$$B = 1 - \frac{C_1}{C_1 + C_2}. \tag{3}$$

Design requirements of similar types of oscillators suppose equal values of both capacitors. We can also use this simplification ($C_1 = C_2 = C$) and (3) reduces to very simple form: $B = 0.5$, which is the only theoretical requirement for sufficient gain to fulfill CO. The FO of the oscillator (Fig. 2) has a typical form for LC oscillators:

$$\omega_0 = \frac{1}{\sqrt{LC}} \sqrt{2}. \tag{4}$$

3 Design of fully electronically controllable oscillator and analysis of its theoretical features

The oscillator obtained in the previous chapter has independently controllable CO and FO, but FO is not controllable electronically. Metal wire inductor is not a very popular component due to its dimension, weight and dependence on mechanical influences (vibration, change of the shape, change of coil distance, etc.). Classical inductor is not suitable for fulfilling our goal of fully electronically controllable oscillator due to impossibility of electronic control of its inductance. Obvious way how to create electronically controllable oscillator from basic circuit in Fig. 2 supposes utilization of a synthetic inductance equivalent. We selected popular and known method for creation of the synthetic inductor [7], where two OTAs [1, 7] and grounded capacitor are used. Two OTA subsections of the voltage differencing

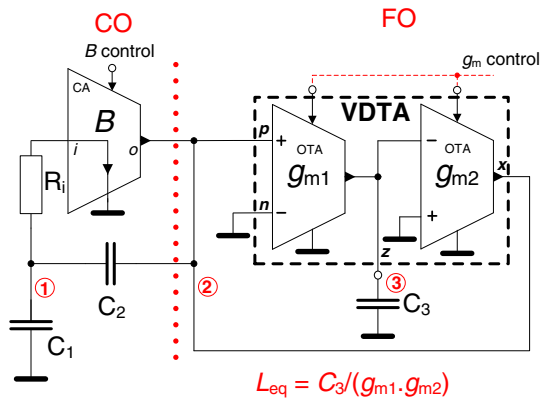


Fig. 3 Modification of the oscillator employing synthetic inductor—final electronically controllable oscillator

transconductance amplifier (VDTA) [31–36] were used for these purposes. Resulting circuit with synthetic inductance simulator is presented in Fig. 3. Inductance replacement brings one or two additional active elements—it depends on VDTA understanding as one device or two OTAs. Nevertheless, we obtained additional node 3, which is very useful as will be discussed later. Equation for FO has now very favorable form:

$$\omega_0 = \frac{1}{\sqrt{\left(\frac{C_1 C_2}{C_1 + C_2}\right) \frac{C_3}{g_{m1} g_{m2}}} \tag{5}$$

Supposing equality of all capacitors ($C_1 = C_2 = C_3 = C$) and both transconductances ($g_{m1} = g_{m2} = g_m$) yields simplification of (5) to form:

$$\omega_0 = \frac{g_m}{C} \sqrt{2} \tag{6}$$

Classical Colpitts circuits (with bipolar transistor) are intended for single-phase generation. Additional node 3 (Fig. 3) is useful for quadrature generation. The relation between nodal voltages V_2 and V_3 has a form:

$$\frac{V_3}{V_2} = \frac{g_{m1}}{s C_3} \tag{7}$$

where substitution of $s = j\omega_0$ gives:

$$\frac{V_3}{V_2} = \frac{1}{j} \sqrt{\left(\frac{C_1 C_2}{C_1 + C_2}\right) \frac{1}{C_3}} \frac{g_{m1}}{g_{m2}} \tag{8}$$

Supposing above noted equality of values of capacitors and transconductances ($C_1 = C_2 = C_3 = C$ and $g_{m1} = g_{m2}$), Eq. (8) reduces to numerical relation between amplitudes and phases:

$$\frac{V_3}{V_2} = \frac{\sqrt{2}}{2} \exp\left(\frac{\pi}{2}j\right) \tag{9}$$

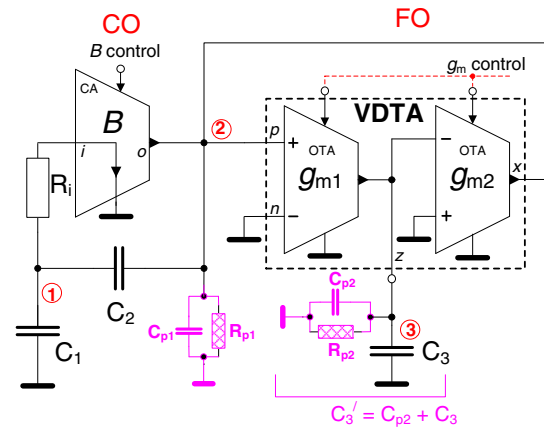


Fig. 4 Model of the circuit for non-ideal analysis

The relation expressed in (9) proves that phase shift between both produced signals is 90° and amplitudes are constant during the tuning process (independent of FO) with constant level difference $\sqrt{2}/2$.

Relation between V_1 and V_2 is given by:

$$\frac{V_1}{V_2} = \frac{s C_2 R_i}{1 + s(C_1 + C_2)R_i} \tag{10}$$

The same kind of simplification leads to:

$$\frac{V_1}{V_2} = \sqrt{\frac{(g_m R_i \sqrt{2})^2}{1 + (g_m R_i 2 \sqrt{2})^2}} \exp\left[\tan^{-1}\left(\frac{1}{g_m R_i 2 \sqrt{2}}\right)j\right] \tag{11}$$

Resulting Eq. (11) can be explained in detail as follows. Amplitude of V_1 reaches approximately 1/2 of V_2 for product $g_m R_i = 1$ and higher values. Steady state oscillation level of V_1 decreases significantly for product $g_m R_i < 1$. Fortunately, high $g_m R_i$ ensures almost constant level of V_1 also in case of tuning. Unfortunately, the node 1 (V_1) is not suitable as output of the multiphase oscillator because phase shift between it and V_2 and therefore also between it and V_3 changes if FO is tuned.

Nodes 2 and 3 are useful to obtain quadrature phase shift with constant amplitude level (9) during the tuning process. In addition, Eqs. (5) and (6) show that linear control of FO is available by $g_{m1} = g_{m2}$. None of these features are available in case of classical Colpitts circuits.

4 Brief study of expected real influences on behavior

This chapter discusses possible problems caused by real influences of parasitic features and inaccuracies of used active elements, considered model of the circuit is shown in Fig. 4, where $C_{p1} = C_{o_CA} + C_{p_VDTA} + C_{x_VDTA}$,

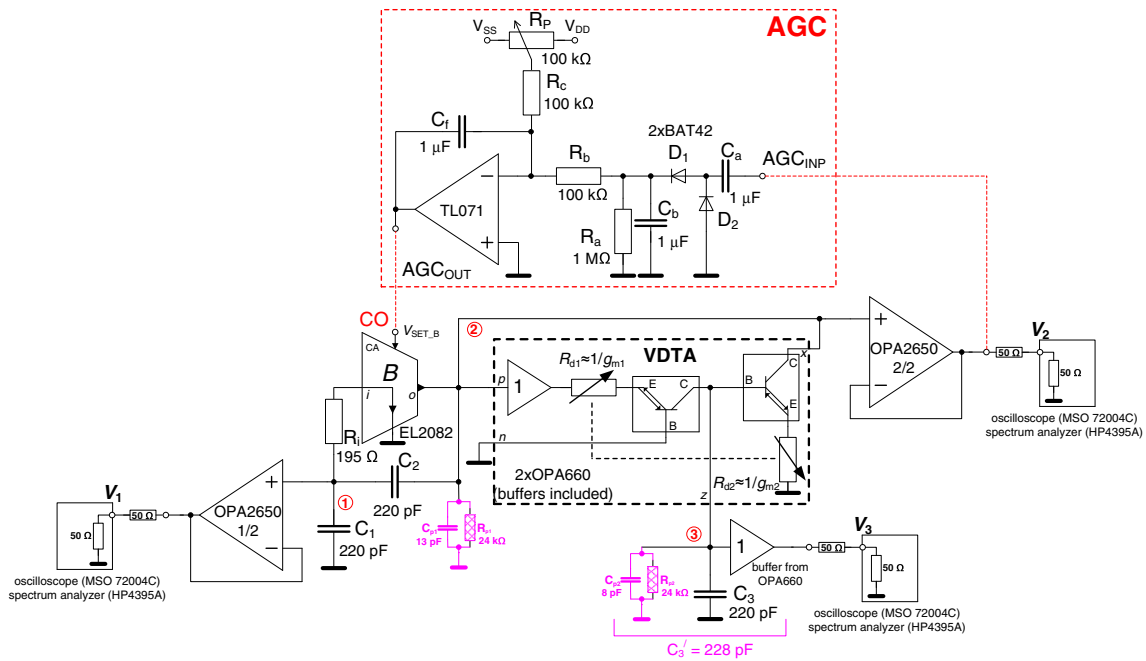


Fig. 5 Measured behavioral model of the complete oscillator

$$R_{p1} = R_{o_CA} \parallel R_{p_VDTA} \parallel R_{x_VDTA}, C_{p2} = C_{z_VDTA} \text{ and } R_{p2} = R_{z_VDTA}.$$

We provide two calculations of expected FO:

- (a) analysis including only parasitic capacitances in high-impedance nodes caused by terminals of active elements:

$$\omega_0' = \sqrt{\frac{g_{m1}g_{m2}(C_1 + C_2)}{C_2C_3C_{p1} + C_1C_3C_{p1} + C_1C_2C_3}} \tag{12}$$

- (b) analysis including all terminal resistances and capacitances of active devices in high-impedance nodes:

$$\omega_0'' = \sqrt{\frac{g_{m1}g_{m2}R_iR_{p1}R_{p2}(C_1 + C_2) + C_2(R_i + R_{p1} + BR_{p1}) + C_1R_i + C_{p1}R_{p1} + C_3R_{p2}}{R_iR_{p1}R_{p2}(C_2C_3C_{p1} + C_1C_3C_{p1} + C_1C_2C_3)}} \tag{13}$$

Parasitic capacitances C_{p1} , C_{p2} and also inequality of $g_{m1} \neq g_{m2}$ have the most significant impact on FO. This inequality depends mainly on accuracy of simultaneous control of both parameters and also manufacturing accuracy of VDTA. Symbol C_3' represents a result of parallel

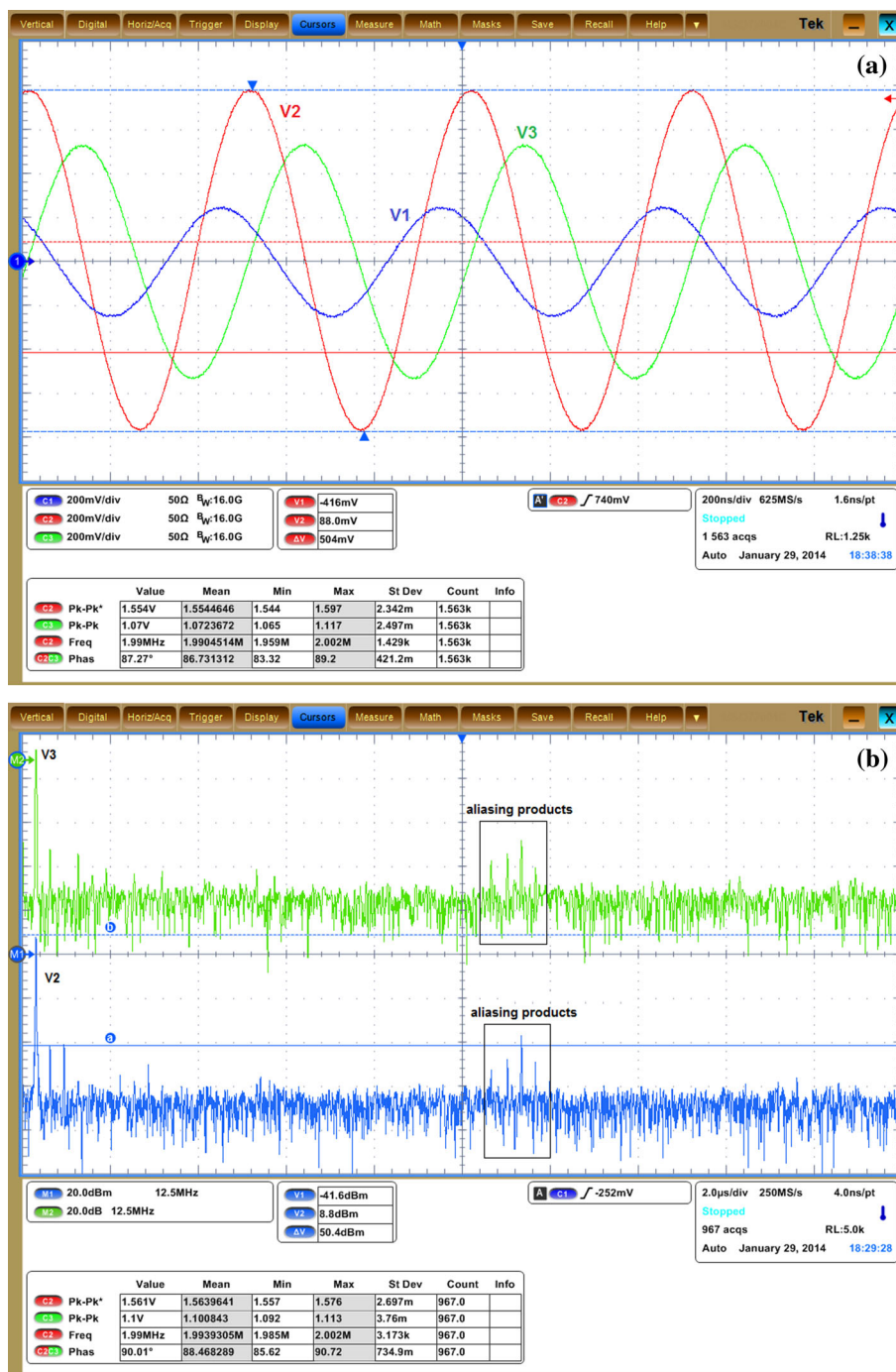
connection of working and parasitic capacitance. These impacts are discussed in more detail in the following chapter.

5 Measurement results with behavioral model employing commercially available devices

Figure 5 includes complete measured circuit of the oscillator based on commercially available devices. We implemented well-known current-mode multiplier EL2082 [37] as adjustable current amplifier (B) and two diamond transistors (OPA660 [38]) to build VDTA. The automatic amplitude gain control circuit (AGC) was created from opamp TL071. Two high-speed opamps OPA2650 [39] and additional high-speed buffer included in OPA660 package were used as supplementary output voltage buffers. Low-

impedance outputs were matched to 50 Ω . Values of passive elements are selected as: $C_1 = C_2 = C_3 = 220$ pF, $R_i = 100 + 95$ Ω (including internal parasitic resistance [37]). Transconductances (g_{m1} , g_{m2}) of the VDTA subsections were adjusted from 0.24 to 8.85 mS.

Fig. 6 Analysis of the oscillator: **a** transient responses, **b** FFT spectrum of V_2 (lower) and V_3 (upper)



Recommended supply voltage is ± 5 V. The rest of parameters is included in Fig. 5.

The AGC circuit provides DC voltage V_{SET_B} derived from output level at node 2 controlling the current gain of the CA (EL2082 has voltage controllable current gain [37]). This voltage V_{SET_B} is approximately equal to current gain B , see [37]. In comparison with transient simulations in [28], real oscillator operates with large time constants ($C_a = C_b = C_f = 1 \mu\text{F}$) for perfect peak

detection and stabilization of amplitude without high amplitude fluctuations. Start of correct operation of AGC requires precise setting of reference voltage from voltage regulator R_p .

We used Tektronix MSO 72004C oscilloscope and HP4395A spectrum analyzer for experimental analyses of the circuit from Fig. 5. As an example, resulting transient responses for $g_{m1,2} = 2.08 \text{ mS}$ are shown in Fig. 6(a). FFT analysis of the output voltages V_2 and V_3 are shown in

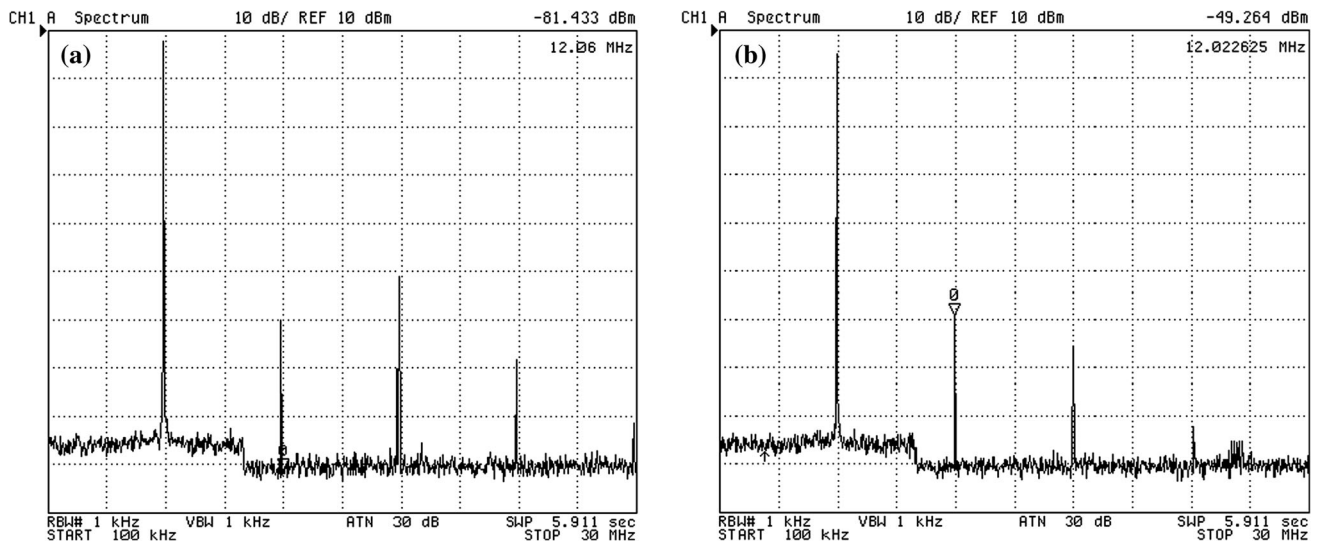


Fig. 7 Spectral analysis obtained by HP4395A ($f_0 = 6.06$ MHz) for voltage: a V_2 , b V_3

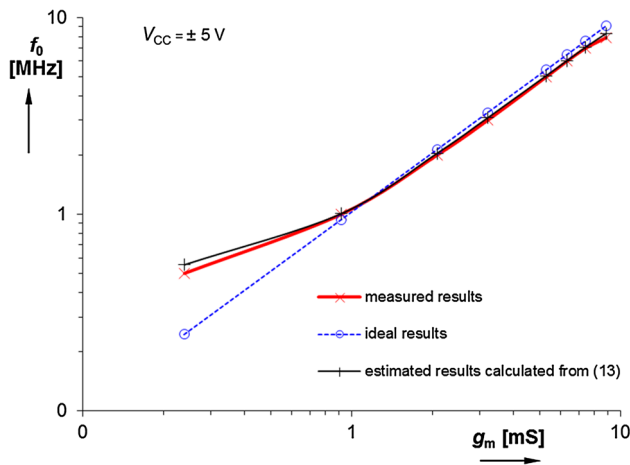


Fig. 8 Dependence of measured, expected/estimated and ideal oscillation frequency on g_m ($g_{m1} = g_{m2} = g_m$)

Fig. 6(b). Oscillation frequency for these values achieved 1.99 MHz. The results from spectrum analyzer provide better resolution in magnitude than digital oscilloscope with limited bit resolution of A/D converter, see Fig. 7 (both useful outputs V_2 and V_3) for another FO example ($f_0 = 6.06$ MHz) obtained by $g_{m1,2} = 6.33$ mS.

Electronic tuning of the oscillator is documented in Fig. 8, where dependence of FO on simultaneous change of $g_{m1,2}$ is shown and compared with ideal and expected trace [calculated from Eq. (13)]. Ideal range of FO control was calculated from 0.245 to 9.06 MHz (for ideally equal capacitors and g_m) for $g_{m1,2}$ adjusted from 0.24 to 8.85 mS. Simple estimation by Eq. (12) yields range from 0.237 to 8.164 MHz and complex estimation with help of (13) gives range from 0.553 to 8.306 MHz. Experimental results of FO are in range between 0.5 and 7.91 MHz.

Difference between expected calculations (12) and (13), considering real parasitic influences, is minimal at frequencies above 1 MHz. However, simpler expression (12) does not represent slope break of the measured trace at low frequencies. Complex non-ideal analysis result (13) models also significant change of the slope. Dependence of the oscillation frequency on $g_{m1,2}$ is almost linear in measured and expected range approximately from 1 MHz to 8 MHz. Analysis shows that the most important impact on FO accuracy has C_{p1} , C_{p2} and disrupted equality $g_{m1} = g_{m2}$ mainly for very high g_m values (see the point at the highest frequency in Fig. 8). An explanation is simple. Transconductance of the diamond transistor (used as subparts of VDTA) is controlled by external so-called degradation resistor (R_d , see Fig. 5). Very low values of R_d comparable to internal emitter resistance $R_E \cong 8\text{--}13 \Omega$ [38] cause inaccuracy (R_E has to be taken into account). In addition, supplementary influence is caused by output resistance of voltage buffer (approximately 7Ω) inside IC package of diamond transistor. At low values of g_m , mainly g_{m2} has slightly higher value than g_{m1} , where problem with additional resistance of buffer output occurs. Importance of this influence increases for increasing g_m value (decreasing R_d). Value of R_{p1} and C_{p1} are determined by output impedance of the CA (EL2082) approximately $1 \text{ M}\Omega/6 \text{ pF}$ [37], input of the buffer in frame of VDTA ($\text{M}\Omega/2 \text{ pF}$ [38]), output (current output of the diamond transistor) of the VDTA ($25\text{--}50 \text{ k}\Omega/4 \text{ pF}$, we considered always the worst case - i.e. $25 \text{ k}\Omega$) and input of the separation buffer created by OPA2650 ($16 \text{ M}\Omega/1 \text{ pF}$ [39]). Overall estimated parasitic value of R_{p1} and C_{p1} is $24 \text{ k}\Omega/13 \text{ pF}$. Values of R_{p2} and C_{p2} are created by output of the diamond transistor in frame of the VDTA ($25\text{--}50 \text{ k}\Omega/4 \text{ pF}$), input of the diamond transistor in frame of the VDTA ($1 \text{ M}\Omega/ 2 \text{ pF}$) and internal

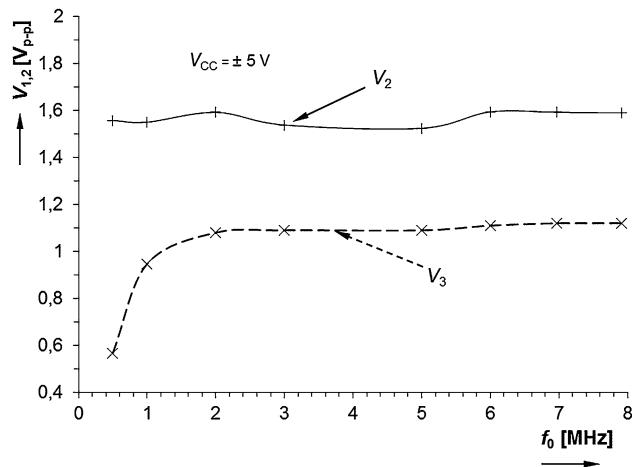


Fig. 9 Dependence of measured output levels V_2 and V_3 on FO tuning

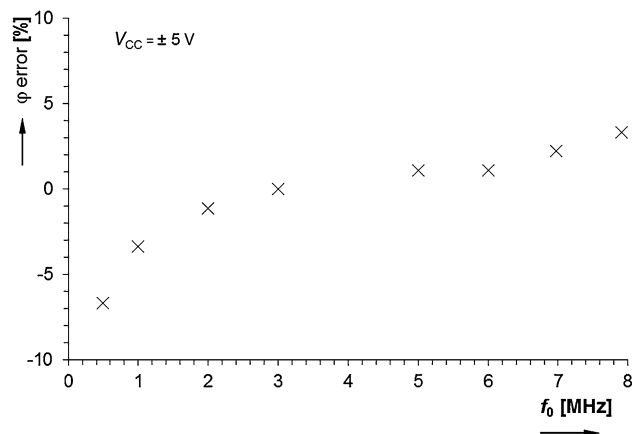


Fig. 10 Dependence of measured phase error of quadrature outputs V_2 and V_3 on FO tuning

voltage buffer of the OPA660 for output separation. Values of R_{p2} and C_{p2} are estimated as 24 k Ω /8 pF. Input capacitance (1 pF) of used separation buffer of V_1 voltage at node 1 has very small impact in comparison to the rest of above discussed problems (resistance is 16 M Ω [39]). Due to minimal influence it can be omitted in analysis.

There is a question about B occurring in (13). Does B change have significant impact on FO accuracy? Change of the B value in really extreme and practically unreal range from 0.1 to 0.9 at fixed f_0 (units of MHz) causes dispersion about units of kHz. Fortunately, around fixed FO, fluctuations of B (caused by AGC response) are many times lower and therefore insignificant. The same testing range of B was used at frequencies of hundreds of kHz, where this impact is significantly higher (dispersion of tens of kHz). However, AGC system operating at stable and

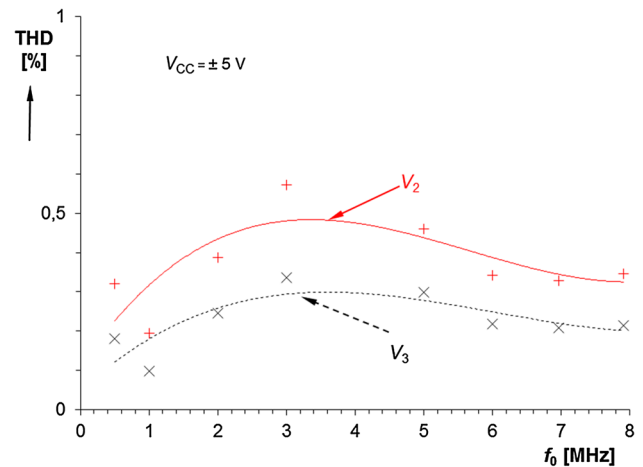


Fig. 11 Measured dependence of THD on FO tuning

fixed f_0 does not evoke so significant change (0.1–0.9) of B , where CO is not practically fulfilled or output levels reach saturation corners of active elements for substantial part of discussed changes. In conclusion we can state that fluctuations of B may influence the lowest frequencies (the lowest corner of the tuning range) but only for high variation of driving DC voltage from AGC (incorrectly selected time constant of AGC for example). Note that this discussion is not related with results in Fig. 12, where FO is intentionally changed in wide range to see AGC response.

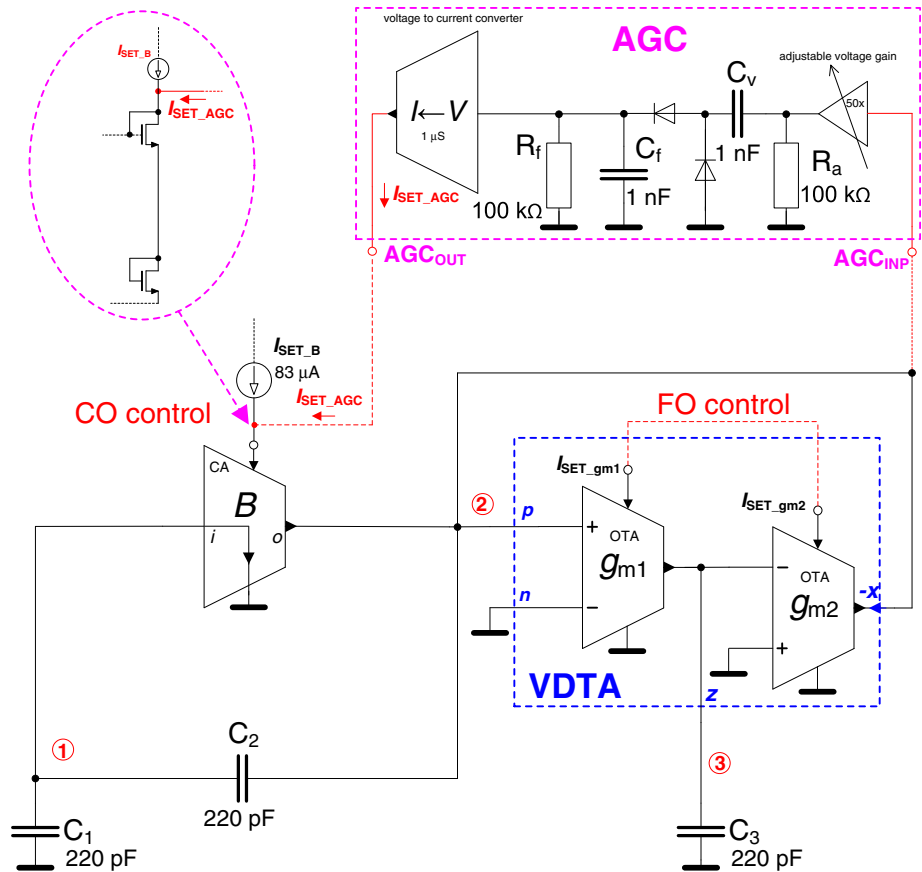
Dependence of the output signal levels of V_2 and V_3 (useful outputs with quadrature phase shift) on FO is given in Fig. 9. When FO above 1 MHz is considered, fluctuations of the output levels are very small (± 34 mV for V_2 and ± 85 mV for V_3).

An accuracy of the quadrature phase shift between V_2 and V_3 during the tuning process was experimentally verified, see Fig. 10. Phase error about ± 3 % in FO range from 1 to 8 MHz was obtained.

Total harmonic distortion (THD) is also very important parameter. We recorded and calculated this parameter from magnitude distance of spectral components (for V_2 and V_3), where magnitude distance of fundamental harmonic component and higher spectral components was about 50 dB and higher. The results calculated from measurement on spectrum analyzer HP4395A are in Fig. 11. THD achieves values lower than 0.5 % in whole range of FO control.

Automatic control of CO provided by the AGC system (shown in Fig. 5) is really necessary. In practice, it is not possible to operate with fixed gain $B = 0.5$ as we derived from ideal condition (3). Tuning of the FO by $g_{m1,2}$ causes gain changes in the loop. These changes have to be compensated. Discontinuation of oscillation, high THD or even saturation of generated signals to supply corners is possible

Fig. 12 Solution of the oscillator based on CA and VDTA suitable for CMOS implementation



when operated without precise auto-compensating AGC systems. This problem is discussed in [12] in detail in case of different circuit structure. Nevertheless, the conclusion of the analysis is similar also for circuit shown in this paper.

6 Possible CMOS implementation

We proposed CMOS solution (Fig. 13) based on utilization of block of adjustable current amplifier (CA) and VDTA (where two OTA subsections are controlled separately as is known from elementary principle of this device [1, 32]) two simple in the complete oscillator. Solution was verified by simulations with Spice models of subblocks based on TSMC LO EPI 0.18 μm technology [40]. Connection of the AGC system to bias control of the CA is shown in detail in Fig. 12 too.

Basic building elements of the proposed circuit (CA or VDTA) or their subblocks eventually are transconductors [1, 7]. Their internal structure is well-known, see Fig. 13(a), where designed aspect ratio of all transistors is also included. We used standard OTA-based subblocks in frame of VDTA due to their possibility of g_m range

extension (to increase FO range) by current mirror gain in comparison with standard Arbel-Goldminz cells that are usually implemented in VDTA element [31], [32]. Transconductance of the OTA in Fig. 13(a) is given by equation:

$$g_m = 2 \sqrt{I_{SET_gm} K_{Pn} \frac{W_{M1,2}}{L_{M1,2}}}, \tag{14}$$

where multiplication by 2 is given by fixed gain of the current mirrors M_4, M_5 and M_3, M_6 . Control of the g_m was tested in range from 0.25 to 2 mS by DC bias current I_{SET_gm} between 10 and 162 μA.

CMOS structure of the adjustable current amplifier is presented in Fig. 13(b). Basic idea of this topology was published in [41]. Our modification consists of adding of input current conveyor section in order to operate with signal of both polarities without DC offset [12]. Input resistance R_i is given by:

$$R_i = \frac{1}{\sqrt{I_{b1} K_{Pn} \frac{W_{M1}}{L_{M1}}} + \sqrt{I_{b1} K_{Pp} \frac{W_{M2}}{L_{M2}}}}. \tag{15}$$

Small-signal value of R_i obtained from simulation is 533 Ω for $I_{b1} = 100 \mu A$. Current gain B of the amplifier is adjusted by DC bias current I_{SET_B} (see Fig. 13b) in accordance with the following equation [41]:

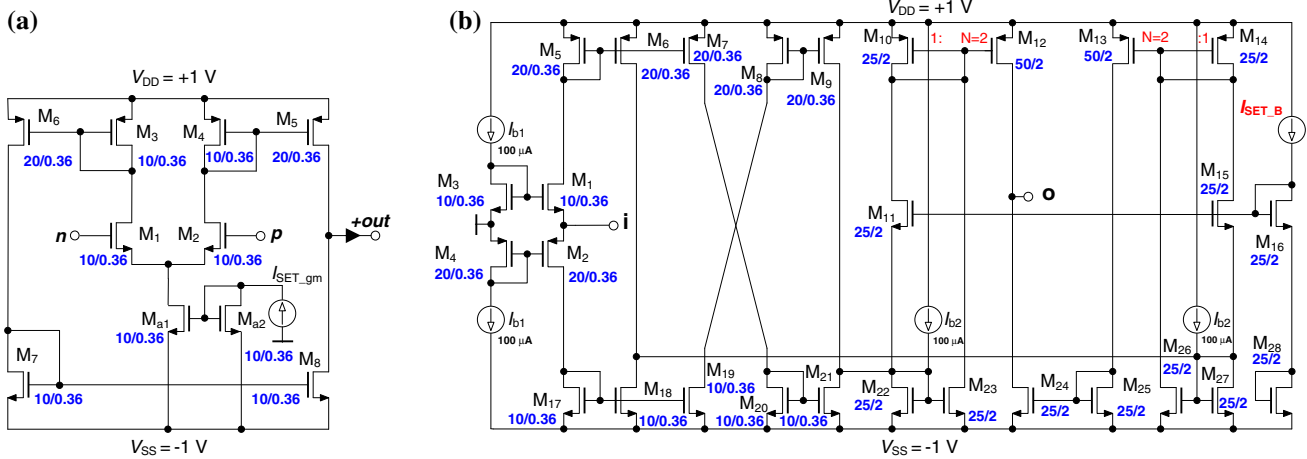


Fig. 13 Possible internal CMOS structures of active elements or their sub-blocks: **a** transconductor, **b** current amplifier

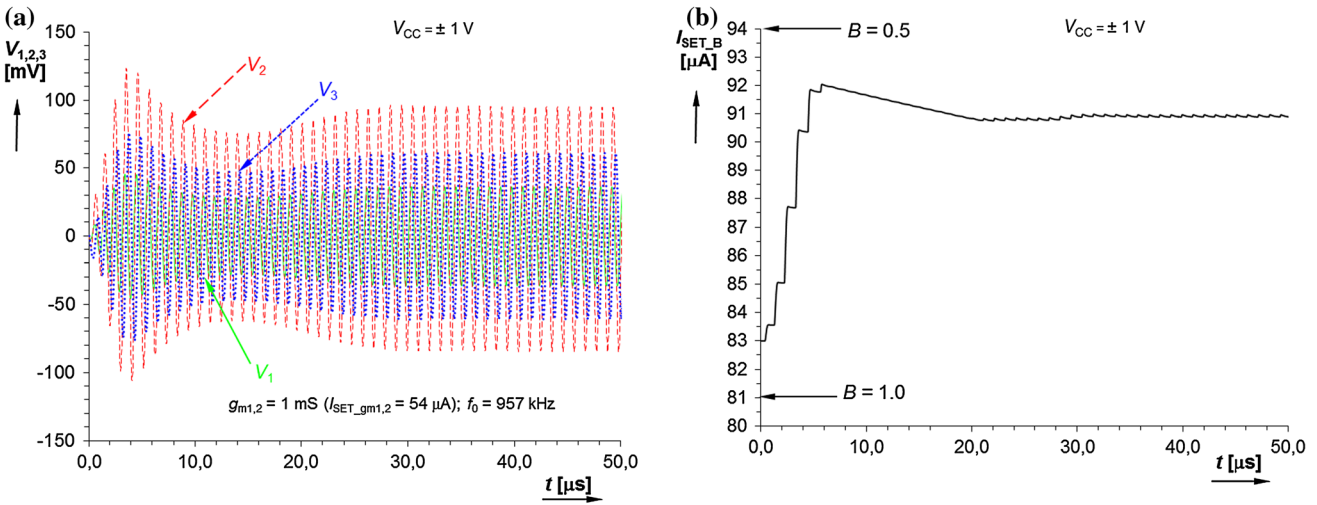


Fig. 14 Startup of the oscillations: **a** transient response, **b** AGC response

$$B = \frac{NI_{b2}}{2I_{set_B}} \cong \frac{I_{b2}}{I_{set_B}}, \tag{16}$$

where N is internal gain of current mirrors, in our case $N = 2$ (Fig. 13b). Simulations showed that adjustable range of B is approximately from 0.4 to 4 by DC control current I_{SET_B} adjusted from 100 to 9.9 μA . Technological constants K_{Pn} , K_{Pp} are given by used technology (TSMC 0.18 μm [40] in our case), and are $K_{Pn} = 170.4 \mu\text{A}/\text{V}^2$ and $K_{Pp} = 35.7 \mu\text{A}/\text{V}^2$.

Circuit shown in Fig. 12 with CMOS structures and models from Fig. 13 was simulated in Spice software. AC coupling was used to remove small additional DC offset of the active devices (several mV). Parameters of the design are following: $C_1 = C_2 = C = 220 \text{ pF}$, $R_i = 533 \Omega$, initial $I_{SET_B} = 83 \mu\text{A}$ ($B \approx 0.85$) and DC supply voltage $\pm 1 \text{ V}$. Initial setting of the oscillator was given by: $g_{m1} = g_{m2} = g_m = 1 \text{ mS}$ ($I_{SET_gm1,2} = 54 \mu\text{A}$). Startup of

the oscillation at all three nodes (V_1, V_2, V_3) is presented in Fig. 14(a) together with initial response of the ideal AGC system (Fig. 14b). Oscillation frequency had value $f_0 = 0.957 \text{ MHz}$. Figure 15 shows steady state transient responses for two discrete oscillation frequencies (0.957 and 1.982 MHz for $g_{m1,2} = 1$ and 2 mS). Dependence of phase distance of V_1 and both other signals (V_2 and V_3) on FO is evident, as was already discussed in chapter 3.

Test of tunability for three selected discrete frequencies (0.482, 0.957, and 1.982 MHz; $g_{m1,2} = 0.5, 1$ and 2 mS) and only for useful nodes (2, 3) is provided in Fig. 16. Results in frequency domain (FFT) for these three g_m values are shown in Fig. 17. Transconductance control of the CMOS VDTA between 0.25 and 2 mS allows FO tuning in range from 0.256 to 2.047 MHz theoretically. Simulations yield range from 0.277 to 1.982 MHz (Fig. 18). The limit of g_m and therefore also of FO on

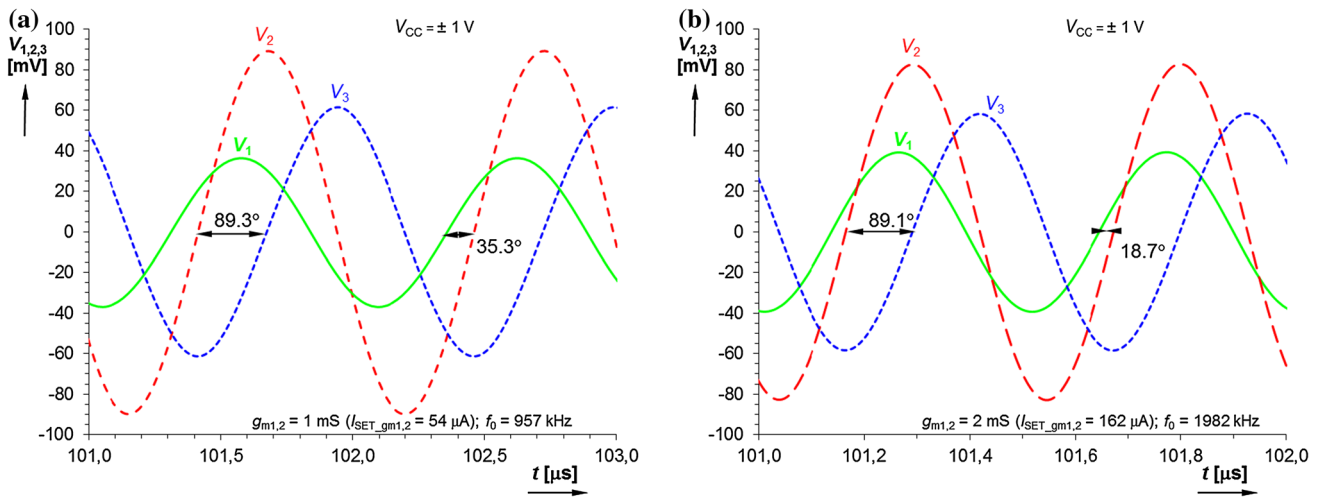


Fig. 15 Steady-state transient responses for two selected FOs: a 0.957 MHz. b 1.982 MHz

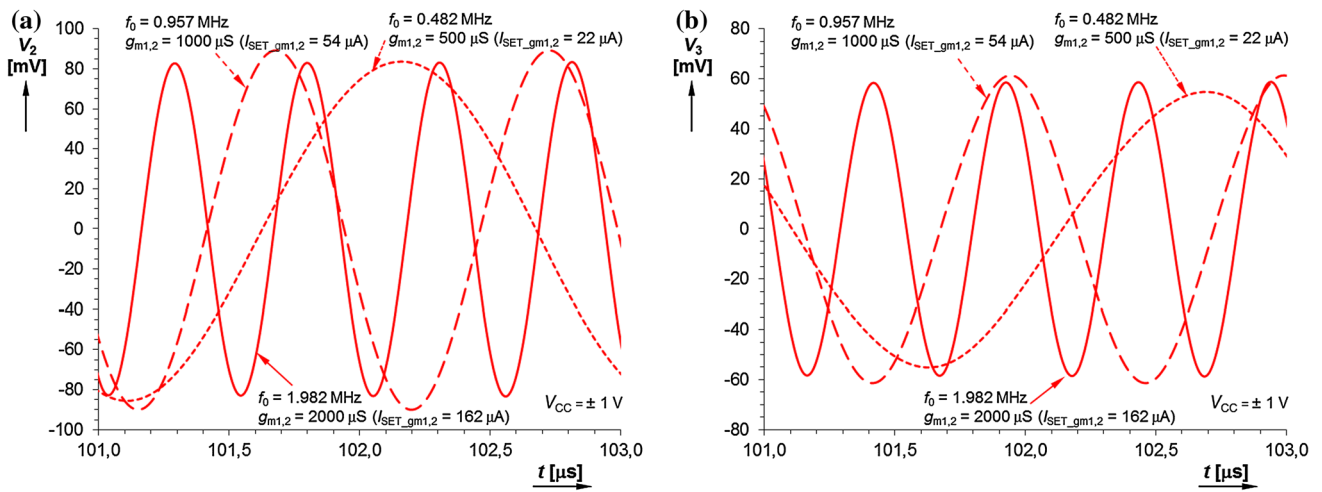


Fig. 16 Tuning of the FO observed on transient responses for: a V_2 , b V_3

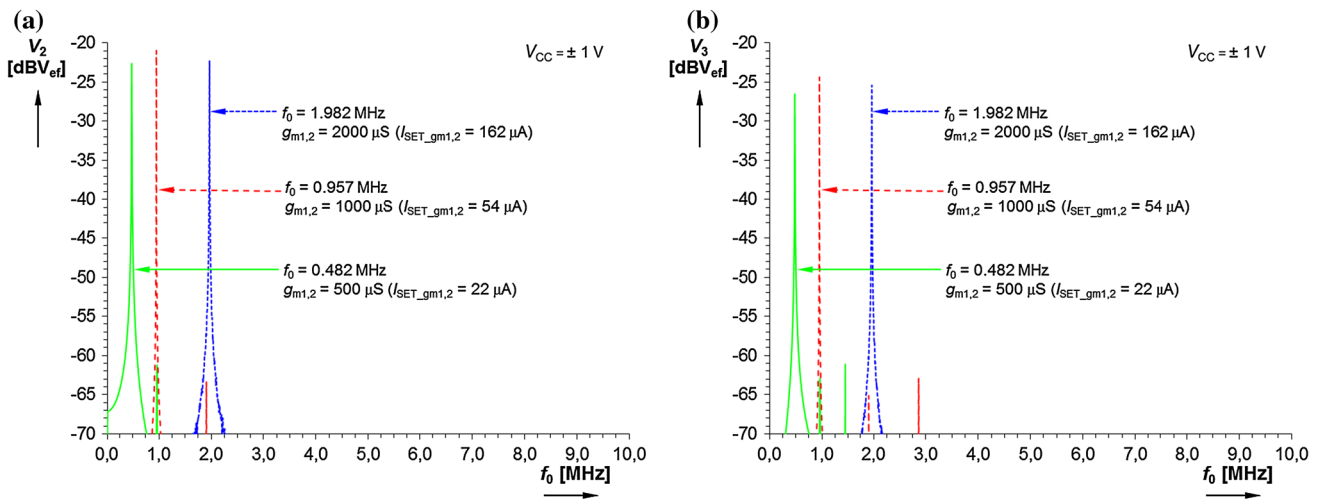


Fig. 17 Tuning of the FO observed in frequency domain for: a V_2 , b V_3

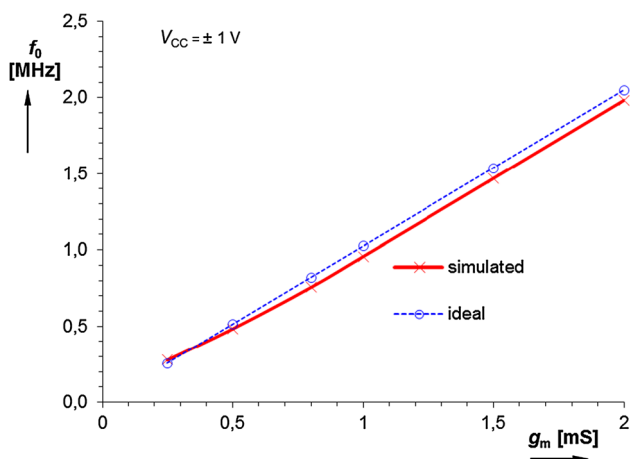


Fig. 18 Simulated dependence of FO on $g_{m1,2}$ values

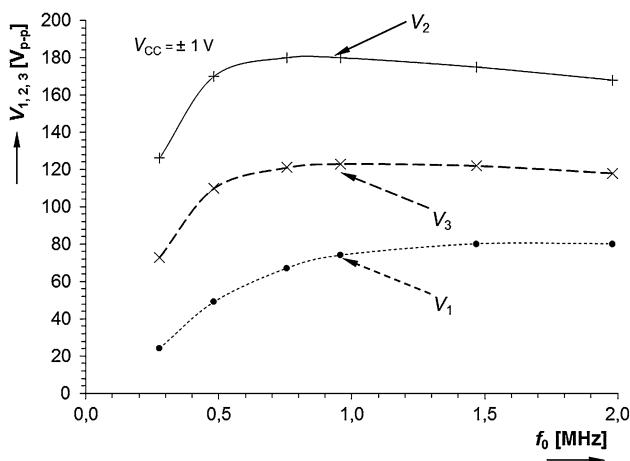


Fig. 19 Simulated dependence of the output levels (voltages V_1 , V_2 , V_3) on FO

higher frequencies is caused by substantial increase of the DC bias current $I_{SET_gm1,2}$.

In comparison with measurement results obtained with behavioral models, where higher g_m and also FO was available, enormous bias current I_{SET_gm} is required for higher g_m . The changes of operation regime of CMOS transistors cause degradation of OTA linearity and also power consumption increases rapidly. Therefore, we cannot reach similar range of FO tuning as when measured (in almost identical conditions) because the maximal value of g_m of presented CMOS OTA model is limited approximately to 2 mS.

Dependence of the output levels on FO is documented in Fig. 19. Operation of the AGC is similar but range of the FO tuning is limited to 2 MHz in this case. Output levels (peak to peak) are substantially lower (hundreds of mV) than in measurements based on commercially available

devices. However, this is unavoidable because of lower supply voltage and 0.18 μm technology.

We also analyzed phase distances of produced signals (Fig. 20a) and dependence of phase error of both quadrature signals V_2 and V_3 on FO (Fig. 20b). As already mentioned, it is clearly seen that phase distance between V_1 and other signals changes if FO is tuned. Therefore, this output is really not useful for multiphase purposes. Phase error of V_2 and V_3 outputs is maximally about $\pm 2\%$ in observed FO range (0.28–2 MHz).

Values of THD in observed FO range are higher (approximately between 0.3 and 3 %) than values obtained from measurement of experimental prototype due to worse and limited linearity of used CMOS models.

Proposed CMOS structure has several parameters that determine key features of the oscillator (FO accuracy and dispersion). Ideal symbolical analysis implies that R_i (input resistance of the used CA) has no impact on function. Nevertheless, study of influences of real nodal impedances caused by terminals of active elements connected to this node reveals that R_i also influences real FO (13). Therefore, further discussion deals with tolerance and thermal dispersion of R_i and also other important parameters (g_m) influencing accuracy of FO.

6.1 Study of independent impacts of R_i and g_m

First of all, we tested impact of bias current I_{b1} (Fig. 14b) on small-signal R_i dispersion in the worst case simulations and found out uncertainty interval of R_i between 476 and 640 Ω for 30 % dispersion of $I_{b1} = 100 \mu\text{A}$ (quite common worst case deviation of IC fabrication process).

Impact of these changes (worst case $\pm 30\%$ deviation of I_{b1} value driving R_i) on the oscillator structure (Fig. 13) consists of very small deviation of FO, approximately from 0.952 to 0.960 MHz (± 4 kHz) from nominal value of $f_0 = 0.957$ MHz ($g_{m1,2} = 1$ mS). The worst case results are very pessimistic and are not likely in practice. We obtained results of the Monte Carlo analysis (for 100 runs) of f_0 samples for 30 % tolerance of I_{b1} with Gaussian distribution. Standard deviation $\Delta f_0 = 1.43$ kHz (sigma) and 4.3 kHz (3 sigma) was obtained. Minimal and maximal value (0.954 and 0.960 MHz) of the f_0 almost corresponds to the worst case results discussed above.

Deviation of g_m of the OTA (Fig. 14a) caused by uncertainty of I_{SET_gm} has significant impact on FO. The deviation of $\pm 30\%$ of $I_{SET_gm1,2}$ results in $g_{m1,2}$ range from 0.772 to 1.206 mS. Deviation of $g_{m1,2}$ is thus more than $\pm 20\%$. Therefore, accuracy of $g_{m1,2}$ is critical for overall FO accuracy. Such tolerance $\pm 30\%$ of $I_{SET_gm1,2}$ causes large deviation = ± 215 kHz (range of FO uncertainty belongs to interval from 0.73 and 1.16 MHz) which

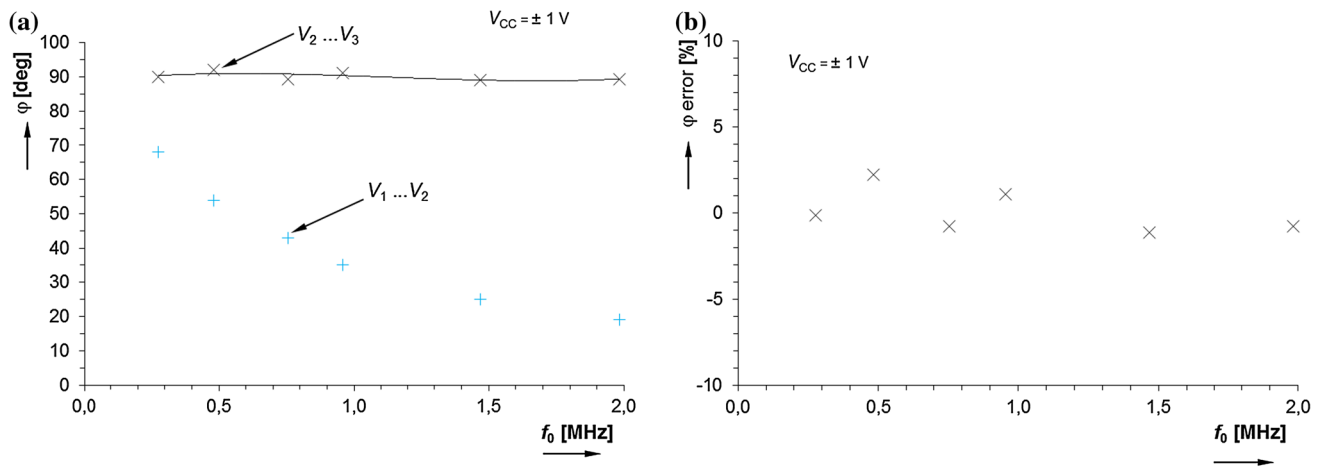


Fig. 20 Simulation results of phase relations in dependence on FO: **a** phase distance **b** phase error between V_2 and V_3

Table 2 Results of the Monte Carlo analysis (100 runs) for FO (nominal $f_0 = 0.957$ MHz)

Tolerances (%)			Mean (MHz)	Min (MHz)	Max (MHz)	Sigma (kHz)
R_i	I_{SET_gm1}, I_{SET_gm2}	C_1, C_2, C_3				
30	5	1	0.955	0.934	0.976	8.6
30	5	5	0.955	0.927	0.989	13.1
30	10	1	0.954	0.911	0.994	16.5
30	10	5	0.953	0.908	1.002	19.7
30	20	5	0.950	0.868	1.033	34.8
30	30	5	0.945	0.818	1.067	50.9

Table 4 Results of the Monte Carlo analysis (100 runs) for phase distance between V_2 and V_3

Tolerances (%)			Mean (deg)	Min (deg)	Max (deg)	Sigma (deg)
R_i	I_{SET_gm1}, I_{SET_gm2}	C_1, C_2, C_3				
30	5	1	89.9	88.6	91.3	1.0
30	5	5	90.0	88.6	91.2	1.0
30	10	1	89.8	88.6	91.2	1.1
30	10	5	90.0	88.6	91.3	1.1
30	20	5	90.0	88.6	91.3	1.0
30	30	5	90.1	88.6	91.3	1.0

Table 3 Results of the Monte Carlo analysis (100 runs) for V_2, V_3 values

Tolerances (%)			$V_2; V_3$ mean (mV _{p-p})	$V_2; V_3$ min (mV _{p-p})	$V_2; V_3$ max (mV _{p-p})	$V_2; V_3$ sigma (mV _{p-p})
R_i	I_{SET_gm1}, I_{SET_gm2}	C_1, C_2, C_3				
30	5	1	180; 123	177; 120	182; 127	1.2; 1.5
30	5	5	180; 123	169; 115	187; 130	3.7; 3
30	10	1	180; 123	177; 118	182; 129	1.2; 2.6
30	10	5	180; 123	169; 115	187; 132	3.7; 3.7
30	20	5	180; 124	169; 114	187; 137	3.7; 5.7
30	30	5	180; 124	169; 109	187; 143	3.7; 8.1

is more than $\pm 20\%$ of nominal f_0 . Standard deviation (Monte Carlo analysis as in the previous case) $\Delta f_0 = 47$ kHz (sigma) and 141 kHz (3 sigma) was achieved, which is significantly higher than impact caused by R_i .

Analyses conclude that R_i impact on function is almost negligible, the most important problem is uncorrelated deviation of g_{m1} and g_{m2} values.

6.2 Study of uncorrelated R_i, g_m and C dispersion simultaneously

We provide the results for tolerances of the most important active and passive parameters noted in Tables 2, 3, 4. Table 2 shows deviation of FO, results in Table 3 focus on changes of output voltages (V_2, V_3) and Table 4 describes impact of parameters distortion on accuracy of the phase shift between V_2 and V_3 . Nominal parameters have values: $g_{m1,2} = 1$ mS ($I_{SET_gm1,2} = 54$ μ A), $C_1 = C_2 = C_3 = 220$ pF, $R_i = 533$ Ω and $f_0 = 0.957$ MHz.

7 Concluding remarks and discussion of achieved results

Oscillator in Fig. 3 proposed as advanced modification of the Colpitts circuit [13] offers interesting advantages that are not available in common Colpitts LC circuits. The first advantage is simple control of the oscillation condition by current gain B of used adjustable current amplifier. The second advantage, coming from replacement of the

inductance by synthetic equivalent based on VDTA, consists of availability of quadrature output signals. Amplitude levels of the both produced quadrature signals are independent of tuning process if simple matching condition (equality of both g_m in frame of VDTA) is ensured. In addition, linear control of oscillation frequency is also allowed. Unfortunately, one disadvantage remains—floating capacitor, but it comes from the principle of the Colpitts oscillator (structure always contains floating capacitor). Current gain B is lower than 1 which is quite favorable feature (lower power requirements) as we showed also in the experiments. Proposed circuit was studied experimentally and also in detailed Spice simulations. Commercially available active devices allowed construction of full behavioral representation (Fig. 5) of the circuit together with precise AGC. Achieved range of tunability was obtained from 0.5 to 7.91 MHz in measurements and 0.277 to 1.982 MHz in simulations with presented CMOS model (Fig. 12). Simulated range is reduced due to the limited value of g_m of used CMOS OTA. Measured behavioral model provides output levels of units of volts (peak-to-peak) with THD below 0.5 %. Simulated CMOS model has several times reduced output levels (hundreds of mV_{p-p}) due to low supply voltage. Therefore, linearity of active elements and THD is also worse (units of %) than in measurements. Phase error obtained in measurements is maximally ± 3 % in observed tuning range (1–8 MHz). Simulations offer slightly better results of ± 2 %. A study presented in this paper gives detailed information about circuit features also in comparison with [28].

Simulations and experiments reveal that parasitic capacitances in high-impedance nodes and inequality of simultaneous change of both g_{m1} , g_{m2} have the most important impact on FO accuracy. Statistical Monte Carlo analysis gives interesting results that there is very weak dependence of phase distance of quadrature signals on tolerances of the most important passive and active parameters. On the other hand, oscillation frequency is the most affected parameter. Minimal impact of real input resistance (R_i) accuracy of the current amplifier is very important finding. Operation of the oscillator and expected features were sufficiently verified by the simulations and experiments.

Acknowledgments Research described in the paper was supported by Czech Science Foundation Project Under No. 14-24186P and by internal Grant No. FEKT-S-14-2281. The support of the project CZ.1.07/2.3.00/20.0007 WICOMT, financed from the operational program Education for competitiveness, is gratefully acknowledged. The described research was performed in laboratories supported by the SIX project; the registration number CZ.1.05/2.1.00/03.0072, the operational program Research and Development for Innovation. Dr. Herencsar was supported by the project CZ.1.07/2.3.00/30.0039 of the Brno University of Technology. A preliminary version of this paper

has been presented at the 8th International Conference on Electrical and Electronics Engineering—ELECO 2013 [28].

References

1. Biolek, D., Senani, R., Biolkova, V., & Kolka, Z. (2008). Active elements for analog signal processing: Classification, review, and new proposal. *Radioengineering*, 17(4), 15–32.
2. Surakamponorn, W., & Thitimajshima, W. (1988). Integrable electronically tunable current conveyors. *IEE Proceedings-G*, 135(2), 71–77.
3. Fabre, A., & Mimeche, N. (1994). Class A/AB second-generation current conveyor with controlled current gain. *Electronics Letters*, 30(16), 1267–1268.
4. Tangsrirat, W. (2008). Electronically tunable multi-terminal floating nullor and its application. *Radioengineering*, 17(4), 3–7.
5. Fabre, A., Saaid, O., Wiest, F., & Boucheron, C. (1996). High frequency applications based on a new current controlled conveyor. *IEEE Transaction on Circuits and Systems-I*, 43(2), 82–91.
6. Sotner, R., Kartci, A., Jerabek, J., Herencsar, N., Dostal, T., & Vrba, K. (2012). An additional approach to model current followers and amplifiers with electronically controllable parameters from commercially available ICs. *Measurement Science Review*, 12(6), 255–265.
7. Geiger, R. L., & Sanchez-Sinencio, E. (1985). Active filter design using operational transconductance amplifier: A tutorial. *IEEE Circuits and Devices Magazine*, 1, 20–32.
8. Minaei, S., Sayin, O. K., & Kuntman, H. (2006). A new CMOS electronically tunable current conveyor and its application to current-mode filters. *IEEE Transaction on Circuits and Systems-I*, 53(7), 1448–1457.
9. Sotner, R., Jerabek J., Herencsar N., Dostal T., Vrba K., Electronically adjustable modification of CFA: Double current controlled CFA (DCC-CFA). In 35th International Conference on Telecommunications and Signal Processing (TSP 2012), Prague, Czech Republic, 2012, pp. 401–405.
10. Sotner, R., Herencsar, N., Jerabek, J., Dvorak, R., Kartci, A., Dostal, T., et al. (2013). New double current controlled CFA (DCC-CFA) based voltage-mode oscillator with independent electronic control of oscillation condition and frequency. *Journal of Electrical Engineering*, 64(2), 65–75.
11. Marcellis, A., Ferri, G., Guerrini, N. C., Scotti, G., Stornelli, V., & Trifiletti, A. (2009). The VGC-CCII: A novel building block and its application to capacitance multiplication. *Analog Integrated Circuits and Signal Processing*, 58(1), 55–59.
12. Sotner, R., Hrubos, Z., Herencsar, N., Jerabek, J., Dostal, T., & Vrba, K. (2014). Precise electronically adjustable oscillator suitable for quadrature signal generation employing active elements with current and voltage gain control. *Circuits Systems and Signal Processing*, 33(1), 1–35.
13. Kennedy, M. P. (1994). Chaos in the Colpitts oscillator. *IEEE Transactions on Circuit and Systems-I*, 41(11), 771–774.
14. Soliman, A. M. (1998). Current mode CCII oscillators using grounded capacitors and resistors. *International Journal of Circuit Theory and Applications*, 26(5), 431–438.
15. Soliman, A. M. (1998). Novel generation method of current mode Wien-type oscillators using current conveyors. *International Journal of Electronics*, 85(6), 737–747.
16. Linares-Barranco, B., Rodriguez-Vazquez, A., Sanchez-Sinencio, E., & Huertas, J. L. (1991). CMOS OTA-C high-frequency sinusoidal oscillators. *IEEE Journal of Solid-State Circuits*, 26(2), 160–165.
17. Horng, J. W. (2009). Current-mode third-order quadrature oscillator using CDTAs. *Active and Passive Electronic Components*, 2009, 1–5.

18. Horng, J. W., Lee, H., & Wu, J. (2010). Electronically tunable third-order quadrature oscillator using CDTAs. *Radioengineering*, 19(2), 326–330.
19. Maheshwari, S. (2010). Current-mode third-order quadrature oscillator. *IET Circuits, Devices and Systems*, 4(3), 188–195.
20. Maheshwari, S., & Khan, I. A. (2005). Current controlled third order quadrature oscillator. *IET Proceeding of Circuits Devices Systems*, 152(6), 605–607.
21. Maheshwari, S. (2009). Quadrature oscillator using grounded components with current and voltage outputs. *IET Circuits Devices Systems*, 3(4), 153–160.
22. Chatuverdi, B., & Maheshwari, S. (2013). Third-order quadrature oscillators circuit with current and voltage outputs. *ISRN Electronics*, 2013, 1–8.
23. Promee, P., & Dejhana, K. (2002). An integrable electronic-controlled quadrature sinusoidal oscillator using CMOS operational transconductance amplifier. *International Journal of Electronics*, 89(5), 365–379.
24. Kwawsibsam, A., Sreewirote, B., Jaikla, W. (2011). Third-order voltage-mode quadrature oscillator using DDCC and OTAs. In *Proceeding of International Conference on Circuits, Systems and Simulation IPCSIT*, vol. 7, Singapore, pp. 317–321.
25. Horng, J. W. (2011). Current/voltage-mode third order quadrature oscillator employing two multiple outputs CCII and grounded capacitors. *Indian Journal of Pure and Applied Physics*, 49(7), 494–498.
26. Kungern M., & Junnapiya S. (2011). Current-mode third-order quadrature oscillator using minimum elements. In *Proceeding of the International Conference on Electrical Engineering and Informatics (ICEEI '11)*, pp. 1–4.
27. Koton, J., Herencsar, N., Vrba, K., & Metin, B. (2012). Current- and voltage-mode third-order quadrature oscillator. In *Proceeding of 13th international Conference on Optimization of Electrical and Electronic Equipment (OPTIM)*, Brasov, pp. 1203–1206.
28. Sotner, R., Jerabek, J., Herencsar, N., Petrzela, J., Vrba, K., Kincl, Z. (2013). Tunable oscillator derived from Colpitts structure with simply controllable condition of oscillation and synthetic inductor based on current amplifier and voltage differencing transconductance amplifier. In *Proceeding of the 8th International Conference on Electrical and Electronics Engineering*, pp. 21–25.
29. Basak, A. (1991). *Analogue electronic circuits and systems* (pp. 153–167). New York: Cambridge University.
30. Gray, P. R., Hurst, P. J., Lewis, S. H., & Meyer, R. G. (2009). *Analysis and design of analog integrated circuits* (5th ed.). USA: Wiley.
31. Yesil, A., Kacar, F., & Kuntman, H. (2011). New simple CMOS realization of voltage differencing transconductance amplifier and its RF filter application. *Radioengineering*, 20(3), 632–637.
32. Satansup, J., Pukkalanun, T., & Tangsrirat, W. (2013). Electronically tunable single-input five-output voltage-mode universal filter using VDTAs and grounded passive elements. *Circuits, Systems, and Signal Processing*, 32(3), 945–957.
33. Prasad, D., Bhaskar, D. R., & Srivastava, M. (2013). Universal current-mode biquad filter using a VDTA. *Circuits and Systems*, 4(1), 32–36.
34. Prasad, D., & Bhaskar, D. R. (2012). Electronically controllable explicit current output sinusoidal oscillator employing single VDTA. *ISRN Electronics*, 2012(382560), 1–5.
35. Herencsar, N., Sotner, R., Koton, J., Misurec, J., & Vrba, K. (2013). New compact VM four-phase oscillator employing only single z-copy VDTA and all grounded passive elements. *Elektronika Ir Elektrotechnika*, 19(10), 87–90.
36. Prasad, D., & Bhaskar, D. R. (2012). Grounded and floating inductance simulation circuits using VDTAs. *Circuits and Systems*, 3(4), 342–347.
37. EL2082: Current-Mode multiplier, intersil (Elantec) [online]. last modified 2003 [cit.27.6.2013]. <<http://www.intersil.com/data/fn/fn7152.pdf>>.
38. OPA660: Wide-bandwidth operational transconductance amplifier and buffer, texas instruments [online]. 1995 [cit.9.2.2014]. <http://www.ti.com/lit/ds/symlink/opa660.pdf>.
39. OPA2650: dual wideband, low power voltage feedback operational amplifier, texas instruments [online]. 2000 [cit.9.2.2014]. <http://www.ti.com/general/docs/lit/getliterature.tsp?genericPartNumber=opa2650&fileType=pdf>.
40. MOSIS parametric test results of TSMC LO EPI SCN018 technology. [ftp://isi.edu/pub/mosis/vendors/tsmc-018/t44e_lo_epi_params.txt]. Cited 24 May 2012.
41. Surakamponorn, W., & Kumwachara, K. (1992). CMOS-based electronically tunable current conveyor. *Electronics Letters*, 28(14), 1316–1317.



Roman Sotner was born in Znojmo, Czech Republic, in 1983. He received the Ph.D. and M.Sc. degree in Electrical Engineering from the Brno University of Technology, Czech Republic, in 2012 and 2008, respectively. Currently, he is a research worker at the Department of Radio Electronics, Faculty of Electrical Engineering and Communication, Brno University of Technology, Brno, Czech Republic. His interests are analogue circuits

(active filters, oscillators, audio, etc.), circuits in the current mode, circuits with direct electronic controlling possibilities especially and computer simulation. He is a member of IEEE.



Jan Jerabek was born in Bruntal, Czech Republic, in 1982. He received the Ph.D. degree in Electrical Engineering in 2011 from the Brno University of Technology, Czech Republic. He is currently assistant professor at the Department of Telecommunications, Faculty of Electrical Engineering and Communication, Brno University of Technology. His research interests are focused on circuit design and applications of modern active elements such as

adjustable current amplifiers and followers, transconductance and transimpedance amplifiers.



Norbert Herencsar was born in Slovak Republic in 1982. He received the M.Sc. and Ph.D. degrees in Electronics and Communication and Teleinformatics from Brno University of Technology, Czech Republic, in 2006 and 2010, respectively. Currently, he is an Assistant Professor at the Department of Telecommunications and employee at the Centre of Sensor, Information and Communication Systems (SIX) of Faculty of Electrical Engineering and

Communication, Brno University of Technology, Brno, Czech Republic. During September 2009–February 2010 and February 2013–May 2013 he was an Erasmus Exchange Student and Visiting Researcher, respectively, with the Department of Electrical and Electronic Engineering, Bogazici University, Istanbul, Turkey. During February 2014–March 2014 he was a Visiting Researcher with the Department of Electronics and Communications Engineering, Dogus University, Istanbul, Turkey. His research interests include analog filters, current-, voltage- and mixed-mode circuits, electronic circuit & system design, new active elements and their circuit applications, and oscillators. He is an author or co-author of 37 research articles published in SCI-E peer-reviewed international journals, 23 articles published in other journals, and 68 papers published in proceedings of international conferences. Dr. Herencsar is Senior Member of the IACSIT and Member of the IEEE, IAENG, and ACEEE.



Jiri Petrzela was born in Brno, Czech Republic, in 1978. He received the M.Sc. and Ph.D. degrees at the Brno University of Technology in 2003 and 2007 respectively. His research interest covers the nonlinear dynamics, chaos theory and analog circuit design. Currently he is an associated professor at Department of Radio Electronics.



Kamil Vrba received the Ph.D. degree in Electrical Engineering in 1976, and the Prof. degree in 1997, both from the Brno University of Technology. Since 1990 he has been Head of the Department of Telecommunications, Faculty of Electrical Engineering and Computer Science, Brno University of Technology, Brno, Czech Republic. His research work is concentrated on problems concerned with accuracy of analog circuits and mutual conversion of analog

and digital signals. In cooperation with AMI Semiconductor Czech, Ltd. (now ON Semiconductor Czech Republic, Ltd.) he has developed number of novel active function blocks for analog signal processing such as universal current conveyor (UCC), universal voltage conveyor (UVC), programmable current amplifier (PCA), and others. He is an author or co-author of more than 650 research articles published in international journals or conference proceedings. Professor Vrba is a Member of IEEE, IEICE, and Associate Member of IET.



Zdenek Kincl was born in Brno, Czech Republic, in 1985. He received the M.Sc. and Ph.D. degrees in Electrical Engineering from the Brno University of Technology, in 2009 and 2013, respectively. Currently, he is a researcher at the Department of Radio electronics, Faculty of Electrical Engineering and Communication, Brno University of Technology and an employee at the SIX research centre. His field of research includes circuit theory,

computer-aided design, optical communications and fault diagnosis. He is also participated on several projects for aerospace applications.

[12] SOTNER, R., JERABEK, J., HERENC SAR, N., HORNG, J-W., VRBA, K. Electronically Linearly Voltage Controlled Second-Order Harmonic Oscillator With Multiples of $\pi/4$ Phase Shifts. In *Proceedings of the 38th International Conference on Telecommunication and Signal Processing (TSP 2014)*, Berlin (Germany), 2014, p. 708-712. ISBN: 978-1-4799-8497-8.

Electronically Linearly Voltage Controlled Second-Order Harmonic Oscillator With Multiples of $\pi/4$ Phase Shifts

Roman Sotner, Jan Jerabek, Norbert Herencsar, Jiun-Wei Horng, and Kamil Vrba

Abstract—Simple multiphase second-order oscillator based on special active device, so-called Z-copy Voltage Controlled Current Follower Differential Input Transconductance Amplifier (ZC-VCCFDITA) is present in this contribution. Simple linear control of oscillation frequency by DC voltage is easily possible. Simple automatic gain control circuit (AGC) for amplitude stabilization is also presented. Three output signals have phase difference (multiples of $\pi/4$) and amplitude of produced signal is not disturbed by the tuning process. Functionality of proposed application is verified by Spice simulations of newly proposed behavioral model based on commercially available devices that predetermines initial practical features of active element for future design or fabrication.

Keywords—Electronic control, current follower, intrinsic resistance control, multiphase oscillators, transconductance control, voltage control, ZC-VCCFDITA, z-copy.

I. INTRODUCTION

MULTIPHASE oscillators are group of circuits that generates at least two output signals with specific phase shift between them [1]. Cascading of lossy blocks (integrators and differentiators) together with positive feedback in the loop is very suitable way of the design [2]-[6]. These structures provide integer multiples of $\pi/2$, $\pi/4$ or $\pi/6$ phase shifts typically. However, the complexity of these structures is large and many output phases cause rapid extension of the structures. This way of synthesis requires many sections. Simultaneous matched control of parameter in

Manuscript received February 18, 2015. Research described in the paper was supported by Czech Science Foundation project under No. 14-24186P and by grant No. FEKT-S-14-2281. The support of the project CZ.1.07/2.3.00/20.0007 WICOMT, financed from the operational program Education for competitiveness, is gratefully acknowledged. The described research was performed in laboratories supported by the SIX project; the registration number CZ.1.05/2.1.00/03.0072, the operational program Research and Development for Innovation. Dr. Herencsar was supported by the project CZ.1.07/2.3.00/30.0039 of the Brno University of Technology.

R. Sotner is with the Brno University of Technology, Department of Radio Electronics, Faculty of Electrical Engineering and Communication, Technická 12, Brno, 616 00, Czech Republic (e-mail: sotner@feec.vutbr.cz).

J. Jerabek, N. Herencsar, and K. Vrba are with the Brno University of Technology, Department of Telecommunications, Faculty of Electrical Engineering and Communication, Technická 12, Brno, 616 00, Czech Republic (e-mails: {jerabekj; herencsn; vrbak}@feec.vutbr.cz).

J.-W. Horng is with the Chung Yuan Christian University, Department of Electronic Engineering, Chung-Li, 32023, Taiwan (e-mail: jwhorng@cycu.edu.tw).

each section for tuning of oscillation frequency (by simultaneous control of each of time constants [3]) can be complicated if special matching conditions are required [2], [4]. The basic three-phase variants presented in [5] require at least circuit of 3rd-order (3 capacitors and 5 transconductors) and sophisticated matching of parameters for their control (tuning).

The second and very extensive possibility to realize multiphase oscillators is utilization of all-pass sections ([7]-[10] for example). However, these circuits realize phase shifts in multiples of $\pi/2$ in the most cases. Solutions presented in [9]-[10] provide also lower minimal phase shift than $\pi/2$ but modification of resulting chain of blocks is required. Ref. [11] presents arbitrary adjustable phase shifts in the oscillator. Unfortunately, only two output signals are available.

The other known way, how to construct oscillator with phase shifted outputs, is combination of all-pass section and loss-less integrator in the loop ([12]-[18] for example). These circuits are substantially simpler, than previously discussed examples, and provide several phase shifts (mainly quadrature - $\pi/2$ multiples). However, condition for oscillation (CO) and frequency of oscillation (FO) are not independently controllable (one of them or both) [13], [18].

Multiphase oscillators could be obtained also by interconnecting of lossy and lossless integrator to one loop (or specific loops), see for example [19]-[22] and references cited therein. However, phase shifts and amplitudes of generated signals depend on tuning process in many cases, [21] for instance.

Simple second-order oscillators that provide $\pi/4$ multiples of phase shifts, were published in [23] and [24]. Unfortunately, both solutions have some drawbacks. These two circuits provide multiphase outputs with elementary phase shift in multiples of $\pi/4$ and allow independent control of CO. However, tuning of FO is not possible. One solution presented in [24] even does not allow independent control of CO.

Our solution of three-phase oscillator solves the main problem of above discussed circuits i.e.: independent control of CO and FO (by independent parameters), linear tuning is ensured by simple matching condition and phase shifts ($\pi/4$) and amplitudes are constant during the tuning process in simple second-order circuit.

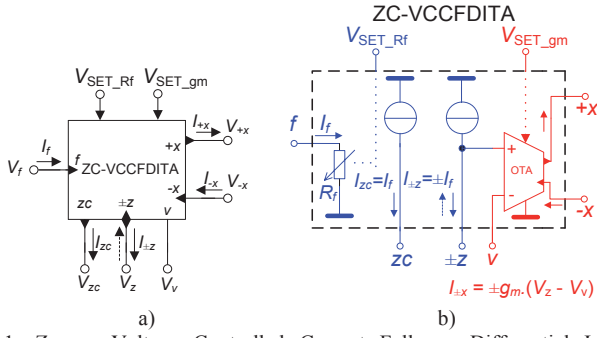


Fig. 1. Z-copy Voltage Controlled Current Follower Differential Input Transconductance Amplifier (ZC-VCCFDITA): a) symbol, b) behavioral model.

II. Z-COPY VOLTAGE CONTROLLED CURRENT FOLLOWER DIFFERENTIAL INPUT TRANSCONDUCTANCE AMPLIFIER

Basic principle of the active device used in proposed design requires brief explanation. Detailed explanation is given in [25]. Z-copy Voltage Controlled Current Follower Differential Input Transconductance Amplifier (ZC-VCCFDITA) is a derivative of the recently introduced active device called Generalized Current Follower Differential Input Transconductance Amplifier (GCFDITA) [26], which belongs to the family of active elements deeply investigated by Herencsar et al. [27]-[29] and Biolek et al [30]. Symbol and behavioral model of the ZC-VCCFDITA is shown in **Fig. 1**. Active device can be divided to two subparts: current follower/inverter section (terminals f , $\pm z$ and zc) and transconductance section (terminals $\pm z$, v , $-x$ and $+x$). Auxiliary terminal $\pm z$ is common for both subparts. Current flowing into terminal f is mirrored (and/or inverted) to two terminals signed as $\pm z$ and zc . The current $\pm I_z$ from auxiliary terminal causes voltage drop on impedance connected to this port. Difference of this voltage and voltage on v terminal is transformed to two output currents of both polarities (I_{+x} , I_{-x}), see **Fig. 1b** for details. Behavioral model of the ZC-VCCFDITA, used for simulations, will be explained later.

III. PROPOSED OSCILLATOR STRUCTURE

The proposed oscillator circuit is available in two variants (**Fig. 2**). The main difference between them is polarity of some output and auxiliary terminals. It is important to know both possible types because fulfilling of CO is not the same despite of fact that characteristic equation is nearly the same for both circuits.

Characteristic equation of the circuit in **Fig. 2a** has form:

$$s^2 + \frac{(C_2 A - C_1) g_m}{C_1 C_2} s + \frac{g_m}{C_1 C_2 R_f} = 0, \quad (1)$$

where CO and FO are as follows:

$$A \leq \frac{C_1}{C_2}, \quad \omega_0 = \sqrt{\frac{g_m}{C_1 C_2 R_f}}. \quad (2), (3)$$

Both parameters (g_m , R_f) are controllable independently or simultaneously with no impact on CO. In addition, their simultaneous control allows linear tuning of the oscillator. CO is adjustable externally (outside of active device) by simple voltage inverting amplifier/attenuator, where

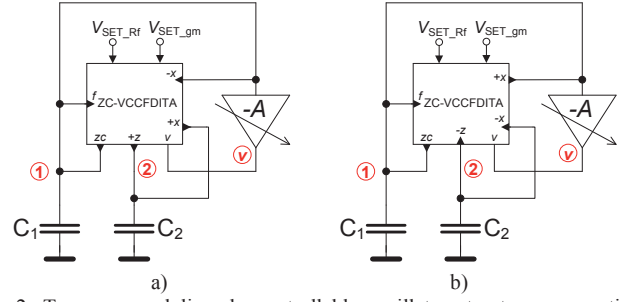


Fig. 2. Two proposed linearly controllable oscillator structures generating phase shift $\pi/4$: a) requires decrease of gain A for startup of oscillations, b) requires increasing gain A for startup of oscillations.

decreasing gain A causes startup of and increases level of oscillations. Therefore, this block can be easily replaced by simple voltage inverter and passive resistive divider (attenuator). Supposing equality of both capacitors, $A \leq 1$ is required for startup of oscillation.

Produced amplitudes (nodes 1 and 2 in **Fig. 2a**) have relation:

$$\frac{V_2}{V_1} = -\frac{g_m R_f + 1}{R_f (g_m - s C_2)}, \quad (4)$$

that gives (supposing equality of both capacitors $C_1 = C_2 = C$ and $g_m = 1/R_f$)

$$\frac{V_2}{V_1} = \frac{2}{-1+j} = -(1+j), \quad (5)$$

that can be transformed to:

$$V_2 = -\sqrt{2} \exp[\tan^{-1}(1)] V_1 = \sqrt{2} \exp\left[j\left(\frac{\pi}{4} + \pi\right)\right] V_1. \quad (6)$$

Phase distance between V_2 and V_1 is 225 (-135) degrees. Voltage at node v of the ZC-VCCFDITA (V_v) is inversion of V_1 voltage:

$$\frac{V_v}{V_1} = -\frac{(-g_m + s C_2)}{(-g_m + s C_2)}, \quad (7)$$

that leads to phase distance of 45 degrees between V_2 and V_v .

Characteristic equation and CO of the solution in **Fig. 3b** have form (only small difference in order of terms in linear coefficient):

$$s^2 + \frac{(C_1 - C_2 A) g_m}{C_1 C_2} s + \frac{g_m}{C_1 C_2 R_f} = 0, \quad A \geq \frac{C_1}{C_2}, \quad (8), (9)$$

and FO has the same form as (3). Required gain A have to be ≥ 1 for startup of oscillations (if $C_1 = C_2 = C$). It is main difference between both solutions of presented structure (**Fig. 2**), except possible phase shifts, but it is really important for practical implementation of automatic amplitude stabilization of oscillations.

Relation between produced amplitudes (**Fig. 2b**) in nodes 1 and 2 has form:

$$\frac{V_2}{V_1} = -\frac{g_m R_f + 1}{R_f (g_m + s C_2)}. \quad (10)$$

Supposing again equality of both capacitors $C_1 = C_2 = C$ and $g_m = 1/R_f$ (simultaneous control for linear tuning), relation simplifies to:

$$\frac{V_2}{V_1} = \frac{-2}{1+j} = -1+j, \quad (11)$$

that gives

$$V_2 = -\sqrt{2} \exp[\tan^{-1}(-1)]V_1 = \sqrt{2} \exp\left[j\left(-\frac{\pi}{4} + \pi\right)\right]V_1. \quad (12)$$

It means that phase shift between V_2 and V_1 is 135 (–225) degrees. Phase distance between voltage at node v of the ZC-VCCFDITA and V_1 is:

$$\frac{V_v}{V_1} = -\frac{g_m + sC_2}{g_m + sC_2}. \quad (13)$$

V_v is inversion of V_1 voltage. Due to this fact, we have also phase shift 45 degree available between V_2 and V_v (180-135).

IV. SIMULATION RESULTS

A. Particular design

Circuit in **Fig. 2b** was further analyzed by PSpice simulation. Active element was created by behavioral model introduced in [25]. Analyzed solution, including behavioral model of the ZC-VCCFDITA, is depicted in **Fig. 3** together with circuit for automatic gain control circuit (AGC) for stabilization of oscillation. Proposed behavioral model utilizes circuit for R_f control [31] based on electronically controllable current conveyors (ECCII_{1,2} - EL2082 [32]), current followers/inverters (CF/I₃ - EL4083 [33]), transconductance section (ECCII₄ and A₆ - VCA610 [34]) with current outputs of both polarities (CF/I₅). Controllable gain of the variable gain amplifier VCA610 is used as advantage for our AGC implementation because this gain A directly controls CO. Value of the gain A is derived from output amplitudes and driven by detected DC voltage (after diode doubler) as: $A \cong 10^{-2(V_{AGC}+1)}$ [34], that is given by constant value V_{const} (slightly higher than 1) which is summed with modified level of detected signal (by R_a) from node 1. Driving voltage V_{AGC} decreases and increases in order to minimize output fluctuations. Some values and parameters of the AGC system are shown directly in **Fig. 3**. Opamp can be implemented by known and high-frequency LT1364 [35], for example. Values of C_r , R_{c1} and R_r are chosen in dependence on required time constants. However, these time constants cannot be long in simulations because steady state in the circuit depends on it and is reached after long time. But in practice, these values are in hundreds of nF (capacitors) and hundreds of kΩ (resistors). Other working values and parameters were set as: $C_1 = C_2 = 100$ pF, $A \cong 1$ (for ideal fulfilling of CO but driven by AGC). Both adjustable parameters g_m and $1/R_f$ ($g_m \cong V_{SET_gm}/R_4$ [32] and $R_f \cong R_1/V_{SET_Rf}$ [31]) are set equal and adjusted simultaneously ($V_{SET_gm} = V_{SET_Rf}$). We can see, that $g_m = 1/R_f$ and equality of $R_1 = R_4 = R_{14}$ modify (3) to form $\omega_0 = V_{SET_f0}/(CR_{14})$, where $V_{SET_f0} = V_{SET_gm} = V_{SET_Rf}$. We suppose simultaneous change (equality) of both voltages.

B. Discussion of nonidealities

Ideal FO for $V_{SET_f0} = 1$ V is equal to 1.592 MHz. However, in the circuit of this complexity there are many real influences. The most important problems and real nonidealities are:

1) Real impedances in both high-impedance nodes 1 and 2

Impedance in node 1 is formed by output resistance of the Z terminal and Y terminal of the ECCII₁ (1 MΩ/ 5 pF and

2 MΩ/ 2 pF) [32], output impedance of the CF/I₃ terminal (1 MΩ/ 9 pF – estimated experimentally, datasheet [33] does not include this information), input impedance (negative input) of VCA₆ (1 MΩ/ 3 pF) [34], output impedance of the CF/I₅ (1 MΩ/ 9 pF) and input impedance of external voltage follower for AGC (5 MΩ/ 1 pF) [35]. Therefore expected impedance in node 1 has parameter values $R_{p1} \cong 213$ kΩ and $C_{p1} \cong 29$ pF.

Impedance in node 2 is formed as follows. There are only output impedance of the CF/I₃ (1 MΩ/ 9 pF) [33], input impedance of the Y terminal ECCII₄ (2 MΩ/ 2 pF) and output impedance of the CF/I₅ (1 MΩ/ 9 pF). Parameters of the impedance in node 2 are $R_{p1} \cong 400$ kΩ, $C_{p1} \cong 20$ pF.

Note that R_1 and R_4 already take into account real input resistance of X terminal (95 Ω [31]) of the ECCII.

2) Tracking errors in the structure of the model

We found out that the most important problem of the follower inaccuracy is in case of both CF/I blocks. Simulation shows that current transfers of the CF/I has non-unity gain (simulated value is about 0.93). It causes decrease of real transconductance (g_m) or resistance R_f as: $g_m' \cong V_{SET_gm}0.93/R_4$ and $R_f' \cong R_1/(0.93 V_{SET_Rf})$.

Following equation for FO respects discussed nonidealities:

$$\omega_0' \cong \sqrt{\frac{g_m' R_f' (R_{p1} + R_{p2}) + g_m' R_{p1} R_{p2} + R_f' + 2R_{p1}}{R_f' R_{p1} R_{p2} (C_1 + C_{p1}) (C_2 + C_{p2})}}. \quad (14)$$

C. Results

Simulation of the oscillator with proposed behavioral model of the ZC-CCCFDITA were provided in OrCAD PSpice and results in time and frequency domain are presented in following graphs. **Figure 4** shows startup of oscillations with reaction of the AGC system (V_{AGC} driving gain A for CO control). Steady state waveforms in all available nodes 1, 2, v , are shown in **Fig. 5**. FO achieved value 1.158 MHz for $V_{SET_f0} = 1$ V ($g_m = 1/R_f = 0.93$ mS) in simulation. In accordance to (14) we obtained expected value 1.197 MHz. Total harmonic distortion at this frequency was calculated as 0.74, 0.47 and 0.92 % for V_1 , V_2 , V_v . According to simulation results, phase shifts are 137 degrees (between V_1 and V_2) and 44 degrees (between V_2 and V_v). Dependence of generated phase differences on FO are depicted in **Fig. 6**. Dependence of FO on V_{SET_f0} and output amplitudes on FO are in **Fig. 7** and **Fig. 8**. Expected trace (in **Fig. 7**) confirms impact of discussed real influences of behavioral model.

V. CONCLUSION

Useful oscillator generating three signals with phases based on multiple of $\pi/4$ was constructed with special active device called z-copy voltage controlled current follower differential input transconductance amplifier. Behavioral model confirmed intention of the design and utilization of controllable features in application. Future work is focused on proposal of CMOS design of discussed active device and its implementation in this application.

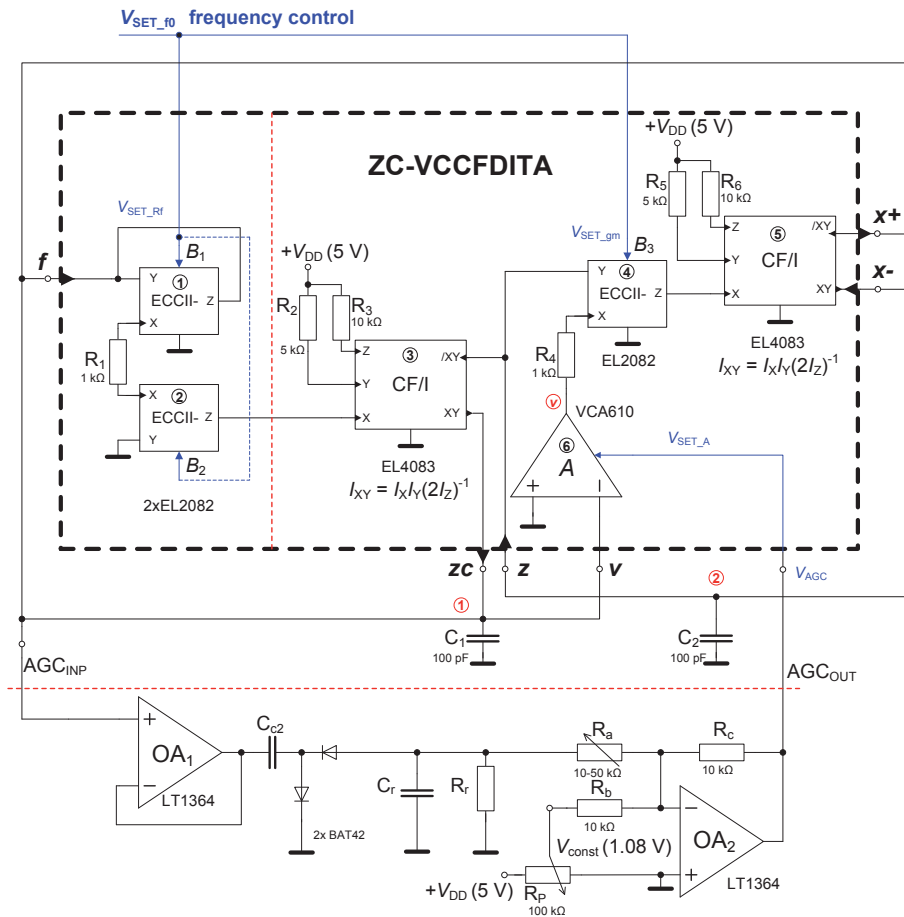


Fig. 3. Simulated circuit (full implementation) consisting of behavioral model of the ZC-CCCFDITA and AGC.

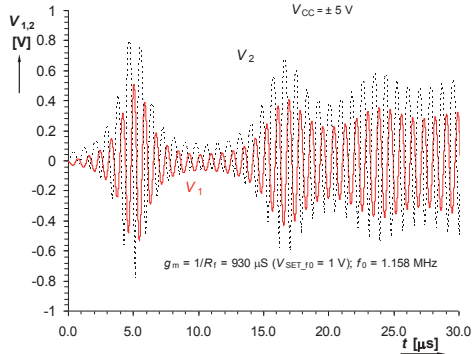


Fig. 4. Startup of oscillations (V_{OUT1} , V_{OUT2}).

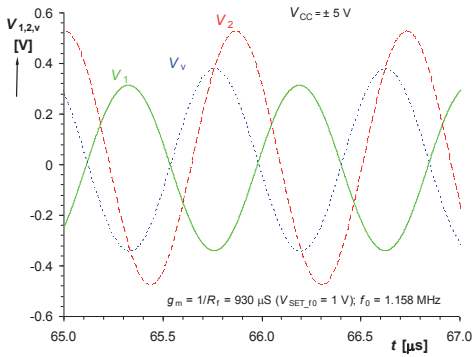


Fig. 5. Steady-state output waveforms at all available nodes.

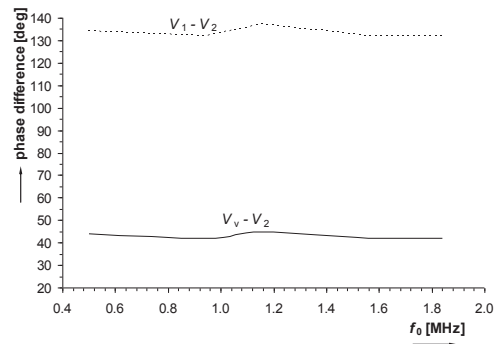


Fig. 6. Phase differences between available nodes in dependence on FO.

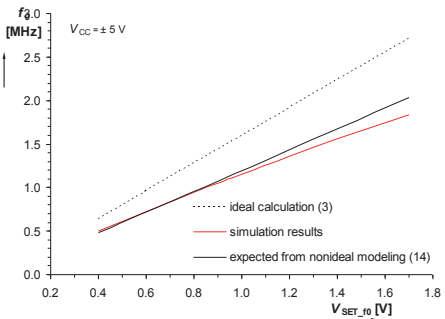


Fig. 7. Dependence of FO on V_{SET_f0} .

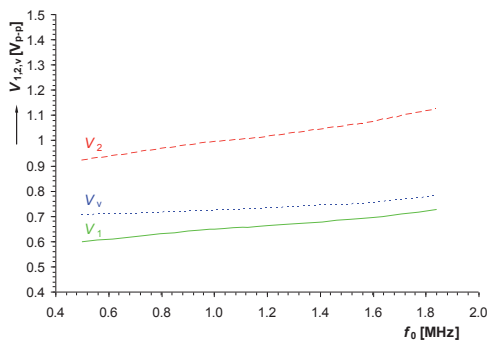


Fig. 8. Dependence of output levels on FO.

REFERENCES

- [1] W. Chen, "The Circuits and Filters Handbook," Boca Raton, FL: CRC Press, 2002.
- [2] M. T. Abuelmaatti, M. A. Al-qahtani, "A New Current-Controlled Multiphase Sinusoidal Oscillator Using Translinear Current Conveyors," *IEEE Transactions on Circuits and Systems II: Analog and Digital Signal Processing*, vol. 45, no. 7, pp. 881–885, 1998.
- [3] G. Souliotis, C. Psychalions, "Electronically controlled multiphase sinusoidal oscillators using current amplifiers," *International Journal of Circuit Theory and Applications*, vol. 37, no. 1, p. 43–52, 2009.
- [4] M. Kumngern, J. Chanwutium, K. Dejhan, "Electronically tunable multiphase sinusoidal oscillator using translinear current conveyors," *Analog Integrated Circuits and Signal Processing*, vol. 65, no. 2, p. 327–334, 2010.
- [5] S-H. Tu, Y-S. Hwang, J-J. Chen, A. M. Soliman, C-M. Chang, "OTA-C arbitrary-phase-shift oscillators," *IEEE Trans. on Instrumentation and Measurement*, vol. 61, no. 8, pp. 2305–2319, 2012.
- [6] M. Sagbas, U. E. Ayten, N. Herencsar, S. Minaei, "Current and Voltage Mode Multiphase Sinusoidal Oscillators Using CBTAs," *Radioengineering*, vol. 22, no. 1, pp. 24–33, 2013.
- [7] S. J. G. Gift, "The application of all-pass filters in the design of multiphase sinusoidal systems," *Microelectronics Journal*, vol. 31, no. 1, p. 9–13, 2000.
- [8] A. U. Keskin, D. Biolek, "Current mode quadrature oscillator using current differencing transconductance amplifiers (CDTA)," *IEE Proc. Circuits Devices and Systems*, vol. 153, no. 3, p. 214–218, 2006.
- [9] W. Jaikla, P. Prommee, "Electronically Tunable Current-mode Multiphase Sinusoidal Oscillator Employing CCCDTA-based Allpass Filters with Only Grounded Passive Elements," *Radioengineering*, vol. 20, no. 3, pp. 594–599, 2011.
- [10] P. Prommee, N. Wongprommoon, "Log-domain All-pass Filter-based Multiphase Sinusoidal Oscillator," *Radioengineering*, vol. 22, no. 1, pp. 14–23, 2013.
- [11] K. Songsuwankit, W. Petchmaneeumka, V. Riewruja, "Electronically adjustable phase shifter using OTAs," in *Proc. of the Int. Conf. on Control, Automation and Systems (ICCAS2010)*, Gyeongju-do (Korea), 2010, p. 1622–1625.
- [12] R. Keawon, W. Jaikla, "A Resistor-less Current-mode Quadrature Sinusoidal Oscillator Employing Single CCCDTA and Grounded Capacitors," *Przegląd Elektrotechniczny*, vol. 87, no. 8, p. 138–141, 2011.
- [13] W. Jaikla, M. Siriruchyanun, J. Bajer, D. Biolek, "A simple current-mode quadrature oscillator using single CDTA," *Radioengineering*, vol. 17, no. 4, p. 33–40, 2008.
- [14] N. Pandey, S. K. Paul, "Single CDTA-based current mode all-pass filter and its applications," *Journal of Electrical and Computer Engineering*, vol. 2011, p. 1–5, 2011.
- [15] A. U. Keskin, C. Aydin, E. Hancioglu, C. Acar, "Quadrature Oscillator Using Current Differencing Buffered Amplifiers (CDBA)," *Frequenz*, vol. 60, no. 3, p. 21–23, 2006.
- [16] S. N. Songkla, W. Jaikla, "Realization of Electronically Tunable Current-mode First-order Allpass Filter and Its Application," *International Journal of Electronics and Electrical Engineering*, vol. 2012, no. 6, p. 40–43, 2012.
- [17] S. Minaei, E. Yuces, "Novel Voltage-Mode All-pass Filter Based on Using DVCCs," *Circuits Systems and Signal Processing*, vol. 29, no. 3, p. 391–402, 2010.
- [18] N. Herencsar, S. Minaei, J. Koton, E. Yuces, K. Vrba, "New resistorless and electronically tunable realization of dual-output VM all-pass filter using VDIBA," *Analog Integrated Circuits and Signal Processing*, vol. 74, no. 1, p. 141–154, 2013.
- [19] V. Biolkova, J. Bajer, D. Biolek, "Four-phase oscillator employing two active elements," *Radioengineering*, vol. 20, no. 1, pp. 334–339, 2011.
- [20] N. Herencsar, R. Sotner, J. Koton, J. Misurec, K. Vrba, "New compact VM four-phase oscillator employing only single z-copy VDTA and all grounded passive elements," *Elektronika IR Elektrotehnika*, vol. 19, no. 10, pp. 87–90, 2013.
- [21] R. Sotner, Z. Hrubos, B. Sevcik, J. Slezak, J. Petrzela, T. Dostal, "An example of easy synthesis of active filter and oscillator using signal flow graph modification and controllable current conveyors," *Journal of Electrical Engineering*, vol. 62, no. 5, pp. 258–266, 2011.
- [22] R. Sotner, Z. Hrubos, N. Herencsar, J. Jerabek, T. Dostal, "Precise electronically adjustable oscillator suitable for quadrature signal generation employing active elements with current and voltage gain control," *Circuits, Systems and Signal Processing*, vol. 33, no. 1, pp. 1–35, 2014.
- [23] R. Sotner, A. Lahiri, J. Jerabek, N. Herencsar, J. Koton, T. Dostal, K. Vrba, "Special type of three-phase oscillator using current gain control for amplitude stabilization," *International Journal of Physical Sciences*, vol. 7, no. 25, pp. 3089–3098, 2012.
- [24] R. Sotner, J. Jerabek, N. Herencsar, "Voltage differencing buffered/inverted amplifiers and their applications for signal generation," *Radioengineering*, vol. 22, no. 2, pp. 490–504, 2013.
- [25] J. Jerabek, R. Sotner, N. Herencsar, W. Jaikla, K. Vrba, "Behavioral model for Z-copy Voltage Controlled Current Follower Differential Input Transconductance Amplifier and its features," in *Proc. of the 37th Int. Conf. on Telecommunications and Signal Processing (TSP2014)*, Berlin, submitted for publication.
- [26] N. Herencsar, J. Koton, K. Vrba, A. Lahiri, "Single GCFDITA and grounded passive elements based general topology for analog signal processing applications," in *Proc. of the 11th International Conference on Networks - ICN 2012*, Saint Gilles, Reunion Island, pp. 59–62, 2012.
- [27] N. Herencsar, J. Koton, I. Lattenberg, K. Vrba, "Signal-flow graphs for current-mode universal filter design using current follower transconductance amplifiers (CFTAs)," in *Proc. of Int. Conf. on Applied Electronics (APPEL2008)*, Pilsen, 2008, pp. 69–72.
- [28] N. Herencsar, J. Koton, K. Vrba, "Electronically tunable phase shifter employing current-controlled current follower transconductance amplifiers (CCCFTAs)," in *Proc. of the 32th Int. Conf. on Telecommunications and Signal Processing (TSP2009)*, Dunakility, 2009, pp. 54–57.
- [29] N. Herencsar, J. Koton, K. Vrba, "Realization of current-mode KHN-equivalent biquad using current follower transconductance amplifiers (CFTAs)," *IEICE Trans. Fundamentals*, vol. E93-A, no. 10, pp. 1816–1819, 2010.
- [30] D. Biolek, R. Senani, V. Biolkova, Z. Kolka, "Active elements for analog signal processing: classification, review and new proposals," *Radioengineering*, vol. 17, no. 4, pp. 15–32, 2008.
- [31] R. Sotner, A. Kartci, J. Jerabek, N. Herencsar, T. Dostal, K. Vrba, "An Additional Approach to Model Current Followers and Amplifiers with Electronically Controllable Parameters from Commercially Available ICs," *Measurement Science Review*, vol. 12, no. 6, pp. 255–265, 2012.
- [32] Intersil (Elantec). EL2082 CN Current-mode multiplier (datasheet), 1996, 14 p., accessible on [www: http://www.intersil.com/data/fn/fn7152.pdf](http://www.intersil.com/data/fn/fn7152.pdf)
- [33] Intersil (Elantec). EL4083 CN Current-mode four-quadrant multiplier (datasheet), 1995, 14 p., accessible on [www: http://www.intersil.com/content/dam/Intersil/documents/fn71/fn7157.pdf](http://www.intersil.com/content/dam/Intersil/documents/fn71/fn7157.pdf)
- [34] Texas Instruments. VCA610 Wideband voltage controlled amplifier (datasheet), 2000, 14 p., accessible on [www: http://www.ti.com/lit/ds/symlink/vca610.pdf](http://www.ti.com/lit/ds/symlink/vca610.pdf)
- [35] Linear Technology, LT1364 CN Dual and quad 70 MHz, 1000 V/us, Op Amps, 1994, 12 p., accessible on [www: http://cds.linear.com/docs/en/datasheet/13645fa.pdf](http://cds.linear.com/docs/en/datasheet/13645fa.pdf)

[13] SOTNER, R., HRUBOS, Z., HERENC SAR, N., JERABEK, J., DOSTAL, T., VRBA, K. Precise Electronically Adjustable Oscillator Suitable for Quadrature Signal Generation Employing Active Elements with Current and Voltage Gain Control. *Circuits Systems and Signal Processing*, 2014, vol. 33, no. 1, p. 1-35. ISSN: 0278-081X.

Precise Electronically Adjustable Oscillator Suitable for Quadrature Signal Generation Employing Active Elements with Current and Voltage Gain Control

Roman Sotner · Zdenek Hrubos ·
Norbert Herencsar · Jan Jerabek · Tomas Dostal ·
Kamil Vrba

Received: 24 October 2012 / Revised: 2 June 2013 / Published online: 9 July 2013
© Springer Science+Business Media New York 2013

Abstract A new oscillator suitable for quadrature and multiphase signal generation is introduced in this contribution. A novel active element, called the controlled gain-buffered current and voltage amplifier (CG-BCVA) with electronic possibilities for current and voltage gain adjustment is implemented together with a controlled gain-current follower differential output buffered amplifier (CG-CFDOBA) for linear adjustment of the oscillation frequency and precise control of the oscillation condition in order to ensure a stable level of generated voltages and sufficient total harmonic distortion. The parameters of the oscillator are directly controllable electronically. Simultaneous changes of two current gains allow linear adjusting of the oscillation frequency, and a controllable voltage gain is intended to control the oscillation con-

R. Sotner (✉) · Z. Hrubos

Department of Radio Electronics, Faculty of Electrical Engineering and Communication, Brno University of Technology (BUT), Technicka 3082/12, Brno, 616 00, Czech Republic
e-mail: sotner@feec.vutbr.cz

Z. Hrubos

e-mail: xhrubo00@stud.feec.vutbr.cz

N. Herencsar · J. Jerabek · K. Vrba

Department of Telecommunications, Faculty of Electrical Engineering and Communication, Brno University of Technology (BUT), Technicka 3082/12, Brno, 616 00, Czech Republic

N. Herencsar

e-mail: herencsn@feec.vutbr.cz

J. Jerabek

e-mail: jerabekj@feec.vutbr.cz

K. Vrba

e-mail: vrba@feec.vutbr.cz

T. Dostal

Department of Electronics and Computer Science, College of Polytechnics Jihlava, Tolsteho 16, Jihlava 586 01, Czech Republic
e-mail: tomas.dostal@vspj.cz

dition. A detailed comparison of the proposed circuits with recently developed and discovered solutions employing the same type of electronic control is provided and shows the useful features of the proposed oscillator and utilized methods of electronic control. Behavioral models based on commercially available ICs have been used for experimental purposes. CMOS implementation of active elements was introduced and utilized for additional simulations and studies. Non-ideal analysis, Monte Carlo statistical evaluations of simulated models, and further analyses were performed for the exact determination of the expected results. Laboratory experiments confirmed the workability and estimated behavior of the proposed circuit as well.

Keywords Electronic control · Adjustable current and voltage gains · Current and voltage amplifier · Current follower differential output buffered amplifier · Quadrature and multiphase oscillators · CG-BCVA · CG-CFDOBA

1 Introduction

Electronic control in modern applications for signal processing in inter-frequency bands is a topic of many research works today. Development in this field started with the discovery and development of current conveyors (CCs) by Smith and Sedra [67, 68], Fabre [21], and Svoboda et al. [82]. Many other active elements with possibilities for electronic adjustability were introduced, innovated, and frequently utilized for circuit synthesis and design in the past, for example, operational transconductance amplifiers (OTAs) [23] and current feedback amplifiers (CFAs) [12, 56, 62], etc. A comprehensive review of old as well as recent discoveries in the field of active elements is summarized in Bielek et al. [12]. Extensive descriptions of many modifications and novel approaches are given in [12] and in references cited therein.

1.1 Methods of Electronic Control in Applications of Modern Active Elements

A basic way to control parameters in applications is by a manual change of values of passive elements—floating or grounded resistors in most cases (see [24, 25, 32, 48, 51, 71], for example). Electronic control requires additional elements (e.g., the FET transistor [24]), and the final solution is generally more complicated. A better way is to use what are called bias currents for direct electronic control of parameters of active elements (OTAs, CCs, etc.). Adjusting the intrinsic resistance (R_X) by the bias current (I_{bias}) is a very common solution for controlling parameters in many applications employing CCs [9, 18, 20, 34, 60] or adjustable CFAs [66, 73, 76]. Similarly, adjusting the transconductance value of an OTA [23] also requires bias current control [10, 15, 22, 41, 43, 46, 59, 65, 69, 72, 85]. Another method which is used is the current gain adjustment. The development of this method started along with the development of current followers (CFs) [12] and their derivatives [1, 13, 26, 27, 35, 50, 70]. Applications of adjustable current followers and amplifiers (used to control current gain) were reported in [58, 61, 84], for example. Many authors have also implemented current gain controlling mechanisms with current conveyors and amplifiers [19, 31, 39, 40, 49, 54, 63, 78, 81, 83]. Several conceptions also utilize a combination

of two methods of adjustment (using two parameters) [40, 49, 54]. Minaei et al. [54], Kumngern et al. [40], and Sotner et al. [73, 76] presented several different design methods for current conveyors with the possibility of intrinsic resistance and current gain control; Marcellis et al. [49] designed a conveyor with simultaneous adjustment of current and voltage gain. Digital control of current gain has achieved increasing attention in recent years. El-Adawy et al. [17] and Alzaher et al. [4–6] introduced digitally programmable CFs, current amplifiers, and CCs, respectively.

1.2 Comparison of Oscillator Solutions Employing Controllable Current Gain

A short comparison of several previous results is now given. The following conceptions that use the possibility to control the current gain of active elements have been introduced.

Sotner et al. [76] engaged three double current-controlled current feedback amplifiers (DCC-CFAs) in a quadrature oscillator solution. This circuit has the advantages of noninteractive electronic controllability of the condition of oscillation (CO) and the oscillation frequency (f_0 , FO) without an impact on the changes of output amplitudes during the tuning process. All parameters of the oscillator are controllable electronically by bias currents (current gains), and additional extension of the tunability range is possible via adjustable intrinsic resistances (R_X).

Three electronically controllable dual output current amplifier-based integrators were utilized by Souliotis et al. [78] in an arbitrary-multiphase (in this particular case, three-phase) current-mode oscillator as an example of a directly electronically tunable oscillator. The CO and FO are tunable via the control current I_{bias} .

Current conveyor-based integrators for a generalized multiphase oscillator design were used by Kumngern et al. [39]. They also designed an internal structure of the current conveyor with an adjustable current gain between the X and Z terminals. Matching of the time constant of each integrator section is ensured by bias control of the current gains. Unfortunately, these results are not focused on electronic adjustment of the oscillation frequency.

Kumngern et al. [40] also proposed a simple oscillator where the intrinsic input resistance was used for f_0 and the current gain for CO control (noninteractive). Only two active elements and two grounded capacitors are necessary in their solution. However, amplitude dependence and nonlinear control of f_0 occurs.

An interesting solution which implements three programmable current amplifiers (PCAs), two resistors, and two capacitors was proposed by Herencsar et al. [31]. The dependence of FO on the current gain is not linear, but FO and CO are controllable by current gains.

Alzaher proposed a very useful oscillator employing digitally adjustable active elements [4]. His oscillator allows operation in both voltage and current modes. Control of f_0 is linear, and the CO is also adjustable via the current gain. Alzaher's solution requires three adjustable elements and six passive elements.

Souliotis et al. [79] also presented two simple solutions for a quadrature oscillator, where two active elements employing current gain adjustment and two grounded capacitors were used.

The current gain type of f_0 control was also used in oscillators employing the Z-copy controlled-gain current differencing buffered amplifier (ZC-CG-CDBA) introduced by Biolek et al. in [8] and [11]. The solution in [8] requires two ZC-CG-CDBAs and six passive elements. CO is controllable by a floating resistor, but f_0 is adjustable digitally (the dependence of f_0 on the current gain is linear). The solutions discussed in [11] engage two ZC-CG-CDBAs and five passive elements, and f_0 is controllable linearly. The output amplitudes are not dependent on the tuning process; however, CO is controllable using floating resistors only.

Electronic control of f_0 in [75] is possible via adjustable current gain, but CO is only available by controllable replacement of a grounded resistor. Our oscillator in [75] employs only one active element, but its disadvantage is the dependence of one of the produced amplitudes on the tuning process and nonlinear control of f_0 .

The lack of electronic controllability of CO in [75] was improved in [77], where an additional active element with controllable gain was used. Two similar solutions, where active elements with low-impedance voltage outputs were utilized in the oscillator design, are discussed in [74]. Table 1 provides a detailed comparison of the aforementioned solutions.

The digital adjustment of current and voltage gains is very useful for FO control (see [4, 8, 11], for example). However, discontinuous adjustment of CO can be insufficient for satisfactory stability of output amplitudes and low total harmonic distortion (THD) in some cases. Sufficient bit resolution of digital control is critical. An analog-to-digital converter is essential if digital control (derived from the output amplitude) of CO is intended for automatic amplitude gain control (an AGC circuit), which causes additional complications and increased power consumption. Therefore, continuous control seems to be better for adjusting CO in order to ensure stable output amplitudes and low THD.

1.3 Comparison of Important Oscillators Based on Other Active Elements

Important solutions reported in the past employing different types of active elements are compared in Table 2, excluding circuits that employed current gain control discussed in Table 1 and the corresponding text. The most important problems concerning these previously published oscillators are: (1) four-phase or differential quadrature signal generation is not easily possible [4, 24–29, 32, 34, 36–38, 41–48, 50, 51, 57, 59, 65, 66, 70–72, 85]; (2) additional modification is necessary (current/voltage transformation and/or voltage buffering) for differential quadrature signal generation [10, 22, 27, 32–34, 36–38, 41–43, 45–48, 57, 59, 65, 72, 85]; (3) some are controllable by passive elements only [13, 25–29, 32, 37, 38, 42, 44, 47, 48, 50, 51, 70]; (4) there are too many passive elements [24, 37, 85]; (5) floating capacitors are required [25, 26, 33, 37, 38, 65, 70]; (6) there are too many active elements [22, 27, 41, 46, 50, 53, 59]. More detailed information is given in Table 2 and the comments below. None of the listed solutions employs current and voltage gain control for adjustment of FO and CO. Most of the discussed solutions are based on the state variable approach [25, 27–29], loop and multi-loop integrator (lossy and lossless) feedbacks [10, 39, 76, 78], all-pass sections [33, 37, 38, 53] (an active element-based solution only, without external components was reported in [53]), resonator equivalents [4], autonomous

Table 1 Comparison of important controllable oscillators employing current gain control

Solution	No. of passive elements	No. and type of active elements	Quadrature solution	Type of control	Amplitude dependent on tuning process/linear control of FO	CO controllable by gain	Type of output signal (current or voltage)	Additional voltage buffers or I/V converters are necessary (for voltage-mode operation)	Possibility of differential voltage quadrature outputs without additional modification and buffering	THD [%]	FO range [MHz]
[76]	5	3 DCC-CFA	Yes	I_{bias}	No/Yes	Yes	Voltage	No	No	1.8	0.25–3.8
[78]	3	3 CA	Yes ^d	I_{bias}	b/No	Yes	Current	Yes	b	2.0	0.091–0.46
[39]	3(5)	3(5) CCCII	bd	I_{bias}	b	Yes	Current	Yes	No	b	b
[40]	2	2 CCCII	No	I_{bias}	Yes/No	Yes	Voltage	Yes	No	1–7	0.2–1.7
[31]	4	3 PCA	Yes	I_{bias}	Yes/No	Yes	Current	Yes	No	< 2	0.05–0.3
[4]	6	3 DCCF+2 VB	Yes	Digital	No/Yes	Yes	Both	No	No	b	0.3–1.6
[79]	2	2 CA	Yes	I_{bias}	c	Yes	Current	Yes	No	b	1.0–2.7
[8]	6	2 ZC-CG-CDBA	Yes	Digital	No/Yes	No	Both	No	No	0.9	0.25–0.47
[11]	5	2 ZC-CG-CDBA	Yes	Digital	No/Yes	No	Both	No	No	0.2–0.3	0.25–2.8
[75]	4	1 CCTA	Yes	V control	Yes/No	No	Voltage	Yes	No	0.6–4.0	0.2–1.2
[77]	5	2 ECCII+1 CCII+2 VB	Yes	V control	Yes/No	Yes	Voltage	Yes	No	0.3–0.9	0.26–1.25

Table 1 (Continued)

Solution	No. of passive elements	No. and type of active elements	Quadrature solution	Type of control	Amplitude dependent on tuning process/linear control of FO	CO controllable by gain	Type of output signal (current or voltage)	Additional voltage buffers or I/V converters are necessary (for voltage-mode operation)	Possibility of differential voltage quadrature outputs without additional modification and buffering	THD [%]	FO range [MHz]
[74]	5	2 (CG-CFDOBA+CG-CIBA/CG-ICVA)	Yes	V_{control}	Yes/No	Yes	Voltage	No	No	0.6–1.3	0.1–1.26
Our design	5	2 (CG-CFDOBA+CG-BCVA)	Yes	V_{control}	No/Yes	Yes ^a	Voltage	No	Yes	0.12–2.5	0.25–8.0

Notes: CA—Current amplifier; CCCII—Current-controlled current conveyor/translinear current conveyor; CCTA—Current conveyor transconductance amplifier (1 current conveyor + 1 transconductance amplifier); CG-BCVA—Controlled gain-current follower differential output buffered amplifier (1 current amplifier + 1 voltage amplifier + 1 voltage buffer + 1 voltage inverter); CG-CFDOBA—Controlled gain-current follower differential output buffered amplifier (1 current amplifier + 1 voltage buffer + 1 voltage inverter); CG-CIBA—Controlled gain-current inverter buffered amplifier (1 current inverter + 1 voltage buffer); CG-ICVA—Controlled gain-inverted current and voltage amplifier (1 inverting current amplifier + 1 voltage amplifier); DCC-CFA—Double current-controlled—current feedback amplifier (2 current conveyors + 2 voltage buffers); DCCCF—Digitally controlled current follower; ECCII/CCII—Electronically controllable current conveyor of second generation/current conveyor of second generation; PCA—Programmable current amplifier; ZC-CG-CDBA—Z-copy controlled gain current differencing buffered amplifier (1 current differencing unit with amplification + 1 voltage buffer)

^aProposed circuit utilized adjustable voltage gain to control CO, other circuits use current gain control

^bInformation is not available or feature is not possible

^cSpecial matching condition must be fulfilled for availability of this feature

^dMultiphase type with different phase shifts other than quadrature

Table 2 Comparison of oscillator solutions based on two active elements and selected types employing one, three, and more active elements (excluding solutions compared in Table 1)

Reference	Active elements	Number of passive/active elements	Quadrature outputs	Independent CO and FO	Amplitude dependent on tuning process/linear control of FO	Type of control	Type of output signal (current or voltage)	Additional voltage buffers or I/V converters are necessary (for voltage-mode operation)	Possibility of differential voltage quadrature outputs without additional modification and buffering	Floating capacitor(s)
[71]	CCII	6/3 (5/2)	Yes	Yes	No/Yes	Passive elements	Voltage	Yes	No	No
[25]	CFA	5/2	No	Yes	No/No	Passive elements	Both	No	No	Yes
[24]	CFA	6/2 (9/3)	No	Yes	No/No	FET (DC voltage)	Voltage	No	No	No
[51]	CFA	5/2	No	Yes	No/No	Passive elements	Voltage	No	No	No
[48]	DVCC	5/3	Yes	Yes	Yes/No	Passive elements	Current	Yes	No ^a	No
[32]	GCFTA, VB	4/2	Yes	Yes	Yes/No	Passive elements	Voltage	Yes ^b	No	No
[34]	CCCII	2/2	No	Yes	Yes/No	R _x	Voltage	Yes	No	No
[66]	CC-CFA	2/2	No	Yes	No/No	R _x	Voltage	No	No	No
[41]	DO-OTA	2/3-6	–	Yes	–	g _m	Current	Yes	No	No
[59]	OTA	2/3(4)	Yes	Yes	No/Yes	g _m	Voltage	Yes	No	No
[65]	OTA	3/2 (5/2)	No	Yes ^c	Yes/No	g _m	Voltage	Yes	No	No
[46]	OTA	2-3/2-4	Yes	Yes ^d	Yes ^d	g _m	Voltage	Yes	No	Yes ^c
[85]	OTA	3-7/2	–	Yes	Yes/No	g _m	Voltage	Yes	No	No
[22]	DO-OTA	4/4	Yes	Yes	No/Yes	g _m	Voltage	Yes	No	No
[10]	MO-OTA	2/3	Yes	Yes	Yes ^f	g _m	Current	Yes	Yes ^e	No
[43]	CCTA	4/1	Yes	Yes	Yes/No	g _m	Both	Yes	No ^f	No
[72]	MO-OTA	3/2	No	No	No/No	g _m	Both	Yes	No ^g	No
[70]	CCII, VB, CFA	4-6/2	No	Yes ^h	–	Passive elements	Both	Yes ^h	No	Yes
[27]	CF, VF (VB)	5/2-4	Yes ⁱ	Yes	Yes/No	Passive elements	Both	Yes	No	No
[26]	CF, VF (VB)	5/2	No	Yes	–	Passive elements	Voltage	No	No	Yes

Table 2 (Continued)

Reference	Active elements	Number of passive/active elements	Quadrature outputs	Independent CO and FO	Amplitude dependent on tuning process/linear control of FO	Type of control	Type of output signal (current or voltage)	Additional voltage buffers or I/V converters are necessary (for voltage-mode operation)	Possibility of differential voltage quadrature outputs without additional modification and buffering	Floating capacitor(s)
[50]	CF, VF (VB)	5/6	No ^j	Yes	–	Passive elements	Voltage	No	No	No
[13]	DO-CIBA	5-6/2	Yes	Yes	No/Yes	Passive elements	Voltage	No	Yes	No
[28]	CFA	5/2	–	Yes	Yes/No	Passive elements	Voltage	No	No	No
[29]	CFA	5/2	k	Yes	Yes/No	Passive elements	Voltage	No	No	No
[57]	ZC-CDTA	2/2	Yes	h	h	g_m	Current	Yes	No	No
[36]	CCCDTA	2/2	Yes	Yes	No/Yes	R_{x+} , g_m	Current	Yes	No	No
[45]	CDTA	3/2	Yes	Yes	Yes/No	g_m	Both	Yes	No ^g	No
[42]	DO/MO-CCII	4/2	Yes	Yes	No/Yes	Passive elements	Current	Yes	No	No
[47]	CCII	5/2	No	Yes	Yes/No	Passive elements	Voltage	Yes	No	No
[44]	CFA	6/3	Yes	Yes	–	Passive elements	Voltage	No	No	No
[38]	CDTA	6/2	Yes	Yes	No/Yes	Passive elements	Current	Yes	No	Yes
[37]	CDBA	8/2	Yes	No	–	Passive elements	Current	Yes	No	Yes
[53]	OTA, OPAMP	0/7	Yes	–	–	Passive elements	Voltage	Yes	No	–
[33]	VDIBA	3/2	Yes	No ^l	–	g_m	Both	No	No	–
PROPOSED						g_m	Voltage	Yes	Yes ^l	Yes
Our	CG-CFDOBA, CG-BCVA	5/2	Yes	Yes	No/Yes	B, A	Voltage	No	Yes	No

Table 2 (Continued)

A—adjustable voltage gain; B —adjustable current gain; g_m —transconductance (controllable by bias current); R_x —intrinsic resistance (controllable by bias current); CCII—second generation current conveyor; CCCII—translinear current conveyor/current-controlled CCII; CCTA—current conveyor transconductance amplifier; CCCTA—current-controlled current conveyor transconductance amplifier; CCCDTA—current-controlled CDTA; CDBA—current differencing buffered amplifier; CDTA—current differencing transconductance amplifier; CFA—current feedback amplifier; CC-CFA—current-controlled current feedback amplifier; DBTA—differential-input buffered and transconductance amplifier; DO-CCII/CCCII—dual output CCII/dual output CCCII; DO-OTA—dual output OTA; DVCC—differential voltage current conveyor; GCFTA—generalized current follower transconductance amplifier; MCDTA—modified CDTA; MO-CCII/CCCII—multiple output CCII/multiple output CCCII; OPAMP—operational amplifier; OTA—operational transconductance amplifier; VB—voltage buffer (or voltage follower—VF); VDIBA—voltage differencing inverting buffered amplifier; – information is not available or feature is not possible

^aFour-phase output available in current-mode (additional IV converters and buffers necessary)

^bOne voltage output is buffered

^cSome of discussed circuits allow independent CO and FO control, some realizations have floating capacitors

^dLiterature [46] deals with several oscillators, one of which is quadrature with linear control of FO and amplitudes independent of tuning process

^eCircuit was designed as differential quadrature type but requires two times higher number of passive elements (capacitors) than single-ended solution presented in [59]

^fSolutions allow linear control of FO, but CO is quite uncomfortable (one g_m must be equal or higher than g_m adjusting FO if linear tuning of FO is required), additional one inverted signal for four-phase (differential current-mode operation) is required

^gFour-phase (diff. quadrature) operation available after additional modification (two voltage output signals available directly, two current output signals required transformation to voltage and buffering)

^hCO is independent of FO if special matching condition (equality of both controllable parameters) is fulfilled, however start of oscillation and CO control is complicated (only value of capacitors influence CO theoretically), some solutions require voltage buffer, some (employing CFA) do not

ⁱTwo realizations in [27] are quadrature, some from other proposed types have quadrature outputs only if matching conditions are fulfilled

^jReplacement of some active elements is necessary (author's recommendation) for generation of quadrature signals

^kSome realizations allow quadrature outputs, some require fulfilling of matching condition

^lFour-phase outputs available simultaneously, but voltage buffers necessary for operation independent of load connection, CO controllable electronically, adjusting of FO not possible in [33]

admittance networks [70], or more complicated synthesis approaches [85], which unfortunately do not always provide solutions which are suitable for our requirements.

Our main required features are: (1) independent CO and FO control, (2) differential quadrature outputs (four-phase) for voltage-mode implementation (buffered for low impedance load), (3) linear control of FO, (4) equal and unchangeable amplitudes during the FO tuning process, (5) no additional matching condition required for linear control of FO, and (6) easily adjustable CO by circuit for amplitude stabilization and simple implementation of AGC.

Several oscillator solutions are compared in the following text. Many of them do not allow quadrature outputs [24–26, 34, 47, 50, 51, 65, 66, 70, 72, 85] or only allow quadrature operation after fulfilling some matching condition [27, 29]. The main problem of the reported solutions is to achieve all the required features simultaneously. If the above-mentioned problems are fulfilled, there are also other drawbacks (additional current-to-voltage (I/V) conversion of output signals [10, 27, 36, 38, 41–43, 45, 48, 53, 57, 70, 72], buffering [22, 27, 32–34, 37, 43, 45–47, 59, 65, 70–72, 85] etc.; see the comments following Table 2). The most similar or the same features and parameters compared with our solution (number of active and passive elements) are offered by the circuits in [22] and [13], as is clear from Table 2. However, the solution discussed in [22] allows differential quadrature generation but requires four active elements and additional buffering of outputs (high impedance nodes). The situation is similar for the oscillator reported in [13], where almost all the discussed problems were solved. However, no type of electronic control is discussed in [13] (simultaneous change of two resistors for linear control of FO is required), and CO is controllable only by the replacement of the floating resistor with an opto-coupler. None of the discussed two active element-based solutions allows similar features to those of our proposed circuit. The situation is simpler in our case. CO is controllable by an adjustable voltage gain in the frame of the CG-BCVA element.

Some simple one- or two-active element-based solutions require special matching conditions (equality of two resistors or parameters of active elements) for linear adjustment of FO and fulfillment of CO (marked by ^c in Table 1, and by ⁱ in Table 2). A typical example in the case of Ref. [57] has the following form (for transconductance control): CO: $C_1 g_{m1} = C_2 g_{m2}$; FO: $\omega_0 = \sqrt{\frac{g_{m1} g_{m2}}{C_1 C_2}}$ (adjustable parameters $g_{m1} = g_{m2}$ for fulfilled CO and for linear FO tuning simultaneously). One transconductance is determined for CO control and the other one for FO adjusting. However, both adjustable parameters (two resistors, two transconductances, etc.) have to be matched if linear control of FO is required; moreover, the CO is given by equality of capacitance values [57, 70, 79]. This is the main drawback of some previously published circuits, because only capacitor values are suitable for the startup of oscillation (implementing an AGC circuit for wideband FO adjustment without fluctuation of the output amplitude is not easy task). Therefore, we used two adjustable current gains for independent linear FO control and one voltage gain for CO control without matching constraints between them in our work.

In this work, we introduce a new type of oscillator utilizing a current follower differential output buffered amplifier (CFDOBA) and a novel modification of the active element, called the controlled gain-buffered current and voltage amplifier (CG-BCVA). We introduced several remarks and possible applications in [74] without

deep analysis and evaluation. In comparison to the conception of the current conveyor presented by Marcellis et al. [49], where the voltage gain was adjusted between the Y and X terminals and the current gain was adjusted between the X and Z ports of the current conveyor, our solution utilizes a different approach. This approach includes separate adjustable current and voltage amplifiers in the frame of the BCVA element. Some similarity to the well-known CFAs [24, 25, 28, 29, 44, 62] exists. However, the CFDOBA and BCVA do not require a current conveyor part [67, 68, 82], unlike the CFA [24, 25, 28, 29, 44, 62]. The CFDOBA, BCVA, and CFA have current-mode and voltage-mode parts, i.e., a current conveyor (voltage and current input terminals) and simple voltage buffer in the case of the CFA, an adjustable current amplifier (only a current input terminal) and a voltage buffer/inverter in the case of the CFDOBA, and an adjustable voltage amplifier in the case of the BCVA. Nevertheless, the standard CFA contains an input voltage terminal Y (this terminal is required in circuit synthesis [24, 25, 28, 29, 44] based on the CFA and its applications), and does not allow buffered direct and inverted voltage outputs simultaneously or any kind of direct electronic control in application. To the best of the authors' knowledge, no similar active element (CG-BCVA) or its application in oscillators with controllable features has been reported in the open literature so far.

2 Active Elements with Gain Control Features

The principle of the active elements used is described in the following text. The current follower differential output buffered amplifier (CFDOBA) was introduced in [12], a similar type, called the current inverter buffered amplifier (CIBA) was introduced in [13], and its controllable derivative was presented in [74] (controlled gain CIBA: CG-CIBA). It seems to be a very suitable active element for electronically adjustable applications in signal processing. We used a modified version of the CFDOBA, called the controlled gain-current follower differential output buffered amplifier (CG-CFDOBA), where current gain (B) adjusting is allowed. The symbol, behavioral model, and a possible construction based on commercially available ICs are depicted in Fig. 1. This active element has the following terminals: a low impedance current input terminal p , an auxiliary high impedance current output terminal z , and two low impedance voltage outputs w (noninverting and inverting). An additional auxiliary terminal allows control of the current gain between terminals p and z . This terminal is called V_{SET_B} in our case, because it provides gain control via DC voltage [74]. The following matrix equations describe the ideal behavior:

$$\begin{bmatrix} I_z \\ V_{w+} \\ V_{w-} \\ V_p \end{bmatrix} = \begin{bmatrix} 0 & 0 & 0 & B \\ 1 & 0 & 0 & 0 \\ -1 & 0 & 0 & 0 \\ 0 & 0 & 0 & 0 \end{bmatrix} \cdot \begin{bmatrix} V_z \\ I_{w+} \\ I_{w-} \\ I_p \end{bmatrix}. \quad (1)$$

An improved conception of the CFDOBA allows controllability of both current and voltage gains simultaneously in the frame of one active element, and it is a useful approach for the design of controllable applications. We called this modification the

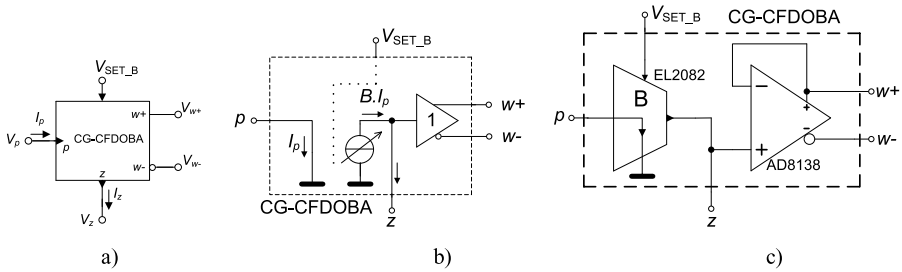


Fig. 1 Controlled gain-current follower differential output buffered amplifier (CG-CFDOBA): (a) symbol, (b) behavioral model, (c) possible implementation using commercially available ICs

controlled gain-buffered current and voltage amplifier (CG-BCVA). A detailed explanation is provided in Fig. 2, where the symbol, behavioral models, and a possible practical implementation employing readily available ICs are shown. The terminals of the presented active element provide more possibilities than CG-CFDOBA; however, many of them have the same purpose. Low impedance current input terminal p , auxiliary high impedance terminal z , and low impedance voltage output terminals w_{\pm} have the same meanings as for the CG-CFDOBA (see Fig. 1). The CG-BCVA has additional dispositions. This active element was first used in [74] only theoretically in the controlled gain-current and voltage amplifier (CG-CVA) and the controlled gain-inverted current and voltage amplifier (CG-ICVA). The CG-CVA and CG-ICVA use a voltage amplifier with adjustable voltage gain (A), unlike the CG-CFDOBA, where only a voltage buffer/inverter is used. Control of current and voltage gains is separated into two auxiliary terminals (two controlling DC voltages, V_{SET_B} and V_{SET_A} , respectively). Terminal w is a low impedance voltage output of the voltage amplifier for the CG-CVA or CG-BCVA. The additional voltage buffer, which can also be used as an inverter (see Fig. 2c), gives an interesting advantage in multi-loop circuit synthesis. The output(s) of the voltage buffer is (are) marked by b .

The ideal behavior of the CG-BCVA is defined by the following matrix equations:

$$\begin{bmatrix} I_z \\ V_w \\ V_b \\ V_p \end{bmatrix} = \begin{bmatrix} 0 & 0 & 0 & B \\ A & 0 & 0 & 0 \\ 1 & 0 & 0 & 0 \\ 0 & 0 & 0 & 0 \end{bmatrix} \cdot \begin{bmatrix} V_z \\ I_w \\ I_b \\ I_p \end{bmatrix}, \tag{2}$$

$$\begin{bmatrix} I_z \\ V_w \\ V_{b+} \\ V_{b-} \\ V_p \end{bmatrix} = \begin{bmatrix} 0 & 0 & 0 & 0 & B \\ A & 0 & 0 & 0 & 0 \\ 1 & 0 & 0 & 0 & 0 \\ -1 & 0 & 0 & 0 & 0 \\ 0 & 0 & 0 & 0 & 0 \end{bmatrix} \cdot \begin{bmatrix} V_z \\ I_w \\ I_{b+} \\ I_{b-} \\ I_p \end{bmatrix}, \tag{3}$$

where Eq. (2) represents the model of the CG-BCVA in Fig. 2b and Eq. (3) the model in Fig. 2c, respectively. Adjustable gains are very useful for oscillator design, as is obvious from the designed solution that will be presented.

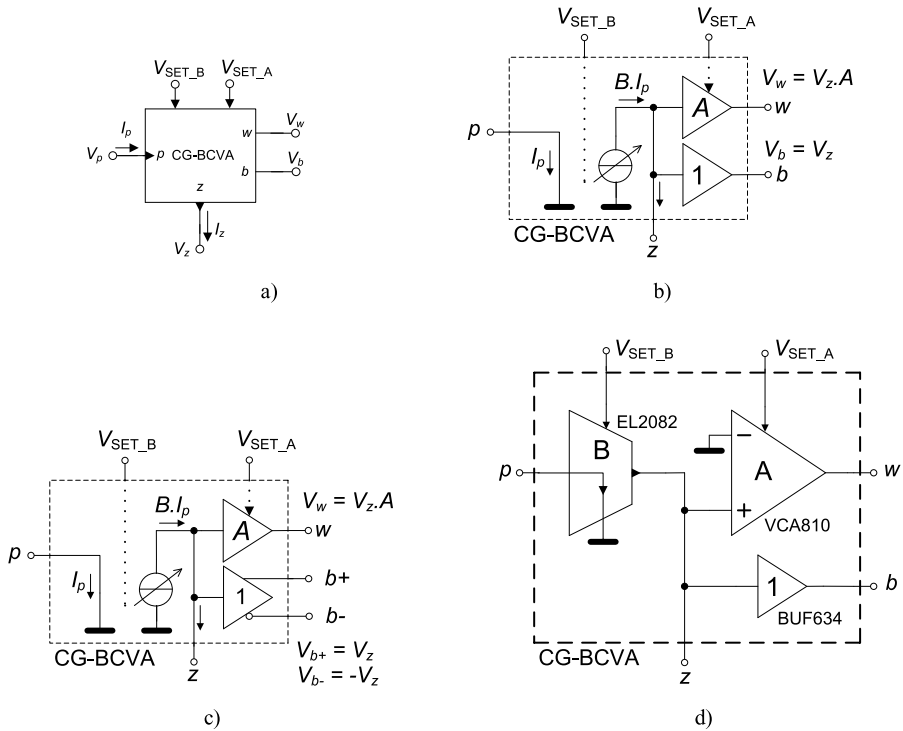


Fig. 2 Controlled gain-buffered current and voltage amplifier (CG-BCVA): (a) symbol, (b) behavioral model, (c) behavioral model with additional inverting buffer output, (d) possible implementation using commercially available ICs (version without additional inverting output)

3 Multiphase Oscillator with Linear Control of Oscillation Frequency and Automatic Control of Oscillation Condition

We used the above discussed active elements to design a precise adjustable oscillator with multiphase output properties. The proposed circuit and its modification are shown in Fig. 3. The theory of the synthesis principle is the following. We put two integrators (lossy and lossless) in a closed loop, where one integrator was complemented by a negative resistance. We created this part by using an adjustable voltage amplifier in the frame of the CG-BCVA and resistor R_3 . The characteristic equation (CE) has the following form:

$$CE: s^2 + \frac{R_1 + R_3 - R_1 A_2}{R_1 R_3 C_2} s + \frac{B_1 B_2}{R_1 R_2 C_1 C_2} = 0. \tag{4}$$

The condition of oscillation (CO) and frequency of oscillation (FO, ω_0 , f_0) are:

$$CO: A_2 \geq 1 + \frac{R_3}{R_1}, \tag{5}$$

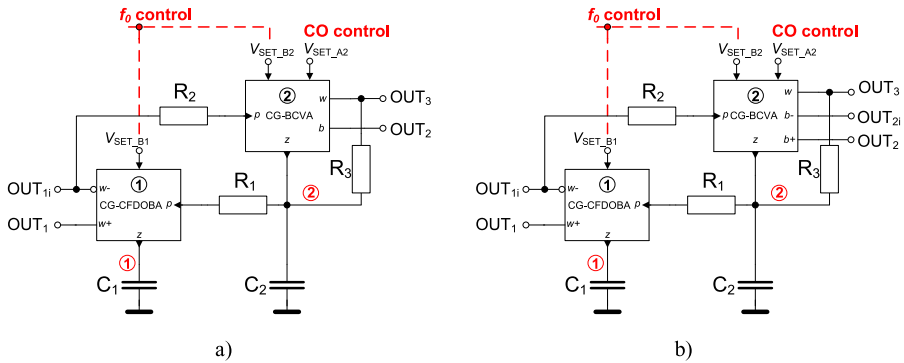


Fig. 3 Tunable multiphase oscillator employing two active elements based on controlled gains: **(a)** basic solution, **(b)** modification for differential quadrature signal generation

$$FO: \omega_0 = \sqrt{\frac{B_1 B_2}{R_1 R_2 C_1 C_2}} \tag{6}$$

The relative sensitivities of oscillation frequency (6) on the values of the passive elements and current gains are theoretically equal to ± 0.5 . An analysis of the relations between generated signals (high impedance nodes, voltage across capacitors) is provided as follows:

$$\frac{V_{C1}}{V_{C2}} = \frac{B_1}{s R_1 C_1} = \frac{B_1}{j \omega R_1 C_1} = -j \sqrt{\frac{R_2 C_2 B_1}{R_1 C_1 B_2}} \tag{7}$$

Considering the equality of both current gains ($B_1 = B_2 = B_{1,2}$), Eq. (7) is simplified as

$$\frac{V_{C1}}{V_{C2}} = -j \sqrt{\frac{R_2 C_2}{R_1 C_1}} \tag{8}$$

A simultaneous change of the current gains of both active elements, i.e., $B_1 = B_2 = B_{1,2}$ ($V_{SET_B1} = V_{SET_B2}$) ensures linear control of FO, and voltage gain A_2 (V_{SET_A2}) allows control of CO and amplitude stability from an external precise (automatic) amplitude gain control circuit (AGC). In the basic variant (Fig. 3a), four low impedance voltage outputs are available. Output voltages V_{OUT1} (terminal $w+$ of CG-CFDOBA) and V_{OUT2} (b terminal of CG-BCVA) have a quadrature phase shift, which is a consequence of (8). Output voltage V_{OUT1i} is available at terminal $w-$ of CG-CFDOBA, and represents inversion of V_{OUT1} . The generated voltage at the w of CG-BCVA has same phase as V_{OUT2} ; the only difference is caused by amplification between w and b of CG-BCVA. The solution in Fig. 3a produces three signals with phase shifts of 90 and 180 degrees. The oscillator introduced in Fig. 3b is suitable for four-phase generation or differential quadrature signal generation because terminals (outputs of CG-BCVA) $b+$ (V_{OUT2}) and $b-$ (V_{OUT2i}) are not influenced by gain A_2 (V_{OUT3}), which sets CO during the tuning process. Differential quadrature signals

are available at OUT_1 , OUT_{1i} and OUT_2 , OUT_{2i} in the case of Fig. 3b. The solution from Fig. 3a is analyzed in detail in the following sections.

The state variable method of synthesis ([28, 29], for example) could also be used to obtain this oscillator. However, such sophisticated methods are not necessary for this quite simple circuit; cascading integrators and negative resistance are sufficient to complete the proposed oscillator. Examples of circuits derived by state variable methods were reported in the impressive works written by Gupta and Senani [28, 29]. Many oscillator structures, including current feedback amplifier (CFA)-based integrators (in fact) in loops constructed by the state variable methods were introduced in the works [28, 29]. The oscillators in [29] utilize simpler active elements (a lower number of outputs) than the solution described in our contribution. Unfortunately, the solutions reported in [28, 29] belong to the family of single resistance controllable types (electronic control is more complicated), and also utilize high impedance voltage inputs (Y terminal of CFA), and relations between amplitudes exist in the case of tuning. Requirements to have both stable quadrature amplitudes while the oscillator is tuned are demanded in many communication systems [11], and our solution fulfills these specifications.

4 Real Behavior and Experimental Results

Knowledge of the expected behavior and influences of real active elements is necessary for practical utilization of the proposed circuit in complex communication systems. Non-ideal models of the active elements are shown in Fig. 4. We can neglect some parameters (for example, the output resistances of w and b —these are very low values below 1Ω) because their effect on function is insignificant. However, the influences of real parameters of the p and z terminals are very important and they affect at least FO (small or large shift) and CO.

We built a behavioral model of both active elements for real laboratory experiments from commercially available ICs in order to verify the functionality (fabrication of one's own IC structures is very time-consuming and expensive). In our opinion, if the circuit built from discrete commercially available elements works well, then the appropriate IC version consisting of current amplifiers, voltage amplifiers,

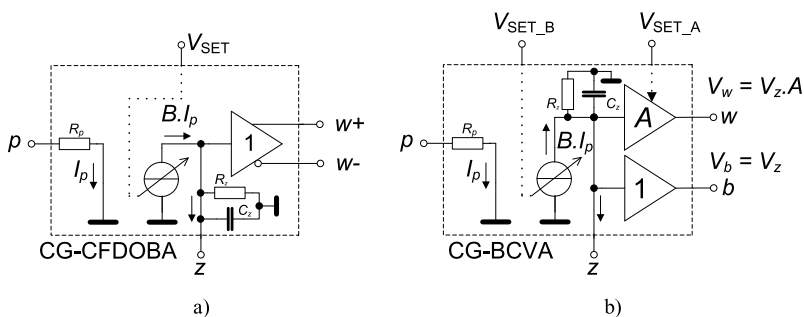
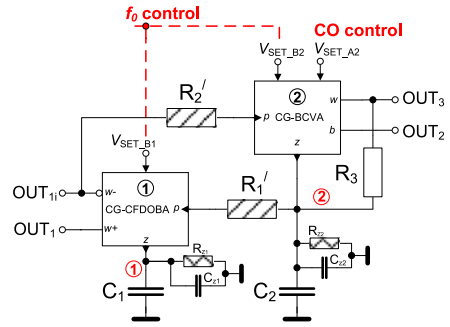


Fig. 4 The most important non-idealities of real active elements: (a) CG-CFDOBA, (b) CG-BCVA

Fig. 5 Model of proposed oscillator for non-ideal analysis



and buffers (designed via actual IC technology) will work even better. A model of the oscillator, where important influences are highlighted by hatched and small elements, is shown in Fig. 5.

We established a behavioral model of the CG-CFDOBA using current-mode multiplier EL2082 [16] and differential voltage amplifier AD8138 [2] as voltage buffer/inverter (full negative feedback). The parameters of the CG-CFDOBA are as follows: intrinsic resistance of current input terminal of current-mode multiplier p is $R_{p1} \approx 95 \Omega$ (EL2082 [16]), resistance of auxiliary high impedance terminal z is $R_{z1} \approx 860 \text{ k}\Omega$ (output impedance of current-mode multiplier and input impedance of voltage buffer: $1 \text{ M}\Omega \parallel 6 \text{ M}\Omega$ in parallel [2, 16]), and capacitance of high-impedance terminal z is $C_{z1} \approx 6 \text{ pF}$ (capacitance of current output of EL2082 and input capacitance of AD8138 in parallel: $5 + 1 \text{ pF}$ [2, 16]).

The real parameters of the CG-BCVA, namely R_{p2} , are similar ($R_{p2} \approx 95 \Omega$) to those for the CG-CFDOBA (the real behavioral model also utilizes EL2082). We expect the main difference to be at terminal z , where three instead of two partial blocks (current amplifier, voltage amplifier, and buffer) are interconnected. The estimated value of the impedance of terminal z is $R_{z2} \approx 470 \text{ k}\Omega$ (current output resistance of EL2082, input resistance of adjustable voltage amplifier VCA810 [86], and input resistance of voltage buffer BUF634 [14]: $1 \text{ M}\Omega \parallel 1 \text{ M}\Omega \parallel 8 \text{ M}\Omega$), $C_{z2} \approx 14 \text{ pF}$ (output capacitance of EL2082, input capacitance of VCA810, and input capacitance of BUF634: $5 + 1 + 8 \text{ pF}$).

We selected the external passive elements as $R_1 = R_2 = 910 \Omega$, $R_3 = 1 \text{ k}\Omega$, and $C_1 = C_2 = 47 \text{ pF}$. The elements highlighted in Fig. 5 have the following estimated values: $R'_1 = R'_2 \approx R_1 + R_{p1} \approx R_2 + R_{p2} \approx 1005 \Omega$ [16], $R_{z1} \approx 860 \text{ k}\Omega$, $C_{z1} \approx 6 \text{ pF}$, and $R_{z2} \approx 470 \text{ k}\Omega$, $C_{z2} \approx 14 \text{ pF}$. We included the values of C_{z1} and C_{z2} to obtain $C'_1 \approx C_1 + C_{z1} \approx 53 \text{ pF}$ and $C'_2 \approx C_2 + C_{z2} \approx 61 \text{ pF}$. The influence of the printed circuit board was not estimated. A careful routine analysis provides the following results in the form of more accurate design equations (CO and frequency) considering important non-idealities:

$$\text{CO: } A'_2 \geq \frac{R'_2 R_{z1} R_{z2} C'_1 (R'_1 + R_3) + R'_1 R'_2 R_3 (R_{z1} C'_1 + R_{z2} C'_2)}{R'_1 R'_2 R_{z1} R_{z2} C'_1}, \tag{9}$$

$$\text{FO: } \omega'_0 = \sqrt{\frac{B_1 B_2 R_3 R_{z1} R_{z2} \alpha_1 + [R'_1 R'_2 R_{z2} (A_2 - 1) - R'_2 R_3 (R'_1 + R_{z2})]}{R'_1 R'_2 R_3 R_{z1} R_{z2} C'_1 C'_2}}, \tag{10}$$

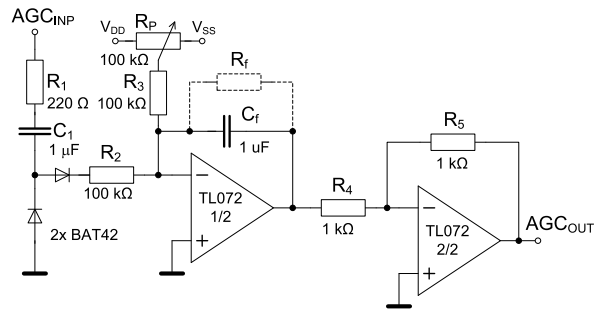
Table 3 Impact of inaccurate voltage buffering on $f_0 = 3$ MHz ($B_{1,2} = 1.1$)

Toler. α_1 [%]	α_1 [-]	$\pm\Delta f_0$ [kHz]
± 10	0.90–1.10	153
± 5	0.95–1.05	77
± 2	0.98–1.02	31

Table 4 Approximate magnitude difference of terms of (9)

$B_{1,2}$ [-]	$B_1 B_2 R_3 R_{z1} R_{z2}$	$R'_1 R'_2 R_{z2} (A_2 - 1) - R'_2 R_3 (R'_1 + R_{z2})$
10	10^{16}	10^9
1	10^{14}	10^9
0.1	10^{12}	10^9
0.01	10^{10}	10^9

Fig. 6 Amplitude-automatic gain control circuit for wideband amplitude stabilization



where α_1 represents the non-ideal voltage gain (transfer) of the voltage buffer (in the frame of the CG-CFDOBA). The expected and measured oscillation frequency achieves a value $f_0 = 3$ MHz for selected parameters ($R_1 = R_2 = 910 \Omega$, $R_3 = 1 \text{ k}\Omega$, $C_1 = C_2 = 47 \text{ pF}$), and $B_1 = B_2 = B_{1,2} = 1.1$ ($V_{SET_B1} = V_{SET_B2} = V_{f0_control} = 1.15 \text{ V}$). Paper [16] explains the relation between the current gain B and control DC voltage ($B \approx V_{SET}$, exactly valid for $V_{SET} < 2 \text{ V}$). The impact of an inaccurate buffer gain (α_1) on the deviation Δf_0 (worst case) based on (9) and for above discussed setting ($f_0 = 3$ MHz) was analyzed, and the results are given in Table 3.

The second term in the numerator of (9) has minimal impact on the overall value of f_0 if $B_{1,2} > 0.1$ ($A_2 = 2$), because it has a lower value (more than 100 times for real parameters, see Table 4) in comparison to the first term (α_1 supposes equality to 1 in this calculation).

The circuit in Fig. 3 requires an amplitude gain control circuit (AGC). We used one of the more suitable solutions, as shown in Fig. 6. Classical low-cost and low-frequency operational amplifiers and diode doublers are sufficient for these purposes. Resistor R_f sets the slope of the input-output characteristic of the AGC circuit (integrator), which ensures smaller or more extensive reactions to amplitude changes (R_f achieves values from ∞ to hundreds of $\text{k}\Omega$). Because VCA810 requires a negative and decreasing DC control voltage to increase the output signal level, a voltage inverter is necessary. The outputs of the multiphase oscillator can be available as the

Fig. 7 Transient responses at all available outputs (V_{OUT1} - blue, V_{OUT1i} - green, V_{OUT2} - red, V_{OUT3} - orange) for $B_{1,2} = 1.1$ ($V_{f0_control} = 1.15$ V)

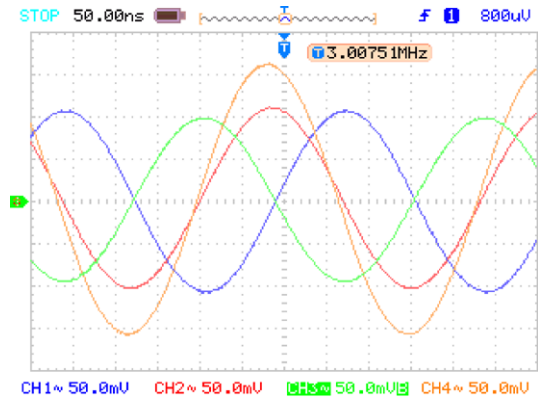
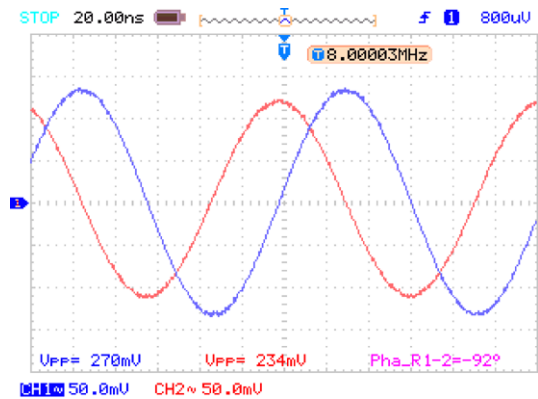


Fig. 8 Transient responses at V_{OUT1} and V_{OUT2} for $B_{1,2} = 2.9$ ($V_{f0_control} = 3.17$ V)



input of the AGC circuit (except for OUT_3), and the output of the AGC is connected to V_{SET_A2} .

Laboratory measurements of the circuit in Fig. 3a showed the following results. We used a RIGOL DS1204B oscilloscope and an HP4395A network vector/spectrum analyzer (50Ω matching of the oscillator outputs) for the experimental tests. The transient responses at all available outputs are depicted in Fig. 7. Detailed measurements for the quadrature signals across the working capacitors (buffered, of course) are shown in Fig. 8 for the highest measured $f_0 = 8$ MHz ($B_{1,2} = 2.9$; $V_{f0_control} = 3.17$ V). The related frequency spectra are shown in Fig. 9.

Figure 10 shows the dependence of f_0 on $B_{1,2}$ ($B_{1,2}$ was adjusted between 0.1–2.9). The ideal trace was calculated from Eq. (6). The ideal range of the f_0 adjustment was calculated as 0.337 to 9.776 MHz. The expected estimation based on the more accurate Eq. (10) provides a range from 0.279 to 8.077 MHz, and a range from 0.250 to 8 MHz was gained and verified by laboratory tests. We also tested the stability of the output level during the tuning process and the total harmonic distortion (THD); see Fig. 11. The stability of the output level during the tuning process changed slightly, and the output voltage of both observed outputs was close to 200 mV_{P-P} (Fig. 11a). The measured THD reached values lower than 0.5 % for f_0 above 2 MHz for both observed output responses (Fig. 11b).

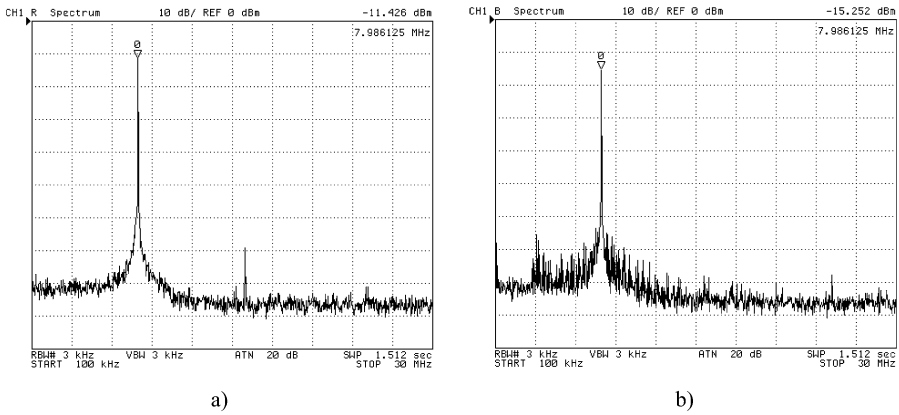


Fig. 9 Measured frequency spectra ($B_{1,2} = 2.9$): (a) for V_{OUT1} , (b) for V_{OUT2}

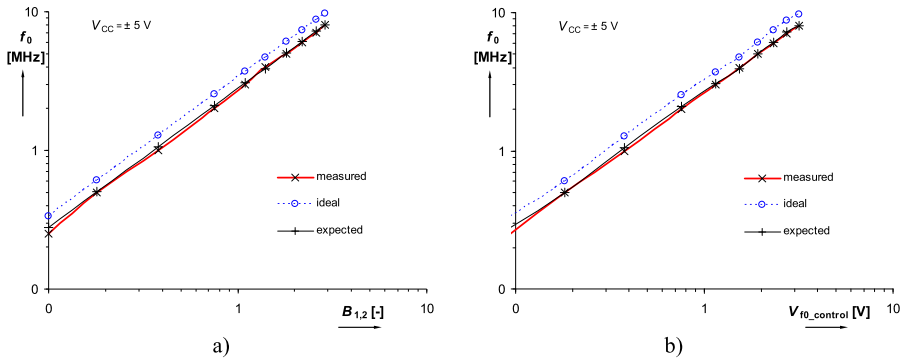


Fig. 10 Dependence of f_0 on: (a) adjustable current gains $B_{1,2}$, (b) control voltage which is setting $B_{1,2}$ ($V_{f0_control}$)

The phase error between available quadrature outputs was measured, and the results are shown in Fig. 12. Maximal deviation from -90° was up to $\pm 3^\circ$ (error $\pm 2.8\%$ from the nominal value).

5 CMOS Structures of Proposed Active Elements and Simulation Results

In this chapter we will present proposed CMOS implementations of the introduced active elements based on their behavioral descriptions shown in Fig. 1 and Fig. 2. We will also provide simulation results of their main features. The TSMC LO EPI 0.18 μm CMOS technology transistor models [55] were used in the simulations.

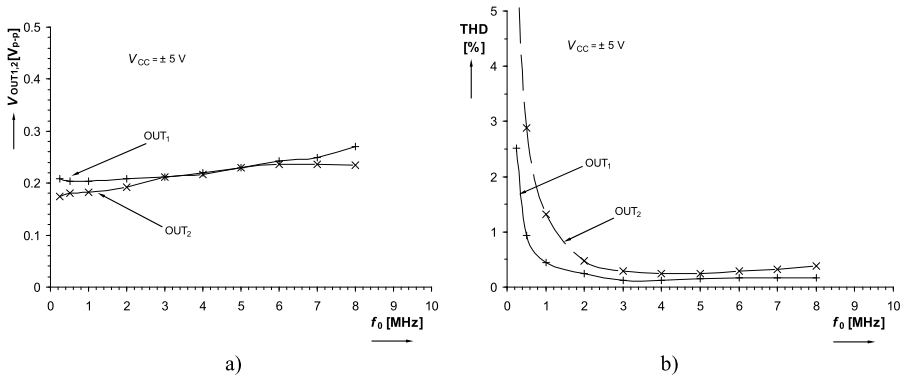


Fig. 11 Additional characteristics: (a) output levels (V_{OUT1} , V_{OUT2}) versus f_0 , (b) THD versus f_0

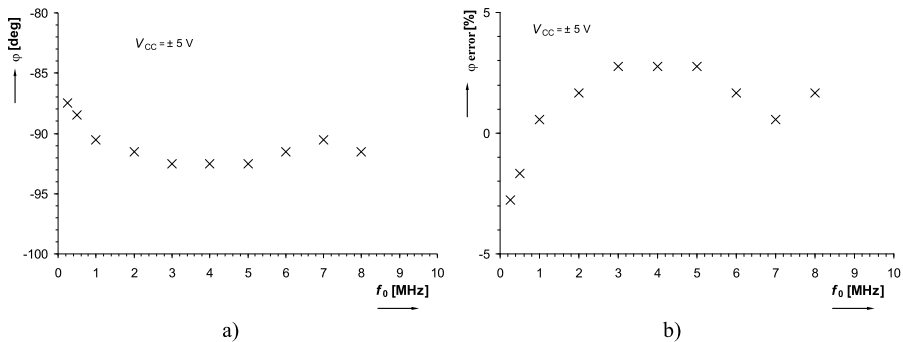


Fig. 12 Study of quadrature outputs: (a) phase shift dependence on f_0 , (b) phase error dependence on f_0

5.1 Controlled Gain-Current Follower Differential Output Buffered Amplifier (CG-CFDOBA)

The proposed CMOS implementation of the CG-CFDOBA is depicted in Fig. 13. The model consists of three important blocks in accordance with Fig. 1. The first part is the adjustable current amplifier. The input stage of this amplifier is solved as the input section of a classical current conveyor [20, 67, 68, 82]. The presented solution of the gain-controllable part is based on principles presented in [80], where bias current I_{SET_B} controls the current gain ($N = 2$, see Fig. 13):

$$B = \frac{N I_{b2}}{2 I_{set_B}} \cong \frac{I_{b2}}{I_{set_B}}. \tag{11}$$

The voltage buffer and inverter sub-blocks complete the whole active element. The buffer employs a simple transconductance amplifier [23] (a special type presented in [7, 89]) and a high-gain complementary MOS inverter in full negative feedback, which is beneficial due to its low output resistance. The voltage inverter utilizes the same structure, but the input signal of this section is inverted by a simple common-emitter follower. It is not favorable to use this common-emitter follower as is, because

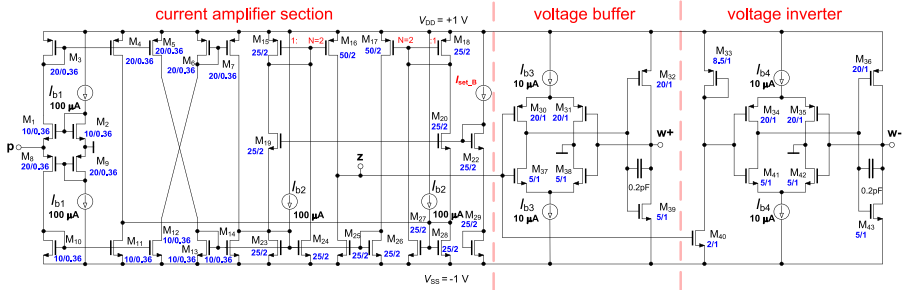


Fig. 13 Proposed CMOS model of the CG-CFDOBA

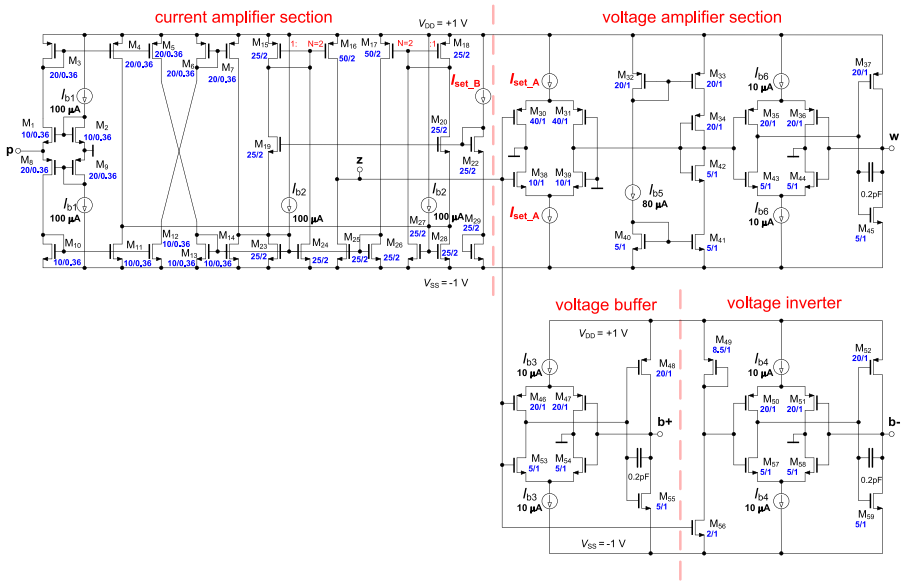


Fig. 14 Proposed CMOS model of the CG-BCVA

it has a quite high output impedance, and increasing the W/L ratio causes a higher drain current with resulting higher power consumption. Therefore, additional buffering is more suitable than using M_{33} and M_{40} transistors only at the location of the voltage inverter. Capacitors (0.2 pF) have frequency compensation purposes (high-frequency resonant peak of transfer characteristics).

5.2 Controlled Gain-Buffered Current and Voltage Amplifier (CG-BCVA)

The proposed CMOS implementation of the CG-BCVA shown in Fig. 14 employs the same sub-blocks as we discussed in the previous section and an additional voltage gain controllable section. The adjustable voltage amplifier utilizes a transconductance section and the electronic equivalent of a resistor [3, 87, 90] (a simple modification of the solution presented in [87]) at the current output terminal of the OTA; i.e.,

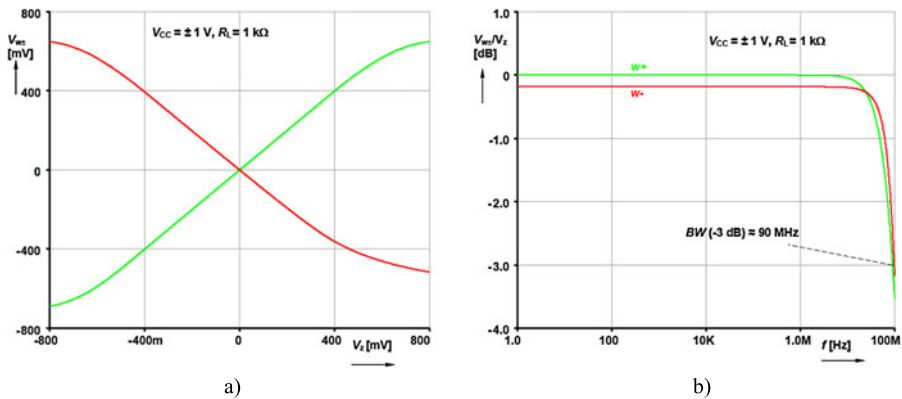


Fig. 15 Transfer characteristics of the voltage buffer/inverter part: (a) DC domain, (b) AC domain

the voltage gain A of this section is given as: $A = g_{mC} \cdot R_{eq}$. The high impedance output (OTA) is buffered. The overall transconductance g_{mC} can be calculated as $g_{mC} = (g_{mP} + g_{mN})/2$, where $g_{mN,P} = \sqrt{2I_{drain}K_{pN,P}W/L}$ ($K_{pN,P}$ is a fabrication constant given by the mobility of carriers and the gate oxide capacitance of the P or N MOS, and I_{drain} is derived from the bias current: $I_{drain} = 1/2I_{SET_A}$). The P and N MOS are supposed to have identical features in most cases; therefore, the W/L ratios (shown in blue in the figures) have to be matched to obtain almost identical P and N types (the P type has a more than four times longer W in comparison to the N type in many cases). An equivalent electronic resistor (R_{eq}) is given by g_m and g_{ds} for both the P and N types (M_{34} , M_{42}) and is controlled by a fixed bias current (small-signal $R_{eq} = 1/(g_{mM34} + g_{dsM34} + g_{mM42} + g_{dsM42})$).

5.3 Main Features of Sub-Blocks Used for Construction of CMOS Models

We have provided PSpice simulations of the presented CMOS models. The main features in the DC and AC domains of the voltage follower (buffer)/inverter sections are presented in Fig. 15.

The simulation results of the adjustable current amplifier are depicted in Fig. 16 for selected gains (B). The current gain adjustment was verified from 3.0 to 0.5 by a change of I_{SET_A} from 37 μA to 93 μA , respectively. The adjustable voltage amplifier was also tested for several selected values of voltage gain A , and the results are given in Fig. 17. The voltage gain was adjusted (in Fig. 17) from 0.5 to 2.5 by changing I_{SET_A} from 10 μA to 100 μA .

Replacement of the bias current by voltage is possible by an interchange of the appropriate illuminating current sources (I_{b3} , I_{b4} in Fig. 13, for example) by current mirrors (this modification was not provided in Figs. 13 and 14 because of their expected complexity and hard readability) and conversion of the bias voltage through a resistor connected to the current input of the mirrors. All the important and some additional (small-signal) parameters are summarized in Table 5 (for both active elements).

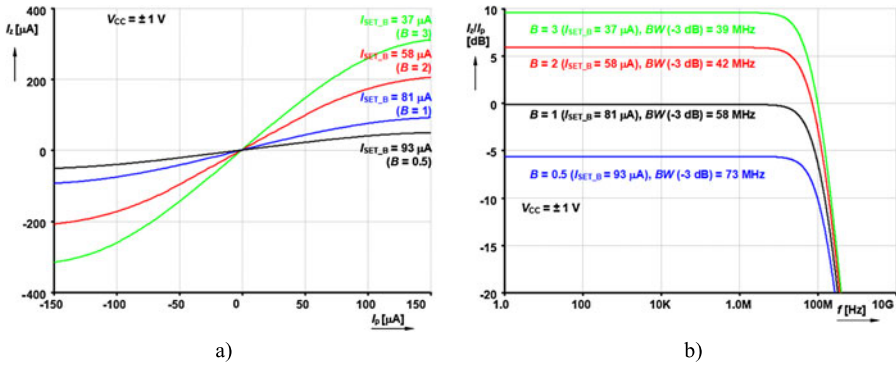


Fig. 16 Transfer characteristics of the adjustable current amplifier: (a) DC domain, (b) AC domain

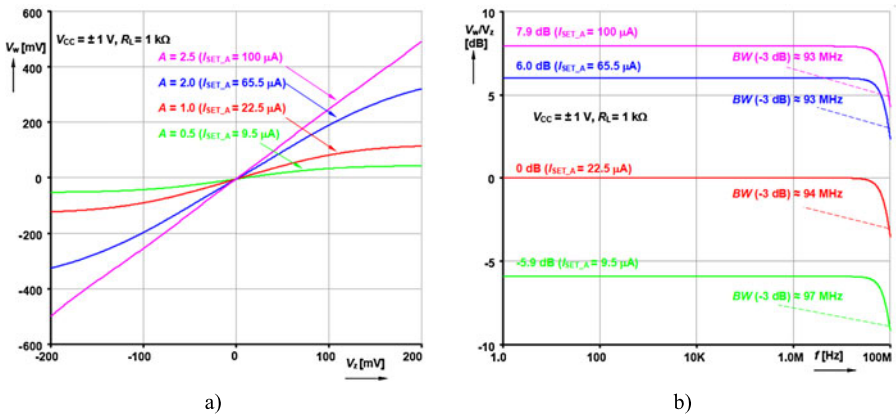


Fig. 17 Transfer characteristics of the adjustable voltage amplifier: (a) DC domain, (b) AC domain

Table 5 Achieved important parameters of sub-blocks of CG-CFDOBA and CG-BCVA

Controllable parameters	
Parameter	Tested range of adjustment
Current gain (B [-])	0.36–3.76 ($I_{SET_B} = 100 \mu\text{A}$ – $20 \mu\text{A}$)
Voltage gain (A [-])	0.3–2.5 ($I_{SET_A} = 5 \mu\text{A}$ – $100 \mu\text{A}$)
DC performances ($I_{SET_B} = 100 \mu\text{A}$, $I_{SET_A} = 22.5 \mu\text{A}$). TF analysis	
Parameter	Value
I_z/I_p [-]	0.35
V_w/V_z [-]	1.00
V_{b+}/V_z [-]	1.00
V_{b-}/V_z [-]	-0.98
R_p [Ω]	533
R_z [$k\Omega$]	55
R_w, R_{b+}, R_{b-} [Ω]	6

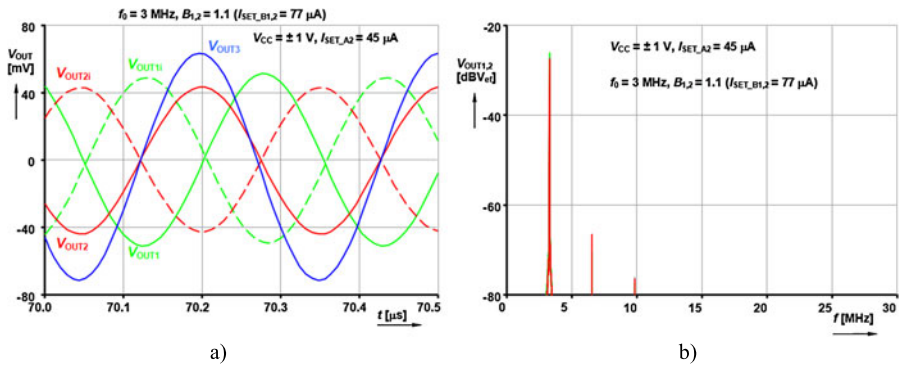


Fig. 18 Simulated responses of the CMOS model-based oscillator from Fig. 3b: (a) transient responses at all available outputs, (b) FFT spectrum for selected outputs

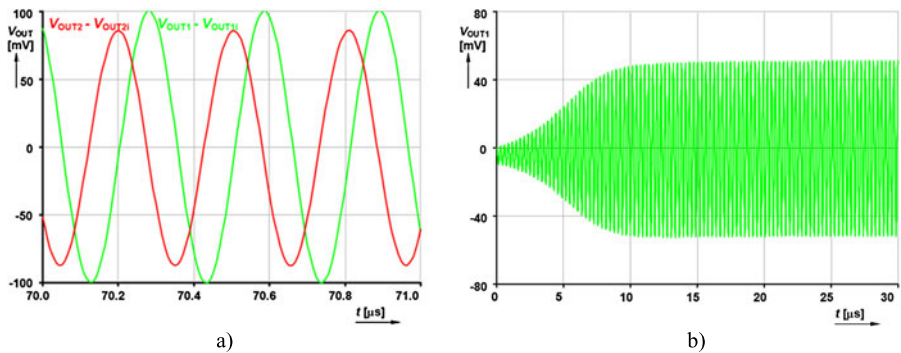


Fig. 19 Additional simulated characteristics: (a) differential-mode operation, (b) initial startup of the oscillation

5.4 Performances and Verifications of the Proposed Oscillator

The oscillator from Fig. 3b employing the above-discussed CMOS models of the CG-CFDOBA and CG-BCVA was analyzed in detail. The parameters of the circuit elements were selected as $R_{1,2} = 1 \text{ k}\Omega$ ($R_p = 533 \Omega + \text{external } 467 \Omega$), $C_{1,2} = 47 \text{ pF}$. The initial PSpice results (the transient responses and spectra are shown in Fig. 18 for all available outputs) are provided for $f_0 = 3 \text{ MHz}$, where the controllable parameters of the active elements had values $B_{1,2} = 1.1$ ($I_{SET,B} = 77 \mu\text{A}$). The calculated THD was 0.7 % (V_{OUT1} , V_{OUT1i}) and 1.1 % (V_{OUT2} , V_{OUT2i}), respectively. Inverting the outputs of both quadrature responses (V_{OUT1i} and V_{OUT2i}) allows differential-mode operation (more resistant to common-mode distortion and noise than single-ended solutions), and it offers the generation of two differential quadrature signals with a two times higher output level (Fig. 19a). Figure 19b shows an example of the initial startup of the oscillations. In the given results (Fig. 18, Fig. 19) the THD is at a sufficient level, but the generated amplitudes reached tens of millivolts only. We note that it is possible to operate with amplitudes of several hundreds of millivolts, but

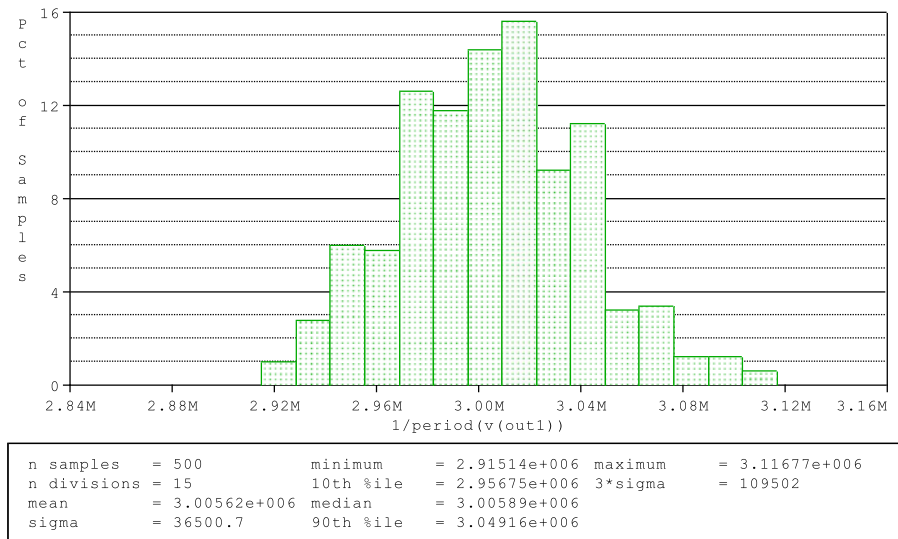


Fig. 20 Histogram of 500 simulation runs for 5 % value dispersion of bias control currents

simultaneously the THD increases rapidly due to nonlinearities of the DC transfer characteristics of the active elements (given by the low supply voltage).

6 Performances of the Oscillator Dependent on Important Mismatches and Temperature

The proposed oscillator was statistically evaluated using a Monte Carlo PSpice analysis. Our main object of interest was the fluctuation of f_0 changes caused by deviations of the control parameters ($B_{1,2}$). A Monte Carlo analysis was provided for the CMOS model-based oscillator as well as for the behavioral model (the same as the one we used for experimental purposes), because commercially available devices are easily accessible as macromodels for PSpice libraries. The influences of temperature change on the whole circuit with these macromodels were also studied.

6.1 Analysis of CMOS Model-Based Simulation Results

A Monte Carlo simulation (Gaussian distribution, 500 runs) was provided for 5, 10, and 20 % tolerances (dispersion of their values) of bias currents I_{SET_B1} and I_{SET_B2} . The obtained standard deviation of the oscillation frequency (FO) from the nominal value was $\Delta f_0 = \pm 37$ kHz (f_0 can be found between the minimal and maximal values, i.e., 2.915 MHz and 3.117 MHz—the worst case) for 5 % dispersion of bias currents (Fig. 20). Standard deviations of $\Delta f_0 = \pm 72$ kHz and ± 132 kHz were gained for 10 and 20 % tolerances, respectively.

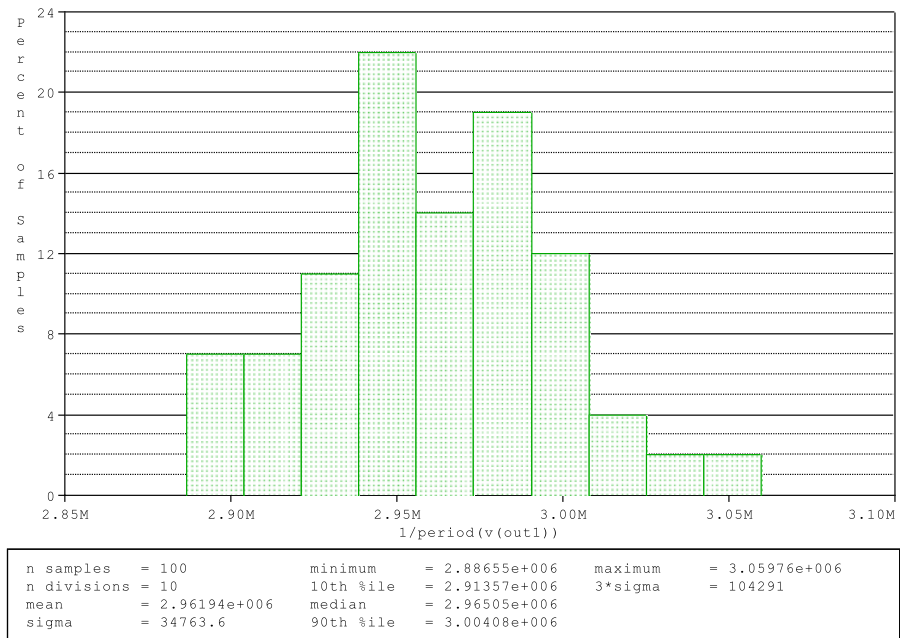


Fig. 21 Histogram of 100 simulation runs for 5 % value dispersion of control voltages

6.2 Analysis of Commercially Available Macromodel-Based Simulation Results

An analysis of behavioral representation, where $B_{1,2}$ gains were controlled by DC voltages (V_{SET_B}), achieved results similar to those presented in the previous section. A standard deviation (for 5 % dispersion of $V_{SET_B1,2}$ values) of $\Delta f_0 = \pm 35$ kHz (min.–max.: 2.887 MHz and 3.060 MHz) was obtained (Fig. 21). The number of runs is lower (only 100) due to the complexity of the simulated circuit (including sufficient time for the amplitude stabilization response of the AGC), and the analyses are very time-consuming (one Monte Carlo analysis set takes about 50 min). Standard deviations $\Delta f_0 = \pm 70$ kHz and ± 140 kHz were gained for 10 and 20 % dispersions of the $V_{SET_B1,2}$ values, respectively. Note that we also assume independent (not simultaneous) fluctuations of V_{SET_B1} and V_{SET_B2} , and hence also B_1 and B_2 . Influencing elements are also the working capacitors and their tolerances. Considering their impact, we find that $\Delta f_0 = \pm 44$ kHz (for 5 % tolerances of $V_{SET_B1,2}$, 5 % tolerances of working capacitors, and 1 % tolerances of working resistors).

6.3 Temperature Impact on Oscillator Performance

Temperature effects on the overall function (FO and CO) were also studied, and the analysis of the simulated behavioral model provided interesting results. We tried to analyze temperature fluctuations about 30 % from the nominal value $\theta = 27$ °C (it is approximately 20 °C to 35 °C). The results are given in Fig. 22. The amplitude of the generated signal changed very slightly (the AGC system compensates these variations very well). The most important impact of temperature change was on f_0 . The

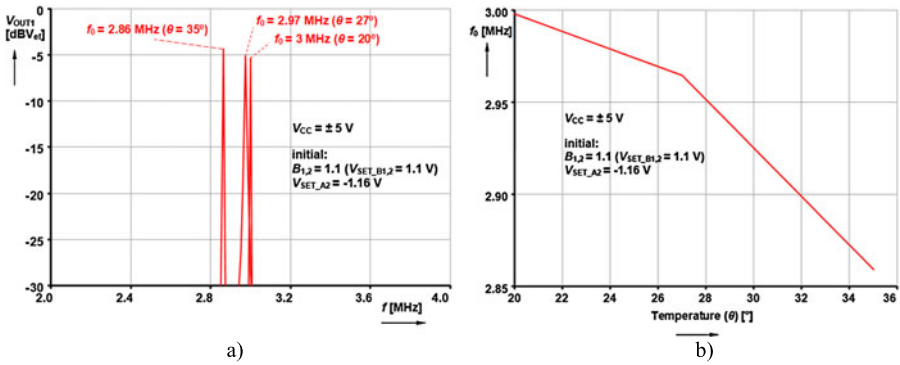
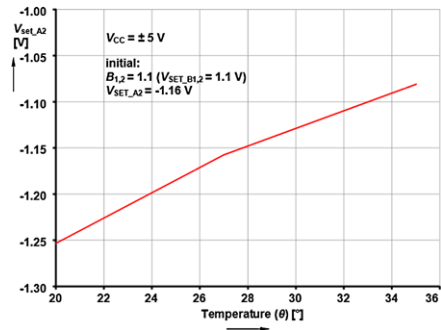


Fig. 22 Temperature effects on oscillation frequency: (a) detail in spectrum, (b) simulated dependence

Fig. 23 Temperature effect on produced DC control voltage V_{SET_A} driving condition of oscillation



obtained change of f_0 comes to 140 kHz, see Fig. 22b. The influence of temperature effect on AGC (fulfillment of CO) does not cause important problems (discontinuation of oscillations) in the observed range. The AGC system reacts to changes (the main consequence of temperature effects is fluctuation of f_0) by automatic driving of V_{SET_A2} (gain A approximately between 1.4 and 3.2, recalculated from V_{SET_A2}); see Fig. 23.

7 Investigation of the Oscillation Condition by Open-Loop Gain Analysis

This analysis is given to explain the behavior and necessity of the automatic AGC system. Many researchers suppose that just reaching $A_2 = 2$ (and keeping it fixed all the time, as was determined from Eq. (5) or (9)), is sufficient for wideband tuning of f_0 . However, this is not entirely true in the detailed view. Let us break the loop between V_{OUTi} and the terminal of R_2 (see Fig. 24) and investigate fulfillment of the loop Barkhausen oscillation criterion [30, 52, 64, 88] (gain and phase shift in the loop) in the ideal case and in the case of simulating the AC model of the proposed oscillator. In the ideal case, CO is fulfilled for the situation shown in Fig. 25a only (for the exact value $A_2 = 1 + R_3/R_1 = 2$) and for all values of $B_{1,2}$. This means that the gain in the loop reaches 1 (0 dB) and phase shift 0° (between V_{OUTi} and V_{INP}).

Fig. 24 Investigation of the oscillation condition in the oscillator by open-loop gain analysis

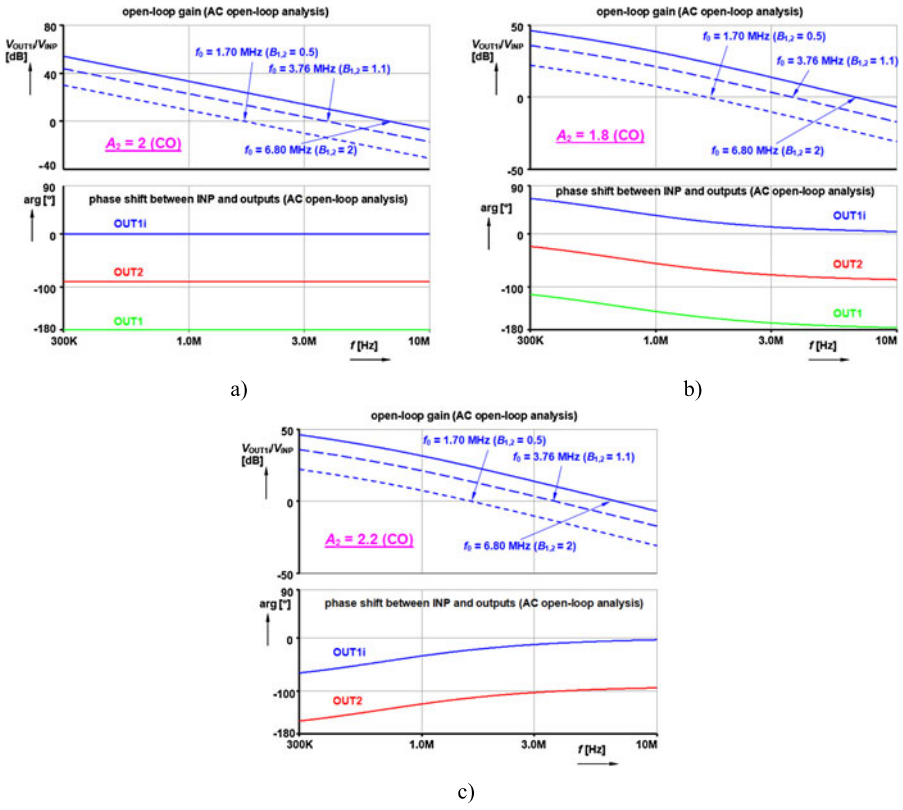
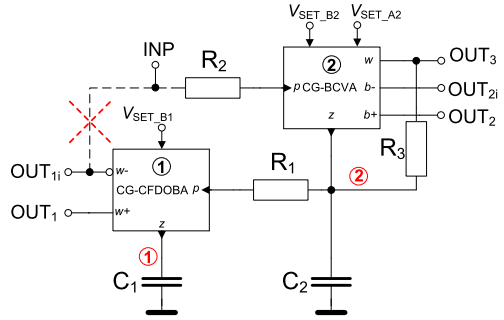


Fig. 25 Ideal behavior of open-loop gain of the oscillator: (a) CO fulfilled $A_2 = 2$, (b) $A_2 < 2$, (c) $A_2 > 2$

Both corresponding outputs in the direction of the loop (V_{OUT2} and V_{OUT1}) are also shown in Fig. 25 and confirm the achieved phase shifts of the generated signals. CO is not fulfilled for different values of A_2 (see Fig. 25b, c) for any value of $B_{1,2}$.

Figure 26 offers more substantial information. To obtain the following results, PSpice simulations of the oscillator were performed with the behavioral model employing macromodels of the active elements. The behavioral model used respects

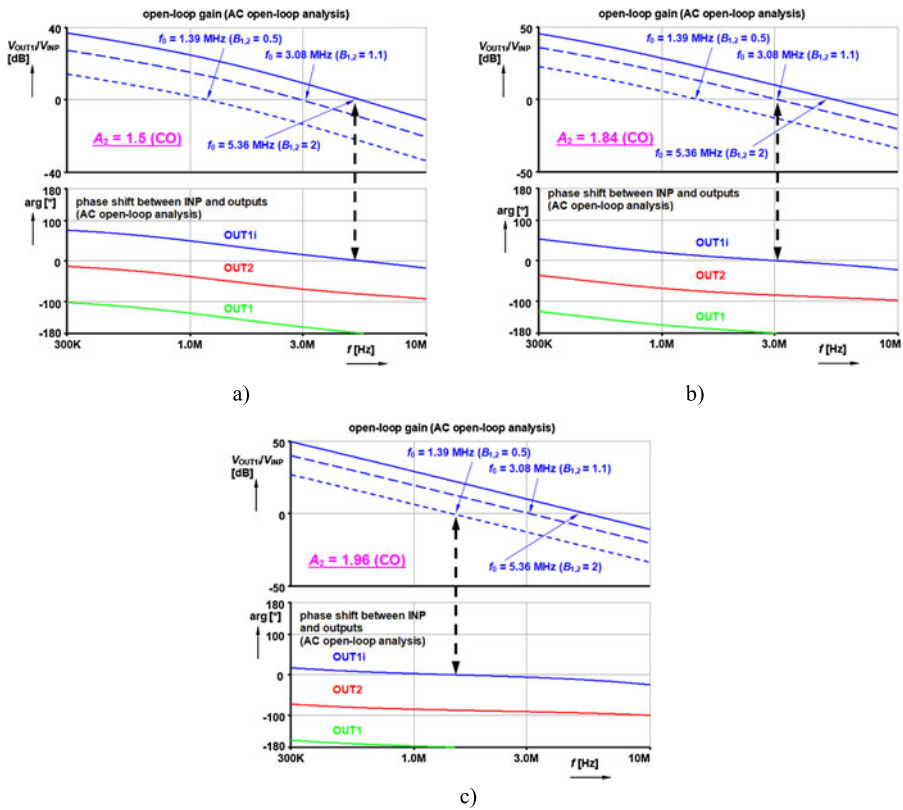


Fig. 26 Open-loop gain of the simulated behavioral model: **(a)** CO fulfilled for $f_0 = 5.36$ MHz, **(b)** CO fulfilled for $f_0 = 3.08$ MHz, **(c)** CO fulfilled for $f_0 = 1.39$ MHz

input and output impedances and frequency limitations of the active devices (see the comments in Sect. 4 concerning Fig. 5). In Fig. 26, three scenarios are given for various A_2 , and from the results we can see that CO is fulfilled only for the frequency (module crossing 0 dB), where the phase of V_{OUT1i} crosses 0° and simultaneously A_2 is fixed. From Fig. 26 it is clearly shown that a smaller or larger change of A_2 is necessary to follow the current amplitude condition (crossing 0 dB) and therefore the actual setting of f_0 . Tuning of f_0 by $B_{1,2}$ without AGC causes two consequences: (1) oscillations may drop down (discontinue operation) in the first case (the phase and amplitude conditions are not fulfilled simultaneously) or (2) amplitudes reach the saturation limits of the DC transfer characteristic of the active elements and the THD is terrible (higher gain than 1 in closed loop—the amplitude condition is not fulfilled for stable sinusoidal oscillations/ limit of stability).

Figure 27 gives the best explanation of the behavior of the circuit. In Fig. 27a the changes of A_2 (driving of V_{SET_A2} manually) are shown. CO (amplitude and phase condition) is only fulfilled for $A_2 = 1.84$ (at $B_{1,2} = 1.1$). A higher gain A_2 than nominal ($A_2 = 1.84$) causes an increase of the output amplitudes and also THD (because the loop gain is higher than 1 at f_0 , the limit of stability is exceeded), and a lower

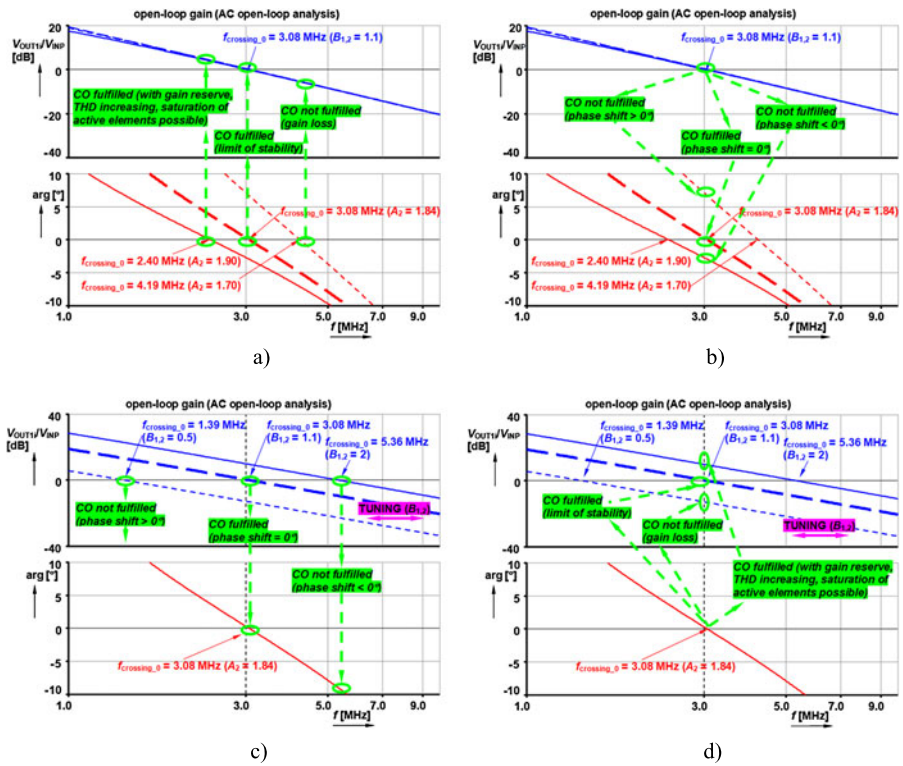


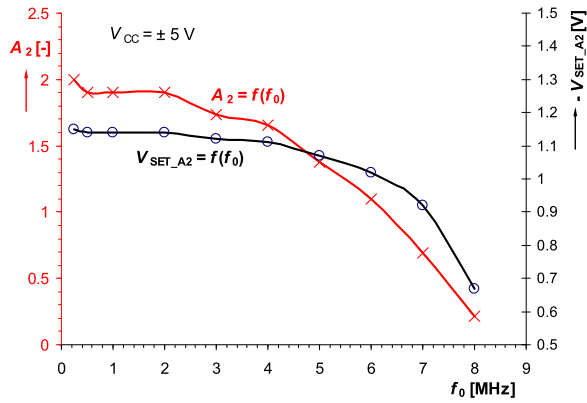
Fig. 27 Investigation of amplitude and phase condition of oscillation in simulated behavioral model (open-loop gain): (a) observation of amplitude condition fulfillment for different values of A_2 and fixed value of $B_{1,2}$, (b) observation of phase condition fulfillment for different values of A_2 and fixed value of $B_{1,2}$, (c) observation of phase condition fulfillment for different values of $B_{1,2}$ and fixed value of A_2 , (d) observation of amplitude condition fulfillment for different values of $B_{1,2}$ and fixed value of A_2

gain than nominal (at $f_0 = 3.08$ MHz for $B_{1,2} = 1.1$ only) causes discontinuation of oscillations (Fig. 27a). Similarly, the phase condition fulfillment can also be studied. From Fig. 27b it can be seen that CO is not fulfilled for different A_2 than the nominal value (the phase shift in the closed loop is different from 0°).

In Fig. 27c, during the tuning of f_0 by $B_{1,2}$, we suppose that A_2 has a fixed value. CO is not fulfilled for different than nominal values of $B_{1,2} = 1.1$, because the phase shift in the loop is always different from 0° . Similarly, CO at $f_0 = 3.08$ MHz ($A_2 = 1.84$) is not fulfilled for $B_{1,2} = 0.5$ (the gain in the loop is too low and <1). On the other hand, a high value of $B_{1,2}$ means high gain at $f_0 = 3.08$ MHz and increasing THD or limitation of amplitudes (Fig. 27d).

The reasons for the necessity of the AGC system seem to be clear. Adjusting $B_{1,2}$ in order to control f_0 causes changes in the gain in the closed loop (decreasing or increasing), and the AGC has to compensate these fluctuations (decreasing or increasing) in the gain by automatic driving of A_2 (through V_{SET_A2}). Therefore, the symbolic CO (5) or (9) does not tell us the complete information and is valid in the ideal case only. This problem is typical for many previously published circuits

Fig. 28 Dependence of automatically adjusted A_2 and $V_{\text{SET_A2}}$ on f_0 ($B_{1,2}$)



(compensation of the loop gain by a directly electronically adjustable parameter of an active element or by a value of the passive element is necessary), but in the past it was not explained in detail.

Figure 28 shows measurement results for a real oscillator (including the response of the AGC circuit in Fig. 6), where the DC voltage driving of gain A_2 in dependence on the current setting of $f_0(B_{1,2})$ is presented.

8 Conclusion

We have presented an interesting oscillator which is suitable for multiphase or differential quadrature signal generation. A very recently defined active element, i.e., the controlled gain-current follower differential output buffered amplifier (CG-CFDOBA) [12, 13], and a newly introduced element, the controlled gain-buffered current and voltage amplifier (CG-BCVA) were used for purposes of oscillator synthesis. Electronic control of two parameters in the frame of one active element is an attractive method which is very useful in particular applications. The proposed methods of gain control allow the synthesis and design of electronically controllable applications (an oscillator in our case) easily and with very favorable features. The main highlighted benefits can be found in the electronic linear control of the oscillation frequency (tested from 0.25 MHz to 8 MHz) and electronic control of the oscillation condition. The output levels were almost constant during the tuning process and reached about 200 mV_{P-P}. THD below 0.5 % in a range above 2 MHz was achieved. In comparison to some previously reported types [40, 74, 75, 77], the dependence of the output amplitudes on the tuning process was eliminated by simultaneous adjustment of both time constants of the integrators [11]. Grounded capacitors are a common requirement in similar types of circuits. A precise analysis of the real parameters and non-idealities of active elements allows the determination of more accurate descriptions and simulations. Laboratory measurements confirmed the validity and workability as well. Four-phase oscillators are useful for some types of modulations (multiples of 90 degrees phase shift are required). An important advantage is also the possibility to generate differential quadrature outputs. This is very important

for low-voltage CMOS solutions, where produced amplitudes reach several tens or hundreds of millivolts only—the differential mode means that one can achieve two times higher output levels than those obtained in single-ended solutions.

Acknowledgements The research described in this paper was supported by Czech Science Foundation projects under No. 102/09/1681 and No. 102/11/P489, by the project (Brno University of Technology) of specific research FEKT-S-11-15 and the project Electronic-biomedical co-operation ELBIC M00176. Dr. Herencsar was supported by the project CZ.1.07/2.3.00/30.0039 of the Brno University of Technology. The support of the project CZ.1.07/2.3.00/20.0007 WICOMT, financed by the operational program Education for Competitiveness is gratefully acknowledged. The described research was performed in laboratories supported by the SIX project, registration number CZ.1.05/2.1.00/03.0072, the operational program Research and Development for Innovation. This research work is also funded by projects EU ECOP EE.2.3.20.0094 and CZ.1.07/2.2.00/28.0062.

The authors also wish to thank the anonymous reviewers for their useful and constructive comments which have helped to improve the paper.

References

1. M.T. Abuelma'atti, Grounded capacitor current-mode oscillator using single current follower. *IEEE Trans. Circuits Syst. I, Fundam. Theory Appl.* **39**(12), 1018–1020 (1992)
2. AD8138, Low distortion differential ADC driver. Analog Devices [online]. Last modified 1/2006 [cit. 28.7.2011]. Available at URL: <http://www.analog.com/static/imported-files/data_sheets/AD8138.pdf>
3. K.M. Al-Ruwaihi, J.M. Noras, A novel linear resistor utilizing MOS transistors with identical sizes and one controlling voltage. *Int. J. Electron.* **76**(6), 1083–1098 (1994)
4. H. Alzaher, CMOS digitally programmable quadrature oscillators. *Int. J. Circuit Theory Appl.* **36**(8), 953–966 (2008)
5. H. Alzaher, N. Tasadduq, O. Al-Ees, F. Al-Ammari, A complementary metal-oxide semiconductor digitally programmable current conveyor. *Int. J. Circuit Theory Appl.* **41**(1), 69–81 (2013)
6. H. Alzaher, N. Tasadduq, Realizations of CMOS fully differential current followers/amplifiers, in *International Symposium ISCAS* (IEEE Press, New York, 2009), pp. 1381–1384
7. A.F. Arbel, L. Goldminz, Output stage for current-mode feedback amplifiers, theory and applications. *Analog Integr. Circuits Signal Process.* **2**(3), 243–255 (1992)
8. J. Bajer, D. Biolek, Digitally controlled quadrature oscillator employing two ZC-CG-CDBAs, in *International Conference Electronic Devices and Systems (EDS09 IMPAPS CS)* (2009), pp. 298–303
9. H. Barthelemy, M. Fillaud, S. Bourdel, J. Gaunery, CMOS inverters based positive type second generation current conveyors. *Analog Integr. Circuits Signal Process.* **50**(2), 141–146 (2007)
10. D.R. Bhaskar, K.K. Abdalla, R. Senani, Electronically-controlled current-mode second order sinusoidal oscillators using MO-OTAs and grounded capacitors. *Circuits Syst.* **2**(2), 65–73 (2011)
11. D. Biolek, A. Lahiri, W. Jaikla, M. Siripruchyanun, J. Bajer, Realisation of electronically tunable voltage-mode/current-mode quadrature sinusoidal oscillator using ZC-CG-CDBA. *Microelectron. J.* **42**(10), 1116–1123 (2011)
12. D. Biolek, R. Senani, V. Biolkova, Z. Kolka, Active elements for analog signal processing: classification, review, and new proposal. *Radioengineering* **17**(4), 15–32 (2008)
13. V. Biolkova, J. Bajer, D. Biolek, Four-phase oscillators employing two active elements. *Radioengineering* **20**(1), 334–339 (2011)
14. BUF634: 250 mA high-speed buffer, Texas Instruments [online]. 1996, last modified 9/2000 [cit. 28.7.2011]. Available at URL: <<http://focus.ti.com/lit/ds/symlink/buf634.pdf>>
15. U. Cam, H. Kuntman, C. Acar, On the realization of OTA-C oscillators. *Int. J. Electron.* **85**(3), 313–326 (1998)
16. EL2082: Current-mode multiplier. Intersil (Elantec) [online]. 1996, last modified 2003 [cit. 28.7.2011]. Available at URL: <<http://www.intersil.com/data/fn/fn7152.pdf>>
17. A. El-Adawy, A.M. Soliman, H.O. Elwan, Low voltage digitally controlled CMOS current conveyor. *AEÜ, Int. J. Electron. Commun.* **56**(3), 137–144 (2002)
18. I. Eldbib, V. Musil, Self-cascoded current controlled CCI based tunable band pass filter, in *18th International Conference Radioelektronika 2008* (IEEE Press, New York, 2008), pp. 1–4

19. A. Fabre, N. Mimeche, Class A/AB second-generation current conveyor with controlled current gain. *Electron. Lett.* **30**(16), 1267–1268 (1994)
20. A. Fabre, O. Saaid, F. Wiest, C. Boucheron, High frequency applications based on a new current controlled conveyor. *IEEE Trans. Circuits Syst. I, Fundam. Theory Appl.* **43**(2), 82–91 (1996)
21. A. Fabre, Third generation current conveyor: a helpful active element. *Electron. Lett.* **31**(5), 338–339 (1995)
22. J. Galan, R.G. Carvalaj, A. Torralba, F. Munoz, J. Ramirez-Angulo, A low-power low-voltage OTA-C sinusoidal oscillator with large tuning range. *IEEE Trans. Circuits Syst. I, Fundam. Theory Appl.* **52**(2), 283–291 (2005)
23. R.L. Geiger, E. Sanchez-Sinencio, Active filter design using operational transconductance amplifier: a tutorial. *IEEE Circuits Devices Mag.* **1**, 20–32 (1985)
24. S.S. Gupta, D.R. Bhaskar, R. Senani, New voltage controlled oscillators using CFOAs. *AEÜ, Int. J. Electron. Commun.* **63**(3), 209–217 (2009)
25. S.S. Gupta, R.K. Sharma, D.R. Bhaskar, R. Senani, Sinusoidal oscillators with explicit current output employing current-feedback op-amps. *Int. J. Circuit Theory Appl.* **38**(2), 131–147 (2010)
26. S.S. Gupta, R. Senani, New single resistance controlled oscillators employing a reduced number of unity-gain cells. *IEICE Electron. Express* **1**(16), 507–512 (2004)
27. S.S. Gupta, R. Senani, New single-resistance-controlled oscillator configurations using unity-gain cells. *Analog Integr. Circuits Signal Process.* **46**(2), 111–119 (2006)
28. S.S. Gupta, R. Senani, State variable synthesis of single resistance controlled grounded capacitor oscillators using only two CFOAs. *IEE Proc., Circuits Devices Syst.* **145**(2), 135–138 (1998)
29. S.S. Gupta, R. Senani, State variable synthesis of single-resistance-controlled grounded capacitor oscillators using only two CFOAs: additional new realizations. *IEE Proc., Circuits Devices Syst.* **145**(6), 415–418 (1998)
30. F. He, R. Ribas, C. Lahuec, M. Jezequel, Discussion on the general oscillation startup condition and the Barkhausen criterion. *Analog Integr. Circuits Signal Process.* **59**(2), 215–221 (2009)
31. N. Herencsar, A. Lahiri, K. Vrba, J. Koton, An electronically tunable current-mode quadrature oscillator using PCAs. *Int. J. Electron.* **99**(5), 609–621 (2012)
32. N. Herencsar, K. Vrba, J. Koton, A. Lahiri, Realizations of single-resistance-controlled quadrature oscillators using a generalized current follower transconductance amplifier and a unity gain voltage-follower. *Int. J. Electron.* **97**(8), 879–906 (2010)
33. N. Herencsar, S. Minaei, J. Koton, E. Yuce, K. Vrba, New resistorless and electronically tunable realization of dual-output VM all-pass filter using VDIBA. *Analog Integr. Circuits Signal Process.* **74**(1), 141–154 (2013)
34. J.W. Horng, A sinusoidal oscillator using current-controlled current conveyors. *Int. J. Electron.* **88**(6), 659–664 (2001)
35. J.J. Chen, C.C. Chen, H.W. Tsao, S.I. Liu, Current-mode oscillators using single current follower. *Electron. Lett.* **27**(22), 2056–2059 (1991)
36. W. Jaikla, A. Lahiri, Resistor-less current-mode four-phase quadrature oscillator using CCCDTA and grounded capacitors. *AEÜ, Int. J. Electron. Commun.* **66**(3), 214–218 (2012)
37. A.U. Keskin, C. Aydin, E. Hancioglu, C. Acar, Quadrature oscillator using current differencing buffered amplifiers (CDBA). *Frequenz* **60**(3), 21–23 (2006)
38. A.U. Keskin, D. Biolek, Current mode quadrature oscillator using current differencing transconductance amplifiers (CDTA). *IEE Proc., Circuits Devices Syst.* **153**(3), 214–218 (2006)
39. M. Kumngern, J. Chanwutium, K. Dejhan, Electronically tunable multiphase sinusoidal oscillator using translinear current conveyors. *Analog Integr. Circuits Signal Process.* **65**(2), 327–334 (2010)
40. M. Kumngern, S. Junnapiya, A sinusoidal oscillator using translinear current conveyors, in *International Conference APPCAS* (IEEE Press, New York, 2010), pp. 740–743
41. H. Kuntman, A. Ozpinar, On the realization of DO-OTA-C oscillators. *Microelectron. J.* **29**(12), 991–997 (1998)
42. A. Lahiri, Current-mode variable frequency quadrature sinusoidal oscillator using two CCs and four passive components including grounded capacitors. *Analog Integr. Circuits Signal Process.* **71**(2), 303–311 (2012)
43. A. Lahiri, Explicit-current-output quadrature oscillator using second-generation current conveyor transconductance amplifier. *Radioengineering* **18**(4), 522–526 (2009)
44. A. Lahiri, M. Gupta, Realizations of grounded negative capacitance using CFOAs. *Circuits Syst. Signal Process.* **30**(1), 134–155 (2011)
45. A. Lahiri, Novel voltage/current-mode quadrature oscillator using current differencing transconductance amplifier. *Analog Integr. Circuits Signal Process.* **61**(2), 199–203 (2009)

46. B. Linarez-Barranco, A. Rodriguez-Vazquez, E. Sanchez-Sinencio, L. Huertas, CMOS OTA-C high frequency sinusoidal oscillators. *IEEE J. Solid-State Circuits* **26**(2), 160–165 (1991)
47. S.I. Liu, Single-resistance-controlled/voltage-controlled oscillator using current conveyors and grounded capacitors. *Electron. Lett.* **31**(5), 337–338 (1995)
48. S. Maheshwari, B. Chatuverdi, High output impedance CMQOs using DVCCs and grounded components. *Int. J. Circuit Theory Appl.* **39**(4), 427–435 (2011)
49. A. Marcellis, G. Ferri, N.C. Guerrini, G. Scotti, V. Stornelli, A. Trifiletti, The VGC-CCII: a novel building block and its application to capacitance multiplication. *Analog Integr. Circuits Signal Process.* **58**(1), 55–59 (2009)
50. P.A. Martinez, B.M. Monge-Sanz, Single resistance controlled oscillator using unity gain cells. *Microelectron. Reliab.* **45**(1), 191–194 (2005)
51. P.A. Martinez, J. Sabadell, C. Aldea, Grounded resistor controlled sinusoidal oscillator using CFOAs. *Electron. Lett.* **33**(5), 346–348 (1997)
52. H. Martinez-Garcia, A. Grau-Saldes, Y. Bolea-Monte, J. Gamiz-Caro, On discussion on Barkhausen and Nyquist stability criteria. *Analog Integr. Circuits Signal Process.* **70**(3), 443–449 (2012)
53. S. Minaei, O. Cicekoglu, New current-mode integrator and all-pass section without external passive elements and their application to design a dual-mode quadrature oscillator. *Frequenz* **57**(1–2), 19–24 (2003)
54. S. Minaei, O.K. Sayin, H. Kuntman, A new CMOS electronically tunable current conveyor and its application to current-mode filters. *IEEE Trans. Circuits Syst. I, Fundam. Theory Appl.* **53**(7), 1448–1457 (2006)
55. MOSIS parametric test results of TSMC LO EPI SCN018 technology. Available on-line [ftp://ftp.isi.edu/pub/mosis/vendors/tsmc-018/t44e_lo_epi-params.txt]. Cited 24.5.2012
56. H. Palouda, National Semiconductors—current feedback amplifiers. *Appl. Note* **597**, 1–10 (1989)
57. N. Pandey, S.K. Paul, Single CDTA-based current mode all-pass filter and its applications. *J. Electr. Comput. Eng.* (2011). doi:[10.1155/2011/897631](https://doi.org/10.1155/2011/897631)
58. C. Psychalinos, A. Spanidou, Current amplifier based grounded and floating inductance simulators. *AEÜ, Int. J. Electron. Commun.* **60**(2), 168–171 (2006)
59. A. Rodriguez-Vazquez, B. Linarez-Barranco, L. Huertas, E. Sanchez-Sinencio, On the design of voltage-controlled sinusoidal oscillators using OTA's. *IEEE Trans. Circuits Syst.* **37**(2), 198–211 (1990)
60. S.B. Salem, M. Fakhfakh, D.S. Masmoudi, M. Loulou, P. Loumeau, N. Masmoudi, A high performance CMOS CCII and high frequency applications. *Analog Integr. Circuits Signal Process.* **49**(1), 71–78 (2006)
61. B. Sedighi, M.S. Bakhtiar, Variable gain current mirror for high-speed applications. *IEICE Electron. Express* **4**(8), 277–281 (2007)
62. R. Senani, Realization of a class of analog signal processing/signal generation circuits: novel configurations using current feedback opamps. *Frequenz* **52**(9–10), 196–206 (1998)
63. S. Shi-Xiang, Y. Guo-Ping, C. Hua, A new CMOS electronically tunable current conveyor based on translinear circuits, in *7th International Conference ASICON 2007* (IEEE Press, New York, 2007), pp. 569–572
64. V. Singh, Discussion on Barkhausen and Nyquist stability criteria. *Analog Integr. Circuits Signal Process.* **62**(3), 327–332 (2010)
65. V. Singh, Equivalent forms of dual-OTA RC oscillators with application to grounded-capacitor oscillators. *IEE Proc., Circuits Devices Syst.* **153**(2), 95–99 (2006)
66. M. Siripruchyanun, C. Chanapromma, P. Silapan, W. Jaikla, BiCMOS current-controlled current feedback amplifier (CC-CFA) and its applications. *WSEAS Trans. Electron.* **6**(5), 203–219 (2008)
67. K.C. Smith, A. Sedra, A second generation current conveyor and its applications. *IEEE Trans. Circuit Theory* **CT-17**(2), 132–134 (1970)
68. K.C. Smith, A. Sedra, The current conveyor: a new circuit building block. *Proc. IEEE* **56**(3), 1368–1369 (1968)
69. A.M. Soliman, CMOS balanced output transconductor and applications for analog VLSI. *Microelectron. J.* **30**(1), 29–39 (1999)
70. A.M. Soliman, Novel oscillators using current and voltage followers. *J. Franklin Inst.* **335**(6), 997–1007 (1998)
71. A.M. Soliman, Synthesis of grounded capacitor and grounded resistor oscillators. *J. Franklin Inst.* **336**(4), 735–746 (1999)
72. R. Sotner, J. Jerabek, J. Petrzela, T. Dostal, K. Vrba, Electronically tunable simple oscillator based on single-output and multiple output transconductor. *IEICE Electron. Express* **6**(20), 1476–1482 (2009)

73. R. Sotner, J. Jerabek, N. Herencsar, T. Dostal, K. Vrba, Electronically adjustable modification of CFA: double current controlled CFA (DCC-CFA), in *35th International Conference on Telecommunications and Signal Processing (TSP 2012)* (IEEE Press, New York, 2012), pp. 401–405
74. R. Sotner, J. Jerabek, N. Herencsar, Z. Hrubos, T. Dostal, K. Vrba, Study of adjustable gains for control of oscillation frequency and oscillation condition in 3R-2C oscillator. *Radioengineering* **21**(1), 392–402 (2012)
75. R. Sotner, J. Jerabek, R. Prokop, K. Vrba, Current gain controlled CCTA and its application in quadrature oscillator and direct frequency modulator. *Radioengineering* **20**(1), 317–326 (2011)
76. R. Sotner, N. Herencsar, J. Jerabek, J. Koton, T. Dostal, K. Vrba, Quadrature oscillator based on modified double current controlled current feedback amplifier, in *22nd International Conference Radioelektronika 2012* (IEEE Press, New York, 2012), pp. 275–278
77. R. Sotner, Z. Hrubos, B. Sevcik, J. Slezak, J. Petrzela, T. Dostal, An example of easy synthesis of active filter and oscillator using signal flow graph modification and controllable current conveyors. *J. Electr. Eng.* **62**(5), 258–266 (2011)
78. G. Souliotis, C. Psychalinos, Electronically controlled multiphase sinusoidal oscillators using current amplifiers. *Int. J. Circuit Theory Appl.* **37**(1), 43–52 (2009)
79. G. Souliotis, C. Psychalinos, Harmonic oscillators realized using current amplifiers and grounded capacitors. *Int. J. Circuit Theory Appl.* **35**(2), 165–173 (2007)
80. W. Surakamponorn, K. Kumwachara, CMOS-based electronically tunable current conveyor. *Electron. Lett.* **28**(14), 1316–1317 (1992)
81. W. Surakamponorn, W. Thitimajshima, Integrable electronically tunable current conveyors. *IEE Proc. G, Electron. Circuits Syst.* **135**(2), 71–77 (1988)
82. J.A. Svoboda, L. McGory, S. Webb, Applications of commercially available current conveyor. *Int. J. Electron.* **70**(1), 159–164 (1991)
83. W. Tangsrirat, Electronically tunable multi-terminal floating nullor and its application. *Radioengineering* **17**(4), 3–7 (2008)
84. W. Tangsrirat, T. Pukkalanun, Digitally programmable current follower and its applications. *AEÜ, Int. J. Electron. Commun.* **63**(5), 416–422 (2009)
85. Y. Tao, J.K. Fidler, Electronically tunable dual-OTA second-order sinusoidal oscillators/filters with non-interacting controls: a systematic synthesis approach. *IEEE Trans. Circuits Syst. I, Fundam. Theory Appl.* **47**(2), 117–129 (2000)
86. VCA810, High gain adjust range, wideband, variable gain amplifier. Texas Instruments [online]. 2003, last modified 12/2010 [cit. 28.7.2011]. Available at URL: <http://focus.ti.com/lit/ds/sbos275f/sbos275f.pdf>>
87. Z. Wang, 2-MOSFET transresistor with extremely low distortion for output reaching supply voltage. *Electron. Lett.* **26**(13), 951–952 (1990)
88. L. Wangenheim, On the Barkhausen and Nyquist stability criteria. *Analog Integr. Circuits Signal Process.* **66**(1), 139–141 (2011)
89. A. Yesil, F. Kacar, H. Kuntman, New simple CMOS realization of voltage differencing transconductance amplifier and its RF filter application. *Radioengineering* **20**(3), 632–637 (2011)
90. E. Yuce, S. Minaei, H. Alpaslan, Novel CMOS technology-based linear grounded voltage controlled resistor. *J. Circuits Syst. Comput.* **20**(3), 447–455 (2011)

[14] SOTNER, R., HERENC SAR, N., JERABEK, J., KOTON. J., DOSTAL, T., VRBA, K. Electronically controlled oscillator with linear frequency adjusting for four-phase or differential quadrature output signal generation. *International Journal of Circuit Theory and Applications*, 2014, vol. 42, no. 12, p. 1264-1289. ISSN: 0098-9886.

Electronically controlled oscillator with linear frequency adjusting for four-phase or differential quadrature output signal generation

Roman Sotner^{1,*†}, Norbert Herencsar², Jan Jerabek², Jaroslav Koton²,
Tomas Dostal^{1,3} and Kamil Vrba²

¹*Department of Radio Electronics, Faculty of Electrical Engineering and Communication, Brno University of Technology, Technicka 12, Brno, 616 00, Czech Republic*

²*Department of Telecommunications, Faculty of Electrical Engineering and Communication, Brno University of Technology, Technicka 12, Brno, 616 00, Czech Republic*

³*Department of Electrical Engineering and Computer Science, College of Polytechnics Jihlava, Tolsteho 16, Jihlava, 586 01, Czech Republic*

ABSTRACT

This paper introduces novel four-phase oscillator employing two Dual-Output Controlled Gain Current Follower Buffered Amplifiers (DO-CG-CFBAs), single Current Amplifier, three resistors, and two grounded capacitors suitable for differential quadrature signal production (floating outputs). To control the frequency of oscillation (FO) and condition of oscillation (CO), only the current gain adjustment of active elements is used. The circuit was designed by well-known state variable approach. The oscillator employs three active elements for linear control of FO and to adjust CO and provides low-impedance voltage outputs. Furthermore, two straightforward ways of automatic amplitude gain control were used and compared. Active elements with very good performance are implemented to fulfill required features. Suitable CMOS implementation of introduced DO-CG-CFBA was shown. Important characteristics of the designed oscillator were verified experimentally and by PSpice simulations to confirm theoretical and expected presumptions. Copyright © 2013 John Wiley & Sons, Ltd.

Received 16 April 2012; Revised 5 September 2012; Accepted 26 March 2013

KEY WORDS: electronic control; adjusting; Current Amplifier; Dual-Output Controlled Gain Current Follower Buffered Amplifier (DO-CG-CFBA); differential signals; quadrature oscillator

1. INTRODUCTION

There are lots of active elements that are available for analog signal processing. A very well-organized overview of active elements was presented in [1] that gives suggestion for possible improvements. Electronic control is very important feature of actual circuit design and synthesis. In general, we can divide ways of electronic control to two groups. The first group provides control by replacing selected passive components by controllable counterpart (FET, digital potentiometer, A/D converter, transconductor, ...). Such oscillators are called as single resistance controlled oscillators (SRCO) [2]. One resistor usually serves for control the frequency of oscillation (FO) and second sets the condition of oscillation (CO). This kind of control is called indirect. That means additional enlargement of whole circuit is needed. The second type of control is direct. These circuits include active elements with possibility of (direct) control of their parameters (i.e. transconductance [3], intrinsic input resistance [4], current gain [5–12], and voltage gain [12]). Many active elements with such a feature were introduced in the past, but attention was focused on quite simple elements only.

*Correspondence to: Roman Sotner, Department of Radio Electronics, Faculty of Electrical Engineering and Communication, Brno University of Technology, Technicka 12, Brno, 616 00, Czech Republic.

†E-mail: sotner@feec.vutbr.cz

Many researchers are still interested in this field. Main focus is given to complicated elements with various types of direct electronic controllability. Controllable current gain is used as a main instrument for direct electronic control of parameters of application in this paper.

1.1. Development of active elements with possibility of current gain control

Surakampontrorn *et al.* [5] introduced electronically tunable Current Conveyor (CC) with possibility of current gain control between X and Z port. Similar active element was proposed by Fabre *et al.* [6]. Possibilities of current control (digital) were expanded into elements with differential signal processing by Mahmoud *et al.* [7]. Finally, Minaei *et al.* [8] designed active element where combination of several types of control was possible. Sedighi *et al.* [9] introduced very interesting approach to current control. A Multi-Terminal Floating Nullor with current gain adjustability was presented by Tangsrirat in [10]. Tangsrirat *et al.* [11] also proposed digitally controllable active element (Current Follower). Several ways of control, including current gain and voltage gain in frame of CC (VGC-CCII), were implemented by Marcellis *et al.* [12]. Alzahrer *et al.* contributed to this field with Fully Differential Digitally Controllable Current Followers, Amplifiers [13], and CCs [14]. El-Adawy *et al.* [15] used similar way of control in Digitally Controlled CC. Similar type of control was also used also in Digitally Adjustable Current Amplifier (DACA) presented by Jerabek *et al.* [16]. Control of current gain has different definitions in hitherto published works but main goal (amplification) is the same. Some papers deal with this active element under the designation 'Adjustable Current Follower', but this is confusing, because adjustability of current active element has wide meaning (adjustable intrinsic resistance for example). Biolek *et al.* [17] implemented digital control of current gain to so-called Z Copy-Controlled Gain-Current Differencing Buffered Amplifier (ZC-CG-CDBA). This element is very complex; however, it provides many application possibilities.

1.2. Oscillator design and structures suitable for direct electronic control

Great attention was given to development of SRCO types of oscillators in the past. Many suitable structures and design methods were introduced by Senani and Gupta [2, 18, 19]. Some solutions in [19, 20] allow design of quadrature oscillators employing two active elements, but controllability of such types is given by changes of resistors (grounded and floating) only, because structures are based on standard Current Feedback Amplifiers (CFAs) and standard CCs of second generation (CCII) [1]. Standard and classical CFA does not allow any electronic control of its parameters. However, described methods of synthesis (state variable approach) [2, 18–20] is very useful for further design of directly electronically adjustable oscillators. Gupta *et al.* [21] also showed how to control these types of oscillators by simple FET. We can find similarities of discussed structures with CFAs in solutions presented in many works, because state variable methods lead to loop and multi-loop systems with integrators (lossy and lossless) [18–20]. Practically same solutions [2, 18–20] are available by several design methods beside state variable synthesis. However, our solution has different characteristic equation (CE) (any from solutions presented in [2, 18–20] do not contain adjustable current gains for non-interactive control of FO and CO and linear tuning of FO). Brief summarization of several important oscillator conceptions employing current gain control follows.

Souliotis *et al.* [22] proposed very simple two-loop oscillator with two Current Amplifiers and two grounded capacitors, where quadrature outputs (current responses) are available. Linear control of FO is possible, but matching between parameters, which control FO, is very important for fulfilling of CO. Alzahrer [23] presented two oscillators (similar to our solution) which are based on combination of active elements (Voltage Followers and Current Amplifiers - Digitally Controllable Current Followers). Both proposed circuits contain four resistors and two capacitors and generate both current and voltage quadrature signals. Biolek *et al.* also used ZC-CG-CDBAs to design of quadrature oscillators in [24] and [25]. Solution in [24] uses two active elements and five or six passive elements (capacitors are grounded). FO is controllable linearly by current gain; CO and FO are independent. Output amplitude is not dependent on tuning process. However, CO is controllable via floating resistors only. In comparison to our solutions presented in this paper, oscillators in [24, 25] require more sophisticated active elements. Very simple oscillator employing only one active element and four passive elements was presented in [26]. Current gain was used for FO control, but CO is still

controlled by grounded resistor. Dependence of FO on gain is not linear. Setting of CO employing current gain control was discussed in [27]. However, nonlinear dependence of FO on current gain still remains in [27]. Herencsar *et al.* [28] presented interesting solution, where three Programmable Current Amplifiers (PCAs), two resistors and two capacitors were implemented. PCA operation is based on DACA principle [16]. Dependence of FO on current gain is not linear but FO and CO are controllable by current gains. Biolkova *et al.* [29] introduced interesting method and oscillators, which provide signals with differential (symmetrical) quadrature outputs, i.e. four phase oscillator, where phase shifts 90, 180 and 270 degrees are accessible simultaneously. Nevertheless, these oscillators were proposed as SRCO types. Detailed comparison of quadrature oscillators employing current gain for FO control, which were published in recent years, is given in Table I. Some solutions allow to generate output signals in current or voltage form simultaneously [23–25]. Additional current to voltage conversion and voltage buffers are required in [23–25] in order to obtain voltage differential (symmetrical) quadrature outputs. It is not necessary in our solution as will be shown later. Many active elements in discussed solutions [22–25, 28, 29] and also in our oscillator do not require voltage inputs in comparison with CFAs extensively used by Gupta and Senani [2, 18, 19]. This means certain simplification of internal structure of active element. Classical CFAs (missing inverted voltage output) used for oscillator design also do not easily allow to obtain differential quadrature signals.

A digital controlling approach is very interesting and profitable in many applications [16, 23–25, 28]. The digital adjusting is very useful for FO control. However, coarse and discontinuous adjusting (steps) of CO (by current gain) could be insufficient for satisfactory fluctuances of output amplitudes and total harmonic distortion (THD) in some cases. Sufficient bit resolution is very important. Additionally, analog-to-digital converter is essential, if digital control (derived from output amplitude) of CO is intended for automatic amplitude control. It means additional complication and power consumption. Therefore, we decided to use continuous control.

1.3. Comparison of one, two, and more active element-based solutions

In this section, we selected several interesting oscillator solutions employing different types and different number of active elements. Selected solutions employing one [30–33], two [34–45], three [44, 46–51], or more [44, 51–60] active elements are listed in Table II and comparison with our approach is provided except solutions that were discussed above in sections 1.1. Recently presented circuits based on Differential-input Buffered and Transconductance Amplifier (DBTA) [30], Current Differencing Transconductance Amplifiers (CDTAs) [31–35, 42], CCs (CC, CCII, CCCII, DVCC) [36–40, 46, 49, 50], Current Feedback Amplifiers (CFAs) [41], Operational Transconductance Amplifiers (OTAs) [44, 45, 47, 48, 51–53], and their modifications are compared. Abbreviations of mentioned active elements are explained below Table II.

Some circuits employ many passive elements [43, 45], and electronic control of their parameters (CO, FO) is not easily possible [43]. Circuits in [31–39, 44] are very simple because for their realization, only minimal number of active and passive elements are necessary. Several solutions belong to types controlled by passive elements [40, 42, 50], where suitable resistors (mainly grounded) can be replaced by adjustable equivalents (FET) [21]. However, the quality of adjusting is limited by features of used additional discrete FET transistor which also means increasing complexity of the circuit in some cases. From historical point of view, the most often used type of electronic control seems to be the transconductance adjusting [31, 34, 38, 44, 45, 47, 48, 51–53]. Intrinsic resistance control of low-impedance current input terminal in oscillators [36, 46] received increasing attention in recent years despite of the fact that discovery of this method is quite old [4]. On the other hand, the idea of combination both discussed methods is quite new [32, 35]. A combination of intrinsic resistance and current gain also allows some benefits from electronic control point of view [37]. Very interesting approach was presented by Lahiri *et al.* [41], where authors implemented adjustable capacitor-simulating circuit to control FO. Another possibility to control FO is switching of capacitances, but it only allows discontinuous changes of FO [39]. Many examples of two OTA-based oscillators were introduced in the past. Nevertheless, some of proposed solutions require huge number of passive elements (many of them are floating resistors [45]), and non-interactive control of CO and FO can be also difficult in some discussed solutions. Several

Table I. Comparison of important controllable quadrature oscillators employing current gain control.

Reference	Active elements	Number of passive elements / active elements	Independent CO and FO	Amplitude dependent on tuning process	CO controllable by gain	Linear control of FO	Type of output signal (current or voltage)	Additional voltage buffers or I/V converters are necessary (for voltage mode operation)	Possibility of differential voltage outputs without additional modification and buffering	FO range [MHz]
[22]	CAs	2/2	^a	^b	Yes	Yes	Current	Yes	No	1.0–2.5
[23]	DCCFs / VFs	6/5	Yes	No	Yes	Yes	Both	No	No	0.3–1.6
[24]	ZC-CG-CDBAs	6/2	Yes	No	No	Yes	Both	No	No	0.25–0.483
[25]	ZC-CG-CDBAs	5/2	Yes	No	No	Yes	Both	No	No	0.25–2.8
[26]	CGCCCTA	4/1	Yes	Yes	No	No	Voltage	Yes	No	0.2–1.2
[27]	ECCII _s	5/3	Yes	Yes	Yes	No	Voltage	No	No	0.26–1.25
[28]	PCAs	4/3	Yes	Yes	Yes	No	Current	Yes	No	0.05–0.3
Proposed	DO-CF-CFBAs	5/3	Yes	No	Yes	Yes	Voltage	No	Yes	0.05–6.8

CA - Current Amplifier

CGCCTA - Current Gain Controlled Current Conveyor Transconductance Amplifier

DCCF/VF - Digitally Controllable Current Follower and Voltage Follower (buffer)

DO-CG-CFBA - Dual-Output Controlled Gain Current Follower Buffered Amplifier

ECCII - Electronically Controllable Current Conveyor of second generation

PCA - Programmable Current Amplifier

ZC-CG-CDBA - Z-copy Controlled-Gain Current Differencing Buffered amplifier

^aspecial matching condition for start of oscillation and linear control of FO simultaneously required^binformation is not available or feature is not possible

Table II. Comparison of selected oscillator solutions based on one, two, and more standard and modified active elements.

Reference	Active elements	Number of passive / active elements	Quadrature outputs	Independent CO and FO	Amplitude dependent on tuning process/ linear control of FO	Type of control	Type of output signal (current or voltage)	Additional voltage buffers or I/V converters are necessary (for voltage mode operation)	Possibility of differential voltage outputs without additional modification and buffering	Only external capacitors required
One active element										
[30]	DBTA	5/1	Yes	Yes	Yes/No	Passive elements	Voltage	No ^a	No	No
[31]	MCDTA	2/1	Yes	^b	No/Yes	g_m	Current	Yes	No	Yes
[32]	CCCDTA	2/1	Yes	^b	No/Yes	R_x, g_m	Current	Yes	No	Yes
[33]	CDTA	3/1	Yes	No	^c	Passive elements	Current	Yes	No	No
Two active elements										
[34]	CDTA	2/2	Yes	^b	No/Yes	g_m	Current	Yes	No	Yes
[35]	CCCDTA	2/2	Yes	Yes	No/Yes	R_x, g_m	Current	Yes	No	Yes
[36]	CCCI	2/2	No	Yes	Yes/No	R_x	Voltage	Yes	No	Yes
[37]	CCCI	2/2	No	Yes	Yes/No	R_x, B	Voltage	Yes	No	Yes
[38]	CDTA	3/2	Yes	Yes	Yes/No	g_m	Both	Yes	No	No
[39]	DO/MO-CCII	4/2	Yes	Yes	No/Yes	Passive elements	Current	Yes	No	No
[40]	CCII	5/2	No	Yes	Yes/No	Passive elements	Voltage	Yes	No	No
[41]	CFA	3+ $C_{eq}/2$ (6/3)	Yes	Yes	^c	CFA replacement of C	Voltage	No	No	No

[42]	CDTA	6/2	Yes	Yes	No/Yes	Passive elements	Current	Yes	No	No
[43]	CDBA	8/2	No	No	^c	Passive elements	Voltage	Yes	No	No
[44]	OTA	2-4/2-4	Yes	Yes	No/Yes	g_m	Voltage	Yes	No	Yes
[45]	OTA	3-7/2	Yes	Yes	Yes/No	g_m	Voltage	Yes	No	No
Three and more active elements										
[46]	CCCII	2/3	Yes	^b	No/Yes	R_x	Current	Yes	No	Yes
[47]	OTA	2/3	No	^b	No/Yes	g_m	Voltage	Yes	No	Yes
[48]	OTA + VB	3/3	No	Yes	Yes/No	g_m	Voltage	No	No	No
[49]	DVCC	4/3	Yes	^b	No/Yes	Passive elements	Voltage	Yes	No	No
[50]	DVCC	5/3	Yes	Yes	Yes/No	Passive elements	Current	Yes	No	No
[51]	DO-OTA	2/3-6	^c	Yes	No/Yes	g_m	Current	Yes	No	Yes
[52]	OTA	2/4	Yes	Yes	No/Yes	g_m	Current	Yes	No	Yes
[53]	DO-OTA	4/4	Yes	Yes	No/Yes	g_m	Voltage	Yes	No	Yes
Active-only										
[54, 55]	OTAs + OPAMPs	0/7	Yes	^c	^c	g_m	Both	No	No	^c
[56]	CCCTAs + OPAMPs	0/4	Yes	Yes	No/Yes	R_x, g_m	Current	Yes	No	^c
[57]	OPAMPs + OTAs	0/5	Yes	Yes	No/Yes	g_m	Voltage	No	No	^c

Continues

Table II. Continued

Reference	Active elements	Number of passive / active elements	Quadrature outputs	Independent CO and FO	Amplitude dependent on tuning process/ linear control of FO	Type of control	Type of output signal (current or voltage)	Additional voltage buffers or I/V converters are necessary (for voltage mode operation)	Possibility of differential voltage outputs without additional modification and buffering	Only external capacitors required
[58]	OPAMPs + OTAs	0/5	Yes	Yes	No/Yes	g_m	Current	Yes	No	c
[59]	CCCTAs + OPAMPs	0/5	Yes	Yes	No/Yes	R_x, g_m	Current	Yes	No	c
[60]	OTAs + OPAMPs + CCII	0/7	Yes	Yes	No/Yes	R_x, g_m	Voltage	No	No	c
Proposed solution										
	DO-CG-CFBAs	5/3	Yes	Yes	No/Yes	B	Voltage	No	Yes	No

g_m - transconductance (controllable by bias current)

R_x - intrinsic resistance (controllable by bias current)

B - adjustable current gain

CCII - second generation current conveyor

CCCII - translinear current conveyor/ current controlled CCII

CCCTA - current controlled current conveyor transconductance amplifier

CCCDTA - current controlled CDTA

CDBA - current differencing buffered amplifier

CDTA - current differencing transconductance amplifier

CFA - current feedback amplifier

DBTA - Differential-input Buffered and Transconductance Amplifier

DO-CCII/CCCII - dual output CCII/ dual output CCCII

DO-OTA - dual output OTA

DVCC - differential voltage current conveyor

MCDTA - modified CDTA

MO-CCII/CCCII - multiple output CCII/ multiple output CCCII

OPAMP - operational amplifier

OTA - operational transconductance amplifier

VB - voltage buffer (or voltage follower - VF)

C_{eq} - equivalent capacitance

^aonly one voltage output is buffered [30]

^bspecial matching condition for start of oscillation and linear control of FO simultaneously required

^cinformation is not available or feature is not possible

realizations based on CFAs [2, 18, 19, 21] always allow non-interactive control of CO and FO (FET replacement of resistor tunes FO), but some of these circuits require high number of passive elements. Furthermore, these circuits do not allow linear control of FO and differential quadrature outputs. Special matching condition of two parameters for correct operation (start of oscillations and linear electronic control) of circuits presented in [31, 32, 34, 46, 47, 49] is required. Example of typical matching condition is the following (in case of transconductance control): CO: $C_1 g_{m1} = C_2 g_{m2}$; FO: $\omega_0 = \sqrt{\frac{g_{m1} g_{m2}}{C_1 C_2}}$ (adjustable parameters $g_{m1} = g_{m2}$ for fulfilled CO and for linear FO tuning simultaneously). Solution presented by Senani [47] can work as electronically controllable system with independent CO and FO control (one transconductance is suitable for CO control and other one for FO adjusting). However, all adjustable parameters have to be matched if linear control of FO is required and moreover the CO is given by equality of capacitance values so as in [31, 32, 34, 46, 49]. This matching condition has to fulfill CO and ensures FO control simultaneously. It is main drawback of some hitherto published two-active-device-based circuits, because only capacitor values are suitable to adjust the startup of oscillation, if matching of all easily controllable parameters (intrinsic resistance and transconductance by bias currents) is required. In such cases from implementation of amplitude gain control (AGC) circuit for wideband FO adjusting without fluctuances of output amplitude point of view, capacitance value adjusting in order to control CO is not easy task. Therefore, in our work, we used three adjustable gains, because they allow simultaneous control of CO and FO without matching constraints between them. Here it is also important noting that any of the given solutions in Table II employing classical active elements and their modifications do not allow obtaining of differential low-impedance voltage outputs, because output signals are available in high-impedance nodes or in form of currents (current-mode realizations) and additional conversion or/and buffers/inverters are necessary. Main disadvantages of discussed oscillators are the following:

1. Too many passive elements [41, 43–45],
2. Non-interactive control of FO and CO is not possible [33, 43],
3. Matching of two parameters is necessary to fulfill CO and tuning of FO simultaneously [31, 32, 34, 46, 49],
4. Linear control of FO is not possible [30, 36–38, 40, 48, 50],
5. Quadrature outputs are not provided [36, 37, 40, 47, 48],
6. Influence of FO control on amplitudes of generated signals [36–38, 40, 45, 48, 50],
7. Problematic implementation of AGC circuit for stable wideband FO adjusting [31, 32, 34, 46, 47, 49],
8. High-impedance voltage outputs - additional buffering necessary [30, 36–38, 40, 43–45, 47, 49, 53],
9. No differential outputs - additional current to voltage converters and/or voltage buffers/inverters necessary [30–60].

Here proposed Dual-Output Controlled Gain Current Follower Buffered Amplifier (DO-CG-CFBA)-based oscillator has none of above listed drawbacks of discussed solutions.

1.4. Active-only oscillator types

Active-only oscillators are very interesting since they operate without any passive elements (even without discrete capacitors). Their behavior is defined by parasitic parameters of active elements (finite frequency features - lossy integrator, parasitic capacitances, etc.). Therefore, we can estimate only expected behavior, because exact description is not possible, and it is given by fabrication tolerances of active elements, parasites on printed circuit board, etc., mainly for high frequencies. Deviation of ideal, expected, and real oscillation frequency can be in tens of percentage. However, active-only solutions are useable for high-frequency design (tens of MHz). Workability of active-only oscillators is based on frequency limitation of used active elements and operational amplifiers (opamps), which pole frequency is used for active-only oscillators design.

Synthesis and design principles are similar to common known approaches. Minaei *et al.* [54, 55] used all-pass section without any external passive elements, for example. In Table II, we have also compared some typical active-only solutions [54–60]. Electronic control of active-only oscillators is

possible by transconductance control [54, 55, 57, 58], or by combination of intrinsic resistance and transconductance control [56, 59, 60]. Linear adjusting of FO and tuning without amplitude fluctuations and dependence on tuning process can also be possible. Benefits of low-impedance voltage outputs are also achievable [54, 55, 60]. However, these solutions require higher number of active elements (in most cases standard opamps [54–60] and additional active devices).

In comparison to our solution, discussed circuits offer similar features from electronic control point of view. Some realizations also have low-impedance voltage outputs (outputs of opamps) [54, 55, 60], but require seven active elements. Complexity of some discussed solutions, higher power consumption (many active elements in some cases) in comparison to standard solutions, and not accurate design based on estimations and large tolerances of parasites are main drawbacks of active-only oscillators. In addition, inverted outputs for differential quadrature signal generation are not available. Solution discussed by Prommee *et al.* [58] allows four quadrature output signals in form of current. Hence, differential output signal generation is also possible after additional modifications, which increase complexity.

1.5. All-pass section-based solutions and multiphase types

All-pass filters are general building blocks of quadrature oscillators. Two all-pass sections are suitable to establish quadrature oscillator (for example Keskin *et al.* [42], Herencsar *et al.* [61] and references cited therein) with controllable features. Other approach requires one all-pass section and lossless integrator ([32–34, 43, 46, 49], for instance). Interesting design approach was presented by Songsuwankit *et al.* in [62], where OTA-based phase shifters were used in order to construct of oscillator with arbitrary adjustable phase shift between both generated signals.

Attention was given to multiphase oscillator design that was also frequently investigated in the past. Interesting approaches were discussed by Abuelmaatti *et al.* [63], Gift [64], Souliotis *et al.* [65], and Kumngern *et al.* [66]. Multiphase approach allows also obtaining of quadrature outputs suitable for differential signal generation. However, circuit realizations in [63–66] seem to be difficult and extensive for quadrature output purposes, if simpler ways exist. In addition, electronic adjusting of FO is not easy, and multiple matching of parameters is required (for example [66]).

Oscillator presented in this paper simultaneously fulfils following requirements: (1) grounded capacitors (preferred for on-chip implementation); (2) direct continuous electronic adjusting; (3) FO and CO control without changes of any passive element; (4) both parameters (FO, CO) controllable by current gain only; (5) linear control of FO; (6) independent control of FO and CO without mutual disturbance; (7) easy implementation of amplitude (automatic) gain control (AGC) for FO adjusting and satisfying THD requirements - only rectified output voltage is sufficient; (8) buffered outputs - no additional buffering is necessary; (9) generated signals with four phase shifts available simultaneously - possibility of differential (symmetrical) quadrature output signals (output level is two times higher in comparison to asymmetrical - single ended solution: very advantageous in low supply voltage CMOS solutions); (10) equal amplitudes of all signals (theoretically); (11) unchangeable amplitudes while FO is tuned; (12) all real current input (intrinsic) resistances of active elements are absorbable to values of working (external) resistors.

The paper is organized as follows: Section 1 describes recent progress of adjustable active elements and oscillator design. Definition and features of new DO-CG-CFBA are given in Section 2. Section 3 deals with proposed four-phase (differential-output) oscillator and its direct electronic controlling possibilities. Real behavior, experimental, and simulation results are discussed in Sections 4 and 5, and concluding remarks are given in Section 6.

2. ACTIVE ELEMENT SUITABLE FOR MULTIPHASE OSCILLATOR DESIGN

So-called Dual-Output Current Inverted Buffered Amplifier (DO-CIBA) was introduced by Biolkova *et al.* in [29]. Dual-Output Current Follower Buffered Amplifier (DO-CFBA) or Current Follower Differential Output Buffered Amplifier (CFDOBA) known from [1] has similar behavior, but only current follower instead of inverter is used. We modified this active element in order to control current gain. We intended

to use current amplifier with controllable gain instead of current follower or inverter in the block. Therefore, we used section of adjustable current amplifier and section of voltage buffer and inverter.

Principle of the so-called DO-CG-CFBA is clear from following hybrid matrix equations:

$$\begin{bmatrix} I_z \\ V_{w+} \\ V_{w-} \\ V_p \end{bmatrix} = \begin{bmatrix} 0 & 0 & 0 & B \\ 1 & 0 & 0 & 0 \\ -1 & 0 & 0 & 0 \\ 0 & 0 & 0 & 0 \end{bmatrix} \cdot \begin{bmatrix} V_z \\ I_{w+} \\ I_{w-} \\ I_p \end{bmatrix}, \tag{1}$$

where B represents adjustable current gain. Port voltages and currents are explained in Figure 1a. From (1) is clear that DO-CG-CFBA consists of two partial blocks: adjustable current amplifier and voltage buffer/inverter. Schematic symbol and behavioral model of DO-CG-CFBA, where possible implementation employs commercially available elements (current-mode multiplier as current amplifier and differential operational amplifier/driver with unity gain as voltage buffer/inverter), is shown in Figure 1. DO-CG-CFBA has low-impedance current input terminal p , high-impedance auxiliary terminal z , and two low-impedance voltage output terminals (direct $w+$ and inverted $w-$). Current gain (B) is controlled by external DC current or voltage.

In fact, we can find some similarity of proposed DO-CG-CFBA to well-known CFA (CFA consists of CCII and also voltage buffer). However, standard CFA contains an input voltage terminal Y . Standard CFA does not allows buffered direct and inverted voltage outputs simultaneously and any kind of direct electronic control (current gain) in oscillator application [2, 18, 19, 21, 41] for example. In addition, CFA-based oscillators [2, 18, 19, 21, 41] require input voltage terminal Y in most cases (to build lossy and lossless integrators), which is not available in DO-CG-CFBA. Our oscillator solution was designed without necessity of this Y terminal.

3. PROPOSED FOUR-PHASE OSCILLATOR

We used standard state-variable approach [2, 18–20] for design of presented circuit. State matrix equations are described generally by form $\dot{x} = A \cdot x$, where:

$$\dot{x} = \begin{bmatrix} \frac{dv_1}{dt} \\ \frac{dv_2}{dt} \end{bmatrix}, \tag{2}$$

$$A = \begin{bmatrix} a_{11} & a_{12} \\ a_{21} & a_{22} \end{bmatrix}, \tag{3}$$

$$x = \begin{bmatrix} v_1 \\ v_2 \end{bmatrix}. \tag{4}$$

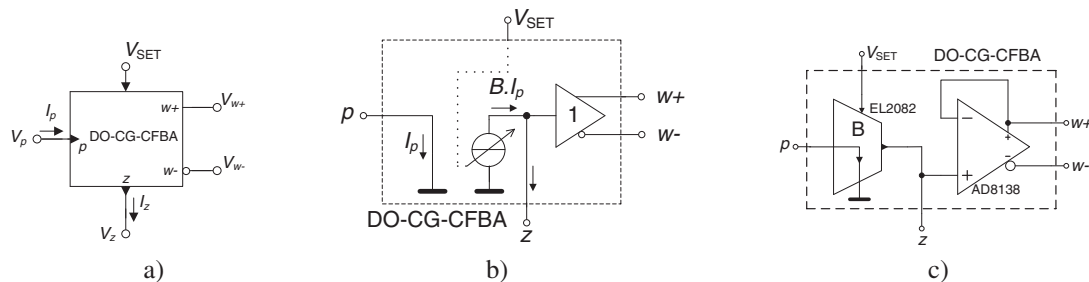


Figure 1. Dual-Output Controlled Gain Current Follower Buffered Amplifier (DO-CG-CFBA): a) schematic symbol, b) behavioral model, c) possible implementation.

Symbol A represents admittance matrix, x is vector of nodal voltages (on grounded capacitors), and \dot{x} is vector of currents through capacitors defined as derivation of state voltages. CE is given by following form:

$$\det(\lambda E - A) = \begin{vmatrix} \lambda - a_{11} & -a_{12} \\ -a_{21} & \lambda - a_{22} \end{vmatrix} = \lambda^2 - (a_{11} + a_{22})\lambda + (a_{11}a_{22} - a_{21}a_{12}) = 0, \quad (5)$$

where λ is eigenvector of A and E is unity matrix. CO and FO are defined as:

$$\text{CO} : a_{11} + a_{22} = 0, \quad (6)$$

$$\text{FO} : \omega_0 = \sqrt{\det(A)} = \sqrt{a_{11}a_{22} - a_{21}a_{12}}. \quad (7)$$

Above discussed approach supposes two grounded capacitors. Specific transfers are created between these two nodes which form state equations (admittance matrix A) appropriately to required features (quadrature, electronic control, simplicity, etc.). Basic building block with transfer $I_z / V_i = G \cdot B$ is shown in Figure 2. This block is the main core of future oscillator.

Matrix state system of our four-phase oscillator has form:

$$\begin{bmatrix} \frac{dv_1}{dt} \\ \frac{dv_2}{dt} \end{bmatrix} = \begin{bmatrix} 0 & -\frac{G_1 B_1}{C_1} \\ \frac{G_2 B_2}{C_2} & -(G_3 - G_3 B_3) / C_2 \end{bmatrix} \cdot \begin{bmatrix} v_1 \\ v_2 \end{bmatrix}, \quad (8)$$

where coefficient a_{11} is intentionally equal to 0. It allows quadrature oscillator design as it is clear from [2, 18–20] for example. CE, CO, and FO (f_0 or angular ω_0) are:

$$\text{CE} : s^2 + s \frac{G(B_3 - 1)}{C_2} + \frac{B_1 B_2 G_1 G_2}{C_1 C_2} = 0, \quad (9)$$

$$\text{CO} : B_3 \leq 1, \quad (10)$$

$$\text{FO} : \omega_0 = \sqrt{\frac{B_1 B_2 G_1 G_2}{C_1 C_2}}. \quad (11)$$

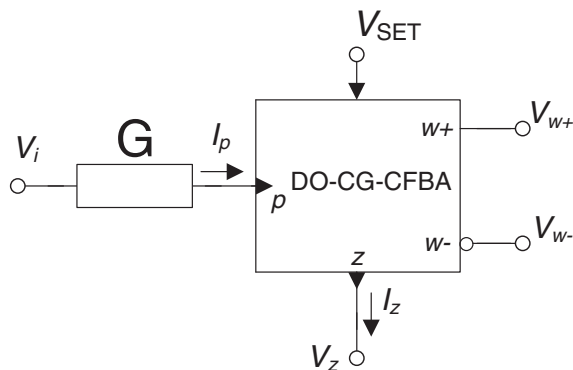


Figure 2. Elementary building block.

The ideal relative sensitivities of FO on circuit parameters are:

$$S_{B_1}^{\omega_0} = S_{B_2}^{\omega_0} = -S_{R_1}^{\omega_0} = -S_{R_2}^{\omega_0} = -S_{C_1}^{\omega_0} = -S_{C_2}^{\omega_0} = 0.5, \tag{12}$$

$$S_{B_3}^{\omega_0} = S_{R_3}^{\omega_0} = 0. \tag{13}$$

The final oscillator is shown in Figure 3. Two lossless voltage integrators are practically connected to one loop and form circuit to ensure the appropriate controllability of time constants, which is also clear from synthesis in (8).

The ratio between output amplitudes V_{OUT1} and V_{OUT2} is given by:

$$\frac{V_{OUT1}}{V_{OUT2}} = \frac{-B_1}{sR_1C_1} = \frac{-B_1}{j\omega R_1C_1}. \tag{14}$$

Substitution of the ω by ω_0 from (11) to (14) leads to:

$$\frac{V_{OUT1}}{V_{OUT2}} = \frac{-B_1}{j\sqrt{\frac{B_1B_2}{R_1R_2C_1C_2}}R_1C_1} = j\sqrt{\frac{R_2C_2B_1}{R_1C_1B_2}}. \tag{15}$$

It is possible to control oscillator by B_1 or B_2 but appropriate output amplitude (V_{OUT1} or V_{OUT2}) is not unchanged during the tuning process and control of FO is not linear. Fulfilling of the equality $B_1 = B_2 = B$ simplifies (15) to:

$$\frac{V_{OUT1}}{V_{OUT2}} = j\sqrt{\frac{R_2C_2}{R_1C_1}}, \tag{16}$$

and produced amplitudes are equal theoretically (if $R_1 = R_2 = R$, $C_1 = C_2 = C$) and constant while oscillator is tuned. The oscillator is tunable linearly by simultaneous change of $B_1 = B_2$ in wider range than by B_1 or B_2 (separately) as is obvious from:

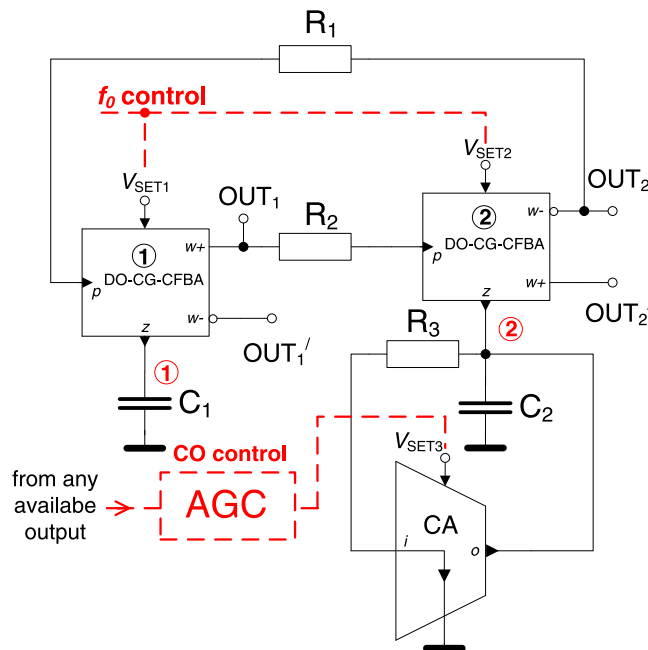


Figure 3. Four-phase oscillator employing two DO-CG-CFBAs and controllable current amplifier.

$$\omega_0 = B \sqrt{\frac{G_1 G_2}{C_1 C_2}} = \frac{B}{\sqrt{R_1 R_2 C_1 C_2}} \tag{17}$$

4. REAL BEHAVIOR AND EXPERIMENTAL RESULTS

Possible CMOS implementation of active elements used for the design of the proposed oscillator were discussed in [5, 6, 8, 10, 14, 15, 23], for example. In order to verify the functionality of the functional block, the fabrication of ICs is very time-consuming and expensive. Therefore active elements used in proposed oscillator were modeled by commercially available current multipliers and voltage buffers/inverters. This approach allows to obtain real laboratory results. In contrast to many research papers, where verification is based on only simulations of model employing specific fabrication technology, analyses obtained by measurement with real elements provide more relevant results. Authors believe that if the circuit built from discrete commercially available elements works well, then appropriate IC version consisting of current amplifiers and voltage buffers/inverters, designed via actual and specific IC technology, will work even better.

We designed oscillator with following values of passive elements: $R_1 = R_2 = R_3 = 820 \Omega$, $C_1 = C_2 = 47 \text{ pF}$. We have built real model of DO-CG-CFBA from current mode multiplier EL2082 [67] and differential opamp AD8138 [68]. Non-ideal model of DO-CG-CFBA is shown in Figure 4a. Current amplifier is characterized by non-ideal model shown in Figure 4b. EL2082 has input resistance 95Ω and output impedance $1 \text{ M}\Omega / 5 \text{ pF}$. Differential opamp AD8138 has input impedance $6 \text{ M}\Omega / 1 \text{ pF}$. Output resistance is very favorable ($< 1 \Omega$ below 20 MHz). We can estimate values of parasitic elements from above discussed parameters: $R_p = R_i \approx 95 \Omega$, $R_z \approx 860 \text{ k}\Omega$, $R_o \approx 1 \text{ M}\Omega$; $C_z \approx 6 \text{ pF}$, $C_o = 5 \text{ pF}$. Proposed oscillator including non-idealities is shown in Figure 5. We are able to include intrinsic resistances of current inputs to working resistor values (it is important for exact calculation): $R'_1 = R'_2 = R'_3 \approx 915 \Omega$ ($R'_{1,2} \approx R_{1,2} + R_{p1,2}$ and $R'_3 = R_3 + R_i$; $R_p = R_i \approx 95 \Omega$). Expected values in high-impedance nodes 1, 2 are: $R_{z1} \approx 860 \text{ k}\Omega$, $C_{z1} \approx 6 \text{ pF}$; therefore, $C'_1 = C_1 + C_{z1} \approx 53 \text{ pF}$; $R_{z2} \parallel R_o \approx 460 \text{ k}\Omega$, $C_{z2} + C_o \approx 11 \text{ pF}$; therefore, $C'_2 = C_2 + C_{z2} + C_o \approx 58 \text{ pF}$. Influence of $R_{w\pm}$ is negligible because $R_{w\pm} < 1 \Omega$ (for frequencies below 20 MHz).

When these non-idealities are taken into account, CO and FO are now in following forms:

$$\text{CO} : B'_3 \leq \frac{R_{z1} \left(\frac{R_{z2} R_o}{R_{z2} + R_o} \right) C'_1 + R'_3 R_{z1} C'_1 + R'_3 \left(\frac{R_{z2} R_o}{R_{z2} + R_o} \right) C'_2}{R_{z1} \left(\frac{R_{z2} R_o}{R_{z2} + R_o} \right) C'_1} \tag{18}$$

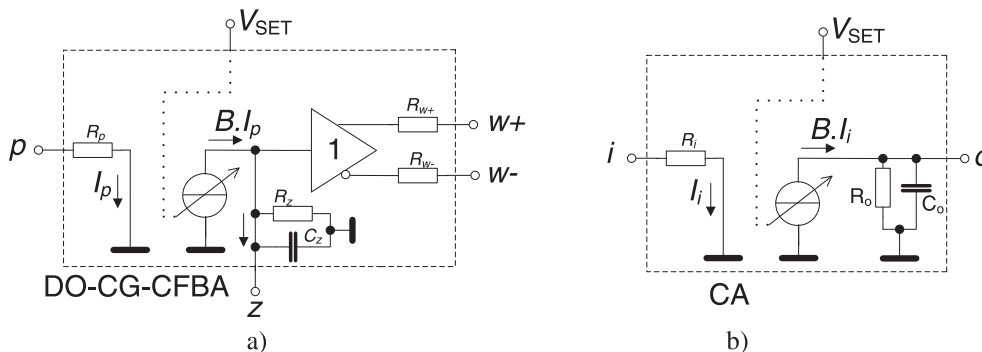


Figure 4. Non-ideal models: a) DO-CG-CFBA, b) CA.

$$FO : \omega'_0 = \sqrt{\frac{B_1 B_2 R'_3 R'_{z1} \left(\frac{R_{z2} R_o}{R_{z2} + R_o}\right) \alpha_1 \alpha_2 - R'_1 R'_2 \left[B'_3 \left(\frac{R_{z2} R_o}{R_{z2} + R_o}\right) + \left(\frac{R_{z2} R_o}{R_{z2} + R_o}\right) + R'_3\right]}{R'_1 R'_2 R'_3 R'_{z1} \left(\frac{R_{z2} R_o}{R_{z2} + R_o}\right) C'_1 C'_2}}, \tag{19}$$

where $\alpha_{1,2}$ are non-ideal voltage gains (transfers) of voltage followers in DO-CG-CFBAs. Practically, these gains are not exactly equal to 1. Second term in numerator of (19) has minimal impact on overall value of FO if $B_{1,2} > 0.2$ because it has lower value (more than hundred times for real parameters, see Table III) in comparison with first term ($\alpha_{1,2}$ are supposed equal to 1 in this calculation). Therefore:

$$B_1 B_2 R'_3 R'_{z1} \left(\frac{R_{z2} R_o}{R_{z2} + R_o}\right) \alpha_1 \alpha_2 \gg R'_1 R'_2 \left[B'_3 \left(\frac{R_{z2} R_o}{R_{z2} + R_o}\right) + \left(\frac{R_{z2} R_o}{R_{z2} + R_o}\right) + R'_3\right]. \tag{20}$$

Second term in numerator of (19) has significant impact on accuracy of FO if $B_{1,2} < 0.1$.

Table IV shows impact of non-accurate buffer gain on deviation Δf_0 (worst case) based on calculation (19) and for $f_0 = 2.507$ MHz. Tolerances of these undesired gains (larger than 5%) could cause significant problems with accuracy of f_0 (Table IV).

Relation between current gain of DO-CG-CFBA and CA (adjustable element is represented by EL2082 multiplier) and DC control voltage is given by simple equation $B \approx V_{SET}$ [67]. However, dependence of B on V_{SET} is quite nonlinear when $V_{SET} > 2$ V, see [67]. Parameters of active elements (current gains of DO-CG-CFBAs and CA) were set as follows: $B_{1,2} = 0.8$ ($V_{SET1,2} = 0.8$ V) and $B_3 \approx 1$. Ideal FO (when only R'_1, R'_2, R'_3 were taken into account) has value 2.962 MHz. Expected FO (19) is 2.507 MHz and value obtained by measurement was 2.503 MHz. Main difference between ideal and measured FO is given by parasitic capacitances C_{z1} and C_{z2} and C_o . Two AGC circuits were used for amplitude stabilization and regulation of CO during tuning process. The first type is based on opamp and the second type is employing common-emitter bipolar transistor. Both methods are shown in Figure 6. All results were carried out for output and load impedances equal to 50 Ω .

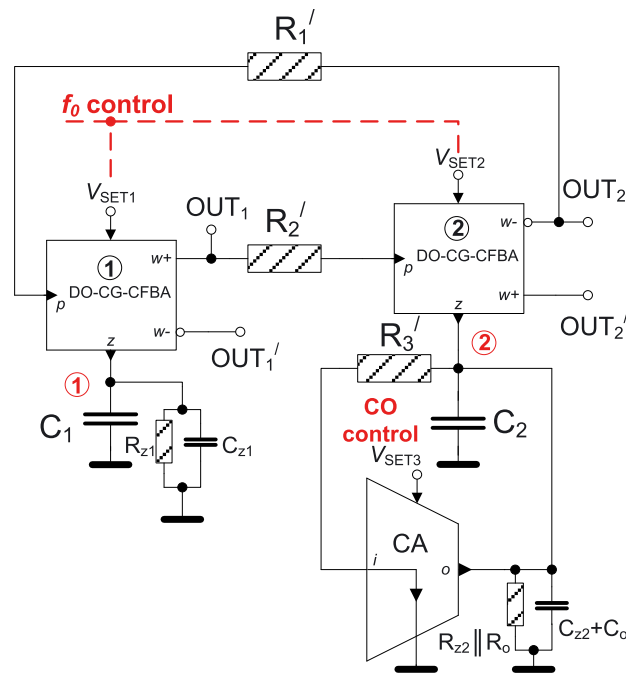


Figure 5. Proposed oscillator from Figure 3 including non-idealities.

Table III. Difference of magnitudes of terms from (20).

$B_{1,2}$ [-]	$B_1 B_2 R_3 R_{z1} \left(\frac{R_2 R_o}{R_{z2} + R_o} \right) \alpha_1 \alpha_2$	$R_1 R_2' \left[B_3' \left(\frac{R_2 R_o}{R_{z2} + R_o} \right) + \left(\frac{R_2 R_o}{R_{z2} + R_o} \right) + R_3' \right]$
10	10^{16}	10^{11}
2	10^{15}	10^{11}
1	10^{14}	10^{11}
0.2	10^{13}	10^{11}
0.1	10^{12}	10^{11}
0.01	10^{10}	10^{11}

Table IV. Impact of non-accurate voltage buffering in DO-CG-CFBA on f_0 .

Toler. $\alpha_{1,2}$ [%]	$\alpha_{1,2}$ [-]	$\pm \Delta f_0$ [kHz]
± 10	0.90–1.10	252
± 5	0.95–1.05	126
± 2	0.98–1.02	51

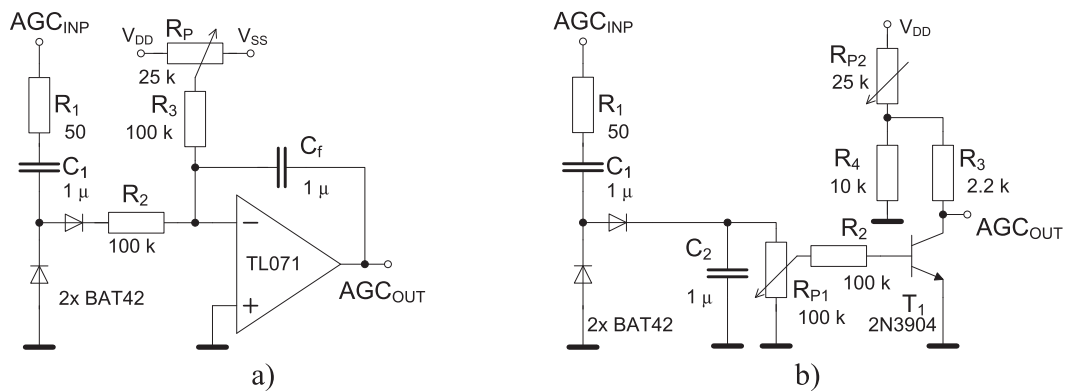


Figure 6. AGC systems used in oscillator employing: a) opamp, b) BJT.

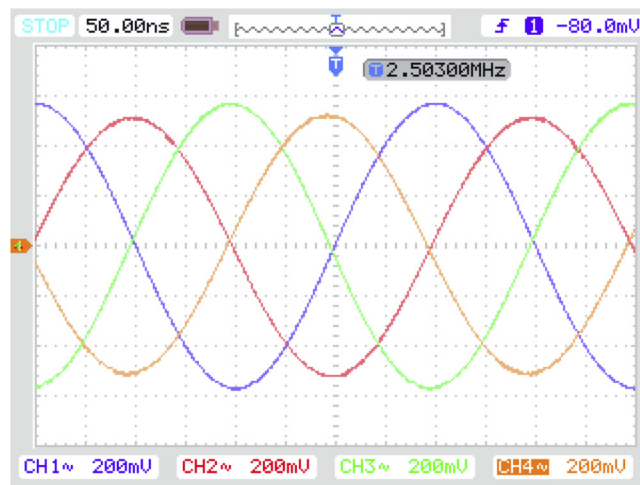


Figure 7. Generated signals at all available outputs (blue - V_{OUT1} , red - V_{OUT2} , green - V'_{OUT1} , orange - V'_{OUT2}).

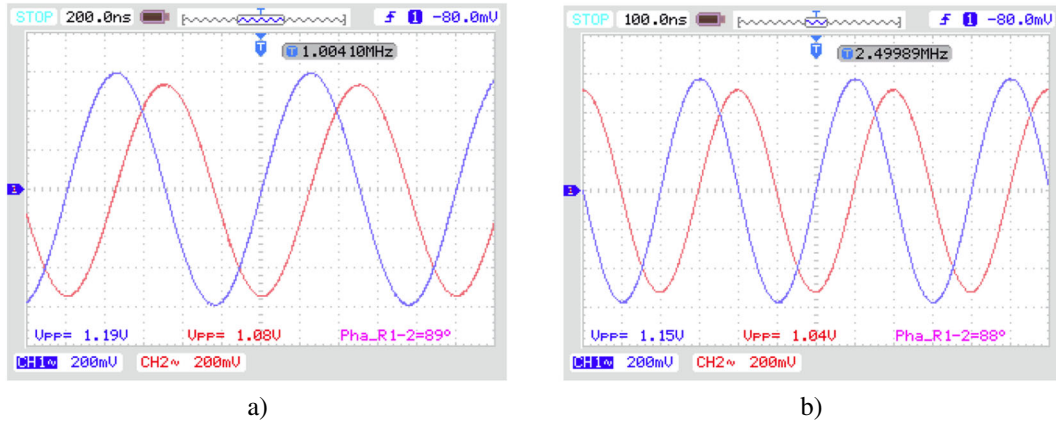


Figure 8. Generated quadrature signals V_{OUT1} and V_{OUT2} (AGC from Figure 6a): a) $f_0=1$ MHz, b) $f_0=2.5$ MHz.

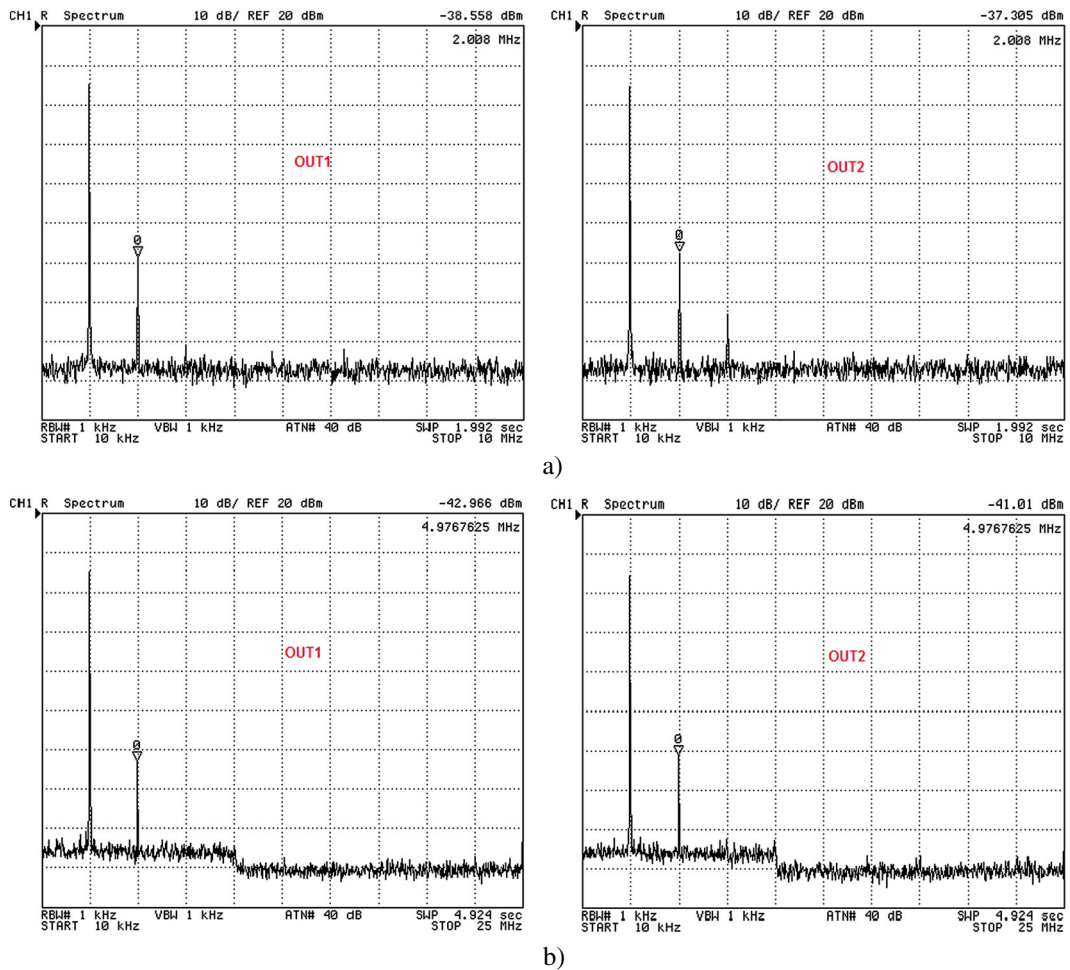


Figure 9. Spectral analyses of generated signals (AGC from Figure 6a): a) $f_0=1$ MHz, b) $f_0=2.5$ MHz.

Figure 7 shows results that were obtained from experiments with active elements discussed above. All responses (both inverted and non-inverted) are shown only in this Figure 7 because their amplitudes are the same and only phases are inverted. Because both inverted and non-inverted

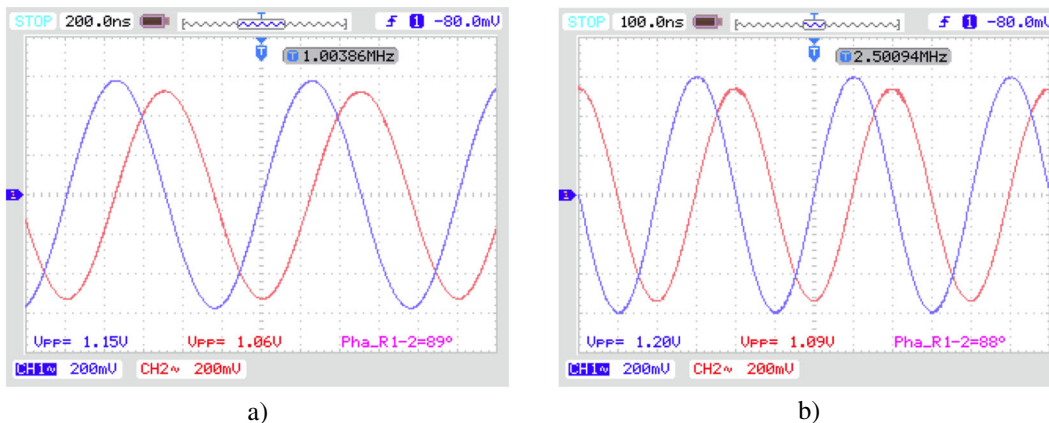


Figure 10. Generated quadrature signals V_{OUT1} and V_{OUT2} (AGC from Figure 6b): a) $f_0=1$ MHz, b) $f_0=2.5$ MHz.

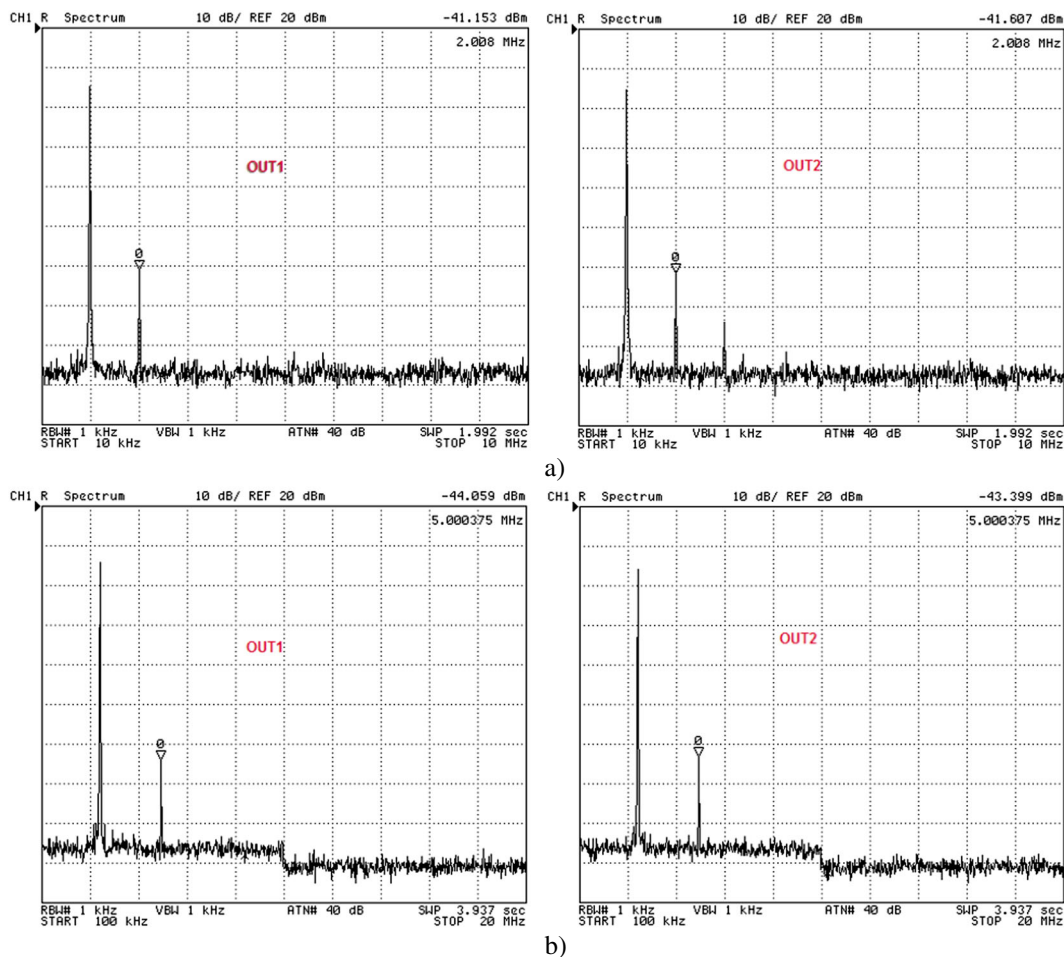


Figure 11. Spectral analyses of generated signals (AGC from Figure 6b): a) $f_0=1$ MHz, b) $f_0=2.5$ MHz.

responses are the same (except phase shift), other figures shows just two curves, each actually representing two responses for better readability. All available output voltages are shown in time domain. Transient responses of V_{OUT1} and V_{OUT2} for two different FO: 1 MHz ($B_{12}=0.323$) and

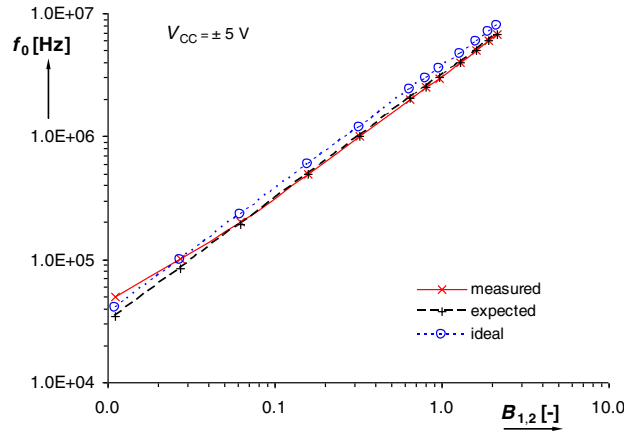


Figure 12. Dependence of FO (f_0) on $B_{1,2}$.

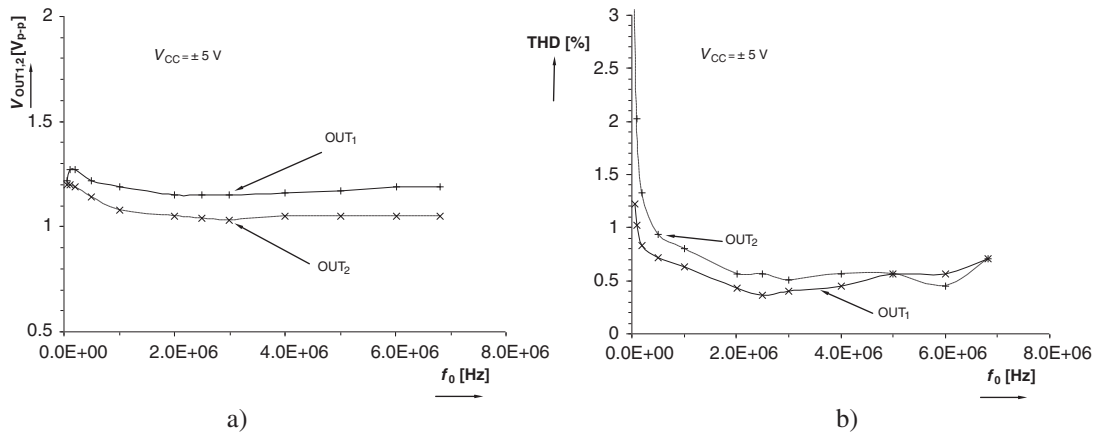


Figure 13. Measured dependences for AGC from Figure 6a: a) voltage level vs. f_0 , b) THD vs. FO.

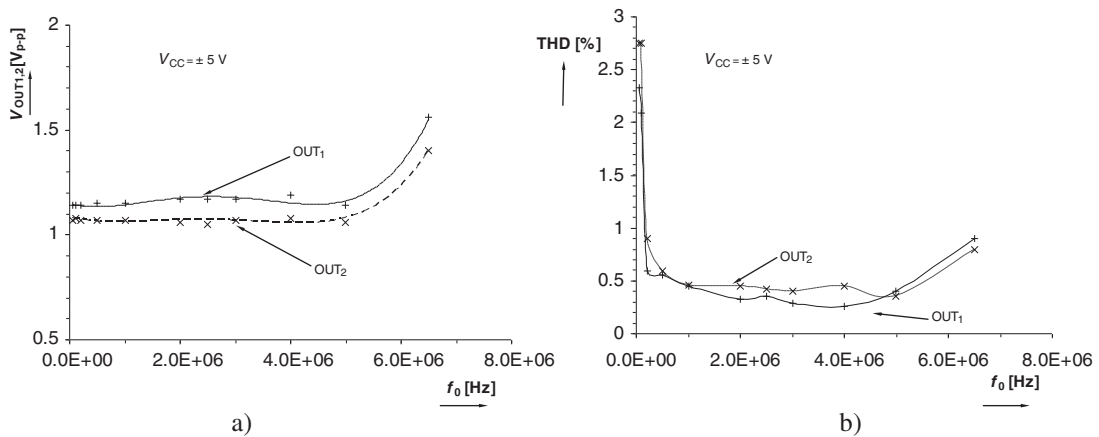


Figure 14. Measured dependences for AGC from Figure 6 b: a) voltage level vs. f_0 , b) THD vs. f_0 .

2.5 MHz ($B_{12}=0.800$) are depicted in Figure 8. AGC from Figure 6a was used. Spectral analyses related to results shown in Figure 8a and Figure 8b are presented in Figure 9. We also tested second type of AGC, which was shown in Figure 6b. Results are summarized in Figure 10 and Figure 11.

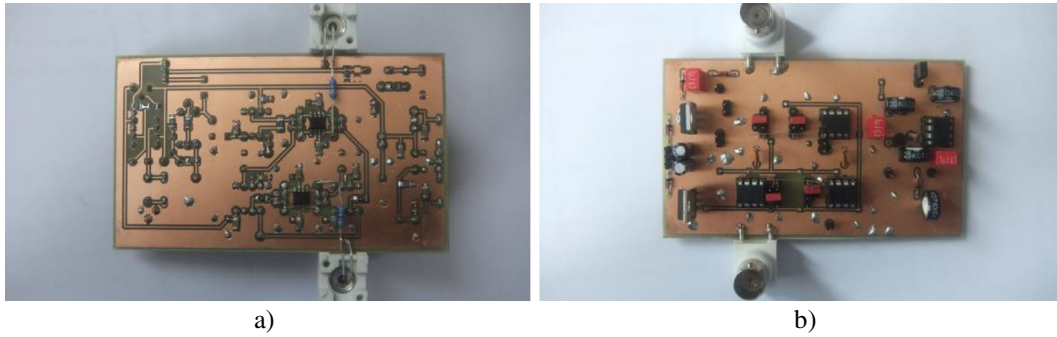


Figure 15. Experimental printed circuit board: a) bottom side, b) top side.

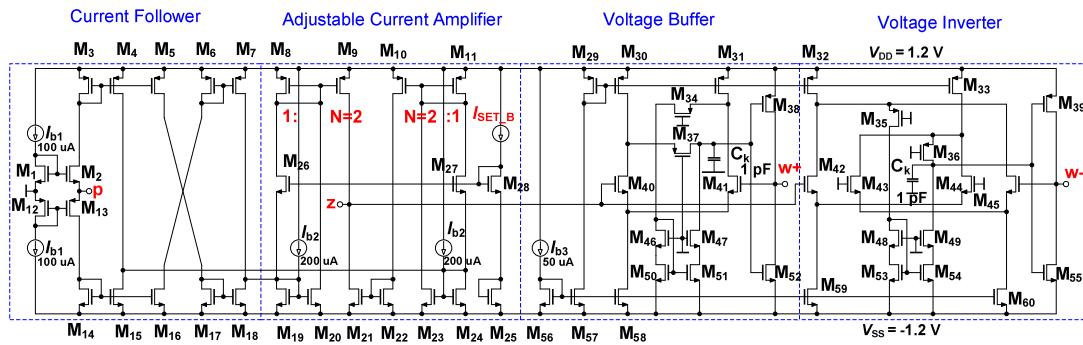


Figure 16. CMOS solution of dual output controlled gain current follower buffered amplifier (DO-CG-CFBA).

Table V. Aspect ratios of transistors in model from Figure 16.

Transistor	W/L [μm]
$M_1, M_2, M_{14}\text{--}M_{18}, M_{29}\text{--}M_{36}$	34/2
$M_3\text{--}M_7, M_{12}, M_{13}, M_{37}$	68/2
$M_8, M_{11}, M_{19}\text{--}M_{22}, M_{24}\text{--}M_{28}$	100/2
M_9, M_{10}	200/2
M_{23}	98/2
M_{38}, M_{39}	16/2
M_{40}, M_{41}	12/2
$M_{42}\text{--}M_{55}$	4/2
$M_{56}\text{--}M_{60}$	6/2

Ideal, expected, and measured dependences of FO on current gains $B_{1,2}$ are compared in Figure 12. Ideal dependence supposes only R'_1, R'_2, R'_3 . Expected results, when all non-idealities are taken into account, were gained from (19). FO adjusting range in ideal case is from 41 kHz to 7.97 MHz, expected range is from 35 kHz to 6.76 MHz and real values, which were obtained from measurement, are 50 kHz to 6.82 MHz. All results were carried out for $B_{1,2} \in \{0.01; 2.15\}$ that corresponds to $V_{\text{SET}1,2} \in \{0.01; 2.31\}$ V. We also evaluated dependences of output level and THD on FO. All results for both AGCs are depicted in Figure 13 and Figure 14. We can observe THD between 0.4 and 0.9% in almost whole range of FO for the first type of AGC (Figure 13). Fluctuations of output signals are $\Delta V_{\text{OUT}1} = \pm 45$ mV_{p-p} and $\Delta V_{\text{OUT}2} = \pm 25$ mV_{p-p} in almost whole range of tuning ($f_0 > 0.5$ MHz). For the second type of AGC, the THD between 0.3 and 0.9% is observed (Figure 14). Fluctuations of output level are smaller ($\Delta V_{\text{OUT}1} = \pm 25$ mV_{p-p} and

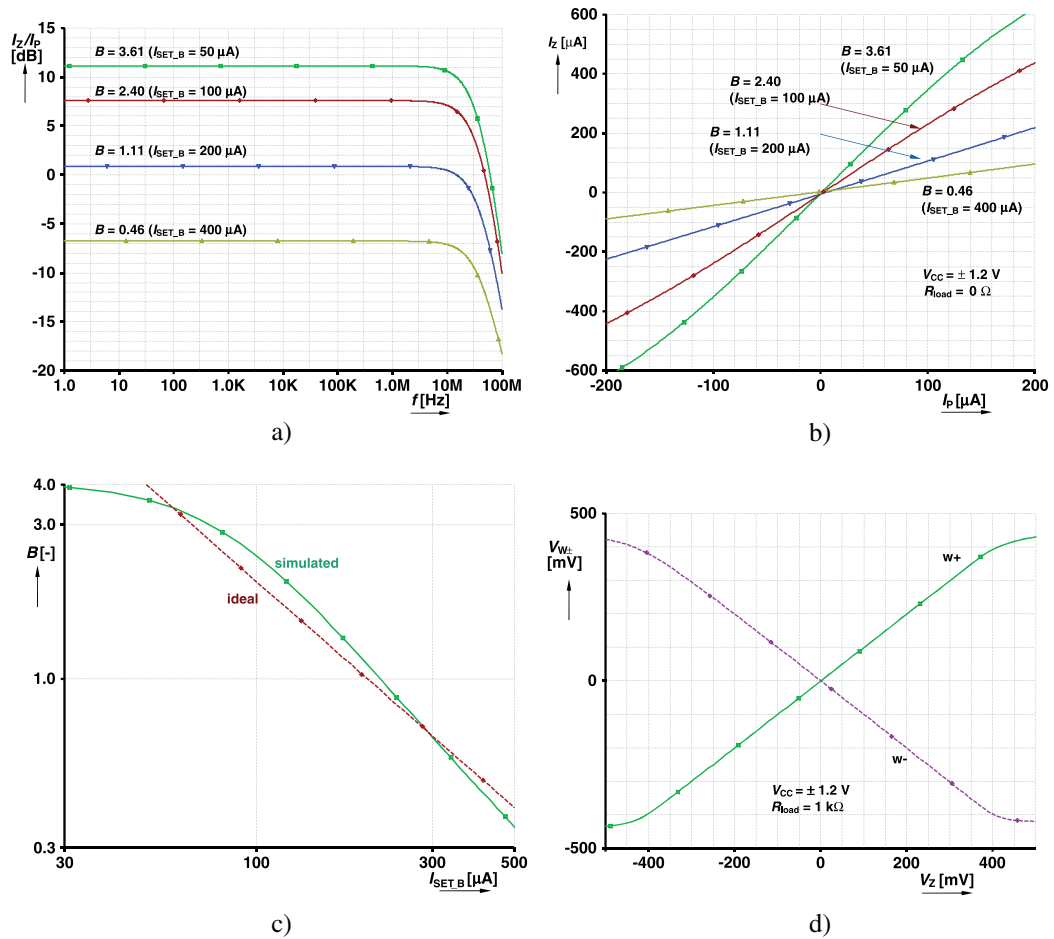


Figure 17. Important characteristics of proposed model: a) dependence of current gain on frequency, b) DC characteristics of current amplifier, c) dependence of current gain on control current, d) DC characteristics of voltage buffer and inverter.

Table VI. Important small-signal parameters.

R_p [Ω]	693
R_z [$k\Omega$]	44
R_{w+} [Ω]	0.9
R_{w-} [Ω]	1.1
f_{-3dB} (CA part) [MHz]	25
f_{-3dB} (buffer/inverter) [MHz]	56/65
for $I_{SET,B} = 200 \mu A$ ($B = 1.11$)	

$\Delta V_{OUT2} = \pm 15 mV_{p-p}$ for $f_0 < 6$ MHz. Significant increase of fluctuations is typical for upper or lower corner of f_0 adjusting (for both AGCs). Amplitudes of generated signals are strictly identical only in ideal case. Difference of output levels during the tuning process is caused by inequality of both gains (B_1 and B_2). Dependences of B_1 and B_2 of both DO-CG-CFBAs on V_{SET} are not exactly the same. Measured prototype is depicted in Figure 15.

5. CMOS IMPLEMENTATION OF DO-CG-CFBA

In this section, we introduce the CMOS structure of proposed DO-CG-CFBA in Figure 1a that is suitable for future on-chip implementation. The proposed model shown in Figure 16 complements

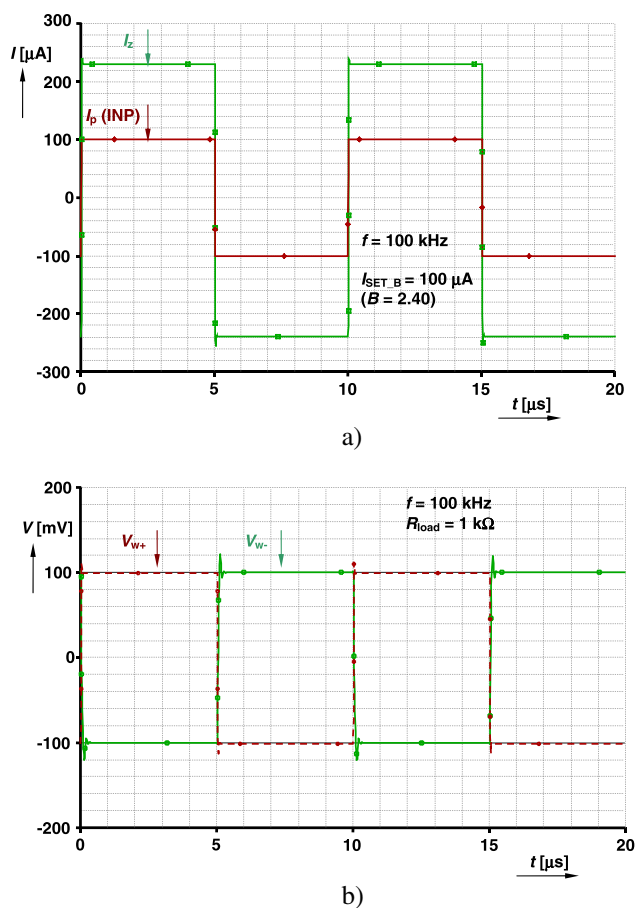


Figure 18. Square response for: a) current amplifier, b) voltage buffer/inverter.

theoretical proposal and behavioral model based on commercially available active elements. Dimensions of transistors are listed in Table V. Our model consists of four parts. The first part is current follower, which is realized by classical CC of second generation [4]. This partial element is necessary because following part (current amplifier) requires symmetrical input signal and two bias current sources. The second part (compact adjustable current amplifier) is based on solution presented by Surakamponorn *et al.* [69]. Authors used this amplifier as a part of CMOS electronically tunable CC. The voltage buffer and inverter were extracted from CMOS transistor implementation of universal voltage conveyor presented by Koton *et al.* [70]. An equation for current gain was noted in [69], and it is also valid for model that was introduced by us:

$$B = \frac{NI_{b2}}{2I_{SET-B}} \approx \frac{I_{b2}}{I_{SET-B}}, \quad (21)$$

where N means multiplication ratio of the current mirrors formed by M_8 – M_9 and M_{10} – M_{11} . Several basic characteristics of proposed CMOS structure are depicted in Figure 17. Computer analyses were performed by PSpice program and with CMOS transistor models of TSMC LO EPI 0.18 μm technology [71].

Small-signal parameters are summarized in Table VI. Responses to square excitation in order to demonstrate stability of designed model are shown in Figure 18. Amplitudes of testing signals are 100 μA (current amplifier section) and 100 mV (voltage buffer and inverter) at $f = 100$ kHz. Compensation capacitors (C_k , units of pF, see Figure 16) are used in order to increase stability of proposed CMOS model (voltage buffer/inverter). Overall power consumption of one DO-CG-CFBA CMOS model achieve 8.5 mW (for $B \approx 1$, $V_{CC} = \pm 1.2$ V). Power consumption decreases for higher current gains [69], and it is an advantage of this solution. However, current gain is theoretically limited to $B \leq 2N$ [69] (Figure 17c).

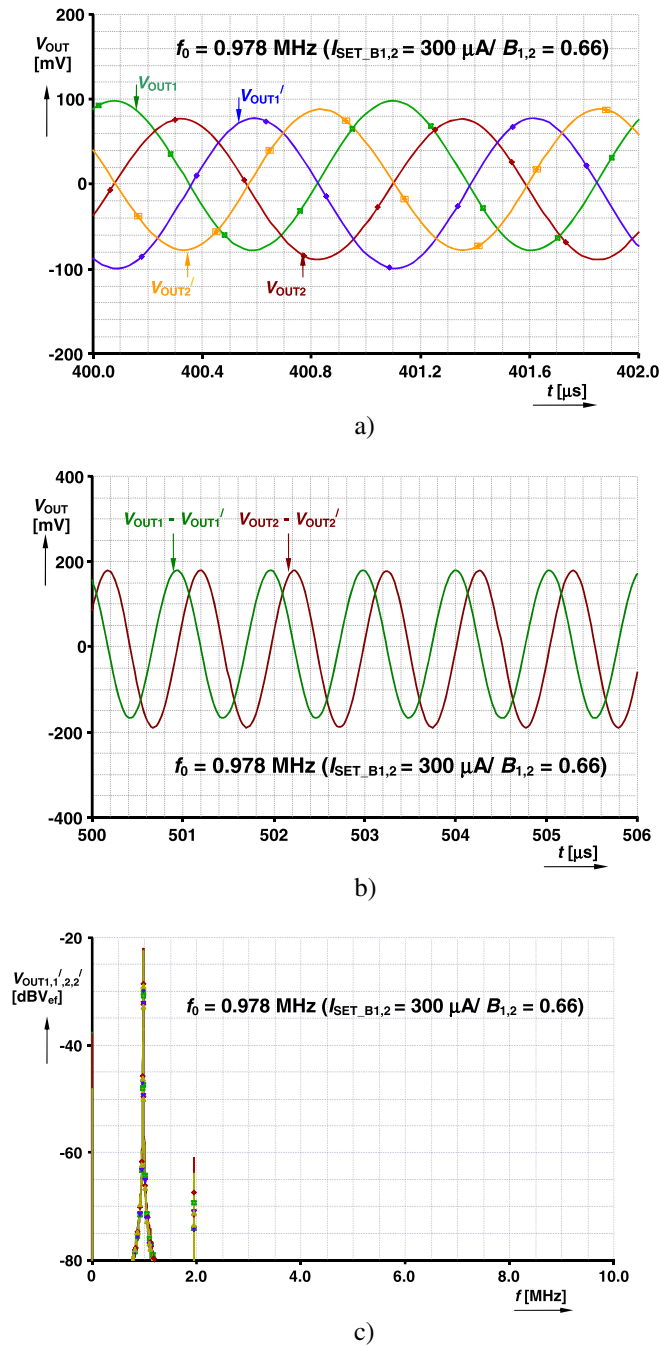


Figure 19. Simulation results of whole oscillator based on presented CMOS model: a) transient responses - single ended mode, b) transient responses - differential mode, c) frequency spectrum.

We used above introduced CMOS model in proposed oscillator shown in Figure 3, and results are given in Figure 19. In the oscillator structure, the current amplifier was simulated by CA part of DO-CG-CFBA in Figure 16, as it is expected. Parameters of design were: $C_1 = C_2 = 100 \text{ pF}$, $R_1 = R_2 = R_3 = 300 \Omega$ (including $R_p = 693 \Omega$ is overall value $R'_{1,2,3} = 993 \Omega$), $B_{1,2} = 0.66$ ($I_{\text{SET_B1,2}} = 300 \mu\text{A}$), $B_3 = 0.98$ ($I_{\text{SET_B3}} = 220 \mu\text{A}$). Ideal value of oscillation frequency achieves $f_0 = 1.058 \text{ MHz}$ (11). Value gained from simulation is 978 kHz. Transient responses of all generated signals are in Figure 19a, differential output responses are shown in Figure 19b and frequency spectrum of all output signals is in Figure 19c. Suppression of higher harmonic components (the most significant was second) was about 38–41 dBc for all available output signals which yields THD $\approx 1\%$.

6. CONCLUSION

In this paper, we presented new quadrature oscillator having following beneficial features: independent and direct electronic control of FO and CO by current gain, linear control of FO, availability of four-phases and buffered voltage outputs, even differential (symmetrical) signals are available. Presented conception provides all features which were defined in introductory section, but careful analyses revealed also some problems. Adjustability range of f_0 is restricted by achievable range of current gain of specific current active element. Inaccurate and unequal gains cause differences between generated amplitudes as well as unequal dependence of both gains on control parameter (DC voltage V_{SET} in our case). In case of on-chip low-voltage and low-power CMOS-VLSI implementation, these problems could be minimized. Main problems in such case could be restricted dynamical range and non-linearities of active elements. Therefore, available output levels will be very low (tens–hundreds of mV maximally), and it is not very favorable for rectifier in AGC system. From THD point of view, both of tested AGCs are very similar (obtained THD dependences are very close to each other), but AGC with bipolar transistor seems to be more suitable. From the stability of output amplitudes point of view (during tuning process), the AGC type with opamp is more suitable. Proposed CMOS model of DO-CG-CFBA and its utilization in oscillator also confirmed its workability and offers solution for future on-chip design. As we expected, in comparison to experimentally measured circuit (DO-CG-CFBAs based on commercially available devices), simulations of low-voltage CMOS implementation of the oscillator provided considerably lower levels of generated output signals.

ACKNOWLEDGEMENTS

Research described in the paper was supported by Czech Science Foundation projects under No. 102/09/1681, No. 102/10/P561, No. 102/11/P489, by project (Brno University of Technology) of specific research FEKT-S-11-15 and project Electronic-biomedical co-operation ELBIC M00176. Dr. Herencsar was supported by the project CZ.1.07/2.3.00/30.0039 of Brno University of Technology. The support of the project CZ.1.07/2.3.00/20.0007 WICOMT, financed from the operational program Education for competitiveness is gratefully acknowledged. The described research was performed in laboratories supported by the SIX project; the registration number CZ.1.05/2.1.00/03.0072, the operational program Research and Development for Innovation. This research work is funded also by projects EU ECOP EE.2.3.20.0094, CZ.1.07/2.2.00/28.0062. Authors also wish to thank the reviewers for their useful comments.

REFERENCES

1. Biolk D, Senani R, Biolkova V, Kolka Z. Active elements for analog signal processing: Classification, Review, and New Proposal. *Radioengineering* 2008; **17**(4):15–32.
2. Senani R, Gupta SS. Synthesis of single-resistance-controlled oscillators using CFOAs: simple state-variable approach. *IEE Proceedings on Circuits Devices and Systems* 1997; **144**(2):104–106, DOI: 10.1049/ip-cds:19971006.
3. Geiger RL, Sanchez-Sinencio E. Active filter design using operational transconductance amplifiers: a tutorial. *IEEE Circuits and Devices Magazine* 1985; **1**:20–32.
4. Fabre A, Saaid O, Wiest F, Boucheron C. High frequency applications based on a new current controlled conveyor. *IEEE Transactions on Circuits and Systems - I* 1996; **43**(2):82–91, DOI: 10.1109/81.486430.
5. Surakampontrorn W, Thitimajshima W. Integrable electronically tunable current conveyors. *IEE Proceedings-G* 1988; **135**(2):71–77.
6. Fabre A, Mimeche N. Class A/AB Second-generation Current Conveyor with Controlled Current Gain. *Electronics Letters* 1994; **30**(16):1267–1268, DOI: 10.1049/el:19940878.
7. Mahmoud SA, Hashies MA, Soliman AM. Low-voltage digitally controlled fully differential current conveyor. *IEEE Transactions on Circuits and Systems I* 2005; **52**(10):2055–2064, DOI: 10.1109/TCSI.2005.852922.
8. Minaei S, Sayin OK, Kuntman H. A new CMOS electronically tunable current conveyor and its application to current-mode filters. *IEEE Transaction on Circuits and Systems I - Regular papers* 2006; **53**(7):1448–1457, DOI: 10.1109/TCSI.2006.875184.
9. Sedighi B, Bakhtiar MS. Variable gain current mirror for high-speed applications. *IEICE Electronics Express* 2007; **4**(8):277–281, DOI: 10.1587/elex.4.277.
10. Tangsrirat W. Electronically Tunable Multi-Terminal Floating Nullor and Its Application. *Radioengineering* 2008; **17**(4):3–7.
11. Tangsrirat W, Pukkalanun T. Digitally programmable current follower and its applications. *AEU International Journal of Electronics and Communications* 2009; **63**(5):416–422, DOI: 10.1016/j.aue.2008.02.014.

12. Marcellis A, Ferri G, Guerrini NC, Scotti G, Stornelli V, Trifiletti A. The VGC-CCII: a novel building block and its application to capacitance multiplication. *Analog Integrated Circuits and Signal Processing* 2009; **58**(1):55–59, DOI: 10.1007/s10470-008-9213-6.
13. Alzaher H, Tasadduq N. Realizations of CMOS Fully Differential Current Followers/Amplifiers. *Int. Symp. On Circuits and Systems (ISCAS 2009)* May 2009; pp. 1381–1384, DOI: 10.1109/ISCAS.2009.5118022.
14. Alzaher H, Tasadduq N, Al-Ees O, Al-Ammari F. A complementary metal–oxide semiconductor digitally programmable current conveyor. *International Journal of Circuit Theory and Applications* 2013; **41**(1):69–81, DOI: 10.1002/cta.786.
15. El-Adawy A, Soliman AM, Elwan HO. Low Voltage Digitally Controlled CMOS Current Conveyor. *AEU International Journal of Electronics and Communications* 2002; **56**(3):137–144, DOI: 10.1078/1434-8411-54100086.
16. Jerabek J, Sotner R, Vrba K. Fully-differential current amplifier and its application to universal and adjustable filter. *In Proceedings of the International Conference on Applied Electronics APPEL2010*, Czech Republic: Pilsen, 2010; pp. 141–144.
17. Birolek D, Bajer J, Biolkova V, Kolka Z, Kubicek M. Z Copy-Controlled Gain-Current Differencing Buffered Amplifier and its applications. *International Journal of Circuit Theory and Applications* 2010; **39**(3):257–274, DOI: 10.1002/cta.632.
18. Gupta SS, Senani R. State variable synthesis of single resistance controlled grounded capacitor oscillators using only two CFOAs. *IEE Proceedings on Circuits, Devices and Systems* 1998; **145**(2):135–138, DOI: 10.1049/ip-cds:19981667.
19. Gupta SS, Senani R. State variable synthesis of single-resistance-controlled grounded capacitor oscillators using only two CFOAs: additional new realisations. *IEE Proceedings on Circuits Devices and Systems* 1998; **145**(6):415–418, DOI: 10.1049/ip-cds:19982393.
20. Petrzela J, Vyskocil P, Prokopec J. Fundamental oscillators based on diamond transistors. *In proceedings of 20th International Conference Radioelektronika 2010*, Czech Republic: Brno, 2010; pp. 217–220, DOI: 10.1109/RADIOELEK.2010.5478555.
21. Gupta SS, Bhaskar DR, Senani R. New voltage controlled oscillators using CFOAs. *AEU International Journal of Electronics and Communications* 2009; **63**(3):209–217, DOI: 10.1016/j.aeue.2008.01.002.
22. Souliotis G, Psychalinos C. Harmonic oscillators realized using current amplifiers and grounded capacitors. *International Journal of Circuit Theory and Applications* 2007; **35**(2):165–173, DOI: 10.1002/cta.386.
23. Alzaher H. CMOS Digitally Programmable Quadrature Oscillators. *International Journal of Circuit Theory and Applications* 2008; **36**(8):953–966, DOI: 10.1002/cta.479.
24. Bajer J, Birolek D. Digitally Controlled Quadrature Oscillator Employing Two ZC-CG-CDBAs. *In Proc. of International Conference on Electronic Devices and Systems EDS'09 IMAPS CS*, Czech Republic: Brno, 2009; pp. 298–303.
25. Birolek D, Lahiri A, Jaikla W, Siripruchyanun M, Bajer J. Realisation of electronically tunable voltage-mode/current-mode quadrature sinusoidal oscillator using ZC-CG-CDBA. *Microelectronics Journal* 2011; **42**(10):1116–1123, DOI: 10.1016/j.mejo.2011.07.004.
26. Sotner R, Jerabek J, Prokop R, Vrba K. Current gain controlled CCTA and its application in quadrature oscillator and direct frequency modulator. *Radioengineering* 2011; **20**(1):317–326.
27. Sotner R, Hrubos Z, Sevcik B, Slezak J, Petrzela J, Dostal T. An example of easy synthesis of active filter and oscillator using signal flow graph modification and controllable current conveyors. *Journal of Electrical Engineering* 2011; **62**(5):258–266, DOI: 10.2478/v10187-011-0041-z.
28. Herencsar N, Lahiri A, Vrba K, Koton J. An electronically tunable current-mode quadrature oscillator using PCAs. *International Journal of Electronics* 2011; **99**(5):609–621, DOI: 10.1080/00207217.2011.643489.
29. Biolkova V, Bajer J, Birolek D. Four-Phase Oscillators Employing Two Active Elements. *Radioengineering* 2011; **20**(1):334–339.
30. Herencsar N, Koton J, Vrba K, Lahiri A. New voltage-mode quadrature oscillator employing single DBTA and only grounded passive elements. *IEICE Electronics Express* 2009; **6**(24):1708–1714.
31. Li Y. Electronically tunable current-mode quadrature oscillator using single MCDTA. *Radioengineering* 2010; **19**(4):667–671.
32. Keawon R, Jaikla W. A Resistor-less Current-mode Quadrature Sinusoidal Oscillator Employing Single CCCDTA and Grounded Capacitors. *Przeglad Elektrotechniczny* 2011; **87**(8):138–141.
33. Jaikla W, Siripruchyanun M, Bajer J, Birolek D. A simple current-mode quadrature oscillator using single CDTA. *Radioengineering* 2008; **17**(4):33–40.
34. Pandey N, Paul SK. Single CDTA-based current mode all-pass filter and its applications. *Journal of Electrical and Computer Engineering* 2011; **2011**:1–5, DOI: 10.1155/2011/897631.
35. Jaikla W, Lahiri A. Resistor-less current-mode four-phase quadrature oscillator using CCCDTA and grounded capacitors. *AEU International Journal of Electronics and Communications* 2012; **66**(3):214–218, DOI: 10.1016/j.aeue.2011.07.001.
36. Horng JW. A sinusoidal oscillator using current-controlled current conveyors. *International Journal of Electronics* 2001; **88**(6):659–664, DOI: 10.1080/00207210110044369.
37. Kumngern M, Junnapiya S. A sinusoidal oscillator using translinear current conveyors. *In Proceedings of Asia Pacific Conference on Circuits and Systems (APCCAS 2010)*, Malaysia: Kuala Lumpur, 2010; pp. 740–743, DOI: 10.1109/APCCAS.2010.5774754.
38. Lahiri A. Novel voltage/current-mode quadrature oscillator using current differencing transconductance amplifier. *Analog Integrated Circuits and Signal Processing* 2009; **61**(2):199–203, DOI: 10.1007/s10470-009-9291-0.

39. Lahiri A. Current-mode variable frequency quadrature sinusoidal oscillator using two CCs and four passive components including grounded capacitors. *Analog Integrated Circuits and Signal Processing* 2012; **71**(2):303–311, DOI: 10.1007/s10470-010-9571-8.
40. Liu SI. Single-resistance-controlled/ voltage-controlled oscillator using current conveyors and grounded capacitors. *Electronics Letters* 1995; **31**(5):337–338, DOI: 10.1049/el:19950259.
41. Lahiri A, Gupta M. Realizations of Grounded negative Capacitance Using CFOAs. *Circuits, Systems and Signal Processing* 2011; **30**(1):134–155, DOI: 10.1007/s00034-010-9215-3.
42. Keskin AU, Biölek D. Current mode quadrature oscillator using current differencing transconductance amplifiers (CDTA). *IEE Proceedings Circuits Devices and Systems* 2006; **153**(3):214–218.
43. Keskin AU, Aydin C, Hancioglu E, Acar C. Quadrature Oscillator Using Current Differencing Buffered Amplifiers (CDBA). *Frequenz* 2006; **60**(3):21–23.
44. Linares-Barranco B, Rodriguez-Vazquez A, Sanches-Sinencio E, Huertas JL. CMOS OTA-C High-Frequency Sinusoidal Oscillators. *IEEE Journal of Solid-State Circuits* 1991; **26**(2):160–165, DOI: 10.1109/4.68133.
45. Tao Y, Fidler JK. Electronically tunable dual-OTA second order sinusoidal oscillators/filters with non-interacting controls: A systematic synthesis approach. *IEEE Transaction on Circuits and Systems I: Fundamental Theory and Applications* 2000; **47**(2):117–129, DOI: 10.1109/81.828566.
46. Songkla SN, Jaikla W. Realization of Electronically Tunable Current-mode First-order Allpass Filter and Its Application. *International Journal of Electronics and Electrical Engineering* 2012; **6**:40–43.
47. Senani R. New electronically tunable OTA-C sinusoidal oscillator. *Electronics Letters* 1989; **25**(4):286–287, DOI: 10.1049/el:19890199.
48. Abuelmaatti MT, Khan MH. New electronically-tunable oscillator circuit using only two OTAs. *Active and Passive Electronic Components* 1998; **20**(4):189–194, DOI: 10.1155/1998/63168.
49. Minaei S, Yuçe E. Novel Voltage-Mode All-pass Filter Based on Using DVCCs. *Circuits Systems and Signal Processing* 2010; **29**(3):391–402, DOI: 10.1007/s00034-010-9150-3.
50. Maheshwari S, Chatuverdi B. High output impedance CMQOs using DVCCs and grounded components. *International Journal of Circuit Theory and Applications* 2011; **39**(4):427–435, DOI: 10.1002/cta.636.
51. Kuntman H, Ozpinar A. On the realization of DO-OTA-C oscillators. *Microelectronics Journal* 1998; **29**(12):991–997, DOI: 10.1016/S0026-2692(98)00063-9.
52. Summart S, Thongsopa Ch, Jaikla W. OTA Based Current-mode Sinusoidal Quadrature Oscillator with Non-interactive Control. *Przeglad Elektrotechniczny* 2012; **88**(7a):14–18.
53. Galan J, Carvajal RG, Torralba A, Munoz F, Ramirez-Angulo J. A low-power low-voltage OTA-C sinusoidal oscillator with large tuning range. *IEEE Transaction on Circuits and Systems I: Fundamental Theory and Applications* 2005; **52**(2):283–291, DOI: 10.1109/TCSI.2004.841599.
54. Minaei S, Cicekoglu O. New current-mode integrator, all-pass section and quadrature oscillator using only active elements. In *proceedings of 1st IEEE International conference on Circuits and Systems for Communications ICCSC02*, 2002; pp. 70–73, DOI: 10.1109/OCCSC.2002.1029047.
55. Minaei S, Cicekoglu O. New Current-Mode Integrator and All-pass Section without External Passive Elements and Their Application to Design a Dual-Mode Quadrature Oscillator. *Frequenz* 2003; **57**(1-2):19–24.
56. Lawanwisut S, Siripruchyanun M. An active-only high-output impedance current-mode quadrature oscillator using CCCCTA based-lossless differentiators. In *Proceedings of the International Conference TENCON 2009*, Republic of Singapore: Singapore, 2009; pp. 1–4, DOI: 10.1109/TENCON.2009.5395861.
57. Abuelmaatti MT, Alzahr HA. Active-only sinusoidal oscillator. *Microelectronics Journal* 1998; **29**(7):461–464, DOI: 10.1016/S0026-2692(97)00104-3.
58. Prommee P, Somdunyanok M, Dejhan K. Universal filter and its oscillator modification employing only active components. In *Proceedings of the International Conference on Intelligent Signal Processing and Communications Systems ISPACS 2008*, Bangkok: Thailand, 2008; pp. 1–4, DOI: 10.1109/ISPACS.2009.4806759.
59. Jantakun A, Pisutthipong N, Siripruchyanun M. An active-only high output-impedance current-mode universal biquad filter and quadrature oscillator based on lossless differentiators. In *Proceedings of the International Conference on Electrical Engineering/ Electronics Computer Telecommunications and Information Technology (ECTI-CON) 2010*, Thailand: Chaing Mai, 2010; pp. 32–36.
60. Abuelmaatti MT. Active-only sinusoidal oscillator with electronically-tunable fully-uncoupled frequency and condition of oscillation. *Active and passive Electronic Components* 2001; **24**(4):233–241, DOI: 10.1155/2001/27076.
61. Herencsar N, Minaei S, Koton J, Yuçe E, Vrba K. New resistorless and electronically tunable realization of dual-output VM all-pass filter using VDIBA. *Analog Integrated Circuits and Signal Processing* 2013; **74**(1):141–154, DOI: 10.1007/s10470-012-9936-2.
62. Songsuwankit K, Petchmaneeumka W, Riewruja V. Electronically adjustable phase shifter using OTAs. In *Proceedings of the International Conference on Control, Automation and Systems (ICCAS2010)*, Gyeongju-do: Korea, 2010; pp. 1622–1625.
63. Abuelmaatti MT, Al-Qahtani MA. A New Current-Controlled Multiphase Sinusoidal Oscillator Using Translinear Current Conveyors. *IEEE Transactions on Circuits and Systems II: Analog and Digital Signal Processing* 1998; **45**(7):881–885, DOI: 10.1109/82.700937.
64. Gift SJG. The application of all-pass filters in the design of multiphase sinusoidal systems. *Microelectronics Journal* 2000; **31**(1):9–13, DOI: 10.1016/S0026-2692(99)00084-1.

65. Souliotis G, Psychalinos C. Electronically controlled multiphase sinusoidal oscillators using current amplifiers. *International Journal of Circuit Theory and Applications* 2009; **37**(1):43–52, DOI: 10.1002/cta.486.
66. Kumngern M, Chanwutium J, Dejhana K. Electronically tunable multiphase sinusoidal oscillator using translinear current conveyors. *Analog Integrated Circuits and Signal Processing* 2010; **65**(2):327–334, DOI: 10.1007/s10470-010-9470-z.
67. EL2082: Current-Mode Multiplier, Intersil (Elantec) [online]. 1996, last modified 2003 [cit.28.7.2011]. Available from: <http://www.intersil.com/data/fn/fn7152.pdf>
68. AD8138: Low Distortion Differential ADC Driver, Analog Devices [online]. last modified 1/2006 [cit.28.7.2011]. Available from: http://www.analog.com/static/imported-files/data_sheets/AD8138.pdf
69. Surakamponorn W, Kumwachara K. CMOS-based electronically tunable current conveyor. *Electronics Letters* 1992; **28**(14):1316–1317, DOI: 10.1049/el:19920836.
70. Koton J, Herencsar N, Vrba K, Metin B. Current- and voltage-mode third-order quadrature oscillator. *In Proceeding of the 13th International Conference on Optimization of Electrical and Electronic Equipment (OPTIM 2012)*, Romania: Brasov, 2012, pp. 1203–1206, DOI: 10.1109/OPTIM.2012.6231795.
71. MOSIS parametric test results of TSMC LO EPI SCN018 technology. Available from: ftp://ftp.isi.edu/pub/mosis/vendors/tsmc-018/t44e_lo_epi-params.txt. Cited 24.5.2012.

[15] SOTNER, R., JERABEK, J., HERENC SAR, N., VRBA, K., DOSTAL, T. Features of multi-loop structures with OTAs and adjustable current amplifier for second-order multiphase/quadrature oscillators. *AEU - International Journal of Electronics and Communications*, 2015, vol. 69, no. 5, p. 814-822. ISSN: 1434-8411.



Features of multi-loop structures with OTAs and adjustable current amplifier for second-order multiphase/quadrature oscillators

Roman Sotner^{a,*}, Jan Jerabek^b, Norbert Herencsar^b, Kamil Vrba^b, Tomas Dostal^{a,c}

^a Department of Radio Electronics, Brno University of Technology, Technická 3082/12, Brno 616 00, Czech Republic

^b Department of Telecommunications, Brno University of Technology, Technická 3082/12, Brno 616 00, Czech Republic

^c Department of Electrical Engineering and Computer Science, College of Polytechnics Jihlava, Tolsteho 16, Jihlava 586 01, Czech Republic

ARTICLE INFO

Article history:

Received 1 October 2014

Accepted 28 January 2015

Keywords:

Current amplifier
Multiphase oscillator
Operational transconductance amplifier
Quadrature oscillator
Signal flow graphs

ABSTRACT

This contribution presents two types of second-order multiphase oscillators based on the multiple-loop transfer modification. The main aim of this paper is to show the possibilities of two structures to generate multiphase outputs (phase shifts of multiples of $\pi/2$ and $\pi/4$) and the features resulting from this type of synthesis. We focused on independently and electronically adjustable oscillation condition for simple implementation of automatic amplitude gain control circuit (AGC) and linear electronic control of oscillation frequency. Basic two-loop structure (typical for band-pass response in multifunctional filtering structures) with additional loop of the feedback for control of oscillation condition was used. There are two different requirements for oscillation condition fulfillment in the same topology. These aspects (actual polarity of the loops transfers) are important for design of the AGC in specific case. Mutual relations between generated signals at available outputs of the circuits are studied. Design is supported by the detailed signal-flow graphs. Final circuits were verified by PSpice simulations.

© 2015 Elsevier GmbH. All rights reserved.

1. Introduction

Tunable oscillators with multiphase character (quadrature, for example) are under increasing attention of many researchers today. Despite the fact there are many interesting multiphase solutions, they are very often based on subsequently shifted phase of elementary blocks (lossy integrators, differentiators) [1–7]. These circuits are typical by easy synthesis, easily controllable condition of oscillation (CO) by gain in the loop, and generate phases in multiples of $\pi/2$, $\pi/4$, $\pi/6$ (phase shift of elementary building block). However, such realizations are very complicated (many cascaded building blocks) and difficult matching of several parameters is required for tuning [2,4]. Possibility of simultaneous adjusting of each time constant is an advantage for tuning of frequency of oscillations (FO) in some cases [3,5].

Another conception is based on utilization of all-pass section and an integrator [8–14]. Oscillators designed in this way produce less number of output phases and independence of CO and FO is problematic in some cases [8,10,12–14].

* Corresponding author. Tel.: +420 541 14 6560.

E-mail addresses: sotner@feec.vutbr.cz (R. Sotner), jerabekj@feec.vutbr.cz (J. Jerabek), herencsn@feec.vutbr.cz (N. Herencsar), vrbak@feec.vutbr.cz (K. Vrba), tomas.dostal@vspj.cz (T. Dostal).

We can also use cascading of two all-pass sections (for example [15,16]). Substantial improvements in separation of CO and FO were shown.

Simple (in comparison with standard multiphase solutions utilizing cascading of sections [1–7]) circuit structures also enable the output signals with multiphase character (not only two quadrature output signals) if specific design requirements (and matching of some parameters) are fulfilled [17]. However, tuning of the oscillator is problematic and only CO is independently settable. Fortunately, recently investigated structures [18] also reveal circuit where independent control of CO and FO occurs. Multiphase features of two simple circuits producing phase shifts of $\pi/4$, $\pi/2$, $3\pi/4$, $5\pi/4$ and π without necessity of cascade of integrators/differentiators were verified in [18]. However, these structures require specific matching of parameters in order to ensure constant and unchangeable output amplitudes during the tuning process and that is the main problem of these circuits. This field requires further attention.

This paper focuses on simple multiphase solutions (simpler than usually used approaches based on cascading of subsections [1–7]) with minimum passive elements that allows obtaining of several outputs typically ($\pi/2$) and non-typically (multiples of $\pi/4$) phase shifted signals without dependence of linear tuning process on output amplitudes. We used a very illustrative way of the synthesis by means of signal-flow graphs (SFG) [19,20] and focused out attention

on the utilization of the proposed structures for differential-voltage mode operation. Many suitable active elements exist and were reported in recent years [21]. We selected operational transconductance amplifiers (OTA) [21,22] and adjustable current amplifier (CA) for the synthesis because they allow simple utilization in systems without necessity of requiring resistors.

We compared known solutions of the similar electronically controllable types of second-order oscillators based on OTAs and several advanced devices based on OTA (partially), i.e. current differencing transconductance amplifiers (CDTA), voltage differencing transconductance amplifiers (VDTA), current follower transconductance amplifiers (CFTA) and current conveyor transconductance amplifiers (CCTA) – extensions of the OTA features by further active elements [21] and our solutions from several aspects, see Table 1. All the circuits (discussed in Table 1) allow at least one phase shift ($\pi/2$ in many cases). Our goal is to find electronically controllable solutions where multiphase (or differential) outputs are available and unchangeable in voltage level under condition of FO tuning which utilize minimal number of active and passive elements and operate without requiring matching of parameters. Many solutions have been compared in detail in Table 1 but they have the following problems: (1) Some circuits employ 4 and more active elements [23–29]; (2) Some solutions are electronically tunable only under very unsuitable conditions [8,30] (see notes in Table 1); (3) Many of the studied circuits do not allow linear control of the FO [31–45]; (4) Many circuits allow linear control of FO under disadvantageous matching condition only – not suitable in practice and for utilization of amplitude automatic gain control circuit (AGC) [8,10,30,46]; (5) There exist several oscillators where all the generated output levels are independent on linear tuning process [8,10,24–26,28,47–49] but almost none of them have multiphase outputs (circuit in [47] has multiphase outputs but produced signals seems to be influenced by CO control, circuit in [28] allows multiphase operation but structure is too complicated); (6) Separated control of CO (by independent parameter suitable for driving) of some solutions (typically in cases discussed in point 6, 7, and 8) is not possible [8,10,30,46]; (7) A majority of solutions is not suitable for differential outputs [8,10,23–27,29–34,36–43,48,49,51,52]; (8) A very small number of studied types of circuits allow multiphase outputs (more than 2) [28,32,35,47] but output amplitudes of some of them vary if FO is tuned [32,35] or do not allow differential outputs [32]; (9) Phase shifts in multiples of $\pi/4$ are possible in a limited number of known circuits (for example [17,18]) except complicated multiphase (higher-order) solutions that employ cascading of integrator/differentiator lossy blocks (for example [7]). As conclusion of such analysis we intended to synthesize second-order oscillator (recapitulation of required specification): (a) allowing linear control of FO, (b) having completely independent parameter for CO setting, (c) having multiphase output character of produced signal (available also for differential/symmetrical operation) with unchangeable output levels during the tuning process (FO change), (d) providing the simplest circuit structure (minimal number of passive and active elements).

Considering these points, we concluded that only two second-order solutions (employing OTAs and OTA-based active elements

[28,47]) fulfill the main above given conditions (but with some drawbacks). A solution introduced by Galan et al. [28] utilizes four OTAs (differential output) and four capacitors. Four additional voltage buffers for impedance separation of four high-impedance output nodes (nodes of capacitors) in case of low-impedance loads are required. Therefore, it is too complex. Circuit presented by Jaikla et al. [47] seems to be useful and beneficial. The authors discuss very simple realization (two active and two passive elements) but output responses are available in form of currents only and further current-to-voltage conversion with additional buffering is necessary. It seems that relations between produced output currents can be influenced by the CO adjusting. In fact, each active element, used in [47], consists of two subsections (current differencing unit [21] and multiple-output OTA). Therefore, there is still scope for improvements in complexity of solution if simple single-purpose active elements (active elements without sub-partial composition by simple active parts) are used.

Our proposal provides all featured benefits (a)–(d) in solutions with minimal number of passive elements (capacitors only) and a sufficiently low number of active elements (always two OTAs with multiple outputs and one adjustable current amplifier). In comparison with the previously reported structures based on OTAs only [23–29,44,47] our solutions utilize also additional current amplifier beneficially. Our proposed structures are comparable to the simplest circuits that allow all the specified features simultaneously [28] and remove some drawbacks of known similar circuits. Nevertheless, same as all other circuitries, also our circuits presented in this paper require additional buffering of high-impedance nodes to obtain low-impedance voltage outputs. Fortunately, as we will see in further text, such buffering by special voltage buffer (non-inverting and inverting output) can be also profitable in order to ensure multiphase features.

The paper is divided as follows: Section 1 introduces recent progress of the research in the field and shows imperfections of available solutions that should be solved. A detailed comparison of various hitherto published circuits is also given. Section 2 deals with the OTAs and CA-based structures leading to featured advantages. Detailed simulation results are shown in Section 3 and concluding remarks are presented in Section 4.

2. Circuit structures

Our derivation is based on a very simple structure employing only one multiple-output OTA and one single-output OTA together with one current amplifier for CO control. A proposal of presented circuits was inspired by interesting work of [44] written by Bhaskar-Abdalla-Senani. The authors proposed several structures that require two functional current outputs of the OTA and employ three active elements. Functional outputs mean a number of outputs required for interconnection between integrators and closing functional loops in the circuit. OTA terminals for additional explicit current outputs are not taken to this group (functional). However, a lack of linear control of oscillation frequency in all the circuits proposed in [44] is evident. All there presented types have frequency of oscillation equal to $\omega_0 = (g_{m1}g_{m2}/(C_1C_2))^{1/2}$.

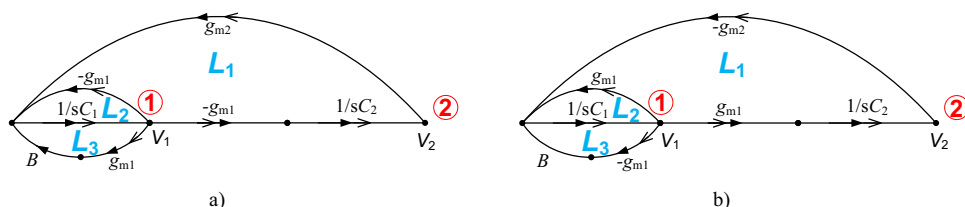


Fig. 1. SFG solutions of the OTA-based and adjustable current amplifier based quadrature oscillator that requires for CO: (a) $B \geq 1$, (b) $B \leq 1$.

Table 1
Comparison of electronically controlled simple second-order OTA (and active block extending OTA element) based solutions generating phase shift of $\pi/2$ or $\pi/4$ that are not employing multiple cascading of integrator/differentiator based building blocks in one loop.

Solution	No. of passive elements	No. and type of active elements	Type of the lowest output phase shift	Linear control of FO possible	Simultaneous adjusting of parameters setting FO and CO for linear control of FO and independent CO required	All produced amplitudes independent on tuning process	Type of output signal (current or voltage)	Separated parameter(s) for CO control without influence on FO	Possibility of differential voltage $\pi/2$ or $\pi/4$ outputs without additional modification	Multiphase type (more than two output responses)
[8]	2	1 CCCDTA		*1	Yes	Yes	Current	No	No	No
[10]	2	2 ZC-CDTA		*2	Yes	Yes	Current	No	No	No
[31]	2	2 CCCDTA		No	–	No	Current	Yes	No	No
[30]	3	1 CDTA		*3	Yes	Yes	Current	No	No	No
[32]	2	1 DVCCCTA		No	–	No	Both	Yes	No	Yes
[47]	2	2 CCCDTA		Yes	No	Yes	Current	Yes	Yes	Yes
[50]	2	2 CCCFTA		Yes	No	No	Current	Yes	No	No
[33]	3	1 CCCFTA		No	–	No	Current	Yes	No	No
[34]	3	1 VDTA		No	–	No	Current	Yes	No	No
[49]	3	1 VDTA, 1 CA		Yes	No	Yes	Voltage	Yes	No	No
[35]	5	1 ZC-VDTA		No	–	No	Voltage	Yes	Yes	Yes
[36]	4	1 CCTA		No	–	No	Voltage	Yes	No	No
[51]	2	2 VDTA		Yes	No	No	Current	Yes	No	No
[37,38]	3	2 CDTA		No	–	No	Current	Yes	No	No
[39]	2	3 CDTA	$\pi/2$	No	–	No	Current	Yes	No	No
[48]	2	2 CDTA	$\pi/2$	Yes	–	Yes	Current	Yes	No	No
[40]	2	3 CDTA	$\pi/2$	No	–	No	Current	Yes	No	No
[41]	2	1 DO-CCCDTA		No	–	N/A	Voltage	Yes	No	No
[52]	2	2 CCCDTA, 1 VB		Yes	No	N/A	Voltage	Yes	No	No
[42]	2	1 MO-CCCDTA (Fig. 2)		No	–	N/A	Current	Yes	No	No
[43]	3	3 CDTA		No	–	No	Both	Yes	No	N/A
[23]	3	4 OTA		Yes	No	N/A	Voltage	Yes	No	No
[24]	2	3-6 OTA (Figs. 5b and 6b)		Yes	No	Yes	Voltage	Yes	No	No
[25]	2	4 OTA (Fig. 2d)		Yes	No	Yes	Voltage	Yes	No	No
[26]	2	4 OTA (Fig. 1c)		Yes	No	Yes	Voltage	Yes	No	No
[27]	2	4-6 DO-OTA (Fig. 1b,c,e,g)		Yes	No	N/A	Current	Yes	No	No
[28]	4	4 DO-OTA		Yes	No	Yes	Voltage	Yes	Yes	Yes
[44]	2	3 MOTA		No	–	No	Current	Yes	No	No
[29]	2	1 MOTA, 1 DO-OTA, 2 OTA		Yes	No	Yes	Current	Yes	No	No
[46]	2	1 MCDTA		*4	Yes	Yes	Current	No	No	No
[45]	2	1 CCCDTA		No	–	No	Current	Yes	No	No
Proposed 1	2	2 OTA, 1 CA	$\pi/2$	Yes	No	Yes	Voltage	Yes	Yes	Yes
Proposed 2	2	2 OTA, 1 CA	$\pi/4$	Yes	No	Yes	Voltage	Yes	Yes	Yes

Abbreviations and explanations: CA – current amplifier; CCCDTA – current controlled current differencing transconductance amplifier; CCCFTA – current controlled current follower transconductance amplifier; CCTA – current conveyor transconductance amplifier; CDTA – current differencing transconductance amplifier; DO-CCCDTA – dual output current controlled current differencing transconductance amplifier; DO-OTA – dual output transconductance amplifier; DVCCCTA – differential voltage current conveyor transconductance amplifier; DVCCTA – differential voltage current controlled current conveyor transconductance amplifier; MCDTA – modified current differencing transconductance amplifier; MOTA – multiple output transconductance amplifier; OTA – operational transconductance amplifier; VB – voltage buffer; VDTA – voltage differencing transconductance amplifier; ZC-CDTA – Z-copy current differencing transconductance amplifier; ZC-VDTA – Z-copy voltage differencing transconductance amplifier.

*1 simultaneous control of R_n and g_m allows linear control of FO independent on CO but in ideal case only (strictly accurate equality both parameters required for CO fulfillment) – no parameters remain for CO control.

*2 simultaneous control of g_{m1} and g_{m2} allows linear control of FO independent on CO but in ideal case only (strictly accurate equality both parameters required for CO fulfillment) – no parameters remain for CO control.

*3 simultaneous control of g_m and R allows linear control of FO independent on CO but in ideal case only (strictly accurate equality both parameters required for CO fulfillment) – no parameters remain for CO control.

*4 simultaneous control of g_{m1} and g_{m2} allows linear control of FO independent on CO but in ideal case only (strictly accurate equality both parameters required for CO fulfillment) – no parameters remain for CO control (capacitance value is not suitable).

2.1. The first type of the multiphase oscillator with the minimal phase shift $\pi/2$

Our solutions focus on multiple-output OTA-based solutions without problems with CO separation from FO and fully electronically adjustable FO by transconductances. Based on interesting structures, that were presented in [44], we provide the improved modification in Fig. 1. Current amplifier is not used for CO control in [44]. Both important nodes of grounded capacitors are only labeled in SFGs in Fig. 1 for better clarity of diagrams. Additional modification of SFGs by explicit current outputs of the OTAs or supplementary voltage buffer/inverters in nodes 1 and 2 in order (to obtain multiphase character of the circuits) is a very easy task that is not necessary to be directly drawn in Fig. 1.

Solution in Fig. 1a has the following characteristic equation:

$$s^2 + \frac{g_{m1}(1-B)}{C_1}s + \frac{g_{m1}g_{m2}}{C_1C_2} = 0, \tag{1}$$

where we can clearly see that CO in form $B \geq 1$ is controllable by current gain B and g_{m1} can be used together with g_{m2} for linear control of FO without affecting CO. Different polarity of the outputs of OTAs allows to obtain different form of oscillation condition in the same circuit structure where polarity (sign) of some loops (L_1, L_2, L_3) in the SFG is opposite. A perfect example is shown in Fig. 1b. The same circuit as in Fig. 1a has almost identical characteristic

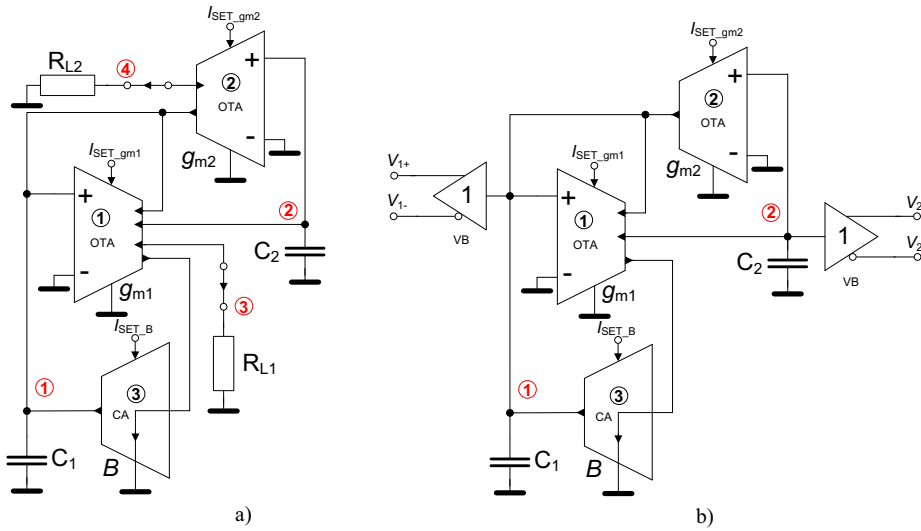


Fig. 2. The full multiphase solutions based on Fig. 1a: (a) utilizes also explicit OTA current outputs and (b) fully differential modification utilizing differential output voltage buffers.

Table 2 Evaluation of amplitude and phase relations for oscillator in Fig. 2a.

	Symbolical relation	Relation for $s=j\omega_0$	Phase shift between two voltages (fulfilled equality of both g_m and $C, B=1$)	Amplitude relation (equality of both g_m and $C, B=1$)
$V_2 - V_1$	$-\frac{g_{m1}}{sC_2}$	$V_2 = \sqrt{\frac{g_{m1}C_1}{g_{m2}C_2}} \exp(j\frac{\pi}{2}) V_1$	$+\pi/2$ ($+90^\circ, V_2$)	1
$V_3 - V_1$	$-g_{m1}R_{L1}$	$V_3 = -g_{m1}R_{L1} V_1$	$-\pi$ ($-180^\circ, V_3$)	$g_{m1}R_{L1}$
$V_4 - V_1$	$g_{m2}R_{L2} \frac{g_{m2}}{sC_2}$	$V_4 = g_{m2}R_{L2} \sqrt{\frac{g_{m1}C_1}{g_{m2}C_2}} \exp(-j\frac{\pi}{2}) V_1$	$-\pi/2$ ($-90^\circ, V_4$)	$g_{m2}R_{L2}$
$V_3 - V_2$	$-g_{m1}R_{L1} (\frac{g_{m2}}{sC_2 + g_{m1}(1-B)})$	$V_3 = g_{m1}R_{L1} \sqrt{\frac{g_{m2}C_1}{g_{m1}C_2}} \exp(j\frac{\pi}{2}) V_2$	$+\pi/2$ ($+90^\circ, V_3$)	$g_{m1}R_{L1}$
$V_4 - V_2$	$-g_{m2}R_{L2}$	$V_4 = -g_{m2}R_{L2} V_2$	$-\pi$ ($-180^\circ, V_4$)	$g_{m2}R_{L2}$

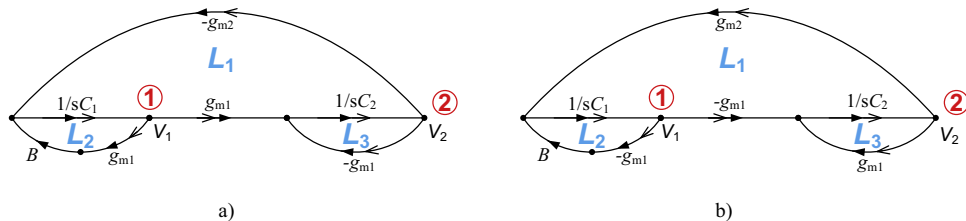


Fig. 3. SFG solutions of the OTA-based and adjustable current amplifier based oscillator (providing $\pi/4$ phase shift) that requires for CO: (a) $B \geq 1$ and (b) $B \leq 1$.

equation formally but CO is different. Characteristic equation of the circuit in Fig. 1b is modified to:

$$s^2 + \frac{g_{m1}(B-1)}{C_1}s + \frac{g_{m1}g_{m2}}{C_1C_2} = 0. \tag{2}$$

Modification is only in sign in linear coefficient. Oscillation condition of this version (Fig. 1b) is fulfilled for $B \leq 1$. It is very useful to know this information because it directly affects selection of the type and the design of automatic amplitude gain control circuit (AGC) for amplitude stabilization.

The structure in Fig. 2a, based on Fig. 1a, was drawn with additional explicit current outputs (mixed mode solution) that can be useful for multiphase or differential voltage-mode purposes (it depends on specific solutions – it will be discussed later) if converter from current to voltage (simple grounded resistor) and appropriate voltage buffering is used. Amplitude and phase relations between available outputs of the oscillator (for oscillation frequency $s=j\omega_0$) in Fig. 2a are given in Table 2.

The previous analysis shows that multiphase or differential quadrature (it depends on utilization of the outputs) is really obtained. The relation on fourth line is valid only for $B=1$. It is clearly seen that many of the relations are directly influenced by g_{m1} or g_{m2} that are used for linear control (simultaneously – $g_{m1} = g_{m2} = g_m$) of FO. Therefore, these outputs are suitable only if the oscillator is working with stable or very slightly (in narrow band) variable FO. Otherwise, phase relations keep unchangeable but output amplitudes of V_3 and V_4 varies in dependence on $g_{m1} = g_{m2} = g_m$. Operation of the oscillator in voltage mode requires additional voltage buffering. It is a disadvantage of such a “mixed-mode” circuit because it allows high-impedance nodes only and

four required voltage buffers are the cost for simplicity of operations (current-mode summing) in the structure. Fortunately, with respect to the availability of differential quadrature outputs, only two differential output buffers are sufficient and the disadvantage of dependencies of the amplitude relations on FO is completely removed if these buffers are connected to nodes 1 and 2, see Fig. 2b.

2.2. The second type of the multiphase oscillator with the minimal phase shift $\pi/4$

It is a generally known fact [1–4,22,24] that the application of lossy integrator in proposed systems allows obtaining phase shifts of output responses with different values than 90 degree. An interesting example also employing multiple-output OTAs is shown in Fig. 3.

The characteristic equation of the oscillator in Fig. 3a (in presented configuration and polarities of outputs of active elements) is almost identical to (1) and has the form:

$$s^2 + \frac{g_{m1}(C_1 - C_2B)}{C_1C_2}s + \frac{g_{m1}g_{m2}}{C_1C_2} = 0, \tag{3}$$

whereas the CO is: $B \geq C_1/C_2$. Therefore, fulfillment of CO (equality of both capacitances $C_1 = C_2 = C$ is supposed) is conditioned by $B \geq 1$. We can obtain reverse type of condition ($B \leq 1$) if characters (polarities) of the functional outputs (interconnections of the loops) of OTAs are opposite, see Fig. 3b.

Fig. 4a presents full multiphase solution utilizing additional explicit current outputs (mixed mode solution) of both OTAs. Amplitude and phase relations between available outputs (Fig. 4a) have forms noted in Table 3. We also suppose simplification

Table 3 Evaluation of amplitude and phase relations for oscillator in Fig. 4a.

Symbolical relation	Relation for $s=j\omega_0$ (fulfilled equality of both g_m and C , $B=1$)	Phase shift between two voltages (fulfilled equality of both g_m and C , $B=1$)	Amplitude relation (equality of both g_m and C , $B=1$)
$V_2 - V_1$	$V_2 = \frac{\sqrt{2}}{2} \exp(-j\frac{\pi}{4}) V_1$	$-\pi/4$ (-45° , V_2)	$\sqrt{2}/2$
$V_3 - V_1$	$V_3 = g_m R_{L1} \frac{\sqrt{2}}{2} \exp(-j\frac{3\pi}{4}) V_1$	$-3\pi/4$ (-135° , V_3)	$g_m R_{L1} \sqrt{2}/2$
$V_4 - V_1$	$V_4 = g_m R_{L2} \frac{\sqrt{2}}{2} \exp(-j\frac{5\pi}{4}) V_1$	$-5\pi/4$ (-225° , V_4)	$g_m R_{L2} \sqrt{2}/2$
$V_3 - V_2$	$V_3 = g_m R_{L1} \exp(-j\frac{\pi}{2}) V_2$	$-\pi/2$ (-90° , V_3)	$g_m R_{L1}$
$V_4 - V_2$	$V_4 = -g_m R_{L2} V_2$	$-\pi$ (-180° , V_4)	$g_m R_{L2}$

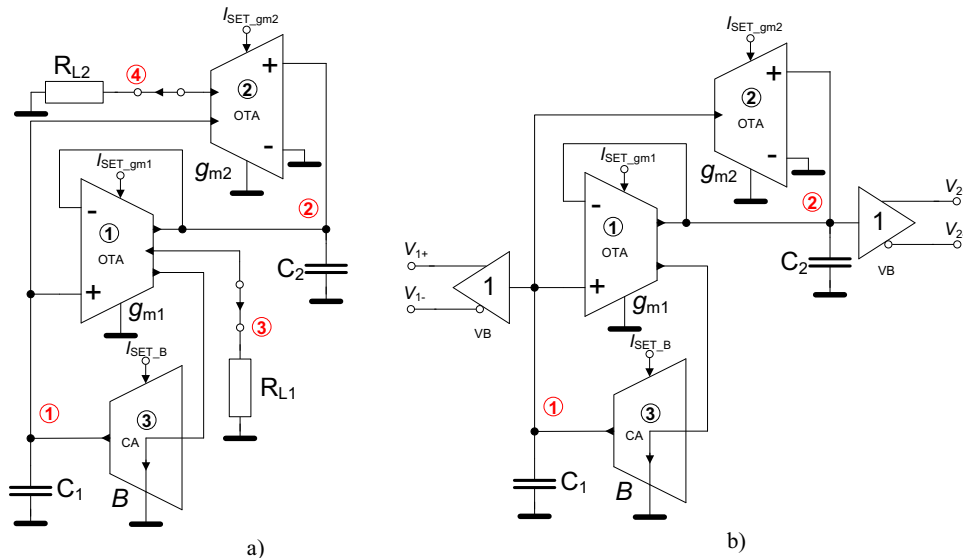


Fig. 4. The full multiphase solution based on Fig. 3a: (a) utilizes also explicit OTA current outputs and (b) fully differential modification utilizing differential output voltage buffers.

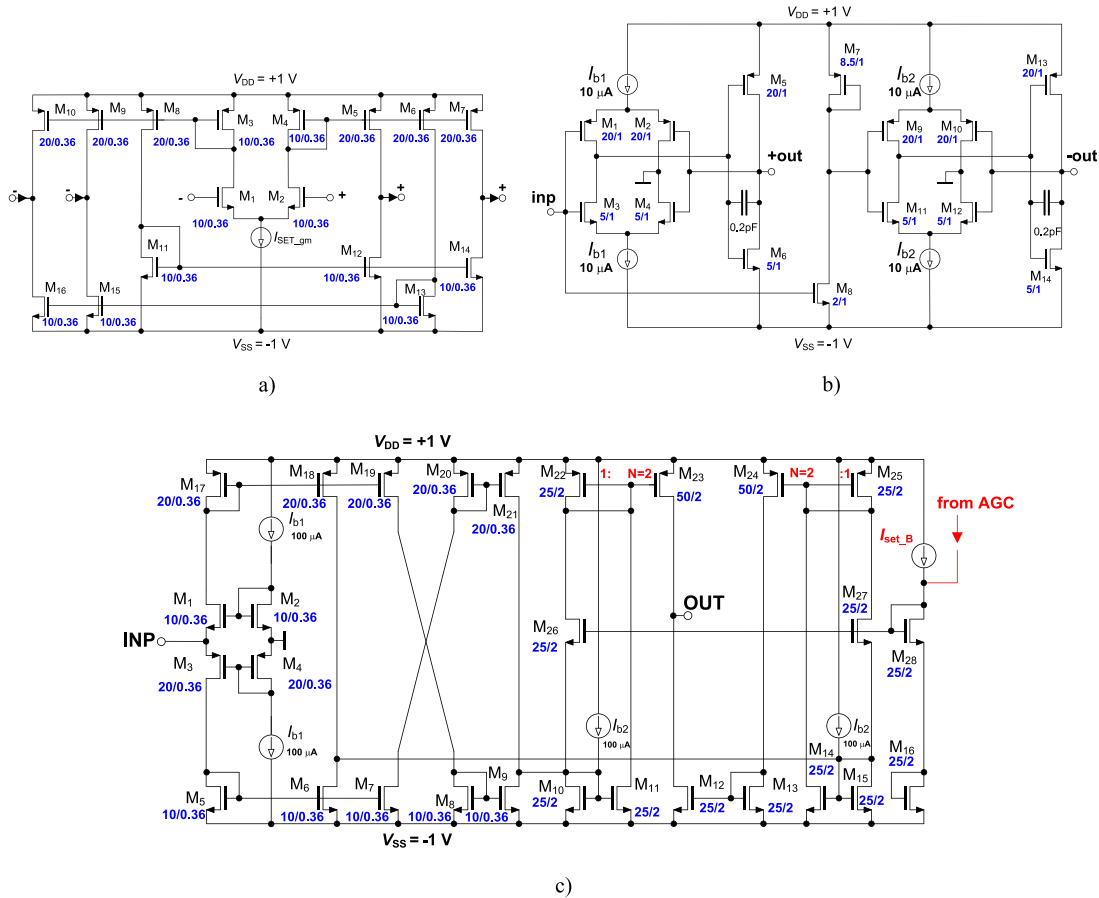


Fig. 5. CMOS structures for modeling of: (a) multiple-output transconductance amplifier, (b) voltage buffer/inverter and (c) adjustable current amplifier.

(equality $C_1 = C_2 = C$, $g_{m1} = g_{m2} = g_m$, $B = 1$) in the third column (for $s = j\omega_0$). Otherwise, relations are very complicated. Oscillator in Fig. 4a is suitable for purposes of multiphase generation only if stable FO is required. Otherwise, the relations of the levels of almost all the outputs depend on tuning process ($g_m = g_{m1} = g_{m2}$). Phase relations keep preserved if the oscillator is tuned. However, small fluctuances of B in order to control CO may cause some problems in the relation between V_2 and V_3 . Voltages V_1 and V_2 only are not dependent on tuning process. In comparison with the previous types in Fig. 2 (phase shifts available in multiples of $\pi/2$) the circuits in Fig. 4 offer finer steps of phase shift (multiples of $\pi/4$). A similar solution (Fig. 2b) with differential voltage buffers (Fig. 4b) is suitable for generation of constant phase shift $\pi/4$ and its multiples (with independent output levels on FO) in multiphase and differential mode. However, the amplitude of V_2 is $\sqrt{2}/2$ times lower than V_1 but, fortunately, independent on FO adjusting.

3. Simulation results

We selected the following design parameters of each of the oscillator: $g_{m1} = g_{m2} = g_m = 0.5\text{--}1.5\text{ mS}$, $C_1 = C_2 = C = 68\text{ pF}$, $B \approx 1$. It allows

theoretical range of f_0 tuning from 1.17 to 3.51 MHz. Supply voltage was $\pm 1\text{ V}$.

3.1. Models of active elements

Active elements appearing in Figs. 2 and 4 were implemented by PSpice models based on TSMC LO EPI 0.18 μm technology process parameters [53]. We used the following elementary CMOS structures of OTAs [18,22,24,25] CA, [49,54] and voltage buffers/inverters [55]. All internal structures are shown in Fig. 5.

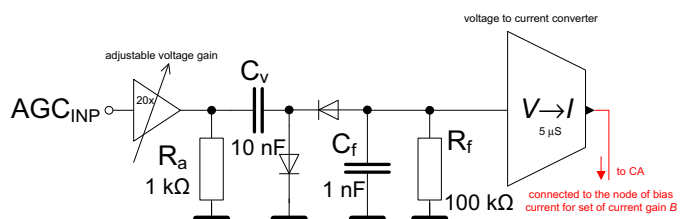


Fig. 6. Amplitude automatic gain control circuit (AGC).

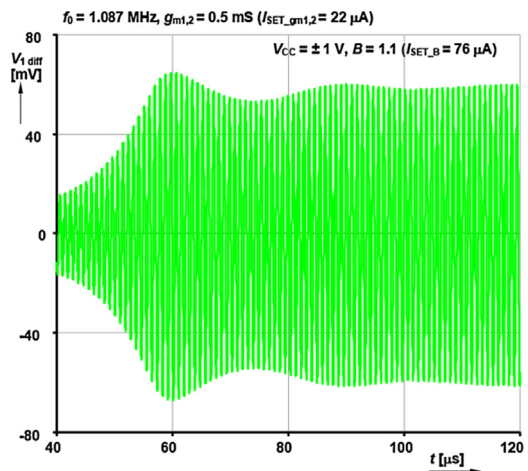


Fig. 7. Startup of the oscillations stabilized by the AGC system.

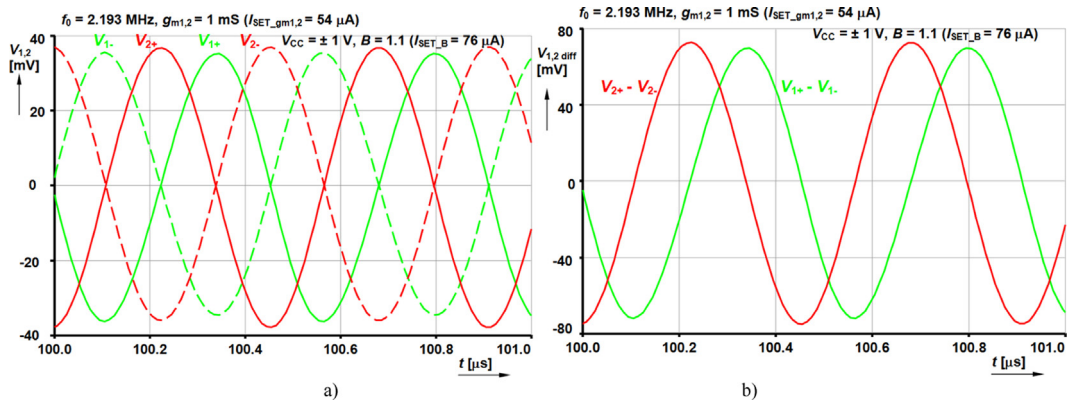


Fig. 8. Transient responses: (a) all available responses in single ended mode and (b) differential mode.

Unused outputs can be grounded or whole mirror section (P and N-MOS) can be removed from the structure to reduce a number of transistors. Overall transconductance (Fig. 5a) [56] is given by:

$$g_m = 2 \sqrt{I_{SET, gm} K_{Pn} \frac{W_{M1,2}}{L_{M1,2}}}, \quad (4)$$

because current gain of the current mirrors is multiplied by 2 (2 times higher W). Fig. 5b focuses on internal topology of adjustable current amplifier (CA) with current gain given by [54]:

$$B = \frac{N I_{b2}}{2 I_{SET, B}} \cong \frac{I_{b2}}{I_{SET, B}}. \quad (5)$$

Fabrication constants [53], given by gate-oxide capacitance and mobility of carriers, have approximate values $K_{Pn} = 170.4$ μ A/V² and $K_{Pp} = 35.7$ μ A/V². Voltage buffers/inverters are easily constructed from the structure in Fig. 5c.

Above discussed parameters (f_0 range) are obtained for $I_{SET, gm} = 22$ – 99 μ A. Implementation of automatic amplitude gain control circuit (AGC) was necessary for oscillations with stable amplitudes and low total harmonic distortion (Fig. 6).

3.2. Simulation results of the quadrature oscillator (first solution)

An oscillator in Fig. 2b was tested with above introduced models of active devices. Startup of the oscillations is depicted in Fig. 7 (differential output: $V_{1+} - V_{1-}$). All available waveforms (single ended) in the output nodes V_{1+} , V_{1-} , V_{2+} , V_{2-} are shown in Fig. 8a, differential-mode operation is then depicted in Fig. 8b. Oscillation

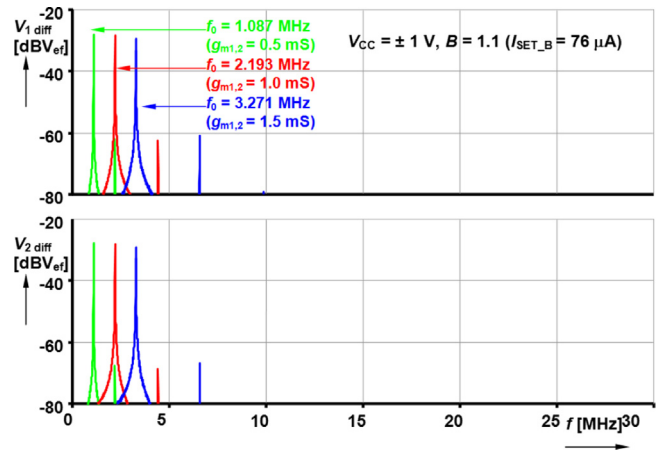


Fig. 9. Tuning example for three discrete oscillation frequencies in differential-mode (FFT spectrum).

frequency gained from simulation for $g_m = 1$ mS ($I_{SET, gm} = 54$ μ A) was 2.193 MHz (ideal value is 2.340 MHz). Tuning of the oscillator was verified in Fig. 9 (frequency spectrum) where three discrete frequencies (1.087, 2.193, 3.271 MHz) were set by $g_m = 0.5, 1, 1.5$ mS ($I_{SET, gm} = 22, 54, 99$ μ A). Output waveforms in differential-mode were unchangeable in amplitude and reaches level about 140 mV_{P-P} with phase shift about 88.3 degrees. Total harmonic distortion (THD) achieves value 1.8–2.2% for $V_{1\pm}$ output and 0.9–1.3% for $V_{2\pm}$ output.

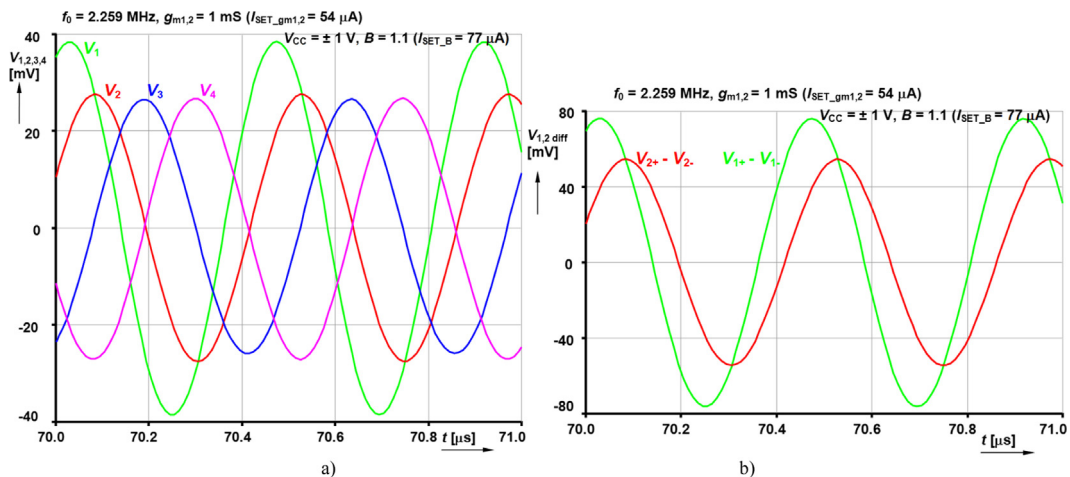


Fig. 10. Transient responses: (a) all available responses in single ended mode and (b) differential mode.

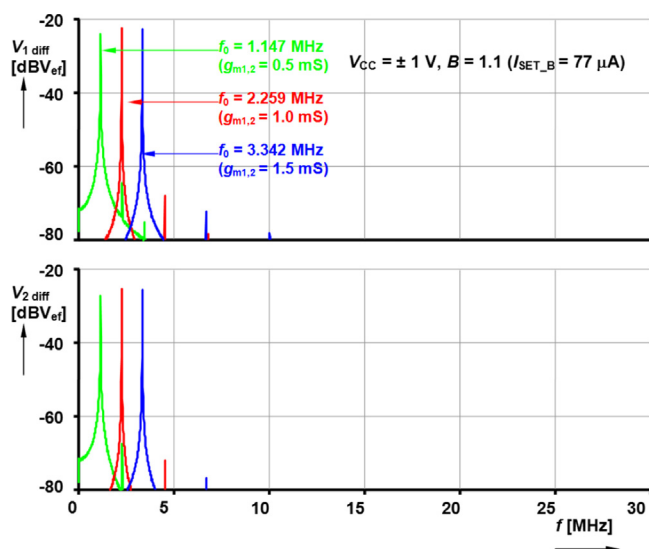


Fig. 11. Tuning example for three discrete oscillation frequencies in differential-mode (FFT spectrum).

The DC current source sets $I_{SET,B}$ to $76 \mu\text{A}$ (approximate value of B is 1.1). Actual value in simulation was slightly different. Tuning of the f_0 causes small changes of this current between 79 and $78 \mu\text{A}$ that was directly driven from the AGC circuit.

3.3. Simulation results of the $\pi/4$ oscillator (second solution)

Design parameters of the type in Fig. 4b are the same as in the previous case. We tested the circuit in Fig. 4b (all available outputs) in single-ended mode to obtain all phase shifts available in the structure. The results shown in Fig. 10a are for $g_m = 1 \text{ mS}$ (achieved $f_0 = 2.259 \text{ MHz}$; ideal frequency is 2.340 MHz). It proves the validity of the calculations of the amplitude relations provided in Table 3. Simulated phase shifts were obtained as: -45 ($V_2 - V_1$), -134 ($V_3 - V_1$), -221 ($V_4 - V_1$), -87 ($V_3 - V_2$) and -177 ($V_4 - V_2$) degrees. Transient responses for differential-mode are shown in Fig. 10b. Tuning of the oscillation frequency was verified also in three discrete values of g_m (the same as in the previous case of quadrature type) and the values gained from simulation are 1.147 , 2.259 and 3.342 MHz . The results in differential-mode are summarized in Fig. 11 (FFT spectrum). Available amplitude levels reach 150 mV_{P-P} for $V_{1\pm}$ and about 110 mV_{P-P} for $V_{2\pm}$. The phase shifts between $V_{1\pm}$ and $V_{2\pm}$ at these three frequencies were 44.4 , 44.3 and 43.8 degrees. THD were in the range of 0.4 to 1% ($V_{1\pm}$) and 0.3 to 0.9% ($V_{2\pm}$). The observed inaccuracies of the FO are caused by inaccurate setting of the $g_{m1,2}$. We estimated the error of the transconductance to be about 5% what is about $70 \mu\text{S}$ lower than the expected value. In our case it means a shift of FO to lower frequencies. Fortunately, each inaccuracy caused by g_m can be easily electronically corrected.

4. Conclusion

Our work brings and confirmed the interesting findings in oscillator circuits with transconductors and current amplifier. First of all, it is clear that the oscillation condition is not the same in practically identical circuit structures if polarities (signs) of the loop transfer(s) are given by different polarities of transfers of active elements. Specific situation requires current gain $B \geq 1$ or $B \geq C_1/C_2$ for fulfilled oscillation condition and the second possibility how to establish oscillator based on the same systems of the loops has opposite form for fulfillment of condition ($B \leq 1$, $B \leq C_1/C_2$). It seems to be quite

important information for designers in practice. It is not sufficient to know only what should be fulfilled for startup of oscillations but what is also correct direction of driving this parameter (increasing or decreasing?) for system of amplitude stabilization (automatic amplitude gain control circuit). It has not been frequently solved in recent research works. All these ideas were realized in two final circuit derivations providing quadrature or $\pi/4$ phase shifts where also amplitude relation were investigated. Phase relations keep unchangeable during the linear tuning process. However, amplitudes of produced signals at all available outputs are not always equal and unchangeable during the tuning process respectively. Fortunately, this problem can be also solvable. We can use simple differential voltage buffers in nodes where produced voltages are not mutually dependent on tuning process to produce required phase shift in single-ended or differential mode and the rest of the outputs is unused or grounded (current outputs). Parasitic analyses show that the function and fulfillment of oscillation condition can be disrupted only for critical values of the resistances in high-impedance nodes (units of $k\Omega$ and lower).

Standard design methods for quadrature or multiphase signal generation were discussed in the introductory section. However, there were also some completely different approaches to the design of quadrature and multiphase oscillators in recent years. For example Maundy et al. [57] presented concept based on fractional-order all-pass transfer sections. In fact, such conception utilizes all-pass section, fractional-order section (transfer containing fractional exponent α of the Laplace operator s) and gain block. Fractional character of the section is given by RC approximation of the fractional order capacitor in the structure of the AP. Such approach allows design of multiphase oscillators with theoretically arbitrary phase shifts between generated amplitudes and extended range of FO control (tuning) proportional to reciprocal time constant exponentiated by $1/\alpha$ [57]. However, only in case of easy change of the exponent of fractional capacitances. It seems to be not possible in presented solution. Interesting unconventional approach was also presented by Ozoguz et al. [58]. The authors used functional blocks operating in approximated square-root domain for the construction of multiphase oscillator. The described proposals are very interesting and have some potential, unfortunately a real application of interesting idea presented for example in [57] is limited by unavailability of simple electronic adjusting of fractional-order capacitor that is very important for real utilization of fractional-order-based circuits in systems for signal generation and processing. There seems to be many unsolved problems for future research.

Acknowledgements

Research described in the paper was supported by Czech Science Foundation projects under No. 14-24186P, by internal grant No. FEKT-S-14-2281 and project Electronic-biomedical co-operation ELBIC M00176. The support of the project CZ.1.07/2.3.00/20.0007 WICOMT, financed from the operational program Education for competitiveness, is gratefully acknowledged. Research described in this paper was financed by Czech Ministry of Education in frame of National Sustainability Program under grant LO1401. For research, infrastructure of the SIX Center was used. Dr. Herencsar was supported by the project CZ.1.07/2.3.00/30.0039 of the Brno University of Technology. We would also like to thanks prof. Raj Senani for his useful comments.

References

- [1] Gift SJG. The application of all-pass filters in the design of multiphase sinusoidal systems. *Microelectron J* 2000;31(1):9–13.

- [2] Abuelmaatti MT, Al-Qahtani MA. A new current-controlled multiphase sinusoidal oscillator using translinear current conveyors. *IEEE Trans Circuits Syst II: Analog Digital Signal Process* 1998;45(7):881–5.
- [3] Souliotis G, Psychalinos C. Electronically controlled multiphase sinusoidal oscillators using current amplifiers. *Int J Circuit Theory Appl* 2009;37(1):43–52.
- [4] Kumngern M, Chanwutium J, Dejhan K. Electronically tunable multiphase sinusoidal oscillator using translinear current conveyors. *Analog Integr Circuits Signal Process* 2010;65(2):327–34.
- [5] Prommee P, Dejhan K. An integrable electronic-controlled quadrature sinusoidal oscillator using CMOS operational transconductance amplifier. *Int J Electron* 2002;89(5):365–79.
- [6] Kumngern M, Dejhan K. Multiphase sinusoidal oscillators using operational transconductance amplifiers. *Thammasat Int J Sci Technol* 2009;14(1):82–94.
- [7] Tu S-H, Hwang Y-S, Chen J-J, Soliman AM, Chang C-M. OTA-C arbitrary-phase-shift oscillators. *IEEE Trans Instrum Meas* 2012;61(8):2305–19.
- [8] Keawon R, Jaikla W. A resistor-less current-mode quadrature sinusoidal oscillator employing single CCCDTA and grounded capacitors. *Prz Elektrotech* 2011;87(8):138–41.
- [9] Jaikla W, Siripruchyanun M, Bajer J, Biolk D. A simple current-mode quadrature oscillator using single CDTA. *Radioengineering* 2008;17(4):33–40.
- [10] Pandey N, Paul SK. Single CDTA-based current mode all-pass filter and its applications. *J Electr Comput Eng* 2011;1–5. <http://dx.doi.org/10.1155/2011/897631>.
- [11] Keskin AU, Aydin C, Hancioglu E, Acar C. Quadrature oscillator using current differencing buffered amplifiers (CDBA). *Frequenz* 2006;60(3):21–3.
- [12] Songkla SN, Jaikla W. Realization of electronically tunable current-mode first-order allpass filter and its application. *Int J Electron Electr Eng* 2012;6:40–3.
- [13] Minaei S, Yuce E. Novel voltage-mode all-pass filter based on using DVCCs. *Circuits Syst Signal Process* 2010;29(3):391–402.
- [14] Herencsar N, Minaei S, Koton J, Yuce E, Vrba K. New resistorless and electronically tunable realization of dual-output VM all-pass filter using VDIBA. *Analog Integr Circuits Signal Process* 2013;74(1):141–54.
- [15] Keskin AU, Biolk D. Current mode quadrature oscillator using current differencing transconductance amplifiers (CDTA). *IEE Proc Circuits Devices Syst* 2006;153(3):214–8.
- [16] Vosper JV, Heima M. Comparison of single- and dual-element frequency control in a CCIL-based sinusoidal oscillator. *Electron Lett* 1996;32(25):2293–4.
- [17] Sotner R, Lahiri A, Jerabek J, Herencsar N, Koton J, Dostal T, et al. Special type of three-phase oscillator using current gain control for amplitude stabilization. *Int J Phys Sci* 2012;7(25):3089–98.
- [18] Sotner R, Jerabek J, Herencsar N. Voltage differencing buffered/inverted amplifiers and their applications for signal generation. *Radioengineering* 2013;22(2):490–504.
- [19] Mason SJ. Feedback theory further properties of signal flow graphs. *Proc IRE* 1956;44(7):920–6.
- [20] Coates CJ. Flow-graph solution of linear algebraic equations. *IRE Trans Circuit Theory* 1959;6(2):170–87.
- [21] Biolk D, Senani R, Biolkova V, Kolka Z. Active elements for analog signal processing: classification, review, and new proposal. *Radioengineering* 2008;17(4):15–32.
- [22] Geiger RL, Sanchez-Sinencio E. Active filter design using operational transconductance amplifier: a tutorial. *IEEE Circuits Devices Mag* 1985;1:20–32.
- [23] Linares-Barranco B, Rodriguez-Vazquez A, Sanchez-Sinencio E, Huertas JL. 10 MHz CMOS OTA-C voltage-controlled quadrature oscillator. *Electron Lett* 1989;25(12):765–7.
- [24] Rodriguez-Vazquez A, Linares-Barranco B, Huertas L, Sanchez-Sinencio E. On the design of voltage-controlled sinusoidal oscillators using OTA's. *IEEE Trans Circuits Syst* 1990;37(2):198–211.
- [25] Linares-Barranco B, Rodriguez-Vazquez A, Sanchez-Sinencio E, Huertas L. CMOS OTA-C high frequency sinusoidal oscillators. *IEEE J Solid-State Circuits* 1991;26(2):160–5.
- [26] Cam U, Kuntman H, Acar C. On the realization of OTA-C oscillators. *Int J Electron* 1998;85(3):313–26.
- [27] Kuntman H, Ozpinar A. On the realization of DO-OTA-C oscillators. *Microelectron J* 1998;29(12):991–7.
- [28] Galan J, Carvalaj RG, Torralba A, Munoz F, Ramirez-Angulo J. A low-power low-voltage OTA-C sinusoidal oscillator with large tuning range. *IEEE Trans Circuits Syst I* 2005;52(2):283–91.
- [29] Summart S, Thongsopa Ch, Jaikla W. OTA based current-mode sinusoidal quadrature oscillator with non-interactive control. *Prz Elektrotech* 2012;88(7a):14–7.
- [30] Jin J, Wang C. Single CDTA-based current-mode quadrature oscillator. *AEU – Int J Electron Commun* 2012;66(11):933–6.
- [31] Sakul C, Jaikla W, Dejhan K. New resistorless current-mode quadrature oscillators using 2 CCCDTAs and grounded capacitors. *Radioengineering* 2011;20(4):890–7.
- [32] Jaikla W, Siripruchyanun M, Lahiri A. Resistorless dual-mode quadrature sinusoidal oscillator using a single active building block. *Microelectron J* 2011;42(1):135–40.
- [33] Srisakultiew S, Siripruchyanun M, Jaikla W. Single-resistance-controlled current-mode quadrature sinusoidal oscillator using single CCCFTA with grounded elements. In: *Proc. of int. conf. on telecommunication and signal processing TSP2013*. 2013. p. 436–9.
- [34] Prasad D, Bhaskar DR. Electronically controllable explicit current output sinusoidal oscillator employing single VDTA. *ISRN Electron* 2012:1–5. ID 382560.
- [35] Herencsar N, Sotner R, Koton J, Misurec J, Vrba K. New compact VM four-phase oscillator employing only single z-copy VDTA and all grounded passive elements. *Elektronika Ir Elektrotechnika* 2013;19(10):87–90.
- [36] Sotner R, Jerabek J, Prokop R, Vrba K. Current gain controlled CCTA and its application in quadrature oscillator and direct frequency modulator. *Radioengineering* 2011;20(1):317–26.
- [37] Lahiri A. Novel voltage/current-mode quadrature oscillator using current differencing transconductance amplifier. *Analog Integr Circuits Signal Process* 2009;61(2):199–203.
- [38] Lahiri A. New current-mode quadrature oscillator using CDTA. *IEICE Electron Express* 2009;6(3):135–40.
- [39] Tangsriat W, Tanjaroen W. Current-mode sinusoidal quadrature oscillator with independent control of oscillation frequency and condition using CDTAs. *Indian J Pure Appl Phys* 2010;48(5):363–6.
- [40] Tanjaroen W, Tangsriat W. Resistorless current-mode quadrature sinusoidal oscillator using CDTAs. In: *Proc. of 2009 APSIPA annual summit and conference*. 2009. p. 307–10.
- [41] Jaikla W, Siripruchyanun M. A versatile quadrature oscillator and universal biquad filter using dual-output current controlled current differencing transconductance amplifier. In: *Proc. of the 2006 international symposium on communications and information technologies*. 2006. p. 1072–5.
- [42] Lahiri A, Misra A, Gupta K. Novel current-mode quadrature oscillators with explicit-current-outputs using CCCDTA. In: *Proceeding of 19th international conference radioelektronika*. 2009. p. 47–50.
- [43] Horng JW, Lee H, Wu JY. Electronically tunable third-order quadrature oscillator using CDTAs. *Radioengineering* 2010;19(2):326–30.
- [44] Bhaskar DR, Abdalla KK, Senani R. Electronically-controlled current-mode second order sinusoidal oscillators using MO-OTAs and grounded capacitors. *Circuits Syst* 2011;2(2):65–73.
- [45] Pinkaew P, Suwanjan P, Jaikla W. Simple quadrature, sinusoidal oscillator with grounded elements. *Int J Comput Electr Eng* 2013;5(4):362–5.
- [46] Li Y. Electronically tunable current-mode quadrature oscillator using single MCDDTA. *Radioengineering* 2010;19(4):667–71.
- [47] Jaikla W, Lahiri A. Resistor-less current-mode four-phase quadrature oscillator using CCCDTA and grounded capacitors. *AEU – Int J Electron Commun* 2012;66(3):214–8.
- [48] Biolk D, Biolkova V, Keskin AU. Current mode quadrature oscillator using two CDTAs and two grounded capacitors. In: *Proc. of the 5th WSEAS international conference on systems, science and simulation in engineering ICOSSE'06*. 2006. p. 368–70.
- [49] Sotner R, Jerabek J, Herencsar N, Petrzela J, Vrba K, Kincl Z. Linearly tunable quadrature oscillator derived from LC Colpitts structure using voltage differencing transconductance amplifier and adjustable current amplifier. *Analog Integr Circuits Signal Process* 2014;81(1):121–36.
- [50] Lamun P, Kumngern M, Tortonchai U, Sarsithithum K. Tunable current-mode quadrature sinusoidal oscillator employing CCCFTAs and grounded capacitors. In: *4th international conference on intelligent systems, modelling and simulation*. 2013. p. 665–8.
- [51] Prasad D, Srivastava M, Bhaskar DR. Electronically controllable fully-uncoupled explicit current-mode quadrature oscillator using VDTAs and grounded capacitors. *Circuits Syst* 2013;4(2):169–72.
- [52] Jaikla W, Siripruchyanun M. CCCDTAs-based versatile quadrature oscillator and universal biquad filter. In: *Proc. of 2007 ECTI conference*. 2007. p. 1065–8.
- [53] MOSIS parametric test results of TSMC LO EPI SCN018 technology. Available from: <https://www.mosis.com/cgi-bin/cgiwrap/umosis/swp/params/tsmc-018>
- [54] Surakamponorn W, Kumwachara K. CMOS-based electronically tunable current conveyor. *Electron Lett* 1992;28(14):1316–7.
- [55] Arbel AF, Goldminz L. Output stage for current-mode feedback amplifiers, theory and applications. *Analog Integr Circuits Signal Process* 1992;2(3):243–55.
- [56] Razavi B. *Design of analog CMOS integrated circuits*. New York: McGraw-Hill; 2001.
- [57] Maundy B, Elwakil A, Gift S. On the realization of multiphase oscillators using fractional-order allpass filters. *Circuits Syst Signal Process* 2012;31(1):3–17.
- [58] Ozoguz S, Abdelrahman TM, Elwakil AS. Novel approximate square-root domain all-pass filter with application to multiphase oscillators. *Analog Integr Circuits Signal Process* 2006;46(3):297–301.

[16] SOTNER, R., JERABEK. J., HERENC SAR, N., VRBA, K. Design of the simple oscillator with linear tuning and $\pi/4$ phase shift based on emulator of the modified current differencing unit. *IEICE Electronics Express*, 2015, vol. 12, no. 19, p. 1-7. ISSN: 1349-2543.

Design of the simple oscillator with linear tuning and pi/4 phase shift based on emulator of the modified current differencing unit

Roman Sotner^{a)}, Jan Jerabek, Norbert Herencsar, and Kamil Vrba

Faculty of Electrical Engineering and Communication, Brno University of Technology, Technicka 12, Brno, 616 00, Czech Republic

a) sotner@feec.vutbr.cz

Abstract: This paper presents a simple oscillator with 45 degrees phase shift between output signals. A Modified Current Differencing Unit (MCDU) was used for its design. The MCDU offers controllability of input resistances of current inputs and controllability of current gains. These features are not available together in the standard current differencing unit and it limits usability in some applications. The proposed oscillator allows linear electronic control of oscillation frequency and independent control of condition of oscillation with simple implementation of amplitude stabilization. The PSpice simulations and measurements in laboratory with manufactured behavioral emulator of the MCDU confirmed the expected features of the solution.

Keywords: electronic control, behavioral model/emulator, oscillator, modified current differencing unit

Classification: Electron devices, circuits, and systems

References

- [1] H. O. Elwan and A. M. Soliman: *Analog Integr. Circuits Signal Process.* **11** (1996) 35. DOI:10.1007/BF00174237
- [2] N. Herencsar, R. Sotner, B. Metin, J. Koton and K. Vrba: 8th International Conference on Electrical and Electronics Engineering (ELECO) (2013) 17. DOI:10.1109/ELECO.2013.6713927
- [3] B. Metin, N. Herencsar and K. Vrba: *Radioengineering* **21** [2] (2012) 718.
- [4] J. Vavra and D. Biolek: *Int. Conf. on Electronic Devices and Systems (EDS IMPAPS)* (2008) 7.
- [5] J. Vavra and J. Bajer: *Analog Integr. Circuits Signal Process.* **74** (2013) 121. DOI:10.1007/s10470-012-9906-8
- [6] D. Biolek, R. Senani, V. Biolkova and Z. Kolka: *Radioengineering* **17** [4] (2008) 15.
- [7] C. Acar and S. Ozoguz: *Microelectron. J.* **30** (1999) 157. DOI:10.1016/S0026-2692(98)00102-5
- [8] A. Toker, S. Ozoguz, O. Cicekoglu and C. Acar: *IEEE Trans. Circuits Syst. II, Analog Digit. Signal Process.* **47** (2000) 949. DOI:10.1109/82.868465

- [9] D. Bielek: Euro. Conf. on Circuit Theory and Design (ECCTD) (2003) 397.
- [10] M. Siripruchyanun and W. Jaikla: Circuits Syst. Signal Process. **27** (2008) 113. DOI:10.1007/s00034-008-9014-2
- [11] R. Sotner, J. Jerabek, N. Herencsar, T. Zak, W. Jaikla and K. Vrba: Adv. Electr. Comp. Eng. **15** (2015) 3. DOI:10.4316/AECE.2015.01001
- [12] Ch. Sakul, W. Jaikla and K. Dejhan: Radioengineering. **20** [4] (2011) 890.
- [13] W. Jaikla and A. Lahiri: AEU, Int. J. Electron. Commun. **66** (2012) 214. DOI:10.1016/j.aeue.2011.07.001
- [14] S.-H. Tu, Y.-S. Hwang, J.-J. Chen, A. M. Soliman and C.-M. Chang: IEEE Trans. Instrum. Meas. **61** (2012) 2305. DOI:10.1109/TIM.2012.2184958
- [15] R. Sotner, J. Jerabek, J. Petrzela, N. Herencsar, R. Prokop and K. Vrba: Elektronika Ir Elektrotechnika **20** (2014) 13. DOI:10.5755/j01.eee.20.9.8709
- [16] R. Sotner, J. Jerabek, N. Herencsar, J. W. Horng and K. Vrba: 37th Int. Conf. on Telecommunications and Signal Processing (TSP) (2014) 396.
- [17] R. Sotner, J. Jerabek, N. Herencsar, K. Vrba and T. Dostal: AEU, Int. J. Electron. Commun. **69** (2015) 814. DOI:10.1016/j.aeue.2015.01.012
- [18] W. Surakampontrorn and W. Thitimajshima: IEE Proc. G **135** (1988) 71. DOI:10.1049/ip-g-1.1988.0010
- [19] A. Fabre and N. Mimeche: Electron. Lett. **30** (1994) 1267. DOI:10.1049/el:19940878
- [20] S. Minaei, O. K. Sayin and H. Kuntman: IEEE Trans. Circuits Syst. I, Reg. Papers **53** (2006) 1448. DOI:10.1109/TCSI.2006.875184
- [21] R. Sotner, A. Kartci, J. Jerabek, N. Herencsar, T. Dostal and K. Vrba: Meas. Sci. Rev. **12** (2012) 255. DOI:10.2478/v10048-012-0035-4

1 Introduction

Development of active devices based on current difference starts with differential current conveyor (DCCII) [1]. A detailed discussion of history of active elements utilizing current difference is provided for example in [2] and [3]. These devices contain so-called current differencing unit (CDU). CDU was studied as an independent building part by Vavra et al. [4] and introduced as a suitable active device for synthesis of applications in [5, 6]. The very-well known active devices utilizing CDU part are so-called a current differencing buffered amplifier (CDBA) [6, 7, 8] and a current differencing transconductance amplifier (CDTA) [6, 9]. There were some attempts to extend the features of control in the frame of the CDU part. For example Siripruchyanun et al. [10] presented modification of the CDTA where the input resistances of both inputs of the CDU part are controllable. However, this extent of control is insufficient for some applications. Therefore, modified current differencing unit (MCDU) was introduced in [11] where the applications in reconfigurable reconnection-less filters were discussed. Except electronic control of the resistances of the input terminals (p and n), the MCDU supposes existence of additional control of current gains in both ways (from p and n) before current subtraction. This extension allows synthesis of the interesting applications especially oscillators.

The oscillators producing output signals with phase shift are required subsystems in communication and measurement. The electronically controllable oscilla-

tors utilizing current difference based devices are designed as quadrature (phase shift equal to 90 degrees), for example [12, 13]. However, simple circuits producing different phase shifts than 90 degrees have not been studied enough. Oscillators with $\pi/4$ phase shift can be used for special modulation purposes. Except multi-phase solutions (sophisticated chains of lossy blocks, for example [14]), where multiples of basic minimal integer phase shift are available, there were not many simple structures reported in the past where 45 degrees phase shift is available. There are some simpler electronically controllable solutions than multiphase chains of blocks, where such phase shift is available. The papers [15, 16, 17] present structures where phase shift 45 deg. and linear electronic control is available. However, the circuit solutions [15, 16, 17] are more complex than presented in this paper (additional passive elements [15] or additional controllable voltage amplifier [16] are required, or more than 2 active devices are necessary for construction and some of them have multiple-outputs [17]), see Table I. Our solution here allows to utilize each of the MCDU parameter (namely: input resistances - R_p , R_n , and current gains - B_1 , B_2) in simple single active device based electronically controllable oscillator where two output amplitudes (unchangeable during the tuning process) with 45 deg. phase distance are available.

Table I. Comparison of simple linearly electronically controllable oscillators providing independent FO and CO generating output voltage amplitudes with $\pi/4$ phase distance.

Reference	Type of active elements	No. of passive elements	No of active elements
[15]	ZC-CG-VDCC	4	1
[16]	ZC-VCCFDITA, VA	2	2
[17]	OTA, CA	2	3
proposed	MCDU	2	1

CA current amplifier; MCDU modified current differencing unit; OTA operational transconductance amplifier; VA voltage amplifier; ZC-CG-VDCC z-copy controlled gain voltage differencing current conveyor; ZC-VCCFDITA z-copy voltage controlled current follower differential input transconductance amplifier.

2 Proposed MCDU-based oscillator

The definition of the MCDU was given in [11]. The basic principle of CDU was clearly explained in [4, 5, 6]. The principle of the MCDU is given in Fig. 1(a) where ideal small-signal model is shown. Presence of two independent Y terminals together with controllable gains B_1 and B_2 in the active device are the new features in comparison to standard CDU. All inter-terminal relations are marked directly in the Fig. 1(a).

We focused our design on special type of the oscillator where constant phase shift $\pi/4$ is available and stays unchanged during the tuning of the frequency of oscillations (FO). The really simple and resistor-less circuit structure of the oscillator in Fig. 1(b) offers this feature. Notice that electronic controllability of

the parameters of the MCDU is indicated by the DC control voltages (V_{SET_B1} , etc.). Characteristic equation and FO of the solution in Fig. 1(b) are of the following forms:

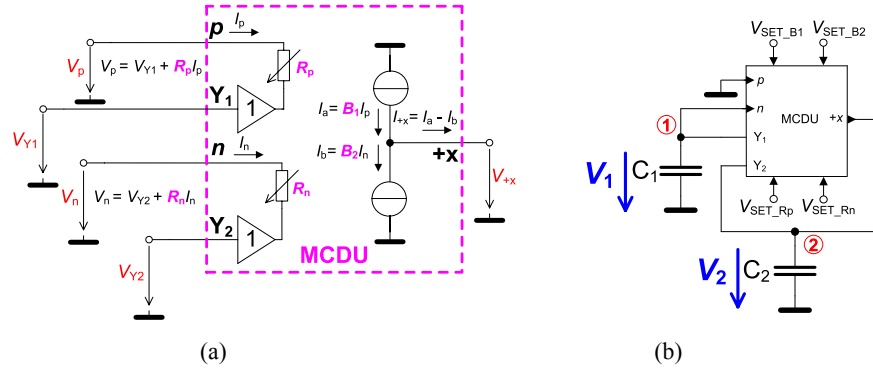


Fig. 1. (a) Ideal model of CDU with advanced features referred as modified CDU (MCDU), (b) Proposed oscillator based on MCDU providing phase shift $\pi/4$ between outputs.

$$s^2 + \frac{(C_2 - C_1 B_2)}{R_n C_1 C_2} s + \frac{B_1}{R_p R_n C_1 C_2} = 0, \quad (1)$$

$$\omega_0 = \sqrt{\frac{B_1}{R_p R_n C_1 C_2}}, \quad (2)$$

where a condition for oscillation (CO) is: $C_2/C_1 \leq B_2$. A concept of the oscillator is based on the electronically controllable parameters available in frame of the MCDU. The controllable current gain B_2 serves for adjusting of CO and simultaneously adjusted intrinsic input resistances ($R_p = R_n = R_{p,n}$) ensure linear control of FO. The generated signals in nodes 1 and 2 are of the following amplitude and phase relation:

$$\frac{V_1}{V_2} = \frac{1}{1 + s C_1 R_n} = \frac{\sqrt{1 + \frac{R_n B_1 C_1}{R_p C_2}}}{2} \exp \left[\tan^{-1} \left(-\sqrt{\frac{R_n B_1 C_1}{R_p C_2}} \right) j \right]. \quad (3)$$

Supposing $R_p = R_n = R_{p,n}$, $C_1 = C_2 = C_{1,2}$, $B_1 = 1$, it leads to:

$$\frac{V_1}{V_2} = \frac{\sqrt{2}}{2} \exp[\tan^{-1}(-1)j] \Rightarrow V_1 = \frac{\sqrt{2}}{2} \exp\left(-\frac{\pi}{4}j\right) V_2. \quad (4)$$

Voltage V_2 foreruns V_1 by phase distance of 45 degrees and their amplitude ratio is constant if FO is tuned and equal to $\sqrt{2}/2$. This ratio can be adjusted by simple attenuator after separation (voltage buffer) of the high-impedance output node 2.

3 Experimental verification by laboratory tests

We prepared following behavioral model/emulator (including system for amplitude stabilization) of the oscillator based on commercially available active elements. The behavioral model (Fig. 2) employs several electronically controllable current con-

veyors of second generation ECCIIs [18, 19, 20]) available in the frame of the current mode multiplier EL2082 and diamond transistor (DT) OPA860. This MCDU model was firstly reported in [11]. Input resistances and current gains are defined as: $R_p \cong R_i'/V_{SET_Rp}$, $R_n \cong R_j'/V_{SET_Rn}$, $B_1 \cong V_{SET_B1}$ and $B_2 \cong V_{SET_B2}$ [21]. Supposing $R_p = R_n = R_{p,n}$ (and $R_i' = R_j' = R_{ij}'$ in frame of the model) and constant $B_1 = 1$ (V_{SET_B1}), we can use specified equation for FO:

$$f_0 \cong \frac{V_{SET_Rp,n}}{2\pi R_{i,j}' C_{1,2}}. \quad (5)$$

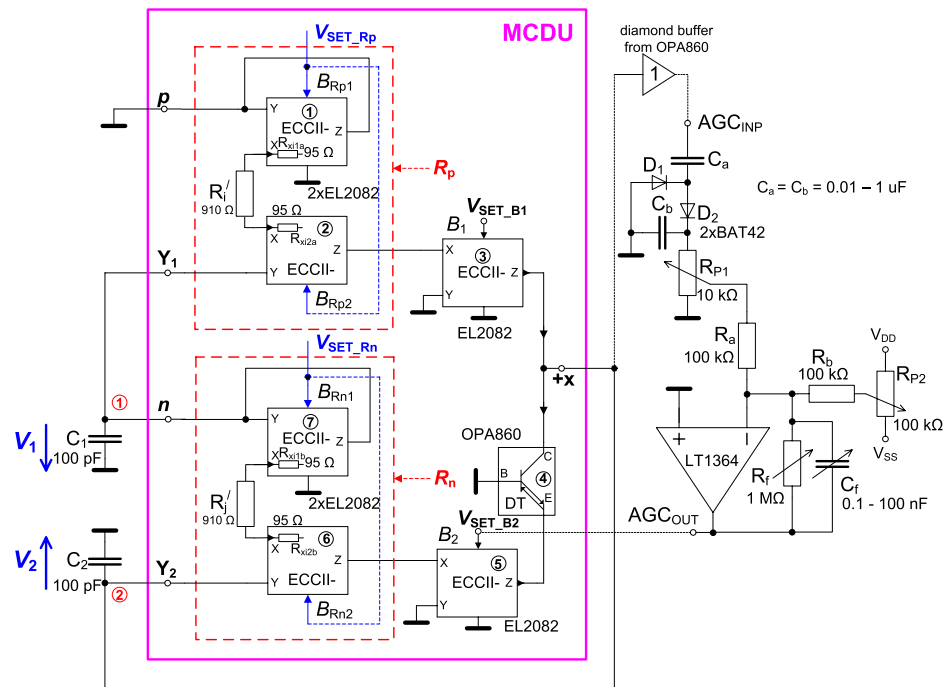


Fig. 2. Manufactured oscillator based on MCDU behavioral model/emulator employing commercially available active devices including automatic gain control (AGC) circuit for laboratory tests.

The parameters of the circuit are selected as $C_{1,2} = 100$ pF, $B_1 = 1$ ($V_{SET_B1} = 1$ V) and $R_{p,n} = 3.2$ k Ω ($V_{SET_Rp,n} = 0.32$ V). Such setting yields ideal $f_0 = 0.507$ MHz, simulations with behavioral model (Fig. 2) provided 0.459 MHz and experimentally measured value was 0.499 MHz. Laboratory results are given in Fig. 3 (we used oscilloscope RIGOL DS1204B and spectrum analyzer HP4395A). An example of both measured transient responses (blue color - V_1 ; red color - V_2) is shown in Fig. 3(a), spectrum of output responses (upper spectrum - V_1 ; lower spectrum - V_2) in Fig. 3(b) and dependence of FO on $V_{SET_Rp,n}$ in Fig. 3(c). Manufactured MCDU module, used for experimental study of the oscillator, is shown in Fig. 3(d). AGC was provided as an independent part. Measured outputs were separated by voltage buffers and matched to 50 Ω load. Phase difference 46 degrees of both signals was observed. Experimental verification in laboratory brings the results that indicate behavioral model/emulator suitability for operation up to units of MHz

(FO was adjusted from 0.147 to 1.911 MHz by DC control voltage from 0.1 to 1.0 V). An analysis of total harmonic distortion yields value about 1.5% (suppression of higher harmonic components more than 35 dBc).

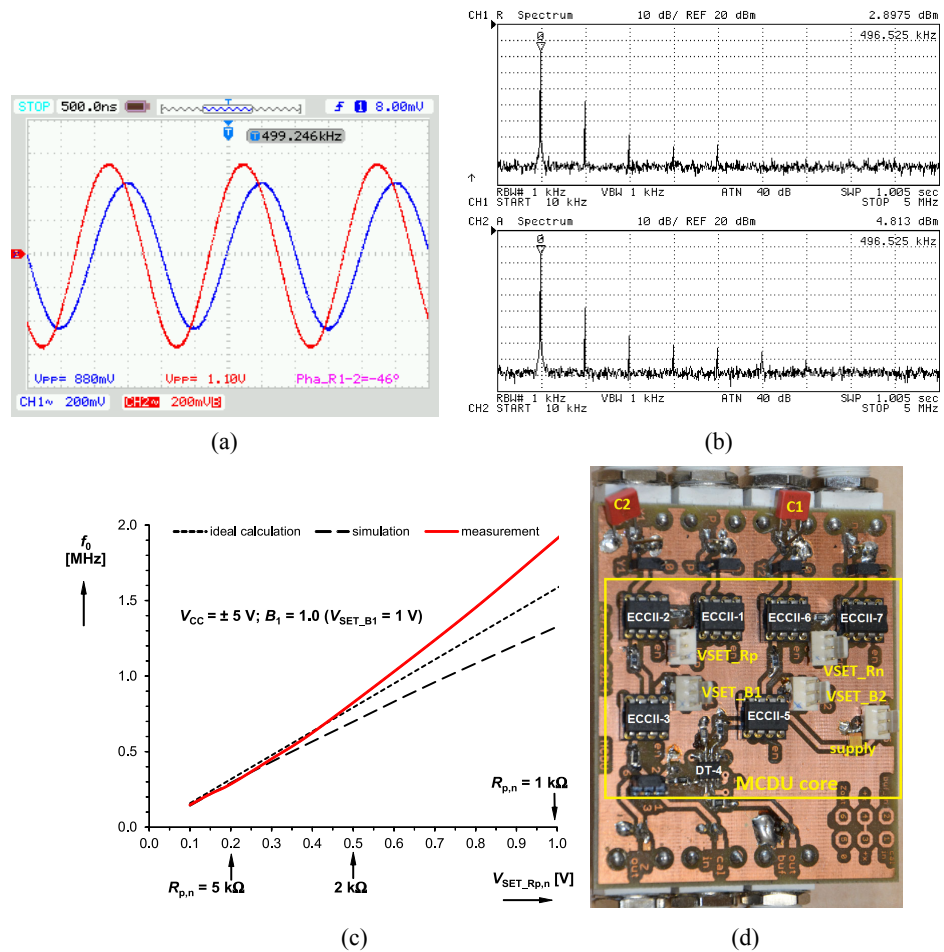


Fig. 3. (a) Measured transient responses of produced signals (blue color - V_1 , red color - V_2), (b) Measured spectrum of both outputs (upper spectrum - V_1 ; lower spectrum - V_2), (c) Ideal, simulated and measured dependence of FO on $V_{SET_Rp,n}$, (d) Manufactured MCDU module used for experimental study of the oscillator.

4 Conclusion

The resulting features of the designed oscillator confirmed usefulness of advanced controllable properties in the frame of the MCDU (behavioral emulator) for the design of the interesting applications and suitability of this active device for future IC implementation. Functionality was verified from frequencies of hundreds of kHz up to units of MHz. Complexity of the MCDU emulator balances its four useful controllable features and it is not an important issue for IC implementation. Except the beneficial features of the MCDU in reconfigurable reconnection-less filters [11], the discussed results here indicate that such advanced active device can offer the useful features also for design of oscillators.

Acknowledgments

Research described in this paper was financed by Czech Ministry of Education in frame of National Sustainability Program under grant LO1401. For research, infrastructure of the SIX Center was used.

[17] SOTNER, R., JERABEK, J., LANGHAMMER, L., POLAK, J., HERENC SAR, N., PROKOP, R., PETRZELA, J., JAIKLA, W. Comparison of two solutions of quadrature oscillators with linear control of frequency of oscillation employing modern commercially available devices. *Circuits Systems and Signal Processing*, 2015, vol. 34, no. 11, p. 3449-3469. ISSN: 0278-081X.

Comparison of Two Solutions of Quadrature Oscillators With Linear Control of Frequency of Oscillation Employing Modern Commercially Available Devices

Roman Sotner¹ · Jan Jerabek² · Lukas Langhammer² · Josef Polak² · Norbert Herencsar² · Roman Prokop³ · Jiri Petrzela¹ · Winai Jaikla⁴

Received: 7 July 2014 / Revised: 27 February 2015 / Accepted: 27 February 2015 /
Published online: 21 March 2015
© Springer Science+Business Media New York 2015

Abstract This paper proposes two circuits of frequency-controlled oscillators, whose structures are based only on simple commercially available active elements with minimum number of terminals, in particular, the differential voltage buffer, controllable

✉ Roman Sotner
sotner@feec.vutbr.cz

Jan Jerabek
jerabekj@feec.vutbr.cz

Lukas Langhammer
langhammer@phd.feec.vutbr.cz

Josef Polak
xpolak24@stud.feec.vutbr.cz

Norbert Herencsar
herencsn@feec.vutbr.cz

Roman Prokop
prokop@feec.vutbr.cz

Jiri Petrzela
petrzelj@feec.vutbr.cz

Winai Jaikla
kawinai@kmitl.ac.th

- ¹ Department of Radio Electronics, Faculty of Electrical Engineering and Communication, Brno University of Technology (BUT), Technicka 3082/12, 616 00 Brno, Czech Republic
- ² Department of Telecommunications, Faculty of Electrical Engineering and Communication, Brno University of Technology (BUT), Technicka 3082/12, 616 00 Brno, Czech Republic
- ³ Department of Microelectronics, Faculty of Electrical Engineering and Communication, Brno University of Technology (BUT), Technicka 3058/10, 616 00 Brno, Czech Republic
- ⁴ Department of Engineering Education, Faculty of Industrial Education, King Mongkut's Institute of Technology Ladkrabang, Ladkrabang, Bangkok 105 20, Thailand

voltage amplifier and electronically controllable current conveyor. Two methods for achieving linear control (tuning) of frequency of oscillations (FO) are discussed. The first method employs a simple structure. However, the generated signal level (amplitude) depends on the tuning process. This is a drawback of this method. The second method solves this drawback completely, and the generated signals have constant amplitudes during the tuning of FO. The expected behavior is confirmed by laboratory experiments utilizing commercially available high-speed active elements (current- and voltage-mode multipliers, video difference amplifier). Operational range was tested from frequencies of hundreds of kHz up to frequencies of tens of MHz.

Keywords Quadrature oscillator · Linear control · Current mode multiplier · Voltage-mode multiplier · Differential voltage buffer · Electronic control

1 Introduction

Many types of harmonic quadrature oscillators utilizing various active elements [6] and design approaches have been presented in the literature. Quadrature oscillators can be divided into two groups when only networks with fully independent conditions of oscillation (CO) and frequency of oscillation (FO) are taken into account. Fully independent CO means the existence of a controllable parameter (intrinsic resistance of current input terminal, R_x , transconductance, g_m , an adjustable current gain, B , an adjustable voltage gain, A) in the equation for CO, and this parameter is not present in the equation for FO. The first group covers oscillators with nonlinear control (square root in almost all cases) of FO by electronically adjustable parameter(s). The second group includes solutions with linear control of FO. A comprehensive review of two-integrator loop-based nonlinearly and linearly controllable quadrature oscillators with various active elements (many of them are commercially available, some of them allow electronic control of application) was published by Soliman in [23]. Many interesting solutions, where FO is controllable even linearly by passive resistors (see [7, 14] and references cited therein), have been introduced in recent research works. However, a more useful method of electronic control is often not discussed or is not easily possible (it requires additional circuitry—digital potentiometers, FET replacements, etc.). A comparison of the important hitherto published results (electronically controllable second-order quadrature oscillators only) is given in Table 1. As can be seen from the comparison in Table 1, there are some issues that should not be overlooked.

- a) Only a few solutions [4, 9, 13, 18, 21, 23, 24] can be implemented by simple commercially available elements because they really do not require any kind of unusual features (multiple outputs, special type of control, conversion of output current signals to voltage form, etc.),
- b) Direct voltage control of FO (to obtain a voltage-controlled oscillator) without additional circuitry is hardly ever available, except in [24, 26, 28],
- c) Some implementations require parameter matching for linear control of FO as well as the ideal fulfillment of CO (no additional parameter for CO driving is available for amplitude stabilization during the tuning process) [11, 17, 20],

- d) Many works deal with solutions based on multi-terminal active element(s) [5, 10, 11, 16, 17, 20, 22, 23, 25–30], which could be a complication because of the interconnection of high-impedance nodes/terminals (it causes decreased impedance and increased parasitic capacitance) especially in the current mode.

Easy implementation of the oscillator by using modern and available components is an important aspect of this work. Proposing a useful, quite simple and high-speed (up to several MHz) voltage-controlled oscillator suitable for designers who do not have access to chip fabrication is the primary goal of our work. The number of known solutions with the following features is quite limited, see, for example, [9, 18, 21]:

- a) truly simple commercially available elements that are easy to apply
- b) solutions that provide required features (linear electronic FO control and independent electronic CO control, quadrature outputs, constant amplitudes during tuning process).

Therefore, there is still scope for further valuable improvements. Our final solution fulfills the standard requirements and can be implemented using commercially available elements with a minimal number of terminals (three terminals per active device at most).

As can be seen from published works, recent research in this field has mostly been focused on linear control of FO because it is quite a common and widely used method of FO control in applications (simple control of FO driven by microprocessor and/or D/A converters). It is worth mentioning that there are also other non-typical methods of oscillator design with modern active elements. The possibility of employing negative capacitance in the design of oscillators [15] is a perfect example. Similarly, active devices based on bulk-driven techniques (for example [12]) offer some benefits, in particular, low power consumption) in such applications as oscillators. However, linear electronic control of FO was not discussed in these works, and therefore, these references are not included in Table 1.

The advantages of the proposals presented below can be briefly summarized. Note that some of the discussed features are available in already known solutions but not all of them are available simultaneously. In comparison with previously reported quadrature systems, our solutions offer simultaneously:

- a) direct and mutually independent voltage control of FO and CO without additional circuitry or modification of the structure,
- b) linear control of FO,
- c) simple active elements (minimal number of terminals),
- d) structure suitable for commercially available active elements,
- e) the second network solution also improves the independence of generated amplitudes of the tuning process.

This paper is divided into sections as follows. Section 2 provides an overview of the active elements used (we have selected only commercially available devices) and explains the principles of the sub-blocks constructed. The basic concept of the novel (unusual) CO control is discussed. Several possible design modifications of the oscillators which are subsequently modified to have the required features are discussed in Sect. 3. Section 4 gives detailed experimental results and a comparison

Table 1 Comparison of important second-order electronically controllable quadrature oscillator solutions with linear control of FO

Reference	Active elements used in oscillator	No. of passive/active elements	Independent CO and FO	Amplitudes independent of tuning process	Commercial availability of active elements	Type of control	Direct voltage control (VCO) possible	Multi-terminal active elements required
[23]	OTA ^a	2/4	Yes	**	Yes	g_m	No	No
[13]	DO-OTA	2/3-6	Yes	*	Yes	g_m	No	No
[21]	OTA	2/3(4)	Yes	Yes	Yes	g_m	No	No
[18]	OTA	2-4/2-4	Yes ^b	Yes	Yes	g_m	No	No
[9]	DO-OTA	4/4	Yes	Yes	Yes	g_m	No	No
[4]	MO-OTA	2/3	Yes	**	Partially	g_m	No	Partially
[20]	ZC-CDTA	2/2	^c	**	No	g_m	No	Yes
[10]	CCCDTA	2/2	Yes	Yes	No	R_x, g_m	No	Yes
[3]	DCCF, VF	6/5	Yes	Yes/Yes	No	B	No	No
[22]	CCCDTA	2/2	Yes	**	No	R_x, g_m	No	Yes
[16]	ZC-CFTA	3/3	Yes	Yes	No	g_m	No	Yes
[11]	CCCDTA	2/1	No ^d	No	No	g_m, R_x	No	Yes
[17]	MCDTA	2/1	No ^c	Yes	No	g_m	No	Yes
[5]	ZC-CG-CDBA	5/2	Yes	Yes	No	B^3	No	Yes
[30]	OTA, DO-OTA, MO-OTA	2/4	Yes	Yes	Partially	g_m	No	Yes
[29]	CCCII	2/4	Yes	Yes	No	R_x	No	Yes
[27]	DCC-CFA	5(3)/2	Yes	Possible	No	R_x, B	No	Yes
[26]	DO-CG-CFBA, CA	5/3	Yes	Yes	No	B	Yes	Yes
[24]	ECCII, CCII	5/4	Yes	Yes	Yes	B	Yes	No

Table 1 continued

Reference	Active elements used in oscillator	No. of passive/active elements	Independent CO and FO	Amplitudes independent of tuning process	Commercial availability of active elements	Type of control	Direct voltage control (VCO) possible	Multi-terminal active elements required
[25]	DO-CG-VDBA/VDBVA	3/2	Yes	Yes	No	A, g_m	No	Yes
[28]	CG-CFDOBA, CG-BCVA	5/2	Yes	Yes	No	A, B	Yes	Yes
Proposed								
Figure 3	DVB, VA, ECCII	4/3	Yes	No	Yes	A, B	Yes	No
Figure 4	DVB, VA, ECCII	4/4	Yes	Yes	Yes	A, B	Yes	No

A, adjustable voltage gain; B, adjustable current gain; g_m , transconductance (controllable by bias current); R_x , intrinsic resistance (controllable by bias current); CA, current amplifier (with adjustable gain); CCII, second generation current conveyor; CCCII, translinear current conveyor/ current controlled CCII; CG-CFDOBA, controlled gain-current follower differential output buffered amplifier; CG-BCVA, controlled gain-buffered current and voltage amplifier; DCCF, digitally controllable current follower; DCC-CFA, double current controlled-current feedback amplifier; DO-CG-CFBA, dual output-controlled gain-current follower buffered amplifier; DO-CG-VDBA, dual output-controlled gain-voltage differencing buffered amplifier; DO-CG-VDBVA, dual output-controlled gain-voltage differencing buffered voltage amplifier; DO-OTA, dual output OTA; ECCII, electronically controllable current conveyor of second generation; MCDTA, modified CDTA; OTA, operational transconductance amplifier; VB, voltage buffer (or voltage follower—VP); ZC-CDTA, z-copy current differencing transconductance amplifier; ZC-CG-CDBA, z-copy-controlled gain-current differencing buffered amplifier; ZC-CFTA, z-copy current follower transconductance amplifier; CFOA, current feedback operational amplifier

* Possible but not verified

** Information is not available or feature is not possible

a Reference [23] deals with many solutions employing various active elements, circuits in Fig. 9 (based on OTAs) are very beneficial, but they do not allow direct voltage control without additional modification of the bias driving system

b Reference [18] deals with several oscillators; one of them is quadrature oscillator with linear control of FO and amplitudes independent of the tuning process

c FO is independent of CO if the special matching condition (equality of both controllable parameters) is fulfilled, but the start of oscillation and CO control is complicated (only the value of capacitors influences CO theoretically)—CO and FO are therefore not fully independent in practice

d CO controlled by replacement of passive element (floating resistor)

with the theoretical results. Finally, an overall discussion and the main conclusions are summarized in the last section.

2 Active Elements and Building Blocks Used for CO Control

2.1 Active Elements

Since our design is based on the application of commercially available active elements such as the difference amplifier AD830 [1], voltage multiplier AD835 [2] and diamond transistors, a description of the principles of the selected active elements is given below.

Difference amplifier AD830 [1] serves as a differential voltage buffer (DVB) and realizes the transfer function: $V_+ - V_- = V_{out}$. Voltage-mode multiplier AD835 [2] is very suitable for constructing a high-speed variable gain amplifier (VGA), where the gain A is driven by the DC voltage V_{SETA} . This VGA (Fig. 1a) can implement positive or negative gain ($\pm A$) in accordance with the polarity of V_{SETA} , as can be seen from the definition [2]: $A = \pm V_{SETA} (R_{f1} + R_{f2}) / R_{f2}$.

We use the current-mode multiplier EL2082 [8] for controlling the current gain and implementing an electronically controllable current conveyor (ECCII). The basic principle of a standard ECCII is given by the simple equations (in an ideal case): $V_Y = V_X$, $I_Y = 0$, $I_Z = BI_X$. The current gain between the X and Z ports (B) is adjustable by DC voltage (V_{SETB}), and the voltage gain (transfer) from the Y port to the X port is fixed (equal to 1). A modified type, shown in Fig. 1b, can offer both

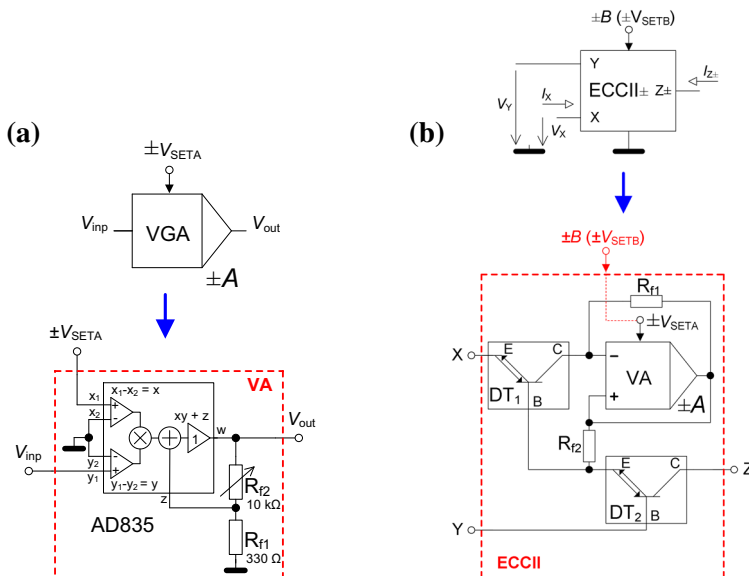
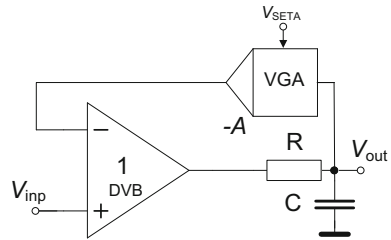


Fig. 1 Active elements with special control functions (gain changeable in both polarities) implemented by commercially available devices: **a** controllable voltage amplifier, **b** electronically controllable current conveyor and one of the possible behavioral representations

Fig. 2 Sub-block suitable for oscillator synthesis



polarities of current transfer in general. This model utilizes two diamond transistors (DT) OPA860 [31] and one controllable voltage amplifier (e.g., VCA810 [32] or AD835 [2]). The ideal current gain B is given by the term: $B = \pm AR_{s1}/R_{s2}$. This “replacement” offers features similar to that offered by ECCII based on EL2082.

2.2 Sub-block for Control of CO in Proposed Oscillators

The proposed implementations of oscillators contain a special feedback part shown in Fig. 2. This part contains DVB and VGA, represented by a voltage-mode multiplier from Fig. 1a and a passive RC network. The voltage transfer function of this sub-block has the form:

$$\frac{V_{\text{out}}}{V_{\text{inp}}} = \frac{1}{sCR + 1 - A}. \quad (1)$$

As is obvious from Eq. (1), the actual value of the controllable voltage gain A of VGA has a direct impact on the character (lossy/loss-less integrator, stable–unstable, non-minimal argument) of this simple transfer section.

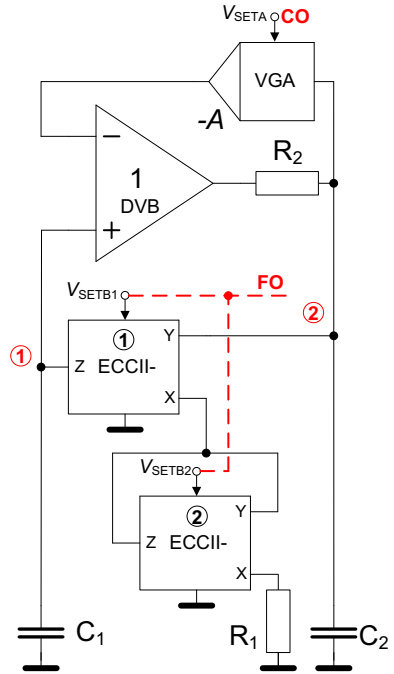
3 Proposed Solutions of Quadrature Oscillators

3.1 First Type of Oscillator

The first type of the proposed circuit is shown in Fig. 3. The sub-block for CO control (shown in Fig. 2), included in the final structure, allows us to obtain oscillators where the dependence of FO on a controllable parameter can be changed/modified easily. In other words, only the integrator (its controllable specification) connected between the input and the output of the sub-block from Fig. 2 determines the character of FO control. Quadratic or higher-order FO control function (i.e. increased tuning sensitivity) can be achieved by using an appropriate number of the blocks (ECCIIs with parameter B) in the integrator (Fig. 3).

An oscillator is obtained if a loss-less integrator is connected between the V_{out} and V_{inp} terminals (Fig. 2). This integrator is also formed by R and C elements (R_1, C_1), and two ECCII elements in order to obtain linear control. The characteristic equation of this oscillator is:

Fig. 3 First type of oscillator designed to obtain linear control



$$s^2 + \frac{(1 - A)}{R_2 C_2} s + \frac{B_1 B_2}{R_1 R_2 C_1 C_2} = 0, \tag{2}$$

where CO is $A \geq 1$; FO and the relation between generated amplitudes are:

$$\omega_0 = \sqrt{\frac{B_1 B_2}{R_1 R_2 C_1 C_2}}, \tag{3}$$

$$\frac{V_{C1}}{V_{C2}} = \frac{-B_1 B_2}{s C_1 R_1}. \tag{4}$$

Truly linear control is available in the case $B_1 = B_2 = B$, in such a case:

$$\omega_0 = \frac{B}{\sqrt{R_1 R_2 C_1 C_2}}, \tag{5}$$

$$\frac{V_{C1}}{V_{C2}} = \frac{-B^2}{s C_1 R_1} \Rightarrow \left. \frac{V_{C1}}{V_{C2}} \right|_{\omega = \omega_0} = -B^{-1} \sqrt{\frac{R_2 C_2}{R_1 C_1}}. \tag{6}$$

As is obvious from (6), B^{-1} causes a change in the amplitude V_{C1} during the tuning process. It could be a very important drawback if both outputs of the oscillator are required. In addition, it causes total harmonic distortion (THD) to increase if the amplitude reaches high levels (simply due to output limitations of the active devices).

3.2 Second Type of Oscillator

In solution depicted in Fig. 4, the relationship of the produced signal level (V_{C1}) and FO is removed, see Eqs. (6) and (7). The control of FO is split into the two integrators, see position of $ECCII_1(B_1)$ and $ECCII_2(B_2)$ in Fig. 4 and compare it to Fig. 3. The sub-block for CO control (Sect. 2; Fig. 2) was modified (Fig. 5). The oscillator of Fig. 4 has the same equation for CO and FO as the circuit in Fig. 3, but the relation between the output amplitudes has a different form:

$$\frac{V_{C1}}{V_{C2}} = \frac{-B_1}{sC_1R_1} \Rightarrow \frac{V_{C1}}{V_{C2}} \Big|_{\substack{\omega = \omega_0 \\ B_1 = B_2 = B}} = -\sqrt{\frac{R_2C_2}{R_1C_1}}, \tag{7}$$

Fig. 4 Second type of controllable oscillator with two ECCIIs (linear control of FO)

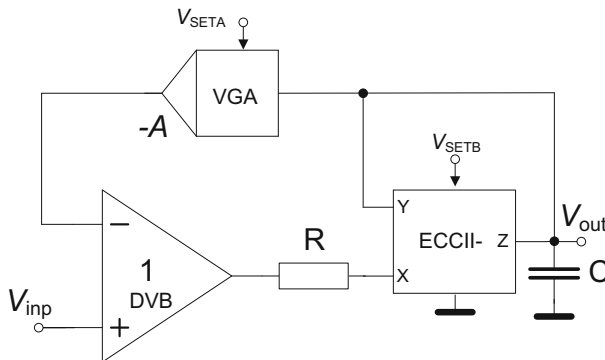
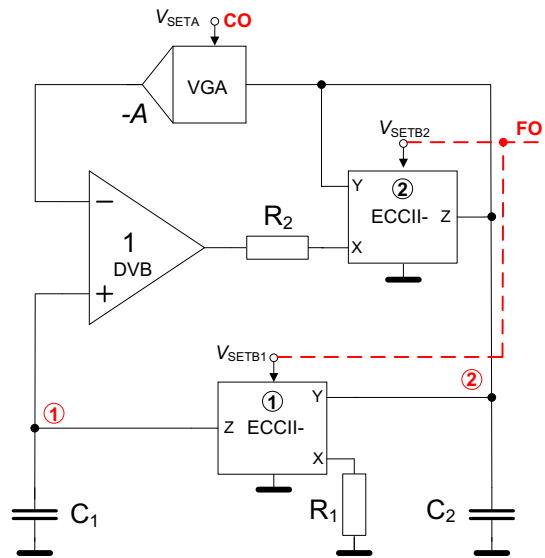


Fig. 5 Modification of sub-block suitable for synthesis of an oscillator with linear control of FO

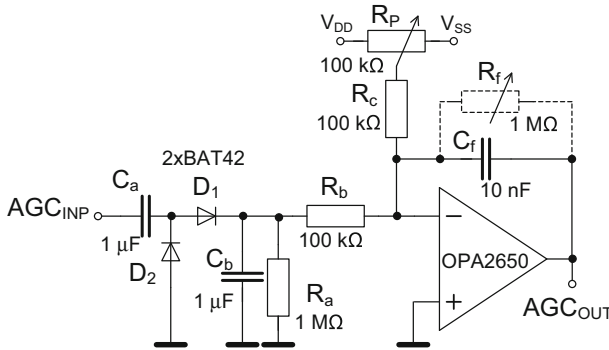


Fig. 6 AGC system for amplitude stabilization used during measurement of both oscillators

which ensures equal generated amplitudes during the tuning process of FO ($B_1 = B_2 = B$).

In comparison with (1), the circuit in Fig. 5 has the following transfer function:

$$\frac{V_{\text{out}}}{V_{\text{inp}}} = \frac{B}{sCR + B(1 - A)}. \quad (8)$$

4 Experimental Verification

Both circuits given in Figs. 3 and 4 were measured. These circuits were supplemented with an amplitude automatic gain control circuit (AGC) shown in Fig. 6, which is necessary for amplitude stabilization during the tuning process. The output DC voltage of the AGC directly drives the V_{SETA} input of VA responsible for CO control of each of the oscillators. Output voltages (V_{C1} , V_{C2}) were buffered by voltage buffers based on high-speed precise op-amp OPA2650 [19], and outputs were matched to 50Ω load. The buffered output of V_{C2} was selected as the input signal for the AGC system in both cases. Both tested solutions were based on a differential voltage buffer made up of AD830 [1], voltage multiplier AD835 [2] and current-mode multipliers (also known as ECCII) EL2082 [8]. The supply voltage was $\pm 5 \text{ V}$. Detailed information about the AGC is provided in Fig. 6.

4.1 The First Oscillator Type from Fig. 3

4.1.1 Low-Frequency Operation

The values of $R_1 = 225 \Omega$ ($130 \Omega +$ internal resistance of ECCII₂, $R_{X2} = 95 \Omega$ [28]) and $R_2 = 220 \Omega$ were selected for verifying the circuit shown in Fig. 3. The capacitance values ($C_1 = C_2 = C$) chosen were 1 nF in this case. The term “low frequency” means in our case that the oscillator operates in the region of gain-bandwidth product (GBW) guaranteed by the manufacturer of the particular active element.

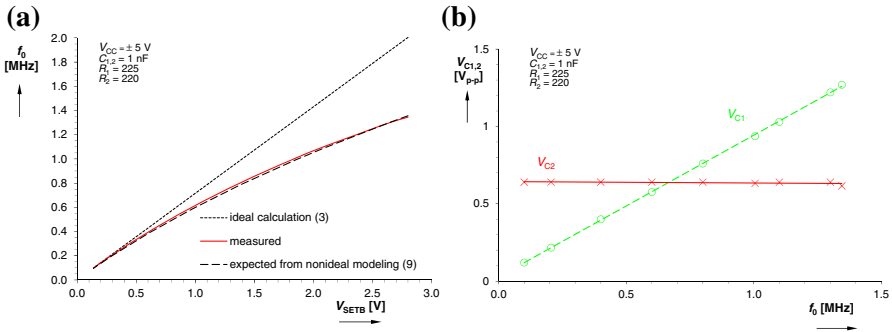


Fig. 7 Low-frequency operation-dependence of: **a** FO on V_{SETB} , **b** $V_{C1,2}$ on FO

The results of behavior in the mentioned low-frequency range are documented in the following figures. The dependence of FO on V_{SETB} is depicted in Fig. 7a, where ideal (5), expected (9) and measured traces are shown. The range of FO control was experimentally verified from 100 kHz to 1.34 MHz. The DC control voltage V_{SETB} of ECCII_s (current gain B) [8] was adjusted from 0.14 to 2.8 V. The difference between the ideal and the measured trace is quite large. Therefore, we studied the non-ideal features of the structure. We concluded that additional parasitic capacitances in high-impedance nodes, where working capacitors are also connected (node 1 and 2), have the most significant effect on FO accuracy together with the R_x value of the real input terminal X of ECCII₁ in Fig. 3. Since working capacitors have values much higher than parasitic capacitances ($1\text{ nF} \times 15\text{ pF}$), in this low-frequency case, it is sufficient to only take into account the R_{X1} ($95\ \Omega$) [8] of ECCII₁ in order to obtain more accurate results for FO:

$$\omega'_0 = \sqrt{\frac{B_1 B_2}{R_2(R_1 + R_{X1} B_2) C_1 C_2}} \tag{9}$$

We need not provide a full parasitic analysis in this case, because the R_{X1} effect has the most important impact on FO accuracy. Fortunately, for the selected values of $C_{1,2}$ ($1\text{ nF} \gg 15\text{ pF}$), the contribution of R_{X1} to the estimation is sufficient to obtain a correct estimation. The estimated range of FO (9) was found to be 96 kHz to 1.36 MHz, which is in good agreement with the measured results, see Fig. 7a. Figure 7b provides the measured dependence of the output amplitudes on FO. It can clearly be seen that V_{C1} depends on FO as was predicted by the theoretical relation (6). The dependence of THD on FO and that of phase shift on FO are shown in Fig. 8. THD, in the case of V_{C1} increasing, increases rapidly in the highest corner of FO due to V_{C1} levels reaching the saturation limits of the active elements used. An example of transient responses (V_{C1} – blue color, V_{C2} – red color) for $f_0 = 1\text{ MHz}$ ($V_{SETB} = 1.85\text{ V}$) are shown in Fig. 9.

4.1.2 High-Frequency Operation

We also verified the correct behavior of this structure at high frequencies of tens of MHz. The weakest cell of the oscillators is DVB (AD830) due to its quite low

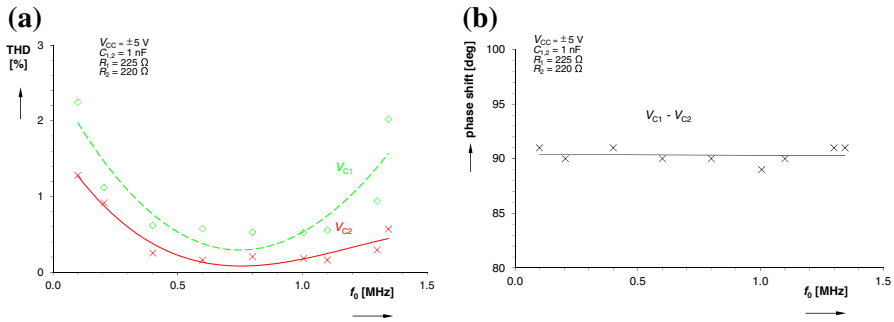


Fig. 8 Low-frequency operation-dependence of: **a** THD on FO, **b** phase difference on FO

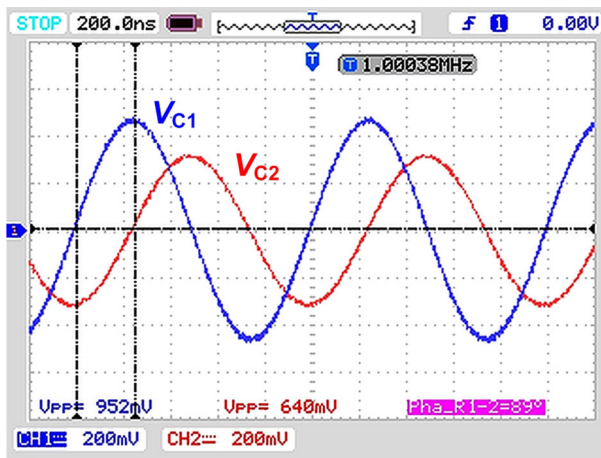


Fig. 9 Example of transient responses for stable FO (1 MHz)

3 dB bandwidth, which is only about 30 MHz for ± 5 V supply. Since the working capacitors have a low capacitance ($C_{1,2} = 33$ pF), additional parasitic capacitances (15 pF) connected to nodes 1 and 2 have a significant impact and should be included in order to get a precise estimation (9). These parasitic capacitances are formed by the real capacitance of input and output terminals of active elements (approximately 8 pF in each node) [1, 2, 8, 19]. The absolute maximum of FO, where amplitudes were stable and minimally distorted, was found to be 20.06 MHz (at $V_{SETB} = 2.05$ V). The measured range of FO was from 4.24 to 20.06 MHz (V_{SETB} from 0.36 to 2.05 V). The expected range, based on the above-discussed estimation, was calculated to be between 4.41 and 19.7 MHz. The results of FO dependence on DC control voltage V_{SETB} and the dependence of produced amplitudes on FO are shown in Fig. 10. Dependence of THD and phase shift between produced signals on FO is demonstrated in Fig. 11. Transient responses for $f_0 = 10$ MHz ($V_{SETB} = 0.91$ V) are provided in Fig. 12. Blue color represents V_{C1} and red color V_{C2} . From Fig. 11b, we can see that the amplitudes and phase shift change during FO tuning. The change in amplitude

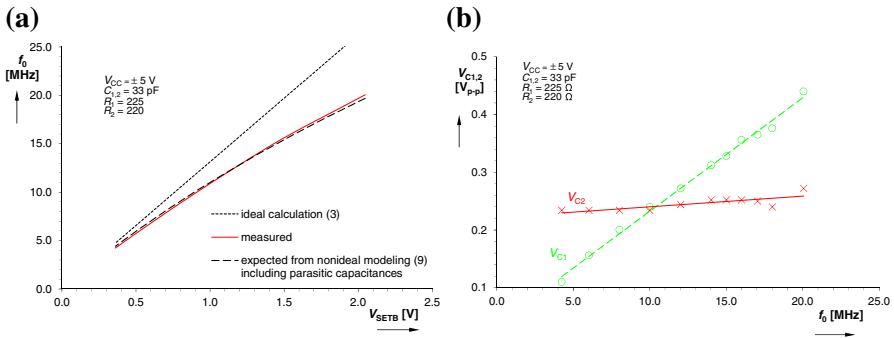


Fig. 10 High-frequency operation-dependence of: a FO on V_{SETB} , b $V_{C1,2}$ on FO

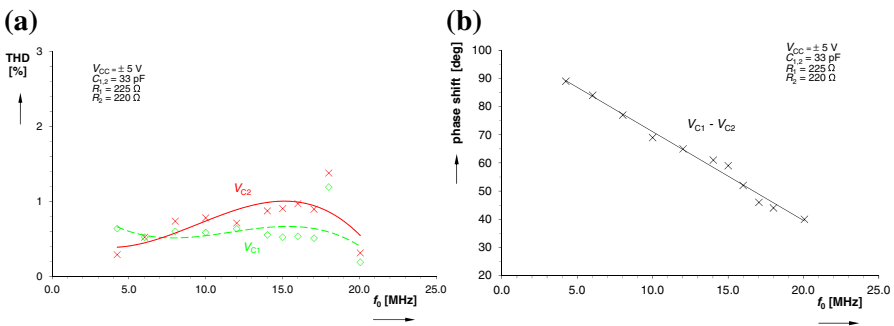


Fig. 11 High-frequency operation-dependence of: a THD on FO, b phase shift on FO

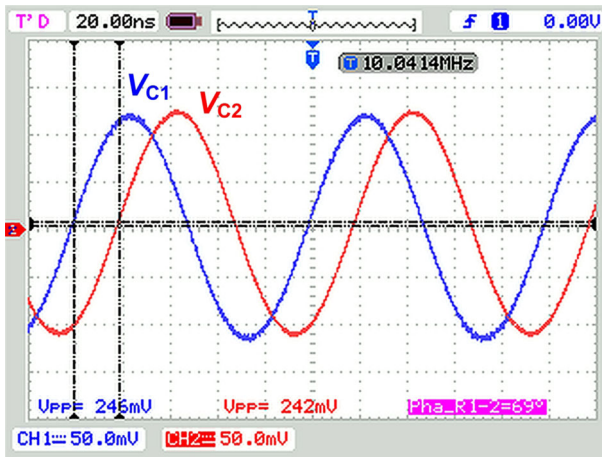


Fig. 12 Example of output transient responses for stable FO (10 MHz)

is given by the theoretical principle (6). Unfortunately, the change in phase shift is caused by a non-ideal frequency response (roll-off at high frequencies) of the AD830 used [1].

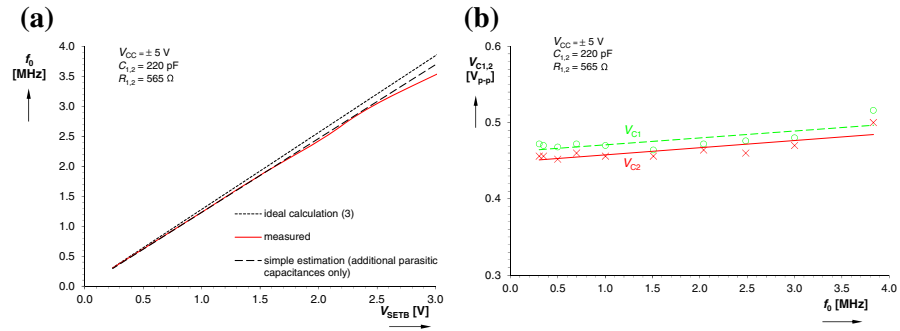


Fig. 13 Low-frequency operation-dependence of: **a** FO on V_{SETB} , **b** $V_{C1,2}$ on FO

4.2 The Second Oscillator Type from Fig. 4

4.2.1 Low-Frequency Operation

The circuit in Fig. 4 was designed for the low-frequency and the high-frequency tests (similar to Sect. 4.1). The values of passive elements were selected taking such requirements into account.

For the so-called low-frequency mode, the following passive components were used: The working resistors were $R_1 = 470$ Ω externally +95 Ω inside ECCII₁ and $R_2 = 470$ Ω externally +95 Ω inside ECCII₂, and therefore, $R_1 = R_2 = R = 565$ Ω . Both working capacitors were selected as $C_1 = C_2 = C = 220$ pF. The DC control voltage was changed from 0.24 to 3.32 V. The ideal range of control between 306 kHz and 4.26 MHz is calculated from (5). Note that the capacitances are lower than in the case of the first oscillator type; therefore, the impact of the parasitic capacitances is significant even in the low-frequency mode. As regards the parasitic capacitances at the nodes of both working capacitors (additional 10 pF in each node), the estimation leads to an expected FO range from 294 kHz to 4.09 MHz. It is close to the measured results that are: 305 kHz–3.83 MHz. The results are shown in Fig. 13, where the dependence of FO on V_{SETB} and the dependence of both produced amplitudes on FO are given. Figure 14 shows the THD values and phase shift for produced signals in the available range of FO. The phase shift is constant below 2 MHz, as can be seen from Fig. 14b. The transient responses for discrete $f_0 = 1.51$ MHz ($V_{SETB} = 1.3$ V) are shown in Fig. 15.

4.2.2 High-Frequency Operation

The values of passive elements in Fig. 4 were calculated for the high-frequency testing: $C_1 = C_2 = C = 33$ pF and $R_1 = R_2 = R = 215$ Ω (external 120 Ω , internal 95 Ω of the intrinsic input resistance of R_x of the ECCIIs). Also, an example of full and precise analysis of the parasitic influences in this circuit is provided, see Fig. 16. The assumed values of parasitic influences (the values are shown in Fig. 16) were always estimated in accordance with datasheets of the active elements used [1, 2, 8, 19].

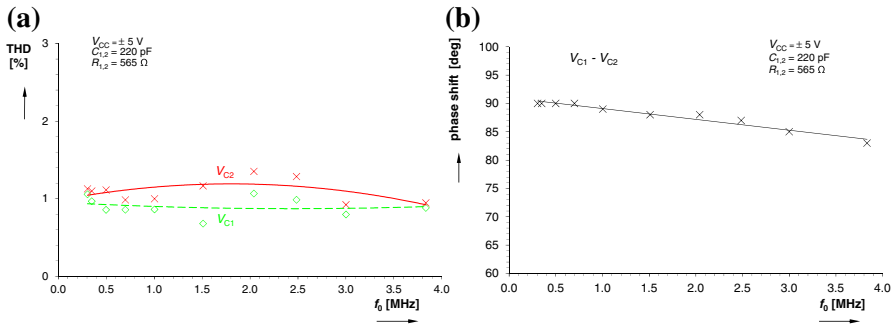


Fig. 14 Low-frequency operation-dependence of: a THD on FO, b phase shift on FO

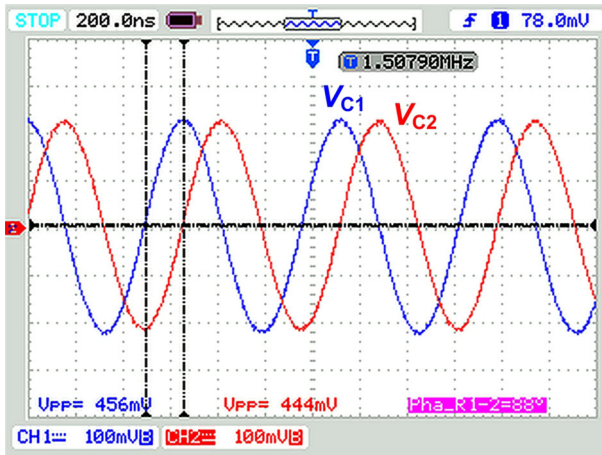


Fig. 15 Exemplary transient results for stable FO (1.51 MHz)

The resulting design equations, based on a routine analysis of the circuit in Fig. 16, for estimating the expected FO and CO are in the form:

$$\omega'_0 = \sqrt{\frac{B_1 B_2 R_{p1} R_{p2} + R_1 R_2 + B_2 R_1 R_{p2} (1 - A')}{R_1 R_2 R_{p1} R_{p2} C'_1 C'_2}}, \tag{10}$$

$$A' \geq \frac{R_1 R_2 (R_{p1} C'_1 + R_{p2} C'_2) + R_1 R_{p1} R_{p2} C'_1}{R_1 R_{p1} R_{p2} C'_1}. \tag{11}$$

Of course, R_1 and R_2 take R_x (95 Ω) into account. This value can be absorbed into the working resistor, which is very useful when compared to the previous solution (Fig. 3), where this absorption is not fully possible and R_{x1} influences the dependence of FO on the DC control voltage significantly. The measured results of FO dependence on V_{SETB} controlled from 0.12 to 1.22 V give a range from 1.97 to 20.18 MHz, see Fig. 17a. Analytical estimation provides a range from 1.82 to 18.76 MHz (10). We found that parasitic capacitances were the most critical parameters influencing FO in

Fig. 16 Modeling of parasitic influences for estimation of real behavior

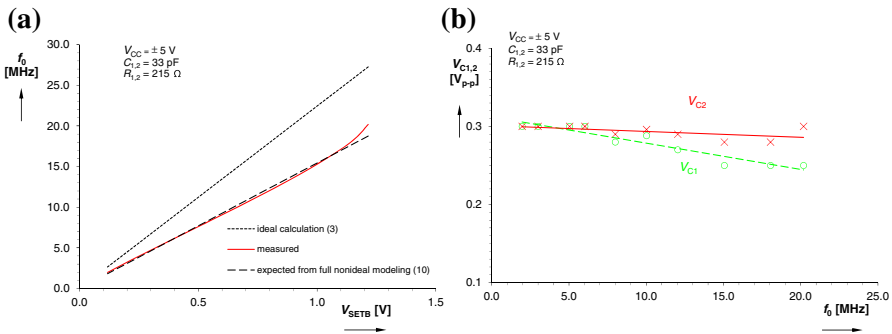
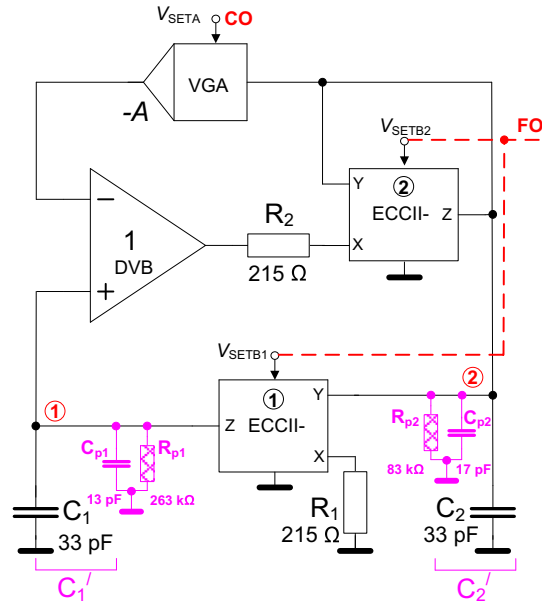


Fig. 17 High-frequency operation-dependence of: **a** FO on V_{SETB} , **b** $V_{C1,2}$ on FO

this circuit. The term $B_2 R_1 R_{p2} (1 - A')$ of (10) has at least a thousand times lower magnitude than the dominant term $B_1 B_2 R_{p1} R_{p2}$. Because $R_{p1} R_{p2} \gg R_1 R_2$, Eq. (10) can be simplified to:

$$\omega'_0 = \sqrt{\frac{B_1 B_2}{R_1 R_{p1} C'_1 C'_2}}, \tag{12}$$

which can also be obtained in a similar way in the previous case (see the note “simple estimation—additional parasitic capacitances only” in the Fig. 13a) and real experiments confirm that this simplification is possible. We show this detailed analysis only for this type of oscillator because this simplification is possible due to the high resistive component of impedance at nodes where both working capacitors are connected. Note

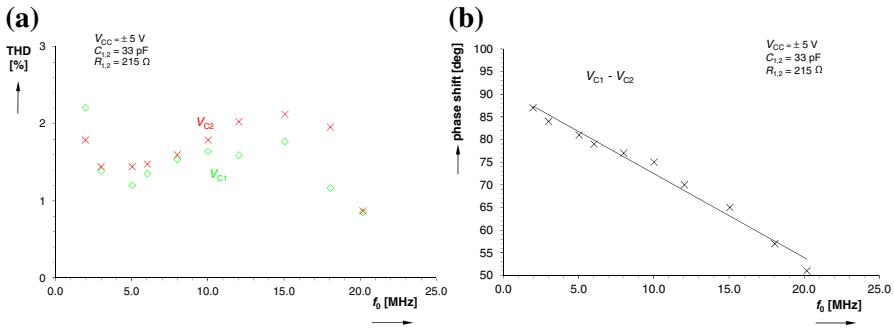


Fig. 18 High-frequency operation-dependence of: a THD on FO, b phase shift on FO

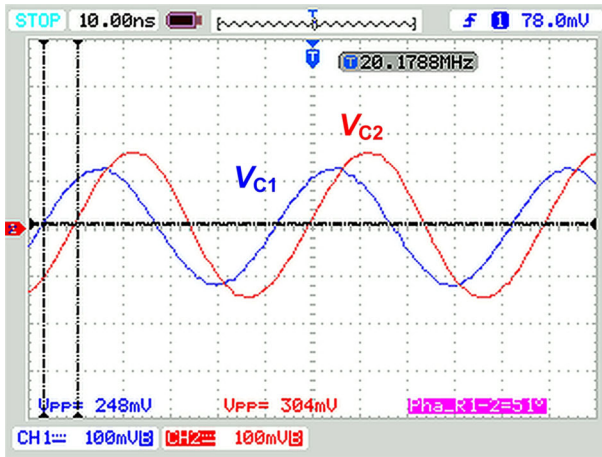


Fig. 19 Transient responses for stable FO (20.18 MHz)

that the solution in Sect. 4.1 is influenced by an additional impact of R_{X1} , see (9). The dependence of the output levels on FO is shown in Fig. 17b. The THD dependence on FO and the evolution of the phase shift between V_{C1} and V_{C2} are documented in Fig. 18. The DVB element of the oscillator must be replaced by a device with better frequency features if quadrature phase shift is strictly required at high FO (tens of MHz). Transient responses are given in Fig. 19 for $V_{SETB} = 1.22\text{ V}$ ($f_0 = 20.18\text{ MHz}$), where the blue line represents V_{C1} and the red one depicts V_{C2} . Figure 20 gives an example of corresponding frequency spectrums of both the generated signals.

4.3 Phase Noise Measurement

We measured the phase noise of both proposed circuits. In practice, the offset frequency is selected as 1/1000 of the fundamental (first) harmonic tone. In the case of operating at $f_0 = 1\text{ MHz}$, the offset frequency is $f_{off} = 1\text{ kHz}$ (1.001 MHz). We provide four results for the first type of circuit from Fig. 3 (two output signals—the

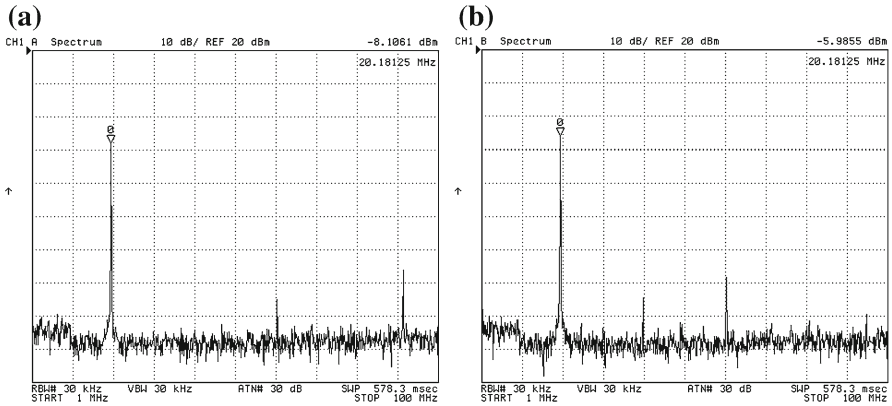


Fig. 20 An example of spectral analysis for stable FO (20MHz): **a** spectrum of V_{C1} , **b** spectrum of V_{C2}

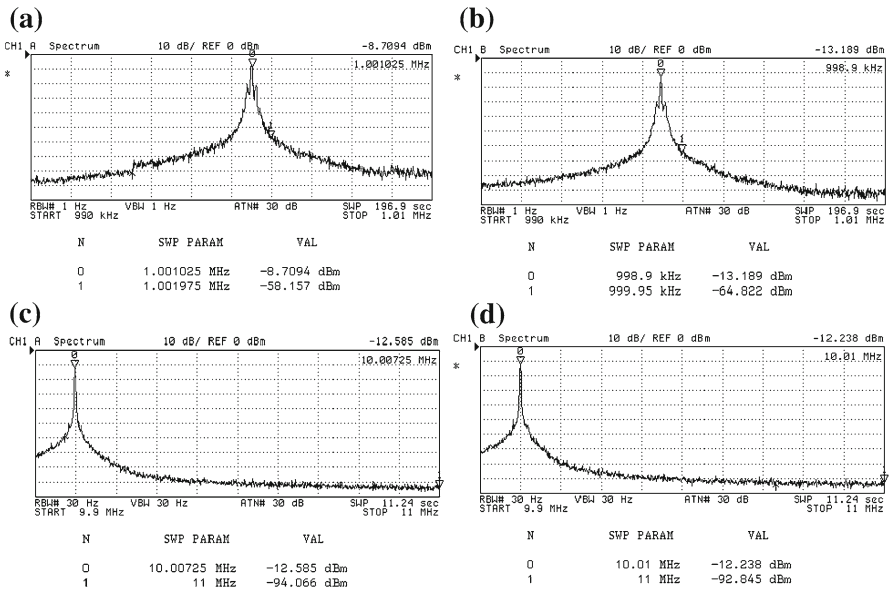


Fig. 21 Phase noise results: detail of spectrum around fundamental tone: **a** $f_0 = 1$ MHz ($R_1 = 220 \Omega$, $R_2 = 225 \Omega$, $C_1 = C_2 = C = 1$ nF, $V_{SETB} = 1.846$ V) and $f_{off} = 1$ kHz for V_{C1} , **b** $f_0 = 1$ MHz and $f_{off} = 1$ kHz for V_{C2} , **c** $f_0 = 10$ MHz ($R_1 = 220 \Omega$, $R_2 = 225 \Omega$, $C_1 = C_2 = C = 33$ pF, $V_{SETB} = 0.91$ V) and $f_{off} = 1$ MHz for V_{C1} , **d** $f_0 = 10$ MHz and $f_{off} = 1$ MHz for V_{C2}

V_{C1} amplitude depends on the tuning process for $f_0 = 1$ MHz, $f_{off} = 1$ kHz and for $f_0 = 10$ MHz, $f_{off} = 1$ MHz). The results of phase noise for V_{C1} are shown in the case of the second oscillator from Fig. 4 (V_{C1} and V_{C2} are not dependent on FO). All results are shown in Figs. 21 and 22.

The evaluated phase noises reach values of 49 dBc/Hz for V_{C1} and 52 dBc/Hz for V_{C2} ($f_0 = 1$ MHz, $f_{off} = 1$ kHz in both cases) for the situation in Fig. 21. Supposing

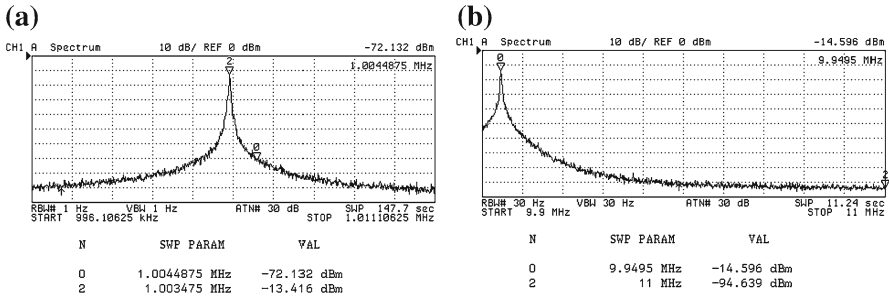


Fig. 22 Phase noise results: detail of spectrum around fundamental tone: **a** $f_0 = 1$ MHz ($R_1 = 565 \Omega$, $R_2 = 565 \Omega$, $C_1 = C_2 = C = 220$ pF, $V_{SETB} = 0.817$ V) and $f_{off} = 1$ kHz for V_{C1} , **b** $f_0 = 10$ MHz ($R_1 = 215 \Omega$, $R_2 = 215 \Omega$, $C_1 = C_2 = C = 33$ pF, $V_{SETB} = 0.665$ V) and $f_{off} = 1$ MHz for V_{C1}

fundamental tone $f_0 = 10$ MHz and $f_{off} = 1$ MHz, we obtained 81 dBc/Hz for V_{C1} and also for V_{C2} .

The phase noise of the second circuit type (Fig. 22) was evaluated for V_{C1} as 59 dBc/Hz ($f_0 = 1$ MHz and $f_{off} = 1$ kHz) and 80 dBc/Hz ($f_0 = 10$ MHz with $f_{off} = 1$ MHz).

5 Conclusion

This paper has presented two solutions as to how to construct linearly controllable quadrature oscillators. The solution in Fig. 3 is based on the product of two simultaneously controllable gains ($B_1 B_2$) in the time constant of the loss-less integrator. However, serious problems occur here. The amplitude of one of the generated signals depends on the tuning process (control of FO is achieved via this controllable gain), and, as a consequence, it changes its value during the tuning process. An additional problem is that THD increases if this amplitude comes near the saturation level of the active elements used. Therefore, the second variant of FO control was studied. The difference from the first oscillator type is that it separates the gain control between the two integrators, which are always required for constructing the oscillator. Both methods were studied in detail via experiments using modern commercially available devices and under similar real world conditions. The experimental results were obtained from frequencies of hundreds of kHz up to frequencies of tens of MHz. A THD of about 1–2 % was obtained for the measured waveforms. The dynamical features of the active devices (the voltage multiplier AD835 especially) are responsible for the worse THD. The bandwidth (–3 dB) of the differential voltage buffer AD830 limits the usability of the presented experimental circuits maximally to 2 MHz. However, a limited utilization of oscillator designs (with particular elements) can be extended to approximately 20 MHz if the drawback of phase shift dependence on FO is not a very important issue.

Acknowledgments Research described in this paper was financed by Czech Ministry of Education in frame of National Sustainability Program under Grant LO1401. For research, infrastructure of the SIX Center was used. Research described in the paper was supported by Czech Science Foundation project

under No. 14-24186P. Grant No. FEKT-S-14-2281 also supported this research. The support of the Project CZ.1.07/2.3.00/20.0007 WICOMT, financed from the operational program Education for competitiveness, is gratefully acknowledged. The authors would like to thank the editor and the anonymous reviewers for their useful and constructive comments that helped to improve the paper.

References

1. AD830: High speed, video difference amplifier, analog devices [online] (2005), last modified 3/2003 [cit.27.4.2014]. http://www.analog.com/static/imported-files/data_sheets/AD830.pdf
2. AD835: 250 MHz, voltage output 4-quadrant, analog devices [online] (1994), last modified 12/2010 [cit. 22.4.2014]. http://www.analog.com/static/imported-files/data_sheets/AD835.pdf
3. H. Alzaher, CMOS digitally programmable quadrature oscillators. *Int. J. Circuit Theory Appl.* **36**(8), 953–966 (2008). doi:10.1002/cta.479
4. D.R. Bhaskar, K.K. Abdalla, R. Senani, Electronically-controlled current-mode second order sinusoidal oscillators using MO-OTAs and grounded capacitors. *Circuits Syst.* **2**(2), 65–73 (2011). doi:10.4236/cs.2011.22011
5. D. Biolek, A. Lahiri, W. Jaikla, M. Siripruchyanun, J. Bajer, Realisation of electronically tunable voltage-mode/current-mode quadrature sinusoidal oscillator using ZC-CG-CDBA. *Microelectron. J.* **42**(10), 1116–1123 (2011). doi:10.1016/j.mejo.2011.07.004
6. D. Biolek, R. Senani, V. Biolkova, Z. Kolka, Active elements for analog signal processing: classification, review, and new proposal. *Radioengineering* **17**(4), 15–32 (2008)
7. V. Biolkova, J. Bajer, D. Biolek, Four-phase oscillators employing two active elements. *Radioengineering* **20**(1), 334–339 (2011)
8. EL2082: Current-Mode Multiplier, Intersil (Elantec) [online] (1996), last modified 2003 [cit.28.7.2011]. <http://www.intersil.com/data/fn/fn7152.pdf>
9. J. Galan, R.G. Carvalaj, A. Torralba, F. Munoz, J. Ramirez-Angulo, A low-power low-voltage OTA-C sinusoidal oscillator with large tuning range. *IEEE Trans. Circuits Syst.* **1** **52**(2), 283–291 (2005). doi:10.1109/TCSI.2004.841599
10. W. Jaikla, A. Lahiri, Resistor-less current-mode four-phase quadrature oscillator using CCCDTA and grounded capacitors. *AEU Int. J. Electron. Commun.* **66**(3), 214–218 (2012). doi:10.1016/j.aeue.2011.07.001
11. R. Keaton, W. Jaikla, A resistor-less current-mode quadrature sinusoidal oscillator employing single CCCDTA and grounded capacitors. *Prz. Elektrotech.* **87**(8), 138–141 (2011)
12. F. Khateb, F. Kacar, N. Khatib, D. Kubanek, High-precision differential-input buffered and external transconductance amplifier for low-voltage low-power applications. *Circuits Syst. Signal Process.* **32**(2), 453–476 (2013). doi:10.1007/s00034-012-9470-6
13. H. Kuntman, A. Ozpinar, On the realization of DO-OTA-C oscillators. *Microelectron. J.* **29**(12), 991–997 (1998). doi:10.1016/S0026-2692(98)00063-9
14. A. Lahiri, Current-mode variable frequency quadrature sinusoidal oscillator using two CCs and four passive components including grounded capacitors. *Analog Integr. Circuits Signal Process.* **71**(2), 303–311 (2012). doi:10.1007/s10470-010-9571-8
15. A. Lahiri, M. Gupta, Realizations of grounded negative capacitance using CFOAs. *Circuits Syst. Signal Process.* **30**(1), 143–155 (2011). doi:10.1007/s00034-010-9215-3
16. Y. Li, Electronically tunable current-mode biquadratic filter and four-phase quadrature oscillator. *Microelectron. J.* **45**(3), 330–335 (2014). doi:10.1016/j.mejo.2013.12.005
17. Y. Li, Electronically tunable current-mode quadrature oscillator using single MCDTA. *Radioengineering* **19**(4), 667–671 (2010)
18. B. Linarez-Barranco, A. Rodriguez-Vazquez, E. Sanchez-Sinencio, L. Huertas, CMOS OTA-C High frequency sinusoidal oscillators. *IEEE J. Solid State Circuits* **26**(2), 160–165 (1991). doi:10.1109/4.68133
19. OPA2652: Dual 700 MHz, Voltage-Feedback Operational Amplifier, Texas Instruments [online]. (2006), last modified 5/2006 [cit.27.4.2014]. <http://www.ti.com/lit/ds/symlink/opa2652.pdf>
20. N. Pandey, S. K. Paul, Single CDTA-based current mode all-pass filter and its applications. *J. Electr. Comput. Eng.* 1–5 (2011). doi:10.1155/2011/897631
21. A. Rodriguez-Vazquez, B. Linarez-Barranco, L. Huertas, E. Sanchez-Sinencio, On the design of voltage-controlled sinusoidal oscillators using OTA's. *IEEE Trans. Circuits Syst.* **1** **37**(2), 198–211 (1990). doi:10.1109/31.45712

22. Ch. Sakul, W. Jaikla, K. Dejhan, New resistorless current-mode quadrature oscillators using 2 CCCD-TAs and grounded capacitors. *Radioengineering* **20**(4), 890–897 (2011)
23. A.M. Soliman, Two integrator loop quadrature oscillators: A review. *J. Adv. Res.* **4**(1), 1–11 (2013). doi:[10.1016/j.jare.2012.03.001](https://doi.org/10.1016/j.jare.2012.03.001)
24. R. Sotner, A. Lahiri, A. Kartci, N. Herencsar, J. Jerabek, K. Vrba, Design of novel precise quadrature oscillators employing ECCIs with electronic control. *Adv. Electr. Comput. Eng.* **13**(2), 65–72 (2013). doi:[10.4316/AECE.2013.02011](https://doi.org/10.4316/AECE.2013.02011)
25. R. Sotner, J. Jerabek, N. Herencsar, Voltage differencing buffered/ inverted amplifiers and their applications for signal generation. *Radioengineering* **22**(2), 490–504 (2013)
26. R. Sotner, N. Herencsar, J. Jerabek, J. Koton, T. Dostal, K. Vrba, Electronically controlled oscillator with linear frequency adjusting for four-phase or differential quadrature output signal generation. *Int. J. Circuit Theory Appl.* **42**(12), 1264–1289 (2014). doi:[10.1002/cta.1919](https://doi.org/10.1002/cta.1919)
27. R. Sotner, N. Herencsar, J. Jerabek, R. Dvorak, A. Kartci, T. Dostal, K. Vrba, New double current controlled CFA (DCC-CFA) based voltage mode oscillator with independent electronic control of oscillation condition and frequency. *J. Electr. Eng.* **64**(2), 65–75 (2013). doi:[10.2478/jee-2013-0010](https://doi.org/10.2478/jee-2013-0010)
28. R. Sotner, Z. Hrubos, N. Herencsar, J. Jerabek, T. Dostal, K. Vrba, Precise Electronically adjustable oscillator suitable for quadrature signal generation employing active elements with current and voltage gain control. *Circuits Syst. Signal Process.* **33**(1), 1–35 (2014). doi:[10.1007/s00034-013-9623-2](https://doi.org/10.1007/s00034-013-9623-2)
29. S. Summart, Ch. Thongsopa, W. Jaikla, CCCIs-based sinusoidal quadrature oscillators with non-interactive control of condition and frequency. *Indian J. Pure Appl. Phys.* **52**(4), 277–283 (2014)
30. S. Summart, S. Tongsoa, W. Jaikla, OTA based current-mode sinusoidal quadrature oscillator with non-interactive control. *Prz. Elektrotech.* **88**(7a), 14–17 (2012)
31. Texas Instruments. OPA860 Wide-bandwidth, operational transconductance amplifier (OTA) and buffer (online), <http://www.ti.com/lit/ds/symlink/opa860.pdf>
32. VCA810: High Gain Adjust Range, Wideband, variable gain amplifier, Texas Instruments [online] (2003), last modified 12/2010 [cit.28.7.2011]. <http://focus.ti.com/lit/ds/sbos275f/sbos275f.pdf>

[18] SOTNER, R., JERABEK, J., PETRZELA, J., PROKOP, R., VRBA, K., KARTCI, A., DOSTAL, T. Quadrature Oscillator Solution Suitable with Arbitrary and Electronically Adjustable Phase Shift. In *Proceedings of the IEEE International Symposium on Circuits and Systems (ISCAS)*, Lisbon (Portugal), 2015, p. 3056-3059. ISBN: 978-1-4799-8391-9, ISSN: 0271-4310.

Quadrature Oscillator Solution Suitable with Arbitrary and Electronically Adjustable Phase Shift

Roman Sotner*, Jan Jerabek*, Jiri Petrzela*, Roman Prokop*, Kamil Vrba*, Aslihan Kartci†, Tomas Dostal**

Email: {sotner, jerabekj, petrzelj, prokop, vrbak}@feec.vutbr.cz aslhankartc@gmail.com dostal@vspj.cz

*Faculty of Electrical Engineering and Communication, Brno University of Technology, Technicka 10, 616 00 Brno, Czech Republic

†Department of Electronics and Communications Engineering, Yildiz Technical University, Esenler, 34222, Istanbul, Turkey

**Department of Electrical Engineering and Computer Science, College of Polytechnics Jihlava, Tolsteho 16, Jihlava 586 01, Czech Republic

Abstract—This paper discusses new quadrature oscillator consisting of two all-pass sections and inverting amplifier that is capable of generating two signals with arbitrary phase shift between them. Constrains and limits of this simple idea are discussed. Verifications of theoretical expectations were provided by Spice simulations based on active devices with TSMC 0.18 μm NMOS and PMOS technological models.

Keywords—Arbitrary phase shift, all-pass section, electronic control, multiphase oscillator, operational transconductance amplifier, quadrature oscillator

I. INTRODUCTION

Harmonic oscillators with multiphase or/and arbitrary adjustable phase shift between output signals are still very interesting areas for many researchers, because many various active elements [1] can be beneficially utilized and allow interesting additional features in some cases. Unfortunately, there is no space for a detailed analysis of already known solutions. Therefore, we will provide discussion of selected typical examples found in recent papers.

Principle of operation of known solutions can be divided to the following groups: a) lossy blocks (integrators or similar selective sections) in stepwise phase shifted cascade and full feedback (for example [2]-[4] and references cited therein); b) all-pass section in combination with integrators/differentiators in simple loops ([5]-[9] for example); c) all-pass sections (APs) in the loop ([10]-[11] for example); d) other principles (see [12] for detailed discussion). Most of discussed simple solutions focus on quadrature oscillator design (for example detailed literature discussion in [13] and [14]). Some attempts to design the simple oscillators with different phase shift than 90 degrees were also provided ([12], [15] for example). However, these solutions suffer from some drawbacks (mutually dependent oscillation condition and frequency of oscillations, required matching of several parameters and amplitudes dependent on tuning process [12]).

Unfortunately, arbitrary setting of the phase shift between output signals is not always ensured [16]. Only typical phase shifts in multiphase types of oscillators are verified (phase shifts given by $2\pi/n$, where n is integer value), typically in

Research described in this paper was financed by the National Sustainability Program under grant LO1401 and by the Czech Science Foundation under grant no. GP14-24186P. For the research, infrastructure of the SIX Center was used. Grant No. FEKT-S-14-2281 and project Electronic-biomedical co-operation ELBIC M00176 also supported this research. The support of the project CZ.1.07/2.3.00/20.0007 WICOMT, financed from the operational program Education for competitiveness, is gratefully acknowledged.

multiples of $\pi/4$, $\pi/3$, etc. Arbitrary phase shift means phase shift may not be in integer multiple of the minimal available phase shift generated by the basic lossy block of the structure. Moreover, solutions in [16] are quite complicated and require many active elements. However, from our point of view, it seems to be possible to generate not only integer multiples of basic phase shifts, as is presented in this contribution on a very simple example of circuit solution.

II. OSCILLATOR ANALYSIS

Implementation of oscillator with shifted phase, as it was introduced for example in [11], was carried out using two proposed AP-s and amplifier in one loop. All-pass sections, used in the design, are based on solution presented by Bajer [17], which was slightly improved (replacement of the current conveyor element by the operational transconductance amplifier (OTA) in order to reduce floating resistor). Very similar AP was presented also by Keskin et al. [18]. However, their AP circuit requires attenuated (1/2) signal from internal high impedance node to negative input terminal of the OTA. Simple block diagram is depicted in Fig. 1. Barkhausen criterion [19]-[22] is supposed for startup of oscillations fulfillment of the following conditions:

$$G(s) = K_{AP1}(s)(-K)K_{AP2}(s) = 1, \quad (1)$$

$$\varphi_{AP1} + \varphi_{AP2} + \varphi_K = 2\pi k, \quad k = 1, 2, \dots \quad (2)$$

In this case we obtain the following equation (we suppose to fulfill oscillation condition $-K = 1$, i.e. gain of the inverting amplifier in positive feedback loop has to be equal to 1 at oscillation frequency):

$$-K \left(\frac{g_{m1} - sC_1}{g_{m1} + sC_1} \right) \left(\frac{g_{m2} - sC_2}{g_{m2} + sC_2} \right) = - \frac{s^2 - \left(\frac{C_1 g_{m2} + C_2 g_{m1}}{C_1 C_2} \right) s + \frac{g_{m1} g_{m2}}{C_1 C_2}}{s^2 + \left(\frac{C_1 g_{m2} + C_2 g_{m1}}{C_1 C_2} \right) s + \frac{g_{m1} g_{m2}}{C_1 C_2}} = 1 \quad (3)$$

Oscillation frequency is given by:

$$\omega_0 = \sqrt{g_{m1} g_{m2} / C_1 C_2}. \quad (4)$$

The first AP section has transfer function:

$$K_{AP1}(s) = \frac{g_{m1} - sC_1}{g_{m1} + sC_1} = \frac{\sqrt{g_{m1}^2 + (\omega_0 C_1)^2} e^{-\tan^{-1}\left(\frac{\omega_0 C_1}{g_{m1}}\right)j}}{\sqrt{g_{m1}^2 + (\omega_0 C_1)^2} e^{\tan^{-1}\left(\frac{\omega_0 C_1}{g_{m1}}\right)j}} = 1 \cdot e^{-2 \tan^{-1}\left(\frac{\omega_0 C_1}{g_{m1}}\right)j}, \quad (5)$$

hence, the gain (modulus) and phase are:

$$|K_{AP1}| = 1, \quad \varphi_{AP1} = -2 \tan^{-1}\left(\frac{\omega_0 C_1}{g_{m1}}\right). \quad (6), (7)$$

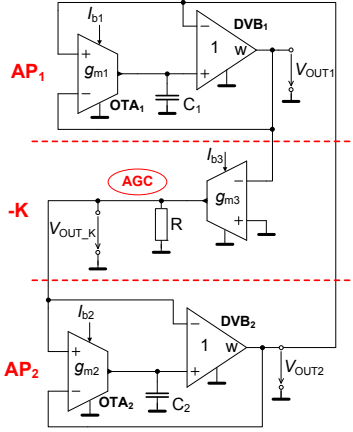


Fig. 1. Multiphase oscillator based on two AP sections and inverter.

Substitution of (4) to (7) gives phase shift (in degrees) of the AP₁ for oscillation frequency as:

$$\varphi_{AP1} = -2 \tan^{-1}\left(\sqrt{\frac{g_{m2} C_1}{g_{m1} C_2}}\right) \frac{180}{\pi}. \quad (8)$$

We can also express analogically phase shift for the second AP section with transfer:

$$K_{AP2}(s) = \frac{g_{m2} - sC_2}{g_{m2} + sC_2}. \quad (9)$$

Inverting voltage amplifier ($-K$) has transfer given by: $-K = g_{m3}R$. It allows very simple utilization of circuit for automatic amplitude stabilization, i.e. automatic gain control (AGC) circuit.

III. ACTIVE ELEMENTS

We used the following CMOS TSMC LO EPI 0.18 μm technology models [23] for implementation of required active elements in PSpice simulations, with supply voltage $\pm 0.9 \text{ V}$. Aspect ratios (W/L) of all transistors used are noted directly in figures (Fig. 2).

OTA is well-known element [1] and suitable for many kinds of design due to its simple structure and controllability (Fig. 2a). Transconductance changes approximately between $60 \mu\text{S}$ and 1 mS by bias current (I_b) adjusted from 5 to $235 \mu\text{A}$. It changes also bandwidth (-3 dB) from 21 to 164 MHz and also output resistance from $1.4 \text{ M}\Omega$ to $90 \text{ k}\Omega$. Input linear dynamical range is limited in the worst case to $\pm 100 \text{ mV}$ (output shorted to ground) due to the low-voltage CMOS technology.

Differential voltage buffer (DVB) is very important for our design. A model shown in Fig. 2b consists of two OTAs (OTA and grounded resistor replacement) and voltage inverter. Transit frequency of the buffer is 195 MHz . Dynamical range is also about $\pm 100 \text{ mV}$. Output resistance (R_w) of the DVB achieves value over 70Ω .

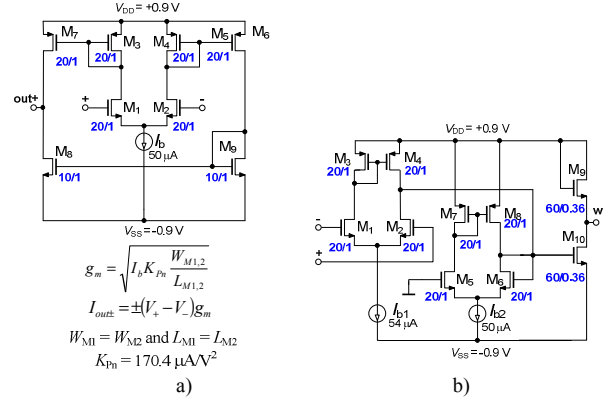


Fig. 2. Simulation models: a) simple OTA, b) DVB.

IV. DESIGN AND SIMULATION RESULTS

AGC circuit is implementable very simply in this case. We used circuit shown in Fig. 3. Produced amplitude levels are quite low (tens of mV), practically under threshold voltage of used diode detector, therefore amplification of the signal for AGC before further processing is required. Diode D₁ is formed by the NMOS transistor and transistor M₁ operates in linear (ohmic) regime (typical example is BF245A). So, AGC operation ensures slightly variable resistor in parallel to R in Fig. 1.

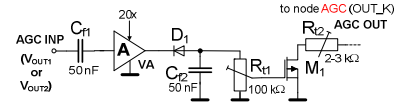


Fig. 3. AGC system used for amplitude stabilization.

The following parameters for the oscillator in standard quadrature phase shift operation regime have been selected: $C_1 = C_2 = C = 47 \text{ pF}$, $g_{m1} = g_{m2} = g_m = 500 \mu\text{S}$ ($I_{b1} = I_{b2} = I_b = 66 \mu\text{A}$), $g_{m3} = 500 \mu\text{S}$ ($I_{b3} = 66 \mu\text{A}$) and $R = 10 \text{ k}\Omega$. Calculated oscillation frequency is $f_0 = 1.693 \text{ MHz}$. Simulation results are in Fig. 4. Simulation with CMOS models lead to value $f_0 = 1.559 \text{ MHz}$.

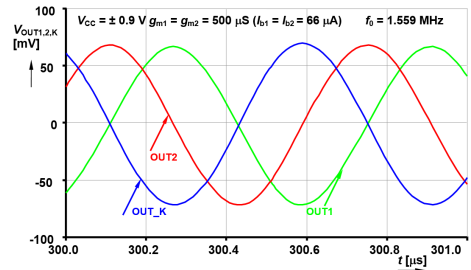


Fig. 4. Transient responses of the proposed oscillator in quadrature operation.

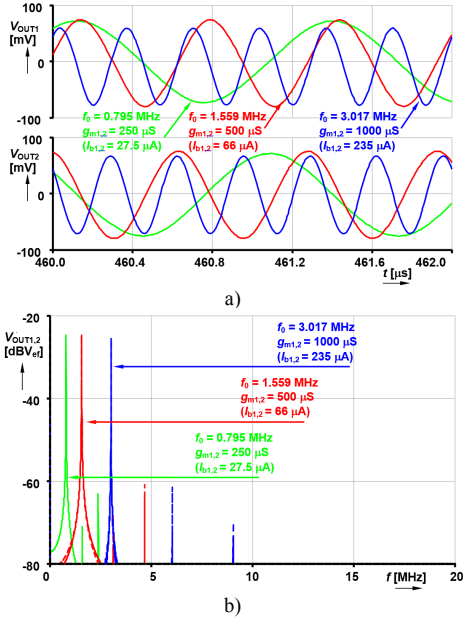


Fig. 5. Oscillation frequency adjusting (quadrature mode) for three different values: a) time domain, b) spectrum.

Electronic control of the oscillation frequency by simultaneous change of both transconductances ($g_{m1,2}$) is presented in Fig. 5 for three different values. Tuning range of oscillation frequency f_0 was verified from 0.194 to 3.016 MHz. Separation of higher harmonics components is 37 dB and higher, thus total harmonic distortion (THD) achieves only values about 1.5%.

Oscillators employing AP sections allow design of oscillators generating signals with easily adjustable phase shift without impact on generated ratio of amplitudes. Our particular setting requires oscillator producing two signals with frequency $f_0 = 1$ MHz and phase shift $\varphi_{OUT1-2} = -55^\circ$. Values of capacitors are again $C_1 = C_2 = C = 47$ pF. We used equation (8) that was slightly modified to form:

$$\left[\tan\left(-\frac{\varphi_{OUT1-2}}{2}\right) \right]^2 = \frac{g_{m2}C_1}{g_{m1}C_2}, \quad (10)$$

if we suppose equality of both capacitors, equation could be rewritten to:

$$g_{m2} = g_{m1} \left[\tan\left(-\frac{\varphi_{OUT1-2}}{2}\right) \right]^2. \quad (11)$$

Resulting equation (12) was obtained by substitution of (4) to (11):

$$g_{m2} = \tan\left(-\frac{\varphi_{OUT1-2}}{2}\right) \omega_0 C. \quad (12)$$

Values of both transconductances were calculated by help of (12) and (4) as $g_{m1} = 566 \mu\text{S}$ ($I_{b1} = 82 \mu\text{A}$) and $g_{m2} = 154 \mu\text{S}$ ($I_{b2} = 16 \mu\text{A}$). At first, we calculated g_{m2} from (12) for known $\varphi_{OUT1-2} = -55^\circ$ and $f_0 = 1$ MHz and selected C , then g_{m1} from (4) was obtained. Simulation results are in Fig. 6. We achieved oscillation frequency 0.945 MHz and phase shift -55.5° from

our simulation. Dependence of phase shifts on ratio of both transconductances is clear from (11). We documented this behavior in Tab. 1, where ideal phase shifts and values obtained from simulation were compared (also demonstrated in Fig. 7). Loop cascading of two APs with controllable features is useful because it provides phase shifts between outputs with arbitrary values (no multiples of minimal and constant phase shift value), in comparison to [2]-[4], [16] for example, where minimal phase shift and its multiples are fixed and determined by lossy blocks.

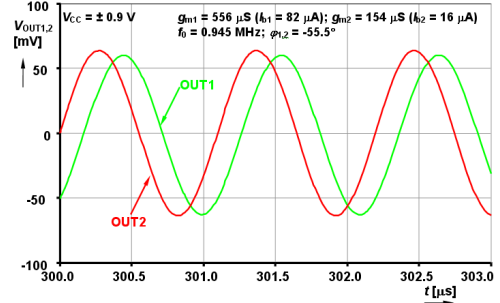


Fig. 6. Transient simulation for designed parameters ("arbitrary" mode).

TABLE I. IDEAL ($\varphi_{OUT1-2i}$) AND SIMULATED ($\varphi_{OUT1-2s}$) PHASE SHIFTS.

g_{m1} [μS]	g_{m2} [μS]	g_{m2}/g_{m1} [-]	f_{0i} [MHz]	f_{0s} [MHz]	$\varphi_{OUT1-2i}$ [$^\circ$]	$\varphi_{OUT1-2s}$ [$^\circ$]
50	1000	1/20	0.757	0.674	-25.2	-23.2
100	1000	1/10	1.071	0.962	-35.1	-32.4
100	500	1/5	0.757	0.733	-48.2	-49.4
250	500	1/2	1.197	1.117	-70.6	-68.8
500	500	1	1.693	1.569	-90.0	-89.0
500	250	2	1.197	1.193	-109.5	-109.1
500	100	5	0.757	0.736	-131.9	-131.6
1000	100	10	1.071	1.024	-145.0	-144.0
1000	50	20	0.757	0.680	-154.9	-151.3

In case we ensure constant g_{m2}/g_{m1} ratio during the tuning process, we can also electronically tune this type of the oscillator with intended phase shift between produced amplitudes. Arbitrariness of the phase shift generation is given by possible g_{m2}/g_{m1} ratio (in fact by minimal and maximal available g_m value of used OTAs). Therefore, ranges of available phase shifts in Tab. 1 and Fig. 7 are also limited by g_m adjustable from $50 \mu\text{S}$ to 1 mS (1:40). This fact also brings some limits for frequency tuning (extremely high ratios of g_{m2}/g_{m1} are problematic but theoretically possible).

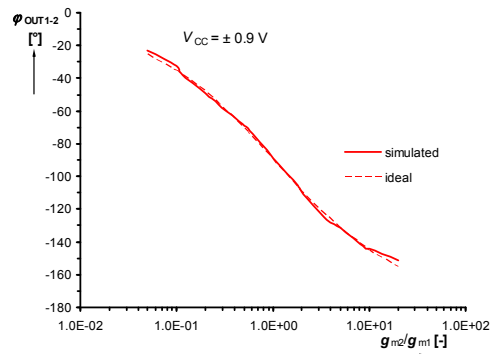


Fig. 7. Dependence of phase shift on g_{m2}/g_{m1} ratio.

Monte Carlo analyses were performed in order to discover parameters variations. Note that all results are actually worse than expected because all variations were mutually uncorrelated during simulation. When tolerance of g_{m1} and g_{m2} is 1% and tolerance of capacitors (C_1 and C_2) is 5%, phase shift results in 54.8 deg. ± 4.0 deg. Temperature variations were also analyzed. For phase shift setting equal to 90 deg. (55 deg. respectively), temperature dependences (0 to 40 deg. Celsius) were in case of phase error ± 2 deg. (± 5 deg. respectively). Frequency errors in the same conditions were $\pm 10\%$ ($\pm 5\%$ respectively). V_{CC} stepping analysis yields that supply voltage should be > 0.75 V for correct operation for both variants (90 deg. and 55 deg. phase shifts).

V. CONCLUSION

Straight-forward modification of quite simple AP-based oscillator structure can provide real arbitrary phase shift between two generated signals. As detailed analysis shows, this modification is based on adjustable ratio of g_{m2} and g_{m1} in AP sections, which are in standard design normally equal to each other. Tuning of the oscillator is provided by g_{m1} and g_{m2} simultaneously. Their ratio has direct impact on the produced phase shift. Note that possibility of the design with very accurate ratios of parameters (and their highly-correlated temperature dependences) is one from main advantages of IC implementation. Therefore this is considered as advantage of our solution. Oscillation frequency with preserved phase shift can be tuned only if condition of constant ratio g_{m2}/g_{m1} is always fulfilled in whole range of tuning. A practical example in our contribution for specific design parameters provides adjustable range of phase shifts between 23 and 151 degrees. Nevertheless, it is worth mentioning again that phase shift can achieve practically any value between these borders, which is a significant feature of our solution. However, there are also some limitations. Range of g_m of the OTA is always restricted by minimal and maximal bias current to ensure operation of MOS differential pair (OTA) in saturation. Therefore, a range of phase shift adjusting is also limited by available minimal and maximal ratio of g_{m2}/g_{m1} in particular solution. Spectral purity and phase noise of produced signals (in this case) is dependent mainly on the AGC circuit. Circuit was designed and simulated in PSpice software therefore study of temperature variations is not meaningful at this phase.

REFERENCES

- [1] D. Biolek, R. Senani, V. Biolkova, Z. Kolka, "Active element for analog signal processing: Classification, review and new proposals," *Radioengineering*, vol. 17, no. 4, pp. 15-32, 2008.
- [2] M. T. Abuelmaatti, M. A. Al-Qahtani, "New current-controlled multiphase sinusoidal oscillator using translinear current conveyors," *IEEE Transactions on Circuits and Systems II: Analog and Digital Signal Processing*, vol. 45, no. 7, pp. 881-885, 1998.
- [3] G. Souliotis, C. Psychalinos, "Electronically controlled multiphase sinusoidal oscillators using current amplifiers," *International Journal of Circuit Theory and Applications*, vol. 37, no. 1, pp. 43-52, 2009.
- [4] M. Kungern, J. Chanwutium, K. Dejhan, "Electronically tunable multiphase sinusoidal oscillator using translinear current conveyors," *Analog Integrated Circuits and Signal Processing*, vol. 65, no. 2, pp. 327-334, 2010.
- [5] R. Keawon, W. Jaikla, "Resistor-less Current-mode quadrature sinusoidal oscillator employing single CCCDTA and grounded capacitors," *Przeglad Elektrotechniczny*, vol. 87, no. 8, pp. 138-141, 2011.
- [6] W. Jaikla, M. Siripruchyanun, J. Bajer, D. Biolek, "A simple current-mode quadrature oscillator using single CDTA," *Radioengineering*, vol. 17, no. 4, pp. 33-40, 2008.
- [7] A. U. Keskin, C. Aydin, E. Hancioglu, C. Acar, "Quadrature oscillator using current differencing buffered amplifiers (CDBA)," *Frequenz*, vol. 60, no. 3, pp. 21-23, 2006.
- [8] S. N. Songkla, W. Jaikla, "Realization of electronically tunable current-mode first-order allpass filter and its application," *International Journal of Electronics and Electrical Engineering*, vol. 2012, no. 6, pp. 40-43, 2012.
- [9] S. Minaei, E. Yuce, "Novel voltage-mode all-pass filter based on using DVCCs," *Circuits Systems and Signal Processing*, vol. 29, no. 3, pp. 391-402, 2010.
- [10] A. U. Keskin, D. Biolek, "Current mode quadrature oscillator using current differencing transconductance amplifiers (CDTA)," *IEE Proc. Circuits Devices and Systems*, vol. 153, no. 3, pp. 214-218, 2006.
- [11] K. Songsuwanit, W. Petchmaneeumka, V. Riewruja, "Electronically adjustable phase shifter using OTAs," In *Proceedings of the International Conference on Control, Automation and Systems (ICCAS2010)*, Gyeonggi-do (Korea), pp. 1622-1625, 2010.
- [12] R. Sotner, J. Jerabek, N. Herencsar, "Voltage differencing buffered/inverted amplifiers and their applications for signal generation," *Radioengineering*, vol. 22, no. 2, pp. 490-504, 2013.
- [13] R. Sotner, N. Herencsar, J. Jerabek, J. Koton, T. Dostal, K. Vrba, "Electronically controlled oscillator with linear frequency adjusting for four-phase or differential quadrature output signal generation," *International Journal of Circuit Theory and Applications*, vol. 42, no. 12, pp. 1264-1289, 2014.
- [14] R. Sotner, Z. Hrubos, N. Herencsar, J. Jerabek, T. Dostal, K. Vrba, "Precise electronically adjustable oscillator suitable for quadrature signal generation employing active elements with current and voltage gain control," *Circuits Systems and Signal Processing*, vol. 33, no. 1, pp. 1-35, 2014.
- [15] R. Sotner, J. Jerabek, N. Herencsar, J-W. Horng, K. Vrba, "Electronically linearly voltage controlled second-order harmonic oscillator with multiples of $\pi/4$ phase shifts," In *Proceedings of the 37th International Conference on Telecommunications and Signal Processing (TSP2014)*, Berlin (Germany), pp. 396-400, 2014.
- [16] S-H. Tu, Y-S. Hwang, J-J. Chen, A. M. Soliman, C-M. Chang, "OTA-C arbitrary-phase-shift oscillators," *IEEE Transactions on Instrumentation and Measurement*, vol. 61, no. 8, pp. 2305-2319, 2012.
- [17] J. Bajer, D. Biolek, "Voltage-mode electronically tunable all-pass filter employing CCCII+, one capacitor and differential-input voltage buffer," In *Proceedings of 26th IEEE Convention of Electrical and Electronics Engineers in Israel (IEEEI2010)*, Eliat (Israel), pp. 934-937, 2010.
- [18] A. U. Keskin, K. Pal, E. Hancioglu, "Resistorless first-order filter with electronic tuning," *AEU - International Journal of Electronics and Communication*, vol. 62, no. 4, pp. 304-306, 2008.
- [19] L. Wangenheim, "On the Barkhausen and Nyquist stability criteria," *Analog Integrated Circuits and Signal Processing*, vol. 66, no. 1, pp. 139-141, 2011.
- [20] F. He, R. Ribas, C. Lahuec, M. Jezequel, "Discussion on the general oscillation startup condition and the Barkhausen criterion," *Analog Integrated Circuits and Signal Processing*, vol. 59, no. 2, pp. 215-221, 2009.
- [21] V. Singh, "Discussion on Barkhausen and Nyquist stability criteria," *Analog Integrated Circuits and Signal Processing*, vol. 62, no. 3, pp. 327-332, 2010.
- [22] H. Martinez-Garcia, A. Grau-Saldes, Y. Bolea-Monte, J. Gamiz-Caro, "Discussion on Barkhausen and Nyquist stability criteria," *Analog Integrated Circuits and Signal Processing*, vol. 70, no. 3, pp. 443-449, 2012.
- [23] MOSIS parametric test results of TSMC LO EPI SCN018 technology. Available on-line [ftp://ftp.isi.edu/pub/mosis/vendors/tsmc-018/t44e_lo_epi-params.txt]. Cited 24.5.2012.

[19] SOTNER, R., KARTCI, A., JERABEK, J., HERENC SAR, N., PETRZELA, J. Modulator Based on Electronic Change of Phase Shift in Simple Oscillator. In *ELECO 2015 9th International Conference on Electrical and Electronics Engineering*, Bursa (Turkey), 2015. p. 101-105. ISBN: 978-605-01-0737-1.

Modulator Based on Electronic Change of Phase Shift in Simple Oscillator

Roman Sotner¹, Aslihan Kartci¹, Jan Jerabek², Norbert Herencsar², Jiri Petrzela¹

¹Dept. of Radio Electronics, Faculty of Electrical Engineering and Communication, Brno University of Technology, Technicka 3082/12, Brno, Czech Republic

sotner@feec.vutbr.cz, aslhankartc@gmail.com, petrzelj@feec.vutbr.cz

²Dept. of Telecommunications, Faculty of Electrical Engineering and Communication, Brno University of Technology, Technicka 3082/12, Brno, Czech Republic

jerabekj@feec.vutbr.cz, herencsn@feec.vutbr.cz

Abstract

In this study, we propose phase shift keying system using an oscillator based on two all-pass filters. The main idea is based on phase commutation by converted data to two pairs of DC control voltages for controlling both all-pass sections. Therefore, the proposal of converter of data to DC control voltages is solved with precise amplitude automatic gain control circuit. The system operation was verified while employing commercially available devices through PSPICE program at the modulation frequencies 1 MHz and 10 kHz with driving signals 0 V (L) and 5 V (H), respectively. The simulation results confirmed the theoretical presumptions.

1. Introduction

The particular problems of multiphase oscillator solutions have been frequently solved in recent works ([1-9] for example). Several works focus on lower multiples of phase shift than of 90 or 60 degrees, for example 45 degrees [6, 8, 9]. There are also implemented some special approaches to the design of the multiphase oscillators [10-12]. For example, Ozoguz *et al.* [10] presented utilization of functional blocks operating in approximated square-root domain for the construction of multiphase oscillator. Maundy *et al.* [11] used fractional-order all-pass (AP) transfer section for the design of multiphase oscillator. Symbolical transfer function of this section contains fractional exponent α of the Laplace operator s , where fractional character is given by RC approximation of the fractional order capacitor in the structure. This feature allows synthesis of the multiphase oscillators with theoretically arbitrary phase shifts between generated signals and extended range of frequency of oscillations (FO) tuning proportional to reciprocal time constant exponentiated by $1/\alpha$. Unfortunately, unavailability of simple electronic adjusting of the fractional-order capacitor limits real utilization of fractional-order-based circuits in systems for the signal generation and processing. There are many problems suitable for future research that have to be solved. A very interesting work regarding multiphase generation based also on non-standard principle was published by Promee *et al.* [12], where log-domain [13] approach was used to obtain reduced complexity of all-pass section, better dynamics of linear operation and wider tunability of oscillation frequency.

Our proposal utilizes the oscillator with theoretically arbitrary phase shift of two generated signals. Generation of arbitrary phase distance between two output signals has been hardly ever solved in simple second-order oscillator structures.

Some notes about arbitrary phase shift generation were given by Tu *et al.* [6]. However, their solutions still produce integer multiples of the minimal phase shift distance between generated amplitudes. The first attempt to really continuously settable phase distance of two produced signals in the frame of the simple oscillator was presented in [14]. However, no other ideas how to utilize oscillator with such feature were discussed. Our question is: What application/system can be prepared with oscillator producing “arbitrary” phase shift? Therefore, the presented work focuses on simple application of the modified oscillator structure (voltage controlled all-pass sections including precise amplitude automatic gain control circuit) in simple phase shift keying modulator system including control logic (converter of data to DC driving voltages).

2. Proposed Solution

Our aim is to design modulator with two outputs providing identical carrier frequency and with digitally controlled phase shift between them (phase shift commutated between two values). We used modification of the simple oscillator based on two all-pass filtering sections [14] as the main building block of the solution. However, several other counterparts are required for the design. First of all, precise automatic amplitude gain control circuit (AGC) has to be designed in order to ensure and preserve stable output levels. We want to implement oscillator solution with voltage-controlled phase shift to achieve the simplest method of driving. In such a case the data (symbols) are represented by square wave with levels 0 V (logic L) and 5 V (logic H). Therefore, the next important task is the proposal of “converter of data (symbol) to DC control voltage”. Therefore, we divided our work to several subparts where all these partial problems will be discussed separately. The block structure of the system is shown in Fig. 1.

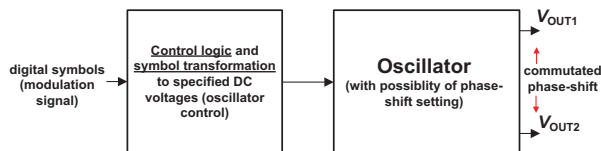


Fig. 1. Proposed concept of digital modulator

2.1. Oscillator with Possibility of Phase Shift Setting

The oscillator structure is shown in Fig. 2. It utilizes a solution based on two AP sections (derived from [15, 16]) and

inverting voltage amplifier presented in [14]. Note that solution in **Fig. 2** has many different features (including controllable amplifier VA and a different type of the phase shifters) than [14].

The condition of oscillation (CO) is fulfilled for $-A \geq 1$. Variable voltage amplifier VCA610 [17], driven by negative DC voltage, serves for control of CO. FO is given by:

$$\omega_0 = \sqrt{\frac{B_1 B_2}{R_1 R_2 C_1 C_2}} \cong \sqrt{\frac{V_{SETB1} V_{SETB2}}{R_1 R_2 C_1 C_2}}. \quad (1)$$

It is clear that FO of the oscillator is electronically adjustable (even linearly if $V_{SETB1} = V_{SETB2} = V_{SETB}$). Phase relations of the operation of this oscillator can be derived from transfer relations of partial AP sections. This construction of AP is based on electronically controllable current conveyor of second generation (ECCII+) [18, 19] built with help of current-mode multiplier EL2082 [20], very popular diamond transistor (DT) OPA660 [21] and differential voltage buffer (DVB) AD830 [22] with unity gain transfer.

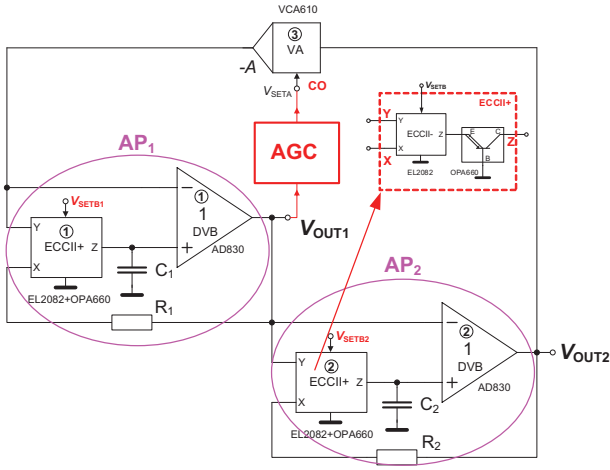


Fig. 2. Oscillator used in proposed solution

By routine analysis we can obtain phase shift between input and output of the AP section (we suppose fulfilled CO, i.e. $-A = 1$):

$$K_{AP1}(s) = \frac{\frac{B_1}{R_1} - sC_1}{\frac{B_1}{R_1} + sC_1} = \frac{\sqrt{\left(\frac{B_1}{R_1}\right)^2 + (\omega_0 C_1)^2} e^{\tan^{-1}\left(\frac{\omega_0 C_1 R_1}{B_1}\right)j}}{\sqrt{\left(\frac{B_1}{R_1}\right)^2 + (\omega_0 C_1)^2} e^{\tan^{-1}\left(\frac{\omega_0 C_1 R_1}{B_1}\right)j}} = 1. \exp\left[-2 \tan^{-1}\left(\frac{\omega_0 C_1 R_1}{B_1}\right)j\right] \quad (2)$$

Supposing insertion of ω_0 from (1) to (2), we obtained argument of the equation in form:

$$\varphi_{1-2} = -2 \tan^{-1}\left(\sqrt{\frac{B_2}{B_1} \frac{R_1 C_1}{R_2 C_2}}\right)_{\substack{R_1=R_2=R \\ C_1=C_2=C}} \cong -2 \tan^{-1}\left(\sqrt{\frac{B_2}{B_1}}\right). \quad (3)$$

It can be seen that phase shift of the produced signals depends on B_2/B_1 ratio. Therefore, we can use these two parameters for electronic control of phase shift between V_{OUT1} and V_{OUT2} and for control of FO (if defined ratio is kept constant during the tuning process). Note that also other parameters (R_1 , R_2 especially) may serve for definition of phase distance (ratio) and

then both identical values of $B_{1,2}$ (adjusted simultaneously) may serve for FO control.

We selected the following parameters for validation and demonstration of the assumed features of the oscillator: $C_1 = C_2 = C = 220$ pF, $R_1 = R_2 = R = 565 \Omega$ ($470 \Omega + 95 \Omega$ of the X terminal [20]). Our design requirements are given as follows: $\varphi_{1-2} = 30$ deg in case of logic L (0 V, as explained in section 2.2) at the data input and $f_0 = 1$ MHz. Supposing that (3) can be rewritten to:

$$\frac{B_2}{B_1} = \tan^2\left(-\frac{\varphi_{1-2}}{2}\right), \quad (4)$$

and considering (1), we have two possibilities of driving the commutation:

$$\frac{B_2}{B_1} = \text{const.}, \quad \frac{B_2}{B_1} = \frac{1}{\text{const.}} \quad (5), (6)$$

while product $B_1 B_2$ is always the same. Therefore, we found out that the second phase distance of V_{OUT1} and V_{OUT2} (for logic H – 5 V at the data input, as explained in section 2.2) is given by mutual dependence of B_1 and B_2 to keep their ratio directly driving FO. We can define only initial phase distance (for L). The second phase distance for H is given by mutual dependence of (1) and (3). Therefore (3) or (4) and (1) does not allow to select the second phase distance, i.e. product of B_1 and B_2 has to be the same in both cases of phase shift commutation to obtain unchangeable FO. The first value of B_1 can be calculated (by substitution of (1) and (4)) as:

$$B_1 = \frac{2\pi f_0 \sqrt{R_1 R_2 C_1 C_2}}{\tan\left(-\frac{\varphi_{1-2}}{2}\right)} \Bigg|_{\substack{R_1=R_2=R \\ C_1=C_2=C}} = \frac{2\pi f_0 RC}{\tan\left(-\frac{\varphi_{1-2}}{2}\right)}. \quad (7)$$

Numerical calculation yields $B_1 = 2.91$ for $\varphi_{1-2} = 30$ deg. Due to nonlinear dependence of B on V_{SETB} [20] above 2 V, V_{SETB1} must be 3.4 V in this case. The second gain/DC voltage can be expressed from (4) as $B_2 = 0.21$ ($V_{SETB2} = 0.21$ V). So, we obtained two sets (pairs) of values $B_1 = 2.91$ ($V_{SETB1} = 3.4$ V), $B_2 = 0.21$ ($V_{SETB2} = 0.21$ V) for L (data) and $B_1 = 0.21$ ($V_{SETB1} = 0.21$ V), $B_2 = 2.91$ ($V_{SETB2} = 3.4$ V) for H from (5) and (6). The phase distance of V_{OUT1} and V_{OUT2} in the H is 150 deg.

2.2. Control Logic – Converter of data symbols to DC control voltage

Due to the requirements on the oscillator and AP blocks of the structure to obtain phase shift commutation, we have to ensure two driving signals for control of the current gains $B_{1,2}$ where two specific values (levels) are available. In other words, our task is to design a controlling logic part or “data to voltage converter” with two outputs, where commutation of two V_{SETB} (0.21 V and 3.4 V) in dependence on the state of input signal (L or H) is possible. Therefore, we designed system shown in **Fig. 3**. The presented solution contains two sections/channels (for V_{SETB1} and V_{SETB2}). The first part of each channel is a comparator part where input modulation signal (data) is compared with reference level 1.5 V (to decide whether input signal is logic 0 or 1, i.e. 0 V or 5 V). In case that input level has character of log. 0, one comparator from the pair has output in high state (saturation – $V_{sat_LM239} = 4.85$ V) and the second in low state (0 V). These results are evaluated by adder/subtractor

based on simple opamp. The amplification/attenuation is set by resistors to ensure the appropriate result of subtraction (0.21 V for L and 3.4 V for H). Therefore, DC voltage of the reference level referencing the both subtraction stages is -4.85 V.

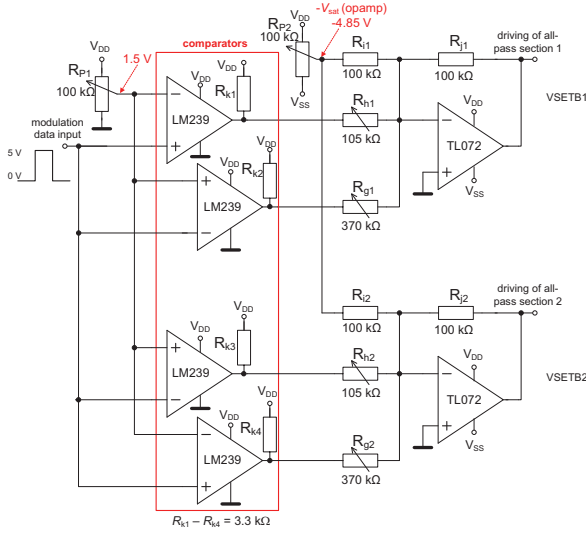


Fig. 3. Designed converter of data symbols to DC control voltage

Based on this, we can calculate values of resistors (resistors $R_{i1} = R_{j1}$ in the direct path with inverting unity gain were selected as 100 kΩ) of the subtractor as:

$$R_{g1} = \frac{R_{j1}}{\left(1 - \frac{V_{SETB1_L}}{V_{sat_LM239}}\right)}, \quad R_{h1} = \frac{R_{j1}}{\left(1 - \frac{V_{SETB1_H}}{V_{sat_LM239}}\right)}, \quad (8), (9)$$

that yields $R_{g1} = 334$ kΩ (for $V_{SETB1_L} = 0.21$ V) and $R_{h1} = 105$ kΩ (for $V_{SETB1_H} = 3.4$ V). Value 334 kΩ was modified to 370 kΩ for correct setting of $V_{SETB1_L} = 0.21$ V in simulations. The second section employs the same values ($R_{h2} = R_{h1}$ and $R_{g2} = R_{g1}$) but their timing is inverted, i.e. while L causes $V_{SETB1} = 0.21$ V, V_{SETB2} has value 3.4 V and in the case of H V_{SETB1} is 3.4 V and $V_{SETB2} = 0.21$ V. Simple modification of R_g , R_h values allows to set up output levels of V_{SETB} quite simply.

2.3. Automatic Amplitude Gain Control Circuit

Practical implementation of each oscillator working in low and middle frequency bands (except GHz band where different principles are used) requires proposal of amplitude automatic gain control circuit (AGC). We implemented simple structure based on the diode doubler (envelope detector) and two simple opamps in **Fig. 4**. DC constant value 1.1 V represents DC voltage for control of CO ($V_{SETA} = -1.1$ V in **Fig. 2**). Output oscillations (at AGC input) are transformed to dynamically (slowly) changing DC voltage signal from rectifier (doubler) and this signal is amplified/attenuated by inverting amplifier and summed with DC constant 1.1 V. Therefore, AGC responses on signal amplitude change by appropriate increase or decrease of the DC control voltage (V_{SETA}) for VA in **Fig. 2**.

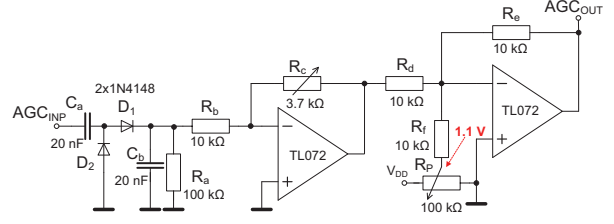


Fig. 4. Automatic amplitude gain control circuit (AGC)

3. Results of Simulations

We verified function of the modulator system in transient responses where digital input data (symbols) with frequency 10 kHz, level 0 V (L) or 5 V (H) and duty cycle 50% are directly driving the phase shift distance of both output signals (V_{OUT1} , V_{OUT2}), **Fig. 5**. It also includes both driving signals from “converter of data to control voltage” used for setting of B_1 (V_{SETB1}) and B_2 (V_{SETB2}). The last result of our simulation is transient response at the both outputs of the oscillator (V_{OUT1} , V_{OUT2}). All these results are shown for FO equal to 1.055 MHz (simulated) in **Fig. 5**. The detail on edge of the driving signal (data) to see the reaction of the oscillator on change of the phase distance is given in **Fig. 6**.

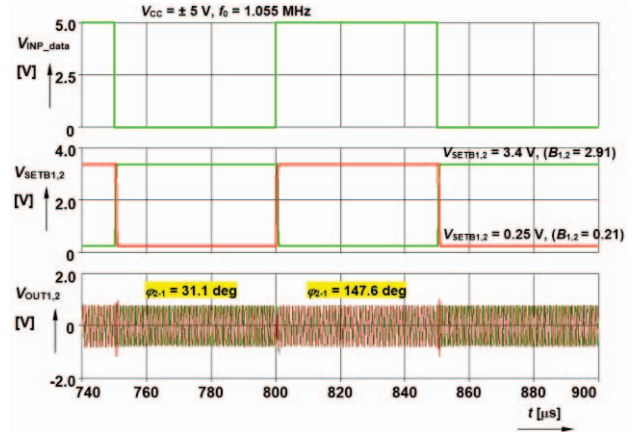


Fig. 5. Transient response of the modulator system on the data input – phase distance commutation

Response seems to be a little bit delayed ($0.5 \mu\text{s}$) due to the delay of the rising and falling edges of the voltages V_{SETB1} and V_{SETB2} from converter part (simple opamps with low slew rate were used in the converter in this particular solution). Stabilization of the level and waveforms takes about $1.5 \mu\text{s}$. FFT spectrum of the output responses (V_{OUT1} , V_{OUT2}) with modulation (**Fig. 6**) is shown in **Fig. 7**. **Figure 8** documents spectrum of the signals without modulation. It is clear and expected that modulation causes worse phase noise features (energy is spread to wider bandwidth), as obvious from the comparison of **Fig. 7** and **Fig. 8**. Spectral purity of the output responses (**Fig. 8**) is very high. Note that values of Y-axis in **Fig. 7** and **Fig. 8** are in dBV ($20\log_{10}(V_{OUT1,2}/1 \text{ V})$). Suppression of higher harmonic components is more than 60 dBc that yields total harmonic distortion below 0.1 %.

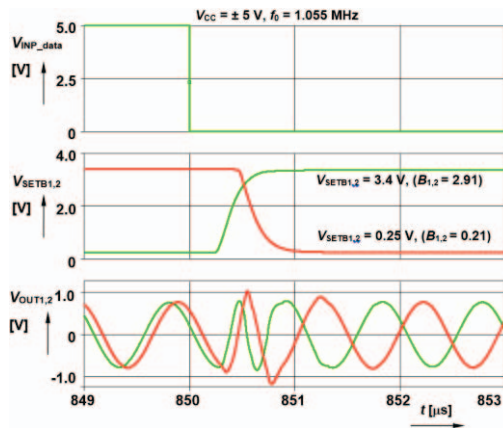


Fig. 6. Detail on the transient effect near to falling edge of the driving signal (data) – phase distance commutation

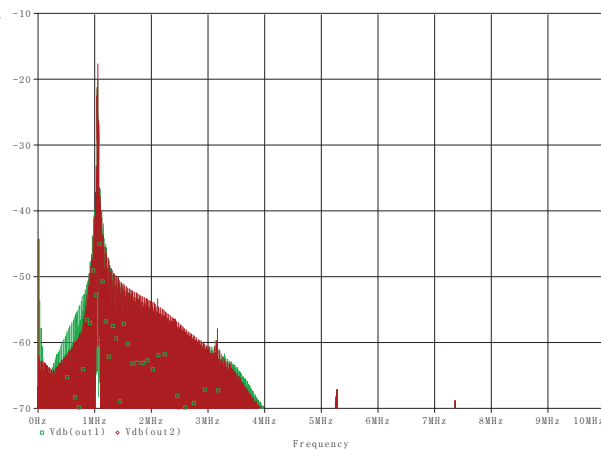


Fig. 7. FFT spectrum of the output signals (VOUT1, VOUT2) under condition of modulation

6. Conclusions

Our work shows how to utilize the interesting oscillator with adjustability of the phase distance between produced signals in the digital phase shift keying modulator. All required construction counterparts were carefully and detailed discussed. Design of the phase commutation was provided for the initial ideal phase shift 30 degrees for input state L and the frequency of oscillation equal to 1 MHz. The second ideal phase shift is 150 degrees in opposite state (assumed for H). The simulations verified and confirmed expected behavior at 1.055 MHz. with two available phase shifts 31.1 and 147.6 degrees. Thus, our verifications confirmed expected behavior of the system. The system has some limitations: the second phase shift (for H) cannot be selected arbitrarily; inaccurate setting (commutation of control levels) may cause parasitic change of FO. These issues are the main aim of our further research and analyses as well as establishment of the experimental verification in order to prove the workability of the design in lab environment.

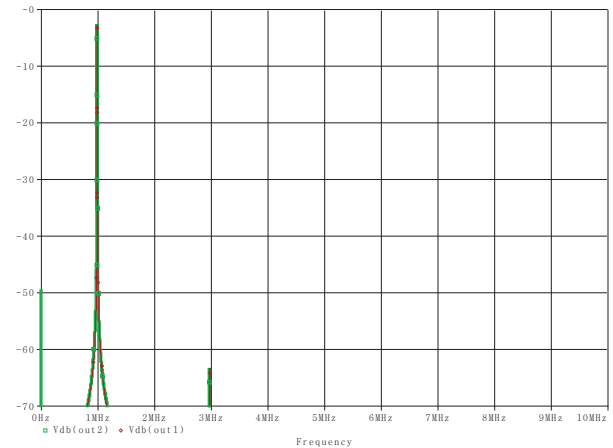


Fig. 8. FFT spectrum of the output signals (VOUT1, VOUT2) without modulation

7. Acknowledgement

Research described in this paper was financed by Czech Ministry of Education in frame of National Sustainability Program under grant LO1401. For research, infrastructure of the SIX Center was used. Research described in the paper was supported by Czech Science Foundation project under No. 14-24186P. Grant No. FEKT-S-14-2281 also supported this research. The support of the project CZ.1.07/2.3.00/20.0007 WICOMT, financed from the operational program Education for competitiveness, is gratefully acknowledged.

8. References

- [1] A. U. Keskin, D. Bielek, "Current mode quadrature oscillator using current differencing transconductance amplifiers (CDTA)", *IEE Proc. Circuits Devices and Systems*, vol. 153, no. 3, pp. 214-218, 2006.
- [2] G. Souliotis, C. Psychalinos, "Electronically controlled multiphase sinusoidal oscillators using current amplifiers", *International Journal of Circuit Theory and Applications*, vol. 37, no. 1, pp. 43-52, 2009.
- [3] W. Tangsrirat, W. Tanjaroen, T. Pukkalanun, "Current-mode multiphase sinusoidal oscillators using CDTA-based allpass sections", *AEU – International Journal of Electronics and Communications*, vol. 63, no. 7, pp. 616-622, 2009.
- [4] M. Kumngern, J. Chanwutium, K. Dejhan, "Electronically tunable multiphase sinusoidal oscillator using translinear current conveyors", *Analog Integrated Circuits and Signal Processing*, vol. 65, no. 2, pp. 327-334, 2010.
- [5] W. Jaikla, P. Promee, "Electronically Tunable Current-mode Multiphase Sinusoidal Oscillator Employing CCCDTA-based Allpass Filters with Only Grounded Passive Elements", *Radioengineering*, vol. 20, no. 3, pp. 594-599, 2011.
- [6] S-H. Tu, Y-S. Hwang, J-J. Chen, A. M. Soliman, C-M. Chang, "OTA-C arbitrary-phase-shift oscillators", *IEEE Transactions on Instrumentation and Measurement*, vol. 61, no. 8, pp. 2305-2319, 2012.

- [7] M. Sagbas, U. E. Ayten, N. Herensar, S. Minaei, "Current and Voltage Mode Multiphase Sinusoidal Oscillators Using CBTAs", *Radioengineering*, vol. 22, no. 1, pp. 24-33, 2013.
- [8] R. Sotner, J. Jerabek, N. Herencsar, "Voltage Differencing Buffered/Inverted Amplifiers and Their Applications for Signal Generation", *Radioengineering*, vol. 22, no. 2, pp. 490-504, 2013.
- [9] R. Sotner, J. Jerabek, N. Herencsar, K. Vrba, T. Dostal, "Features of multi-loop structures with OTAs and adjustable current amplifier for second-order multiphase/quadrature oscillators", *AEU – International Journal of Electronics and Communications*, vol. 69, no. 5, pp. 814-822, 2015.
- [10] S. Ozoguz, T. M. Abdelrahman, A. S. Elwakil, "Novel Approximate Square-Root Domain All-Pass Filter with Application to Multiphase Oscillators", *Analog Integrated Circuits and Signal Processing*, vol. 46, no. 3, pp. 297-301, 2006.
- [11] B. Maundy, A. Elwakil, S. Gift, "On the Realization of Multiphase Oscillators Using Fractional-Order Allpass Filters", *Circuits Systems and Signal Processing*, vol. 31, no. 1, pp. 3-17, 2012.
- [12] P. Promee, N. Wongprommoon, "Log-domain All-pass Filter-based Multiphase Sinusoidal Oscillators", *Radioengineering*, vol. 22, no. 1, pp. 14-23, 2013.
- [13] D. Frey, "Log-domain filtering: An approach to current-mode filtering", *IEE part-G*, vol. 140, no. 6, pp. 406-416, 1993.
- [14] R. Sotner, J. Jerabek, J. Petrzela, R. Prokop, K. Vrba, A. Kartci, T. Dostal, "Quadrature Oscillator Solution Suitable with Arbitrary and Electronically Adjustable Phase Shift", in *proc. of IEEE International Symposium on Circuits and Systems 2015*, Lisbon, Portugal, 2015, pp. 3056-3059.
- [15] A. U. Keskin, K. Pal, E. Hancioglu, "Resistorless first-order filter with electronic tuning", *AEU - International Journal of Electronics and Communications*, vol. 62, no. 4, pp. 304-306, 2008.
- [16] J. Bajer, D. Biolek, "Voltage-mode electronically tunable all-pass filter employing CCCII+, one capacitor and differential-input voltage buffer", in *Proceedings of 26th IEEE Convention of Electrical and Electronics Engineers in Israel (IEEEI2010)*, Eliat, Israel, 2010, pp. 934-937.
- [17] VCA610: Wideband voltage controlled amplifier, Texas Instruments [online]. 2000, last modified 11/2000. URL: <http://www.ti.com/lit/ds/symlink/vca610.pdf>
- [18] W. Surakamponporn, W. Thitimajshima, "Integrable electronically tunable current conveyors", *IEE Proceedings-G*, vol. 135, no. 2, pp. 71-77, 1988.
- [19] A. Fabre, N. Mimeche, "Class A/AB second-generation current conveyor with controlled current gain", *Electronics Letters*, vol. 30, no. 16, pp. 1267-1268, 1994.
- [20] Intersil (Elantec). EL2082 CN Current-mode multiplier (datasheet), 1996, 14 p., accessible on [www.intersil.com](http://www.intersil.com/data/fn/fn7152.pdf)
- [21] OPA660: Wide Bandwidth Operational Transconductance Amplifier and Buffer, Texas Instruments [online], 1995, last modified 9/2000 [cit.22.10.2012]. available at URL: <http://www.ti.com/lit/ds/symlink/opa660.pdf>
- [22] AD830: High Speed, Video Difference Amplifier, Analog Devices [online], 2003, last modified 1/2003. URL: http://www.analog.com/static/imported-files/data_sheets/AD830.pdf

[20] KARTCI, A., SOTNER, R., JERABEK, J., HERENC SAR, N., PETRZELA, J. Phase shift keying modulator design employing electronically controllable all- pass sections. *Analog Integrated Circuits and Signal Processing*, 2016, online first (in press), p. 1-20. ISSN: 0925-1030.

Phase shift keying modulator design employing electronically controllable all-pass sections

Aslihan Kartci¹ · Roman Sotner¹ · Jan Jerabek² · Norbert Herencsar² · Jiri Petrzela¹

Received: 1 March 2016/Revised: 19 May 2016/Accepted: 23 May 2016
© Springer Science+Business Media New York 2016

Abstract This paper presents two techniques of implementation of phase shift keying modulator. Both techniques are focused on the utilization of special features of an oscillator, which is based on first-order all-pass filters. The first method leads to modulators having generated signals with arbitrary phase shift between two outputs using only special features of oscillators in order to use less number of components in the structure. The second approach utilizes the same oscillator and also additional all-pass filter that increases the complexity of the circuitry, but eliminates requirements for extra-complicated driving circuit (control logic) and removes some undesired aspects of the first solution. The related circuits and subsystems are discussed in detail. Finally, features of all proposed

structures are verified via PSpice using TSMC 0.18 um CMOS technology parameters and also by laboratory experiments with commercially available active devices. The experimental results agree both with simulation and theoretical analysis.

Keywords Phase shift keying · Modulation · All-pass filter · Electronic control · Operational transconductance amplifier · Electronically controllable second generation current conveyor

1 Introduction

Analog circuits used for signal generation are very important in practice. Simple sinusoidal oscillators are highly required in many areas of applied circuit theory. Multiphase sinusoidal oscillators (MSOs) are specific types of these systems. They are useful in areas of instrumentation applications, in wireless transceivers, direct conversion transmitters (mixers), frequency synthesizers, switched-capacitor filters, measurement purposes (selective voltmeters), even in the study of biological systems and many others [1]. Generally, MSO is a circuit providing simultaneously more than one output, each having generated sine waveform with different phase shift. They are determined mainly for applications in modern digital multi-state modulations and demodulations (quadrature phase shift keying—QPSK for example) as source of carrier signal (coherent cosine and sine wave components). Therefore, MSOs represent an important unit in these general engineering areas [2].

Typical examples of the multiphase sinusoidal oscillators can be found in [3–8] for instance. Quadrature oscillators ([9] for example) belongs to group of MSO

A preliminary version of this paper has been presented at the 9th International Conference on Electrical and Electronics Engineering—ELECO 2015 [29].

✉ Roman Sotner
sotner@feec.vutbr.cz

Aslihan Kartci
aslhankartc@gmail.com

Jan Jerabek
jerabekj@feec.vutbr.cz

Norbert Herencsar
herencsn@feec.vutbr.cz

Jiri Petrzela
petrzelj@feec.vutbr.cz

¹ Department of Radio Electronics, Faculty of Electrical Engineering and Communication, Brno University of Technology, Technicka 3082/12, Brno, Czech Republic

² Department of Telecommunications, Faculty of Electrical Engineering and Communication, Brno University of Technology, Technicka 3082/12, Brno, Czech Republic

systems offering generally two outputs with $\pi/2$ phase shift. Principles of operation of known solutions can be divided to the following groups: (a) lossy blocks (integrators or similar selective sections) in stepwise phase shifted cascade and full feedback (for example [3–8] and references cited therein); (b) all-pass filters (APFs) in combination with integrators/differentiators in simple loops ([9, 10] for example); (c) APFs in the loop ([11–14] for example); (d) two APFs and inverting [15, 16] or non-inverting amplifier [17]; and (e) other principles (see [17–19] for detailed discussion).

Moreover, there were introduced few multiphase oscillators implementing some other approaches [17–19]. Maundy et al. [17] constructed multiphase oscillator using fractional-order all-pass filters. The transfer function of this filter has fractional exponent α as Laplace operator s , where the fractional character is given by approximation of fractional capacitor using RC emulator. This feature allows synthesis of the multiphase oscillators with theoretically arbitrary phase shifts between generated signals and obtaining much higher oscillation frequencies when the oscillation frequency is proportional to reciprocal time constant exponentiated by $1/\alpha$. Unfortunately, the fractional-order capacitor limits real utilization of fractional-order-based circuits in systems for signal generation and processing due to unavailability of simple electronic adjusting. There are still many open issues to be solved in the future and also different interesting approaches. For example, Ozoguz et al. [18] proposed approximate square-root domain all-pass filter to construct multiphase oscillator. Promee and Wongprommoon [19] used log-domain approach [20] for multiphase generation, which reduce complexity of all-pass filter and it has better dynamics of linear operation, and wider tunability of oscillation frequency.

Discussed approaches for multiphase solutions (explained in [7]) allow the design of oscillator with arbitrary phase shifts between outputs. However, in the most cases there is minimal (integer value) available phase step such as $\pi/6$, $\pi/4$, $\pi/3$, or $\pi/2$. Additional multiples of the phase shift can be done by auxiliary blocks (integrators, differentiators in loop(s)) and appropriate feedbacks. Requirements on arbitrary setting of the phase shift between produced signals are not solved very often directly in second-order oscillator structures. Not many structures that allow this feature have been presented in the open literature [12, 15, 16]. However, to the best of authors' knowledge, the possibility of arbitrary setting of phase shift was not the main goal of researchers in the past. Brief comparison of these solutions (representing topology based on two all-pass filters and inverting amplifier in one loop) is provided in Table 1.

Selected solutions of typical MSO concepts published in recent literature can be (after several minor modifications) used for design of similar oscillator structure as used in this paper. Therefore it is worth to discuss their benefits for such type of synthesis. Tangsrirat et al. [5] published MSO based on APFs (with two controllable current differencing transconductance amplifiers—CDTAs and floating capacitor). Similarly structure presented by Gift et al. [11] may create suitable oscillator with arbitrary phase shift setting (2 APFs based on opamps and many passive elements). Unfortunately, control of oscillation frequency and phase shift is possible only through values of passive elements. Keskin et al. [12] uses only two APs based on CDTAs to create quadrature oscillator that can be modified to generate arbitrary phase shifts. Similarly, Jaikla et al. [13] employs APFs (based also on CDTAs) in chain/loop of blocks creating MSO. However, controllability is limited with the values of passive elements only. Modification of active device and AP section allows electronic control by intrinsic resistance of low impedance input terminal(s) (see [14]). Table 1 includes only solutions representing the same block topology as we are beneficially using also in this study [15, 16] and also structure reported in [12], because it offers theoretical possibility to fulfill requirements for electronically settable arbitrary setting of phase shift.

This paper is divided as follows: In the introduction section, we discuss the issues regarding to arbitrary phase shift difference between generated waveforms in multiphase oscillators, features of the latest, attractive multiphase solutions, and few special approaches. A possible topology of MSO based on all-pass filters as a special application of configuration of arbitrary phase shift is presented in Sect. 2. Beside this, the main feature of the proposed simple second-order oscillator with theoretically arbitrary phase shift of two generated signals is implemented in phase shift keying modulator and related subsystems are also discussed together with simulations and experimental results. The performances of oscillator are tested both in quadrature and arbitrary mode. In Sect. 3, we present alternative solution based on more common concept (oscillator and all-pass filter) including its simulation and experimental results. Finally, the main features are summarized and both designed solution are compared in conclusion (Sect. 4).

2 General concept of the oscillator based on two-all-pass sections and inverting amplifier in the loop

The first idea of electronically adjustable phase shift in the oscillator structure was presented in [21] and is based on two APFs and electronically controllable inverting variable

Table 1 Comparison of electronically controllable oscillators providing two outputs having features for arbitrary phase shift between them based on two all-pass filters and inverting amplifier in one loop

Features of sub-building APFs					Features of oscillator				
Solution	Type of active element	Floating C	Number of active/passive (R + C) elements	Parameter(s) for control	Overall number of active and passive elements	Arbitrary phase shift available/ tested	Tested phase shifts (°)	Linear/electronic control of FO	Type of output signal (current/voltage)
[12]	CDTA	Yes	1/2 + 1	passive/ R_x	2/6	Yes/no	N/A	Yes	Current
[15]	OTA	Yes	3/0 + 1	g_m	7/3	Yes/no	N/A	Yes	Voltage
[16]	DDCC	No	2/0 + 1	R_x	5/2	Yes/no	N/A	Yes	Voltage
[25]	ICDBA	Yes	1/0 + 1	$2x R_x$	N/A	N/A	N/A	N/A	N/A
[26]	DVCC	No	2/0 + 1	R_x	N/A	N/A	N/A	N/A	N/A
[27]	FDCCII	No	1/1 + 1	Passive R	N/A	N/A	N/A	N/A	N/A
[28]	DXCCII	No	1/2 + 2 1/3 + 1	Passive R	N/A	N/A	N/A	N/A	N/A
<i>Proposed</i>									
Figure 1	DVB, OTA	No	2/0 + 1	g_m	5/3	Yes/yes	-23 to -151 [21]	Yes	Voltage
Figure 8	DVB, ECCII	No	2/1 + 1	B	5/4	Yes/yes	-17 to -141	Yes	Voltage

CDTA current differencing transconductance amplifier, OTA operational transconductance amplifier, DDCC differential difference current conveyor, DVCC differential voltage current conveyor, FDCCII fully differential current conveyor, DXCCII dual-X second generation current conveyor, ICDBA inverting current differencing buffered amplifier, DVB differential voltage buffer, ECCII electronically controllable second generation current conveyor, R_x resistance of current input terminal, g_m transconductance, B controllable current gain

gain voltage amplifier implemented in CMOS technology. Each of all-pass sections [22, 23] utilizes operational transconductance amplifier (OTA) [24], and differential voltage buffer (DVB). Similarly as in our approach, many recent works are indicated possible design of all-pass sections utilizing intentional voltage [25–28] or current input difference [28] in frame of active device of its sub-part. However, some of them does not allow electronic tunability directly [27, 28]. To do it, the replacements of elements that are not controllable electronically are

necessary [27]. These solution are also added to Table 1 for qualitative comparison.

The first solution of the oscillator based on OTAs and DVBs that is shown in Fig. 1 was derived from solution presented in [21] (similar concept used also in [29]). The circuit is divided to three parts in the loop: APF₁ with transfer K_{APF1} , APF₂ with transfer K_{APF2} , and inverting amplifier allowing gain control ($-K$). This type of the oscillator is analyzed for fulfilments of Barkhausen criterion [30–33]. The relation between them is:

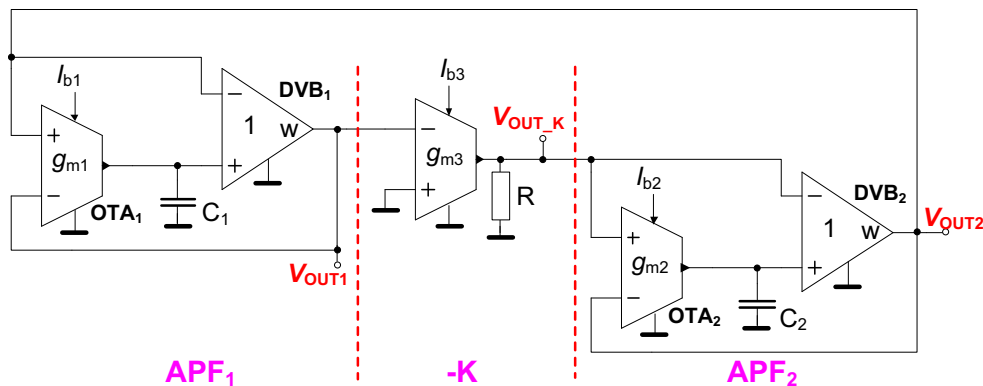


Fig. 1 Oscillator based on two all-pass sections and inverting amplifier in the loop [21]

$$G(s) = K_{APF1}(s)(-K)K_{APF2}(s) = 1, \tag{1}$$

$$\phi_{APF1} + \phi_{APF2} + \phi_K = 2\pi k, \quad k = 1, 2, \dots, \tag{2}$$

where ϕ_i for $i \in \{APF_1, APF_2, K\}$ are partial phase shifts of blocks in the loop. It is clear that combination of $\phi_{APF1} + \phi_{APF2} = \pi$ (180°). If the condition of oscillations (CO) is fulfilled (the gain of inverting amplifier is equal to 1), the following expression can be given:

$$\begin{aligned} & -K \left(\frac{g_{m1} - sC_1}{g_{m1} + sC_1} \right) \left(\frac{g_{m2} - sC_2}{g_{m2} + sC_2} \right) \\ &= - \frac{s^2 - \left(\frac{C_1 g_{m2} + C_2 g_{m1}}{C_1 C_2} \right) s + \frac{g_{m1} g_{m2}}{C_1 C_2}}{s^2 + \left(\frac{C_1 g_{m2} + C_2 g_{m1}}{C_1 C_2} \right) s + \frac{g_{m1} g_{m2}}{C_1 C_2}} = 1. \end{aligned} \tag{3}$$

The transfers of both APFs have typical forms:

$$\begin{aligned} K_{APF1}(s) &= \frac{g_{m1} - sC_1}{g_{m1} + sC_1} \\ &= \frac{\sqrt{g_{m1}^2 + (\omega_0 C_1)^2} \exp \left[\tan^{-1} \left(-\frac{\omega_0 C_1}{g_{m1}} \right) j \right]}{\sqrt{g_{m1}^2 + (\omega_0 C_1)^2} \exp \left[\tan^{-1} \left(\frac{\omega_0 C_1}{g_{m1}} \right) j \right]} \\ &= 1 \cdot \exp \left[-2 \tan^{-1} \left(\frac{\omega_0 C_1}{g_{m1}} \right) j \right], \end{aligned} \tag{4}$$

$$\begin{aligned} K_{APF2}(s) &= \frac{g_{m2} - sC_2}{g_{m2} + sC_2} \\ &= 1 \cdot \exp \left[-2 \tan^{-1} \left(\frac{\omega_0 C_2}{g_{m2}} \right) j \right]. \end{aligned} \tag{5}$$

Hence, the gain and phase are:

$$|K_{APF1}| = 1, \tag{6}$$

$$\phi_{APF1} = -2 \tan^{-1} \left(\frac{\omega_0 C_1}{g_{m1}} \right), \tag{7}$$

and analogically valid for the APF2. Frequency of oscillation (FO) of the circuit in Fig. 1 has the following common form:

$$\omega_0 = \sqrt{\frac{g_{m1} g_{m2}}{C_1 C_2}}. \tag{8}$$

Substitution of (8) to (7) results in phase shift at oscillation frequency expressed as:

$$\phi_{APF1} = -2 \tan^{-1} \left(\sqrt{\frac{g_{m2} C_1}{g_{m1} C_2}} \right) \frac{180}{\pi}, \tag{9}$$

and

$$\phi_{APF2} = -2 \tan^{-1} \left(\sqrt{\frac{g_{m1} C_2}{g_{m2} C_1}} \right) \frac{180}{\pi}. \tag{10}$$

Inverting variable gain of voltage amplifier is created by OTA (g_{m3}) and resistance R ($-K = g_{m3}R$). This design

allows very simple utilization of the circuit for amplitude stabilization (automatic gain control circuit—AGC) as will be shown later.

2.1 Design of parameters for arbitrary phase shift setting

Considering (9) and (10) and $\phi_{APF1} = 180 - \phi_{APF2} = \phi_{OUT1-2}$, we can express relation between target phase shift and parameters of the circuit elements required for design. Modification of (9) leads to:

$$\left[\tan \left(-\frac{\phi_{OUT1-2}}{2} \right) \right]^2 = \frac{g_{m2} C_1}{g_{m1} C_2}. \tag{11}$$

Taking into account equality of both capacitors $C_1 = C_2 = C$, (11) can be modified to:

$$g_{m2} = g_{m1} \left[\tan \left(-\frac{\phi_{OUT1-2}}{2} \right) \right]^2, \tag{12}$$

and by substituting (8)–(12) is rewritten to:

$$g_{m2} = \tan \left(-\frac{\phi_{OUT1-2}}{2} \right) \omega_0 C. \tag{13}$$

Equation (9) or (10), i.e. phase shift as the function of ratio of g_{m1} and g_{m2} is illustrated in Fig. 2. The trace is close to both corners (0° and 180°) only theoretically for very large ratio of both parameters that is practically not available. The limitations are caused by practical restriction of available range of g_m values. However, possibility of arbitrary adjustable phase shift (given by ratio g_{m1} and g_{m2}) between produced sine waveforms is evident. Using common types of OTAs, we practically cannot ensure ratios of g_{m1} and g_{m2} larger than 1/20 or 20. If $g_{m1} = g_{m2}$ is simultaneously changed, i.e. $g_{m1}/g_{m2} = 1$, this type of

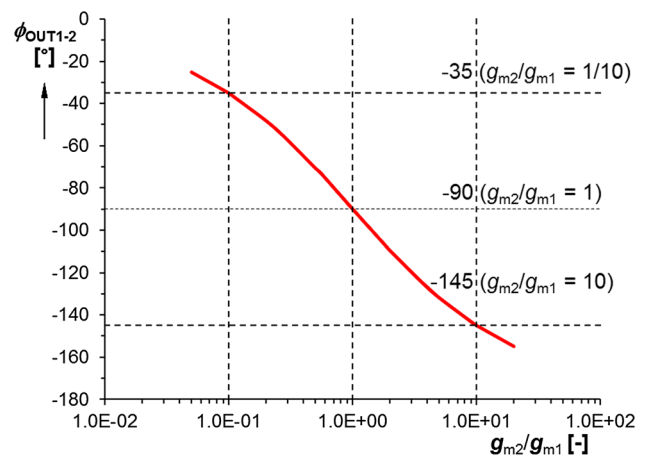


Fig. 2 Theoretical dependence of phase shift of APFs (ϕ_{OUT1-2}) on g_{m1} and g_{m2} ratio in case of oscillator shown in Fig. 1

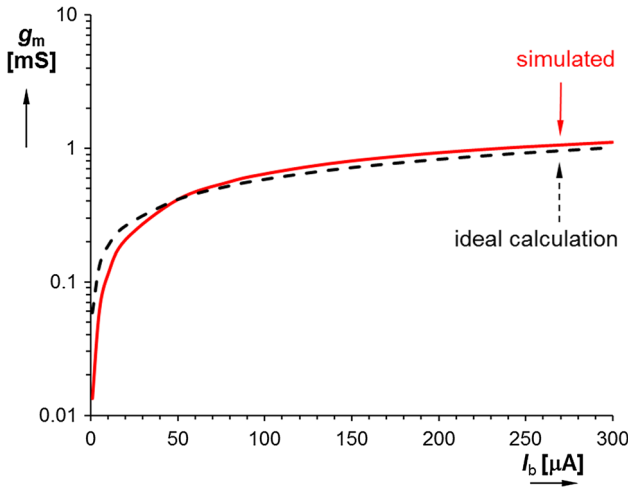


Fig. 3 Dependence of g_m on bias current for CMOS OTA reported in [21]

oscillator operates in quadrature mode, as obvious from Fig. 2.

Internal CMOS structures of active devices OTA and DVB are discussed in detail in [21]. We have availability of g_m setting from $10 \mu\text{S}$ to 1.1 mS controlled by bias current adjusted in range from 1 to $300 \mu\text{A}$ (see Fig. 3). General circuit including also amplitude stabilization part is shown in Fig. 4. AGC circuit employs voltage amplifier (VA), diode detector and unipolar transistor working as adjustable resistor. Its system operates as variable resistor in parallel with the resistor in inverting amplifier (set by $g_{m3} = 500 \mu\text{S}$ for $I_{b\text{APF}} = 66 \mu\text{A}$ and $R = 10 \text{ k}\Omega$) driven from output signal.

3 Application of the oscillator in phase shift keying modulator: the first solution

The arbitrarily adjustable phase shift between generated signals in this type of the oscillator was explained in detail in [21]. Above discussed setting of the quadrature oscillator (itself) cannot be used for purposes of modulation with alternating phase shift. Based on (8) and Fig. 2, we can see that two different phase shifts appear for two different g_{m2}/g_{m1} , but FO has still the same value. This feature is useful for modulation purposes. The initial phase shift of generated waveforms (if $C_1 = C_2 = C$) can be chosen to obtain values for the first state based on (13) and (8). In this case, the second parameter g_{m1} can be calculated from (8). The design example has been chosen as: $f_0 = 1 \text{ MHz}$, $\phi_{\text{OUT1-2}} = -50^\circ$, $C_1 = C_2 = C = 47 \text{ pF}$, $R = 10 \text{ k}\Omega$. Power supply voltage is $\pm 0.9 \text{ V}$. The parameters are found as:

$$g_{m2}(-50^\circ) = \tan\left(-\frac{\phi_{\text{OUT1-2}}}{2}\right)\omega_0 C$$

$$= \tan\left(-\left(\frac{-50}{2}\right)\right)2\pi \cdot 1 \cdot 10^6 \cdot 47 \cdot 10^{-12} = 138 \mu\text{S},$$
(14)

$$g_{m1} = \frac{(\omega_0 C)^2}{g_{m2}} = \frac{(2\pi \cdot 1 \cdot 10^6 \cdot 47 \cdot 10^{-12})^2}{138 \cdot 10^{-6}} = 632 \mu\text{S}.$$
(15)

Driving bias currents are approximately $I_{b1} = 100 \mu\text{A}$ ($g_{m1} = 632 \mu\text{S}$) and $I_{b2} = 18 \mu\text{A}$ ($g_{m2} = 138 \mu\text{S}$). Phase shift $\phi_{\text{OUT1-2}} = -50^\circ$ is valid for $g_{m2} = 138 \mu\text{S}$ and $g_{m1} = 638 \mu\text{S}$ ($g_{m1}/g_{m2} \cong 1/5$). The second state occurs if

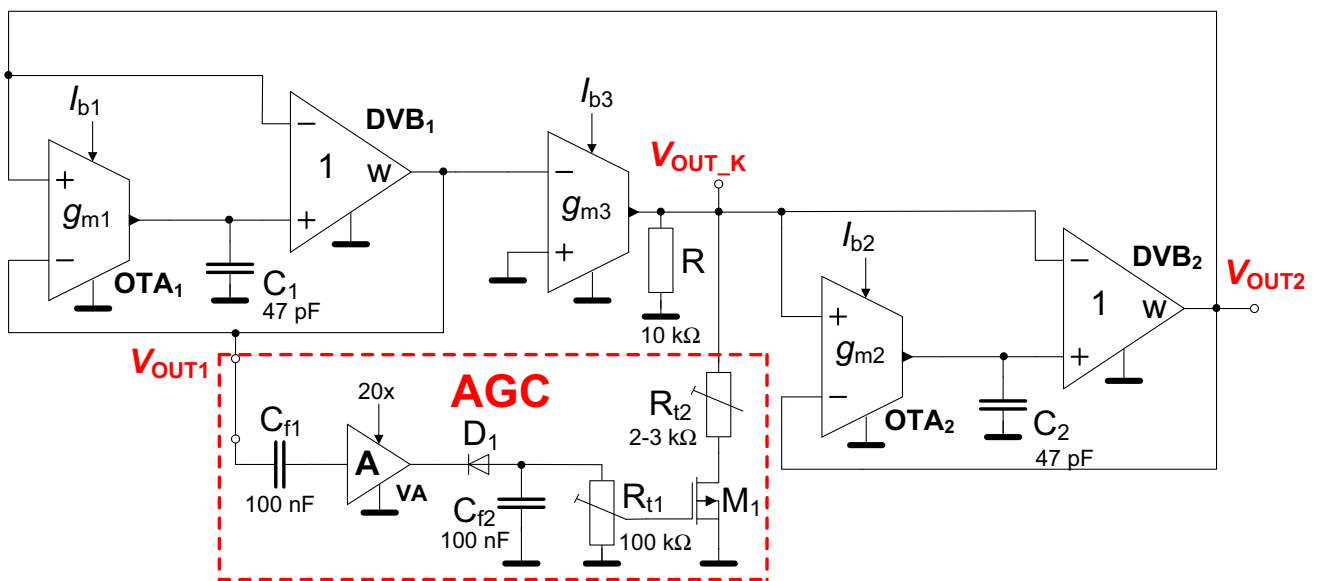


Fig. 4 Final structure of first oscillator including AGC circuit for amplitude stabilization

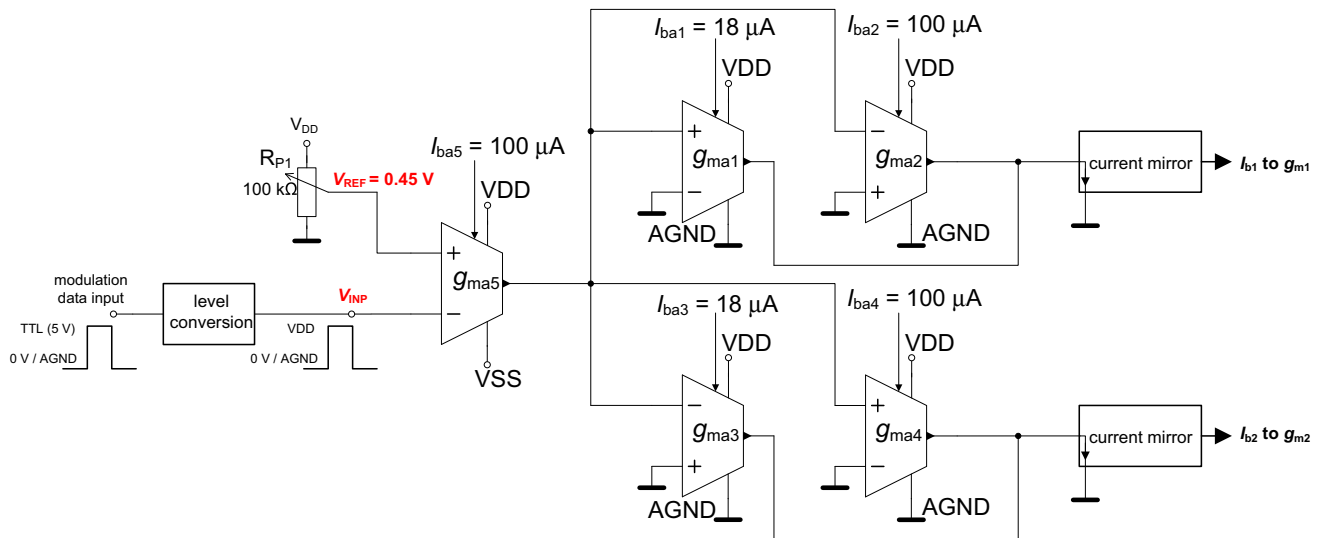


Fig. 5 Converter of digital data to bias driving currents for OTAs in the oscillator (control logic)

g_m ratio is opposite: $g_{m1}/g_{m2} = 632/138 \cong 5$, hence phase shift is calculated from (9) or (10) as -130° .

The transconductance ratio must be switched correctly in order to ensure proper conversion of digital data symbols (TTL logic 0 for L and 5 V for H as well) during modulation. The adequate system to convert digital data to bias current via OTAs in the oscillator is shown in Fig. 5.

Principle of the operation is as the following: Input data in TTL logic (high—5 V, low—0 V) is converted to respect maximal available voltage in the used technology (TSMC 0.18 μm in our case [34]), which is +0.9 V (maximal positive supply voltage). Then, the input data is compared in comparator based on OTA (g_{ma5}) with reference level. Output of the comparator provides high or low saturation, which means that for $V_{INP} > V_{REF}$ is output in $V_{DD} = +0.9$ V and for $V_{INP} < V_{REF}$ in $V_{SS} = -0.9$ V. In order to reach both polarities, g_{ma5} stage is supplied by both the positive and negative voltage. Bias current $I_{ba5} = 100 \mu\text{A}$ is selected appropriately for sufficiently high open-loop voltage gain (with very high impedance at the output) of the OTA, which is important in order to reach both saturation levels. On the other hand, further OTAs in this system are supplied by only single supply branch (positive V_{DD}). Logic L causes saturation of g_{ma5} to V_{DD} , while logic H turns g_{ma5} to V_{SS} . If high state (V_{DD}) occurs at the output of g_{ma5} , then g_{ma1} and g_{ma4} (fully saturated) are providing current flowing to output current mirrors. This current is equal to maximal bias I_{ba1} and I_{ba4} set in accordance to calculations of g_{m2} and g_{m1} of the oscillator from (14) and (15). Remaining OTAs (g_{ma2} , g_{ma3}) are not providing output currents, because positive input voltage (V_{DD}) at inverting inputs keeps them inactive. Situation analogically repeats vice versa when V_{SS} occurs

at the output of g_{ma5} (H at the modulation data input). This leads to effective alternation of ratio in the oscillator in order to change phase shift between produced waveforms. System serving for phase shift keying purposes based on proposed data symbol converter and oscillator is shown as block diagram in Fig. 6.

3.1 Simulation results

The proposed circuit in Fig. 6 is simulated via using PSpice with previously discussed parameters and settings. Transient domain results are shown in Fig. 7 for $f_{mod} = 10$ kHz. Due to many inaccuracies in the system, bias currents I_{b1} and I_{b2} are not exactly identical as theoretically calculated but results confirm the circuit capability of the modulator and phase shifts are 135° (from left side) and 51° in this particular case. Inaccuracy in bias currents leads to errors in both phase shifts (in comparison to theoretical calculation), and simultaneously there is also inaccuracy of FO (960 kHz was simulated). Overshoots at the moment of phase shift alternation are caused by response of AGC system due to step change of g_{m1} and g_{m2} affecting energy conditions in the oscillator, but this issue is relevant for very high speed of alternation (high value of modulation frequency f_{mod}) as well as final construction of the system and selection of proper technology.

3.2 Experimental results: detailed explanation of subparts

The proposed oscillator working as phase shift modulator is designed with commercially available devices. These devices serve for initial experiments confirming validity of

Fig. 6 Block concept of proposed phase shift modulation system

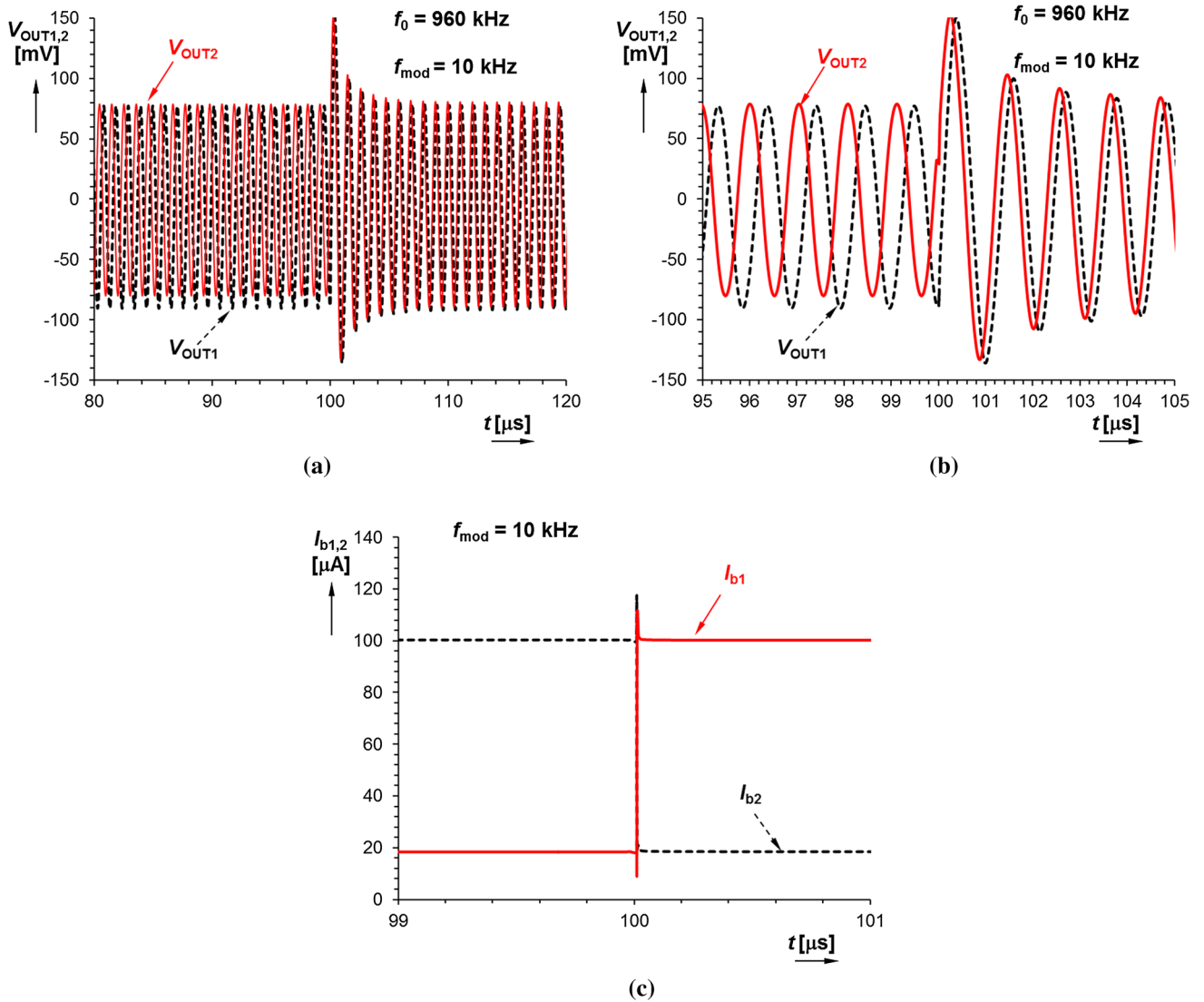
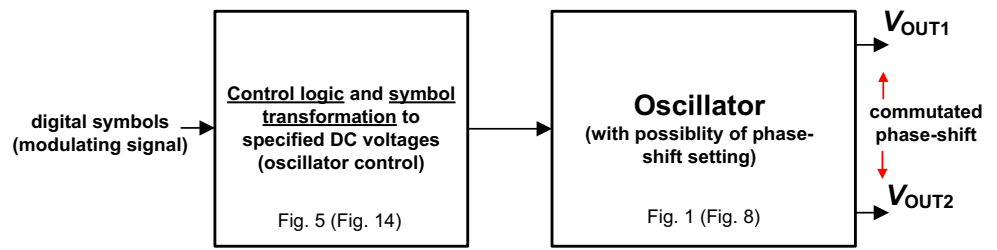


Fig. 7 Simulation results of the modulator: **a** transient response in larger scale around change of the phase shift, **b** detail on moment of the phase shift alternation, **c** driving bias currents I_{b1} and I_{b2} in moment of phase alternation

simulation results and also offer good opportunity for designers to create such type of complex system without expensive fabrication in form of integrated circuit. The verified oscillator employing commercially available active devices has been modified such that in the all-pass blocks instead of OTA elements, electronically controllable current conveyors have been used [29].

3.2.1 The oscillator realization using commercially available devices

Both APFs, used in Fig. 1, can be replaced by APFs (derived from [22, 23]) based on electronically controllable second generation current conveyor (ECCII) [35–37] providing controllable current gain (B) tuning and voltage

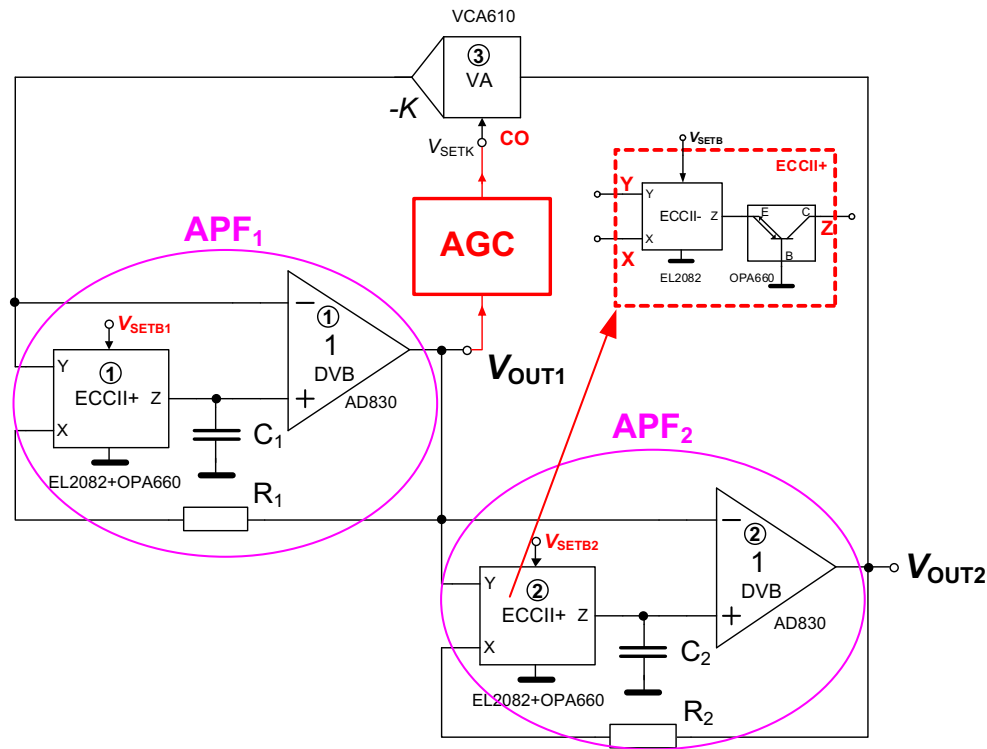


Fig. 8 Structure of the oscillator based on commercially available devices for measurement purposes [29]

amplifier (VA) with electronically controllable gain (A) in order to simplify the controllability of the oscillator (DC voltage). The oscillator structure based on commercial devices is shown in Fig. 8. It is equivalent to solution which is previously described in Fig. 1. We used current-mode multipliers EL2082 [38], diamond transistors OPA660 [39] to construct APFs including one floating resistor and variable gain amplifier VCA610 [40] to realize transfer of inverting amplifier ($-K$). The EL2082 itself represents ECCII-, therefore to create ECCII+, output inversion is required using additional current inverter based on diamond transistor, as shown in Fig. 8.

The transfer function of the single APF (for example APF₁) is:

$$K_{APF1}(s) = \frac{\frac{B_1}{R_1} - sC_1}{\frac{B_1}{R_1} + sC_1} = \frac{g_{m1} - sC_1}{g_{m2} + sC_1}, \tag{16}$$

which can be rewritten similarly as (4) to:

$$K_{APF1}(s) = \frac{\sqrt{\left(\frac{B_1}{R_1}\right)^2 + (\omega_0 C_1)^2} \exp\left[\tan^{-1}\left(-\frac{\omega_0 C_1 R_1}{B_1}\right)j\right]}{\sqrt{\left(\frac{B_1}{R_1}\right)^2 + (\omega_0 C_1)^2} \exp\left[\tan^{-1}\left(\frac{\omega_0 C_1 R_1}{B_1}\right)j\right]} = 1 \cdot \exp\left[-2 \tan^{-1}\left(\frac{\omega_0 C_1 R_1}{B_1}\right)j\right]. \tag{17}$$

It is clear that operation of APFs in Figs. 1 and 8 is identical because $g_{m1} = B_1/R_1 \cong V_{SETB1}/R_1$ and $-K = 10^{2(V_{SETK}-1)}$ [40]. Thus, we can use this behavioral representation in Fig. 8 as fully functional replacement of system in Fig. 1. Now, the equation for FO is slightly modified to:

$$\omega_0 = \sqrt{\frac{B_1 B_2}{R_1 R_2 C_1 C_2}} \cong \sqrt{\frac{V_{SETB1} V_{SETB2}}{R_1 R_2 C_1 C_2}}. \tag{18}$$

The oscillator is linearly tunable if $V_{SETB1} = V_{SETB2} = V_{SETB}$, as obvious from (18) as well as if constant ratio of V_{SETB1} and V_{SETB2} (as ratio g_{m1} and g_{m2} discussed in previous sections) remains preserved in the tuning process. Generated phase shift expressed by current gains B_1, B_2 instead of g_{m} s has the following form (supposing equality of capacitors and resistors):

$$\begin{aligned} \varphi_{OUT1-2} &= -2 \tan^{-1}\left(\sqrt{\frac{B_2 R_1 C_1}{B_1 R_2 C_2}}\right) \Big|_{\substack{R_1=R_2=R \\ C_1=C_2=C}} \\ &\cong -2 \tan^{-1}\left(\sqrt{\frac{B_2}{B_1}}\right). \end{aligned} \tag{19}$$

Note that also other parameters (R_1, R_2 especially) may serve for definition of phase shifts (ratios) and then keeping $B_1 = B_2$ and adjusting these parameters simultaneously may serve for linear FO control. This is obvious advantage with respect to solution in Fig. 1 employing OTAs, although two additional resistors are required.

3.2.2 System for amplitude stabilization

Practical implementation of each oscillator working in low and middle frequency bands (except GHz bands, where different principles are used) requires design of amplitude automatic gain control (AGC) circuit. The CMOS solution in Fig. 4 is based on control of resistance, therefore alternative solution is required. We implemented AGC structure based on the diode doubler (envelope detector) and two simple opamps shown in Fig. 9. DC constant value 1.1 V represents DC voltage for control of CO ($V_{SETK} = -1.1$ V in Fig. 8). Output oscillations (at AGC input) are transformed to slowly and dynamically changing DC voltage signal from rectifier (doubler) and this signal is amplified/attenuated by inverting amplifier and summed with DC constant 1.1 V. Therefore, AGC responses on signal amplitude change by appropriate increase or decrease of the DC control voltage (V_{SETK}) for VA in Fig. 8.

3.2.3 The oscillator operating in quadrature mode

Our first tests are focused on quadrature mode only. The required passive component values have been determined as follows: $C_1 = C_2 = C = 220$ pF, $R_1 = R_2 = R = 565 \Omega$ ($470 \Omega + 95 \Omega$ of the X terminal [38]) and supply voltages ± 5 V. Using (18), we obtain $V_{SETB1} = V_{SETB2} = V_{SETB} = 0.79$ V for $f_0 = 1$ MHz. Results of both output waveforms and their spectral analyses are shown in Fig. 10. Tunability, spectral purity and changes of output amplitudes are studied in Fig. 11, when FO was changed from 0.23 to 2.0 MHz by V_{SETB} adjusted from 0.2 to 1.9 V.

3.2.4 Arbitrary phase shift mode

This operation mode allows us to select FO and phase shift of generated signals. The second phase shift is determined by mutual dependence of (18) and (19) or (20), respectively. Our design requirements are given as follows:

$\phi_{OUT1-2} = -50^\circ$ at $f_0 = 1$ MHz. Hence, (19) can be rewritten as:

$$\frac{B_2}{B_1} = \tan\left(-\frac{\phi_{OUT1-2}}{2}\right)^2. \tag{20}$$

By substitution (18)–(20), the value of B_1 can be calculated as:

$$B_1 = \frac{2\pi f_0 \sqrt{R_1 R_2 C_1 C_2}}{\tan\left(-\frac{\phi_{OUT1-2}}{2}\right)} \Bigg|_{\substack{R_1=R_2=R \\ C_1=C_2=C}} = \frac{2\pi f_0 RC}{\tan\left(-\frac{\phi_{OUT1-2}}{2}\right)}. \tag{21}$$

Numerical calculation yields $B_1 = 1.67$ ($V_{SETB1} = 1.67$ V) for $\phi_{OUT1-2} = -50^\circ$. The second gain/DC voltage can be calculated from (20) as $B_2 = 0.36$ ($V_{SETB2} = 0.36$ V). The transient response of output signals is shown in Fig. 12 and the measured phase shift is -47° while the FO is slightly decreased to 937 kHz. Figure 13 shows the measured dependence of phase shift on B_2/B_1 (V_{SETB2}/V_{SETB1}) ratio.

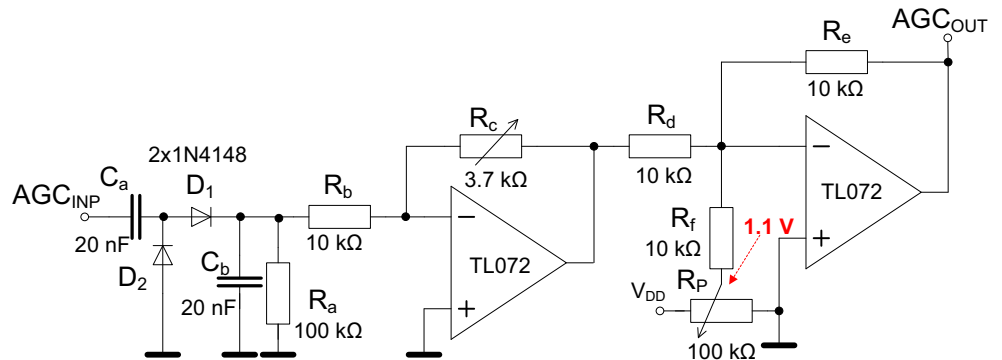
Considering Eq. (18), we have two possibilities for phase shift driving for modulation purposes:

$$\frac{B_2}{B_1} = const., \tag{22}$$

$$\frac{B_2}{B_1} = \frac{1}{const.}, \tag{23}$$

while product $B_1 B_2$ is always the same in order to keep the FO constant. When we define the first (initial) phase shift then the second phase shift is given by mutual dependence of (18) and (19). Therefore, (18) or (19) and (20) do not allow selecting the second phase shift, i.e. product of B_1 and B_2 have to be the same in both cases to obtain stable FO. Note that the change of state is referred as commutation in further text. Therefore, we obtained two pairs of values $B_1 = 1.67$ ($V_{SETB1} = 1.67$ V), $B_2 = 0.36$ ($V_{SETB2} = 0.36$ V) for L (data) and $B_1 = 0.36$ ($V_{SETB1} = 0.36$ V), $B_2 = 1.67$ ($V_{SETB2} = 1.67$ V) for H from (20) to (22). Hence, the phase shift of V_{OUT1} and V_{OUT2} in the H is -130° (19) and -50° for the L.

Fig. 9 Automatic AGC circuit for amplitude stabilization designed for oscillator in Fig. 8



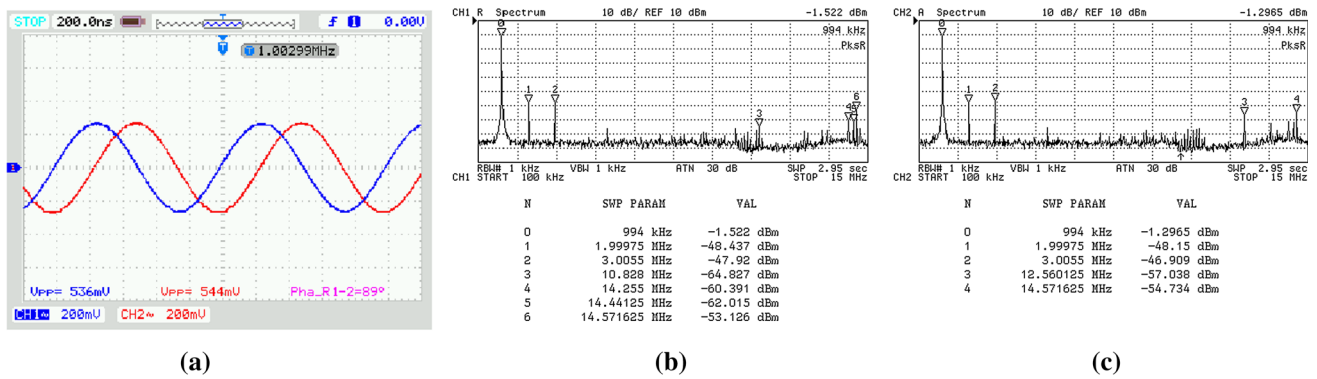


Fig. 10 Experimental results of the oscillator in quadrature mode: **a** output waveforms, **b** spectral analysis of V_{OUT1} , **c** spectral analysis of V_{OUT2}

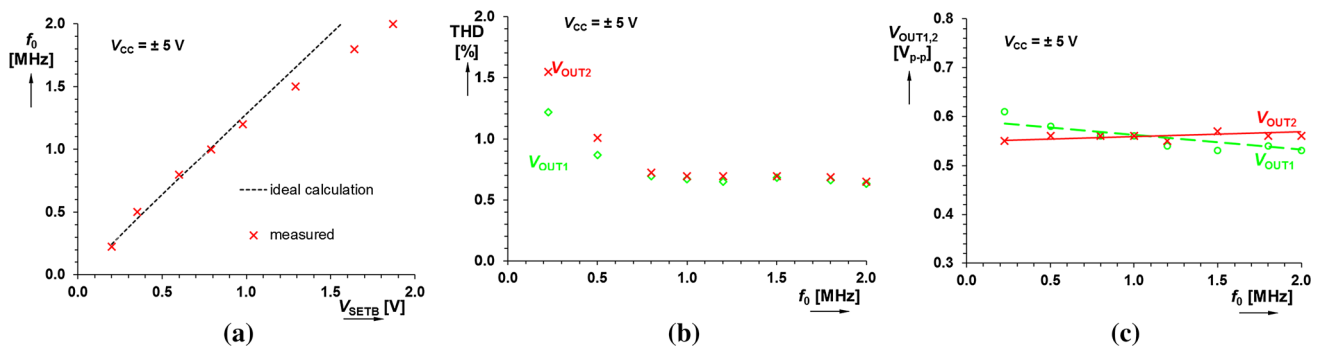


Fig. 11 Tuning process of the oscillator: **a** dependence of FO on V_{SETB} , **b** dependence of THD on FO, **c** dependence of amplitude level (V_{P-P}) on FO

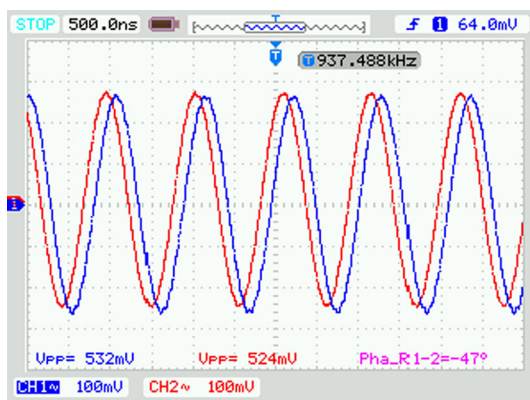


Fig. 12 Output transient response for arbitrary adjustable phase shift

3.2.5 Control logic: digital data to DC control voltages converter

Due to requirements on the oscillator and APF blocks of the structure (Fig. 8) to obtain phase shift commutation, we have to ensure two driving signals for control of the current gains B_1, B_2 where two specific values (levels) are required. In other words, our task is to design controlling logic part (similarly as in Fig. 5 for CMOS solution) or “data to

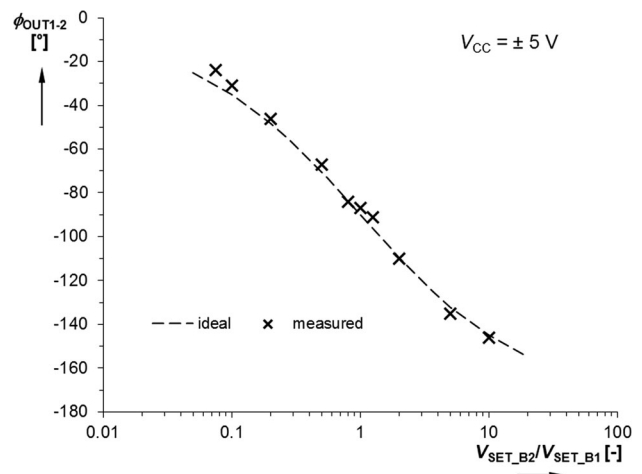
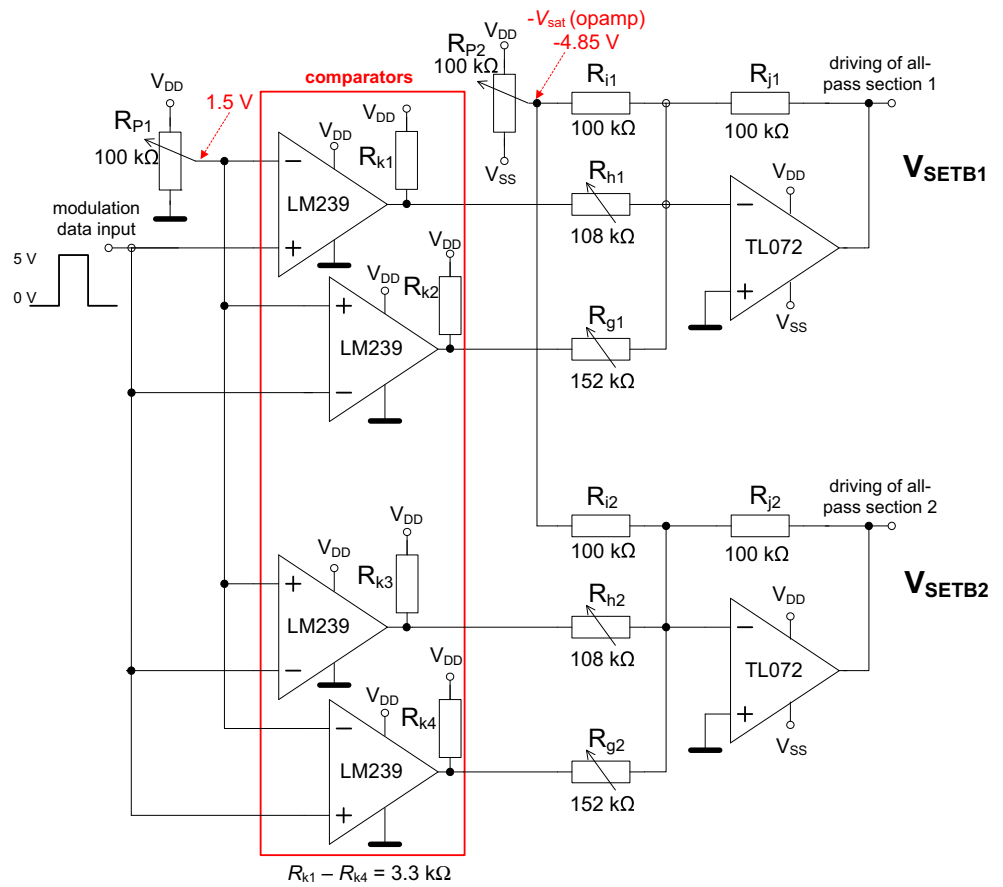


Fig. 13 Comparison of theoretical and measured dependence of phase shift of APF (ϕ_{OUT1-2}) on B_1 and B_2 ratio

voltage converter” with two outputs, where commutation of two V_{SETB} (0.36 and 1.67 V) in dependence on the state of input signal (L or H) is possible. Therefore, we designed system based on low-cost components (opamps and comparators) shown in Fig. 14 for our laboratory experiments. Proposed solution contains two channels, i.e. one for

Fig. 14 Generation of two pairs of adjustable DC voltages in phase shift commutation control logic



V_{SETB1} and another for V_{SETB2} . The first section of each channels is comparator part, where input modulation signal (TTL data) is compared with reference level 1.5 V hence to decide whether input signal is logic 0 or 1, i.e. 0 or 5 V. In case that input level has character of log. 0, one of the comparators has output in high state (saturation— $V_{sat_LM239} = 4.85$ V), while the second is in low state (0 V). These results are evaluated by adder/subtractor based on simple opamp. The amplification/attenuation is set by resistors to ensure appropriate result of subtraction (0.36 V for L and 1.67 V for H). Therefore, DC voltage of the reference level coming to both subtraction stages is -4.85 V. Based on this, selecting $R_{i1} = R_{j1}$ in the direct path with inverting unity gain as 100 k Ω , we can calculate resistor values of the subtractor as:

$$R_{g1} = \frac{R_{j1}}{\left(1 - \frac{V_{SETB1_L}}{V_{sat_LM239}}\right)}, \quad (24)$$

$$R_{h1} = \frac{R_{j1}}{\left(1 - \frac{V_{SETB1_H}}{V_{sat_LM239}}\right)}, \quad (25)$$

that yields $R_{g1} = 152$ k Ω (for $V_{SETB1_L} = 0.36$ V) and $R_{h1} = 108$ k Ω (for $V_{SETB1_H} = 1.67$ V). In order to ensure correct setting of operation in experiments, resistor values

can be modified by trimmers to compensate influences of real active and passive devices. The second section employs the same values ($R_{h2} = R_{h1}$ and $R_{g2} = R_{g1}$), but its logic is inverted, i.e. while L causes $V_{SETB1} = 0.36$ V and $V_{SETB2} = 1.67$ V and in case of H $V_{SETB1} = 1.67$ V and $V_{SETB2} = 0.36$ V. Modification of R_g , R_h values allow to set output levels of V_{SETB} easily.

3.2.6 Operation of the full system as phase shift keying modulator

The phase shift keying modulator has been designed by interconnection of proposed oscillator (Fig. 8), AGC (Fig. 9), and control logic (Fig. 14). At the input of control logic in Fig. 14, data input signal in TTL levels (0; 5 V) and 1 kHz frequency were used. Obtained transient responses are shown in Fig. 15. Driving voltages V_{SETB1} and V_{SETB2} are shown on the upper half of the figure (green and orange color). Modulated signals V_{OUT1} and V_{OUT2} are given in the lower part of the figure together with zoomed details of both states of phase shifts. Zoomed change of the state, Lissajous plot, and spectral analysis of both outputs (upper— V_{OUT1} , lower— V_{OUT2}) are given in Fig. 16.

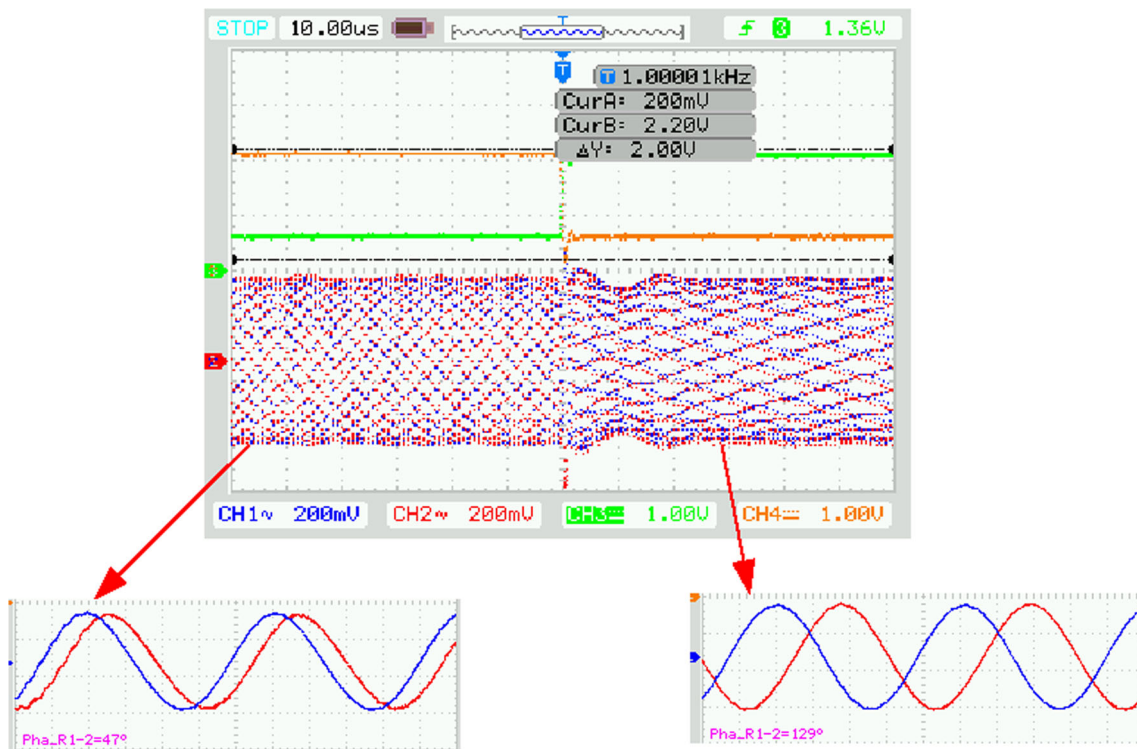


Fig. 15 Transient responses of the phase shift keying modulator in operation mode

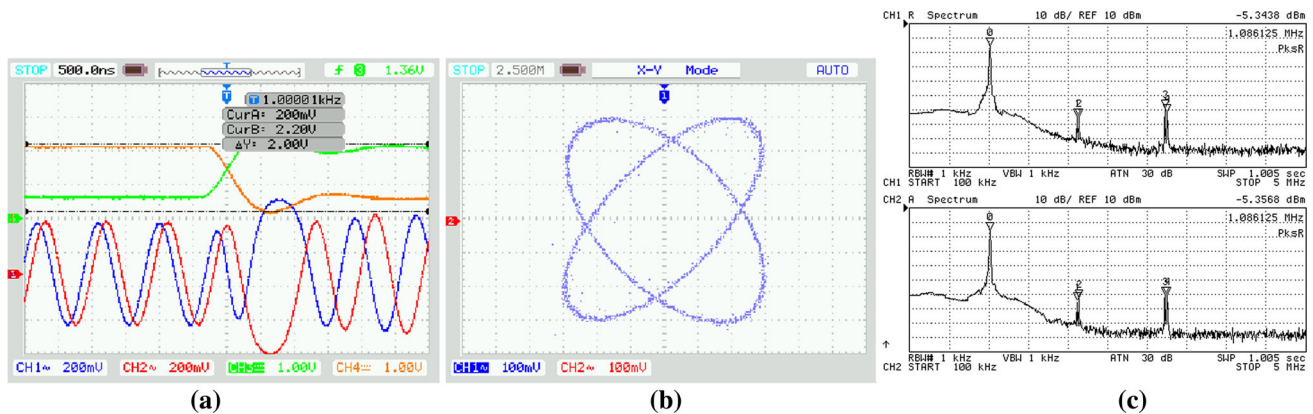


Fig. 16 Detailed analyses: **a** zoomed change of the state, **b** Lissajous plot, **c** spectral analysis

3.3 Discussion

The workability of the proposed circuits is confirmed by experimental measurements. Significant advantage is simple design based on oscillator with AGC and control logic for data to driving voltages conversion. However, there are also drawbacks. Range of B (g_m in case of CMOS solution) is always restricted. Therefore, adjusting of phase shift is also limited by available minimal and maximal ratio in particular solution (B_2/B_1 , g_{m2}/g_{m1} , approximately 1/20–20). Second value of phase shift for H cannot be set

arbitrarily, i.e. independently on initial phase shift for L. In addition, nonlinearity of dependence of B on control voltage (for $B > 2$ especially) as well as g_m on I_b must be considered for accurate design. Otherwise, as it has been observed in experiments, substantial problems may occur, for example two tone modulation, because commutation of $g_{m1,2}$ or $B_{1,2}$ causes also parasitic change of FO. It is possible to avoid it for very accurate design and trimming. Due to the discussed issues, we prepared the second solution that exhibits better features and removes many discussed disadvantages for the cost of the slightly higher complexity.

4 The oscillator with additional APF to provide electrical set of phase shift in modulator: the second solution

The second solution is logically established by using the oscillator (Figs. 1, 8) with additional all-pass filter connected to one available output in the oscillator structure. The block concept is given in Fig. 17.

4.1 Simulation results

In the design, we used the same block as were reported in detail in Fig. 1, therefore many parameters remain the same (oscillator is operating in quadrature regime because $g_{m1} = g_{m2}$) and therefore design steps and considerations will be provided in brief form. In the second concept of the phase shift keying modulator, the oscillator is the same structure as in Fig. 1 and only additional APF₃, identical to APF_{1,2} used for construction of the oscillator, is connected to V_{OUT1} and forms V_{OUT2} (see Fig. 18). Considering initial design parameters $f_0 = 1$ MHz and $g_{m1} = g_{m2} = g_m$, the recalculated values are $g_m = 300 \mu S$ ($I_{b1} = I_{b2} = I_b = 41 \mu A$).

The transconductance of the APF₃ (C_3 has also 47 pF as in APFs in the oscillating core) for two possible states (we selected 30° and 120°) can be calculated as follows:

$$g_{mAPF}(-30^\circ) = \frac{\omega_0 C_3}{\tan\left(-\frac{\varphi_{OUT1-2}}{2}\right)} = \frac{2\pi \cdot 10^6 \cdot 47 \cdot 10^{-12}}{\tan\left(-\left(\frac{-30}{2}\right)\right)} = 1100 \mu S, \tag{26}$$

Fig. 17 The block diagram of the second solution of proposed phase shift keying modulator

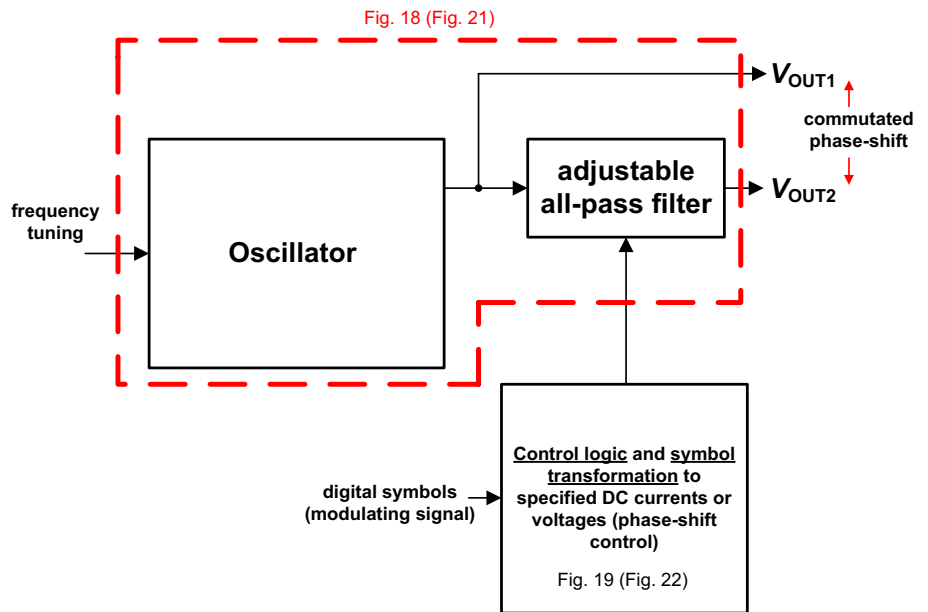
$$g_{mAPF}(-120^\circ) = \frac{\omega_0 C_3}{\tan\left(-\frac{\varphi_{OUT1-2}}{2}\right)} = \frac{2\pi \cdot 10^6 \cdot 47 \cdot 10^{-12}}{\tan\left(-\left(\frac{-120}{2}\right)\right)} = 170 \mu S. \tag{27}$$

Hence, I_{bAPF} is set as 300 μA (−30°) and 20 μA (−120°), respectively. The control logic for this oscillator in Fig. 18 must be slightly modified, see Fig. 19. It should be noted that it is significantly simpler than solution in Fig. 5, since only half of overall circuitry is used, because only single driving bias current I_{bAPF} is required.

PSpice simulations of the CMOS model provided transient responses shown in Fig. 20. Here the selected time segment and detail on moment of the commutation of phase shift are highlighted. Overshoot is significantly reduced because there is no disruption of oscillation condition in the oscillator loop in case of this solution when compared to the circuit in Figs. 1 or 6. APF₃ provides independent control of phase shift at the output V_{OUT2} as well as FO is now independent on phase shift setting. Simulated $f_0 = 992$ kHz and the first state for L achieves phase shift between V_{OUT1} and V_{OUT2} 26°. The phase shift in the second state (H) reaches 127°.

4.2 Experimental results

Experimental results are performed for circuit structure shown in Fig. 21. AGC system used in these experiments is the same as in Fig. 9. Figure 22 introduces simplified control logic system (data to DC voltage V_{SETB3} converter) for phase shift keying modulator. The design of the oscillator part in Fig. 21 is provided with the same values as in



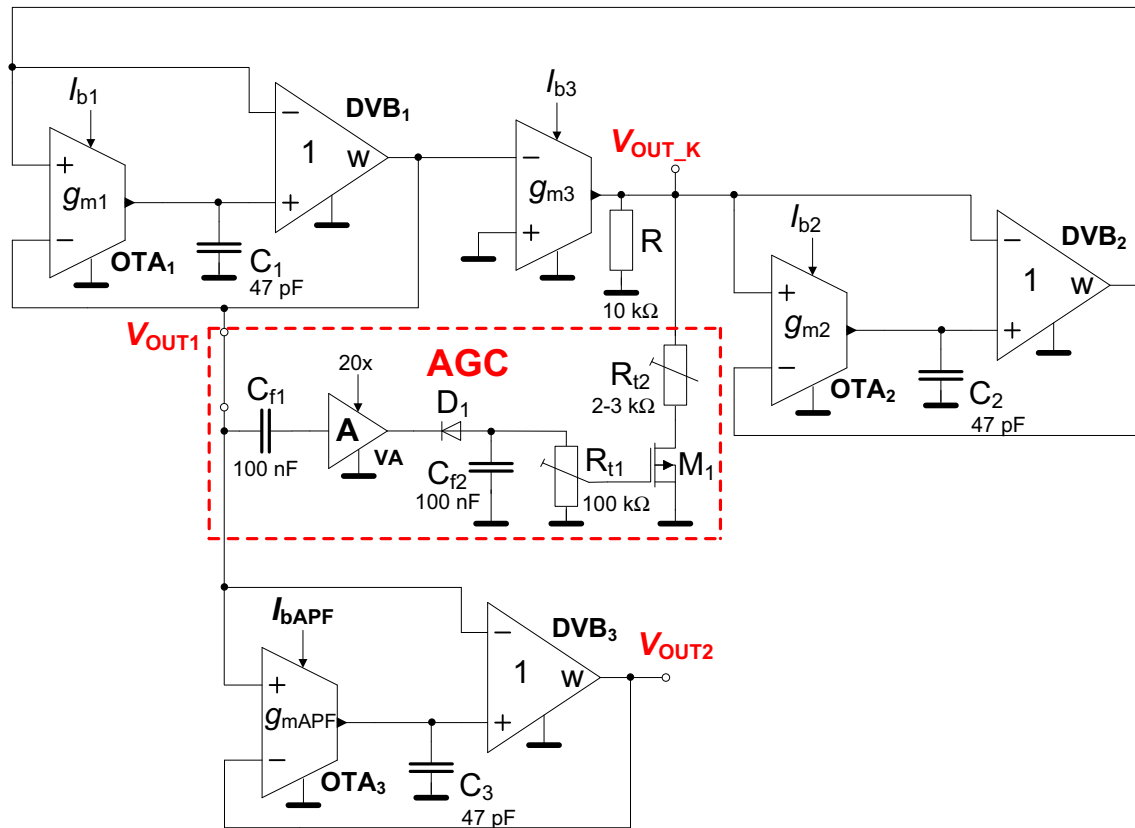


Fig. 18 Oscillator with additional APF₃ to provide adjustable phase shift

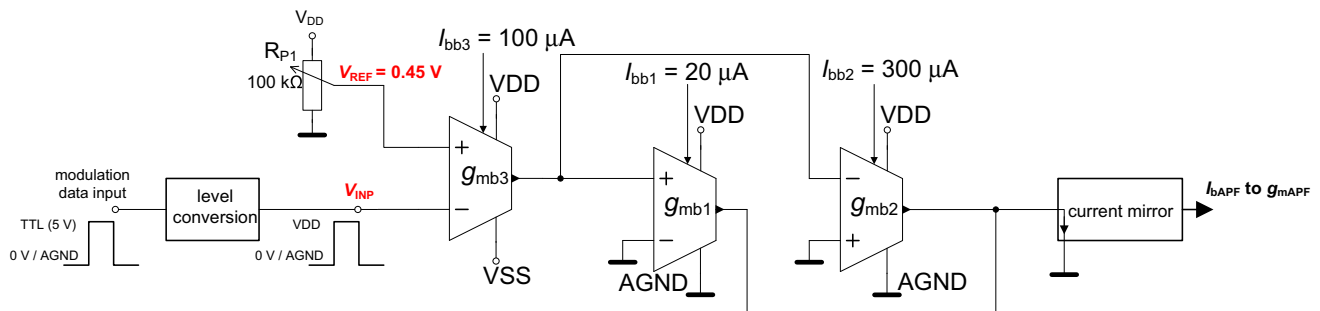


Fig. 19 Control logic: converter of digital data to bias driving current for g_{mAPF} in the all-pass filter

Sect. 2.3.3 (all $C = 220$ pF, all $R = 565 \Omega$, $B_1 = B_2 = B = 0.79$, $f_0 = 1$ MHz). The all-pass filter discussed in chapter 2.3.1 (Eq. 17) allows to calculate value of B_3 for AP₃ as $B_3 = 2.91$ ($V_{SETB_3} = 3.4$ V due to significant nonlinearity of dependence of B on V_{SET} [38] for $B > 2$, for L state $\phi_{OUT1-2} = -30^\circ$) and $B_3 = 0.45$ ($V_{SETB_3} = 0.45$ V, for state H, $\phi_{OUT1-2} = -120^\circ$). Except simplification of control logic to single channel solution, resistor values of R_g and R_h had to be recalculated as 334 and 110 k Ω , respectively.

In this solution, the modulation signal has also $f_{mod} = 1$ kHz. Transient responses are shown in Fig. 23. Labelling is as follows: green curve is modulation signal with TTL levels (0; 5 V), and orange color is driving signal of V_{SETB_3} . Lower traces are both output waveforms V_{OUT1} and V_{OUT2} together with details in both states (L, H). Detail on change of the phase shift (from H to L), Lissajous plot and spectral analysis of both outputs (upper— V_{OUT1} , lower— V_{OUT2}) are depicted in Fig. 24.

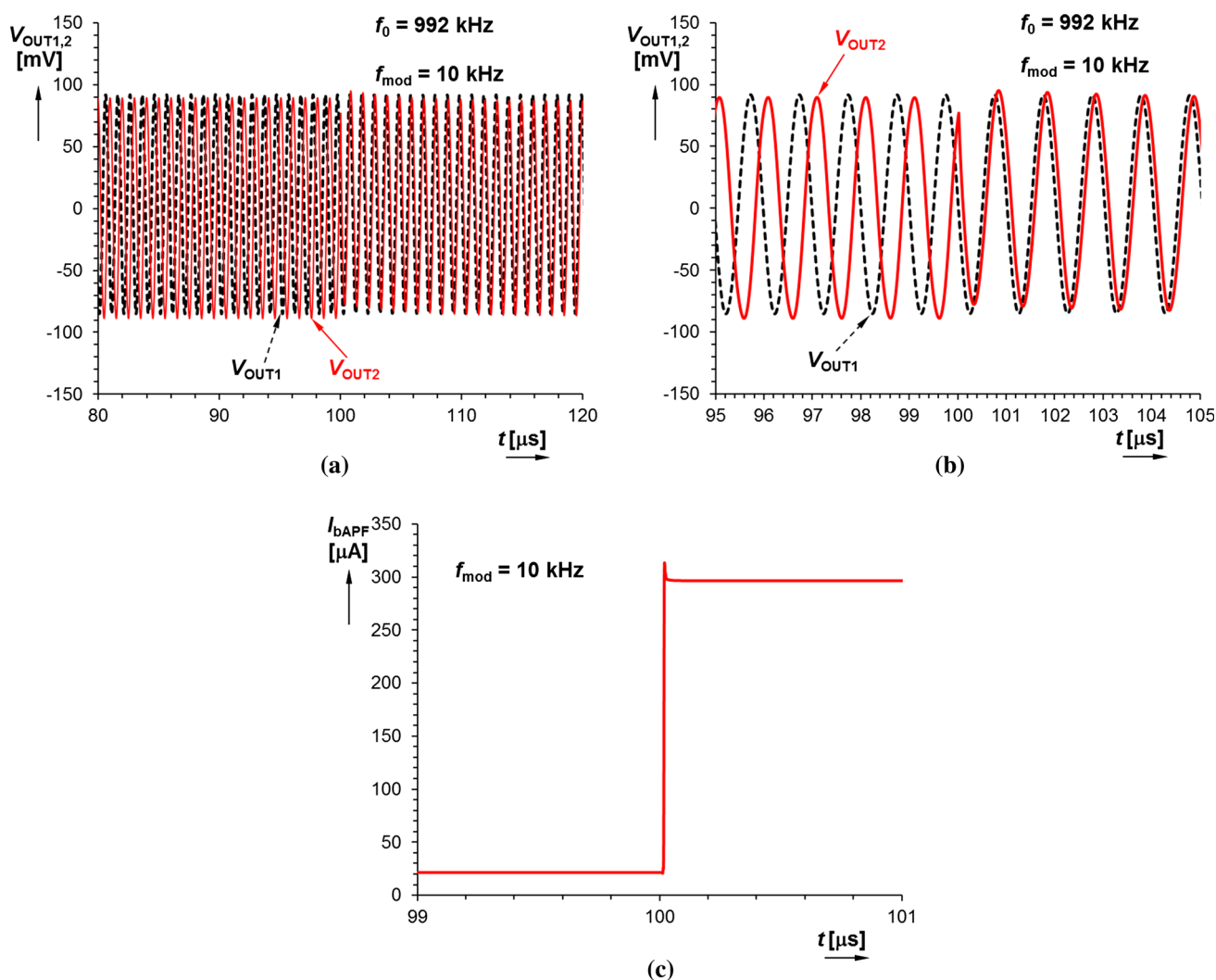


Fig. 20 Simulation results of the second modulator: **a** transient response in larger scale around change of the phase shift, **b** detail on moment of the phase shift commutation, **c** driving bias current I_{bAPF} in moment of phase shift change

4.3 Discussion

The second solution removes many of previously discussed drawbacks of the first solution, such as mutual dependence of FO and phase shift setting—i.e. impossibility of the setting the second state, disruption of driving to oscillator system—closed loop, overshoots, two tone production etc. Hence, the second solution really offers independent tuning of FO, both states of phase shift are selectable and control logic is simpler. However, it is not driving directly the phase shift between produced signals in the oscillator structure anymore. Additional APF performs these operations. Therefore, despite of fact that control logic has half complexity in comparison to the first solution, overall circuitry is more extensive. Hence, it is on the designer's choice which solution will be better for particular purposes in the application.

5 Conclusion

Availability of arbitrary phase shift setting in the simple second-order oscillator can reduce the number of active devices and device's power consumption. Theoretically, any phase shift can be achieved between 0° and -180° and not only minimal phase step given by lossy blocks in known multiphase/multi-loop structures. It was tested from -17° to -141° (due to max. available ratio of g_{m1}/g_{m2} ; B_1/B_2 respectively, see Fig. 13) in experiments. In the first case, tuning of the oscillator is provided by g_{m1} (B_1 in discrete solution) and g_{m2} (B_2), simultaneously. Their ratio has direct impact on the produced phase shift and it has to be ensured as constant, if frequency is tuned. Second type of modulator allows independent setting of frequency and both phase shifts, however, it is more complex since additional APF is required. Our computer and experimental

Fig. 21 Structure of the phase shift keying modulator based on commercially available components

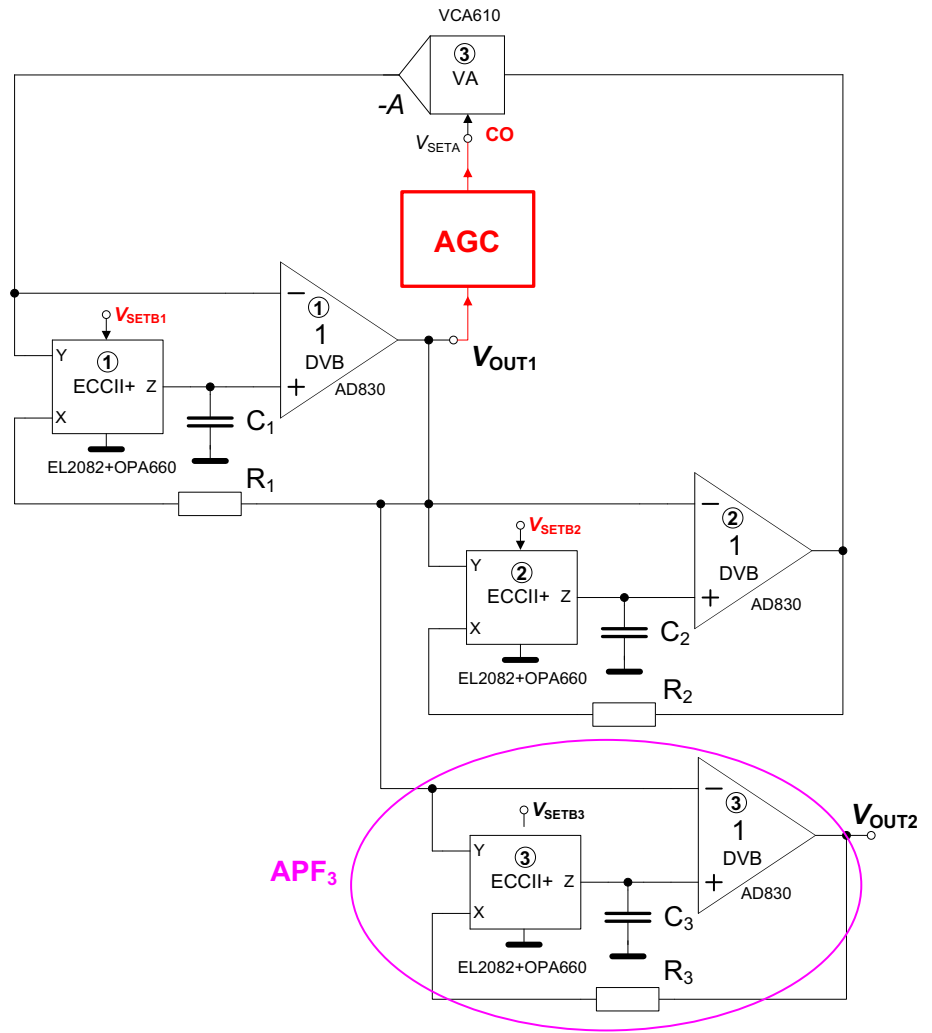
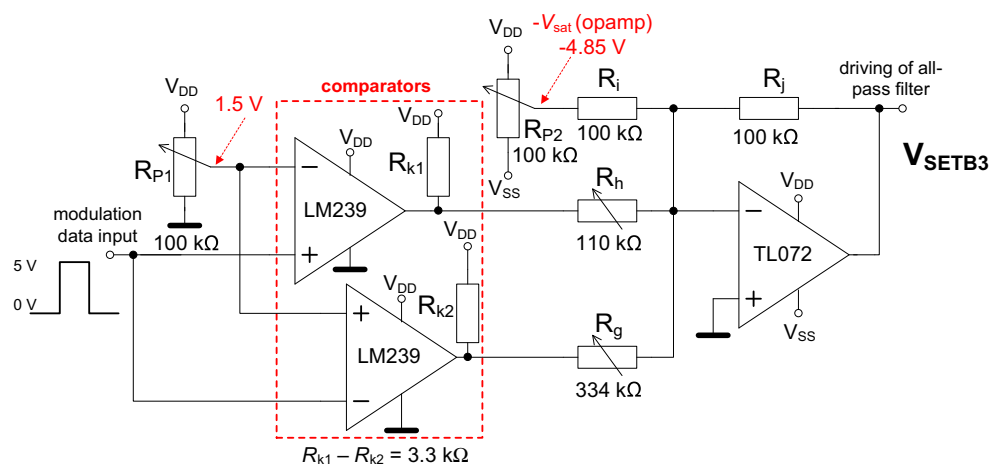


Fig. 22 Control logic: Data to DC voltage converter



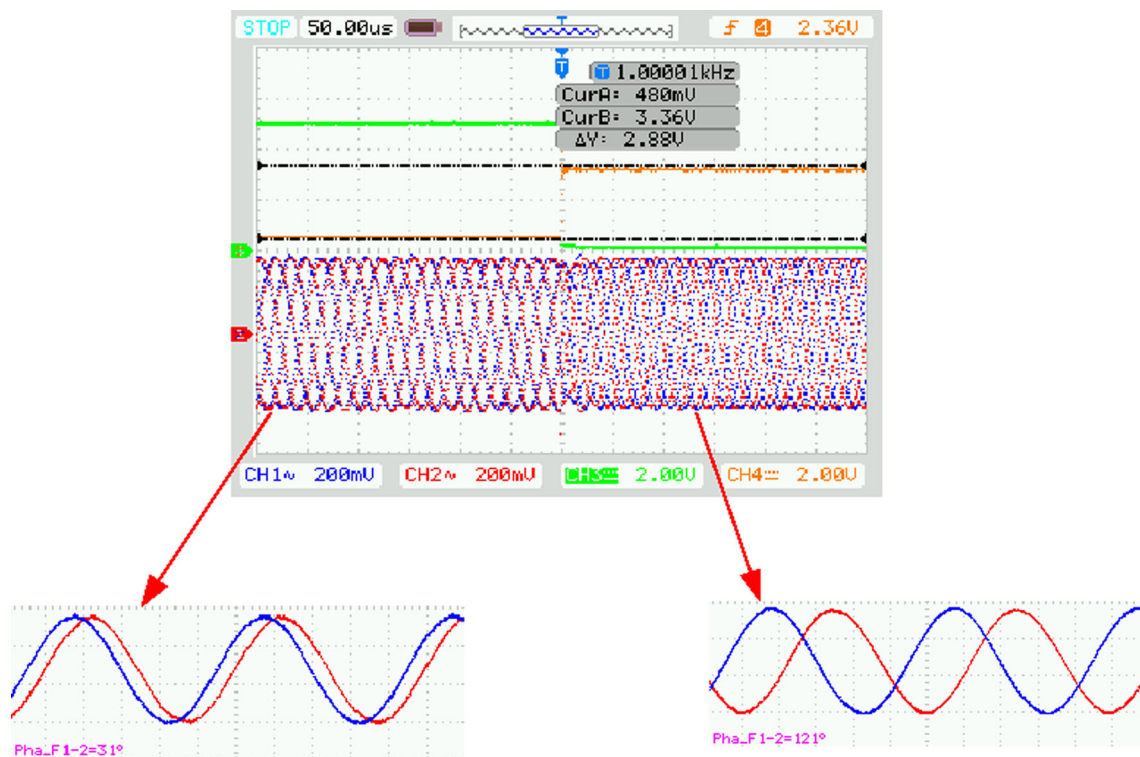


Fig. 23 Transient responses of the phase shift keying modulator

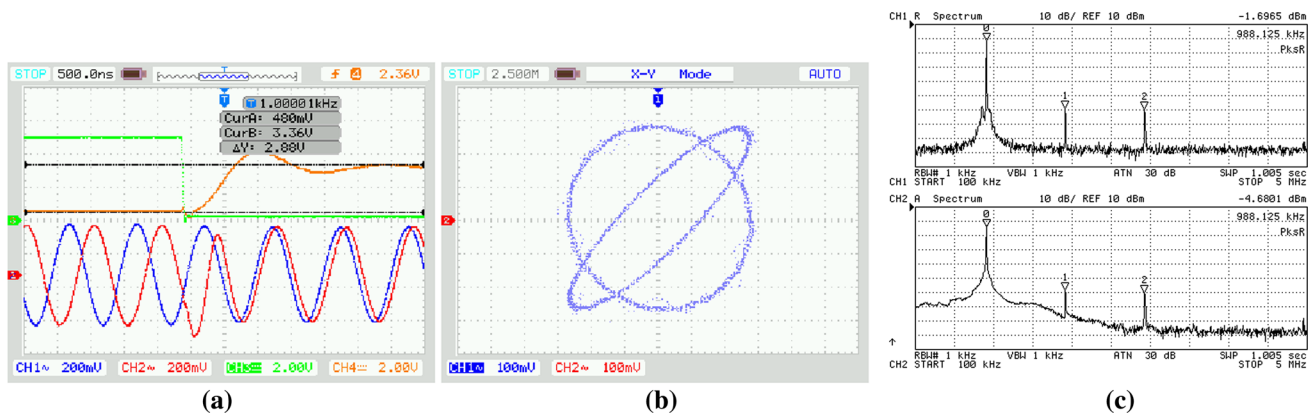


Fig. 24 Detailed results of measurement: **a** focused on state change, **b** Lissajous plot, **c** spectral analysis

Table 2 Comparison of ideal design and results obtained from simulations and measurements

	TYPE1		TYPE2	
	f_0 (MHz)	φ_{OUT1-2} (°)	f_0 (MHz)	φ_{OUT1-2} (°)
Ideal	1.00	50/130	1.00	30/120
CMOS simulated	0.96	51/135	0.99	26/127
Experimental results	1.09	47/129	0.99	31/121

verifications confirmed expected behavior of both systems. Comparison of simulated and measured features for both modulation systems with both different approaches is provided in Table 2.

Acknowledgments Research described in this paper was financed by Czech Ministry of Education in frame of National Sustainability Program under Grant LO1401. For research, infrastructure of the SIX Center was used. Research described in the paper was supported by Czech Science Foundation Project under No. 14-24186P.

References

- Li, R. C.-H. (2012). *RF circuit design*. Wiley series on information and communication technology (2nd ed.). Wiley. ISBN 978-1-118-30990-2. <http://eu.wiley.com/WileyCDA/WileyTitle/productCd-1118309901.html>.
- Razavi, B. (2009). *Fundamentals of microelectronics*. Hoboken: Wiley.
- Abuelma'atti, M. T., & Al-Qahtani, M. A. (1998). A new current-controlled multiphase sinusoidal oscillator using translinear current conveyors. *IEEE Transactions on Circuits and Systems*, 2, *Analog and Digital Signal Processing*, 45(7), 881–885.
- Souliotis, G., & Psychalinos, C. (2009). Electronically controlled multiphase sinusoidal oscillators using current amplifiers. *International Journal of Circuit Theory and Applications*, 37(1), 43–52.
- Tangsrirat, W., Tanjaroen, W., & Pukkalanun, T. (2009). Current-mode multiphase sinusoidal oscillator using CDTA-based allpass sections. *AEU-International Journal of Electronics and Communications*, 63(7), 616–622.
- Kumngern, M., Chanwutitum, J., & Dejhan, K. (2010). Electronically tunable multiphase sinusoidal oscillator using translinear current conveyors. *Analog Integrated Circuits and Signal Processing*, 65(2), 327–334.
- Tu, S. H., Hwang, Y. S., Chen, J. J., Soliman, A. M., & Chang, C. M. (2012). OTA-C arbitrary-phase-shift oscillators. *IEEE Transactions on Instrumentation and Measurement*, 61(8), 2305–2319.
- Sagbas, M., Ayten, U. E., Herencsar, N., & Minaei, S. (2013). Current and voltage mode multiphase sinusoidal oscillators using CBTAs. *Radioengineering*, 22(1), 24–33.
- Keskin, A. U., Aydin, C., Hancioglu, E., & Acar, C. (2006). Quadrature oscillator using current differencing buffered amplifiers (CDBA). *Frequenz*, 60(3–4), 57–60.
- Herencsar, N., Minaei, S., Koton, J., Yuce, E., & Vrba, K. (2013). New resistorless and electronically tunable realization of dual-output VM all-pass filter using VDIBA. *Analog Integrated Circuits and Signal Processing*, 74(1), 141–154.
- Gift, S. J. G. (2000). The application of all-pass filters in the design of multiphase sinusoidal systems. *Microelectronics Journal*, 31(1), 9–13.
- Keskin, A. U., & Biolek, D. (2006). Current mode quadrature oscillator using current differencing transconductance amplifiers (CDTA). *IEEE Proceedings on Circuits Devices and Systems*, 153(3), 214.
- Jaikla, W., Siripruchyanun, M., Biolek, D., & Biolkova, V. (2010). High-output-impedance current-mode multiphase sinusoidal oscillator employing current differencing transconductance amplifier-based allpass filters. *International Journal of Electronics*, 97(7), 811–826.
- Jaikla, W., & Prommee, P. (2011). Electronically tunable current-mode multiphase sinusoidal oscillator employing CCCDTA-based allpass filters with only grounded passive elements. *Radioengineering*, 20(3), 594–599.
- Songsuwankit, K., Petchmaneeumka, W., & Riewruja, V. (2010). Electronically adjustable phase shifter using OTAs. In *Proceedings of IEEE international conference in control automation and systems* (pp. 1622–1625).
- Chaturvedi, B., & Maheshwari, S. (2012). An ideal voltage-mode all-pass filter and its application. *Journal of Communication and Computer*, 9, 613–623.
- Maundy, B., Elwakil, A., & Gift, S. (2012). On the realization of multiphase oscillators using fractional-order allpass filters. *Circuits, Systems, and Signal Processing*, 31(1), 3–17.
- Ozoguz, S., Abdelrahman, T. M., & Elwakil, A. S. (2006). Novel approximate square-root domain all-pass filter with application to multiphase oscillators. *Analog Integrated Circuits and Signal Processing*, 46(3), 297–301.
- Prommee, P., & Wongprommoon, N. (2013). Log-domain all-pass filter-based multiphase sinusoidal oscillators. *Radioengineering*, 22(1), 14–23.
- Frey, D. R. (1993). Log-domain filtering: an approach to current-mode filtering. *IEEE Proceedings in Circuits, Devices and Systems, Part G*, 140(6), 406–416.
- Sotner, R., Jerabek, J., Petrzela, J., Prokop, R., Vrba, K., Kartci, A., & Dostal, T. (2015). Quadrature oscillator solution suitable with arbitrary and electronically adjustable phase shift. In *IEEE international symposium on circuits and systems* (pp. 3056–3059).
- Keskin, A. Ü., Pal, K., & Hancioglu, E. (2008). Resistorless first-order all-pass filter with electronic tuning. *AEU-International Journal of Electronics and Communications*, 62(4), 304–306.
- Bajer, J., & Biolek, D. (2010). Voltage-mode electronically tunable all-pass filter employing CCCII+, one capacitor and differential-input voltage buffer. In *Proceedings of IEEE 26th convention of electrical and electronics engineers in Israel* (pp. 934–937).
- Biolek, D., Senani, R., Biolkova, V., & Kolka, Z. (2008). Active elements for analog signal processing: classification, review, and new proposals. *Radioengineering*, 17(4), 15–32.
- Metin, B., Pal, K., & Cicekoglu, O. (2011). CMOS controlled inverting CDBA with a new all-pass filter application. *International Journal of Circuit Theory and Applications*, 39(4), 417–425.
- Maheshwari, S. (2008). A canonical voltage-controlled VM-APS with grounded capacitor. *Circuits, Systems, and Signal Processing*, 27(1), 123–132.
- Metin, B., Herencsar, N., & Pal, K. (2011). Supplementary first-order all-pass filters with two grounded passive elements using FDCCII. *Radioengineering*, 20(2), 433–437.
- Minaei, S., & Yuce, E. (2010). Unity/variable-gain voltage-mode/current-mode first-order all-pass filters using single dual-X second-generation current conveyor. *IETE Journal of Research*, 56(6), 305–312.
- Sotner, R., Kartci, A., Jerabek, J., Herencsar, N., & Petrzela, J. (2015). Modulator based on electronic change of phase shift in simple oscillator. In *Proceedings of international conference on electrical and electronics engineering (ELECO)* (pp. 101–105).
- von Wangenheim, L. (2011). On the Barkhausen and Nyquist stability criteria. *Analog Integrated Circuits and Signal Processing*, 66(1), 139–141.
- He, F., Ribas, R., Lahuec, C., & Jézéquel, M. (2009). Discussion on the general oscillation startup condition and the Barkhausen criterion. *Analog Integrated Circuits and Signal Processing*, 59(2), 215–221.
- Singh, V. (2010). Discussion on Barkhausen and Nyquist stability criteria. *Analog Integrated Circuits and Signal Processing*, 62(3), 327–332.

33. Martinez-Garcia, H., Grau-Saldes, A., Bolea-Monte, Y., & Gamiz-Caro, J. (2012). On discussion on Barkhausen and Nyquist stability criteria. *Analog Integrated Circuits and Signal Processing*, 70(3), 443–449.
34. MOSIS parametric test results of TSMC LO EPI SCN018 technology. <https://www.mosis.com/cgi-bin/cgiwrap/umosis/swp/params/tsmc-018>.
35. Surakamponorn, W., & Thitimajshima, P. (1988). Integrable electronically tunable current conveyors. *IEEE Proceedings on Electronic Circuits and Systems, Part G*, 135(2), 71–77.
36. Fabre, A., & Mimeche, N. (1994). Class A/AB second-generation current conveyor with controlled current gain. *Electronics Letters*, 30(16), 1267–1269.
37. Minaei, S., Sayin, O. K., & Kuntman, H. (2006). A new CMOS electronically tunable current conveyor and its application to current-mode filters. *IEEE Transactions on Circuits and Systems I: Regular Papers*, 53(7), 1448–1457.
38. Intersil (Elantec). EL2082 CN Current-mode multiplier (datasheet), 1996. <http://www.intersil.com/data/fn/fn7152.pdf>.
39. OPA660: Wide Bandwidth Operational Transconductance Amplifier and Buffer, Texas Instruments [online], 1995, last modified 9 2000 [cit.22.10.2012]. <http://www.ti.com/lit/ds/sym link/opa660.pdf>.
40. VCA610: Wideband voltage controlled amplifier, Texas Instruments [online], 2000, last modified 11 2000. <http://www.ti.com/lit/ds/sym link/vca610.pdf>.



Aslihan Kartci received M.Sc. degree in Electronics from Yildiz Technical University, Turkey in 2015. Currently, she is working toward the Ph.D. degree in Radio Electronics from Brno University of Technology, Czech Republic. Her research interests include analog integrated circuits with modern active elements, and their applications as filters and oscillators, general element simulator, numerical methods for analysis of electronic networks,

and computer-aided methods for simulation of electronic circuits. She is a student member of IEEE.



Roman Sotner was born in Znojmo, Czech Republic, in 1983. He received the Ph.D. and M.Sc. degree in Electrical Engineering from the Brno University of Technology, Czech Republic, in 2012 and 2008, respectively. Currently, he is a research worker at the Department of Radio Electronics, Faculty of Electrical Engineering and Communication, Brno University of Technology, Brno, Czech Republic. His interests are analogue circuits

(active filters, oscillators, audio, etc.), circuits in the current mode, circuits with direct electronic controlling possibilities especially and computer simulation. He is a member of IEEE.



adjustable current amplifiers and followers, transconductance and transimpedance amplifiers.



Norbert Herencsar was born in Slovak Republic, in 1982. He received the M.Sc. and Ph.D. degrees in Electronics and Communication and Teleinformatics from Brno University of Technology, Czech Republic, in 2006 and 2010, respectively. Since December 2015, he is an Associate Professor at the Department of Telecommunications of Brno University of Technology, Brno, Czech Republic. During September 2009–February 2010 and February 2013–May 2013 he was an Erasmus Exchange Student and Visiting Researcher, respectively, with the Department of Electrical and Electronic Engineering, Bogazici University, Istanbul, Turkey. During January 2014–April 2014 he was a Visiting Researcher with the Department of Electronics and Communications Engineering, Dogus University, Istanbul, Turkey. His research interests include analog filters, current-, voltage- and mixed-mode circuits, new active elements and their circuit applications, low transistor count circuits, MOS-only circuits, oscillators, and inductor simulators. He is an author or co-author of 56 research articles published in SCI-E peer-reviewed international journals, 24 articles published in other journals, and 89 papers published in proceedings of international conferences. Since 2010, Dr. Herencsar is Deputy-Chair of the International Conference on Telecommunications and Signal Processing (TSP). Since 2012, he is Co-Editor of the International Journal of Advances in Telecommunications, Electrotechnics, Signals and Systems. Since 2014, he is Associate Editor of the Journal of Circuits, Systems and Computers (JCSC). Dr. Herencsar is Senior Member of the IEEE, IACSIT, and IRED, and Member of the IAENG, ACEEE, and RS. Since 2015, he serves as IEEE Czechoslovakia Section SP/CAS/COM Joint Chapter Chair as well as Membership Development Officer.



Jiri Petrzela was born in Brno, Czech Republic, in 1978. He received the M.Sc. and Ph.D. degrees at the Brno University of Technology in 2003 and 2007 respectively. His research interest covers the nonlinear dynamics, chaos theory and analog circuit design. Currently he is an associated professor at Department of Radio Electronics.

[21] SOTNER, R., JERABEK, J., HERENCŠAR, N., PROKOP, R., VRBA, K., PETRZELA, J., DOSTAL, T. Simply Adjustable Triangular and Square Wave Generator Employing Controlled Gain Current and Differential Voltage Amplifier. In *Proceedings of the 23th international conference Radioelektronika 2013*, Pardubice (Czech Republic), 2013, p. 109-114. ISBN: 978-1-4673-5517-9.

Simply Adjustable Triangular and Square Wave Generator Employing Controlled Gain Current and Differential Voltage Amplifier

R. Sotner, J. Jerabek, N. Herencsar, R. Prokop,
K. Vrba, J. Petrzela
Faculty of Electrical Engineering and Communication
Brno University of Technology
Brno, Czech Republic
sotner@feec.vutbr.cz

T. Dostal
Dept. of Electrical Engineering and Computer Science
College of Polytechnics Jihlava
Jihlava, Czech Republic

Abstract—Our contribution deals with combination of controllable current and voltage gain in frame of active element called controlled gain current and differential voltage amplifier (CG-CDVA). Proposed behavioral model was used for construction of very simple and electronically controllable triangle and square wave generator. Simulation results supported theoretical presumptions and confirmed workability.

Keywords—adjustable current and voltage gain; electronic control; triangle and square wave generator

I. INTRODUCTION

Many possible ways of control of active elements were studied in the past. Interesting theoretical overview of useful approaches provided Bielek et al. [1]. We can recapitulate significant ideas very briefly. Searching for suitable ways of control of active elements started after discovery of current conveyor (CCII) by Sedra et al. [2]. Intrinsic resistance control [3]-[4] belongs to frequently used methods. Transconductance (g_m) control [5] allows benefits of the wide range adjusting (several decades) as we can see in [6]-[7]. An attention was also given to development of elements with controlled current gain. Electronically controllable current conveyors were introduced by Surakampontorn et al. [8] and Fabre et al. [9]. The author's interest in this area has survived to the present time. Many interesting solutions of elements with controllable gain were introduced quite recently, for example simple controllable current amplifiers [10]-[12]. Advanced active elements utilizing current gain control in frame of more complicated structure offer more benefits than simple amplifiers, for example [13]-[14]. Digitally controllable equivalents are also interesting for many researchers [15]-[16].

Development of active elements with more than one way of electronic control started to be popular quite recently. Important progress attained Minaei et al. [17] with electronically controllable current conveyor of second generation (ECCII) where combination of current gain (B) and intrinsic resistance (R_x) control was proposed. De Marcellis et al. [18] enhanced possibilities of control in frame of current conveyor and implemented also voltage gain control.

Kumngern et al. [19] proposed in their conveyor also intrinsic resistance and current gain control with different structure (in comparison to [17]). Electronic control of parameters was proposed in so-called current conveyor transconductance amplifier (CCTA) [20] where intrinsic resistance and transconductance control was realized separately by Siripruchyanun et al. [21]. Both methods of control were used in modification of the current differencing transconductance amplifier (CDTA) [22] presented by Jaikla et al. [23] and Sakul et al. [24].

Many solutions of generators allow only control of repeating (oscillation) frequency (f_0) by change of resistor value [25]-[31]. Bielek et al. [25] presented interesting simple solutions generating non-harmonic signal. Generator employs one CDTA, grounded capacitor and three resistors. De Marcellis et al. [26] utilized two CCII, six resistors and floating capacitor. Solution presented by Chien et al. [27] requires two differential voltage current conveyors (DVCCs) [1], three resistors and control of duty cycle is also allowed. Almashary et al. [28] presented generator based on two CCII, three resistors and two capacitors. Pal et al. [29] employed two CCII, three resistors and floating capacitor. Two current feedback operational amplifiers (CFOAs) [1] were used in solution presented by Saque et al. [30] where four resistors and floating capacitor are required. Minaei et al. [31] used similar way based on CFOAs and DVCCs. Engagement of two operational transresistance amplifiers (OTRAs), three resistors and one floating capacitor was shown by Lo et al. [32].

Possibilities of direct electronic control were also studied. Interesting solutions were presented quite recently. The perfect example of design and theoretical background was given by Chung et al. [33] where three transconductors (OTAs) [1] and two resistors are sufficient for control of repeating frequency and also duty cycle by DC bias currents of transconductors, similarly Siripruchyanun et al. [34]. Some solutions were designed with current-mode outputs. Kumbun et al. [35] used two multiple output through transconductance amplifiers (MO-CTTAs) only to realize generator tuneable by bias currents. Two multiple output current controlled current differencing transconductance amplifiers (MO-CCCDTAs) are also suitable

Research described in the paper was supported by Czech Science Foundation projects under No. 102/09/1681 and by internal grant No. FEKT-S-11-13. The support of the project CZ.1.07/2.3.00/20.0007 WICOMT, financed from the operational program Education for competitiveness, is gratefully acknowledged. The described research was performed in laboratories supported by the SIX project; the registration number CZ.1.05/2.1.00/03.0072, the operational program Research and Development for Innovation.

for discussed purposes as shown by Silapan et al. [36] and Sristakul et al. [37].

Our contribution has advantages of simple circuitry, low number of active and passive elements and simple electronic control by current gain in comparison to many discussed solutions.

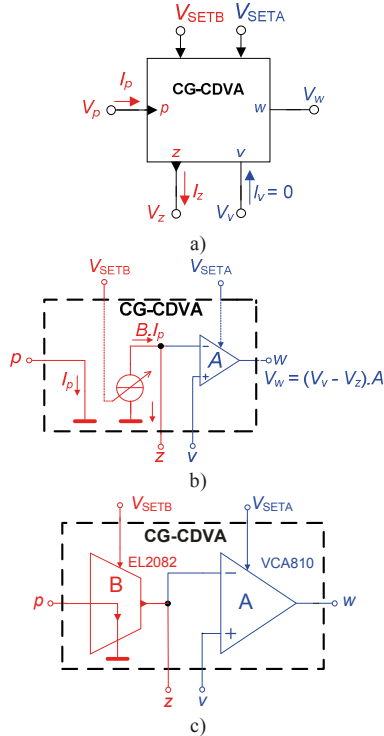


Figure 1. Proposed controlled gain current and differential voltage amplifier (CG-CDVA): a) symbol, b) behavioral, c) possible behavioral implementation employing commercially available devices.

II. CONTROLLED GAIN CURRENT AND DIFFERENTIAL VOLTAGE AMPLIFIER

We identified lack of the voltage gain controllability in many recently introduced active elements [1] and find similarity of our approach to some discussed elements, of course without possibility of voltage gain control or even without any control. The most similar active elements are: so-called current differencing differential input buffered amplifier (CDDIBA), current differencing differential input differential output buffered amplifier (CDDIDIBA), current differencing operational amplifier (CDOA) and current voltage differential input buffered amplifier (CVDIBA). All discussed elements are based on two partial sections (current differencing unit [1], [25] and differential output voltage buffer in most cases). The similarity of our solution to above discussed elements consists of using of voltage differencing input of second section of active element. Nevertheless, the rest of significant characters is different. We utilized only one current input terminal p (not current differencing unit, which utilizing two ports), auxiliary terminal (output of section of current amplifier) z , auxiliary terminal v (voltage terminal) and output terminal w . Two supplementary terminals V_{SETA} and V_{SETB} provide voltage

control of parameters (current gain B and voltage gain A). Similar element, so-called controlled gain current and voltage amplifier (CG-CVA), was firstly discussed in [38]. However, the name for this modification was not clear and therefore we called this device as the controlled gain current and differential voltage amplifier (CG-CDVA). Discussed active element is shown in Fig. 1. Basic principle of operation is obvious: input current is amplified by controllable current gain $-I_p B = I_z$ and through impedance connected to terminal z transferred to voltage output as amplified difference $(V_v - V_z) A = V_w$.

III. PROPOSED TRIANGLE AND SQUARE WAVE GENERATOR

Key block of the whole generator is comparator with hysteresis (so-called Schmitt trigger [33]). Our active element has capabilities to realize the comparator using controllable voltage amplifier section without necessity of any additional resistor, see Fig. 2.

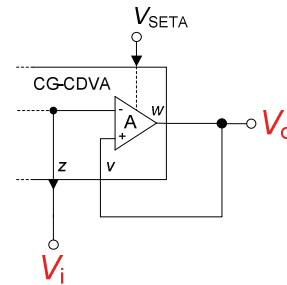


Figure 2. Comparator with hysteresis (partial section of CG-CDVA).

A positive feedback causes operation of output at two saturation levels ($\pm V_{o_sat}$) defined by catalogue parameters (between ± 1.3 to ± 1.8 V) [39]. Relation between input threshold voltages (marked as $\pm V_i$) and output saturation $\pm V_{o_sat}$ level has form:

$$\left(\mp V_{o_sat}\right) = \frac{A}{A-1} (\pm V_i) \cong \frac{10^{-2(V_{SETA}+1)}}{10^{-2(V_{SETA}+1)} - 1} (\pm V_i), \quad (1)$$

High gain A means equality of V_o (referencing value) to V_i causing turnover of V_o from $-V_{o_sat}$ to $+V_{o_sat}$ respectively. Equation $A = 10^{-2(V_{SETA}+1)}$ [39] between voltage gain A and control voltage V_{SETA} is valid and allows adjusting of gain from -40 to 40 dB ($0.01x$ to $100x$) by negative DC voltage changed from 0 to -2 V [39]. DC transfer characteristics of the comparator with hysteresis for selected gains A are shown in Fig. 3. However, term $A/(A-1)$ is valid only in ideal case and is subject to significant inaccuracy. Therefore, very accurate calculations require knowledge of DC transfer characteristic shown in Fig. 3.

Triangle and square wave generator based on CG-CDVA is depicted in Fig. 4. Maximal current through capacitor is proportional $(1/R)$ to value limited by $V_{SQ} = \pm V_{o_sat}$ and current gain B of current amplifier section. Linear dynamical range of current amplifier is sufficient and current limitation occurs at higher level than saturation limitation of V_o (voltage amplifier) because current gain is quite low (units) and dynamical range of current amplifier is very favorable therefore it influences

charging of C minimally. Maximal current limitation is given by:

$$I_{C_max} = \pm \left(\frac{V_{SQ}}{R} + I_{duty} \right) B, \quad (2)$$

where voltage limitation given by saturation level can be found above ± 1 V [39] and highly depends on A (1).

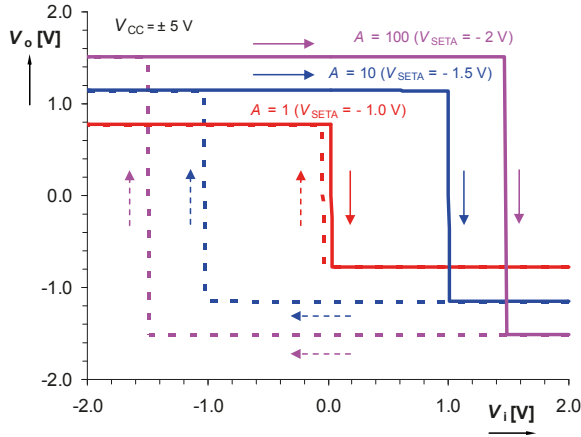


Figure 3. Simulated DC transfer characteristics of the comparator with hysteresis (Schmitt trigger) based on partial section of CG-CDVA.

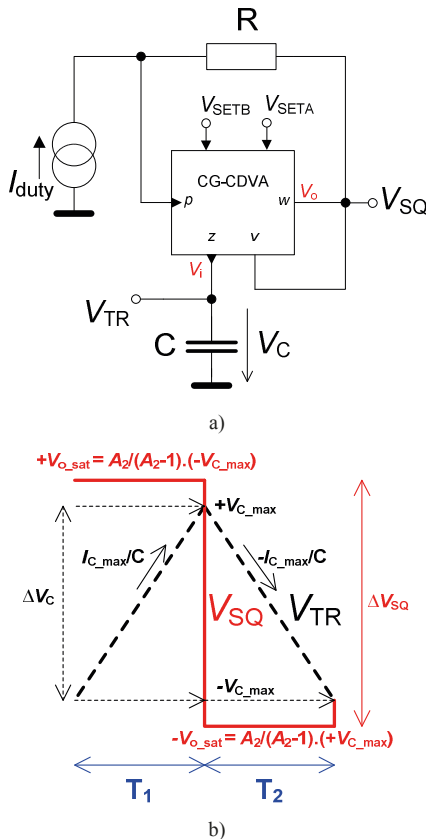


Figure 4. Simple triangle and square generator using CG-CDVA: a) proposed circuit, b) output waveforms, time sections and thresholds.

The change of voltage across the capacitor increases linearly from $-V_{C_max}$ to $+V_{C_max}$ (reference voltage thresholds of the comparator) respectively:

$$\Delta V_C = +V_{C_max} - (-V_{C_max}) = 2V_{C_max}. \quad (3)$$

where difference between V_C and V_{SQ} is given by equation (1):

$$\pm V_{C_max} = \left(\frac{A-1}{A} \right) (\mp V_{o_sat}). \quad (4)$$

Output square wave voltage changes between saturation levels of output of comparator:

$$\Delta V_{SQ} = +V_{o_sat} - (-V_{o_sat}) = 2V_{o_sat}. \quad (5)$$

Therefore we can generalize (3)-(5) to:

$$\Delta V_{SQ} = \left(\frac{A}{A-1} \right) \Delta V_C. \quad (6)$$

It is very easy to derive equation for repeating frequency (f_0) because voltage across capacitor increases or decreases linearly between $\pm V_{C_max}$ limits all the time. Charging and discharging intervals (Fig. 4b) can be derived from following expressions by help of (2) as:

$$2V_{o_sat} \left(\frac{A-1}{A} \right) = \frac{I_{C_max}}{C} T_1 = \frac{\left(\frac{+V_{o_sat}}{R} + I_{duty} \right) B}{C} T_1, \quad (7)$$

$$2V_{o_sat} \left(\frac{A-1}{A} \right) = -\frac{I_{C_max}}{C} T_2 = \frac{\left(\frac{V_{o_sat}}{R} - I_{duty} \right) B}{C} T_2. \quad (8)$$

Both intervals are given by:

$$T_1 = \frac{2V_{o_sat} \left(\frac{A-1}{A} \right) RC}{(V_{o_sat} + I_{duty} R) B}, \quad (9)$$

$$T_2 = \frac{2V_{o_sat} \left(\frac{A-1}{A} \right) RC}{(V_{o_sat} - I_{duty} R) B}. \quad (10)$$

Repeating frequency and duty cycle have forms:

$$f_0 = \frac{1}{T_1 + T_2} = \frac{B(V_{o_sat} + I_{duty} R)(V_{o_sat} - I_{duty} R)}{4RC(V_{o_sat})^2} \left(\frac{A}{A-1} \right), \quad (11)$$

$$D = \frac{T_1}{T} = \frac{1}{2} \left(1 - \frac{I_{duty} R}{V_{o_sat}} \right). \quad (12)$$

Theoretical limits of I_{duty} ($D = 0; 100\%$) are $\pm V_{o_sat}/R$. Repeating frequency is controllable without affect on duty cycle. Equation (11) simplifies to following form for $D = 50\%$ without DC current source ($I_{duty} = 0$):

$$f_0 = \frac{1}{T} = \frac{B}{4RC} \left(\frac{A}{A-1} \right) \cong \frac{V_{SETB}}{4RC} \left(\frac{10^{-2(V_{SETA}+1)}}{10^{-2(V_{SETA}+1)} - 1} \right). \quad (13)$$

Repeating frequency is controllable by current gain B directly driven by V_{SETB} [40].

IV. SIMULATION RESULTS

Preliminary simulation results were given by PSpice program with macromodels of current-mode multiplier EL2082 [40] (classified as obsolete by manufacturer but available and sufficient for preliminary behavioral modeling) and voltage controllable amplifier VCA810 [39], that were used for behavioral modeling of CG-CDVA element. Parameters of design of the generator are following: $R = 390 + 95 \Omega$ (intrinsic resistance of current input of EL2082 [40]), $C = 100 \text{ pF} + 6 \text{ pF}$ (parasitic [39], [40]), $B = 1$ ($V_{SETB} = 1 \text{ V}$), $A = 10$ ($V_{SETA} = -1.5 \text{ V}$), $D = 50\%$ ($I_{duty} = 0 \text{ mA}$), term $A/(A-1) \approx 1$ in accordance with Fig. 3.

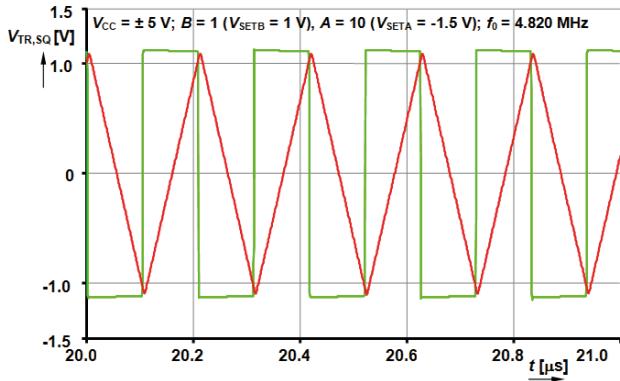


Figure 5. Simulated transient responses of both output voltages.

Discussed design was focused on application in frequency band of units of MHz. Ideal calculation of repeating frequency (including 95Ω of intrinsic resistance [40]) achieves $f_0 = 4.863 \text{ MHz}$. Simulated value of f_0 was 4.820 MHz . Simulated transient responses of both outputs are depicted in Fig. 5. Simulations provided value of $\pm V_{o_sat}$ equal to $\pm 1.15 \text{ V}$.

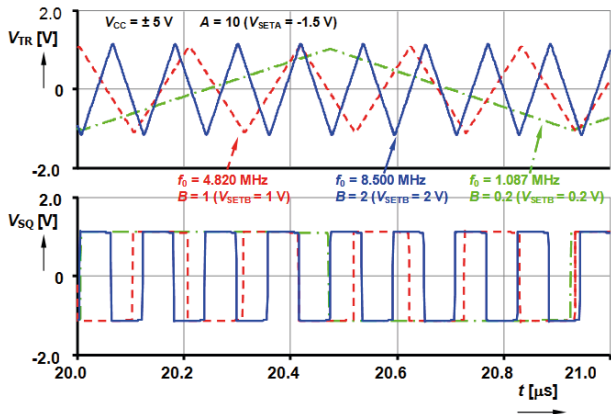


Figure 6. Simulated transient responses for three different values of repeating frequency and current gain B .

Proposed oscillator has also very favorable adjustable features, i.e. electronic control of repeating frequency is very simple (11). We tested adjusting of current gain B in range from 0.1 to 2.7 (V_{SETB} between 0.1 to 3 V) and repeating frequency was adjusted from 0.56 MHz to 11.39 MHz . Corresponding results are in Fig. 6 where waveforms for three selected discrete frequencies (three values of B) are shown.

Dependence of repeating frequency on current gain B and control voltage V_{SETB} is presented in Fig. 7. Important difference between ideal and simulated trace for higher gain B is caused by nonlinear dependence of current gain on V_{SETB} and finite frequency features of used VCA810 (GBW trace does not stay flat perfectly for frequencies above 10 MHz [39], and impact of finite slew rate is also very important).

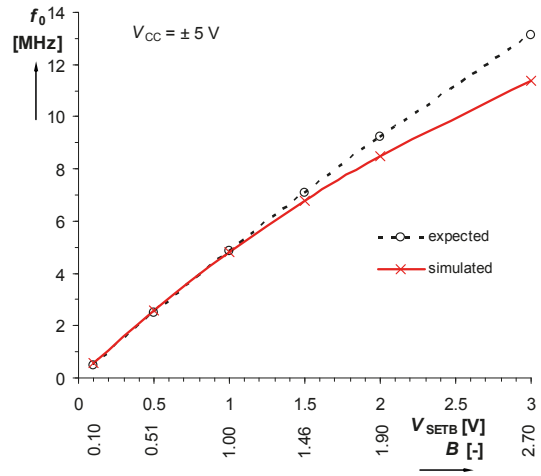


Figure 7. Dependence of repeating frequency on control voltage V_{SETB} and current gain B .

An example of operation with different duty cycle ($D = 25\%$) is shown in Fig. 8, for $f_0 = 3.528 \text{ MHz}$.

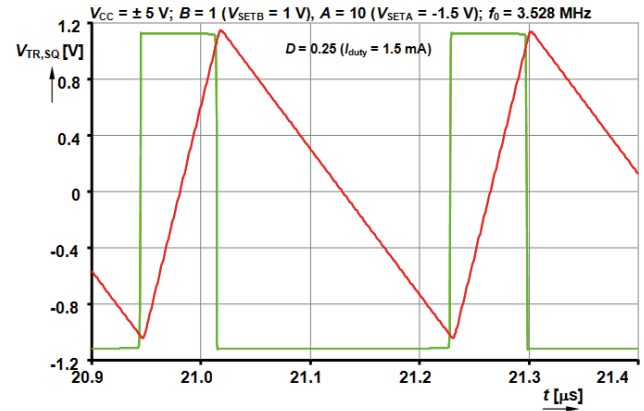


Figure 8. Simulated transient responses of non-symmetric ramps.

Amplitudes of produced signals in dependence on repeating frequency are shown in Fig. 9.

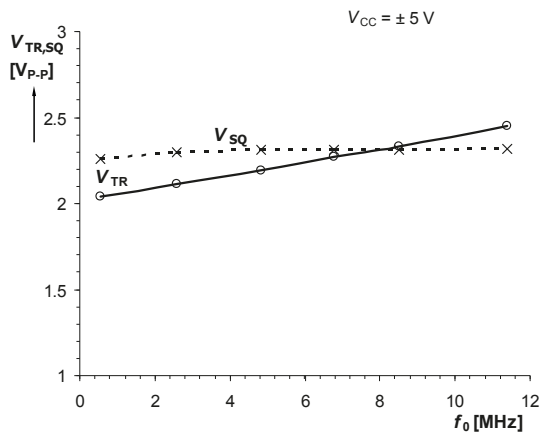


Figure 9. Dependences of output amplitudes on repeating frequency.

V. CONCLUSION

Novel adjustable active element which combines two ways of control (current and voltage gain) was introduced and its behavioral model discussed. A simple application example of advantageous features of proposed active element was discussed and analyzed in detail. Proposed generator offers very simple circuitry, minimal number of active and passive elements and simple electronic control by DC voltage. Range of repeating frequency control wider than 10 MHz was obtained by simulations with suitable behavioral model of proposed active element employing commercially available devices. It confirms workability of circuit and validity of theoretical assumptions. Future work supposes proposal of CMOS structure of CG-CDVA and additional tests.

REFERENCES

- [1] D. Biolek, R. Senani, V. Biolkova, Z. Kolka, "Active elements for analog signal processing: Classification, Review and New Proposals," *Radioengineering*, vol. 17, no. 4, pp. 15–32, 2008.
- [2] A. Sedra, K. C. Smith, "A second generation current conveyor and its applications," *IEEE Transaction on Circuit Theory*, vol. CT-17, no. 2, pp. 132–134, 1970.
- [3] A. Fabre, O. Saaid, F. Wiest, C. Boucheron, "High frequency applications based on a new current controlled conveyor," *IEEE Trans. on Circuits and Systems - I*, vol. 43, no. 2, pp. 82–91, 1996.
- [4] J. W. Horng, "A sinusoidal oscillator using current-controlled current conveyors," *Int. Journal of Electronics*, vol. 88, no. 6, pp. 659–664, 2001.
- [5] R. L. Geiger, E. Sánchez-Sinencio, "Active filter design using operational transconductance amplifiers: a tutorial," *IEEE Circ. and Devices Magazine*, vol. 1, pp. 20–32, 1985.
- [6] A. Rodríguez-Vázquez, B. Linares-Barranco, J. L. Huertas, E. Sánchez-Sinencio, E. "On the design of voltage-controlled sinusoidal oscillators using OTAs," *IEEE Trans. Circuits and Systems*, vol. 37, no. 2, pp. 198–211, 1990.
- [7] B. Linares-Barranco, A. Rodríguez-Vázquez, E. Sánchez-Sinencio, J. L. Huertas, "CMOS OTA-C high-frequency sinusoidal oscillators," *IEEE Journal of Solid-State Circuits*, vol. 26, no. 2, pp. 160–165, 1991.
- [8] W. Surakampontorn, W. Thitimajshima, "Integrable electronically tunable current conveyors," *IEE Proceedings-G*, vol. 135, no. 2, pp. 71–77, 1988.

- [9] A. Fabre, N. Mimeche, "Class A/AB Second-generation Current Conveyor with Controlled Current Gain," *Electronics Letters*, vol. 30, no. 16, pp. 1267–1268, 1994.
- [10] G. Soulitis, C. Psychalinos, "Electronically controlled multiphase sinusoidal oscillators using current amplifiers," *International Journal of Circuit Theory and Applications*, vol. 37, no. 1, pp. 43–52, 2009.
- [11] N. Herencsar, A. Lahiri, K. Vrba, J. Koton, "An electronically tunable current-mode quadrature oscillator using PCAs," *Int. Journal of Electronics*, vol. 99, no. 5, pp. 609–621, 2012.
- [12] J. Jerabek, J. Koton, R. Sotner, K. Vrba, "Adjustable band-pass filter with current active elements: two fully-differential and single-ended solutions," *Analog Integrated Circuits and Signal Processing*, vol. 74, no. 1, pp. 129–139, 2013.
- [13] W. Tangsrirat, "Electronically Tunable Multi-Terminal Floating Nullor and Its Application," *Radioengineering*, vol. 17, no. 4, pp. 3–7, 2008.
- [14] D. Biolek, A. Lahiri, W. Jaikla, M. Siripruchyanun, J. Bajer, "Realisation of electronically tunable voltage-mode/current-mode quadrature sinusoidal oscillator using ZC-CG-CDBA," *Microelectronics Journal*, vol. 42, no. 10, pp. 1116–1123, 2011.
- [15] W. Tangsrirat, T. Pukkalanun, "Digitally programmable current follower and its applications," *AEU – International Journal of Electronics and Communications*, vol. 63, no. 5, pp. 416–422, 2009.
- [16] H. Alzahr, N. Tasadduq, O. Al-Ees, F. Al-Ammari, "A complementary metal–oxide semiconductor digitally programmable current conveyor," *International Journal of Circuit Theory and Applications*, available online, 2011, DOI: 10.1002/cta.786.
- [17] S. Minaei, O. K. Sayin, H. Kuntman, "A new CMOS electronically tunable current conveyor and its application to current-mode filters," *IEEE Trans. on Circuits and Systems - I*, vol. 53, no. 7, pp. 1448–1457, 2006.
- [18] A. Marcellis, G. Ferri, N. C. Guerrini, G. Scotti, V. Stornelli, A. Trifiletti, "The VGC-CCII: a novel building block and its application to capacitance multiplication," *Analog Integrated Circuits and Signal Processing*, vol. 58, no. 1, pp. 55–59, 2009.
- [19] M. Kumngern, S. Junnapiya, "A sinusoidal oscillator using translinear current conveyors," in *Proc. Asia Pacific Conf. on Circuits and Systems APPCAS2010*, Kuala Lumpur, 2010, pp. 740–743.
- [20] R. Prokop, V. Musil, "Modular approach to design of modern circuit blocks for current signal processing and new device CCTA," in *Proc. Conf. on Signal and Image Processing IASTED*, Anaheim, 2005, pp. 494–499.
- [21] M. Siripruchyanun, W. Jaikla, "Current controlled current conveyor transconductance amplifier (CCCCTA): a building block for analog signal processing," *Electrical Engineering*, vol. 90, no. 6, pp. 443–453, 2008.
- [22] D. Biolek, "CDTA – building block for current-mode analog signal processing," in *Proc. European Conf. Circuits Theory and Design ECCTD03*, Krakow, 2003, pp. 397–400.
- [23] W. Jaikla, A. Lahiri, "Resistor-less current-mode four-phase quadrature oscillator using CCCDTAs and grounded capacitors," *AEU - International Journal of Electronics and Communications*, vol. 66, no. 3, pp. 214–218, 2011.
- [24] Ch. Sakul, W. Jaikla, K. Dejhan, "New resistorless current-mode Quadrature Oscillators Using 2 CCCDTAs and Grounded Capacitors," *Radioengineering*, vol. 20, no. 4, pp. 890–896, 2011.
- [25] D. Biolek, V. Biolkova, "Current-mode CDTA-based comparators," in *Proc. of the 13th Int. Conf. on Electronic Devices and Systems EDS IMAPS*, Brno, 2006, pp. 6–10.
- [26] A. De Marcellis, C. Di Carlo, G. Ferri, V. Stornelli, "A CCII-based wide frequency range square waveform generator," *International Journal of Circuit Theory and Applications*, available online, 2011, DOI: 10.1002/cta.781.
- [27] H-Ch. Chien, "Voltage-controlled dual slope operation square/triangular wave generator and its application as a dual mode operation pulse width modulator employing differential voltage current conveyors," *Microelectronics Journal*, vol. 43, no. 12, pp. 962–974, 2012.

- [28] B. Almashary, H. Alhokail, "Current-mode triangular wave generator using CCIIIs," *Microelectronics Journal*, vol. 31, no. 4, pp. 239-243, 2000.
- [29] D. Pal, A. Srinivasulu, B. B. Pal, A. Demosthenous, B. N. Das, "Current Conveyor-Based Square/Triangular Waveform Generators With Improved Linearity," *IEEE Transaction on Instrumentation and Measurement*, vol. 58, no. 7, pp. 2174-2180, 2009.
- [30] A. S. Saque, M. M. Hossain, W. A. Davis, H. T. Russell, R. L. Carter, "Design of sinusoidal, triangular, and square wave generator using current feedback amplifier (CFOA)," in *Proc. of IEEE Region 5 Conference*, Kansas City, 2008, pp. 1-5.
- [31] S. Minaei, E. Yuce, "A simple Schmitt trigger circuit with grounded passive elements and its application to square/triangular wave generator," *Circuits, Systems, and Signal Processing*, vol. 31, no. 3, pp. 877-888, 2012.
- [32] Y. K. Lo, H. C. Chien, "Switch-controllable OTRA-based square/triangular waveform generator," *IEEE Transaction on Circuits Systems and Signal Processing II*, vol. 54, no. 12, pp. 1110-1114, 2007.
- [33] W. S. Chung, H. Kim, H. W. Cha, H.J. Kim, "Triangular/square-wave generator with independently controllable frequency and amplitude," *IEEE Transactions on Instrumentation and Measurement*, vol. 54, no. 1, pp. 105-109, 2005.
- [34] M. Siripruchyanun, P. Wardkein, "A full independently adjustable, integrable simple current controlled oscillator and derivative PWM signal generator," *IEICE Trans. Fundam. Electron. Commun. Comput. Sci.*, vol. E86-A, no. 12, pp. 3119-3126, 2003.
- [35] J. Kumbun, M. Siripruchyanun, "MO-CTTA-based electronically controlled current-mode square/triangular wave generator," in *Proc. of the 1st International Conf. on Technical Education (ICTE2009)*, 2010, pp. 158-162.
- [36] P. Silapan, M. Siripruchyanun, "Fully and electronically controllable current-mode Schmitt triggers employing only single MO-CCDTA and their applications," *Analog Integrated Circuits and Signal Processing*, vol. 68, no. 11, pp. 111-128, 2011.
- [37] T. Srisakul, P. Silapan, M. Siripruchyanun, "An electronically controlled current-mode triangular/square wave generator employing MO-CCCCTAs," in *Proc. of the 8th Int. Conf. on Electrical Engineering/ Electronics, Computer, Telecommunications, and Information Technology*, 2011, pp. 82-85.
- [38] R. Sotner, J. Jerabek, N. Herencsar, Z. Hrubos, T. Dostal, K. Vrba, "Study of Adjustable Gains for Control of Oscillation Frequency and Oscillation Condition in 3R-2C Oscillator," *Radioengineering*, vol. 21, no. 1, pp. 392-402, 2012.
- [39] Texas Instruments. VCA810H High Gain Adjustable Wideband, variable gain amplifier (datasheet), 2003, 30 p., accessible on [www: http://focus.ti.com/lit/ds/sbos275f/sbos275f.pdf](http://focus.ti.com/lit/ds/sbos275f/sbos275f.pdf)
- [40] Intersil. E.L2082 CNC Current-mode multiplier (datasheet), 1996, 14 p., accessible on [www: http://www.intersil.com/data/fn/fn7152.pdf](http://www.intersil.com/data/fn/fn7152.pdf)

[22] SOTNER, R., JERABEK, J., HERENCŠAR, N., DOSTAL, T., VRBA, K. Design of Z-copy controlled- gain voltage differencing current conveyor based adjustable functional generator. *Microelectronics Journal*, 2015, vol. 46, no. 2, p. 143-152. ISSN: 0026-2692.



ELSEVIER

Contents lists available at ScienceDirect

Microelectronics Journal

journal homepage: www.elsevier.com/locate/mejo

Design of Z-copy controlled-gain voltage differencing current conveyor based adjustable functional generator



Roman Sotner^{a,*}, Jan Jerabek^b, Norbert Herencsar^b, Tomas Dostal^c, Kamil Vrba^b

^a Department of Radio Electronics, Brno University of Technology, Brno, Technická 12, 616 00 Czech Republic

^b Department of Telecommunications, Brno University of Technology, Brno, Technická 12, 616 00 Czech Republic

^c Department of Electrical Engineering and Computer Science, College of Polytechnics Jihlava, Jihlava, Tolsteho 16, 586 01 Czech Republic

ARTICLE INFO

Article history:

Received 14 May 2014

Received in revised form

1 November 2014

Accepted 27 November 2014

Available online 29 December 2014

Keywords:

Square and triangular wave generator

PWM

Differential mode

Electronic Control

Voltage- and current-mode

Transconductance

Current gain

Voltage differencing current conveyor

ABSTRACT

This paper introduces interesting active element and its application in the field of square and triangular wave generators. Active element, so-called Z-Copy Controlled Gain Voltage Differencing Current Conveyor (ZC-CG-VDCC), has availability of three mutually independently and electronically adjustable parameters (transconductance, intrinsic resistance of the current input terminal and current gain between two terminals) that are very popular for control of applications today. In addition, a proposed device utilizes very useful z-copy (additional auxiliary terminal) features and two terminals providing voltage difference. All mentioned features are beneficial in mixed-mode circuit synthesis and design of adjustable applications (active filters, oscillators, generators, modulators, etc.). Electronically adjustable properties of the device are involved in the design of an adjustable generator. The generator provides voltage- and current-mode square wave outputs that can be also used for differential square wave output when very simply modified. Application of the generator in simple pulse width modulator (PWM) is also introduced. A detailed analysis and Spice simulation results are given and main features of the circuits are compared to electronically controllable solutions of recent development in this field.

© 2014 Elsevier Ltd. All rights reserved.

1. Introduction

Applications of electronically controllable active elements [1] in the field of signal generation allow interesting benefits such as: simple controllability of oscillation/repeating frequency, independent control of oscillation condition, control of output amplitudes (or ratios of amplitudes), duty cycle control, etc. by electronically adjustable parameter that is controlled externally by DC bias current or voltage [1]. We focused our attention on electronically controllable functional (triangular and square wave) generator with differential square wave outputs in this work because square wave signals are important in many analog and digital communication subsystems (clock generators, pulse width modulators, DC–DC converters, TTL and CMOS logic, etc.). Differential outputs are beneficial mainly in low-voltage technologies (output level rapidly decreases with decreasing power supply voltage – even tens of mV in some cases) due to availability of two-times higher output level and lower additional common-mode distortion and better noise immunity. Table 1 compares several recently reported solutions of generators [2–11]. We focused our overview on

electronically controllable solutions only. There are two ways of understanding the number of active devices. Table 1 includes solutions based on discrete active elements and also active elements involving several (typically two) active subparts, in Table 1 noted in separated columns.

Circuit presented in [2] allows differential triangle and square wave outputs. However, circuit requires two active elements based on composition of two subparts used in frame of the voltage differencing buffered/inverted amplifiers (VDDBA/VDIBA). Therefore, solution presented here seems to be simpler. Chung et al. [3] utilizes three OTAs (controllable by bias currents), two grounded resistors and capacitor. A number of active elements (considered also subparts of our device) in [3] is also higher than in our case. Very similar solution to [3] was also proposed by Siripruchyanun et al. [4]. An approach presented by Kumbun et al. [5] is based on two so-called multiple-output through transconductance amplifiers (MO-CTTAs) and grounded capacitor. These MO-CTTAs are complemented by current follower with two inputs having special features ($I_{inp+} = -I_{inp-}$) and output transconductance section. Therefore, our solution is less complex than realization in [5]. Silapan et al. [6] and Sristakul et al. [7] also proposed interesting solutions (similar to [5]), where two multiple-output current controlled current differencing amplifiers (MO-CCDTAs) and grounded capacitor were used. The CDTA device is also based

* Corresponding author.

E-mail address: sotner@feec.vutbr.cz (R. Sotner).

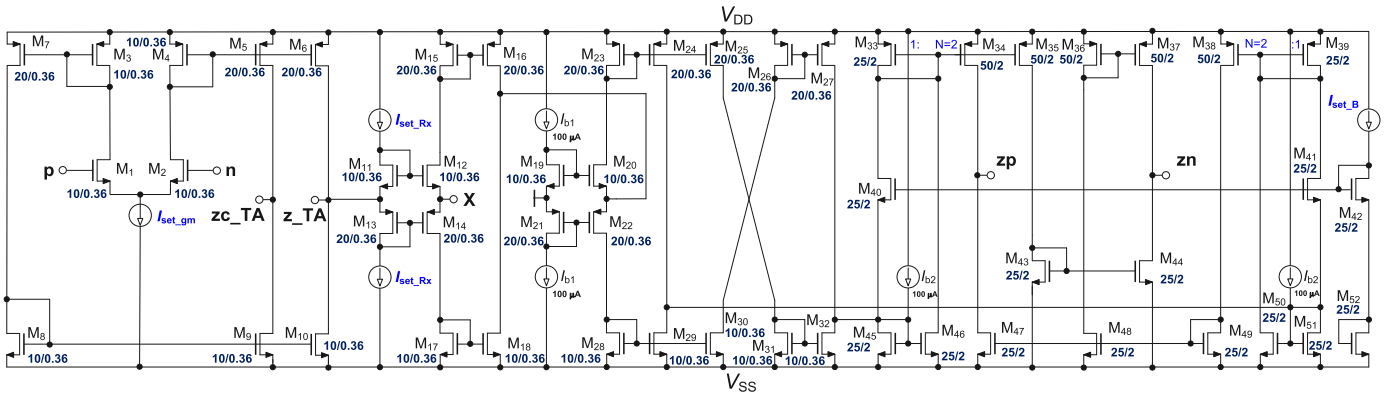


Fig. 2. Proposed CMOS structure of ZC-CG-VDCC element ($V_{DD} = -V_{SS} = 1\text{ V}$).

Table 2
Selected important features of the ZC-CG-VDCC CMOS model.

Controllable parameters	
parameter	tested range of adjusting
current gain $I_{z_{p,n}}/I_x$ (B [-])	0.36–3.76 ($I_{set_B} = 100\ \mu\text{A} - 20\ \mu\text{A}$, $BW = 39\text{--}73\ \text{MHz}$)
transconductance $I_{z_TA}, zc_TA/V_p$ (g_m [μS])	255–1919 ($I_{set_gm} = 10\ \mu\text{A} - 150\ \mu\text{A}$, $BW = 209\text{--}505\ \text{MHz}$)
intrinsic resistance V_x/I_x (R_x [$\text{k}\Omega$])	2.53–0.451 ($I_{set_Rx} = 10\ \mu\text{A} - 150\ \mu\text{A}$)
Other DC performances ($I_{set_gm} = I_{set_Rx} = I_{set_B} = 100\ \mu\text{A}$)	
parameter	value
V_{z_TA}/V_x [-]	0.98
$R_{p,n}$ [Ω]	1E20
$R_{\pm z_TA}, zc_TA$ [$\text{k}\Omega$]	34.6
R_x [Ω]	533
R_{zp} [$\text{k}\Omega$]	55.0
R_{zn} [$\text{k}\Omega$]	53.1
Other AC performances ($I_{set_gm} = I_{set_Rx} = I_{set_B} = 100\ \mu\text{A}$)	
parameter	value
$R_{\pm z_TA}$ (R_{zc_TA}) [$\text{k}\Omega$]	> 35 for $I_{set_gm} \leq 100\ \mu\text{A}$ ($f < 10\ \text{MHz}$)
R_{zp}, R_{zn} [$\text{k}\Omega$]	> 50 for $I_{set_B} \leq 100\ \mu\text{A}$ ($f < 1\ \text{MHz}$)
$C_{p,n}$ [fF]	30
$C_{\pm z_TA}, C_{zc_TA}$ [fF]	110
C_{zp} [fF]	120
C_{zn} [fF]	190

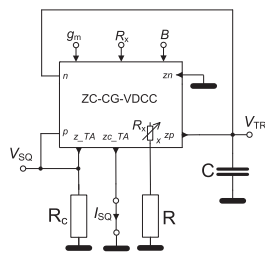


Fig. 3. ZC-CG-VDCC-based triangle and square wave generator.

Table 3
Design parameters of the generator.

$C = 40\ \text{pF}$
$R_c = 5\ \text{k}\Omega$
$R = 1\ \text{k}\Omega$
$R_x = 1\ \text{k}\Omega$ ($I_{set_Rx} = 34\ \mu\text{A}$)
$g_m = 1\ \text{mS}$ ($I_{set_gm} = 54\ \mu\text{A}$)
$B = 1$ ($I_{set_B} = 81\ \mu\text{A}$)

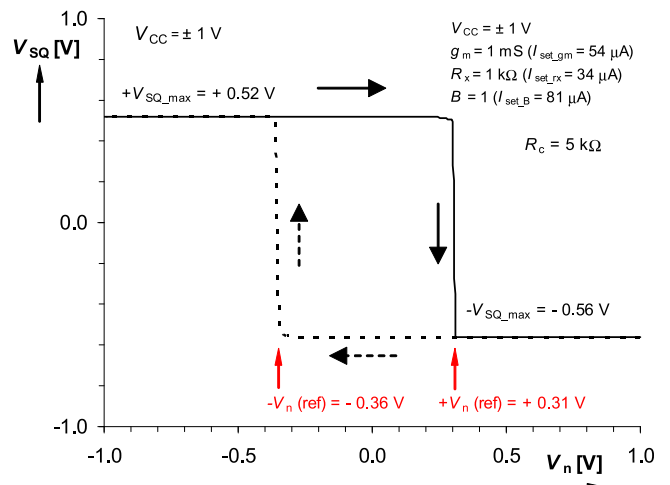


Fig. 4. DC characteristic of the comparator as part of ZC-CG-VDCC.

very complex, the solutions of generators discussed in [5–7] also require two active elements, which already combine at least two elementary building sub-blocks. Therefore, generator utilizing only one ZC-CG-VDCC seems to be simpler and more flexible from the controllable features point of view. Our solution offers similar

benefits as some of the previously reported circuits, but in addition it allows current output of square wave signal as well, which (after transformation to voltage through resistor) can be useful for differential (symmetrical) purposes.

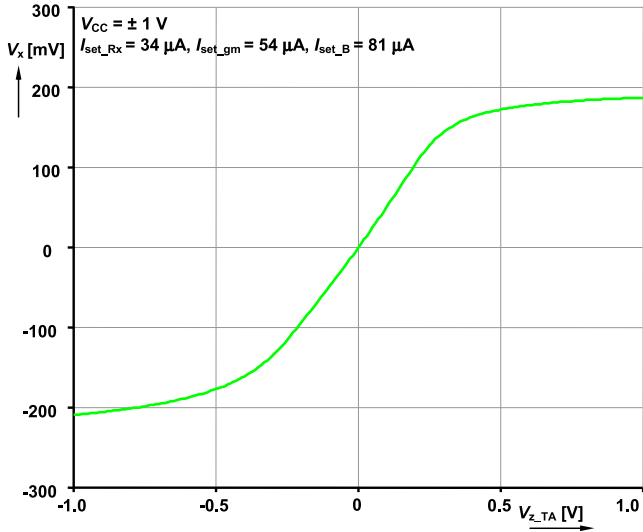


Fig. 5. DC transfer characteristic of the transfer between V_{z_TA} and V_x ($R=1\text{ k}\Omega$).

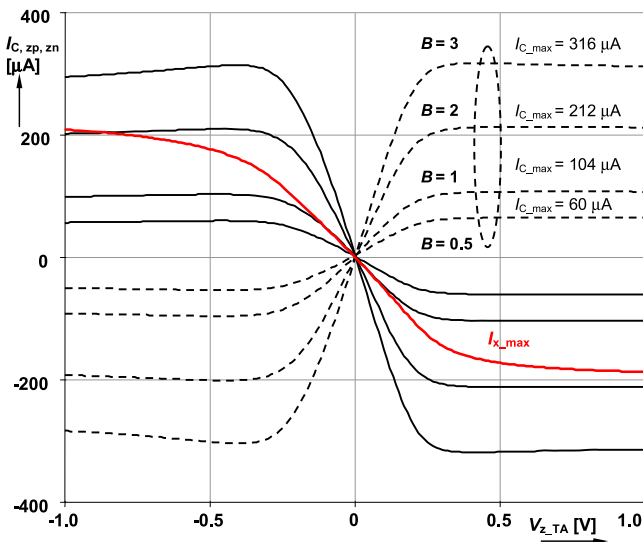


Fig. 6. Simulated corners of DC transfer characteristic required for explanation of integrator functionality and exact determination of repeating frequency.

Organization of this work is following: Section 1 explains the reasons for presented development and features (and comparison) of several important hitherto published solutions. Basic behavior of the proposed active device is explained in Section 2. Section 3 introduces and investigates design of a generator based on ZC-CG-VDCC in detail, including graphical simulation results (step-by-step for better understanding of principle) and simple experimental test. Concluding remarks and overall summarization of obtained results are given in Section 4.

2. Z-copy controlled gain voltage differencing current conveyor (ZC-CG-VDCC)

ZC-CG-VDCC is multi-terminal active device with three types of electronic control (three adjustable parameters of the active element are available and controllable mutually independently). Behavior of the model of ZC-CG-VDCC is shown in Fig. 1. In fact, there are two functional parts: operational transconductance amplifier (OTA) [1,14] followed by electronically controllable current conveyor of second generation (ECCII) [1,15–19]. The OTA has typical adjustable parameter referred as transconductance (g_m) [14]. The ECCII part offers typically one adjustable parameter: current input intrinsic resistance (R_x) [15] of terminal X or current gain between X and Z terminals (B) [16,17]. Rarely, these two parameters are adjustable in frame of one active device [18–21]. All discussed parameters (g_m , R_x , B) are controllable by DC bias currents (I_{set_gm} , I_{set_Rx} , I_{set_B}). Our proposal combines all available ways of control in one compact solution that offers differential voltage input terminals (p , n), current input terminal (X), auxiliary high-impedance terminal (z_TA) and its direct copy (z_c_TA) [1] and two high-impedance current outputs (zp , zn).

A composition of two active elements in one structure means an additional complication in some point of view (realization from discrete components). However, standard CMOS VLSI design is beneficial for these and similar approaches to electronically controllable active elements, because design and realization is quite simple and increasing complexity of the active device is not so significant. Fig. 2 shows proposed CMOS structure [26] (aspect ratios in $\mu\text{m}/\mu\text{m}$ units of transistors are included directly in Fig. 2).

Eqs. (1–5) from [14,22–24] define behavior of this structure. Ideal relation between terminal voltages and currents is:

$$I_{z_TA} = I_{z_c_TA} = (V_p - V_n)g_m, \tag{1}$$

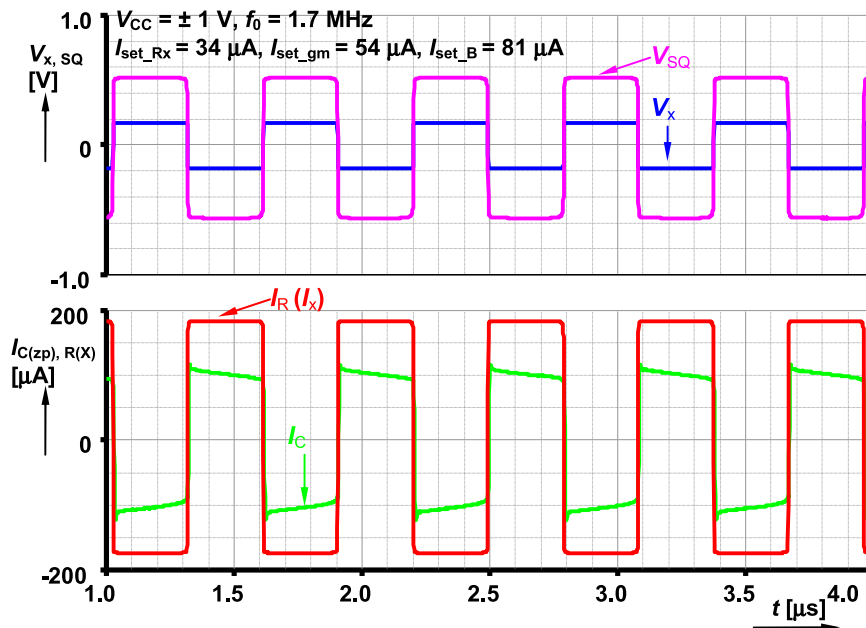


Fig. 7. Transient responses of currents and voltages thru/on important passive elements/nodes and parts (generator is running).

where

$$g_m = 2\sqrt{I_{set_gm}K_{Pn}\frac{W_{M1,2}}{L_{M1,2}}} \quad (2)$$

Multiplication by current mirrors causes two time higher output current (constant 2 in Eq. (2)) of the OTA section in Fig. 2. Control of the both remaining parameters is focused on ECCII part as:

$$V_x = V_{z_TA} + R_x I_x, \quad (3)$$

where

$$R_x = \frac{1}{\sqrt{I_{set_Rx}K_{Pn}(W_{M11,12}/L_{M11,12})} + \sqrt{I_{set_Rx}K_{Pp}(W_{M13,14}/L_{M13,14})}}, \quad (4)$$

and

$$I_{zp} = -I_{zn} = B \cdot I_x, \quad (5)$$

where $B = NI_{b2}/(2I_{set_B}) \cong I_{b2}/I_{set_B}$ (see Fig. 2). Technological constants K_{Pn} , K_{Pp} are given differently for specific technology (in our case: $K_{Pn} = 170.4 \mu A/V^2$ and $K_{Pp} = 35.7 \mu A/V^2$ [25] for CMOS TSMC LO EPI 0.18 μm technology). All parameters (bias currents/current sources) in Eqs. (1)–(5) are noted in Fig. 2. Parameters, ranges of

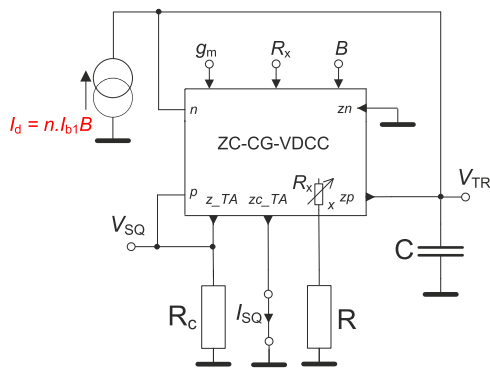


Fig. 8. Modification of the generator having possibility of duty cycle control.

control and other features (AC, DC, dynamics, time domain ...) of proposed ZC-CG-VDCC CMOS model are given in [26,27]. Some of them are summarized in Table 2.

3. Adjustable functional generator

Proposed ZC-CG-VDCC is also applicable in triangle and square wave (functional) generator by very simply way. The circuit is shown in Fig. 3 and it provides also current output of square wave signal. OTA part of the VDCC serves as Schmitt comparator [3,28] with hysteresis (parameters of the hysteresis window of the comparator are adjustable by transconductance g_m and I_{set_gm}) and ECCII part forms loss-less integrator with electronically adjustable time constant set by B .

A detailed explanation of principle is supplemented by design steps. The parameters of our design are summarized in Table 3.

The transconductance section with R_c forms Schmitt trigger (comparator), where ideal relation between thresholds and output

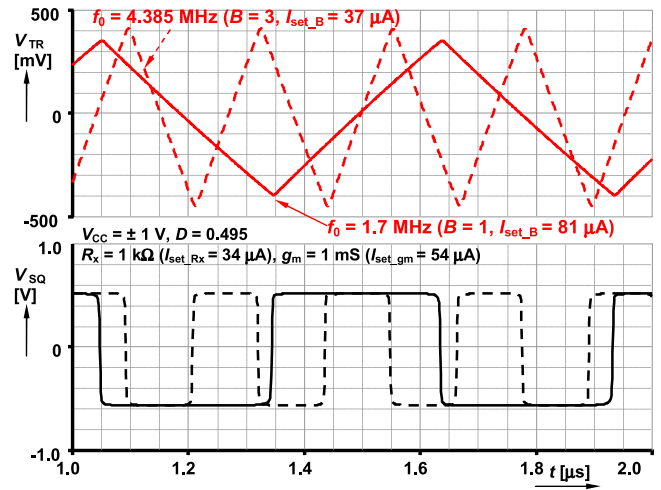


Fig. 10. Example of the tuning of the generator for two discrete values of B .

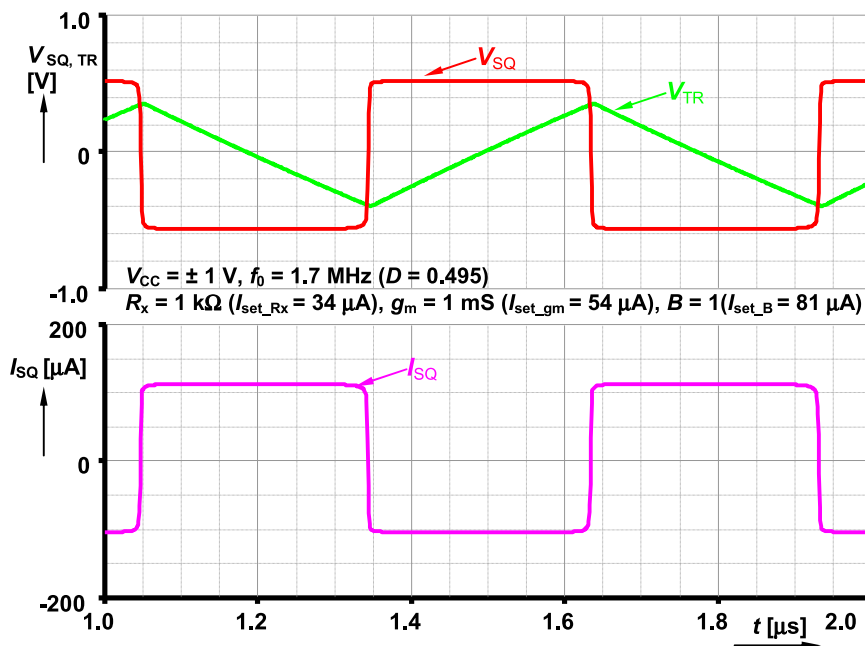


Fig. 9. Available output transient responses V_{SQ} , I_{SQ} and V_{TR} .

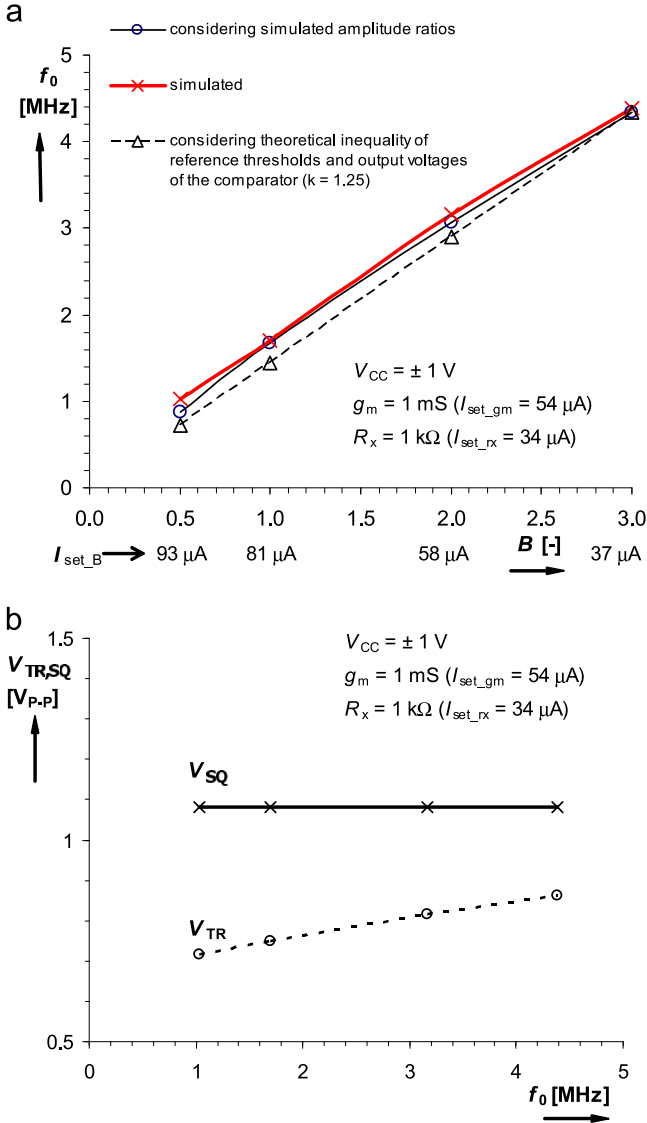


Fig. 11. Tuning of the generator: (a) repeating frequency vs. current gain and (b) output amplitudes in dependence on repeating frequency.

levels has form:

$$\pm V_{SQ_max} \cong \mp V_{TR_max} \cdot k = \mp V_{TR_max} \left(\frac{g_m R_C}{g_m R_C - 1} \right), \quad (6)$$

which gives $\pm V_{SQ_max} \cong \mp V_{TR_max} \cdot 1.25$. Starting information is saturation output voltage of the comparator. This voltage achieves two saturation corners $\pm V_{SQ_max}$ that are given by $V_{SQ_max} = 2I_{set_gm}R_C$. The constant 2 comes from current multiplication by current mirrors in OTA section (Fig. 2). Expected value is $V_{SQ_max} = 2 \times 54e-6 \times 5e3 = 0.54$ V. In accordance with (6), we can calculate estimated value of $V_{TR_max} = 0.54/1.25 = 0.43$ V. The dynamical characteristic of the comparator is depicted in Fig. 4.

Inaccuracy of thresholds and saturation corners is caused by parasitic voltage offset. Additionally, R_c is smaller than 5 k Ω because node of z_{TA} has DC resistance (internal parameters of CMOS model of VDCC $R_{z_TA} \approx 50$ k Ω (for $I_{set_gm} = 54$ μ A)). Therefore, overall value of the resistance in the node is smaller (≈ 4.55 k Ω and $k = 1.28$).

We can use limited dynamical ranges of active element or its subsection as advantages. It seems to be a good idea for generator design, because this application is nonlinear in general principle. The voltage at z_{TA} terminal is the same as V_{SQ} and because for CCII in

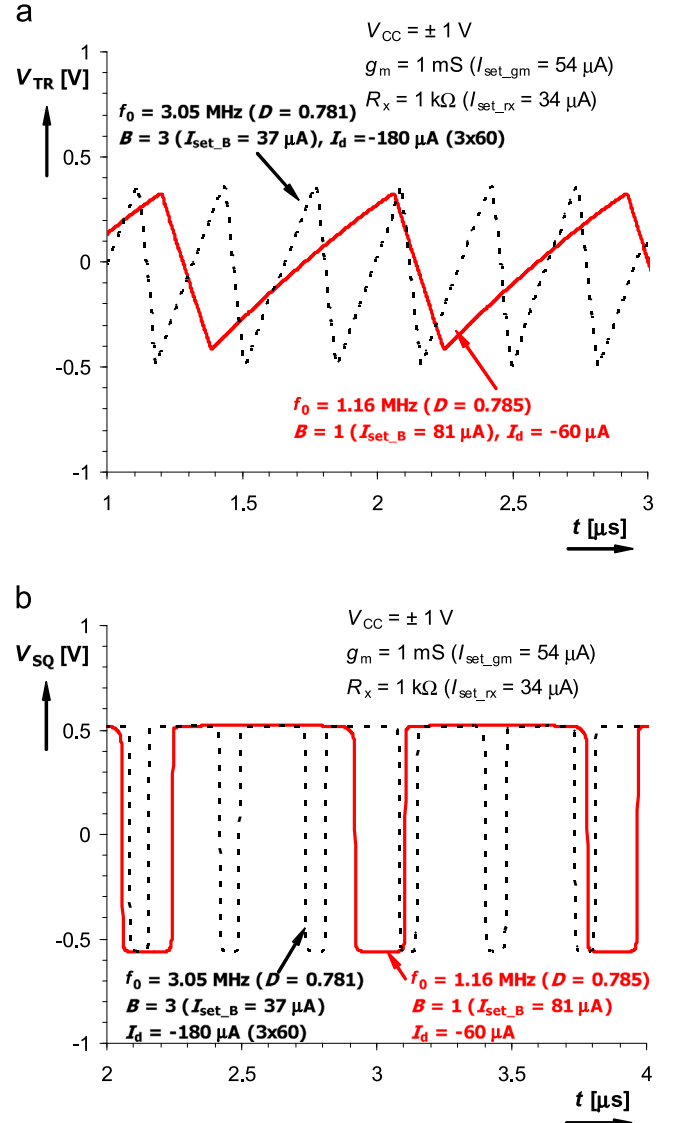


Fig. 12. Transient response for f_0 adjusting with $D=80\%$: (a) triangle wave and (b) square wave.

internal structure of VDCC it is valid that $V_{z_TA} = V_x + V_{R_x}$. Therefore, we can state that $I_x = I_R = (V_x + V_{R_x})/R'$, where $R' = R + R_x$ or also $I_x = I_R = V_x/R$. However, it is valid only if voltage V_{SQ_max} is found in linear range of $V_x = f(V_{z_TA})$ characteristic, see Fig. 5 (for $R = 1$ k Ω).

Input voltage V_{SQ_max} (input voltage in integrator point of view) is in saturation corner of voltage buffer between V_{z_TA} and V_x terminal of conveyer part of VDCC (we suppose theoretically $V_{SQ_max} = 0.54$ V at the output of comparator) and voltage at X terminal is near to 200 mV. This setting was ensured by the intended design of comparator to high output voltage (higher than linear range of V_x). This fact also defines current I_x , which is also out of linear range ($I_{x_max} = V_{x_max}/R = 0.2/1.10^3 = 200$ μ A) of characteristic I_{zp} (or $I_{zn}) = f(I_x)$. Maximal saturation current limit of I_C (capacitor) is defined by current sources I_{b1} in CMOS model (Fig. 2), in fact $I_{b1,B}$ (where I_{b1} in Fig. 2 has value 100 μ A) [26]. We can observe this behavior also in Fig. 6. The maximal current I_C charging the working capacitor is directly determined by $I_{b1,B}$.

We can determine equations for both half periods (in our case in Fig. 3) as:

$$\frac{2V_{TR_max}}{T_1} = \frac{I_{C_max}}{C}, \quad (7)$$

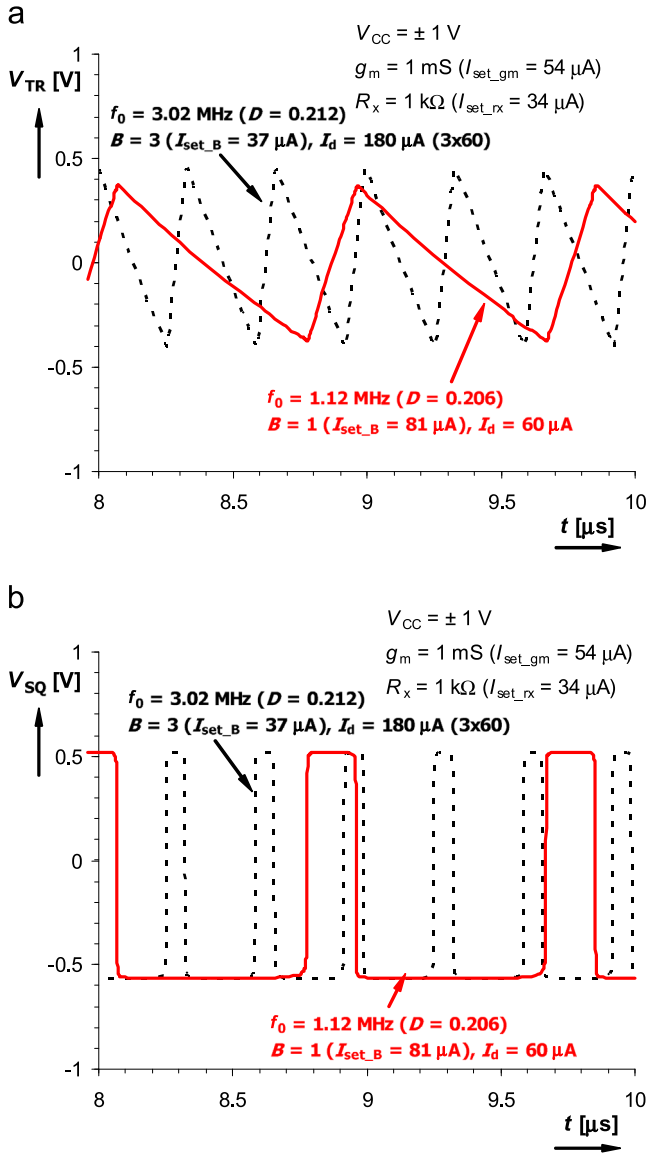


Fig. 13. Transient response for f_0 adjusting with $D=20\%$: (a) triangle wave and (b) square wave.

$$\frac{2V_{TR_max}}{T_2} = \frac{-I_{C_max}}{C}, \quad (8)$$

where

$$T_1 = \frac{2V_{TR_max}C}{I_{C_max}} \cong \frac{2V_{TR_max}C}{I_{b1}B}, \quad (9)$$

$$T_2 = \frac{2V_{TR_max}C}{-I_{C_max}} \cong \frac{2V_{TR_max}C}{-(-I_{b1}B)}, \quad (10)$$

and overall period is

$$T = T_1 + T_2 = \frac{4V_{TR_max}C}{I_{b1}B}. \quad (11)$$

Repeating frequency can be expressed as:

$$f_0 = \frac{I_{b1}B}{4V_{TR_max}C} = \frac{I_{b1}B}{4(I_{set_gm}2R_C/k)C}, \quad (12)$$

where k means real ratio of both produced amplitudes. The simulated results for above discussed design parameters are in Fig. 7. The results presented in Fig. 7 are important for further discussion. The results in Fig. 7 support validity of Eq. (12) and

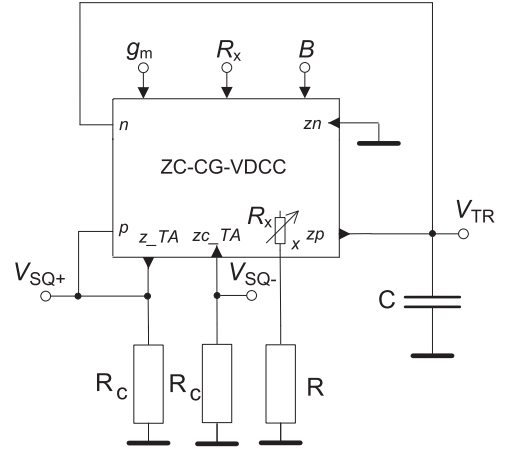


Fig. 14. Generator providing symmetrical (differential) square wave output (V_{SQ+} , V_{SQ-}).

further presumptions (Fig. 5) for design parameters. Repeating frequency f_0 calculated by help of $V_{TR_max}=0.35$ V (also observable in Fig. 9 where amplitude of triangle wave is $2 \times V_{TR_max}$) has value 1.776 MHz and f_0 calculated from the right side of Eq. (12) has value 1.628 MHz. Simulation provided $f_0=1.7$ MHz.

Proposed generator can be modified for duty cycle (D) control. Modification of circuit includes DC current I_d connected to the node of capacitor and it causes offset of current I_C and therefore allows driving of the duty cycle. Modified version in Fig. 8 has both time intervals and repeating period as follows:

$$T_1 = \frac{2V_{TR_max}C}{I_{C_max}} = \frac{2V_{TR_max}C}{I_{b1}B + I_d}, \quad (13)$$

$$T_2 = \frac{2V_{TR_max}C}{-I_{C_max}} = \frac{2V_{TR_max}C}{I_{b1}B - I_d}, \quad (14)$$

$$T = T_1 + T_2 = \frac{4V_{TR_max}I_{b1}BC}{(I_{b1}B + I_d)(I_{b1}B - I_d)}, \quad (15)$$

and repeating frequency has then the following form:

$$f_0 = \frac{1}{T} = \frac{I_{b1}B(1 + (I_d/I_{b1}B))(1 - (I_d/I_{b1}B))}{4V_{TR_max}C} \cong \frac{I_{b1}B(1 + (I_d/I_{b1}B))(1 - (I_d/I_{b1}B))k}{4(2I_{set_gm}R_C)C}, \quad (16)$$

where k is amplitude relation (6) between V_{SQ_max} and V_{TR_max} . The ratio k can be used as a result of approximate Eq. (6) or as real ratio of produced signal amplitudes. The duty cycle is defined as:

$$D = \frac{T_1}{T} = \frac{1}{2} \left(1 - \frac{I_d}{I_{b1}B} \right) = 0.5(1-n), \quad (17)$$

where parameter $n=I_d/I_{b1}B$ represents relation between duty cycle and repeating frequency. Limits of I_d (and also D) are theoretically restricted to maximal value given by $\pm I_{b1}B$. Available setting of the repeating frequency independently on duty cycle is also possible if matching condition of constant ratio n keeps fulfilled ($I_d=(1-2D)I_{b1}B$). Repeating frequency can also be rewritten to simplified form:

$$f_0 = \frac{I_{b1}B(1-D)Dk}{2I_{set_gm}R_C C}. \quad (18)$$

A possibility of simple control f_0 independently of D also by I_{set_gm} is obvious. However, such adjusting (g_m) also changes level of produced amplitudes, see (6).

The simulation results of available output signals are in Fig. 9 for $D=50\%$. Tuning of the generator is documented in Fig. 10, for two discrete values of $B=1$ and 3. Repeating frequency was 1.7 and 4.385 MHz. Simulated dependences of repeating frequency on B and output amplitudes (peak-to-peak values) on repeating frequency are in Fig. 11. Simulations prove that repeating frequency is

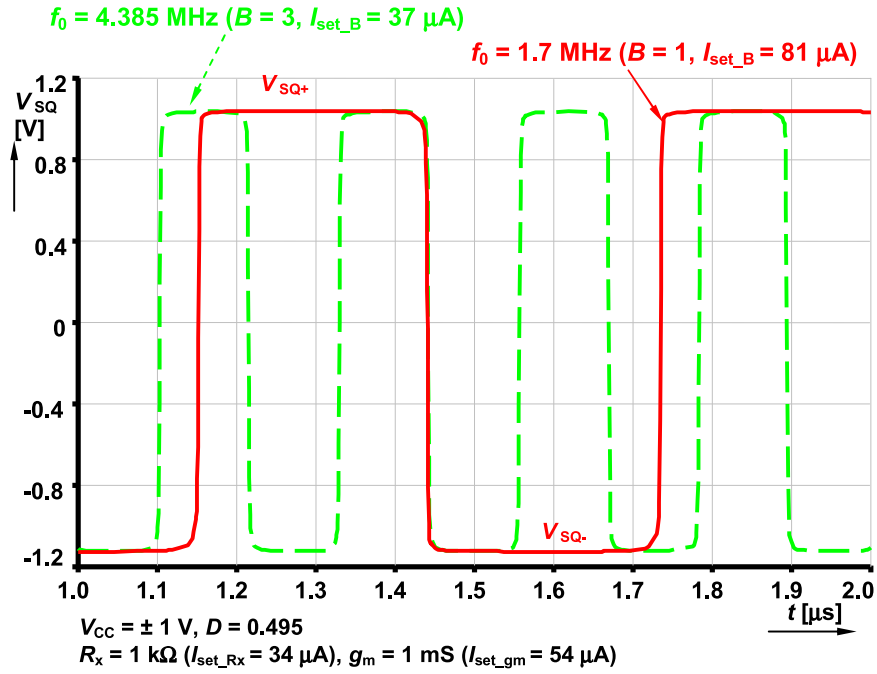


Fig. 15. Transient responses of differential square wave output for two selected frequencies.

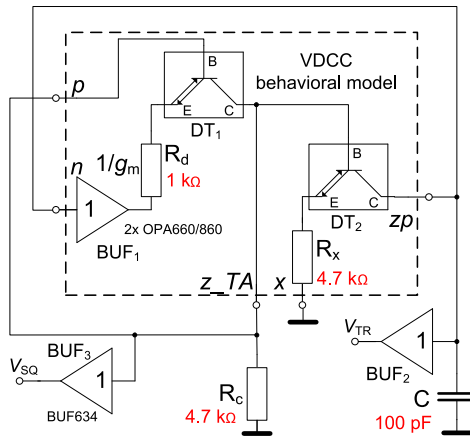


Fig. 16. Behavioral model of the generator employing DT-s for preliminary experimental tests.

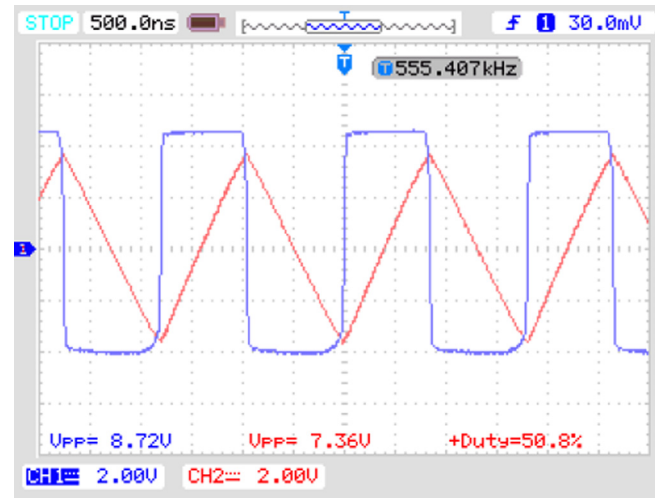


Fig. 17. Measured transient responses of the triangle and square wave generator.

tunable approximately from 1 MHz to 4.385 MHz for B adjusted between 0.5 and 3 ($I_{\text{set}_B}=93 \mu\text{A}$, $I_{\text{set}_B}=37 \mu\text{A}$). Expected range of f_0 is from 0.723 to 4.34 MHz, see Fig. 11a and b shows dependences of output amplitudes on repeating frequency.

We also tested an operation for setting of two different frequencies and constant duty cycle $D=80\%$. The source I_d has to provide DC current: $I_d = I_{b1}B(1-2D)$ if independent control of f_0 with differently set D is required. The results are in Fig. 12 (D was 78.5% in particular simulation). A similar test was provided for ideal $D=20\%$ (simulation as 20.6%), see Fig. 13.

The circuit in Fig. 3 offers differential voltage output if conversion of I_{SQ} current responses to voltage through resistor (additional R_c from z_c_TA terminal – both equal values) is provided (Fig. 14). It is very useful because it means two-times higher amplitude for further application (beneficial mainly in low-voltage and low-power solutions) and additional benefits like immunity to common mode distortion and noises if symmetrical output is used. Exemplary results ($D=50\%$, $I_d=0$) are shown in Fig. 15.

3.1. Simple experimental test

We have verified experimentally the proposed conception of VDC in non-tunable generator circuit based on concept presented in Fig. 3. A model of the VDC implemented in the generator was based on diamond transistors (DT-s) [29,30] see Fig. 16. Voltage buffers BUF_1 and BUF_2 were implemented using internal parts of OPA660 [29] and BUF_3 was external type BUF634 [31]. We used RIGOL DS 1204B oscilloscope for measurement of transient responses. Design parameters of the model are: $R_c=4.7 \text{ k}\Omega$, $R_x=4.7 \text{ k}\Omega$, $g_m=1/R_d=1 \text{ mS}$, and $C=100 \text{ pF}+8 \text{ pF}$ parasitic capacitance (estimated from [29–31]). The repeating frequency was calculated from:

$$f_0 = \frac{V_{SQ}}{V_{TR}} \frac{1}{4R_x C} = \frac{1}{4R_x C} \left(\frac{R_c/R_d}{(R_c/R_d) - 1} \right) \approx \frac{1.27}{4R_x C} \quad (19)$$

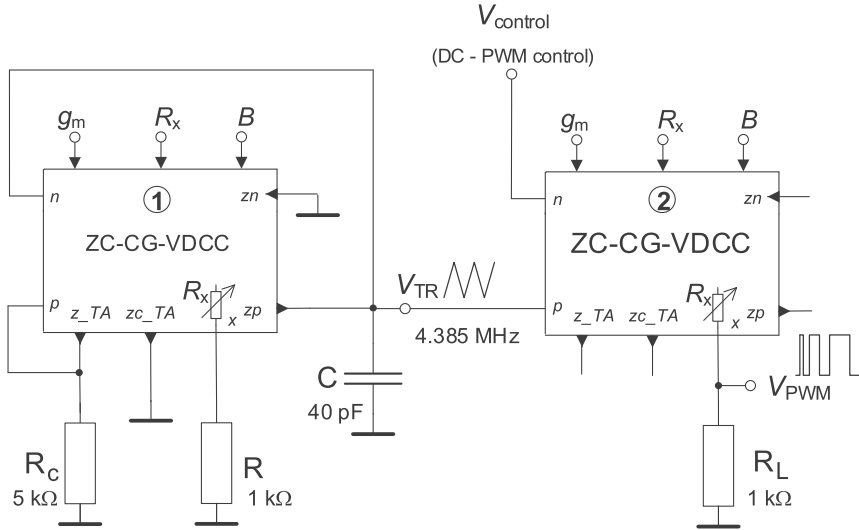


Fig. 18. ZC-CG-VDCC-based pulse width modulator utilizing generator from Fig. 3.

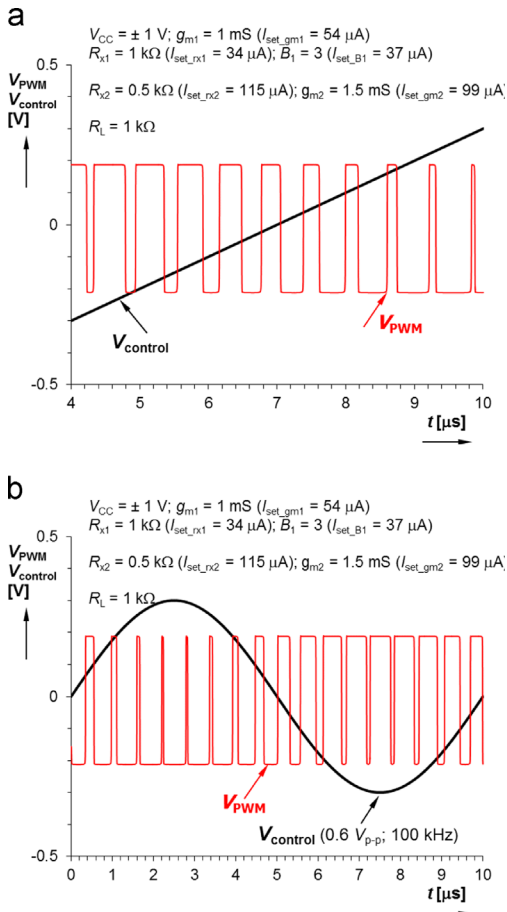


Fig. 19. Results of the PWM simulation – solution from Fig. 18: (a) example of linear sweep and (b) example of harmonic excitation.

and it provided the resulting repeating frequency 625 kHz. Measurement results are in Fig. 17, where $f_0=555$ kHz was obtained. Estimation (the first part of (19)) of repeating frequency from produced amplitudes (V_{SQ} , V_{TR}) provides value of 583 kHz. The results prove workability of the concept.

4. Pulse width modulator as exemplary application of the designed generator

Functional generators providing triangular and square wave outputs are applicable in many areas of signal processing, for example as sources of clock timing, in pulse width modulators (PWM), in serial sigma-delta converters, etc. We proposed the following very simple pulse width modulator as very typical example of utilization of triangular wave output of the generator. Two ZC-CG-VDCCs are sufficient to provide simple PWM modulator, proposed solution is shown in Fig. 18. PWM generators are very frequently used and very important for power supply sources and converters (DC-DC, AC-DC) and high-efficient amplifiers (D class for example).

Simple comparator without hysteresis was formed by input OTA section of the ZC-CG-VDCC which is directly connected to the current conveyor CCII input Y (z_{TA}). Thus, output response is obtained after buffering by internal voltage buffer in frame of CCII part (at x terminal). This terminal (output of the PWM) is terminated by load resistance 1 kΩ. Unused terminals of the ZC-CG-VDCCs are kept unconnected (open) or grounded. Values of used passive elements are noted in figures (Fig. 18). Repeating frequency of the generator was set as 4.385 MHz ($C=40$ pF). The rest of used constant values (bias currents) are noted in figures including simulation results. The results of the PWM modulator in (a) linear sweep of DC control voltage ($V_{control}$) from -0.3 to 0.3 V and (b) harmonic excitation (0.6 V_{p-p}, 100 kHz). Black traces show the $V_{control}$ and the red colored traces represent output PWM signals.

5. Conclusion

The details of designed generator are summarized in Table 4. Our solution is useful for voltage- and current-mode signal processing, where square wave input signal is required. Simulations confirmed analytical presumptions and expectations. Note that functions of internal sections of ZC-CG-VDCC can be interchanged (integrator is created by OTA and comparator by ECCII section, see Fig. 1b) in order to obtain another solution of the generator. Simple exemplary application of ZC-CG-VDCC in electronically controllable

Table 4
Summarization of gained features from analysis and simulations.

	No. of passive elements	Repeating frequency $D=50\%$	Range of parameter control	Frequency range [MHz]	Output levels in single-ended mode [V_{P-P}] V_{TR}/V_{SQ}	Power consumption for min. f_0 [mW] $D=50\%$	Power consumption for max. f_0 [mW] $D=50\%$
Fig. 3 ^a	3	$f_0 = I_{b1}B/4V_{TR_max}C$	B (1; 3) I_{set_B} (81; 37) μA	1.0–4.385	0.78/1.10	6.28	4.94

^a $C=40$ pF, $R_x=1$ k Ω ($I_{set_Rx}=34$ μA), $R=1$ k Ω , $g_m=1$ mS ($I_{set_gm}=54$ μA)

nonlinear circuits, as triangular and square wave generators is shown. However, all controllable features of the device were not fully engaged. Moreover, presented ZC-CG-VDCC offers interesting features if all its controllable parameters are employed. It is useful in reconfigurable and adjustable filters and harmonic signal generation [26,27].

Acknowledgment

Research described in the paper was supported by Czech Science Foundation project under GP14-24186P and by internal grant no. FEKT-S-14-2281 and project Electronic-biomedical co-operation ELBIC M00176. The support of the project CZ.1.07/2.3.00/20.0007 WICOMT, financed from the operational program Education for Competitiveness, is gratefully acknowledged. The described research was performed in laboratories supported by the SIX project; the registration number CZ.1.05/2.1.00/03.0072, the operational program Research and Development for Innovation. Dr. Herencsar was supported by the project CZ.1.07/2.3.00/30.0039 of the Brno University of Technology.

References

- [1] D. Biolek, R. Senani, V. Biolkova, Z. Kolka, Active elements for analog signal processing: classification, review and new proposals, *Radioengineering* 17 (4) (2008) 15–32.
- [2] R. Sotner, J. Jerabek, N. Herencsar, Voltage differencing buffered/inverted amplifiers and their applications for signal generation, *Radioengineering* 22 (2) (2013) 490–504.
- [3] W.S. Chung, H. Kim, H.W. Cha, H.J. Kim, Triangular/square-wave generator with independently controllable frequency and amplitude, *IEEE Trans. Instr. Measur.* 54 (1) (2005) 105–109.
- [4] M. Siripruchyanun, P. Wardkein, A full independently adjustable, integrable simple current controlled oscillator and derivative PWM signal generator, *IEICE Trans. Fundam. Electron. Commun. Comput. Sci.* E86-A (12) (2003) 3119–3126.
- [5] J. Kumbun, M. Siripruchyanun, MO-CTTA-based electronically controlled current-mode square/triangular wave generator, in: *Proceedings of the 1st International Conference on Technical Education (ICTE2009)*, Bangkok, 2010, pp. 158–162.
- [6] P. Silapan, M. Siripruchyanun, Fully and electronically controllable current-mode Schmitt triggers employing only single MO-CCCDTA and their applications, *Analog Integr. Circuits Signal Process.* 68 (11) (2011) 111–128.
- [7] T. Srisakul, P. Silapan, M. Siripruchyanun, An electronically controlled current-mode triangular/square wave generator employing MO-CCCTAs, in: *Proceedings of the 8th International Conference on Electrical Engineering/Electronics, Computer, Telecommunications, and Information Technology*, Khon Kaen, 2011, pp. 82–85.
- [8] H.-Ch. Chien, Voltage-controlled dual slope operation square/triangular wave generator and its application as a dual mode operation pulse width modulator employing differential voltage current conveyors, *Microelectron. J.* 43 (12) (2012) 962–974.
- [9] M. Janeczek, D. Kubanek, K. Vrba, Voltage-controlled square/triangular wave generator with current conveyors and switching diodes, *Int. J. Adv. Telecommun. Electrochem. Signals Syst.* 1 (2–3) (2012) 1–4. <http://dx.doi.org/10.11601/ijates.v1i2-3.33>.
- [10] R. Sotner, J. Jerabek, N. Herencsar, A. Lahiri, J. Petrzela, K. Vrba, Practical aspects of operation of simple triangular and square wave generator employing diamond transistor and controllable amplifiers, in: *Proceedings of the 36th International Conference on Telecommunications And Signal Processing (TSP 2013)*, 2013, pp. 431–435.
- [11] R. Sotner, J. Jerabek, N. Herencsar, R. Prokop, K. Vrba, J. Petrzela, T. Dostal, Simply adjustable triangular and square wave generator employing controlled gain current and differential voltage amplifier, in: *Proceedings of the 23th International Conference Radioelektronika 2013*, 2013, pp. 109–114.
- [12] W. Chiu, S.I. Liu, H.W. Tsao, CMOS differential difference current conveyors and their applications, *IEE Proc. Circuits Dev. Syst.* 143 (2) (1996) 91–96.
- [13] H.O. Elwan, A.M. Soliman, A novel CMOS differential voltage current conveyor and its applications, *IEE Proc. Circuits Dev. Syst.* 144 (3) (1997) 195–200.
- [14] R.L. Geiger, E. Sánchez-Sinencio, Active filter design using operational transconductance amplifiers: a tutorial, *IEEE Circ. Dev. Mag.* 1 (1985) 20–32.
- [15] A. Fabre, O. Saadi, F. Wiest, C. Boucheron, High frequency applications based on a new current controlled conveyor, *IEEE Trans. Circuits Syst. I* 43 (2) (1996) 82–91.
- [16] W. Surakamponorn, W. Thitimajshima, Integrable electronically tunable current conveyors, *IEE Proceedings-G* 135 (2) (1988) 71–77.
- [17] A. Fabre, N. Mimeche, Class A/AB second-generation current conveyor with controlled current gain, *Electron. Lett.* 30 (16) (1994) 1267–1268.
- [18] S. Minaei, O.K. Sayin, H. Kuntman, A new CMOS electronically tunable current conveyor and its application to current-mode filters, *IEEE Trans. Circuits Syst. I* 53 (7) (2006) 1448–1457.
- [19] M. Kumngern, S. Junnapiya, A sinusoidal oscillator using translinear current conveyors, in: *Proceedings of the Asia Pacific Conference on Circuits and Systems APPCAS2010*, Kuala Lumpur, 2010, pp. 740–743.
- [20] R. Sotner, J. Jerabek, N. Herencsar, T. Dostal, K. Vrba, Electronically adjustable modification of CFA: Double Current Controlled CFA (DCC-CFA), in: *Proceedings of the 35th International Conference on Telecommunications and Signal Processing (TSP 2012)*, Prague, 2012, pp. 401–405.
- [21] R. Sotner, A. Kartci, J. Jerabek, N. Herencsar, T. Dostal, K. Vrba, An additional approach to model current followers and amplifiers with electronically controllable parameters from commercially available ICs, *Meas. Sci. Rev.* 12 (6) (2012) 255–265. <http://dx.doi.org/10.2478/v10048-012-0035-4>.
- [22] J. Baker, *CMOS Circuit Design, Layout and Simulation*, Wiley-IEEE Press, West Sussex (2005) 1039.
- [23] I. Eldbib, V. Musil, Self-cascoded Current Controlled CCII Based Tunable Band Pass Filter, in: *Proceedings of the 18th International Conference Radioelektronika, Praha*, 2008, pp. 1–4.
- [24] W. Surakamponorn, K. Kumwachara, CMOS-based electronically tunable current conveyor, *Electron. Lett.* 28 (14) (1992) 1316–1317. <http://dx.doi.org/10.1049/el:19920836>.
- [25] MOSIS parametric test results of TSMC LO EPI SCN018 technology. Available on-line {ftp://ftp.isi.edu/pub/mosis/vendors/tsmc-018/t44e_lo_epi-params.txt} (Cited 24.5.12).
- [26] R. Sotner, N. Herencsar, J. Jerabek, R. Prokop, A. Kartci, T. Dostal, K. Vrba, Z-copy controlled-gain voltage differencing current conveyor: advanced possibilities in direct electronic control of first-order filter, *Elektronika IR Elektrotechnika* 20 (6) (2014) 77–83. <http://dx.doi.org/10.5755/j01.eee.20.6.7272>.
- [27] R. Sotner, J. Jerabek, J. Petrzela, N. Herencsar, R. Prokop, K. Vrba, Second-order simple multiphase oscillator using Z-copy controlled-gain voltage differencing current conveyor, *Elektronika IR Elektrotechnika* 20 (9) (2014) 13–18. <http://dx.doi.org/10.5755/j01.eee.20.9.8709> (in press).
- [28] J. Misurec, J. Koton, Schmitt trigger with controllable hysteresis using current conveyors, *Int. J. Adv. Telecommun. Electrochem., Signals Syst.* 1 (1) (2012) 1–5. <http://dx.doi.org/10.11601/ijates.v1i1.9>.
- [29] Texas Instruments, OPA660 Wide bandwidth operational transconductance amplifier and buffer (datasheet), 2000, 20 p., accessible on www: (<http://www.ti.com/lit/ds/symlink/opa660.pdf>).
- [30] Texas Instruments, OPA860 Wide-bandwidth, operational transconductance amplifier (OTA) and buffer (datasheet), 2008, 33 p., accessible on www: (<http://www.ti.com/lit/ds/symlink/opa860.pdf>).
- [31] Texas Instruments, BUF 634 250 mA High-speed buffer (datasheet), 1996, 20 p., accessible on www: (<http://focus.ti.com/lit/ds/symlink/buf634.pdf>).

[23] JERABEK, J., SOTNER, R., DOSTAL, T., VRBA, K. Simple Resistor-less Generator Utilizing Z- copy Controlled Gain Voltage Differencing Current Conveyor for PWM Generation. *Elektronika Ir Elektrotechnika*, 2015, vol. 21, no. 5, p. 28-34. ISSN: 1392-1215.

Simple Resistor-less Generator Utilizing Z-copy Controlled Gain Voltage Differencing Current Conveyor for PWM Generation

Jan Jerabek¹, Roman Sotner², Tomas Dostal³, Kamil Vrba¹

¹Department of Telecommunications, Faculty of Electrical Engineering and Communication, Brno University of Technology, Technicka 12, Brno, 616 00, Czech Republic

²Department of Radio Electronics, Faculty of Electrical Engineering and Communication, Brno University of Technology, Technicka 12, Brno, 616 00, Czech Republic

³Department of Electrical Engineering and Computer Science, College of Polytechnics Jihlava, Tolsteho 16, Jihlava 586 01, Czech Republic
sotner@feec.vutbr.cz

Abstract—This paper deals with a very simple functional generator employing single multi-terminal advanced active device, so-called z-copy controlled gain voltage differencing current conveyor (ZC-CG-VDCC). This active element offers various inter-terminal relations and interesting possibilities of multi-parameter electronic control, which are utilized to control resulting application (triangular and square wave generator). Simple pulse width modulator (PWM) based on two ZC-CG-VDCCs is a further application example of presented generator. Verification of expected behavior was performed by simulation based on CMOS model of the ZC-CG-VDCC and also by lab measurement.

Index Terms—Electronic control, functional generator, multiple-terminal advanced active element, PWM, voltage differencing current conveyor, ZC-CG-VDCC.

I. INTRODUCTION

Advanced or special active elements [1] are useful in circuit synthesis and design from many substantial reasons. First of all, they dispose of various interesting terminal relations [1] useful for simplification of circuit synthesis of standard, advanced or special applications. The next beneficial feature of advanced active elements consists in direct independent electronic control of several parameters included in frame of active device, for example [2]–[5]. Common active elements for circuit design (operational amplifiers for example) realize only one and very simple signal operation ($V_{out} = (V_+ - V_-) \cdot A$, where A) [6], [7] without possibility of electronic control of its parameter(s) in

many cases. Beneficial features of advanced active elements can be also used in the design of functional generators.

Electronically controllable functional (triangular and square wave) generators are widely employed in many analog and digital communication subsystems (clock generation, pulse width modulation, TTL or CMOS logic, DC-DC, AC-DC converters, etc.) [6], [7].

Operational transconductance amplifiers (OTA) [1], [8] were the first active elements that were very suitable for design of generators.

II. DISCUSSION OF RELATED RESEARCH

Siripruchyanun *et al.* [9] and Chung *et al.* [10] proposed a generator based on three adjustable OTAs and three passive elements. Three commercially available active elements were utilized in solution presented in [11], where electronic controllability of the solution was the main contribution.

Another solution employing two (indivisible to sub-blocks) active elements and four passive elements was reported by Janecek *et al.* [12]. However, his work does not focus on electronic controllability. Chien [13] proposed a generator based on two differential voltage current conveyors (DVCCs) that are multi-terminal active elements, and four passive elements.

Kumbun *et al.* [14] starts with utilization of electronically controllable active elements with active subsections. Their active element, referred to as multiple-output through transconductance amplifiers (MO-CTTA) employs current amplifier with special input feature (sCA) and OTA. Two MO-CTTA are required for construction of the generator. The same number of active devices is required for generators presented by Silapan *et al.* [15]. Silapan *et al.* [15] used two multiple-output current controlled current differencing amplifiers (MO-CCDTAs) which consist of current differencing unit (CDU) [1], [16], [17] and OTA subsections. A solution presented by Srisakul [18] is based

Manuscript received March 9, 2015; accepted June 29, 2015.

Research described in this paper was financed by Czech Ministry of Education in frame of National Sustainability Program under grant LO1401. For research, infrastructure of the SIX Center was used. Research described in the paper was supported by Czech Science Foundation projects under No. 14-24186P. Grant No. FEKT-S-14-2281 also supported this research. The support of the project CZ.1.07/2.3.00/20.0007 WICOMT, financed from the operational program Education for competitiveness, is gratefully acknowledged.

on multiple-output current controlled current conveyor transconductance amplifier (MO-CCCCTA) where current controlled current conveyor of second generation (CCCII) [1], [19], [20] and OTA create subsections.

Two active elements are sufficient for construction of a functional generator presented in [21], where dual-output voltage differencing buffered amplifier (DO-VDBA) and fully balanced voltage differencing amplifier (FB-VDBA) were employed. These elements are created by internal subsections in a form of operational transconductance amplifier and voltage buffer (VB) or voltage inverter (VI). The proposed generator allows differential outputs of both generated responses.

Single active element, so-called controlled gain current and differential voltage amplifier (CG-CDVA) is sufficient for construction of the generator presented in [22]. Active devices consist of adjustable current amplifier (aCA) and adjustable differential voltage amplifier (DVCA) subsections.

Therefore, a solution of generator, introduced in this paper, offers some significant improvements. Employed active element is not complex and only one element is enough in order to form the generator. Number of external passive elements is decreased to only one grounded capacitor and both signals (square and triangle wave) are available in both voltage and current form. Moreover, functions of our solution are experimentally verified in order to prove the correctness of our concept.

III. ACTIVE ELEMENT DESCRIPTION

Z-copy Controlled Gain Voltage Differencing Current Conveyor (ZC-CG-VDCC) is an active device covering high variability of terminal relations and controllable parameters itself that is highly beneficial for many applications. A detailed principle is discussed in [4] and [5], where we can find also internal CMOS structure that was used for simulations also in this paper. Therefore, we provide only brief explanation of ideal behavior of this multi-terminal active element. Simplified behavioral block model is shown in Fig. 1. In fact, ZC-CG-VDCC is interconnection of two main sub-blocks: OTA and electronically controllable current conveyor of second generation (ECCII) [1]–[3].

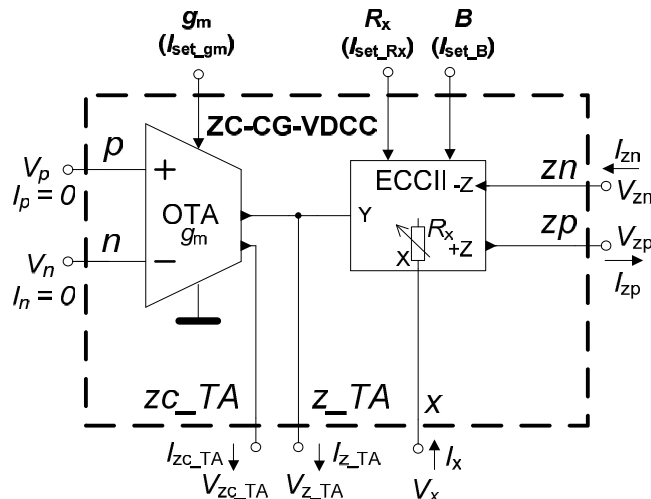


Fig. 1. Behavioral sub-block model of the ZC-CG-VDCC.

Behavior of model in Fig. 1 is defined by:

$$I_{z_TA} = I_{zc_TA} = (V_p - V_n) g_m, \quad (1)$$

$$V_x = V_{z_TA} + R_x I_x, \quad (2)$$

$$I_{zp} = -I_{zn} = B \times I_x, \quad (3)$$

where controllable parameters are transconductance (g_m)

$$g_m = 2 \sqrt{I_{set_gm} K_{Pn} \frac{W_{M1,2}}{L_{M1,2}}}, \quad (4)$$

internal resistance of current input terminal X (R_x)

$$R_x = \frac{1}{\sqrt{I_{set_Rx} K_{Pn} \frac{W_{M11,12}}{L_{M11,12}}} + \sqrt{I_{set_Rx} K_{Pp} \frac{W_{M13,14}}{L_{M13,14}}}}, \quad (5)$$

and current gain B

$$B = \frac{NI_{b2}}{2I_{set_B}} \cong \frac{I_{b2}}{I_{set_B}}. \quad (6)$$

Parameters I_{set_gm} , I_{set_Rx} , I_{set_B} , I_{b2} are values of internal bias sources of the CMOS structure, W_M and L_M are dimensions of used transistors and K_P are transconductance parameters for used fabrication technology (for more details see [5]).

IV. FUNCTIONAL GENERATOR

The proposed generator in Fig. 2 is formed by two parts: integrator and comparator (Schmitt trigger). We can form these subparts very simply by internal sections of the ZC-CG-VDCC (integrator = capacitor + OTA section, comparator = ECCII section). Square wave is available also in form of current flowing from zc_TA terminal.

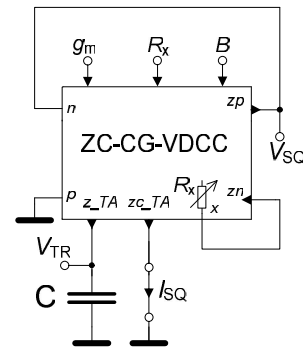


Fig. 2. Triangle and square wave generator based on ZC-CG-VDCC.

A part of the comparator (input z_TA , output zp) has the following principle. The highest current gain in structure of ZC-CG-VDCC has theoretical maximum limited to $B_{max} = 4$ [4], [5] for very low DC bias current I_{set_B} . Voltage transfer between z_TA and zn terminals has ideal formula

$$\frac{V_{zn}}{V_{z_TA}} = \frac{1-B}{1+B}, \quad (7)$$

where transfer has character of unity gain voltage amplifier for $B < 1$. In case of $B = 1$, this part of active element behaves as comparator with hysteresis [10]. Direct copy of current I_x (in saturation given by $I_{b1} = 100 \mu\text{A}$ in [5]) multiplied by gain B is available at terminal zp . Voltage at this terminal is in saturation corner without load resistance. Between zn and z_{TA} terminals unity gain (7) still persists, therefore threshold input voltages are equal to saturation corners $\pm V_{zn/zn_sat}$ (approximately $\pm 0.8 \text{ V}$ to $\pm 0.9 \text{ V}$ in our case). Due to this fact, we can obtain equal amplitudes of triangular and square wave response. This statement is valid only for $B = 1$ in real case.

Supposing equality of threshold and output level of the repeating frequency is given (for 50 % duty cycle) as

$$f_0 = \frac{I_{set_gm}}{2V_{TR_max}C}, \quad (8)$$

where $V_{TR_max} = V_{SQ_max}$ and 2 in denominator comes from current mirror ratio in CMOS structure [5]. The proposed variant of the generator can also operate with different duty cycle (D) than 50 %, see Fig. 3. Only one additional DC current source is supplemented into the structure.

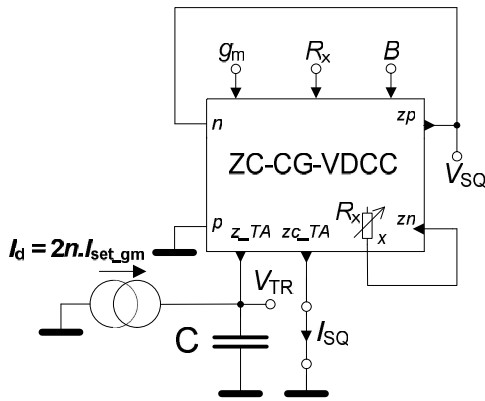


Fig. 3. Triangle and square wave generator with duty cycle control based on ZC-CG-VDCC.

Using routine analysis, we obtain the following expression for repeating frequency

$$f_0 = \frac{I_{z_TA_max} \left(1 - \frac{I_d}{I_{z_TA_max}} \right) \left(1 + \frac{I_d}{I_{z_TA_max}} \right)}{4V_{TR_max}C} = \frac{I_{set_gm} \left(1 - \frac{I_d}{2I_{set_gm}} \right) \left(1 + \frac{I_d}{2I_{set_gm}} \right)}{2V_{TR_max}C}, \quad (9)$$

and duty cycle ($I_{z_TA_max} = 2I_{set_gm}$)

$$D = \frac{1}{2} \left(1 + \frac{I_d}{2I_{set_gm}} \right) = \frac{1}{2} (1 + n), \quad (10)$$

where $n = I_d/2I_{set_gm}$ and represents relation between D and f_0 . (I_d is theoretically limited to $\pm 2I_{set_gm}$). Constant 2 is also given by multiplication of current mirrors in OTA section in

frame of the ZC-CG-VDCC element (see [5]). Setting of D independently of f_0 is also possible for constant ratio $n = 2D - 1$ ($I_d = 2I_{set_gm}(2D - 1)$). Accurate ratio of two DC currents is quite easily available in IC design.

V. SIMULATION RESULTS

A. Functional Generator

We obtained the following simulation results for parameters: $C = 40 \text{ pF}$, $R_x = 1 \text{ k}\Omega$ ($I_{set_Rx} = 34 \mu\text{A}$), $g_m = 1 \text{ mS}$ ($I_{set_gm} = 54 \mu\text{A}$), $B = 2$ ($I_{set_B} = 58 \mu\text{A}$). Transient responses (V_{TR} , V_{SQ}) are given in Fig. 4 for theoretical $f_0 = 0.844 \text{ MHz}$. The repeating frequency obtained from simulation was 0.904 MHz . The triangle wave signal has inverting polarity (consequence of inverting Schmitt trigger). Tuning of the generator (Fig. 5) was verified from 109 kHz to 1479 kHz by adjusting of I_{set_gm} from $5 \mu\text{A}$ to $99 \mu\text{A}$ (ideal range of f_0 control is $78 \text{ kHz} - 1547 \text{ kHz}$). Range of the adjusting is proportional to I_{set_gm} .

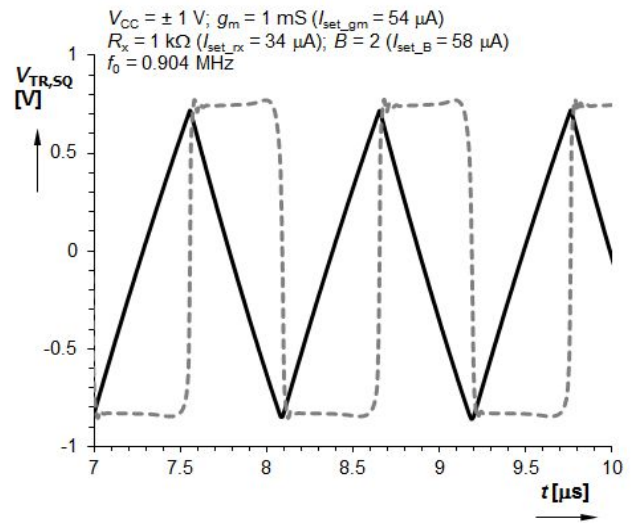


Fig. 4. Transient responses of the generator from Fig. 2 (V_{TR} , V_{SQ}).

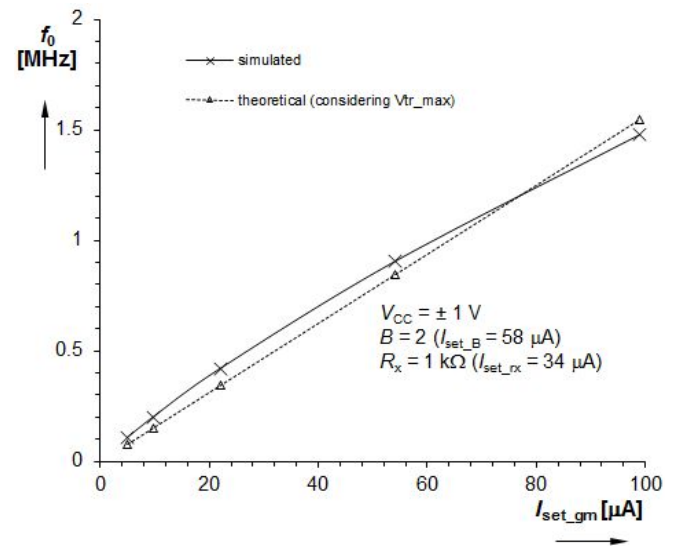


Fig. 5. Dependence of the repeating frequency on DC bias current I_{set_gm} .

The results of exemplary f_0 tuning for two different frequencies and $D = 30 \%$ or 70% (simulated as 29.7% and 30.8% or 66.9% and 69.7%) are given in Fig. 6 and Fig. 7. Utilization of current output terminal zc_TA (resistive load at

this terminal) allows to obtain differential voltage output of the square wave that is useful in low-voltage and low power applications, where voltage swing is very limited.

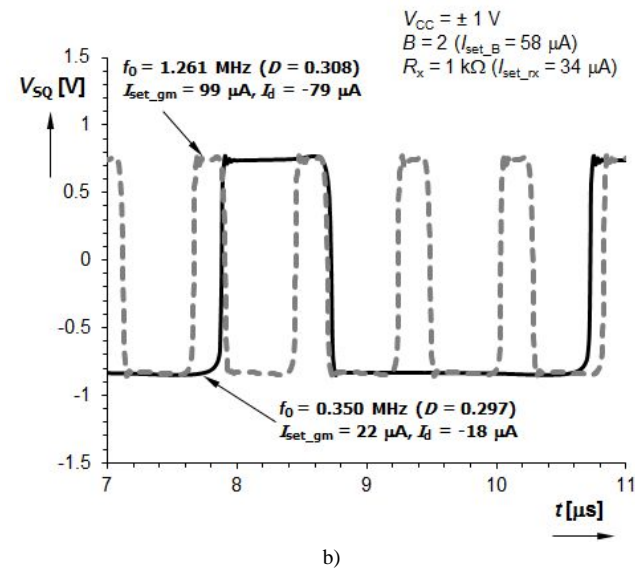
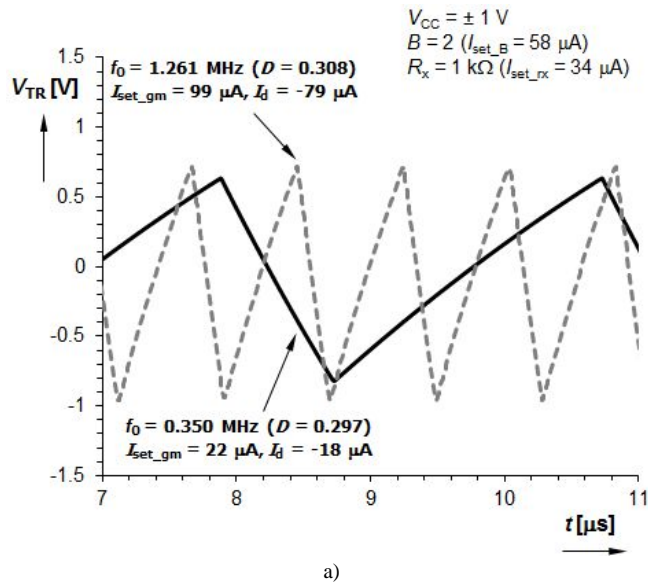


Fig. 6. Transient response for f_0 adjusting with $D = 30\%$: a) triangle wave, b) square wave.

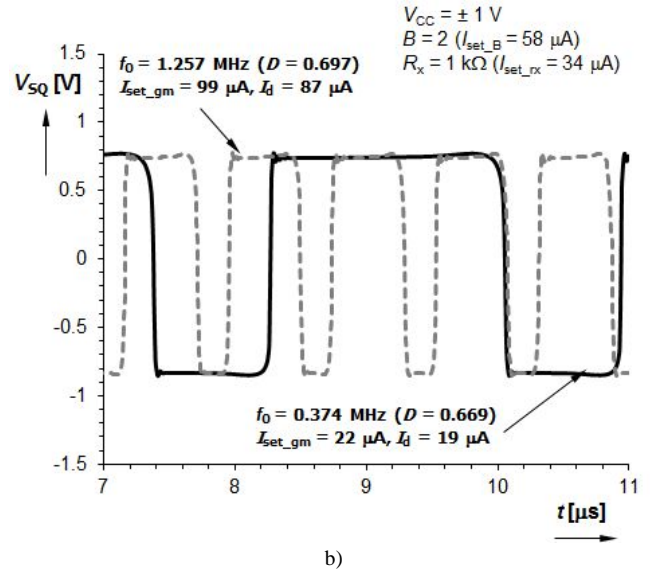
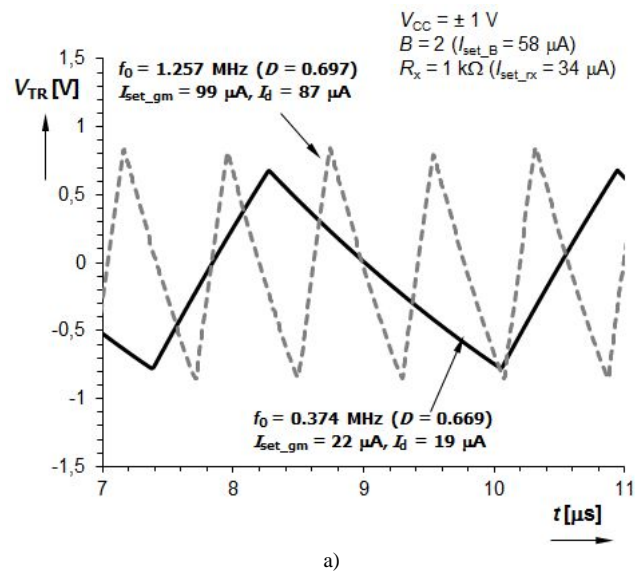


Fig. 7. Transient response for f_0 adjusting with $D = 70\%$: a) triangle wave, b) square wave.

B. PWM Modulator

Pulse width modulator (PWM) [23] is both quite important and typical application of the functional generator. PWM modulators are frequently used in power supply sources/converters (DC-DC, AC-DC) and high-efficient audio amplifiers (D class) for example. We established the following PWM modulator (Fig. 8) as a simple example of utilization of the triangular wave output of the generator. Two ZC-CG-VDCCs are sufficient to provide simple PWM modulator employing low number of passive elements (one R and one C only). Input OTA section of the ZC-CG-VDCC₂ which is directly connected to the current conveyor CCII input Y (z_{TA}) forms simple comparator without hysteresis. Output response is available after internal voltage buffer in frame of CCII part (at X terminal).

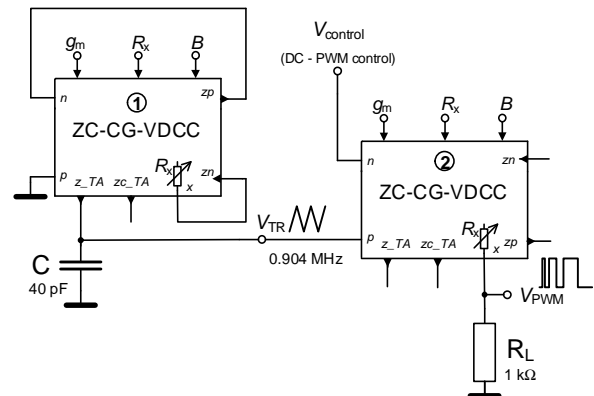


Fig. 8. A simple pulse width modulator based on two ZC-CG-VDCC.

Output of the PWM is terminated by load resistance $1\text{ k}\Omega$ and rest of terminals (ZC-CG-VDCCs) was kept unconnected or grounded. Configuration of the modulator was set as: repeating frequency 0.904 MHz , $C = 40\text{ pF}$. Additional parameters (bias currents) are noted in figures including simulation results (Fig. 9). We tested system in two situations: a) linear sweep of DC control voltage (V_{control}) from -0.8 V to 0.8 V and b) harmonic excitation ($1.1\text{ V}_{\text{p-p}}$, 50 kHz).

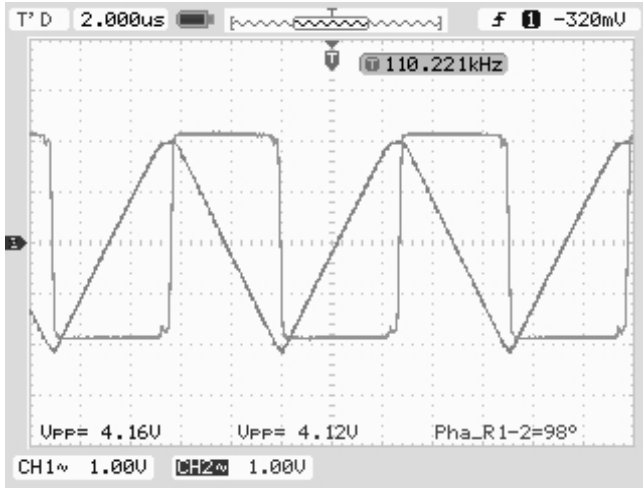


Fig. 11. Measured transient responses for f_0 adjusting with $D = 50\%$ of the generator from Fig. 2 based on behavioral model in Fig. 10: a) $f_0 = 11$ kHz, b) $f_0 = 110$ kHz.

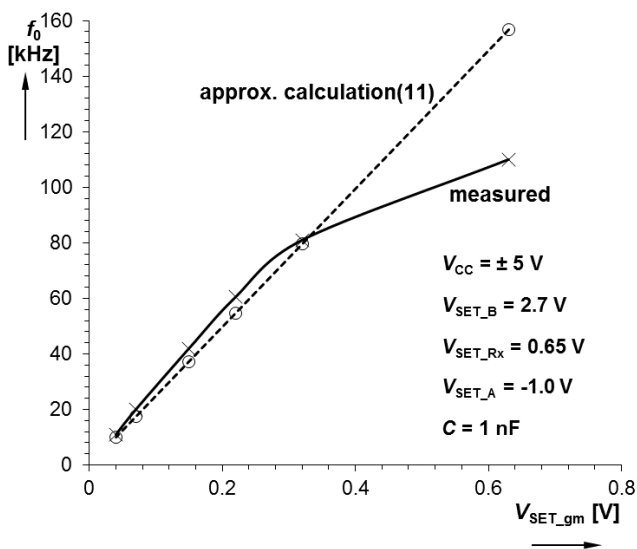
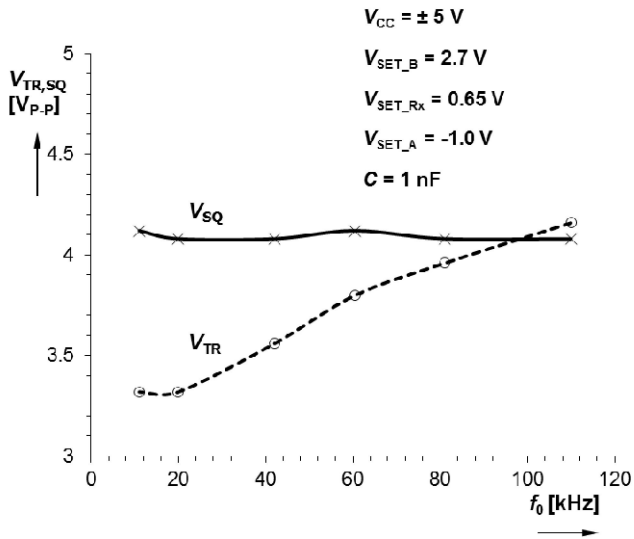


Fig. 12. Measured dependences of: a) output levels on f_0 , b) f_0 on V_{SET_gm} .

VII. CONCLUSIONS

Presented functional generator requires only one active

element and really low number of external passive elements (one capacitor only) and moreover it provides outputs (square and triangle wave) in both voltage and current form. By utilizing CMOS model of the active device from [5] we obtained very large adjustability range from 109 kHz to 1479 kHz by adjusting of I_{set_gm} from $5 \mu A$ to $99 \mu A$. For comparison with already published solutions see Table I, where a brief overview was provided. Note that our work includes also real measurement results that prove the design correctness. Behavioral model suffers from the significant parasitics that limit useful bandwidth in this case, as was discussed in previous section, therefore it was measured in 11 kHz to 110 kHz range. Proposed generator can be used for PWM modulation by a very simple way – a part of additional active device is used for comparisons of triangular wave with constant DC component to create PWM signal. All adjustable parameters (g_m , R_x , B) of the ZC-CG-VDCC were not necessary in the presented applications. Engagement of all controllable features is fully utilized in reconnection-less reconfigurable active filters [5] or multiphase oscillators [4] for example. Note that the generator can be obtained also if internal subsections (Fig. 1) of the ZC-CG-VDCC are interchanged (integrator is created by ECCII and comparator by OTA section) [25]. However, solution presented here saves two resistors.

TABLE I. COMPARISON OF SELECTED GENERATOR SOLUTIONS.

Reference	No. of active/passive elements	Abbreviation of active element or elements	Internal subsections	Available current and voltage output of square wave type	Differential square wave outputs available	Type of output signals (current or voltage)
[9], [10]	3/3	OTA	-	No	No	Voltage
[11]	3/2	2x VCA + DT + VB	-	No	No	Voltage
[12]	2/4	CCII + UCC + 4 diodes	-	N/A	Yes	Voltage
[13]	2/4	DVCC	-	No	N/A	Voltage
[14]	2/1	MO-CTTA	sCA+OTA	N/A	N/A	Current
[15]	2/1	MO-CCCDDTA	CDU+OTA	N/A	N/A	Current
[18]	2/1	MO-CCCCTA	CCCII+OTA	N/A	N/A	Current
[21]	2/3	DO-VDBA, FB-VDBA	OTA+VB+V I	Yes	Yes	Both
[22]	1/2	CG-CDVA	aCA+DVCA	No	No	Voltage
[25]	1/3	ZC-CG-VDCC	OTA+ECCII	Yes	Yes	Both
Fig. 2	1/1	ZC-CG-VDCC	OTA+ECCII	Yes	Yes	Both

Note: N/A – information is not available or verified

REFERENCES

- [1] D. Biolek, R. Senani, V. Biolkova, Z. Kolka, "Active elements for analog signal processing: classification, review and new proposals", *Radioengineering*, vol. 17, no. 4, pp. 15–32, 2008.
- [2] S. Minaei, O. K. Sayin, H. Kuntman, "A new CMOS electronically tunable current conveyor and its application to current-mode filters", *IEEE Trans. on Circuits and Systems - I*, vol. 53, no. 7, pp. 1448–1457, 2006. [Online]. Available: <http://dx.doi.org/10.1109/TCSI.2006.875184>

- [3] A. Marcellis, G. Ferri, N. C. Guerrini, G. Scotti, V. Stornelli, A. Trifiletti, "The VGC-CCII: a novel building block and its application to capacitance multiplication", *Analog Integrated Circuits and Signal Processing*, vol. 58, no. 1, pp. 55–59, 2009. [Online]. Available: <http://dx.doi.org/10.1007/s10470-008-9213-6>
- [4] R. Sotner, J. Jerabek, J. Petrzela, N. Herencsar, R. Prokop, K. Vrba, "Second-order simple multiphase oscillator using z-copy controlled-gain voltage differencing current conveyor", *Elektronika Ir Elektrotechnika*, vol. 20, no. 9, pp. 13–18, 2014. [Online]. Available: <http://dx.doi.org/10.5755/j01.eee.20.9.8709>
- [5] R. Sotner, N. Herencsar, J. Jerabek, R. Prokop, A. Kartci, T. Dostal, K. Vrba, "Z-copy controlled-gain voltage differencing current conveyor: advanced possibilities in direct electronic control of first-order filter", *Elektronika Ir Elektrotechnika*, vol. 20, no. 6, pp. 77–83, 2014. [Online]. Available: <http://dx.doi.org/10.5755/j01.eee.20.6.7272>
- [6] A. Basak, *Analogue electronic circuits and systems*. Cambridge University Press: New York, USA, 1991, p. 376. [Online]. Available: <http://dx.doi.org/10.1017/CBO9781139168069>
- [7] P. R. Gray, P. J. Hurst, S. H. Lewis, R. G. Meyer, *Analysis and design of analog integrated circuits*. John Wiley and Sons, Inc.: USA, 2009, p. 896.
- [8] R. L. Geiger, E. Sanchez-Sinencio, "Active filter design using operational transconductance amplifiers: a tutorial", *IEEE Circ. and Devices Magazine*, vol. 1, pp. 20–32, 1985. [Online]. Available: <http://dx.doi.org/10.1109/MCD.1985.6311946>
- [9] M. Siripruchyanun, P. Wardkein, "A full independently adjustable, integrable simple current controlled oscillator and derivative PWM signal generator", *IEICE Trans. Fundam. Electron. Commun. Comput. Sci.*, vol. E86-A, no. 12, pp. 3119–3126, 2003.
- [10] W. S. Chung, H. Kim, H. W. Cha, H. J. Kim, "Triangular/square-wave generator with independently controllable frequency and amplitude", *IEEE Trans. Instrumentation and Measurement*, vol. 54, no. 1, pp. 105–109, 2005. [Online]. Available: <http://dx.doi.org/10.1109/TIM.2004.840238>
- [11] R. Sotner, J. Jerabek, N. Herencsar, A. Lahiri, J. Petrzela, K. Vrba, "Practical aspects of operation of simple triangular and square wave generator employing diamond transistor and controllable amplifiers", in *Proc. 36th Int. Conf. Telecommunications and Signal Processing (TSP 2013)*, Rome, 2013, pp. 431–435. [Online]. Available: <http://dx.doi.org/10.1109/tsp.2013.6613968>
- [12] M. Janecek, D. Kubanek, K. Vrba, "Voltage-controlled square/triangular wave generator with current conveyors and switching diodes", *International Journal of Advances in Telecommunications Electrotechnics, Signals and Systems*, vol. 1, no. 2-3, pp. 1–4, 2012.
- [13] H-Ch. Chien, "Voltage-controlled dual slope operation square/triangular wave generator and its application as a dual mode operation pulse width modulator employing differential voltage current conveyors", *Microelectronics Journal*, vol. 43, no. 12, pp. 962–974, 2012. [Online]. Available: <http://dx.doi.org/10.1016/j.mejo.2012.08.005>
- [14] J. Kumbun, M. Siripruchyanun, "MO-CTTA-based electronically controlled current-mode square/triangular wave generator", in *Proc. of the 1st Int. Conf. on Technical Education (ICTE 2009)*, Bangkok, 2010, pp. 158–162.
- [15] P. Silapan, M. Siripruchyanun, "Fully and electronically controllable current-mode Schmitt triggers employing only single MO-CCCDTA and their applications", *Analog Integrated Circuits and Signal Processing*, vol. 68, no. 11, pp. 111–128, 2011. [Online]. Available: <http://dx.doi.org/10.1007/s10470-010-9593-2>
- [16] J. Vavra, J. Bajer, D. Biolek, V. Biolkova, "Current-mode quadrature oscillator employing ZC-CDU based all-pass filter", in *Proc. IEEE Int. Conf. on Electronics Engineering and Signal Processing (EESP)*, 2011, Male, pp. 640–644.
- [17] J. Vavra, D. Biolek, "OTA-based current differencing unit", in *Proc. Int. Conf. on Electronic Devices and Systems (EDS IMPAPS)*, Brno, 2008, pp. 7–12.
- [18] T. Srisakul, P. Silapan, M. Siripruchyanun, "An electronically controlled current-mode triangular/square wave generator employing MO-CCCTAs", in *Proc. 8th Int. Conf. on Electrical Engineering/Electronics, Computer, Telecommunications, and Information Technology*, Khon Kaen, 2011, pp. 82–85. [Online]. Available: <http://dx.doi.org/10.1109/ecticon.2011.5947776>
- [19] A. Sedra, K. C. Smith, "A second generation current conveyor and its applications", *IEEE Trans. Circuit Theory*, vol. CT-17, no. 2, pp. 132–134, 1970. [Online]. Available: <http://dx.doi.org/10.1109/TCT.1970.1083067>
- [20] A. Fabre, O. Saaid, F. Wiest, C. Boucheron, "High frequency applications based on a new current controlled conveyor", *IEEE Trans. on Circuits and Systems - I*, vol. 43, no. 2, pp. 82–91, 1996. [Online]. Available: <http://dx.doi.org/10.1109/81.486430>
- [21] R. Sotner, J. Jerabek, N. Herencsar, "Voltage differencing buffered/inverted amplifiers and their applications for signal generation", *Radioengineering*, vol. 22, no. 2, pp. 490–504, 2013.
- [22] R. Sotner, J. Jerabek, N. Herencsar, R. Prokop, K. Vrba, J. Petrzela, T. Dostal, "Simply adjustable triangular and square wave generator employing controlled gain current and differential voltage amplifier", in *Proc. 23th Int. Conf. Radioelektronika 2013*, Pardubice, 2013, pp. 109–114.
- [23] J. Caldwell, "Analog pulse width modulation", TI precision Designs: Verified Design (Texas Instruments application recommendations), pp. 1–21, 2013. [Online]. Available: <http://www.ti.com/lit/ug/slau508/slau508.pdf>
- [24] R. Sotner, A. Kartci, J. Jerabek, N. Herencsar, T. Dostal, K. Vrba, "An additional approach to model current followers and amplifiers with electronically controllable parameters from commercially available ICs", *Measurement Science Review*, vol. 12, no. 6, pp. 255–265, 2012. [Online]. Available: <http://dx.doi.org/10.2478/v10048-012-0035-4>
- [25] R. Sotner, J. Jerabek, N. Herencsar, T. Dostal, K. Vrba, "Design of Z-copy controlled-gain voltage differencing current conveyor based adjustable functional generator", *Microelectronics Journal*, vol. 46, no. 2, pp. 143–152, 2015. [Online]. Available: <http://dx.doi.org/10.1016/j.mejo.2014.11.008>

[24] SOTNER, R., HERENC SAR, N., JERABEK, J., PROKOP, R., KARTCI, A., DOSTAL, T., VRBA, K. Z-Copy Controlled-Gain Voltage Differencing Current Conveyor: Advanced Possibilities in Direct Electronic Control of First- Order Filter. *Elektronika Ir Elektrotechnika*, 2014, vol. 20, no. 6, p. 77-83. ISSN: 1392-1215.

Z-Copy Controlled-Gain Voltage Differencing Current Conveyor: Advanced Possibilities in Direct Electronic Control of First-Order Filter

R. Sotner¹, N. Herencsar², J. Jerabek², R. Prokop³, A. Kartci⁴, T. Dostal⁵, K. Vrba²

¹Department of Radio Electronics, Faculty of Electrical Engineering and Communication, Brno University of Technology, Technicka 12, Brno, 616 00, Czech Republic

²Department of Telecommunications, Faculty of Electrical Engineering and Communication, Brno University of Technology, Technicka 12, Brno, 616 00, Czech Republic

³Department of Microelectronics, Faculty of Electrical Engineering and Communication, Brno University of Technology, Technicka 10, Brno, 616 00, Czech Republic

⁴Department of Electronics and Communication Engineering, Faculty of Electrical & Electronics, Yildiz Technical University, Davutpasa Mah., 34220-Esenler, Istanbul, Turkey

⁵Department of Electrical Engineering and Computer Science, College of Polytechnics Jihlava, Tolsteho 16, Jihlava 586 01, Czech Republic
sotner@feec.vutbr.cz

Abstract—A modified version of voltage differencing current conveyor (VDCC) and its performance in detail is presented in this paper. Modified VDCC, so-called z-copy controlled gain voltage differencing current conveyor (ZC-CG-VDCC), offers interesting features from adjustability point of view. The active element allows independent electronic control of three adjustable parameters: intrinsic resistance of current input terminal, transconductance and current gain of the output stage which is not possible in case of conventional VDCC. The characteristics of proposed CMOS implementation designed using TSMC LO EPI 0.18 μ m technology process parameters are shown and discussed. Simple application in reconfigurable reconnection-less first-order voltage-mode multifunctional filter is shown and verified by SPICE simulations and experimentally. The filter tuning and change of the transfer function type is allowed by the controllable parameters of the ZC-CG-VDCC.

Index Terms—Electronic control, current conveyor, current gain, first order, intrinsic resistance, multifunctional filter, reconfiguration, transconductance, voltage differencing current conveyor, voltage-mode, z-copy, ZC-CG-VDCC.

I. INTRODUCTION

Active elements [1] with more than one controllable parameter are very important for technical progress in this field, because they allow more effective electronic control,

increasing variability in applications, simple circuit design and simple circuit structure. Frequently discussed active elements use principles based on electronic control of the intrinsic resistance (R_x) of the current input terminal x [2] (in the frame of current conveyor [3]) and control of the transconductance section (g_m) [4]. Active elements with possibility of current gain (B) control were presented by Surakamponporn et al. [5] and Fabre et al. [6]. However, only the current gain control is realized.

Some active elements that combine two externally controllable parameters (by bias voltage or current) were already discussed in applications of analog circuits and systems [7]–[9]. Minaei et al. [7] proposed current conveyor with adjustable properties i.e. adjustable B between x and z terminals and adjustable intrinsic resistance of the current input terminal x . Marcellis et al. [8] introduced modified conveyor with controllable features of voltage gain between y a x and current gain between x and z terminals. Kumngern et al. [9] also combined R_x and B control in their version of translinear current conveyor.

Several combined active elements, based on transconductance section (OTA) [1], [4] and current conveyor of second generation (CCII) [2], [3], were already proposed. Typical examples of active elements with two-parameter control are some modifications of the very known current differencing transconductance amplifier (CDTA) [1], [10], where R_x and g_m control is implemented by DC bias currents [11], [12]. For example, the current conveyor transconductance amplifier (CCTA) [1], [13] also utilizes independent R_x and g_m control in some of its modifications [14]. One modification of CCTA [15] also employs current gain control, where current conveyor with gain-adjustable properties was used. Controllable current gain in frame of current conveyor [5], [6] seems to be an interesting and

Manuscript received January 13, 2014; accepted April 9, 2014.

Research described in the paper was supported by Czech Science Foundation project under No. 14-24186P, by internal grant No. FEKT-S-14-2281, and project Electronic-biomedical co-operation ELBIC M00176. The support of the project CZ.1.07/2.3.00/20.0007 WICOMT, financed from the operational program Education for competitiveness, is gratefully acknowledged. The described research was performed in laboratories supported by the SIX project; the registration number CZ.1.05/2.1.00/03.0072, the operational program Research and Development for Innovation. Dr. Herencsar was supported by the project CZ.1.07/2.3.00/30.0039 of the Brno University of Technology.

valuable advantage. Active elements having this advantage attained many innovative modifications [16], [17].

The main aim of this paper is a design of an enhanced active element with useful and feasible controllable features. A voltage differencing current conveyor (VDCC) belongs to family of novel hybrid elements presented by Biolek et al. [1]. In this contribution the VDCC, used as main core of the proposed new active device, is presented as z -copy variant with controllable parameters. We refer this modification as z -copy controlled gain voltage differencing current conveyor (ZC-CG-VDCC). Hitherto published works have already discussed so-called differential voltage current conveyor (DVCC) [1], [18]–[21]. Nevertheless, both elements (VDCC and DVCC) have different behaviour and also different block structure that inheres from basic behaviour. The DVCC has two differential voltage input terminals y and realizes difference of two voltages [18]–[21]. The rest of the conception is identical to common current conveyor [2], [3]. One current input terminal x and current output terminal z (or multiple terminals $\pm z$) are available. In comparison to discussed DVCC, the VDCC also consists of transconductance section (OTA) [1], [4] and offers additional auxiliary terminal for more universality of such element. Very interesting active elements, which belong to this family, were also proposed by Soliman [22] under designation pseudo-differential current conveyors (PDCCs). For example, the CCTA [13]–[15] utilizes same types of sub-blocks (CCII and OTA) as VDCC, however in reverse order of interconnection. This different order of interconnection also brings interesting features in applications. However, any of above discussed active elements and approaches do not allow control of three parameters within the frame of one active device as is presented in this paper. This approach allows construction of very simple applications with minimum number of passive elements.

II. Z-COPY CONTROLLED-GAIN VOLTAGE DIFFERENCING CURRENT CONVEYOR

Proposed active element, so-called z -copy controlled gain voltage differencing current conveyor (ZC-CG-VDCC) is shown in Fig. 1. This element was derived from basic theoretical concept of VDCC [1]. The conventional VDCC consist of a transconductance amplifier [1], [4] connected to the y terminal of classical second generation current conveyor [3]. Important fact is that only transconductance control is available in frame of conventional VDCC. Our modification allows simultaneous and mutually independent control of three important parameters, i.e. g_m , R_x of current input terminal x in frame of the CCII section [2], and also B between x and z terminals of the CCII section [5]–[9]. Behavioural model consists of the transconductor OTA-DISO (differential input and single output) and electronically controllable CCII (ECCII) [5]–[7], [9]. The OTA section allows g_m control and ECCII section realizes control of R_x and B .

Symbol of ZC-CG-VDCC in Fig. 1(a) utilizes high impedance voltage differencing inputs p , n , auxiliary terminals $\pm z_{TA}$, z_{cTA} (outputs of transconductance

section), high impedance positive and negative current outputs of section of current conveyors z_p , z_n , low-impedance current input / voltage output x (current conveyor part) and three terminals for external control of B , intrinsic resistance, and transconductance by bias currents. Following equations describe inter-terminal relations: $V_x = V_{z_{TA}} + R_x I_x$, $I_{z_{TA}} = -I_{z_{TA}} = I_{z_{cTA}} = (V_p - V_n)g_m$, $I_{z_p} = I_x B$, $I_{z_n} = -I_x B$.

Figure 1(b) explains behaviour of the proposed device in details and its possible block diagram is given in Fig. 1(c). Such active element seems to be complex, but internal CMOS topology is not challenging, see Fig. 2. Basic block structure form Fig. 1(c) was taken into account for design of CMOS realization in Fig. 2. There are three important parts (transconductor, current conveyor of second generation and adjustable current amplifier). The first part is the transconductance amplifier [1], [4], [23] with differential NMOS pair connected to a voltage input of CMOS current conveyor. Intrinsic resistance control was performed in frame of the current conveyor section [2], [23], which is separated from the last block forming adjustable current amplifier [24]. The reason for this subdivision is simple. Bias control of intrinsic resistance in frame of current conveyor with current amplifier section influences at least dependence of current gain on control bias current significantly as was discussed in [25]. Therefore, independent current conveyor and independent bias current serves for intrinsic resistance controlling purposes.

The transconductance of the OTA section is given by ideal equation [23]

$$g_m = 2\sqrt{I_{set_gm} K_{Pn} \frac{W_{M1,2}}{L_{M1,2}}}, \quad (1)$$

where constant 2 is given by current mirror gain (see Fig. 2). Intrinsic resistance of current input x has expression [23]

$$R_x = \frac{1}{\sqrt{I_{set_Rx} K_{Pn} \frac{W_{M11,12}}{L_{M11,12}}} + \sqrt{I_{set_Rx} K_{Pp} \frac{W_{M13,14}}{L_{M13,14}}}}, \quad (2)$$

and adjustable current gain has form [24]

$$B = \frac{N I_{b2}}{2 I_{set_B}} \cong \frac{I_{b2}}{I_{set_B}}, \quad (3)$$

where $N = 2$ (see Fig. 2). Proposed CMOS model was simulated and analysed with TSMC LO EPI 0.18 μm technology process parameters [26], where fabrication constants (given by gate-oxide capacitance and mobility of carriers) have approximate values of $K_{Pn} = 170.4 \mu\text{A}/\text{V}^2$ and $K_{Pp} = 35.7 \mu\text{A}/\text{V}^2$.

III. SPICE SIMULATION RESULTS OF THE ZC-CG-VDCC

Main parameters of the proposed ZC-CG-VDCC with power supply voltages ± 1 V are given in following figures. Gain control of current from x to z terminals was verified by adjusting of bias current I_{set_B} from 20 μA to 100 μA in range of B from 3.76 to 0.36 (Fig. 3).

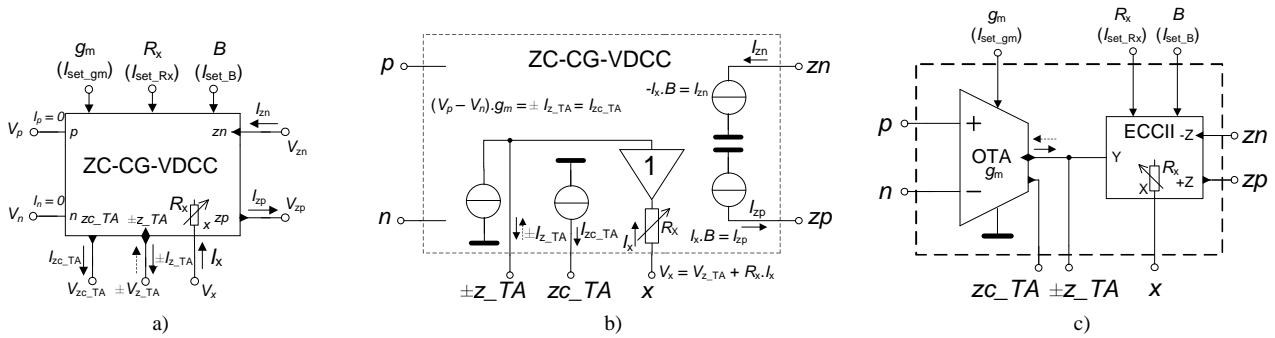


Fig. 1. Proposed ZC-CG-VDCC with independent control of three parameters: a) symbol, b) behavioral model, c) possible block conception.

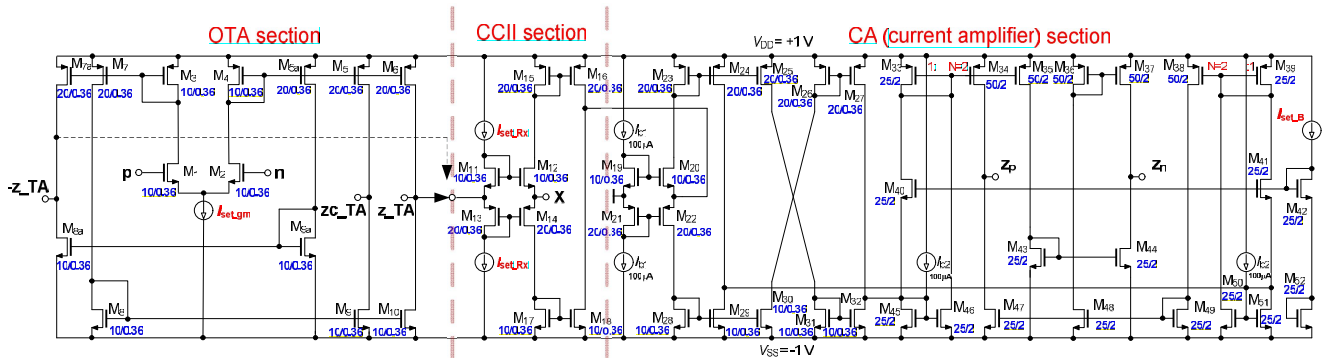


Fig. 2. CMOS realization of proposed ZC-CG-VDCC.

Selected transfers for $B = 3, 2, 1, 0.5$ are shown in Fig. 3 (DC transfer characteristic and frequency response).

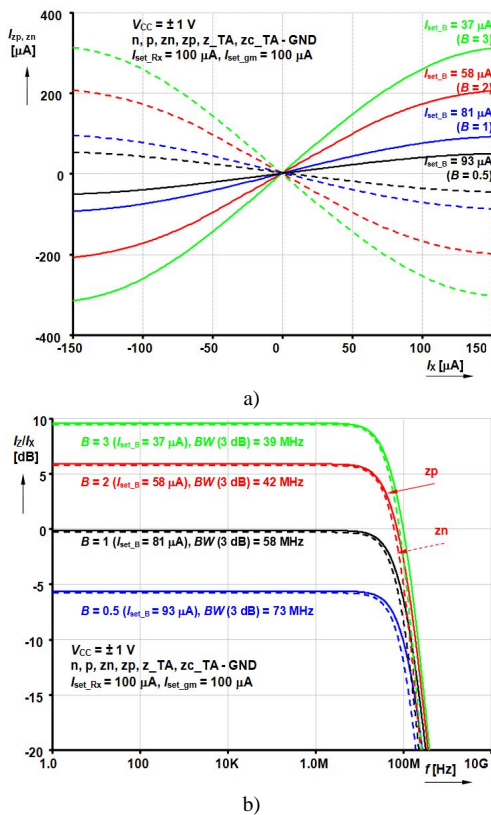


Fig. 3. Transfer characteristics of controlled current amplification for selected values of gain: a) DC transfers, b) AC frequency responses.

Linear dynamical range of input current (I_x) is almost $\pm 100 \mu A$ and bandwidth 39 MHz for $B = 3$. The second important adjustable parameter of presented active element

is transconductance. Bias control of I_{set_gm} from $10 \mu A$ to $150 \mu A$ allows changes of g_m from $255 \mu S$ to $1919 \mu S$. Dynamical range of V_p is approximately ± 100 mV and bandwidth 505 MHz for $g_m = 1.5$ mS. Characteristics in DC and AC domain are shown in Fig. 4 in detail for three selected values (0.5, 1.0 and 1.5 mS) of g_m . DC characteristic of voltage gain between z_TA and x port is shown in Fig. 5(a).

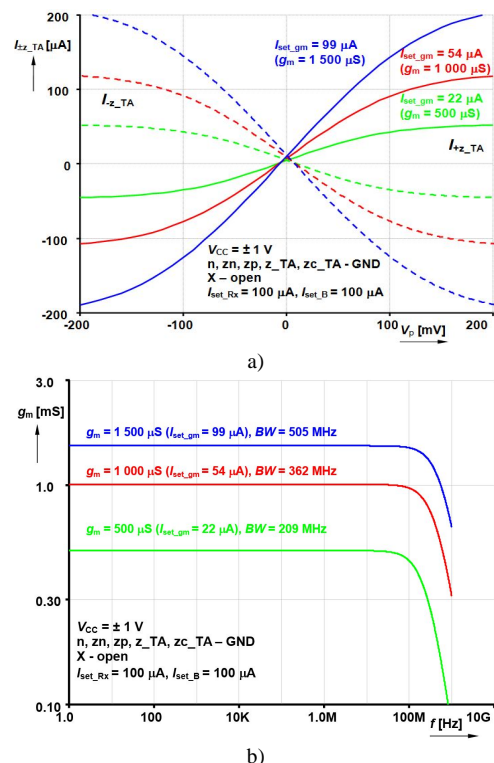


Fig. 4. Transconductance characteristics for selected values of g_m : a) DC transfers, b) AC frequency responses.

Figure 5(b) shows dependence of R_x on I_{set_RX} . Input resistance is controllable from 2.53 k Ω to 451 Ω by I_{set_RX} adjusted from 10 to 150 μ A. Important parameters of the proposed ZC-CG-VDCC model are summarized in Table I. Notes in Fig. 3–Fig. 5 mean information for connection of remaining terminals for presented set of analyses.

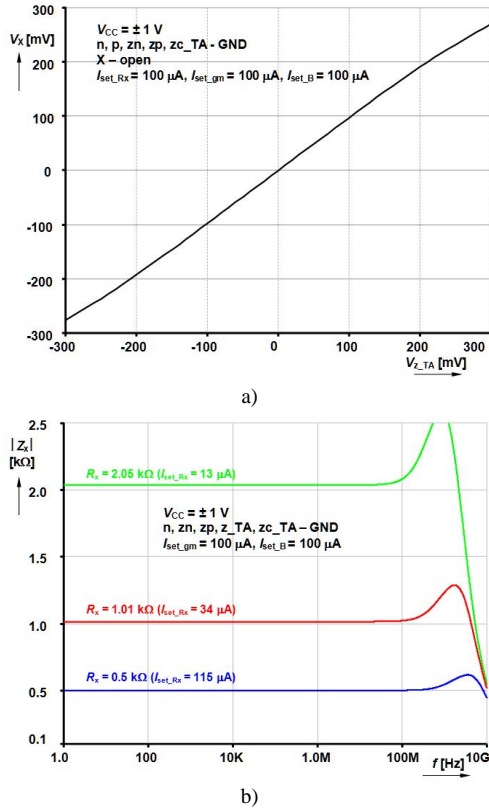


Fig. 5. Important characteristics of the current conveyor part (R_x terminal): a) DC transfer between z_TA and x terminal, b) dependence of R_x on I_{set_RX} .

IV. APPLICATION EXAMPLE:

RECONFIGURABLE FIRST-ORDER MULTIFUNCTION FILTER

Controllable features of proposed active device can be used in so-called reconfigurable reconnection-less tunable multifunctional filter (no change of output or input terminal or change of structure is required for change of the transfer function [27] – electronic control allows contactless reconfiguration) very beneficially. These solutions were not studied in detail in the past and our initial experience shows that such active elements like ZC-CG-VDCC with variety of controllable possibilities are very useful for their synthesis.

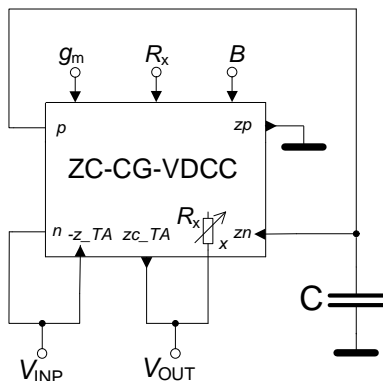


Fig. 6. Reconnection-less reconfigurable and tunable low-pass and all-pass filter.

Proposed solution is shown in Fig. 6. Note that circuit in Fig. 6 requires z_TA terminal with opposite (negative) polarity. It is indicated by dashed line in CMOS structure in Fig. 2. Transfer function (TF) of the circuit in Fig. 6 has form

$$K(s) = \frac{V_{OUT}}{V_{INP}} = \frac{Bg_m - sC(R_x g_m - 1)}{Bg_m + sC}, \quad (4)$$

where zero and pole frequencies (f_z , f_p) are given as: $\tilde{S}_z = Bg_m/(C(R_x g_m - 1))$ and $\tilde{S}_p = Bg_m/C$. It is clearly seen that current gain B serves for simultaneous control of $f_{p,z}$. The R_x configures type of the transfer function electronically independently on other parameters. The all-pass (AP) filter response is available in case when $g_m R_x = 2$ and its TF has a form

$$K_{AP}(s) = \frac{V_{OUT}}{V_{INP}} = \frac{Bg_m - sC}{Bg_m + sC}, \quad (5)$$

TABLE I. SUMMARIZATION OF IMPORTANT FEATURES OF THE ZC-CG-VDCC CMOS MODEL.

Controllable parameters	
parameter	tested range of adjusting
current gain (B [-])	0.36 – 3.76 ($I_{set_B} = 100 \mu\text{A} - 20 \mu\text{A}$)
transconductance (g_m [μS])	255 – 1 919 ($I_{set_gm} = 10 \mu\text{A} - 150 \mu\text{A}$)
intrinsic resistance (R_x [$\text{k}\Omega$])	2.53 – 0.451 ($I_{set_Rx} = 10 \mu\text{A} - 150 \mu\text{A}$)
DC performances ($I_{set_gm} = I_{set_Rx} = I_{set_B} = 100 \mu\text{A}$). TF analysis	
parameter	value
I_{zp}/I_x [-]	0.36
I_{zn}/I_x [-]	0.35
I_{z_TA}/V_p (g_m) [μS]	1 517
V_{z_TA}/V_x [-]	0.98
$R_{p,n}$ [Ω]	1E20
R_{z_TA, zc_TA} [$\text{k}\Omega$]	34.6
R_x [Ω]	533
R_{zp} [$\text{k}\Omega$]	55.0
R_{zn} [$\text{k}\Omega$]	53.1
AC performances ($I_{set_gm} = I_{set_Rx} = I_{set_B} = 100 \mu\text{A}$)	
parameter	value
$R_{z_TA}(R_{zc_TA})$ [$\text{k}\Omega$]	> 35 for $I_{set_gm} = 100 \mu\text{A}$ ($f < 10 \text{ MHz}$)
R_{zp}, R_{zn} [$\text{k}\Omega$]	> 50 for $I_{set_B} = 100 \mu\text{A}$ ($f < 1 \text{ MHz}$)
$C_{p,n}$ [fF]	30
C_{z_TA}, C_{zc_TA} [fF]	110
C_{zp} [fF]	120
C_{zn} [fF]	190

And if $g_m R_x = 1$, the low-pass (LP) filter response is obtained

$$K_{LP}(s) = \frac{V_{OUT}}{V_{INP}} = \frac{Bg_m}{Bg_m + sC}. \quad (6)$$

Special type of TF so-called inverting direct transfer (iDT) is available for $g_m R_x = 2$ and $B = 0$. In these conditions the circuit works as direct connection (constant magnitude and phase response) between input and output terminal. Pure direct transfer (non-inverting) is available for $g_m R_x \rightarrow 0$ together with any value of positive gain B .

We provided simulations of the circuit in Fig. 6 with proposed CMOS model (Fig. 2) and experimental verifications with behavioural model of ZC-CG-VDCC based on commercially available devices called diamond transistor (DT) OPA860 and multiplier EL2082 (ECCII-), see Fig. 7. Results presented in further text were gained for

$C = 470$ pF and $g_m = 1$ mS, see comments in figures (figure captions) for obtained values and setting of parameters in simulations and experiments. Supply voltage of the behavioural model was ± 5 V (± 1 V for CMOS model).

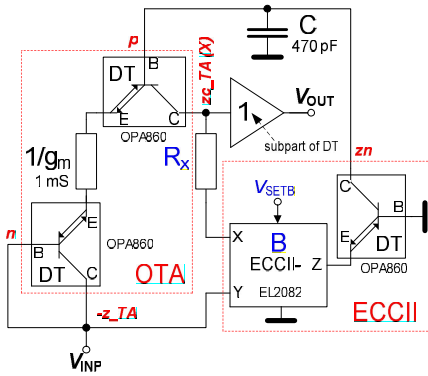


Fig. 7. Behavioral model of the ZC-CG-VDCC in proposed reconfigurable filtering application employing commercially available active devices.

Frequency responses of the TF change between AP, LP, DT and iDT were recorded by network analyser E5071C ($f_{min} = 9$ kHz, $P_{in} = -15$ dBm/50 Ω), see Fig. 8–Fig. 11.

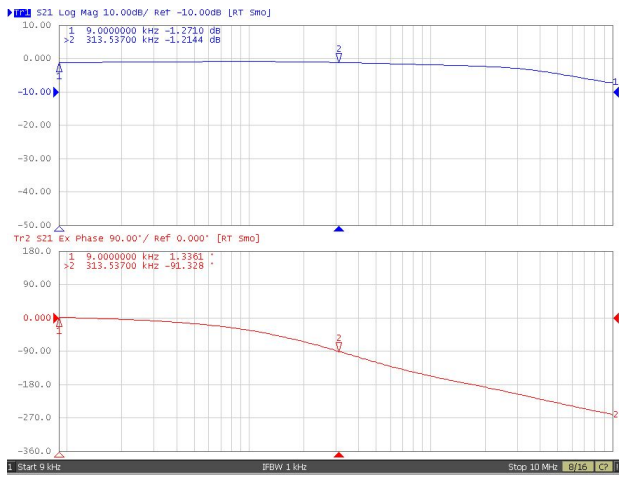


Fig. 8. All-pass filter response for $g_m = 1$ mS, $R_x = 2$ k Ω and $B = 1$.

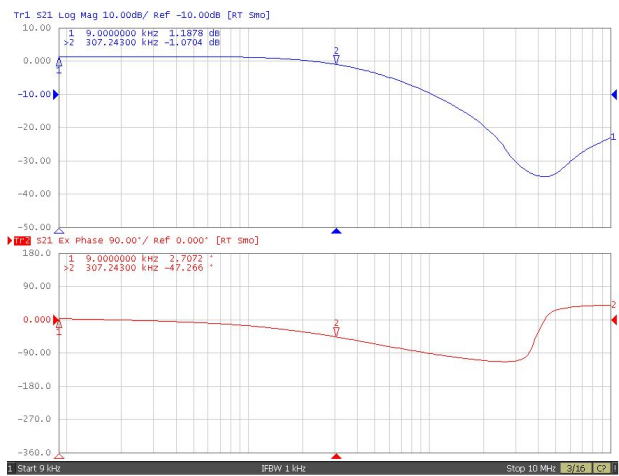


Fig. 9. Low-pass filter response for $g_m = 1$ mS, $R_x = 1$ k Ω and $B = 1$.

Phase responses in Fig. 12 document electronic reconfiguration between iDT, DT transfer and LP and AP response for specific set of R_x and B values, see details in Fig. 12 where also comparison of ideal, simulated (proposed CMOS model of the ZC-CG-VDCC) and measured

(behavioural model) traces is given. Validity of the behavioural model is supposed approximately to 1 MHz. Features of the CMOS model (R_x , B) do not allow operation of the filter (Fig. 6) in iDT and DT regime.

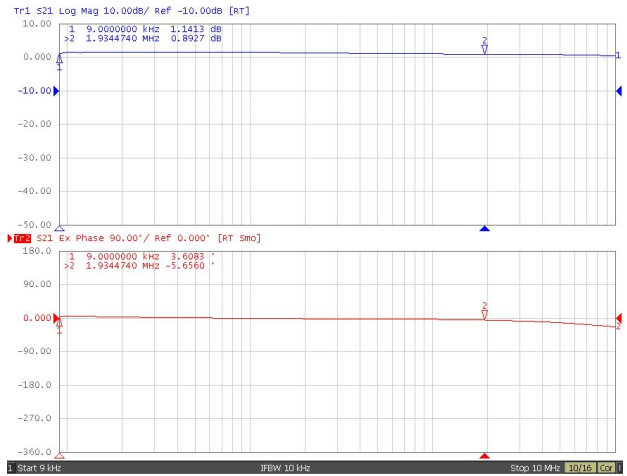


Fig. 10. Direct transfer response for $g_m = 1$ mS, $R_x = 0$ k Ω and $B = 1$.

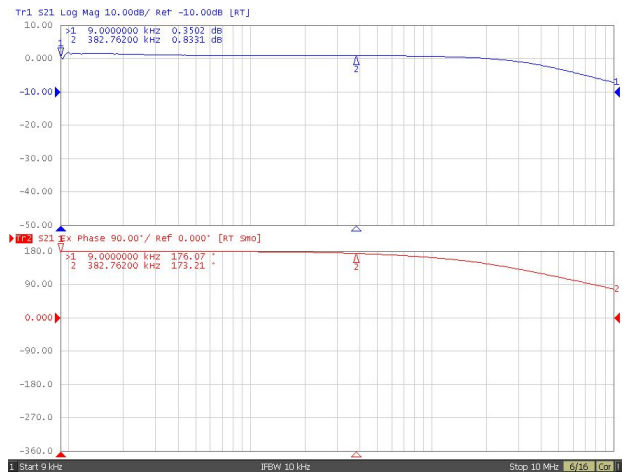


Fig. 11. Inverting direct transfer response ($g_m = 1$ mS, $R_x = 2$ k Ω and $B = 0$).

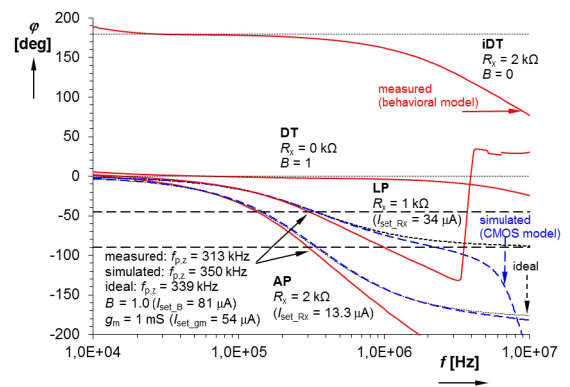


Fig. 12. Reconfiguration between iDT, DT, LP and AP (phase responses).

Transient response (oscilloscope Rigol DS1204B) of the AP filter is shown in Fig. 13 ($f_{in} = 313$ kHz, AP has the same setting as we give in caption of Fig. 8). Tuning features for AP and LP responses are shown in Fig. 14 and Fig. 15. Ideal values of pole/zero frequencies ($f_{p,z}$) are 169, 339 and 667 kHz ($B = 0.5, 1, 2$). Values of $f_{p,z}$, obtained from simulations were 187 kHz, 350 kHz and 696 kHz and experiments yield values 166 kHz, 313 kHz and 610 kHz

(see also Fig. 14).

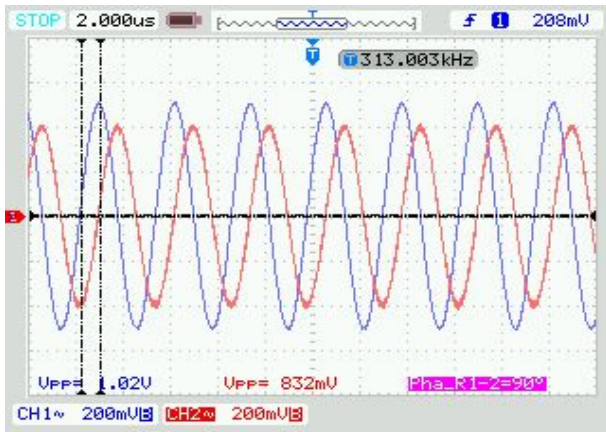


Fig. 13. Transient response of the AP filter for $f_{in} = 313$ kHz ($g_m = 1$ mS, $R_x = 2$ k Ω and $B = 1$).

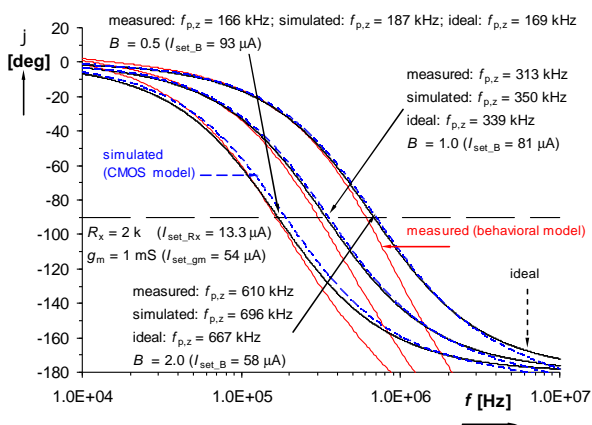


Fig. 14. Tuning of the AP filter (phase responses).

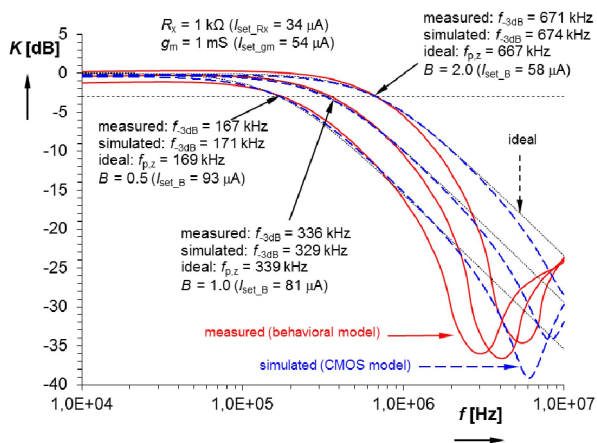


Fig. 15. Tuning of the LP filter (magnitude responses).

V. CONCLUSIONS

Our work is focused on design of modification of the voltage differencing current conveyor, proposal of its model and example of its useful features in simple application. The most important advantages of proposed active element are availability of three types of independent electronic control and useful z-copy technique. Range of the B control of the CMOS model was verified between 0.36 and 3.76 ($I_{set,B}$ from 100 μ A to 20 μ A), control of the g_m value between 255 μ S and 1 919 μ S ($I_{set,gm}$ from 10 μ A to 150 μ A) and R_x value in range from 2.53 k Ω to 0.451 k Ω ($I_{set,Rx}$ from 10 μ A to 150 μ A). Frequency features allow operation of CMOS

simulation model to tens of MHz. Bandwidth (3 dB) of the ZC-CG-VDCC model is determined by current amplifier block, where minimal value 39 MHz was obtained for $B = 3$, see Fig. 3(b). Further details are summarized in Table I. Proposed active element was implemented in simple electronically reconfigurable reconnection-less first-order multifunctional filtering structure working in voltage-mode which features were verified in frequency band of hundreds of kHz by Spice simulations and experimentally with behavioural model of the proposed active device employing commercially available devices. Electronic control allows change of the transfer type (direct transfer, inverting direct transfer, all-pass and low-pass response) and tuning of the $f_{p,z}$ frequency (even independent control of f_z). Tuning was tested for three values of B (0.5, 1, 2) that results in simulated $f_{p,z}$ (187, 350, 696 kHz). Measurements provide 166 kHz, 313 kHz and 610 kHz (Fig. 14). Behavioural and CMOS models of the ZC-CG-VDCC represent expected behaviour of filtering application and confirm our assumptions. ZC-CG-VDCC seems to be interesting choice for circuit synthesis and possible fabrication.

REFERENCES

- [1] D. Biolek, R. Senani, V. Biolkova, Z. Kolka, "Active elements for analog signal processing: classification, review and new proposals", *Radioengineering*, vol. 17, no. 4, pp. 15–32, 2008.
- [2] A. Fabre, O. Saaid, F. Wiest, C. Boucheron, "High frequency applications based on a new current controlled conveyor", *IEEE Trans. on Circuits and Systems - I*, vol. 43, no. 2, pp. 82–91, 1996.
- [3] A. Sedra, K. C. Smith, "A second generation current conveyor and its applications", *IEEE Trans. Circuit Theory*, vol. CT-17, no. 2, pp. 132–134, 1970. [Online]. Available: <http://dx.doi.org/10.1109/TCT.1970.1083067>
- [4] R. L. Geiger, E. Sanchez-Sinencio, "Active filter design using operational transconductance amplifiers: a tutorial", *IEEE Circ. and Devices Magazine*, vol. 1, pp. 20–32, 1985. [Online]. Available: <http://dx.doi.org/10.1109/MCD.1985.6311946>
- [5] W. Surakampontorn, W. Thitimajshima, "Integrable electronically tunable current conveyors", *IEE Proc.-G*, vol. 135, no. 2, 1988, pp. 71–77. [Online]. Available: <http://dx.doi.org/10.1049/ip-g-1.1988.0010>
- [6] A. Fabre, N. Mimeche, "Class A/AB second-generation current conveyor with controlled current gain", *Electronics Letters*, vol. 30, no. 16, pp. 1267–1268, 1994. [Online]. Available: <http://dx.doi.org/10.1049/el:19940878>
- [7] S. Minaei, O. K. Sayin, H. Kuntman, "A new CMOS electronically tunable current conveyor and its application to current-mode filters", *IEEE Trans. on Circuits and Systems - I*, vol. 53, no. 7, pp. 1448–1457, 2006.
- [8] A. Marcellini, G. Ferri, N. C. Guerrini, G. Scotti, V. Stornelli, A. Trifiletti, "The VGC-CCII: a novel building block and its application to capacitance multiplication", *Analog Integrated Circuits and Signal Processing*, vol. 58, no. 1, pp. 55–59, 2009. [Online]. Available: <http://dx.doi.org/10.1007/s10470-008-9213-6>
- [9] M. Kummern, S. Junnapiya, "A sinusoidal oscillator using translinear current conveyors", in *Proc. Asia Pacific Conf. on Circuits and Systems (APCCAS 2010)*, Kuala Lumpur, 2010, pp. 740–743. [Online]. Available: <http://dx.doi.org/10.1109/APCCAS.2010.5774754>
- [10] A. U. Keskin, D. Biolek, E. Hancioglu, V. Biolkova, "Current-mode KHN filter employing current differencing transconductance amplifiers", *AEU – Int. Journal of Electronics and Communications*, vol. 60, no. 6, pp. 443–446, 2006. [Online]. Available: <http://dx.doi.org/10.1016/j.aue.2005.09.003>
- [11] W. Jaikla, A. Lahiri, "Resistor-less current-mode four-phase quadrature oscillator using CCCDTAs and grounded capacitors", *AEU – Int. Journal of Electronics and Communications*, vol. 66, no. 3, pp. 214–218, 2011. [Online]. Available: <http://dx.doi.org/10.1016/j.aue.2011.07.001>
- [12] Ch. Sakul, W. Jaikla, K. Dejhan, "New resistorless current-mode

- quadrature oscillators using 2 CCCDTAs and grounded capacitors”, *Radioengineering*, vol. 20, no. 4, pp. 890–896, 2011.
- [13] R. Prokop, V. Musil, “Modular approach to design of modern circuit blocks for current signal processing and new device CCTA”, in *Proc. Conf. on Signal and Image Processing (IASTED)*, Anaheim, 2005, pp. 494–499.
- [14] M. Siripruchyanun, W. Jaikla, “Current controlled current conveyor transconductance amplifier (CCCCTA): a building block for analog signal processing”, *Electrical Engineering Springer*, vol. 90, no. 6, pp. 443–453, 2008. [Online]. Available: <http://dx.doi.org/10.1007/s00202-007-0095-x>
- [15] R. Sotner, J. Jerabek, R. Prokop, K. Vrba, “Current gain controlled CCTA and its application in quadrature oscillator and direct frequency modulator”, *Radioengineering*, vol. 20, no. 1, pp. 317–326, 2011.
- [16] R. Sotner, J. Jerabek, N. Herencsar, Z. Hrubos, T. Dostal, K. Vrba, “Study of adjustable gains for control of oscillation frequency and oscillation condition in 3R-2C oscillator”, *Radioengineering*, vol. 21, no. 1, pp. 392–402, 2012.
- [17] J. Jerabek, J. Koton, R. Sotner, K. Vrba, “Adjustable band-pass filter with current active elements: two fully-differential and single-ended solutions”, *Analog Integrated Circuits and Signal Processing*, vol. 74, no. 1, pp. 129–139, 2013. [Online]. Available: <http://dx.doi.org/10.1007/s10470-012-9942-4>
- [18] S. Minaei, M. A. Ibrahim, “General configuration for realizing current-mode first-order all-pass filter using DVCC”, *Int. Journal of Electronics*, vol. 92, no. 6, pp. 347–356, 2005. [Online]. Available: <http://dx.doi.org/10.1080/00207210412331334798>
- [19] S. Maheshwari, “A canonical voltage-mode-controlled VM-APS with grounded capacitors”, *Circuits Systems and Signal Processing*, vol. 27, no. 1, pp. 123–132, 2008. [Online]. Available: <http://dx.doi.org/10.1007/s00034-008-9015-1>
- [20] S. Minaei, E. Yuce, “Novel voltage-mode all-pass filter based on using DVCCs”, *Circuits Systems and Signal Processing*, vol. 29, no. 3, pp. 391–402, 2010. [Online]. Available: <http://dx.doi.org/10.1007/s00034-010-9150-3>
- [21] J. W. Horng, “DVCCs based high input impedance voltage-mode first-order allpass, highpass and lowpass filters employing grounded capacitor and resistor”, *Radioengineering*, vol. 19, no. 4, pp. 653–656, 2010.
- [22] A. M. Soliman, “Wide dynamic range CMOS pseudo-differential current conveyors: CMOS realizations and applications”, *Circuits Systems and Signal Processing*, vol. 32, no. 2, pp. 477–497, 2013. [Online]. Available: <http://dx.doi.org/10.1007/s00034-012-9478-y>
- [23] J. Baker, *CMOS Circuit Design, Layout and Simulation*. Wiley-IEEE Press, West Sussex, 2005, p. 1039.
- [24] W. Surakamponorn, K. Kumwachara, “CMOS-based electronically tunable current conveyor”, *Electronics Letters*, vol. 28, no. 14., pp. 1316–1317, 1992. [Online]. Available: <http://dx.doi.org/10.1049/el:19920836>
- [25] R. Sotner, J. Jerabek, N. Herencsar, T. Dostal, K. Vrba, “Electronically adjustable modification of CFA: Double Current Controlled CFA (DCC-CFA)”, in *Proc. of the 35th Int. Conf. on Telecommunications and Signal Processing (TSP 2012)*, Prague, 2012, pp. 401–405.
- [26] MOSIS parametric test results of TSMC LO EPI SCN018 technology. [Online]. Available: ftp://ftp.isi.edu/pub/mosis/vendors/tsmc-018/t44e_lo_epi-params.txt
- [27] R. Sotner, J. Jerabek, B. Sevcik, T. Dostal, K. Vrba, “Novel solution of notch/all-pass filter with special electronic adjusting of attenuation in the stop band”, *Elektronika ir Elektrotechnika*, vol. 17, no. 7, pp. 37–42, 2011.

[25] SOTNER, R., JERABEK, J., HERENC SAR, N., PROKOP, R., VRBA, K., DOSTAL, T. Resistor-less First- Order Filter Design with Electronical Reconfiguration of its Transfer Function. In *Proceedings of the 24th International Conference Radioelektronika 2014*, Bratislava (Slovakia), 2014. p. 63-66. ISBN: 978-1-4799-3715-8.

Resistor-less First-Order Filter Design with Electronical Reconfiguration of its Transfer Function

R. Sotner, J. Jerabek, N. Herencsar, R. Prokop, K. Vrba
 Faculty of Electrical Engineering and Communication
 Brno University of Technology
 Brno, Czech Republic
 sotner@feec.vutbr.cz

T. Dostal
 Dept. of Electrical Engineering and Computer Science
 College of Polytechnics Jihlava
 Jihlava, Czech Republic
 tomas.dostal@vspj.cz

Abstract—This contribution deals with special first-order filtering structure design based on two operational transconductance amplifiers (OTAs) and single electronically controllable current conveyor of second generation (ECCII). Controllable parameters of OTAs and ECCII allow electronic reconnection-less reconfiguration among several types of transfer functions. Theoretical assumptions are supported by PSpice simulations with models of commercially available real devices.

Keywords—Adjustable filters; current conveyor; current gain control; first-order filter; multifunctionality; reconfigurability; transconductor

I. INTRODUCTION

Electronic filters [1] are widespread group of systems used in many various applications and subparts of communication systems. However, some features are not available or even possible in the simplest passive RC and RLC structures. Active elements [2] offer interesting features in controllability of many types of circuits [3]. However, current research and published works in the field of electronically controllable filters with active elements are mostly focused on solutions of control of filtering application parameters, i.e. pole frequency (f_p) and quality factor (Q) independently and also above all on multifunctionality (several types of transfer functions available in frame of one structure). Many solutions use well known principle presented by Kerwin, Huelsman and Newcomb [4]. Immense amount of recent works deal with various circuit structures using various active elements [2] that provide independent control of f_p and/or of Q [3], [4]. However, proposals, that allow also electronic control of the transfer type, are not often discussed. To the best of author's knowledge and with respect to second-order all-pass/band-reject solution in [5], circuits providing electronically reconfigurable features in order to change type of the transfer function without reconnection of signal source and output node are not available in the open literature. Such reconfigurable features (reconnection-less change of the type of the transfer function between several filtering responses) can be useful for on-chip application. Unfortunately, these features seem to be not feasible by standard opamps due to lack of electronically controllable parameters. Special active elements [2] with controllable features are very useful for purposes of this synthesis. Our aim is to suggest one from many possible

solutions of first-order filter realization, which allows reconnection-less reconfiguration across several transfer types.

II. RECONFIGURABLE MULTIFUNCTIONAL STRUCTURE

General structure of presented circuit is depicted in Fig. 1. Two OTAs [6] and one ECCII [7], [8] are employed in quite simple circuitry using only one grounded capacitor and one resistor. OTA has classical definition: $(V_+ - V_-)g_m = I_o$ and ECCII is defined by following inter-terminal relations: $V_Y = V_X$, $I_Z = B.I_X$, $I_Y = 0$. We have two possibilities to build ECCII and R_X area of this circuit. The first way supposes commercially available elements and external parts. The second way takes benefits of the some recently introduced active devices [9] into account. In such modification, externally connected resistor is replaced by intrinsic current input resistance of ECCII, ($I_X = (V_X - V_Z)/R_x$), at the X terminal (R_x) [10] that is controlled by DC bias current similarly as current gain B between X and Z terminal. Therefore, also resistor-less variant is available for further (mainly on-chip) implementation, see Fig. 1. Except CMOS solutions [9], [10], we can obtain electronically adjustable R_x also by implementation of commercially available devices. However, such solution requires at least two active devices [11].

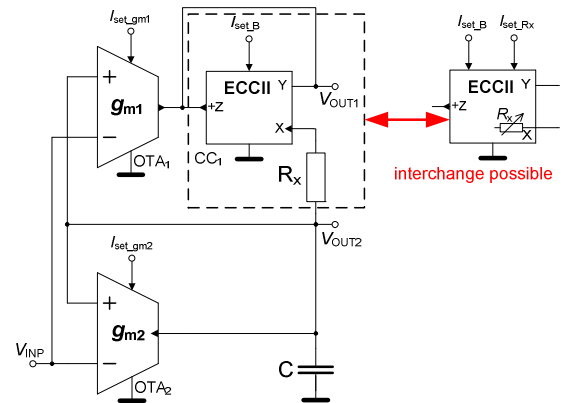


Fig. 1. General circuit structure for realization of specific first-order filters.

The circuit in Fig.1 has two possible output nodes. Transfer functions of this circuit have forms:

$$K_1(s) = \frac{V_{OUT1}}{V_{INP}} = \frac{Bg_{m2} - g_{m1} - sCR_x g_{m1}}{Bg_{m2} - g_{m1} + sCB}, \quad (1)$$

Research described in the paper was supported by Czech Science Foundation project under No. 14-24186P and by grant No. FEKT-S-14-2281 and project Electronic-biomedical co-operation ELBIC M00176. The support of the project CZ.1.07/2.3.00/20.0007 WICOMT, financed from the operational program Education for competitiveness, is gratefully acknowledged. The described research was performed in laboratories supported by the SIX project; the registration number CZ.1.05/2.1.00/03.0072, the operational program Research and Development for Innovation. Dr. Herencsar was supported by the project CZ.1.07/2.3.00/30.0039 of the Brno University of Technology.

$$K_2(s) = \frac{V_{OUT2}}{V_{INP}} = \frac{Bg_{m2} - g_{m1}}{Bg_{m2} - g_{m1} + sCB}. \quad (2)$$

There are three adjustable parameters in this structure: R_x , $g_{m1,2}$ and B . First set of graphs (Fig. 2) illustrates the function $K_1(s)$ for stepping of parameter B and $g_{m2} = 2g_{m1} = 1$ mS ($C = 100$ pF, $R_x = 1$ k Ω). Figure 3 shows behavior of the circuit for constant $B = 1$ and change of the g_{m2} . Magnitude response is always constant and equal to one in this case.

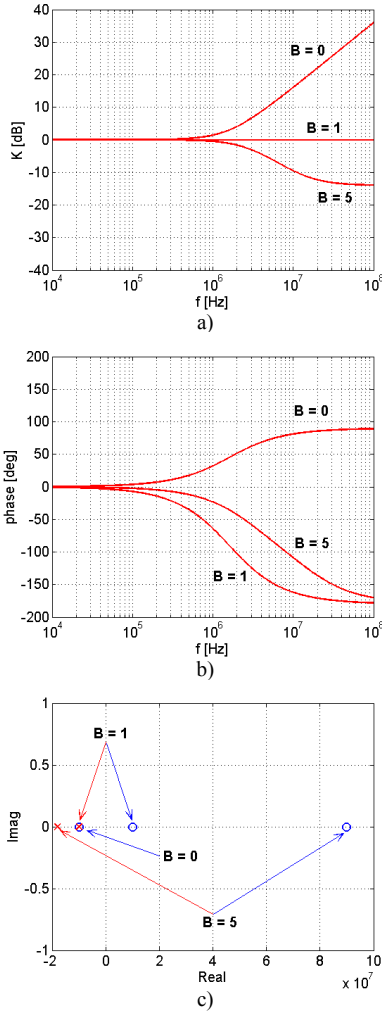


Fig. 2. Behavior of the circuit (V_{OUT1}) for B adjusting ($g_{m2} = 2g_{m1} = 1$ mS): a) magnitude responses, b) phase responses, c) complex plot ($C = 100$ pF, $R_x = 1$ k Ω).

The circuit structure offers several electronically reconfigurable types of the transfer. We can obtain:

A. All-pass (V_{OUT1}) and low-pass filter (V_{OUT2})

These responses are available for $B = 1$, $g_{m1} = 1/R_x$, and $g_{m2} > g_{m1}$ in forms:

$$K_{AP}(s) = \frac{V_{OUT1}}{V_{INP}} = \frac{g_{m2} - g_{m1} - sC}{g_{m2} - g_{m1} + sC}, \quad (3)$$

$$K_{LP}(s) = \frac{V_{OUT2}}{V_{INP}} = \frac{g_{m2} - g_{m1}}{g_{m2} - g_{m1} + sC}, \quad (4)$$

where g_{m1} and R_x have fixed value and g_{m2} serves for electronic tuning of the pole frequency (zero and pole in case of AP filter). In both cases, pole frequency has form:

$$\omega_p = \frac{g_{m2} - g_{m1}}{C}. \quad (5)$$

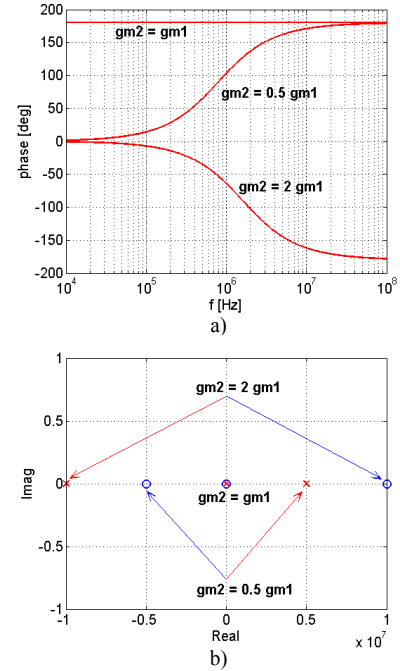


Fig. 3. Behavior of the circuit (V_{OUT1}) for g_{m2} adjusting ($B = 1$): a) phase responses, c) complex plot ($C = 100$ pF, $R_x = 1$ k Ω)

B. Direct inverting gain (V_{OUT1})

The desired transfer function is obtained for $g_{m2} = g_{m1}$ and $B = 1$ as: $K_{iDT} = -R_x g_{m1}$ ($K_{iDT} = -1$ for $g_{m1} = 1/R_x$). This function allows independent adjusting of the gain by R_x control.

C. Adjustable zero (V_{OUT1})

This function is possible for $B = 0$ in form:

$$K_Z(s) = \frac{V_{OUT1}}{V_{INP}} = 1 + sCR_x. \quad (6)$$

It is not pure filtering function but transfer with adjustable zero (6) is very useful for synthesis of so-called bilinear filters [12]-[15]. This form of adjustable zero is practically unavailable in classical passive structures. However, operation in this configuration is very hazardous (in proposed circuit structure) due to the high gain in positive feedback loop (possible instability and limitation of the output to saturation corners).

D. Adjustable low-pass filter with zero (V_{OUT1})

The filter with zero (and finite attenuation in the stop-band) is available also for $B = 1$ and $g_{m2} > g_{m1}$. However, R_x value has to be different and higher than $1/g_{m1}$ as we can see in:

$$K_{LP-z}(s) = \frac{V_{OUT1}}{V_{INP}} = \frac{g_{m2} - g_{m1} - sCR_x g_{m1}}{g_{m2} - g_{m1} + sC}, \quad (7)$$

where R_x serves for zero frequency control and attenuation/gain control with no influence on pole frequency.

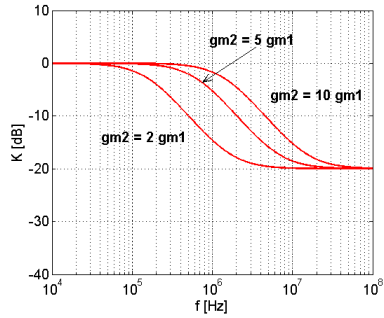


Fig. 4. Controllable features of the LP filter (V_{OUT1}) with control of the pole and zero frequency by g_{m2} ($R_x = 100 \Omega$, $g_{m1} = 1 \text{ mS}$, $C = 1 \text{ nF}$, $B = 1$).

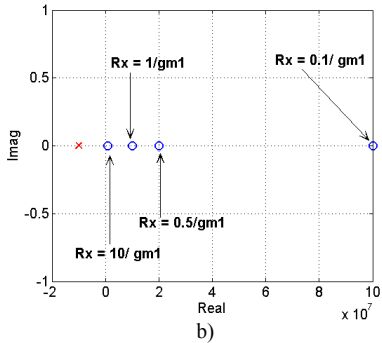
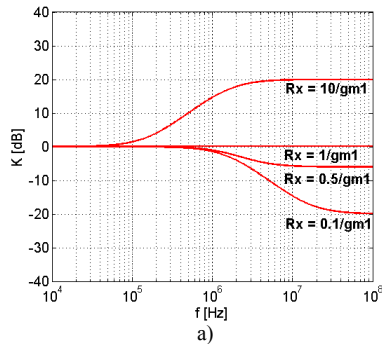


Fig. 5. Features of the filter (V_{OUT1}) with control of the pole and zero frequency by R_x : a) magnitude responses, b) complex plot ($g_{m2} = 2g_{m1} = 1 \text{ mS}$, $C = 100 \text{ pF}$, $B = 1$).

Zero frequency is given by:

$$\omega_z = \frac{g_{m2} - g_{m1}}{C R_x g_{m1}}, \quad (8)$$

which depends on relation of R_x and g_{m1} ($K(\omega \rightarrow \infty) = R_x g_{m1}$) in stop-band control, see example in Fig. 4 ($R_x = 100 \Omega$, $g_{m1} = 1 \text{ mS}$, $C = 1 \text{ nF}$). Distance of both frequencies (zero and pole) is given by $R_x g_{m1}$. The pole and zero frequencies have equal values and structure behaves as AP filter for $R_x = 1/g_{m1}$ only. Adjusting of the R_x ($g_{m2} = 2g_{m1} = 1 \text{ mS}$, $C = 100 \text{ pF}$, $B = 1$) causes change of the gain at the high frequencies, see Fig. 5.

III. BEHAVIORAL MODEL AND SIMULATION RESULTS

Model of the circuit with commercially available active elements (their models in OrCAD PSpice) is shown in Fig. 6. We used diamond transistors (DT) OPA860 [16] as OTAs and current-mode multiplier EL2082 [17] as electronically controllable current conveyor (ECCII). Passive elements were selected as: $R_x = 1 \text{ k}\Omega$, $C = 1 \text{ nF}$. Other parameters were adjusted to obtain specific transfers in simulated experiments (see comments in figures and figure captions). Basic default characteristics at both available outputs for $g_{m2} = 2g_{m1} = 1 \text{ mS}$ are in Fig. 7.

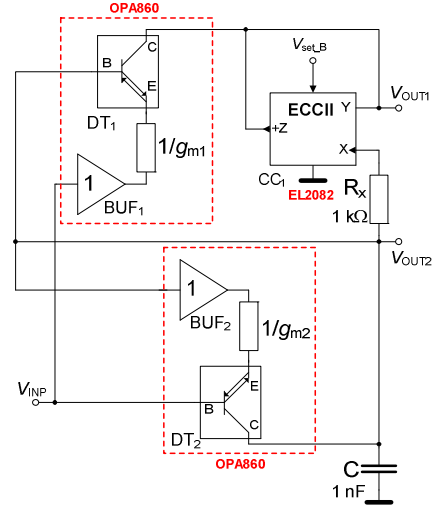


Fig. 6. Simulation model of the designed circuit based on commercially available devices.

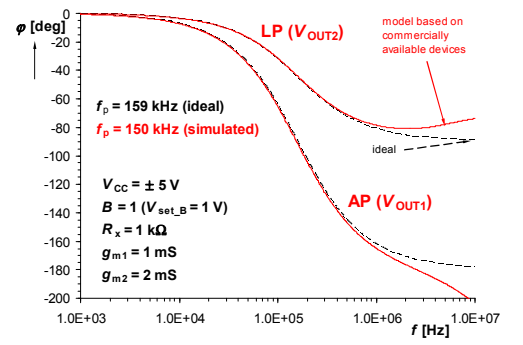
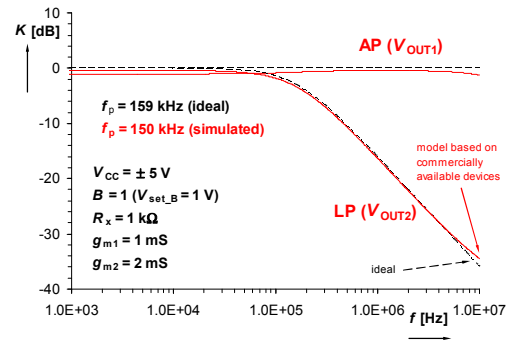


Fig. 7. Basic configuration of the filter: a) magnitude responses, b) phase responses.

Tuning of the filter by g_{m2} was verified for LP response (Fig. 8). Change of the transfer function between direct inversion ($g_{m2} = g_{m1}$) and AP response tuned by increasing g_{m2} when $g_{m2} > g_{m1}$ is shown in Fig. 9 (phase responses). Example of modification of the output response at V_{OUT1} by adjustable zero (regulation of zero location and stop-band attenuation by R_x) is proved in Fig. 10.

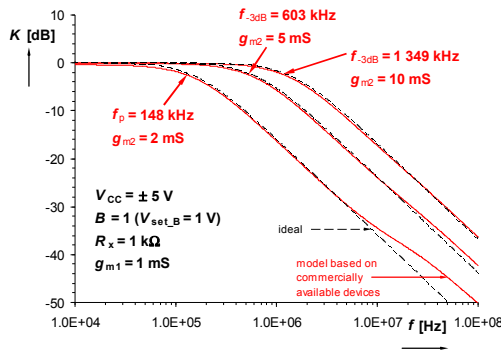


Fig. 8. Tuning of the LP response (V_{OUT2}).

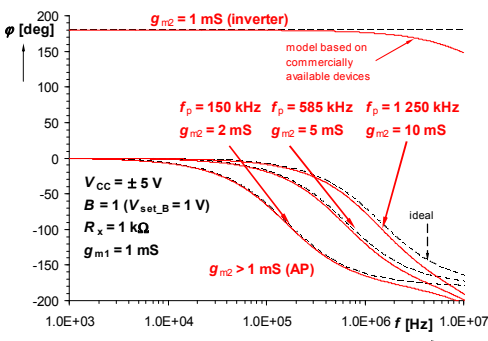


Fig. 9. Change of type of the transfer function and tuning of the AP response by g_{m2} (V_{OUT1}).

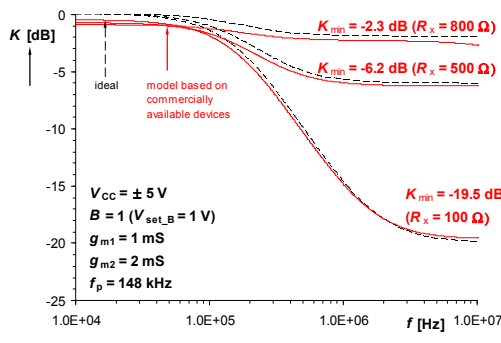


Fig. 10. Modification of the AP response to obtain LP response with adjustable zero (V_{OUT1}).

IV. CONCLUSION

We can obtain all-pass filter, low-pass filter with zero, inverting amplification and adjustable zero function in one structure only by changes of electronically controllable

parameters g_{m2} , R_x and B . Input (excitation) or output node is not moved to obtain these features (reconnection-less operation). In addition, classical low-pass filter is available at the second output. These features of the proposed circuit structure were confirmed by PSpice simulations.

REFERENCES

- [1] W. Chen, *The Circuits and Filters Handbook*. Boca Raton, FL: CRC Press, 2002.
- [2] D. Birolek, R. Senani, V. Biolkova, Z. Kolka, "Active elements for analog signal processing: Classification, Review and New Proposals," *Radioengineering*, vol. 17, no. 4, pp. 15-32, 2008.
- [3] R. Raut, M. N. S. Swamy, *Modern Analog Filter Analysis and Design: A practical approach*, many, Weinheim, Germany: Wiley-VCH Verlag GmbH and Co., 2010.
- [4] W. J. Kerwin, L. P. Huelsman, W. R. Newcomb, "State variable synthesis for insensitive integrated circuit transfer functions," *IEEE Journal of Solid State Circuits*, vol. 2, no. 3, pp. 87-92, 1967.
- [5] R. Sotner, J. Jerabek, B. Sevcik, T. Dostal, K. Vrba, "Novel solution of notch/all-pass filter with special electronic adjusting of attenuation in the stop band," *Elektronika Ir Elektrotechnika*, vol. 17, no. 7, pp. 37-42, 2011.
- [6] R. L. Geiger, E. Sánchez-Sinencio, "Active filter design using operational transconductance amplifiers: a tutorial," *IEEE Circ. and Devices Magazine*, vol. 1, pp. 20-32, 1985.
- [7] W. Surakamponorn, W. Thitimajshima, "Integrable electronically tunable current conveyors," *IEE Proceedings-G*, vol. 135, no. 2, pp. 71-77, 1988.
- [8] A. Fabre, N. Mimeche, "Class A/AB second-generation current conveyor with controlled current gain," *Electronics Letters*, vol. 30, no. 16, pp. 1267-1268, 1994.
- [9] S. Minaei, O. K. Sayin, H. Kuntman, "A new CMOS electronically tunable current conveyor and its application to current-mode filters," *IEEE Trans. on Circuits and Systems - I*, vol. 53, no. 7, pp. 1448-1457, 2006.
- [10] A. Fabre, O. Saaid, F. Wiest, C. Boucheron, "High frequency applications based on a new current controlled conveyor," *IEEE Trans. on Circuits and Systems - I*, vol. 43, no. 2, pp. 82-91, 1996.
- [11] R. Sotner, A. Kartci, J. Jerabek, N. Herencsar, T. Dostal, K. Vrba, "An Additional Approach to Model Current Followers and Amplifiers with Electronically Controllable Parameters from Commercially Available ICs," *Measurement Science Review*, vol. 12, no. 6, pp. 255-265, 2012.
- [12] A. Fernandez-Vazquez, R. Rosas-Romero, J. Rodriguez-Asomoza, "A New Method for Designing Flat Shelving and Peaking Filter Based on Allpass Filters," in *proc. of 17th int. conf. on Electronics, Communications and Computers CONIELECOMP2007*, pp. 1-10, 2007.
- [13] J. Valsa, J. Vlach, "RC models of a constant phase elements," *International Journal of Circuit Theory and Applications*, vol. 41, no. 1, pp. 59-67, 2013.
- [14] J. Petrzela, "Fundamental Analog Cells for Fractional-Order Two-Port Synthesis," in *proc. of 23th Int. Conf. Radioelektronika 2013*, pp. 182-187, 2013.
- [15] B. M. Vinagre, I. Podlubny, A. Hernandez, V. Feliu, "Some approximations of fractional order operators used in control theory and applications," *Fractional calculus and applied analysis*, vol. 3, no. 3, pp. 231-248, 2000.
- [16] Texas Instruments. OPA860 Wide-bandwidth, operational transconductance amplifier (OTA) and buffer (datasheet), 2008, 33 p., accessible on [www: http://www.ti.com/lit/ds/symlink/opa860.pdf](http://www.ti.com/lit/ds/symlink/opa860.pdf)
- [17] Intersil (Elantec). EL2082 CN Current-mode multiplier (datasheet), 1996, 14 p., accessible on [www: http://www.intersil.com/data/fn/fn7152.pdf](http://www.intersil.com/data/fn/fn7152.pdf)

[26] SOTNER, R., JERABEK, J., HERENC SAR, N., ZAK, T., JAIKLA, W., VRBA, K. Modified Current Differencing Unit and its Application for Electronically Reconfigurable Simple First-order Transfer Function. *Advances in Electrical and Computer Engineering*, 2015, vol. 15, no. 1, p. 3-10. ISSN: 1582-7445.

Modified Current Differencing Unit and its Application for Electronically Reconfigurable Simple First-order Transfer Function

Roman SOTNER¹, Jan JERABEK², Norbert HERENC SAR², Tomas ZAK¹, Winai JAIKLA³, Kamil VRBA²

¹*Dept. of Radio Electronics, Faculty of Electrical Engineering and Communication, Brno University of Technology, Technicka 3082/12, 61600, Brno, Czech Republic*

²*Dept. of Telecommunications, Faculty of Electrical Engineering and Communication, Brno University of Technology, Technicka 3082/12, 61600, Brno, Czech Republic*

³*Dept. of Engineering Education, Faculty of Industrial Education, King Mongkut's Institute of Technology Ladkrabag, 10520, Bangkok, Thailand*

sotner@feec.vutbr.cz

Abstract—Modified current differencing unit (MCDU) and its simple filtering application are introduced in this paper. Modification of the well-known current differencing unit consists in weighted difference of both input currents controlled by adjustable current gain, controllable intrinsic resistance of both current input terminals, and availability of additional voltage terminal(s). Definition of MCDU therefore requires four adjustable parameters (B_1 , B_2 , R_p , R_n). A presented active element offers and combines benefits of electronically controllable current conveyor of second generation and current differencing unit and allows synthesis of interesting adjustable applications, which are not available by classical approaches based on simple elements. MCDU brings variability of the transfer function into the structure. It provides several transfer types without necessity of input or output node change by simple electronic tuning. A presented structure represents so-called reconnection-less reconfigurable current-mode filter for realization of all-pass, inverting high-pass, low-pass and direct transfer response. Behavioral model of the MCDU was prepared and carefully tested in filtering application. Spice simulations and measurements confirmed theoretical assumptions.

Index Terms—Current differencing unit, controllable current gain, controllable intrinsic current input resistance, reconfigurability, multifunctional filter.

I. INTRODUCTION

Reconfigurability of the systems is generally a very important requirement of present-day applications (on-chip especially). Microelectronic design of on-chip systems focused on analog parts and signal processing before digitization (A/D conversion) always uses filters, amplifiers, coupling blocks with defined bandwidth, etc. However, chip development is very expensive and, unfortunately, also the results are sometimes inaccurate. Enormous fabrication tolerances cause the main problems with accuracy (deviation of parameters) of analog systems. Therefore, electronically controllable systems based on electronically controllable

active elements [1] are really important. We selected active filters as a perfect example of utilization of modern active elements.

A. Classical example of approach to obtain different transfer types in multifunctional filters

There are multifunctional or universal types of the filters in voltage- (examples [2-6]) and also current-mode (examples [3,4,7-10]) providing low-pass (LP), band-pass (BP), high-pass (HP), band-reject (BR) and all-pass (AP) filtering transfer function simultaneously at several output nodes [2-4] or current output terminals (see [10,11] for example and references cited therein). There are two possibilities of the synthesis of multifunctional multi-loop structures [8-10]. The first approach supposes one input and several outputs (so-called Follow the Leader Feedback state variable structure [4,10]) or several inputs and one output (so-called modified or inverting Follow the Leader Feedback structure [4,10]). The perfect practical example of mutual relation, similarity and difference of both approaches is shown in [12]. Therefore, the types of the filter with one input and several outputs are abbreviated as SIMO (Single Input - Multiple Output) and filters with several inputs and one output are abbreviated MISO (Multiple Input - Single Output). Generally, it does not mean that multi-loop state variable approach was used for their synthesis but it is one of the possible and best known way to obtain tunable multifunctional filtering structures [2-6]. Based on the discussion above, the most important information is that a classical multifunctional filter requires a change of the input or output in structure to obtain different transfer characteristic.

B. Reasons for implementation of reconnection-less multifunctional filtering solutions

Practical utilization of multifunctional filters in many analog systems is sufficient until a change of transfer function is required and we have no simple way to change input or output physically – in order to introduce galvanic connection (it is a typical problem for on-chip implementation – after fabrication when changes of topology are not possible). We can imagine useful signal, which is to be digitized in A/D and some undesirable low-

Research described in this paper was financed by the National Sustainability Program under grant LO1401 and by the Czech Science Foundation under grant no. GP14-24186P. For the research, infrastructure of the SIX Center was used. Grant No. FEKT-S-14-2281 also supported this research. The support of the project CZ.1.07/2.3.00/20.0007 WICOMT, financed from the operational program Education for competitiveness, is gratefully acknowledged.

Digital Object Identifier 10.4316/AECE.2015.01001

or high-frequency components suddenly occur. Now, the signal line with constant frequency response should be changed to HP or LP response and tuned (bandwidth change) in order to remove undesired signals and noises – it is no problem with reconnection of input or output terminals and electronic control of pole frequency in discrete solution of the filter. Required change of the filtering function can be realized also by switches. However, switching of inputs or outputs is not very favorable and brings the additional problems (power consumption and place on PCB or on chip). Additionally, some effects caused by discontinuous regime of operation and mechanical switching are undesired. Chip design requires the best effort to reduce occupied area and additional switches and their control cannot be in compliance with this requirement. We can also set a type of transfer function of the filter directly by controllable parameters of suitable active device. This idea has not been discussed in the literature very often [13-17]. Our paper focuses on filtering solution that allows control of type of the transfer function electronically by parameter(s) of advanced active element.

C. Brief recapitulation of multi-parameter controllability in known active elements

Electronic control of parameters in active circuit design came up from first type of rapidly used active devices, operational transconductance amplifier (OTA) [18], where electronic adjusting of the transconductance (g_m) between input voltage and output current is possible. Discovery of OTA starts the era of amazing development in the circuit applications and active analog signal processing. Active elements with controllable current gain (B) [19,20] and controllable intrinsic resistance of the current input terminal (R_x) [21] came after short time.

Combination of several controllable parameters in frame of one active device is quite a common way of development of new and improved (from controllability point of view) circuit structures and analog systems in the field of active filters, oscillators, generators, modulators, etc. Minaei et al. [22] proposed the first type of controllable active device that offers R_x and B control. The interesting features of electronic driving are also possible in a proposal published by Kumngern et al. in [23], where translinear current conveyor with similar possibilities has been shown. Marcellis et al. [24] created an active element with voltage and current gain control. Combination of g_m and R_x control can be found many times in literature. Many recently developed active devices combine this way of control, for example several modifications of current differencing transconductance amplifier (CDTA) [1,25], see for example [28-30] and references cited therein. The same method of control was used in modifications of so-called current conveyor transconductance amplifier (CCTA) [1,31], see for example [32].

Despite the fact that a possible way to construct electronically controllable intrinsic resistance of the current input terminal (R_x) of active element from commercially available devices has been shown quite recently [33,34], many applications were designed with these controllable parameters as a primary mechanism of tuning or adjusting other parameters of filtering transfer function, for example

[21,30,32]. However, control of DC bias current in the structure of current conveyor (allowing R_x or g_m control typically) causes undesired influences of output resistance which damages stop band attenuation due to their effect in high-impedance nodes of filtering structure [35]. The development of multi-parameter controllable features of active elements was discussed also in [36] where active element also offers control of B and R_x in frame of special modification of current feedback amplifier (CFA) [1] without impact of R_x control on output resistance [36]. Advanced active element referred to as dual-output controlled-gain voltage-differencing buffered/inverted amplifier (DO-CG-VDBVA) [37] was designed with intention of voltage gain (A) and g_m control. Electronically adjustable voltage and current gain was implemented in so-called controlled-gain buffered current and voltage amplifier (CG-BCVA) [38]. A brief comparison of already known controllable active devices is provided in Table I.

TABLE I. BASIC COMPARISON OF ACTIVE ELEMENTS WITH MULTI-PARAMETER CONTROL (IT MEANS MORE THAN ONE)

Ref.	Abbrev. of active element	Controllable parameters	Typical type of control
[22,28-30,32]	ECCII; CCCDTA; CCCTA	R_x, g_m	two DC bias currents
[23,36]	CCCII; DCC-CFA	R_x, B	two DC bias currents
[37]	DO-CG-VDBVA	A, g_m	-
[24,38]	VGC-CCII; CG-BCVA	B, A	two DC bias currents; DC control voltages
proposed	MCDU	two R_x , two B	DC control voltages

Explanations:
 ECCII – electronically controllable current conveyor of second generation
 CCCDTA – current-controlled current differencing transconductance amplifier
 CCCTA – current-controlled current conveyor transconductance amplifier
 CCCII – current-controlled current conveyor of second generation
 DCC-CFA – double current-controlled current feedback amplifier
 DO-CG-VDBVA – controlled gain voltage-differencing buffered/inverted amplifier
 VGC-CCII – voltage and current gain second generation current conveyor
 CG-BCVA – controlled gain buffered current and voltage
 MCDU – modified current differencing unit
 A – general controllable voltage gain
 B – general controllable current gain
 R_x – intrinsic resistance of current input terminal(s)
 g_m – transconductance

The main contribution of this paper is a design of simple first-order reconfigurable filter employing modified version of current differencing unit (CDU) [1,25,27]. Despite the same basic principle (difference of two currents), the modified version of CDU (MCDU) is significantly useful for an application discussed in this paper. The paper is divided as follows: introduction and presentation of MCDU (section 2), reconfigurable filtering solution providing features interesting for practical applications (section 3), proposal of suitable behavioral model of the MCDU and simulation results of the application (section 4), study of important parasitic influences (section 5) and conclusion (section 6).

II. MODIFIED CDU

Basic behavioral model of the CDU, presented by Biolek et al. [1,25-27] as a subpart of the CDTA element, utilizes two current conveyors of second generation (CCII+). Both voltage input terminals are grounded, see Fig. 1. The basic definition of the classic CDU operation is explained by equation: $I_x = I_p - I_n$. Current differencing buffered amplifier (CDBA) also offers very similar features, for example [1,39]. Classical CDU also does not provide possibility of control of input terminal resistances [21], which is very popular today in advanced types of CDTAs (for example [28-30]). A solution of differential current conveyor (DCC) presented in [40] also allows very similar possibilities (as standard CDTA). Unfortunately, very limited electronically adjustable parameters of the DCC (or its applications) are presented in [40].

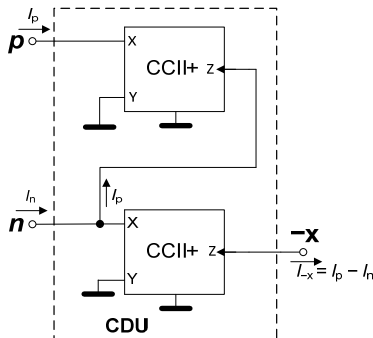


Figure 1. Basic definition of CDU employing two positive current conveyors of second generation

The introduced MCDU also utilizes voltage input terminals Y (two terminals, Y_1 and Y_2 are now available, not grounded as in Fig. 1), see Fig. 2. Ideal behavioral model is shown in Fig. 2a. Figure 2b shows a symbol of the MCDU and possible practical utilization based on commercially available active devices is introduced in Fig. 2c. Diamond transistor is used as a simple current inverter. Note that an order of the blocks (ECCII and diamond transistor) can be interchanged in the structure.

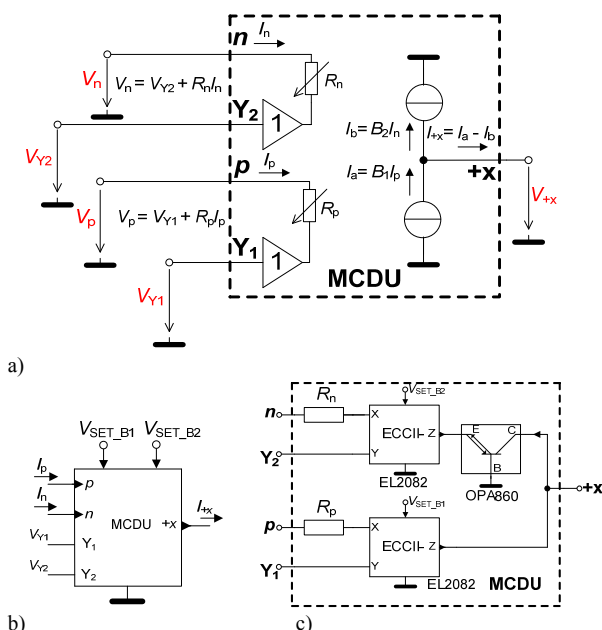


Figure 2. MCDU circuit: a) ideal behavioral model, b) symbol, c) possible practical utilization

MCDU allows independent control of current gain in both current paths as:

$$I_{+x} = I_p B_1 - I_n B_2, \tag{1}$$

that brings that interesting features in application which will be introduced later together with controllable input resistances R_p and R_n as is obvious from these relations:

$$V_p = V_{Y1} + R_p I_p, \tag{2}$$

$$V_n = V_{Y2} + R_n I_n. \tag{3}$$

III. APPLICATIONS OF MCDU IN ELECTRONICALLY RECONFIGURABLE FIRST-ORDER TRANSFER FUNCTION

The proposed MCDU provides the useful features in simple active filters. Utilization of one or both Y terminals (Y_1 and Y_2) can bring the interesting features that are not available in applications of basic CDU. The MCDU (Fig. 2) was used in current-mode solution shown in Fig. 3. The additional feedbacks bring opportunity to obtain simple transfer function in a form:

$$K_I(s) = \frac{B_2 - sCR_n B_1}{1 + sCR_n}, \tag{4}$$

Pole and zero frequencies are of the following form:

$$\omega_z = \frac{B_2}{CR_n B_1}, \quad \omega_p = \frac{1}{CR_n}. \tag{5}, (6)$$

Current-mode filtering solution from Fig. 3 provides the following transfer functions:

- a) all-pass (AP) response for $B_1 = 1$ and $B_2 = 1$; zero/pole frequency is controllable by R_n value,
- b) inverting high-pass (iHP) response is available for $B_2 = 0$, $B_1 = 1$ (for unity pass-band gain); pole frequency control is possible by R_n ,
- c) low-pass (LP) response for $B_1 = 0$, $B_2 = 1$; pole frequency controllable by R_n ,
- d) direct transfer (DT) for $B_1 = -1$, $B_2 = 1$ and inverting direct transfer (iDT) for $B_1 = 1$ and $B_2 = -1$.

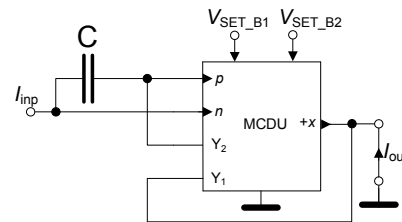


Figure 3. Multifunctional reconfigurable filter utilizing the MCDU circuit

Independent control of zero frequency by B_1 and B_2 is possible as is obvious from (5).

IV. BEHAVIORAL MODEL AND SIMULATION RESULTS

We used structure from Fig. 3 for further analysis. Commercially available devices allow quite easy controllability in applications. Current-mode multiplier EL2082 [41] is very favorable for purposes of behavioral modeling of active elements and applications together with diamond transistors OPA860 [42]. Behavioral model of the MCDU in filtering application (Fig. 3) is shown in Fig. 4. The circuit in Fig. 3 does not require control of R_p . Therefore, this element was represented only by fixed passive resistor (its controllability is not necessary in this particular case). Controllable part R_n (dashed red color line)

was created by sub-block ($R_n \cong (R_1 + R_{x1} + R_{x2}) / V_{set_Rn}$) discussed in detail in [33,34]. All parameters required for control (B_1, B_2, R_n) are adjustable electronically by DC voltages ($V_{set_B1}, V_{set_B2}, V_{set_Rn}$).

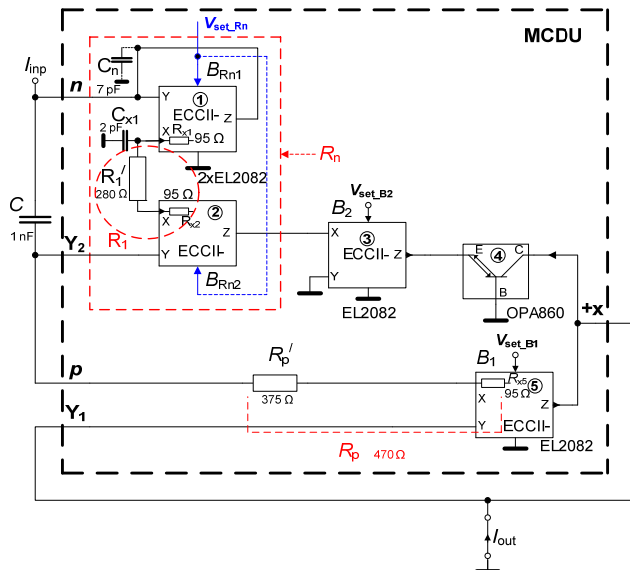
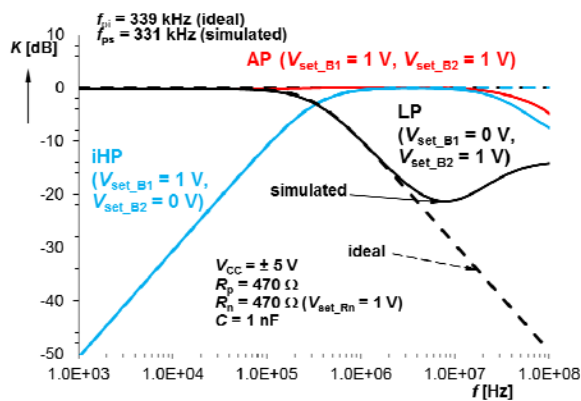


Figure 4. Proposed filter including simplified behavioral model of the MCDU

The values of passive elements are selected as follows: $R_p = 470 \Omega$ (including resistance $R_{x5} = 95 \Omega$ of the terminal X of the EL2082 [41]), $C = 1 \text{ nF}$. The R_n control was set and verified in range between 235Ω and $4.7 \text{ k}\Omega$ by V_{set_Rn} between 2 and 0.1 V. Figure 5 shows the available types of adjustable transfer functions for particular values of V_{set_B1} and V_{set_B2} ($B \cong V_{set_B}$ for EL2082 [41]). Ideal pole frequency (f_{pi}) is 339 kHz for setting: $V_{set_B1} = V_{set_B2} = 1 \text{ V}$, $V_{set_Rn} = 1 \text{ V}$ (470Ω). Value 331 kHz was obtained from simulation (f_{ps}). Transfers DT and iDT could not be analyzed because this particular behavioral model (Fig. 4) does not allow to set negative gains (B). Tuning of the pole frequency is illustrated in Fig. 6 and Fig. 7. Figure 6 shows adjusting of pole frequency of the AP response and Fig. 7 of the iHP response. The value of resistance R_n was adjusted as: 235Ω ($V_{set_Rn} = 2 \text{ V}$), 470Ω ($V_{set_Rn} = 1 \text{ V}$), 940Ω ($V_{set_Rn} = 0.5 \text{ V}$) and $4.7 \text{ k}\Omega$ ($V_{set_Rn} = 0.1 \text{ V}$) in both cases. A range of the pole frequency (f_{ps}) control from 35 kHz to 623 kHz was obtained, which is very close to ideal values $f_{pi} = 34 \text{ kHz}$ to 677 kHz . The filter was tested also in time domain in regime of AP function at frequency 339 kHz . The results are shown in Fig. 8.



a)

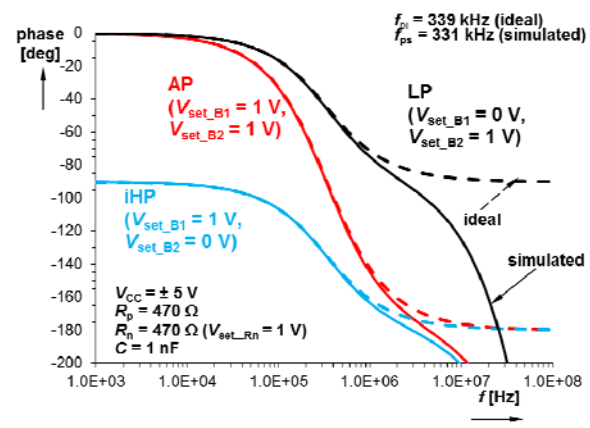
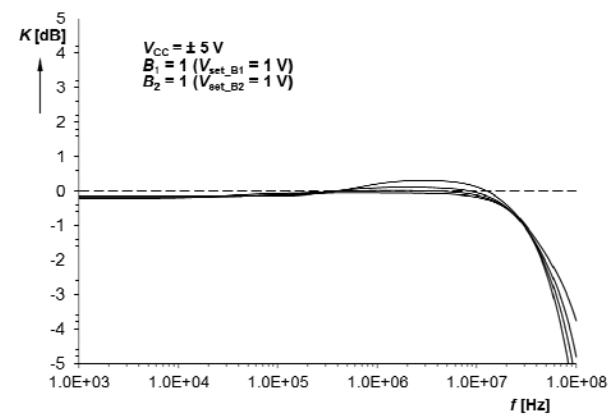
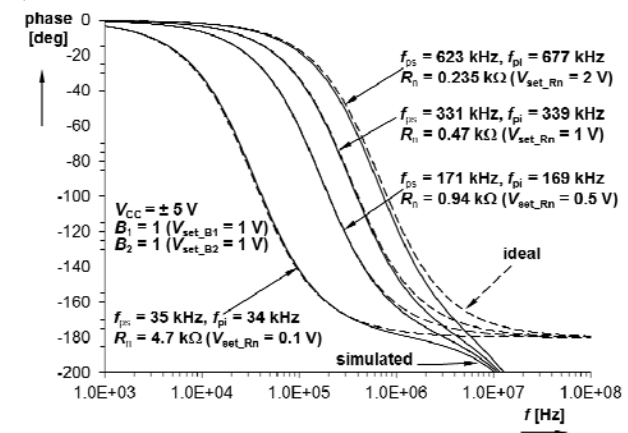


Figure 5. Simulated frequency characteristics of proposed filter in Fig. 4: a) magnitude responses, b) phase responses

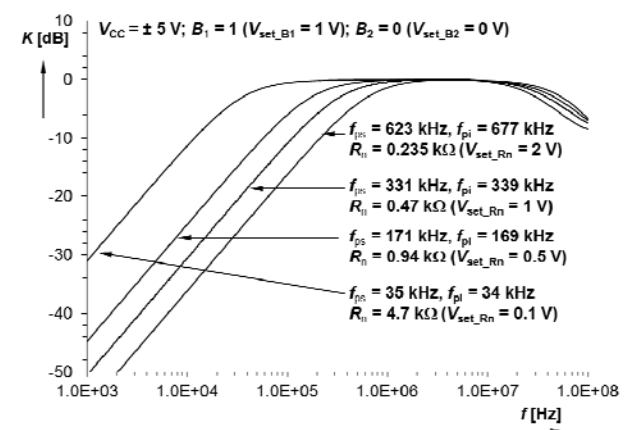


a)

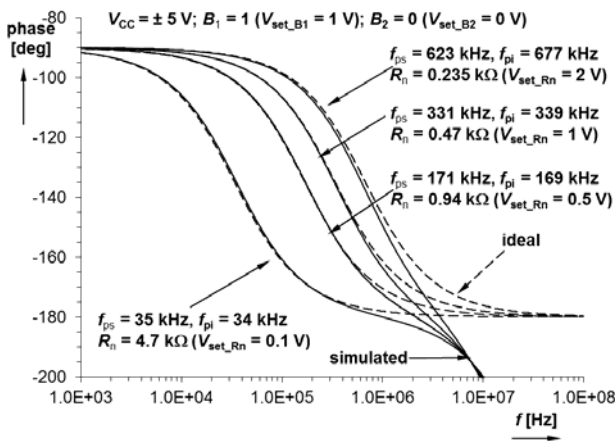


b)

Figure 6. Simulation results in case of tuning of the AP transfer: a) magnitude responses, b) phase responses



a)



b) Figure 7. Simulation results in case of tuning of the iHP transfers: a) magnitude responses, b) phase responses

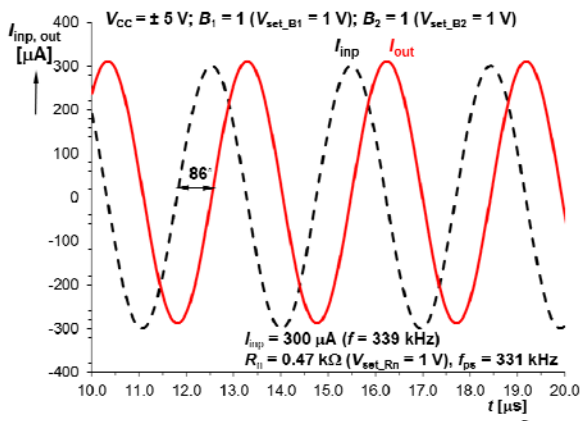


Figure 8. Transient response of the input and output current for AP function (simulation results)

V. STUDY OF PARASITIC INFLUENCES

Discussion of parasitic influences is really important. It helps us to understand the real behavior of the circuit. Finite bandwidth of the iHP and AP response at the high frequencies is one of them. This gain drop is not caused by finite frequency features of the used active elements in behavioral model (Fig. 4). The most influencing is parasitic capacitor C_n (see Fig. 4) in the current input terminal n . High impedance input and output terminals of the subparts of the behavioral model have sufficiently high values of impedance and their impact in studied bandwidth is not so important, and therefore we can neglect them. Equation (4) is now of the following form:

$$K_I'(s) \cong \frac{B_2 - sCR_n B_1}{1 + sR_n(C_n + C) + s^2 CC_p R_p} \quad (7)$$

$$= \frac{B_2 - sCR_n B_1}{(1 + sCR_n)(1 + sC_n R_p)}$$

We can see an additional pole ($\omega_{pp} = 1/C_n R_p$) that was created by combination of fixed R_p and parasitic C_n . Value of C_n is given by capacitances of Y and Z terminals of EL2082 ($C_n \cong 5-7$ pF [41] without additional influences on PCB, etc.). Based on this discussion, expected high frequency gain drop should be obtained between 48 and 68 MHz. A simulation result is 68 MHz (for example from Fig. 5, Fig. 6).

Capacitance C_n is given by parasitic features - it cannot be optimized or reduced under minimal limit 5-7 pF if EL2082

is used. Nevertheless, precise PCB design should minimize an additional influences. However, resistance R_p (positive current input terminal) can be adjusted or selected in order to control ω_{pp} . We can see the impact of R_p value on overall frequency performance in Fig. 9 (observed at AP response).

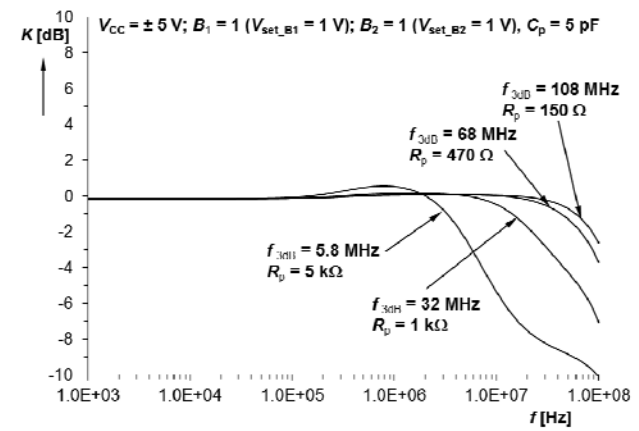


Figure 9. Impact of R_p value on overall frequency performances (AP response)

A problem with parasitic zeros of the LP filter in case of $B_1 = 0$ (Fig. 5) is caused by the used model of controllable R_n (highlighted part in Fig. 4 – ECCII₁ and ECCII₂). In such case, transfer function (4) in LP configuration ($B_1 = 0$) is now of a form (including the main affecting parameters R_1 , R_{x1} and C_{x1}):

$$K_I''(s) \cong \frac{B_2(1 - s^2 CC_{x1} R_{x1} R_p)}{D''(s)} \quad (8)$$

where

$$D''(s) \cong 1 + s(C_n R_{x1} + CR_1 + C_{x1} R_1 + CR_{x1} + C_n R_1) + s^2 [CC_{x1} R_1 (R_{x1} + R_p) + CC_n R_p (R_1 + R_{x1}) + C_{x1} C_n R_1 R_{x1}] + s^3 CC_{x1} C_n R_1 R_{x1} R_p \quad (9)$$

Location of parazitic zero (zeros – two roots symmetrical around y axis) is given by $\omega_z = \pm 1/\sqrt{CC_{x1} R_{x1} R_p}$. Minimal gain

$K_I''(\omega_z)_{\min} = \lim_{\omega \rightarrow \omega_z} K_I''(s)$ calculated from (8) at zero

frequency is approximately -28 dB. We obtained $f_z = 16.8$ MHz from (8). It is in quite good correspondence with the results in Fig. 6. Of course, utilization of other possibilities to control R_n or active devices (ECCII) with lower R_x than behavioral model from [33,34] reduces the impact of this problem significantly.

VI. EXPERIMENTAL RESULTS

We prepared a measurement setup based on ENA E5071C network vector analyzer and two converters employing diamond transistors OPA860 [42]. Established setup is shown in Fig. 10. Device under test (DUT) is based on behavioral model in Fig. 4 with the same values of external passive components. A knowledge of R_p and R_n is critical for estimation of the accurate operation of the MCDU. We measured frequency dependent impedance Z_p and Z_n typical of proposed MCDU (impedance analyzer HP4294A). An example of several traces for selected values of V_{set_Rn} (V_{set_Rp}) is plotted in Fig. 11.

The controllable parameters of the circuit were adjusted

to confirm expected behavior. However, real values of control voltages are slightly different in comparison with the simulation results. This inaccuracy is given by nonlinear dependence of current gains of the EL2082 [41] on control voltages V_{set_Rn} , V_{set_Rp} , V_{set_B1} and V_{set_B2} and its fabrication deviations. Hardly estimable values of parasitic impedances of PCB (additional parasitic capacitances mainly) in high-impedance nodes have also additional and very important impact on accuracy.

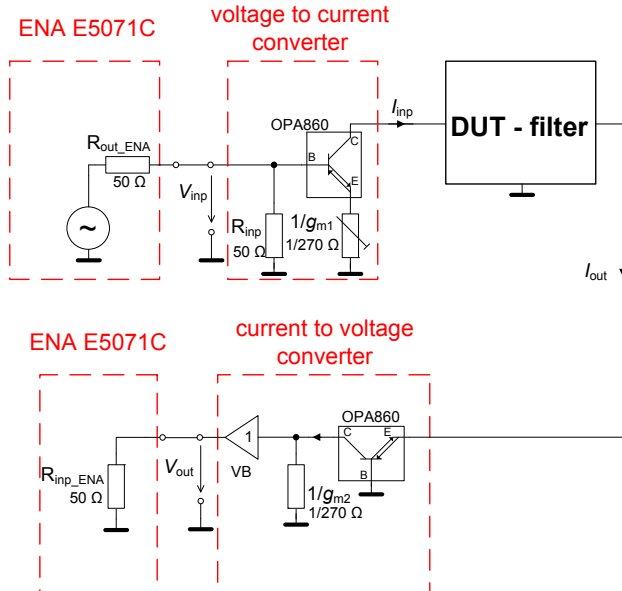


Figure 10. Established measurement setup of the designed filter from Fig. 4

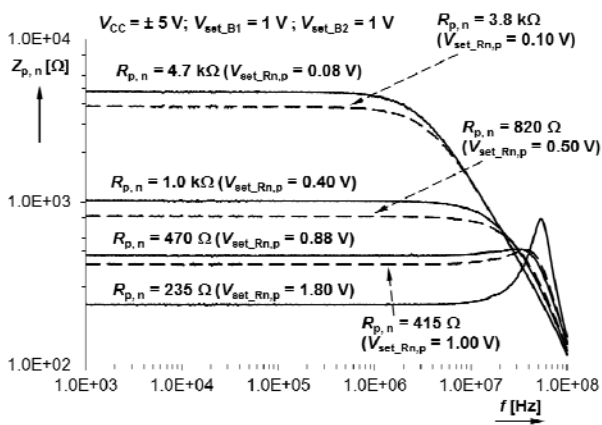


Figure 11. Measured impedances of n, p terminals in dependence on $V_{set_Rp,n}$

Despite some differences, we can conclude that the experiments confirmed and verified functionality of the reconfigurable filtering structure and we have really emulated behavior of reconfigurable filter based on ideal conception of MCDU device. The results of the experimental tests are given in Fig. 12 – Fig. 14, where magnitude and phase responses of filter in all three basic configurations are shown. Tuning of the filter was verified in case of AP and iHP responses. Frequency characteristics for V_{set_Rn} stepping are given in Fig. 15 and Fig. 16. All constants and parameters of measurements are directly noted in figures.

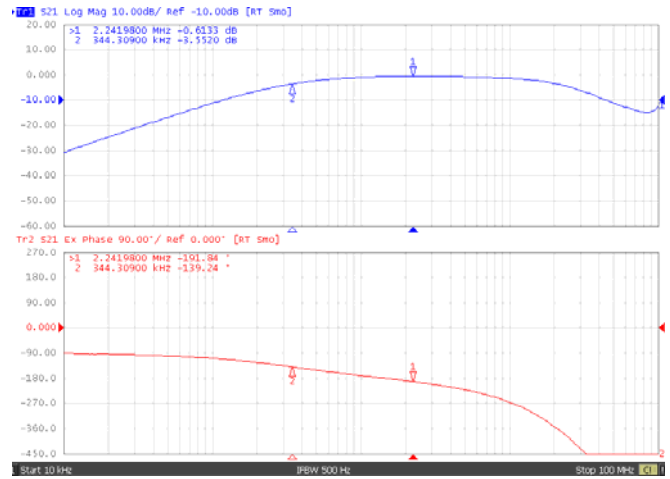


Figure 12. Frequency response of the iHP filter ($V_{set_Rn} = 0.65$ V, $V_{set_Rp} = 0.89$ V, $V_{set_B1} = 1.23$ V, $V_{set_B2} = 0$ V)

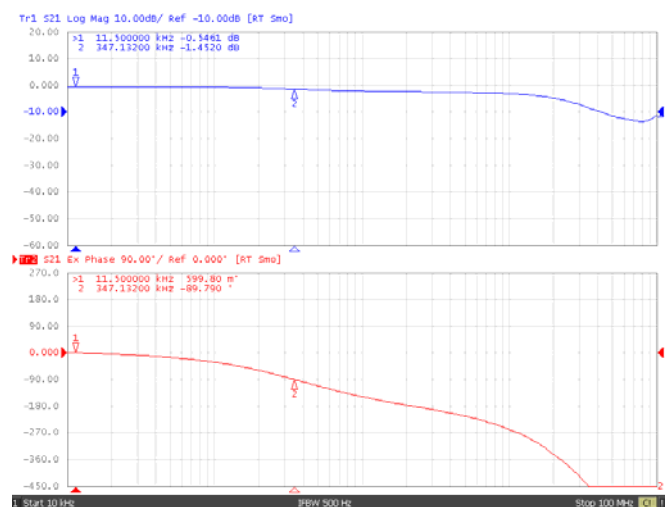


Figure 13. Frequency response of the AP filter ($V_{set_Rn} = 0.62$ V, $V_{set_Rp} = 0.89$ V, $V_{set_B1} = 1$ V, $V_{set_B2} = 1$ V)

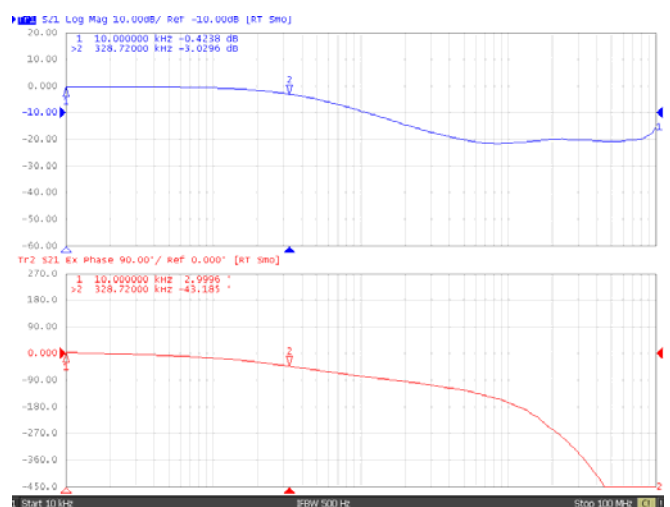


Figure 14. Frequency response of the LP filter ($V_{set_Rn} = 0.69$ V, $V_{set_Rp} = 0.89$ V, $V_{set_B1} = 0$ V, $V_{set_B2} = 1.1$ V)

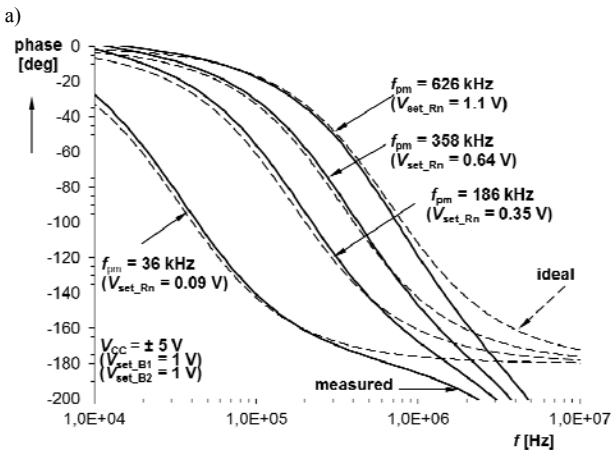
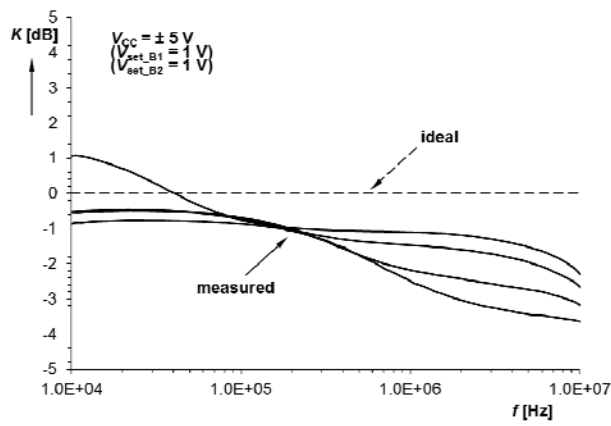


Figure 15. Tuning of the AP filter response by stepping of $V_{set,Rn}$: a) magnitude responses, b) phase responses

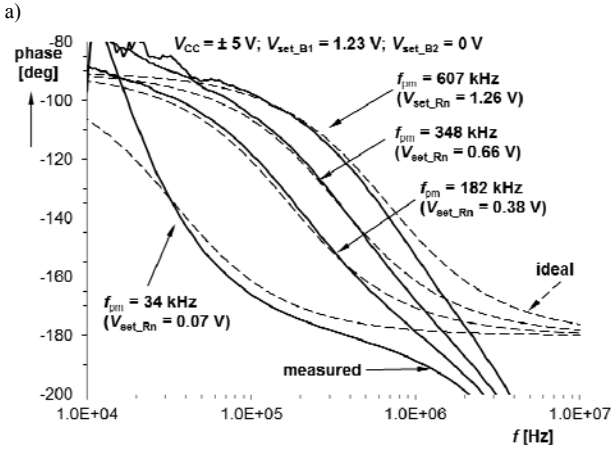
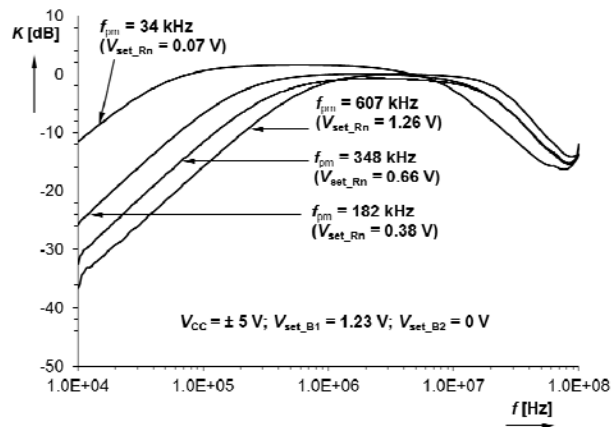


Figure 16. Tuning of the iHP filter response by stepping of $V_{set,Rn}$: a) magnitude responses, b) phase responses

VII. CONCLUSION

The definition of the MCDU brings beneficial advantages in comparison with classic simple active elements and basic CDU that does not allow the above discussed controllable features in the filtering applications. The filtering application of the MCDU in Fig. 3 seems to be very interesting because no matching condition for tuning is required and circuit provides all filtering functions that are theoretically available in the first-order filter (namely iHP, LP and AP). Even direct transfer (or inverting direct transfer) is available. Proposed behavioral model of the MCDU allows electronic control of the required parameters (R_n , B_1 , B_2) in proposed filter (Fig. 4) and operation sustainable up to tens of MHz. Moreover, the proposed structure allows independent pole and zero setting (pole has to be set at first and zero setting does not influence it). Therefore, LP and HP responses with intentional zero (finite attenuation in stop band) are also available from AP response. Simulation and measurement results confirmed theoretical hypotheses and validity of the synthesis.

REFERENCES

- [1] D. Bielek, R. Senani, V. Biolkova, Z. Kolka, "Active elements for analog signal processing: classification, review and new proposals," *Radioengineering*, vol. 17, no. 4, pp. 15–32, 2008.
- [2] J. W. Kerwin, L. P. Hulesman, W. R. Newcomb, "State variable synthesis for insensitive integrated circuit transfer functions," *IEEE Journal of Solid State Circuits*, vol. 2, no. 3, pp. 87–92, 1967. [Online]. Available: <http://dx.doi.org/10.1109/JSSC.1967.1049798>
- [3] R. Raut, M. N. S. Swamy, *Modern Analog Filter Analysis and Design: A practical approach*. Weinheim, Germany: Wiley-VCH Verlag GmbH and Co. KGaA, 355 p., 2010.
- [4] Y. Sun, J. K. Fidler, "Some design methods of OTA-C and CCII-RC filters," in *Proc. of IEE Colloquium on Digital and Analogue Filters and Filtering*, London, 1993, pp. 7/1-7/8.
- [5] R. Nawrocky, U. Klein, "New OTA-capacitor realisation of a universal biquad," *Electronics Letters*, vol. 22, no. 15, pp. 50–51, 1986. [Online]. Available: <http://dx.doi.org/10.1049/el:19860034>
- [6] Y. Sun, "Second-order OTA-C filters derived from Nawrocky-Klein biquad," *Electronics Letters*, vol. 34, no. 15, pp. 1449–1450, 1998. [Online]. Available: <http://dx.doi.org/10.1049/el:19981036>
- [7] Y. Sun, J. K. Fidler, "Structure Generation of Current-Mode Two Integrator Dual output-OTA Grounded Capacitor Filters," *IEEE Transaction on Circuits and Systems II: Analog and Digital Signal Processing*, vol. 43, no. 9, pp. 659–663, 1996. [Online]. Available: <http://dx.doi.org/10.1109/82.536762>
- [8] Y. Sun, J. K. Fidler, "Current-mode OTA-C realization of arbitrary filter characteristics," *Electronics Letters*, vol. 32, no. 13, pp. 1181–1182, 1996. [Online]. Available: <http://dx.doi.org/10.1049/el:19960807>
- [9] Y. Sun, J. K. Fidler, "Current-mode multiple-loop feedback filters using dual output OTAs and grounded capacitors," *International Journal of Circuit Theory and Applications*, vol. 25, no. 2, pp. 69–80, 1997. [Online]. Available: [http://dx.doi.org/10.1002/\(SICI\)1097-007X\(199703/04\)25:2<69::AID-CTA950>3.0.CO;2-9](http://dx.doi.org/10.1002/(SICI)1097-007X(199703/04)25:2<69::AID-CTA950>3.0.CO;2-9)
- [10] T. Dostal, "Filters with Multi-Loop Feedback Structure in Current Mode," *Radioengineering*, vol. 12, no. 3, pp. 6–11, 2003.
- [11] R. Sotner, J. Petrzela, J. Slezak, "Current-Controlled Current-Mode Universal Biquad Employing Multi-Output Transconductors," *Radioengineering*, vol. 18, no. 3, s. 285–294, 2009.
- [12] R. Sotner, B. Sevcik, L. Brancik, T. Dostal, "Multifunctional Adjustable Biquadratic Active RC Filters: Design Approach by Modifying of Corresponding Signal Flow Graphs," *Przeglad Elektrotechniczny*, vol. 87, no. 2, pp. 225–229, 2011.
- [13] R. Sotner, J. Jerabek, B. Sevcik, T. Dostal, K. Vrba, "Novel Solution of Notch/All-pass Filter with Special Electronic Adjusting of Attenuation in the Stop Band," *Elektronika Ir Elektrotechnika*, vol. 17, no. 7, p. 37–42, 2011.
- [14] J. Petrzela, R. Sotner, "Systematic design procedure towards reconfigurable first-order filters," in *Proc. 24th International Conference Radioelektronika 2014, Bratislava, 2014*, pp. 237–240.

- [Online]. Available: <http://dx.doi.org/10.1109/Radioelek.2014.6828462>
- [15] R. Sotner, J. Jerabek, N. Herencsar, R. Prokop, K. Vrba, T. Dostal, "Resistor-less First-Order Filter Design with Electronical Reconfiguration of its Transfer Function," in Proc. 24th International Conference Radioelektronika 2014, 2014, pp. 63–66. [Online]. Available: <http://dx.doi.org/10.1109/Radioelek.2014.6828417>
- [16] R. Sotner, J. Jerabek, J. Petrzela, K. Vrba, T. Dostal, "Design of Fully Adjustable Solution of Band-Reject/All-Pass Filter Transfer Function Using Signal Flow Graph Approach," in Proc. 24th International Conference Radioelektronika 2014, 2014, pp. 67–70. [Online]. Available: <http://dx.doi.org/10.1109/Radioelek.2014.6828418>
- [17] R. Sotner, N. Herencsar, J. Jerabek, R. Prokop, A. Kartci, T. Dostal, K. Vrba, "Z-Copy Controlled-Gain Voltage Differencing Current Conveyor: Advanced Possibilities in Direct Electronic Control of First-Order Filter," Elektronika Ir Elektrotechnika, vol. 20, no. 6, p. 77–83, 2014. [Online]. Available: <http://dx.doi.org/10.5755/j01.eee.20.6.7272>
- [18] S. E. Sanchez, R. L. Geiger, L. H. Nevarez, "Generation of continuous-time two integrator loop OTA filter structures," IEEE Transactions on Circuits and Systems, vol. 35, no. 8, pp. 936–946, 1988. [Online]. Available: <http://dx.doi.org/10.1109/31.1840>
- [19] W. Surakampontorn, W. Thitimaishima, "Integrable electronically tunable current conveyors," IEE Proceedings-G, vol. 135, no. 2, pp. 71–77, 1988.
- [20] A. Fabre, N. Mimeche, "Class A/AB second-generation current conveyor with controlled current gain," Electronics Letters, vol. 30, no. 16, pp. 1267–1268, 1994. [Online]. Available: <http://dx.doi.org/10.1049/el:19940878>
- [21] A. Fabre, O. Saaid, F. Wiest, C. Boucheron, "High frequency applications based on a new current controlled conveyor," IEEE Trans. on Circuits and Systems - I, vol. 43, no. 2, pp. 82–91, 1996. [Online]. Available: <http://dx.doi.org/10.1109/81.486430>
- [22] S. Minaei, O. K. Sayin, H. Kuntman, "A new CMOS electronically tunable current conveyor and its application to current-mode filters," IEEE Trans. on Circuits and Systems - I, vol. 53, no. 7, pp. 1448–1457, 2006. [Online]. Available: <http://dx.doi.org/10.1109/TCSI.2006.875184>
- [23] M. Kumngern, S. Junnapiya, "A sinusoidal oscillator using translinear current conveyors," in Proc. Asia Pacific Conf. on Circuits and Systems APPCAS2010, Kuala Lumpur, 2010, pp. 740–743. [Online]. Available: <http://dx.doi.org/10.1109/APCCAS.2010.5774754>
- [24] A. Marcellis, G. Ferri, N. C. Guerrini, G. Scotti, V. Stornelli, A. Trifiletti, "The VGC-CCII: a novel building block and its application to capacitance multiplication," Analog Integrated Circuits and Signal Processing, vol. 58, no. 1, pp. 55–59, 2009. [Online]. Available: <http://dx.doi.org/10.1007/s10470-008-9213-6>
- [25] J. Vavra, J. Bajer, D. Biolek, V. Biolkova, "Current-mode Quadrature Oscillator Employing ZC-CDU Based All-Pass Filter," in Proc. IEEE Int. Conf. on Electronics Engineering and Signal Processing (EESP), 2011, Male, pp. 640–644.
- [26] J. Vavra, D. Biolek, "OTA-based current differencing unit," in Proc. of int. conf. on Electronic Devices and Systems (EDS IMPAPS), Brno, 2008, pp. 7–12.
- [27] W. Jaikla, M. Siripruchyanun, J. Bajer, D. Biolek, "A Simple Current-mode Quadrature Oscillator Using Single CDTA," Radioengineering, vol. 17, no. 4, pp. 33–40, 2008.
- [28] W. Jaikla, P. Prommee, "Electronically Tunable Current-mode Multiphase Sinusoidal Oscillator Employing CCCDTA-based Allpass Filters with Only Grounded Passive Elements," Radioengineering, vol. 20, no. 3, pp. 594–599, 2011.
- [29] W. Jaikla, A. Lahiri, "Resistor-less current-mode four-phase quadrature oscillator using CCCDTA and grounded capacitors," AEU-International Journal of Electronics and Communications, vol. 66, no. 3, pp. 214–218, 2012. [Online]. Available: <http://dx.doi.org/10.1016/j.aeue.2011.07.001>
- [30] M. Siripruchyanun, W. Jaikla, "Electronically Controllable Current-Mode Universal Biquad Filter Using DO-CCCDTA," Circuits Systems and Signal Processing, vol. 27, no. 1, pp. 113–122, 2008. [Online]. Available: <http://dx.doi.org/10.1007/s00034-008-9014-2>
- [31] R. Prokop, V. Musil, "Modular approach to design of modern circuit blocks for current signal processing and new device CCTA," in Proc. Conf. on Signal and Image Processing IASTED, Anaheim, 2005, pp. 494–499.
- [32] M. Siripruchyanun, W. Jaikla, "Current controlled current conveyor transconductance amplifier (CCCCTA): a building block for analog signal processing," Electrical Engineering Springer, vol. 90, no. 6, pp. 443–453, 2008. [Online]. Available: <http://dx.doi.org/10.1007/s00202-007-0095-x>
- [33] R. Sotner, J. Jerabek, N. Herencsar, T. Dostal, K. Vrba, "Additional Approach to the Conception of Current Follower and Amplifier with Controllable Features," in Proc. of the 34th Int. Conf. on Telecommunications and Signal Processing (TSP2011), Budapest, 2011, pp. 279–283. [Online]. Available: <http://dx.doi.org/10.1109/TSP.2011.6043726>
- [34] R. Sotner, A. Kartci, J. Jerabek, N. Herencsar, T. Dostal, K. Vrba, "An Additional Approach to Model Current Followers and Amplifiers with Electronically Controllable Parameters from Commercially Available ICs," Measurement Science Review, vol. 12, no. 6, pp. 255–265, 2012. [Online]. Available: <http://dx.doi.org/10.2478/v10048-012-0035-4>
- [35] J. Jerabek, R. Sotner, K. Vrba, "Tunable universal filter with current follower and transconductance amplifiers and study of parasitic influences," Journal of Electrical Engineering, vol. 62, no. 6, s. 317–326, 2011. [Online]. Available: <http://dx.doi.org/10.2478/v10187-011-0051-x>
- [36] R. Sotner, N. Herencsar, J. Jerabek, R. Dvorak, A. Kartci, T. Dostal, K. Vrba, "New double current controlled CFA (DCC-CFA) based voltage-mode oscillator with independent electronic control of oscillation condition and frequency," Journal of Electrical Engineering, vol. 64, no. 2, s. 65–75, 2013. [Online]. Available: <http://dx.doi.org/10.2478/jee-2013-0010>
- [37] R. Sotner, J. Jerabek, N. Herencsar, "Voltage differencing buffered/inverted amplifiers and their applications for signal generation," Radioengineering, vol. 22, no. 2, pp. 490–504, 2013.
- [38] R. Sotner, Z. Hrubos, N. Herencsar, J. Jerabek, T. Dostal, "Precise electronically adjustable oscillator suitable for quadrature signal generation employing active elements with current and voltage gain control," Circuits Systems and Signal Processing, vol. 33, no. 1, pp. 1–35, 2014. [Online]. Available: <http://dx.doi.org/10.1007/s00034-013-9623-2>
- [39] H. O. Elwan, A. M. Soliman, "CMOS differential current conveyors and applications for analog VLSI," Analog Integrated Circuits and Signal Processing, vol. 11, no. 1, pp. 35–45, 1996.
- [40] A. Toker, "Current-mode allpass filters using current differencing buffered amplifier and a new high-Q bandpass filter configuration," IEEE Transactions on Circuits and Systems II, vol. 47, no. 9, pp. 949–954, 2000. [Online]. Available: <http://dx.doi.org/10.1109/82.868465>
- [41] Intersil (Elantec). EL2082 CN Current-mode multiplier (datasheet), 1996, 14 p., accessible on [www: http://www.intersil.com/data/fn/fn152.pdf](http://www.intersil.com/data/fn/fn152.pdf)
- [42] Texas Instruments. OPA860 Wide-bandwidth, operational transconductance amplifier (OTA) and buffer (datasheet), 2008, 33 p., accessible on [www: http://www.ti.com/lit/ds/symlink/opa860.pdf](http://www.ti.com/lit/ds/symlink/opa860.pdf)

[27] SOTNER, R., JERABEK, J., HERENC SAR, N., PROKOP, R., VRBA, K., DOSTAL, T. First-order Reconfigurable Reconnection-less Filters Using Modified Current Differencing Unit. In *Proceedings of 25th International Conference Radioelektronika 2015*. Pardubice (Czech Republic), 2015, p. 46-50. ISBN: 978-1-4799-8117-5.

First-order Reconfigurable Reconnection-less Filters Using Modified Current Differencing Unit

R. Sotner, J. Jerabek, N. Herencsar, R. Prokop, K. Vrba
Faculty of Electrical Engineering and Communication
Brno University of Technology
Brno, Czech Republic
sotner@feec.vutbr.cz

T. Dostal
Dept. of Electrical Engineering and Computer Science
College of Polytechnics Jihlava
Jihlava, Czech Republic
tomas.dostal@vspj.cz

Abstract—This paper presents simple electronically reconfigurable and reconnection-less filtering applications based on useful modification of current differencing unit (CDU). Modified CDU improves its controllable features and bring some other advantages. Three examples of first-order filtering structure in voltage- and current-mode were studied and compared. The last presented solution providing all-pass, inverting high-pass and low-pass (and theoretically also direct transfer) responses was investigated by PSpice simulations using complex behavioral model of the modified CDU, based on commercially available devices. It confirmed theoretically expected behavior.

Keywords—Current differencing unit; CDU; electronic control; reconfigurability; reconnection-less filter; transfer function adjusting; tuning

I. INTRODUCTION

Current difference seems to be quite important operation for analog signal processing [1]-[3]. It is commonly required in filtering structures [2], [3] working in current-mode. Active device [4] with this feature has some importance for field of electronically reconfigurable reconnection-less structures and its design. Presented approach utilizes multi-parameter control in frame of one active device. It was sufficiently used for applications of interesting synthesis several times, as was shown in works presented by Minaei et al. [5], Kumngern et al. [6] and Marcellis et al. [7] for example. However, their applications were focused on different types of applications, not on reconfigurability of reconnection-less structures of active filters. In this contribution, useful combination of electronically controllable features are discussed and implemented in advanced and improved type of current differencing unit (CDU) [4], [8], [9].

Classical multifunctional filters (for example [2], [3]) offer one input and several outputs or several inputs and one output. It means that such structure require reconnection of input/output terminal in order to obtain different transfer response. Therefore, such approach is not very beneficial for solutions of systems where additional mechanical change in circuitry (reconnection) is not easily allowed. However,

electronically controllable reconnection-less filters allow multifunctionality even in case when one input and one output terminal are the same for all the time. Of course, there are some ways how to provide reconnection in frame of chip, however switching may bring some undesired problems – increasing of level of distortion from interferences of clock and useful signal (if required changes are fast), overshoots, additional complication of the design, additional power consumption, etc. Beneficial behavior of reconnection-less reconfigurable filters allow immediate and continuous reaction on changes in processed useful signal (temporarily increasing distortion, noise floor, undesired spectral components in some parts of band) – suitable also for some kind of adaptive control. We can expect following transfer functions in the first-order structures: low-pass (LP), high-pass (HP), all-pass (AP) response and direct transfer (DT), in non-inverting or inverting form (iLP, iHP, iAP, iDT).

II. DISCUSSION OF RECENTLY PUBLISHED WORKS

Reconfigurable first-order transfer functions were discussed also in several of our previously published works. The research started in [10] where several solutions reconfigurable reconnection-less filters based on the operational transconductance amplifiers (OTA) [4], [11] were synthesized by matrix method of the unknown nodal voltages. However, because OTA cannot reach transconductance $g_m = 0$ S, utilization is partially limited (for instance by maximal stop-band attenuation in case of some transfer types). Solutions in [10] also offer quite restricted possibilities of reconfigurations between transfer characteristics (mainly AP, HP and LP with zero). The second and more important problem is the mutual dependence of the parameters serving for reconfiguration and for tuning of the filter. For example (Fig. 1 and equation (2) in [10]) g_{m1} can be used for control of the pole frequency but meanwhile we require fulfilled equality $g_{m1} = g_{m2}$ in configuration of the filter as HP. Therefore solutions, where reconfiguration is based on different controllable parameters and mutual independence of tuning and reconfiguration, should be designed. Our following work [12] reflects these requirements. We implemented also controllable current gain (B) and resistance of the current input terminal R_X (in frame of the single additional electronically controllable current conveyor of second generation – ECCII [4], [5]) to the transfer

Research described in this paper was financed by Czech Ministry of Education in frame of National Sustainability Program under grant LO1401. For research, infrastructure of the SIX Center was used. Research described in the paper was supported by Czech Science Foundation projects under No. 14-24186P. Grant No. FEKT-S-14-2281 also supported this research. The support of the project CZ.1.07/2.3.00/20.0007 WICOMT, financed from the operational program Education for competitiveness, is gratefully acknowledged.

function to obtain wider features of reconnection-less reconfigurability. The solution employs three active elements. We have available AP, LP, LP with zero, pure adjustable zero and iDT in [12] but, unfortunately, at two independent outputs (all responses are not available on single output) that is quite important drawback. However it was good start for the following work. Our following research was focused on implementation of single active element (so-called z-copy controlled-gain voltage differencing current conveyor) with three independently adjustable parameters (B , R_X , g_m) into the design of the reconnection-less reconfigurable filter presented in [13]. Two parameters allow reconfiguration between AP, LP, DT and iDT (pole frequency of the LP and zero/pole location of the AP can be controlled independently on configuration – mutual influence of parameters for configuration and tuning was removed). In presented work, we started to search solutions where also HP is available without mutual influence of parameters as in [10]).

An active device with special current differencing features (CDU) seems to be very useful for these purposes after certain modification leading to advanced variability of the adjustable parameters was prepared (modified CDU - MCDU). Two filters (voltage-mode and current-mode operation – general symbolical transfer functions are slightly different) in this work offer iAP, HP, DT and AP, iHP, and iDT. Mutual influence of tuning and reconfiguration is also eliminated, only simple matching $R_p = R_n$ is required for tuning of (i)HP. The third (current-mode) solution offers DT, LP, iHP and AP response (all transfers available in first-order filters) that was not obtained in any of previous works [10], [12], [13]. Third solution presented in this paper is similar to solution (in current-mode) published quite recently in [14]. The filter in [14] offers the same transfers as presented in this contribution (DT, LP, iHP and AP). The difference between circuits is in slightly different interconnection of input terminals (solution in [14] requires utilization of Y terminal of MCDU). This difference leads to completely different general symbolical transfer function. In addition, there is also difference in MCDU conception. MCDU circuit, presented in this contribution, has full electronic adjustability of both current input resistances (R_p , R_n). In case of MCDU behavioral model in [14], current input p has fixed (and nonadjustable) resistance R_p . Verifications of the filtering solution in [14] reveal impact of parasitic influences on LP that seems to be substantially larger than in particular solution presented in this paper (Fig. 6).

III. MODIFIED CURRENT DIFFERENCING UNIT

Biolek et al. presented current differencing unit [4], [8], [9] as the first part of so-called current differencing transconductance amplifier (CDTA) [4], [15]. General behavioral model supposes interconnection of two current conveyors of second generation (CCII) [16]. However, their voltage input terminals are intentionally grounded to perform the main definition equation of the CDU behavior: $I_x = I_p - I_n$. Modification (Fig. 1), presented in this contribution, supposes availability of one voltage input terminal that is normally contained in CCII device. Of course, as known from some works [17] (or modified versions of the CDTA [18]-[20] for

example), both current input terminals have controllable resistance:

$$V_p = V_Y + R_p I_p, \quad V_n = R_n I_n \quad (1), (2)$$

In addition, current transfer of both inputs p and n can be adjusted and their difference is available at the current output terminal x :

$$I_{+x} = I_p B_1 - I_n B_2. \quad (3)$$

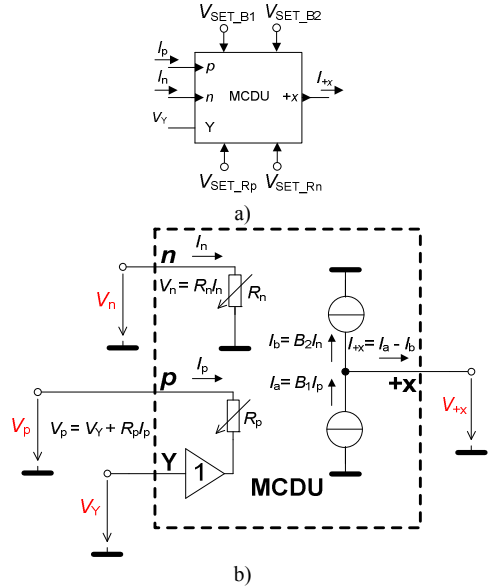


Fig. 1. Modified current differencing unit: a) symbol, b) ideal behavioral model.

IV. FIRST-ORDER RECONFIGURABLE FILTER APPLICATIONS OF THE MCDU

Proposed MCDU provides useful features for application in reconfigurable reconnection-less filtering structures that are not available in applications with basic CDU. We prepared three interesting examples in voltage- and also current-mode of circuit operation, where only one MCDU and one floating capacitor is required. Demonstration of ideal features of proposed applications were provided for $C = 1$ nF, and default values $R_p = R_n = 1$ k Ω , $B_1 = B_2 = 1$, unless otherwise stated.

A. The first solution

Simple but interesting circuit operating in voltage-mode is shown in Fig. 2. This solution has following transfer function:

$$K_V(s) = \frac{R_n B_1 - R_p B_2 + s C R_p R_n}{R_n B_1 + s C R_p R_n}, \quad (4)$$

where zero and pole frequency are given by:

$$\omega_z = \frac{R_n B_1 - R_p B_2}{C R_p R_n}, \quad \omega_p = \frac{B_1}{C R_p}. \quad (5), (6)$$

The parameter B_2 is very useful for direct control of type of the transfer function. There are available three types of operations (filtering functions): a) inverting AP (iAP) response for $B_2 = 2$

($B_1 = 1$); b) HP response for $B_1 = B_2 = 1$ and $R_p = R_n$, control of pole frequency is available by simultaneous change of $R_p = R_n$; c) direct transfer (DT), for $B_2 = 0, B_1 = 1$ (if $R_p = R_n$).

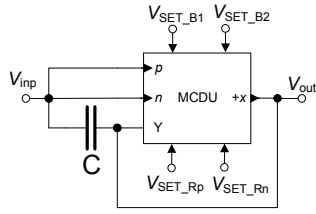


Fig. 2. Voltage-mode multifunctional filter with controllable features.

Details about ideal behavior of this solution are given in Fig. 3, where example magnitude and phase responses and also complex plot are given for $f_p = 159$ kHz. Example of control of pole frequency of iAP response (in case of phase response) and pole frequency of HP (in case of magnitude response) are given in Fig. 4.

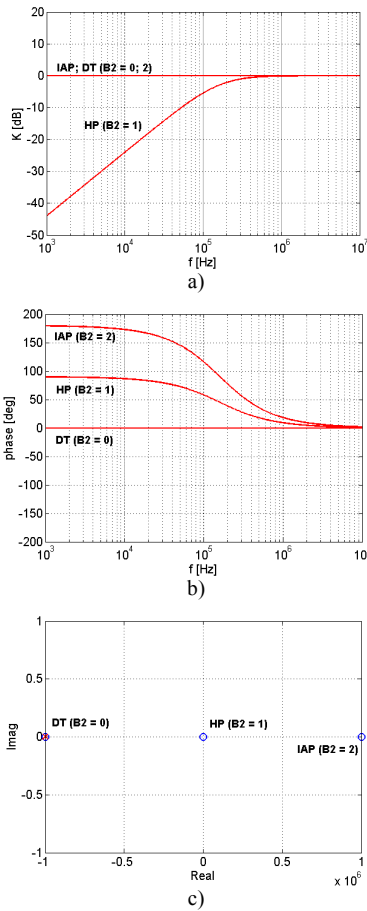


Fig. 3. Ideal analysis of proposed filter in Fig. 2: a) magnitude responses, b) phase responses, c) complex plot.

B. The second solution

The current-mode type of the filter is available from the same circuit structure (the same position of input and output terminal), see Fig. 5.

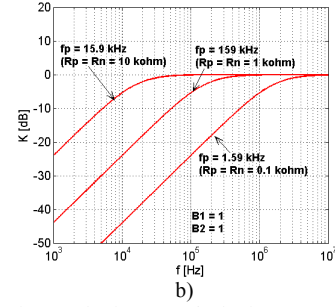
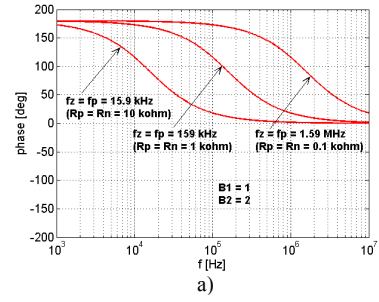


Fig. 4. Example of control of: a) zero/pole frequency of the iAP response, b) pole frequency of the HP response.

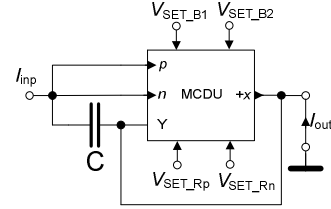


Fig. 5. Current-mode implementation of the same structure as in Fig. 2.

The type has transfer, where important differences are evident:

$$K_I(s) = \frac{R_p B_2 - R_n B_1 - s C R_p R_n}{R_p + R_n + s C R_p R_n}. \quad (7)$$

Zero frequency has the same form as (5). Formula for pole frequency is different:

$$\omega_p = \frac{R_p + R_n}{C R_n}. \quad (8)$$

The second structure also offers three types of the transfers (the lowest possible gains B are preferred): a) AP response for $B_1 = -1$ ($B_2 = 1$) or $B_2 = 3$ ($B_1 = 1$), control of zero/pole frequency is possible by $R_p = R_n$, or by R_p or R_n separately; b) inverting HP response (iHP) for $B_1 = 1$ ($B_2 = 1$) and $R_p = R_n$, control of pole frequency by simultaneous control of $R_p = R_n$; c) inverting DT response (iDT) for $B_1 = 3$ ($B_2 = 1$) and $R_p = R_n$ or $B_2 = -1$ ($B_1 = 1$). Theoretical results of this type of the filter are similar to simulation results of filter from Fig. 2, therefore it is omitted.

C. The third solution

Different and interesting current-mode circuit, that has also reconfigurable features, is shown in Fig. 6 (terminal Y is not used in this case). Transfer function has form:

$$K_I(s) = \frac{B_2 + s C (R_p B_2 - R_n B_1)}{1 + s C (R_p + R_n)}, \quad (11)$$

where zero and pole frequencies are:

$$\omega_z = \frac{B_2}{C(R_p B_2 - R_n B_1)}, \quad \omega_p = \frac{1}{C(R_p + R_n)}. \quad (12),(13)$$

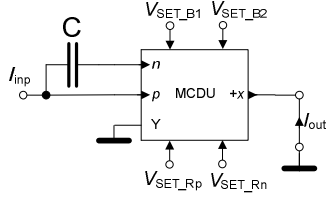


Fig. 6. Another structure of current-mode filter with reconfigurable features.

Circuit in Fig. 6 produces: a) DT function for $B_1 = -1$ ($B_2 = 1$); b) LP response for $B_1 = 1$ ($B_2 = 1$), control of pole frequency is possible by simultaneous adjusting of $R_p = R_n$; c) iHP response for $B_2 = 0$ ($B_1 = 1$); d) AP response for $B_1 = 3$ ($B_2 = 1$) and $R_p = R_n$; simultaneous $R_p = R_n$ allows control of zero/pole frequency.

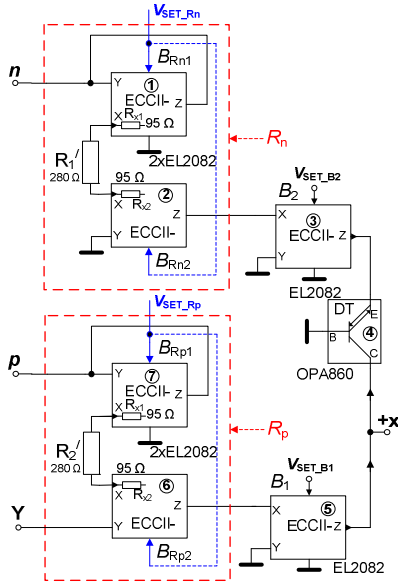


Fig. 7. Behavioral model of the MCDU.

V. SIMULATION RESULTS

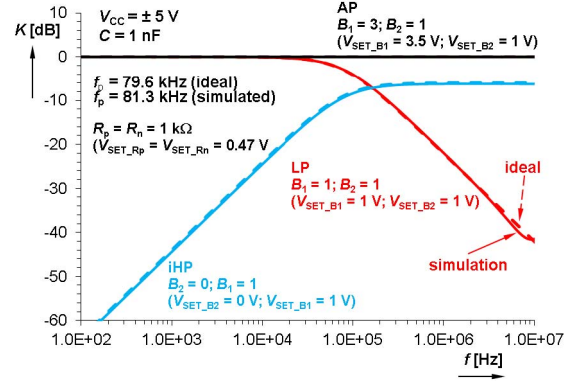
A. MCDU behavioral model

We prepared following model (Fig. 7) of the MCDU based on ECCIIs [21], [22] utilizing current gain control between terminal X and Z as main controllable feature, utilizing commercially available devices (EL2082 [23] OPA860 [24]). Control of R_p and R_n values was solved by subpart presented in [25], [26]. Relation between control voltage V_{SET_Rn} and V_{SET_Rp} has form:

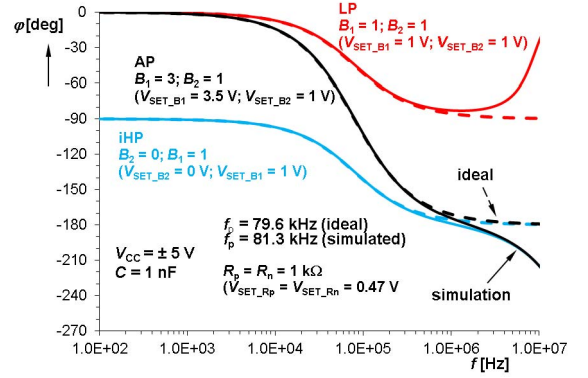
$$R_p \cong \frac{R'_1 + 2R_X(ECCI)}{V_{SET_Rp}}, \quad R_n \cong \frac{R'_2 + 2R_X}{V_{SET_Rn}}, \quad (14), (15)$$

Values of passive parameters are given in Fig. 7. Current gains B_1, B_2 are equal to V_{SET_B1}, V_{SET_B2} up to value 2 V, dependence is quite nonlinear above this value [23]. Change of $V_{SET_Rp,n}$ from 0.1 to 2 V allows control of $R_{p,n}$ in range from 4.7 k Ω to

235 Ω (it is used for demonstration of filter adjusting as follows). Diamond transistor (in the structure of model) serves as current inverter to generate negative current in output summing node.



a)



b)

Fig. 8. Frequency responses of available transfers: a) magnitude responses, b) phase responses.

B. Filter performance

We selected solution in Fig. 6 for detailed analysis, where above presented model was implemented. Values of passive elements were set as in ideal study ($C = 1$ nF, and initial values $R_p = R_n = 1$ k Ω , $B_1 = B_2 = 1$, unless otherwise stated). All parameters are noted directly in figures. Available transfer responses are shown in Fig. 8. We can ensure operation of the iHP response without gain-loss for $B_1 = 2$, but we intentionally analyzed state when $B_1 = 1$ to see 6.2dB attenuation, that corresponds to ratio of coefficients of linear member of transfer function in numerator and denominator (pass-band gain). Figure 9 shows tuning of the pole frequency by $R_p = R_n$ change (by $V_{SET_Rp} = V_{SET_Rn}$), observed at the LP response. Note that DT is not available in this case due to unavailability of negative (inverting) gain B in presented behavioral model of the MCDU.

VI. CONCLUSION

Improved features (controllability of parameters) of MCDU overcomes standard CDU and allow design of interesting applications. We presented several simple structures of the filtering applications based on one MCDU and one floating capacitor. The first solution operates in voltage-mode and offers iAP, HP and DT transfer functions. Requirements on

current gain ($B_{1,2}$ values) are the lowest from the presented solutions. The second solution was derived as current-mode equivalent of the first circuit. However, transfer function is slightly different in detail and allows iDT, iHP and AP response. The third (also current-mode) solution seems to be the most beneficial. It provides iHP, AP and LP transfers (theoretically also DT). Transfer functions of the third solution were verified by PSpice simulations utilizing behavioral model of the MCDU based on commercially available devices. This behavioral model allows full control of current gains $B_{1,2}$ and also R_p and R_n .

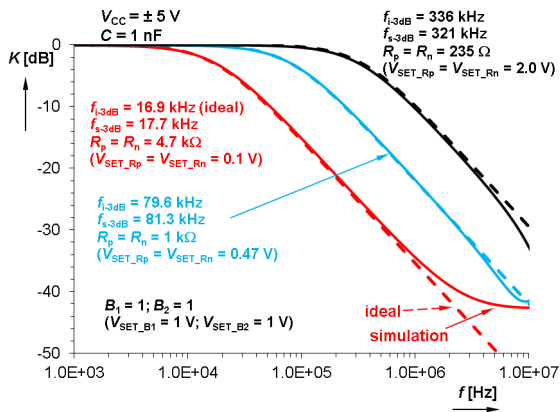


Fig. 9. Tuning of the LP response.

REFERENCES

- [1] W. Chen, *The Circuits and Filters Handbook*. Boca Raton, FL: CRC Press, 2002.
- [2] R. Raut, M. N. S. Swamy, *Modern Analog Filter Analysis and Design: A practical approach*. Weinheim, Wiley, 2010.
- [3] T. Dostal, "Filters with Multi-Loop Feedback Structure in Current Mode," *Radioengineering*, vol. 12, no. 3, pp. 6-11, 2003.
- [4] D. Biolk, R. Senani, V. Biolkova, Z. Kolka, "Active elements for analog signal processing: Classification, Review and New Proposals," *Radioengineering*, vol. 17, no. 4, pp. 15-32, 2008.
- [5] S. Minaei, O. K. Sayin, H. Kuntman, "A new CMOS electronically tunable current conveyor and its application to current-mode filters," *IEEE Trans. on Circuits and Systems - I*, vol. 53, no. 7, pp. 1448-1457, 2006.
- [6] M. Kumngern, S. Junnapiya, "A sinusoidal oscillator using translinear current conveyors," in *Proc. Asia Pacific Conf. on Circuits and Systems APCAS2010*, pp. 740-743, 2010.
- [7] A. Marcellis, G. Ferri, N. C. Guerrini, G. Scotti, V. Stornelli, A. Trifiletti, "The VGC-CCII: a novel building block and its application to capacitance multiplication," *Analog Integrated Circuits and Signal Processing*, vol. 58, no. 1, pp. 55-59, 2009.
- [8] J. Vavra, D. Biolk, "OTA-based current differencing unit," in *Proc. of int. conf. on Electronic Devices and Systems (EDS IMPAPS)*, Brno, pp. 7-12, 2008.
- [9] J. Vavra, J. Bajer, D. Biolk, V. Biolkova, "Current-mode Quadrature Oscillator Employing ZC-CDU Based All-Pass Filter," in *Proc. IEEE Int. Conf. on Electronics Engineering and Signal Processing (EESP)*, pp. 640-644, 2011.

- [10] J. Petrzela, R. Sotner, "Systematic design procedure towards reconfigurable first-order filters," in *Proc. 24th International Conference Radioelektronika 2014*, pp. 237-240, 2014.
- [11] R. L. Geiger, E. Sanchez-Sinencio, "Active filter design using operational transconductance amplifiers: a tutorial," *IEEE Circuits and Devices Magazine*, vol. 1, pp. 20-32, 1985.
- [12] R. Sotner, J. Jerabek, N. Herencsar, R. Prokop, K. Vrba, T. Dostal, "Resistor-less First-Order Filter Design with Electronical Reconfiguration of its Transfer Function," in *Proc. 24th International Conference Radioelektronika 2014*, pp. 63-66, 2014.
- [13] R. Sotner, N. Herencsar, J. Jerabek, R. Prokop, A. Kartci, T. Dostal, K. Vrba, "Z-Copy Controlled-Gain Voltage Differencing Current Conveyor: Advanced Possibilities in Direct Electronic Control of First-Order Filter," *Elektronika Ir Elektrotechnika*, vol. 20, no. 6, pp. 77-83, 2014.
- [14] R. Sotner, J. Jerabek, N. Herencsar, T. Zak, W. Jaikla, K. Vrba, "Modified Current Differencing Unit and its Application for Electronically Reconfigurable Simple First-order Transfer Function," *Advances in Electrical and Computer Engineering*, vol. 15, no. 1, pp. 3-10, 2015.
- [15] D. Biolk, "CDTA – Building Block for Current-Mode Analog Signal Processing," in *Proc. Of the European Conference on Circuit Theory and Design ECCTD2003*, pp. 397-400, 2003.
- [16] A. Sedra, K. C. Smith, "A second generation current conveyor and its applications," *IEEE Transaction on Circuit Theory*, vol. CT-17, no. 2, pp. 132-134, 1970.
- [17] A. Fabre, O. Saaid, F. Wiest, C. Boucheron, "High frequency applications based on a new current controlled conveyor," *IEEE Trans. on Circuits and Systems - I*, vol. 43, no. 2, pp. 82-91, 1996.
- [18] W. Jaikla, P. Prommee, "Electronically Tunable Current-mode Multiphase Sinusoidal Oscillator Employing CCCDTA-based Allpass Filters with Only Grounded Passive Elements," *Radioengineering*, vol. 20, no. 3, pp. 594-599, 2011.
- [19] W. Jaikla, A. Lahiri, "Resistor-less current-mode four-phase quadrature oscillator using CCCDTA and grounded capacitors," *AEU-International journal of Electronics and Communications*, vol. 66, no. 3, pp. 214-218, 2012.
- [20] M. Siripruchyanun, W. Jaikla, "Electronically Controllable Current-Mode Universal Biquad Filter Using DO-CCCDTA," *Circuits Systems and Signal Processing*, vol. 27, no. 1, pp. 113-122, 2008.
- [21] W. Surakamponorn, W. Thitimajshima, "Integrable electronically tunable current conveyors," *IEE Proceedings-G*, vol. 135, no. 2, pp. 71-77, 1988.
- [22] A. Fabre, N. Mimeche, "Class A/AB second-generation current conveyor with controlled current gain," *Electronics Letters*, vol. 30, no. 16, pp. 1267-1268, 1994.
- [23] Intersil (Elantec). EL2082 CN Current-mode multiplier (datasheet), 1996, 14 p., accessible on [www: http://www.intersil.com/data/fn/fn7152.pdf](http://www.intersil.com/data/fn/fn7152.pdf)
- [24] Texas Instruments. OPA860 Wide-bandwidth, operational transconductance amplifier (OTA) and buffer (datasheet), 2008, 33 p., accessible on [www: http://www.ti.com/lit/ds/symlink/opa860.pdf](http://www.ti.com/lit/ds/symlink/opa860.pdf)
- [25] R. Sotner, J. Jerabek, N. Herencsar, T. Dostal, K. Vrba, "Additional Approach to the Conception of Current Follower and Amplifier with Controllable Features," in *Proc. of the 34th Int. Conf. on Telecommunications and Signal Processing (TSP2011)*, pp. 279-283, 2011.
- [26] R. Sotner, A. Kartci, J. Jerabek, N. Herencsar, T. Dostal, K. Vrba, "An Additional Approach to Model Current Followers and Amplifiers with Electronically Controllable Parameters from Commercially Available ICs," *Measurement Science Review*, vol. 12, no. 6, pp. 255-265, 2012.

[28] SOTNER, R., JERABEK, J., HERENC SAR, N., PROKOP, R., LAHIRI, A., DOSTAL, T., VRBA, K. First-order transfer sections with reconnection-less electronically reconfigurable high-pass, all-pass and direct transfer character. *Journal of Electrical Engineering*, 2016, vol. 67, no. 1, p. 12-20. ISSN: 1335-3632.

FIRST-ORDER TRANSFER SECTIONS WITH RECONNECTION-LESS ELECTRONICALLY RECONFIGURABLE HIGH-PASS, ALL-PASS AND DIRECT TRANSFER CHARACTER

Roman Sotner^{*} — Jan Jerabek^{**} — Norbert Herencsar^{**}
 — Roman Prokop^{***} — Abhirup Lahiri^{****}
 — Tomas Dostal^{*****} — Kamil Vrba^{**}

Presented research introduces active filtering circuits which allow change of the transfer type without necessity of reconnection of the input or output terminal that can be very useful for on-chip applications. Our attention is focused on simple first-order filters that allow high-pass response (HP), all-pass response (AP) and also direct transfer (DT) with constant magnitude and phase characteristics between two terminals (input and output) by adjusting of one controllable parameter (current gain B in our case). Useful modification of the well-known current follower transconductance amplifier (CFTA), the so-called Z-copy current-controlled current follower differential input transconductance amplifier (ZC-CCCFDITA) and adjustable current amplifier were utilized in these circuits. Interesting possibilities (crossing between several transfer functions) of presented circuits require different values of B to obtain desired transfer function that is very important for practice and selection of specific way of control. Requirements on value of this continuously controllable gain B differ among presented structures. Theory is supported by simulation and measurement results with behavioral models utilizing commercially available active elements and simulation results with active elements based on CMOS models.

Key words: active filters, electronic control, reconfiguration, reconnection-less multifunction, Z-copy current-controlled current follower differential input transconductance amplifier, ZC-CCCFDITA

1 INTRODUCTION

Many suitable active elements for circuit synthesis of various applications have been presented in literature [1]. Some of them allow interesting features and give useful possibilities of electronic control in applications. However, their further modifications bring some additional advantages that are not available in their basic forms and definitions. These improvements mean additional implementation of controllable parameters in the active element in the most cases. We know four types of electronic control in frame of the active element. The first group utilizes controllable transconductance (g_m) [1, 2]. The second group deals with controllable intrinsic resistance (R_x) of the current input terminal (mainly in current-mode active elements) [3]. Control of current gain (B) [4] becomes very popular in recent years mainly [5–11]. Utilization of the adjustable voltage gain (A) is also very useful in many cases, but complexity of active elements is worse [12] than basic structures utilizing g_m or R_x control [2, 3]. Design of active elements in combination of several (at least two) types of control in frame of one active element is one of today's trends [13–19].

We prepared overview of combined active elements employing current follower/inverter and transconductance subparts. Active elements combining current inverter and transconductance amplifier have been already investigated precisely. For example current inverter transconductance amplifier (CITA) and its modifications (using so-called Z-copy technique [20]) were reported in recent literature [21]. Active elements presented in previously discussed work have only one possibility of control by electronically adjustable transconductance.

We provided detailed comparison of the CFTA/CITA-based circuit structures (or their modifications) that provide first- and/or second- order transfer functions, to see recent progress in the field of CFTA/CITA-based first-order filters. Solutions discussed in [21–25] are simple first-order circuits. Some of them provide also universal [23] or multifunctional filtering characteristics [24]. Typical distinctiveness of the multifunctional/universal filters is the necessity of physical reconnection of the input or output terminal for change of the transfer type.

Change of the transfer function of the filter is quite important feature of applications on the chip. This feature is required if direct connection between two nodes

^{*} Department of Radio Electronics, ^{**} Department of Telecommunications, Faculty of Electrical Engineering and Communication, Brno University of Technology, Technická 3082/12, 616 00 Brno, Czech Republic, sotner@feec.vutbr.cz; ^{***} Department of Microelectronics, Faculty of Electrical Engineering and Communication, Brno University of Technology, Technická 3058/10, 616 00 Brno, Czech Republic; ^{****} D3-Friends Apartments, IP Extension, Delhi, India ^{*****} Department of Technical Studies, College of Polytechnics, Jihlava, Tolsteho, 16, 586 01, Jihlava, Czech republic

Table 1. Comparison of the parameters of presented solutions to recently reported reconnection-less voltage-mode filtering structures based on other active elements

	Active elements (number)	Type of functions	Available transfer functions
[26]	ECCII- (1), VB (1)	biquadratic (2 nd order)	AP, BR
[27]	ECCII- (4), MO-CF/I (2), VB (1) or OTA (5), VB (1)	biquadratic (2 nd order)	AP, BR
[28]	OTA (2), ECCII-(1)	1 st order	AP, LP, iDT
[29]	ZC-CG-VDCC (1)	1 st order	AP, LP, iDT, DT
Fig. 3a	ZC-CCCFDITA (1), CA (1)	1 st order	iHP, AP, iDT
Fig. 3b	ZC-CCCFDITA (1), CA (1)	1 st order	HP, iAP, DT

Abbreviations:

- ECCII- Current Conveyor of Second Generation (negative) with possibility of gain adjusting between X and Z terminal
- OTA Operational Transconductance Amplifier
- VB Voltage Buffer
- CA Current Amplifier (adjustable gain B)
- MO-CF/I Multiple-output Current Follower/Inverter
- ZC-CG-VDCC Z-copy Controlled-Gain Voltage Differencing Current Conveyor
- DT direct transfer
- iDT inverted direct transfer
- BR band reject transfer function
- AP all-pass transfer function
- iAP inverting all-pass transfer function
- LP low-pass transfer function
- HP high-pass transfer function
- iHP inverting high-pass transfer function

(in frame of the complex communication system — sub-blocks) have to be replaced by HP or other filter response in order to reject some type of wide-band or selective noise or distortion. It is necessary to provide reconnection of the output by switches, it practice. However, some types of the filter with specific features (reconnection-less reconfigurable) allow change of the transfer function by simple tuning of externally adjustable parameter [26] — no physical/electrical reconnection is necessary. Recently reported reconnection-less filtering circuits were summarized in Tab. 1 for easy comparison. Solution discussed in [26] allows change of the 2nd-order transfer function

between AP and BR by adjustable current gain. Solution of some drawbacks of [26] was discussed in full state variable follow the leader structure presented in [27]. However, circuit is quite complicated. The first order reconnection less filters were presented also in [28,29]. Both realizations, are focused on reconfiguration between AP, LP and direct transfer (DT). Unfortunately, no realization reported in the past (Tab. 1) was focused on AP, HP and DT transfer functions that can be changed electronically. For more details see Tab. 1.

This paper is focused on simple 1st-order circuits where additional adjustable current amplifier was en-

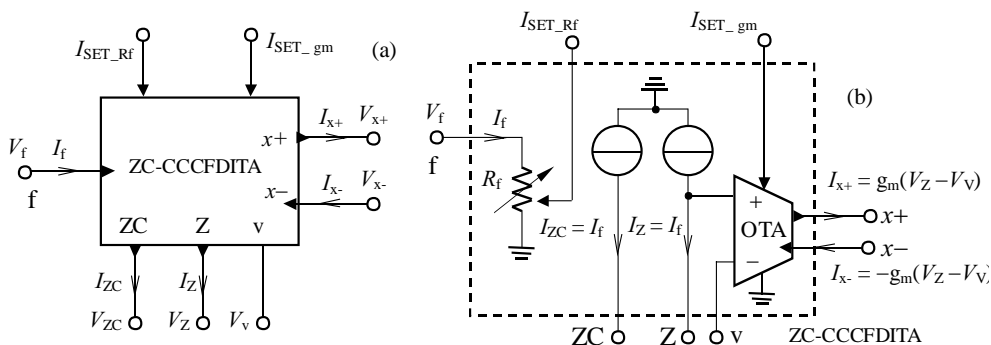


Fig. 1. Principle of the ZC-CCCFDITA: (a) — symbol, (b) — behavioral model

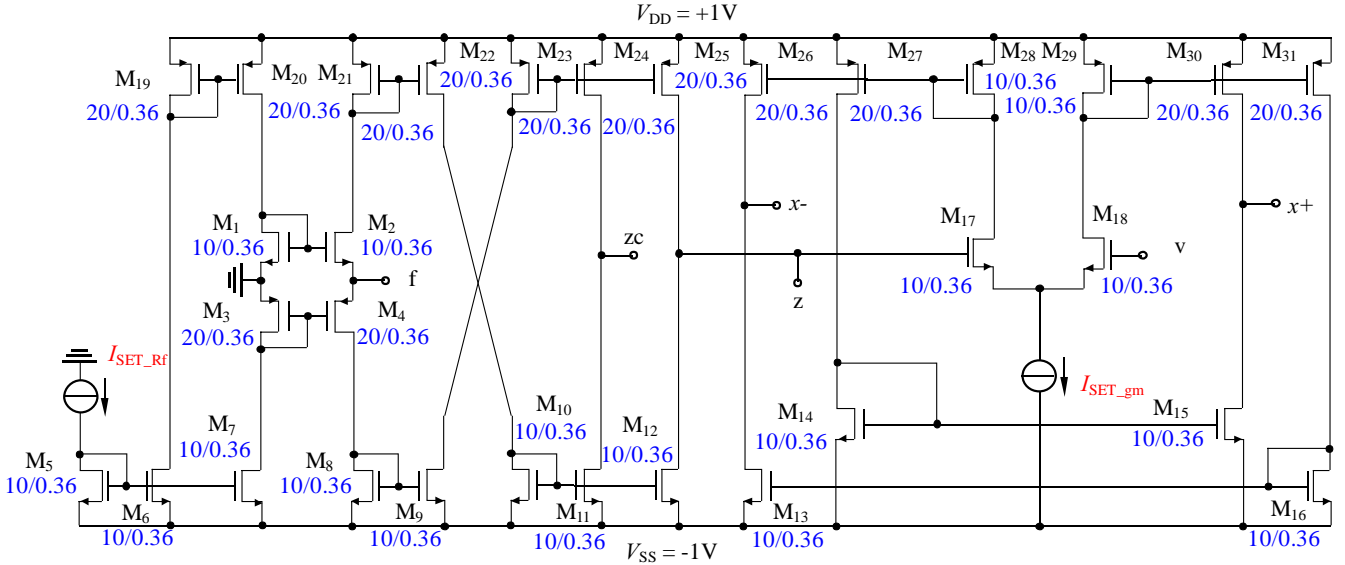


Fig. 2. Possible internal CMOS topology of proposed ZC-CCCFDITA active element

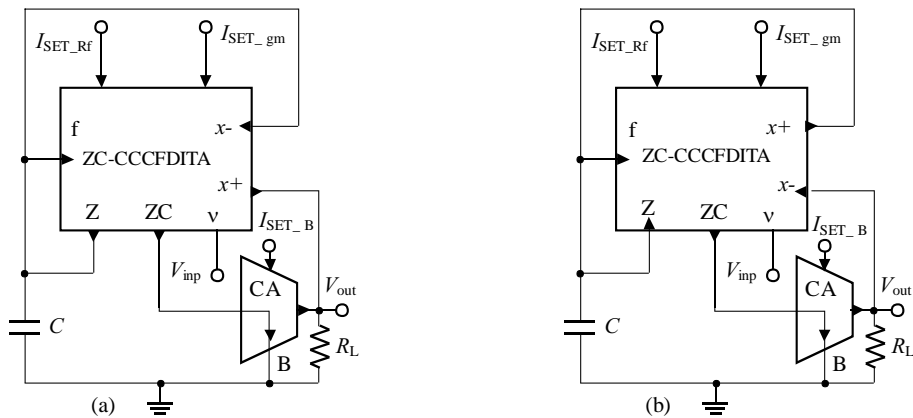


Fig. 3. HP/AP structures utilizing single ZC-CCCFDITA and adjustable current amplifier: (a) — using non-inverting controllable current amplifier, (b) — using inverting current amplifier

gaged to obtain several types of transfer characteristics including direct connection (non-inverting or inverting) between input and output terminal (the same form of the numerator and denominator of the transfer function — transfer with constant magnitude and phase characteristic) in several very simple circuits.

The paper is organized as follows: Section 2 shows definition of presented modification of active element (so-called Z-copy current-controlled current follower differential input transconductance amplifier — ZC-CCCFDITA) and possible way of its CMOS implementation. Chapter 3 deals with 1st-order electronically reconfigurable transfers (HP, AP, DT) in simple circuits based on ZC-CCCFDITA and adjustable current amplifier with minimal number of passive elements and their theoretical analysis. Section 4 introduces method of implementation of the ZC-CCCFDITA by commercially available active elements (behavioral model) and its application in selected type of the reconfigurable filtering solution to-

gether with CMOS implementation. Comparison of ideal and simulated results with CMOS and behavioral model is also presented. Exemplary experimental results are given in Section 5. Summarization of achieved features, requirements and results is provided in conclusion.

2 Z-COPY CURRENT-CONTROLLED CURRENT FOLLOWER DIFFERENTIAL INPUT TRANSCONDUCTANCE AMPLIFIER

The Z-copy current-controlled current follower differential input transconductance amplifier (ZC-CCCFDITA) belongs to family of modern active elements [1] deeply investigated by Herencsar *et al.*, [30]. Principle of this useful modification of basic CFTA is in controllable input intrinsic resistance R_f , transconductance (g_m) of the output section and additional differential voltage input [25] of the output (transconductance section – OTA). Basic CFTA does not use fully-differential input of the OTA

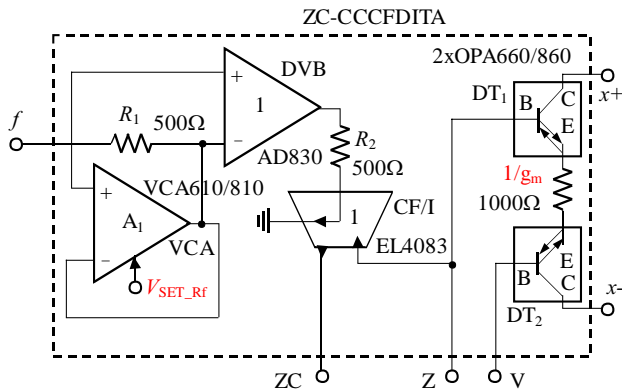


Fig. 4. Behavioral model of the ZC-CCCFDITA employing commercially available active devices

section (one input terminal is grounded) [1], however, it seems to be advantageous. Principal conception of the ZC-CCCFDITA is shown in Fig. 1.

Input current I_f is mirrored to two output terminals of the first section (current follower). One current output is connected directly to the second (output) section based on operational transconductance amplifier (OTA) and called z . The second auxiliary current output of the first section is identical copy of the input current I_f , this output is called zc . Negative input of the OTA section lead out of the device and noted as v . Two current outputs of the OTA section have both polarities or we can use multiple-output OTA section. Principle is clear from Fig. 1b. The CMOS structure utilizing current controlled current conveyor of second generation [3] connected as multiple-output current follower and dual-output OTA section [2, 22] is shown in Fig. 2.

Controllable intrinsic resistance is given by [31, 32]

$$R_f = \frac{1}{\sqrt{I_{SET_Rf} K_{Pn} \frac{W_{M1,2}}{L_{M1,2}}} + \sqrt{I_{SET_Rf} K_{Pp} \frac{W_{M3,4}}{L_{M3,4}}}}, \quad (1)$$

and transconductance of the output OTA section has known expression [31]

$$g_m = 2\sqrt{I_{SET_gm} K_{Pn} \frac{W_{M17,18}}{L_{M17,18}}} \quad (2)$$

where constant 2 is given by gain of current mirrors (P-MOS: M_{28} – M_{27} and M_{29} – M_{30}) and $K_{Pn,p}$ are technological constants ($\mu_0 C_{ox}$) of used fabrication technology [33] (TSMC 0.18 μm).

3 FIRST-ORDER FILTERS WITH ELECTRONICALLY RECONFIGURABLE TYPE OF THE TRANSFER FUNCTION

Almost all active electronic systems are integrated on chip today. Electronic adjustability of the systems is important for control of bandwidth, pole frequency, oscillation frequency, quality factor, *etc.* However, extensive

reconfiguration like change of the transfer function of the frequency filter is not possible because it requires change of topology, reconnection of input/output nodes (SIMO, MISO types) very often. Unfortunately, after fabrication no change of the internal structures is possible. We present simple 1st-order transfer functions that are available in advanced circuitry as HP or AP response without necessity of changing the topology or reconnection of nodes (SISO — single input and single output type). Only electronically adjustable parameter is used for change type of the transfer function. Therefore this way can be very useful for on-chip subsystems. We will demonstrate principle on two solutions both are practically the same but different configurations of polarities of the outputs of active elements give us significantly different possibilities.

Circuit in Fig. 3a is HP/AP filter and DT based on ZC-CCCFDITA and Adjustable Current Amplifier. It has both of the z and zc terminals with positive polarity. Transfer function has form

$$K_1(s) = \frac{g_m R_L}{R_f} \frac{B - sCR_f}{g_m + sC}. \quad (3)$$

The circuit structure behaves as inverting HP (iHP) section for $B = 0$. AP section is available for $B = 1$ for a condition $g_m = 1/R_f$. Inverting direct transfer (iDT) is set by $B = -1$. Zero and pole frequencies are given by $\omega_z = B/R_f C$ and $\omega_p = g_m/C$.

Independent control of the zero and pole location (outside pure AP behavior) is possible also by R_f and g_m (bilinear filter). However, both parameters influence pass-band gain.

The second solution of the filter has the same circuit solution but direction (polarity) of output currents from outputs and auxiliary terminal z are opposite, see Fig. 3b. This difference is important for type (polarity) and value of controllable current gain B . Despite the fact that both circuits have the same structure, transfer function of the solution in Fig. 3b is slightly different

$$K_2(s) = \frac{g_m R_L}{R_f} \frac{2 - B + sCR_f}{g_m + sC}, \quad (4)$$

where $B = 1$ gives DT response (constant unity magnitude and phase equal to 0 degrees) if $g_m = 1/R_f$. The transfer function of HP response is obtained in case of $B = 2$ and the inverting AP (iAP) response is available for $B = 3$ ($g_m = 1/R_f$). Zero frequency is given by $\omega_z = (2 - B)/R_f C$ and pole frequency is the same as in the previous case ($\omega_p = g_m/C$).

The first case (Fig. 3a) requires controllable parameter $B \geq 0$ for change of the transfer type from HP to AP response, the second case (Fig. 3b) allows change also from HP to AP, but for $B \geq 2$. Migration of zero from left to the right side of the complex space is conditioned by both polarities of B ($B = \pm 1$) in the first case in Fig. 3a, which is sophisticated task for current amplifier. Fortunately, solution in Fig. 3b allows migration of zero just

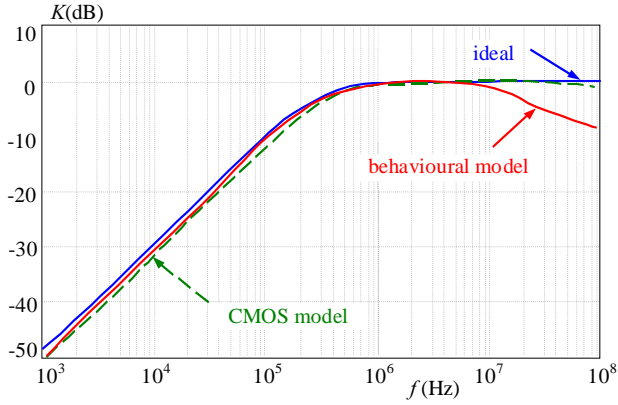


Fig. 5. HP magnitude response obtained from structure utilizing behavioral or CMOS model of ZC-CCCFDITA and adjustable current amplifier

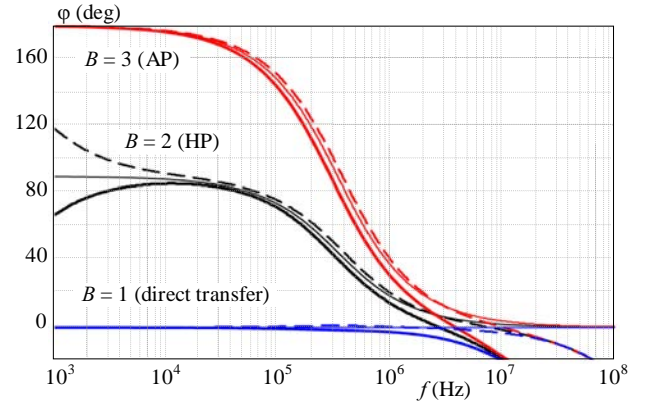


Fig. 6. AP and DT magnitude responses obtained from structure utilizing behavioral and CMOS models of ZC-CCCFDITA and adjustable current amplifier

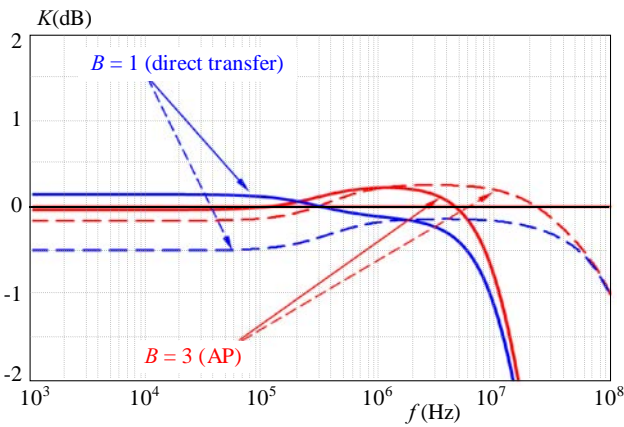


Fig. 7. All phase responses obtained from structure utilizing behavioral and CMOS models of ZC-CCCFDITA and adjustable current amplifier (three discrete current gains)

in one polarity of the B . Necessity of higher gain $B = 3$ (for AP response) is small disadvantage of this solution (higher gain = higher power consumption in many cases). Both circuits are suitable for cascading (high-impedance input terminal). This solution will be analyzed in more details in Chapter 4.

4 SIMULATION RESULTS

4.1 Simulation of the selected filtering solution

Circuit in Fig. 3b was chosen for detailed study. Its features are interesting for investigation because it allows HP, AP and DT functions simultaneously in one circuit structure (without reconnection) only by change of parameter B (in one polarity). The rest of parameters was selected as: $R_f = R_L = 1 \text{ k}\Omega$, $C = 470 \text{ pF}$, $g_m = 1 \text{ mS}$. Current amplifier constructed from EL2082 [35] was used for control of loop-gain and type of the transfer (commercially available devices-based behavioral model).

We prepared the following behavioral model (Fig. 4) of the ZC-CCCFDITA based on commercially available devices (VCA610/810 [36], AD830 [37], EL4083 [38],

EL2082 [35] and diamond transistor OPA860 [39,40]). Supply voltage of the behavioral model was $\pm 5 \text{ V}$. Discussed model employs controllable current amplifier/follower part that allows voltage control of the R_f based on voltage controllable amplifier (VCA) (method firstly proposed in [41]). The resistance R_f is given by [41] as

$$R_f = R_1(1 + 10^{-2(V_{\text{SET_rf}}+1)}). \quad (5)$$

Differential voltage amplifier (DVB) can be easily replaced by the second VCA to control also the current gain [41]. Resistor R_2 serves as voltage/current converter. Transconductance section is utilized by two diamond transistors (DTs).

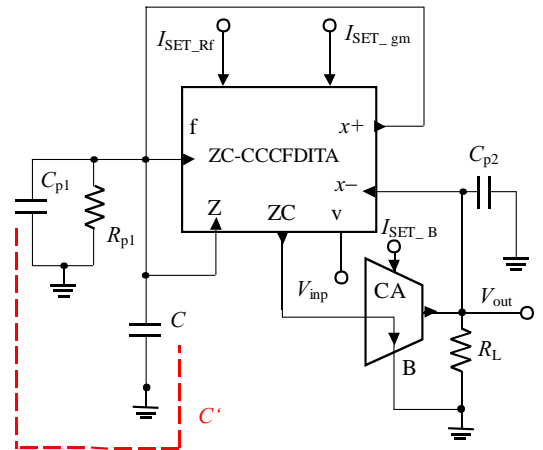


Fig. 8. Model representing the most important parasitic influences in circuit from Fig. 3b

CMOS structure from Fig. 2 was also used (after appropriate changes of polarities of the outputs and auxiliary terminals in accordance to Fig. 3b) for simulation together with CMOS current amplifier based on section used also in [11,12] and [29] especially for example. Its current gain [34] is given by

$$B = \frac{NI_{b2}}{2I_{\text{set}_B}} \cong \frac{I_{b2}}{I_{\text{set}_B}}. \quad (6)$$

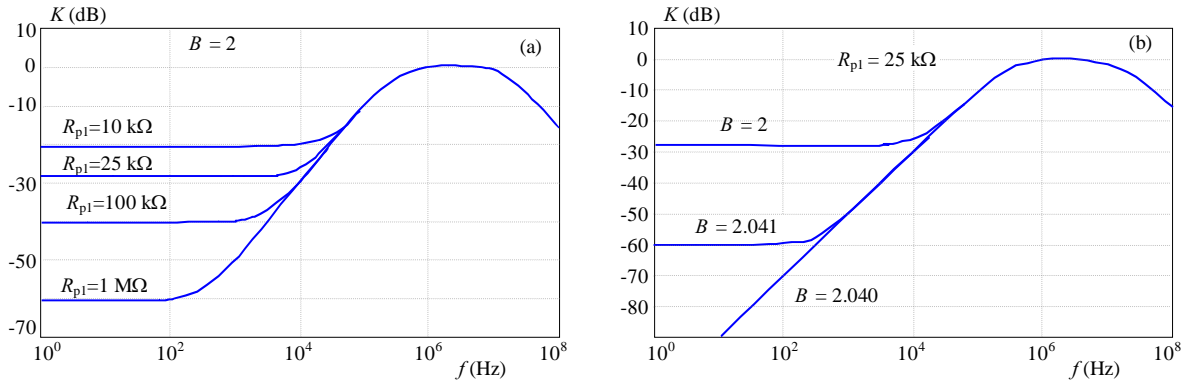


Fig. 9. HP response behavior under conditions of parasitic elements: (a) — stepping of R_{p1} while B is constant, (b) — stepping of B while R_{p1} is constant

Figure 5 shows magnitude HP response for three traces: ideal ($f_p = 339$ kHz for $B = 2$, $g_m = 1$ mS, $R_f = 1$ k Ω), simulation with behavioural model ($f_p = 296$ kHz for $V_{SET_B} = 2.46$ V, $g_m = 1$ mS, $V_{SET_Rf} = 1$ V) and simulation with CMOS model ($f_p = 378$ kHz for $I_{SET_B} = 56.5$ μ A, $I_{SET_gm} = 54$ μ A, $I_{SET_Rf} = 34$ μ A) using the ZC-CCCFDITA device. Figure 6 indicates reconfigurability between AP, HP and direct transfer in phase response. There ideal traces, simulation results with behavioural model and simulation results with CMOS model of the ZC-CCCFDITA are compared. The ideal trace, behavioural model and CMOS model responses are distinguished by style of the line (ideal trace - thin solid line, behavioural model thick line, CMOS model thick dashed line). Sets of parameters (in order to obtain AP for ideal $B = 3$, HP for ideal $B = 2$ and direct transfer for ideal $B = 1$) are following: AP (behavioural model - $f_p = 292$ kHz, $V_{SET_B} = 4$ V, $g_m = 1$ mS, $V_{SET_Rf} = 1$ V; CMOS model - $f_p = 373$ kHz, $I_{SET_B} = 35$ μ A, $I_{SET_gm} = 54$ μ A, $I_{SET_Rf} = 34$ μ A), HP (behavioural model - $f_{3dB} = 296$ kHz, $V_{SET_B} = 2.46$ V, $g_m = 1$ mS, $V_{SET_Rf} = 1$ V; CMOS model - $f_{3dB} = 378$ kHz, $I_{SET_B} = 56.5$ μ A, $I_{SET_gm} = 54$ μ A, $I_{SET_Rf} = 34$ μ A), direct transfer (behavioural model - $V_{SET_B} = 1.15$ V, $g_m = 1$ mS, $V_{SET_Rf} = 1$ V; CMOS model - $I_{SET_B} = 81$ μ A; $I_{SET_gm} = 54$ μ A; $I_{SET_Rf} = 34$ μ A). Magnitude responses for DT and HP configuration are given in Fig. 7. Sets of parameters is the same as note above (for AP and DT). Supply voltage was always ± 5 V for behavioural model and ± 1 V for CMOS model.

4.2 Parasitic analysis of selected filtering solution

We provided detailed analysis of important parasitic influences in the selected structure (Fig. 3b). Main problems create additional impedance in high-impedance node of working capacitor and parasitic capacitance in node of working resistor R_L (in parallel). Model representing these problems is depicted in Fig. 8. We suppose following simplifications, because they are nearly always fulfilled: $R_{ZC} \gg R_{inpCA}$, $R_{x-} \gg R_L$ therefore, we can

suppose R_L in node operating as only dominant resistance. Parasitic elements are estimated (determined from behavioral model in Fig. 4 for example) as follows: $R_{p1} \approx R_f \parallel R_z \parallel R_{x+} \approx R_f \parallel 25$ k Ω , $C_{p1} \approx C_f + C_z + C_{x+} \approx 10$ pF, $C_{p2} \approx C_{out_CA} + C_{x-} \approx 10$ pF. We used also simplification $C' = C + C_{p1}$. The rest of parameters was used as in case of Section 4.1. Low value of $R_{x\pm}$ (25 k Ω [39, 40]) seems to be the most important problem for us. Approximate equation for overall transfer function of the filter has form in this case

$$K'_2(s) = g_m R_L (R_{p1}(2 - B) + R_f + sC'R_f R_{p1}) / (g_m R_f R_{p1} + R_f + s[R_f R_{p1} C' + R_L C_{p2}(g_m R_f R_{p1} + 2R_{p1} + R_f)] + s^2 C' C_{p2} R_f R_{p1} R_L). \quad (7)$$

Simulation results of the HP response (that is the most influenced by parasitic behavior) we have shown in Fig. 9. Of course R_{p1} has direct impact on zero location and value of finite attenuation in the stop band, see Fig. 9a.

Ideal value $B = 2$ is expected for pure HP response without zero. Existence of real R_{p1} causes unintentional creation of zero also for $B = 2$. However, problem of low $R_{x\pm}$ (the most important contributor of R_{p1}) can be still easily solved by B control (as we suppose to utilize for reconfiguration) to compensate impact of R_{p1} and to obtain pure HP again (for $B = 2.04$), see Fig. 9b.

Second order denominator of influenced transfer function has also impact on pass-band transfer drop at higher frequencies (but maybe lower than available bandwidth of active elements in some cases) that is visible in all transfer responses (HP, iAP, DT). Estimation of this pole frequency can be provided from: $\omega_{p2} \cong 1/R_L C_{p2} \cong 16$ MHz.

5 EXPERIMENTAL RESULTS

We measured discussed type of the filter (Fig. 3b) based on behavioral model from Fig. 4 and additional current amplifier (EL2082) under the same conditions as described in Section 4. Measurements were provided by network vector analyzer ENA E5071C. Brief exemplary results of the filter configurations, particularly HP, iAP

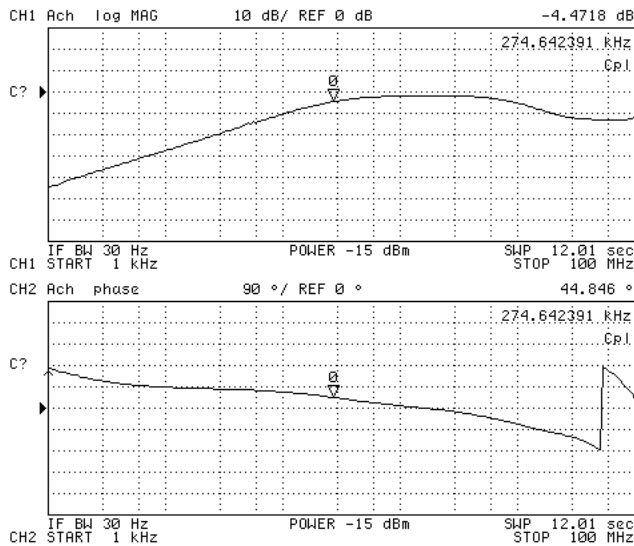


Fig. 10. Measured magnitude and phase response of HP configuration, $V_{\text{set}_B} = 2.6$ V

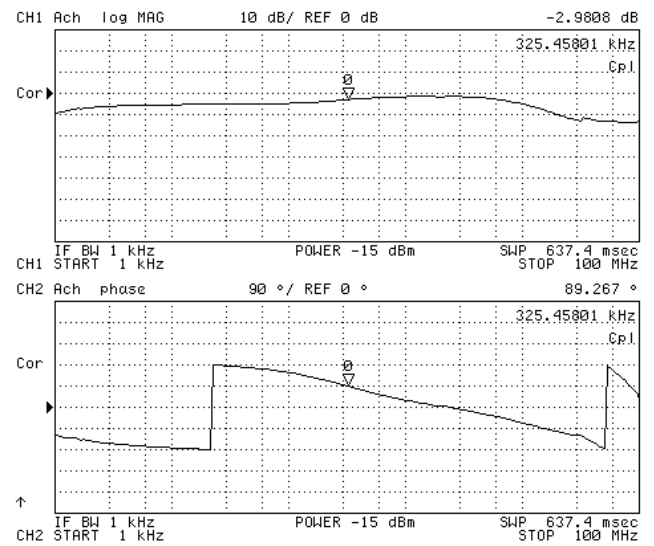


Fig. 11. Measured magnitude and phase response of iAP configuration, $V_{\text{set}_B} = 4.3$ V

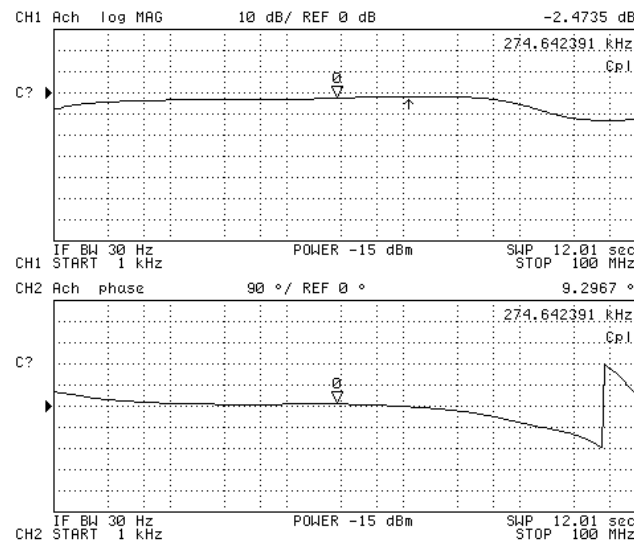


Fig. 12. Measured magnitude and phase response of DT configuration, $V_{\text{set}_B} = 1$ V

and DT transfers, are shown in Figs. 10–12. Experimental results are close to expectations and behavior of simulated case.

Acknowledgement

Research described in this paper was financed by Czech Ministry of Education in frame of National Sustainability Program under grant LO1401. For research, infrastructure of the SIX Center was used. Research described in the paper was supported by Czech Science Foundation project under No. 14-24186P.

REFERENCES

- [1] BIOLEK, D.—SENANI, R.—BIOLKOVA, V.—KOLKA, Z.: Active Elements for Analog Signal Processing: Classification, Review and New Proposals, *Radioengineering* **17** No. 4 (2008), 15–32.
- [2] GEIGER, R. L.—SÁNCHEZ-SINENCIO, E.: Active Filter Design using Operational Transconductance Amplifiers: a Tutorial, *IEEE Circ. and Devices Magazine* **1** (1985), 20–32.
- [3] FABRE, A.—SAAID, O.—WIEST, F.—BOUCHERON, C.: High Frequency Applications based on a New Current Controlled Conveyor, *IEEE Trans. on Circuits and Systems - I* **43** No. 2 (1996), 82–91.
- [4] SURAKAMPONTORN, W.—THITIMAJSHIMA, W.: Integrable Electronically Tunable Current Conveyors, *IEE Proceedings-G* **135** No. 2 (1988), 71–77.
- [5] H. ALZAHER: CMOS Digitally Programmable Quadrature Oscillators, *International Journal of Circuit Theory and Applications* **36** No. 8 (2008), 935–966, DOI: 10.1002/cta.479.
- [6] ALZAHER, H.—TASADDUQ, N.—AL-EES, O.—AL-AMMARI, F.: A Complementary Metal-Oxide Semiconductor Digitally Programmable Current Conveyor, *International Journal of Circuit Theory and Applications* **41** No. 1 (2013), 69–81, DOI: 10.1002/cta.786.
- [7] BIOLEK, D.—LAHIRI, A.—JAIKLA, W.—SIRIPRUCHYANUN, M.—BAJER, J.: Realisation of Electronically Tunable Voltage-Mode/Current-Mode Quadrature Sinusoidal Oscillator using ZC-CG-CDBA, *Microelectronics Journal* **42** No. 10 (2011), 1116–1123.
- [8] SOULITIS, G.—PSYCHALINOS, C.: Electronically Controlled Multiphase Sinusoidal Oscillators using Current Amplifiers, *International Journal of Circuit Theory and Applications* **37** No. 1 (2009), 43–52.
- [9] HERENC SAR, N.—LAHIRI, A.—VRBA, K.—KOTON, J.: An Electronically Tunable Current-Mode Quadrature Oscillator using PCAs, *Int. Journal of Electronics* **99** No. 5 (2011), 609–621, DOI: 10.1080/00207217.2011.643489.
- [10] SOTNER, R.—LAHIRI, A.—KARTCI, A.—HERENC SAR, N.—JERABEK, J.—VRBA, K.: Design of Novel Precise Quadrature Oscillators Employing ECCIs with Electronic Control, *Advances in Electrical and Computer Engineering* **13** No. 2 (2013), 65–72.
- [11] SOTNER, R.—HERENC SAR, N.—JERABEK, J.—KOTON, J.—DOSTAL, T.—VRBA, K.: Electronically Controlled Oscillator with Linear Frequency Adjusting for Four-Phase or Differential Quadrature Output Signal Generation, *International Journal of Circuit Theory and Applications*, **42** No. 12 (2014), 1264–1289.
- [12] SOTNER, R.—HRUBOS, Z.—HERENC SAR, N.—JERABEK, J.—DOSTAL, T.: Precise Electronically Adjustable Oscillator

- Suitable for Quadrature Signal Generation Employing Active Elements with Current and Voltage Gain Control, *Circuits Systems and Signal Processing* **33** No. 1 (2014), 1–35.
- [13] MINAEI, S.—SAYIN, O. K.—KUNTMAN, H.: A New CMOS Electronically Tunable Current Conveyor and its Application to Current-Mode Filters, *IEEE Trans. on Circuits and Systems - I* **53** No. 7 (2006), 1448–1457.
- [14] SIRIPRICHYANUN, M.—JAIKLA, W.: Current Controlled Current Conveyor Transconductance Amplifier (CCCCTA): a Building Block for Analog Signal Processing, *Electrical Engineering Springer* **90** No. 6 (2008), 443–453.
- [15] KUMNGERN, M.—JUNNAPIYA, S. A.: Sinusoidal Oscillator using Translinear Current Conveyors, *Proceedings of Asia Pacific Conference on Circuits and Systems (APCCAS 2010)*, Malaysia, Kuala Lumpur, 2010, pp. 740–743, DOI: 10.1109/APCCAS.2010.5774754.
- [16] JAIKLA, W.—LAHIRI, A.: Resistor-Less Current-Mode Four-Phase Quadrature Oscillator using CCCDTAs and Grounded Capacitors, *AEU – International Journal of Electronics and Communications* **66** No. 3 (2011), 214–218.
- [17] SAKUL, C.—JAIKLA, W.—DEJHAN, K.: New Resistorless Current-Mode Quadrature Oscillators using 2 CCCDTAs and Grounded Capacitors, *Electrical Engineering Springer* **90** No. 6 (2008), 443–453.
- [18] SOTNER, R.—JERABEK, J.—HERENC SAR, N.—DOSTAL, T.—VRBA, K.: Electronically Adjustable Modification of CFA: Double Current Controlled CFA (DCC-CFA), *Proceedings of the 35th International Conference on Telecommunications and Signal Processing*, Prague, Czech Republic, 2012, pp. 401–405.
- [19] SOTNER, R.—HERENC SAR, N.—JERABEK, J.—DVORAK, R.—KARTCI, A.—DOSTAL, T.—VRBA, K.: New Double Current Controlled CFA (DCC-CFA) based Voltage-Mode Oscillator with Independent Electronic Control of Oscillation Condition and Frequency, *Journal of Electrical Engineering* **64** No. 2 (2013), 65–75.
- [20] BIOLEK, D.—BAJER, J.—BIOLKOVA, V.—KOLKA, Z.—KUBICEK, M.: Z Copy-Controlled Gain-Current Differencing Buffered Amplifier and its applications, *International Journal of Circuit Theory and Applications* **39** No. 3 (2011), 257–274.
- [21] BIOLEK, D.—BIOLKOVA, V.: Electronically Tunable Phase Shifter Employing Current-Controlled Current Follower Transconductance Amplifiers (CCCFTAs), *Proceedings of the 32th International Conference on Telecommunications and Signal Processing - TSP'09*, Dunakility, Hungary, 2009, pp. 54–57.
- [22] HERENC SAR, N.—KOTON, J.—VRBA, K.: Current Controlled Current Conveyor Transconductance Amplifier (CCCCTA): a Building Block for Analog Signal Processing, *Electrical Engineering Springer* **90** No. 6 (2008), 443–453.
- [23] LI, Y.: A Series of New Circuits based on CFTAs, *AEU – International Journal of Electronics and Communications* **66** No. 7 (2012), 587–592.
- [24] IAMAREJIN, A.—MANE EWAN, S.—SUWANJAN, P.—JAIKLA, W.: Current-Mode Variable Current Gain First-Order Allpass Filter Employing CFTAs, *Prezglad Elektrotechniczny* **89** No. 2a (2013), 238–241.
- [25] HERENC SAR, N.—KOTON, J.—VRBA, K.—LAHIRI, A.: Single GCFDITA and Grounded Passive Elements based General Topology for Analog Signal Processing Applications, *Proceedings of the 11th International Conference on Networks - ICN 2012*, Saint Gilles, Reunion Island, 2012, pp. 59–62.
- [26] SOTNER, R.—JERABEK, J.—SEVCIK, B.—DOSTAL, T.—VRBA, K.: Novel Solution of Notch/All-Pass Filter with Special Electronic Adjusting of Attenuation in the Stop Band, *Elektronika Ir Elektrotechnika* **17** No. 7 (2011), 37–42.
- [27] SOTNER, R.—JERABEK, J.—PETRZELA, J.—VRBA, K.—DOSTÁL, T.: Design of Fully Adjustable Solution of Band-Reject/All-Pass Filter Transfer Function using Signal Flow Graph Approach, In *Proceedings of the 24th International Conference Radioelektronika 2014*, pp. 67–70.
- [28] SOTNER, R.—JERABEK, J.—HERENC SAR, N.—PROKOP, R.—VRBA, K.—DOSTAL, T.: Resistor-Less First-Order Filter Design with Electronical Reconfiguration of its Transfer Function, *Proceedings of the 24th International Conference Radioelektronika 2014*, 2014, pp. 63–66.
- [29] SOTNER, R.—HERENC SAR, N.—JERABEK, J.—PROKOP, R.—KARTCI, A.—DOSTAL, T.—VRBA, K.: Z-Copy Controlled-Gain Voltage Differencing Current Conveyor: Advanced Possibilities in Direct Electronic Control of First-Order Filter, *Elektronika Ir Elektrotechnika* **20** No. 6 (2014), 77–83.
- [30] HERENC SAR, N.—KOTON, J.—LATTENBERG, I.—VRBA, K.: Signal-Flow Graphs for Current-Mode Universal Filter Design using Current Follower Transconductance Amplifiers (CF-TAs), *Proc. of Applied Electronics APPEL2008*, Pilsen, 2008, pp. 69–72.
- [31] BAKER, J.: *CMOS Circuit Design, Layout and Simulation*, Wiley-IEEE Press, West Sussex, 2008.
- [32] ELDBIB, I.—MUSIL, V.: Self-Cascoded Current Controlled CCII Based Tunable Band Pass Filter, *Proc. 18th Int. Conf. Radioelektronika*, Praha, 2008, pp. 1–4.
- [33] MOSIS Parametric Test Results of TSMC LO EPI SCN018 Technology, ftp://ftp.isi.edu/pub/mosis/vendors/tsmc-018/t44e_lo_epi-params.txt Available on-line, cited 24.5.2012.
- [34] SURAKAMPONTORN, W.—KUMWACHARA, K.: CMOS-Based Electronically Tunable Current Conveyor, *Electronics Letters* **14** No. 28 (1992), 1316–1317, DOI: 10.1049/el:19920836.
- [35] Intersil (Elantec) EL2082 CN Current-Mode Multiplier (datasheet),.
- [36] Texas Instruments. VCA810: High Gain Adjust Range, Wideband, variable gain amplifier, <http://www.ti.com/lit/ds/symlink/vca810.pdf> 2003 (last modified 12/2010), 30 p.
- [37] Analog Devices. AD830 High Speed, Video Difference Amplifier (datasheet), http://www.analog.com/static/imported-files/data_sheets/AD830.pdf 2010 (Rev. C, 03/2010), 20 p.
- [38] Current-mode four-quadrant multiplier EL 4083 (datasheet), <http://www.elantec.com> 1995, 16 p.
- [39] Texas Instruments. OPA660 Wide bandwidth operational transconductance amplifier and buffer (datasheet), [www: http://www.ti.com/lit/ds/symlink/opa660.pdf](http://www.ti.com/lit/ds/symlink/opa660.pdf) 2000, 20 p.
- [40] Texas Instruments. OPA860 Wide-bandwidth, operational transconductance amplifier (OTA) and buffer (datasheet), [www: http://www.ti.com/lit/ds/symlink/opa860.pdf](http://www.ti.com/lit/ds/symlink/opa860.pdf) 2008, 33 p.
- [41] SOTNER, R.—KARTCI, A.—JERABEK, J.—HERENC SAR, N.—DOSTAL, T.—VRBA, K.: An Additional Approach to Model Current Followers and Amplifiers with Electronically Controllable Parameters from Commercially Available ICs, *Measurement Science Review* **12** No. 6 (2012), 255–265.

Received 28 December 2014

Roman Šotner was born in Znojmo, Czech Republic, in 1983. He received the PhD degree in Electrical Engineering in 2012 from the Brno University of Technology, MSc degree in 2008 and BSc degree in 2006. Currently, he is a research worker at the Department of Radio electronics, Faculty of Electrical Engineering and Communication, Brno University of Technology, Brno, Czech Republic. His interests are analogue circuits (active filters, oscillators, audio, *etc*), circuits in the current mode, circuits with direct electronic controlling possibilities especially and computer simulation.

Jan Jeřábek was born in Bruntal, Czech Republic, in 1982. He received the PhD degree in Electrical Engineering in 2011 from the Brno University of Technology, Czech Republic. He is currently assistant professor at the Department of Telecommunications, Faculty of Electrical Engineering and

Communication, Brno University of Technology. His research interests are focused on circuit design and applications of modern active elements such as adjustable current amplifiers and followers, transconductance and transimpedance amplifiers.

Norbert Herencsar was born in Slovakia, in 1982. He received the MSc and PhD degrees in Electronics & Communication and Teleinformatics from Brno University of Technology, Czech Republic, in 2006 and 2010, respectively. Since December 2015, he is an Associate Professor at the Department of Telecommunications of Brno University of Technology, Brno, Czech Republic. During September 2009-February 2010 and February 2013-May 2013 he was an Erasmus Exchange Student and Visiting Researcher, respectively, with the Department of Electrical and Electronic Engineering, Bogazici University, Istanbul, Turkey. During January 2014 – April 2014 he was a Visiting Researcher with the Department of Electronics and Communications Engineering, Dogus University, Istanbul, Turkey. His research interests include analog filters, current-, voltage- and mixed-mode circuits, new active elements and their circuit applications, low transistor count circuits, MOS-only circuits, oscillators, and inductor simulators. He is an author or co-author of 56 research articles published in SCI-E peer-reviewed international journals, 24 articles published in other journals, and 89 papers published in proceedings of international conferences. Since 2010, he is Deputy-Chair of the International Conference on Telecommunications and Signal Processing (TSP). Since 2012, is Co-editor of the International Journal of Advances in Telecommunications, Electrotechnics, Signals and Systems. Since 2014, he is Associate Editor of the Journal of Circuits, Systems and Computers (JCSC). Dr. Herencsar is Senior Member of the IEEE, IACSIT, and IRED, and Member of the IAENG, ACEEE, and RS. Since 2015, he serves as IEEE Czechoslovakia Section SP/CAS/COM Joint Chapter Chair as well as Membership Development Officer.

Roman Prokop was born in Velké Meziříčí in 1971. He received the MSc and PhD degrees in Electrical Engineering from the Brno University of Technology, Czech Republic, in 1995 and 2009, respectively. He is currently working as Assistant at the Dept. of Microelectronics, Brno University of Technology. His research is in the field of integrated circuit design, where his interests include modern innovative analog circuits, current mode circuits, analog signal processing and digitally tunable analog circuits.

Abhirup Lahiri received Bachelor of Engineering (BE) degree with the highest honors from the Division of Electronics and Communications, Netaji Subhas Institute of Technology (erstwhile, Delhi Institute of Technology), University of Delhi, India. His past research works include design of compact analog circuit solutions using novel voltage-mode and current-mode active elements. His current research interests include low-power and low-voltage analog circuit design and precision voltage and current reference generation. He has authored/co-authored more than thirty international journal/conference papers (including fifteen SCI/SCI-E publications) and has acted as a reviewer (by editor's invitation) for numerous international journals and conferences of repute. He served as a program committee member for the International Conference on Telecommunications and Signal Processing (TSP). He is an editorial board member of Radioengineering Journal for the years 2011-2012. His biography is included in Marquis Who's Who in the World 2011- (28th Edition).

Tomáš Dostál born in 1943, received his PhD (1976) and DrSc degree (1989). He was with the University of Defense Brno (1976-1978 and 1980-1984), with the Military Technical College Baghdad (1978-1980), with the Brno University of Technology (1984-2008) and with the European Polytechnic Institute (2008 - 2009). Since 2009 he has been with the College of Polytechnics, Jihlava as Professor of Electronics. His interests are in circuit theory, analog filters, switched capacitor networks and circuits in the current mode.

Kamil Vrba received the PhD degree in Electrical Engineering in 1976, and the Prof degree in 1997, both from the Technical University of Brno. Since 1990 he has been Head of the Dept. of Telecommunications, Faculty of Electrical Engineering and Computer Science, Brno University of Technology, Brno, Czech Republic. His research work is concentrated on problems concerned with accuracy of analog circuits and mutual conversion of analog and digital signals. In cooperation with AMI Semiconductor Czech, Ltd. (now ON Semiconductor Czech Republic, Ltd.) he has developed number of novel active function blocks for analog signal processing such as universal current conveyor (UCC), universal voltage conveyor (UVC), programmable current amplifier (PCA), and others. He is an author or co-author of more than 650 research articles published in international journals or conference proceedings. Professor Vrba is a Member of IEEE, IEICE, and Associate Member of IET.

[29] SOTNER, R., JERABEK, J., SEVCIK, B., DOSTAL, T., VRBA, K. Novel Solution of Notch/All- pass Filter with Special Electronic Adjusting of Attenuation in the Stop Band. *Elektronika Ir Elektrotechnika*, 2011, vol. 17, no. 7, p. 37-42. ISSN: 1392- 1215.

Novel Solution of Notch/All-pass Filter with Special Electronic Adjusting of Attenuation in the Stop Band

R. Sotner, J. Jerabek, B. Sevcik, T. Dostal, K. Vrba

Faculty of Electrical Engineering and Communication, Brno University of Technology,

Purkynova 118, 612 00 Brno, Czech Republic, phone: +420 541 149 140, e-mail: xsotne00@stud.feec.vutbr.cz

Introduction

There are many suitable active elements for electronic adjusting in the signal processing (high-speed data communication systems, regulation and measurement techniques, electro-acoustics, etc.). We can introduce for example operational transconductance amplifiers (OTA-s) [1], current differencing transconductance amplifiers (CDTA-s) [2], differential input buffered and transconductance amplifiers (DBTA-s) [3], current follower transconductance amplifier (CFTA-s) [4], single, dual and multi-output controlled current conveyors (ECCII-s, VCG-CCII-s, DO-CCCCII-s, MO-CCCCII-s) [5–9] or current controlled current feedback amplifiers (CC-CFA-s) [10]. Many another novel active elements and their properties are summarized in [11], unfortunately many of them are not commercially available yet. Electronic control of the parameters of mentioned active elements is possible due to the DC bias control current or voltage.

A lot of applications are focused on sinusoidal oscillators [12–15] and filters [16–20], in the voltage, current and also mixed mode. Many of active filters are multifunctional or universal (we can obtain low-pass, band-pass, high-pass, all-pass and band reject/notch filter within the same circuit) and sometimes there is a possibility of electronic tuning. Practically, there is no necessity to have all transfer functions in one circuitry. In particular applications, one type of filtering function is usually required. Main aim of this work is not to show multifunctional or fully adjustable circuit but to introduce a simple approach in case of the electronic adjusting of the stop-band attenuation. Some recent solutions are compared in the following text.

Except circuits shown in [16–20, 30–32] realizations of single-purpose filters (all pass/notch filter) were published in [21–29]. Solution of the all-pass and notch filter based on single CCII- and 6 passive elements is described in [21]. Complicated solution is presented in [22] and is based on CCII- and CCII+ and 5 passive elements. Publication [23] presents multifunctional filter based on

single CCII- and 5 passive elements where notch response is also possible. Ref. [24] deals with quite complicated all-pass/notch filter employing two CCII+ and one CCII- and 6 grounded passive elements. In [25, 26] multifunctional filters with notch response with CCII+ and CCII- and 5-6 passive elements were also introduced. Solution described in [27] shows all-pass, notch and band-pass filter using single CCII+ and 7-9 passive elements. Similarly, one and two current-conveyor-based filter structures providing notch/all-pass responses were reported in [28, 29]. Other universal structures with CCII+ and CCCII- using minimum passive components are in [30, 31]. Circuit in [30] is quite similar to the presented solution but it has different configuration of ports of used current conveyor. Some mentioned solutions [21–27] do not provide capability of tuning the natural frequency. Control of the natural frequency in recent papers is often not possible. If it is present, it is based on the external control of current input resistance (R_x) [33] that is achieved by control of the bias current (I_b) of proposed active element or by change of the value of passive element or elements simultaneously.

Multi-loop integrator structures allow (in specific cases) control of the stop-band attenuation in case of notch filter, for example, but circuit solution is quite complicated in comparison with our solution. Example of principle signal-flow graph (SFG) of common KHN state-variable realization is shown in Fig. 1. These types of solution (and also other derived canonical forms) are very popular [2, 20, 32, 34–38].

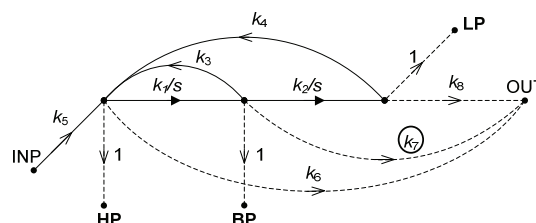


Fig. 1. An example of multi-loop commonly-used realization of universal biquad

Structure contains two loss-less integrators in two feedback loops. Structure is universal and therefore we can obtain all biquadratic filtering responses. All-pass and notch responses are available on node designed as OUT in Fig. 1. Adjusting of the band-stop attenuation is possible due to change of k_7 path transfer. Structure works as notch with adjustable stop-band transfer for $k_7 > 0$ and for $k_7 < 0$ it works as all-pass filter. Maximal attenuation in stop band of the notch filter is obtained for $k_7 = 0$. This path transfer represents middle coefficient of numerator of the biquadratic transfer function. However, this solution requires minimally three active elements to ensure mentioned adjustability. Of course, there main transfer functions like high-pass (HP), low-pass (LP), band-pass (BP) or also notch/band reject (BR) and all-pass (AP) are available. Tuning and quality factor Q adjusting is possible easily, but it requires additional active elements which complicates final circuit realization. Similar universal or multifunctional filter solutions can be found for example in [4, 6, 16–19, 32, 36].

Our novel solution is much simpler. It contains only one current conveyor (CC) and one voltage buffer (VB). Variable current gain of the current conveyor allows electronic change between BR and AP response. Although there are some disadvantages described in following text (i.e. only one passive element is grounded, unsuitable for Q changes) it is very interesting and simple solution with electronic control that can be useful in special cases. Simple notch filter which provides a possibility of electronic control of the stop-band attenuation can be important for exact suppression of some frequency components for example in radio-frequency devices (suppression of interferences, mirrored frequencies, etc.) in the base band or the inter-frequency band (IF). It is usually necessary to keep given frequency mask in these cases. Our solution has some drawbacks that are discussed in further text but some of them are compensated by the simplicity and also by some special features (attenuation control) which are not commonly included in reported approaches.

Notch filter based on controllable current conveyor and buffer

Fig. 2a shows principle of used active element CCII- (negative). This controllable element is called electronically controlled current conveyor of second generation (ECCII) in [5] or voltage and current gain controlled current conveyor of second generation VCG-CCII in [7]. In our case we suppose controllable current

transfer (B) of CCII via external control force (DC control voltage V_g , $B = f(V_g)$). Proposed notch filter (Fig. 2b) with electronically adjustable attenuation was designed by modification of the autonomous circuit structure with partial admittance network and two CCII- (similarly technique in [39]). There are two resistors and two capacitors, one of them is floating. Resistor-less variant is shown in Fig. 2c. R_z represents real part of internal CCII output impedance of unused output. VB is implemented by part of the CCII-. In this case, filter uses only internal R_x resistances ($R_1 = R_{x1}$ and $R_2 = R_{x2}$ in the following equations) of the current input of the CCII-. The transfer function, angular frequency, quality factor and sensitivities are expressed as:

$$K(s) = \frac{V_{OUT}}{V_{INP}} = \frac{s^2 + \frac{-R_2 C_1 B + R_2 C_2}{R_1 R_2 C_1 C_2} s + \frac{1}{R_1 R_2 C_1 C_2}}{s^2 + \frac{R_1 C_1 + R_2 C_2}{R_1 R_2 C_1 C_2} s + \frac{1}{R_1 R_2 C_1 C_2}}, \quad (1)$$

$$\omega_C = \sqrt{\frac{1}{R_1 R_2 C_1 C_2}}, \quad (2)$$

$$Q = \frac{R_1 R_2 C_1 C_2}{R_1 C_1 + R_2 C_2} \sqrt{\frac{1}{R_1 R_2 C_1 C_2}}, \quad (3)$$

$$S_{R_1}^{\omega_C} = S_{R_2}^{\omega_C} = S_{C_1}^{\omega_C} = S_{C_2}^{\omega_C} = -0.5, \quad (4)$$

$$S_B^{\omega_C} = 0, \quad (5)$$

$$S_{R_2}^Q = -S_{R_1}^Q = 0.5, \quad (6)$$

$$S_{C_1}^Q = -S_{C_2}^Q = 0.5 \left(\frac{R_2 C_2 - R_1 C_1}{R_2 C_2 + R_1 C_1} \right), \quad (7)$$

$$S_B^Q = 0, \quad (8)$$

where B represents current transfer of CC. The middle coefficient in the numerator in (1) contains controllable current transfer B which can be used for adjusting of the maximal attenuation of proposed notch filter. If the coefficient is equal to 0 we can obtain the utmost attenuation. It is fulfilled for $B = 1$ (when $R_2 C_1 = R_2 C_2$ is valid). The circuit works as adjustable notch filter if $B \leq 1$. If $B > 1$ filter works as all-pass filter or circuit with non-minimal argument (zeros are in right complex half plane).

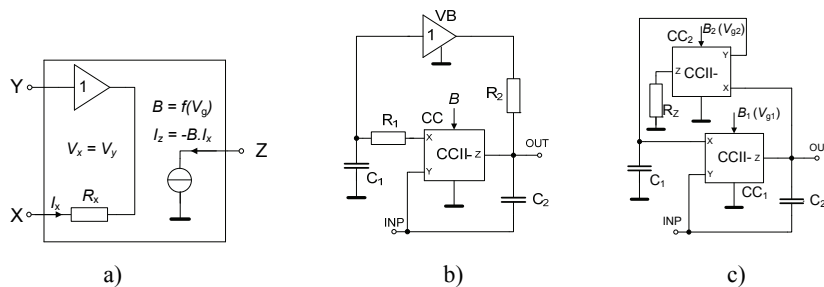


Fig. 2. Proposed solution of notch filter with electronically adjustable stop-band attenuation: a –the CCII- without fixed current transfer; b – notch filter employing negative CCII, voltage buffer and four passive elements; c – resistor-less variant of proposed filter

Design of the filter parameters and influences of real active blocks

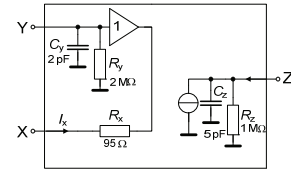
Passive elements of structure from Fig. 2b have been selected as $R_1 = R_2 = R = 100 \Omega + 95 \Omega$ (R_x), capacitors as $C_1 = C_2 = C = 470 \text{ pF}$. CCII- device known as current mode multiplier EL 2082 [40] was used for the verification purposes. Second CCII- is connected as voltage buffer (only Y a X ports) or it is possible to replace it by any voltage buffer. We can control current transfer of the CC via DC control voltage V_g between 0 - 2 where $B = f(V_g)$. $B_1 = 1$ was set by $V_g = 1 \text{ V}$. For higher values of V_g , dependence $B = f(V_g)$ is nonlinear [40]. Parameters $f_c = 1.737 \text{ MHz}$ and $Q = 0.5$ have been calculated from (2, 3).

Parasitic influences are caused by the real input and output properties (R_x , R_y , R_z , C_y , C_z) of used active elements (Fig. 3a). They were added to filtering structure as shown in Fig. 3b. The voltage buffer as a part of CC₂ (Y, X) was used. Real parameters have been taken into account and eq. (1) changed to following eqs. (9-15) where $R_1^* = R_1 + R_{x1}$, $R_2^* = R_2 + R_{x2}$, $C_1^* = C_1 + C_{y2}$,

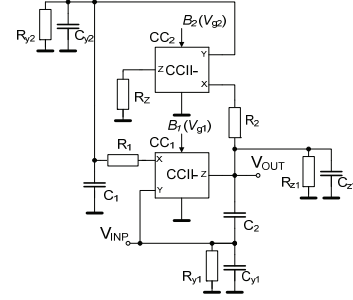
$B_1^* = \frac{B_1 \omega_T}{s + \omega_T}$. Transfer function and coefficients of

transfer function in eqs. (9-15) do not contain R_{y1} and C_{y1} , therefore they can be neglected. All equations contain frequency dependent current transfers B_1^* . Real R_y and R_z resistances of EL 2082 are quite high (hundreds of k Ω) [18] and therefore the influence on f_c and Q should be minimal. But results showed impact on max. achievable attenuation in the stop band. In ideal case it should be more than 60 dB, in real (and simulation) case less than 50 dB.

Capacitances C_y and C_z caused slight shift of characteristic frequency f_c .



a)



b)

Fig. 3. Non-ideal features: a – non-ideal model of CCII-; b – parasitic input and output properties of active elements are included

Characteristic frequency is about 50 kHz lower (1.687 MHz) than theoretically. It is also partly caused by inequality of $R_{x1} \neq R_{x2}$ (then $R_1 \neq R_2$). Manufacturing tolerance of R_x (EL 2082 [40]) is quite large (about $\pm 20 \%$). Real R_x value is about 95Ω and therefore cannot be omitted:

$$K^*(s) = \frac{a_2^* s^2 + a_1^* s + a_0^*}{b_2^* s^2 + b_1^* s + b_0^*}, \quad (9)$$

where

$$b_2^* = 1, \quad (10)$$

$$b_1^* = \frac{R_1^* C_1^* R_{y2} (R_2^* + R_{z1}) + R_2^* R_{z1} (R_{y2} C_{z1} + R_1^* C_2 + R_{y2} C_2 + R_1^* C_{z1})}{R_1^* R_2^* R_{y2} R_{z1} C_1^* (C_2 + C_{z1})}, \quad (11)$$

$$b_0^* = \frac{R_1^* R_2^* + R_1^* R_{z1} + R_2^* R_{y2} + R_{y2} R_{z1}}{R_1^* R_2^* R_{y2} R_{z1} C_1^* (C_2 + C_{z1})}, \quad (12)$$

$$a_2^* = \frac{C_2}{(C_2 + C_{z1})}, \quad (13)$$

$$a_1^* = \frac{(R_{y2} C_2 + R_1^* C_2 - R_{y2} B_1 C_1^*)}{R_1^* R_{y2} C_1^* (C_2 + C_{z1})}, \quad (14)$$

$$a_0^* = \frac{(R_{y2} - R_2^* B_1)}{R_1^* R_2^* R_{y2} C_1^* (C_2 + C_{z1})}. \quad (15)$$

Experimental results and discussion

Network analyzer Agilent E5071C, two negative CCII- EL 2082 [40] and common FET (BF 245A)

transistors (two and two parallel for lower resistance value) were used for the experimental and computer (simulation) verification. Adjustment of the characteristic frequency (f_c) is possible only by floating resistors R_1 and R_2 but if we

replace them by FET transistors, we can control the f_c by the DC voltage V_C , see Fig. 4a. Another approach (Fig. 4b) to f_c -control is to use modified CCII- element with the possibility of control of the current input resistance R_x by DC bias current I_b (similarly like in [5, 7-8, 10, 33], for instance), where $R_x = f(I_b)$. There is necessary to simultaneously change the R_1 and R_2 or $R_{x1}(I_{b1})$ and $R_{x2}(I_{b2})$ values. The results are summarized in Fig. 5. The simulation results were obtained in PSpice with professional macro-models. Notch filter from Fig. 2b was also measured. In Fig. 5a, comparison of ideal, simulated and measured magnitude responses is given, in Fig. 5b measured electronic adjusting of max. attenuation is shown, Fig. 5c shows dependence of the max. attenuation on the control voltage V_g . Finally, in Fig. 5d, example of adjusting the f_c is included. Measured phase response of the notch filter is depicted in Fig. 6. Greater difference between simulated and measured traces at minimal transfers (over -40 dB) in stop band (Fig. 5c) is caused by non-accurate relation between B and control voltage in the real scenario. It is given by one of used active element EL 2082 and it is significantly influenced by $R_x = 95 \Omega$ (CCII) causing $R_1 \neq R_2$. Theoretically, using of FET transistor as replacement of R_1 and R_2 for tuning purposes is very easy. In final application, we are limited by nonlinearities caused by them, because they increase total harmonic distortion of whole application. Described solution is suitable only for small signal levels. Second possible solution (Fig. 4b) based on extended CCII with R_x control is widely used in present literature [8, 10]. It is better than the first one in some applications, but these active elements [11] are not commonly available. However, for microelectronic experts there is no problem

to implement similar device directly on chip with adequate active element. When the control voltage exceeds $V_g = 1 \text{ V}$ ($B > 1$) zeros are shifting to the right complex half plane and filter produces all-pass response. Inequality $R_2 C_2 < R_2 C_1$ is valid for $B > 1$ and the middle numerator coefficient of (1) is then negative. Pure AP response is available for $B = 3$. Measured filter output response for $V_g = 2.65 \text{ V}$ is shown in Fig. 7. This feature of this filter realization with controllable current gain is very interesting and could be really useful in particular application.

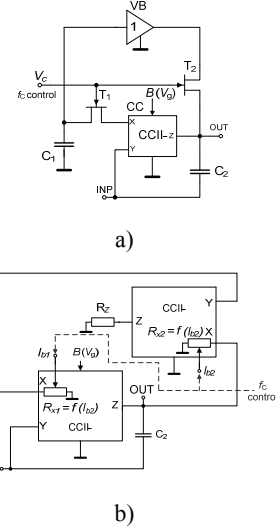


Fig. 4. Tunable variants of proposed notch filter: a - f_c tunable by two FET transistors; b - tunable by extended CCII with R_x control

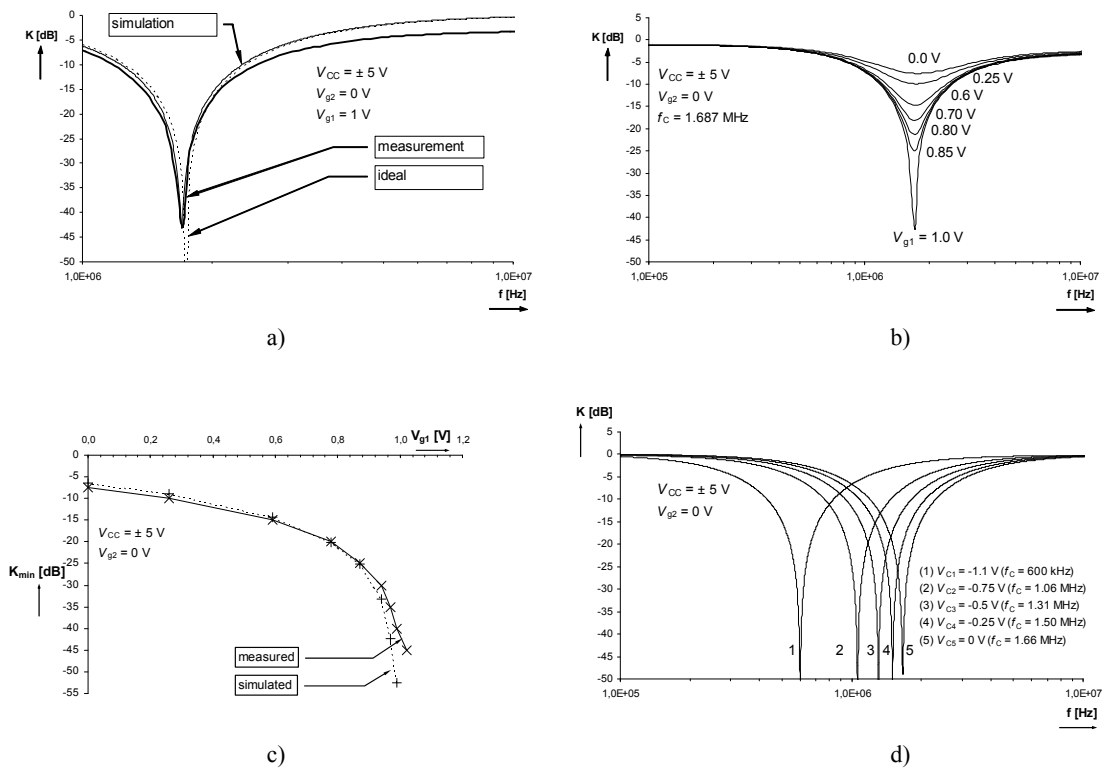


Fig. 5. Experimental and simulation results: a – detail of comparison of the simulated and measured magnitude response; b – measured adjusting of the max. attenuation; c – dependence of the max. attenuation on V_{g1} ; d – simulated tuning of f_c by FET transistors

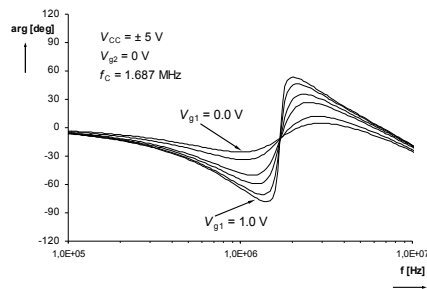


Fig. 6. Measured phase response of the notch filter

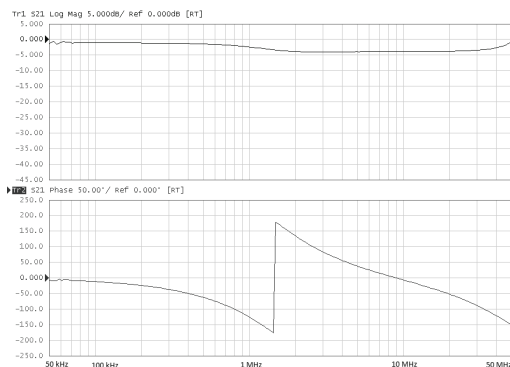


Fig. 7. Measured all-pass response ($V_g = 2.65$ V)

Conclusions

Novel structure of the notch/all-pass filter with electronically adjustable attenuation in the stop band based on two negative current conveyors or one negative conveyor and voltage buffer and minimum number of the passive elements has been proposed. Resistor-less variant is also possible but it depends a lot on accuracy and tolerances of internal current input resistances (R_x) of used active elements. The macromodel of EL 2082 was used in order to obtain simulation results and EL 2082 served as real device for measurement purposes. Measured attenuation varied from 7 to 45 dB without disturbance of the characteristic frequency or the quality factor. Of course, there are also some drawbacks. Change of the quality factor is not easy (maximal achievable value is 0.5), tuning and adjusting is possible only in limited range. However, main aim of this work is to show simple solution of notch filter with attenuation adjusting and electronic control of transfer function (from notch to AP). Presented solution could be useful in particular cases because of its simplicity. In recent literature there are many other filtering solutions which provide other transfer functions except notch response, but these usually multi-loop feedback conceptions are quite complicated (many active and passive elements) or electronic adjusting of attenuation is not easy. Presented conception is based only on adjustable conveyor and voltage buffer.

Acknowledgements

Research described in the paper was supported by the Czech Ministry of Education under research program MSM 0021630513 and by Czech Science Foundation projects under No. 102/08/H027 and No. 102/09/1681.

Research described in the paper is a part of the COST Action IC0803 RF/Microwave communication subsystems for emerging wireless technologies, financed by the Czech Ministry of Education by the grant no. OC09016. This research was financially supported by the project CZ.1.07/2.3.00/20.0007 WICOMT in frame of the operational program Education for competitiveness.

References

1. **Randall L.G., Sanchez-Sinencio E.** Active Filter Design Using Operational Transconductance Amplifiers: A Tutorial // IEEE Circuits and Devices Magazine, 1985. – Vol. 1. – P. 20–32.
2. **Keskin A. U., Bielek D., Hancioglu E., Biolkova V.** Current-mode KHN filter employing Current Differencing Transconductance Amplifiers // AEU – Int J of Electronics and Communications, 2006. – Vol. 60. – No. 6. – P. 443–446.
3. **Herencsar N., Vrba K., Koton J., Lattenberg I.** The conception of differential-input buffered and transconductance amplifier (DBTA) and its application // IEICE Electronics Express, 2009. – Vol. 6. – No. 6. – P. 329–334.
4. **Herencsar N., Koton J., Vrba K., Misurec J.** A novel Current-Mode SIMO Type Universal Filter Using CFTAs // Contemporary Engineering Sciences, 2009. – Vol. 2. – No. 2. – P. 59–66.
5. **Minaei S., Sayin O. K., Kuntman H.** A new CMOS electronically tunable current conveyor and its application to current-mode filters // IEEE Transaction on Circuits and Systems I – Regular papers, 2006. – Vol. 53. – No. 7. – P. 1448–1457.
6. **Koton J., Herencsar N., Cicekoglu O., Vrba K.** Current-mode KHN equivalent frequency filter using ECCIIs // Proceedings of the 33th International Conference on Telecommunications and Signal Processing (TSP 2010). – Baden, Austria, 2010. – P. 27–30.
7. **Marcellis A., Ferri G., Guerrini N. C., Scotti G., Stornelli V., Trifiletti A.** The VGC-CCII: a novel building block and its application to capacitance multiplication // Analog Integrated Circuits and Signal Processing, 2009. – Vol. 58. – No. 1. – P. 55–59.
8. **Tangsrirat W.** Current-tunable current-mode multifunctional filter based on dual-output current-controlled conveyors // AEU – International Journal of Electronics and Communications, 2007. – Vol. 61. – No. 8. – P. 528–533.
9. **Bielek D., Siripruchyanun M., Jaikla W.** CCII and OTA based Current-mode Universal Biquadratic Filter // The sixth PSU Engineering Conference, 2008. – P. 238–241.
10. **Siripruchyanun M., Chanapromma C., Silapan P., Jaikla W.** BiCMOS Current-Controlled Current Feedback Amplifier (CC-CFA) and Its Applications // WSEAS Trans on Electronics, 2008. – Vol. 5. – No. 6. – P. 203–219.
11. **Bielek D., Senani R., Biolkova V., Kolka Z.** Active elements for analog signal processing: Classification, Review, and New Proposals // Radioengineering, 2008. – Vol. 17. – No. 4. – P. 15–32.
12. **Abuelmaatti M., Bentrchia A.** A New Mixed-Mode OTA-C Filter/Oscillator Circuit // Journal of Active and Passive Electronic Devices, 2008, Vol. 3. – P. 211–221.
13. **Hong J. W., Lin S., Yang C.** Sinusoidal Oscillators Using Current Conveyors and Grounded Capacitors // Journal of Active and Passive Electronic Devices, 2007. – Vol. 2. – P. 127–136.

14. **Senani R., Sharma R. K.** Explicit-current-output sinusoidal oscillators employing only a single current-feedback op-amp // *IEICE Electronics Express*, 2004. – Vol. 2. – No. 1. – P. 14–18.
15. **Lahiri A.** New current-mode quadrature oscillators using CDTA // *IEICE Electronics Express*, 2009. – Vol. 6. – No. 3. – P. 135–140.
16. **Abuelmaatti M. T., Bentrchia A.** A novel mixed-mode OTA-C universal filter // *International Journal of Electronics*, 2005. – Vol. 92. – No. 7. – P. 375–383.
17. **Bhaskar D. R., Singh A. K., Sharma R. K., Senani R.** New OTA-C universal current-mode/trans-admittance biquad // *IEICE Electronics Express*, 2005. – Vol. 2. – No. 1. – P. 8–13.
18. **Chen H., Shen S., Wang J.** Electronically tunable versatile voltage-mode universal filter // *AEU – Int Journal of Electronics and Communications*, 2008. – Vol. 62. – No. 4. – P. 316–319.
19. **Wang C., Zhou L., Li T.** A new OTA-C current-mode biquad filter with single input and multiple outputs // *AEU – International Journal of Electronics and Communications*, 2008. – Vol. 62. – No. 3. – P. 232–234.
20. **Biolek D., Biolkova V., Kolka Z.** Universal Current-Mode OTA-C KHN Biquad // *International Journal of Electronics, Circuits and Systems*, 2007. – Vol. 1. – No. 4. – P. 214–217.
21. **Chang, C. M.** Current mode allpass/notch and bandpass filter using single CCII // *Electronics Letters*, 1991. – Vol. 27. – No. 20. – P. 1812–1813.
22. **Liu S., Kuo J., Tsay J.** New CCII- based current-mode biquadratic filters // *International Journal of Electronics*, 1992. – Vol. 72. – No. 2. – P. 243–252.
23. **Chen H. P.** Single CCII- based voltage-mode universal filter // *Analog Integrated Circuits Signal Processing*, 2010. – Vol. 62. – No. 2. – P. 259–262.
24. **Sharma S., Rajput S. S., Pal K., Mangotra L. K., Jamuar S. S.** Low-voltage CCII based all-pass/ notch filter // *Indian Journal of Pure and Applied Physics*, 2006. – Vol. 44. – No. 11. – P. 871–874.
25. **Kumar M., Sristava M. C., Kumar U.** Tunable Multifunctional Filter Using Current Conveyor // *International Journal of Computer Science and Information Security*, 2010. – Vol. 8. – No. 1. – P. 95–98.
26. **Liu S., Lee L.** Voltage-mode universal filters using two current conveyors // *International Journal of Electronics*, 1997. – Vol. 82. – No. 2. – P. 145–149.
27. **Kumar P., Pal K.** Variable Q all-pass, notch and band-pass filters using single CCII // *Frequenz*, 2005. – Vol. 59. – No. 9–10. – P. 235–239.
28. **Soliman A. M.** New all-pass and notch filters using current conveyors // *Frequenz*, 1999. – Vol. 53. – No. 3–4. – P. 84–86.
29. **Higashimura M., Fukui Y.** Realization of all-pass and notch filters using a single current conveyor // *International Journal of Electronics*, 1988. – Vol. 65. – No. 4. – P. 823–828.
30. **Minaei S., Yuce E., Cicekoglu O.** Electronically tunable multi-input single-output voltage-mode filter // *Proceedings of the 2005 European Conference on Circuit Theory and Design*, 2005. – Vol. 3. – P. III/401–III/404.
31. **Pandey N., Paul S. K., Jain S. B.** Voltage Mode Universal Filter using two Plus Type CCII // *Int. J. of Active and Passive Electronic Devices*, 2008. – Vol. 3. – No. 2. – P. 165–173.
32. **Biolek D., Biolková V., Kolka Z.** Universal Current-Mode Gm-C Biquad // *In Proceedings of the 18th International Conference Radioelektronika'2008*, 2008. – P. 137–139.
33. **Fabre A., Saaid O., Wiest F., Boucheron C.** High frequency applications based on a new current controlled conveyor // *IEEE Trans. on CAS-I*, 1996. – Vol. 43. – No. 2. – P. 82–91.
34. **Jerabek J., Vrba K.** SIMO type low-input and high-output impedance current-mode universal filter employing three universal current conveyors // *International Journal of Electronics and Communications (AEU)*, 2010. – Vol. 64. – No. 6. – P. 588–593.
35. **Sotner R., Petrzela J., Slezak J.** Current-Controlled Current-Mode Universal Biquad Employing Multi-Output Transconductors // *Radioengineering*, 2009. – Vol. 18. – No. 3. – P. 285–294.
36. **Herencsar N., Koton J., Vrba K.** Realization of current-mode KHN-equivalent biquad using current follower transconductance amplifiers (CFTAs) // *IEICE Trans. Fundamentals*, 2010. – Vol. E93-A. – No. 10. – P. 1816–1819.
37. **Sotner R., Jerabek J., Dostal T., Vrba K.** Multifunctional adjustable CM biquads based on distributed feedback VM prototype with OTA-s // *International Journal of Electronics*, 2010. – Vol. 97, No. 7. – P. 797–809.
38. **Sotner R., Slezak J., Dostal T., Petrzela J.** Universal tunable current-mode biquad employing distributed feedback structure with MO-CCII // *Journal of Electrical Engineering*, 2010. – Vol. 61. – No. 1. – P. 52–56.
39. **Koton J., Vrba, K.** New Multifunctional Frequency Filter Working in Current-mode // in *IFIP International Federation for Information Processing, Personal Wireless Communications*, eds. Simak, B., Bestak, R., Kozowska, E., (Boston: Springer), 2007. – Vol. 245. – P. 569–577.
40. **Intersil (Elantec). EL 2082CN** Current-Mode Multiplier. – 1996. – 16 p. Online: <http://www.intersil.com>

Received 2010 09 04

R. Sotner, J. Jerabek, B. Sevcik, T. Dostal, K. Vrba. Novel Solution of Notch/All-pass Filter with Special Electronic Adjusting of Attenuation in the Stop Band // *Electronics and Electrical Engineering*. – Kaunas: Technologija, 2011. – No. 7(113). – P. 37–42.

The notch/all-pass filter with two electronically adjustable three-port current conveyors of the second generation (CCII) or one conveyor and one voltage buffer employing only four passive elements is presented in this paper. Used active elements allow the control of current transfer via DC control voltage. Therefore an adjusting of the attenuation in the stop band of the notch filter is possible. The transfer function and major parasitic influences of real active parts are discussed. The verification includes PSpice simulation with professional macromodels and measurement with available current conveyors in frequency domain. III. 7, bibl. 40 (in English; abstracts in English and Lithuanian).

R. Sotner, J. Jerabek, B. Sevcik, T. Dostal, K. Vrba. Užtvarinio filtro slopinimo užtvarinėje juostoje specialaus elektroninio valdymo tyrimas // *Elektronika ir elektrotechnika*. – Kaunas: Technologija, 2011. – Nr. 7(113). – P. 37–42.

Analizuojami užtvariniai elektroniniu būdu valdomi filtrai. Naudojant aktyviuosius elementus galima valdyti srovės perdavimą. Užtvariniame filtre slopinimą galima valdyti užtvarinėje juostoje. Analizuojama perdavimo funkcija ir aktyviųjų elementų parazitiniai ryšiai. Atliktas modeliavimas naudojantis programų paketu „PSpice“. II. 7, bibl. 40 (anglų kalba; santraukos anglų ir lietuvių k.).

[30] SOTNER, R., JERABEK, J., PETRZELA, J., VRBA, K., DOSTAL, T. Design of Fully Adjustable Solution of Band-Reject/All-Pass Filter Transfer Function Using Signal Flow Graph Approach. In *Proceedings of the 24th International Conference Radioelektronika 2014*, Bratislava (Slovakia), 2014. p. 67-70. ISBN: 978-1-4799-3715-8.

Design of Fully Adjustable Solution of Band-Reject/All-Pass Filter Transfer Function Using Signal Flow Graph Approach

R. Sotner, J. Jerabek, J. Petrzela, K. Vrba

Faculty of Electrical Engineering and Communication
Brno University of Technology
Brno, Czech Republic
sotner@feec.vutbr.cz

T. Dostal

Dept. of Electrical Engineering and Computer Science
College of Polytechnics Jihlava
Jihlava, Czech Republic
tomas.dostal@vspj.cz

Abstract—The main aim of this paper is to show logical method how to obtain fully electronically adjustable active filter with electronic control of type of the transfer function without any change of topology and change of input excitation or reconnection of output. It is important for on-chip applications especially. Results of synthesis are demonstrated on biquadratic filter (band-reject and all-pass response) structure and two equivalent solutions are introduced and discussed. Achievable features are confirmed by PSpice simulations.

Keywords—All-pass; band-reject; current conveyor; electronic control; transconductor; signal flow graph

I. INTRODUCTION

Active filters and their transfer functions, namely low-pass (LP), band-pass (BP), high-pass (HP), and mainly band reject (BR) and all-pass (AP) transfers are important topic in analog signal processing. Realization of transfers as AP and BR simultaneously requires sophisticated approach and circuits are not so simple in many cases. Some filtering structures (so-called multifunctional or universal) allow to achieve some or even all transfer functions simultaneously. The first approach, that allows this possibility, was provided as non-electronically tunable solution with operational amplifiers known as Kerwin-Huelsman-Newcomb type (KHN) [1]. Possibilities of electronic control in filtering circuits attain substantial attention for many years. The most often used active elements are transconductors (OTAs) [2], [3]. These elements bring some advantages of biquadratic filtering structures namely in electronically adjustable parameters (some or all) as: the characteristic cutoff or pole frequency (f_c), the quality factor (Q), the bandwidth of the BP response (BW) and the pass-band gain (K_0).

Almost all multifunctional filters are based on loop and multi-loop integrator structures [4]-[6]. The basic building (integrating or biquadratic) sections were formed with OTAs ([7]-[10] for example). Design and synthesis principles of more complicated multi-loop OTA-based structures (also higher orders) were introduced in [11], [12] for example. These principles are important because describe pure mathematical approach to the design of multi-loop filters. We used signal flow graphs (SFGs) [4], [5], [13], [14] in this contribution. The

idea of circuit principle is clear because SFG allows visualization of transfers in the multi-loop system. Symbolical transfer functions obtained by more designer-friendly SFG approach correspond to mathematical approaches [11], [12] and both methods can offer the same resulting circuit.

Works [4]-[12] show that sufficient number of active elements allows availability of various transfer functions (also asymmetrical BPs) [5], [11], [12] and many possibilities of control of parameters (f_c , Q , K_0). However, increased number (several-times higher compared to [1], [7]-[8] in some cases) of active elements is the main drawback [15]. Some of discussed realizations are electronically controllable. In fact, in multifunctional filters two conceptions are possible: the first has only single input and offers more (in many cases at least three - HP, BP, LP) output responses (transfer characteristics) and the second has more inputs and only one output. However, none of proposed approaches was modified to provide control of the transfer by only electronic way.

We can recapitulate all typical features of standard multifunctional filtering circuits: transfer functions are available separately in one structure but at least interconnection (change of input or output or both) or even change of structure is necessary for switching the transfer function. A fully adjustable BR and AP filter is subject of our discussion. In comparison to standard approaches, our solution does not require any physical changes of inputs or outputs. But there only electronic control of parameters allows a change of the transfer function and also ensures other adjustable properties (f_c , Q , etc.). Method of "contact-less change" of the transfer type can be very useful in modern variable on-chip CMOS applications because no additional easy modification of filtering systems inside chip is available without expensive technological intervention (laser trimming, probe bonding) from manufacturer. Very simple solution of the filter, where electronic change of the transfer type between AP and BR was allowed, was discussed in [16]. However, the solution in [16] has some drawbacks namely only frequency f_c is tunable and achievable quality factor is very low. It is given by the simplicity and different design approach. Despite of larger complexity, the BR/AP filter studied in this contribution removes many drawbacks of the simple solution given in [16].

Research described in the paper was supported by Czech Science Foundation project under No. 14-24186P and by grant No. FEKT-S-14-2281 and project Electronic-biomedical co-operation ELBIC M00176. The support of the project CZ.1.07/2.3.00/20.0007 WICOMT, financed from the operational program Education for competitiveness, is gratefully acknowledged. The described research was performed in laboratories supported by the SIX project; the registration number CZ.1.05/2.1.00/03.0072, the operational program Research and Development for Innovation.

Our synthesis and filter solution derived from SFG representation uses modification of the most known active three-port (voltage input Y, current input X, current output Z), so-called current conveyor of second generation (CCII) [17], where adjusting of current gain between Y and Z terminal is possible. Adjustable modification is called electronically controllable CCII (ECCII) [18]-[21]. There are transfers between terminals are: $V_X = V_Y$, $I_Y = 0$, $I_Z = -BI_X$, where parameter B represents electronically adjustable current gain. Other blocks used in discussed structures are simple current followers and inverters and voltage buffers.

II. BAND-REJECT AND ALL-PASS STRUCTURE WITH ADJUSTABLE PROPERTIES

Specific solution of the filter structure discussed in [22] derived from [9] that has multifunctional features and follows fundamentals of synthesis studied in [4]-[6], [11], [12] is the core of presented solution, where only electronic control of specific parameter changes transfer type between AP and BR response and other parameters control filter features (Q , f_c , etc.). Interesting equivalent of KHN filter using ECCIIs was already introduced in [23]. However, structure was not exactly the same and discussion of only electronic control of change of the transfer function was not provided. We have used specific drawing of SFG, based on mutual conversion of voltage to current respectively [24], due to simplifying graph and better explaining principles in our two-loop structure. Note that a conversion between node variables (V and I) is marked by open and closed arrows. SFG and circuit representation of the proposed solution is shown in Fig. 1. The filter has also outputs of BP and LP responses but they are not subject of interest in our discussion.

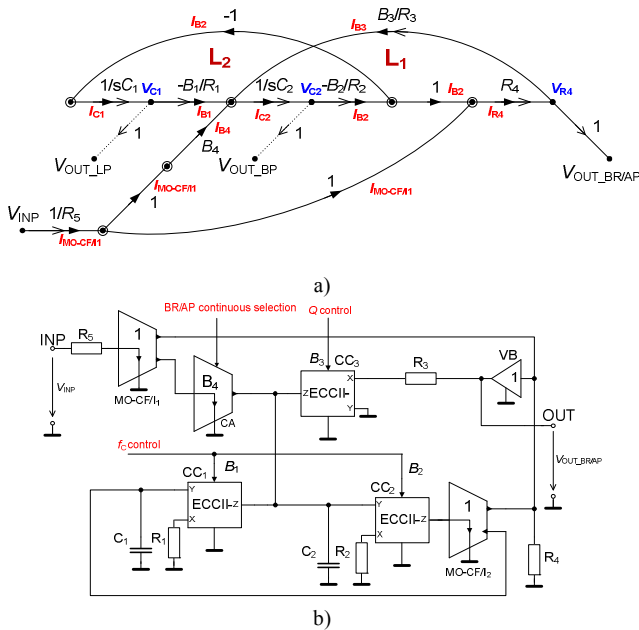


Fig. 1. Fully adjustable BR/AP filter: a) SFG representation, b) complete circuit.

Solution uses two loss-less integrators with CC_1 , CC_2 and R_1 , R_2 , C_1 , C_2 . Feedback loops are created by voltage to current conversion realized by voltage buffer (VB), R_3 and CC_3 (this loop-gain allows control of Q) and multi-output current follower/inverter (MO-CF/ I_2). Feed-forward loops are formed by MO-CF/ I_1 which is directly connected to node of resistor R_4 and by current-amplifier (can be realized also by ECCII element - Y terminal is grounded) connected to specific node between both integrators. Resistor R_5 serves as conversion of input voltage to current (mirrored and inverted by MO-CF/ I_1) and determines input impedance. The transfer function derived from SFG in Fig. 1a by Mason rule [13], [14] has form:

$$K_{BR/AP}(s) = \frac{R_4}{R_5} \left(\frac{s^2 - \frac{B_2 B_4}{R_2 C_2} s + \frac{B_1 B_2}{R_1 R_2 C_1 C_2}}{s^2 + \frac{R_4 B_2 B_3}{R_2 R_3 C_2} s + \frac{B_1 B_2}{R_1 R_2 C_1 C_2}} \right), \quad (1)$$

where angular pole frequency, quality factor and pass-band gain are:

$$\omega_c = \sqrt{\frac{B_1 B_2}{R_1 R_2 C_1 C_2}}, \quad Q = \frac{R_3}{R_4 B_3} \sqrt{\frac{B_1 R_2 C_2}{B_2 R_1 C_1}}, \quad (2), (3)$$

$$K_0 = \frac{R_4}{R_5}. \quad (4)$$

Possible equivalent circuit using single-input and single-output type of transconductors (OTA) is depicted in Fig. 2. This solution saves some additional and auxiliary blocks and elements (mainly resistors).

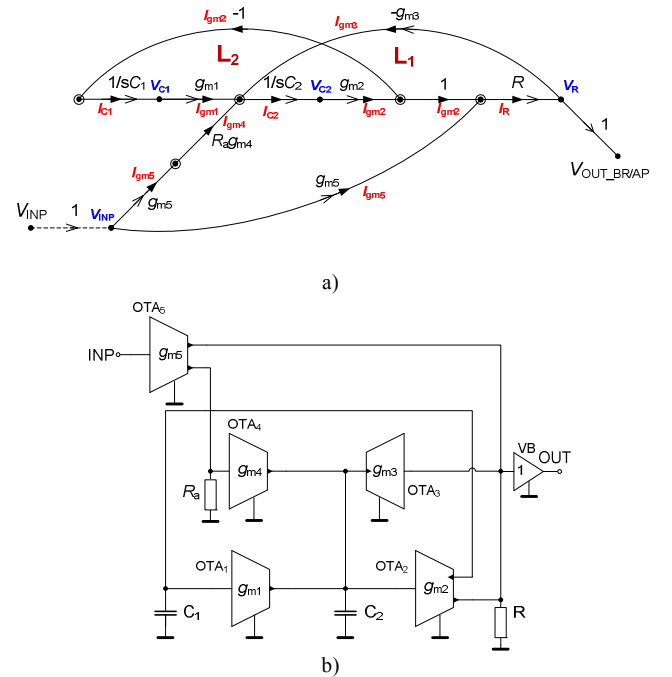


Fig. 2. Simplified representation of the structure with OTAs: a) SFG, b) circuit.

Resulting transfer function of the modification from Fig. 2 is:

$$K_{BR/AP}(s) = g_{m5}R \frac{\left(s^2 - \frac{g_{m2}g_{m4}R_a}{C_2} s + \frac{g_{m1}g_{m2}}{C_1C_2} \right)}{s^2 + R \frac{g_{m2}g_{m3}}{C_2} s + \frac{g_{m1}g_{m2}}{C_1C_2}}, \quad (5)$$

where parameters of the filter are as follows:

$$\omega_c = \sqrt{\frac{g_{m1}g_{m2}}{C_1C_2}}, \quad Q = \frac{1}{g_{m3}R} \sqrt{\frac{g_{m1}C_2}{g_{m2}C_1}}, \quad (6), (7)$$

$$K_0 = g_{m5}R. \quad (8)$$

This circuit is shown just for reference and will not be analyzed any further in this paper.

Coefficient of the linear member of the transfer function in numerator allows control by current gain B_4 (or transconductance g_{m4}) as it is clear from both SFGs and equations (1) and (5). This control realizes changes of the transfer type. All-pass filter response (Fig. 1) supposes $B_4 = 1$ and band-reject response requires $B_4 = 0$, similarly for g_{m4} from Fig. 2.

III. SIMULATION RESULTS

In order to obtain realistic results, we performed simulations with PSpice models of commercially available devices (that are very suitable for presented behavioral modeling) to verify features of proposed solution from Fig. 1. Current-mode multiplier EL2082 [25] was used at the place of ECCII elements (CC_1 - CC_3) and both MO-CF/I-s were modeled by current-mode multiplier EL4083 [26] with fixed unity gain and CA was modeled also by EL4083 where gain (in our case B_4) was adjustable by DC control voltage from 0 to +1. BUF634 [27] was used as voltage buffer. Parameters of the design are following: $f_c = 370$ kHz, $Q = 1$, $K_0 = 1$. Selected values of passive elements are: $R_4 = R_5 = 220 \Omega$, $R_1 = R_2 = R_3 = 195 \Omega$ (including 95Ω of intrinsic resistance of EL2082 [25]) and $C_1 = C_2 = 2.2$ nF. Initial controllable parameters had values: $B_1 = B_2 = B_3 = B_4 = B_5 = 1$.

Results of simulation are in Fig. 3. Real center frequency is $f_c = 360$ kHz and quality factor is $Q = 1.1$. Both transfer functions are shown in magnitude and phase responses. Values of adjustable parameters of the circuit are always noted in figures.

Change of stop-band transfer leads to change of the transfer type as we documented in Fig. 4, where step changes of B_4 are observed in magnitude and phase responses. Phase characteristics confirm behavior where BR response passes to the AP response (circuit with non-minimal argument). Conjugate zeros of the transfer function migrate from location on imaginary axis (or close neighborhood of imaginary axis) to LHP of complex space.

Proposed filter offers some benefits that are not available in solution discussed in [16]. Following examples prove these possibilities. Tuning of the pole frequency of BR response by change of $B_1 = B_2$ from 0.1 to 1.5 is demonstrated in Fig. 5. Pole frequency was adjusted from 38 kHz to 529 kHz. Electronic adjusting of the quality factor allows bandwidth

(BW) control of the BR response between 31 kHz ($Q = 12$, $B_3 = 0.1$) and 651 kHz ($Q = 0.7$, $B_3 = 2$), see Fig. 6.

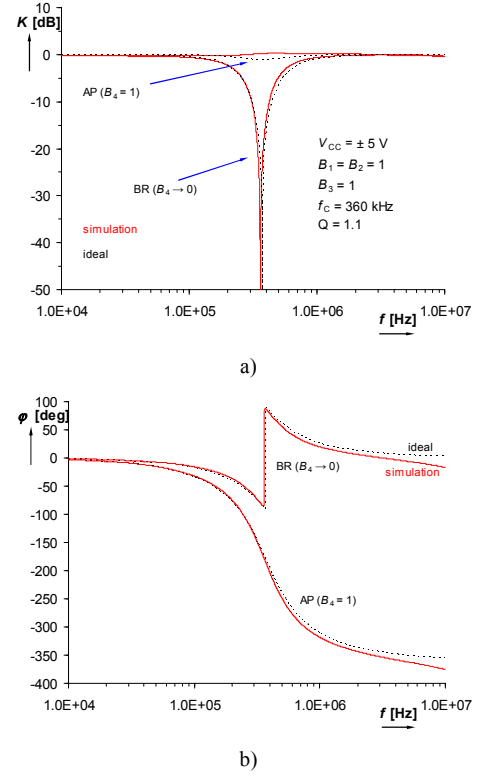


Fig. 3. Electronically adjustable transfer function between BR and AP response : a) magnitudes, b) phases.

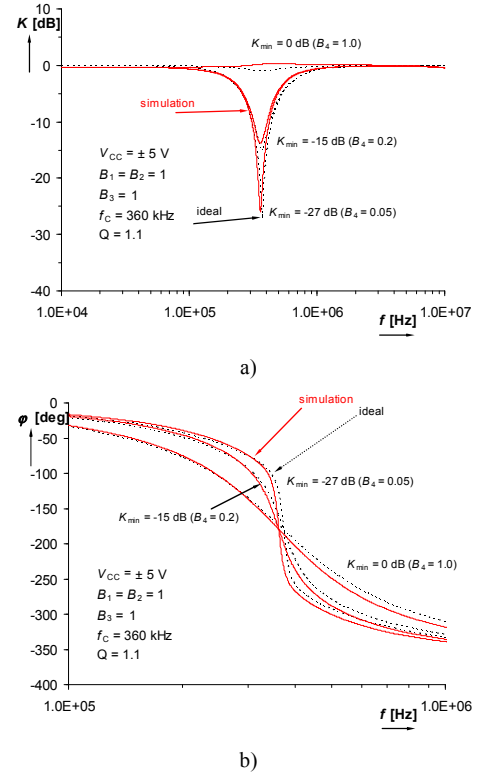


Fig. 4. Observation of stepwise adjusting of B_4 : a) magnitude responses, b) phase responses.

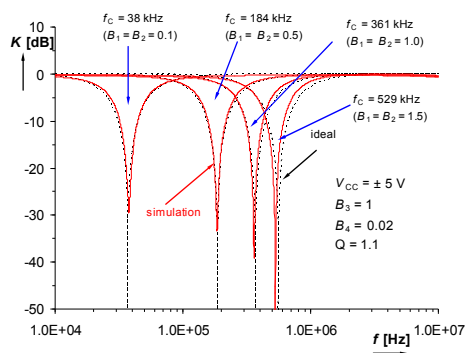


Fig. 5. Tuning of the pole frequency at BR response.

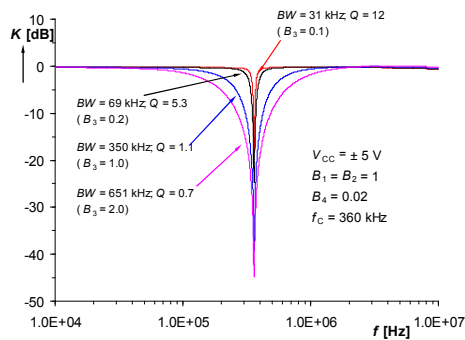


Fig. 6. Adjusting of Q and BW of the BR response.

IV. CONCLUSION

Electronic configurability is very important for on-chip applications. Main intention of this contribution is idea leading to simple synthesis of fully adjustable solution with possibilities of electronic change of transfer function and also all advantages of electronic control of filter parameters. Workability was confirmed by simulations. Despite of fact of complexity of this circuit, simpler realization presented in [16] does not provide benefits of very simple BW , Q and f_c control.

REFERENCES

- [1] J. W. Kerwin, L. P. Hulesman, W. R. Newcomb, "State variable synthesis for insensitive integrated circuit transfer functions," *IEEE Journal of Solid State Circuits*, vol. 2, no. 3, pp. 87-92, 1967.
- [2] R. L. Geiger, E. Sánchez-Sinencio, "Active filter design using operational transconductance amplifiers: a tutorial," *IEEE Circ. and Devices Magazine*, vol. 1, pp. 20-32, 1985.
- [3] D. Bielek, R. Senani, V. Biolkova, Z. Kolka, "Active elements for analog signal processing: Classification, Review and New Proposals," *Radioengineering*, vol. 17, no. 4, pp. 15-32, 2008.
- [4] Y. Sun, J. K. Fidler, "Some design methods of OTA-C and CCII-RC filters," in *proc. of IEE Colloquium on Digital and Analogue Filters and Filtering*, London, 1993, pp. 7/1-7/8.
- [5] T. Dostal, "Filters with Multi-Loop Feedback Structure in Current Mode," *Radioengineering*, vol. 12, no. 3, pp. 6-11, 2003.
- [6] R. Raut, M. N. S. Swamy, *Modern Analog Filter Analysis and Design: A practical approach*. Germany, Weinheim: Wiley-VCH Verlag GmbH and Co. KGaA, 2010, 355 p.
- [7] R. Nawrocky, U. Klein, "New OTA-capacitor realisation of a universal biquad," *Electronics Letters*, vol. 22, no. 15, pp. 50-51, 1986.

- [8] Y. Sun, "Second-order OTA-C filters derived from Nawrocky-Klein biquad," *Electronics Letters*, vol. 34, no. 15, pp. 1449-1450, 1998.
- [9] S. E. Sanchez, R. L. Geiger, L. H. Nevarez, "Generation of continuous-time two integrator loop OTA filter structures," *IEEE Transactions on Circuits and Systems*, vol. 35, no. 8, pp. 936-946, 1988.
- [10] Y. Sun, J. K. Fidler, "Structure Generation of Current-Mode Two Integrator Dual output-OTA Grounded Capacitor Filters," *IEEE Transaction on Circuits and Systems II: Analog and Digital Signal Processing*, vol. 43, no. 9, pp. 659-663, 1996.
- [11] Y. Sun, J. K. Fidler, "Current-mode OTA-C realization of arbitrary filter characteristics," *Electronics Letters*, vol. 32, no. 13, pp. 1181-1182, 1996.
- [12] Y. Sun, J. K. Fidler, "Current-mode multiple-loop feedback filters using dual output OTAs and grounded capacitors," *International Journal of Circuit Theory and Applications*, vol. 25, no. 2, pp. 69-80, 1997.
- [13] S. J. Mason, "Feedback Theory: Further properties of Signal Flow Graphs," *Proceedings of IRE*, vol. 44, no. 7, pp. 920-926, 1956.
- [14] C. L. Coates, "Flow-graph Solution of Linear Algebraic Equations," *IRE Transactions on Circuit Theory*, vol. 6, no. 2, pp. 170-187, 1959.
- [15] M. T. Abuelmaatti, A. Bentrchia, "A novel mixed-mode OTA-C universal filter," *International Journal of Electronics*, vol. 92, no. 7, pp. 375-383, 2005.
- [16] R. Sotner, J. Jerabek, B. Sevcik, T. Dostal, K. Vrba, "Novel Solution of Notch/All-pass Filter with Special Electronic Adjusting of Attenuation in the Stop Band," *Elektronika Ir Elektrotehnika*, vol. 16, no. 7, pp. 37-42, 2011.
- [17] A. Sedra, K. C. Smith, "A second generation current conveyor and its applications," *IEEE Transaction on Circuit Theory*, vol. CT-17, no. 2, pp. 132-134, 1970.
- [18] W. Surakampontrorn, W. Thitimajshima, "Integrable electronically tunable current conveyors," *IEE Proceedings-G*, vol. 135, no. 2, pp. 71-77, 1988.
- [19] A. Fabre, N. Mimeche, "Class A/AB Second-generation Current Conveyor with Controlled Current Gain," *Electronics Letters*, vol. 30, no. 16, pp. 1267-1268, 1994.
- [20] S. Minaei, O. K. Sayin, H. Kuntman, "A new CMOS electronically tunable current conveyor and its application to current-mode filters," *IEEE Trans. on Circuits and Systems - I*, vol. 53, no. 7, pp. 1448-1457, 2006.
- [21] A. Marcellis, G. Ferri, N. C. Guerrini, G. Scotti, V. Stornelli, A. Trifiletti, "The VGC-CCII: a novel building block and its application to capacitance multiplication," *Analog Integrated Circuits and Signal Processing*, vol. 58, no. 1, pp. 55-59, 2009.
- [22] R. Sotner, J. Jerabek, T. Dostal, K. Vrba, "Multifunctional adjustable CM biquads based on distributed feedback VM prototype with OTA-s," *International Journal of Electronics*, vol. 97, no. 7, pp. 797-809, 2010.
- [23] J. Koton, N. Herencsar, O. Cicekoglu, K. Vrba, "Current-mode KHN equivalent frequency filter using ECCIIs," in *Proc. of the 33th Int. Conf. on Telecommunications and Signal Processing (TSP 2010)*, Baden, 2010, pp. 27-30.
- [24] R. Sotner, B. Sevcik, L. Brancik, T. Dostal, "Multifunctional Adjustable Biquadratic Active RC Filters: Design Approach by Modification of Corresponding Signal Flow Graphs," *Przegląd Elektrotechniczny*, vol. 87, no. 2, pp. 225-229, 2011.
- [25] Intersil (Elantec). EL2082 CN Current-mode Multiplier (datasheet), 1995, 14 p., accessible on [www: http://www.intersil.com/data/fn/fn7152.pdf](http://www.intersil.com/data/fn/fn7152.pdf)
- [26] Intersil (Elantec). EL4083 CN Current-mode Four Quadrant multiplier (datasheet), 1996, 14 p., accessible on [www: http://www.intersil.com/content/dam/Intersil/documents/fn71/fn7157.pdf](http://www.intersil.com/content/dam/Intersil/documents/fn71/fn7157.pdf)
- [27] Texas Instruments. BUF 634 250 mA High-speed buffer (datasheet), 1996, 20 p., accessible on [www: http://focus.ti.com/lit/ds/symlink/buf634.pdf](http://focus.ti.com/lit/ds/symlink/buf634.pdf)

[31] SOTNER, R., PETRZELA, J., JERABEK, J., VRBA, K., DOSTAL, T. Solutions of Reconnection-less OTA- based Biquads with Electronical Transfer Response Reconfiguration. In *Proceedings of 25th International Conference Radioelektronika 2015*, Pardubice (Czech Republic), 2015. p. 40-45. ISBN: 978-1-4799-8117-5.

Solutions of Reconnection-less OTA-based Biquads with Electronical Transfer Response Reconfiguration

R. Sotner, J. Petrzela, J. Jerabek, K. Vrba

Faculty of Electrical Engineering and Communication
Brno University of Technology
Brno, Czech Republic
sotner@feec.vutbr.cz

T. Dostal

Dept. of Electrical Engineering and Computer Science
College of Polytechnics Jihlava
Jihlava, Czech Republic
tomas.dostal@vspj.cz

Abstract—This contribution deals with special second-order (biquadratic) single-input and single-output filtering structures employing operational transconductance amplifiers (OTAs) for various electronic variation of parameters that leads to reconnection-less transfer response and is tunable. Structures allows change of transfer type between several types of responses (all or some of them) particularly high-pass, all-pass, band-reject, band-pass and low-pass and high-pass response with intended zero in transfer function. PSpice simulations with models of commercially available real devices support theoretical presumptions.

Keywords—Adjustable filters; biquads; electronic control; method of unknown nodal voltages; multifunctionality; reconfigurability; second-order filter; transconductor

I. INTRODUCTION

Modification of signal features is always very important requirement in signal processing. Filtering of the signal belongs to basic operation where we intend to remove, suppress or amplify some spectral components or part of bandwidth. Classical electronically controllable multifunctional filters [1], [2] can be utilized beneficially in discrete form of realization. In most cases, filter has one input and several outputs where different transfer responses are available. Inverse case is also possible (several inputs and one output). Examples of both types can be found in [3]-[6], for example. However, manual galvanic reconnection is always necessary to change type of the transfer response. Unfortunately, manual reconnection is usually not possible or suitable in some cases (on-chip implementation of the system for example). We can implement controllable switches to the system, etc. Unfortunately, some undesired products of switching (overshoots, interferences of clock signal to analog way) may degrade correct operation of the overall system. In addition, if we require many changes in a little time, such behavior is really disturbing. A question is: Why we need reconfiguration (response or other parameters) of the filter? Self-adjusting system with reconnection-less reconfiguration can react on changes in useful signal immediately and continuously. It evolves idea of adaptive filtering that is

known from digital filters [7]. These specific changes in signal are temporarily appearing undesired spectral components, increased noise floor or distortion-interference level in useful bandwidth, etc. Several filtering systems with single input and single output, where reconfigurability was intentionally designed, were already introduced.

We start our explanation with first-order solutions in [8] where general view on two active elements based solutions with reconnection-less electronically controllable features and their systematic synthesis is described. Circuits presented in [8] offer high-pass (HP), low-pass (LP) and all-pass (AP) or bilinear filter responses. Electronically adjustable first order AP, LP, inverting direct transfer (iDT), adjustable zero and low-pass filter with zero (LPZ) filter is presented in [9] and offers high variability but requires three active elements. Interesting solution was presented in [10], where one single active device allows utilization of its three adjustable parameters for control of reconfigurability in order to obtain AP, LP, iDT and direct transfer (DT). Second order (biquadratic) solution of the reconfigurable filter was introduced in [11], where solution based on two active devices providing AP and band-reject (BR) response was introduced. Unfortunately, quality factor is very low and limited in control and other transfer functions are not available. Problems of low quality factor and other issues were solved in [12]. However, circuit is very complicated and provides only AP and BR response.

Design of single-input and single-output second-order filters with electronically reconfigurable features, allowing more types of transfer responses, is the main aim of this contribution.

II. SECOND-ORDER FILTERS BASED ON INTERCONNECTION OF FIRST-ORDER SECTIONS

Enquiring reader can raise a question if it is possible to get fully reconfigurable biquad by a suitable interconnection of bilinear filters [8]. For these filters a transfer function is much simpler, contains only three free parameters and final circuit realization will be simpler and coherent as well. To obtain a full control of the frequency responses of the first-order filter it is sufficient to adjust two parameters of bilinear filter,

Research described in this paper was financed by Czech Ministry of Education in frame of National Sustainability Program under grant LO1401. For research, infrastructure of the SIX Center was used. Research described in the paper was supported by Czech Science Foundation projects under No. 14-24186P. Grant No. FEKT-S-14-2281 also supported this research. The support of the project CZ.1.07/2.3.00/20.0007 WICOMT, financed from the operational program Education for competitiveness, is gratefully acknowledged.

namely a_0 and b_0 , as follows directly from:

$$K(s) = \frac{a_1s + a_0}{b_1s + b_0} = K_0 \frac{s + \omega_z}{s + \omega_p}, \quad \omega_z \in (-\omega_p, \infty), \quad (1)$$

where K_0 is a transfer constant of pass-band gain. Using a cascade synthesis [13] of these fundamental filters we can form band-pass filter, additional operation of summation at the output allows us to construct BR response as shown in Fig. 1. However the main drawback of this concept lies in the low quality factor since all poles are placed on the real negative axis of the complex plane leading to $Q_p \leq 0.5$.

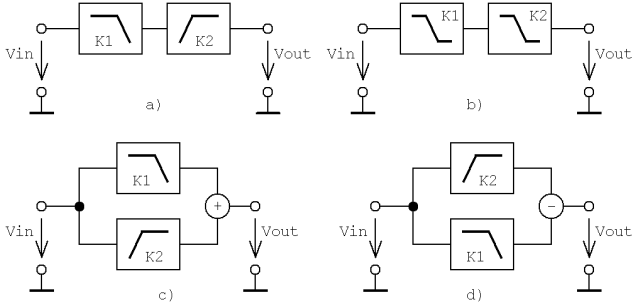


Fig. 1. The possibility to realize low quality factor reconfigurable biquads by a combination of first-order blocks: (a) cascade of LP and HP, (b) cascade of general bilinear filters, (c) summation of LP and HP, (d) subtraction of HP and LP.

Cascade connection of LP and HP filters with adjustable poles always results into BP where only bandwidth can be adjusted. When cascading two bilinear filters with electronically adjustable zero and pole we obtain a general second-order filter having transfer function:

$$K(s) = \frac{N(s)}{D(s)} = \frac{a_2s^2 + a_1s + a_0}{b_2s^2 + b_1s + b_0} = K_0 \frac{s^2 + \frac{\omega_z}{Q_z}s + \omega_z^2}{s^2 + \frac{\omega_p}{Q_p}s + \omega_p^2}, \quad (2)$$

with parameters [13]:

$$\omega_z = \sqrt{\omega_{z1}\omega_{z2}} \quad Q_z = \frac{\sqrt{\omega_{z1}\omega_{z2}}}{\omega_{z1} + \omega_{z2}}, \quad (3)$$

$$\omega_p = \sqrt{\omega_{p1}\omega_{p2}} \quad Q_p = \frac{\sqrt{\omega_{p1}\omega_{p2}}}{\omega_{p1} + \omega_{p2}}$$

where number in lower index corresponds to a position of the particular filter in a cascade. At this point it is evident that, with exception of HPZ and LPZ, any filter type can be obtained if both transfer zeroes are properly positioned. For example choice $-\omega_{z1} = \omega_{p1}$ together with $-\omega_{z2} = \omega_{p2}$ leads to AP filter, by setting $-\omega_{z1} = \omega_{z2}$ we obtain BP filter, equality $\omega_{z1}\omega_{z2} = \omega_{p1}\omega_{p2}$ simultaneously with $Q_z > Q_p$ results into BR filter, typical situation for LP is when the angular frequencies of zeroes are much bigger than poles. Finally configuration for HP filter is achieved if angular frequencies of both transfer zeroes tend to zero. In spite of this universality realization of two filters implies the necessity of two active elements.

Another possibility for reconfigurable biquad filter is to

employ a summation block as shown in Fig. 1c and it seems as a promising idea. Assume a standard transfer function for LP and HP first-order filter, i.e.:

$$K_{LP}(s) = K_1 \frac{\omega_1}{s + \omega_1} \quad K_{HP}(s) = K_2 \frac{s}{s + \omega_2}. \quad (4)$$

Manual analysis gives an improper form of the polynomial $N(s)$ exploitable from the viewpoint of full reconfigurability:

$$N(s) = s^2 + \left(\frac{K_1}{K_2} + 1 \right) \omega_1 s + \frac{K_1}{K_2} \omega_1 \omega_2. \quad (5)$$

If we design LP and HP filter, electronically change gain factor can automatically sweep between particular types of filters (beside cutoff frequencies). Of course this does not aid to improve poor quality factor performance. Almost exactly the same situation arises if we replace summation operation with subtraction block. There is only a slight change in polynomial $N(s)$, in detail:

$$N(s) = s^2 + \left(1 - \frac{K_1}{K_2} \right) \omega_1 s + \frac{K_1}{K_2} \omega_1 \omega_2, \quad (6)$$

while denominator remains unchanged

$$D(s) = s^2 + (\omega_1 + \omega_2)s + \omega_1\omega_2. \quad (7)$$

According to (7) this biquadratic filter is always stable with overdamped impulse response. The polynomial (6) can be easily interpreted as follows. Choice of $K_1 = K_2$ leads to BR frequency response, by substituting $K_1 = 0$ into (6) we learn that first transfer zero at location ω_1 is compensated by first pole, second zero is at origin and second pole is at ω_2 and such configuration leads to HP filter. Setting $K_2 = 0$ causes similar situation except zero at origin and it results into LP. AP filter can be obtained only if $K_1/K_2 = -1$.

As a consequence of above discussion we need to build the biquadratic filtering section as the natural second-order non-autonomous deterministic dynamical system in order to design reconnection-less filter.

III. MATRIX METHOD OF UNKNOWN NODAL VOLTAGES FOR SPECIFIC DESIGN OF RECONFIGURABLE FILTERS

Matrix method of the unknown nodal voltages (MUNV) [13] is very useful approach suitable for symbolical analysis and also synthesis of linear circuits. Rules of this method directly follow from first Kirchhoff's laws [13]. MUNV is especially powerful in the case when networks contains only active elements having self-admittance matrix such as operational transconductance amplifier (OTA) with single, balanced or multiple outputs [14], [15]. In MUNV, we suppose well known relation:

$$\mathbf{Y} \cdot \mathbf{V} = \mathbf{I}, \quad (8)$$

where \mathbf{Y} is square admittance matrix, \mathbf{V} is column vector of unknown nodal voltages and \mathbf{I} is column vector of exciting current sources (only one in case of the filter with single input and single output as required). MUNV can be used for a task of naturally linear circuit synthesis like analog oscillators, filters, amplifiers or linear building blocks of the complex nonlinear systems. MUNV applied on the handmade process

of the reconfigurable biquadratic filter construction is more likely intuitive task than systematic procedure.

IV. RECONFIGURABLE BIQUADRATIC OTA-BASED FILTERS

In order to preserve four degrees of arbitrariness and to keep minimum number of active elements, each synthesized network must contain at least four OTA elements. We suppose existence of three independent nodes in the circuits. Then expected system of equation of MUNV has the following form:

$$\begin{pmatrix} Y_{11} & Y_{12} & Y_{13} \\ Y_{21} & Y_{22} & Y_{23} \\ Y_{31} & Y_{32} & Y_{33} \end{pmatrix} \begin{pmatrix} V_1 \\ V_2 \\ V_3 \end{pmatrix} = \begin{pmatrix} I_1 \\ 0 \\ 0 \end{pmatrix}. \quad (9)$$

We can expect transfer function (2) as division of two sub-determinants:

$$K(s) = \frac{V_{out}}{V_{in}} = \frac{V_3}{V_1} = \frac{\Delta_{1,3}}{\Delta_{1,1}}, \quad (10)$$

where $\Delta_{1,3}$ is sub-determinant of admittance matrix \mathbf{Y} after omitting 1st row and 3rd column and $\Delta_{1,1}$ is sub-determinant of admittance matrix \mathbf{Y} after omitting 1st row and 1st column (in system of three nodes).

A. The first type of reconfigurable filter solution

The first type of our particular transfer function for synthesis of related circuit has form:

$$K(s) = \frac{s^2 - \frac{g_{m3}}{C_1}s + \frac{g_{m1}g_{m4}}{C_1C_2}}{s^2 + \frac{g_{m1}}{C_1}s + \frac{g_{m1}g_{m2}}{C_1C_2}}, \quad (11)$$

where we can see, compared to general form (2), that parameter Q_p is adjusted by g_{m1} , ω_p is tuned by g_{m2} , subsequently numerator parameter Q_z and ω_z is changed by g_{m3} and g_{m4} respectively. Parameter configuration of $g_{m3} \rightarrow 0$, $g_{m2} = g_{m4}$ leads to BR filter, $g_{m3} = g_{m1}$ leads to AP filter, and $g_{m3} = g_{m4} \rightarrow 0$ configures HP filter. Special situations occurs for $g_{m3} \rightarrow 0$ and $g_{m2} < g_{m4}$ resulting in LPZ, $g_{m3} \rightarrow 0$ and $g_{m1} > g_{m4}$ resulting in HPZ. Unfortunately, inverting band-pass response (note that it is not pure BP) has asymmetrical low- and high-frequency behavior. Finite attenuation in the high frequency stop band occurs.

Supposing one floating capacitor C_1 between nodes 1 and 3, one grounded capacitor C_2 in node 2 we can obtain result in:

$$\begin{pmatrix} sC_1 & 0 & -sC_1 \\ 0 & sC_2 & 0 \\ -sC_1 & 0 & sC_1 \end{pmatrix} \cdot \begin{pmatrix} V_1 \\ V_2 \\ V_3 \end{pmatrix} = \begin{pmatrix} I_1 \\ 0 \\ 0 \end{pmatrix}. \quad (12)$$

To obtain (11), $\Delta_{1,1}$ and $\Delta_{1,3}$ should be in forms:

$$\begin{aligned} \Delta_{1,1} &= Y_{22}Y_{33} - Y_{32}Y_{23} = b_2s^2 + b_1s + b_0 = \\ &= s^2C_1C_2 + g_{m1}sC_2 + g_{m1}g_{m2} = \\ &= sC_2(sC_1 + g_{m1}) - [(-g_{m1})(g_{m2})] \end{aligned}, \quad (13)$$

$$\begin{aligned} \Delta_{1,3} &= Y_{21}Y_{32} - Y_{31}Y_{22} = a_2s^2 + a_1s + a_0 = \\ &= s^2C_1C_2 - g_{m3}sC_2 + g_{m1}g_{m4} = \\ &= (-g_{m4})(-g_{m1}) - [(-sC_1 + g_{m3})sC_2] \end{aligned}, \quad (14)$$

Therefore (12) has to be modified to final form:

$$\begin{pmatrix} sC_1 & 0 & -sC_1 \\ -g_{m4} & sC_2 & g_{m2} \\ -sC_1 + g_{m3} & -g_{m1} & sC_1 + g_{m1} \end{pmatrix} \cdot \begin{pmatrix} V_1 \\ V_2 \\ V_3 \end{pmatrix} = \begin{pmatrix} I_1 \\ 0 \\ 0 \end{pmatrix}. \quad (15)$$

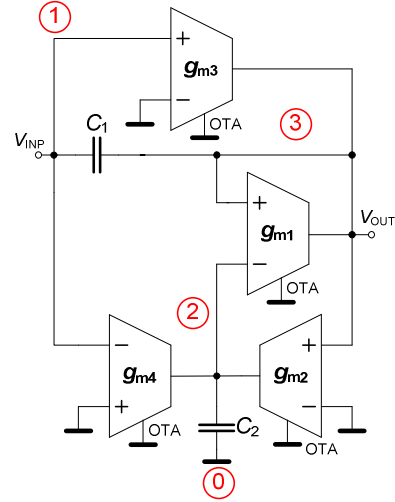


Fig. 2. Circuit implementation of the first type of OTA-based reconnection-less reconfigurable second-order filter.

Because both conditions (13) and (14) must be valid together to obtain required transfer function (term at position Y_{22} and Y_{32} has the same symbol in both cases), we have reached location of controllable transconductances (other way of location is not possible in (15)). Matrix system equations (15) can be directly used for circuit diagram preparation, see Fig. 2.

B. The second type of reconfigurable filter solution

We can derive filter topology (by similar way), where coefficient of linear member of numerator has form of difference of two parameters in comparison to (11). Thus, particular configuration leading to BR supposes equality of two parameters. Circuit is shown in Fig. 3 and is described by following transfer function:

$$K(s) = \frac{s^2 + \frac{g_{m2} - g_{m4}}{C_1}s + \frac{g_{m2}g_{m3}}{C_1C_2}}{s^2 + \frac{g_{m1}}{C_1}s + \frac{g_{m2}g_{m3}}{C_1C_2}}. \quad (16)$$

Matrix equations of this system has form:

$$\begin{pmatrix} sC_1 & 0 & -sC_1 \\ g_{m3} & sC_2 & -g_{m3} \\ -sC_1 - g_{m2} + g_{m4} & g_{m2} & sC_1 + g_{m1} \end{pmatrix} \cdot \begin{pmatrix} V_1 \\ V_2 \\ V_3 \end{pmatrix} = \begin{pmatrix} I_1 \\ 0 \\ 0 \end{pmatrix}. \quad (17)$$

It comes directly from this formula that we can change Q_p via g_{m1} . Equality $\omega_z = \omega_p$ means that we can change between AP filter ($g_{m4} = g_{m1} + g_{m2}$), BR filter ($g_{m4} = g_{m2}$) or BP response ($g_{m2} - g_{m4} > g_{m1}$). On the other hand it is impossible to reach LP and HP frequency response in this case. Note that first OTA (g_{m1}) is nothing more than electronically adjustable grounded resistor.

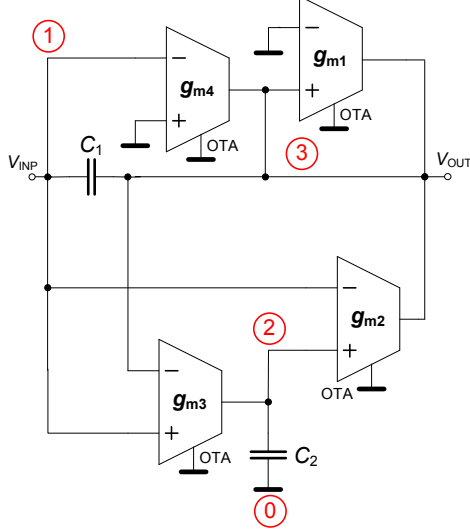


Fig. 3. Circuit implementation of the second type of OTA-based reconnection-less reconfigurable second-order filter.

C. The third type of reconfigurable filter solution

This structure was established to remove one of drawbacks of previous solution, when even HP response is not available. Supposing existence of passive resistor between nodes 1 and 2, we can modify (12) to

$$\begin{pmatrix} sC_1 + G & -G & -sC_1 \\ -G & sC_2 + G & 0 \\ -sC_1 & 0 & sC_1 \end{pmatrix} \cdot \begin{pmatrix} V_1 \\ V_2 \\ V_3 \end{pmatrix} = \begin{pmatrix} I_1 \\ 0 \\ 0 \end{pmatrix}. \quad (18)$$

Future transfer function has form:

$$K(s) = \frac{s^2 + \frac{G - g_{m3}}{C_1} s + \frac{G(g_{m2} - g_{m3}) + g_{m2}g_{m4}}{C_1 C_2}}{s^2 + \frac{G}{C_1} s + \frac{g_{m1}g_{m2}}{C_1 C_2}}. \quad (19)$$

Then sub-determinants are as follows:

$$\begin{aligned} \Delta_{1,1} &= Y_{22}Y_{33} - Y_{32}Y_{23} = s^2 C_1 C_2 + G s C_2 + g_{m1} g_{m2} = \\ &= (sC_2 + G)(sC_1) - [(-g_{m1})(g_{m2})] \end{aligned}, \quad (20)$$

$$\begin{aligned} \Delta_{1,3} &= Y_{21}Y_{32} - Y_{31}Y_{22} = \\ &= s^2 C_1 C_2 + (G - g_{m3})sC_2 + G(g_{m2} - g_{m3}) + g_{m2}g_{m4} = \\ &= (-G - g_{m4})(-g_{m2}) - [(-sC_1 - g_{m3})(sC_2 + G)] \end{aligned}. \quad (21)$$

Complete matrix form obtained from (20) and (21) directly reflects positions of operational transconductance amplifiers:

$$\begin{pmatrix} sC_1 + G & -G & -sC_1 \\ -G - g_{m4} & sC_2 + G & g_{m1} \\ -sC_1 - g_{m3} & -g_{m2} & sC_1 \end{pmatrix} \cdot \begin{pmatrix} V_1 \\ V_2 \\ V_3 \end{pmatrix} = \begin{pmatrix} I_1 \\ 0 \\ 0 \end{pmatrix}. \quad (22)$$

Schematic representation of matrix (22) is shown in Fig. 4. This filter has fixed ratio ω_p/Q_p (controllability of independent Q_p and ω_p is limited). Thus value of resistor R should be calculated after pole frequency and quality factor. The HP response is available for $g_{m2} = g_{m3} = G$ and $g_{m4} \rightarrow 0$. BR response is available for $G = g_{m3}$, BP for $g_{m2} = g_{m3}$ and $g_{m4} \rightarrow 0$. AP, LPZ or HPZ configuration is possible but not very favorable due to high mutual dependence of parameters.

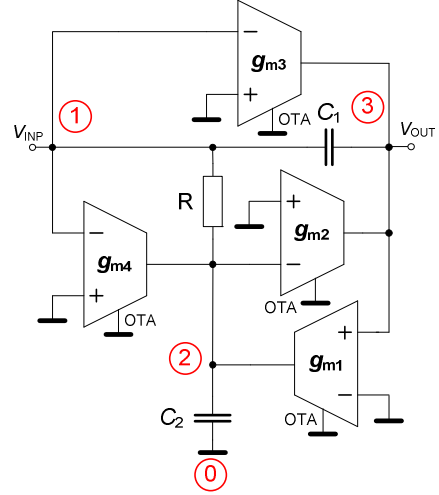


Fig. 4. Circuit implementation of the third type of OTA-based reconnection-less reconfigurable second-order filter.

V. SIMULATION RESULTS

We selected solution in Fig. 2 for detailed analysis due to it's the best variability from discussed circuits. This circuit was established by utilization of diamond transistors (DTs) OPA860 [16] and simulated in PSpice. Values of passive elements were set as: $C_1 = C_2 = 100$ pF. Actual values of transconductances and pole or zero frequencies are directly noted in results (figures). Electronic reconfiguration between AP, BR, iBP and HP response is documented in Fig. 5. LPZ and HPZ behavior can be observed in Fig. 6. Figure 7 shows reconfiguration between BR and AP response. Figure 8 indicates possibility to continuously change the slope of the transfer characteristic between pass and stop band in case of the HP response caused by pole migration (g_{m3}). Tuning of the HP response is verified in Fig. 9 for simultaneous change of g_{m1} and g_{m2} .

VI. DISCUSSION

The core idea (reconnection-less electronic reconfiguration of the filter) is the topic of several previously presented papers. Our team started research in the field of the reconfigurable filtering networks in [11]. Unfortunately, simple reconfigurable biquad from [11], based on two active

devices, has very limited usability (AP and BR only) and several drawbacks (low and uncontrollable quality factor value). Reconfigurability is obtained by the current gain of the electronically controllable current conveyor (ECCII [17], [18]).

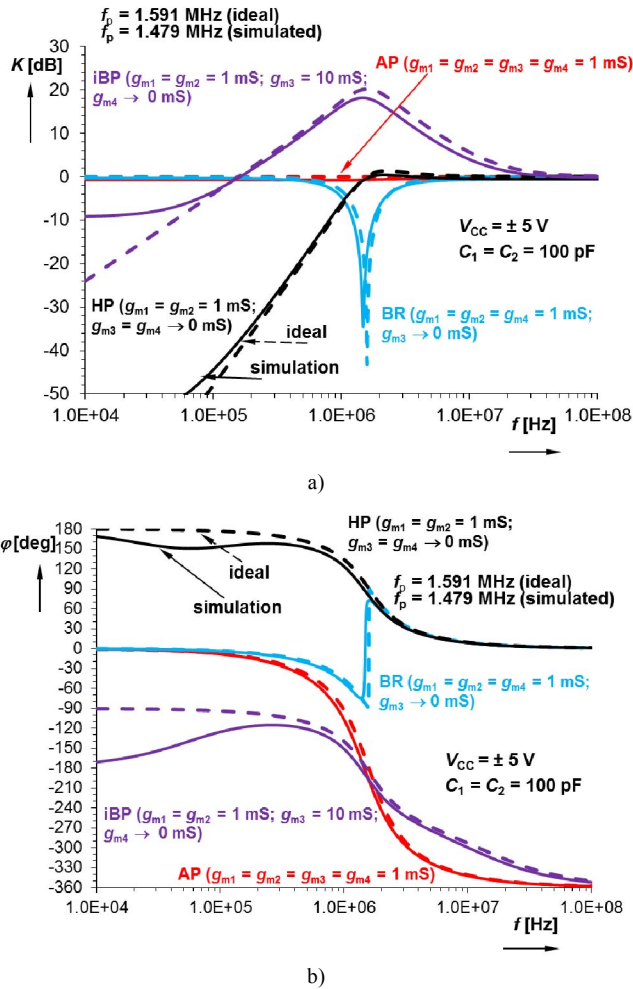


Fig. 5. Results of AC analysis of the filter in four different configurations (AP, BR, HP, iBP): a) magnitude responses, b) phase responses.

Work [9] deals with solution of the first-order filter employing two OTAs and ECCII where transfer type is adjustable between LP, LPZ, pure adj. zero and AP response or filter provides iDT. Unfortunately, all these responses are not available on single output that is quite important drawback. Our paper [12] focuses on systematic synthesis of the reconfigurable biquads by the signal-flow graph approach. The structure can be established by current and voltage followers/inverters, current amplifiers and ECCIIs. Equivalent based on OTAs was also presented. Unfortunately, presented circuits offer only electronic change between AP and BR transfer response and require large number of active devices (more than 5). Reconfigurability is controlled by one parameter of active element. On the other hand, in comparison to [11], quality factor and pole frequency can be adjusted mutually independently. Solutions presented in [8] utilize two OTAs. Systematic synthesis of presented filters is based on

matrix method of the unknown nodal voltages. However, paper [8] is focused on simple first-order reconfigurable filters only. All previously discussed works [8], [9], [11], [12] utilize commercially available active devices. Paper [10] presents active device referred as z-copy controlled gain voltage differencing current conveyor (three independently controllable active parameters are available in the frame of this device) that forms core of the simple reconfigurable first-order filter (providing iDT, DT, LP and AP response). Reconfigurability and tuning are controlled by two electronically adjustable parameters of the active device.

Due to the restricted reconfigurability in case of the previously reported reconnection-less biquadratic solutions [11], [12] (very limited possibilities of transfer response selection), we presented new solutions in this paper that have improved features. For example, biquad filter in Fig. 2 offers simple electronic reconfigurability between BR, AP, HP, iBP, LPZ and HPZ responses. All solutions of reconfigurable biquads presented in this contribution provide substantially extended features then already studied types reported in [11] and [12]. Note that previously discussed structures are completely different (interconnections, active elements and symbolical transfers) in comparison to this work where significant improvements are achieved.

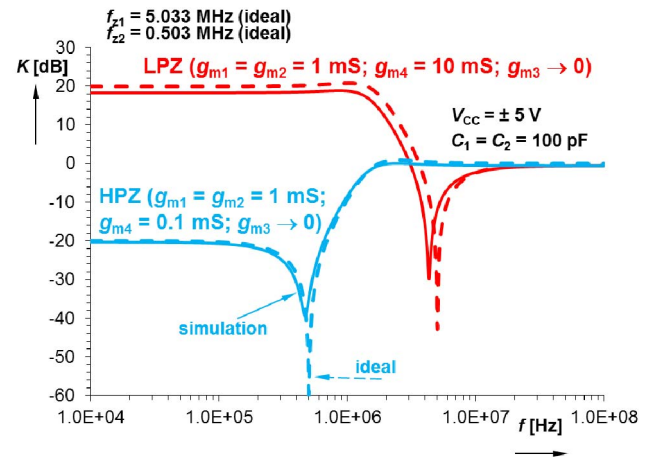


Fig. 6. LPZ and HPZ magnitude responses.

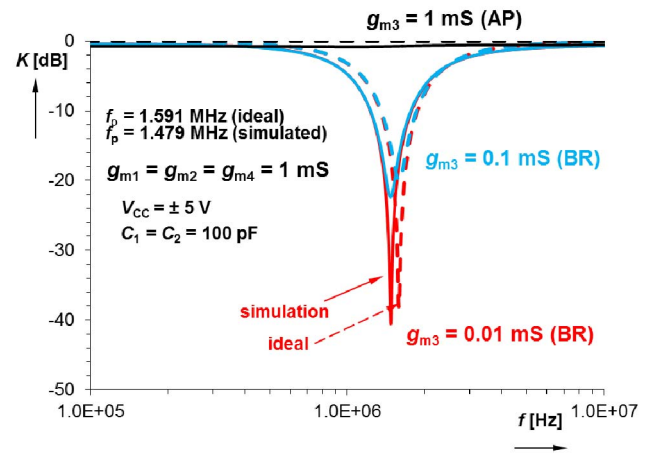


Fig. 7. Reconfiguration between BR and AP response.

VII. CONCLUSION

Simple cascading or interconnection of first-order basic blocks together with mathematical operation (subtraction, summing) can be used for synthesis of second-order systems. Unfortunately, limitation of quality factor to very low values (impossibility to obtain complex conjugate poles) and limited multifunctionality/ reconfigurability of solutions is very important disadvantage of such way of synthesis and design. Better method of synthesis, supposing direct construction of second order systems, is utilization of well-known method of unknown nodal voltages. Using MUNV and regular active devices (OTAs) can be efficiently applied also in circuit synthesis, not only in analysis as is widely used. However, fast hand solution of this task is restricted to three-nodal systems maximally. With respect to computer supported synthesis, this task can be of course extended to more complex systems.

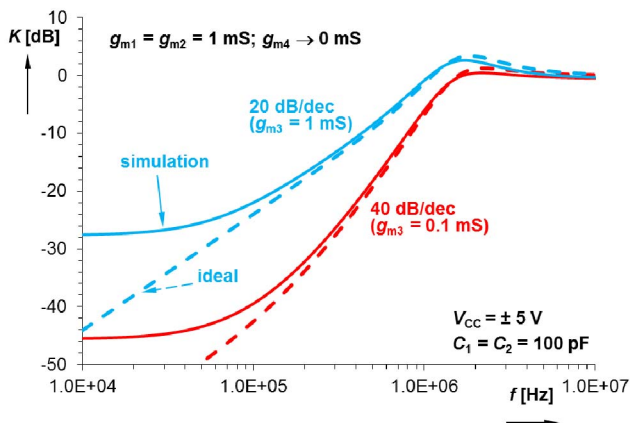


Fig. 8. Slope change at the HP response characteristic.

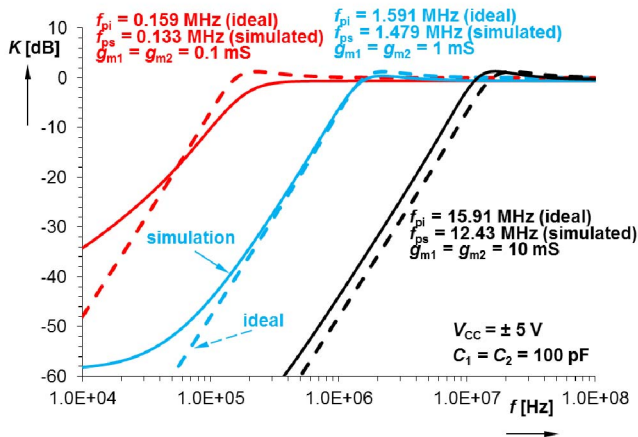


Fig. 9. Tuning observed in the case of the HP response.

We obtained three solutions where multifunctionality and electronic control is possible. Presented circuits can be used for purposes of electronic reconfigurability of transfer function type and other parameters of the filter. The first of them was analyzed in detail by PSpice simulations and expected

operation of designed filtering structure verified. One disadvantage is presence of one floating capacitor, but it was directly appointed by design specification to find very simple solutions. We expect some modifications of synthesis to obtain structures without this possible drawback in future. However, we expect these solution will be more complicated than circuits presented here.

REFERENCES

- [1] T. Deliyannis, Y. Sun, J. K. Fidler, Continuous-Time Active Filter Design. Boca Raton, CRC Press, 1999.
- [2] R. Raut, M. N. S. Swamy, Modern Analog Filter Analysis and Design: A practical approach. Weinheim, Wiley, 2010.
- [3] Y. Sun, J. K. Fidler, "Some design methods of OTA-C and CCII-RC filters," in Proc. IEE Colloquium on Digital and Analogue Filters and Filtering, pp. 1-8, 1993.
- [4] Y. Sun, J. K. Fidler, "Current-mode OTA-C realization of arbitrary filter characteristics," Electronics Letters, vol. 32, no. 13, pp. 1181-1182, 1996.
- [5] Y. Sun, J. K. Fidler, "Current-mode multiple-loop feedback filters using dual output OTAs and grounded capacitors," International Journal of Circuit Theory and Applications, vol. 25, no. 2, pp. 69-80, 1997.
- [6] T. Dostal, "Filters with Multi-Loop Feedback Structure in Current Mode," Radioengineering, vol. 12, no. 3, pp. 6-11, 2003.
- [7] R. G. Lyons, Understanding Digital Signal Processing, Prentice Hall, 2010.
- [8] J. Petrzela, R. Sotner, "Systematic design procedure towards reconfigurable first-order filters," in Proc. 24th International Conference Radioelektronika 2014, pp. 1-4, 2014.
- [9] R. Sotner, J. Jerabek, N. Herencsar, R. Prokop, K. Vrba, T. Dostal, "Resistor-less First-Order Filter Design with Electrical Reconfiguration of its Transfer Function," in Proc. 24th International Conference Radioelektronika 2014, pp. 63-66, 2014.
- [10] R. Sotner, N. Herencsar, J. Jerabek, R. Prokop, A. Kartci, T. Dostal, K. Vrba, "Z-Copy Controlled-Gain Voltage Differencing Current Conveyor: Advanced Possibilities in Direct Electronic Control of First-Order Filter," Elektronika Ir Elektrotechnika, vol. 20, no. 6, pp. 77-83, 2014.
- [11] R. Sotner, J. Jerabek, B. Sevcik, T. Dostal, K. Vrba, "Novel Solution of Notch/All-pass Filter with Special Electronic Adjusting of Attenuation in the Stop Band," Elektronika Ir Elektrotechnika, vol. 17, no. 7, pp. 37-42, 2011.
- [12] R. Sotner, J. Jerabek, J. Petrzela, K. Vrba, T. Dostal, "Design of Fully Adjustable Solution of Band-Reject/All-Pass Filter Transfer Function Using Signal Flow Graph Approach," in Proc. 24th International Conference Radioelektronika 2014, pp. 67-70, 2014.
- [13] W. Chen, The Circuits and Filters Handbook. Boca Raton, FL: CRC Press, 2002.
- [14] R. L. Geiger, E. Sanchez-Sinencio, "Active filter design using operational transconductance amplifiers: a tutorial," IEEE Circuits and Devices Magazine, vol. 1, pp. 20-32, 1985.
- [15] D. Biolek, R. Senani, V. Biolkova, Z. Kolka, "Active elements for analog signal processing: Classification, Review and New Proposals," Radioengineering, vol. 17, no. 4, pp. 15-32, 2008.
- [16] Texas Instruments. OPA860 Wide-bandwidth, operational transconductance amplifier (OTA) and buffer (datasheet), 2008, 33 p., accessible on www: <http://www.ti.com/lit/ds/symlink/opa860.pdf>
- [17] W. Surakamponorn, W. Thitimajshima, "Integrable electronically tunable current conveyors," IEE Proceedings-G, vol. 135, no. 2, pp. 71-77, 1988.
- [18] A. Fabre, N. Mimeche, "Class A/AB second-generation current conveyor with controlled current gain," Electronics Letters, vol. 30, no. 16, pp. 1267-1268, 1994.

[32] SOTNER, R., PETRZELA, J., JERABEK, J., DOSTAL, T. Reconnection-less OTA- based Biquad Filter with Electronically Reconfigurable Transfers. *Elektronika Ir Elektrotechnika*, 2015, vol. 21, no. 3, p. 33-37. ISSN: 1392-1215.

Reconnection-less OTA-based Biquad Filter with Electronically Reconfigurable Transfers

Roman Sotner¹, Jiri Petrzela¹, Jan Jerabek², Tomas Dostal³

¹*Department of Radio Electronics, Faculty of Electrical Engineering and Communication, Brno University of Technology, Technicka 12, Brno, 616 00, Czech Republic*

²*Department of Telecommunications, Faculty of Electrical Engineering and Communication, Brno University of Technology, Technicka 12, Brno, 616 00, Czech Republic*

³*Department of Electrical Engineering and Computer Science, College of Polytechnics Jihlava, Tolsteho 16, Jihlava 586 01, Czech Republic
sotner@feec.vutbr.cz*

Abstract—This paper deals with operational transconductance amplifiers (OTAs) -based active voltage-mode biquad filter with electronically reconfigurable transfer functions. Due to utilization of the very favourable active devices, this design is ready for immediate CMOS design. Presented filtering solution contains four active elements where each of them is directly used for reconnection-less change of transfer function or modification including electronic control of quality factor and tuning. The filter offers availability of all-pass, high-pass, band-pass, band-reject transfer response and special transfers as high-pass with zero and low-pass with zero. Measurement results based on utilization of diamond transistors confirmed expected behaviour of the circuit.

Index Terms—Active filter, biquad, circuit synthesis, electronic control, multifunctionality, operational transconductance amplifier, OTA, reconfiguration, reconnection-less.

I. INTRODUCTION

Reconfigurability is a very useful feature of the analog filters since it represents the possibility of immediate change of type of the frequency response of two-port structure without changing internal topology or a position of input or output port. Its importance even grows in the case of full on-chip implementation of complex electronic system comprising one or several filtering stages where continuous and smooth variability of their behaviour in the frequency domain by the external dc sources became highly necessary. It is not only trend in microelectronic design but also in practical applications focused on effective high-speed signal processing. Many recent scientific publications solve simplified problem since these multifunctional second-order

filters have particular transfer functions available between different nodes of the network. Many methods useful for design of “standard” multifunctional filtering functions have been published [1]–[10]. Signal flow graph synthesis [1], [2] is very useful and illuminating for these purposes. Perfect explanations of synthesis of multifunctional filters based on multiple-loop structures of integrators were given for example in [3]–[10]. Many of them are based on operational transconductance amplifiers (OTAs) [11], [12]. Unfortunately, reconnection-less reconfiguration of the filter response is not discussed in basic literature [3]–[10]. However, our aim is to avoid using the filtering structures where change of required transfer function is obtained by manual reconnection of output (so called single-input and multiple-output types - SIMO) or input (multiple-input and single-output - MISO) terminal.

Research for these structures has real importance due to complicated change of filter type in realization on chip. We can use these filters beneficially when some undesirable frequency components or distortions/noises occur in processed signal and we have to modify (tune) or change type of the transfer function (magnitude response) immediately. Physical reconnection of appropriate output/input of the filter by switches is traditional way how to provide this intentional change. However, it means additional problems (additional chip area for control logic and switches, power consumption, additional distortion from switching mechanisms – discontinuous operation – undesirable frequency components).

Several works dealing with this topic were already published in recent years. However, many of them are focused only on the first-order filters [13]–[15].

Second-order solution of the reconfigurable filtering structure was firstly reported in [16], where circuit based on two active devices providing all-pass (AP) and band-reject (BR) response was introduced. Continuous change of the AP to BR response is possible together with electronic tuning. However, quality factor of proposed solution is very low and limited and other transfer functions are not available.

Manuscript received November 3, 2014; accepted February 25, 2015.

Research described in this paper was financed by Czech Ministry of Education in frame of National Sustainability Program under grant LO1401. For research, infrastructure of the SIX Center was used. Research described in the paper was supported by Czech Science Foundation projects under No. 14-24186P. Grant No. FEKT-S-14-2281 also supported this research. The support of the project CZ.1.07/2.3.00/20.0007 WICOMT, financed from the operational program Education for competitiveness, is gratefully acknowledged.

Problems of low quality factor and other problems in tuning are solved in [17]. However, circuit is very complicated (at least five active elements) and provides again only AP and BR responses. Multiple-loop integrator structure [3]–[10] was used for synthesis in [17].

In this paper, we present structure of the reconnection-less reconfigurable biquad (second-order) filter based on four OTAs, that allows more types of transfer characteristic and more possibilities of electronic control than previously reported solutions. The paper has following structure: Section I gives detailed introduction to this area and reasons for this research, Section II deals with method of synthesis, Section III introduces behavioural model and experimental results and Section IV summarizes main findings of synthesis and main features of proposed circuit.

II. METHOD OF SYNTHESIS

We used matrix method of the unknown nodal voltages (MUNV) [18]–[21] to obtain discussed circuit. MUNV is a widely used approach dedicated to symbolical analysis of the linearized circuits. Its rules directly result from first Kirchhoff's laws [21], the individual equations represent current balance at the particular nodes. To preserve a system of the linear non-homogenous equations solvable, these nodes must be independent on each other. This property is indicated by regularity of the square admittance matrix \mathbf{Y} .

The proposed design procedure starts with a defined transfer function which must be as general as possible in order to alternate transfer zeroes and poles independently on each other. Design itself starts with defined form of the voltage transfer function which should correspond to equation

$$K(s) = \frac{N(s)}{D(s)} = \frac{a_2s^2 + a_1s + a_0}{b_2s^2 + b_1s + b_0} = K_0 \frac{s^2 + \frac{\tilde{S}_Z}{Q_Z}s + \tilde{S}_Z^2}{s^2 + \frac{\tilde{S}_P}{Q_P}s + \tilde{S}_P^2}, \quad (1)$$

where K_0 is pass-band gain and $Q_Z > 0$ and $Q_P > 0$ are zero and pole quality factors. Note that term (1) contains four parameters (\tilde{S}_Z , Q_Z , \tilde{S}_P , Q_P) and this compact set covers all possible frequency responses. Let us imagine a complex plane ready to be filled by transfer zeroes and poles. To preserve some degree of stability the poles should be real or a pair of complex conjugated values but always placed in the left half-plane of the complex plane. This implies that polynomial $D(s)$ have only positive coefficients with the possibility to minimize linear part b_1 down to a reasonable value. In order to obtain all-pass filter we must be able to set a negative value of coefficient $a_1 = -b_1$. For ideal high-pass filter it is necessary to achieve equality $a_0 = a_1 = 0$ and for ideal low-pass we must be able to set $a_1 = a_2 = 0$. Typical configuration of band-pass (BP) filter is $a_0 = a_2 = 0$. Situation is a little bit confusing in the case of band-reject filter because it is bounded to the same circles of constant angular frequency for zeroes and poles, i.e. to the relations $\tilde{S}_Z = \tilde{S}_P$ and $Q_Z > Q_P$. In some specific situations, the so-called low-pass filter with zero (LPZ) and high-pass filter with zero (HPZ) is required. First of them has $\tilde{S}_Z > \tilde{S}_P$ and

$Q_Z > Q_P$ and the second case $\tilde{S}_Z < \tilde{S}_P$ and $Q_Z > Q_P$.

Thus we will focus on circuits which contain just three independent nodes oriented to the overall ground reference. Marking input and output node as first and third unknown voltage respectively, Cramer rule [18] gives following formula for the voltage transfer function:

$$\mathbf{V} = (V_1 \ V_2 \ V_3)^T, \quad (2)$$

$$K(s) = \frac{V_{OUT}}{V_{INP}} = \frac{V_3}{V_1} = \frac{\Delta_{1,3}}{\Delta_{1,1}}, \quad (3)$$

where \mathbf{V} is a column vector of the unknown voltages and $\Delta_{i,j}$ is a sub-determinant of admittance matrix after omitting i -th row and j -th column. Input impedance can be established as

$$Z(s) = \frac{V_{INP}}{I_{INP}} = \frac{1}{I_{INP}} \times \frac{I_{in}(-1)^{1+1} \Delta_{1,1}}{\Delta} = \frac{\Delta_{1,1}}{\Delta}, \quad (4)$$

where I_{in} is arbitrary input current and Δ is full determinant of admittance matrix. We used described approach in system of three nodal voltages where OTAs are used. The basic OTA has differential voltage input and single current output to provide: $(V_+ - V_-) \cdot g_m = I_{out}$, where g_m ($A \cdot V^{-1}$) is electronically adjustable transconductance [11], [12]. Our intended and specific transfer function has form

$$K(s) = \frac{s^2 - \frac{g_{m3}}{C_1}s + \frac{g_{m2}g_{m4}}{C_1C_2}}{s^2 + \frac{g_{m1}}{C_1}s + \frac{g_{m1}g_{m2}}{C_1C_2}}. \quad (5)$$

Supposing presence of floating capacitor between node 1 and 3 (C_1) and grounded capacitor (C_2) in node 2, we have system of linear equations in form

$$\begin{pmatrix} sC_1 & 0 & -sC_1 \\ 0 & sC_2 & 0 \\ -sC_1 & 0 & sC_1 \end{pmatrix} \times \begin{pmatrix} V_1 \\ V_2 \\ V_3 \end{pmatrix} = \begin{pmatrix} I_1 \\ 0 \\ 0 \end{pmatrix}. \quad (6)$$

Fixing this degree of freedom, we have to select correct positions in admittance matrix where specific transconductances (g_{m1} to g_{m4}) are located. In accordance to (3), it leads to sub-determinants:

$$\begin{aligned} \Delta_{1,1} &= s^2C_1C_2 + g_{m1}sC_2 + g_{m1}g_{m2} = \\ &= sC_2(sC_1 + g_{m1}) - g_{m1}(-g_{m2}), \end{aligned} \quad (7)$$

$$\begin{aligned} \Delta_{1,3} &= s^2C_1C_2 - g_{m3}sC_2 + g_{m2}g_{m4} = \\ &= (-g_{m4})(-g_{m2}) - (-sC_1 + g_{m3})sC_2. \end{aligned} \quad (8)$$

We can really see where particular transconductances have to be located in final admittance matrix:

$$\begin{pmatrix} sC_1 & 0 & -sC_1 \\ -g_{m4} & sC_2 & g_{m1} \\ -sC_1 + g_{m3} & -g_{m2} & sC_1 + g_{m1} \end{pmatrix} \times \begin{pmatrix} V_1 \\ V_2 \\ V_3 \end{pmatrix} = \begin{pmatrix} I_1 \\ 0 \\ 0 \end{pmatrix}, \quad (9)$$

and prepare schematic of the solution (Fig. 1). Such biquad filter has significant degree of reconfigurability because g_{m1} influence both Q_P and \tilde{S}_P while g_{m2} affects zero and pole frequency simultaneously. The relation between frequency radius for transfer zeroes and poles are uniquely controlled through g_{m4} since $\tilde{S}_P/\tilde{S}_Z = (g_{m4}/g_{m1})^{1/2}$ while Q_Z is adjusted only by g_{m3} change. This filter realizes these transfers:

1. AP response for $g_{m1} = g_{m2} = g_{m3} = g_{m4}$,
2. BR response for $g_{m1} = g_{m2} = g_{m4}$, $g_{m3} \rightarrow 0$,
3. high-pass (HP) response for $g_{m1} = g_{m2}$, $g_{m3} = g_{m4} \rightarrow 0$,
4. iBP (inverting) response for $g_{m1} = g_{m2}$, $g_{m4} \rightarrow 0$,
5. HPZ (derived from BR) and for $g_{m1} > g_{m4}$, $g_{m3} \rightarrow 0$,
6. LPZ (derived from BR) for $g_{m1} < g_{m4}$, $g_{m3} \rightarrow 0$.

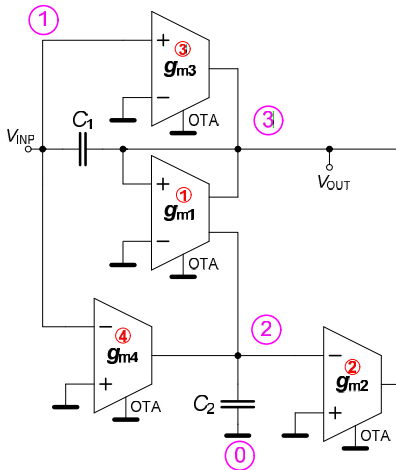


Fig. 1. Synthesized reconfigurable biquad filter based on OTAs.

Note that iBP response is not pure BP (with symmetrical sidebands – slope 20 dB/dec) because it has finite attenuation at the high-frequency stop-band (intentionally – resulting from design equations).

III. BEHAVIOURAL MODEL AND EXPERIMENTAL RESULTS

Five single-output diamond transistors OPA860 [22] were used for implementation of transconductance amplifiers as evident from Fig. 2. Supply voltage became $V_{DD} = V_{SS} = 5$ V and both working capacitors have value $C_1 = C_2 = 470$ pF. Transconductances are given approximately by the so-called degradation resistors $R_{deg} = 1/g_m$ which were set to get $g_{m1} = g_{m2} = 0.91$ mS. This design suppose ideal pole frequency located at $f_p = 339$ kHz and quality factor $Q = 1$. The rest of parameters (g_{m3} and g_{m4}) were changed in order to show the overall filter performances in frequency domain. Diamond transistors are beneficial due to high-frequency features and variability. Unfortunately, wide-range control of their basic parameter is possible only by changing value of the passive resistor.

Results of the measurements are given in Fig. 3 up to Fig. 10. Figure 3 shows configuration of the filter as HP response ($g_{m3} = g_{m4} = 0$ mS), see (5) for clarity. BR response is available for $g_{m3} = 0$ mS simultaneously with $g_{m1,2,4} = 0.91$ mS and is shown in Fig. 4. Attenuation control of the minimal gain of the BR response is possible as we can see in Fig. 5. Maximal measured available attenuation 40 dB was obtained for $g_{m1,2,4} = 0.91$ mS and $g_{m3} = 0.1$ mS (Fig. 5).

Example of attenuation control is shown in Fig. 6, where attenuation is set to be 30 dB were obtained for $g_{m3} = 0.16$ mS. iBP response (with gain 20 dB) for $g_{m3} = 13.7$ mS and $g_{m4} = 0.1$ mS is shown in Fig. 7. AP response is shown in Fig. 8 for $g_{m1,2,3,4} = 0.91$ mS.

Presented filter example is also easily configurable as HP or LP response both with transfer zero. Frequency responses for the first case (HPZ) is achievable for $g_{m3} = 0$ mS, $g_{m4} = 0.1$ mS and is depicted in Fig. 9. Particular results for the second case (LPZ) is reached by setting $g_{m3} = 0$ mS, $g_{m4} = 7.1$ mS and is demonstrated in Fig. 10. Of course, electronic tuning (of pole frequency) is possible, but due to limited space, we restricted our analyses to presentation of reconnection-less filter reconfiguration only.

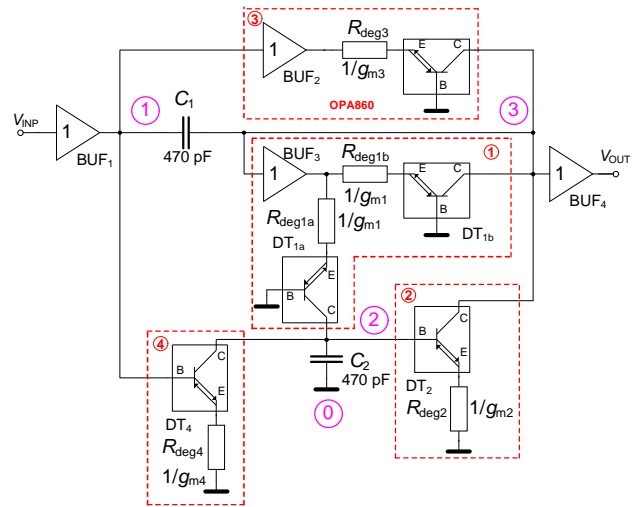


Fig. 2. Behavioural model of the biquadratic filter based on diamond transistors and voltage buffers (available in the single package).

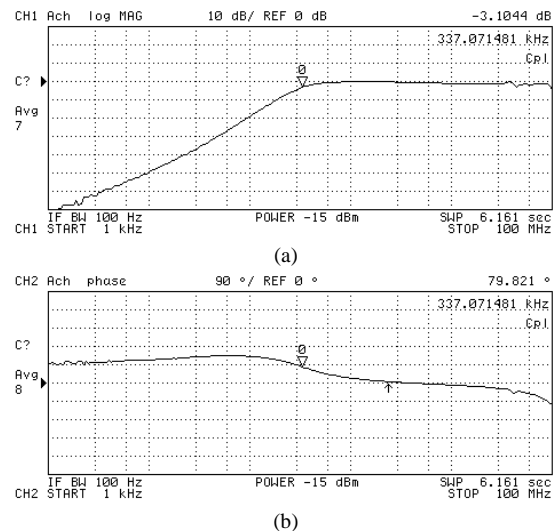
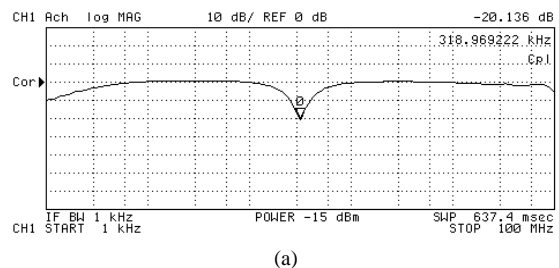
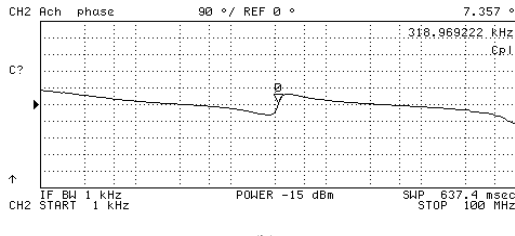


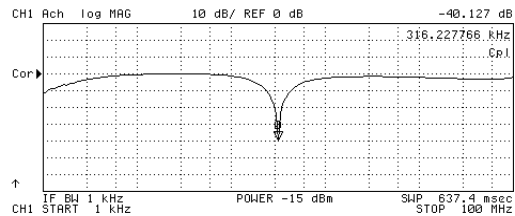
Fig. 3. High-pass configuration ($g_{m3} = g_{m4} = 0$ mS): a) magnitude response; b) phase response.



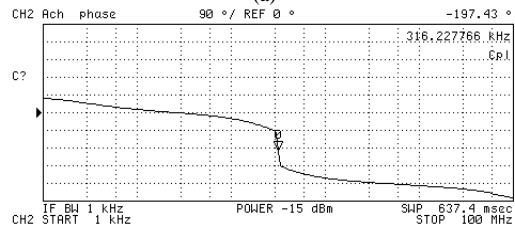


(b)

Fig. 4. Band-reject configuration ($g_{m3} = 0$ mS, $g_{m1,2,4} = 0.91$ mS): a) magnitude response; b) phase response.

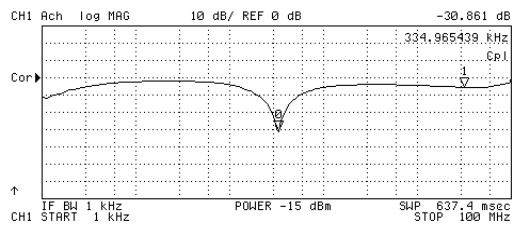


(a)

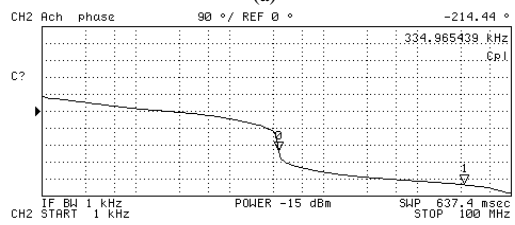


(b)

Fig. 5. Band-reject configuration ($g_{m3} = 0.1$ mS, $g_{m1,2,4} = 0.91$ mS) employing 40 dB attenuation: a) magnitude response; b) phase response.

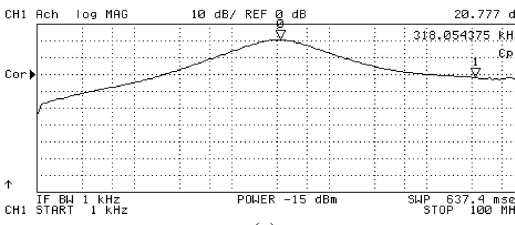


(a)

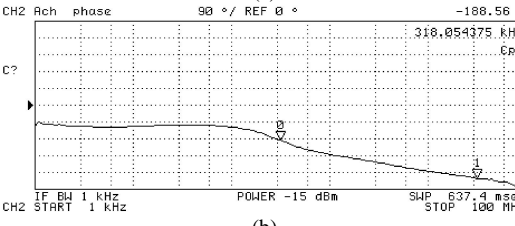


(b)

Fig. 6. Band-reject configuration ($g_{m3} = 0.16$ mS, $g_{m1,2,4} = 0.91$ mS) employing 30 dB attenuation: a) magnitude response; b) phase response.

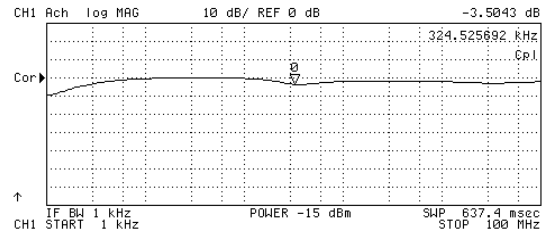


(a)

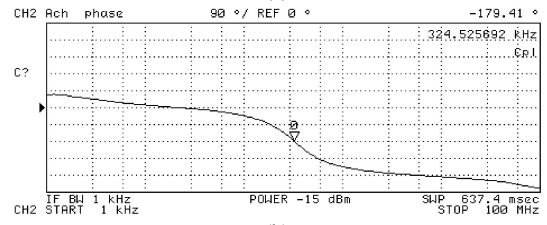


(b)

Fig. 7. Inverting band-pass configuration ($g_{m3} = 13.7$ mS, $g_{m4} = 0.16$ mS): a) magnitude response; b) phase response.

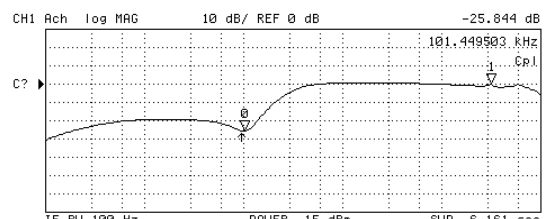


(a)

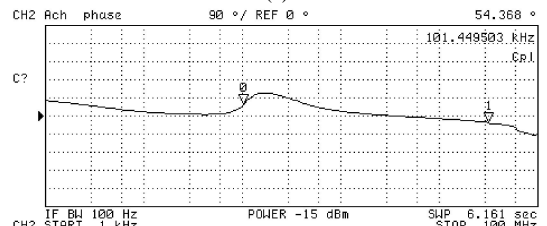


(b)

Fig. 8. All-pass configuration ($g_{m1,2,3,4} = 0.91$ mS): a) magnitude response; b) phase response.

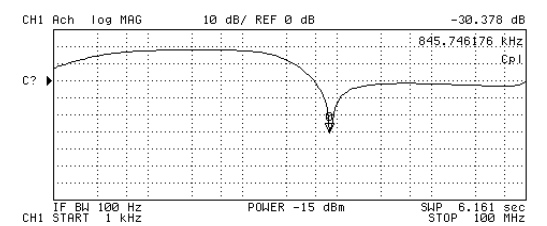


(a)

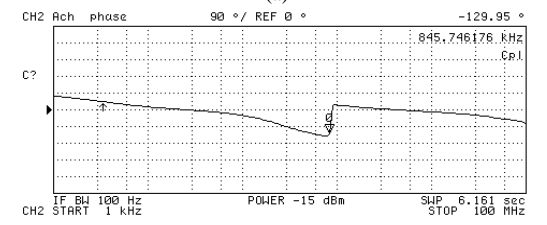


(b)

Fig. 9. High-pass with transfer zero configuration ($g_{m3} = 0$ mS, $g_{m4} = 0.1$ mS): a) magnitude response; b) phase response.



(a)



(b)

Fig. 10. Low-pass with transfer zero configuration ($g_{m3} = 0$ mS, $g_{m4} = 7.1$ mS): a) magnitude response; b) phase response.

Measurement results given above were obtained by network-vector/spectrum analyser HP4395A with input power level -15 dBm, i.e. input voltage 40 mV_{ef} on 50 Ω . Magnitude drop in some results at low frequencies $f_{-3dB} = 2.1$ kHz is given by coupling capacitance (foil 1 μ F) at the output terminal of the filter to avoid DC component dangerous for input of the analyser.

IV. CONCLUSIONS

The presented second-order filtering stage has four parameters which should be externally adjusted independently of each other. Therefore, the voltage transfer function allows setting zeroes and poles independently on each other but still being part of the group of the complex numbers. The transfer poles should be placed firstly with the possibility to achieve the complex conjugated values to get higher quality factors than 0.5; otherwise a structure becomes useless. To preserve a certain degree of stability, the migration of poles should be strictly limited in the left half-plane of the complex plane. The transfer zeros should be complex numbers as well as it is necessary to be able to move them from left to right half-plane of complex space and back in order to obtain all-pass frequency response. Several scenarios for moving zeroes can be arranged. If such movement is along a circle of the constant significant angular frequency we are able to realize continuous change of frequency response from band-reject to all-pass. If couple of the transfer zeroes are created at the origin of the imaginary axis and move towards high angular frequency we change filter nature from high-pass through modified high-pass and band-reject up to low-pass. The complexity of the directions for transfer zeros migration indicates that at least four active elements are needed for practical design of this type of the reconfigurable filter. MUNV is also very suitable for study of real parasitic influences in structures (all undesired effects – parasitic resistances and capacitances - can be simply and directly reflected to the matrix \mathbf{Y}). Measurement results confirm availability of all possible transfer functions (AP, HP, iBP, BR, LPZ, HPZ) in structure based on one single input and single output from frequencies of several kHz to several tens of MHz.

REFERENCES

- [1] S. J. Mason, "Feedback Theory: Further properties of Signal Flow Graphs", in *Proc. IRE*, vol. 44, no. 7, pp. 920–926, 1956. [Online]. Available: <http://dx.doi.org/10.1109/jrproc.1956.275147>
- [2] C. J. Coates, "Flow-graph solution of linear algebraic equations", *IRE Trans. Circuit Theory*, vol. 6, no. 2, pp. 170–187, 1959. [Online]. Available: <http://dx.doi.org/10.1109/TCT.1959.1086537>
- [3] T. Dostal, "All-pass filter in current mode", *Radioengineering*, vol. 14, no. 3, pp. 48–53, 2005.
- [4] C. M. Chang, C. L. Hou, W. Y. Chung, J. W. Horng, C. K. Tu, "Analytical synthesis of high-order single-ended-input OTA-grounded C all-pass and band-reject filter structures", *IEEE Trans. Circuits and Systems: Regular Papers*, vol. 53, no. 3, pp. 489–498, 2006. [Online]. Available: <http://dx.doi.org/10.1109/TCSI.2005.859057>
- [5] C. M. Chang, B. M. Al-Hashimi, "Analytical synthesis of current-mode high-order OTA-C filters", *IEEE Trans. Circuits and Systems: Regular Papers*, vol. 50, no. 9, pp. 1188–1192, 2003. [Online]. Available: <http://dx.doi.org/10.1109/TCSI.2003.816327>
- [6] T. Tsukutani, M. Higashimura, M. Ishida, S. Tsuiki, Y. Fukui, "A general class of current-mode high-order OTA-C filters", *International Journal of Electronics*, vol. 81, no. 6, pp. 663–669, 1996. [Online]. Available: <http://dx.doi.org/10.1080/002072196136355>
- [7] Y. Sun, J. K. Fidler, "Some design methods of OTA-C and CCII-RC filters", in *Proc. IEE Colloquium on Digital and Analogue Filters and Filtering*, London, 1993, pp. 1–8.
- [8] Y. Sun, J. K. Fidler, "Current-mode multiple-loop feedback filters using dual output OTAs and grounded capacitors", *International Journal of Circuit Theory and Applications*, vol. 25, no. 2, pp. 69–80, 1997. [Online]. Available: [http://dx.doi.org/10.1002/\(SICI\)1097-007X\(199703/04\)25:2<69::AID-CTA950>3.0.CO;2-9](http://dx.doi.org/10.1002/(SICI)1097-007X(199703/04)25:2<69::AID-CTA950>3.0.CO;2-9)
- [9] Y. Sun, J. K. Fidler, "Current-mode OTA-C realization of arbitrary filter characteristics", *Electronics Letters*, vol. 32, no. 13, pp. 1181–1182, 1996. [Online]. Available: <http://dx.doi.org/10.1049/el:19960807>
- [10] Y. Sun, J. K. Fidler, "Structure generation of current-mode two integrator dual output-OTA grounded capacitor filters", *IEEE Trans. Circuits and Systems II: Analog and Digital Signal Processing*, vol. 43, no. 9, pp. 659–663, 1996. [Online]. Available: <http://dx.doi.org/10.1109/82.536762>
- [11] R. L. Geiger, E. Sanchez-Sinencio, "Active filter design using operational transconductance amplifiers: a tutorial", *IEEE Circuits and Devices Magazine*, vol. 1, pp. 20–32, 1985. [Online]. Available: <http://dx.doi.org/10.1109/MCD.1985.6311946>
- [12] D. Biolek, R. Senani, V. Biolkova, Z. Kolka, "Active elements for analog signal processing: Classification, Review and New Proposals", *Radioengineering*, vol. 17, no. 4, pp. 15–32, 2008.
- [13] J. Petrzela, R. Sotner, "Systematic design procedure towards reconfigurable first-order filters", in *Proc. 24th Int. Conf. Radioelektronika 2014*, Bratislava, 2014, pp. 1–4. [Online]. Available: <http://dx.doi.org/10.1109/radioelek.2014.6828462>
- [14] R. Sotner, J. Jerabek, N. Herencsar, R. Prokop, K. Vrba, T. Dostal, "Resistor-less first-order filter design with electronical reconfiguration of its transfer function", in *Proc. 24th Int. Conf. Radioelektronika 2014*, Bratislava, 2014, pp. 63–66. [Online]. Available: <http://dx.doi.org/10.1109/radioelek.2014.6828417>
- [15] R. Sotner, N. Herencsar, J. Jerabek, R. Prokop, A. Kartci, T. Dostal, K. Vrba, "Z-copy controlled-gain voltage differencing current conveyor: advanced possibilities in direct electronic control of first-order filter", *Elektronika Ir Elektrotechnika*, vol. 20, no. 6, pp. 77–83, 2014. [Online]. Available: <http://dx.doi.org/10.5755/j01.eee.20.6.7272>
- [16] R. Sotner, J. Jerabek, B. Sevcik, T. Dostal, K. Vrba, "Novel solution of notch/all-pass filter with special electronic adjusting of attenuation in the stop band", *Elektronika Ir Elektrotechnika*, vol. 17, no. 7, pp. 37–42, 2011. [Online]. Available: <http://dx.doi.org/10.5755/j01.eee.113.7.609>
- [17] R. Sotner, J. Jerabek, J. Petrzela, K. Vrba, T. Dostal, "Design of fully adjustable solution of band-reject/all-pass filter transfer function using signal flow graph approach", in *Proc. 24th Int. Conf. Radioelektronika 2014*, Bratislava, 2014, pp. 67–70. [Online]. Available: <http://dx.doi.org/10.1109/radioelek.2014.6828418>
- [18] A. Basak, *Analogue electronic circuits and systems*. Cambridge University Press, New York, USA, 1991, p. 376. [Online]. Available: <http://dx.doi.org/10.1017/CBO9781139168069>
- [19] P. R. Gray, P. J. Hurst, S. H. Lewis, R. G. Meyer, *Analysis and design of analog integrated circuits*. John Wiley and Sons, Inc: USA, 2009, p. 896.
- [20] R. Raut, M. N. S. Swamy, *Modern Analog Filter Analysis and Design: A practical approach*. Willey-VCH Verlag GmbH and Co. KGaA, Germany, Weinheim, 2010, p. 35. [Online]. Available: <http://dx.doi.org/10.1002/9783527631506>
- [21] W. Chen, *The Circuits and Filters Handbook*. Florida: CRC Press, Boca Raton, 2009, p. 3364.
- [22] OPA860: Wide Bandwidth Operational Transconductance Amplifier and Buffer, Texas Instruments. 2005, last modified 8/2008.

[33] SOTNER, R., JERABEK, J., HERENC SAR, N., PETRZELA, J., DOSTAL, T., VRBA, K. First-order adjustable transfer sections for synthesis suitable for special purposes in constant phase block approximation. *AEU - International Journal of Electronics and Communications*, 2015, vol. 69, no. 9, p. 1334-1345. ISSN: 1434-8411.



REGULAR PAPER

First-order adjustable transfer sections for synthesis suitable for special purposes in constant phase block approximation



Roman Sotner^{a,*}, Jan Jerabek^b, Norbert Herencsar^b, Jiri Petrzela^a, Tomas Dostal^{a,c}, Kamil Vrba^b

^a Department of Radio Electronics, Brno University of Technology, Technicka 3082/12, 616 00 Brno, Czech Republic

^b Department of Telecommunications, Brno University of Technology, Technicka 3082/12, 616 00 Brno, Czech Republic

^c Department of Electrical Engineering and Computer Science, College of Polytechnics Jihlava, Tolsteho 16, 586 01 Jihlava, Czech Republic

ARTICLE INFO

Article history:

Received 7 February 2015

Accepted 26 May 2015

Keywords:

All-pass sections

Bilinear section

Fractional-order circuit

Voltage controllable phase shifter

Two-port constant phase element/block

ABSTRACT

The main aim of this work is to investigate electronically adjustable properties of discussed simple transfer sections i.e. all-pass and bilinear filters and their practical verification. Signal-flow graph (SFG) approach was used for better understanding of circuit design and its principle. Simultaneous and separated control of the zero and pole frequencies is available, thus this circuit is favorable for design of both classical and special applications such as constant phase elements/blocks and fractional-order synthesis. Interesting example of operation in two-port block (so-called half integrator) with approximation of constant phase character (shift) is given. Our intentions are supported by PSpice simulation results prepared with active elements modeled on CMOS transistor level in low-voltage TSMC LO EPI 0.18 μm process and also by experimental laboratory tests employing commercially available active elements.

© 2015 Elsevier GmbH. All rights reserved.

1. Introduction

All-pass filters are specific types of filtering circuits that have constant magnitude response during the wide frequency range while phase (argument) characteristic changes. It allows correction of phase shift in many applications utilizing analog signal processing. All-pass (AP) circuits are well-known blocks that have pole(s) in the left-half-plane of complex space and zero(s) in the right-half-plane of complex space (so-called RHP zero). Such situation is called as non-minimal argument circuit. On the other hand, rest of the most known filtering systems such as low-pass, high-pass, band-pass, and band-reject transfer functions are so-called minimal argument circuits wherein zeros and poles are in the left-half-plane. In recent years, an important attention was given to circuit systems with constant phase character [1] (and references cited therein) and systems with special type of transfer characteristic in fractional-order applications [2–4]. Synthesis of some from these specific active circuits requires building blocks similar to AP sections [4]. However, zeros and poles of these sub-blocks are in the left-half-plane. Additionally, location of pole(s) and zero(s) must be independently

and continuously adjustable. These sections also allow simple reconfiguration from classical AP circuit to general bilinear section that has zero and pole in the left-half-plane. Electronic adjusting of discussed parameters brings possibility to utilize these partial circuits in complex structures and chains with simple access to their control or contactless reconfiguration. Mostly in case of AP solutions, modern voltage- and current-mode active elements [5] allow simple electronic control of pole/zero frequency by transconductance (g_m) [5,6] or intrinsic resistance of current input (R_x) [5,7] by bias current.

1.1. State-of-the-art of methodology based on general loop-feedback approaches

First of all, it is necessary to mention useful and known methods for synthesis with signal flow graphs [8,9] and multiple feedback and feed-forward loops of integrators. These methods are necessary for synthesis of classical multi-loop filters (high-orders mainly). Perfect explanations were provided by Dostal [10], Chang et al. [11,12] and Tsukutani et al. [13]. Unfortunately, materials [10–13] do not support special synthesis of simple first-order AP/bilinear filters with separated electronic control of zero and pole frequency. Thus, this possibility is rather accidental in a few specific hitherto published works as will be discussed later. In addition, some authors of works focused on standard AP synthesis understand

* Corresponding author. Tel.: +420 541 14 6560.

E-mail address: sotner@feec.vutbr.cz (R. Sotner).

existence of separated zero and pole adjusting as inconvenient drawback due to necessity of perfect matching of two parameters for tuning. However, some applications require this feature as will be discussed.

Paper [10] describes general method of multiple feedback loops of integrators, summing points and distributions to obtain canonical multi-loop integrator structures (follow the leader feedback and inverse follow the leader feedback realization with transconductors [5] and current differencing transconductance amplifiers [5] as building elements). Approach is intended for high-order AP structures. Impressive work [11] also deals with analytical approach to synthesis of high-order filters based on transconductors only in current-mode with output signal distribution especially. Similar approach is used in work [12] where high-order AP synthesis employs also specific multi-loop based method with current summation and distribution of many signal paths simultaneously. Ref. [13] is focused also on general approach to synthesis of high-order current-mode transfer functions (multifunctional in general) by classical follow the leader feedback (with input summation and multi-output-terminal active elements) approach with transconductor-based integrators. A way how to separate zero and pole frequency control in one general loop was not discussed in these works because standard general multi-loop synthesis of AP or other filtering transfer functions does not require this feature. Our proposal, presented in this manuscript, requires special modification of feedback and feed-forward path-gains. In addition, methods presented in [10–13] utilize active elements with generally multiple-outputs to realize all essential feedbacks with constant transfers equal to 1, -1 or 0. We try to avoid this necessity of active devices with many outputs and many feedback paths in our proposals. It is worth mentioning that none from important theoretical works [10–13] reports intentional separation of zero and pole frequency control (by g_m of transconductor – electronically) in simple first-order systems.

1.2. Discussion of specific hitherto published solutions of first-order AP sections

Detailed comparison of previously reported first-order voltage-mode AP solutions [14–43] is provided in Table 1. Our comparison is restricted to controllable solutions only. Detailed study of previously reported solutions of AP section reveals important issues:

- (1) Some solutions require many active [19] or passive elements [19,20,27,33,42].
- (2) Cascadability, that is important for example for constant phase elements (CPEs) synthesis, is problematic [25,28,39] – input and output impedance of AP block has impact on overall transfer function (previous section influences the following section).
- (3) Many solutions have frequency dependent input impedance in real case (grounded or floating capacitor is connected to the high-impedance input terminal or between input node and active element) [14,20,23–25,28,30,31] – additional pre-buffering is required.
- (4) Many solutions have frequency dependent output impedance in real case (passive elements including capacitors connected to the high-impedance output nodes without buffering) [28,38,41,42] – buffering is required.
- (5) Many voltage-mode solutions do not dispose by separated low-impedance output(s) [17,18,25,28,35,38,39,41,42].
- (6) Selected solutions have input impedance also dependent on parameter serving for tunability in real case [16,28–31,39] (input impedance influenced by synthetic resistor $1/g_m$ created by transconductor with direct feedback or by intrinsic

resistance R_x of current input terminal in the same node as capacitor).

- (7) Selected solutions have output impedance also dependent on parameter serving for tunability [17,18,25,35,38,41,42].
- (8) Grounded capacitors that are usually required for IC design, are not available in many cases [14,20,23–26,28,30,31,33–35,37,38].
- (9) Independent control of pole (f_p) and zero (f_z) frequency was not proposed nor tested in studied solutions, only some works [15,18,28] indicated these possibilities symbolically without further discussion.
- (10) Reconfiguration of published solutions between minimal and non-minimal argument is not discussed or solved (reconfiguration between AP and bilinear system).

Very useful AP circuits, where independent control of f_p and f_z is possible, have already been published in open literature [15,18,28]. Unfortunately, these solutions have many drawbacks. For example, circuit discussed by Biolek et al. [15] allows control of f_p by g_m . However, control of f_z is available only by floating resistor. Replacement of floating resistance by electronically controllable equivalent is complicated task (for example two additional transconductors [6]). Tanaphatsiri et al. [28] proposed circuit, where f_p is controllable by g_m and f_z by R_x (R_x is general notation of control by intrinsic current input resistance). Unfortunately, circuit in [28] utilizes floating capacitor, is not suitable for full cascability – it has frequency dependent input and output impedances and input impedance is influenced by tuning in real case and without additional buffering. Transconductor-based solutions allowing independent electronic control of pole and zero frequency can be found also in work presented by Kushar et al. [18]. Unfortunately, term g_{m1}/g_{m2} in front of the main fraction of transfer function in form: $K(s) = g_{m1}/g_{m2}(s - g_{m2}/C)/(s + g_{m1}/C)$ is not useful for applications in constant phase blocks and similar systems. It complicates design due to additional influence on gain/attenuation. In addition, other drawbacks limit utilization of solution in [18], see Table 1. Demanded transfer function has form: $K(s) = (s \pm g_{m2}/C)/(s + g_{m1}/C)$ or $K(s) = (s \pm g_{m1}/C)/(s + g_{m2}/C)$, which is required for synthesis with bilinear systems [1,4]. All intentionally designed AP/bilinear sections in this paper have this form of transfer function.

Detailed study of above discussed hitherto published papers revealed space for further improvements. Therefore, the main aim of this paper is simple utilization of signal-flow graphs (SFG) [8,9] to the design of electronically controllable AP (circuit with non-minimal argument) and pseudo AP sections (circuits with minimal argument) and their application. A substantial attention is given to separated control of zero and pole frequency of AP sections that could be very useful in some cases for diverse forms of adjusting and control in the circuit synthesis (circuits with minimal and non-minimal argument for so-called CPEs [1], blocks and special types of transfer characteristics in fractional-order applications [2–4]). All circuits discussed in this paper offer commonly required benefits: (I) Grounded capacitors. (II) Minimal number of passive elements. (III) Simple active elements with minimal number of terminals, which are also easily commercially available. (IV) Full input and output separation (cascadability always possible, even simple matching to 50Ω in voltage-mode structures – required in RF chains). (V) Independence of input and output features (impedances) on electronic control (tuning). (VI) Independent/separated control of pole and zero frequency. (VII) Simple reconfiguration from “classical” AP section to bilinear (pseudo-AP) section.

The paper is organized as follows: Section 2 discusses design of all-pass/bilinear sections by help of SFG, where specific solutions are commented. Section 3 brings models for representation of active elements and computer analysis of selected solution.

Table 1
Detailed comparison of the most of hitherto published first-order voltage-mode all-pass solutions.

Ref	No. and type of active elements	No. of passive elements	Grounded C	All R grounded?	Type of control	Separate control of f_z and f_p	Reconfiguration between minimal and non-minimal argument	Full cascability	Frequency dependent input impedance ^a	Frequency dependent output impedance ^a	Input impedance dependent on parameter serving for control	Output impedance dependent on parameter serving for control	Separated low-impedance output
[14]	1 OTA, 1 VB	2	No	N/A	g_m	No	N/A	Yes	Yes	No	No	No	Yes
[15]	1 FB-VDBA	2	Yes	No	g_m	Possible ^a	N/A	Yes	No	No	No	No	Yes
[16]	2 OTA, 1 OPAMP	3	Yes	No	g_m	No	N/A	Yes	No	No	Yes	No	Yes
[17]	3 OTA	1	Yes	N/A	g_m	No	N/A	Yes	No	No	No	Yes	No
[18]	2 OTA	1	Yes	N/A	g_m	Yes ^b	N/A	Yes	No	No	No	Yes	No
[19]	6 OTA, 1 OPAMP ^c	3	Yes	No	g_m	No	N/A	Yes	No	No	No	No	Yes
[20]	2 OTA, 1 OPAMP	2(4) ^d	No	N/A	g_m	No	N/A	Yes	Yes	No	No	No	Yes
[21]	1 OTA, 1 DVB	1	Yes	N/A	g_m	No	N/A	Yes	No	No	No	No	Yes
[22]	1 VD-DIBA	1	Yes	N/A	g_m	No	N/A	Yes	No	No	No	No	Yes
[23]	1 VDIBA	1	No	N/A	g_m	No	N/A	Yes	Yes ^e	e	No	No	e
[24]	1 OTA, 1 VB	2	No	N/A	g_m	No	N/A	Yes	Yes	No	No	No	Yes
[25]	3 OTA	1	No	N/A	g_m	No	N/A	No	Yes	No	No	Yes	No
[26]	1 UVC, 1 OTA	1	No	N/A	g_m	No	N/A	Yes	No	No	No	No	Yes
[27]	1 VGC-MCFOA	4	Yes	No	V gain	No	N/A	Yes	No	No	No	No	Yes
[28]	1 CCCDTA	1	No	N/A	g_m, R_x	Yes ^f	N/A	No	Yes	Yes	Yes	No	No
[29]	2 DVCC	1	Yes	N/A	R_x	No	N/A	Yes	No	No	Yes	No	Yes
[30]	1 CC-VCIII	1	No	N/A	R_x	No	N/A	Yes	Yes	No	Yes	No	Yes
[31]	1 C-ICDBA	1	No	N/A	R_x	No	N/A	Yes	Yes	No	Yes	No	Yes
[32]	1 CCCII, 1 DVB	1	Yes	N/A	R_x	No	N/A	Yes	No	No	No	No	Yes
[33]	1 UVC	3	No	Yes	R_{eq}	No	N/A	Yes	No	No	No	No	Yes
[34]	1 CCCII, 1 OPAMP	1	No	N/A	R_x	No	N/A	Yes	No	No	No	No	Yes
[35]	IVB-ORC	1	No	N/A	R_x	No	N/A	Yes	No	No	No	Yes	No
[36]	2 DDCC	1	Yes	N/A	R_{eq}	No	N/A	Yes	No	No	No	No	Yes
[37]	1 UVC	1	No	N/A	R_{eq}	No	N/A	Yes	No	No	No	No	Yes
[38]	5 MOS transistors	1	No	N/A	R_{eq}	No	N/A	Yes	No	Yes	No	Yes	No
[39]	1 MO-CCCCTA	1	Yes	N/A	R_x, g_m	No	N/A	No	No	No	Yes	No	No
[40]	2 DVCC	2	Yes	Yes	N/A	No	N/A	Yes	No	No	No	No	Yes
[41]	FDCCII	2	Yes	Yes	R_{eq}	No	N/A	No	No	Yes	No	Yes	No
[42]	2 DVCC	3	Yes	Yes	N/A	No ^g	N/A	No	No	Yes	No	Yes	No
[43]	2 DVCC	2	Yes	Yes	N/A	No	N/A	Yes	No	No	No	No	Yes
Proposed													
Fig. 1	2 OTA, 1 DVB	1	Yes	N/A	g_m	Yes	Yes	Yes	No	No	No	No	Yes
Fig. 2	2 OTA, 1 DVB	1	Yes	N/A	g_m	Yes	Yes	Yes	No	No	No	No	Yes

Abbreviations: CCCII, current-controlled-second-generation current conveyor; CC-VCIII, current controlled third-generation voltage conveyor; C-ICDBA = CMOS controlled inverting Current differencing buffered amplifier; DDCC, differential difference current conveyor; DVB, differential voltage buffer; DVCC, differential voltage current conveyor; FB-VDBA, fully balanced voltage differencing buffered amplifier; FDCCII, fully differential current conveyor of second generation; IVB-ORC, inverting voltage buffer with output resistance control – similar to R_x ; MO-CCCCTA, multiple-output current controlled current transconductance amplifier; OPAMP, operational amplifier; OTA, operational transconductance amplifier; UVC, universal voltage conveyor; VB, voltage buffer; VD-DIBA, voltage differencing-differential input buffered amplifier; VDIBA, voltage differencing inverting buffered amplifier; VGC-MCFOA, voltage gain-controlled modified current feedback amplifier.

g_m – transconductance(s).

R_{eq} – electronically controllable resistance equivalent(s).

R_x – intrinsic current input resistance(s).

N/A – not available, not tested.

^a means that input/output high-impedance node is connected to capacitor (grounded or floating in feedback).

^a Possible in case of electrical replacement of resistor.

^b Possible in form: $K(s) = g_{m1}/g_{m2}(sC \pm g_{m2})/(sC + g_{m1})$.

^c Complicated solution requires floating capacitance multiplier – several additional OTAs required.

^d Differential solution requires four floating capacitors.

^e One output is frequency dependent high-impedance node, the second is low-impedance output; impact on frequency dependence of input impedance is critical for low values of real z-terminal resistance.

^f Separated control f_p, f_z possible in [28] but not tested.

^g Separated control of f_z only is possible by value of resistor or capacitor in some cases, pole frequency change influences also zero frequency.

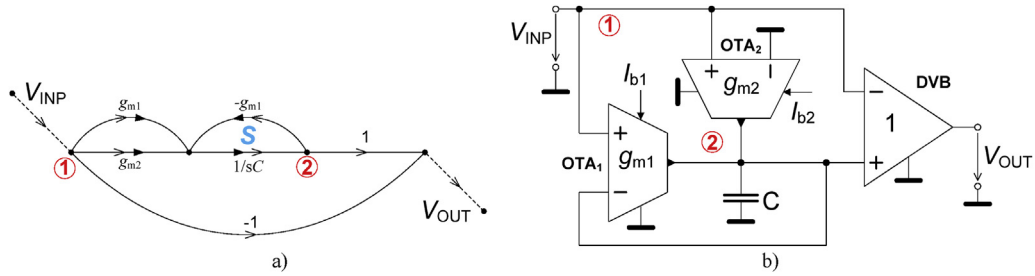


Fig. 1. AP/bilinear section with separated zero and pole frequency control: (a) SFG, (b) its circuit realization.

Section 3 includes also application in presetable phase shifter, proves independent zero and pole frequency control and example of utilization of selected structure in system with constant phase character. Experimental results are presented in Section 4. Some examples of tolerance analysis, variation of conditions (supply voltage) and nonlinear effects on selected solution are presented in Section 5. Concluding remarks and summary is provided in Section 6.

2. Electronically adjustable AP/bilinear transfer sections

Solutions of AP section presented in [21,32] inspired our work and allowed to introduce interesting structure. Authors use so-called diamond transistor (DT) and differential voltage buffer (DVB) in their solutions. DVB is very important active element for this synthesis. However, separated control of pole and zero frequency was not supposed in [21,32]. Simultaneous control is suitable for AP filter-based applications (phase shifters). However, it is not sufficient for some special purposes [1–4]. Special magnitude and phase frequency responses suitable for advanced circuit synthesis of CPE and fractional systems are available from AP or bilinear/pseudo-AP (positive sign between absolute and linear coefficient of the numerator – zeros are in left half-plane of complex space) response, if zero frequency (ω_z, f_z) is adjustable separately from pole frequency (ω_p, f_p). Solutions in Figs. 1 and 2 have this feature. Transfer function was obtained by using of Mason rule [8,9] and for this type of circuit (Fig. 1) is very simple:

$$K_{AP1}(s) = \frac{g_{m2} - sC}{g_{m1} + sC}, \tag{1}$$

where $\omega_z = g_{m2}/C$ and $\omega_p = g_{m1}/C$ (and s is complex frequency). The circuit with minimal argument is available, if transfer constant (g_{m2}) of OTA_2 is negative (interchanged inputs). Interchange of the DVB inputs is also necessary for positive transfer. Matching of $g_{m1} = g_{m2}$ is required for operation of the each section just as pure AP filter. However, our goal is a solution with mutually independent controllable zero and pole frequency for utilization in special synthesis as will be explained in application example.

Separated electronic adjusting of the zero and pole frequency is also possible in structure in Fig. 2. Its transfer function has a form:

$$K_{AP2}(s) = \frac{g_{m1} - sC}{g_{m2} + sC}, \tag{2}$$

where the zero and pole frequency can be respectively expressed as $\omega_z = g_{m1}/C$ and $\omega_p = g_{m2}/C$. Interchange of polarity of inputs of the OTA_1 causes transposition of zeros to the left half-plane of complex space (circuit with minimal argument), but overall sign of the Eq. (2) is then negative (interchange of DVB inputs is required for positive transfer). Advantage of the second solution consists in less complicated structure of loops (see SFGs in Figs. 1 and 2).

3. Application examples of presented AP/bilinear transfer section

3.1. Models of active elements

Practical verification and utilization of discussed circuits require proper models of active elements. All circuits presented in previous chapter are based on single-output OTAs and DVB. We used transistor models of TSMC LO EPI 0.18 μm technology [44] to establish following simulation models. Basic dual-input and dual-output transconductor (OTA-DIDO) uses common internal structure [6], which is shown in Fig. 3a, where I_b is bias current and aspect ratios of used CMOS transistors are included. DVB block was implemented by very useful active element (in fact based on OTA), the so-called voltage differencing inverted buffered amplified (VDIBA) [23], see Fig. 3b. Modified version with better low-impedance output features is shown in Fig. 3c.

All features of the models were achieved for $V_{CC} = \pm 0.9\text{V}$. The important input resistance of both OTA and DVB is very high $R_{in} \rightarrow \infty$. Transconductance of the OTA (Fig. 3a) changes approximately between 60 μS and 1 mS by bias current (I_b) adjusted from 5 to 235 μA . It changes also bandwidth (-3 dB) from 21 to 164 MHz and also output resistance from 1.4 M Ω to 90 k Ω . Input linear dynamical range is limited to $\pm 100\text{mV}$ due to the low-voltage

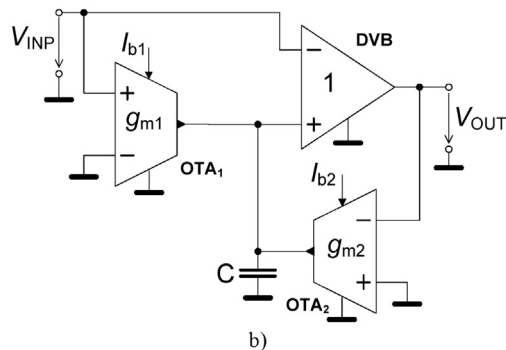


Fig. 2. AP/bilinear section with separated zero and pole frequency control (reduced complexity of branches): (a) SFG, (b) circuit realization.

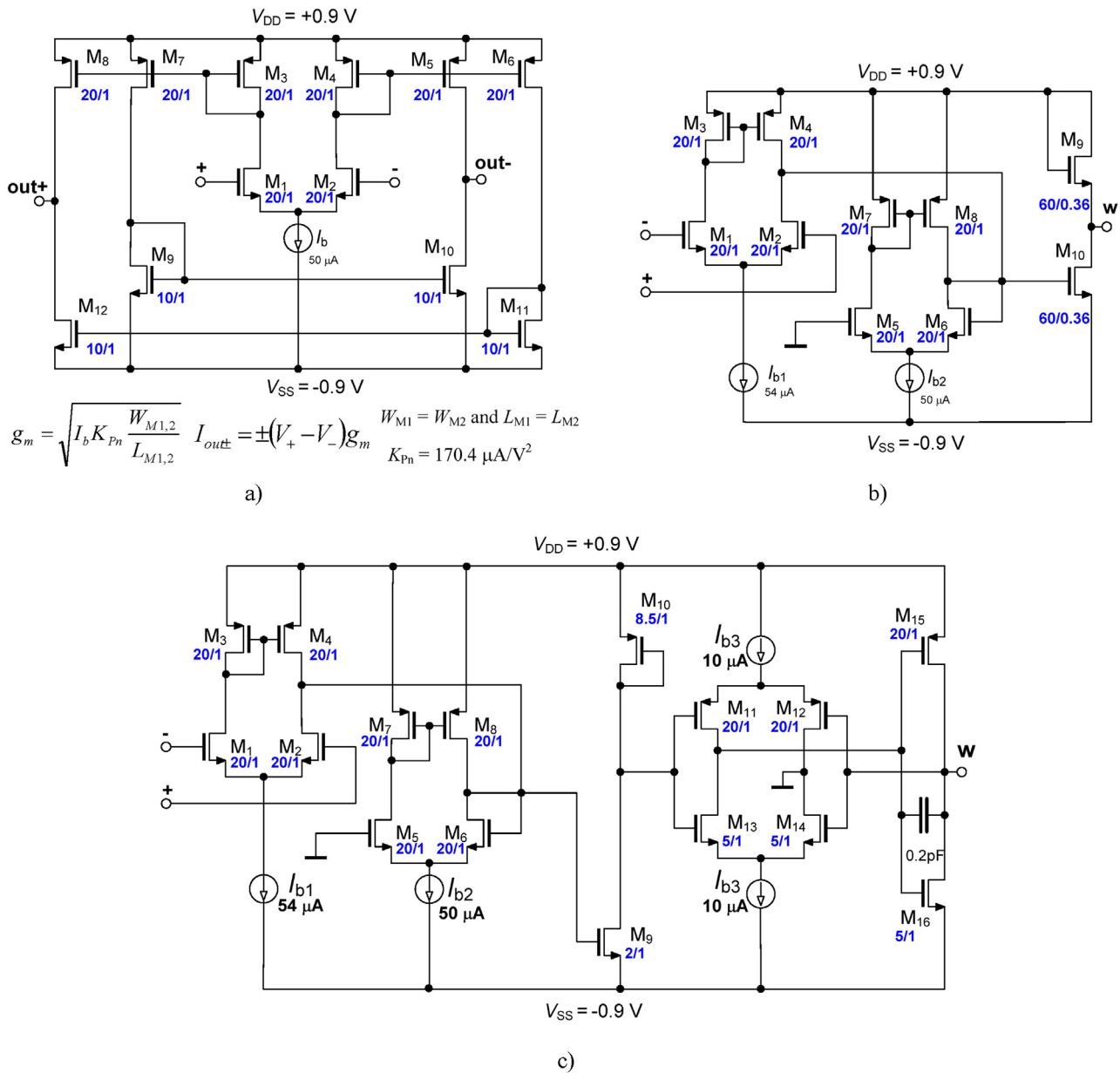


Fig. 3. Simulation models of active elements which are necessary for discussed constructions: (a) OTA-DIDO, (b) DVB type 1, (c) DVB type 2.

CMOS technology and nonlinearity of the basic OTA concept. Transit frequency of the DVB (Fig. 3b) is 195 MHz. Dynamical range is also about ± 100 mV. Output resistance (R_w) of the DVB achieves value over 70Ω . It is possible to decrease this value, but aspect ratios (ratio of W/L of M_9 and M_{10}) are very high for low R_w and it causes increasing of transistor dimensions. Note that the modified DVB from Fig. 3c achieves lower output impedance about $\approx 6 \Omega$.

3.2. Adjustable phase shifter

We used model of the OTA and DVB (Fig. 3a and b) in these simulations. We selected AP/bilinear solution in Fig. 1b and values of $C = 47$ pF and $f_z = f_p = 1.693$ MHz (ideal value) for $g_{m1} = g_{m2} = g_m = 500 \mu\text{S}$ ($I_b = I_{b2} = I_b = 66 \mu\text{A}$). The zero and pole frequency obtained from simulation was $f_z = f_p = 1.658$ MHz. Adjustability of the phase shifter was verified by simultaneous change of both

$g_{m1} = g_{m2} = g_m$ from $100 \mu\text{S}$ to 1 mS by bias current ($I_b = I_{b2} = I_b$) between 9 and $235 \mu\text{A}$. Graphical results are in Fig. 4.

3.3. Separated zero and pole frequency control

Separated adjustability of the zero (f_z) and pole (f_p) frequency in circuit from Fig. 1b was verified by using models of two OTAs and DVB from Fig. 3a (negative output of the OTA-DIDO was grounded) and Fig. 3b. Adjusting of the zero frequency is also observed in Fig. 5a and control of pole frequency is documented in Fig. 5b. Phase responses have similar form as results in Fig. 4b (tunability range is lower).

Interchange of inputs of OTA_2 (g_{m2}) from Fig. 1b and inputs of DVB (in order to achieve positive transfer) leads to transfer with minimal argument, which can be used for special applications such as modeling of transfer lines, CPEs, or fractional-order circuits synthesis [1–4]. Phase responses are depicted in

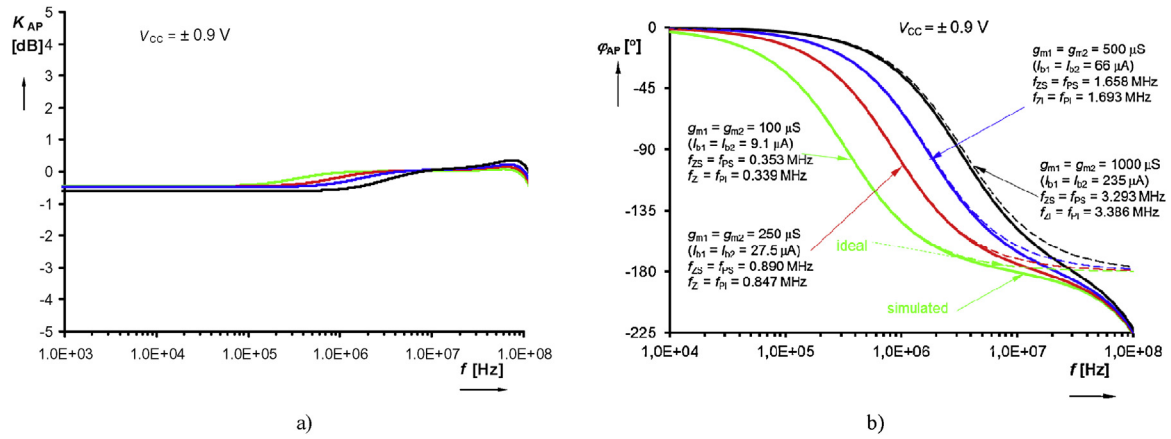


Fig. 4. Simultaneous adjusting of the zero and pole frequency of the AP section: (a) magnitude responses, (b) phase responses.

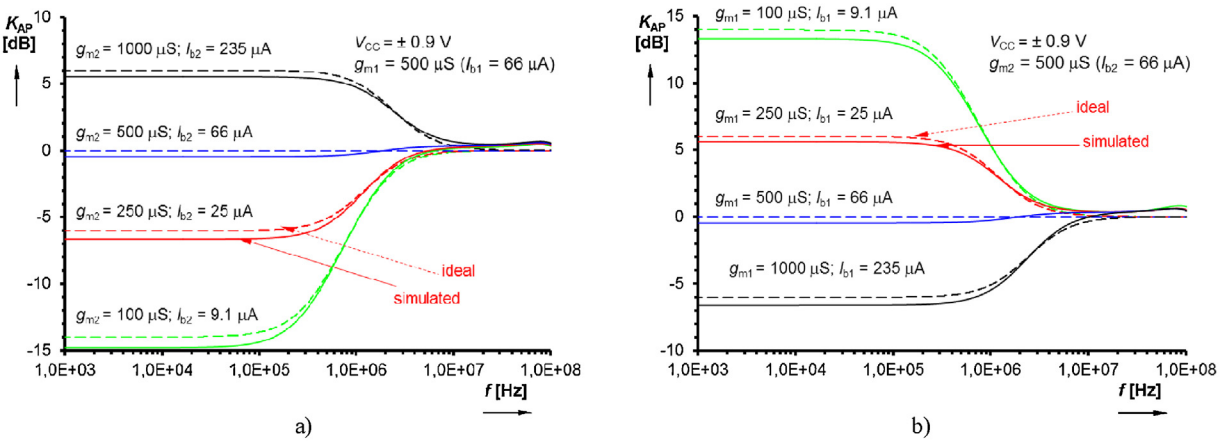


Fig. 5. Separated control of parameters of transfer section – magnitude responses: (a) zero frequency, (b) pole frequency.

Fig. 6. Magnitude responses are the same as results shown in Fig. 5.

3.4. Example of the constant phase two-port block

Proposed two-port blocks with separately adjustable zeros and poles (Fig. 1) can be used in so-called CPE structures [1,4] (and references cited therein) generating constant phase shift (45° , in our case the so-called half integrator; ideal symbolical transfer: $K_{CPE}(s) = k_0 s^{-0.5}$ – typical building block with fractional order character) in specified frequency range. Such two-port transfer function

(consisting of cascade connection of first-order sections) has following obvious approximating mathematical expression [4]:

$$K_{CPE_approx}(s) = \frac{\prod_{i=1}^m (s - z_i)}{\prod_{j=1}^n (s - p_j)} = \frac{\sum_{i=1}^m a_i s^i}{\sum_{j=1}^n b_j s^j} \quad \left. \begin{matrix} \\ \\ \\ \end{matrix} \right|_{z_i, p_j \in \mathbb{R}} \quad (3)$$

Our example that is shown in Fig. 7a requires five sections from Fig. 1b (see Fig. 7b for exact connection), where DVB from Fig. 3c was

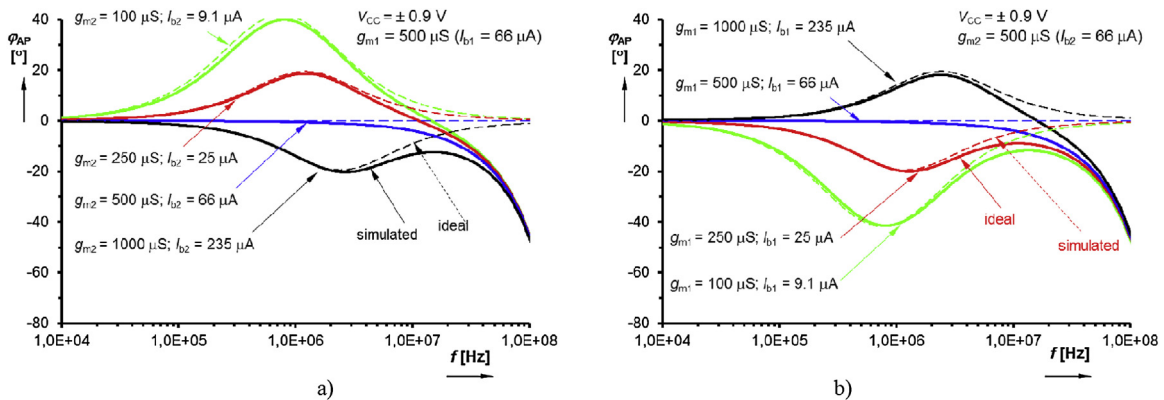


Fig. 6. Separated control of parameters of transfer section – phase responses: (a) zero frequency, (b) pole frequency.

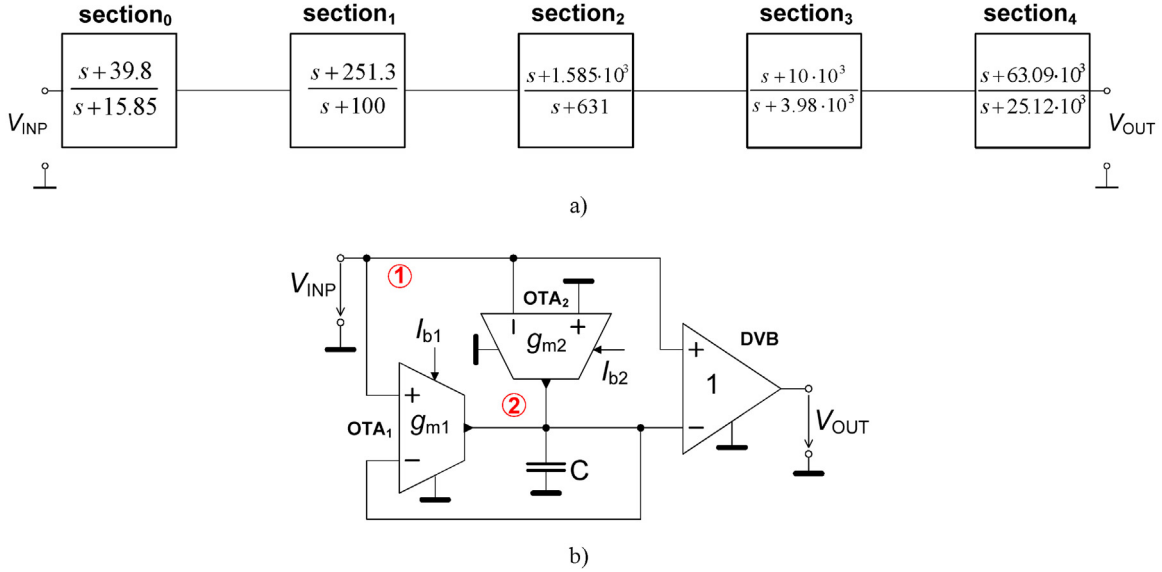


Fig. 7. Synthesis of CPE structure: (a) chain of 1st order transfer sections, (b) one transfer section utilizing circuit from Fig. 1b.

used. Therefore, final transfer function has total of five zeros and the same number of the poles. We used approximation (Oustaloup's method) discussed in Ref. [45] and established following semi-symbolical transfer function:

$$K_{CPE_approx}(s) = \left(\frac{s+39.8}{s+15.85} \right) \left(\frac{s+251.3}{s+100} \right) \left(\frac{s+1.585 \cdot 10^3}{s+631} \right) \times \left(\frac{s+10 \cdot 10^3}{s+3.98 \cdot 10^3} \right) \left(\frac{s+63.09 \cdot 10^3}{s+25.12 \cdot 10^3} \right), \quad (4)$$

where it is possible to find all zeros and poles located to the left-half-plane of complex space. The zeros and poles are located at frequencies: $f_{z1} = 6.3$ Hz, $f_{z2} = 40$ Hz, $f_{z3} = 252$ Hz, $f_{z4} = 1.591$ kHz, $f_{z5} = 10.04$ kHz; $f_{p1} = 2.5$ Hz, $f_{p2} = 15.9$ Hz, $f_{p3} = 100.4$ Hz, $f_{p4} = 633.4$ Hz, $f_{p5} = 4$ kHz. We selected working capacitor of each section (Fig. 7b) as (taken from the left side in Fig. 7a) $C_1 = 1$ μ F, $C_2 = 680$ nF, $C_3 = 100$ nF, $C_4 = 68$ nF, $C_5 = 10$ nF. Each next section was connected to the output of the previous section by AC coupling (10 μ F capacitor) in order to avoid the influence of the DC offset (limitation/saturation of section for reason of high gain). Relatively simple calculation allows determining of g_{m2} (zero) and g_{m1} (pole) values for each section as (see Eq. (1); signs in numerator and denominator are positive for circuit in Fig. 7b now): section₀ – $g_{m2} = z_0 \cdot C_1 = 39.8 \cdot 1 \cdot 10^{-6} = 39.8$ μ S, $g_{m1} = p_0 \cdot C_1 = 15.85 \cdot 1 \cdot 10^{-6} = 15.85$ μ S; section₁ – $g_{m2} = 171$ μ S, $g_{m1} = 68$ μ S; section₂ – $g_{m2} = 158.5$ μ S, $g_{m1} = 63.1$ μ S; section₃ – $g_{m2} = 680$ μ S, $g_{m1} = 271$ μ S; section₄ – $g_{m2} = 631$ μ S, $g_{m1} = 251$ μ S. The bias control current (setting of $g_{m1,2}$ of each section) was adjusted carefully to set exact zeros and poles location (electronically) in following values (again from the left side): section₀ – $I_{b2} = 3.16$ μ A, $I_{b1} = 1.195$ μ A; section₁ – $I_{b2} = 5.61$ μ A, $I_{b1} = 15.95$ μ A; section₂ – $I_{b2} = 5.18$ μ A, $I_{b1} = 14.5$ μ A; section₃ – $I_{b2} = 28.17$ μ A, $I_{b1} = 110.3$ μ A; section₄ – $I_{b2} = 25.55$ μ A, $I_{b1} = 96.9$ μ A. The important results of AC analysis are summarized in Fig. 8 where magnitude and phase responses are shown. The approximation of constant phase characteristic is valid approximately from 20 Hz to 1.17 kHz (obtained phase shift is about 43° with ripple 2.5°), which is close to theory. Overall phase ripple and frequency features depend on number of used first-order transfer sections, their properties and type of approximation. Complex CPE chain is very

suitable for possible synthesis of IC form. Appropriate design of active elements with reduced or eliminated temperature dependence together with minimized fabrication mismatch of g_m -s and other parameters may ensure sufficiently accurate setting of zeros and poles locations in CPE approximation.

4. Laboratory results

A modification done by SFG of circuit from Fig. 1a is depicted in Fig. 9a. SFG was modified to obtain phase shifter with voltage controllable parameters (zero and pole frequency). This modification was established because of experimental verification by commercially available active elements and contains two adjustable voltage amplifiers VCA610 [46], diamond transistor OPA660 [47], and voltage differential amplifier AD830 [48], see Fig. 9b. Modified transfer function has a form:

$$K_{AP}(s) = \frac{V_{OUT}}{V_{INP}} = \frac{\frac{A_2}{RC} - s}{\frac{A_1}{RC} + s}, \quad (5)$$

where the voltage gain is $A = 10^{-2(V_C+1)}$ [46]. Therefore, we can rewrite (5) as:

$$K_{AP}(s) = \frac{V_{OUT}}{V_{INP}} = \frac{\frac{10^{-2(V_{C2}+1)}}{RC} - s}{\frac{10^{-2(V_{C1}+1)}}{RC} + s}, \quad (6)$$

from which zero and pole frequencies are $\omega_z = \frac{10^{-2(V_{C2}+1)}}{RC}$, $\omega_p = \frac{10^{-2(V_{C1}+1)}}{RC}$.

Parameters of the circuit in Fig. 9 are following: $R = 100$ Ω , $C = 1$ nF. Measured magnitude and phase response for $A_1 = A_2 = 0.1$ ($V_{C1} = V_{C2} = 0.5$ V) are available in Fig. 10. Supply voltage was ± 5 V. Ideal $f_p = f_z$ frequency has value 159 kHz, measured value equal to 145 kHz was obtained.

Simultaneous control of f_z and f_p ($V_{C1} = V_{C2} = V_C$) allows tuning of the phase shifter by very easy way. Voltage gains (A) were adjusted approximately from 0.01 to 2.5 by DC voltage V_C changed from -0.1 to -1.2 V (control voltage is negative [46]). Achieved values of zero/pole (simultaneous control) frequency are summarized in Fig. 11. Active elements used for construction of the phase shifter have quite low gain-bandwidth (GBW), therefore, higher

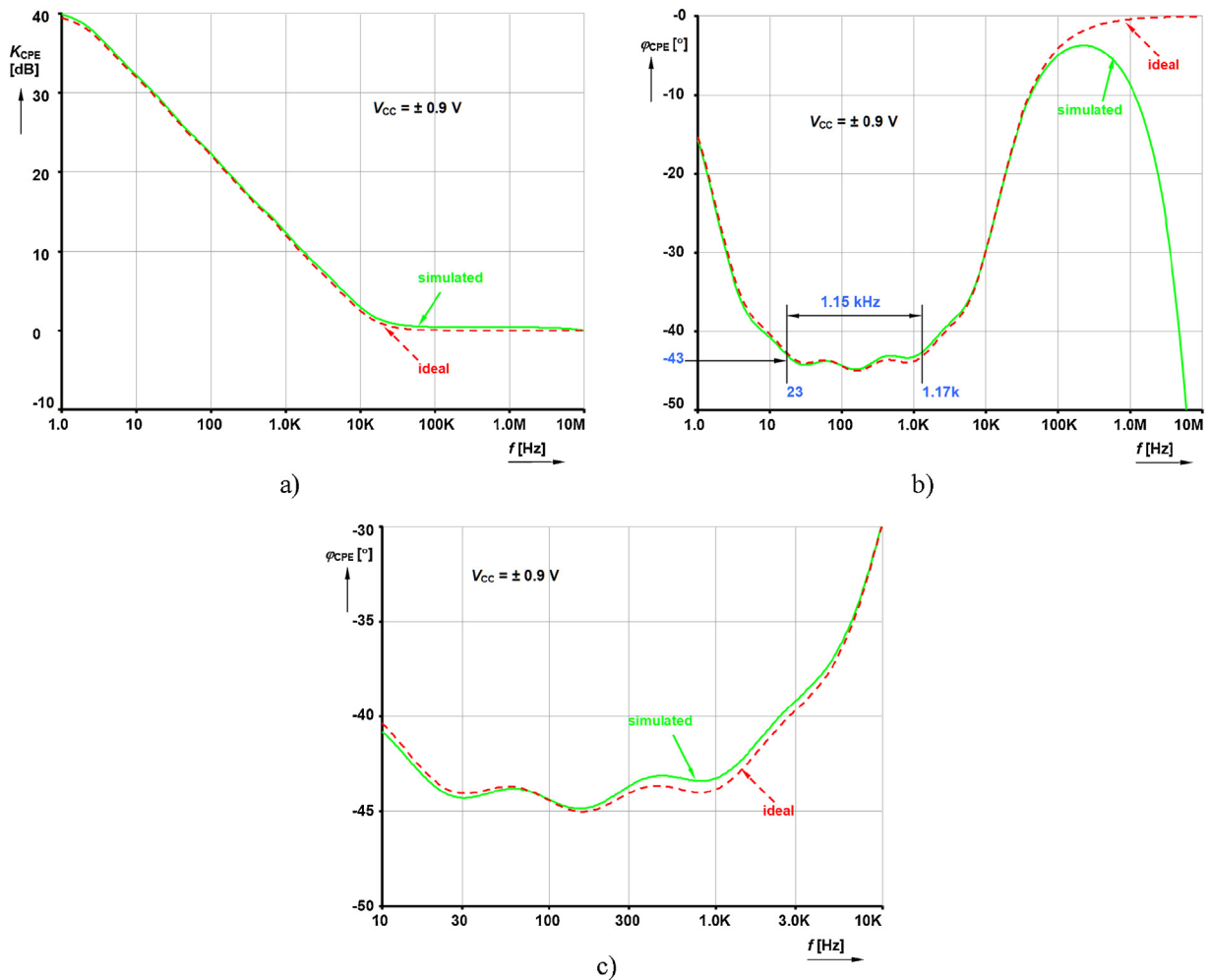


Fig. 8. Simulated results of CPE structure: (a) magnitude response, (b) phase response, (c) detail of useful bandwidth.

difference between ideal and measured results at higher frequencies was expected. Results confirm this fact.

Separated control of the zero and pole frequency was also verified and results are shown in Fig. 12. One DC control voltage was kept constant while second was changed through several discrete values.

During measurement we used HP4395A and Agilent E5071C vector network/spectrum analyzers. Many results were recorded starting from 10 kHz, because it is the lowest frequency measured by the E5071C analyzer. Provided analyzes confirmed our intention to design controllable (zero and pole frequency) transfer section.

5. Analysis of real influence on performances of selected AP/bilinear example

5.1. Monte Carlo analysis

We simulated process variation of main parameters of circuit in Fig. 1b in two situations. The first results are provided by behavioral models of transconductors and DVB with controlled sources (voltage controlled current source, voltage controlled voltage source) for PSpice, where impact of both g_m -s and non-unity-gain tracking of DVB (uncorrelated) are taken into account. Results were prepared

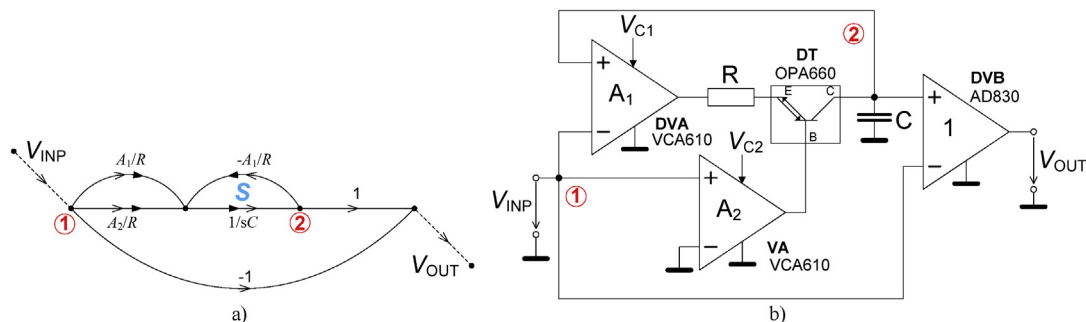


Fig. 9. Voltage controllable prototype of the circuit from Fig. 1: (a) SFG, (b) circuit realization.

Table 2
Monte Carlo tolerance analysis results (AP from Fig. 1b) – behavioral models of transconductors and DVB.

Analysis type	Tol. g_{m1} [%]	Tol. g_{m2} [%]	Tol. voltage follower [%]	Tol. C [%]	$f_{p,min}$ [kHz] ($g_{m1,2} = 100 \mu S$)				$f_{p,max}$ [kHz] ($g_{m1,2} = 1000 \mu S$)			
					Mean	Min	Max	Sigma	Mean	Min	Max	Sigma
Nominal	–	–	–	–	339	–	–	–	3386	–	–	–
Monte Carlo (Gaussian, 1000 runs)	5	5	5	1	339	299	376	12	3388	2992	3765	122
	5	5	5	5	340	276	417	21	3404	2762	4167	205
	10	10	10	5	340	247	443	29	3399	2473	4427	289
	10	10	30	5	340	247	443	29	3400	2473	4427	289
	20	20	20	5	338	182	506	51	3377	1816	5060	505

Table 3
Monte Carlo tolerance analysis results (AP from Fig. 1b) – CMOS models of transconductors and DVB.

Analysis type	Tol. I_{b1} [%]	Tol. I_{b2} [%]	Tol. C [%]	$f_{p,min}$ [kHz] ($I_{b1,2} = 9.1 \mu A$)				$f_{p,max}$ [kHz] ($I_{b1,2} = 235 \mu A$)			
				Mean	Min	Max	Sigma	Mean	Min	Max	Sigma
NOMINAL	–	–	–	353	–	–	–	3295	–	–	–
Monte Carlo (Gaussian, 1000 runs)	5	5	1	353	321	388	11	3295	3135	3470	57
	5	5	5	355	304	424	20	3309	2867	3852	165
	10	10	1	353	286	419	21	3291	2968	3597	102
	10	10	5	354	283	443	27	3305	2841	3937	183
	20	20	5	352	202	501	46	3284	2383	4093	253

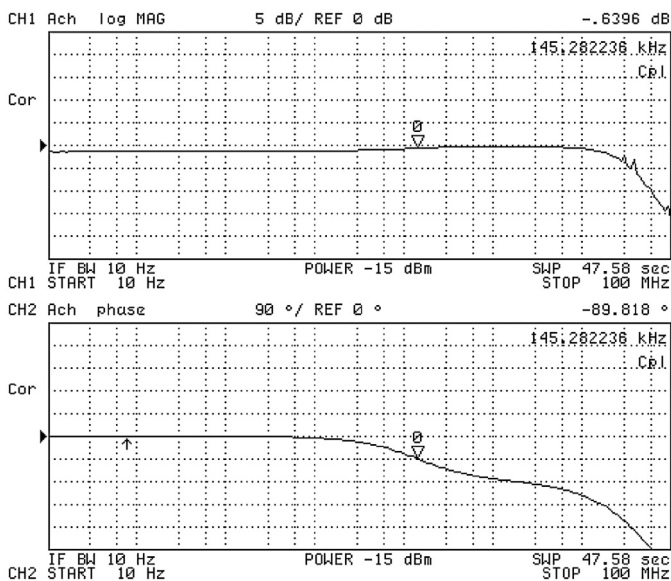


Fig. 10. Measured magnitude and phase response of the phase shifter ($V_{C1,2} = 0.5 V$).

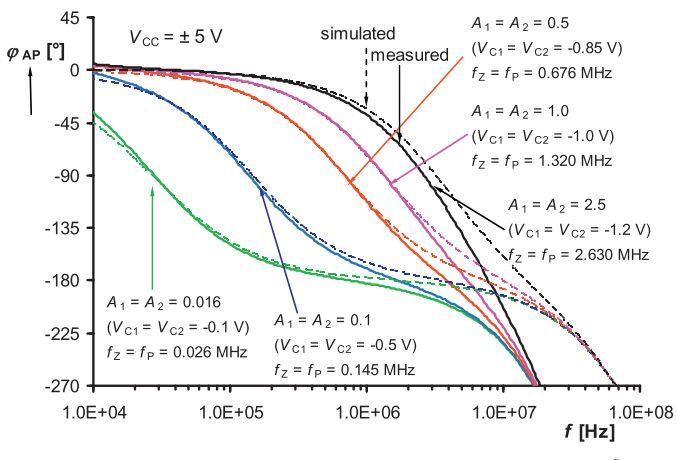


Fig. 11. Comparison of simulated and measured phase responses in case of adjusting of the phase shifter.

for both corners of $f_{p,z}$ ($g_{m1,2} = 100$ and $1000 \mu S$, $C = 47 pF$ – nominal values) and they are given in **Table 2** for initial comparison. Therefore, subject of our attention are real influences (inaccuracies and tolerances) in discussed tuning range. Accuracy of pole/zero frequency is mainly given by tolerance of both transconductances and capacity value uncertainty, as is expected.

The most important fact seems to be minimal influence of tracking error of DVB, see bold values in **Table 2**. Therefore we can omit this parameter from further analysis. **Table 3** shows results of analyses, where results were performed by simulations with presented CMOS models. Values of bias currents (I_{b1} , I_{b2}) for g_m control and capacitance were varied by Gaussian distribution in noted tolerance intervals. The third line of **Table 3** is documented graphically as example. Illustrative example of magnitude and phase responses together with histograms are given in **Figs. 13 and 14**.

5.2. Variation of supply voltage

We tested also impact of supply voltage on AC performances and both corners of tuning range, see **Fig. 15**. Filter operates from $V_{CC} = V_{DD} = -V_{SS} = 0.4 V$ at low corner of tuning range. If supply voltage is increased from 0.4 to 1.2 V, frequency changes from 323 to 368 kHz. In the second case (high corner of tuning range) is situation slightly worse. CMOS transistors in transconductance amplifiers pass into different regime than required saturation for lower values of V_{CC} due to high value of bias currents $I_{b1,2}$. Voltage 0.7 V and higher seems to be sufficient for correct operation. Insufficient features for lower supply voltages than 0.7 V are evident from **Fig. 15b** (see red arrow). Pole/zero frequency varies from 3.21 to 3.37 MHz in this corner of tunability range for voltage from 0.7 to 1.2. Important impact of supply voltage also causes obvious problems with available dynamical range. Nominal supply voltage allows input voltage about 200 mV_{p-p} maximally (higher input levels cause substantial limitation and distortion of output voltage). Supply voltage has to be at least $\pm 0.5 V$ to ensure operation with this input level. As conclusion, we have to ensure that supply voltage does not drop under $\pm 0.7 V$ for correct operation of the AP.

5.3. Dynamic features including intermodulation products

We studied also dynamic range under conditions of two signal voltage sources of signals with slightly different frequencies ($f_1 = 1.6 MHz$, $f_2 = 1.65 MHz$ – selected around pole/zero frequency

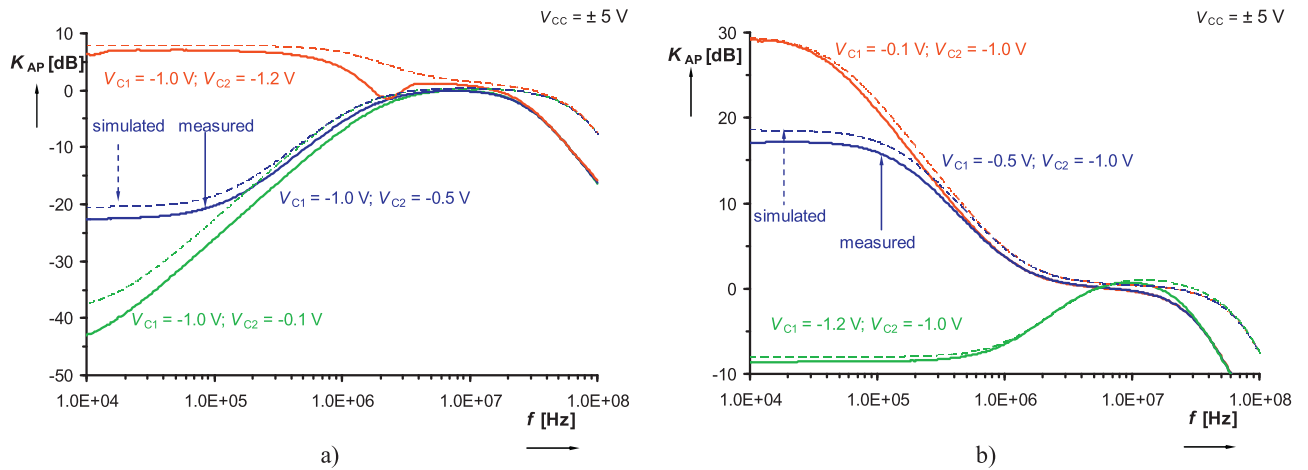


Fig. 12. Measured and simulated magnitude responses for separate control of: (a) zero frequency, (b) pole frequency.

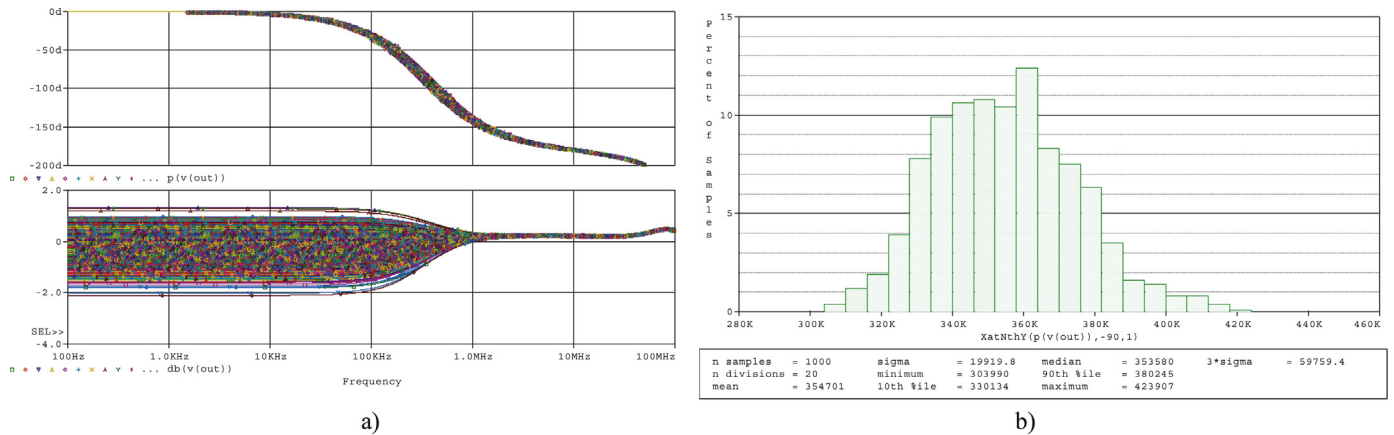


Fig. 13. Monte Carlo simulation: (a) frequency responses (phase and magnitude), (b) histogram of pole/zero frequency ($I_{b1,2} = 9.1 \mu A, f_{p,min} = 353$ kHz) variation.

at 1.658 MHz for $I_{b1,2} = 66 \mu A$ and equal amplitudes to obtain dynamic features including nonlinearity. Matching to 50Ω is easily provided due to beneficially high input and low output impedance of proposed AP (Fig. 1b). Intermodulation product (IM_3) is expected as $2f_2 - f_1 = 1.7$ MHz. Input amplitude varied from 10 to 200 mV.

Results in power scale (effective/RMS value of voltages recalculated to dBm) are shown in Fig. 16. Selected AP solution in Fig. 1b achieves IIP_3 value about -1 dBm. Similar analysis is not commonly available in recent works in the field but it can be also very useful for designers.

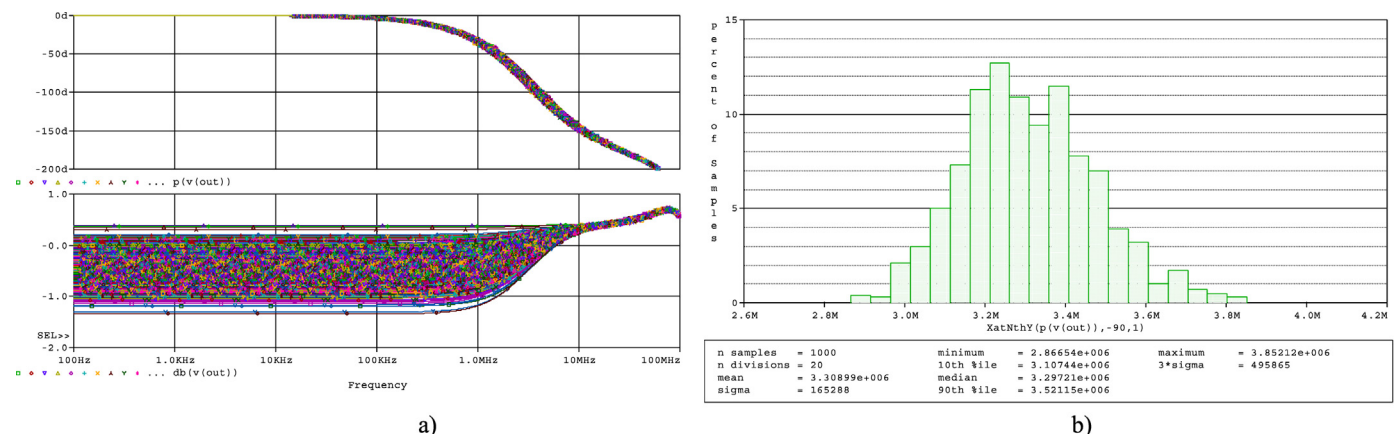


Fig. 14. Monte Carlo simulation: (a) frequency responses (phase and magnitude), (b) histogram of pole/zero frequency ($I_{b1,2} = 235 \mu A, f_{p,min} = 3309$ kHz) variation.

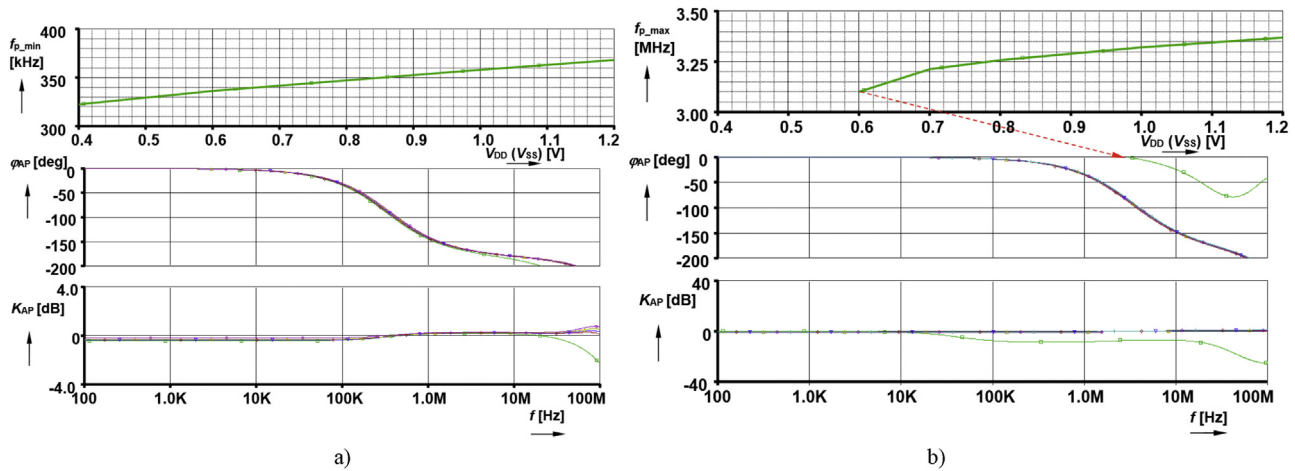


Fig. 15. Supply voltage dependence of pole/zero frequency for: (a) the lowest corner, (b) the highest corner. (For interpretation of the references to color in this figure legend, the reader is referred to the web version of this article.)

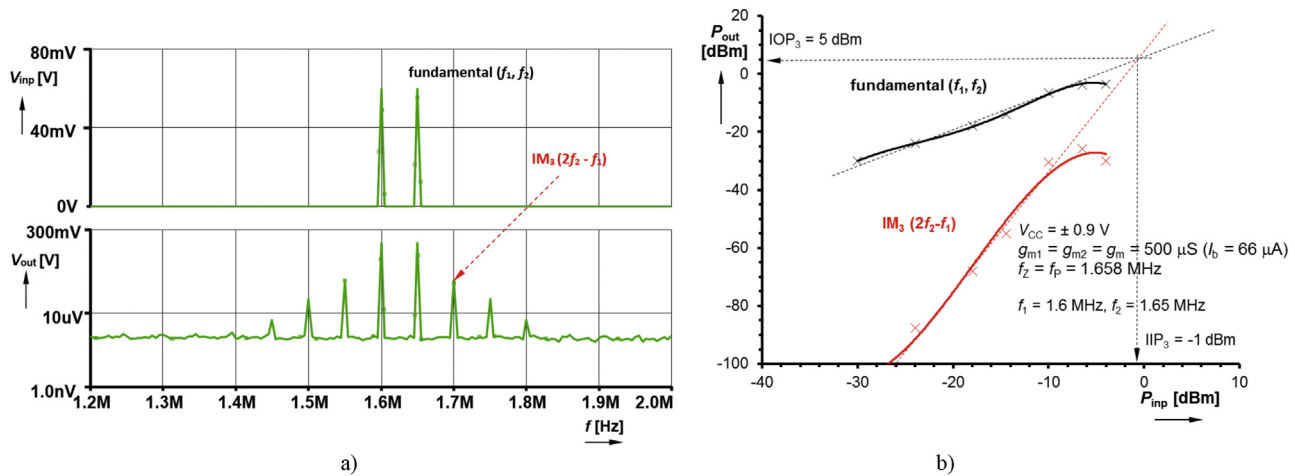


Fig. 16. Dynamic features of the AP including intermodulation products: (a) spectrum detail on fundamental and higher-order products, (b) determination of intercept point for specific case of simulated model.

6. Conclusion

The SFGs were used to demonstrate design and transfers inside loop of AP and general bilinear transfer sections with OTAs and differential voltage buffer. Designed circuits offer all commonly required features that are: (i) simple electronic control, (ii) input and output features suitable for cascading, (iii) grounded capacitors, and (iv) separated control of zero and pole frequency with simple availability of their migration between minimal and non-minimal argument circuit's character especially. Note that simple interchanges of current output polarity or voltage inputs of used active elements allow to design transfers, where zeros are located in left half-plane of complex space in comparison to true (general) AP section, where zeros are located in right half-plane. Separated zero and pole frequency control in AP (bilinear section) allows design of special circuits which generate constant phase shift between output and input voltage and synthesis of fractional-order dynamical systems. Selected AP/bilinear section was verified experimentally in all regimes of operation (simultaneous and separated control of pole/zero frequency). CPE could be implemented by discrete (commercially available) devices. However, the best possible way of its implementation seems to be in CMOS technology. In this case, active elements are simpler than in case of discrete form. In addition, IC implementation of whole CPE system (chain of five subsections) is less impacted by real influences of parasitic factors.

Acknowledgements

Research described in this paper was financed by the National Sustainability Program under grant LO1401 and by the Czech Science Foundation under grant No. GP14-24186P. For the research, infrastructure of the SIX Center was used. Grant No. FEKT-S-14-2281 also supported this research. The support of the project CZ.1.07/2.3.00/20.0007 WICOMT, financed from the Operational Program Education for Competitiveness, is gratefully acknowledged.

References

- [1] Valsa J, Vlach J. RC models of a constant phase elements. *Int J Circuit Theory Appl* 2013;41(1):59–67.
- [2] Radwan AG, Elwakil AS, Soliman AM. Fractional-order sinusoidal oscillators: design procedure and practical examples. *IEEE Trans Circuits Syst* 2008;55(7):2051–63.
- [3] Radwan AG, Elwakil AS, Soliman AM. First-order filters generalized to the fractional domain. *J Circuits Syst Comput* 2008;17(1):55–66.
- [4] Petrzela J. Fundamental analog cells for fractional-order two-port synthesis. In: *Proceedings of 23rd international conference radioelektronika 2013*. 2013. p. 182–7.
- [5] Bielek D, Senani R, Biolkova V, Kolka Z. Active elements for analog signal processing: classification, review, and new proposal. *Radioengineering* 2008;17(4):15–32.
- [6] Geiger RL, Sanchez-Sinencio E. Active filter design using operational transconductance amplifiers: a tutorial. *IEEE Circuits Devices Mag* 1985;1:20–32.

- [7] Fabre A, Saaid O, Wiest F, Boucheron C. High frequency applications based on a new current controlled conveyor. *IEEE Trans Circuits Syst* 1996;43(2):82–91.
- [8] Mason SJ. Feedback Theory: Further properties of signal flow graphs. *Proc IRE* 1956;44(7):920–6.
- [9] Coates CJ. Flow-graph solution of linear algebraic equations. *IRE Trans Circuit Theory* 1959;6(2):170–87.
- [10] Dostal T. All-pass filter in current mode. *Radioengineering* 2005;14(3):48–53.
- [11] Chang CM, Hou CL, Chung WY, Horng JW, Tu CK. Analytical synthesis of high-order single-ended-input OTA-grounded C all-pass and band-reject filter structures. *IEEE Trans Circuits Syst* 2006;53(3):489–98.
- [12] Chang CM, Al-Hashimi BM. Analytical synthesis of current-mode high-order OTA-C filters. *IEEE Trans Circuits Syst* 2003;50(9):1188–92.
- [13] Tsukutani T, Higashimura M, Ishida M, Tsuiki S, Fukui Y. A general class of current-mode high-order OTA-C filters. *Int J Electron* 1996;81(6):663–9.
- [14] Jovanovic GS, Mitic DB, Stojcev MK, Antic DS. Phase-synchronizer based on gm-C all-pass filter chain. *Adv Electric Comput Eng* 2012;12(1):39–44.
- [15] Biolek D, Biolkova V, Kolka Z. All-pass filter employing fully balanced voltage differential buffered amplifier. In: *Proceedings of the international conference LASCAS2010*. 2010. p. 232–5.
- [16] Das BP, Watson N, Liu Y. Simulation of voltage controlled tunable all-pass filter using LM13700 OTA. *World Acad Sci Eng Technol* 2010;2010(44):560–4.
- [17] Kumngern M, Chanwutitum J, Dejhan K. Electronically tunable voltage-mode all-pass filter using simple CMOS OTAs. In: *International symposium on communications and information technologies ISCIT2008*. 2008. p. 1–5.
- [18] Kushar K, Varun K. Resistor less voltage mode first order all pass filter employing grounded capacitor. *VSRD Int J Electric Electron Commun Eng* 2012;2(1):22–6.
- [19] Das BP, Watson N, Liu Y. Wide tunable all pass filter using OTAs as active component. In: *Proceedings of international conference on signals and electronics systems*. 2010. p. 379–82.
- [20] Acosta L, Ramirez-Angulo J, Martin-Lopez AJ, Carvajal RG. Low-voltage first-order differential CMOS all-pass filter with programmable pole-zero. *Electron Lett* 2009;45(8):385–6.
- [21] Keskin AU, Pal K, Hancioglu E. Resistorless first-order filter with electronic tuning. *AEU Int J Electron* 2008;62(4):304–6.
- [22] Biolek D, Biolkova V. First-order voltage-mode all-pass filter employing one active element and one grounded capacitor. *Analog Integr Circuits Signal Process* 2010;65(1):123–9.
- [23] Herencsar N, Minaei S, Koton J, Yuce E, Vrba K. New resistorless and electronically tunable realization of dual-output VM all-pass filter using VDIBA. *Analog Integr Circuits Signal Process* 2013;74(1):141–54.
- [24] Khan IA, Ahmed MT. Electronically tunable first-order OTA-capacitor filter sections. *Int J Electron* 1986;61(2):233–7.
- [25] Songsuwankit K, Petchmaneelumka W, Riewruja V. Electronically adjustable phase shifter using OTAs. In: *Proceedings of the international conference on control, automation and systems (ICCAS2010)*. 2010. p. 1622–5.
- [26] Herencsar N, Koton J, Vrba K. A new electronically tunable voltage-mode active-C phase shifter using UVC and OTA. *IEICE Electron Express* 2009;6(17):1212–8.
- [27] Herencsar N, Koton J, Lahiri A, Metin B, Vrba K. A voltage gain-controlled modified CFOA and its application in electronically tunable four-mode all-pass filter design. *Int J Adv Telecommun Electrotech Signals Syst* 2012;1(1):20–5.
- [28] Tanaphatsiri C, Jaikla W, Sirirpruchyanun M. An electronically controllable voltage-mode first order all-pass filter using only single CCCDTA. In: *International symposium on communications and information technologies ISCIT 2008*. 2008. p. 305–9.
- [29] Maheshwari S. A canonical voltage-controlled VM-APS with grounded capacitor. *Circuits Syst Signal Process* 2008;27(1):123–32.
- [30] Herencsar N, Koton J, Vrba K, Metin B. Novel voltage conveyor with electronic tuning and its application to resistorless all-pass filter. In: *Proceedings of 34th international conference on telecommunications and signal processing (TSP2011)*. 2011. p. 265–8.
- [31] Metin B, Pal K, Cicekoglu O. CMOS-controlled inverting CDBA with a new all-pass filter application. *Int J Circuit Theory Appl* 2011;39(4):417–25.
- [32] Bajer J, Biolek D. Voltage-mode electronically tunable all-pass filter employing CCCII+, one capacitor and differential-input voltage buffer. In: *Proceedings of 26th IEEE convention of electrical and electronics engineers in Israel (IEEEI2010)*. 2010. p. 934–7.
- [33] Herencsar N, Koton J, Jerabek J, Vrba K, Cicekoglu O. Voltage-mode all-pass filters using universal voltage conveyor and MOSFET-based electronic resistors. *Radioengineering* 2011;20(1):10–8.
- [34] Biolkova V, Kolka Z, Biolek D. Dual-output all-pass filter employing fully-differential operational amplifier and current-controlled current conveyor. In: *Proceedings of the 7th international conference on electrical and electronics engineering – ELECO 2011*. 2011. p. 319–23.
- [35] Toker A, Ozoguz S. Tunable allpass filter for low voltage operation. *Electron Lett* 2003;39(2):175–6.
- [36] Metin B, Pal K, Cicekoglu O. All-pass filters using DDCC- and MOSFET-based electronic resistor. *Int J Circuit Theory Appl* 2011;39(8):881–91.
- [37] Herencsar N, Koton J, Vrba K, Minaei S. Electronically tunable MOSFET-C voltage-mode all-pass filter based on universal voltage conveyor. In: *Proceedings of IEEE 3rd international conference on communication software and networks (ICCSN 2011)*. 2011. p. 442–5.
- [38] Minaei S, Yuce E. High input impedance NMOS-based phase shifter with minimum number of passive elements. *Circuits Syst Signal Process* 2012;31(1):51–60.
- [39] Pandey N, Arora P, Kapur S, Malhotra S. First order voltage mode MO-CCCCTA based all pass filter. In: *Proceedings of international conference on communications and signal processing (ICCSP 2011)*. 2011. p. 535–7.
- [40] Horng JW. DVCCs based high input impedance voltage-mode first-order all-pass. Highpass and lowpass filters employing grounded capacitor and resistor. *Radioengineering* 2010;19(4):653–6.
- [41] Metin B, Herencsar N, Pal K. Supplementary first-order all-pass filters with two grounded passive elements using FDCCII. *Radioengineering* 2011;20(2):433–7.
- [42] Maheshwari S. High input impedance VM-APs with grounded passive elements. *IET Circuits Devices Syst* 2007;1(2):72–8.
- [43] Ibrahim M, Minaei S, Yuce E. All-pass sections with rich cascading and IC realization suitability. *Int J Circuit Theory Appl* 2012;40(5):461–72.
- [44] MOSIS parametric test results of TSMC LO EPI SCN018 technology; 2012. Available from <https://www.mosis.com/cgi-bin/cgiwrap/umosis/swp/params/tsmc-018> [cited 09.06.15].
- [45] Vinagre BM, Podlubny I, Hernandez A, Feliu V. Some approximations of fractional order operators used in control theory and applications. *Fract Calculus Appl Anal* 2000;3(3):231–48.
- [46] VCA610: wideband voltage controlled amplifier. Texas Instruments; 2000. Available from: <http://www.ti.com/lit/ds/symlink/vca610.pdf> [cited 22.10.12].
- [47] OPA660: wide bandwidth operational transconductance amplifier and buffer. Texas Instruments; 1995. Available from: <http://www.ti.com/lit/ds/symlink/opa660.pdf> [cited 22.10.12].
- [48] AD830: high speed, video difference amplifier. Analog Devices; 1995. Available from: http://www.analog.com/static/imported-files/data_sheets/AD830.pdf [cited 22.10.12].

[34] SOTNER, R., JERABEK, J., PETRZELA, J., DOSTAL, T. Simple Approach for Synthesis of Fractional- Order Grounded Immittances Based on OTAs. In *Proceedings of 39th International Conference on Telecommunications and Signal Processing (TSP 2016)*, Vienna (Austria), 2016, p. 563-568. ISBN: 978-1-5090-1287-9.

Simple Approach for Synthesis of Fractional-Order Grounded Immittances Based on OTAs

Roman Sotner, Jan Jerabek, Jiri Petrzela

Faculty of Electrical Engineering and Communication
Brno University of Technology
Brno, Czech Republic
sotner@feec.vutbr.cz

Tomas Dostal

Dept. of Technical Studies
College of Polytechnics
Jihlava, Czech Republic
tomas.dostal@vspj.cz

Abstract—This paper briefly introduces an approach towards a simple synthesis of the grounded fractional-order immittances. Proposed method is based on multiplication of partial grounded immittance emulators with mutually independent electronic control of zero and pole location. General structure is based on the operational transconductance amplifiers (OTAs) while practical realization implements the so-called diamond transistors OPA860. Workability of the proposed concepts in the frequency domain was verified in Orcad PSpice simulations.

Keywords—behavioral modeling; circuit behavioral emulator; electronic control; fractional-order component; gyrator; immittance multiplication; impedance converter; zero and pole adjusting

I. INTRODUCTION

Synthesis of active and passive circuits characterized by fractional-order (FO) dynamics [1]-[3] is receiving significant attention nowadays. A reason for this is that many emerging applications from the area of continuous-time analog signal processing have been reported in the past; for example FO filters [4]-[10], FO harmonic oscillators [11]-[12], two-ports described by FO transfer function (integrators, differentiators or phase shifters capable to asymptotically change phase shift in user defined range) [13]-[16] and two-terminal elements with fractional immittance function [8], [17].

Since FO circuit devices are not commercially available, these fractional-order elements (FOEs) need to be approximated in the frequency domain by suitable circuitry network topologies. This approximation necessarily causes phase frequency response being rippled around theoretical value while it should be almost constant over operational frequency range. Several approaches towards FOE design are used in recent works: 1) utilization of integer-order transfers to substitute coefficients in filter of the fractional order [10], [18]; 2) utilization of bilinear section to provide direct configuration of zeros and poles location (mainly for all-pass filters and phase shifters [12], [13], two-port blocks – integrator, differentiator [14]-[16], [19], [20], leading to fractional-order $PI^{\alpha}D^{\beta}$ regulators [21]); 3) direct utilization of bilinear impedances/admittances (immittances) for emulation of immittance of fractional character. A successive solution of synthesis problem probably leads through the consideration of

the general biquadratic impedances.

Selection of proper approximation (coefficients/roots of the transfer or impedance function, a number and location of zero and poles [22], [23], etc.) is always a key factor having direct impact on accuracy (phase ripple) and achieved frequency range of emulator. This way of construction of FOEs is very complex but there is no other way until commercially available FOEs are available. They are based on different principles (layers of organic and inorganic materials [24], [25]), far away from analog behavioral emulation and mathematic approximations. In spite of the fact, it offers further space for synthesis of novel FOEs-based circuits and their applications, which will attract significant increase of attention when some FOEs are accessible for common designers.

This work presents quite simple approach to synthesis of these devices based on impedance/admittance multiplication and proper emulation of partial impedance/admittance by sub-circuit allowing independent adjusting of zero and pole frequency. To the best of author's knowledge, there are no similar previously published works regarding the latest research focusing on synthesis of grounded immittances with electronically settable fractional-order character.

II. IMPEDANCE MULTIPLICATION

The most straightforward synthesis of FO immittances is based on multiplication of partial immittances of fundamental elements, no matter if impedances or admittances are considered. It helps to obtain final positive and real immittance function with desired complexity. The basic circuit building block, where this feature is provided, is structure well known as general Antoniou impedance converter (gyrator) [26] (Fig. 1). It contains two operational amplifiers and five passive elements (only one of them is grounded) – impedances. However, it offers only a limited number of multiplied elements (the same relation is valid for both variants in Fig. 1a and b):

$$Z_{INP}(s) = \frac{Z_1(s)Z_3(s)Z_5(s)}{Z_2(s)Z_4(s)}. \quad (1)$$

This synthesis of Z_{INP} in case of solution in Fig. 1b can be easily extended to arbitrary degree by utilization of additional

Research described in this paper was financed by Czech Ministry of Education in frame of National Sustainability Program under grant LO1401. For research, infrastructure of the SIX Center was used. Research described in the paper was supported by Czech Science Foundation project under No. 14-24186P.

opamps (Fig. 2). Note that final impedance should be still considered as grounded.

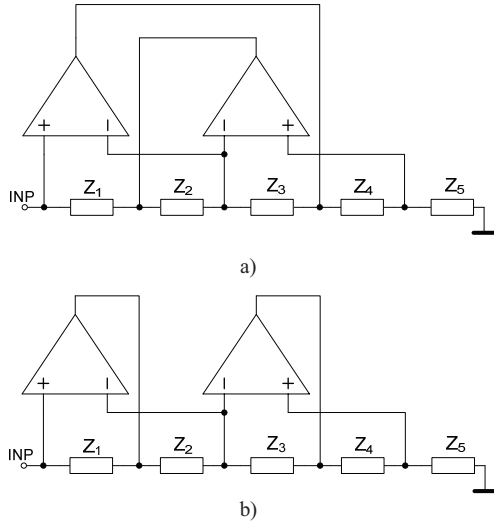


Fig. 1. Antoniou impedance converters: a) standard feedback, b) equivalent modified feedback.

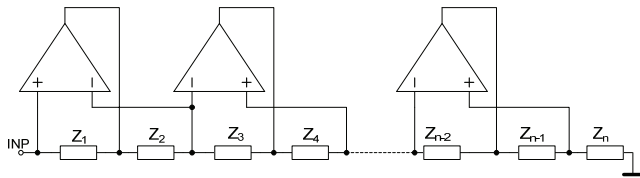


Fig. 2. Generalized chain of multiplied floating impedances based on Antoniou impedance converter.

We obtained the following formula for input impedance:

$$Z_{INP}(s) = \frac{\prod_{i=1}^{\frac{n+1}{2}} Z_{2i-1}(s)}{\prod_{i=1}^{\frac{n-1}{2}} Z_{2i}(s)} \quad (2)$$

However, impedance multiplication in form (2) is not very suitable due to product of odd impedances in the numerator divided by product of even impedances in the denominator. Moreover, electronic change of zeros and poles locations is not possible.

Our effort focused on searching simpler structure and moreover with grounded passive elements, where product of an unlimited number of impedances/admittances can be expected. The synthesis of single Z_n element with electronically adjustable zero and pole frequency will be very difficult as well as very complicated circuitry will be required. Therefore, we studied other possibilities and carried out following generalized circuit (Fig. 3) based on operational transconductance amplifiers (OTAs) and grounded impedances. The main idea was inspired by [27] where simple OTA-based impedance converter was presented. The formula for input impedance of the circuit in Fig. 3 has the following expression:

$$Z_{INP}(s) = \frac{1}{\pm g_{mn+1} \prod_{i=1}^n g_{mi} Z_i(s)} \quad (3)$$

Advantage of this form is evident at first sight. All impedances Z_n are multiplied in a different way than in (2) where only odd n are in numerator divided by even n in the denominator. Polarity of the Z_{INP} can be easily selected by polarity of the selected OTA in the chain (g_{mn+1} in Fig. 3 for example).

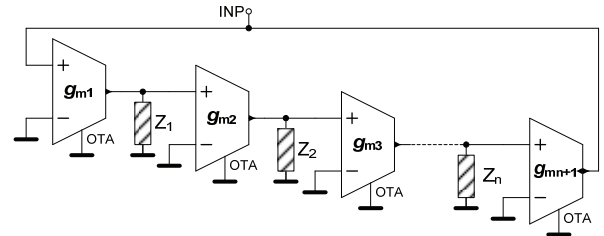


Fig. 3. Generalized impedance converter/multiplier employing OTAs and grounded impedances.

III. EMULATOR OF THE GROUNDED BILINEAR IMPEDANCE

This section is very important for further synthesis of FO grounded impedance. In fact, it is basic building block capable of creating a pair of independently adjustable zero and pole of the input impedance. The suitable circuit solution, fulfilling the above mentioned requirements, can be found in Fig. 4. It utilizes three OTAs and single grounded capacitor. Input impedance of the emulator can be expressed as follows:

$$Z_n(s) = \frac{sC + g_{me2}}{g_{me3}(sC + g_{me1})} = \frac{s + \frac{g_{me2}}{C}}{g_{me3} \left(s + \frac{g_{me1}}{C} \right)} = \frac{s + \omega_Z}{g_{me3}(s + \omega_P)} \quad (4)$$

where pole frequency ($\omega_P = g_{me1}/C$) can be adjusted by g_{me1} and zero frequency ($\omega_Z = g_{me2}/C$) by g_{me2} . Any transconductance parameter in this structure g_{me} can be simply electronically controlled. Therefore, pole and zero location can be independently and continuously varied by DC bias currents for example.

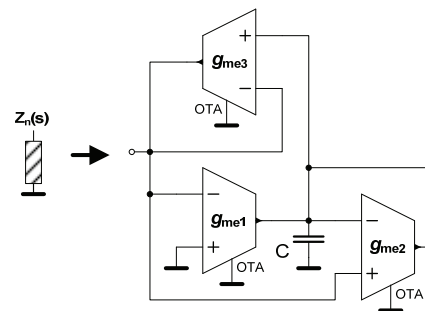


Fig. 4. Emulator of the grounded impedance with mutually independently and electronically adjustable zero and pole.

IV. PRACTICAL EXAMPLE

Let us assume FO approximant having mathematical order $n = 7$. This leads to seven impedances generated by structure in

Fig. 4 and eight OTAs required for their multiplication, according to Fig. 3. In this particular case we have:

$$Z_{INP}(s) = \frac{1}{g_{m1}g_{m2}g_{m3}g_{m4}g_{m5}g_{m6}g_{m7}g_{m8}Z_1Z_2Z_3Z_4Z_5Z_6Z_7}. \quad (5)$$

The situation can be significantly simplified if g_{m1} through g_{m8} as well as g_{me3} in Z_n emulators have the same value g_{mC} . Then (5) reduces to:

$$Z_{INP}(s) = \frac{1}{g_{mC}Z_1Z_2Z_3Z_4Z_5Z_6Z_7}. \quad (6)$$

This can be rewritten to:

$$Z_{INP}(s) = \frac{1}{g_{mC}} \left(\frac{sC_a + g_{me1a}}{sC_a + g_{me2a}} \right) \left(\frac{sC_b + g_{me1b}}{sC_b + g_{me2b}} \right) \left(\frac{sC_c + g_{me1c}}{sC_c + g_{me2c}} \right) \cdot \left(\frac{sC_d + g_{me1d}}{sC_d + g_{me2d}} \right) \left(\frac{sC_e + g_{me1e}}{sC_e + g_{me2e}} \right) \left(\frac{sC_f + g_{me1f}}{sC_f + g_{me2f}} \right) \left(\frac{sC_g + g_{me1g}}{sC_g + g_{me2g}} \right). \quad (7)$$

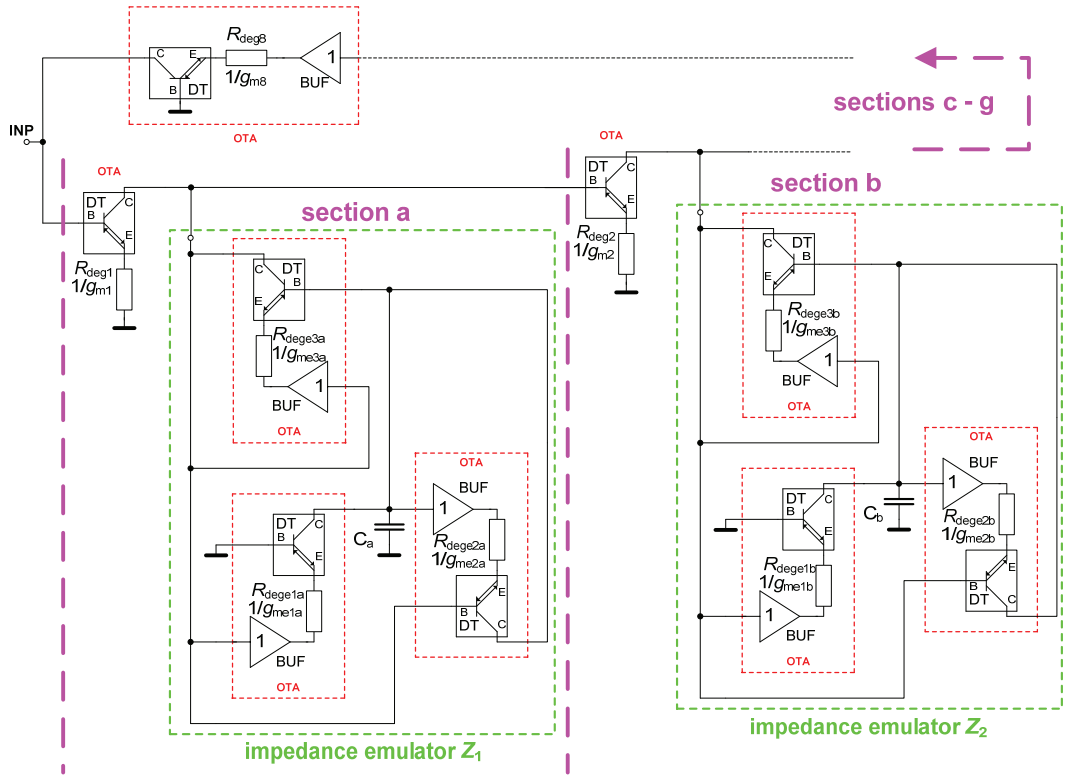


Fig. 5. Partial illustration of fractional-order immittance for $n = 7$ including OTAs created by commercially available OPA860.

V. RESULTS OF SIMULATION

Orcad PSpice circuit simulator has been utilized for the FO immittance concept presented in the previous section. Diamond transistors (DT) and diamond buffers (OPA860) were utilized to create OTAs introduced in the above discussed figures (Fig. 3 and Fig. 4). Operation of DT as OTA is clear from Fig. 5, where we present a part of whole structure of fractional-order immittance for $n = 7$ including particular OTAs

where indexes $a - g$ indicate specific section of emulator (Fig. 4). To obtain approximation with minimal phase ripple in wide frequency range we used approximation based on formulas given in [22], [23] and recalculated passive ladder structure to get location of zeros and poles as follows:

$$Z_{INP}(s) = \frac{1}{g_{mC}} \left(\frac{s + 35.5}{s + 100} \right) \left(\frac{s + 212.1}{s + 458} \right) \left(\frac{s + 980.4}{s + 2100.7} \right) \cdot \left(\frac{s + 4497.4}{s + 9628.2} \right) \left(\frac{s + 20630.7}{s + 44129.1} \right) \left(\frac{s + 95377.9}{s + 202250.8} \right) \left(\frac{s + 569943}{s + 3 \cdot 10^6} \right). \quad (8)$$

Specific values of the parameters can be easily established as $g_{me1a} = \omega_{z1}C_a$, $g_{me2a} = \omega_{p1}C_a$ for the first section (based on Fig. 4) and analogically for other sections ($g_{me1b} - g_{me1g}$ for poles and $g_{me2b} - g_{me2g}$ for zeros). Capacitor value is always the same for calculation of the parameters for pole and zero frequency in the particular section.

implementation for the first two sections of the immittance (section a and b).

Verification of the Z_n emulator (Fig. 4) is provided for $C = 100$ nF, $g_{me3} = 1\,000$ μ S, and g_{me1} and g_{me2} achieves 450 μ S or 963 μ S (first setting and second setting) alternately (first setting represents section $d - Z_4$ in (7) and (8)). The exemplary simulation results are shown in Fig. 6 and Fig. 7 for indicated combinations of g_{me1} and g_{me2} - pole

foregoing zero (used in section d) and an example of zero foregoing pole in observed frequency range.

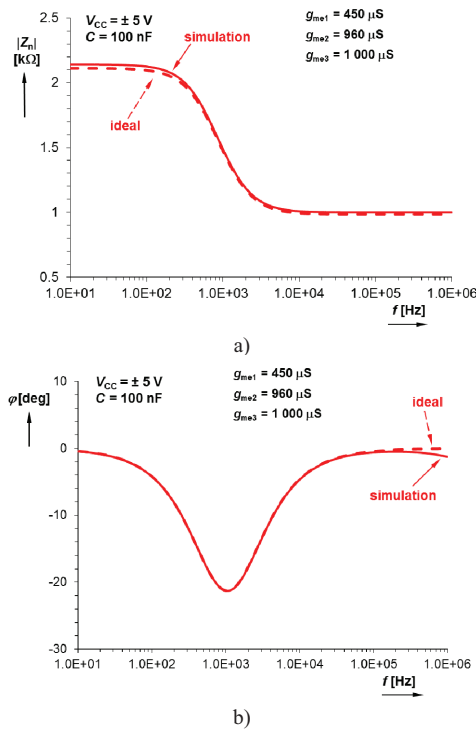


Fig. 6. Exemplary results of Z_n emulator in first setting configured for pole foregoing zero: a) magnitude response, b) phase response.

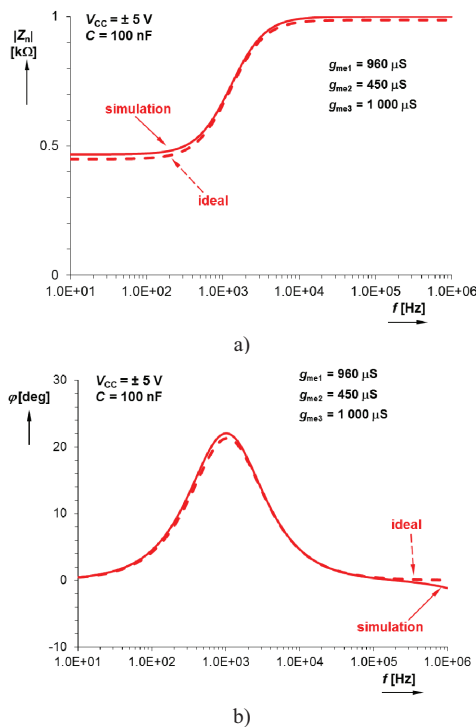


Fig. 7. Exemplary results of Z_n emulator in second setting configured for zero foregoing pole: a) magnitude response, b) phase response.

Above noted approximation (8) is used for calculation of the circuit parameters. We selected values of capacitors to be easily selectable from production series (E12) and transconductances to be feasible in commonly available ranges of commercially available active devices emulating behavior of the OTA (OPA860). Selected and calculated parameters, given in Fig. 5, are summarized in Table 1. The simulation results of the fractional element emulating impedance (fractal inductance) proportional to $k \cdot s^{1/2}$ are given in Fig. 8 where magnitude and phase response are shown for all these cases. Ideal trace represents ideal inductance, theoretical trace stands for the results of ideal simulation when particular approximation is used and the simulation results represent the results of the same simulation but with realistic behavioral models.

TABLE I. PARAMETERS OF THE DESIGNED EXAMPLE (FIG. 5)

Section	Selected parameters	Calculated parameters	
	C_{a-g} [nF]	$g_{m1a-g} [\mu S] / R_{dege1a-g} [k\Omega]$ (zeros)	$g_{m2a-g} [\mu S] / R_{dege2a-g} [k\Omega]$ (poles)
a	2 200	78.1 / 22	220 / 4.55
b	1 000	212.1 / 5.56	458 / 2.18
c	470	461 / 2.44	987 / 1.01
d	100	449.7 / 2.5	962.8 / 1.04
e	47	969.9 / 1.11	2 074 / 0.44
f	10	953.8 / 1.05	2 022 / 0.45
g	1	569.9 / 2.04	3 000 / 0.4
$g_{m3a-g} [\mu S]$	1 000	$g_m \cong 1/R_{deg}$	
$g_{m1-8} [\mu S]$	1 000		

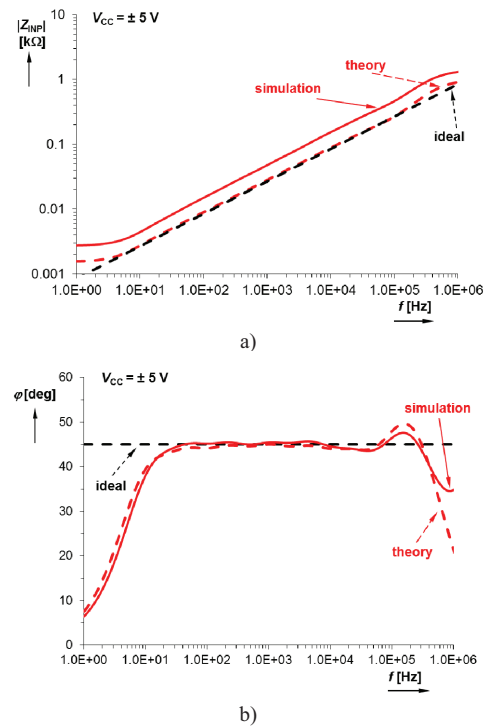


Fig. 8. Emulated fractional positive impedance ($n = 7$): a) magnitude responses, b) phase responses.

The ideal values of the parameters (g_m -s) noted above require certain readjustment especially for accurate locations of

zeros and poles specified in theory. The reasons for this deviation are dependent on existence of real nodal impedances of high-impedance nodes (not only capacitors are connected in nodes where inputs and outputs of used DTs as OTAs are interconnected together). Output impedance of the DT OPA860 is reported as 55 k Ω that is really low value if two outputs are connected in parallel. The precise small-signal parasitic analysis is too complicated in such extensive circuitry our system presents. Values of degradation resistances (Fig. 5) used in simulation of full chain of elements forming fractional-order inductance are also given in Tab. 1 (already optimized values). Fortunately, electronic controllability of the g_m -s allows very simple correction if necessary.

VI. CONCLUSION

We selected an interesting example of utilization of OTAs for special synthesis of FO grounded passive element with specific character of the impedance. The important information has been carried out from the point of view of the impedance multiplication. We started with Antoniou impedance converter (its generalized chain) as the possible solution but product of all immittances in the circuit structure is not pure (there are even elements divided by odd elements). Odd elements in denominator of Z_{INP} (2) are useless (and they increase complexity of the circuitry only) for our aims in the fractional-order synthesis. Therefore, derived immittance multiplier based on OTA has significant importance for our approach. It allows easier multiplication (3) than modification of the Antoniou chain, grounded elements Z_n (it simplifies proposal of emulator of the Z_n – it can be grounded) and electronic controllability (magnitude/impedance norm compensation or setting), if necessary. The design steps are quite simple: 1) selection of meaningful values of $g_{m1} - g_{m8}$ (physically suitable values in frame of possibility of active device – OPA860), 2) approximation (taking bandwidth of “constant” phase and phase ripple into account) based on [22] and [23] determines the number of sections (zero and pole coordinates – angular frequencies), 3) proper selection of working capacitors in order to ensure meaningful values of g_m -s, 4) comparison of roots (8) and form (7) to calculate g_{me1a-g} , g_{me2a-g} ($R_{dege1a-g}$, $R_{dege2a-g}$) values. Validity of the approximation was verified in the band approximately from 30 Hz to 100 kHz with phase error (phase ripple) ± 1.5 deg. maximally. It is quite large bandwidth in comparison to [19], for instance. Easy correction of disrupted characteristic due to real behavior of active devices is simply allowed by g_m . The most important drawback is complexity of this type of approximation. Design approach is simple but the presented circuit requires 29 OTAs ($8 + 3 \cdot 7$) and 7 grounded capacitors to emulate device with fractional character in above mentioned bandwidth. Unfortunately, there is no other possibility until FOEs will be commercially available. In addition, power consumption will also be enormous. Preliminary estimation from PSpice simulation, taking all active devices into account, indicates power consumption about 1 W (5 V, 210 mA) per supply branch.

Discussed research in active fractional-order immittance emulators is very actual as can be seen from [28] where grounded fractional inductor has been proposed by using of known opamp-based Antoniou converter [26]. Current

feedback operational amplifiers (CFOAs) that offer better features than standard operational amplifiers, have been utilized in fractional inductor and capacitor emulators [29]. The interesting concept of floating fractional (constant phase) element has been shown in [30]. Circuit structure is simpler than presented in this paper. However, proposal has lower bandwidth and higher phase ripple of used approximation than our solution. Fractional-order systems receive increasing attention as can be seen from the recent application examples in filters [31] and oscillators [32].

REFERENCES

- [1] M. Ortigueira, “An Introduction to the fractional continuous-time linear systems: The 21st century systems,” IEEE Circuits and Systems Magazine, vol. 8, no. 3, pp. 19-26, 2008.
- [2] A. S. Elwakil, “Fractional-order circuits and systems: An emerging interdisciplinary research area,” IEEE Circuits and Systems Magazine, vol. 10, no. 4, pp. 40-50, 2010.
- [3] T. Freeborn, “A survey of fractional-order circuit models for biology and biomedicine,” IEEE Journal on Emerging and Selected Topics in Circuits and Systems, vol. 3, no. 3, pp. 416-424, 2013.
- [4] A. G. Radwan, A. M. Soliman, A. S. Elwakil, “First-order filters generalized to the fractional domain,” Journal of Circuits, Systems and Computers, vol. 17, no. 1, pp. 55-66, 2008.
- [5] A. G. Radwan, A. S. Elwakil, A. M. Soliman, “On the generalization of second-order filters to the fractional-order domain,” Journal of Circuits, Systems and Computers, vol. 18, no. 2, pp. 361-386, 2009.
- [6] T. Freeborn, B. Maundy, A. S. Elwakil, “Field programmable analogue array implementation of fractional step filters,” IET Circuits, Devices and Systems, vol. 4, no. 6, pp. 514-524, 2010.
- [7] B. Maundy, A. S. Elwakil, T. Freeborn, “On the practical realization of higher-order filters with fractional stepping,” Signal Processing, vol. 91, no. 3, pp. 484-491, 2011.
- [8] P. Ahmadi, B. Maundy, A. S. Elwakil, “High quality factor asymmetric slope band-pass filters: fractional-order capacitor approach,” IET Circuits, Devices & Systems, vol. 6, no. 3, pp. 1-11, 2011.
- [9] A. Ali, A. G. Radwan, A. M. Soliman, “Fractional order Butterworth filter: Active and passive realizations,” IEEE Journal on Emerging and Selected Topics in Circuits and Systems, vol. 3, no. 3, pp. 346-354, 2013.
- [10] G. Tsirimokou, C. Laoudias, C. Psychalinos, “0.5-V fractional-order companding filters,” International Journal of Circuit Theory and Applications, vol. 43, no. 9, pp. 1105-1126, 2015.
- [11] A. G. Radwan, A. S. Elwakil, A. M. Soliman, “Fractional-order sinusoidal oscillators: design procedure and practical examples,” IEEE Transactions on Circuits and Systems I: Regular papers, vol. 55, no. 7, pp. 2051-2063, 2008.
- [12] B. Maundy, A. S. Elwakil, S. Gift, “On the realization of multiphase oscillators using fractional-order allpass filters,” Circuits, Systems and Signal Processing, vol. 31, no. 1, pp. 3-17, 2012.
- [13] J. Petrzela, “Arbitrary phase shifters with decreasing phase,” In Proceedings of 37th International Conference on Telecommunications and Signal Processing (TSP 2014), Berlin, Germany, pp. 329-333, 2014.
- [14] D. Mondal, K. Biswas, “Performance study of fractional order integrator using single-component fractional order element,” IET Circuits, Devices and Systems, vol. 5, no. 4, pp. 334-342, 2011.
- [15] B. Krishna, “Studies on fractional order differentiators and integrators: A survey,” Signal Processing, vol. 91, no. 3, pp. 386-426, 2011.
- [16] G. Tsirimokou, C. Psychalinos, “Ultra-low voltage fractional-order differentiator and integrator topologies: an application for handy noisy ECGs,” Analog Integrated Circuits and Signal Processing, vol. 81, no. 2, pp. 393-405, 2014.
- [17] A. G. Radwan, K. Salama, “Fractional-order RC and RL circuits,” Circuits Systems and Signal Processing, vol. 31, no. 6, pp. 1901-1915, 2012.

- [18] G. Tsirimokou, C. Psychalinos, A. S. Elwakil, "Digitally programmed fractional-order Chebyshev filters realizations using current-mirrors," In Proceedings of IEEE Int. symposium on Circuits and Systems (ISCAS), Lisbon, Portugal, pp. 2337-2340, 2015.
- [19] R. Sotner, J. Jerabek, N. Herencsar, J. Petrzela, T. Dostal, K. Vrba, "First-order adjustable transfer sections for synthesis suitable for special purposes in constant phase block approximation," *AEU – International Journal of Electronics and Communications*, vol. 69, no. 9, pp. 1334-1345, 2015.
- [20] G. Tsirimokou, C. Psychalinos, "Ultra-Low Voltage Fractional-Order Circuits Using Current-Mirrors," *International Journal of Circuit Theory and Applications*, vol. 44, no.1 pp. 109-126, 2016.
- [21] I. Podlubny, I. Petras, B. Vinage, P. O'Leary, L. Dorcak, "Analogue realization of fractional-order controllers," *Nonlinear Dynamics*, vol. 29, no. 1, pp. 281-296, 2002.
- [22] J. Valsa, J. Vlach, "RC models of a constant phase element," *International Journal of Circuit Theory and Applications*, vol. 41, no. 1, pp. 59-67, 2013.
- [23] J. Valsa, P. Dvorak, M. Friedel, "Network model of CPE," *Radioengineering*, vol. 20, no. 3, pp. 619-626, 2011.
- [24] A. Adhikary, M. Khanra, S. Sen, K. Biswas, "Realization of carbon nanotube based electrochemical fractor," In Proceedings of IEEE Int. symposium on Circuits and Systems (ISCAS), Lisbon, Portugal, pp. 2329-2332, 2015.
- [25] A. M. Elshurafa, M. N. Almadhoun, K. N. Salama, H. N. Alshareef, "Microscale electrostatic fractional capacitors using reduced graphene oxide percolated polymer composites," *Applied Physics Letters*, vol. 102, no. 102, pp. 232901, 2013.
- [26] Antoniou, A. "Gyrator using operational amplifier," *Electronics Letters*, vol. 3, no. 8, pp. 350-352, 1967.
- [27] R. L. Geiger, E. Sanchez-Sinencio, "Active filter design using operational transconductance amplifiers: a tutorial," *IEEE Circ. And Devices Magazine*, vol. 1, no. 2, pp. 20-32, 1985.
- [28] M. Tripathy, D. Mondal, K. Biswas, S. Sen, "Experimental studies on realization of fractional inductors and fractional-order bandpass filters," *International Journal of Circuit Theory and Applications*, vol. 43, pp. 1183-1196, 2015.
- [29] I. Dimeas, G. Tsirimokou, C. Psychalinos, A. Elwakil, "Realization of Fractional-Order Capacitor and Inductor Emulators Using Current Feedback Operational Amplifiers," In Proceedings of Int. Symposium on Nonlinear Theory and its Applications (NOLTA2015), Hong Kong, China, pp. 237-240, 2015.
- [30] G. Tsirimokou, C. Psychalinos, A. Elwakil, "Emulation of a Constant Phase Element Using Operational Transconductance Amplifiers," *Analog Integrated Circuits and Signal Processing*, vol. 85, no. 3, pp 413-423, 2015.
- [31] F. Khateb, D. Kubanek, G. Tsirimokou, C. Psychalinos, "Fractional-order filters based on low-voltage DDCCs," *Microelectronics Journal*, vol. 50, pp. 50-59, 2016.
- [32] D. Kubanek, F. Khateb, G. Tsirimokou, C. Psychalinos, "Practical design and evaluation of fractional-order oscillator using differential voltage current conveyors," *Circuits Systems and Signal Processing Journal*, DOI: 10.1007/s00034-016-0243-5, 2016.

[35] SOTNER, R., KARTCI, A., JERABEK, J., HERENC SAR, N., DOSTAL, T., VRBA, K. An Additional Approach to Model Current Followers and Amplifiers with Electronically Controllable Parameters from Commercially Available ICs. *Measurement Science Review*, 2012, vol. 12, no. 6, p. 255-265. ISSN: 1335-8871.

An Additional Approach to Model Current Followers and Amplifiers with Electronically Controllable Parameters from Commercially Available ICs

R. Sotner¹, A. Kartci², J. Jerabek³, N. Herencsar³, T. Dostal^{1,4}, K. Vrba³

¹Dept. of Radio Electronics, Faculty of Electrical Engineering and Communications, Brno University of Technology, Purkynova 118, 612 00, Brno, Czech Republic, sotner@feec.vutbr.cz

²Dept. of Electronics and Telecommunication Engineering, Corlu Engineering Faculty, Namik Kemal University, Cerkezkooy, Yolu, 3. km, 598 60 Corlu, Turkey, aslhankartc@gmail.com

³Dept. of Telecommunications, Faculty of Electrical Engineering and Communications, Brno University of Technology, Purkynova 118, 612 00, Brno, Czech Republic, {jerabekj; herencsn; vrbak}@feec.vutbr.cz

⁴Dept. of Electronics and Computer Science, College of Polytechnics Jihlava, Tolsteho 16, 586 01, Jihlava, Czech Republic, dostal@vspj.cz

Several behavioral models of current active elements for experimental purposes are introduced in this paper. These models are based on commercially available devices. They are suitable for experimental tests of current- and mixed-mode filters, oscillators, and other circuits (employing current-mode active elements) frequently used in analog signal processing without necessity of on-chip fabrication of proper active element. Several methods of electronic control of intrinsic resistance in the proposed behavioral models are discussed. All predictions and theoretical assumptions are supported by simulations and experiments. This contribution helps to find a cheaper and more effective way to preliminary laboratory tests without expensive on-chip fabrication of special active elements.

Keywords: Intrinsic resistance, current and voltage gain control, current follower and amplifier, behavioral modeling

1. INTRODUCTION

MANY WORKS deal with specific applications of modern active elements [1]. Methods of intrinsic resistance adjusting (for example Fabre et al. [2], Siripruchyanun et al. [3]) by bias current in many novel and standard active elements are very popular. This kind of control was mainly the domain of current conveyors (CC-s) and its applications (Sedra et al. [4], Svoboda et al. [5]). However, this parameter (intrinsic resistance - labeled as R_i or R_x) is given by technological aspects and is dependent on temperature. Some designers consider this parameter as parasitic. It is correct in some cases, mainly in active elements where the R_i value is not adjustable [5]. In addition, this resistance is considered as small-signal parameter. Behavior of R_i for higher signal levels has nonlinear character.

In the last three decades considerable attention was given to the active elements with electronic possibility of current gain control (Surakamponorn et al. [6], Fabre et al. [7], Minaei et al. [8]). It seems to be a very interesting topic for researchers. Some novel types of current conveyors (Mahmound et al. [9], Kumngern et al. [10]), so-called current followers and nullors (Sedighi et al. [11], Tangsrirat [12], Tangsrirat et al. [13]), have been published quite recently. Alzaher et al. [14, 15] and Koton et al. [16] utilized digital control of current gain in their active elements and applications. Current gain control received important attention also in more complicated active elements formed by basic functional components, for example current differencing buffered amplifier (CDBA) presented by Biolek et al. in [17] and [18], programmable current amplifier

(PCA) introduced by Herencsar et al. [19], current gain controlled current conveyor transconductance amplifier (CGCCCTA) discussed in [20], etc.

Some attempts to use several methods of control in frame of one active element have been solved in recent years. For example Marcellis et al. [21] proposed an approach to control current gain and voltage gain independently in frame of one active element. Kumngern et al. [22] proposed an interesting conception of current conveyor with intrinsic resistance and current gain controlling possibilities. Similar approach was used in [23], where both methods of control were used in the so-called double current controlled current feedback amplifier (DCC-CFA). Jaikla et al. [24] implemented the so-called current controlled current differencing transconductance amplifiers (CCCDTA-s) where intrinsic resistance and transconductance [1] adjusting is possible.

Discussed approaches have been widely investigated in recent years. However, all discussed elements and approaches require fabrication of designed internal implementation or we have to rely only on simulation results. Nevertheless, experimental verification is necessary or beneficial in many cases. It provides a more realistic view on behavior of the proposed application. Experimental tests with available devices are more reliable despite the accuracy and exactness of some simulation results. However, fabrication of on-chip implementation is very expensive and therefore not suitable for preliminary tests of application in the most cases. Accessibility of specialized models used for realistic modeling seems to be an advantage for designers. Practically, precise models of active elements with exactly defined and controllable intrinsic resistance complemented

by adjustable current gain are missing in available literature. Therefore in this paper we implemented and verified several conceptions of current followers and amplifiers. The first two solutions employ electronically controllable current conveyors (ECCII) and current gain control. The current gain (B) is controllable by DC voltage. The second type utilizes voltage gain (A) in voltage controllable voltage amplifier (VCA) and diamond transistor (DT).

2. MODEL OF CURRENT FOLLOWERS AND AMPLIFIERS WITH ADJUSTABLE FEATURES

General description and behavior of single-input and single-output (SISO) current follower (CF) with controllable intrinsic resistance $R_i = f(V_{Ri})$ or current amplifier (CA) with controllable intrinsic resistance and current gain $k_i = f(V_{ki})$ is shown in Fig.1.

Main reasons for the proposal of behavioral models are following:

a) This approach allows the design of application, experimental verification of features and optimization without fabrication of particular active element in phase of first tests, which is very economical.

b) There are not many ways in literature explaining how to model electronically controllable intrinsic resistance in real experimental tests without chip and fabrication.

c) Small-signal resistance R_i is suitable only for small-signal operation in many cases. Our solution provides large range of input signals without significant increase of total harmonic distortion (THD).

d) Key features of models are independent on technology and fabrication process (R_i parameter is defined by external components and control voltage). Only restrictions of gain control of active elements limit achievable R_i of the model. Many on-chip implementations have intrinsic resistance dependent on the technology used. This intrinsic resistance is controllable by bias voltage or current [2, 3]. Nevertheless, adjusting of these bias values has negative effect on other parameters (output resistance, linearity, dynamic,...). In addition, temperature dependence of R_i is obvious. One example is the equation $R_i = V_t/2I_b$ (known for Sedra's conveyor [4] and in similar form for many other works e.g. [2-3]) which is valid in BJT technology where $V_t \approx 26$ mV is thermal voltage (temperature dependent), and I_b is bias current. In our models, intrinsic resistance is not directly defined by temperature-dependent parameter (V_t). Therefore, in our case the dependence on fabrication technology is not so important.

A. Adjustable Current Followers and Amplifiers based on Controllable Current Gains

The first part of this work deals with utilization of a negative-type electronically controllable second generation current conveyor (ECCII-). Behavior of ECCII- is explained in Fig.2. The transfers between terminal voltages and currents are as follows (Surakampontrorn et al. [6]; Minaei et al. [8]): $V_Y = V_X + R_x I_X$, $I_Y = 0$, $I_Z = -B I_X$, where R_x is intrinsic resistance of ECCII- [4, 5]. R_x has fixed value in this case, therefore it is considered as parasitic element. There is no possibility to change the value of R_x electronically, except by bias current [2, 3] in some

integrated implementation, but it is not generally valid for all cases of CCII [4, 5].

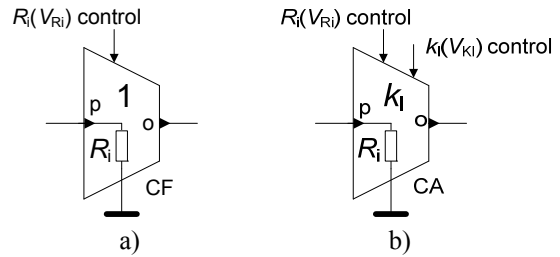


Fig.1. Symbol of: a) the current follower with only input resistance control, b) the current amplifier with current gain and input resistance control.

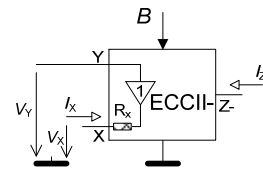


Fig.2. Symbol of ECCII-.

1) Solution Employing Two External Resistors

The possible conception of the inverting CF (CA) utilizing ECCII- and employing two resistors is depicted in Fig.3. The first section of the circuit in Fig.3 (without CC_3) represents simple non-inverting CF with controllable intrinsic resistance (at p terminal). Note that this part could be used independently, because in some applications only CF is sufficient instead of the whole current amplifier. The input resistance is defined as $R_i = R_1/B_1$. If the whole structure from Fig.3 is considered, overall current gain has the following form:

$$k_i = -\frac{B_2 B_3}{B_1} \frac{R_1}{R_2}. \quad (1)$$

Assuming $B_1 = B_2$ (adjusting of B_1 only in order to change R_i value causes unintentional affection on k_i - therefore simultaneous control of both B) and $R_1 = R_2$, the overall current gain in Eq. (1) simplifies to $k_i = -B_3$. Effects of the non-ideal properties (R_{x1} , R_{x2} , R_{x3}) cause minor modification of adjustable intrinsic resistance:

$$R_i = \frac{(R_1 + R_{x1})}{B_1}. \quad (2)$$

Now, the current transfer including the discussed non-idealities has the following form:

$$k_i = -\frac{B_2 B_3}{B_1} \frac{(R_1 + R_{x1})}{(R_2 + R_{x2})}, \quad (3)$$

where we have to ensure that $R_1 = R_2$ and $R_{1,2} \gg R_{x1,2}$, if no significant impact on gain is required. The output impedance (resistance) of CC_2 has multiple times higher value than R_{x3} .

One disadvantage of such approach is the necessity of simultaneous change of both current gains (B_1 and B_2) for R_i control without impact on current gain.

2) Solution Employing One External Resistor

The next interesting type including ECCII- is shown in Fig.4a. This variant is also easily applicable as controlled negative resistor, if the outputs of CC_1 and CC_2 are swapped (see Fig.4b). The CC_3 (B_3) is necessary only for current gain control. It is obvious that this model also works as CF with controllable R_i without CC_3 . Input resistance of the p terminal is given by $R_i = R_1/B_1$ (similarly as in previous case) and current gain has the form $k_i = B_2B_3/B_1$. Simultaneous change of both B_1 and B_2 is also required for operation without influence on overall k_i .

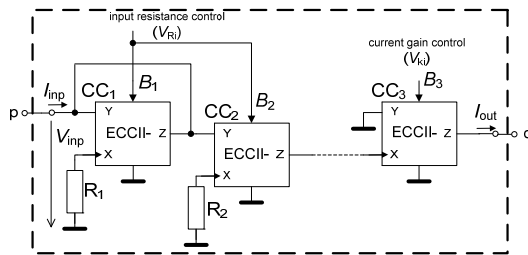


Fig.3. Solution employing two external resistors.

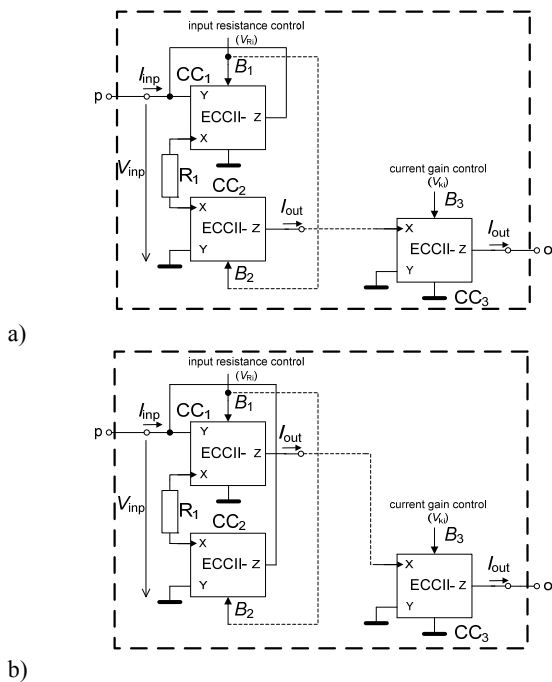


Fig.4. Solution employing one external resistor: a) for positive R_i value adjusting, b) for negative R_i value adjusting.

Considering the R_x of both CC_1 and CC_2 , the input resistance can be expressed as:

$$R_i = \pm \frac{(R_1 + R_{x1} + R_{x2})}{B_1}. \quad (4)$$

It is obvious that R_i is more dependent on input resistances of partial CCs ($R_{x1,2}$) than in the previous case.

B. Adjustable Current Amplifiers Based on Controllable Voltage Gains

Two interesting solutions are given in this part of our work. Main core of models consists of two voltage controllable amplifiers (VCA) and diamond transistor (DT). Their schematic symbols are shown in Fig.5. The voltage controllable amplifier with differential input and single output is defined by well-known equation: $V_{out} = (V_+ - V_-)A$, where $A = f(V_c)$. The principle of the diamond transistor is very similar to the second generation current conveyor [4, 5]. Transfers between terminal (E - current input, B - voltage input, C - current output) voltages and currents are ideally very similar to the CCII: $V_B = V_E$, $I_B = 0$, and $I_C = I_E$.

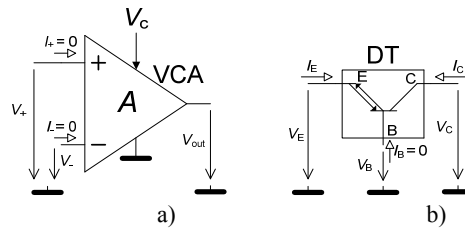


Fig.5. Symbols of: a) voltage controllable amplifier, b) diamond transistor.

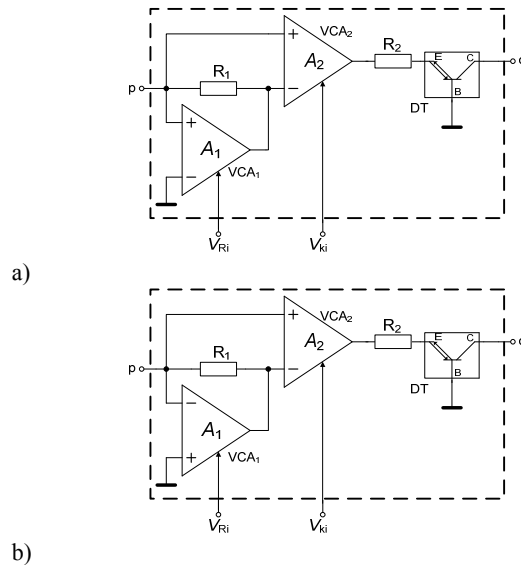


Fig.6. Solution utilizing VCA and DT where R_i could be adjusted to be: a) positive and negative, b) positive only.

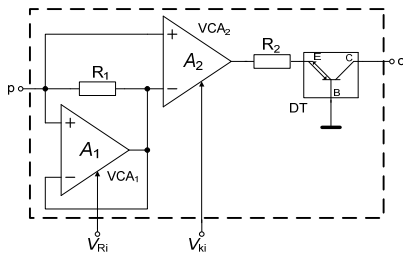
1) Solution Using Two VCAs and one DT

The models shown in Fig.6 are based on voltage-mode operation. The VCA_1 has feedback resistor R_1 between positive input and output. Voltage drop at resistor R_1 is processed by differential input of the VCA_2 . The VCA_2 provides voltage output and, therefore, conversion to the current mode is necessary. This conversion is made by DT through resistor R_2 . Intrinsic resistance of the p port of both solutions from Fig.6 is defined by the following equations:

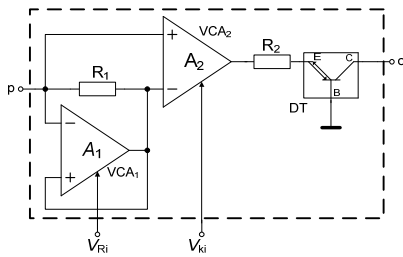
$$R_i = \frac{R_1}{1-A_1}, \quad R_i = \frac{R_1}{1+A_1}. \quad (5), (6)$$

Equation (5) is valid for solution shown in Fig.6a and Eq. (6) for the solution in Fig.6b. The circuit in Fig.6a provides interesting features (curiosity) in electronic control of R_i . Intrinsic resistance has positive character for $A_1 < 1$. The value of R_i increases if A_1 is nearly equal to 1. For higher values of A_1 the R_i value decreases and the whole input resistance is negative. However, the circuit is not stable for $A_1 > 1$. Overall current transfer of both solutions is given by:

$$k_i = -\frac{R_1}{R_2} A_2. \quad (7)$$



a)



b)

Fig.7. Solution utilizing VCA and DT with additional feedback where R_i could be adjusted to be: a) positive only, b) positive and negative.

Adjustable gain of VC_2 (A_2) allows electronic current gain control. In comparison to previous solutions with ECCII-s, the simultaneous change of two parameters is not necessary.

2) Solution Using Two VCAs, one DT and Additional Voltage Feedback

Modifications of circuits from Fig.6 were obtained when additional feedback was used. Modified version is shown in Fig.7. In this case the inverting input of VCA_1 is not grounded but connected to the output of VCA_1 .

Presented modifications (Fig.7) provide following equations for R_i :

$$R_i = R_1(1 + A_1), \quad R_i = R_1(1 - A_1). \quad (8), (9)$$

Equation (8) is valid for solution shown in Fig.7a and Eq. (9) for Fig.7b. Circuit in Fig.7a allows only increase of R_i values but solution in Fig.7b (interchanged terminals of VCA_1) allows similar type of control as the conception in Fig.6a. Unfortunately, the amplifier is then unstable. Current gain of the whole model is the same as in the previous case (7).

3. VERIFICATION AND PRACTICALLY ACHIEVABLE PERFORMANCES

All the above discussed models of CF (CA) were verified experimentally. An experimental board was designed for these purposes. Measuring setup for experimental verification was established. The voltage to current and current to voltage converters were necessary at the input and output of the device under test (DUT). The grounded resistance (R_{k2}) and voltage buffer was sufficient at the output, and voltage follower and resistor (R_{k1}) were required for input conversion, see Fig.8. We used very good high-speed voltage followers OPA633 [25] or BUF634 [26]. This equipment allows measurement with vector/spectral network analyzer (50 Ω matching). The transfer function has to be recalculated from voltage transfer which is measured by vector-network analyzer Agilent E5071C.

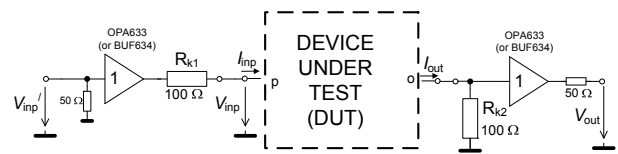


Fig.8. Measuring setup (testing equipment) for experimental tests.

Proper current transfers were recalculated from the following equations:

$$I_{inp} = \frac{V_{inp}'}{R_{k1} + R_i}, \quad I_{out} = \frac{V_{out}}{R_{k2}}, \quad (10), (11)$$

$$K_I = \frac{V_{out}}{V_{inp}'} = \frac{V_{out}}{V_{inp}'} \frac{R_{k1} + R_i}{R_{k2}} = K_V \frac{R_{k1} + R_i}{R_{k2}}. \quad (12)$$

It is obvious that if $R_{k1} = R_{k2} = R_k$, then Eq. (12) reduces to:

$$K_I = K_V \left(1 + \frac{R_i}{R_k} \right). \quad (13)$$

A. Adjustable Current Followers or Amplifiers Based on Controllable Current Gains

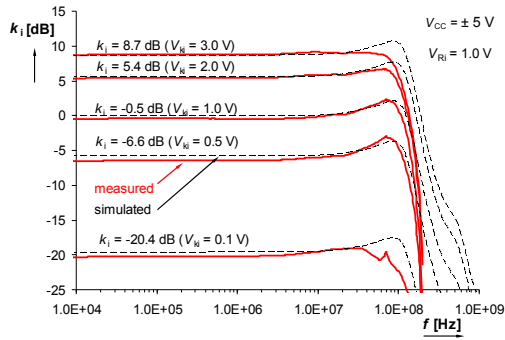
1) Solution Employing Two External Resistors

Solution shown in Fig.3 was built by three EL2082-s [27] (current mode multiplier) as ECCII-s. Current gain B is proportional to DC control voltage (and equal in range from 0 to 2 V). For current gain and intrinsic resistance the following relations are valid:

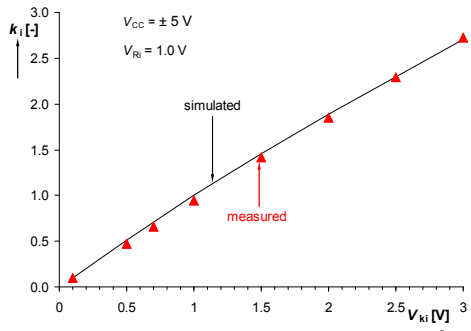
$$k_i \cong -V_{ki} \frac{(R_1 + R_{x1})}{(R_2 + R_{x2})}, \quad R_i \cong \frac{(R_1 + R_{x1})}{V_{Ri}}. \quad (14), (15)$$

Following values of passive elements: $R_1 = R_2 = 220 \Omega$ ($R_{x1,2} = 95 \Omega$ [27]) were selected. Experimental results are summarized in Fig.9 - Fig.12. Magnitude responses for

different values of current gain controlled by V_{ki} ($B_2 \approx V_{ki}$) and dependence of current gain k_i on control voltage V_{ki} are shown in Fig.9.

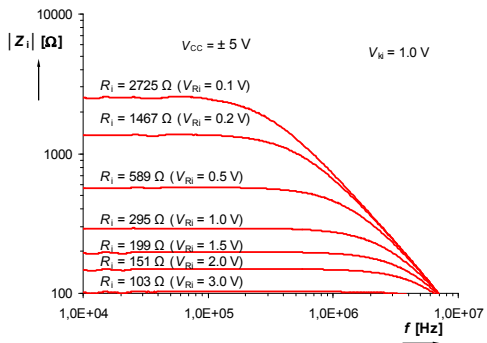


a)

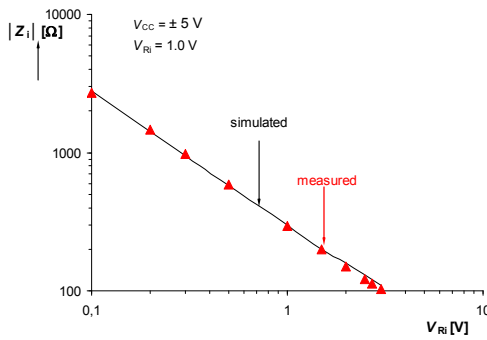


b)

Fig.9. Measured and simulated results: a) current gain magnitude response, b) dependence of current gain on control voltage.

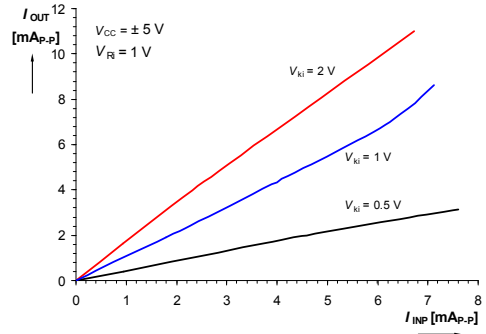


a)

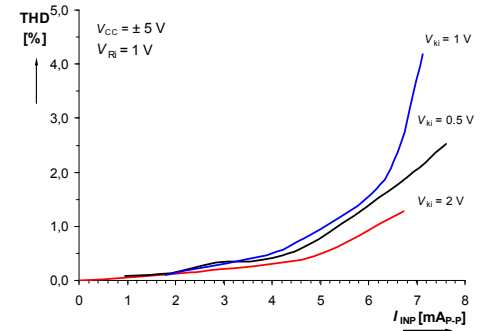


b)

Fig.10. Experimental results: a) measured frequency dependence of intrinsic resistance, b) dependence of intrinsic resistance on control voltage.

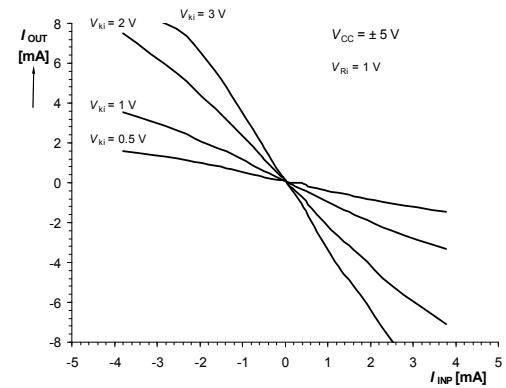


a)

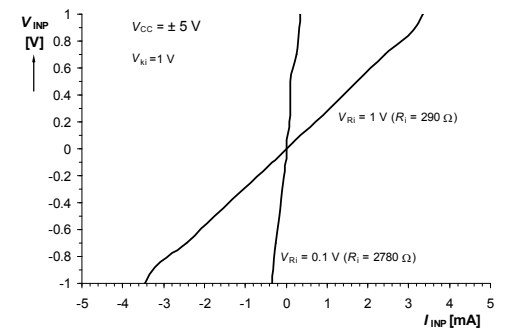


b)

Fig.11. Experimental results for harmonics excitation (1 MHz): a) measured dynamical characteristics, b) THD dependence on input level.



a)



b)

Fig.12. Measured DC characteristics: a) I_{out} vs. I_{inp} , b) V_{inp} vs. I_{inp} for R_i calculation.

Fig.10 shows frequency dependence of the intrinsic resistance (R_i) and dependence of R_i ($|Z_i|$ at 10 kHz respectively) on control voltage V_{Ri} . These results were obtained by network analyzer. However, capacity of the coaxial cable influences overall value of parasitic capacitance of current input (p) for higher values of R_i . Therefore, frequency bandwidth (flatness) of the R_i is lower than in the case where input terminal (p) is directly connected to another analog system on printed circuit board. Nevertheless, results confirm workability of the proposed CA model.

Dynamical characteristics and dependence of total harmonic distortion (THD) on input current level (recalculated from voltage) for harmonic excitation (sine wave) are given in Fig.11. THD seems to be maximally 0.2% for amplitude lower than 0.5 mA.

Static DC characteristics of CA and dependence of V_{imp} on I_{imp} for R_i calculation from DC values (traces for two R_i values are depicted) are shown in Fig.12.

2) Solution Employing One External Resistor

Current mode multipliers EL2082 were used also for the solution depicted in Fig.4a ($R_1 = 100 \Omega$, $R_{x1,2} = 95 \Omega$ [27]). Equations for current gain k_i and intrinsic resistance (R_i) have forms:

$$k_i \cong V_{ki}, \quad R_i \cong \frac{(R_1 + R_{x1} + R_{x2})}{V_{Ri}}. \quad (16), (17)$$

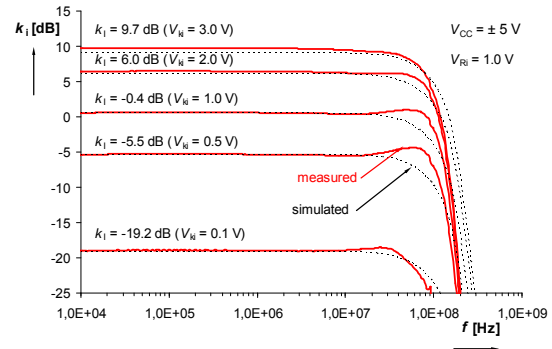
The current gain k_i is not dependent and influenced by R_1 or both parasitic intrinsic resistances of ECCII-s ($R_{x1,2}$), which is an important advantage in comparison to the previous case. Nevertheless, we have to consider $R_{x1,2}$ which increase resulting R_i twice more in comparison with the previous solution. Results are presented in Fig.13 - Fig.16.

B. Adjustable Current Amplifiers Based on Controllable Voltage Gains

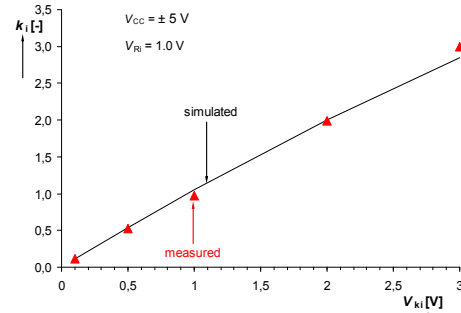
1) Solution Using Two VCAs and One DT

Solution employing voltage controllable (voltage mode) amplifiers (VCA-s) and diamond transistor is better from the electronic control point-of-view. Main advantage is that no matching condition is necessary. External resistors have values $R_1 = R_2 = 100 \Omega$. Two voltage controllable amplifiers VCA810 [28] and one diamond transistor OPA860 [29] were used in the solution depicted in Fig.6a. Following formulas for k_i and R_i are valid in accordance to [28]:

$$k_i \cong -\frac{R_1}{R_2} 10^{-2(V_{ki}+1)}, \quad R_i \cong \frac{R_1}{1-10^{-2(V_{Ri}+1)}}. \quad (18), (19)$$

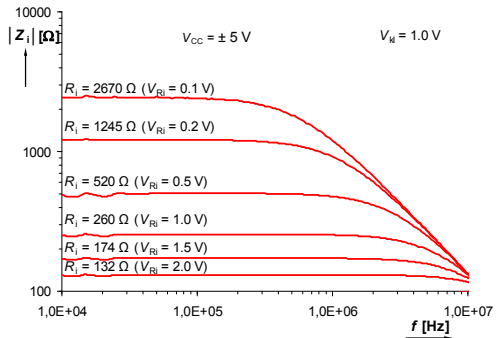


a)

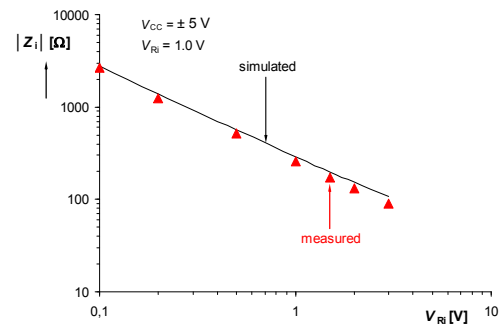


b)

Fig.13. Measured and simulated results: a) current gain magnitude response, b) dependence of current gain on control voltage.

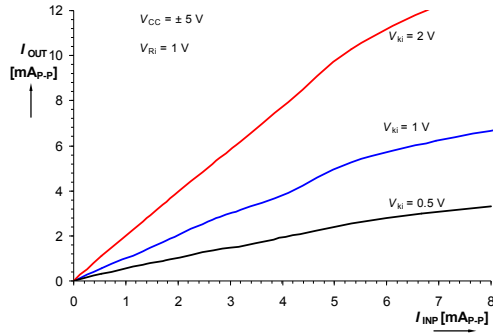


a)

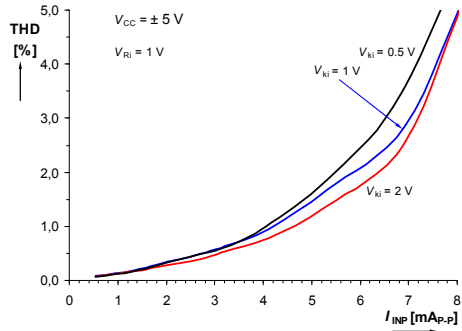


b)

Fig.14. Experimental results: a) measured frequency dependence of intrinsic resistance, b) dependence of intrinsic resistance on control voltage.

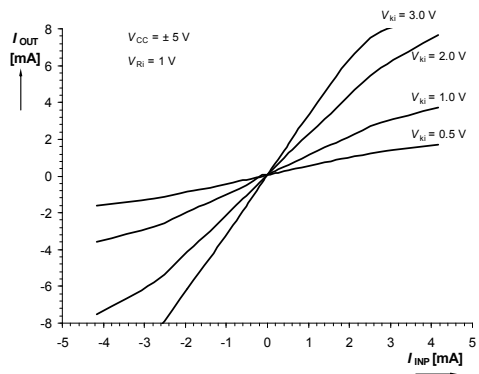


a)

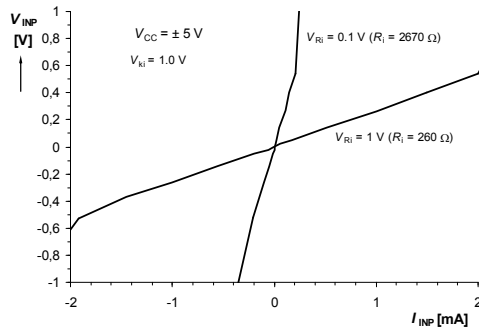


b)

Fig. 15. Experimental results for harmonics excitation (1 MHz): a) measured dynamical characteristics, b) THD dependence on input level.

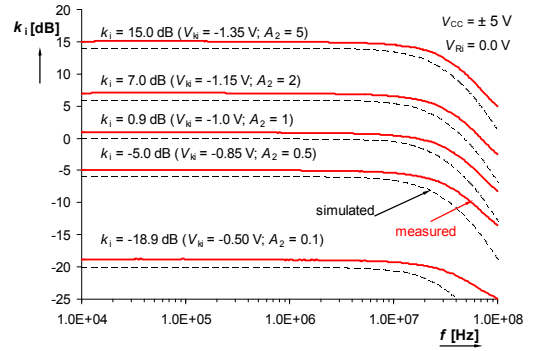


a)

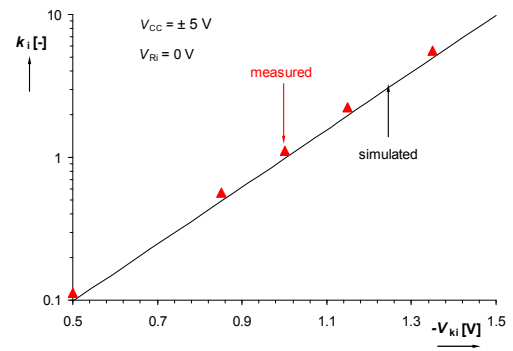


b)

Fig. 16. Measured DC characteristics: a) I_{out} vs. I_{inp} , b) V_{inp} vs. I_{inp} for R_i calculation.

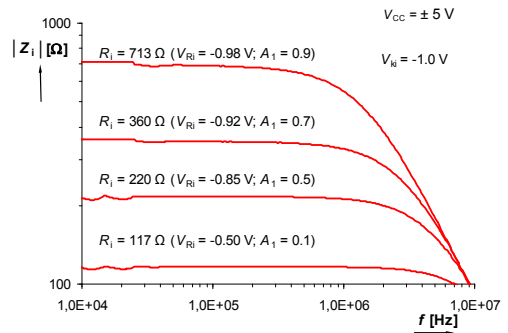


a)

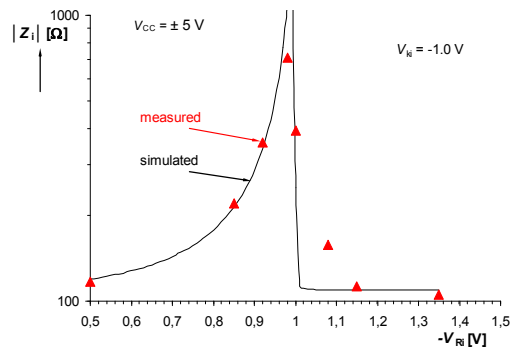


b)

Fig. 17. Measured and simulated results: a) current gain magnitude response, b) dependence of current gain on control voltage.

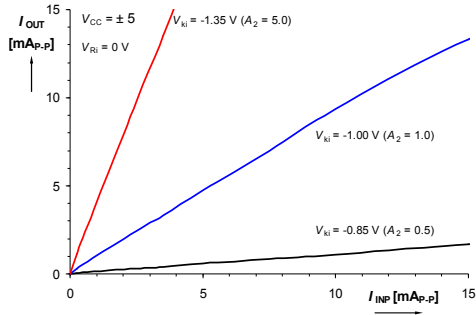


a)

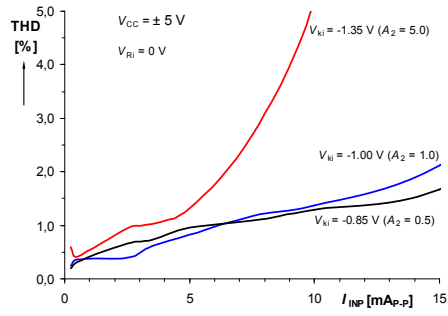


b)

Fig. 18. Experimental results: a) measured frequency dependence of intrinsic resistance, b) dependence of intrinsic resistance on control voltage.



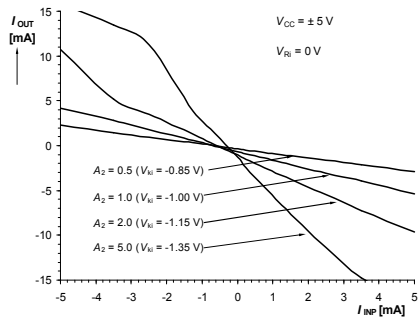
a)



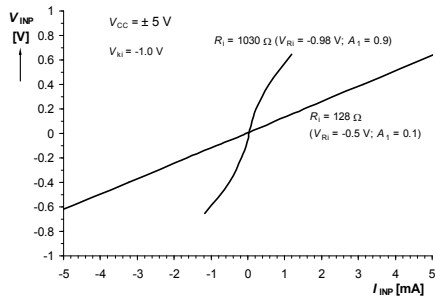
b)

Fig.19. Experimental results for harmonics excitation: a) measured dynamical characteristics, b) THD dependence on input level.

Results are shown in Fig.17 - Fig.20. Change of the resistance R_i is documented in Fig.18. The value increases till V_{Ri} achieves value close to 1 V. If V_{Ri} gets over 1 V, resistance decreases and it has negative character.

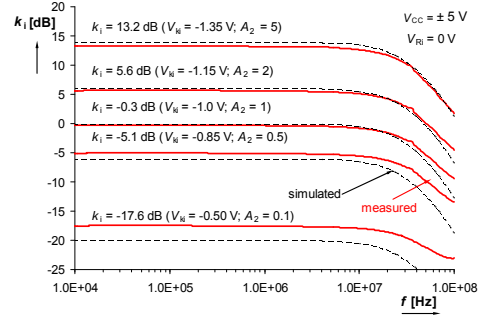


a)

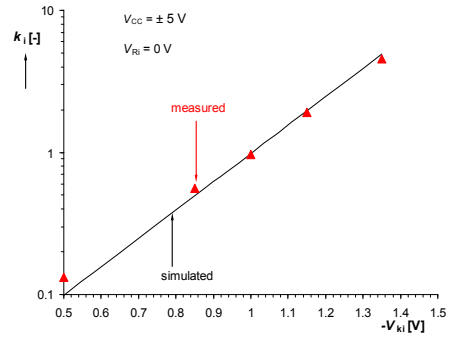


b)

Fig.20. Measured DC characteristics: a) I_{out} vs. I_{inp} , b) V_{inp} vs. I_{inp} for R_i calculation.



a)

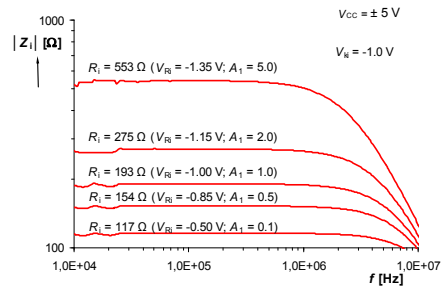


b)

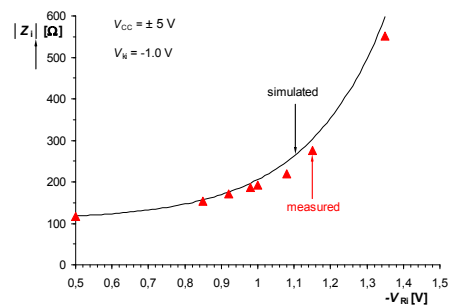
Fig.21. Measured and simulated results: a) current gain magnitude response, b) dependence of current gain on control voltage.

2) Solution Using Two VCAs, One DT and Additional Voltage Feedback

The last presented solution (Fig.7a) was also built with VCA810 and OPA860 and specific equation valid for R_i of this type of CA has the form:



a)



b)

Fig.22. Experimental results: a) measured frequency dependence of intrinsic resistance, b) dependence of intrinsic resistance on control voltage.

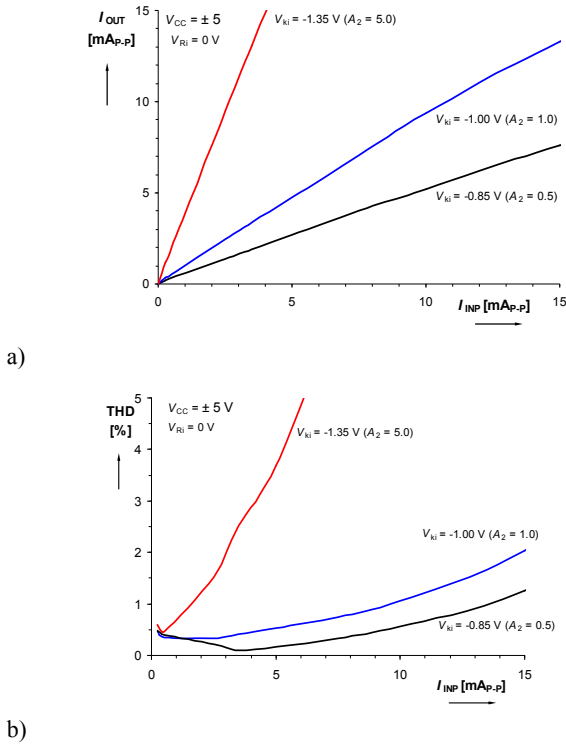


Fig.23. Experimental results for harmonics excitation: a) measured dynamical characteristics, b) THD dependence on input level.

$$R_i \cong R_1 \left(1 + 10^{-2(V_{Ri}+1)}\right). \quad (20)$$

The current gain k_i has the same form as (18). Results are presented in Fig.21 - Fig.24.

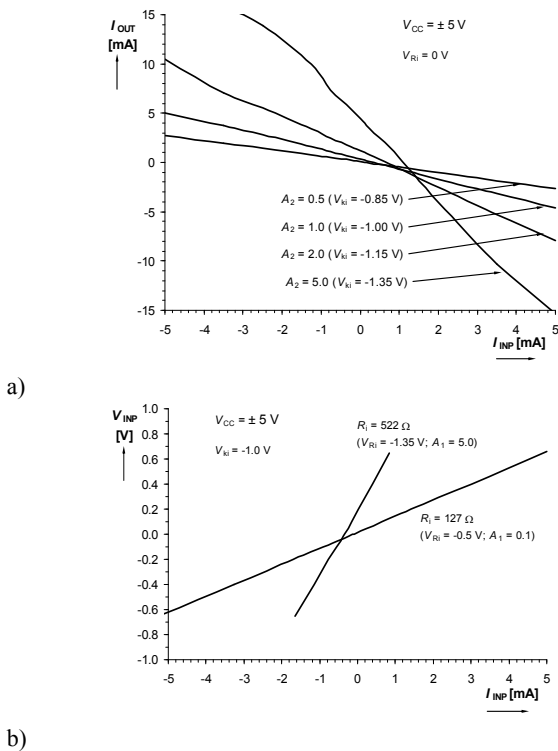


Fig.24. Measured DC characteristics: a) I_{OUT} vs. I_{INP} , b) V_{INP} vs. I_{INP} for R_i calculation.

Table 1. Comparison of main features of proposed solutions

Solution	Fig. 3	Fig. 4a	Fig. 6a	Fig. 7a
No. passive elements	2 grounded	1 floating	2 floating	2 floating
No. active elements	3 ECCII-s	3 ECCII-s	2 VCA, DT	2 VCA, DT
Matching of parameters required	yes	yes	no	no
k_i GBW [MHz]	100-140	70-110	35-45	25-45
k_i [-]	0.1-2.7 V_{ki} (0.1-3V)	0.1-2.8 V_{ki} (0.1-3V)	0.1-5.6 V_{ki} (0.5-1.35V)	0.1-4.6 V_{ki} (0.5-1.35V)
R_i [k Ω]	2.7-0.1 V_{Ri} (0.1-3V)	2.7-0.13 V_{Ri} (0.1-2V)	0.11-0.71 V_{Ri} (0.5-0.98V)	0.16-0.55 V_{Ri} (0.5-1.35 V)
Type of k_i control	linear	linear	exponential	exponential
Type of R_i control	hyperbolic	hyperbolic	hyperbolic/ exponential	exponential

C. Comparison of Proposed Solutions

All presented and measured solutions are compared in Table 1. Number of active and passive elements, necessity of matching of parameters (for example $B_1 = B_2$ in Fig.3 and Fig.4a), gain bandwidth (-3 dB), range of k_i , input resistance R_i , and type of control are the main attributes of the comparison. The solution from Fig.3 requires three ECCII-s and two grounded resistors for adjusting of k_i and R_i . The solution from Fig.4a provides the same benefits, but it consists of only one resistor. Frequency features and range of control of both important parameters (R_i , k_i) for selected values (R_1 , R_2) are similar. The most important drawback of the first solution is influence of intrinsic resistances of ECCII ($R_{x1,2}$) and external resistors R_1 and R_2 on k_i . This drawback was removed in model of CA from Fig.4a, where only one resistor is required. The worst disadvantage is the necessity of matching $B_1 = B_2$ for control of R_i without influence on k_i in both solutions. Solutions with VCA-s and DT-s from Fig.6a and Fig.7a solve this problem and no matching condition is required. However, the gain-bandwidth is lower, because VCA810 has lower GBW (30 MHz only [28]).

4. CONCLUSION

We designed and analyzed different varieties of circuit solutions that model current follower (or amplifier) and showed their performances. These circuits could be used as simulation models and mainly experimental (laboratory) models in development of applications with current active elements. They are useful in cases when we do not have any possibilities to fabricate current amplifiers or followers in specific applications like current-mode and mixed-mode filters, oscillators, sensor technique [30-31] (mainly in current-mode), and other circuits in complex systems (for example [32]) and in the first phase of tests (verification of expected behavior). Beyond using powerful simulation programs it allows to reveal important problems in the design without expensive fabrication of chip. Therefore, the presented approaches offer an easy way how to verify the proposed application using special active element with discussed features in a very simple and low-cost solution.

Because EL2082 multiplier is classified as an obsolete part, two further approaches based on voltage controllable voltage amplifiers and diamond transistors (these parts are easily accessible) were tested and they provided similar benefits. We hope that the presented approaches will be helpful for design, modeling and experiments employing novel types of active elements, which are using the discussed methods of control (k_i , R_i). Several application examples of such elements were given in [33].

5. ACKNOWLEDGEMENT

Research described in the paper was supported by Czech Science Foundation projects under No. 102/09/1681 and No. 102/11/P489. The support of the project CZ.1.07/2.3.00/20.0007 WICOMT, financed from the operational program Education for competitiveness, is gratefully acknowledged. Dr. Norbert Herencsar was supported by the project CZ.1.07/2.3.00/30.0039 of Brno University of Technology. The described research was performed in laboratories supported by the SIX project; the registration number CZ.1.05/2.1.00/03.0072, the operational program Research and Development for Innovation.

REFERENCES

- [1] Biolek, D., Senani, R., Biolkova, V., Kolka, Z. (2008). Active elements for analog signal processing: Classification, review, and new proposal. *Radioengineering*, 17 (4), 15-32.
- [2] Fabre, A., Saaid, O., Wiest, F., Boucheron, C. (1996). High frequency applications based on a new current controlled conveyor. *IEEE Transactions on Circuits and Systems I: Fundamental Theory and Applications*, 43 (2), 82-91.
- [3] Siripruchyanun, M., Chanapromma, C., Silapan, P., Jaikla, W. (2008). BiCMOS current-controlled current feedback amplifier (CC-CFA) and its applications. *WSEAS Transactions on Electronics*, 6 (5), 203-219.
- [4] Sedra, A., Smith, K.C. (1970). A second generation current conveyor and its applications. *IEEE Transaction on Circuit Theory*, 17 (1), 132-134.
- [5] Svoboda, J.A., McGory, L., Webb, S. (1991). Applications of a commercially available current conveyor. *International Journal of Electronics*, 70 (1), 159-164.
- [6] Surakamponorn, W., Thitimajshima, W. (1988). Integrable electronically tunable current conveyors. *IEE Proceedings G: Electronic Circuits & Systems*, 135 (2), 71-77.
- [7] Fabre, A., Mimeche, N. (1994). Class A/AB second-generation current conveyor with controlled current gain. *Electronics Letters*, 30 (16), 1267-1268.
- [8] Minaei, S., Sayin, O.K., Kuntman, H. (2006). A new CMOS electronically tunable current conveyor and its application to current-mode filters. *IEEE Transaction on Circuits and Systems I: Regular Papers*, 53 (7), 1448-1457.
- [9] Mahmoud, S., Hashies, M., Soliman, A. (2005). Low-voltage digitally controlled fully differential current conveyor. *IEEE Transactions on Circuits and Systems I: Regular Papers*, 52 (10), 2055-2064.
- [10] Kumngern, M., Chanwutium, J., Dejhan, K. (2010). Electronically tunable multiphase sinusoidal oscillator using translinear current conveyors. *Analog Integrated Circuits and Signal Processing*, 65 (2), 327-334.
- [11] Sedighi, B., Bakhtiar, M.S. (2007). Variable gain current mirror for high-speed applications. *IEICE Electronics Express*, 4 (8), 277-281.
- [12] Tangsrirat, W. (2008). Electronically tunable multi-terminal floating nullor and its application. *Radioengineering*, 17 (4), 3-7.
- [13] Tangsrirat, W., Pukkalanun, T. (2009). Digitally programmable current follower and its applications. *AEU – International Journal of Electronics and Communications*, 63 (5), 416-422.
- [14] Alzahr, H., Tasadduq, N. (2009). Realizations of CMOS fully differential current followers/amplifiers. In *IEEE International Symposium on Circuits and Systems (ISCAS 2009)*, 24-27 May, 2009. IEEE, 1381-1384.
- [15] Alzahr, H., Tasadduq, N., Al-Ees, O., Al-Ammari, F. (2011). A complementary metal-oxide semiconductor digitally programmable current conveyor. *International Journal of Circuit Theory and Applications*. Accepted for publication (2011). DOI: 10.1002/cta.786.
- [16] Koton, J., Herencsar, N., Jerabek, J., Vrba, K. (2010). Fully differential current-mode band-pass filter: Two design solutions. In *Proceedings of the 33rd International Conference on Telecommunications and Signal Processing (TSP 2010)*, 17-20 August, 2010, 1-4.
- [17] Biolek, D., Bajer, J., Biolkova, V., Kolka, Z., Kubicek, M. (2010). Z copy-controlled gain-current differencing buffered amplifier and its applications. *International Journal of Circuit Theory and Applications*, 39 (3), 257-274.
- [18] Biolek, D., Lahiri, A., Jaikla, W., Siripruchyanun, M., Bajer, J. (2011). Realisation of electronically tunable voltage-mode/current-mode quadrature sinusoidal oscillator using ZC-CG-CDBA. *Microelectronics Journal*, 42 (10), 1116-1123.
- [19] Herencsar, N., Lahiri, A., Vrba, K., Koton, J. (2012). An electronically tunable current-mode quadrature oscillator using PCAs. *International Journal of Electronics*, 99 (5), 609-621.
- [20] Sotner, R., Jerabek, J., Prokop, R., Vrba, K. (2011). Current gain controlled CCTA and its application in quadrature oscillator and direct frequency modulator. *Radioengineering*, 20 (1), 317-326.
- [21] Marcellis, A., Ferri, G., Guerrini, N.C., Scotti, G., Stornelli, V., Trifiletti, A. (2009). The VGC-CCII: A novel building block and its application to capacitance multiplication. *Analog Integrated Circuits and Signal Processing*, 58 (1), 55-59.
- [22] Kumngern, M., Junnapiya, S. (2010). A sinusoidal oscillator using translinear current conveyors. In *IEEE Asia Pacific Conference on Circuits and Systems (APCCAS 2010)*, 6-9 December 2010. IEEE, 740-743.

- [23] Sotner, R., Herencsar, N., Jerabek, J., Koton, J., Dostal, T., Vrba, K. (2012). Quadrature oscillator based on modified double current controlled current feedback amplifier. In *Radioelektronika 2012: Proceedings of 22nd International Conference*. IEEE, 275-278.
- [24] Jaikla, W., Lahiri, A. (2011). Resistor-less current-mode four-phase quadrature oscillator using CCCDTAs and grounded capacitors. *AEU - International Journal of Electronics and Communications*, 66 (3), 214-218.
- [25] Texas Instruments. (1993). *OPA633: High speed buffer amplifier*. Last modified 9/2000.
- [26] Texas Instruments. (1996). *BUF634: 250 mA High-speed buffer*. Last modified 9/2000.
- [27] Intersil (Elantec). (1996). *EL2082: Current-mode multiplier*. Last modified 2003.
- [28] Texas Instruments. (2003). *VCA810: High gain adjust range, wideband, variable gain amplifier*. Last modified 12/2010.
- [29] Texas Instruments. (2005). *OPA860: Wide bandwidth operational transconductance amplifier and buffer*. Last modified 8/2008.
- [30] Odon, A. (2010). Modelling and simulation of the pyroelectric detector using MATLAB/Simulink. *Measurement Science Review*, 10 (6), 195-199.
- [31] Deng, X., Yang, W.Q. (2012). Fusion research of electrical tomography with other sensors for two-phase flow measurement. *Measurement Science Review*, 12 (2), 62-67.
- [32] Abu-Al-Aish, A., Rehman, M., Abdullah, Z., Abu-Hassan, H. (2010). Microcontroller based capacitive mass measuring system. *Measurement Science Review*, 10 (1), 15-18.
- [33] Sotner, R., Jerabek, J., Herencsar, N., Dostal, T., Vrba, K. (2011). Additional approach to the conception of current follower and amplifier with controllable features. In *Proceedings of the 34th International Conference on Telecommunications and Signal Processing (TSP 2011)*, 279-283.

Received July 02, 2012.

Accepted November 25, 2012.

[36] SOTNER, R., JERABEK, J., KARTCI, A., HERENC SAR, N., PROKOP, R., PETRZELA, J., VRBA, K. Behavioral Models of Current Conveyor of Second Generation with Advanced Controllable Inter-Terminal Relations. In *Proceedings of the 38th International Conference on Telecommunications and Signal Processing (TSP 2015)*, Prague (Czech Republic), 2015, p. 360-365. ISBN: 978-1-4799-8497-8.

Behavioral Models of Current Conveyor of Second Generation with Advanced Controllable Inter-Terminal Relations

Roman Sotner, Jan Jerabek, Aslihan Kartci, Norbert Herencsar, Roman Prokop, Jiri Petrzela, and Kamil Vrba

Abstract—This paper introduces behavioral model of advanced type of current conveyor with extended controllable inter-terminal features. This type of active device offers three independent current input terminals (X), all with adjustable input resistance R_X where currents from all X terminals are weighted in independent branches by electronically adjustable current gains (B) and summed in the output node. Voltage inter-terminal relations are advanced because of controllable voltage difference of two pairs of input voltages. This advanced active device offers interesting features for future applications in analog signal processing. The functionality of the model was verified by PSpice simulations.

Keywords—Advanced features, electronic control, current conveyor, current gain control, intrinsic resistance control, inter-terminal transfers, voltage gain control.

I. INTRODUCTION

ACTIVE DEVICES [1] like current conveyors [2] are very important for various areas of analog signal processing, especially in the filters, oscillators, and other applications [3]. The current conveyor of second generation (CCII) [4], [5] is used very frequently in many applications. It is quite important to recapitulate the main features of an ideal generalized three-port current conveyor [2], [6], [7]. Classical generalized current conveyor has three terminals (voltage/current input – Y, current input – X, current output – Z) and provides transfers between terminals Y and X (voltage transfer α and also current transfer β) and between terminals X and Z (current transfer γ). In accordance to definition [6], [7] transfers α , β , γ achieve values 0 or ± 1 but in general, they can have an arbitrary value. The transfer β is set to 0 in the CCII specification. Parameters α and γ are referred by another

way in our work. In our definition of the current conveyor, where also intentional, real and non-zero input resistance of the X terminal (R_X) is supposed, following general relations are valid. The current transfer notation γ was replaced by controllable parameter B ($I_Z = BI_X$) between X and Z terminal. Relation between X and Y terminals is represented by $V_X = AV_Y - I_X R_X$. Parameters B (current gain [8]-[10]), A (voltage gain [11]) and R_X (resistance of the current input terminal X [10]-[12]) are generally arbitrarily adjustable constants with positive value (in the most cases).

Note there are still three input/output terminals in the generalized CCII (GCCII). However, increase of number of the Z terminals is also well-known. We can provide multiple output copies with positive or negative transfer [2] or we can modify this type to have mutually independently controllable gain (including polarity) of all available outputs [13]. Also some modifications offering two Y terminal inputs with specific relation $V_{Y1} - V_{Y2} = V_X$, known as differential voltage current conveyor (DVCC) [14], differential difference current conveyor (DDCC) [15] allowing relation $V_{Y1} - V_{Y2} + V_{Y3} = V_X$ were presented in the past. However, none of them includes adjustable parameter in relation for these terminal ($Y_1 - Y_n$) voltages and/or other values of the GCCII. Attempt to obtain controllable feature regarding difference of two voltages was provided in so-called z-copy controlled-gain voltage differencing current conveyor (ZC-CG-VDCC) [16]. However, current conveyor is only subpart of the active device and voltage difference was realized by controllable operational transconductance amplifier. The next possibility how to improve transfer features (electronically controllable) of the GCCII is in the case of terminal X. Only single X terminal (with controllable R_X in some cases) was present in discussed DDCCs, DVCCs, VDCCs, etc. There are also devices referred as dual-X current conveyor of second generation (DXCCII) [17], [18] where two X terminals are available to provide function $V_{Xp} = -V_{Xn} = V_Y$. So-called fully differential current conveyor of second generation (FDCCII) [19], [20] offers four Y type terminals (voltage inputs) and implements operations utilizing of two X terminals in the form: $V_{Xp} = V_{Y1} - V_{Y2} + V_{Y3}$ and $V_{Xn} = V_{Y2} - V_{Y1} + V_{Y4}$.

Based on the study provided, there is still scope for valuable improvements and implementation of advanced features improving also performance of the previously reported types of advanced CCs (DXCCII, FDCCII, etc.). In some cases, we require some special features that are useful for simplification of some signal operations intended in the

Manuscript received February 18, 2015. Research described in this paper was financed by the National Sustainability Program under grant LO1401. For the research, infrastructure of the SIX Center was used. Research described in the paper was supported by Czech Science Foundation project under No. 14-24186P. Grant No. FEKT-S-14-2281 also supported this research. The support of the project CZ.1.07/2.3.00/20.0007 WICOMT, financed from the operational program Education for competitiveness, is gratefully acknowledged.

R. Sotner, J. Jerabek, N. Herencsar, R. Prokop, Jiri Petrzela and K. Vrba are with the Brno University of Technology, Faculty of Electrical Engineering and Communication, Technicka 3082/12, Brno, 616 00, Czech Republic (e-mails: {sotner; jerabekj; herencsn; prokop; petrzelj; vrbak}@feec.vutbr.cz).

A. Kartci is with the Yildiz Technical University, Department of Electronics and Communications Engineering, Esenler, 34222, Istanbul, Turkey (e-mail: aslhankartc@gmail.com).

synthesis and design of application. Therefore, we defined useful modification of the GCCII. Our contribution presents new behavioral model designed for the representation of GCCII with direct electronic (voltage) control of all discussed features (B , A , R_X) and also with advanced features of transfers regarding X and Y controllable terminal relations.

II. BEHAVIORAL MODELS OF THE GCCII WITH ADVANCED CONTROLLABLE FEATURES BETWEEN TERMINALS

Behavioral models are based on commercially available active devices that are easily accessible for fast experimental tests. Main characteristics of complex devices constructed from such elements are given by their parameters. We can expect that integrated solution of such active element will always offer better performance from many points of view. This approach has many advantages. First of all, expensive design and fabrication of IC prototype is not necessary in starting phase of the development or for preliminary tests. Subsection A describes basic principle and controllable $X \rightarrow Z$ transfers, the following subsection B describes controllable $Y \rightarrow X$ transfers (extension of core section).

A. Advanced Inter-Terminal Relations of $X \rightarrow Z$ Transfer

Despite of wide and various utilization of previously reported types (FDCCII) allowing some operations (difference of currents to X) there electronic control of such type of relation is missing. We proposed model of the CC with three X terminals with three independently controllable R_X -s in form:

$$V_{X1} = V_Y - I_{X1} R_{X1}, \quad (1)$$

$$V_{X2} = V_Y - I_{X2} R_{X2}, \quad (2)$$

$$V_{X3} = V_Y - I_{X3} R_{X3}. \quad (3)$$

All input currents participate on output operation ($X \rightarrow Z$):

$$I_Z = B_1 k_1 I_{X1} + B_2 k_2 I_{X2} + B_3 k_3 I_{X3}. \quad (4)$$

This relation includes interesting features for applications because it represents weighting function of input currents (k_{1-3} are general constants of particular solution) from three independent branches (gain of each current is independently adjustable before final summarization in high-impedance current output terminal Z). Ideal model of the designed CC with advanced features is shown in Fig. 1.

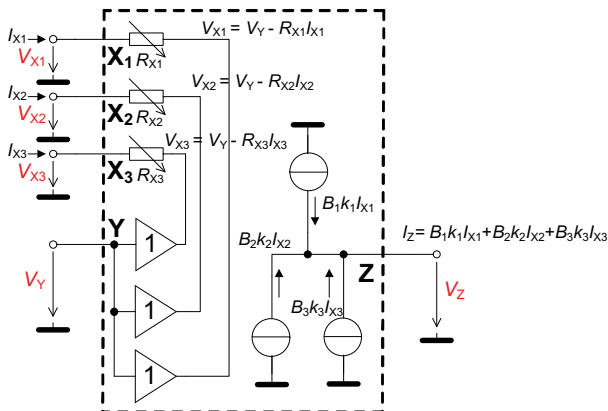


Fig. 1. Ideal principle of the CC with advanced features concerning the $X \rightarrow Z$ terminal relations.

Final behavioral model based on commercially available elements is shown in Fig. 2. The model utilizes six resistors, six electronically controllable current conveyors of second generation (ECCII) [8], [10] known also under designation current-mode multiplier EL2082 [21] and six simple voltage buffers (VBs). As a VB, we can chose for example OPA633 [22], BUF634 [23] or excellent buffer included in OPA660 package [24]). Such setup can really cover the above discussed features (1)-(4). Particular equations specified for presented model from Fig. 2 (basic idea explained in [25], [26]) are in following forms:

$$V_{X1} \cong V_Y - I_{X1} \left(\frac{R'_{ja}}{V_{SET_Rx1}} \right), \quad (5)$$

$$V_{X2} \cong V_Y - I_{X2} \left(\frac{R'_{jb}}{V_{SET_Rx2}} \right), \quad (6)$$

$$V_{X3} \cong V_Y - I_{X3} \left(\frac{R'_{jc}}{V_{SET_Rx3}} \right), \quad (7)$$

because partial $R_X \cong R'_j / V_{SET_Rx}$ in accordance to [25] and [26]. Therefore:

$$I_Z \cong \frac{V_{SET_B1} R'_{ja}}{V_{SET_Rx1} R'_{ia}} I_{X1} + \frac{V_{SET_B2} R'_{jb}}{V_{SET_Rx2} R'_{ib}} I_{X2} + \frac{V_{SET_B3} R'_{jc}}{V_{SET_Rx3} R'_{ic}} I_{X3}, \quad (8)$$

due to approximate validity of $B \cong V_{SET_B}$ [21].

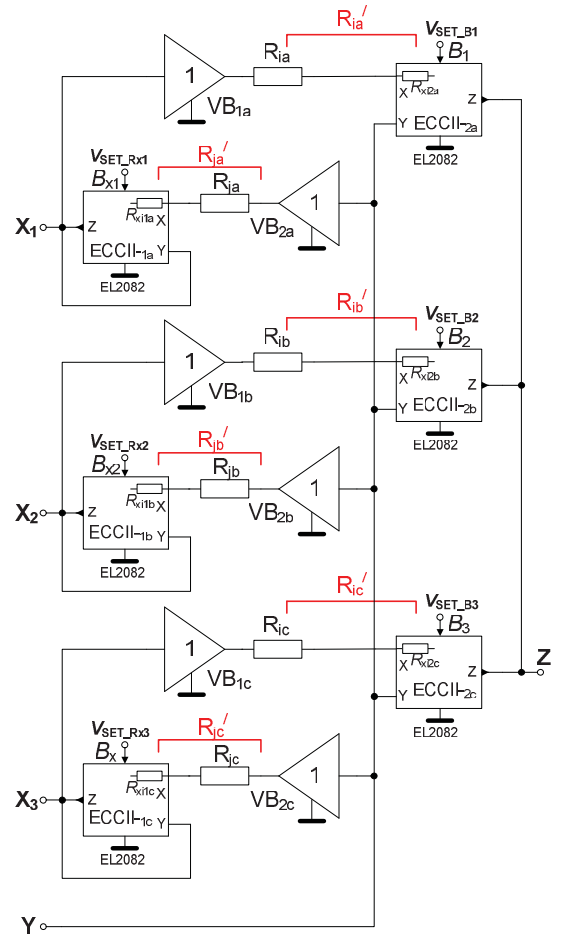


Fig. 2. Behavioral model of the CC with advanced features concerning the $X \rightarrow Z$ terminal relation.

B. Advanced Inter-Terminal Relations of $Y \rightarrow X$ Transfer

This extension of the features supposes voltage operation (difference or sum) of the voltage transfer in $Y \rightarrow X$ direction. Commercially available variable gain voltage amplifiers of various type (abbreviated as VA in our explanation), controllable by DC voltage or digitally, can be easily employed. Features of CC presented in Fig. 2 can be extended also by active subpart given in Fig. 3. We implemented precise, reliable and quite known VCA610 [27] amplifiers in our case. Additional difference of resulting differences ($V_{Y1} - V_{Y2}$ and $V_{Y3} - V_{Y4}$) from VA_1 and VA_2 is performed by the differential voltage buffer (DVB) AD830 [28]. Ideal relations between $V_{Y1,2,3,4}$ and $V_{X1,2,3}$ (for $X_{1,2,3}$ open) have the following form:

$$V_{X1} = [(V_{Y1} - V_{Y2})A_1 - (V_{Y3} - V_{Y4})A_2] - I_{X1}R_{X1}, \quad (9)$$

$$V_{X2} = [(V_{Y1} - V_{Y2})A_1 - (V_{Y3} - V_{Y4})A_2] - I_{X2}R_{X2}, \quad (10)$$

$$V_{X3} = [(V_{Y1} - V_{Y2})A_1 - (V_{Y3} - V_{Y4})A_2] - I_{X3}R_{X3}, \quad (11)$$

where exact transfers for specific active elements (Fig. 3) are given by:

$$V_{X1} \cong [(V_{Y1} - V_{Y2})10^{-2(V_{SET_A1+1})} - (V_{Y3} - V_{Y4})10^{-2(V_{SET_A2+1})}] - I_{X1} \left(\frac{R'_{ja}}{V_{SET_RX1}} \right)^{\frac{1}{\beta}}, \quad (12)$$

$$V_{X2} \cong [(V_{Y1} - V_{Y2})10^{-2(V_{SET_A1+1})} - (V_{Y3} - V_{Y4})10^{-2(V_{SET_A2+1})}] - I_{X2} \left(\frac{R'_{jb}}{V_{SET_RX2}} \right)^{\frac{1}{\beta}}, \quad (13)$$

$$V_{X3} \cong [(V_{Y1} - V_{Y2})10^{-2(V_{SET_A1+1})} - (V_{Y3} - V_{Y4})10^{-2(V_{SET_A2+1})}] - I_{X3} \left(\frac{R'_{jc}}{V_{SET_RX3}} \right)^{\frac{1}{\beta}}, \quad (14)$$

where V_{SET_A} is DC control voltage [27]. It achieves range from -2 to 0 V and allows to change voltage gain A from 100 to 1/100 (± 40 dB).

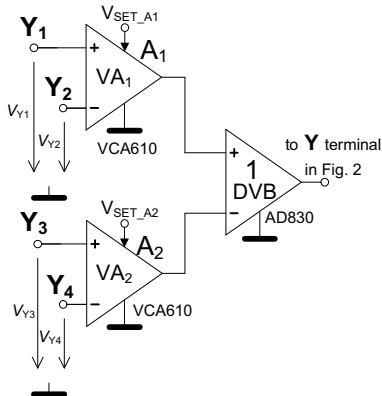


Fig. 3. Extension of the behavioral model from Fig. 2 by additional advanced $Y \rightarrow X$ inter-terminal relations.

III. SIMULATION RESULTS OF THE PROPOSED BEHAVIORAL MODEL

We tested functionality of proposed model (Fig. 2) by PSpice simulations in this preliminary stage. All resistors in the model were chosen as $R_i = R_j = 910 \Omega$ (overall values $R'_i = R'_j = 1005 \Omega$). The DC characteristic of the $X_1 \rightarrow Z$

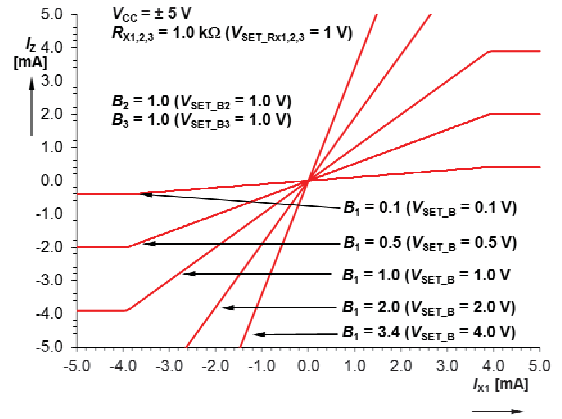


Fig. 4. DC transfer characteristic of $X_1 \rightarrow Z$ for several steps of B_1 .

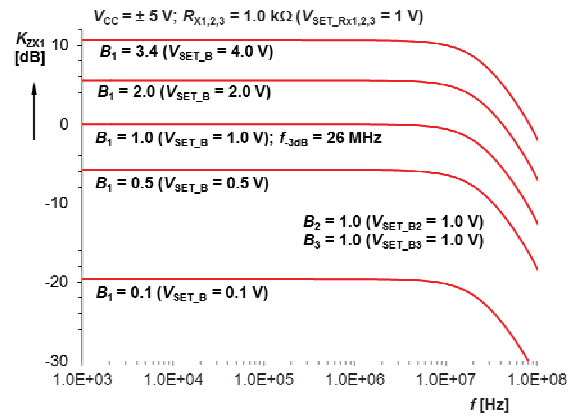


Fig. 5. AC transfer responses of $X_1 \rightarrow Z$ for several steps of B_1 .

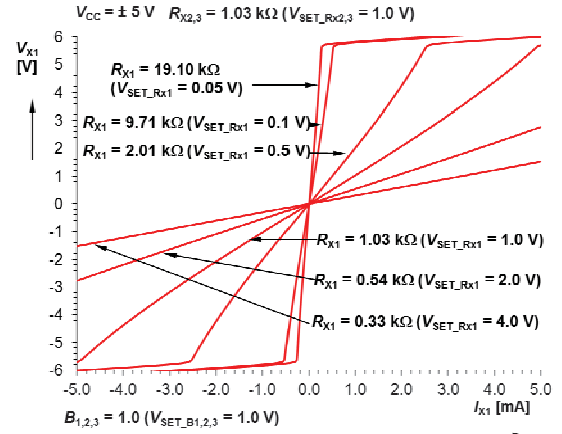


Fig. 6. DC dependence of V_{X1} on I_{X1} for X_1 terminal and stepped V_{SET_RX1} value.

transfer for several values of B_1 is shown in Fig. 4. Only “channel” with input X_1 (driving current through X_1) was tested. The rest (X_2 and X_3) of channels is analogical to X_1 . AC responses for stepping of B_1 are shown in Fig. 5.

Features of X terminals for stepped V_{SET_RX1} value (again identical for all - $X_{1,2,3}$) are documented by dependence of terminal voltage on input current in Fig. 6 (for X_1 only). Magnitude of impedance of the X_1 terminal are shown in Fig. 7 (the rest of current inputs provides the same behavior). DC characteristic of the $Y \rightarrow X$ (all X terminals) transfer has limits of linearity around ± 4 V (at the input Y and also at the

output X - open). Frequency response of this transfer function depends on actual setting of $V_{SET_R_X}$ (R_X). We tested transfer $Y \rightarrow X_1$ as an example. The first parasitic pole frequency is:

$$\omega_p = \frac{1}{2\pi R_X C_p} \cong \frac{V_{SET_R_X}}{2\pi R_X' C_p}, \quad (15)$$

where C_p is parasitic capacitance in node of X terminal (approximately 7 pF [21], [24]) and it decreases for large values of R_X . Hand calculation from equation (15) provides theoretical value $f_p = 995$ kHz and simulation gives $f_p = 1.135$ MHz (Fig. 8). Note that peak for $R_{X1} = 0.33$ k Ω (Fig. 8) is caused by complex conjugated character of poles in this particular configuration. Transient response for square wave excitation at all X terminals is shown in Fig. 9 to verify summing operation between X terminals. Note that this relation can be easily modified to obtain also different relation (difference) than sum of all currents from X_1 , X_2 and X_3 . Summing features of all three current inputs are also tested in Fig. 10 where sine wave excitation was used. Two inputs, X_1 and X_2 , are driven by current signal having amplitude level 150 μ A (100 kHz) and the third is driven by 300 μ A (200 kHz). Figure 10 indicates two situations. The first result (red solid line) is outcome of simple sum of input currents ($B_{1,2,3} = 1$). Result for weighted summing operation ($B_2 = 0.5$ and $B_{1,3} = 1$) is depicted by red dashed line.

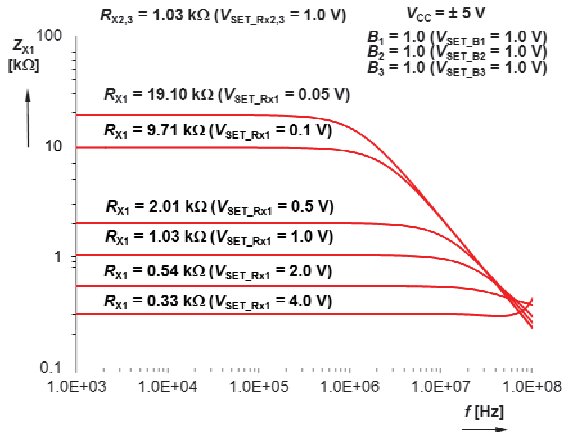


Fig. 7. Magnitude of impedance of X_1 terminal for stepped $V_{SET_R_{X1}}$ value.

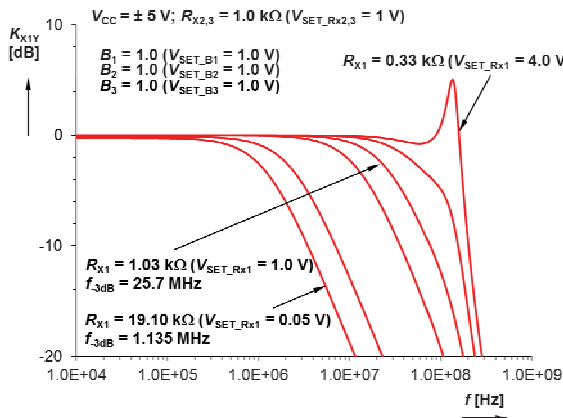


Fig. 8. AC response of $Y \rightarrow X_1$ transfer in dependence on R_{X1} .

Additional extension of the $Y \rightarrow X$ voltage inter-terminal transfer (Fig. 3) in combination with part in Fig. 2 provides following results. Fig. 11 shows results of test of Y_1 terminal ($V_{Y2} = V_{Y3} = V_{Y4} = 0$) in DC domain and for different values of V_{SET_A1} (gains A_1). The magnitude and frequency responses of the $Y_1 \rightarrow X_{1,2,3}$ transfer are given in Fig. 12. Example of transient responses for $V_{Y1} - V_{Y3}$ and $V_{Y1} + V_{Y4}$ operations are shown in Fig. 13 and Fig. 14 (all detailed specifications are noted in figures). An example of the signal operation with adjusted A_1 and A_2 (V_{SET_A1} , V_{SET_A2}) is shown in Fig. 15.

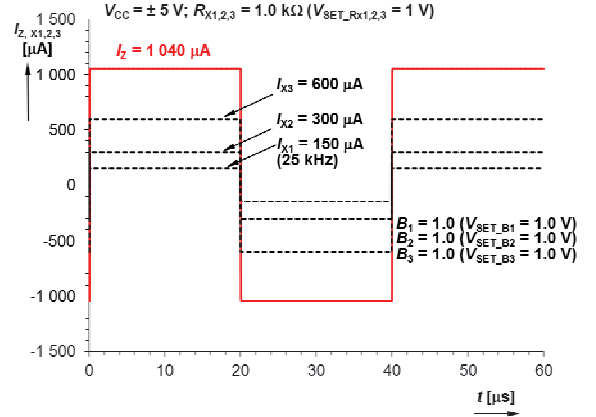


Fig. 9. Transient response ($X \rightarrow Z$) of the current sum in node Z for square wave excitation (three different input currents).

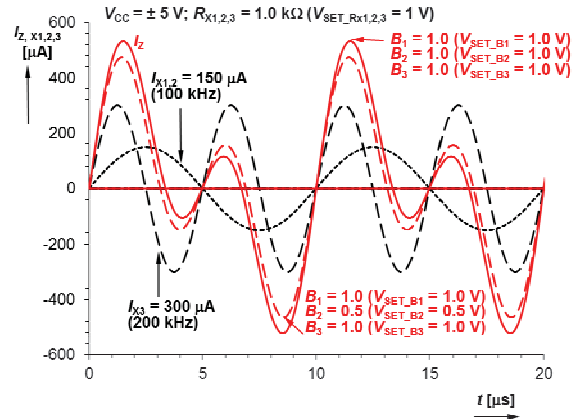


Fig. 10. Transient response ($X \rightarrow Z$) of the current sum in node Z for sine wave excitation (three different input currents, balanced and weighted gain).

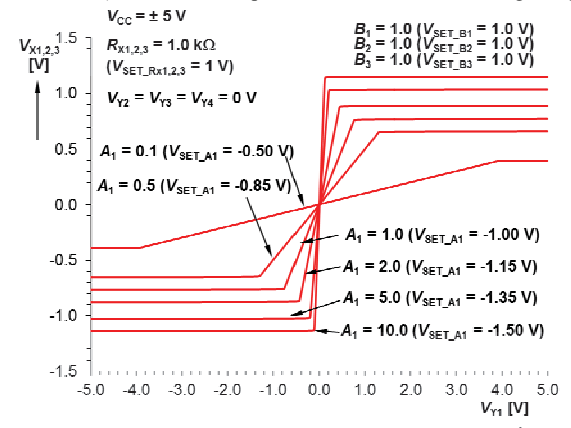


Fig. 11. DC transfer characteristic $Y_1 \rightarrow X_{1,2,3}$ for several steps of A_1 (V_{SET_A1}).

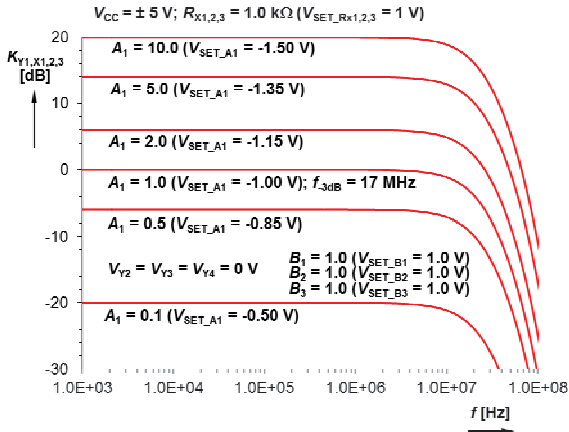


Fig. 12. Magnitude of $Y_1 \rightarrow X_{1,2,3}$ transfer responses for several steps of A_1 (V_{SET_A1}).

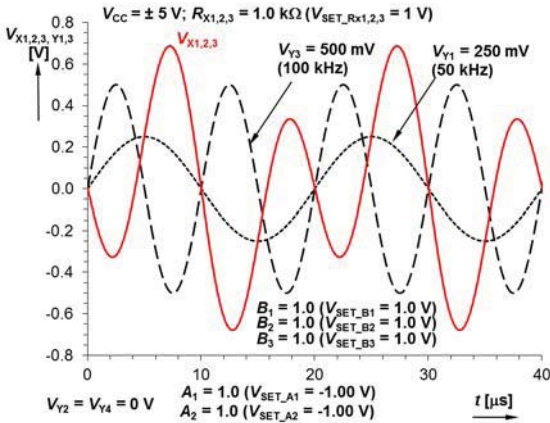


Fig. 13. Transient response ($Y_{1,3} \rightarrow X_{1,2,3}$) of the voltage difference results in nodes $X_{1,2,3}$ for sine wave excitation for different input voltage levels and frequencies.

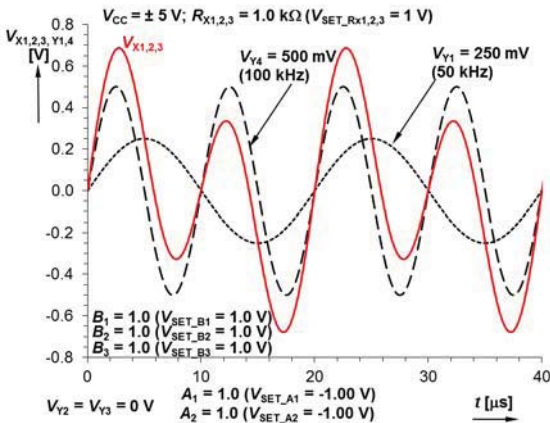


Fig. 14. Transient response ($Y_{1,4} \rightarrow X_{1,2,3}$) of the voltage difference results in nodes $X_{1,2,3}$ for sine wave excitation for different input voltage levels and frequencies.

IV. CONCLUSION

Presented complex behavioral model of the CC offers various interesting features of electronic controllability of the main features (B , A , R_X) and also allows advanced inter-terminal features. All these features are very useful in future applications of filters, oscillators, modulators, etc. The model represents advanced active device and facilitates very

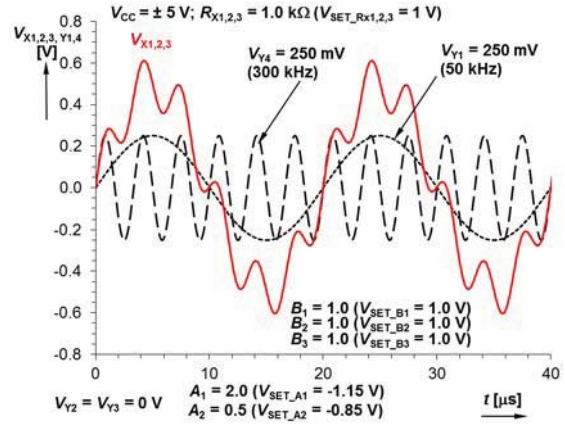


Fig. 15. Transient response ($Y_{1,4} \rightarrow X_{1,2,3}$) of the voltage difference results in nodes $X_{1,2,3}$ for sine wave excitation for different input frequencies and adjusted A_1 (V_{SET_A1}), A_2 (V_{SET_A2}).

inexpensive verification of various theories and hypotheses without requirement of the system implementation on IC at this stage. In other words, it allows the very first but real experimental verification of the system and foregoing expensive IC fabrication. However, the model has also some limitations. Dynamical range seem to be quite large (units of mA and units of V). Controllability of B is limited approximately to 3.5. Voltage gains A are available up to 100, however input dynamical features reduces to mV level. Frequency limit of the model is around 1 MHz. It is given by R_X dependence on frequency and magnitude response of the $Y \rightarrow X$ transfer and by V_{SET_RX} versus parasitic pole frequency). The higher limit of the R_X control is about 10–20 k Ω . Simulations confirmed functionality of the model and its suitability for further experiments in the research of electronically adjustable applications. Transient responses are shown in order to prove the functionality of mathematical operations and amplitudes were selected sufficiently low to obtain negligible total harmonic distortion (THD).

REFERENCES

- [1] D. Biolk, R. Senani, V. Biolkova, Z. Kolka, "Active elements for analog signal processing: Classification, Review and New Proposals", *Radioengineering*, vol. 17, no. 4, pp. 15–32, 2008.
- [2] R. Senani, D. R. Bhaskar, A. K. Singh, "Current conveyors: Variants, Applications and Hardware Implementations", Springer International Publishing Switzerland, 2015.
- [3] W. Chen, "The Circuits and Filters Handbook," Boca Raton, FL: CRC Press, 2002.
- [4] A. Sedra, K. C. Smith, "A second generation current conveyor and its applications", *IEEE Transaction on Circuit Theory*, vol. CT-17, no. 2, pp. 132–134, 1970.
- [5] J. A. Svoboda, L. McGory, S. Webb, "Applications of a commercially available current conveyor," *Int. Journal of Electronics*, vol. 70, no. 1, pp. 159–164, 1991.
- [6] D. Biolk, K. Vrba, J. Cajka, T. Dostal, "General three-port current conveyor: a useful tool for network design", *Journal of Electrical Engineering*, vol. 51, no. 1–2, pp. 36–39, 2000.
- [7] J. Cajka, T. Dostal, K. Vrba, "General view on current conveyors" *International Journal of Circuit Theory and Applications*, vol. 32, no. pp. 133–138, 2004.
- [8] W. Surakamponorn, W. Thitimajshima, "Integrable electronically tunable current conveyors", *IEE Proceedings-G*, vol. 135, no. 2, pp. 71–77, 1988.

- [9] A. Fabre, N. Mimeche, "Class A/AB second-generation current conveyor with controlled current gain", *Electronics Letters*, vol. 30, no. 16, pp. 1267–1268, 1994.
- [10] S. Minaei, O. K. Sayin, H. Kuntman, "A new CMOS electronically tunable current conveyor and its application to current-mode filters", *IEEE Trans. on Circuits and Systems - I*, vol. 53, no. 7, pp. 1448–1457, 2006.
- [11] A. Marcellis, G. Ferri, N. C. Guerrini, G. Scotti, V. Stornelli, A. Trifiletti, "The VGC-CCII: a novel building block and its application to capacitance multiplication", *Analog Integrated Circuits and Signal Processing*, vol. 58, no. 1, pp. 55–59, 2009.
- [12] A. Fabre, O. Saaïd, F. Wiest, C. Boucheron, "High frequency applications based on a new current controlled conveyor", *IEEE Trans. on Circuits and Systems - I*, vol. 43, no. 2, pp. 82–91, 1996.
- [13] J. Jerabek, R. Sotner, K. Vrba, "TISO Adjustable filter with controllable controlled-gain voltage differencing current conveyor", *Journal of Electrical Engineering*, vol. 65, no. 3, pp. 137-143, 2014.
- [14] H. O. Elwan, A. M. Soliman, "A novel CMOS differential voltage current conveyor and its applications", *IEE Proceedings on Circuits Devices and Systems*, vol. 144, no. 3, pp. 195-200, 1997.
- [15] W. Chiu, S. I. Liu, H. W. Tsao, "CMOS differential difference current conveyors and their applications", *IEE Proceedings on Circuits Devices and Systems*, vol. 143, no. 2, pp. 91-96, 1996.
- [16] R. Sotner, N. Herencsar, J. Jerabek, R. Prokop, A. Kartci, T. Dostal, K. Vrba, "Z-copy Controlled-Gain Voltage Differencing Current Conveyor: Advanced Possibilities in Direct Electronic Control of First-order Filter", *Elektronika IR Elektrotechnika*, vol. 20, no. 6, pp. 77-83, 2014.
- [17] F. Kacar, B. Metin, H. Kuntman, "A new CMOS dual-X second generation current conveyor (DCCCII) with and FDNR circuit application", *AEU – International Journal of Electronics and Communications*, vol. 64, no. 8, pp. 774-778, 2010.
- [18] S. Maheshwari, M. S. Ansari, "Catalog of Realizations for DXCCII using Commercially Available ICs and Applications", *Radioengineering*, vol. 21, no. 1, pp. 281-289, 2012.
- [19] A. A. El-Adawy, A. M. Soliman, H. O. Elwan, "A Novel Fully Differential Current Conveyor and Applications for Analog VLSI", *IEEE Transactions on Circuits and Systems – II: Analog and Signal Digital Processing*, vol. 47, no. 4, pp. 306-313, 2000.
- [20] F. Kacar, A. Yesil, H. Kuntman, "Current-Mode Biquad Filters Employing Single FDCCII", *Radioengineering*, vol. 21, no. 4, pp. 1269-1278, 2012.
- [21] Intersil (Elantec). EL2082 CN Current-mode multiplier (datasheet), 1996, 14 p., accessible on [www: http://www.intersil.com/data/fn/fn7152.pdf](http://www.intersil.com/data/fn/fn7152.pdf)
- [22] Texas Instruments. OPA633 High Speed Buffer Amplifier (datasheet), 1993, 9 p., accessible on [www: http://www.ti.com/lit/ds/sbos150/sbos150.pdf](http://www.ti.com/lit/ds/sbos150/sbos150.pdf)
- [23] Texas Instruments. BUF634 250 mA high-speed buffer (datasheet), 1996, 20 p., accessible on [www: http://www.ti.com/lit/ds/symlink/buf634.pdf](http://www.ti.com/lit/ds/symlink/buf634.pdf)
- [24] Texas Instruments. OPA660 Wide bandwidth operational transconductance amplifier and buffer (datasheet), 1993, 8 p., accessible on [www: http://www.ti.com/lit/ds/symlink/opa860.pdf](http://www.ti.com/lit/ds/symlink/opa860.pdf)
- [25] R. Sotner, A. Kartci, J. Jerabek, N. Herencsar, T. Dostal, K. Vrba, "An Additional Approach to Model Current Followers and Amplifiers with Electronically Controllable Parameters from Commercially Available ICs," *Measurement Science Review*, vol. 12, no. 6, pp. 255–265, 2012.
- [26] J. Jerabek, R. Sotner, A. Kartci, N. Herencsar, R. Prokop, T. Dostal, K. Vrba, "Commercially Available Behavioral Models of the Voltage Controllable Generalized Current Conveyor of Second Generation" in *Proc. of the 38th Int. Conf. on Telecommunications and Signal Processing (TSP2015)*, Prague, submitted for publication,
- [27] Texas Instruments. VCA610 Wideband voltage controlled amplifier (datasheet), 2000, 14 p., accessible on [www: http://www.ti.com/lit/ds/symlink/vca610.pdf](http://www.ti.com/lit/ds/symlink/vca610.pdf)
- [28] Analog Devices. AD830 High Speed, Video Difference Amplifier (datasheet), 2003, 20 p. accessible on [www: http://www.ti.com/lit/ds/symlink/opa860.pdf](http://www.ti.com/lit/ds/symlink/opa860.pdf)

[37] SOTNER, R., HERENC SAR, N., JERABEK, J., VRBA, K., DOSTAL, T., JAIKLA, W., METIN, B. Novel first-order all-pass filter applications of z- copy voltage differencing current conveyor. *Indian Journal of Pure and Applied Physics*, 2015, vol. 53, no. 8, p. 537-545. ISSN: 0019-5596.

Novel first-order all-pass filter applications of z-copy voltage differencing current conveyor

Roman Sotner¹, Norbert Herencsar², Jan Jerabek², Kamil Vrba², Tomas Dostal¹, Winai Jaikla^{3*} & Bilgin Metin⁴

¹Department of Radio Electronics, Brno University of Technology, Technicka 3082/12, 616 00 Brno, Czech Republic

²Department of Telecommunications, Brno University of Technology, Technicka 3082/12, 616 00 Brno, Czech Republic

³Department of Engineering Education, Faculty of Industrial Education, King Mongkut's Institute of Technology Ladkrabag, Ladkrabag, Bangkok 105 20, Thailand

⁴Department of Management Information Systems, Bogazici University, Hisar Campus, 34342-Bebek-Istanbul, Turkey

*E-mail: winai.ja@hotmail.com, bilgin.metin@boun.edu.tr

Received 18 April 2014; revised 27 November 2014; accepted 18 February 2015

The application of z-copy voltage differencing current conveyor (ZC-VDCC) in simple and interesting first-order all-pass sections has been studied in the present paper. The solutions presented here have presumptions for direct electronic control. Some of proposed circuits offer curious possibilities of control. Electronic controllability of the VDCC allows simultaneous zero and pole frequency adjusting, separated zero or pole frequency adjusting or migration of zero from left half plane to right half plane of complex space. Behavioral models of VDCC based on commercially available devices are proposed and selected type of all-pass section was verified by simulations and also by measurements. Results of simulations, experiments, and theoretical proposal are compared. Experiments confirm workability of proposed behavioral equivalent circuit in bandwidths to units of MHz.

Keywords: All-pass section, Behavioral modeling, Electronic control, Voltage differencing current conveyor, Z-copy, VDCC, Zero/pole location control

1 Introduction

Simple and tunable or partially adjustable active filters in both current- or voltage-mode are very useful for applications in communication subsystems like anti-aliasing or reconstruction filters and smoothers, band selection, signal generation in sine wave oscillators (all-pass or band-pass sections), etc. Simple all-pass sections are core elements of multiphase generating solutions¹⁻³. Moreover, they can be used as sub-blocks for construction of the fractional order synthesis^{4,7} as an example. When cascaded or interconnected, sub-blocks with adjustable location of zeros or poles can be used for approximation of fractional order "passive" elements and two-ports^{4,7} or whole applications^{5,6,8}.

Active element used as the main core of proposed applications, is known as voltage differencing current conveyor (VDCC) and belongs to family of hybrid elements introduced by Biolek *et al*⁹. The VDCC is presented as z-copy (ZC-VDCC) variant⁹ in this contribution. Several solutions of active element based on current conveyor of second generation⁹⁻¹³ (CCII) and transconductance section^{9,14} (OTA) were

theoretically proposed. Some basic elements offer benefits of simple electronic control of intrinsic resistance (R_x) of current input terminal¹¹ X or current gain between X and Z terminals^{12,13} by bias current. The basic building parts have been already used for construction of combined active elements with many benefits. For example, current conveyor transconductance amplifier^{9,15} (CCTA) utilizes same types of sub-blocks (CCII and OTA) as VDCC, but in different order of interconnection. However, basic CCTA does not provide differential voltage input and internal transfers between main and auxiliary terminals that are important for applications.

Many all-pass structures were proposed in recent years. However, some of them are too complicated (many active and passive elements) and focused on second-order types^{16,17} for example or are not supposed for direct electronic control of their parameters (neither zero/pole frequency adjusting). Of course, all-pass response is also available in second-order multi-functional biquad systems¹⁸, but independent control of pole/zero frequency in such systems is too complex. Really simple first-order all-

pass circuits exist in the literature¹⁹ electronic controllability is still challenging question in the hitherto literature.

The difference between VDCC and DVCC inheres from basic behaviour. The DVCC realizes subtraction of two voltages¹⁶⁻¹⁹ (two differential voltage input terminals Y) and the rest of ideal behaviour is identical to classical current conveyor⁹ with one current input terminal X and current output terminal Z (or multiple terminals $\pm Z$). In comparison to DVCC, the VDCC element contains transconductance section⁹ and offers additional terminal, which increases the universality of this element. Advanced CCTA with differential difference¹⁸ CCTA (DDCCTA) has similar input features as DDCC (three Y terminals). However, ZC-VDCC proposed in this paper is more suitable for our purpose (differential input section is sufficient in many cases).

Our work is focused mainly on discussion of simple first-order all-pass sections. Therefore, a short comparison of previously published works in this field (all-pass structures based on devices similar to proposed VDCC) is necessary at this place.

Let us compare circuits based on DVCC with similar complexity: Minaei *et al*²⁰. proposed general admittance networks employing one DVCC leading to specific selection of non-controllable all-pass filters, where three passive elements were required. Two DVCCs with two Y terminals (Y_1, Y_2) and one grounded capacitor were utilized in controllable (by intrinsic resistance R_x) all-pass section presented by Maheshwari *et al*²¹. The all-pass filter with the same number of active elements with one floating resistor and grounded capacitor was introduced by Minaei *et al*²². Horng *et al*²³. proposed all-pass filter only with grounded passive elements, where again two DVCCs were necessary. DVCCs are useful for synthesis of the universal second-order systems, where all-pass responses are available. Interesting current-mode example has been presented by Ibrahim *et al*²⁴., where three these DVCCs elements together with four grounded resistors and two grounded capacitors were used to realize all transfer characteristics.

Similar constructions of simple first-order all-pass sections are available by using of differential difference current conveyor⁹ (DDCC), where not only subtraction but also addition (three or more Y terminals) is allowed. Ibrahim *et al*²⁵. used one DDCC which utilizes three Y terminals, floating capacitor, and grounded resistor to realize inverting non-

adjustable all-pass section. Some other solutions utilize one or two DDCCs. Combination of one floating or grounded resistor and capacitor have been introduced by Metin *et al*²⁶. Solutions presented by Krishna *et al*²⁷. require two DDCCs, grounded resistor and capacitor. Chatuverdi *et al*²⁸. presented two DDCCs-based solutions using grounded capacitors in inverting all-pass section controllable by intrinsic resistance R_x . DDCC found its utilization also in universal second-order filtering structures. For example Ibrahim *et al*²⁹. utilized dual-output DDCCs in classical KHN voltage-mode biquad solution that allows also all-pass response.

Our contribution presents several interesting current-, voltage-, and mixed-mode solutions of simple first-order all-pass transfer section employing VDCC element. Some of circuits have special electronically adjustable possibilities, e.g. zero (ω_z, f_z) or pole (ω_p, f_p) frequency control or interesting feature of their separated control. All studied circuits require minimum number of external components (only capacitors in most cases). Our solutions are simple, only differential voltage input (two voltage input terminals) is sufficient in comparison to the most similar DVCC and DDCC based solutions, where three voltage input terminals are often utilized. In addition, simple DVCC and DDCC do not have possibility of electronic control and therefore, do not provide special adjustable features.

2 Z-copy Voltage Differencing Current Conveyor

The principle of the ZC-VDCC is shown in Fig. 1, where symbol, behavioural model, and possible implementation by commercially available devices is shown. The first part of ZC-VDCC consists of OTA section with two current outputs (identical or inverted polarities) and the second part is formed by CCII section (it is current-controlled variant CCCII¹¹). The active element has two voltage inputs p, n , one current input x , auxiliary (high-impedance) terminal z_TA , its copy zc_TA and two current outputs zp and zn . The bi-directional arrows mean both possible polarities (generally) of currents (from terminals z_TA and zc_TA).

3 Proposed Simple Filtering Applications

3.1 Current-Mode All-pass Sections

In recent years, these circuits received attention mainly as parts of multiphase oscillators¹⁻³. The first example of using ZC-VDCC is shown in Fig. 2. It is

simple current-mode all-pass section with independently electronically pole frequency and also zero frequency. Transfer function of proposed circuit has form:

$$K_{AP_CM1}(s) = \frac{I_{OUT}}{I_{INP}} = \frac{g_m - sC}{g_m(1 + sCR_x)} \quad \dots (1)$$

where zero frequency is adjustable by g_m as $\omega_z = g_m/C$ and pole frequency $\omega_p = 1/R_x C$ can be adjusted by R_x . Disadvantage is direct influence of g_m change on dc gain (at low frequencies), but it can be useful for some systems, where behaviour in magnitude responses is not so important⁷. Input impedance (resistance) of this solution is proportional to $\sim 1/g_m$.

The next circuit shown in Fig. 3 is modification of previous solution, where different interconnection of terminals was used in order to obtain possibility of zero frequency control. Only one parameter (R_x) allows adjusting of zero frequency in inverting all-pass section.

Transfer function has form:

$$K_{AP_CM2}(s) = \frac{I_{OUT}}{I_{INP}} = \frac{sC(1 - g_m R_x) - g_m}{sC + g_m} \quad \dots (2)$$

from which zero frequency is $\omega_z = \frac{g_m}{(1 - g_m R_x)C}$.

Zero is in right-half-plane (RHP) of the complex space for typical all-pass configuration ($g_m R_x > 1$). Controllable parameter R_x allows change of transfer function from all-pass section to inverting transfer section with migration of zero to left-half-plane (LHP). Input impedance of this circuit is frequency dependent and directly proportional to R_x value.

The circuit shown in Fig. 4 has advantage of independent zero and also pole frequency control. We can found transfer function in the form:

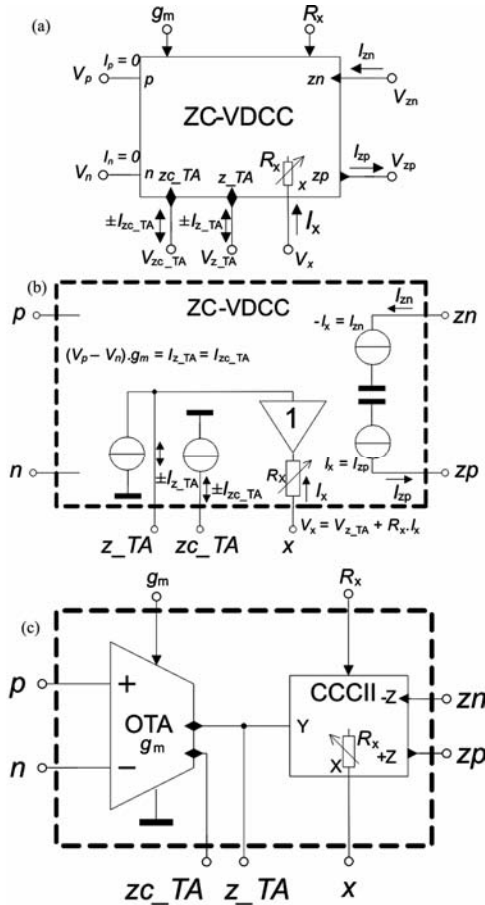


Fig. 1 — Z-copy voltage differencing current conveyor (VDCC): (a) symbol, (b) behavioral model, (c) block implementation

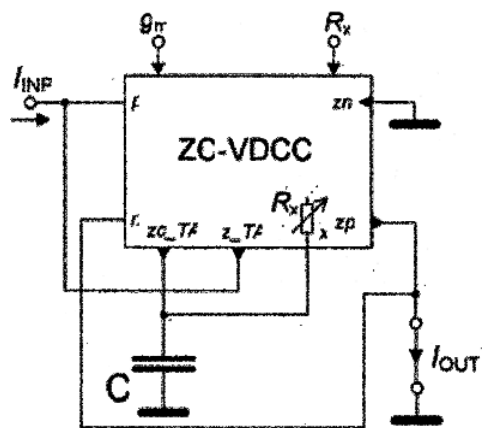


Fig. 2 — Current-mode all-pass section with independent pole and/or zero frequency control

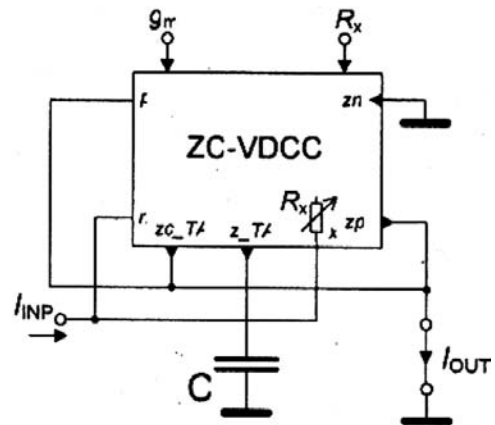


Fig. 3 — Current-mode all-pass section with independent zero frequency control

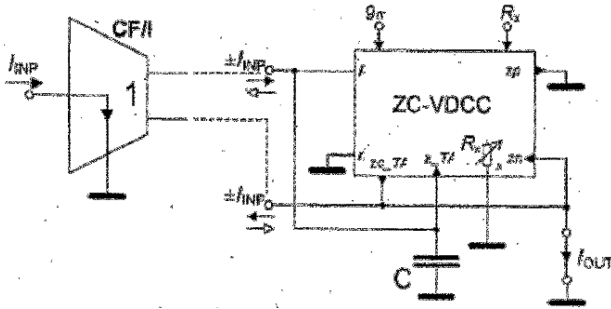


Fig. 4 — Current-mode non-inverting/inverting all-pass section with independent zero and/or pole frequency control and low-impedance input

$$K_{AP_CM3}(s) = \frac{I_{OUT}}{I_{INP}} = \pm \frac{1 - sCR_x}{R_x(g_m + sC)} \quad \dots (3)$$

where $\omega_z = 1/R_xC$ and $\omega_p = g_m/C$. Hence, both adjustable parameters of the VDCC are used effectively. On the other hand, this structure requires current excitation to two nodes (input currents of both polarities). Interchange of their polarity changes overall polarity of the transfer (as included in Eq. 3). The current distributor (current follower/inverter – CF/I with two outputs) is required for this operation. Simultaneous control of R_x and g_m allows to work as typical all-pass filter. Influence of R_x on dc gain is the drawback of this solution. However, it is not critical problem in some cases⁷. Input impedance of this circuit is low (given by input impedance of used CF/I). Therefore, solution is immediately suitable for cascading.

Output of discussed solutions has frequency dependent high-impedance character given by parameters and values of passive elements. It is not important if next connected block has sufficiently low-impedance current input. Output node of all proposed circuits in this subsection has to be connected to the low-impedance input (shorted in ideal case) of following system for correct operation.

3.2 Mixed-Mode All-pass Section

Interesting mixed-mode solution of all-pass filter is shown in Fig. 5. The circuit behaves as voltage to current converter with all-pass characteristic. The trans-admittance-mode (TAM) transfer function has the following form:

$$K_{AP_TAM}(s) = \frac{I_{OUT}}{V_{INP}} = g_m \left(\frac{1 - sCR_x}{1 + sCR_x} \right) \quad \dots (4)$$

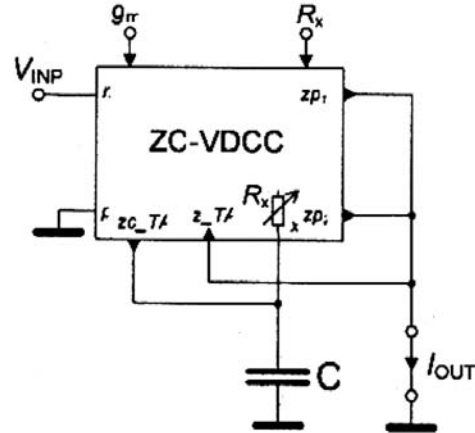


Fig. 5 — Mixed-mode all-pass section with electronic control of zero/pole frequency and also of conversion gain

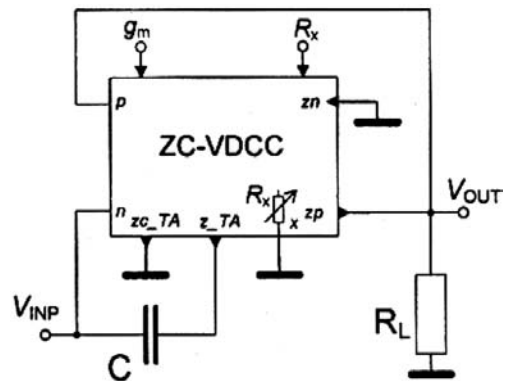


Fig. 6 — Voltage-mode all-pass section utilizing floating capacitor and grounded resistor.

Electronic control of zero/pole frequency by R_x and also independent electronic control of conversion dc gain by g_m are the main advantages of this circuit. Presented structure requires two positive z_p terminals in comparison to the rest of discussed solutions in this section. Current-mode all-pass section is also possible in this structure, when grounded resistor (small value) is connected to the input terminal (V_{INP}) – this resistance realizes current to voltage conversion.

Input impedance of the solution shown in Fig. 5 is high (and frequency independent) and character of the output of the circuit is similar to current-mode solutions in section 3.1 (low-impedance input of a following block is required).

3.3 Voltage-Mode All-pass Sections

Very simple utilization of ZC-VDCC in voltage-mode all-pass sections is also possible. Circuit shown in Fig. 6 uses floating capacitor and grounded external resistor. Despite fact of floating capacitor, it allows

simultaneous control of both pole and zero frequency and therefore, simple application as adjustable phase shifter. Similar method of utilizing OTA section and inverting buffered amplifier with floating capacitor was proposed by Herencsar *et al*³⁰.

Transfer function was obtained as:

$$K_{AP_VM1}(s) = \frac{V_{OUT}}{V_{INP}} = \frac{R_L(g_m - sC)}{g_m R_L + sCR_x} \quad \dots (5)$$

where simple simultaneous tuning of zero and pole by g_m is allowed, if we suppose matching of $R_L = R_x$. Generally, pole frequency is controllable

independently by R_x ($\omega_p = \frac{g_m R_L}{CR_x}$). Input impedance

of this circuit is frequency dependent, but buffering is not required in case of excitation from standard low-impedance voltage source – output of the operational amplifier in previous sub-system for example. Similarly, buffering is necessary in case of low-impedance load at the output.

Grounded resistor (which can be considered as disadvantage of this solution) can be also easily removed as presented in solution shown in Fig. 7. Modified circuit has transfer function:

$$K_{AP_VM2}(s) = \frac{V_{OUT}}{V_{INP}} = - \frac{R_x(g_m - sC)}{1 - g_m R_x + sCR_x} \quad \dots (6)$$

and it behaves as inverting all-pass section if $g_m R_x = 0.5$. However, electronic controllability of this circuit is complicated due to this matching condition. Character of the input and output and their interconnection with other systems is similar to previous situation (Fig. 6).

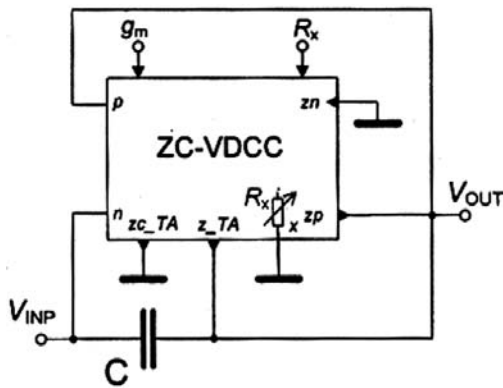


Fig. 7 — Modified voltage-mode all-pass section from Fig. 6 utilizing only floating capacitor.

Figure 8 shows better solution than circuits depicted in Figs 6 and 7. External resistor R_L is not required in this modification. Nevertheless, advantage of independent pole frequency control by R_x (Fig. 6) is missing. However, additional voltage buffer/inverter (VB/I) is necessary. Low-impedance output (practically given by output impedance of the external inverter) is substantial advantage of the solution. Transfer function is given by equation:

$$K_{AP_VM3}(s) = \frac{V_{OUT}}{V_{INP}} = \frac{g_m - sC}{g_m + sC} \quad \dots (7)$$

External voltage inverter can be omitted if current conveyor part in frame of the VDCC (Fig. 1c) has inverting transfer between Y and X terminals (so called inverting current conveyor⁹-ICCI). In such case output impedance of the all-pass section is determined by actual R_x value. Due to low-impedance output (solution with voltage inverter in Fig. 8) cascading of these blocks is easily possible.

The circuit in Fig. 9 shows the next unusual example of ZC-VDCC application and has non-typical transfer function:

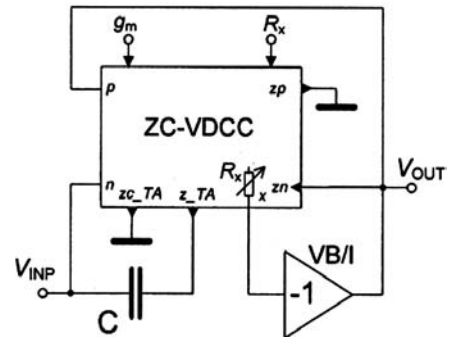


Fig. 8 — Resistor-less modification of the voltage-mode all-pass section from Fig. 6 without matching conditions.

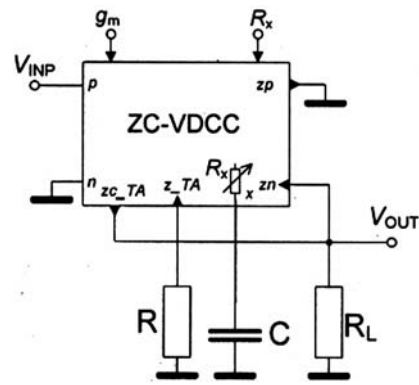


Fig. 9 — Modified voltage-mode all-pass section with independent zero frequency control.

$$K_{AP_VM4}(s) = \frac{V_{OUT}}{V_{INP}} = g_m R_L \left[\frac{1 + sC(R - R_x)}{1 + sCR_x} \right] \quad \dots(8)$$

that has interesting feature of continuous controllability of the zero location $\omega_z = \frac{1}{(R - R_x)C}$ by grounded resistance R . Similarly as in Eq.(2), it allows change the zero location from RHP to LHP. Input impedance of the circuit is frequency independent and high; therefore, cascading of such blocks is also possible. However, low-impedance load influences output significantly (voltage buffer required).

4 Experimental Verification of Selected Filter

All-pass filter from Fig. 6 was selected for experimental verification because it has advantage of simple simultaneous electronic control of zero and pole frequency. We proposed following behavioral models of VDCC based on commercially available devices employing diamond transistors^{31,32} (DT) OPA660/860 and current-mode multiplier³³ (or conveyor) EL2082 in order to test selected circuit by PSpice simulations and also lab measurements.

4.1 Proposed Behavioral Models

The all-pass filter from Fig. 6 does not require all terminals (z_{c_TA} and z_n), therefore, suitable behavioral model can be simpler than proposed device as shown in Fig. 1. Two possible implementations of behavioral model of VDCC element based on DTs and EL2082 are shown in Fig. 10. Despite of fact that EL2082 is classified as obsolete element without proper replacement, this device is still available from some distributors and very useful for behavioral experiments.

These preliminary tests with both behavioral models of VDCC suppose R_x and g_m parameters controllable as external parts. Both g_m and also R_x parameter should be controllable by bias currents in practical CMOS utilization of VDCC element, but that is not the purpose of the present paper.

4.2 Measurement and Simulation Results

All-pass filter as shown from Fig. 6 was designed with following parameters: $f_p = f_z = 1.59$ MHz, $C = 100$ pF, $R = R_x = 1$ k Ω , $g_m = 1$ mS. Proposed application was verified with behavioral model shown in Fig. 10b by simulations and experiments with commercially available devices, oscilloscope

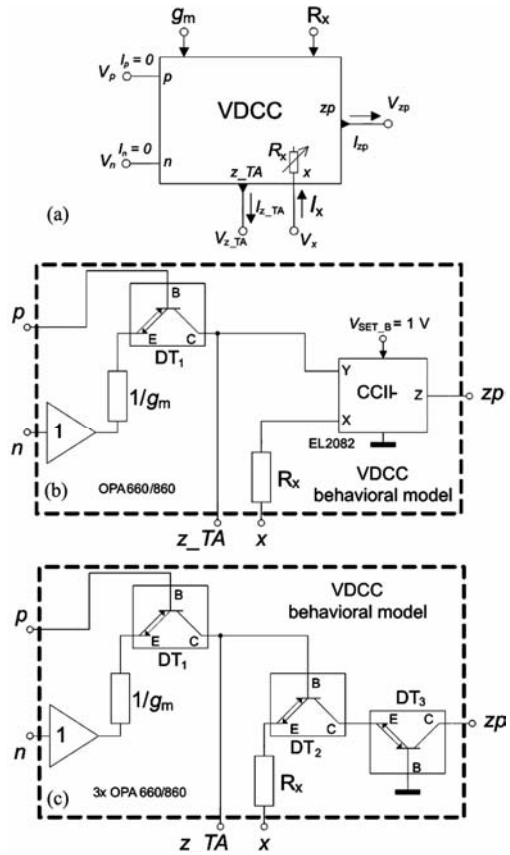


Fig. 10 — Possible implementation of reduced behavioral model of ZC-VDCC: (a) symbol, (b) using OPA 660/860 and EL2082, (c) utilizing OPA660/860 only.

DS1204B, and vector-network analyzer Agilent E5071C. Supply voltage was ± 5 V. Measured results in frequency domain (magnitude and phase characteristics in detail from 100 kHz to 100 MHz) are shown in Fig. 11. Available frequency bandwidth of the proposed prototype is about 20 MHz. Measured value of $f_p = f_z$ was 1.525 MHz. Transient response of the output signal for excitation frequency 1.5 MHz, that is very close to pole and zero frequency of the all-pass section, as shown in Fig. 12. Input signal (CH1) is plotted by blue colour and output signal by red colour (CH2). Tune ability of the section was verified by discrete changes of transconductance g_m with particular values: 0.21, 0.45, 1.0 and 2.21 mS (by resistor $1/g_m$ in Fig. 10b). Ideal $f_p = f_z$ values are 0.334, 0.716, 1.591, and 3.374 MHz, while by simulations provided values are 0.349, 0.707, 1.494, and 3.088 MHz. Results obtained from experimental tests with behavioral model are: 0.367, 0.683, 1.525, and 3.261 MHz. Simulated and measured phase characteristics of the all-pass section are compared in

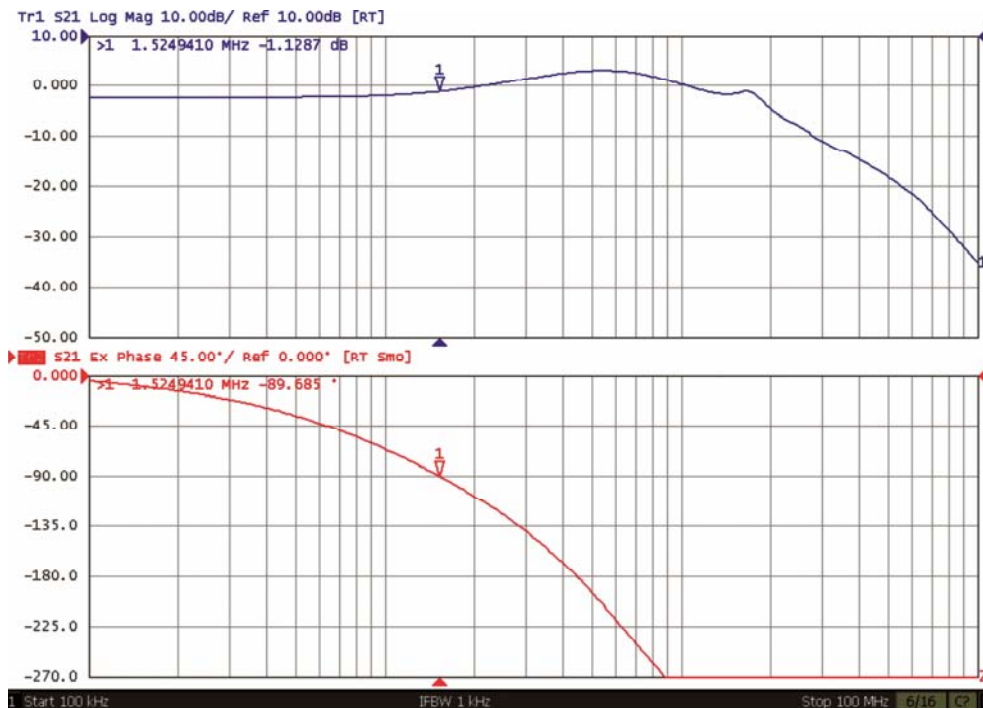


Fig. 11 — Measured results of the all-pass section – detail of magnitude and phase response

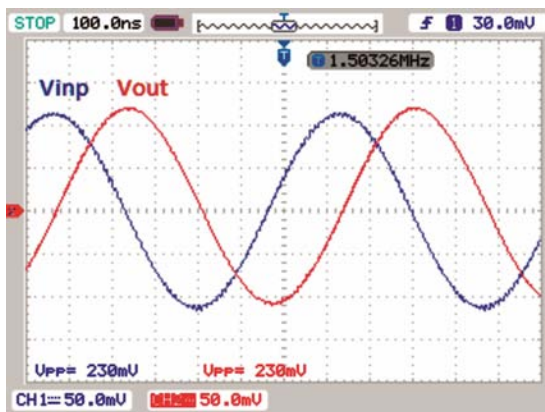


Fig. 12 — Input and output transient responses of AP filter for sine wave excitation

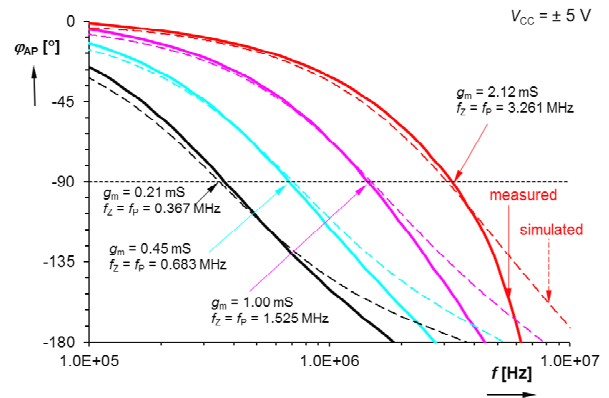


Fig. 13 — Comparison of simulated and measured phase responses for different values of g_m .

Fig. 13. All results were obtained for 50 Ω input and output matching conditions.

4.3 Analysis of Parasitic Effects

The circuit model of the all-pass section (Fig. 6) including real parasitics is shown in Fig. 14. Current and voltage error of current conveyor section in frame of ZC-VGCC are signed as α (voltage tracking error between z_{TA} and x terminal) and β (current tracking error between x and z_p terminal). Their values are given by: $\alpha = 1 - \varepsilon$ and $\beta = 1 - \delta$, where $|\varepsilon| \ll 1$ and

$|\delta| \ll 1$. Parasitic elements have values determined from interconnection of terminals of commercially available devices that were selected for experimental verification. We expect $R_{p1} \approx 25$ k Ω (output³¹ of the OPA660 and input³⁵ Y of the EL2082 are in parallel), $C_{p1} \approx 6$ pF (4+2 pF), $R' = R_L \parallel R_p \parallel R_{zp} \approx 1$ k Ω ($R \ll R_p \parallel R_{zp}$ and has dominant impact) and $C_{p2} \approx 7$ pF (2+5 pF). Resistance R_x (95+910 Ω) is considered as parasitic in many works in the field. However, it is used often for electronic control³⁴. In this case, R_x is

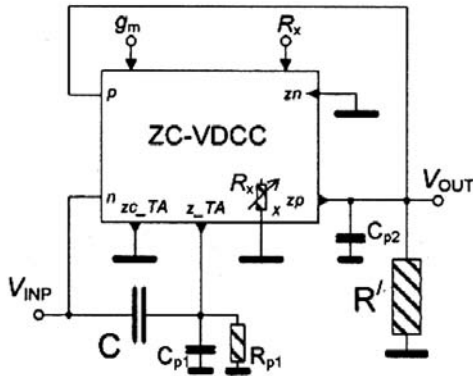


Fig. 14 — Filter from Fig. 6 including parasitics for study of parasitic influences.

correct function of the proposed circuit. Transfer function including above discussed parasitic elements and parameters have form:

$$K'_{AP_VM1}(s) = \frac{\alpha\beta R_{p1}(R'g_m - sC_1R')}{s^2C_{p2}(C_1 + C_{p1})R'R_xR_{p1} + s(C_{p1}R_{p1} + C_1R_{p1} + C_{p2}R')R_x + R_x + \alpha\beta R_{p1}R'g_m} \dots(9)$$

necessary for Eq. (9) has the denominator of the second order. The zero is still located at $f_z \cong 1.591$ MHz, but two poles exist in real case. Numerical calculation provided their values as $f_{p1} \cong 1.67$ MHz and $f_{p2} \cong 21.1$ MHz. Therefore, drop of magnitude response in direction to the high frequencies is caused mainly by the second pole. The main source of this problem is C_{p2} . The frequency where phase shift is equal to 90 degree was found as 1.518 MHz (first pole). Therefore, measurement results (Figs 11 and 13) are quite near to real behaviour expectation from this non-ideal analysis.

5 Conclusions

Several introduced simple applications of VDCC prove suitability of this active element for design of special and simple parts of communication sub-systems (in this contribution all-pass sections). The circuit in Fig. 2 allows completely independent electronic control of the zero and pole frequencies. Circuit in Fig. 3 has benefit of simple electronic control of migration of zero from RHP to the LHP. The solution in Fig. 4 also allows independent zero and pole control, but circuit requires additional

current distribution to two input nodes. Figure 5 shows circuit with mixed-mode application (voltage input and current output). Zero and pole frequency are adjustable simultaneously and *dc* gain constant between input voltage and output current is controllable independently. Figure 6 offers solution, where simultaneous control of zero/pole frequency is easily possible by g_m . Separated pole frequency control is also possible in this case. External resistor could be saved, but matching condition is more complicated than in previous type of all-pass filter, see Fig. 7. Resistor-less all-pass filter was introduced also in Fig. 8. However, correct operation of such system requires additional external voltage inverter. Fortunately, the same function is available, if in internal VDCC topology the current conveyor (CCII) is changed to ICCII (but we lost advantage of low-impedance output consequently). All-pass filter in Fig. 9 provides control of zero migration by grounded resistor that allows to implement external system for its control (digital potentiometer, digital to analog converter, CMOS resistance equivalent, ...) independent on features of VDCC fabricated in specific topology. One of presented solution was chosen (Fig. 6) to be verified experimentally and results confirmed expected behaviour and also tunability of all-pass filter. Proposed behavioral model of VDCC allows operation of circuit in bandwidth of units MHz with sufficient dynamics and it is suitable also for preliminary experimental tests of other applications.

Acknowledgement

Research described in this paper was financed by Czech Ministry of Education in frame of National Sustainability Program under grant LO1401. For research, infrastructure of the SIX Center was used.

References

- 1 Gift S J G, *Microelectronics Journal*, 31 (2000) 9.
- 2 Jaikla W & Promee P, *Radioengineering*, 20 (2011) 594.
- 3 Promee P & Somdunyanok M, *35th Int Conf on Telecommunications and Signal Processing (TSP2012)*, Prague, (2012) 355.
- 4 Valsa J & Vlach J, *Int J of Circuit Theory & Applications*, 41 (2013) 59.
- 5 Radwan A G, Elwakil A S & Soliman A M, *IEEE Trans on Circuits & Sys*, 55 (2008) 2051.
- 6 Radwan A G, Elwakil A S & Soliman A M, *J of Circuits, Sys & Computers*, 17 (2008) 55.
- 7 Petrzela J, *23th Int Conf Radioelektronika*, Czech Republic, (2013) 182.
- 8 Maundy B, Elwakil A & Gift S, *Circuits Systems & Signal Proc*, 31 (2012) 3.

- 9 Bielek D, Senani R, Biolkova V & Kolka Z, *Radioengineering*, 17 (2008) 15.
- 10 Sedra A & Smith K C, *IEEE Trans on Circuit Theory*, 17 (1970) 132.
- 11 Fabre A, Saaid O, Wiest F & Boucheron C, *IEEE Trans on Circuits & Sys*, 43 (1996) 82.
- 12 Surakamponorn W & Thitimajshima W, *IEE Proceedings-G*, 135 (1988) 71.
- 13 Fabre A & Mimeche N, *Electronics Lett*, 30 (1994) 1267.
- 14 Geiger R L & Sánchez-Sinencio E, *IEEE Circ & Devices Magazine*, 1 (1985) 20.
- 15 Prokop R & Musil V, *Proc Conf on Signal & Image Proc IASTED*, Anaheim, (2005) 494.
- 16 Kumar P, Pal K & Gupta G K, *Indian J of Pure & Appl Phys*, 44 (2006) 398.
- 17 Sharma S, Rajput S S, Pal K, Mangotra L K & Jamuar S S, *Indian J of Pure & Appl Phys*, 44 (2006) 871.
- 18 Tangsrirat W, Channumsin O & Pukkalanun T, *Indian J of Pure & Appl Phys*, 51 (2013) 516.
- 19 Shah N A, Quadri M & Iqbal S Z, *Indian J of Pure & Appl Phys*, 46 (2013) 893.
- 20 Minaei S & Ibrahim M A, *Int J Electronics*, 92 (2005) 347.
- 21 Maheshwari S, *Circuits Sys & Signal Proc*, 27 (2008) 123.
- 22 Minaei S & Yuce E, *Circuits Sys & Signal Proc*, 29 (2010) 391.
- 23 Hornig J W, *Radioengineering*, 19 (2010) 653.
- 24 Ibrahim M A, S Minaei & Kuntman H, *Int J of Electronics & Communi*, 59 (2005) 311.
- 25 Ibrahim A M, Kuntman H & Cicekoglu O, *Circuits Sys & Signal Processing*, 22 (2003) 525.
- 26 Metin B, Cicekoglu O & Pal K, *Midwest Symposium on Circuits & Sys*, Montreal, (2007) 518.
- 27 Krishna M, Kumar N, A Srinivasulu & Lal R K, *Int Conference on Circuits, Systems*, (2011) 128.
- 28 Chatuverdi B & Maheshwari S, *J Communication & Computer*, 9 (2012) 613.
- 29 Ibrahim M A, Kuntman H, *Int J Electronics & Communication*, 58 (2004) 429.
- 30 Herencsar N, Minaei S, Koton J, Yuce E & Vrba K, *Analog Integrated Circuits & Signal Proc*, 74 (2013) 141.
- 31 Texas Instruments. *OPA660 Wide bandwidth operational transconductance amplifier and buffer (datasheet)*, (2000) 20, accessible on www: <http://www.ti.com/lit/ds/symlink/opa660.pdf>
- 32 Texas Instruments. *OPA860 Wide-bandwidth, operational transconductance amplifier (OTA) and buffer (datasheet)*, (2008) 33, accessible on www: <http://www.ti.com/lit/ds/symlink/opa860.pdf>
- 33 Intersil (Elantec). *EL2082 CN Current-mode multiplier (datasheet)*, (1996) 14, accessible on www: <http://www.intersil.com/data/fn/fn7152.pdf>
- 34 Sotner R, Kartci A, Jerabek J, Herencsar N, Dostal T & Vrba K, *Measurement Sci Review*, 12 (2012) 255.

[38] SOTNER, R., PROKOP, R., JERABEK, J., KLEDROWETZ, V., FUJCIK, L., DOSTAL, T. Design of Current-Controlled Current Conveyor Stage With Systematic Current Offset Reduction. In *Proceedings of International Conference on Applied Electronics (APPEL 2015)*, Pilsen (Czech Republic), 2015, p. 225-228. ISBN: 978-80-261-0385-1.

Design of Current-Controlled Current Conveyor Stage With Systematic Current Offset Reduction

Roman Sotner, Roman Prokop, Jan Jerabek,
Vilem Kledrowetz, Lukas Fuceik
Faculty of Electrical Engineering and
Communication
Brno University of Technology
Brno, Czech Republic
sotner@feec.vutbr.cz

Tomas Dostal
Dept. of Electrical Engineering and Computer
Science
College of Polytechnics Jihlava
Jihlava, Czech Republic
tomas.dostal@vspj.cz

Abstract – This contribution presents modification of current-controlled current conveyor (CCCII) designed in order to reduce the systematic DC current offset of transfer between X and Z terminal and also an example of practical design including practical guideline and recommendations. Simulations in Cadence Spectre simulator with ON Semiconductor/AMIS I2T100 based on 0.7 μm technology CMOS07 were provided for verification of discussed features.

Keywords–CCCII; CMOS; current conveyor; electronic control; offset reduction

I. INTRODUCTION

Current conveyors (CC) [1]-[4] have attracted attention of researchers for many years. There are many interesting modifications of basic structures defined by Sedra et al. [1]. However, elementary definitions [1]-[4] does not suppose any kind of electronic control of any parameter of the circuit. Several modifications were introduced in order to improve electronic controllability of their parameters. Intrinsic small-signal resistance of the current input terminal X (R_X) is the parameter which was explored in applications of so-called current controlled current conveyor of second generation (CCCII) [4]-[7]. An attention was also focused on current gain control

between X and Z terminal (B) [8]-[10] in so-called electronically controllable current conveyor (ECCII). Many interesting conceptions followed, where combined methods of two parameters control were solved. Minaei et al. [11] introduced CMOS ECCII with independent electronic control of R_X and B . Similarly Kumngern et al. [12] defined control of these parameters in simple bipolar solution of the CC. De Marcellis et al. [13] contributed with voltage gain control (A). These ideas were also utilized in further complex elements for example in advanced current feedback amplifiers [14]-[15].

Unfortunately, many of the presented solutions were designed only for computer analysis and do not solve some practical requirements, e.g. minimization of DC offset and appropriate DC accuracy (very small transistors are used, which cause unacceptable matching offset and too low dynamic impedance in some cases). Our solution supposes practical utilization of the CC, expects practical design and later silicon implementation. Our circuit has very good accuracy of the current transfers and significantly improved (decreased) systematic DC current offset between X and Z terminal in frame of CCCII (controllable R_X), which is always present.

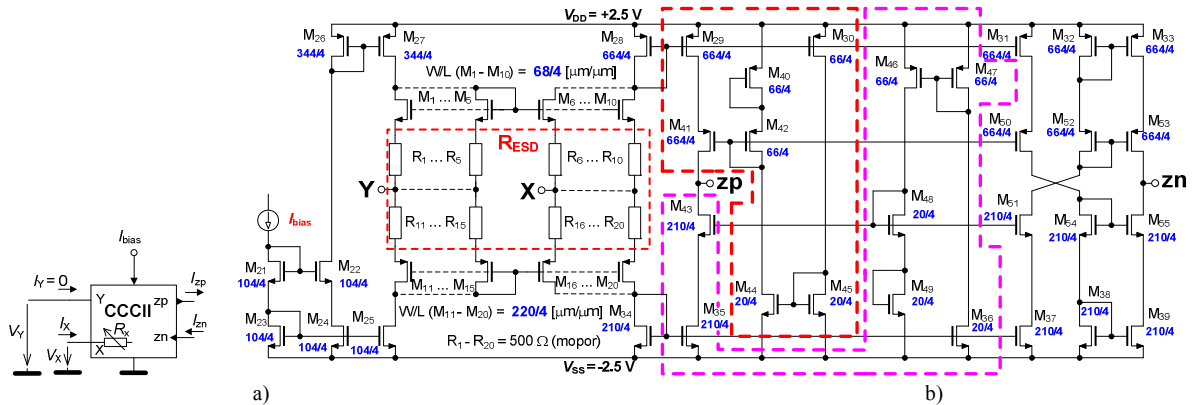


Figure 1. Current-controlled current conveyor (CCCII) with systematic DC current offset reduction: a) schematic symbol, b) cell structure.

Research described in this paper was financed by Czech Ministry of Education in frame of National Sustainability Program under grant LO1401. For research, infrastructure of the SIX Center was used. Research described in the paper was supported by Czech Science Foundation project under No. 14-24186P. Grant No. FEKT-S-14-2281 also supported this research. The support of the project CZ.1.07/2.3.00/20.0007 WICOMT, financed from the operational program Education for competitiveness, is gratefully acknowledged.

Schematic symbol and internal structure of the CCCII cell with improved features are shown in Fig. 1. Definition of the CCCII behavior is well known [4]-[7]: $V_X = V_Y + R_X I_X$, $I_Y = 0$, $I_{zp} = -I_{zn} = I_X$.

II. DESIGN OF THE CCCII CELL

We have used ON Semiconductor/AMIS I2T100 fabrication technology available in frame of Europractice academic consortium. This technology is precise, verified and perfect for similar analog and mixed-mode designs. In case of smaller technologies, we always have to design W and L dimensions large enough for sufficient DC accuracy in the case of analog circuits. Thus, simply put, when only analog design is considered, there is usually no point in using smaller technology (benefit vs. cost is usually not balanced).

The CCCII contains three main subparts. The first of them is biasing circuit (M_{21-27}). This part has to provide bias current for the rest of the structure. Design of this section was provided by following specifications: overdrive voltage $\Delta V_{GS} = V_{Dsat} = V_{GS} - V_{th} = 0.4$ V (where V_{th} is threshold voltage: 0.74 V for NMOS and 1.1 V for PMOS typically), we can use larger ΔV_{GS} because there is not amplitude swing (signal) and voltage space given by supply voltage corners ($V_{DD} = -V_{SS} = 2.5$ V) is sufficient, this fact also reduces overall W/L ratio of transistors (better noise features, saving of the chip area); maximal bias current $I_{bias} = 200$ μ A; length of transistors $L = 4$ μ m was chosen for sufficiently high MOS output resistance. Transconductance parameters (fabrication constants given by gate-oxide capacitance and mobility of carriers) for hand calculations are approximately $K_{pN} = 95$ μ A/V² and $K_{pP} = 29$ μ A/V². Based on equations [16]:

$$W_{M21-25} = \frac{2I_{bias}}{K_{pN}(V_{GS_M21-25} - V_{thN})^2} L, \quad (1)$$

$$W_{M26-27} = \frac{2I_{bias}}{K_{pP}(V_{GS_M26-27} - V_{thP})^2} L, \quad (2)$$

we calculated widths: $W_{M21-25} = 105$ μ m and $W_{M26-27} = 345$ μ m.

The second part is so-called translinear section [5], [17]-[19], where we suppose R_X control. Generally known CCCII contains only four transistors (2 NMOS and 2 PMOS) in translinear section. However, we have to match recommended ESD requirements. Therefore, this part consists of ten ‘‘fingers’’ M_{1-10} and M_{11-20} where additional resistors R_{1-20} are required due to the ESD protection of the inputs. Unfortunately, resistance (500 Ω) of R_{6-10} and R_{16-20} directly influences overall value of the R_X . This additional resistance is noted as R_{ESD} in further text. Overall value of small-signal R_X can be expressed as:

$$R_X \cong \frac{0.2}{\frac{1}{R_{ESD} + 1/g_{mP}} + \frac{1}{R_{ESD} + 1/g_{mN}}}, \quad (3)$$

where

$$g_{mP} = \sqrt{2K_{pP}\left(\frac{W}{L}\right)_P 0.2I_{bias}}, \quad g_{mN} = \sqrt{2K_{pN}\left(\frac{W}{L}\right)_N 0.2I_{bias}}. \quad (4),(5)$$

Parameters g_{mP} and g_{mN} are partial transconductances of the single finger (M_{6-10} , M_{16-20}). Constant 0.2 in (3)-(5) is given by division of R_X to five fingers (I_{bias} is also divided to five branches). We expect $g_{mP} = g_{mN} = g_{mNP}$ for simple design of R_X value. Then, we can simplify (3) to form:

$$R_X \cong 0.1 \cdot (R_{ESD} + 1/g_{mNP}). \quad (6)$$

We can express direct relation for W/L ratio of partial finger NMOS (M_{1-10}) and PMOS (M_{11-20}) as:

$$\left(\frac{W}{L}\right)_{N,P} = \frac{1}{2K_{pN,P} 0.2I_{bias}} \left(\frac{1}{0.1} - R_{ESD}\right)^2. \quad (7)$$

Design requirements are: maximal $I_{bias} = 200$ μ A (40 μ A in each of 5 branches); $R_{ESD} = 500$ Ω ; $R_X = 330$ Ω , $L = 4$ μ m. We calculated $W_{M11-20} = 220$ μ m (PMOS) and $W_{M1-10} = 67$ μ m (NMOS) from (7). Supposing typical $\Delta V_{GS} = 0.25$ V (this part is processing signal with amplitude swing, we cannot allow bigger value of ΔV_{GS}), we verified that transistors should operate in saturation up to $I_{bias} = 50$ μ A in each finger (for $\Delta V_{GS} = 0.25$ V), calculated from equation [16]:

$$I_{bias} = \frac{K_{pN,P}}{2} \left(\frac{W}{L}\right)_{N,P} (\Delta V_{GS})^2. \quad (8)$$

Our design supposes I_{bias} should reach 40 μ A in each finger for $R_X = 330$ Ω .

The last part of the CCCII contains output section (mirrors) with DC current offset reduction auxiliary circuits. We used the same equations (1) and (2) for calculation of dimensions of the main transistors of the output section, similarly as at the beginning of our discussion (we suppose $\Delta V_{GS} = 0.29$ V, $L = 4$ μ m). We obtained from the calculation $W_{M34,35,37,38,39,43,51,54,55} = 200$ μ m, $W_{M28,29,31,32,33,41,50,52,53} = 656$ μ m. Explanation of the auxiliary circuits design is given in following section.

III. DC CURRENT OFFSET REDUCTION

Standard cascoding of CMOS current mirrors [16] is very well-known method how to increase output resistance of the current mirror in order to ensure high accuracy of mirroring. However, there are situations where standard approach cannot be applied due to limited voltage space in the structure. Fortunately, there are some methods (different way of cascode biasing), that can be very useful in particular solutions. We used auxiliary networks (red- and pink-colored parts) in our solution of the CCCII (Fig. 1). Partial schematic diagram of the auxiliary circuit for current offset reduction between X and zp , zn terminals is shown in Fig. 2b (for half of the section, the second part is analogical). The circuit operation is based on additional supporting MOS transistor connected to the output drive. It works very similarly as standard cascoding (Fig. 2a) of current mirrors [16] but this

arrangement does not consume so large voltage space in translinear loop as standard cascoded current mirror.

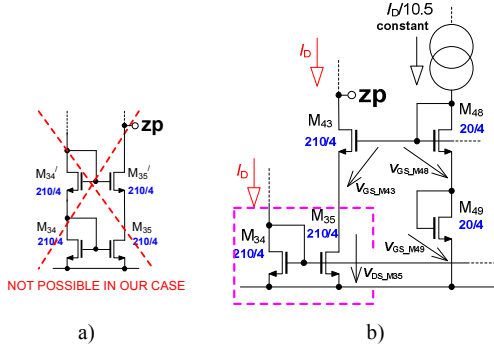


Figure 2. Basic principle of static DC current offset reduction: a) standard cascoding, b) cascoding with different way of biasing.

Our goal is to design current mirror M_{34} , M_{35} (and others if more outputs of this mirror are required) with very accurate relation (unity gain in our case) between input and output current to minimize systematic DC offset. Therefore, V_{DS} of both transistors must be almost equal. We will suppose constant bias current I_{bias} (fixed R_X value) in the first case of our discussion. Auxiliary network (M_{43} , M_{48} , M_{49}) of the output drive provides following relation:

$$V_{GS_M43} + V_{DS_M35} = V_{GS_M48} + V_{GS_M49} \quad (9)$$

Additional section sufficiently increases output impedance of the mirror. Thus, voltage drop across V_{DS_M35} is almost equal to voltage drop across diode M_{34} (if W/L and drain currents of M_{49} and M_{34} are identical then $V_{GS_M34} = V_{DS_M35} = V_{GS_M49}$). Very similar situation (well-known fact) occurs in case of constant ratio of current through branch M_{48} and M_{49} (diodes) and current through M_{34} , M_{35} , M_{43} ($k_1 = I_{D_M34,35,43}/I_{D_M48,49}$) and aspect ratios W/L of M_{43} , M_{35} , M_{48} and M_{49} ($k_2 = (W/L_{M34,35,43})/(W/L_{M48,49})$). We obtained:

$$V_{DS_M35} = V_{GS_M34} = V_{GS_M49} = \sqrt{\frac{2I_D}{k_1} \left(K_{PN} \frac{\left(\frac{W}{L}\right)_{M49}}{k_2} \right)^{-1}} + V_{th_N} \quad (10)$$

where we can see that this V_{GS} is not dependent on k if W/L and current gain of the mirror are designed as equal ($k_1 = k_2 = k$).

Above discussed system for DC offset reduction works properly if constant I_D is available. However, additional circuitry is required to ensure sufficiently low offset also if biasing conditions are changed. We suppose intentional control of I_{bias} in order to adjust R_X value. The current through branch M_{48} and M_{49} ($I_D/10.5$) should be also adjusted in accordance with I_{bias} (I_D in explanatory Fig. 2b and Fig. 3). Otherwise, V_{GS_M48} and V_{GS_M49} are not changed simultaneously with others – directly influenced by I_D . Thus, V_{DS_M35} is not almost equal to V_{GS_M34} for large changes of I_D anymore (offset increases in specific range of I_{bias} adjusting) and transistors may even left their operation region (saturation) in the worst case. Additional current mirrors (M_{34} - M_{36} , M_{46} - M_{47}) in Fig. 3 solve this problem partially. It seems to be sufficient solution in required range of I_{bias} adjusting. Our design example

supposes 10.5-times smaller transistors of auxiliary network (M_{46} , M_{47} , M_{48} , M_{49} , M_{36}) to save chip area. For additional information see comparison of the simulation results (Fig. 5) based on CCCII utilized solutions in Fig. 2b and Fig. 3.

Calculated W/L ratios together with final W/L (see Fig. 1) modified in accordance to the precise layout guidelines (division of active areas of transistors to fingers, matching-interdigitation, dummy, ESD recommendations, etc. [16]) are summarized in Tab. 1.

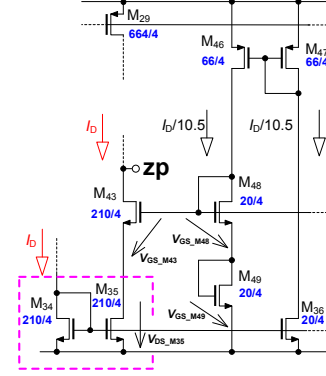


Figure 3. Principle of DC current offset reduction with dynamical response on bias current changes.

TABLE I. CALCULATED AND FINAL W/L RATIOS

Transistor	W/L ratio [-]	
	calculated	final
M_{1-10}	67/4	68/4
M_{11-20}	220/4	220/4
M_{21-25}	105/4	104/4
M_{26-27}	345/4	344/4
$M_{28,29,31,32,33,41,50,52,53}$	656/4	664/4
$M_{34,35,37,38,39,43,51,54,55}$	200/4	210/4
$M_{30,40,42,46,47}$	66/4	66/4
$M_{36,44,45,48,49}$	20/4	20/4

IV. SIMULATION RESULTS

Detail of the DC transfer characteristic between X and zp (zn) terminals for standard CCCII (without offset reduction) and CCCII presented in Fig. 1 is shown in Fig. 4.

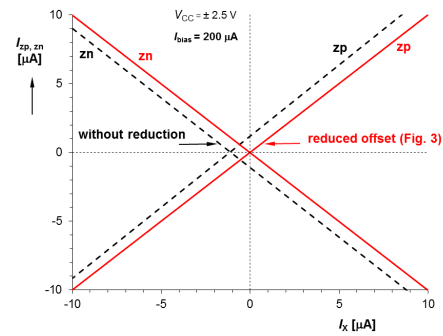


Figure 4. Detail of DC transfer between X and zp, zn terminals.

We analyzed the systematic DC current offset of the standard CCCII topology without offset minimization (for our design parameters). Figure 5 indicates dependence of this DC offset on I_{bias} adjusted from 1 μA to 200 μA . The smallest value of the DC offset of the standard CCCII (without reduction) achieves about 50 nA ($I_{bias} = 1 \mu A$) but all transistors of CCCII are not operating in saturation regime anymore) and the highest value is 1.15 μA (200 μA). The solution with reduced offset (Fig. 3) offers values 0.66 – 20 nA in discussed I_{bias} range. Dependence of small-signal R_X

on I_{bias} in the same range is shown in Fig. 6. Theoretical (ideal) trace was achieved from (3)-(5). Simulated value $R_X = 306 \Omega$ for $I_{bias} = 200 \mu A$ was obtained. Hand calculation gives value 330Ω . AC responses of the transfer between X and zp and zn terminals are in Fig. 7 (18.5 and 12.1 MHz -3 dB bandwidths were achieved for $I_{bias} = 200 \mu A$).

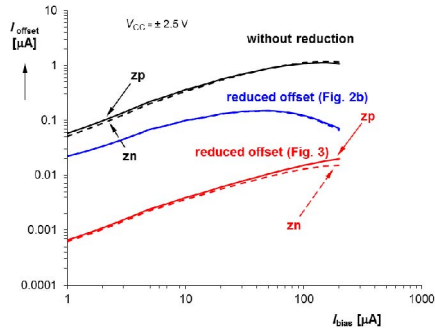


Figure 5. Dependence of current offset value on I_{bias} adjusting.

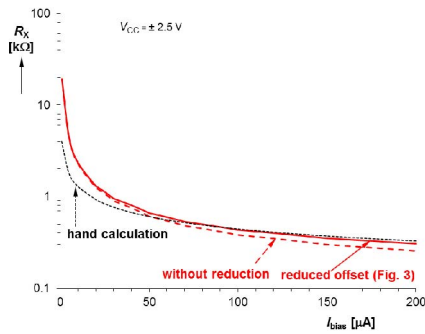


Figure 6. Dependence of R_X on I_{bias} adjusting.

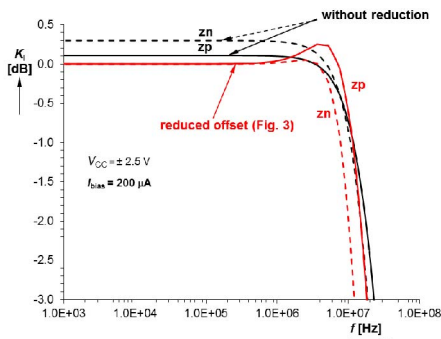


Figure 7. AC transfer between X and zp, zn terminals.

V. CONCLUSION

We have discussed solution how to improve DC accuracy of the standard CMOS CCCII. DC offset of the transfer between X and zp or zn terminals can be significantly reduced (from 1.15 μA in basic CCCII to 20 nA in variant with systematic offset reduction for the highest value of the $I_{bias} = 200 \mu A$). It is worth to solve the systematic offset reduction because matching offset analysis (CCCII with or without systematic offset reduction) revealed comparable offset dispersions (sigma around 1 μA) to unreduced systematic value. Our topology improves also accuracy of the unity current transfer significantly (Fig. 7). Our future work expects analysis of fabricated prototype.

REFERENCES

- [1] A. Sedra, K. C. Smith, "A second generation current conveyor and its applications," IEEE Transaction on Circuit Theory, vol. CT-17, no. 2, pp. 132-134, 1970.
- [2] J. A. Svoboda, L. Mcgory, S. Webb, "Applications of commercially available current conveyor," Int. Journal of Electronics, vol. 70, no. 1, pp. 159-164, 1991.
- [3] H. Barthelemy, M. Fillaud, S. Bourdel, J. Gaunery, "CMOS inverters based positive type second generation current conveyors," Analog Integrated Circuits and Signal Processing, vol. 50, no. 2, pp. 141-146, 2007.
- [4] D. Biolek, R. Senani, V. Biolkova, Z. Kolka, "Active elements for analog signal processing: Classification, Review, and New Proposal," Radioengineering, vol. 17, no. 4, pp. 15-30, 2008.
- [5] A. Fabre, O. Saaid, F. Wiest, C. Boucheron, "High frequency applications based on a new current controlled conveyor," IEEE Trans. on Circuits and Systems - I, vol. 43, no. 2, pp. 82-91, 1996.
- [6] S. B. Salem, M. Fakhfakh, D. S. Masmoudi, M. Loulou, P. Loumeau, N. Masmoudi, "A high performance CMOS CCI and high frequency applications," Analog Integrated Circuits and Signal Processing, vol. 49, no. 1, pp. 71-78, 2006.
- [7] I. Eldbib, V. Musil, "Self-cascoded Current Controlled CCI Based Tunable Band Pass Filter," in Proc. 18th Int. Conf. Radioelektronika, Praha, 2008, pp. 1-4.
- [8] W. Surakamponorn, W. Thitimajshima, "Integrable electronically tunable current conveyors," IEE Proceedings-G, vol. 135, no. 2, pp. 71-77, 1988.
- [9] W. Surakamponorn, K. Kumwachara, "CMOS-based electronically tunable current conveyor," Electronics Letters, vol. 28, no. 14, pp. 1316-1317, 1992.
- [10] A. Fabre, N. Mimeche, "Class A/AB second-generation current conveyor with controlled current gain," Electronics Letters, vol. 30, no. 16, pp. 1267-1268, 1994.
- [11] S. Minaei, O. K. Sayin, H. Kuntman, "A new CMOS electronically tunable current conveyor and its application to current-mode filters," IEEE Trans. on Circuits and Systems - I, vol. 53, no. 7, pp. 1448-1457, 2006.
- [12] M. Kumngern, S. Junnapiya, "A sinusoidal oscillator using translinear current conveyors," in Proc. Asia Pacific Conference on Circuits and Systems (APCCAS), Kuala Lumpur, 2010, pp. 740-743.
- [13] A. Marcellis, G. Ferri, N. C. Guerrini, V. Scotti, A. Trifiletti, "The VGC-CCII: a novel building block and its application to capacitance multiplication," Analog Integrated Circuits and Signal Processing, vol. 58, no. 1, pp. 55-59, 2009.
- [14] R. Sotner, J. Jerabek, N. Herensar, T. Dostal, K. Vrba, "Electronically adjustable modification of CFA: Double Current Controlled CFA (DCC-CFA)," in Proc. 35th Int. Conf. on Telecommunications and Signal Processing (TSP2012), Prague, 2012, pp. 401-405.
- [15] R. Sotner, N. Herensar, J. Jerabek, R. Dvorak, A. Kartci, T. Dostal, K. Vrba, "New double current controlled CFA(DCC-CFA) based voltage-mode oscillator with independent electronic control of oscillation condition and frequency," Journal of Electrical Engineering, vol. 64, no. 2, pp. 65-75, 2013.
- [16] B. Razavi, Design of analog CMOS integrated circuits, New York, McGraw-Hill, 2001.
- [17] B. Gilbert, "Translinear Circuits: a Historical Overview," Analog Integrated Circuits Signal Processing, vol. 9, no. 2, pp. 95-118, 1996.
- [18] A. Bradley, "MOS Translinear Principle for All Inversion Levels," IEEE Trans. on Circuits and Systems-II: vol. 55, no. 2, pp. 121-125, 2008.
- [19] R. Prokop, V. Musil, "Modular approach to design of modern circuit blocks for current signal processing and new device CCTA," Seventh International Conference on Signal and Image Processing (IASTED 2005), Honolulu, 2005, pp. 494-499.

[39] SOTNER, R., JERABEK, J., PROKOP, R., KLEDROWETZ, V., FUJCIK, L., DOSTAL, T. Reconfigurable 1st Order Filters Based on Differential Voltage Input and a Single Current Output Transconductance Multiplier. In *PROCEEDINGS EUROCON 2015 (IEEE Region 8, 16th International Conference on Computer as a Tool)*, Salamanca (Spain), 2015, p. 324-327. ISBN: 978-1-4799-8569-2.

Reconfigurable 1st Order Filters Based on Differential Voltage Input and a Single Current Output Transconductance Multiplier

Roman Sotner, Jan Jerabek, Roman Prokop, Vilem Kledrowetz, Lukas Fucik
Faculty of Electrical Engineering and Communication
Brno University of Technology
Brno, Czech Republic
sotner@feec.vutbr.cz

Tomas Dostal
Dept. of Electrical Engineering and Computer Science
College of Polytechnics Jihlava
Jihlava, Czech Republic
tomas.dostal@vspj.cz

Abstract—This paper deals with reconnection-less electronically reconfigurable filtering applications of the differential voltage input and single current output transconductance multiplier. A voltage-mode and mixed-mode filter solutions are presented and their electronically configurable features (change of transfer type and adjustment) are verified by simulations in a Cadence Spectre simulator with I2T100 0.7 μm technology.

Keywords—Active element; electronic control; reconfiguration; reconnection-less filter; transconductance multiplier

I. INTRODUCTION

Many useful active elements for analog signal processing are known today [1]. However, most of them focus on linear operation and linear relations (summation, difference, subtraction, amplification, attenuation, etc.) between inter-terminal voltages and currents (transfers in general). Nonlinear operation may bring forth interesting features to an active device as well as the whole application. The first attempt to allow advanced signal operation between terminal transfers is multiplication. Of course, there are many known approaches how to construct voltage-mode multipliers (for example [2]-[6]). Research in this field is still open for improvement (see, for example, the quite recent work [7] and references cited therein). Some commercially available devices have also been manufactured (EL2082, EL4083, AD834). However, they focus directly on voltage mode operation (input and output signals are voltages) [8] or provide pure current mode operation [9]. There are also mixed-mode solutions [10] (also known as electronically controllable current conveyor) but multiplication is possible only between input voltage and input current. Applications in frequency filters, oscillators, modulators, etc. require current output terminal(s) in many cases. It was also discussed, for example, in [7], where a similar multiplier based on the same principle of the multiplication core was presented. However, in [7] and many similar cases, the range of output current change is very small in relation to multiplied input voltages (low tens of μA maximally) that is insufficient in many applications. Our

modification supposes an additional transconductance section [1], [11] in order to boost output current to a level that is more appropriate for real applications (variable gain amplifiers/transconductors with both polarities of the output response). This feature allows to construct interesting filtering applications, for example, a section with easy reconfiguration between minimal and non-minimal arguments.

The constructed CMOS transconductance multiplier allows us to design the applications which are not easily available with a classic operational transconductance amplifier (OTA) [11]. For example, reconfigurable frequency filters require such active elements where continuous change of the controllable parameter (even including change of polarity) of the active element is available. Electronically adjustable filters with the reconnection-less feature of transfer characteristic reconfiguration are very useful for on-chip design – electronic change of the transfer function is really useful because no physical (galvanic) change of structure or selection of the input/output terminal (by electronic switching causing possible-limited dynamic range and high distortion, etc.) is required. Input and output terminals are always the same (single-input and single-output type). Several works presenting this topic have already been published [12]-[16]. Works [12], [13] focus on second-order structures. Works [14]-[15] deal with 1st-order filters reconfigurable between all-pass (AP), low-pass (LP) and direct or inverting transfer (DT, iDT) functions. However, a solution also implementing high-pass (HP) response has not been discussed. Structures presented in this paper also allow HP transfer function to be available in voltage-mode. A sophisticated active device (modified current differencing unit allowing electronic control of four parameters) was presented in [16] to obtain LP, inverting HP and AP transfers simultaneously in a reconfigurable 1st-order current-mode filter

II. MULTIPLIER DEFINITION

A basic symbol of the multiplier is shown in Fig. 1. It implements transfer function in form:

$$I_z = (V_{x1} - V_{x2})(V_{y1} - V_{y2})k, \quad (1)$$

Research described in this paper was financed by Czech Ministry of Education in frame of National Sustainability Program under grant LO1401. For research, infrastructure of the SIX Center was used. Research described in the paper was supported by Czech Science Foundation projects under No. 14-24186P. Grant No. FEKT-S-14-2281 also supported this research. The support of the project CZ.1.07/2.3.00/20.0007 WICOMT, financed from the operational program Education for competitiveness, is gratefully acknowledged.

where k is the conversion transfer constant given by the specific solution and topology of the multiplier.

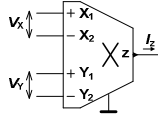


Fig. 1. Symbol of the transconductance multiplier.

Figure 2 shows the CMOS structure of the multiplier based on the standard multiplying core (so-called folded MOS Gilbert's cell) [5] with resistive loads (R_1 and R_2) and an additional transconductance section with cascoded mirrors (cascoded OTA) designed in order to provide boosted output current, good dynamics and linearity of the active device. Lower bandwidth is cost for these benefits.

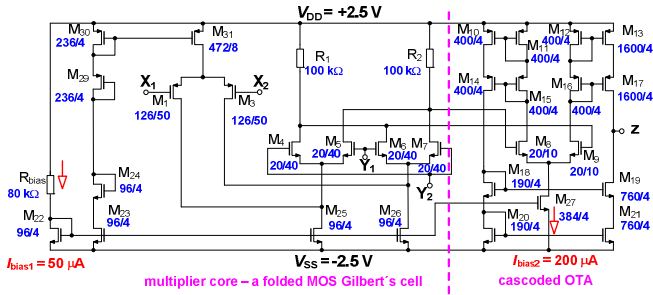


Fig. 2. CMOS structure of the transconductance multiplier.

The behavior of the multiplier is very similar to the standard OTA [11], where $I_{OUT} = (V_+ - V_-)g_m$. However, a standard OTA has only one polarity g_m and $g_m = 0$ is not possible as is obvious. Interchanging the input terminals is required for changing g_m (output current) polarity. Therefore, electronically adjustable availability of the transconductance value (g_m) in both polarities (and easy accessibility of $g_m = 0$) is a very important advantage of a transconductance amplifier based on a multiplier core. Constant transconductance of the multiplier is given by:

$$k = \sqrt{2k_{pN} \left(\frac{W}{L}\right)_{M1,2} k_{pP} \left(\frac{W}{L}\right)_{M4,5,6,7}} \sqrt{k_{pN} \left(\frac{W}{L}\right)_{M8,9}} I_{bias2} 4R_f, \quad (2)$$

where $k_{pN} = 67 \mu A/V^2$ and $k_{pP} = 27 \mu A/V^2$ are the transconductance parameters (approximated values considering different source and bulk potential of NMOS and PMOS) for ON Semiconductor/AMIS I2T100 0.7 μm technology used for simulation and potential fabrication because of its well-verified behavior and precise performance in analog signal processing. Constant value 4 in (2) is given by the gain of current mirrors of the output OTA section. The numerical value of k achieves 2.2 mS in our particular case.

III. APPLICATION EXAMPLES – RECONFIGURABLE FILTERS

The beneficial features of the transconductance multiplier (both polarities or zero value of g_m) allow to design an interesting filtering structure which may also serve as a bilinear section for the design of so-called constant phase elements or blocks (two-ports) and special fractional-order synthesis [17], [18] as the elementary building blocks in many resulting applications (for

example [18], [19]). This structure is presented in Fig. 3. The available transfer function has a general form:

$$K(s) = \frac{sC \pm g_{m1}}{sC \pm g_{m2}}. \quad (3)$$

However, we will mainly discuss practically interesting configurations. For $g_{m1} = g_{m2}$, the voltage-mode filter in Fig. 3 allows the following transfer - DT (bilinear filter [18] type 1):

$$K_{DT}(s) = \frac{sC + g_{m1}}{sC + g_{m2}}. \quad (4)$$

Inverting all-pass filter (iAP) for $g_{m2} = -g_{m1}$:

$$K_{iAP}(s) = \frac{sC - g_{m1}}{sC + g_{m2}}, \quad (5)$$

HP response for $g_{m1} = 0$:

$$K_{HP}(s) = \frac{sC}{sC + g_{m2}}, \quad (6)$$

and bilinear filter (type 2) in the form:

$$K_{DT}(s) = \frac{sC - g_{m1}}{sC - g_{m2}}. \quad (7)$$

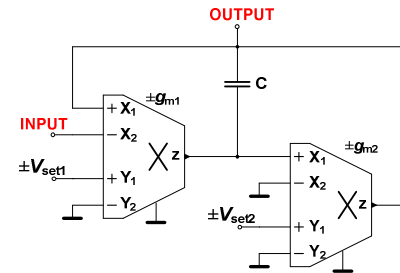


Fig. 3. Reconfigurable reconnection-less 1st-order voltage-mode filter.

All combinations of g_m polarities are easily available due to utilizing a transconductance multiplier. Additionally, independent or simultaneous control of zero ($\omega_p = g_{m1}/C$) and pole ($\omega_z = g_{m2}/C$) is easily available, which is very beneficial for classic electronic tuning and also for synthesis of the constant phase blocks [18].

The second example of application is the mixed-mode filtering structure shown in Fig. 4. The general available transfer function has the form:

$$G(s) = \frac{I_{OUT}}{V_{INP}} = \frac{sC(g_{m2} - g_{m1}) + g_{m1}g_{m2}}{sC + g_{m1}}. \quad (8)$$

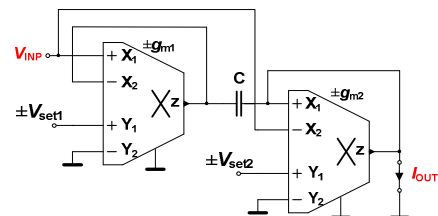


Fig. 4. Reconfigurable reconnection-less 1st-order mixed-mode filter.

This transfer function offers (for $g_{m2} = g_{m1}$) the following interesting configurations – low-pass filter:

$$G_{LP}(s) = \frac{g_{m1}g_{m2}}{sC + g_{m1}} \quad (9)$$

The all-pass filter is available for $g_{m1} = 2g_{m2} = g_m$:

$$G_{AP}(s) = g_m \frac{-sC + 2g_m}{sC + g_m}, \quad (10)$$

and the inverting high-pass filter:

$$G_{HP}(s) = \frac{-sCg_m}{sC + g_m} \quad (11)$$

IV. SIMULATION RESULTS

Both circuits were simulated in a Cadence Spectre simulator. The results are given for the following specifications: $C = 10$ nF, ideal pole/zero frequency 15.9 kHz, supply voltage ± 2.5 V and initial condition $g_{m1} = g_{m2} = 1$ mS ($V_{set1} = V_{set2} = 0.46$ V).

The results for the circuit from Fig. 3 are given in Fig. 5, where magnitude responses for g_{m1} (V_{set1}) stepping (see Tab. 1) are given (3 discrete values of g_{m1}). Phase responses are shown in Fig. 6. Simulated pole/zero frequency has a value of 15.1 kHz. The results confirm eq. (4)-(6) and illustrate the reconfigurable features of the structure. For negative g_{m1} , the filter operates in the regime of non-minimal argument (see detailed stepping of g_{m1} for several values in Fig. 7 and Fig. 8). For positive g_{m1} , the filter changes transfer from HP response to iAP response.

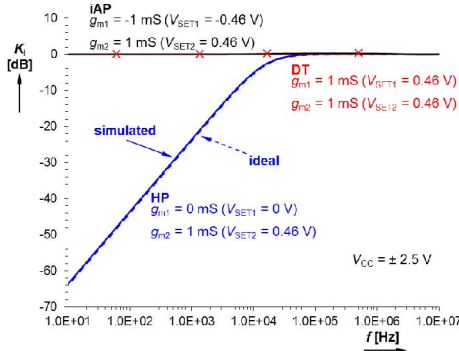


Fig. 5. Magnitude responses of the voltage-mode reconfigurable filter presented in Fig. 3 in iAP, DT and HP configuration.

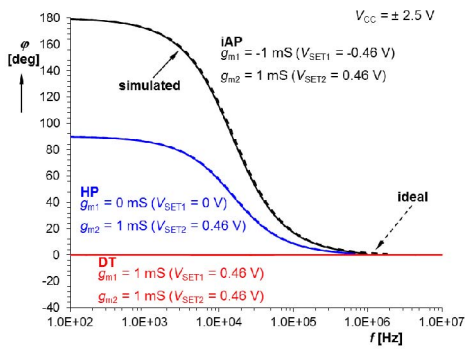


Fig. 6. Phase responses of the voltage-mode reconfigurable filter from Fig. 3 in iAP, DT and HP configuration.

TABLE I. SMALL-SIGNAL TRANSCONDUCTANCE VS. CONTROL VOLTAGE

g_m [mS]	± 0.25	± 0.5	± 1.0	± 2.0
V_{set} [V]	± 0.113	± 0.226	± 0.46	± 0.90

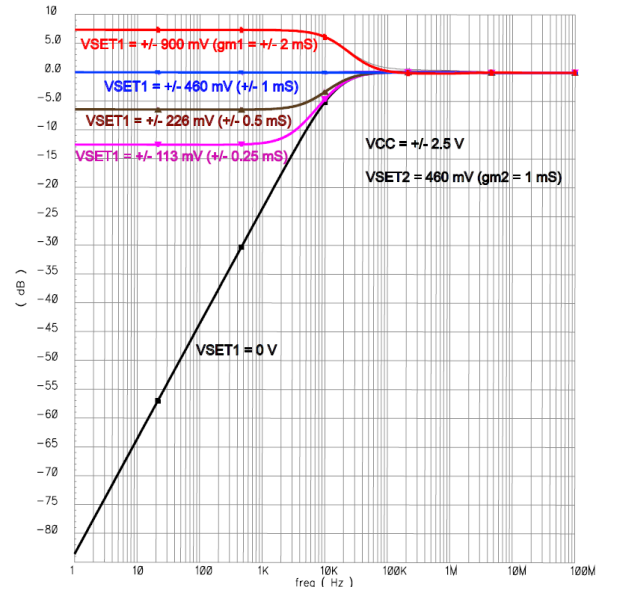


Fig. 7. Magnitude responses of the g_{m1} stepping in the voltage-mode reconfigurable filter from Fig. 3.

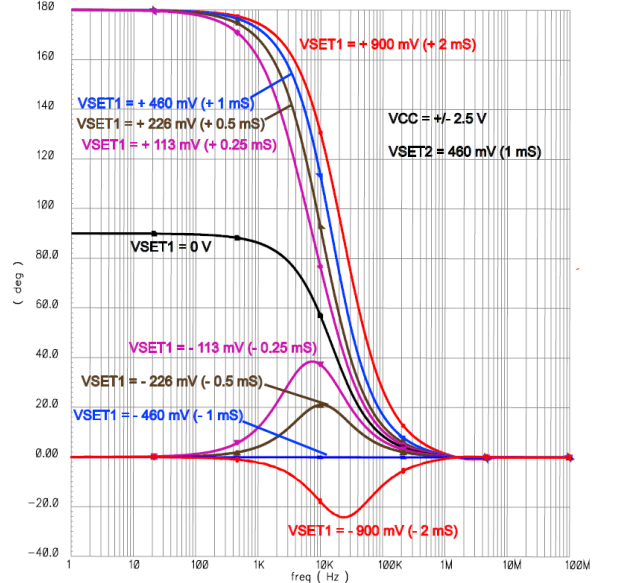


Fig. 8. Phase responses of the g_{m1} stepping in the voltage-mode reconfigurable filter from Fig. 3.

An example of electronic adjustments of the zero/pole frequency of the iAP response is given in Fig. 9. The frequency was altered between four discrete values: 3.54 kHz ($g_{m1} = g_{m2} = 0.25$ mS), 7.17 kHz (0.5 mS), 15.1 kHz (1 mS) and 34.9 kHz (2 mS). Appropriate setting (depending on required zero location, attenuation in the stop band, etc.) of both parameters (g_{m1} , g_{m2}) allows operation of the filter as HP with transfer zero (HPZ). An example of the simulation results of the second structure (Fig. 4) is shown in Fig. 10 and Fig. 11.

REFERENCES

- [1] D. Biolek, R. Senani, V. Biolkova, Z. Kolka, "Active elements for analog signal processing: classification, review, and new proposals," *Radioengineering*, vol. 17, no. 4, pp. 15-30, 2008.
- [2] B. Gilbert, "A precise four-quadrant multiplier with subnanosecond response," *IEEE Journal of Solid-State Circuits*, vol. SC-3, no. 4, pp. 365-373, 1968.
- [3] B. Gilbert, "A high-performance monolithic multiplier using active feedback," *IEEE Journal of Solid-State Circuits*, vol. SC-9, no. 6, pp. 364-373, 1974.
- [4] D. C. Soo, R. G. Meyer, "A four-quadrant NMOS analog multiplier," *IEEE Journal of Solid-State Circuits*, vol. SC-17, no. 6, pp. 1174-1178, 1982.
- [5] J. N. Babanezhad, G. C. Themes, "A 20-V four-quadrant CMOS analog multiplier," *IEEE Journal of Solid-State Circuits*, vol. SC-20, no. 6, pp. 1158-1168, 1985.
- [6] S-C. Qin, R. L. Geiger, "A +/- 5-V CMOS analog multiplier," *IEEE Journal of Solid-State Circuits*, vol. SC-22, no. 6, pp. 1143-1146, 1987.
- [7] S. Keles, H. Kuntman, "Four quadrant FG MOS analog multiplier," *Turkish Journal of Electrical Engineering and Computer Science*, vol. 19, no. 2, pp. 291-301, 2011.
- [8] Analog Devices. AD835 250 MHz, Voltage output 4-quadrant multiplier (datasheet), 2010, 16 p., accessible on [www: http://www.analog.com/static/imported-files/data_sheets/AD835.pdf](http://www.analog.com/static/imported-files/data_sheets/AD835.pdf)
- [9] Intersil (Elantec). EL4083 CN Current-mode four quadrant multiplier (datasheet), 1995, 14 p., accessible on [www: http://www.intersil.com/content/dam/Intersil/documents/el40/el4083.pdf](http://www.intersil.com/content/dam/Intersil/documents/el40/el4083.pdf)
- [10] Intersil (Elantec). EL2082 CN Current-mode multiplier (datasheet), 1996, 14 p., accessible on [www: http://www.intersil.com/data/fn/fn7152.pdf](http://www.intersil.com/data/fn/fn7152.pdf)
- [11] R. L. Geiger, E. Sánchez-Sinencio, "Active filter design using operational transconductance amplifiers: a tutorial," *IEEE Circ. and Devices Magazine*, vol. 1, pp. 20-32, 1985.
- [12] R. Sotner, J. Jerabek, B. Sevcik, T. Dostal, K. Vrba, "Novel solution of notch/all-pass filter with special electronic adjusting of attenuation in the stop band," *Elektronika Ir Elektrotechnika*, vol. 17, no. 7, pp. 37-42, 2011.
- [13] R. Sotner, J. Jerabek, J. Petrzela, K. Vrba, T. Dostal, "Design of fully adjustable solution of band-reject/all-pass filter transfer function using signal flow graph approach," In *Proceedings of the 24th International Conference Radioelektronika 2014*, 2014, p. 67-70.
- [14] R. Sotner, J. Jerabek, N. Herencsar, R. Prokop, K. Vrba, T. Dostal, "Resistor-less first-order filter design with electrical reconfiguration of its transfer function," In *Proceedings of the 24th International Conference Radioelektronika 2014*, 2014, p. 63-66.
- [15] R. Sotner, N. Herencsar, J. Jerabek, R. Prokop, A. Kartci, T. Dostal, K. Vrba, "Z-copy controlled-gain voltage differencing current conveyor: advanced possibilities in direct electronic control of first-order filter," *Elektronika Ir Elektrotechnika*, vol. 20, no. 6, p. 77-83, 2014.
- [16] R. Sotner, J. Jerabek, N. Herencsar, T. Zak, W. Jaikla, K. Vrba, "Modified Current Differencing Unit and its Application for Electronically Reconfigurable Simple First-order Transfer Function", *Advances in Electrical and Computer Engineering*, vol. 15, no. 1, pp. 3-10, 2015.
- [17] B. M. Vinagre, I. Podlubny, A. Hernandez, V. Feliu, "Some approximations of fractional order operators used in control theory and applications," *Fractional calculus and applied analysis*, vol. 3, no. 3, pp. 231-248, 2000.
- [18] J. Petrzela, "Fundamental analog cells for fractional-order two-port synthesis," in *Proc. of 23th Int. Conf. Radioelektronika 2013*, Pardubice, Czech Republic, pp. 182-187, 2013.
- [19] B. Maundy, A. Elwakil, S. Gift, "On the realization of multiphase oscillators using fractional-order allpass filters," *Circuits Systems and Signal Processing*, vol. 31, no. 1, pp. 3-17, 2012.

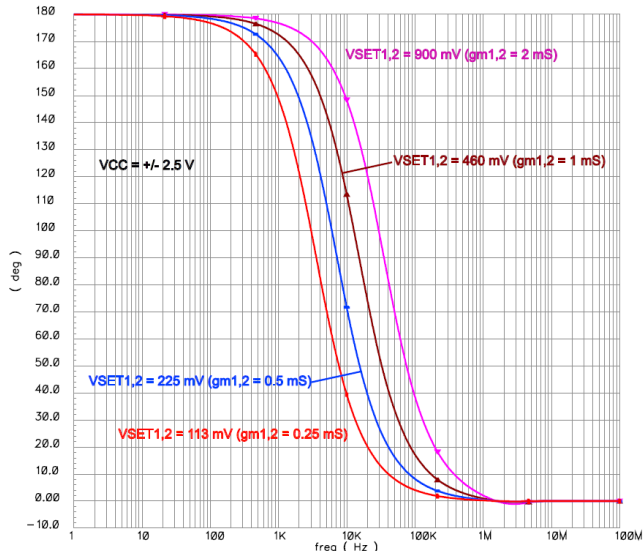


Fig. 9. Electronic adjustments of the zero/pole frequency of the iAP (phase responses) from Fig. 3.

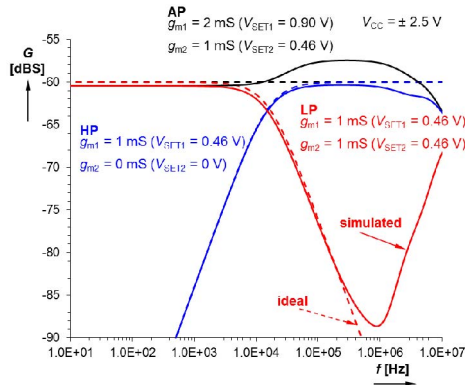


Fig. 10. Magnitude responses of the mixed-mode filter from Fig. 4.

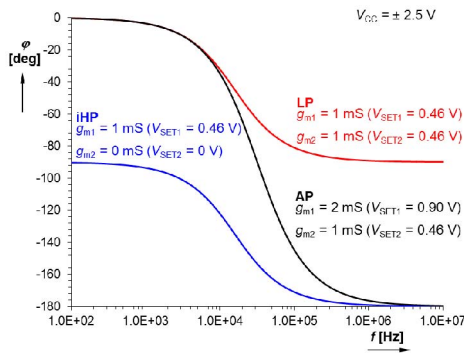


Fig. 11. Phase responses of the mixed-mode filter from Fig. 4.

V. CONCLUSION

We have shown that a transconductance multiplier brings wide variability into filtering structures where reconnection-less features are possible. The circuit in Fig. 3 can work in several transmission modes, i.e., DT, iDT, iAP and HP, and independent control of zero and pole frequency is also allowed. Therefore, this circuit (in bilinear mode) is also suitable for special types of nonstandard synthesis. The circuit in Fig. 4 allows reconfiguration between LP, AP and iHP.